

**Ongoing Face Recognition
Vendor Test (FRVT)**
Part 1: Verification

Patrick Grother
Mei Ngan
Kayee Hanaoka
Joyce C. Yang
Austin Hom

*Information Access Division
Information Technology Laboratory*

This publication is available free of charge from:
<https://www.nist.gov/programs-projects/face-recognition-vendor-test-frvt-ongoing>

2022/11/06



ACKNOWLEDGMENTS

The authors are grateful for the long-standing support and collaboration of the the Department of Homeland Security's Science & Technology Directorate (S&T) and the Office of Biometric Identity Management (OBIM).

Additionally, the authors are grateful to staff in the NIST Biometrics Research Laboratory for infrastructure supporting rapid evaluation of algorithms.

DISCLAIMER

Specific hardware and software products identified in this report were used in order to perform the evaluations described in this document. In no case does identification of any commercial product, trade name, or vendor, imply recommendation or endorsement by the National Institute of Standards and Technology, nor does it imply that the products and equipment identified are necessarily the best available for the purpose.

INSTITUTIONAL REVIEW BOARD

The National Institute of Standards and Technology's Research Protections Office reviewed the protocol for this project and determined it is not human subjects research as defined in Department of Commerce Regulations, 15 CFR 27, also known as the Common Rule for the Protection of Human Subjects (45 CFR 46, Subpart A).

FRVT STATUS

This report is a draft NIST Interagency Report, and is open for comment. It is the thirty sixth edition of the report since the first was published in June 2017. Prior editions of this report are maintained on the FRVT [website](#), and may contain useful information about older algorithms and datasets no longer used in FRVT.

FRVT remains open: All [four tracks](#) of the FRVT are open to new algorithm submissions.

2022-11-06 changes since 2022-09-26:

- ▷ We have added results for first algorithms from six developers: AFR Engine, CMC Institute of Science and Technology, Saga Densan Center, Turkcell Technology, UXLabs, and Wise AI SDN BHD.
- ▷ We have added results for new algorithms from 14 returning developers: Coretech Knowledge, Cloudwalk - Moontime, Cloudmatrix, Deepglint, Guangzhou Pixel Solutions, Hangzhou Allu Network Information Technology, NEO Systems, One More Security, Palit Microsystems, Panasonic R+D Center Singapore, Samsung S1, Seventh Sense Artificial Intelligence, Touchless ID, and Veridas Digital Authentication Solutions S.L.
- ▷ We have retired results for 10 algorithms per our policy to only list results for two algorithms per developer. Results for retired algorithms appear in prior versions of this report in the [archive](#).

2022-09-26 changes since 2022-08-30:

- ▷ We have added results for first algorithms from three developers: Codeline, First Credit Bureau Kazakhstan, and InfoCert.
- ▷ We have added results for new algorithms from 14 returning developers: Advancegroup, Armatura LLC, Beijing Hisign Technology, Cybercore, Cyberlink Corp, Herta Security, ICM Airport Technics, InsightFace AI, Metsakuur, NSENSE Corp, Samsung-SDS, Videmo Intelligente Videoanalyse, Vietnam Posts and Telecommunications Group, and Vision Intelligence Center of Meituan.
- ▷ We have retired results for 11 algorithms per our policy to only list results for two algorithms per developer. Results for retired algorithms appear in prior versions of this report in the [archive](#).

2022-08-30 changes since 2022-07-29:

- ▷ We have added results for first algorithms from two developers: Aximetria, Intellibrain Technological Projects
- ▷ We have added results for new algorithms from twelve returning developers: Alchera Inc, Dermalog, Idemia, Incode Technologies Inc, Intellivision, Kasikorn Labs, Megvii/Face++, Techsign, TuringTech.vip, Universidade de Coimbra, Verijelais, Vixvizon
- ▷ We have retired results for six algorithms per our policy to only list results for two algorithms per developer. Results for retired algorithms appear in prior versions of this report in the [archive](#).

2022-07-29 changes since 2022-06-27:

- ▷ We have added results for first algorithms from seven developers: FRP LLC (Hawaii), IMDS Software, Inspur (Beijing) Electronic Information Industry, Intema - LGL Group, PAPAGO, Qaz Biometric Systems, and VIDA-Digital Identity

- ▷ We have added results for new algorithms from nine returning developers: Cyberextruder, Glory, Maxvision Technology, Rank One Computing, Securif AI, Suprema AI, Suprema ID, Toshiba, and Yuan High-Tech Development.
- ▷ We have retired results for nine algorithms per our policy to only list results for two algorithms per developer. Results for retired algorithms appear in prior versions of this report in the [archive](#).

2022-07-29 changes since 2022-06-27:

- ▷ We have added results for first algorithms from seven developers: FRP LLC (Hawaii), IMDS Software, Inspur (Beijing) Electronic Information Industry, Intema - LGL Group, PAPAGO, Qaz Biometric Systems, and VIDA-Digital Identity
- ▷ We have added results for new algorithms from nine returning developers: Cyberextruder, Glory, Maxvision Technology, Rank One Computing, Securif AI, Suprema AI, Suprema ID, Toshiba, and Yuan High-Tech Development.
- ▷ We have retired results for nine algorithms per our policy to only list results for two algorithms per developer. Results for retired algorithms appear in prior versions of this report in the [archive](#).

2022-06-27 changes since 2022-06-03:

- ▷ We have added results for first algorithms from two developers: Krungthai Bank, and Smartbiometrik.
- ▷ We have added results for new algorithms from thirteen returning developers: Aiseemu, Corsight, Digidata, Griaule, Guangzhou Pixel Solutions, Hangzhuo AI Network Information Technology, Neurotechnology, Real Networks, Samsung S1, Sensetime Group, Smart Engines, Verihubs Inteligensia, and VinBigData.
- ▷ We have retired results for eight algorithms per our policy to only list results for two algorithms per developer. Results for retired algorithms appear in prior versions of this report in the [archive](#).

2022-06-03 changes since 2022-05-05:

- ▷ We have added results for first algorithms from seven developers: Jaak IT, Metsakuur, Palit Microsystems, Smarvist Teknoloji, and Touchless ID.
- ▷ We have added results for new algorithms from sixteen returning developers: Cyberlink, FaceOnLive, Kakao Enterprise, Line Corporation (Line Clova), Multi-Modality Intelligence, NEO Systems, and Unissey
- ▷ We have retired results for four algorithms per our policy to only list results for two algorithms per developer. Results for retired algorithms appear in prior versions of this report in the [archive](#).
- ▷ We have moved the results for the twenty human-difficult pairs used in the May 2018 paper [*Face recognition accuracy of forensic examiners, superrecognizers, and face recognition algorithms*](#) by Phillips et al. [1]. to the algorithm-specific report cards (example: [PDF](#)).
- ▷ Likewise, we have added figures showing impostor distribution shifts across demographics to the report card.

2022-05-05 changes since 2022-03-18:

- ▷ We have added results for first algorithms from seven developers: Accurascan, DICIO, FacePhi, Pangiam, University of Surrey-CVSSP, and Veridium.
- ▷ We have added results for new algorithms from sixteen returning developers: ACI Software, Canon Inc, Cloudwalk - Moontime Smart Technology, Cybercore,

2022-05-05 changes since 2022-03-18:

- ▷ We have added results for first algorithms from seven developers: Accurascan, DICIO, FacePhi, Pangiam, University of Surrey-CVSSP, and Veridium.
- ▷ We have added results for new algorithms from sixteen returning developers: ACI Software, Canon Inc, Cloudwalk - Moontime Smart Technology, Cybercore, Cyberextruder, Gemalto Cogent, HyperVerge Inc, KuKe3D Technology, Megvii/Face++, Mobbeel Solutions, Panasonic R+D Center Singapore, Qnap Security, Samsung-SDS, Vietnam Posts and Telecommunications Group, Viettel Group, and Vision Intelligence Center of Meituan.
- ▷ We have retired results for 12 algorithms per our policy to only list results for two algorithms per developer. Results for retired algorithms appear in prior versions of this report in the [archive](#).

2022-03-18 changes since 2022-02-23:

- ▷ We have added support for the detection of multiple people in a single image (see Section 1.2). Specifically the API allows an algorithm to extract features from one or more faces it detects in an image. NIST scores such cases as a correct match when any detected face matches the reference photo, and as a false positive when either face matches a non-mated reference photo. The expected effect of doing this will be to improve reported false non-match rates, and to minimally elevate false match rates. This technique was only applied to images of type "border" and "kiosk".
- ▷ We have added results for first algorithms from four developers: IntelliVIX, Kasikorn Labs, Lebentech Biometrics, and Wicket.
- ▷ We have added results for new algorithms from 10 returning developers: Chunghwa Telecom, Cloudmatrix, Beijing DeepSense Technologies, FarBar Inc, Imagus Technology Pty, Intellivision, Maxvision Technology, NHN Corp, Seventh Sense Artificial Intelligence, and Verigram.
- ▷ We have retired results for 4 algorithms per our policy to only list results for two algorithms per developer. Results for retired algorithms appear in prior versions of this report in the [archive](#).

2022-02-23 changes since 2022-01-24:

- ▷ We have added results for first algorithms from four developers: AFIS and Biometrics Consulting, Digidata, Graymatics, Hangzhuo Allu Network Information Technology, KnowUTech LLC, Sukshi Technology Innovation, T4iSB, and TuringTech.vip
- ▷ We have added results for new algorithms from 18 returning developers: Cognitec Systems GmbH, GeoVision Inc, Glory, Herta Security, Intel Research Group, InsightFace AI, Kakao Enterprise, N-Tech Lab, Omnidarde Ltd, Papilon Savunma, Paravision, Reveal Networks Inc, Reveal Media Ltd, Shenzhen Inst Adv Integrated Tech CAS, Suprema AI Inc, Toshiba, Universidade de Coimbra, and Yuan High-Tech Development
- ▷ We have retired results for 14 algorithms per our policy to only list results for two algorithms per developer. Results for retired algorithms appear in prior versions of this report in the [archive](#).

2022-01-24 changes since 2022-01-20:

- ▷ We have added results for new algorithms from one returning developer: Vocord.

2022-01-20 changes since 2021-12-18:

- ▷ We have added results for first algorithms from four developers: Armatura, Beyne.AI, One More Security, and VinBigData
- ▷ We have added results for new algorithms from 19 returning developers: AuthenMetric, BOE Technology Group, Cybercore, Cyberlink, Dahua Technology, FaceTag Co, Innovatrics, Megvii, Mobbeel Solutions, Neurotechnology, Oz Forensics, Rank One Computing, Regula Forensics, Samsung S1, Securif AI, Sensetime Group, TigerIT Americas, Videmo Intelligent Videoanalyse, and YooniK.
- ▷ We have retired results for 14 algorithms per our policy to only list results for two algorithms per developer. Results for retired algorithms appear in prior versions of this report in the [archive](#).

: 2021-12-16 changes since 2021-11-22:

- ▷ We have added results for first algorithms from five developers: Alfabeto, Cloudmatrix, Euronovate SA, FaceOnLive Inc, and Mobiclip Technology.
- ▷ We have added results for new algorithms from ten returning developers: ACI Software, ITMO University, NEO Systems, Guangzhou Pixel Solutions, Panasonic R+D Center Singapore, Qnap Security, Scanovate, Tevian, Unissey, and Vietnam Posts and Telecommunications Group.
- ▷ We have retired results for eight algorithms per our policy to only list results for two algorithms per developer. Results for retired algorithms appear in prior versions of this report in the [archive](#).
- ▷ We have revamped the figure showing performance on 20 pairs of open-source images. It now color-codes false negatives and positives against a default threshold value.

2021-11-22 changes since 2021-10-28:

- ▷ We have added results to the [website](#) for kiosk-collected images where the design and geometry configuration mean that many images have considerable downward pitch angle. In some images, the face is partially cropped. Some images have other background faces.
- ▷ We have stopped using child exploitation images in FRVT, as we lost access to the imagery. All results for that set have been removed from the [website](#), and will be removed from future PDF reports.
- ▷ We have added results for first algorithms from seven new developers: CUDO Communication, Daon, KuKe3D Technology, Mantra Softtech India, Maxvision Technology, Multi-Modality Intelligence, and Samsung-SDS.
- ▷ We have added results for new algorithms from seven returning developers: Acer Incorporated, Cloudwalk-Moontime Smart Technology, Gorilla Technology, ID3 Technology, Incode Technologies, NSENSE Corp., and SQIssoft.
- ▷ We have retired results for six algorithms per our policy to only list results for two algorithms per developer. Results for retired algorithms appear in prior versions of this report in the [archive](#).

2021-10-28 changes since 2021-09-08:

- ▷ We have substantially revised the algorithm-specific report cards that are linked from the [FRVT results page](#). (Example: [HTML](#)).
- ▷ We have added results for first algorithms from eight new developers: Beijing Mendaxia Technology, Beijing Hisign Technology, Biocube Matrics, Clearview AI, Reveal Media, Toppan ID Gate, Verigram, and Viettel High Technology.
- ▷ We have added results for new algorithms from thirty returning developers: 20Face, 3divi, Canon Inc Chunghwa Telecom, Corsight, Decatur Industries, Deepglint, Dermalog, FaceTag, Fiberhome Telecommunication Technologies, GeoVision, ICM Airport Technics, Imagus Technology, InsightFace AI, Kakao Enterprise, Kookmin University, Line Corporation, N-Tech Lab, NotionTag Technologies, Realnetworks, Suprema ID, Taiwan-Certificate Authority, Toshiba, Tripleize, Trueface.ai, Veridas Digital Authentication, Visidon, VisionLabs, YooniK, and Yuan High-Tech Development.
- ▷ We have retired results for twenty algorithms per our policy to only list results for two algorithms per developer. Results for retired algorithms appear in prior versions of this report in the [archive](#).

2021-09-08 changes since 2021-08-02:

- ▷ We have added results for first algorithms from seven new developers: Griaule, SQISoft, Qnap Security, Techsign, Smart Engines, Verihubs, and Wuhan Tianyu Information Industry.
- ▷ We have added results for new algorithms from sixteen returning developers: ADVANCE.AI, AuthenMetric, CloudSmart Consulting, Code Everest Pvt, Cognitec Systems, Thales Gemalto Cogent, Intel Research Group, Omnidarde, Oz Forensics, Rank One Computing, Samsung S1 Corp, Securif AI, Tevian, TigerIT Americas, Universidade de Coimbra, and Vigilant Solutions
- ▷ We have retired results for eleven algorithms per our policy to only list results for two algorithms per developer. Results for retired algorithms appear in prior versions of this report in the [archive](#).

2021-08-02 changes since 2021-06-25:

- ▷ We have added results for first algorithms from eight new developers: Bee the Data, Closeli Inc, Coretech Knowledge Inc, Deepsense (France), ioNetworks Inc, Kakao Pay Corp, Seventh Sense Artificial Intelligence, and SK Telecom.
- ▷ We have added results for new algorithms from fifteen returning developers: Alchera Inc, Adera Global PTE, Aware, Bresee Technology, Cyberlink Corp, Expasoft LLC, Fujitsu Research and Development Center, Gorilla Technology, Idemia, Neurotechnology, NEO Systems, NHN Corp, Paravision, Panasonic R+D Center Singapore, and Shenzhen University-Macau University of Science and Technology.
- ▷ We have retired results for twelve algorithms per our policy to only list results for two algorithms per developer. Results for retired algorithms appear in prior versions of this report in the [archive](#).

2021-06-25 changes since 2021-05-21:

- ▷ We have added results for first algorithms from six new developers: Alice Biometrics, BOE Technology Group, Fincore, Neosecu, Sodec App, and Yuntu Data and Technology.

- ▷ We have added results for new algorithms from seven returning developers: Incode Technologies, HyperVerge, Mobbeel Solutions, Guangzhou Pixel Solutions, Remark Holdings, Sensetime, and Vietnam Posts and Telecommunications Group.
- ▷ We have retired results for four algorithms per our policy to only list results for two algorithms per developer. Results for retired algorithms appear in prior versions of this report in the [archive](#).

2021-05-21 changes since 2021-04-26:

- ▷ We have added results for first algorithms from five new developers: Ekin Smart City Technologies, Suprema ID, Tripleize, Taiwan-Certificate Authority, and Vision Intelligence Center of Meituan.
- ▷ We have added results for new algorithms from eight returning developers: ID3 Technology, Imagus Technology, Momentum Digital, N-Tech Lab, NSENSE, Shanghai Jiao Tong University, Vision-Box, and Yuan High-Tech Development
- ▷ We have retired results for seven algorithms per our policy to only list results for two algorithms per developer. Results for retired algorithms appear in prior versions of this report in the [archive](#).

2021-04-26 changes since 2021-04-16:

- ▷ We have added results for first algorithms from three new developers: Quantasoft, Rendip, and NEO Systems.
- ▷ We have added results for new algorithms from four returning developers: 3Divi, Realnetworks, Veridas Digital Authentication Solutions, and Universidade de Coimbra.
- ▷ We have retired results for three algorithms per our policy to only list results for two algorithms per developer. Results for retired algorithms appear in prior versions of this report in the [archive](#).

2021-04-16 changes since 2021-03-19:

- ▷ We have added results for first algorithms from six new developers: 20Face, Beijing DeepSense Technologies, BitCenter UK, Enface, FaceTag, InsightFace AI, Line Corporation, Lema Labs, Nanjing Kiwi Network Technology, Omnidarde, Regula Forensics, and Suprema.
- ▷ We have added results for new algorithms from ten returning developers: CloudSmart Consulting, Dermalog, GeoVision, Neurotechnology, Panasonic R+D Center Singapore, Samsung S1, Securif AI, Trueface.ai, Vigilant Solutions, and Visidon.
- ▷ We have retired results for ten algorithms per our policy to only list results for two algorithms per developer. Results for retired algorithms appear in prior versions of this report in the [archive](#).

2021-03-19 changes since 2021-03-05:

- ▷ We have added results for first algorithms from six new developers: Ajou University, AuthenMetric, Code Everest, Corsight, Papilon Savunma, and NHN Corp
- ▷ We have added results for new algorithms from seven returning developers: Alchera, Deepglint, Fiber-home Telecommunication Technologies, Kakao Enterprise, Kookmin University, Megvii/Face++, and NotionTag Technologies.

- ▷ We have updated many of the hyperlinked HTML report-cards to include seven figures on demographic dependence. Figures of this kind first appeared, and are documented in, the December 2019 document, [NIST Interagency Report 8280](#) on demographic differentials in face recognition. The figures quantify false negative dependence on demographics using “visa-border” comparisons, and false positive dependence using comparisons of “application” photos that uniformly of quality and similar to visa photos.

2021-03-05 changes since 2021-01-19:

- ▷ We have added results for first algorithms from three new developers: IVA Cognitive, Mobbeel, and MoreDian Technology.
- ▷ We have added results for new algorithms from returning developers: Ability Enterprise - Andro Video, ACI Software, Adera Global, AnyVision, BioID Technologies, China Electronics Import-Export, Cognitec Systems, Fujitsu Research and Development Center, Glory, Guangzhou Pixel Solutions, Hengrui AI Technology, Incode Technologies, Intel Research, iQIYI, Mobai, Oz Forensics, Paravision, VisionLabs, and Xforward AI Technology.
- ▷ We have added a new “resources” tab to the main [webpage](#). It includes sortable columns for data related to speed, model size, storage, and memory consumption.
- ▷ We have retired results for 13 algorithms per our policy to only list results for two algorithms per developer. Results for retired algorithms appear in prior versions of this report in the [archive](#).

2021-01-19 changes since 2020-12-18:

- ▷ This report adds results for first algorithms from four developers: Herta Security, Irex AI, Shenzhen University-Macau University of Science and Technology, and Vietnam Posts and Telecommunications Group. See Table 7 for more information.
- ▷ The report also includes results for thirteen developers who have previously submitted algorithms: Bresee Technology, Canon (previously Canon Information Technology (Beijing)), Cyberlink, CSA IntelliCloud Technology, Dahua Technology, ID3 Technology, Imagus Technology (Vixvizon), Moontime Smart Technology, N-Tech Lab, Thales Cogent, Veridas Digital Authentication Solutions, Vocord, and Yuan High-Tech Development.
- ▷ We have retired results for ten algorithms per our policy to only list results for two algorithms per developer. Results for retired algorithms appear in prior versions of this report in the [archive](#).

2020-12-18 changes since 2020-10-09:

- ▷ This report adds results for first algorithms from ten developers: BitCenter UK, CloudSmart Consulting, Cubox, Institute of Computing Technology, Naver Corp, Minivision, NSENSE Corp, Viettel Group, Visage Technologies, and Xiamen University. See Table 7 for more information.
- ▷ The report also includes results for eighteen developers who have previously submitted algorithms: ADVANCE.AI, Awidit Systems, Chosun University, Dermalog, GeoVision, ICM Airport Technics, Idemia, Institute of Information Technologies, Kakao Enterprise, Neurotechnology, Panasonic R+D Center Singapore, Rank One Computing, SenseTime Group, Shanghai Jiao Tong University, TigerIT Americas LLC, Vigilant Solutions, Winsense, and YooniK

- ▷ We have retired results for twelve algorithms per our policy to only list results for two algorithms per developer. Results for retired algorithms appear in prior versions of this report in the [archive](#).

Changes since September 18, 2020:

- ▷ This report adds results for first algorithms from five developers: Aigen, Cortica, Kookmin University, Securif AI and Vinai.
- ▷ The report also includes results for three developers who have previously submitted algorithms: Fujitsu Laboratories, Hengrui AI, and X-Forward AI.
- ▷ In the per-algorithm report-cards linked from tables and the main webpage, we have added a chart to showing reduction in error rates over the course of FRVT i.e. from 2017 onwards for all algorithms supplied by that developer. Similarly we have added a chart showing error rate reductions for our test of protective face mask verification.
- ▷ We plan to continue evaluating algorithms on various mask datasets. We hold that algorithms should be capable of detecting masks and verifying identity of all combinations of masked and unmasked faces. We have accordingly increased the amount of time allowed to extract those features from 1.0 to 1.5 seconds.

Changes since August 25, 2020:

- ▷ This report adds results for first algorithms from eight new developers. Akurat Satu Indonesia, Cybercore, Decatur Industries, Innef Labs, Satellite Innovation/Eocortex, Expasoft, and Mobai.
- ▷ The report includes results for seven developers who have previously submitted algorithms: 3Divi, BioID Technologies, Incode Technologies, Innovatrics, iSAP Solution, Synology, and Tevian.
- ▷ We have retired results for five algorithms per our policy to only list results for two algorithms per developer. Results for retired algorithms appear in prior versions of this report in the [archive](#).

Changes since July 27, 2020:

- ▷ We have introduced per-algorithm report sheets. These are HTML documents linked from the accuracy tables in this report (i.e. Table 29) and on the FRVT 1:1 [homepage](#). The sheets contain interactive graphics allowing, for example, mouseover exploration of FNMR(T) and FMR(T). Some of their content had previously appeared in this document.
- ▷ This report adds results for algorithms from six new developers. ACI Software, Bresee Technology, Fiberhome Telecommunication Technologies, Imageware Systems, Oz Forensics, and Pensees.
- ▷ The report includes results for thirteen developers who have previously submitted algorithms: Canon Information Technology (Beijing), Cyberlink, Dahua Technology, Gorilla Technology, ID3 Technology, Intel Research Group, iQIYI Inc, Momentum Digital, Netbridge Technology, Tech5 SA, Shenzhen AiMall Tech, Vigilant Solutions, and VisionLabs.
- ▷ We have retired results for nine algorithms per our policy to only list results for two algorithms per developer. Results for retired algorithms appear in prior versions of this report in the [archive](#).

Changes since May 18, 2020:

- ▷ The report is the first FRVT update since the pandemic closed it from March to June 2020.

- ▷ This report includes results for algorithms from nine new developers: GeoVision Inc, Su Zhou NaZhi-TianDi Intelligent Technology, YooniK, AYF Technology, PXL Vision AG, Yuan High-Tech Development, Beihang University-ERCACAT, ICM Airport Technics, and Staqu Technologies
- ▷ This report includes results for algorithms from 15 returning developers Acer Incorporated, Antheus Technologia, Chosun University, Chunghwa Telecom, Idemia, Moontime Smart Technology, Neurotechnology, Guangzhou Pixel Solutions, Panasonic R+D Center Singapore, Rank One Computing, Scanovate, Shanghai University - Shanghai Film Academy, Synesis, Trueface.ai, and Veridas Digital Authentication Solutions
- ▷ We have retired results for ten algorithms per our policy to only list results for two algorithms per developer. Results for retired algorithms appear in prior versions of this report in the [archive](#).
- ▷ We separated timing and other resource consumption from the main participation table. The new Table 18 includes template generation durations for four kinds of images, not just mugshots.
- ▷ We have published a separate report, [NIST Interagency Report 8311](#) on accuracy of pre-pandemic algorithms on subjects wearing face masks. We plan to track improvements in accuracy on masked images going forward. In particular, we invite submission of algorithms that can detect whether a person is wearing a mask, extract features from the full face or the exposed periocular region, and do appropriate comparison. We do not intend to evaluate algorithms that assume 100% of images will be of masked individuals.

Changes since March 25, 2020:

- ▷ The report is a maintenance release - it does not add any new algorithms, and FRVT has been closed to new algorithms since mid March 2020.
- ▷ We modified the primary accuracy summary, Table 29, as follows:
 - ▷▷ For visa images, the column for FNMR at FMR = 0.0001 has been removed. The visa images are so highly controlled that the error rates for the most accurate algorithms are dominated by false rejection of very young children and by the presence of a few noisy greyscale images. For now, two visa columns remain: FNMR at $FMR = 10^{-6}$ and, for matched covariates, FNMR at $FMR = 10^{-4}$.
 - ▷▷ We have inserted a new column labelled "BORDER" giving accuracy for comparison of moderately poor webcam border-crossing photos that exhibit pose variations, poor compression, and low contrast due to strong background illumination. The accuracies are the worst from all cooperative image datasets used in FRVT.
- ▷ Accordingly, we updated the failure-to-template rates in Table 37.
- ▷ We withdrew a figure showing how false matches are concentrated in certain visa images used in cross-comparison, because it didn't attempt to include demographic information.

Changes since February 27, 2020:

- ▷ The report adds results algorithms from two new developers: Beijing Alleyes Technology, and the Chinese University of Hong Kong. Results for newly submitted algorithms from two other developers will appear in the next report.
- ▷ The report adds results for algorithms from thirteen returning developers: ASUSTek Computer, Aware, Cyberlink Corp, Gorilla Technology, Innovative Technology, Kakao Enterprise, Lomonosov Moscow State University, Panasonic R+D Center Singapore, Shenzhen AiMall Technology, Shenzhen Intellifusion Technologies, Synology, Tech5 SA, and Via Technologies.

- ▷ Per policy to only list results for two algorithms per developer, we have dropped results for algorithms from Aware, Cyberlink, Gorilla Technology, Kakao Enterprise, Lomonosov Moscow State University, Panasonic R+D Center Singapore, and Tech5 SA.

Changes since January 20, 2020:

- ▷ The report adds results for five new developers: Ability Enterprise (Andro Video), Chosun University, Fujitsu Research and Development Center, University of Coimbra, and Xforward AI Technology.
- ▷ The report adds results for algorithms from six returning developers: AlphaSSTG, Incode Technologies, Kneron, Shanghai Jiao Tong University, Vocord, and X-Laboratory.
- ▷ We have corrected template comparison timing numbers for algorithms submitted September 2019 to January 2020. The values reported previously were slower due to a software bug.
- ▷ We have dropped results for algorithms from Vocord and Incode per policy to only list results for two algorithms per developer.
- ▷ The [FRVT 1:1 homepage](#) has been updated with latest accuracy results.
- ▷ The [FRVT 1:N homepage](#) now includes an update to the September 2019 NIST Interagency Report 8271. The new report adds results for one-to-many search algorithms submitted to NIST from June 2019 to January 2020.

Changes since January 6, 2020:

- ▷ Section 2 has been updated to better describe the Visa and Border images. The caption for Table 29 has been updated to better relate the accuracy values to particular image comparisons.
- ▷ The report adds results for five new developers: Acer, Advance.AI, Expasoft, Netbridge Technology, and Videmo Intelligent Videoanalyse.
- ▷ The report adds results for algorithms from 7 returning developers: China Electronics Import-Export Corp, Intel Research Group, ITMO University, Neurotechnology, N-Tech Lab, Rokid, and VisionLabs.
- ▷ We have dropped results from this edition of the report per policy to only list results for two algorithms per developer: N-Tech Lab, Neurotechnology, ITMO, Visionlabs, and CEIEC.
- ▷ The [FRVT homepage](#) has been updated with latest accuracy results.

Changes since November 11, 2019:

- ▷ Table 18 has been updated to include runtime memory usage. This is the first time such a quantity has been reported. The value is the peak size of the resident set size logged during enrollment of single images.
- ▷ We have migrated summary results table to a new platform that supports sortable tables:
<https://pages.nist.gov/frvt/html/frvt11.html>
- ▷ The report adds results for four new developers: Antheus Technologia, BioID Technologies SA, Canon Information Tech. (Beijing), Samsung S1 (listed in the tables as S1), and Taiwan AI Labs.
- ▷ The report adds results for algorithms from 13 returning developers: Anke Investments, Chunghwa Telecom, Deepglint, Institute of Information Technologies, iQIYI, Kneron, Ping An Technology, Paravision, KanKan Ai, Rokid Corporation, Shanghai Universiy - Shanghai Film Academy, Veridas Digital Authentication Solutions, and Videonetics Technology.

- ▷ We have dropped results from this edition of the report per policy to only list results for two algorithms per developer: remarkai-000, veridas-001, sensetime-001, iit-000, anke-003, and everai-002. Results for these are available in prior editions of this report linked from the FRVT page.
- ▷ We issued [NIST Interagency Report 8280: FRVT Part 3: Demographics](#) on 2019-12-19. It includes results for many of the algorithms covered by this report.

Changes since October 16, 2019:

- ▷ The report adds results for ten new developers: Ai-Union Technology, ASUSTek Computer, DiDi ChuXing Technology, Innovative Technology, Luxand, MVision, Pyramid Cyber Security + Forensic, Scanovate, Shenzhen AiMall Tech, and TUPU Technology.
- ▷ The report adds results for 12 returning developers: CTBC Bank Glory Gorilla Technology Guangzhou Pixel Solutions Imagus Technology Incode Technologies Lomonosov Moscow State University Rank One Computing Samtech InfoNet Shanghai Ulucu Electronics Technology Synesis, and Winsense.
- ▷ We have dropped results from this edition of the report per policy to only list results for two algorithms per developer: glory-000, gorilla-002, incode-003, rankone-006, and synesis-004.
- ▷ Results for five recently submitted algorithms will appear in the next report.

Changes since September 11, 2019:

- ▷ The report adds results for five new participants: Awidit Systems (Awiros), Momenmtum Digital (Sertis), Trueface AI, Shanghai Jiao Tong University, and X-Laboratory.
- ▷ The reports adds results for five new algorithms from returning developers: Cyberlink, Hengrui AI Technology, Idemia, Panasonic R+D Singapore, and Tevian. This causes three algorithm, to be de-listed from the report per policy to list results for two algorithms per developer.

Changes since July 31 2019:

- ▷ The HTML table on the [FRVT 1:1 homepage](#) has been updated to include a column for cross-domain Visa-Border verification. Results for this new dataset appeared in the July 29 report under the name "CrossEV" - these are now renamed "Visa-Border".
- ▷ The [FRVT 1:1 homepage](#) lists algorithms according to lowest mean rank accuracy:

$$\begin{aligned} & \text{Rank(FNMR}_{\text{VISA}} \text{ at FMR = 0.000001}) + \\ & \text{Rank(FNMR}_{\text{VISA-BORDER}} \text{ at FMR = 0.000001}) + \\ & \text{Rank(FNMR}_{\text{MUGSHOT}} \text{ at FMR = 0.00001 after 14 years}) + \\ & \text{Rank(FNMR}_{\text{WILD}} \text{ at FMR = 0.00001}) \end{aligned}$$

This ordering rewards high accuracy across all datasets.
- ▷ The main results in Table 29 is now in landscape format to accomodate extra columns for the Visa-Border set, and mugshot comparisons after at least 12 years.
- ▷ The report adds results for nine new participants: Alpha SSTG, Intel Research, ULSee, Chungwa Telecon, iSAP Solution, Rokid, Shenzhen EI Networks, CSA Intellicloud, Shenzhen Intellifusion Technologies.
- ▷ The reports adds results for six new algorithms from returning developers: Innovatrics, Dahua Technology, Tech5 SA, Intellivision, Nodeflux and Imperial College, London. One algorithm, from Imperial has been retired, per policy to list results for two algorithms per developer.
- ▷ The cross-country false match rate heatmaps have been replotted to reveal more structure by listing countries by region instead of alphabetically.

- ▷ The next version of this report will be posted around October 18, 2019.

Changes since July 3 2019:

- ▷ The HTML table on the [FRVT 1:1 homepage](#) has been updated to list the 20 most accurate developers rather than algorithms, choosing the most accurate algorithm from each developer based on visa and mugshot results. Also, the algorithms are ordered in terms of lowest mean rank across mugshot, visa and wild datasets, rewarding broad accuracy over a good result on one particular dataset.
- ▷ This report includes results for a new dataset - see the column labelled "visa-border" in Table 5. It compares a new set of high quality visa-like portraits with a set webcam border-crossing photos that exhibit moderately poor pose variations and background illumination. The two new sets are described in sections [2.2](#) and [2.3](#). The comparisons are "cross-domain" in that the algorithm must compare "visa" and "wild" images. Results for other algorithms will be added in future reports as they become available.
- ▷ This report adds results for algorithms from 9 developers submitted in early July 2019. These are from 3DiVi, Camvi, EverAI-Paravision, Facesoft, Farbar (F8), Institute of Information Technologies, Shanghai U. Film Academy, Via Technologies, and Ulucu Electronics Tech. Six of these are new participants.
- ▷ Several other algorithms have been submitted and are being evaluated. Results will be released in the next report, scheduled for September 5. That report will include results for new datasets.
- ▷ Older algorithms from Everai, Camvi and 3DiVi, have been retired, per the policy to list only two algorithms per developer.

Changes since June 20 2019:

- ▷ This report adds results for algorithms from 18 developers submitted in early June 2019. These are from CTBC Bank, Deep Glint, Thales Cogent, Ever AI Paravision, Gorilla Technology, Imagus, Incode, Kneron, N-Tech Lab, Neurotechnology, Notiontag Technologies, Star Hybrid, Videonetics, Vigilant Solutions, Winsense, Anke Investments, CEIEC, and DSK. Nine of these are new participants.
- ▷ Several other algorithms have been submitted and are being evaluated. Results will be released in the next report, scheduled for August 1.
- ▷ Older algorithms from Everai, Thales Cogent, Gorilla Technology, Incode, Neurotechnology, N-Tech Lab and Vigilant Solutions have been retired, per the policy to list only two algorithms per developer.

Changes since April 2019:

- ▷ This report adds results for nine algorithms from nine developers submitted in early June 2019. These are from Tencent Deepsea, Hengrui, Kedacom, Moontime, Guangzhou Pixel, Rank One Computing, Synesis, Sensetime and Vocord.
- ▷ Another 23 algorithms have been submitted and are being evaluated. Results will be released in the next report, scheduled for July 3.
- ▷ Older algorithms for Rank One, Synesis, and Vocord have been retired, per the policy to list only two algorithms per developer.

Changes since February 2019:

- ▷ This report adds results for 49 algorithms from 42 developers submitted in early March 2019.
- ▷ This report omits results for algorithms that we retired. We retired for three reasons: 1. The developer submitted a new algorithm, and we only list two. 2. The algorithm needs a GPU, and we no longer allow GPU-based algorithms. 3. Inoperable algorithms.
- ▷ Previous results for retired algorithms are available in older editions of this report linked [here](#).
- ▷ The mugshot database used from February 2017 to January 2019 has been replaced with an extract of the mugshot database documented in NIST Interagency Report 8238, November 2018. The new mugshot set is described in section [2.4](#) and is adopted because:

- ▷▷ It has much better identity label integrity, so that false non-match rates are substantially lower than those reported in FRVT 1:1 reports to date - see Figure 110.
- ▷▷ It includes images collected over a 17 year period such that ageing can be much better characterized - - see Figure 355.
- ▷ Using the new mugshot database, Figure 355 shows accuracy for four demographic groups identified in the biographic metadata that accompanies the data: black females, black males, white females and white males.
- ▷ The report added a figure (now moved to web) with results for the twenty human-difficult pairs used in the May 2018 paper *Face recognition accuracy of forensic examiners, superrecognizers, and face recognition algorithms* by Phillips et al. [1].
- ▷ The report uses an update to the wild image database that corrects some ground truth labels.
- ▷ Some results for the child exploitation database are not complete. They are typically updated less frequently than for other image sets.

Contents

ACKNOWLEDGMENTS	1
DISCLAIMER	1
INSTITUTIONAL REVIEW BOARD	1
1 METRICS	55
1.1 CORE ACCURACY	55
1.2 MULTI-TEMPLATE SCORING METHODOLOGY	55
2 DATASETS	56
2.1 VISA IMAGES	56
2.2 APPLICATION IMAGES	56
2.3 BORDER CROSSING IMAGES	56
2.4 MUGSHOT IMAGES	57
2.5 KIOSK IMAGES	57
2.6 WILD IMAGES	57
3 RESULTS	58
3.1 TEST GOALS	58
3.2 TEST DESIGN	58
3.3 FAILURE TO ENROLL	61
3.4 RECOGNITION ACCURACY	70
3.5 GENUINE DISTRIBUTION STABILITY	355
3.5.1 EFFECT OF BIRTH PLACE ON THE GENUINE DISTRIBUTION	355
3.5.2 EFFECT OF AGEING	395
3.5.3 EFFECT OF AGE ON GENUINE SUBJECTS	425
3.6 IMPOSTOR DISTRIBUTION STABILITY	466
3.6.1 EFFECT OF BIRTH PLACE ON THE IMPOSTOR DISTRIBUTION	466
3.6.2 EFFECT OF AGE ON IMPOSTORS	469

List of Tables

1 PARTICIPANT INFORMATION	24
2 PARTICIPANT INFORMATION	25
3 PARTICIPANT INFORMATION	26
4 PARTICIPANT INFORMATION	27
5 PARTICIPANT INFORMATION	28
6 PARTICIPANT INFORMATION	29
7 PARTICIPANT INFORMATION	30
8 ALGORITHM SUMMARY	31
9 ALGORITHM SUMMARY	32
10 ALGORITHM SUMMARY	33
11 ALGORITHM SUMMARY	34
12 ALGORITHM SUMMARY	35
13 ALGORITHM SUMMARY	36
14 ALGORITHM SUMMARY	37
15 ALGORITHM SUMMARY	38
16 ALGORITHM SUMMARY	39
17 ALGORITHM SUMMARY	40
18 ALGORITHM SUMMARY	41
19 FALSE NON-MATCH RATE	42

20	FALSE NON-MATCH RATE	43
21	FALSE NON-MATCH RATE	44
22	FALSE NON-MATCH RATE	45
23	FALSE NON-MATCH RATE	46
24	FALSE NON-MATCH RATE	47
25	FALSE NON-MATCH RATE	48
26	FALSE NON-MATCH RATE	49
27	FALSE NON-MATCH RATE	50
28	FALSE NON-MATCH RATE	51
29	FALSE NON-MATCH RATE	52
30	FAILURE TO ENROL RATES	62
31	FAILURE TO ENROL RATES	63
32	FAILURE TO ENROL RATES	64
33	FAILURE TO ENROL RATES	65
34	FAILURE TO ENROL RATES	66
35	FAILURE TO ENROL RATES	67
36	FAILURE TO ENROL RATES	68
37	FAILURE TO ENROL RATES	69

List of Figures

1	PERFORMANCE SUMMARY: FNMR VS. TEMPLATE SIZE TRADEOFF	53
2	PERFORMANCE SUMMARY: FNMR VS. TEMPLATE TIME TRADEOFF	54
3	EXAMPLE IMAGES	58
(A)	VISA	58
(B)	MUGSHOT	58
(C)	WILD	58
(D)	BORDER	58
4	PERFORMANCE ON 20 HUMAN-DIFFICULT PAIRS	71
5	PERFORMANCE ON 20 HUMAN-DIFFICULT PAIRS	72
6	PERFORMANCE ON 20 HUMAN-DIFFICULT PAIRS	73
7	PERFORMANCE ON 20 HUMAN-DIFFICULT PAIRS	74
8	PERFORMANCE ON 20 HUMAN-DIFFICULT PAIRS	75
9	PERFORMANCE ON 20 HUMAN-DIFFICULT PAIRS	76
10	PERFORMANCE ON 20 HUMAN-DIFFICULT PAIRS	77
11	PERFORMANCE ON 20 HUMAN-DIFFICULT PAIRS	78
12	PERFORMANCE ON 20 HUMAN-DIFFICULT PAIRS	79
13	PERFORMANCE ON 20 HUMAN-DIFFICULT PAIRS	80
14	PERFORMANCE ON 20 HUMAN-DIFFICULT PAIRS	81
15	PERFORMANCE ON 20 HUMAN-DIFFICULT PAIRS	82
16	PERFORMANCE ON 20 HUMAN-DIFFICULT PAIRS	83
17	PERFORMANCE ON 20 HUMAN-DIFFICULT PAIRS	84
18	PERFORMANCE ON 20 HUMAN-DIFFICULT PAIRS	85
19	PERFORMANCE ON 20 HUMAN-DIFFICULT PAIRS	86
20	PERFORMANCE ON 20 HUMAN-DIFFICULT PAIRS	87
21	PERFORMANCE ON 20 HUMAN-DIFFICULT PAIRS	88
22	PERFORMANCE ON 20 HUMAN-DIFFICULT PAIRS	89
23	PERFORMANCE ON 20 HUMAN-DIFFICULT PAIRS	90
24	PERFORMANCE ON 20 HUMAN-DIFFICULT PAIRS	91
25	PERFORMANCE ON 20 HUMAN-DIFFICULT PAIRS	92
26	PERFORMANCE ON 20 HUMAN-DIFFICULT PAIRS	93
27	PERFORMANCE ON 20 HUMAN-DIFFICULT PAIRS	94
28	PERFORMANCE ON 20 HUMAN-DIFFICULT PAIRS	95
29	PERFORMANCE ON 20 HUMAN-DIFFICULT PAIRS	96
30	PERFORMANCE ON 20 HUMAN-DIFFICULT PAIRS	97

31	PERFORMANCE ON 20 HUMAN-DIFFICULT PAIRS	98
32	PERFORMANCE ON 20 HUMAN-DIFFICULT PAIRS	99
33	PERFORMANCE ON 20 HUMAN-DIFFICULT PAIRS	100
34	PERFORMANCE ON 20 HUMAN-DIFFICULT PAIRS	101
35	PERFORMANCE ON 20 HUMAN-DIFFICULT PAIRS	102
36	PERFORMANCE ON 20 HUMAN-DIFFICULT PAIRS	103
37	PERFORMANCE ON 20 HUMAN-DIFFICULT PAIRS	104
38	PERFORMANCE ON 20 HUMAN-DIFFICULT PAIRS	105
39	PERFORMANCE ON 20 HUMAN-DIFFICULT PAIRS	106
40	ERROR TRADEOFF CHARACTERISTIC: VISA IMAGES	107
41	ERROR TRADEOFF CHARACTERISTIC: VISA IMAGES	108
42	ERROR TRADEOFF CHARACTERISTIC: VISA IMAGES	109
43	ERROR TRADEOFF CHARACTERISTIC: VISA IMAGES	110
44	ERROR TRADEOFF CHARACTERISTIC: VISA IMAGES	111
45	ERROR TRADEOFF CHARACTERISTIC: VISA IMAGES	112
46	ERROR TRADEOFF CHARACTERISTIC: VISA IMAGES	113
47	ERROR TRADEOFF CHARACTERISTIC: VISA IMAGES	114
48	ERROR TRADEOFF CHARACTERISTIC: VISA IMAGES	115
49	ERROR TRADEOFF CHARACTERISTIC: VISA IMAGES	116
50	ERROR TRADEOFF CHARACTERISTIC: VISA IMAGES	117
51	ERROR TRADEOFF CHARACTERISTIC: VISA IMAGES	118
52	ERROR TRADEOFF CHARACTERISTIC: VISA IMAGES	119
53	ERROR TRADEOFF CHARACTERISTIC: VISA IMAGES	120
54	ERROR TRADEOFF CHARACTERISTIC: VISA IMAGES	121
55	ERROR TRADEOFF CHARACTERISTIC: VISA IMAGES	122
56	ERROR TRADEOFF CHARACTERISTIC: VISA IMAGES	123
57	ERROR TRADEOFF CHARACTERISTIC: VISA IMAGES	124
58	ERROR TRADEOFF CHARACTERISTIC: VISA IMAGES	125
59	ERROR TRADEOFF CHARACTERISTIC: VISA IMAGES	126
60	ERROR TRADEOFF CHARACTERISTIC: VISA IMAGES	127
61	ERROR TRADEOFF CHARACTERISTIC: VISA IMAGES	128
62	ERROR TRADEOFF CHARACTERISTIC: VISA IMAGES	129
63	ERROR TRADEOFF CHARACTERISTIC: VISA IMAGES	130
64	ERROR TRADEOFF CHARACTERISTIC: VISA IMAGES	131
65	ERROR TRADEOFF CHARACTERISTIC: VISA IMAGES	132
66	ERROR TRADEOFF CHARACTERISTIC: VISA IMAGES	133
67	ERROR TRADEOFF CHARACTERISTIC: VISA IMAGES	134
68	ERROR TRADEOFF CHARACTERISTIC: VISA IMAGES	135
69	ERROR TRADEOFF CHARACTERISTIC: VISA IMAGES	136
70	ERROR TRADEOFF CHARACTERISTIC: VISA IMAGES	137
71	ERROR TRADEOFF CHARACTERISTIC: VISA IMAGES	138
72	ERROR TRADEOFF CHARACTERISTIC: VISA IMAGES	139
73	ERROR TRADEOFF CHARACTERISTIC: VISA IMAGES	140
74	ERROR TRADEOFF CHARACTERISTIC: VISA IMAGES	141
75	ERROR TRADEOFF CHARACTERISTIC: VISA IMAGES	142
76	ERROR TRADEOFF CHARACTERISTIC: VISA IMAGES	143
77	ERROR TRADEOFF CHARACTERISTIC: VISA IMAGES	144
78	ERROR TRADEOFF CHARACTERISTIC: VISA IMAGES	145
79	ERROR TRADEOFF CHARACTERISTIC: VISA IMAGES	146
80	ERROR TRADEOFF CHARACTERISTIC: VISA IMAGES	147
81	ERROR TRADEOFF CHARACTERISTIC: VISA IMAGES	148
82	ERROR TRADEOFF CHARACTERISTIC: VISA IMAGES	149
83	ERROR TRADEOFF CHARACTERISTIC: VISA IMAGES	150
84	ERROR TRADEOFF CHARACTERISTIC: VISA IMAGES	151
85	ERROR TRADEOFF CHARACTERISTIC: VISA IMAGES	152
86	ERROR TRADEOFF CHARACTERISTIC: VISA IMAGES	153

87	ERROR TRADEOFF CHARACTERISTIC: MUGSHOT IMAGES	154
88	ERROR TRADEOFF CHARACTERISTIC: MUGSHOT IMAGES	155
89	ERROR TRADEOFF CHARACTERISTIC: MUGSHOT IMAGES	156
90	ERROR TRADEOFF CHARACTERISTIC: MUGSHOT IMAGES	157
91	ERROR TRADEOFF CHARACTERISTIC: MUGSHOT IMAGES	158
92	ERROR TRADEOFF CHARACTERISTIC: MUGSHOT IMAGES	159
93	ERROR TRADEOFF CHARACTERISTIC: MUGSHOT IMAGES	160
94	ERROR TRADEOFF CHARACTERISTIC: MUGSHOT IMAGES	161
95	ERROR TRADEOFF CHARACTERISTIC: MUGSHOT IMAGES	162
96	ERROR TRADEOFF CHARACTERISTIC: MUGSHOT IMAGES	163
97	ERROR TRADEOFF CHARACTERISTIC: MUGSHOT IMAGES	164
98	ERROR TRADEOFF CHARACTERISTIC: MUGSHOT IMAGES	165
99	ERROR TRADEOFF CHARACTERISTIC: MUGSHOT IMAGES	166
100	ERROR TRADEOFF CHARACTERISTIC: MUGSHOT IMAGES	167
101	ERROR TRADEOFF CHARACTERISTIC: MUGSHOT IMAGES	168
102	ERROR TRADEOFF CHARACTERISTIC: MUGSHOT IMAGES	169
103	ERROR TRADEOFF CHARACTERISTIC: MUGSHOT IMAGES	170
104	ERROR TRADEOFF CHARACTERISTIC: MUGSHOT IMAGES	171
105	ERROR TRADEOFF CHARACTERISTIC: MUGSHOT IMAGES	172
106	ERROR TRADEOFF CHARACTERISTIC: MUGSHOT IMAGES	173
107	ERROR TRADEOFF CHARACTERISTIC: MUGSHOT IMAGES	174
108	ERROR TRADEOFF CHARACTERISTIC: MUGSHOT IMAGES	175
109	ERROR TRADEOFF CHARACTERISTIC: MUGSHOT IMAGES	176
110	ERROR TRADEOFF CHARACTERISTIC: MUGSHOT IMAGES	177
111	ERROR TRADEOFF CHARACTERISTIC: WILD IMAGES	178
112	ERROR TRADEOFF CHARACTERISTIC: WILD IMAGES	179
113	ERROR TRADEOFF CHARACTERISTIC: WILD IMAGES	180
114	ERROR TRADEOFF CHARACTERISTIC: WILD IMAGES	181
115	ERROR TRADEOFF CHARACTERISTIC: WILD IMAGES	182
116	ERROR TRADEOFF CHARACTERISTIC: WILD IMAGES	183
117	ERROR TRADEOFF CHARACTERISTIC: WILD IMAGES	184
118	ERROR TRADEOFF CHARACTERISTIC: WILD IMAGES	185
119	ERROR TRADEOFF CHARACTERISTIC: WILD IMAGES	186
120	ERROR TRADEOFF CHARACTERISTIC: WILD IMAGES	187
121	ERROR TRADEOFF CHARACTERISTIC: WILD IMAGES	188
122	ERROR TRADEOFF CHARACTERISTIC: WILD IMAGES	189
123	ERROR TRADEOFF CHARACTERISTIC: WILD IMAGES	190
124	ERROR TRADEOFF CHARACTERISTIC: WILD IMAGES	191
125	ERROR TRADEOFF CHARACTERISTIC: WILD IMAGES	192
126	ERROR TRADEOFF CHARACTERISTIC: WILD IMAGES	193
127	ERROR TRADEOFF CHARACTERISTIC: WILD IMAGES	194
128	ERROR TRADEOFF CHARACTERISTIC: WILD IMAGES	195
129	ERROR TRADEOFF CHARACTERISTIC: WILD IMAGES	196
130	ERROR TRADEOFF CHARACTERISTIC: WILD IMAGES	197
131	FALSE MATCH RATES WITHIN AND ACROSS DEMOGRAPHIC GROUPS	198
132	FALSE MATCH RATES WITHIN AND ACROSS DEMOGRAPHIC GROUPS	199
133	FALSE MATCH RATES WITHIN AND ACROSS DEMOGRAPHIC GROUPS	200
134	FALSE MATCH RATES WITHIN AND ACROSS DEMOGRAPHIC GROUPS	201
135	FALSE MATCH RATES WITHIN AND ACROSS DEMOGRAPHIC GROUPS	202
136	FALSE MATCH RATES WITHIN AND ACROSS DEMOGRAPHIC GROUPS	203
137	FALSE MATCH RATES WITHIN AND ACROSS DEMOGRAPHIC GROUPS	204
138	FALSE MATCH RATES WITHIN AND ACROSS DEMOGRAPHIC GROUPS	205
139	FALSE MATCH RATES WITHIN AND ACROSS DEMOGRAPHIC GROUPS	206
140	FALSE MATCH RATES WITHIN AND ACROSS DEMOGRAPHIC GROUPS	207
141	FALSE MATCH RATES WITHIN AND ACROSS DEMOGRAPHIC GROUPS	208
142	FALSE MATCH RATES WITHIN AND ACROSS DEMOGRAPHIC GROUPS	209
143	FALSE MATCH RATES WITHIN AND ACROSS DEMOGRAPHIC GROUPS	210

144	FALSE MATCH RATES WITHIN AND ACROSS DEMOGRAPHIC GROUPS	211
145	FALSE MATCH RATES WITHIN AND ACROSS DEMOGRAPHIC GROUPS	212
146	FALSE MATCH RATES WITHIN AND ACROSS DEMOGRAPHIC GROUPS	213
147	FALSE MATCH RATES WITHIN AND ACROSS DEMOGRAPHIC GROUPS	214
148	FALSE MATCH RATES WITHIN AND ACROSS DEMOGRAPHIC GROUPS	215
149	FALSE MATCH RATES WITHIN AND ACROSS DEMOGRAPHIC GROUPS	216
150	FALSE MATCH RATES WITHIN AND ACROSS DEMOGRAPHIC GROUPS	217
151	FALSE MATCH RATES WITHIN AND ACROSS DEMOGRAPHIC GROUPS	218
152	FALSE MATCH RATES WITHIN AND ACROSS DEMOGRAPHIC GROUPS	219
153	SEX AND RACE EFFECTS: MUGSHOT IMAGES	220
154	SEX AND RACE EFFECTS: MUGSHOT IMAGES	221
155	SEX AND RACE EFFECTS: MUGSHOT IMAGES	222
156	SEX AND RACE EFFECTS: MUGSHOT IMAGES	223
157	SEX AND RACE EFFECTS: MUGSHOT IMAGES	224
158	SEX AND RACE EFFECTS: MUGSHOT IMAGES	225
159	SEX AND RACE EFFECTS: MUGSHOT IMAGES	226
160	SEX AND RACE EFFECTS: MUGSHOT IMAGES	227
161	SEX AND RACE EFFECTS: MUGSHOT IMAGES	228
162	SEX AND RACE EFFECTS: MUGSHOT IMAGES	229
163	SEX AND RACE EFFECTS: MUGSHOT IMAGES	230
164	SEX AND RACE EFFECTS: MUGSHOT IMAGES	231
165	SEX AND RACE EFFECTS: MUGSHOT IMAGES	232
166	SEX AND RACE EFFECTS: MUGSHOT IMAGES	233
167	SEX AND RACE EFFECTS: MUGSHOT IMAGES	234
168	SEX AND RACE EFFECTS: MUGSHOT IMAGES	235
169	SEX AND RACE EFFECTS: MUGSHOT IMAGES	236
170	SEX AND RACE EFFECTS: MUGSHOT IMAGES	237
171	SEX AND RACE EFFECTS: MUGSHOT IMAGES	238
172	SEX AND RACE EFFECTS: MUGSHOT IMAGES	239
173	SEX AND RACE EFFECTS: MUGSHOT IMAGES	240
174	SEX AND RACE EFFECTS: MUGSHOT IMAGES	241
175	SEX AND RACE EFFECTS: MUGSHOT IMAGES	242
176	SEX AND RACE EFFECTS: MUGSHOT IMAGES	243
177	SEX EFFECTS: VISA IMAGES	244
178	SEX EFFECTS: VISA IMAGES	245
179	SEX EFFECTS: VISA IMAGES	246
180	SEX EFFECTS: VISA IMAGES	247
181	SEX EFFECTS: VISA IMAGES	248
182	SEX EFFECTS: VISA IMAGES	249
183	SEX EFFECTS: VISA IMAGES	250
184	SEX EFFECTS: VISA IMAGES	251
185	SEX EFFECTS: VISA IMAGES	252
186	SEX EFFECTS: VISA IMAGES	253
187	SEX EFFECTS: VISA IMAGES	254
188	SEX EFFECTS: VISA IMAGES	255
189	SEX EFFECTS: VISA IMAGES	256
190	SEX EFFECTS: VISA IMAGES	257
191	SEX EFFECTS: VISA IMAGES	258
192	SEX EFFECTS: VISA IMAGES	259
193	SEX EFFECTS: VISA IMAGES	260
194	SEX EFFECTS: VISA IMAGES	261
195	SEX EFFECTS: VISA IMAGES	262
196	SEX EFFECTS: VISA IMAGES	263
197	SEX EFFECTS: VISA IMAGES	264
198	SEX EFFECTS: VISA IMAGES	265
199	SEX EFFECTS: VISA IMAGES	266
200	SEX EFFECTS: VISA IMAGES	267

201 SEX EFFECTS: VISA IMAGES	268
202 SEX EFFECTS: VISA IMAGES	269
203 SEX EFFECTS: VISA IMAGES	270
204 SEX EFFECTS: VISA IMAGES	271
205 SEX EFFECTS: VISA IMAGES	272
206 SEX EFFECTS: VISA IMAGES	273
207 SEX EFFECTS: VISA IMAGES	274
208 SEX EFFECTS: VISA IMAGES	275
209 SEX EFFECTS: VISA IMAGES	276
210 SEX EFFECTS: VISA IMAGES	277
211 SEX EFFECTS: VISA IMAGES	278
212 SEX EFFECTS: VISA IMAGES	279
213 SEX EFFECTS: VISA IMAGES	280
214 SEX EFFECTS: VISA IMAGES	281
215 SEX EFFECTS: VISA IMAGES	282
216 FALSE MATCH RATE CALIBRATION: MUGSHOT IMAGES	283
217 FALSE MATCH RATE CALIBRATION: MUGSHOT IMAGES	284
218 FALSE MATCH RATE CALIBRATION: MUGSHOT IMAGES	285
219 FALSE MATCH RATE CALIBRATION: MUGSHOT IMAGES	286
220 FALSE MATCH RATE CALIBRATION: MUGSHOT IMAGES	287
221 FALSE MATCH RATE CALIBRATION: MUGSHOT IMAGES	288
222 FALSE MATCH RATE CALIBRATION: MUGSHOT IMAGES	289
223 FALSE MATCH RATE CALIBRATION: MUGSHOT IMAGES	290
224 FALSE MATCH RATE CALIBRATION: MUGSHOT IMAGES	291
225 FALSE MATCH RATE CALIBRATION: MUGSHOT IMAGES	292
226 FALSE MATCH RATE CALIBRATION: MUGSHOT IMAGES	293
227 FALSE MATCH RATE CALIBRATION: MUGSHOT IMAGES	294
228 FALSE MATCH RATE CALIBRATION: MUGSHOT IMAGES	295
229 FALSE MATCH RATE CALIBRATION: MUGSHOT IMAGES	296
230 FALSE MATCH RATE CALIBRATION: MUGSHOT IMAGES	297
231 FALSE MATCH RATE CALIBRATION: MUGSHOT IMAGES	298
232 FALSE MATCH RATE CALIBRATION: MUGSHOT IMAGES	299
233 FALSE MATCH RATE CALIBRATION: MUGSHOT IMAGES	300
234 FALSE MATCH RATE CALIBRATION: MUGSHOT IMAGES	301
235 FALSE MATCH RATE CALIBRATION: MUGSHOT IMAGES	302
236 FALSE MATCH RATE CALIBRATION: MUGSHOT IMAGES	303
237 FALSE MATCH RATE CALIBRATION: MUGSHOT IMAGES	304
238 FALSE MATCH RATE CALIBRATION: MUGSHOT IMAGES	305
239 FALSE MATCH RATE CALIBRATION: MUGSHOT IMAGES	306
240 FALSE MATCH RATE CALIBRATION: VISA IMAGES	307
241 FALSE MATCH RATE CALIBRATION: VISA IMAGES	308
242 FALSE MATCH RATE CALIBRATION: VISA IMAGES	309
243 FALSE MATCH RATE CALIBRATION: VISA IMAGES	310
244 FALSE MATCH RATE CALIBRATION: VISA IMAGES	311
245 FALSE MATCH RATE CALIBRATION: VISA IMAGES	312
246 FALSE MATCH RATE CALIBRATION: VISA IMAGES	313
247 FALSE MATCH RATE CALIBRATION: VISA IMAGES	314
248 FALSE MATCH RATE CALIBRATION: VISA IMAGES	315
249 FALSE MATCH RATE CALIBRATION: VISA IMAGES	316
250 FALSE MATCH RATE CALIBRATION: VISA IMAGES	317
251 FALSE MATCH RATE CALIBRATION: VISA IMAGES	318
252 FALSE MATCH RATE CALIBRATION: VISA IMAGES	319
253 FALSE MATCH RATE CALIBRATION: VISA IMAGES	320
254 FALSE MATCH RATE CALIBRATION: VISA IMAGES	321
255 FALSE MATCH RATE CALIBRATION: VISA IMAGES	322
256 FALSE MATCH RATE CALIBRATION: VISA IMAGES	323
257 FALSE MATCH RATE CALIBRATION: VISA IMAGES	324

258	FALSE MATCH RATE CALIBRATION: VISA IMAGES	325
259	FALSE MATCH RATE CALIBRATION: VISA IMAGES	326
260	FALSE MATCH RATE CALIBRATION: VISA IMAGES	327
261	FALSE MATCH RATE CALIBRATION: VISA IMAGES	328
262	FALSE MATCH RATE CALIBRATION: VISA IMAGES	329
263	FALSE MATCH RATE CALIBRATION: VISA IMAGES	330
264	FALSE MATCH RATE CALIBRATION: VISA IMAGES	331
265	FALSE MATCH RATE CALIBRATION: VISA IMAGES	332
266	FALSE MATCH RATE CALIBRATION: VISA IMAGES	333
267	FALSE MATCH RATE CALIBRATION: VISA IMAGES	334
268	FALSE MATCH RATE CALIBRATION: VISA IMAGES	335
269	FALSE MATCH RATE CALIBRATION: VISA IMAGES	336
270	FALSE MATCH RATE CALIBRATION: VISA IMAGES	337
271	FALSE MATCH RATE CALIBRATION: VISA IMAGES	338
272	FALSE MATCH RATE CALIBRATION: VISA IMAGES	339
273	FALSE MATCH RATE CALIBRATION: VISA IMAGES	340
274	FALSE MATCH RATE CALIBRATION: VISA IMAGES	341
275	FALSE MATCH RATE CALIBRATION: VISA IMAGES	342
276	FALSE MATCH RATE CALIBRATION: VISA IMAGES	343
277	FALSE MATCH RATE CALIBRATION: VISA IMAGES	344
278	FALSE MATCH RATE CALIBRATION: VISA IMAGES	345
279	FALSE MATCH RATE CALIBRATION: VISA IMAGES	346
280	FALSE MATCH RATE CALIBRATION: VISA IMAGES	347
281	FALSE MATCH RATE CALIBRATION: VISA IMAGES	348
282	FALSE MATCH RATE CALIBRATION: VISA IMAGES	349
283	FALSE MATCH RATE CALIBRATION: VISA IMAGES	350
284	FALSE MATCH RATE CALIBRATION: VISA IMAGES	351
285	FALSE MATCH RATE CALIBRATION: VISA IMAGES	352
286	FALSE MATCH RATE CALIBRATION: VISA IMAGES	353
287	FALSE MATCH RATE CALIBRATION: VISA IMAGES	354
288	EFFECT OF COUNTRY OF BIRTH ON FNMR	356
289	EFFECT OF COUNTRY OF BIRTH ON FNMR	357
290	EFFECT OF COUNTRY OF BIRTH ON FNMR	358
291	EFFECT OF COUNTRY OF BIRTH ON FNMR	359
292	EFFECT OF COUNTRY OF BIRTH ON FNMR	360
293	EFFECT OF COUNTRY OF BIRTH ON FNMR	361
294	EFFECT OF COUNTRY OF BIRTH ON FNMR	362
295	EFFECT OF COUNTRY OF BIRTH ON FNMR	363
296	EFFECT OF COUNTRY OF BIRTH ON FNMR	364
297	EFFECT OF COUNTRY OF BIRTH ON FNMR	365
298	EFFECT OF COUNTRY OF BIRTH ON FNMR	366
299	EFFECT OF COUNTRY OF BIRTH ON FNMR	367
300	EFFECT OF COUNTRY OF BIRTH ON FNMR	368
301	EFFECT OF COUNTRY OF BIRTH ON FNMR	369
302	EFFECT OF COUNTRY OF BIRTH ON FNMR	370
303	EFFECT OF COUNTRY OF BIRTH ON FNMR	371
304	EFFECT OF COUNTRY OF BIRTH ON FNMR	372
305	EFFECT OF COUNTRY OF BIRTH ON FNMR	373
306	EFFECT OF COUNTRY OF BIRTH ON FNMR	374
307	EFFECT OF COUNTRY OF BIRTH ON FNMR	375
308	EFFECT OF COUNTRY OF BIRTH ON FNMR	376
309	EFFECT OF COUNTRY OF BIRTH ON FNMR	377
310	EFFECT OF COUNTRY OF BIRTH ON FNMR	378
311	EFFECT OF COUNTRY OF BIRTH ON FNMR	379
312	EFFECT OF COUNTRY OF BIRTH ON FNMR	380
313	EFFECT OF COUNTRY OF BIRTH ON FNMR	381
314	EFFECT OF COUNTRY OF BIRTH ON FNMR	382

315	EFFECT OF COUNTRY OF BIRTH ON FNMR	383
316	EFFECT OF COUNTRY OF BIRTH ON FNMR	384
317	EFFECT OF COUNTRY OF BIRTH ON FNMR	385
318	EFFECT OF COUNTRY OF BIRTH ON FNMR	386
319	EFFECT OF COUNTRY OF BIRTH ON FNMR	387
320	EFFECT OF COUNTRY OF BIRTH ON FNMR	388
321	EFFECT OF COUNTRY OF BIRTH ON FNMR	389
322	EFFECT OF COUNTRY OF BIRTH ON FNMR	390
323	EFFECT OF COUNTRY OF BIRTH ON FNMR	391
324	EFFECT OF COUNTRY OF BIRTH ON FNMR	392
325	EFFECT OF COUNTRY OF BIRTH ON FNMR	393
326	EFFECT OF COUNTRY OF BIRTH ON FNMR	394
327	ERROR TRADEOFF CHARACTERISTIC: MUGSHOT IMAGES	396
328	ERROR TRADEOFF CHARACTERISTIC: MUGSHOT IMAGES	397
329	ERROR TRADEOFF CHARACTERISTIC: MUGSHOT IMAGES	398
330	ERROR TRADEOFF CHARACTERISTIC: MUGSHOT IMAGES	399
331	ERROR TRADEOFF CHARACTERISTIC: MUGSHOT IMAGES	400
332	ERROR TRADEOFF CHARACTERISTIC: MUGSHOT IMAGES	401
333	ERROR TRADEOFF CHARACTERISTIC: MUGSHOT IMAGES	402
334	ERROR TRADEOFF CHARACTERISTIC: MUGSHOT IMAGES	403
335	ERROR TRADEOFF CHARACTERISTIC: MUGSHOT IMAGES	404
336	ERROR TRADEOFF CHARACTERISTIC: MUGSHOT IMAGES	405
337	ERROR TRADEOFF CHARACTERISTIC: MUGSHOT IMAGES	406
338	ERROR TRADEOFF CHARACTERISTIC: MUGSHOT IMAGES	407
339	ERROR TRADEOFF CHARACTERISTIC: MUGSHOT IMAGES	408
340	ERROR TRADEOFF CHARACTERISTIC: MUGSHOT IMAGES	409
341	ERROR TRADEOFF CHARACTERISTIC: MUGSHOT IMAGES	410
342	ERROR TRADEOFF CHARACTERISTIC: MUGSHOT IMAGES	411
343	ERROR TRADEOFF CHARACTERISTIC: MUGSHOT IMAGES	412
344	ERROR TRADEOFF CHARACTERISTIC: MUGSHOT IMAGES	413
345	ERROR TRADEOFF CHARACTERISTIC: MUGSHOT IMAGES	414
346	ERROR TRADEOFF CHARACTERISTIC: MUGSHOT IMAGES	415
347	ERROR TRADEOFF CHARACTERISTIC: MUGSHOT IMAGES	416
348	ERROR TRADEOFF CHARACTERISTIC: MUGSHOT IMAGES	417
349	ERROR TRADEOFF CHARACTERISTIC: MUGSHOT IMAGES	418
350	ERROR TRADEOFF CHARACTERISTIC: MUGSHOT IMAGES	419
351	ERROR TRADEOFF CHARACTERISTIC: MUGSHOT IMAGES	420
352	ERROR TRADEOFF CHARACTERISTIC: MUGSHOT IMAGES	421
353	ERROR TRADEOFF CHARACTERISTIC: MUGSHOT IMAGES	422
354	ERROR TRADEOFF CHARACTERISTIC: MUGSHOT IMAGES	423
355	ERROR TRADEOFF CHARACTERISTIC: MUGSHOT IMAGES	424
356	EFFECT OF SUBJECT AGE ON FNMR	426
357	EFFECT OF SUBJECT AGE ON FNMR	427
358	EFFECT OF SUBJECT AGE ON FNMR	428
359	EFFECT OF SUBJECT AGE ON FNMR	429
360	EFFECT OF SUBJECT AGE ON FNMR	430
361	EFFECT OF SUBJECT AGE ON FNMR	431
362	EFFECT OF SUBJECT AGE ON FNMR	432
363	EFFECT OF SUBJECT AGE ON FNMR	433
364	EFFECT OF SUBJECT AGE ON FNMR	434
365	EFFECT OF SUBJECT AGE ON FNMR	435
366	EFFECT OF SUBJECT AGE ON FNMR	436
367	EFFECT OF SUBJECT AGE ON FNMR	437
368	EFFECT OF SUBJECT AGE ON FNMR	438
369	EFFECT OF SUBJECT AGE ON FNMR	439

370	EFFECT OF SUBJECT AGE ON FNMR	440
371	EFFECT OF SUBJECT AGE ON FNMR	441
372	EFFECT OF SUBJECT AGE ON FNMR	442
373	EFFECT OF SUBJECT AGE ON FNMR	443
374	EFFECT OF SUBJECT AGE ON FNMR	444
375	EFFECT OF SUBJECT AGE ON FNMR	445
376	EFFECT OF SUBJECT AGE ON FNMR	446
377	EFFECT OF SUBJECT AGE ON FNMR	447
378	EFFECT OF SUBJECT AGE ON FNMR	448
379	EFFECT OF SUBJECT AGE ON FNMR	449
380	EFFECT OF SUBJECT AGE ON FNMR	450
381	EFFECT OF SUBJECT AGE ON FNMR	451
382	EFFECT OF SUBJECT AGE ON FNMR	452
383	EFFECT OF SUBJECT AGE ON FNMR	453
384	EFFECT OF SUBJECT AGE ON FNMR	454
385	EFFECT OF SUBJECT AGE ON FNMR	455
386	EFFECT OF SUBJECT AGE ON FNMR	456
387	EFFECT OF SUBJECT AGE ON FNMR	457
388	EFFECT OF SUBJECT AGE ON FNMR	458
389	EFFECT OF SUBJECT AGE ON FNMR	459
390	EFFECT OF SUBJECT AGE ON FNMR	460
391	EFFECT OF SUBJECT AGE ON FNMR	461
392	EFFECT OF SUBJECT AGE ON FNMR	462
393	EFFECT OF SUBJECT AGE ON FNMR	463
394	EFFECT OF SUBJECT AGE ON FNMR	464
395	IMPOSTOR COUNTS FOR CROSS COUNTRY FMR CALCULATIONS	468

	Location	Developer Name	Short Name	Seq. Num.	Validation Date
1	NL	20Face	20face-000	000	2021-04-12
2	NL	20Face	20face-001	001	2021-09-29
3	US	3DVi	3divi-006	006	2021-04-14
4	US	3DVi	3divi-007	007	2021-09-27
5	TH	ACI Software	acisw-007	007	2021-11-15
6	TH	ACI Software	acisw-008	008	2022-03-22
7	US	AFIS and Biometrics Consulting	afisbiometrics-000	000	2022-01-27
8	US	AFR Engine	afrengine-000	000	2022-09-29
9	TW	ASUSTek Computer Inc	asusaics-000	000	2019-10-24
10	TW	ASUSTek Computer Inc	asusaics-001	001	2020-02-25
11	CN	AYF Technology	ayftech-001	001	2020-07-06
12	TW	Ability Enterprise - Andro Video	androvideo-000	000	2021-01-25
13	TW	Acer Incorporated	acer-001	001	2020-06-30
14	TW	Acer Incorporated	acer-002	002	2021-11-10
15	SG	Adera Global PTE	ader-002	002	2021-02-16
16	SG	Adera Global PTE	ader-003	003	2021-07-12
17	SG	Advancegroup	advance-003	003	2021-08-05
18	SG	Advancegroup	advance-004	004	2022-09-06
19	TH	Ai First	aifirst-001	001	2019-11-21
20	TW	AiUnion Technology	aiunionface-000	000	2019-10-22
21	TH	Aigen	aigen-001	001	2020-10-06
22	TH	Aigen	aigen-002	002	2021-03-15
23	CN	Aiseemu Technology	aiseemu-001	001	2022-06-16
24	KR	Ajou University	ajou-001	001	2021-03-08
25	ID	Akurat Satu Indonesia	ptakuratsatu-000	000	2020-09-11
26	KR	Alchera Inc	alchera-003	003	2021-07-13
27	KR	Alchera Inc	alchera-004	004	2022-08-12
28	ID	Alfabeta	alfabeta-001	001	2021-12-02
29	ES	Alice Biometrics	alice-000	000	2021-06-15
30	RU	Alivia / Innovation Sys	isystems-001	001	2018-06-12
31	RU	Alivia / Innovation Sys	isystems-002	002	2018-10-18
32	IN	AllGoVision	allgovision-000	000	2019-03-01
33	CN	AlphaSSTG	alphaface-001	001	2019-09-03
34	CN	AlphaSSTG	alphaface-002	002	2020-02-20
35	GB	Amplified Group	amplifiedgroup-001	001	2019-03-01
36	CN	Anke Investments	anke-004	004	2019-06-27
37	CN	Anke Investments	anke-005	005	2019-11-21
38	BR	Antheus Technologia	antheus-000	000	2019-12-05
39	BR	Antheus Technologia	antheus-001	001	2020-06-25
40	GB	AnyVision	anyvision-004	004	2018-06-15
41	GB	AnyVision	anyvision-005	005	2021-02-03
42	US	Armatura LLC	armatura-001	001	2022-01-04
43	US	Armatura LLC	armatura-002	002	2022-09-16
44	CN	AuthenMetric	authenmetric-003	003	2021-08-09
45	CN	AuthenMetric	authenmetric-004	004	2022-01-03
46	US	Aware	aware-005	005	2020-02-27
47	US	Aware	aware-006	006	2021-07-03
48	IN	Awidit Systems	awidit-001	001	2019-09-23
49	IN	Awidit Systems	awidit-002	002	2020-10-28
50	CH	Aximetria	aximetria-001	001	2022-08-10
51	JP	Ayonix	ayonix-000	000	2017-06-22
52	CN	BOE Technology Group	boetech-001	001	2021-06-22
53	CN	BOE Technology Group	boetech-002	002	2021-12-21
54	ES	Bee the Data	beethedata-000	000	2021-07-26
55	CN	Beihang University-ERCACAT	ercacat-001	001	2020-07-06
56	CN	Beijing Alleyes Technology	alleyes-000	000	2020-03-09
57	CN	Beijing DeepSense Technologies	deepsense-000	000	2021-03-19
58	CN	Beijing DeepSense Technologies	deepsense-001	001	2022-03-11
59	CN	Beijing Hisign Technology	hisign-001	001	2021-09-24
60	CN	Beijing Hisign Technology	hisign-002	002	2022-09-09
61	CN	Beijing Mendaxia Technology	mendaxiatech-000	000	2021-09-15
62	CN	Beijing Vion Technology Inc	vion-000	000	2018-10-19
63	KZ	Beyne.AI	beyneai-000	000	2022-01-03
64	CH	BioID Technologies SA	bioidechswiss-001	001	2020-08-28
65	CH	BioID Technologies SA	bioidechswiss-002	002	2021-02-17
66	IN	Biocube Matrics	biocube-001	001	2021-09-08
67	UK	BitCenter UK	farfaces-001	001	2021-04-09
68	CN	Bitmain	bm-001	001	2018-10-17
69	CN	Bresee Technology	bresee-001	001	2020-12-30
70	CN	Bresee Technology	bresee-002	002	2021-06-30

Table 1: Summary of participant information included in this report.

	Location	Developer Name	Short Name	Seq. Num.	Validation Date
71	VN	CMC Institute of Science and Technology	cist-001	001	2022-10-20
72	CN	CSA IntelliCloud Technology	intellicloudai-001	001	2019-08-13
73	CN	CSA IntelliCloud Technology	intellicloudai-002	002	2020-12-17
74	TW	CTBC Bank	ctbcbank-000	000	2019-06-28
75	TW	CTBC Bank	ctbcbank-001	001	2019-10-28
76	KR	CUDO Communication	cudocommunication-001	001	2021-10-20
77	US	Camvi Technologies	camvi-002	002	2018-10-19
78	US	Camvi Technologies	camvi-004	004	2019-07-12
79	JP	Canon Inc	canon-003	003	2021-09-15
80	JP	Canon Inc	canon-004	004	2022-04-25
81	CN	China Electronics Import-Export Corp	ceiec-003	003	2020-01-06
82	CN	China Electronics Import-Export Corp	ceiec-004	004	2021-01-18
83	CN	China University of Petroleum	upc-001	001	2019-06-05
84	CN	Chinese University of Hong Kong	cuhkee-001	001	2020-03-18
85	KR	Chosun University	chosun-001	001	2020-07-01
86	KR	Chosun University	chosun-002	002	2020-11-25
87	TW	Chunghwa Telecom	chtface-004	004	2021-10-08
88	TW	Chunghwa Telecom	chtface-005	005	2022-03-09
89	US	Clearview AI Inc	clearviewai-000	000	2021-09-22
90	CN	Closeli Inc	closeli-001	001	2021-07-15
91	US	CloudSmart Consulting LLC	csc-002	002	2021-03-24
92	US	CloudSmart Consulting LLC	csc-003	003	2021-08-26
93	TW	Cloudmatrix	cloudmatrix-001	001	2022-02-16
94	TW	Cloudmatrix	cloudmatrix-002	002	2022-10-17
95	CN	Cloudwalk - Hengrui AI Technology	cloudwalk-hr-003	003	2020-09-25
96	CN	Cloudwalk - Hengrui AI Technology	cloudwalk-hr-004	004	2021-02-10
97	CN	Cloudwalk - Moontime Smart Technology	cloudwalk-mt-005	005	2022-03-29
98	CN	Cloudwalk - Moontime Smart Technology	cloudwalk-mt-006	006	2022-10-20
99	IN	Code Everest Pvt	facex-001	001	2021-03-08
100	IN	Code Everest Pvt	facex-002	002	2021-08-24
101	KR	Codeline	codeline-000	000	2022-09-13
102	DE	Cognitec Systems GmbH	cognitec-003	003	2021-07-30
103	DE	Cognitec Systems GmbH	cognitec-004	004	2022-02-10
104	TW	Coretech Knowledge Inc	coretech-000	000	2021-07-12
105	TW	Coretech Knowledge Inc	coretech-001	001	2022-09-29
106	IL	Corsight	corsight-002	002	2021-09-01
107	IL	Corsight	corsight-003	003	2022-06-09
108	IL	Cortica	cor-001	001	2020-09-24
109	KR	Cubox	cubox-001	001	2020-12-07
110	KR	Cubox	cubox-002	002	2021-08-24
111	JP	Cybercore	cybercore-002	002	2022-04-25
112	JP	Cybercore	cybercore-003	003	2022-08-31
113	US	Cyberextruder	cyberextruder-003	003	2022-03-16
114	US	Cyberextruder	cyberextruder-004	004	2022-07-20
115	TW	Cyberlink Corp	cyberlink-009	009	2022-05-12
116	TW	Cyberlink Corp	cyberlink-010	010	2022-09-16
117	MX	DICIO	dicio-001	001	2022-03-22
118	CN	DSK	dsk-000	000	2019-06-28
119	CN	Dahua Technology	dahua-006	006	2020-12-30
120	CN	Dahua Technology	dahua-007	007	2021-12-20
121	IE	Daon	daon-000	000	2021-11-03
122	US	Decatur Industries Inc	decatur-000	000	2020-08-18
123	US	Decatur Industries Inc	decatur-001	001	2021-09-27
124	CN	Deepglint	deepglint-004	004	2021-09-17
125	CN	Deepglint	deepglint-005	005	2022-10-17
126	FR	Deepsense	dps-000	000	2021-07-16
127	DE	Dermalog	dermalog-009	009	2021-10-06
128	DE	Dermalog	dermalog-010	010	2022-07-25
129	CN	DiDi ChuXing Technology	didiglobalface-001	001	2019-10-23
130	IN	Digidata	digidata-000	000	2022-01-27
131	IN	Digidata	digidata-001	001	2022-06-10
132	GB	Digital Barriers	digitalbarriers-002	002	2019-03-01
133	TR	Ekin Smart City Technologies	ekin-002	002	2021-05-04
134	RU	Enface	enface-000	000	2021-04-09
135	RU	Enface	enface-001	001	2021-12-17
136	CH	Euronovate SA	euronovate-001	001	2021-11-15
137	RU	Expasoft LLC	expasoft-001	001	2020-09-03
138	RU	Expasoft LLC	expasoft-002	002	2021-07-26
139	US	FRP LLC	frpkauai-001	001	2022-07-18
140	DE	FaceOnLive Inc	faceonlive-001	001	2021-11-23

Table 2: Summary of participant information included in this report.

	Location	Developer Name	Short Name	Seq. Num.	Validation Date
141	DE	FaceOnLive Inc	faceonlive-002	002	2022-04-11
142	ES	FacePhi	facephi-000	000	2022-04-06
143	GB	FaceSoft	facesoft-000	000	2019-07-10
144	KR	FaceTag Co	facetag-000	000	2021-03-22
145	KR	FaceTag Co	facetag-002	002	2022-01-06
146	TW	FarBar Inc	f8-001	001	2019-07-11
147	TW	FarBar Inc	f8-002	002	2022-03-02
148	CN	Fiberhome Telecommunication Technologies	fiberhome-nanjing-003	003	2021-03-12
149	CN	Fiberhome Telecommunication Technologies	fiberhome-nanjing-004	004	2021-09-14
150	UK	Fincore Ltd	fincore-000	000	2021-06-07
151	KZ	First Credit Bureau Kazakhstan	firstcreditKZ-001	001	2022-08-22
152	CN	Fujitsu Research and Development Center	fujitsulab-002	002	2021-02-24
153	CN	Fujitsu Research and Development Center	fujitsulab-003	003	2021-07-12
154	US	Gemalto Cogent	cogent-006	006	2021-07-28
155	US	Gemalto Cogent	cogent-007	007	2022-04-11
156	TW	GeoVision Inc	geo-002	002	2021-04-01
157	TW	GeoVision Inc	geo-004	004	2022-02-10
158	JP	Glory	glory-004	004	2022-02-08
159	JP	Glory	glory-005	005	2022-07-08
160	TW	Gorilla Technology	gorilla-007	007	2021-06-28
161	TW	Gorilla Technology	gorilla-008	008	2021-11-08
162	US	Graymatics	graymatics-001	001	2022-01-13
163	US	Griaule	griaule-000	000	2021-08-20
164	US	Griaule	griaule-001	001	2022-05-31
165	CN	Guangzhou Pixel Solutions	pixelall-008	008	2022-06-16
166	CN	Guangzhou Pixel Solutions	pixelall-009	009	2022-10-26
167	CN	Hangzhuo Allu Network Information Technology	hzailu-002	002	2022-06-02
168	CN	Hangzhuo Allu Network Information Technology	hzailu-003	003	2022-10-11
169	ES	Herta Security	hertasecurity-001	001	2022-01-18
170	ES	Herta Security	hertasecurity-002	002	2022-09-02
171	CN	Hikvision Research Institute	hik-001	001	2019-03-01
172	IN	HyperVerge Inc	hyperverge-002	002	2021-05-27
173	IN	HyperVerge Inc	hyperverge-003	003	2022-04-11
174	AU	ICM Airport Technics	icm-003	003	2021-09-06
175	AU	ICM Airport Technics	icm-004	004	2022-09-07
176	FR	ID3 Technology	id3-006	006	2020-12-17
177	FR	ID3 Technology	id3-008	008	2021-11-10
178	CA	IMDS Software	imds-software-001	001	2022-07-06
179	RU	ITMO University	itmo-007	007	2020-01-06
180	RU	ITMO University	itmo-008	008	2021-11-19
181	RU	IVA Cognitive	ivacognitive-001	001	2021-01-29
182	FR	Idemia	idemia-008	008	2021-07-07
183	FR	Idemia	idemia-009	009	2022-07-27
184	US	Imageware Systems	iws-000	000	2020-08-12
185	GB	Imperial College London	imperial-000	000	2019-03-01
186	GB	Imperial College London	imperial-002	002	2019-08-28
187	US	Incode Technologies Inc	incode-010	010	2021-10-22
188	US	Incode Technologies Inc	incode-011	011	2022-08-10
189	IT	InfoCert	infocert-001	001	2022-09-08
190	IN	Innef Labs	innefulabs-000	000	2020-09-04
191	GB	Innovative Technology	innovativetechnologyltd-001	001	2019-10-22
192	GB	Innovative Technology	innovativetechnologyltd-002	002	2020-02-26
193	SK	Innovatrics	innovatrics-007	007	2020-08-19
194	SK	Innovatrics	innovatrics-008	008	2021-12-15
195	CN	InsightFace AI	insightface-001	001	2021-09-27
196	CN	InsightFace AI	insightface-003	003	2022-08-23
197	CN	Inspur (Beijing) Electronic Information Industry Co	inspur-000	000	2022-07-19
198	CN	Institute of Computing Technology	icthtc-000	000	2020-11-29
199	RU	Institute of Information Technologies	iit-002	002	2019-12-04
200	RU	Institute of Information Technologies	iit-003	003	2020-12-01
201	IS	Intel Research Group	intelresearch-004	004	2021-08-24
202	IS	Intel Research Group	intelresearch-005	005	2022-02-13
203	KR	IntelliVIX	intellivix-001	001	2022-02-25
204	KR	IntelliVIX	intellivix-002	002	2022-07-14
205	AE	Intellibrain Technological Projects	g42-intellibrain-001	001	2022-07-27
206	US	Intellivision	intellivision-003	003	2022-03-07
207	US	Intellivision	intellivision-004	004	2022-07-28
208	LU	Intema-LGL Group	intema-000	000	2022-07-15
209	US	IrexAI	irex-000	000	2020-12-17
210	IL	Is It You	isityou-000	000	2017-06-26

Table 3: Summary of participant information included in this report.

	Location	Developer Name	Short Name	Seq. Num.	Validation Date
211	MX	Jaak IT	jaakit-001	001	2022-05-20
212	KR	Kakao Enterprise	kakao-007	007	2022-01-12
213	KR	Kakao Enterprise	kakao-008	008	2022-05-12
214	KR	Kakao Pay Corp	kakaopay-001	001	2021-07-06
215	TH	Kasikorn Labs	kasikornlabs-000	000	2022-03-02
216	TH	Kasikorn Labs	kasikornlabs-001	001	2022-07-26
217	SG	Kedacom International Pte	kedacom-000	000	2019-06-03
218	US	Kneron Inc	kneron-003	003	2019-07-01
219	US	Kneron Inc	kneron-005	005	2020-02-21
220	US	KnowUTech LLC	knowutech-000	000	2022-02-13
221	KR	Kookmin University	kookmin-002	002	2021-03-05
222	TH	Krunghai	krungthai-002	002	2022-06-21
223	CN	KuKe3D Technology	kuke3d-001	001	2021-10-28
224	CN	KuKe3D Technology	kuke3d-002	002	2022-04-14
225	MX	Lebentech Biometrics	lebentech-000	000	2022-02-16
226	IN	Lema Labs	lemalabs-001	001	2021-04-13
227	JP	Line Corporation	lineclova-001	001	2021-09-26
228	JP	Line Corporation	lineclova-002	002	2022-05-18
229	RU	Lomonosov Moscow State University	intsysmsu-001	001	2019-10-22
230	RU	Lomonosov Moscow State University	intsysmsu-002	002	2020-03-12
231	IN	Lookman Electroplast Industries	lookman-002	002	2018-06-13
232	IN	Lookman Electroplast Industries	lookman-004	004	2019-06-03
233	US	Luxand Inc	luxand-000	000	2019-11-07
234	RU	MVision	mvision-001	001	2019-11-12
235	IN	Mantra Softech India	mantra-000	000	2021-10-28
236	CN	Maxvision Technology	maxvision-001	001	2022-03-03
237	CN	Maxvision Technology	maxvision-002	002	2022-07-12
238	CN	Megvii/Face++	megvii-005	005	2022-03-28
239	CN	Megvii/Face++	megvii-006	006	2022-08-08
240	KR	Metsakuur	metsakuurcompany-001	001	2022-05-12
241	KR	Metsakuur	metsakuurcompany-002	002	2022-09-14
242	GB	MicroFocus	microfocus-001	001	2018-06-13
243	GB	MicroFocus	microfocus-002	002	2018-10-17
244	CN	Minivision	minivision-000	000	2020-10-28
245	NO	Mobai	mobai-000	000	2020-08-26
246	NO	Mobai	mobai-001	001	2021-02-17
247	ES	Mobbeel Solutions	mobbl-001	001	2021-06-16
248	ES	Mobbeel Solutions	mobbl-003	003	2022-04-19
249	KR	Mobipin Technology	mobilpintech-000	000	2021-11-23
250	TH	Momentum Digital	sertis-000	000	2019-10-07
251	TH	Momentum Digital	sertis-002	002	2021-05-13
252	CN	MoreDian Technology	moreedian-000	000	2021-02-24
253	US	Mukh Technologies	mukh-001	001	2022-03-22
254	CN	Multi-Modality Intelligence	multimodality-000	000	2021-10-19
255	CN	Multi-Modality Intelligence	multimodality-001	001	2022-05-16
256	RU	N-Tech Lab	ntechlab-011	011	2021-09-13
257	RU	N-Tech Lab	ntechlab-012	012	2022-01-20
258	CA	NEO Systems	neosystems-004	004	2022-05-02
259	CA	NEO Systems	neosystems-005	005	2022-09-20
260	KR	NHN Corp	nhn-002	002	2021-07-15
261	KR	NHN Corp	nhn-003	003	2022-02-22
262	KR	NSENSE Corp	nsensecorp-003	003	2021-10-29
263	KR	NSENSE Corp	nsensecorp-004	004	2022-09-08
264	CN	Nanjing Kiwi Network Technology	kiwitech-000	000	2021-03-19
265	KR	Neosecu Co	openface-001	001	2021-06-15
266	TW	Netbridge Technology Incoporation	netbridgetech-001	001	2020-01-08
267	TW	Netbridge Technology Incoporation	netbridgetech-002	002	2020-08-11
268	LT	Neurotechnology	neurotechnology-013	013	2022-01-07
269	LT	Neurotechnology	neurotechnology-015	015	2022-06-07
270	ID	Nodeflux	nodeflux-002	002	2019-08-13
271	IN	NotionTag Technologies Private Limited	notionntag-001	001	2021-03-04
272	IN	NotionTag Technologies Private Limited	notionntag-002	002	2021-09-17
273	US	Omnigarde Ltd	omnigarde-001	001	2021-08-23
274	US	Omnigarde Ltd	omnigarde-002	002	2022-01-19
275	KR	One More Security	omface-000	000	2021-12-15
276	KR	One More Security	omface-001	001	2022-10-21
277	RU	Oz Forensics LLC	oz-003	003	2021-08-09
278	RU	Oz Forensics LLC	oz-004	004	2021-12-13
279	TW	PAPAGO Inc	papago-001	001	2022-07-19
280	CH	PXL Vision AG	pxl-001	001	2020-06-30

Table 4: Summary of participant information included in this report.

	Location	Developer Name	Short Name	Seq. Num.	Validation Date
281	TW	Palit Microsystems	palit-000	000	2022-05-16
282	TW	Palit Microsystems	palit-001	001	2022-09-26
283	SG	Panasonic R+D Center Singapore	psl-010	010	2022-04-19
284	SG	Panasonic R+D Center Singapore	psl-011	011	2022-10-06
285	US	Pangiam	pangiam-000	000	2022-04-04
286	TR	Papilon Savunma	papsav1923-001	001	2021-03-10
287	TR	Papilon Savunma	papsav1923-002	002	2022-01-20
288	US	Paravision	paravision-008	008	2021-06-30
289	US	Paravision (EverAI)	paravision-010	010	2022-02-02
290	SG	Pensees Pte	pensees-001	001	2020-08-17
291	IN	Pyramid Cyber Security + Forensic (P)	pyramid-000	000	2019-11-04
292	KZ	Qaz Biometric Systems	qazbs-000	000	2022-06-22
293	TW	Qnap Security	qnap-001	001	2021-12-09
294	TW	Qnap Security	qnap-002	002	2022-04-15
295	CZ	Quantasoft	quantasoft-003	003	2021-04-19
296	US	Rank One Computing	rankone-012	012	2021-12-27
297	US	Rank One Computing	rankone-013	013	2022-07-09
298	US	Realnetworks Inc	realnetworks-006	006	2022-02-09
299	US	Realnetworks Inc	realnetworks-007	007	2022-06-14
300	US	Regula Forensics	regula-000	000	2021-04-13
301	US	Regula Forensics	regula-001	001	2021-12-14
302	CN	Remark Holdings	remarkai-001	001	2019-03-01
303	CN	Remark Holdings	remarkai-003	003	2021-06-22
304	SG	Rendip	rendip-000	000	2021-04-19
305	UK	Reveal Media Ltd	revealmedia-005	005	2021-09-24
306	UK	Reveal Media Ltd	revealmedia-006	006	2022-01-26
307	CN	Rokid Corporation	rokid-000	000	2019-08-01
308	CN	Rokid Corporation	rokid-001	001	2019-12-13
309	KR	SK Telecom	sktelecom-000	000	2021-07-09
310	KR	SQIsoft	sqisoft-001	001	2021-07-27
311	KR	SQIsoft	sqisoft-002	002	2021-11-03
312	DE	Saffe	saffe-001	001	2018-10-19
313	DE	Saffe	saffe-002	002	2019-03-01
314	JP	Saga Densan Center Co Ltd	sdc-000	000	2022-10-18
315	KR	Samsung S1 Corp	s1-005	005	2022-06-17
316	KR	Samsung S1 Corp	s1-006	006	2022-10-17
317	KR	Samsung-SDS	samsungsds-001	001	2022-04-18
318	KR	Samsung-SDS	samsungsds-002	002	2022-09-16
319	IN	Samtech InfoNet Limited	samtech-001	001	2019-10-15
320	RU	Satellite Innovation/Eocortex	eocortex-000	000	2020-08-26
321	IL	Scanovate	scanovate-002	002	2020-06-26
322	IL	Scanovate	scanovate-003	003	2021-11-15
323	RO	Securif AI	securifai-004	004	2021-12-21
324	RO	Securif AI	securifai-005	005	2022-05-16
325	CN	Sensemte Group	sensemte-006	006	2021-12-28
326	CN	Sensemte Group	sensemte-007	007	2022-06-17
327	SG	Seventh Sense Artificial Intelligence	seventhsense-001	001	2022-03-04
328	SG	Seventh Sense Artificial Intelligence	seventhsense-002	002	2022-10-17
329	US	Shaman Software	shaman-000	000	2017-12-05
330	US	Shaman Software	shaman-001	001	2018-01-13
331	CN	Shanghai Jiao Tong University	sjtu-003	003	2020-11-02
332	CN	Shanghai Jiao Tong University	sjtu-004	004	2021-05-13
333	CN	Shanghai Ulucu Electronics Technology	uluface-002	002	2019-07-10
334	CN	Shanghai Ulucu Electronics Technology	uluface-003	003	2019-11-12
335	CN	Shanghai University - Shanghai Film Academy	shu-002	002	2019-12-10
336	CN	Shanghai University - Shanghai Film Academy	shu-003	003	2020-06-24
337	CN	Shanghai Yitu Technology	yitu-003	003	2019-03-01
338	CN	Shenzhen AiMall Tech	aimall-002	002	2020-03-12
339	CN	Shenzhen AiMall Tech	aimall-003	003	2020-08-12
340	CN	Shenzhen EI Networks	einetworks-000	000	2019-08-13
341	CN	Shenzhen Inst Adv Integrated Tech CAS	siat-002	002	2018-06-13
342	CN	Shenzhen Inst Adv Integrated Tech CAS	siat-005	005	2022-02-08
343	CN	Shenzhen Intellifusion Technologies	intellifusion-001	001	2019-08-22
344	CN	Shenzhen Intellifusion Technologies	intellifusion-002	002	2020-03-18
345	CN	Shenzhen University-Macau University of Science and Technology	sztu-000	000	2020-12-17
346	CN	Shenzhen University-Macau University of Science and Technology	sztu-001	001	2021-07-13
347	RU	Smart Engines	smartengines-000	000	2021-08-25
348	RU	Smart Engines	smartengines-001	001	2022-05-31
349	ES	Smartbiometrik	smartbiometrik-001	001	2022-05-16
350	TR	Smarvist Teknoloji	smartvist-000	000	2022-05-10

Table 5: Summary of participant information included in this report.

	Location	Developer Name	Short Name	Seq. Num.	Validation Date
351	DE	Smilart	smilart-002	002	2018-02-06
352	DE	Smilart	smilart-003	003	2019-03-01
353	TR	Sodec App Inc	sodec-000	000	2021-06-02
354	IN	StaQu Technologies	staqu-000	000	2020-07-15
355	CN	Star Hybrid Limited	starhybrid-001	001	2019-06-19
356	CN	Su Zhou NaZhiTianDi intelligent technology	nazhai-000	000	2020-06-25
357	IN	Sukshi Technology Innovation	sukshi-000	000	2022-02-13
358	KR	Suprema AI Inc	suprema-002	002	2022-02-11
359	KR	Suprema AI Inc	suprema-003	003	2022-07-20
360	KR	Suprema ID Inc	supremaid-001	001	2021-05-04
361	KR	Suprema ID Inc	supremaid-002	002	2022-06-24
362	RU	Synesis	synesis-006	006	2019-10-10
363	RU	Synesis	synesis-007	007	2020-06-24
364	TW	Synology Inc	synology-000	000	2019-10-23
365	TW	Synology Inc	synology-002	002	2020-08-20
366	BR	T4iSB	t4isb-000	000	2022-01-28
367	CN	TUPU Technology	tuputech-000	000	2019-10-11
368	TW	Taiwan AI Labs	ailabs-001	001	2019-12-18
369	TW	Taiwan-Certificate Authority Incorporation	twface-000	000	2021-05-14
370	TW	Taiwan-Certificate Authority Incorporation	twface-001	001	2021-09-14
371	CH	Tech5 SA	tech5-004	004	2020-03-09
372	CH	Tech5 SA	tech5-005	005	2020-07-24
373	TR	Techsign	techsign-000	000	2021-08-25
374	TR	Techsign	techsign-001	001	2022-07-01
375	CN	Tencent Deepsea Lab	deepsea-001	001	2019-06-03
376	RU	Tevian	tevian-007	007	2021-08-06
377	RU	Tevian	tevian-008	008	2021-12-06
378	US	TigerIT Americas LLC	tiger-005	005	2021-07-29
379	US	TigerIT Americas LLC	tiger-006	006	2021-12-13
380	RU	Tinkoff Bank	tinkoff-001	001	2021-05-13
381	CN	TongYi Transportation Technology	tongyi-005	005	2019-06-12
382	TW	Toppan ID Gate	toppanidgate-000	000	2021-09-28
383	JP	Toshiba	toshiba-004	004	2021-09-27
384	JP	Toshiba	toshiba-006	006	2022-06-29
385	ES	Touchless ID	touchlessid-000	000	2022-05-02
386	ES	Touchless ID	touchlessid-001	001	2022-09-21
387	JP	Tripleize	aize-001	001	2021-04-23
388	JP	Tripleize	aize-002	002	2021-10-08
389	US	Trueface.ai	trueface-002	002	2021-03-29
390	US	Trueface.ai	trueface-003	003	2021-09-30
391	CN	TuringTech.vip	turingtechvip-001	001	2022-02-03
392	CN	TuringTech.vip	turingtechvip-002	002	2022-07-27
393	TR	Turkcell Technology	turkcell-000	000	2022-10-11
394	CN	ULSee Inc	ulsee-001	001	2019-07-31
395	TW	UXLabs	uxlabs-001	001	2022-09-19
396	FR	Unissey	unissey-001	001	2021-11-29
397	FR	Unissey	unissey-002	002	2022-04-29
398	PT	Universidade de Coimbra	visteam-003	003	2022-01-31
399	PT	Universidade de Coimbra	visteam-004	004	2022-08-01
400	UK	University of Surrey-CVSSP	surrey-cvssp-000	000	2022-03-25
401	UK	University of Surrey-CVSSP	surrey-cvssp-001	001	2022-09-22
402	US	VCognition	vcog-002	002	2017-06-12
403	ES	Veridas Digital Authentication Solutions S.L.	veridas-007	007	2021-09-02
404	ES	Veridas Digital Authentication Solutions S.L.	veridas-008	008	2022-10-17
405	UK	Veridium	veridium-000	000	2022-03-28
406	KZ	Verigram	verigram-000	000	2021-09-06
407	KZ	Verigram	verigram-001	001	2022-03-09
408	ID	Verihubs	verihubs-inteligensia-000	000	2021-07-27
409	ID	Verihubs	verihubs-inteligensia-001	001	2022-06-16
410	ID	Verijelas	verijelas-000	000	2022-08-01
411	TW	Via Technologies Inc	via-000	000	2019-07-08
412	TW	Via Technologies Inc	via-001	001	2020-01-08
413	DE	Videmo Intelligent Videoanalyse	videmo-001	001	2021-12-22
414	DE	Videmo Intelligent Videoanalyse	videmo-002	002	2022-08-31
415	IN	Videonetics Technology Pvt	videonetics-001	001	2019-06-19
416	IN	Videonetics Technology Pvt	videonetics-002	002	2019-11-21
417	VN	Vietnam Posts and Telecommunications Group	vnpt-004	004	2022-04-15
418	VN	Vietnam Posts and Telecommunications Group	vnpt-005	005	2022-08-24
419	VN	Viettel Group	vts-000	000	2020-11-04
420	VN	Viettel Group	vts-001	001	2022-04-20

Table 6: Summary of participant information included in this report.

	Location	Developer Name	Short Name	Seq. Num.	Validation Date
421	VN	Viettel High Technology	viettelhightech-000	000	2021-08-04
422	US	Vigilant Solutions	vigilantsolutions-010	010	2021-04-07
423	US	Vigilant Solutions	vigilantsolutions-011	011	2021-08-07
424	VN	VinAI Research VietNam	vinai-000	000	2020-09-24
425	VN	VinBigData	vinbigdata-001	001	2022-01-06
426	VN	VinBigData	vinbigdata-002	002	2022-06-07
427	SE	Visage Technologies	visage-000	000	2020-12-09
428	FI	Visidon	vd-002	002	2021-04-12
429	FI	Visidon	vd-003	003	2021-10-12
430	CN	Vision Intelligence Center of Meituan	meituan-001	001	2022-03-25
431	CN	Vision Intelligence Center of Meituan	meituan-002	002	2022-09-14
432	PT	Vision-Box	visionbox-001	001	2019-03-01
433	PT	Vision-Box	visionbox-002	002	2021-04-29
434	RU	VisionLabs	visionlabs-010	010	2021-01-25
435	RU	VisionLabs	visionlabs-011	011	2021-10-13
436	AU	Vixvizon	vixvizion-005	005	2022-03-03
437	AU	Vixvizon	vixvizion-006	006	2022-08-11
438	RU	Vocord	vocord-009	009	2020-12-28
439	RU	Vocord	vocord-010	010	2021-12-20
440	US	Wicket	wicket-000	000	2022-02-14
441	CN	Winsense	winsense-001	001	2019-10-16
442	CN	Winsense	winsense-002	002	2020-11-20
443	MY	Wise AI SDN BHD	wiseai-001	001	2022-10-25
444	CN	Wuhan Tianyu Information Industry	wuhantianyu-001	001	2021-08-05
445	CN	X-Laboratory	x-laboratory-000	000	2019-09-03
446	CN	X-Laboratory	x-laboratory-001	001	2020-01-21
447	CN	Xforward AI Technology	xforwardai-001	001	2020-09-25
448	CN	Xforward AI Technology	xforwardai-002	002	2021-02-10
449	CN	Xiamen Meiya Pico Information	meiya-001	001	2019-03-01
450	CN	Xiamen University	xm-000	000	2020-10-19
451	PT	YooniK	yoonik-002	002	2021-09-06
452	PT	YooniK	yoonik-003	003	2022-01-06
453	TW	Yuan High-Tech Development	yuan-004	004	2022-01-14
454	TW	Yuan High-Tech Development	yuan-005	005	2022-06-22
455	CN	Yuntu Data and Technology	ytu-000	000	2021-06-16
456	CN	Zhuhai Yisheng Electronics Technology	yisheng-004	004	2018-06-12
457	CN	iQIYI Inc	iqface-000	000	2019-06-04
458	CN	iQIYI Inc	iqface-003	003	2021-02-23
459	TW	iSAP Solution Corporation	isap-001	001	2019-08-07
460	TW	iSAP Solution Corporation	isap-002	002	2020-09-01
461	TW	ioNetworks Inc	ionetworks-000	000	2021-07-20

Table 7: Summary of participant information included in this report.

	ALGORITHM	CONFIG	LIBRARY	TEMPLATE								COMPARISON ⁴					
				NAME	DATA	DATA	MEMORY	SIZE	GENERATION TIME (ms) ⁴				TIME (ns) ⁵				
									(KB) ¹	(KB) ²	(MB) ³	(B)	MUGSHOT	480x720	960x1440	1600x2400	3000x4500
1	20face-000	117155	324083	²⁰⁹ 905	³¹⁹ 2048 ± 0	⁴⁰ 232 ± 1	²⁹ 223 ± 1	²⁵ 226 ± 4	²¹ 222 ± 1	¹⁵ 224 ± 1	⁴³⁶ 44880 ± 134	⁴³⁵ 44462 ± 163					
2	20face-001	226824	324119	³⁶⁴ 1940	⁴⁰⁰ 4096 ± 0	⁵¹ 279 ± 2	³⁵ 266 ± 1	²⁷ 266 ± 1	²⁶ 267 ± 1	²¹ 267 ± 0	³³⁹ 5553 ± 54	³³⁷ 5541 ± 65					
3	3divi-006	273866	52656	⁸⁵ 472	²⁴⁸ 2048 ± 0	²⁰⁸ 654 ± 1	¹⁷³ 651 ± 0	¹⁵⁴ 660 ± 1	¹³⁷ 678 ± 2	¹³⁷ 759 ± 13	¹¹¹ 775 ± 19	¹¹⁰ 770 ± 22					
4	3divi-007	483115	24723	²⁸⁶ 1285	³¹⁴ 2048 ± 0	¹⁸⁹ 615 ± 1	¹⁶⁰ 616 ± 1	¹⁴¹ 623 ± 1	¹²⁸ 644 ± 1	¹²⁷ 727 ± 5	⁹⁶ 707 ± 31	⁹⁷ 712 ± 25					
5	acer-001	36650	66086	⁷⁰ 417	¹⁹ 512 ± 0	³⁶ 199 ± 0	³¹ 237 ± 28	²⁶ 229 ± 26	²⁵ 242 ± 37	¹⁹ 259 ± 21	²⁵⁵ 2453 ± 44	²⁵⁶ 2461 ± 62					
6	acer-002	43922	624858	³⁷ 187	²⁵⁷ 2048 ± 0	³⁰ 184 ± 0	²³ 184 ± 0	¹⁶ 185 ± 0	¹³ 185 ± 0	¹² 186 ± 0	²⁹⁵ 3370 ± 47	²⁹⁵ 3350 ± 54					
7	acisw-007	267619	36111	⁵¹ 286	²²⁹ 2048 ± 0	⁵⁶ 283 ± 0	⁴⁵ 293 ± 3	⁶¹ 414 ± 0	⁵³ 404 ± 0	⁵⁵ 484 ± 1	¹⁶⁷ 1316 ± 22	¹⁶⁷ 1297 ± 23					
8	acisw-008	171703	39359	²⁵² 1101	²⁷⁷ 2048 ± 0	⁹³ 400 ± 1	⁶⁴ 362 ± 28	⁴⁸ 369 ± 9	³¹ 300 ± 2	²⁶ 336 ± 5	¹⁶⁸ 1327 ± 19	¹⁷⁰ 1337 ± 32					
9	adera-002	0	749797	²¹⁵ 921	⁴⁴⁶ 5120 ± 0	⁴³⁸ 1394 ± 11	³⁹⁹ 1381 ± 1	³⁹⁵ 1393 ± 1	³⁷⁵ 1403 ± 1	³²³ 1464 ± 2	²⁴¹ 2163 ± 32	²⁴³ 2158 ± 28					
10	adera-003	0	749778	²¹³ 917	⁴⁴⁵ 5120 ± 0	⁴³⁰ 1381 ± 12	⁴⁰⁰ 1385 ± 1	³⁹⁸ 1394 ± 1	³⁷³ 1401 ± 1	³²⁴ 1469 ± 1	²⁴⁰ 2148 ± 34	²⁴⁰ 2130 ± 32					
11	advance-003	258867	78699	¹⁰⁰ 518	¹⁸⁸ 2048 ± 0	¹⁷⁵ 586 ± 0	¹⁴⁶ 584 ± 0	¹²⁵ 583 ± 0	¹⁰³ 588 ± 0	⁸³ 591 ± 1	²¹⁵ 1813 ± 17	²¹⁰ 1788 ± 26					
12	advance-004	803133	954494	¹⁴³ 679	¹⁷⁹ 2048 ± 0	³⁶¹ 1099 ± 20	³²⁷ 1107 ± 15	³⁰⁷ 1093 ± 21	²⁷³ 1103 ± 21	²³³ 1138 ± 21	²²⁷ 1935 ± 35	²²⁹ 1936 ± 32					
13	afisbiometrics-000	545886	32882	²⁴⁹ 1088	²⁴ 512 ± 0	³⁹¹ 1219 ± 1	³³⁴ 1135 ± 1	³¹⁹ 1137 ± 2	²⁸³ 1137 ± 1	²³⁴ 1147 ± 1	¹⁷⁴ 1400 ± 29	¹⁷¹ 1357 ± 32					
14	affengine-000	151875	382842	³⁶ 177	⁴⁰⁴ 4096 ± 0	¹³ 107 ± 0	¹² 112 ± 0	³ 284 ± 2	¹⁴⁸ 697 ± 2	³⁹⁶ 3299 ± 17	⁴⁴² 54329 ± 140	⁴⁴² 56195 ± 256					
15	aifirst-001	224157	808777	⁸⁷ 485	¹⁰⁴ 2048 ± 0	¹⁷⁶ 587 ± 2	¹³⁸ 568 ± 2	¹²⁶ 584 ± 3	¹¹⁰ 601 ± 6	¹³⁵ 755 ± 5	¹⁴⁸ 1099 ± 14	¹⁵⁰ 1087 ± 45					
16	aigen-001	256958	595227	²⁶⁰ 1136	²⁴⁰ 2048 ± 0	⁴⁵⁰ 1448 ± 9	⁴¹⁹ 1451 ± 8	⁴²⁶ 1759 ± 6	⁴²² 2594 ± 4	⁴⁰⁸ 5691 ± 44	³¹⁰ 3772 ± 57	³⁰⁹ 3736 ± 56					
17	aigen-002	205300	1316138	²⁰³ 874	¹⁵⁴ 2048 ± 0	¹⁷⁴ 586 ± 24	¹⁴⁵ 582 ± 4	²³⁸ 920 ± 4	⁴⁰⁶ 1758 ± 5	⁴⁰⁷ 5427 ± 17	³⁰⁶ 3678 ± 44	³⁰⁵ 3646 ± 48					
18	ailabs-001	1054663	338989	²⁷⁸ 1252	²⁰⁰ 2048 ± 0	²¹⁶ 664 ± 4	²¹³ 774 ± 50	³²³ 1145 ± 12	⁴¹² 1972 ± 74	⁴⁰⁴ 5205 ± 272	⁴⁵⁴ 104034 ± 661	⁴⁵⁴ 103415 ± 7722					
19	aimall-002	370156	25210	³²⁶ 1576	¹¹⁶ 2048 ± 0	²⁵² 776 ± 4	²⁷¹ 927 ± 27	²⁴⁶ 940 ± 21	²²⁸ 955 ± 34	¹⁹⁶ 1003 ± 75	⁴⁵¹ 72811 ± 7399	⁴⁵⁰ 71216 ± 6286					
20	aimall-003	504324	171935	³⁶⁰ 1913	⁷⁰ 1024 ± 0	²¹² 662 ± 1	²⁰² 740 ± 51	¹⁸⁵ 752 ± 62	¹⁶² 741 ± 46	¹⁴⁶ 807 ± 47	⁴²⁹ 34565 ± 93	⁴³⁰ 34598 ± 118					
21	aiseemu-001	0	1005354	³⁹⁶ 2697	³⁹⁰ 4096 ± 0	³⁴² 1001 ± 1	³⁰³ 1017 ± 0	²⁸³ 1014 ± 5	²⁵³ 1022 ± 2	²¹² 1059 ± 4	³²⁷ 4864 ± 25	³²⁷ 4855 ± 32					
22	aiunionface-000	241642	840295	⁶⁷ 402	¹²⁹ 2048 ± 0	²⁰¹ 637 ± 13	²⁰⁷ 754 ± 41	²⁸⁵ 1025 ± 28	²⁹⁸ 1179 ± 29	³⁵¹ 1639 ± 47	¹⁴² 1072 ± 19	¹⁴⁸ 1080 ± 47					
23	aize-001	268456	168970	³¹⁰ 1436	¹¹⁸ 2048 ± 0	¹¹¹ 437 ± 10	⁹⁰ 440 ± 8	¹¹¹ 542 ± 17	¹⁶⁵ 756 ± 27	³⁴⁵ 1583 ± 53	²²⁹ 1937 ± 22	²²³ 1919 ± 23					
24	aize-002	257106	182517	¹²⁰ 586	²⁹⁹ 2048 ± 0	¹²³ 467 ± 1	¹⁰² 479 ± 1	¹⁸⁶ 756 ± 1	³⁹² 1477 ± 1	⁴⁰¹ 4617 ± 41	⁵⁹ 597 ± 16	⁶⁷ 598 ± 14					
25	ajou-001	363257	31734	⁷⁸ 442	¹⁸⁶ 2048 ± 0	¹⁴⁷ 530 ± 0	¹²⁴ 536 ± 0	¹⁰⁷ 535 ± 0	⁹³ 549 ± 0	⁸⁰ 577 ± 0	⁶² 597 ± 19	⁶⁵ 596 ± 13					
26	alchera-003	487718	24613	²⁹⁸ 1376	²³⁰ 2048 ± 0	²⁸⁵ 854 ± 3	²⁴¹ 862 ± 2	²¹⁷ 870 ± 1	²⁰² 882 ± 2	¹⁷⁶ 918 ± 1	²⁹⁸ 3426 ± 57	²⁹⁶ 3383 ± 53					
27	alchera-004	1001019	388616	²⁸² 1270	²¹⁹ 2048 ± 0	³³¹ 975 ± 0	²⁸⁰ 955 ± 0	²⁵⁷ 960 ± 0	²⁴⁰ 989 ± 0	²³⁵ 1152 ± 1	³⁰¹ 3529 ± 54	³⁰³ 3530 ± 63					
28	alfabeta-001	128232	21780	⁸⁷ 3	¹⁷ 512 ± 0	⁴⁷ 271 ± 0	⁴⁰ 276 ± 2	⁷⁷ 459 ± 2	²⁰⁸ 886 ± 2	³⁸² 2547 ± 9	⁴² 470 ± 25	⁴⁴ 458 ± 20					
29	alice-000	1741293	19355	³⁴⁶ 1732	⁴⁰⁵ 4096 ± 0	³²² 950 ± 2	²⁷³ 933 ± 1	²⁵¹ 949 ± 1	²⁵² 1011 ± 3	²⁶³ 1264 ± 8	³⁹⁷ 14975 ± 201	³⁹⁷ 14890 ± 229					
30	alleyes-000	507636	997090	²⁰⁰ 857	¹¹⁰ 2048 ± 0	²⁵⁷ 784 ± 1	²⁸⁶ 970 ± 61	²⁶¹ 974 ± 62	²²⁴ 943 ± 69	²¹⁰ 1057 ± 23	¹⁶⁶ 1298 ± 34	¹⁶⁸ 1303 ± 51					
31	allgovision-000	172509	155862	¹¹² 561	¹⁴⁹ 2048 ± 0	⁸⁹ 384 ± 8	⁷² 395 ± 17	⁶⁰ 413 ± 14	⁷⁰ 471 ± 14	¹²² 710 ± 21	⁴²⁰ 29903 ± 406	⁴²¹ 29735 ± 194					
32	alphaface-001	259849	81636	¹⁰³ 527	²⁴⁶ 2048 ± 0	¹⁸⁴ 612 ± 1	¹⁵⁵ 613 ± 3	¹³⁷ 612 ± 1	¹¹⁵ 619 ± 1	¹⁰³ 640 ± 2	¹³³ 1008 ± 10	¹³³ 1002 ± 19					
33	alphaface-002	768995	70692	³⁰⁹ 1434	²⁸² 2048 ± 0	¹⁹⁶ 628 ± 2	²⁰⁴ 746 ± 19	¹⁸⁴ 751 ± 18	¹⁷⁰ 779 ± 22	¹⁵¹ 828 ± 40	¹²⁸ 945 ± 25	¹²⁶ 935 ± 17					
34	amplifiedgroup-001	0	47053	¹² 81	⁶² 866 ± 2	¹² 93 ± 0	-	-	-	-	⁴⁴⁴ 57803 ± 4210	⁴⁴³ 56365 ± 1196					
35	androvideo-000	174847	585063	⁶⁸ 403	³⁰⁷ 2048 ± 0	⁵⁰ 277 ± 0	⁴³ 285 ± 0	³⁶ 314 ± 0	⁴² 372 ± 1	⁹³ 620 ± 0	²⁷⁴ 2860 ± 28	²⁷³ 2847 ± 22					
36	anke-004	349388	410776	¹⁵⁵ 706	³⁵⁹ 2056 ± 0	¹⁹³ 625 ± 1	¹⁶³ 627 ± 2	¹⁴⁸ 635 ± 3	¹³⁰ 653 ± 2	¹⁹¹ 982 ± 8	⁸¹ 633 ± 22	⁸¹ 632 ± 34					
37	anke-005	328553	429160	²⁵⁸ 1134	³⁴⁹ 2056 ± 0	¹⁷⁷ 590 ± 2	¹⁵² 594 ± 5	¹³⁴ 601 ± 3	¹²⁴ 638 ± 4	¹⁵⁰ 821 ± 24	⁹⁰ 685 ± 19	⁹³ 687 ± 26					
38	antheus-000	119453	41994	²⁰ 116	⁵⁰ 520 ± 0	¹⁶ 109 ± 1	²⁴ 187 ± 1	¹⁸ 189 ± 1	¹⁴ 195 ± 1	¹⁷ 236 ± 2	³⁵⁷ 6901 ± 268	³⁵⁷ 6936 ± 103					
39	antheus-001	119453	41962	²¹ 118	⁵¹ 520 ± 0	¹⁹ 120 ± 1	³⁴ 265 ± 13	⁸³ 468 ± 22	³¹³ 1223 ± 27	³⁸³ 2660 ± 87	³⁵² 6218 ± 47	³⁵¹ 6216 ± 45					
40	anyvision-004	401001	630797	²⁵³ 1102	⁶⁹ 1024 ± 0	⁷⁷ 355 ± 1	-	-	-	-	²²⁴ 1891 ± 51	²¹⁵ 1829 ± 85					
41	anyvision-005	190979	116595	²²² 963	⁷¹ 1024 ± 0	³³⁶ 985 ± 1	²⁹³ 997 ± 1	²⁷⁸ 1004 ± 1	²⁴² 995 ± 1	¹⁹⁴ 995 ± 1	¹⁰⁴ 733 ± 14	¹⁰⁴ 733 ± 16					
42	armatura-001	0	374608	²⁶⁴ 1151	¹¹² 2048 ± 0	²²⁶ 688 ± 1	¹⁸⁷ 689 ± 1	¹⁶⁹ 693 ± 1	¹⁵¹ 708 ± 3	¹³⁶ 756 ± 13	¹⁹ 270 ± 17	²¹ 268 ± 11					
43	armatura-002	0	1258644	²⁷⁵ 1222	⁴⁴⁸ 6144 ± 0	⁴⁵⁶ 1476 ± 3	⁴²² 1458 ± 5	³⁹⁵ 1505 ± 12	³⁴⁷ 1605 ± 26	¹⁹¹ 1605 ± 26	¹⁹¹ 1589 ± 25						
44	asusaics-000	257418	245320	¹²⁷ 605	³²⁰ 2048 ± 0	¹³⁴ 484 ± 13	¹¹⁸ 506 ± 21	²¹² 850 ± 26	⁴⁰⁸ 1789 ± 61	⁴¹⁰ 6305 ± 188							

	ALGORITHM	CONFIG	LIBRARY	TEMPLATE								COMPARISON ⁴									
				NAME	DATA	DATA	MEMORY	SIZE	GENERATION TIME (ms) ⁴				TIME (ns) ⁵								
									(KB) ¹	(KB) ²	(MB) ³	(B)	MUGSHOT	480x720	960x1440	1600x2400	3000x4500	GENUINE	IMPOSTOR		
45	asusaics-001	257418	245330	124	595	392	4096 ± 0	281	842 ± 17	301	1008 ± 20	389	1377 ± 28	421	2423 ± 90	415	7284 ± 277	367	8618 ± 42	367	8638 ± 136
46	authenmetric-003	293599	39492	226	982	225	2048 ± 0	339	992 ± 1	299	1006 ± 1	277	1003 ± 2	247	1002 ± 1	203	1036 ± 1	205	1757 ± 19	205	1755 ± 19
47	authenmetric-004	381165	39492	272	1214	176	2048 ± 0	306	910 ± 1	266	909 ± 1	234	915 ± 1	216	921 ± 2	184	950 ± 1	200	1724 ± 14	198	1691 ± 29
48	aware-005	300017	26320	280	1265	98	1572 ± 0	302	886 ± 23	311	1038 ± 21	313	1121 ± 22	348	1337 ± 58	368	2195 ± 144	184	1475 ± 63	180	1427 ± 115
49	aware-006	298543	14124	219	943	14	352 ± 0	376	1148 ± 3	339	1146 ± 2	337	1190 ± 2	335	1306 ± 20	360	1754 ± 84	263	2598 ± 42	263	2559 ± 60
50	awiros-001	15499	87480	14	88	23	512 ± 0	12	97 ± 6	10	98 ± 4	11	138 ± 6	22	225 ± 7	75	556 ± 8	145	1079 ± 44	142	1050 ± 45
51	awiros-002	289016	203723	113	562	196	2048 ± 0	129	479 ± 0	114	500 ± 0	106	534 ± 0	114	618 ± 0	181	946 ± 1	230	1966 ± 31	231	1957 ± 25
52	aximetria-001	408902	487912	142	674	291	2048 ± 0	346	1013 ± 1	304	1023 ± 21	288	1029 ± 5	245	999 ± 2	222	1091 ± 5	320	4401 ± 94	319	4490 ± 80
53	ayftech-001	195423	43580	164	731	28	512 ± 0	100	408 ± 23	100	476 ± 52	200	814 ± 108	410	1827 ± 384	406	5412 ± 1029	71	615 ± 16	122	885 ± 44
54	ayonix-000	58505	5252	69	83	1036 ± 0	2	18 ± 2	-	-	-	-	-	-	-	-	-	73	621 ± 23	77	620 ± 26
55	beethedata-000	227849	1087592	111	555	215	2048 ± 0	120	465 ± 0	99	467 ± 0	81	468 ± 0	69	467 ± 0	52	467 ± 0	237	2121 ± 34	238	2110 ± 38
56	beyneai-000	256958	591433	256	1124	239	2048 ± 0	114	451 ± 8	92	449 ± 1	188	767 ± 7	402	1603 ± 25	402	4669 ± 124	308	3730 ± 57	306	3668 ± 54
57	biocube-001	25030	6192987	82	458	399	4096 ± 0	54	282 ± 22	44	292 ± 24	104	521 ± 57	138	684 ± 59	270	1282 ± 68	411	21787 ± 96	411	21812 ± 109
58	bioittechswiss-001	1178769	120811	312	1455	32	512 ± 0	329	966 ± 4	371	1270 ± 270	364	1294 ± 96	376	1409 ± 157	363	1793 ± 79	264	2610 ± 25	264	2624 ± 32
59	bioittechswiss-002	744786	114842	231	993	38	512 ± 0	311	917 ± 2	272	930 ± 2	252	952 ± 2	226	947 ± 3	211	1058 ± 11	244	2177 ± 29	245	2170 ± 31
60	bm-001	287734	38076	27	148	1	64 ± 0	112	444 ± 88	-	-	-	-	-	-	-	223	1887 ± 31	221	1877 ± 26	
61	boetech-001	261376	88710	301	1384	247	2048 ± 0	46	271 ± 1	36	268 ± 1	28	273 ± 0	29	286 ± 1	23	318 ± 1	448	68519 ± 1921	448	67648 ± 822
62	boetech-002	294347	88710	317	1489	197	2048 ± 0	63	305 ± 4	47	296 ± 1	32	302 ± 1	313	31 ± 1	28	348 ± 2	449	68921 ± 2137	449	69473 ± 2104
63	bresee-001	287880	23227	273	1214	140	2048 ± 0	393	1223 ± 3	356	1216 ± 1	374	1331 ± 1	316	1227 ± 1	291	1360 ± 1	431	37240 ± 655	432	37167 ± 584
64	bresee-002	313627	30902	366	1956	133	2048 ± 0	243	743 ± 4	337	1143 ± 2	324	1146 ± 2	286	1148 ± 2	247	1176 ± 2	208	1778 ± 22	208	1775 ± 23
65	camvi-002	236278	225285	165	737	67	1024 ± 0	220	677 ± 7	200	726 ± 36	216	869 ± 28	278	1129 ± 43	388	2785 ± 113	70	612 ± 26	70	603 ± 20
66	camvi-004	280733	615819	214	919	167	2048 ± 0	246	759 ± 10	240	861 ± 17	269	986 ± 34	331	1279 ± 51	390	2891 ± 158	126	948 ± 40	127	963 ± 31
67	canon-003	2550850	101378	444	5472	449	6180 ± 0	403	1263 ± 3	369	1263 ± 1	359	1283 ± 1	343	1320 ± 1	328	1482 ± 2	325	4783 ± 17	322	4780 ± 19
68	canon-004	2399160	114188	446	5956	450	6200 ± 0	320	948 ± 4	279	955 ± 3	256	959 ± 3	233	977 ± 3	217	1064 ± 2	363	7172 ± 63	362	7169 ± 51
69	ceiec-003	260371	88707	74	430	190	2048 ± 0	269	817 ± 4	256	883 ± 57	227	897 ± 60	210	899 ± 72	180	944 ± 72	250	2256 ± 38	250	2241 ± 54
70	ceiec-004	263476	67011	69	408	252	2048 ± 0	348	1024 ± 1	306	1027 ± 1	287	1027 ± 1	255	1030 ± 1	207	1055 ± 1	217	1844 ± 26	216	1836 ± 20
71	chosun-001	765615	707	91	491	216	2048 ± 0	255	783 ± 2	228	826 ± 4	425	1662 ± 13	427	3679 ± 67	423	11694 ± 243	130	998 ± 25	140	1035 ± 11
72	chosun-002	234001	31875	79	450	193	2048 ± 0	42	248 ± 3	37	273 ± 3	419	1495 ± 14	428	7920 ± 90	424	80302 ± 1349	75	623 ± 17	83	634 ± 13
73	chtface-004	409656	311027	316	1487	254	2048 ± 0	70	332 ± 0	53	323 ± 1	40	329 ± 1	37	335 ± 1	33	377 ± 1	201	1727 ± 17	200	1720 ± 16
74	chtface-005	408364	311100	305	1412	175	2048 ± 0	67	322 ± 0	51	316 ± 1	38	325 ± 2	34	324 ± 1	40	411 ± 2	225	1907 ± 19	222	1898 ± 23
75	cist-001	0	300551	117	583	158	2048 ± 0	330	972 ± 0	288	977 ± 1	263	981 ± 0	236	983 ± 0	214	1061 ± 0	279	2947 ± 20	278	2940 ± 22
76	clearviewai-000	342491	211852	403	2750	171	2048 ± 0	441	1402 ± 1	410	1403 ± 1	406	1412 ± 1	379	1420 ± 1	310	1418 ± 1	190	1592 ± 37	188	1561 ± 37
77	closedi-001	420342	9851	173	773	410	4096 ± 0	280	839 ± 1	234	843 ± 1	210	841 ± 1	190	845 ± 1	162	865 ± 1	336	5404 ± 17	335	5400 ± 25
78	cloudmatrix-001	10390	542121	44	249	121	2048 ± 0	18	114 ± 1	13	117 ± 0	10	118 ± 0	9	123 ± 1	10	169 ± 1	439	50263 ± 212	439	50243 ± 237
79	cloudmatrix-002	256635	693318	235	1030	309	2048 ± 0	92	395 ± 1	73	398 ± 1	56	399 ± 1	51	402 ± 1	47	437 ± 20	438	49578 ± 120	438	49602 ± 180
80	cloudwalk-hr-003	383739	144263	229	984	371	2057 ± 0	183	606 ± 0	148	588 ± 0	130	594 ± 0	113	612 ± 1	-	359	6982 ± 80	358	6972 ± 84	
81	cloudwalk-hr-004	502916	520169	304	1394	325	2049 ± 0	294	873 ± 1	251	877 ± 1	222	876 ± 1	201	879 ± 1	172	902 ± 3	382	11652 ± 127	382	11608 ± 123
82	cloudwalk-mt-005	846026	573253	411	2928	192	2048 ± 0	381	1179 ± 3	353	1200 ± 3	342	1209 ± 3	314	1226 ± 5	259	1229 ± 3	389	12525 ± 225	388	12394 ± 152
83	cloudwalk-mt-006	563322	480071	406	2836	289	2048 ± 0	433	1385 ± 0	404	1392 ± 1	400	1398 ± 1	371	1397 ± 4	318	1444 ± 2	294	3364 ± 96	293	3324 ± 83
84	codeline-000	361659	138388	270	1188	278	2048 ± 0	451	1453 ± 0	421	1456 ± 2	415	1456 ± 0	383	1457 ± 0	329	1483 ± 1	242	2171 ± 69	246	2194 ± 84
85	cogent-006	1078167	58108	323	1547	86	1062 ± 0	250	768 ± 0	217	789 ± 1	206	831 ± 2	218	930 ± 1	189	971 ± 1	211	1802 ± 17	211	1797 ± 23
86	cogent-007	621565	72316	359	1884	59	550 ± 0	422	1329 ± 2	391	1333 ± 5	377	1337 ± 4	352	1353 ± 5	302	1390 ± 4	31	355 ± 8	34	367 ± 14
87	cognitec-003	471458	62502	188	817	342	2052 ± 0	83	366 ± 9	77	403 ± 9	58	408 ± 9	57	424 ± 9	58	509 ± 13	297	3417 ± 51	299	3433 ± 53
88	cognitec-004	705645	62678	119	585	341	2052 ± 0	118	463 ± 9	110	497 ± 9	95	504 ± 10	84	521 ± 10	94	631 ± 12	285	3028 ± 197	286	3059 ± 238

Notes

- 1 The configuration size does not capture static data included in libraries.
- 2 The library size is the combined total of all files provided in the submission lib folder. These libraries e.g. OpenCV may or may not be installed on any end user's platform natively and would not need to be installed with the algorithm. Some developers put neural network models in their libraries.
- 3 The memory usage is the peak resident set size reported by the ps system call during template generation.
- 4 The median template creation times are measured on Intel®Xeon®CPU E5-2630 v4 @ 2.20GHz processors.
- 5 The comparison durations, in nanoseconds, are estimated using std::chrono::high_resolution_clock which on the machine in (2) counts 1ns clock ticks. Precision is somewhat worse than that however. The ± value is the median absolute deviation times 1.48 for Normal consistency.

	ALGORITHM	CONFIG	LIBRARY	TEMPLATE								COMPARISON ⁴									
				NAME	DATA	DATA	MEMORY	SIZE	GENERATION TIME (ms) ⁴				TIME (ns) ⁵								
									(KB) ¹	(KB) ²	(MB) ³	(B)	MUGSHOT	480x720	960x1440	1600x2400	3000x4500	GENUINE	IMPOSTOR		
89	cor-001	1194948	11240	277	1249	373	2060 ± 0	234	699 ± 3	243	863 ± 76	214	865 ± 80	197	872 ± 89	185	952 ± 39	457	270145 ± 2259	457	282686 ± 11788
90	coretech-000	186423	43964	66	393	15	512 ± 0	182	602 ± 15	174	659 ± 12	320	1139 ± 24	287	1149 ± 25	241	1165 ± 23	26	333 ± 14	27	321 ± 13
91	coretech-001	235361	305490	321	1524	163	2048 ± 0	227	688 ± 7	190	695 ± 7	218	870 ± 17	200	879 ± 15	165	877 ± 15	76	625 ± 25	85	641 ± 25
92	corsight-002	1474921	32093	371	2061	377	2080 ± 0	411	1290 ± 1	376	1287 ± 1	360	1290 ± 1	336	1307 ± 2	301	1388 ± 4	415	24953 ± 637	414	24263 ± 578
93	corsight-003	1413063	32198	334	1637	376	2080 ± 0	388	1202 ± 2	352	1190 ± 5	340	1199 ± 3	317	1236 ± 3	288	1349 ± 7	419	28754 ± 434	420	28279 ± 446
94	csc-002	0	519768	299	1376	55	544 ± 0	125	473 ± 0	109	494 ± 0	87	481 ± 1	74	490 ± 1	61	514 ± 5	34	367 ± 11	35	371 ± 10
95	csc-003	0	400435	332	1609	56	544 ± 0	138	499 ± 0	113	500 ± 1	94	502 ± 0	81	508 ± 1	68	535 ± 4	37	393 ± 8	38	397 ± 7
96	ctcbcank-000	257208	599238	115	570	202	2048 ± 0	164	568 ± 43	168	690 ± 38	152	711 ± 50	152	831 ± 51	302	3551 ± 87	324	4805 ± 209		
97	ctcbcank-001	275511	599238	125	603	211	2048 ± 0	206	652 ± 35	214	781 ± 30	209	898 ± 51	202	1030 ± 47	311	3926 ± 45	310	3924 ± 56		
98	cubox-001	369627	75427	135	649	265	2048 ± 0	304	907 ± 1	263	902 ± 1	230	903 ± 0	219	917 ± 0	177	931 ± 0	170	1379 ± 37	177	1417 ± 38
99	cubox-002	542254	90975	367	1964	305	2048 ± 0	312	921 ± 1	268	921 ± 1	239	922 ± 1	220	933 ± 1	197	1003 ± 1	233	2008 ± 72	233	1969 ± 57
100	cudocommunication-001	385258	341277	246	1077	182	2048 ± 0	314	925 ± 1	269	923 ± 1	245	928 ± 1	219	932 ± 0	186	964 ± 1	259	2534 ± 20	261	2537 ± 20
101	cuhkee-001	787853	74917	389	2515	331	2052 ± 0	333	977 ± 31	-	-	-	-	-	-	-	266	2719 ± 60	270	2783 ± 56	
102	cybercore-002	166096	7374	392	2564	269	2048 ± 0	136	489 ± 1	112	500 ± 4	93	500 ± 1	79	499 ± 2	67	528 ± 1	387	12389 ± 123	387	12352 ± 112
103	cybercore-003	289176	7969	433	4310	397	4096 ± 0	282	844 ± 2	239	855 ± 4	213	864 ± 4	195	862 ± 4	166	878 ± 2	343	5744 ± 41	345	5737 ± 31
104	cyberextruder-003	253300	12354	76	437	16	512 ± 0	90	390 ± 1	71	388 ± 1	55	393 ± 1	49	399 ± 1	46	435 ± 1	10	198 ± 4	11	189 ± 8
105	cyberextruder-004	169301	12354	61	349	2	128 ± 0	37	206 ± 0	27	208 ± 0	23	209 ± 0	24	229 ± 0	18	249 ± 1	5	145 ± 14	6	155 ± 14
106	cyberlink-009	588443	102201	339	1704	438	4164 ± 0	431	1384 ± 2	407	1395 ± 2	399	1398 ± 2	372	1401 ± 2	321	1456 ± 2	23	299 ± 17	24	304 ± 16
107	cyberlink-010	1590818	102180	422	3672	456	8260 ± 0	404	1265 ± 2	383	1314 ± 5	363	1294 ± 2	329	1273 ± 2	278	1305 ± 2	43	476 ± 23	46	472 ± 14
108	dahua-006	831641	119261	440	5068	122	2048 ± 0	439	1398 ± 2	409	1397 ± 1	403	1404 ± 1	374	1402 ± 1	306	1402 ± 1	18	249 ± 13	20	250 ± 11
109	dahua-007	1578737	119418	451	7237	408	4096 ± 0	437	1393 ± 2	398	1373 ± 1	391	1378 ± 1	362	1378 ± 1	297	1379 ± 2	35	367 ± 102	39	434 ± 108
110	daon-000	280726	2307	370	2013	375	2065 ± 0	159	562 ± 3	143	581 ± 5	191	791 ± 9	187	838 ± 15	208	1055 ± 32	400	16052 ± 88	400	16041 ± 85
111	decatur-000	350495	171271	210	907	430	4100 ± 0	349	1024 ± 2	-	-	-	-	-	-	-	380	11439 ± 80	381	11418 ± 112	
112	decatur-001	342866	253734	318	1507	327	2052 ± 0	362	1103 ± 2	316	1064 ± 2	300	1063 ± 2	265	1067 ± 2	219	1084 ± 2	68	610 ± 19	69	602 ± 8
113	deepglint-004	1073382	261571	414	3084	298	2048 ± 0	453	1470 ± 1	425	1474 ± 1	418	1485 ± 1	391	1474 ± 1	331	1492 ± 2	348	5961 ± 34	349	5955 ± 29
114	deepglint-005	960326	213877	413	2947	189	2048 ± 0	444	1408 ± 1	416	1431 ± 2	408	1424 ± 3	381	1424 ± 3	319	1446 ± 2	355	6765 ± 38	354	6765 ± 40
115	deepsea-001	147497	336250	63	358	74	1024 ± 0	197	630 ± 7	206	752 ± 37	183	746 ± 30	157	727 ± 32	149	820 ± 32	175	1401 ± 37	182	1467 ± 50
116	deeepsense-000	357113	936618	452	7618	114	2048 ± 0	213	664 ± 3	172	645 ± 1	155	660 ± 2	140	687 ± 2	147	808 ± 3	44	480 ± 22	45	459 ± 34
117	deeepsense-001	73173	1288355	441	5314	41	512 ± 0	373	1142 ± 2	342	1164 ± 3	336	1183 ± 3	308	1201 ± 3	283	1323 ± 2	253	2356 ± 35	253	2354 ± 42
118	dermalog-009	0	319363	138	664	18	512 ± 0	76	349 ± 0	60	351 ± 0	44	352 ± 0	39	357 ± 0	36	389 ± 0	46	487 ± 34	37	385 ± 29
119	dermalog-010	0	525908	234	1023	40	512 ± 0	200	635 ± 0	170	640 ± 1	149	639 ± 4	126	647 ± 3	115	691 ± 5	39	444 ± 13	31	341 ± 26
120	dicio-001	61751	119517	11	77	49	520 ± 0	151	538 ± 0	137	563 ± 10	235	915 ± 3	409	1800 ± 7	405	5286 ± 30	270	2818 ± 20	271	2807 ± 31
121	digidglobalface-001	259849	70680	102	527	128	2048 ± 0	185	612 ± 1	167	633 ± 3	146	634 ± 3	128	650 ± 15	109	666 ± 4	128	973 ± 20	128	988 ± 20
122	digidata-000	133370	30249	47	257	271	2048 ± 0	82	361 ± 0	62	360 ± 0	46	361 ± 0	40	363 ± 0	34	380 ± 0	236	2084 ± 37	235	2039 ± 42
123	digidata-001	254564	33036	64	367	153	2048 ± 0	158	559 ± 1	135	561 ± 1	117	562 ± 1	95	564 ± 1	88	602 ± 1	377	10308 ± 102	377	10301 ± 121
124	digitalbarriers-002	83002	598577	362	1930	354	2056 ± 0	38	209 ± 11	32	250 ± 19	59	411 ± 37	176	808 ± 72	370	13409 ± 228	390	13267 ± 206		
125	dps-000	0	2211812	240	1058	427	4096 ± 0	287	868 ± 2	260	893 ± 6	412	1445 ± 9	424	2910 ± 38	417	9345 ± 17	183	1473 ± 37	184	1479 ± 37
126	dsk-000	11967	782905	46	252	39	512 ± 0	61	304 ± 47	52	317 ± 33	276	1001 ± 96	423	2660 ± 170	421	10451 ± 832	362	7152 ± 115	360	7134 ± 111
127	einetworks-000	372608	219883	206	880	350	2056 ± 0	204	645 ± 3	-	-	-	-	-	-	-	328	4876 ± 66	330	5156 ± 77	
128	ekin-002	51434	278	24	139	385	3072 ± 0	385	1186 ± 13	349	1180 ± 12	333	1181 ± 11	306	1191 ± 11	254	1207 ± 8	318	4294 ± 80	339	5569 ± 112
129	enface-000	369598	153781	137	662	77	1024 ± 0	157	555 ± 4	134	558 ± 4	159	669 ± 6	239	987 ± 15	373	2349 ± 54	360	7059 ± 62	359	6980 ± 65
130	enface-001	370710	173609	141	670	73	1024 ± 0	155	550 ± 4	133	555 ± 3	158	668 ± 7	234	981 ± 15	378	2416 ± 59	354	6734 ± 68	355	6766 ± 69
131	eocortex-000	255937	59432	42	224	292	2048 ± 0	62	305 ± 22	57	341 ± 25	73	440 ± 47	67	464 ± 45	60	513 ± 44	124	923 ± 11	125	918 ± 11
132	ercacat-001	811623	58012	405	2816	329	2052 ± 0	355	1052 ± 3	-	-	-	-	-	-	-	260	2551 ± 62	258	2501 ± 81	

Notes

- 1 The configuration size does not capture static data included in libraries.
- 2 The library size is the combined total of all files provided in the submission lib folder. These libraries e.g. OpenCV may or may not be installed on any end user's platform natively and would not need to be installed with the algorithm. Some developers put neural network models in their libraries.
- 3 The memory usage is the peak resident set size reported by the ps system call during template generation.
- 4 The median template creation times are measured on Intel®Xeon®CPU E5-2630 v4 @ 2.20GHz processors.
- 5 The comparison durations, in nanoseconds, are estimated using std::chrono::high_resolution_clock which on the machine in (2) counts 1ns clock ticks. Precision is somewhat worse than that however. The ± value is the median absolute deviation times 1.48 for Normal consistency.

Table 10: Summary of algorithms and properties included in this report. The red superscripts give ranking for the quantity in that column.

ALGORITHM		CONFIG	LIBRARY	TEMPLATE								COMPARISON ⁴									
NAME		DATA	DATA	MEMORY	SIZE	GENERATION TIME (ms) ⁴				TIME (ns) ⁵											
	(KB) ¹	(KB) ²	(MB) ³	(B)	MUGSHOT	480x720	960x1440	1600x2400	3000x4500	GENUINE	IMPOSTOR										
133	euronovate-001	0	1774966	291	1308	89	1177 ± 0	351	1034 ± 2	343	1165 ± 3	328	1160 ± 3	297	1177 ± 3	244	1172 ± 2	453	81294 ± 591	453	81631 ± 931
134	expasoft-001	39057	983064	25	142	205	2048 ± 0	8	70 ± 0	674 ± 0	677 ± 0	5	73 ± 0	4	74 ± 0	194	1660 ± 35	195	1676 ± 48		
135	expasoft-002	38760	59825	32	168	212	2048 ± 0	5	34 ± 0	34 ± 0	34 ± 0	2	34 ± 0	2	34 ± 0	369	8870 ± 78	369	8838 ± 77		
136	f8-001	272977	19668	283	1276	204	2048 ± 0	275	822 ± 39	-	-	-	-	-	399	15262 ± 139	399	15277 ± 212			
137	f8-002	28278	215616	13	83	217	2048 ± 0	6	39 ± 0	441 ± 0	575 ± 0	17	197 ± 1	119	702 ± 1	396	14765 ± 131	396	14790 ± 133		
138	faceonline-001	0	71529	55	302	357	2056 ± 0	27	179 ± 0	19	179 ± 0	20	190 ± 0	10	217 ± 0	27	343 ± 1	141	1064 ± 37	139	1033 ± 35
139	faceonline-002	155220	141019	232	995	127	2048 ± 0	256	783 ± 1	220	797 ± 2	193	794 ± 2	177	809 ± 3	171	901 ± 2	391	13798 ± 197	391	13743 ± 127
140	facephi-000	148904	5219	455	11481	260	2048 ± 0	290	871 ± 2	253	881 ± 3	224	880 ± 4	206	888 ± 4	183	949 ± 12	316	4067 ± 53	315	4047 ± 53
141	facesoft-000	370120	10612	178	796	243	2048 ± 0	218	675 ± 18	178	669 ± 3	165	686 ± 3	135	675 ± 5	112	687 ± 2	249	2239 ± 28	252	2277 ± 96
142	facetag-000	1232331	4022	224	965	62	2048 ± 0	78	355 ± 17	65	369 ± 8	271	989 ± 33	420	2408 ± 91	416	7930 ± 316	450	72003 ± 625	451	71912 ± 612
143	facetag-002	819806	4021	160	726	105	2048 ± 0	152	544 ± 1	128	544 ± 0	110	542 ± 0	92	545 ± 0	74	554 ± 0	202	1730 ± 25	202	1733 ± 25
144	facex-001	305074	930372	412	2931	132	2048 ± 0	105	422 ± 4	88	434 ± 4	103	520 ± 7	161	737 ± 13	353	1670 ± 27	220	1871 ± 23	218	1846 ± 29
145	facex-002	305074	928334	415	3095	213	2048 ± 0	106	426 ± 5	80	429 ± 4	101	516 ± 8	159	730 ± 12	359	1738 ± 36	79	631 ± 25	75	614 ± 19
146	farfaces-001	346494	44581	48	261	20	512 ± 0	380	1179 ± 1	350	1180 ± 1	332	1180 ± 0	301	1185 ± 1	255	1209 ± 2	120	855 ± 25	119	860 ± 31
147	fiberhome-nanjing-003	352895	1482309	196	845	162	2048 ± 0	369	1136 ± 7	333	1134 ± 4	318	1132 ± 3	285	1139 ± 3	236	1154 ± 5	147	1097 ± 38	149	1083 ± 42
148	fiberhome-nanjing-004	443779	1482313	238	1048	391	4960 ± 0	419	1321 ± 5	380	1304 ± 3	368	1307 ± 2	338	1308 ± 3	285	1326 ± 5	165	1276 ± 40	165	1265 ± 38
149	fincore-000	256615	19409	107	535	244	2048 ± 0	142	508 ± 3	117	505 ± 0	97	508 ± 1	83	513 ± 2	69	535 ± 1	206	1765 ± 31	206	1763 ± 22
150	firstcreditKZ-001	553811	24803	255	1112	168	2048 ± 0	264	808 ± 0	294	997 ± 0	299	1061 ± 1	295	1174 ± 1	362	1774 ± 54	122	904 ± 20	123	903 ± 23
151	frpkauai-001	507771	24807	245	1076	224	2048 ± 0	228	689 ± 1	189	691 ± 0	171	697 ± 2	155	714 ± 6	141	775 ± 31	107	752 ± 29	109	764 ± 23
152	fujitsulab-002	0	1088887	333	1613	436	4104 ± 0	396	1237 ± 2	359	1222 ± 2	345	1236 ± 1	320	1251 ± 2	286	1327 ± 2	271	2836 ± 25	272	2809 ± 44
153	fujitsulab-003	662263	318209	450	6907	435	4104 ± 0	324	951 ± 20	275	941 ± 19	253	952 ± 19	232	971 ± 20	205	1045 ± 21	273	2855 ± 16	274	2849 ± 19
154	g42-intelbrain-001	1031335	235521	460	25628	8	269 ± 0	332	976 ± 6	287	975 ± 1	275	997 ± 2	266	1068 ± 3	294	1362 ± 8	340	5878 ± 96	348	5865 ± 71
155	geo-002	369903	98667	233	1018	250	2048 ± 0	259	791 ± 1	219	793 ± 0	192	794 ± 0	172	795 ± 1	144	803 ± 1	296	3407 ± 45	298	3422 ± 65
156	geo-004	168980	107714	285	1280	236	2048 ± 0	405	1268 ± 1	374	1279 ± 1	336	1274 ± 0	324	1259 ± 1	275	1296 ± 1	136	1023 ± 20	138	1028 ± 22
157	glory-004	0	999639	378	2181	440	4182 ± 0	225	688 ± 0	209	759 ± 1	24	941 ± 1	415	2134 ± 4	418	9360 ± 47	330	4982 ± 66	328	4990 ± 63
158	glory-005	0	999999	384	2428	441	4182 ± 0	236	703 ± 1	216	789 ± 0	259	972 ± 1	417	2200 ± 25	419	9679 ± 22	333	5224 ± 93	332	5176 ± 81
159	gorilla-007	441058	708166	337	1691	451	6288 ± 0	179	592 ± 1	150	592 ± 1	120	603 ± 1	126	722 ± 9	307	3686 ± 37	308	3709 ± 36		
160	gorilla-008	450175	707000	352	1789	457	8338 ± 0	181	595 ± 1	149	590 ± 0	130	600 ± 1	118	621 ± 2	124	720 ± 9	322	4530 ± 44	320	4524 ± 38
161	graymatrics-001	13095	70406	22	127	395	4096 ± 0	32	191 ± 1	25	203 ± 1	129	592 ± 5	404	1698 ± 9	414	7150 ± 34	433	39874 ± 309	433	39762 ± 295
162	griaule-000	0	598214	239	1054	333	2052 ± 0	103	416 ± 6	84	425 ± 7	190	770 ± 14	405	1749 ± 43	412	6406 ± 189	314	3987 ± 42	311	3938 ± 38
163	griaule-001	0	412061	281	1269	344	2052 ± 0	378	1164 ± 1	326	1096 ± 5	308	1099 ± 4	282	1136 ± 2	333	1509 ± 2	313	3948 ± 23	313	3957 ± 32
164	hertasecurity-001	0	944427	269	1183	33	512 ± 0	75	346 ± 0	58	345 ± 0	43	349 ± 0	38	354 ± 0	35	388 ± 0	207	1770 ± 45	201	1726 ± 48
165	hertasecurity-002	0	944582	268	1177	42	512 ± 0	133	484 ± 7	101	478 ± 3	85	480 ± 3	78	495 ± 3	65	520 ± 3	252	2289 ± 40	251	2267 ± 48
166	hik-001	667866	9290	448	6597	93	1408 ± 0	205	651 ± 0	177	667 ± 8	162	677 ± 16	139	686 ± 13	130	737 ± 12	47	488 ± 19	47	477 ± 22
167	hisign-001	732412	167488	324	1553	378	2080 ± 0	414	1306 ± 1	384	1320 ± 1	369	1315 ± 1	341	1312 ± 1	284	1325 ± 1	13	201 ± 10	9	185 ± 13
168	hisign-002	1014906	102652	375	2123	379	2080 ± 0	261	797 ± 0	221	800 ± 5	195	800 ± 0	173	801 ± 0	143	803 ± 1	17	232 ± 11	13	207 ± 11
169	hyperverge-002	2951900	198832	368	1975	78	1024 ± 0	316	938 ± 1	274	939 ± 1	248	941 ± 1	225	945 ± 1	190	975 ± 1	350	6023 ± 37	350	5966 ± 40
170	hyperverge-003	1167779	281256	402	2748	65	1024 ± 0	457	1477 ± 2	426	1503 ± 3	421	1520 ± 3	397	1525 ± 4	343	1565 ± 3	54	566 ± 11	55	561 ± 8
171	hzailu-002	1515880	74047	437	4715	363	2056 ± 0	377	1150 ± 5	332	1127 ± 6	315	1129 ± 7	284	1137 ± 7	245	1172 ± 3	144	1079 ± 53	145	1070 ± 31
172	hzailu-003	1923030	222185	438	4817	386	3080 ± 0	435	1389 ± 5	390	1331 ± 7	375	1334 ± 2	351	1349 ± 6	313	1424 ± 8	185	1483 ± 35	181	1464 ± 31
173	icm-003	1513988	940	93	500	184	2048 ± 0	221	681 ± 6	180	672 ± 4	178	714 ± 11	185	837 ± 41	298	1381 ± 131	414	24351 ± 161	413	24227 ± 146
174	icm-004	2012129	1089	237	1040	270	2048 ± 0	104	419 ± 6	78	407 ± 6	76	454 ± 15	111	603 ± 51	338	1527 ± 235	395	14730 ± 154	395	14521 ± 152
175	ichttc-000	172459	1471004	353	1805	228	2048 ± 0	73	338 ± 11	56	338 ± 9	70	437 ± 16	148	705 ± 24	357	1719 ± 44	335	5284 ± 63	334	5290 ± 54
176	id3-006	210116	7706	227	982	52	520 ± 0	222	683 ± 0	319	1088 ± 1	338	1192 ± 1	311	1209 ± 1	267	1270 ± 1	338	5547 ± 34	338	5563 ± 34

Notes

- 1 The configuration size does not capture static data included in libraries.
- 2 The library size is the combined total of all files provided in the submission lib folder. These libraries e.g. OpenCV may or may not be installed on any end user's platform natively and would not need to be installed with the algorithm. Some developers put neural network models in their libraries.
- 3 The memory usage is the peak resident set size reported by the ps system call during template generation.
- 4 The median template creation times are measured on Intel®Xeon®CPU E5-2630 v4 @ 2.20GHz processors.
- 5 The comparison durations, in nanoseconds, are estimated using std::chrono::high_resolution_clock which on the machine in (2) counts 1ns clock ticks. Precision is somewhat worse than that however. The ± value is the median absolute deviation times 1.48 for Normal consistency.

Table 11: Summary of algorithms and properties included in this report. The red superscripts give ranking for the quantity in that column.

NAME	ALGORITHM	CONFIG	LIBRARY	TEMPLATE								COMPARISON ⁴	
				SIZE				GENERATION TIME (ms) ⁴				TIME (ns) ⁵	
				(KB) ¹	(KB) ²	(MB) ³	(B)	MUGSHOT	480x720	960x1440	1600x2400	3000x4500	GENUINE
177	id3-008	242416	8151	²⁴³ 1068	⁷ 264 ± 0	²⁷⁰ 819 ± 0	³⁵⁴ 1209 ± 2	³⁶⁶ 1297 ± 2	³⁴⁶ 1329 ± 1	³¹⁷ 1433 ± 1	³⁴¹ 5658 ± 44	³⁴² 5624 ± 40	
178	idemia-008	374017	69922	²⁷¹ 1194	¹³ 348 ± 0	¹¹⁶ 457 ± 1	⁹⁷ 461 ± 0	⁸⁰ 466 ± 1	⁷¹ 476 ± 2	⁵⁹ 513 ± 10	²⁸⁸ 3080 ± 41	²⁸⁴ 3046 ± 56	
179	idemia-009	1066728	70572	³⁹⁷ 2702	⁶¹ 636 ± 0	³⁸⁹ 1207 ± 1	³⁵⁷ 1218 ± 1	³⁴³ 1222 ± 2	³¹² 1222 ± 3	²⁶⁸ 1280 ± 10	³⁴² 5664 ± 84	³⁴¹ 5597 ± 90	
180	iit-002	259579	52070	¹⁶² 731	²⁶³ 2048 ± 0	¹⁴³ 514 ± 1	¹²⁰ 531 ± 2	¹¹⁴ 547 ± 1	¹⁰¹ 583 ± 1	¹²⁸ 733 ± 2	¹³⁷ 1023 ± 7	¹³⁴ 1011 ± 66	
181	iit-003	261288	53791	¹⁸⁹ 817	¹⁰⁹ 2048 ± 0	¹³¹ 482 ± 0	¹⁰⁷ 493 ± 0	⁹⁸ 509 ± 0	⁹⁰ 541 ± 0	¹⁰⁷ 661 ± 0	²⁵ 324 ± 17	²⁸ 326 ± 8	
182	imds-software-001	373399	352623	¹⁷² 772	²⁶⁴ 2048 ± 0	¹²¹ 465 ± 1	²⁸² 958 ± 6	³¹⁷ 1131 ± 5	²⁸¹ 1134 ± 2	²²⁸ 1119 ± 10	³⁸⁴ 11885 ± 120	³⁸³ 11779 ± 174	
183	imperial-000	370120	10623	¹⁷⁹ 796	¹⁸⁷ 2048 ± 0	²¹⁷ 669 ± 1	¹⁸¹ 675 ± 3	¹⁶⁴ 683 ± 17	¹³⁶ 676 ± 2	¹¹³ 689 ± 2	²³⁸ 2130 ± 32	²³⁶ 2052 ± 100	
184	imperial-002	472327	16134	³⁵⁴ 1826	¹¹⁹ 2048 ± 0	¹⁶⁸ 569 ± 1	¹⁴⁴ 581 ± 15	¹²² 575 ± 5	⁹⁸ 576 ± 2	⁸² 588 ± 3	²⁵¹ 2278 ± 90	²⁴¹ 2131 ± 44	
185	incode-010	627808	21014	³⁹⁴ 2628	¹⁷⁷ 2048 ± 0	³⁸³ 1180 ± 2	³⁴⁷ 1178 ± 1	³³⁴ 1182 ± 1	²⁹⁹ 1184 ± 1	²⁵⁶ 1221 ± 1	¹⁵⁸ 1164 ± 32	¹⁵⁷ 1144 ± 32	
186	incode-011	477280	21781	³⁴² 1708	²⁶⁷ 2048 ± 0	²⁹² 872 ± 0	²⁴⁹ 875 ± 0	²²⁵ 881 ± 1	²⁰⁸ 892 ± 1	¹⁷⁸ 939 ± 0	¹⁵¹ 1117 ± 31	¹⁵² 1109 ± 37	
187	infocert-001	1204340	38972	³¹⁵ 1483	¹⁹³ 2048 ± 0	²⁹⁶ 874 ± 1	²⁵⁷ 891 ± 1	²⁹⁵ 1050 ± 5	³⁹⁰ 1473 ± 2	³⁹⁴ 3174 ± 8	³³¹ 5055 ± 108	³²⁹ 5008 ± 100	
188	innefulabs-000	370588	162172	⁷⁷ 439	¹⁴⁸ 2048 ± 0	³⁴⁴ 1006 ± 3	³⁰⁵ 1025 ± 3	²⁸⁹ 1030 ± 4	²⁵⁸ 1041 ± 2	²³¹ 1135 ± 3	³⁴⁴ 5782 ± 41	³⁴⁰ 5741 ± 45	
189	innovativetechnologyltd-001	177232	335757	⁵⁹ 341	¹⁵⁶ 2048 ± 0	¹⁰⁹ 433 ± 7	⁹¹ 446 ± 8	⁷¹ 439 ± 4	⁶² 452 ± 4	⁵⁶ 485 ± 7	²²² 1877 ± 42	²²⁶ 1924 ± 97	
190	innovativetechnologyltd-002	173939	372324	²¹¹ 912	¹²⁰ 2048 ± 0	²¹⁰ 661 ± 2	²⁰¹ 726 ± 4	²⁶⁰ 981 ± 27	²⁴³ 997 ± 40	¹³⁹ 766 ± 3	²¹⁶ 1841 ± 50	²²⁰ 1857 ± 59	
191	innovatrics-007	0	493269	³⁶³ 1937	⁸⁷ 1064 ± 0	⁴⁶⁰ 1485 ± 7	⁴²⁹ 1785 ± 184	⁴²⁸ 2078 ± 24	⁴¹⁴ 2123 ± 15	³⁶⁹ 2210 ± 42	³⁴⁹ 5978 ± 88	³⁴⁴ 5690 ± 102	
192	innovatrics-008	307323	59842	³⁰⁷ 1424	⁵³ 538 ± 0	²⁵⁴ 778 ± 6	²¹⁰ 767 ± 3	¹⁸⁹ 770 ± 3	¹⁷⁵ 803 ± 3	¹⁵⁸ 853 ± 10	²⁸³ 3021 ± 66	²⁶⁶ 2673 ± 88	
193	insightface-001	776777	16606	⁴²⁴ 3852	²⁵⁶ 2048 ± 0	⁴²⁵ 1366 ± 2	³⁹⁶ 1368 ± 3	³⁸⁶ 1372 ± 3	³⁶¹ 1375 ± 5	³⁰⁰ 1386 ± 4	¹⁵² 1119 ± 29	¹⁵¹ 1108 ± 34	
194	insightface-003	1016917	26668	³¹⁹ 1515	³⁰² 2048 ± 0	³⁵⁸ 1073 ± 0	³²⁰ 1092 ± 2	³⁰³ 1070 ± 1	²⁶⁹ 1082 ± 1	²²³ 1101 ± 1	⁶⁰ 597 ± 16	⁶⁴ 595 ± 17	
195	inspur-000	364844	91926	¹⁸³ 808	⁴¹³ 4096 ± 0	⁴²⁶ 1367 ± 1	³⁸⁹ 1331 ± 2	³⁸² 1368 ± 2	³⁸⁹ 1465 ± 1	³⁶⁵ 1861 ± 3	³⁷⁵ 9831 ± 37	³⁷⁴ 9860 ± 40	
196	intellicloudai-001	220831	868246	¹³⁶ 655	²²⁰ 2048 ± 0	¹²⁴ 468 ± 2	⁹⁴ 456 ± 1	⁷⁹ 466 ± 3	⁷⁷ 492 ± 1	⁹⁵ 632 ± 2	¹³⁸ 1056 ± 4	¹⁴³ 1051 ± 72	
197	intellicloudai-002	259047	58559	⁴²⁰ 3584	⁴³¹ 4100 ± 0	²⁸³ 847 ± 1	²³⁵ 847 ± 2	²¹¹ 849 ± 1	¹⁹² 853 ± 1	¹⁶⁷ 878 ± 4	¹¹⁷ 822 ± 28	¹¹⁶ 818 ± 23	
198	intellifusion-001	271872	289387	¹⁶⁹ 762	¹⁸³ 2048 ± 0	²⁴⁷ 764 ± 38	²¹² 774 ± 39	¹⁹⁴ 797 ± 42	¹⁷⁴ 803 ± 34	¹⁴⁵ 805 ± 33	¹⁵⁰ 1112 ± 28	¹⁵⁴ 1128 ± 41	
199	intellifusion-002	762731	385841	²¹⁸ 941	⁴²³ 4096 ± 0	³²¹ 950 ± 2	³²⁵ 1096 ± 42	³⁰⁵ 1088 ± 33	²⁹³ 1168 ± 31	²⁴² 1171 ± 10	¹⁹⁹ 1713 ± 57	¹⁹⁴ 1665 ± 87	
200	intellivision-003	64023	133748	¹⁸¹ 799	³⁵⁶ 2056 ± 0	⁹⁸ 407 ± 3	⁷⁴ 398 ± 2	⁶⁴ 418 ± 2	⁶¹ 450 ± 1	⁸⁴ 591 ± 4	³⁷⁸ 11069 ± 56	³⁷⁵ 11066 ± 75	
201	intellivision-004	117727	131310	⁹⁹ 515	³⁶⁶ 2056 ± 0	⁶⁹ 330 ± 0	⁵⁵ 330 ± 0	⁴² 347 ± 0	⁴⁴ 382 ± 0	⁶² 514 ± 0	³⁷⁹ 11197 ± 63	³⁷⁹ 11165 ± 72	
202	intellivision-001	256654	111858	¹⁹⁴ 842	²⁷⁴ 2048 ± 0	⁸⁵ 378 ± 1	⁶⁶ 379 ± 1	⁵⁰ 381 ± 1	⁴⁵ 384 ± 1	⁴⁴ 421 ± 3	¹⁴⁹ 1100 ± 16	¹⁵³ 1109 ± 22	
203	intellivix-002	361566	116162	²⁶⁷ 1172	²³⁸ 2048 ± 0	³²⁶ 956 ± 0	²⁷⁸ 947 ± 6	²⁶² 976 ± 0	²³⁷ 984 ± 4	²²¹ 1089 ± 1	⁴²¹ 30096 ± 128	⁴²³ 31287 ± 140	
204	intelresearch-004	646918	85290	³⁵⁷ 1856	¹⁴⁷ 2048 ± 0	⁴¹⁸ 1319 ± 2	³⁸³ 1322 ± 3	³⁷² 1330 ± 3	³⁵⁰ 1345 ± 3	³⁰⁹ 1411 ± 5	³²³ 4696 ± 63	³²¹ 4692 ± 66	
205	intelresearch-005	398137	85290	²⁶⁵ 1158	¹³⁰ 2048 ± 0	⁴²¹ 1328 ± 1	³⁹² 1334 ± 2	³⁷⁸ 1344 ± 2	³⁵³ 1356 ± 2	³¹² 1423 ± 4	³²¹ 4524 ± 87	³¹⁸ 4461 ± 74	
206	intemta-000	1532392	19488	²⁵¹ 1097	⁴⁴ 513 ± 0	³⁴⁵ 1010 ± 0	²⁹⁶ 1001 ± 4	²⁷⁴ 994 ± 0	²⁴¹ 993 ± 5	²⁰⁹ 1056 ± 1	¹²³ 910 ± 29	¹²⁴ 906 ± 32	
207	intsysmsu-001	384409	172480	¹⁷⁷ 789	¹⁵⁷ 2048 ± 0	¹⁸⁸ 614 ± 2	¹⁵⁹ 615 ± 2	¹⁵² 642 ± 2	¹⁶³ 750 ± 3	²³⁹ 1159 ± 4	⁷⁴ 621 ± 8	⁷² 611 ± 31	
208	intsysmsu-002	765921	172298	¹⁷⁶ 786	⁷² 1024 ± 0	¹⁸⁰ 593 ± 1	²¹⁸ 793 ± 2	²⁰³ 827 ± 1	¹⁹⁸ 875 ± 104	²⁷⁴ 1293 ± 3	⁵⁰ 549 ± 25	⁵³ 548 ± 29	
209	ionetworks-000	287609	51236	⁶² 351	²⁹³ 2048 ± 0	¹⁰⁸ 430 ± 0	⁸⁹ 435 ± 0	⁶⁹ 433 ± 0	⁴⁹ 432 ± 0	⁴⁹ 444 ± 0	³⁵⁸ 6913 ± 102	³⁶¹ 7150 ± 160	
210	iqface-000	268819	596337	¹⁵⁴ 704	⁴⁴³ 4750 ± 32	¹⁵⁰ 538 ± 26	¹⁰⁸ 494 ± 2	¹¹² 543 ± 3	¹⁶⁰ 734 ± 4	³⁰³ 1393 ± 4	⁴⁶⁰ 636433 ± 38446	⁴⁶⁰ 632654 ± 85615	
211	iqface-003	370803	963398	¹⁸⁷ 817	⁴⁴⁴ 4763 ± 37	¹⁴⁵ 529 ± 1	¹²² 532 ± 2	¹³² 599 ± 8	¹⁹¹ 850 ± 2	³⁵⁴ 1694 ± 2	⁴⁵⁹ 575924 ± 2601	⁴⁵⁹ 576653 ± 2051	
212	irex-000	741899	47419	³⁷³ 2086	³⁸⁸ 3080 ± 0	²⁸⁴ 852 ± 2	²³⁷ 850 ± 1	²²⁰ 874 ± 2	²²² 939 ± 1	²⁶¹ 1249 ± 5	¹¹ 201 ± 11	¹⁴ 208 ± 8	
213	isap-001	99049	204201	¹ 18	⁴¹⁴ 4096 ± 0	¹ 0 ± 0	-	-	-	-	⁴⁰ 459 ± 17	⁴² 456 ± 11	
214	isap-002	256765	49931	⁵³ 288	¹⁹¹ 2048 ± 0	²⁵¹ 769 ± 3	³⁰⁷ 1027 ± 2	²²³ 877 ± 2	¹⁶⁸ 761 ± 1	¹⁷³ 912 ± 2	²⁸⁶ 3045 ± 94	²⁸⁰ 2973 ± 66	
215	isityou-000	48010	36621	¹⁷ 110	⁴⁵⁸ 19200 ± 0	¹⁷ 113 ± 5	-	-	-	-	⁴⁵⁶ 237517 ± 1318	⁴⁵⁶ 237374 ± 1279	
216	isystems-001	274621	639268	²⁵⁰ 1091	³⁰³ 2048 ± 0	⁵⁷ 291 ± 9	-	-	-	-	⁵² 557 ± 16	⁵⁶ 564 ± 22	
217	isystems-002	358984	803389	³³⁰ 1595	²⁵⁹ 2048 ± 0	²⁷⁴ 822 ± 8	-	-	-	-	¹⁰⁶ 749 ± 31	⁸² 632 ± 28	
218	itmo-007	415979	245376	³⁸¹ 2199	¹⁷⁰ 2048 ± 0	²⁴² 741 ± 2	-	-	-	-	²⁶¹ 2551 ± 50	²⁶⁰ 2529 ± 80	
219	itmo-008	726866	318238	³⁰⁰ 1377	⁴¹⁹ 4096 ± 0	³⁵⁷ 1060 ± 1	³¹⁴ 1058 ± 1	²⁹⁸ 1059 ± 1	²⁶⁷ 1072 ± 4	²²⁵ 1104 ± 1	³⁰⁴ 3578 ± 25	³⁰⁴ 3580 ± 28	
220	ivacognitive-001	256958	62791	²²¹ 947	²¹⁰ 2048 ± 0	⁴¹² 1292 ± 3	³⁷⁷ 1289 ± 4	³⁶¹ 1292 ± 4	³³⁴ 1292 ± 3	²⁸¹ 1321 ± 4	³¹⁷ 4228 ± 41	³¹⁶ 4226 ± 41	

Notes

- 1 The configuration size does not capture static data included in libraries.
- 2 The library size is the combined total of all files provided in the submission lib folder. These libraries e.g. OpenCV may or may not be installed on any end user's platform natively and would not need to be installed with the algorithm. Some developers put neural network models in their libraries.
- 3 The memory usage is the peak resident set size reported by the ps system call during template generation.
- 4 The median template creation times are measured on Intel®Xeon®CPU E5-2630 v4 @ 2.20GHz processors.
- 5 The comparison durations, in nanoseconds, are estimated using std::chrono::high_resolution_clock which on the machine in (2) counts 1ns clock ticks. Precision is somewhat worse than that however. The ± value is the median absolute deviation times 1.48 for Normal consistency.

Table 12: Summary of algorithms and properties included in this report. The red superscripts give ranking for the quantity in that column.

	ALGORITHM	CONFIG	LIBRARY	TEMPLATE								COMPARISON ⁴			
				NAME		DATA		MEMORY		SIZE		GENERATION TIME (ms) ⁴			
				(KB) ¹	(KB) ²	(MB) ³	(B)	MUGSHOT	480x720	960x1440	1600x2400	3000x4500	GENUINE	IMPOSTOR	
221	iws-000	30875	3063	10 ⁷⁷	37 ^{512 ± 0}	49 ^{277 ± 5}	42 ^{283 ± 1}	91 ^{494 ± 3}	238 ^{984 ± 3}	391 ^{2987 ± 39}	131 ^{999 ± 40}	130 ^{992 ± 22}			
222	jaakit-001	99024	24754	45 ²⁵¹	36 ^{512 ± 0}	9 ^{76 ± 0}	7 ^{77 ± 0}	79 ^{0 ± 0}	6 ^{81 ± 0}	6 ^{93 ± 0}	256 ^{2466 ± 57}	257 ^{2465 ± 66}			
223	kakao-007	526993	129545	431 ³⁹⁵³	108 ^{2048 ± 0}	329 ^{952 ± 1}	284 ^{961 ± 1}	258 ^{958 ± 1}	230 ^{962 ± 1}	188 ^{968 ± 1}	139 ^{1056 ± 16}	141 ^{1047 ± 28}			
224	kakao-008	734583	104820	426 ³⁸⁷⁶	107 ^{2048 ± 0}	368 ^{1135 ± 3}	340 ^{1148 ± 3}	325 ^{1150 ± 3}	289 ^{1156 ± 1}	246 ^{1175 ± 1}	105 ^{736 ± 23}	101 ^{727 ± 22}			
225	kakaopay-001	397864	179869	146 ⁶⁸⁴	421 ^{4096 ± 0}	113 ^{448 ± 0}	126 ^{542 ± 0}	91 ^{542 ± 0}	72 ^{553 ± 0}	80 ^{633 ± 22}	79 ^{630 ± 22}				
226	kasikornlabs-000	256471	61000	150 ⁶⁹³	288 ^{2048 ± 0}	305 ^{908 ± 36}	252 ^{878 ± 22}	258 ^{969 ± 39}	300 ^{1184 ± 54}	375 ^{2382 ± 145}	423 ^{31669 ± 188}	424 ^{31714 ± 182}			
227	kasikornlabs-001	256471	61037	144 ⁶⁸¹	208 ^{2048 ± 0}	308 ^{912 ± 38}	245 ^{868 ± 10}	280 ^{1005 ± 50}	296 ^{1176 ± 44}	376 ^{2387 ± 147}	422 ^{30759 ± 198}	422 ^{30867 ± 174}			
228	kedacom-000	245292	37401	459 ²³⁵⁷⁴	11 ^{292 ± 0}	140 ^{506 ± 3}	131 ^{547 ± 10}	139 ^{614 ± 9}	104 ^{588 ± 10}	108 ^{605 ± 24}	88 ^{684 ± 14}	91 ^{682 ± 16}			
229	kiwitech-000	369711	21375	184 ⁸⁰⁸	173 ^{2048 ± 0}	178 ^{591 ± 0}	151 ^{594 ± 0}	131 ^{595 ± 1}	109 ^{596 ± 0}	90 ^{609 ± 0}	204 ^{1755 ± 20}	204 ^{1734 ± 16}			
230	kneron-003	58366	1747	38 ¹⁸⁸	174 ^{2048 ± 0}	53 ^{281 ± 3}	41 ^{280 ± 1}	37 ^{315 ± 13}	41 ^{365 ± 7}	258 ^{1224 ± 30}	334 ^{5237 ± 63}	333 ^{5274 ± 99}			
231	kneron-005	375374	13633	81 ⁴⁵⁷	166 ^{2048 ± 0}	144 ^{518 ± 2}	119 ^{522 ± 4}	116 ^{556 ± 5}	166 ^{757 ± 19}	361 ^{1760 ± 25}	226 ^{1922 ± 11}	227 ^{1926 ± 20}			
232	knowutech-000	808045	32886	290 ¹³⁰³	94 ^{1536 ± 0}	446 ^{1419 ± 2}	397 ^{1372 ± 1}	390 ^{1377 ± 1}	363 ^{1382 ± 2}	299 ^{1386 ± 2}	309 ^{3743 ± 31}	307 ^{3693 ± 38}			
233	kookmin-002	371771	30734	190 ⁸²⁷	276 ^{2048 ± 0}	353 ^{1038 ± 2}	313 ^{1047 ± 1}	293 ^{1045 ± 1}	263 ^{1061 ± 1}	226 ^{1116 ± 1}	83 ^{638 ± 19}	84 ^{636 ± 20}			
234	krungthai-002	2360957	15033	266 ¹¹⁷¹	180 ^{2048 ± 0}	64 ^{308 ± 0}	50 ^{314 ± 5}	33 ^{309 ± 0}	31 ^{319 ± 0}	31 ^{362 ± 0}	282 ^{3014 ± 20}	281 ^{2980 ± 22}			
235	kuke3d-001	403462	68786	105 ⁵³⁰	425 ^{4096 ± 0}	267 ^{814 ± 2}	223 ^{811 ± 2}	190 ^{814 ± 2}	178 ^{814 ± 1}	156 ^{834 ± 1}	353 ^{6412 ± 57}	353 ^{6413 ± 51}			
236	kuke3d-002	270544	1227855	185 ⁸⁰⁹	322 ^{2048 ± 0}	139 ^{504 ± 3}	116 ^{504 ± 1}	99 ^{511 ± 1}	86 ^{523 ± 2}	81 ^{585 ± 1}	278 ^{2943 ± 22}	279 ^{2966 ± 38}			
237	lebtech-000	0	10360	18 ¹¹⁰	21 ^{512 ± 0}	32 ^{22 ± 0}	12 ^{22 ± 0}	12 ^{22 ± 0}	13 ^{23 ± 0}	13 ^{23 ± 0}	115 ^{801 ± 42}	117 ^{825 ± 51}			
238	lemalabs-001	748400	198794	401 ²⁷³⁸	113 ^{2048 ± 0}	269 ^{810 ± 0}	224 ^{812 ± 0}	198 ^{813 ± 0}	180 ^{819 ± 0}	15 ^{844 ± 1}	385 ^{11930 ± 35}	385 ^{11913 ± 37}			
239	lineclova-001	944355	407058	383 ²³⁷³	203 ^{2048 ± 0}	278 ^{833 ± 10}	231 ^{830 ± 3}	208 ^{828 ± 4}	186 ^{838 ± 8}	154 ^{833 ± 4}	265 ^{2696 ± 23}	267 ^{2677 ± 35}			
240	lineclova-002	475779	406756	294 ¹³⁵³	185 ^{2048 ± 0}	409 ^{1284 ± 1}	373 ^{1275 ± 2}	357 ^{1275 ± 1}	328 ^{1273 ± 2}	269 ^{1281 ± 2}	269 ^{2765 ± 10}	269 ^{2767 ± 31}			
241	lookman-002	138200	25410	457 ¹⁶⁵¹⁸	57 ^{548 ± 0}	25 ^{173 ± 1}	-	-	-	-	69 ^{610 ± 19}	74 ^{612 ± 22}			
242	lookman-004	244775	37401	458 ²³⁵⁴⁸	58 ^{548 ± 0}	141 ^{507 ± 5}	129 ^{545 ± 12}	138 ^{613 ± 12}	106 ^{590 ± 11}	104 ^{656 ± 16}	121 ^{871 ± 29}	121 ^{878 ± 29}			
243	luxand-000	0	57908	297 ¹³⁶⁶	84 ^{1040 ± 0}	97 ^{407 ± 23}	87 ^{433 ± 11}	74 ^{444 ± 14}	66 ^{464 ± 14}	77 ^{562 ± 25}	118 ^{828 ± 28}	118 ^{828 ± 32}			
244	mantra-000	471458	62566	16 ⁷⁴⁹	328 ^{2052 ± 0}	101 ^{413 ± 18}	106 ^{487 ± 19}	92 ^{494 ± 18}	82 ^{511 ± 18}	86 ^{598 ± 19}	290 ^{3151 ± 51}	289 ^{3127 ± 63}			
245	maxvision-001	256146	61793	409 ²⁸⁸⁰	120 ^{2048 ± 0}	48 ^{275 ± 3}	39 ^{274 ± 2}	29 ^{277 ± 4}	28 ^{280 ± 4}	24 ^{325 ± 3}	97 ^{714 ± 13}	99 ^{717 ± 13}			
246	maxvision-002	171894	60623	358 ¹⁸⁶³	233 ^{2048 ± 0}	24 ^{172 ± 0}	18 ^{171 ± 0}	15 ^{172 ± 0}	12 ^{174 ± 0}	14 ^{221 ± 0}	100 ^{725 ± 5}	100 ^{725 ± 5}			
247	megvii-005	1378009	44038	433 ⁴⁰³⁶	324 ^{2049 ± 0}	417 ^{1319 ± 5}	365 ^{1247 ± 6}	346 ^{1240 ± 2}	319 ^{1245 ± 2}	276 ^{1298 ± 3}	427 ^{32025 ± 121}	428 ^{32008 ± 114}			
248	megvii-006	1554938	44038	436 ⁴³⁵⁴	323 ^{2049 ± 0}	410 ^{1287 ± 3}	375 ^{1286 ± 0}	397 ^{1393 ± 5}	342 ^{1319 ± 1}	292 ^{1360 ± 1}	423 ^{31845 ± 100}	426 ^{31872 ± 118}			
249	meituan-001	615387	333249	254 ¹¹⁰⁶	150 ^{2048 ± 0}	347 ^{1017 ± 4}	300 ^{1008 ± 3}	282 ^{1010 ± 2}	251 ^{1010 ± 3}	198 ^{1011 ± 4}	85 ^{654 ± 10}	88 ^{658 ± 14}			
250	meituan-002	686111	244091	379 ²¹⁹¹	398 ^{4096 ± 0}	356 ^{1052 ± 0}	318 ^{1086 ± 1}	301 ^{1064 ± 2}	262 ^{1060 ± 5}	216 ^{1063 ± 1}	140 ^{1064 ± 10}	144 ^{1070 ± 16}			
251	meiya-001	280055	264913	95 ⁵⁰⁷	326 ^{2049 ± 0}	192 ^{622 ± 12}	-	-	-	-	365 ^{8356 ± 615}	365 ^{8134 ± 97}			
252	mendaxiatech-000	1941475	45484	418 ³¹⁹⁵	429 ^{4097 ± 0}	398 ^{1243 ± 2}	367 ^{1255 ± 1}	388 ^{1373 ± 2}	401 ^{1598 ± 3}	384 ^{2689 ± 8}	437 ^{46906 ± 275}	437 ^{46872 ± 217}			
253	metsakuurcompany-001	445177	1091558	325 ¹⁵⁷²	360 ^{2056 ± 0}	168 ^{578 ± 1}	147 ^{587 ± 3}	127 ^{590 ± 1}	131 ^{659 ± 1}	159 ^{854 ± 1}	366 ^{8600 ± 192}	366 ^{8155 ± 298}			
254	metsakuurcompany-002	0	957558	228 ⁹⁸³	361 ^{2056 ± 0}	334 ^{980 ± 1}	290 ^{978 ± 1}	263 ^{976 ± 2}	248 ^{1005 ± 1}	224 ^{1103 ± 2}	368 ^{8766 ± 326}	368 ^{8786 ± 324}			
255	microfocus-001	104524	27242	39 ¹⁹⁰	3 ^{256 ± 0}	45 ^{264 ± 18}	-	-	-	-	16 ^{215 ± 8}	17 ^{217 ± 10}			
256	microfocus-002	96288	27362	35 ¹⁷⁶	4 ^{256 ± 0}	43 ^{259 ± 18}	-	-	-	-	27 ^{337 ± 34}	18 ^{230 ± 25}			
257	minivision-000	836697	16597	432 ⁴⁰¹³	413 ^{4096 ± 0}	352 ^{1035 ± 1}	309 ^{1033 ± 2}	290 ^{1035 ± 1}	257 ^{1037 ± 1}	213 ^{1059 ± 2}	257 ^{2466 ± 26}	255 ^{2460 ± 25}			
258	mobai-000	365451	80573	175 ⁷⁸⁶	447 ^{6144 ± 0}	249 ^{766 ± 8}	240 ^{869 ± 6}	341 ^{1205 ± 31}	411 ^{1867 ± 45}	399 ^{3549 ± 190}	401 ^{16458 ± 333}	401 ^{16423 ± 1473}			
259	mobai-001	265297	60164	106 ⁵³⁴	143 ^{2048 ± 0}	186 ^{612 ± 3}	157 ^{614 ± 3}	167 ^{687 ± 9}	204 ^{886 ± 31}	355 ^{1707 ± 103}	171 ^{1386 ± 25}	177 ^{1377 ± 26}			
260	mobb1l-001	231160	58706	41 ²²³	283 ^{2048 ± 0}	29 ^{183 ± 32}	22 ^{184 ± 25}	45 ^{354 ± 76}	182 ^{823 ± 396}	387 ^{2781 ± 1166}	383 ^{11832 ± 109}	384 ^{11851 ± 88}			
261	mobb1l-003	172248	60960	50 ²⁷⁰	146 ^{2048 ± 0}	215 ^{664 ± 6}	175 ^{661 ± 5}	157 ^{663 ± 5}	133 ^{665 ± 6}	114 ^{691 ± 5}	388 ^{12506 ± 111}	389 ^{12509 ± 100}			
262	mobilpintech-000	370514	303291	257 ¹¹³⁰	308 ^{2048 ± 0}	399 ^{1245 ± 1}	360 ^{1234 ± 1}	353 ^{1264 ± 1}	357 ^{1360 ± 1}	356 ^{1707 ± 1}	394 ^{14506 ± 214}	394 ^{14433 ± 197}			
263	moreidian-000	525259	21374	217 ⁹³²	285 ^{2048 ± 0}	232 ^{694 ± 0}	191 ^{698 ± 0}	173 ^{699 ± 0}	146 ^{700 ± 0}	123 ^{713 ± 1}	212 ^{1803 ± 11}	209 ^{1779 ± 23}			
264	mukh-001	866223	451194	335 ¹⁶³⁷	76 ^{1024 ± 0}	427 ^{1375 ± 17}	402 ^{1390 ± 12}	404 ^{1406 ± 8}	368 ^{1394 ± 10}	293 ^{1360 ± 11}	38 ^{433 ± 14}	40 ^{435 ± 14}			

Notes

- 1 The configuration size does not capture static data included in libraries.
- 2 The library size is the combined total of all files provided in the submission lib folder. These libraries e.g. OpenCV may or may not be installed on any end user's platform natively and would not need to be installed with the algorithm. Some developers put neural network models in their libraries.
- 3 The memory usage is the peak resident set size reported by the ps system call during template generation.
- 4 The median template creation times are measured on Intel®Xeon®CPU E5-2630 v4 @ 2.20GHz processors.
- 5 The comparison durations, in nanoseconds, are estimated using std::chrono::high_resolution_clock which on the machine in (2) counts 1ns clock ticks. Precision is somewhat worse than that however. The ± value is the median absolute deviation times 1.48 for Normal consistency.

Table 13: Summary of algorithms and properties included in this report. The red superscripts give ranking for the quantity in that column.

	ALGORITHM	CONFIG	LIBRARY	TEMPLATE								COMPARISON ⁴			
				NAME		DATA		MEMORY		SIZE		GENERATION TIME (ms) ⁴			
				(KB) ¹	(KB) ²	(MB) ³	(B)	MUGSHOT	480x720	960x1440	1600x2400	3000x4500	GENUINE	IMPOSTOR	
265	multimodality-000	0	503924	³⁰⁶ 1417	²²⁷ 2048 ± 0	¹⁰² 416 ± 0	⁸³ 420 ± 0	⁶⁵ 423 ± 0	⁵⁸ 427 ± 0	⁵¹ 463 ± 0	¹¹⁹ 848 ± 25	¹¹⁴ 800 ± 28			
266	multimodality-001	185719	545045	³⁰² 1388	⁴⁰⁶ 4096 ± 0	³⁸⁷ 1190 ± 2	³⁴⁴ 1169 ± 2	³²⁹ 1165 ± 2	²⁹² 1167 ± 2	²⁴⁸ 1177 ± 2	¹⁷⁸ 1424 ± 35	¹⁷⁴ 1384 ± 42			
267	mvision-001	227502	149531	¹⁵⁹ 723	³⁰ 512 ± 0	²³¹ 691 ± 21	¹⁹³ 702 ± 19	¹⁷² 697 ± 24	¹⁶⁰ 708 ± 29	¹²¹ 710 ± 27	¹⁵³ 1123 ± 40	¹⁵⁸ 1154 ± 38			
268	nazhiai-000	547484	16141	³⁹⁸ 2716	¹⁹⁸ 2048 ± 0	²²³ 683 ± 3	¹⁸⁶ 687 ± 2	²⁰⁸ 835 ± 27	¹⁸⁹ 840 ± 31	¹⁵⁵ 834 ± 34	²⁴⁸ 2230 ± 34	²⁴² 2133 ± 81			
269	neosystems-004	243546	352623	¹⁰⁴ 529	¹⁴⁴ 2048 ± 0	⁶⁸ 324 ± 0	¹⁹⁰ 711 ± 3	²⁰⁴ 827 ± 7	¹⁹³ 854 ± 2	¹⁷⁴ 916 ± 2	³⁹³ 14437 ± 176	³⁹³ 14355 ± 173			
270	neosystems-005	373632	352627	¹⁹¹ 834	¹¹⁷ 2048 ± 0	¹²⁸ 479 ± 2	²⁸³ 958 ± 6	³¹⁰ 1108 ± 5	²⁷¹ 1098 ± 5	²³⁸ 1158 ± 4	³⁸¹ 11571 ± 152	³⁸⁰ 11410 ± 163			
271	netbridgetech-001	133108	205875	⁹⁶ 508	³⁹⁶ 4096 ± 0	¹¹ 85 ± 1	⁹ 83 ± 0	⁸ 84 ± 0	⁸ 92 ± 0	⁸ 113 ± 4	³⁷⁰ 9280 ± 74	³⁷⁰ 9446 ± 512			
272	netbridgetech-002	257687	49931	⁵⁴ 299	²⁰⁶ 2048 ± 0	²⁷⁹ 838 ± 6	²³³ 838 ± 2	²⁰⁹ 839 ± 1	¹⁸⁸ 839 ± 3	¹⁶⁰ 859 ± 3	²⁷⁶ 2893 ± 65	²⁸⁵ 3050 ± 123			
273	neurotechnology-013	474749	85552	⁴¹⁰ 2894	⁴⁶ 514 ± 0	³⁴⁰ 1000 ± 1	²⁹⁸ 1006 ± 2	²⁸⁴ 1022 ± 2	²⁶⁰ 1053 ± 2	²⁴⁹ 1195 ± 8	² 109 ± 4	¹ 110 ± 4			
274	neurotechnology-015	474782	86045	³⁹¹ 2564	⁴⁷ 515 ± 0	³⁵⁰ 1028 ± 3	³¹⁰ 1033 ± 3	²⁹⁷ 1055 ± 4	²⁷⁰ 1097 ± 4	²⁷⁷ 1304 ± 18	⁴ 130 ± 2	⁴ 130 ± 4			
275	nhn-002	363471	817674	¹⁴⁰ 667	⁴¹² 4096 ± 0	³⁷¹ 1141 ± 3	³³⁵ 1138 ± 2	³²¹ 1141 ± 2	²⁸⁸ 1151 ± 6	²⁵³ 1203 ± 2	⁴⁴³ 56608 ± 579	⁴⁴⁴ 56549 ± 606			
276	nhn-003	933665	432730	³¹³ 1464	⁴¹⁶ 4096 ± 0	³⁹⁴ 1229 ± 2	³⁶⁸ 1261 ± 1	³⁵² 1263 ± 3	³³² 1279 ± 2	²⁹⁶ 1375 ± 3	⁴⁴⁰ 50560 ± 105	⁴⁴⁰ 50592 ± 142			
277	nodeflux-002	774668	690213	⁸⁴ 466	²⁰¹ 2048 ± 0	²³⁸ 708 ± 4	¹⁹⁵ 709 ± 4	¹⁷⁹ 716 ± 5	¹⁵⁶ 716 ± 7	¹²⁹ 736 ± 3	³⁰⁰ 3475 ± 62	²⁹⁷ 3408 ± 143			
278	notiontag-001	92753	427967	¹¹⁴ 566	⁶⁰ 584 ± 0	³¹⁵ 929 ± 35	³²¹ 1092 ± 39	⁴²⁹ 3709 ± 81	⁴²⁹ 10233 ± 180	-	⁴³⁴ 43636 ± 286	⁴³⁴ 43724 ± 330			
279	notiontag-002	271987	967207	⁴⁰⁷ 2840	³⁸² 2120 ± 0	¹¹⁷ 453 ± 2	⁹³ 453 ± 3	⁷⁵ 453 ± 3	⁶³ 458 ± 2	⁵² 471 ± 3	⁴⁰⁹ 20278 ± 194	⁴⁰⁹ 20195 ± 186			
280	nsensemcorp-003	199895	117041	¹⁵⁷ 710	¹³¹ 2048 ± 0	²¹¹ 661 ± 0	¹⁷⁶ 664 ± 0	¹⁵⁶ 662 ± 1	¹³² 659 ± 1	¹⁰⁶ 659 ± 0	⁴³⁵ 44658 ± 51	⁴³⁶ 44654 ± 72			
281	nsensemcorp-004	513276	139178	³³⁶ 1663	³¹¹ 2048 ± 0	⁴⁴⁷ 1433 ± 0	⁴¹⁷ 1445 ± 7	⁴¹³ 1450 ± 3	³⁹⁴ 1487 ± 5	-	²⁵⁴ 2388 ± 42	²⁵⁴ 2385 ± 63			
282	ntechlab-011	786933	209458	⁴⁴⁹ 6867	⁹¹ 1280 ± 0	³⁷⁵ 1148 ± 2	³³⁶ 1142 ± 1	³²⁷ 1159 ± 1	³⁰³ 1185 ± 1	²⁷² 1290 ± 3	⁷ 179 ± 11	⁸ 173 ± 11			
283	ntechlab-012	570796	212350	⁴⁴³ 5451	³⁸³ 2560 ± 0	⁴¹⁶ 1309 ± 1	³⁸⁶ 1323 ± 1	³⁷³ 1331 ± 1	³⁵⁸ 1360 ± 1	³²² 1460 ± 3	¹⁵ 211 ± 8	¹⁶ 211 ± 7			
284	omface-000	459459	844976	²⁹ 150	⁷⁵ 1024 ± 0	³¹ 185 ± 1	²⁶ 206 ± 2	²¹ 203 ± 1	¹⁵ 195 ± 1	¹³ 193 ± 1	⁴⁵ 481 ± 42	⁴³ 456 ± 20			
285	omface-001	146370	1799745	²⁶ 145	⁶⁶ 1024 ± 0	³³ 194 ± 2	²⁸ 222 ± 2	²² 209 ± 0	¹⁸ 216 ± 1	¹⁶ 233 ± 1	⁴⁰³ 18369 ± 19	⁴⁰³ 18366 ± 32			
286	omnigarde-001	200523	32882	⁸³ 464	³⁶ 512 ± 0	³¹⁷ 941 ± 0	²⁵⁵ 883 ± 1	²²⁶ 886 ± 1	²⁰⁷ 891 ± 1	¹⁶⁹ 898 ± 0	¹⁷⁶ 1405 ± 31	¹⁷³ 1379 ± 26			
287	omnigarde-002	368860	32882	¹⁶⁸ 757	⁶⁴ 1024 ± 0	⁴¹³ 1303 ± 1	³⁶⁴ 1246 ± 1	³⁵⁰ 1249 ± 1	³²¹ 1253 ± 1	²⁶⁴ 1261 ± 1	²⁶⁸ 2727 ± 34	²⁶⁸ 2686 ± 32			
288	openface-001	0	40111	¹⁶ 100	²¹⁴ 2048 ± 0	²¹ 148 ± 1	¹⁵ 154 ± 0	⁴⁷ 365 ± 3	⁵⁵ 409 ± 9	⁹² 616 ± 31	⁶⁷ 608 ± 14	⁷¹ 604 ± 13			
289	oz-003	484147	519652	⁴⁵⁶ 11949	³⁴⁸ 2053 ± 0	⁴²⁸ 1375 ± 12	⁴⁰¹ 1388 ± 3	⁴²⁷ 1773 ± 16	⁴¹³ 2039 ± 6	³⁹⁵ 3209 ± 5	⁴⁵² 73905 ± 456	⁴⁵² 73892 ± 444			
290	oz-004	373982	1075452	⁴⁵³ 8071	³⁴⁷ 2053 ± 0	²⁷⁷ 832 ± 7	²⁴⁷ 871 ± 6	²²⁸ 899 ± 10	²⁶⁸ 1078 ± 12	³⁴⁸ 1608 ± 10	⁴⁴⁶ 61654 ± 418	⁴⁴⁶ 61749 ± 450			
291	palit-000	428754	144958	²⁹⁶ 1355	⁴⁰⁷ 4096 ± 0	¹⁶⁷ 570 ± 1	¹⁴¹ 578 ± 1	¹²³ 576 ± 3	¹⁰⁰ 583 ± 1	⁹¹ 614 ± 1	²⁴⁷ 2227 ± 16	²⁴⁹ 2226 ± 16			
292	palit-001	173886	145564	¹¹⁸ 583	¹⁴² 2048 ± 0	³⁹ 227 ± 0	³⁰ 224 ± 1	²⁴ 224 ± 1	²³ 229 ± 3	²⁰ 262 ± 2	¹⁵⁴ 1150 ± 16	¹⁵⁵ 1135 ± 23			
293	pangiam-000	464252	24512	⁴³⁰ 3919	¹⁶⁹ 2048 ± 0	¹⁹⁵ 627 ± 5	¹⁶¹ 618 ± 4	¹⁴⁰ 615 ± 3	¹¹⁶ 620 ± 3	¹⁰¹ 639 ± 3	³ 118 ± 7	³ 113 ± 7			
294	papago-001	669274	52817	³⁸² 2341	¹³⁵ 2048 ± 0	⁴⁰⁶ 1272 ± 6	³⁷⁹ 1296 ± 7	³⁶⁵ 1295 ± 6	³³³ 1281 ± 3	²⁸⁷ 1345 ± 3	³⁹⁸ 15236 ± 169	³⁹⁸ 15184 ± 142			
295	papsav1923-001	279210	52652	⁸⁶ 473	²⁶² 2048 ± 0	¹⁹⁴ 626 ± 1	¹⁶⁴ 628 ± 1	¹⁴³ 630 ± 1	¹²⁷ 648 ± 2	¹³³ 744 ± 3	¹⁰¹ 725 ± 25	¹⁰³ 731 ± 28			
296	papsav1923-002	491185	24727	²⁵⁹ 1136	³⁴³ 2052 ± 0	²⁶⁰ 792 ± 1	²⁸⁹ 978 ± 1	²⁹² 1042 ± 1	²⁹⁰ 1158 ± 1	³⁵² 1641 ± 19	¹⁶⁰ 1209 ± 29	¹⁶² 1206 ± 38			
297	paravision-008	542190	204400	³¹¹ 1448	⁴⁰⁹ 4096 ± 0	²³⁵ 699 ± 0	¹⁹² 700 ± 0	¹⁷⁴ 701 ± 0	¹⁴⁷ 702 ± 1	¹¹⁸ 702 ± 0	²⁸ 337 ± 17	³⁰ 330 ± 13			
298	paravision-010	688291	205854	³⁷⁶ 2150	⁴³⁴ 4100 ± 0	¹⁹⁹ 634 ± 0	¹⁶⁹ 635 ± 0	¹⁴⁷ 635 ± 0	¹²² 635 ± 0	⁹⁹ 635 ± 1	¹⁸⁹ 1577 ± 35	¹⁸⁹ 1571 ± 32			
299	pensees-001	1619431	408932	³⁶¹ 1922	⁴⁵⁴ 8200 ± 0	³⁶⁴ 1108 ± 3	⁴¹⁸ 1448 ± 17	⁴⁰⁹ 1439 ± 10	³⁸⁸ 1464 ± 5	³⁴¹ 1546 ± 9	²⁹¹ 3151 ± 34	²⁹⁰ 3143 ± 25			
300	pixelall-008	0	992249	³⁴⁹ 1741	⁴⁵³ 8192 ± 0	⁴⁵⁴ 1471 ± 3	⁴¹² 1405 ± 4	⁴⁰⁵ 1409 ± 4	³⁷⁸ 1413 ± 3	³¹⁴ 1426 ± 4	²¹⁰ 1799 ± 50	²¹⁴ 1807 ± 48			
301	pixelall-009	0	100914	³⁴⁵ 1731	⁴⁵² 8192 ± 0	⁴⁵⁹ 1484 ± 3	⁴⁰⁸ 1395 ± 3	⁴⁰¹ 1400 ± 4	³⁶⁶ 1391 ± 3	³¹⁶ 1433 ± 3	²¹⁸ 1848 ± 13	²¹⁷ 1842 ± 19			
302	psl-010	411027	591157	⁴⁴² 5361	⁴³⁹ 4168 ± 0	⁴⁴² 1403 ± 9	⁴⁰⁶ 1393 ± 3	³⁹⁴ 1392 ± 3	³⁶⁹ 1395 ± 3	³⁰⁵ 1396 ± 3	³⁰ 354 ± 53	²⁹ 329 ± 29			
303	psl-011	814579	606050	⁴³⁹ 4984	⁴⁵⁵ 8248 ± 0	⁴²⁰ 1324 ± 2	³⁸⁷ 1323 ± 8	³⁷¹ 1326 ± 8	³⁴⁴ 1324 ± 8	²⁸² 1322 ± 4	¹⁹⁶ 1680 ± 37	¹⁹⁷ 1688 ± 40			
304	ptakuratsatu-000	0	585434	²⁹³ 1347	⁵⁴ 538 ± 0	²⁹ 875 ± 3	²⁴² 863 ± 48	²⁴⁴ 928 ± 9	²²⁹ 958 ± 17	²¹⁸ 1066 ± 26	³⁴⁷ 5900 ± 103	³⁴³ 5687 ± 167			
305	pxl-001	110116	78231	³¹ 168	³¹ 512 ± 0	¹⁴ 101 ± 5	¹¹ 104 ± 5	¹⁹ 189 ± 12	⁵⁴ 408 ± 27	³²⁵ 1470 ± 144	³⁴⁰ 5598 ± 45	³⁴⁰ 5590 ± 68			
306	pyramid-000	372608	219883	¹⁸¹ 804	³⁷⁰ 2056 ± 0	¹⁷¹ 583 ± 2	-	-	-	-	³⁶¹ 7147 ± 59	³⁶³ 7586 ± 425			
307	qazbs-000	362015	805258	¹⁹⁹ 856	²⁷² 2048 ± 0	⁴¹⁵ 1307 ± 1	³⁶³ 1243 ± 0	³⁴⁹ 1248 ± 9	³²² 1253 ± 1	²⁶⁶ 1270 ± 0	³³² 5181 ± 62	³³¹ 5167 ± 93			
308	qnap-001	196210	13399	⁵² 286	²⁵⁸ 2048 ± 0	¹⁸⁷ 614 ± 1	¹⁵⁸ 615 ± 1	¹⁴² 627 ± 1	¹¹⁹ 623 ± 1	⁹⁷ 634 ± 2	⁸⁴ 649 ± 11	⁸⁶ 648 ± 14			

Notes

- 1 The configuration size does not capture static data included in libraries.
- 2 The library size is the combined total of all files provided in the submission lib folder. These libraries e.g. OpenCV may or may not be installed on any end user's platform natively and would not need to be installed with the algorithm. Some developers put neural network models in their libraries.
- 3 The memory usage is the peak resident set size reported by the ps system call during template generation.
- 4 The median template creation times are measured on Intel®Xeon®CPU E5-2630 v4 @ 2.20GHz processors.
- 5 The comparison durations, in nanoseconds, are estimated using std::chrono::high_resolution_clock which on the machine in (2) counts 1ns clock ticks. Precision is somewhat worse than that however. The ± value is the median absolute deviation times 1.48 for Normal consistency.

Table 14: Summary of algorithms and properties included in this report. The red superscripts give ranking for the quantity in that column.

	ALGORITHM	CONFIG	LIBRARY	TEMPLATE								COMPARISON ⁴	
	NAME	DATA	DATA	MEMORY	SIZE	MUGSHOT	480x720	960x1440	1600x2400	3000x4500	GENUINE	IMPOSTOR	TIME (ns) ⁵
		(KB) ¹	(KB) ²	(MB) ³	(B)	MUGSHOT	480x720	960x1440	1600x2400	3000x4500	GENUINE	IMPOSTOR	
309	qnap-002	346963	33284	152 ⁷⁰⁰	2048 ± 0	273 ^{821 ± 1}	227 ^{824 ± 1}	202 ^{824 ± 1}	184 ^{826 ± 1}	153 ^{832 ± 1}	21 ^{293 ± 13}	22 ^{287 ± 17}	
310	quantasoft-003	370518	211354	241 ¹⁰⁵⁸	2048 ± 0	198 ^{632 ± 2}	168 ^{634 ± 0}	144 ^{632 ± 0}	121 ^{631 ± 1}	96 ^{634 ± 0}	12 ^{201 ± 7}	12 ^{203 ± 8}	
311	rankone-012	0	264182	23 ¹³⁴	5 ^{261 ± 0}	160 ^{564 ± 3}	132 ^{554 ± 1}	118 ^{564 ± 1}	102 ^{586 ± 1}	116 ^{695 ± 1}	20 ^{273 ± 17}	19 ^{231 ± 14}	
312	rankone-013	0	228729	28 ¹⁴⁹	6 ^{261 ± 0}	229 ^{690 ± 5}	179 ^{672 ± 1}	177 ^{712 ± 1}	171 ^{780 ± 1}	227 ^{1118 ± 3}	32 ^{356 ± 23}	25 ^{304 ± 23}	
313	realnetworks-006	466225	56771	328 ¹⁵⁸⁸	35 ^{2056 ± 0}	202 ^{638 ± 4}	165 ^{630 ± 3}	160 ^{672 ± 5}	149 ^{706 ± 5}	140 ^{774 ± 5}	41 ^{469 ± 19}	48 ^{478 ± 25}	
314	realnetworks-007	570797	101527	416 ³¹³⁷	36 ^{2056 ± 0}	423 ^{1348 ± 2}	395 ^{1358 ± 11}	384 ^{1363 ± 10}	364 ^{1386 ± 9}	335 ^{1517 ± 6}	53 ^{559 ± 31}	52 ^{539 ± 35}	
315	regula-000	262444	29384	129 ⁶¹⁰	316 ^{2048 ± 0}	386 ^{1187 ± 1}	331 ^{1126 ± 1}	316 ^{1129 ± 0}	279 ^{1132 ± 1}	240 ^{1159 ± 1}	49 ^{491 ± 16}	50 ^{500 ± 22}	
316	regula-001	256075	25980	225 ⁹⁷⁶	287 ^{2048 ± 0}	408 ^{1284 ± 1}	358 ^{1220 ± 1}	344 ^{1222 ± 1}	315 ^{1226 ± 1}	262 ^{1255 ± 1}	33 ^{361 ± 10}	32 ^{342 ± 25}	
317	remarkai-001	241857	868314	161 ⁷³⁰	346 ^{2052 ± 0}	276 ^{831 ± 6}	236 ^{849 ± 18}	296 ^{1055 ± 25}	307 ^{1198 ± 34}	330 ^{1519 ± 38}	163 ^{1229 ± 20}	115 ^{805 ± 56}	
318	remarkai-003	280516	58559	428 ³⁸⁹⁶	43 ^{2100 ± 0}	337 ^{986 ± 1}	292 ^{993 ± 1}	272 ^{992 ± 1}	244 ^{999 ± 3}	199 ^{1019 ± 2}	113 ^{787 ± 20}	112 ^{793 ± 22}	
319	rendip-000	0	437653	145 ⁶⁸²	296 ^{2048 ± 0}	119 ^{464 ± 2}	95 ^{458 ± 0}	84 ^{473 ± 0}	72 ^{483 ± 1}	76 ^{556 ± 4}	55 ^{576 ± 13}	57 ^{573 ± 11}	
320	revealmedia-005	293933	202465	171 ⁷⁶³	433 ^{4100 ± 0}	107 ^{428 ± 0}	85 ^{428 ± 0}	68 ^{430 ± 0}	60 ^{433 ± 0}	48 ^{442 ± 0}	234 ^{2023 ± 38}	234 ^{2009 ± 26}	
321	revealmedia-006	293933	200912	166 ⁷⁴¹	339 ^{2052 ± 0}	87 ^{381 ± 0}	67 ^{381 ± 0}	51 ^{382 ± 0}	46 ^{384 ± 0}	38 ^{394 ± 0}	77 ^{626 ± 35}	68 ^{600 ± 2}	
322	rokid-000	258612	396624	274 ¹²¹⁸	362 ^{2056 ± 0}	153 ^{546 ± 3}	127 ^{542 ± 2}	113 ^{545 ± 1}	85 ^{522 ± 3}	78 ^{563 ± 4}	299 ^{3457 ± 62}	300 ^{3463 ± 77}	
323	rokid-001	641223	413733	244 ¹⁰⁷¹	374 ^{2060 ± 0}	307 ^{911 ± 2}	262 ^{901 ± 5}	229 ^{899 ± 2}	211 ^{900 ± 3}	170 ^{901 ± 3}	293 ^{3345 ± 50}	294 ^{3346 ± 149}	
324	s1-005	482369	95685	262 ¹¹³⁷	317 ^{2048 ± 0}	341 ^{1001 ± 0}	297 ^{1002 ± 0}	279 ^{1004 ± 0}	249 ^{1008 ± 0}	201 ^{1029 ± 2}	78 ^{626 ± 74}	59 ^{589 ± 14}	
325	s1-006	482372	95681	261 ¹¹³⁷	249 ^{2048 ± 0}	323 ^{951 ± 0}	281 ^{956 ± 0}	254 ^{957 ± 0}	231 ^{962 ± 0}	192 ^{983 ± 0}	92 ^{696 ± 23}	95 ^{696 ± 29}	
326	saffe-001	85973	62488	33 ¹⁶⁸	92 ^{1280 ± 0}	52 ^{281 ± 1}	-	-	-	-	164 ^{1274 ± 19}	166 ^{1277 ± 26}	
327	saffe-002	260622	28285	198 ⁸⁵⁵	106 ^{2048 ± 0}	268 ^{817 ± 11}	222 ^{805 ± 15}	197 ^{809 ± 19}	179 ^{815 ± 29}	148 ^{813 ± 23}	98 ^{717 ± 7}	98 ^{714 ± 29}	
328	samsungsds-001	1189592	147444	427 ³⁸⁹³	40 ^{4096 ± 0}	370 ^{1140 ± 3}	338 ^{1145 ± 4}	379 ^{1344 ± 5}	360 ^{1366 ± 5}	334 ^{1514 ± 7}	441 ^{51559 ± 773}	441 ^{51721 ± 1003}	
329	samsungsds-002	1040732	147475	385 ²⁴³¹	358 ^{2056 ± 0}	367 ^{1118 ± 1}	345 ^{1175 ± 12}	387 ^{1372 ± 6}	343 ^{1324 ± 2}	330 ^{1489 ± 4}	430 ^{35803 ± 266}	431 ^{36181 ± 674}	
330	samtech-001	288082	219883	126 ⁶⁰⁵	369 ^{2056 ± 0}	58 ^{294 ± 3}	-	-	-	-	364 ^{7694 ± 59}	364 ^{7678 ± 91}	
331	scanovate-002	256986	457227	197 ⁸⁵⁰	209 ^{2048 ± 0}	233 ^{696 ± 32}	197 ^{713 ± 33}	182 ^{738 ± 28}	169 ^{779 ± 32}	243 ^{1172 ± 53}	284 ^{3021 ± 38}	288 ^{3120 ± 163}	
332	scanovate-003	135585	89469	182 ⁸⁰⁸	136 ^{2048 ± 0}	172 ^{585 ± 1}	156 ^{613 ± 12}	128 ^{591 ± 1}	112 ^{610 ± 2}	111 ^{684 ± 1}	277 ^{2926 ± 22}	277 ^{2925 ± 20}	
333	sdc-000	256814	481583	174 ⁷⁸⁶	241 ^{2048 ± 0}	309 ^{913 ± 14}	265 ^{906 ± 9}	322 ^{1142 ± 19}	407 ^{1774 ± 45}	403 ^{4719 ± 222}	428 ^{32645 ± 93}	429 ^{32653 ± 112}	
334	securifai-004	282177	12027	133 ⁶³⁶	134 ^{2048 ± 0}	288 ^{869 ± 1}	244 ^{867 ± 1}	215 ^{867 ± 1}	196 ^{867 ± 1}	163 ^{865 ± 1}	198 ^{1711 ± 19}	199 ^{1705 ± 29}	
335	securifai-005	252532	81777	101 ⁵²⁵	321 ^{2048 ± 0}	429 ^{1377 ± 2}	394 ^{1355 ± 1}	382 ^{1353 ± 0}	355 ^{1357 ± 0}	290 ^{1356 ± 0}	221 ^{1873 ± 25}	219 ^{1847 ± 35}	
336	sensetime-006	765353	37673	447 ⁵⁹⁹⁴	79 ^{1028 ± 0}	424 ^{1352 ± 17}	382 ^{1311 ± 1}	370 ^{1323 ± 1}	354 ^{1357 ± 1}	337 ^{1523 ± 2}	159 ^{1179 ± 28}	160 ^{1157 ± 29}	
337	sensetime-007	765353	37533	445 ⁵⁶⁹⁹	80 ^{1028 ± 0}	434 ^{1386 ± 41}	388 ^{1323 ± 2}	380 ^{1347 ± 2}	359 ^{1366 ± 2}	346 ^{1593 ± 8}	180 ^{1460 ± 29}	179 ^{1425 ± 26}	
338	sertis-000	265572	68770	72 ⁴²⁷	235 ^{2048 ± 0}	245 ^{754 ± 0}	208 ^{759 ± 0}	187 ^{764 ± 0}	167 ^{760 ± 0}	138 ^{763 ± 0}	186 ^{1497 ± 29}	190 ^{1582 ± 38}	
339	sertis-002	460790	68929	303 ¹³⁹¹	301 ^{2048 ± 0}	384 ^{1181 ± 1}	346 ^{1178 ± 0}	335 ^{1183 ± 0}	305 ^{1187 ± 0}	257 ^{1221 ± 0}	146 ^{1086 ± 32}	146 ^{1076 ± 31}	
340	seventhssense-001	369850	3183365	186 ⁸¹¹	335 ^{2052 ± 0}	402 ^{1255 ± 2}	378 ^{1294 ± 15}	358 ^{1277 ± 3}	330 ^{1275 ± 2}	271 ^{1288 ± 3}	228 ^{1936 ± 26}	230 ^{1943 ± 34}	
341	seventhssense-002	452197	1567903	220 ⁹⁴⁴	338 ^{2052 ± 0}	401 ^{1252 ± 1}	372 ^{1271 ± 1}	355 ^{1269 ± 1}	327 ^{1272 ± 1}	273 ^{1290 ± 1}	239 ^{2131 ± 45}	239 ^{2123 ± 45}	
342	shaman-000	0	120033	94 ⁵⁰⁷	426 ^{4096 ± 0}	207 ^{653 ± 16}	-	-	-	-	36 ^{380 ± 25}	36 ^{379 ± 31}	
343	shaman-001	0	174446	98 ⁵¹¹	429 ^{4096 ± 0}	59 ^{294 ± 2}	-	-	-	-	82 ^{635 ± 19}	41 ^{441 ± 25}	
344	shu-002	731250	148309	207 ⁸⁹⁰	403 ^{4096 ± 0}	244 ^{751 ± 2}	211 ^{769 ± 4}	240 ^{922 ± 4}	383 ^{1431 ± 9}	398 ^{3489 ± 47}	461 ^{2930763 ± 47355}	461 ^{2929759 ± 39149}	
345	shu-003	428774	146940	97 ⁵¹¹	123 ^{2048 ± 0}	271 ^{820 ± 6}	230 ^{828 ± 3}	249 ^{941 ± 9}	339 ^{1308 ± 15}	392 ^{3045 ± 44}	258 ^{2506 ± 26}	259 ^{2512 ± 38}	
346	siat-002	486842	7738	386 ²⁴³⁴	345 ^{2052 ± 0}	169 ^{579 ± 0}	-	-	-	-	110 ^{769 ± 13}	107 ^{750 ± 13}	
347	siat-005	380936	16935	289 ¹²⁹⁸	294 ^{2048 ± 0}	95 ^{403 ± 0}	76 ^{400 ± 0}	57 ^{401 ± 0}	52 ^{403 ± 1}	45 ^{422 ± 7}	56 ^{577 ± 13}	58 ^{580 ± 17}	
348	sjtu-003	480795	148243	109 ⁵³⁸	226 ^{2048 ± 0}	272 ^{821 ± 2}	225 ^{820 ± 2}	241 ^{923 ± 3}	309 ^{1201 ± 3}	374 ^{2373 ± 9}	188 ^{1560 ± 20}	187 ^{1560 ± 14}	
349	sjtu-004	1953267	241108	399 ²⁷²⁷	442 ^{4608 ± 0}	395 ^{1236 ± 2}	355 ^{1209 ± 2}	362 ^{1294 ± 4}	399 ^{1554 ± 5}	386 ^{2738 ± 8}	287 ^{3057 ± 14}	287 ^{3070 ± 20}	
350	sktelecom-000	527132	298496	292 ¹³¹¹	95 ^{1536 ± 0}	366 ^{1110 ± 1}	328 ^{1113 ± 1}	311 ^{1114 ± 1}	274 ^{1120 ± 1}	237 ^{1155 ± 1}	418 ^{26583 ± 128}	417 ^{26508 ± 126}	
351	smartbiometrik-001	30875	92620	71 ²⁷	512 ± 0	191 ^{620 ± 7}	162 ^{625 ± 7}	151 ^{640 ± 4}	158 ^{728 ± 6}	206 ^{1047 ± 8}	94 ^{703 ± 31}	96 ^{710 ± 40}	
352	smartengines-000	1711	3025	450	10 ^{288 ± 0}	23 ^{168 ± 7}	20 ^{180 ± 1}	17 ^{188 ± 3}	20 ^{217 ± 3}	22 ^{275 ± 1}	9 ^{197 ± 5}	7 ^{167 ± 11}	

Notes
 1 The configuration size does not capture static data included in libraries.
 2 The library size is the combined total of all files provided in the submission lib folder. These libraries e.g. OpenCV may or may not be installed on any end user's platform natively and would not need to be installed with the algorithm. Some developers put neural network models in their libraries.
 3 The memory usage is the peak resident set size reported by the ps system call during template generation.
 4 The median template creation times are measured on Intel®Xeon®CPU E5-2630 v4 @ 2.20GHz processors.
 5 The comparison durations, in nanoseconds, are estimated using std::chrono::high_resolution_clock which on the machine in (2) counts 1ns clock ticks. Precision is somewhat worse than that however. The ± value is the median absolute deviation times 1.48 for Normal consistency.

	ALGORITHM	CONFIG	LIBRARY	TEMPLATE								COMPARISON ⁴								
				NAME	DATA	DATA	MEMORY	SIZE	GENERATION TIME (ms) ⁴				TIME (ns) ⁵							
									(KB) ¹	(KB) ²	(MB) ³	(B)	MUGSHOT	480x720	960x1440	1600x2400	3000x4500	GENUINE	IMPOSTOR	
353	smartengines-001	7095	4601	³ ₄₆	⁹ ₂₈₈	⁰ _±	⁷² ₃₃₃	⁸⁹ ₄₀₈	¹ _±	⁶⁷ ₄₂₃	¹ _±	⁶⁴ ₄₆₀	² _±	⁷¹ ₅₅₃	⁵ _±	⁶ ₁₅₃	¹¹ _±	⁵ ₁₄₃	¹³ _±	
354	smartvist-000	5959	134084	³⁰ ₁₆₅	²⁹ ₅₁₂	⁰ _±	⁷ ₅₉	⁰ _±	⁵ ₅₆	⁰ _±	⁴ ₅₆	⁰ _±	⁴ ₅₈	⁰ _±	⁵ ₉₀	¹ _±	¹⁷⁹ ₁₄₃₅	³¹ _±	¹⁷⁸ ₁₄₂₂	⁴⁸ _±
355	smilart-002	111826	87805	⁴⁹ ₂₆₃	⁶⁸ ₁₀₂₄	⁰ _±	²⁶ ₁₇₆	¹⁶ _±	-	-	-	-	-	-	-	⁴⁰⁴ ₁₈₇₈₄	¹³⁶ _±	⁴⁰⁸ ₁₈₇₉₅	¹⁵¹ _±	
356	smilart-003	67339	91670	⁴⁰ ₁₉₂	³⁴ ₅₁₂	⁰ _±	²⁸ ₁₈₀	¹² _±	²¹ ₁₈₁	¹⁰ _±	³⁵ ₃₁₃	²² _±	¹³⁴ ₆₆₅	⁴⁹ _±	³⁷¹ ₂₂₉₉	¹⁹⁶ _±	¹⁷² ₁₃₉₅	⁷⁴ _±	¹³⁷ ₁₀₂₇	⁶⁶ _±
357	sodec-000	836592	13142	⁴¹⁷ ₃₁₈₆	³⁹³ ₄₀₉₆	⁰ _±	³⁵⁴ ₁₀₄₁	² _±	³⁰⁸ ₁₀₃₂	¹ _±	²⁹¹ ₁₀₃₅	¹ _±	²⁵⁶ ₁₀₃₇	² _±	²¹⁵ ₁₀₆₁	² _±	²⁰⁹ ₁₇₉₄	³⁷ _±	²⁰⁷ ₁₇₇₅	²³ _±
358	sqisoft-001	278968	386291	¹⁴⁸ ₆₈₈	³⁶⁴ ₂₀₅₆	⁰ _±	¹²⁶ ₄₇₇	⁵ _±	³⁹³ ₁₃₄₈	¹⁸ _±	³⁸¹ ₁₃₅₃	²⁶ _±	³⁴⁹ ₁₃₄₀	¹⁴ _±	³⁰⁴ ₁₃₉₃	²⁸ _±	¹¹⁴ ₇₉₇	²² _±	¹¹¹ ₇₈₈	²² _±
359	sqisoft-002	278039	386291	¹³⁹ ₆₆₆	³⁵² ₂₀₅₆	⁰ _±	¹²² ₄₆₆	⁸ _±	⁹⁸ ₄₆₆	² _±	⁸² ₄₆₈	¹¹ _±	⁶⁵ ₄₆₁	⁶ _±	⁵⁴ ₄₇₂	⁴ _±	¹⁰⁸ ₇₅₈	¹¹ _±	¹⁰⁸ ₇₆₀	²³ _±
360	stauq-000	879661	624676	²⁴² ₁₀₆₄	⁴¹⁷ ₄₀₉₆	⁰ _±	²⁶⁶ ₈₁₃	²⁵ _±	-	-	-	-	-	-	-	²⁸⁰ ₂₉₇₉	³¹ _±	²⁸³ ₃₀₀₇	⁷⁵ _±	
361	starhybrid-001	100509	289356	¹⁹⁵ ₈₄₅	¹⁶⁴ ₂₀₄₈	⁰ _±	⁸⁰ ₃₅₈	⁸² _±	⁶¹ ₃₅₅	⁴⁹ _±	⁴⁹ ₃₇₉	⁵⁸ _±	⁵⁰ ₄₀₁	⁷⁹ _±	³⁷ ₃₉₃	⁶⁷ _±	¹⁴³ ₁₀₇₅	⁵¹ _±	¹⁴⁷ ₁₀₇₈	⁵³ _±
362	sukshi-000	94035	688738	⁶⁵ ₃₇₂	⁴⁶⁰ ₃₂₇₆₈	⁰ _±	⁹⁶ ₄₀₇	¹¹ _±	⁸⁰ ₄₁₃	⁸ _±	⁹⁶ ₅₀₄	⁸ _±	¹⁴¹ ₆₈₉	¹¹ _±	³⁴⁴ ₁₅₇₄	²⁸ _±	³⁷⁴ ₉₈₁₇	⁵⁰ _±	³⁷³ ₉₇₈₇	⁶² _±
363	suprema-002	373808	41473	³⁴⁴ ₁₇₃₁	¹³⁸ ₂₀₄₈	⁰ _±	²⁵⁸ ₇₈₇	³ _±	²³² ₈₃₃	³ _±	²⁴² ₉₂₄	⁴ _±	³⁰² ₁₁₈₅	⁶ _±	³⁸¹ ₂₄₇₉	³ _±	²⁹² ₃₂₅₅	¹⁷ _±	²⁹² ₃₂₅₃	¹⁴ _±
364	suprema-003	498231	116054	²⁷⁶ ₁₂₃₉	²²³ ₂₀₄₈	⁰ _±	⁴⁴⁹ ₁₄₄₈	¹ _±	⁴¹⁴ ₁₄₁₇	⁴ _±	⁴⁰⁷ ₁₄₁₈	³ _±	³⁸⁰ ₁₄₂₁	⁴ _±	³²⁰ ₁₄₅₁	⁵ _±	²⁴⁵ ₂₂₀₁	¹⁰ _±	²⁴⁷ ₂₁₉₈	¹³ _±
365	supremaid-001	258193	23479	¹¹⁰ ₅₄₁	²⁹⁷ ₂₀₄₈	⁰ _±	¹²⁷ ₄₇₉	¹ _±	¹⁰³ ₄₈₁	⁰ _±	⁸⁶ ₄₈₁	⁰ _±	⁷⁵ ₄₉₀	⁰ _±	⁶⁶ ₅₂₂	⁰ _±	⁹⁵ ₇₀₄	¹⁹ _±	⁸⁷ ₆₅₂	¹⁹ _±
366	supremaid-002	256273	23899	⁵⁸ ₃₃₅	¹⁹⁹ ₂₀₄₈	⁰ _±	¹³² ₄₈₃	⁰ _±	¹¹⁵ ₅₀₁	⁰ _±	⁹⁰ ₄₈₈	⁰ _±	⁸⁰ ₅₀₃	⁰ _±	⁷⁹ ₅₆₅	⁰ _±	²³² ₁₉₉₀	¹⁹ _±	²²⁵ ₁₉₂₃	²⁹ _±
367	surrey-cvssp-000	158030	70795	²⁰⁵ ₈₇₉	¹⁴⁵ ₂₀₄₈	⁰ _±	³⁷² ₁₁₄₁	³ _±	³⁴¹ ₁₁₅₇	³ _±	³²⁰ ₁₁₅₈	⁴ _±	²⁹¹ ₁₁₆₃	³ _±	²⁶⁰ ₁₂₄₅	³ _±	³⁷² ₉₅₅₇	¹⁴³ _±	³⁷¹ ₉₆₀₂	¹⁸⁶ _±
368	surrey-cvssp-001	900280	76392	³⁴¹ ₁₇₀₇	²⁷³ ₂₀₄₈	⁰ _±	³⁹² ₁₂₂₁	¹ _±	³⁶¹ ₁₂₃₈	² _±	³⁴⁷ ₁₂₄₀	⁰ _±	³¹⁸ ₁₂₄₃	⁰ _±	²⁶³ ₁₂₅₇	⁰ _±	⁴⁰⁶ ₁₈₉₇₀	¹⁶¹ _±	⁴⁰⁶ ₁₈₉₉₉	¹⁷⁶ _±
369	synesis-006	731941	21817	³¹⁴ ₁₄₇₂	⁴³⁷ ₄₁₀₄	⁰ _±	¹⁵⁴ ₅₄₉	¹ _±	¹³⁰ ₅₄₆	¹ _±	¹¹⁵ ₅₅₂	¹ _±	⁹⁴ ₅₅₈	² _±	¹⁰² ₆₃₉	²⁸ _±	⁹³ ₆₉₇	³² _±	⁹⁴ ₆₈₈	³¹ _±
370	synesis-007	1442961	24145	³⁸⁷ ₂₄₄₃	³⁸⁷ ₃₀₈₀	⁰ _±	³⁹⁰ ₁₂₁₅	⁵ _±	³⁷⁰ ₁₂₆₈	³⁰ _±	³⁶⁷ ₁₃₀₆	⁶⁷ _±	³⁴⁰ ₁₃₁₁	⁵⁸ _±	³¹¹ ₁₄₂₃	⁵² _±	⁸⁹ ₆₈₄	³² _±	⁹² ₆₈₆	²⁵ _±
371	synology-000	221021	25809	⁸⁰ ₄₅₃	¹⁶⁵ ₂₀₄₈	⁰ _±	⁹⁹ ₄₀₇	¹⁴ _±	⁸¹ ₄₁₅	¹⁴ _±	¹⁷⁰ ₆₉₄	³¹ _±	³⁷⁰ ₁₃₉₆	⁵⁸ _±	⁴⁰⁰ ₄₅₆₈	²¹¹ _±	⁴⁰⁸ ₁₉₇₂₀	²⁰³ _±	⁴⁰⁷ ₁₉₇₆₇	³⁷⁹ _±
372	synology-002	256713	25943	⁸⁹ ₄₈₈	²⁷⁹ ₂₀₄₈	⁰ _±	³⁰³ ₈₈₆	⁴ _±	²⁵⁸ ₈₉₂	³ _±	²³⁷ ₉₂₀	² _±	²⁴⁶ ₁₀₀₀	⁵ _±	²⁷⁹ ₁₃₁₇	¹² _±	¹⁸² ₁₄₆₆	³² _±	¹⁸⁵ ₁₄₉₆	⁴⁵ _±
373	sztu-000	338637	15871	²⁸⁷ ₁₂₉₈	²⁸⁴ ₂₀₄₈	⁰ _±	¹⁴⁸ ₅₃₁	⁰ _±	¹²¹ ₅₃₂	⁰ _±	¹⁰⁵ ₅₃₃	⁰ _±	⁸⁷ ₅₃₇	⁰ _±	⁷⁰ ₅₄₈	⁰ _±	⁵⁷ ₅₈₅	¹¹ _±	⁶² ₅₉₂	¹³ _±
374	sztu-001	338650	15871	²⁸⁸ ₁₂₉₈	²⁸⁶ ₂₀₄₈	⁰ _±	¹⁴⁹ ₅₃₅	⁰ _±	¹²⁵ ₅₃₇	⁰ _±	¹⁰⁸ ₅₃₈	⁰ _±	⁸⁹ ₅₄₀	⁰ _±	⁷³ ₅₅₃	⁰ _±	⁶³ ₅₉₉	¹⁰ _±	⁶⁶ ₅₉₈	¹⁰ _±
375	t4isb-000	234227	115237	⁶⁰ ₃₄₃	³⁰⁴ ₂₀₄₈	⁰ _±	³⁴³ ₁₀₀₆	⁵ _±	²⁹⁵ ₁₀₀₁	¹ _±	²⁸¹ ₁₀₀₆	¹ _±	²⁰⁰ ₁₀₂₂	² _±	³⁰⁸ ₁₀₅₈₆	³⁴ _±	³⁰² ₃₅₃₄	³⁴ _±	³⁰² ₃₅₃₄	³⁴ _±
376	tech5-004	2410272	118858	⁴⁰⁰ ₂₇₃₃	¹² ₃₂₁	⁰ _±	²⁹³ ₈₇₂	² _±	³²⁹ ₁₁₁₇	¹⁶⁴ _±	³¹² ₁₁₁₄	¹⁸² _±	²⁸⁰ ₁₁₃₄	¹⁷⁹ _±	¹⁹⁵ ₉₉₉	⁴⁴ _±	⁶¹ ₅₉₇	¹³ _±	⁶¹ ₅₉₂	¹⁶ _±
377	tech5-005	1178769	120517	³⁰⁸ ₁₄₂₆	²² ₅₁₂	⁰ _±	⁴⁰⁷ ₁₂₇₂	¹⁰⁹ _±	³¹² ₁₀₃₈	⁶³ _±	²⁹⁴ ₁₀₄₆	³⁹ _±	²⁷⁹ ₁₁₂₄	³⁸ _±	²⁸⁹ ₁₃₅₁	⁴⁴ _±	²⁶² ₂₅₇₃	³⁷ _±	²⁶² ₂₅₄₅	³² _±
378	techsign-000	0	1101622	³⁶⁵ ₁₉₅₅	¹⁵⁵ ₂₀₄₈	⁰ _±	⁸⁴ ₃₆₆	¹ _±	⁷⁵ ₃₉₈	¹ _±	³³⁰ ₁₁₇₂	³ _±	⁴²⁰ ₃₀₆₅	¹⁸ _±	⁴²² ₁₀₄₆₀	⁶⁵ _±	³²⁴ ₄₇₅₈	¹¹² _±	³²³ ₄₇₈₉	⁹³ _±
379	techsign-001	0	586983	³⁴⁸ ₁₇₄₁	²⁹⁰ ₂₀₄₈	⁰ _±	²⁵² ₇₇₂	³⁵ _±	²¹⁵ ₇₈₈	²³ _±	¹⁹⁶ ₈₀₂	⁴² _±	²²⁷ ₉₄₉	¹⁰ _±	³⁰⁸ ₁₄₀₉	²⁶ _±	⁵⁸ ₅₉₂	¹¹ _±	⁶³ ₅₉₂	¹³ _±
380	tevian-007	779934	19523	³⁴³ ₁₇₁₄	⁸¹ ₁₀₃₂	⁰ _±	¹⁷⁰ ₅₈₃	¹ _±	¹⁴² ₅₇₉	⁰ _±	¹²⁴ ₅₈₀	⁰ _±	¹⁰⁵ ₅₈₈	¹ _±	¹⁰⁰ ₆₃₆	⁰ _±	³²⁹ ₄₈₉₄	⁶⁵ _±	³²⁶ ₄₈₄₁	⁸³ _±
381	tevian-008	847177	19519	⁴¹⁹ ₃₄₉₀	⁸² ₁₀₃₂	⁰ _±	³⁰¹ ₈₈₄	² _±	²⁶⁴ ₉₀₃	¹ _±	²³¹ ₉₀₃	¹ _±	²¹³ ₉₁₁	¹ _±	¹⁸² ₉₄₆	¹ _±	³²⁶ ₄₈₂₈	⁴⁰ _±	³²⁵ ₄₈₁₁	⁴¹ _±
382	tiger-005	342866	253734	³²² ₁₅₃₁	³³² ₂₀₅₂	<														

ALGORITHM			CONFIG	LIBRARY	TEMPLATE						COMPARISON ⁴		
NAME		DATA	DATA	MEMORY	SIZE	GENERATION TIME (ms) ⁴				TIME (ns) ⁵			
		(KB) ¹	(KB) ²	(MB) ³	(B)	MUGSHOT	480x720	960x1440	1600x2400	3000x4500	GENUINE	IMPOSTOR	
397	twface-000	661735	11782	393 2610	242	2048 ± 0	289 871 ± 1	248 873 ± 1	219 873 ± 2	199 876 ± 2	168 898 ± 1	187 1504 ± 29	186 1510 ± 34
398	twface-001	671511	11782	408 2855	266	2048 ± 0	313 923 ± 1	270 925 ± 2	243 926 ± 1	217 929 ± 2	179 940 ± 2	173 1400 ± 32	175 1402 ± 37
399	ulsee-001	370519	57261	-	124	2048 ± 0	209 654 ± 2	-	-	-	-	351 6065 ± 94	352 6228 ± 77
400	uluface-002	0	480761	248 1088	310	2048 ± 0	295 873 ± 42	238 855 ± 9	264 978 ± 24	325 1271 ± 40	372 2333 ± 68	407 19207 ± 1114	404 18501 ± 274
401	uluface-003	97357	529422	279 1264	384	3072 ± 0	328 965 ± 11	285 968 ± 10	304 1087 ± 20	365 1387 ± 36	380 2469 ± 86	417 26057 ± 195	419 26865 ± 566
402	unissey-001	0	1956593	327 1584	402	4096 ± 0	300 880 ± 3	259 892 ± 3	414 1452 ± 8	425 3048 ± 12	420 10017 ± 387	181 1463 ± 35	183 1471 ± 34
403	unissey-002	0	1443765	170 763	424	4096 ± 0	241 736 ± 1	205 752 ± 1	273 994 ± 1	397 1426 ± 1	3331 ± 2	386 12308 ± 91	386 12302 ± 137
404	upc-001	0	89914	247 1077	89	1052 ± 0	156 551 ± 15	194 703 ± 56	180 724 ± 51	164 751 ± 49	161 863 ± 33	289 3114 ± 44	291 3165 ± 97
405	uxlabs-001	291127	39378	153 700	422	4096 ± 0	91 395 ± 0	70 387 ± 0	53 388 ± 0	48 390 ± 0	39 396 ± 0	219 1863 ± 31	224 1921 ± 45
406	vcoog-002	3229434	118946	421 3666	461	61504 ± 5	79 357 ± 25	-	-	-	-	458 296154 ± 3077	458 296436 ± 4183
407	vd-002	254498	34389	149 688	48	516 ± 0	224 684 ± 5	184 679 ± 4	161 676 ± 5	143 693 ± 5	134 754 ± 5	24 300 ± 14	26 319 ± 32
408	vd-003	254505	44051	151 696	334	2052 ± 0	230 691 ± 5	188 690 ± 5	163 683 ± 4	142 691 ± 5	125 722 ± 5	132 1003 ± 11	132 1001 ± 7
409	veridas-007	355105	891492	390 2527	222	2048 ± 0	291 872 ± 9	250 875 ± 8	351 1261 ± 18	418 2238 ± 38	411 6374 ± 147	86 655 ± 16	89 660 ± 19
410	veridas-008	1100495	1190915	454 8932	194	2048 ± 0	319 944 ± 12	277 945 ± 11	376 1334 ± 27	419 2382 ± 48	413 6959 ± 172	99 723 ± 14	102 731 ± 16
411	veridium-000	0	47198	15 98	459	29399 ± 2045	10 79 ± 0	8 80 ± 0	9 89 ± 0	7 90 ± 0	7 111 ± 0	447 64880 ± 171	447 64697 ± 247
412	verigram-000	256209	7798	355 1842	231	2048 ± 0	262 807 ± 1	226 821 ± 1	260 972 ± 2	356 1358 ± 3	389 2848 ± 13	162 1222 ± 17	163 1219 ± 17
413	verigram-001	282155	11773	395 2638	141	2048 ± 0	214 664 ± 2	182 675 ± 2	207 833 ± 4	310 1202 ± 7	385 2733 ± 32	195 1664 ± 60	193 1648 ± 56
414	verihubs-inteligensia-000	209562	51877	73 427	278	2048 ± 0	162 567 ± 0	428 1558 ± 8	424 1560 ± 8	400 1568 ± 8	349 1621 ± 8	412 22351 ± 91	412 22371 ± 81
415	verihubs-inteligensia-001	216524	51916	75 437	280	2048 ± 0	161 564 ± 0	136 562 ± 0	119 566 ± 1	96 566 ± 0	87 600 ± 0	410 21770 ± 84	410 21735 ± 102
416	verijelas-000	254540	10322	347 1736	101	2048 ± 0	66 321 ± 0	54 325 ± 1	41 329 ± 0	36 335 ± 5	30 360 ± 0	376 10267 ± 143	376 10218 ± 109
417	via-000	124422	11151	223 964	137	2048 ± 0	237 707 ± 8	203 740 ± 5	232 906 ± 41	223 941 ± 40	204 1040 ± 5	127 966 ± 28	135 1021 ± 44
418	via-001	370255	11151	338 1697	172	2048 ± 0	327 964 ± 3	302 1011 ± 3	286 1026 ± 4	259 1045 ± 3	232 1137 ± 28	129 983 ± 31	129 989 ± 40
419	videmo-001	212051	95063	56 304	237	2048 ± 0	34 199 ± 0	16 164 ± 0	13 164 ± 0	10 164 ± 0	9 165 ± 0	22 296 ± 17	23 288 ± 16
420	videmo-002	212053	32963	51 332	255	2048 ± 0	35 199 ± 0	17 169 ± 0	14 169 ± 0	11 170 ± 0	11 170 ± 0	14 209 ± 7	18 208 ± 8
421	videonetics-001	30875	5963	5 61	26	512 ± 0	44 262 ± 3	38 273 ± 1	72 439 ± 3	181 820 ± 3	377 2393 ± 43	155 1153 ± 38	156 1142 ± 65
422	videonetics-002	121981	6289	19 115	337	2052 ± 0	55 282 ± 5	46 295 ± 1	100 513 ± 4	254 1029 ± 3	393 3151 ± 46	161 1219 ± 57	164 1262 ± 56
423	vettelhightech-000	259471	215557	71 419	102	2048 ± 0	117 461 ± 1	96 461 ± 2	78 461 ± 1	68 467 ± 2	57 494 ± 0	64 599 ± 11	60 591 ± 13
424	vigilantsolutions-010	348798	49973	193 840	98	1548 ± 0	190 615 ± 0	166 631 ± 0	148 632 ± 0	123 636 ± 0	105 659 ± 0	48 490 ± 13	49 488 ± 11
425	vigilantsolutions-011	255661	49973	122 591	97	1548 ± 0	94 402 ± 0	82 418 ± 0	63 418 ± 0	56 422 ± 0	50 445 ± 0	29 339 ± 20	33 366 ± 37
426	vinaai-000	402391	866522	236 1032	306	2048 ± 0	360 1099 ± 1	324 1095 ± 1	306 1093 ± 1	272 1099 ± 1	230 1126 ± 1	281 2996 ± 20	282 2993 ± 26
427	vinbigdata-001	271405	44746	121 589	315	2048 ± 0	440 1400 ± 5	405 1393 ± 2	393 1391 ± 2	367 1393 ± 1	307 1404 ± 1	169 1351 ± 50	169 1310 ± 38
428	vinbigdata-002	256322	138864	128 606	151	2048 ± 0	166 569 ± 2	140 572 ± 1	120 571 ± 1	97 572 ± 1	85 596 ± 1	243 2175 ± 44	244 2160 ± 53
429	vion-000	228219	7533	92 498	330	2052 ± 0	71 333 ± 1	-	-	-	-	432 39839 ± 3561	418 26830 ± 2241
430	visage-000	49218	70150	9 73	25	512 ± 0	4 27 ± 0	2 27 ± 0	2 31 ± 0	3 38 ± 0	3 63 ± 0	246 2220 ± 14	248 2218 ± 14
431	visionbox-001	256869	190645	116 579	318	2048 ± 0	335 983 ± 7	322 1093 ± 46	383 1360 ± 68	416 2181 ± 105	409 5955 ± 281	157 1161 ± 22	159 1154 ± 20
432	visionbox-002	259063	135281	130 612	372	2059 ± 0	130 482 ± 1	105 482 ± 0	88 484 ± 1	76 492 ± 1	64 517 ± 3	231 1969 ± 44	228 1931 ± 42
433	visionlabs-010	1067280	19357	208 902	45	513 ± 0	239 730 ± 0	198 717 ± 1	175 709 ± 0	153 713 ± 1	131 739 ± 0	65 600 ± 41	78 626 ± 35
434	visionlabs-011	1067280	19353	201 862	43	513 ± 0	240 731 ± 1	199 717 ± 1	176 710 ± 1	154 714 ± 1	132 741 ± 1	51 556 ± 26	54 559 ± 25
435	visteam-003	215359	33730	90 489	394	4096 ± 0	400 1249 ± 4	366 1251 ± 4	354 1266 ± 5	326 1272 ± 5	295 1370 ± 9	356 6816 ± 111	356 6816 ± 105
436	visteam-004	61594	35369	34 168	268	2048 ± 0	60 303 ± 5	49 313 ± 6	30 278 ± 4	30 288 ± 4	32 377 ± 7	312 3936 ± 72	312 3938 ± 79
437	vixvizacion-005	38886	534579	163 731	161	2048 ± 0	110 433 ± 4	68 381 ± 3	52 383 ± 3	43 373 ± 1	42 411 ± 1	103 731 ± 63	80 632 ± 32
438	vixvizacion-006	594053	396294	212 914	218	2048 ± 0	298 876 ± 9	220 828 ± 3	201 817 ± 1	183 825 ± 2	164 871 ± 1	66 600 ± 23	73 611 ± 25
439	vnpt-004	370110	240841	230 988	313	2048 ± 0	397 1238 ± 1	362 1241 ± 1	348 1242 ± 2	337 1307 ± 2	332 1505 ± 2	312 4047 ± 48	314 4008 ± 108
440	vnpt-005	560630	240888	263 1141	248	2048 ± 0	443 1403 ± 0	411 1404 ± 6	402 1403 ± 6	384 1456 ± 0	350 1630 ± 10	303 3562 ± 23	303 3554 ± 29

Notes

- 1 The configuration size does not capture static data included in libraries.
- 2 The library size is the combined total of all files provided in the submission lib folder. These libraries e.g. OpenCV may or may not be installed on any end user's platform natively and would not need to be installed with the algorithm. Some developers put neural network models in their libraries.
- 3 The memory usage is the peak resident set size reported by the ps system call during template generation.
- 4 The median template creation times are measured on Intel®Xeon®CPU E5-2630 v4 @ 2.20GHz processors.
- 5 The comparison durations, in nanoseconds, are estimated using std::chrono::high_resolution_clock which on the machine in (2) counts 1ns clock ticks. Precision is somewhat worse than that however. The ± value is the median absolute deviation times 1.48 for Normal consistency.

Table 17: Summary of algorithms and properties included in this report. The red superscripts give ranking for the quantity in that column.

ALGORITHM			CONFIG	LIBRARY	TEMPLATE						COMPARISON ⁴	
NAME		DATA	DATA	MEMORY	SIZE	GENERATION TIME (ms) ⁴				TIME (ns) ⁵		
		(KB) ¹	(KB) ²	(MB) ³	(B)	MUGSHOT	480x720	960x1440	1600x2400	3000x4500	GENUINE	IMPOSTOR
441	vocord-009	1380132	201560	⁴³⁴ 4162	⁹⁹ 1920 ± 0	⁴⁵⁵ 1472 ± 2	⁴²⁴ 1472 ± 1	⁴²³ 1549 ± 1	⁴⁰³ 1667 ± 2	³⁶⁷ 2064 ± 2	²³⁵ 2052 ± 50	²³⁷ 2056 ± 39
442	vocord-010	902552	206873	⁴²⁵ 3858	⁸⁸ 1088 ± 0	⁴⁵² 1459 ± 2	⁴²³ 1459 ± 1	⁴¹⁷ 1463 ± 2	³⁹³ 1484 ± 1	³³⁹ 1535 ± 3	²⁶⁷ 2724 ± 31	²⁶⁵ 2653 ± 45
443	vts-000	256589	169760	³⁴⁰ 1704	²⁰⁷ 2048 ± 0	¹³⁵ 486 ± 1	¹⁰⁴ 481 ± 0	⁸⁹ 484 ± 0	⁷³ 485 ± 1	⁶³ 517 ± 0	⁴⁵⁵ 124209 ± 352	⁴⁵⁵ 123652 ± 358
444	vts-001	293000	475743	¹³² 618	¹³⁹ 2048 ± 0	²¹⁹ 676 ± 1	¹⁸⁵ 683 ± 6	¹⁶⁶ 687 ± 3	¹⁴⁴ 695 ± 2	¹²⁰ 709 ± 2	³⁷³ 9620 ± 44	³⁷² 9618 ± 54
445	wicket-000	826392	641802	³⁷² 2071	²⁶¹ 2048 ± 0	⁴⁴⁵ 1419 ± 2	⁴¹⁵ 1429 ± 3	⁴¹⁰ 1444 ± 4	³⁸⁷ 1460 ± 3	³⁴⁰ 1537 ± 6	⁴⁴⁵ 60976 ± 232	⁴⁴⁵ 61096 ± 323
446	winsense-001	264428	32035	²¹⁶ 922	⁹⁰ 1280 ± 0	²⁴⁸ 766 ± 7	³¹⁵ 1058 ± 47	²⁶⁷ 983 ± 97	²⁶¹ 1053 ± 119	²⁸⁰ 1320 ± 84	¹⁹² 1631 ± 28	²³² 1964 ± 171
447	winsense-002	281379	25780	³⁵⁰ 1781	²²¹ 2048 ± 0	¹³⁷ 494 ± 2	¹¹¹ 498 ± 1	¹⁰² 519 ± 1	⁸⁸ 537 ± 1	⁹⁸ 634 ± 1	¹⁹⁷ 1683 ± 8	¹⁹⁶ 1685 ± 7
448	wiseai-001	189467	60781	⁴³ 245	¹¹¹ 2048 ± 0	⁴¹ 240 ± 0	³³ 251 ± 0	³⁹ 328 ± 1	³⁵ 327 ± 0	²⁵ 332 ± 0	²⁷² 2850 ± 29	²⁷⁵ 2852 ± 31
449	wuhantianyu-001	465118	66457	²⁰² 866	¹⁸¹ 2048 ± 0	²⁰³ 642 ± 1	¹⁷¹ 642 ± 1	¹⁵³ 644 ± 0	¹²⁹ 652 ± 0	¹¹⁷ 697 ± 0	³⁷¹ 9502 ± 151	³⁷⁵ 9920 ± 253
450	x-laboratory-000	520020	197310	³²⁰ 1524	³⁵⁵ 2056 ± 0	²⁶³ 808 ± 7	²⁶¹ 897 ± 113	²³³ 907 ± 103	²⁰³ 886 ± 103	¹¹⁰ 673 ± 39	¹⁰² 725 ± 19	¹⁰⁶ 749 ± 34
451	x-laboratory-001	625140	398792	³⁵⁶ 1844	³⁵³ 2056 ± 0	¹⁷³ 586 ± 2	¹⁵³ 596 ± 5	¹³⁶ 603 ± 6	¹¹⁷ 620 ± 7	¹⁴² 793 ± 14	¹¹⁶ 813 ± 28	¹²⁰ 872 ± 32
452	xforwardai-001	340100	51163	³⁷⁷ 2173	²⁹⁵ 2048 ± 0	³⁸² 1180 ± 2	³⁵¹ 1182 ± 1	³³⁹ 1194 ± 1	³⁰⁴ 1186 ± 2	²⁵² 1203 ± 1	¹¹² 779 ± 17	¹¹³ 797 ± 13
453	xforwardai-002	707715	51163	³⁶⁹ 1989	⁴¹⁸ 4096 ± 0	³¹⁸ 944 ± 1	²⁷⁶ 942 ± 1	²⁵⁰ 943 ± 4	²²¹ 935 ± 1	¹⁸⁷ 967 ± 1	¹⁷⁷ 1406 ± 8	¹⁷⁶ 1405 ± 13
454	xm-000	578041	148920	¹⁴⁷ 688	³³⁶ 2052 ± 0	²⁹⁹ 878 ± 2	²⁵⁴ 882 ± 1	²⁷⁰ 988 ± 2	³²³ 1258 ± 3	³⁷⁹ 2434 ± 7	¹⁹³ 1634 ± 17	¹⁹² 1632 ± 20
455	yisheng-004	486351	38653	²⁸⁴ 1279	³⁸⁹ 3704 ± 0	⁸⁶ 378 ± 12	-	-	-	-	⁹¹ 693 ± 137	⁵¹ 526 ± 34
456	yitu-003	1525719	138919	⁴²³ 3737	³⁸⁰ 2082 ± 0	²⁸⁶ 860 ± 0	-	-	-	-	⁴⁰² 18305 ± 71	⁴⁰² 18286 ± 62
457	yoonik-002	453720	265415	⁴⁰⁴ 2755	¹⁵⁹ 2048 ± 0	³⁷⁴ 1145 ± 4	³³⁰ 1123 ± 2	³¹⁴ 1124 ± 2	²⁷⁶ 1125 ± 2	²²⁹ 1126 ± 3	¹⁰⁹ 761 ± 32	¹⁰⁵ 736 ± 32
458	yoonik-003	346691	265415	³⁸⁰ 2196	²³⁴ 2048 ± 0	³³⁸ 991 ± 3	²⁹¹ 980 ± 1	²⁶⁸ 984 ± 4	²³⁵ 982 ± 1	¹⁹³ 983 ± 1	⁸⁷ 684 ± 45	⁹⁰ 678 ± 41
459	ytu-000	1477360	44032	³⁸⁸ 2484	¹²⁵ 2048 ± 0	¹⁴⁶ 530 ± 0	¹²³ 533 ± 0	¹⁵⁰ 640 ± 0	¹⁹⁴ 861 ± 2	³⁶⁶ 1949 ± 8	⁴²⁴ 31797 ± 131	⁴²⁵ 31794 ± 133
460	yuan-004	428665	50011	²⁹⁵ 1353	⁴¹¹ 4096 ± 0	¹⁶³ 567 ± 0	¹³⁹ 569 ± 0	¹²¹ 573 ± 0	⁹⁹ 579 ± 0	⁸⁹ 607 ± 0	³⁴⁵ 5816 ± 35	³⁴⁷ 5800 ± 31
461	yuan-005	258312	145564	¹⁹² 839	¹¹⁵ 2048 ± 0	⁸⁸ 381 ± 0	⁶⁹ 386 ± 0	⁵³ 387 ± 2	⁴⁷ 390 ± 4	⁴³ 421 ± 3	¹⁵⁶ 1156 ± 8	¹⁶¹ 1196 ± 26

Notes

- 1 The configuration size does not capture static data included in libraries.
- 2 The library size is the combined total of all files provided in the submission lib folder. These libraries e.g. OpenCV may or may not be installed on any end user's platform natively and would not need to be installed with the algorithm. Some developers put neural network models in their libraries.
- 3 The memory usage is the peak resident set size reported by the ps system call during template generation.
- 4 The median template creation times are measured on Intel® Xeon® CPU E5-2630 v4 @ 2.20GHz processors.
- 5 The comparison durations, in nanoseconds, are estimated using std::chrono::high_resolution_clock which on the machine in (2) counts 1ns clock ticks. Precision is somewhat worse than that however. The ± value is the median absolute deviation times 1.48 for Normal consistency.

Table 18: Summary of algorithms and properties included in this report. The red superscripts give ranking for the quantity in that column.

	Algorithm	FALSE NON-MATCH RATE (FNMR)										LESS CONSTRAINED, NON-COOP.					
		CONSTRAINED, COOPERATIVE								WILD							
		Name	VISAMC	VISA	MUGSHOT	MUGSHOT12+YRS	VISABORDER	BORDER	BORDER	1E-05							
	FMR	0.0001	1E-06	1E-05	1E-05	1E-06	1E-06	1E-06	1E-05	0.0001							
1	20face-000	0.1268	404	0.1828	398	0.1748	405	0.2768	405	0.1765	390	0.1864	300	0.0927	334	0.0405	284
2	20face-001	0.0521	380	0.0732	380	0.1414	403	0.2549	404	0.0769	366	0.1354	291	0.0419	292	0.0295	172
3	3divi-006	0.0064	190	0.0094	190	0.0047	170	0.0066	174	0.0091	179	0.0191	156	0.0113	151	0.0289	146
4	3divi-007	0.0024	56	0.0038	60	0.0028	63	0.0034	59	0.0046	92	0.0101	81	0.0082	97	0.0300	187
5	acer-001	0.0294	360	0.0504	362	0.0240	354	0.0463	356	0.0436	346	0.0622	259	0.0360	286	0.0307	201
6	acer-002	0.0169	328	0.0262	327	0.0103	288	0.0167	299	0.0182	280	0.0281	197	0.0159	206	0.0297	179
7	acisw-007	0.4276	431	0.5493	433	0.8425	446	0.9185	446	0.8424	430	0.9976	418	0.9930	435	0.4963	430
8	acisw-008	0.0100	258	0.0147	253	0.0094	284	0.0126	253	0.1740	389	0.6651	358	0.4545	387	0.0925	365
9	ader-a-002	0.0052	145	0.0071	144	0.0047	167	0.0064	168	0.0087	170	0.0159	132	0.0136	179	0.0990	368
10	ader-a-003	0.0043	124	0.0059	124	0.0036	121	0.0043	103	0.0076	149	0.0151	121	0.0128	171	0.0989	367
11	advance-003	0.0060	182	0.0087	177	0.0052	187	0.0067	175	0.0389	339	0.4914	340	0.1291	340	0.0508	314
12	advance-004	0.0083	235	0.0101	205	0.0037	128	0.0054	137	0.0051	105	0.3555	328	0.1088	338	0.1635	387
13	afisbiometrics-000	0.0051	144	0.0073	149	0.0030	82	0.0050	126	0.0044	86	0.0077	47	0.0057	42	0.0282	95
14	afrengine-000	0.6244	451	0.7336	450	0.8318	445	0.9083	444	0.8122	427	0.9980	420	0.9895	433	0.6480	437
15	aifirst-001	0.0119	283	0.0170	274	0.0084	263	0.0127	259	0.0131	237	0.0212	167	0.0138	182	0.0432	298
16	aigen-001	0.0124	291	0.0219	305	0.0143	325	0.0217	322	0.0236	307	0.8960	387	0.3255	373	0.0681	340
17	aigen-002	0.0192	340	0.0343	344	0.0256	355	0.0402	350	0.0389	338	0.9196	391	0.3876	381	0.1096	373
18	ailabs-001	0.0158	322	0.0276	333	0.0192	341	0.0317	342	0.0352	333	0.0608	256	0.0434	295	0.0338	245
19	aimall-002	0.0119	284	0.0167	272	0.0224	349	0.0411	352	0.0233	304	0.0373	230	0.0235	256	0.0327	232
20	aimall-003	0.0033	87	0.0041	66	0.0033	107	0.0035	70	0.0056	117	0.0109	88	0.0087	110	0.0312	211
21	aiseemu-001	0.0021	45	0.0029	39	0.0027	50	0.0033	54	0.0038	65	0.0339	219	0.0057	43	0.0282	86
22	aiunionface-000	0.0104	263	0.0154	262	0.0082	260	0.0122	248	0.0141	244	0.0243	180	0.0169	212	0.0306	199
23	aize-001	0.0223	347	0.0344	345	0.0199	342	0.0313	341	0.0367	335	0.0522	250	0.0359	285	0.0446	303
24	aize-002	0.0210	345	0.0327	341	0.0280	358	0.0489	359	0.0504	352	0.0692	263	0.0434	294	0.0854	360
25	ajou-001	0.0093	248	0.0147	254	0.0071	237	0.0126	254	0.0173	277	0.0274	192	0.0186	230	0.0348	252
26	alchera-003	0.0044	126	0.0055	116	0.0031	88	0.0039	87	0.0042	82	0.0077	49	0.0065	60	0.0339	246
27	alchera-004	0.0035	100	0.0052	111	0.0028	69	0.0039	88	0.0029	25	0.0075	43	0.0044	14	0.0304	194
28	alfabeta-001	0.4867	438	0.5831	436	0.6855	431	0.8156	433	0.8253	429	0.7765	374	0.6416	401	0.3427	419
29	alice-000	0.0119	285	0.0192	292	0.0106	295	0.0170	300	0.0167	268	0.0265	188	0.0150	200	0.0288	135
30	alleyes-000	0.0058	172	0.0090	185	0.0055	197	0.0087	217	0.0068	137	0.0105	86	0.0076	85	0.0282	94
31	allgovision-000	0.0346	370	0.0527	366	0.0232	351	0.0339	343	0.0372	337	0.0620	258	0.0443	299	0.0607	330
32	alphaface-001	0.0065	193	0.0097	198	0.0039	134	0.0063	167	0.0083	163	-	-	-	-	0.0280	76
33	alphaface-002	0.0052	149	0.0075	154	0.0030	76	0.0044	108	1.0000	452	0.0115	97	0.0084	103	0.0279	64
34	amplifiedgroup-001	0.5034	440	0.5848	437	0.6973	434	0.8316	434	0.7807	424	0.7724	372	0.6354	398	0.4250	425
35	androvideo-000	0.0243	350	0.0438	357	0.0239	353	0.0365	347	0.0483	351	0.1870	301	0.0635	318	0.1163	376
36	anke-004	0.0080	227	0.0154	261	0.0073	239	0.0112	240	0.0102	205	0.0178	150	0.0118	160	0.0288	138
37	anke-005	0.0070	201	0.0109	218	0.0059	208	0.0094	223	0.0105	207	0.0142	112	0.0102	132	0.0289	145
38	antheus-000	0.2564	416	0.3776	419	0.7240	435	0.8699	439	0.8899	437	0.9872	409	0.9483	425	0.7668	441
39	antheus-001	0.1311	405	0.2306	406	0.5113	423	0.6797	425	0.8748	436	0.9908	413	0.9649	429	0.7586	440
40	anyvision-004	0.0267	355	0.0385	353	0.0258	356	0.0487	358	0.0234	306	0.0301	203	0.0191	234	0.0470	307
41	anyvision-005	0.0023	53	0.0037	59	0.0027	60	0.0035	66	0.0049	100	0.0084	59	0.0069	71	0.0285	111
42	armatura-001	0.0033	91	0.0042	77	0.0031	86	0.0037	77	0.0056	116	0.0110	89	0.0092	118	0.0815	357
43	armatura-002	0.0041	121	0.0052	107	0.0034	112	0.0044	105	0.0040	71	0.8502	385	0.0275	269	0.0753	348
44	asusaics-000	0.0125	295	0.0209	300	0.0085	265	0.0134	267	0.0143	248	0.7189	362	0.0285	270	0.0295	171

Table 19: FNMR is the proportion of mated comparisons below a threshold set to achieve the FMR given in the header on the fourth row. FMR is the proportion of impostor comparisons at or above that threshold. The light grey values give rank over all algorithms in that column. The pink columns use only same-sex impostors; others are selected regardless of demographics. The exception, in the green column, uses “matched-covariates” i.e. impostors of the same sex, age group, and country of birth. The second pink column includes effects of extended ageing. Missing entries for border, visa, mugshot and wild images generally mean the algorithm did not run to completion. The VISA columns compare images described in section 2.1. The MUGSHOT columns compare images described in section 2.4. The VISA-BORDER column compare images described in section 2.2 with those of section 2.3. The BORDER column compares images described in section 2.3. The WILD columns compare images described in section 2.6.

	Algorithm	FALSE NON-MATCH RATE (FNMR)										LESS CONSTRAINED, NON-COOP.					
		CONSTRAINED, COOPERATIVE								WILD							
		Name	VISAMC	VISA	MUGSHOT	MUGSHOT12+YRS	VISA BORDER	BORDER	BORDER	WILD							
	FMR	0.0001	1E-06	1E-05	1E-05	1E-06	1E-06	1E-06	1E-05	0.0001							
45	asusaics-001	0.0125	293	0.0210	301	0.0085	267	0.0134	268	0.0143	249	0.7437	366	0.0289	272	0.0295	170
46	authenmetric-003	0.0036	107	0.0053	113	0.0039	140	0.0051	128	0.0095	192	0.9930	414	0.5932	395	0.0290	149
47	authenmetric-004	0.0027	67	0.0042	78	0.0033	103	0.0036	74	0.0083	166	0.9879	410	0.4058	383	0.0290	154
48	aware-005	0.0457	377	0.0643	375	0.0603	385	0.1094	387	0.0613	358	0.1075	283	0.0491	302	0.0314	217
49	aware-006	0.0487	378	0.0819	383	0.0529	379	0.1090	385	0.1011	378	0.1058	280	0.0502	305	0.0317	222
50	awiros-001	0.4044	429	0.4622	425	0.5530	425	0.6518	422	0.2008	394	0.1994	304	0.1386	345	0.5584	433
51	awiros-002	0.1990	410	0.2561	408	0.3319	412	0.4411	412	0.3821	410	0.9938	415	0.2634	364	0.0997	369
52	aximetria-001	0.0111	272	0.0186	286	0.0110	301	0.0148	284	0.0170	272	0.3928	331	0.2090	357	0.0409	288
53	ayftech-001	0.0946	397	0.1941	400	0.2438	408	0.3625	408	0.1558	386	0.1589	295	0.0936	335	0.0785	350
54	ayonix-000	0.4351	433	0.4872	427	0.6150	430	0.7510	430	0.6557	419	0.6361	354	0.4981	388	0.3635	421
55	beethedata-000	0.0127	298	0.0195	293	0.0092	278	0.0157	290	0.0171	274	0.0306	205	0.0204	243	0.0285	115
56	beyneai-000	0.0071	208	0.0107	215	0.0104	292	0.0131	265	0.0170	273	0.9837	407	0.6171	397	0.0597	329
57	biocube-001	0.5596	446	0.6834	445	0.7700	442	0.8712	440	0.8446	431	0.9661	403	0.7922	412	0.2377	403
58	bioidtechswiss-001	0.0054	158	0.0072	147	0.0069	230	0.0124	251	0.0060	124	0.0094	73	0.0065	63	0.0313	215
59	bioidtechswiss-002	0.0049	136	0.0067	138	0.0064	216	0.0116	243	0.0067	136	0.0117	99	0.0086	107	0.0279	55
60	bm-001	0.7431	455	0.9494	456	0.9586	451	0.9843	450	0.9049	439	0.9021	390	0.8395	418	0.9935	451
61	boetech-001	0.0662	389	0.0802	382	0.0493	377	0.0791	376	0.0682	363	0.1074	282	0.0758	325	0.1719	389
62	boetech-002	0.0535	383	0.0565	371	0.0114	309	0.0136	270	0.0403	340	0.0650	260	0.0606	316	0.1697	388
63	bresee-001	0.0085	236	0.0143	249	0.0086	270	0.0153	288	0.0108	211	0.0168	140	0.0115	156	0.0355	265
64	bresee-002	0.0079	225	0.0101	204	0.0065	220	0.0079	201	0.0129	232	0.0263	187	0.0224	253	0.0327	233
65	camvi-002	0.0125	294	0.0221	307	0.0089	275	0.0145	282	0.0142	246	0.2650	316	0.0166	211	0.0288	133
66	camvi-004	0.0171	332	0.0316	340	0.0042	150	0.0049	124	0.0097	198	0.6636	357	0.0141	187	0.0284	103
67	canon-003	0.0041	123	0.0059	122	0.0030	74	0.0040	91	0.0040	70	0.0073	40	0.0059	47	0.0274	21
68	canon-004	0.0052	151	0.0091	187	0.0033	106	0.0058	152	0.0037	60	0.0770	267	0.0494	303	0.0267	3
69	ceiec-003	0.0071	209	0.0107	212	0.0061	213	0.0079	204	0.0160	260	0.0316	208	0.0260	264	0.0308	207
70	ceiec-004	0.0038	114	0.0051	105	0.0045	163	0.0053	132	0.0062	131	0.3939	332	0.0104	138	0.0325	229
71	chosun-001	0.0525	381	0.0936	385	0.0742	390	0.1263	393	0.0978	377	1.0000	444	0.9354	423	0.4446	427
72	chosun-002	0.0390	372	0.0646	376	0.0339	369	0.0576	368	0.0455	350	0.6904	360	0.1746	354	0.0696	342
73	chtface-004	0.0046	131	0.0062	130	0.0052	186	0.0080	205	0.0088	175	0.0152	122	0.0106	141	0.0306	200
74	chtface-005	0.0033	92	0.0049	99	0.0029	71	0.0041	95	0.0044	85	0.0317	209	0.0066	66	0.0306	198
75	cist-001	0.0046	129	0.0065	135	0.0042	151	0.0063	165	0.9675	446	0.9997	430	0.9994	443	0.0407	285
76	clearviewai-000	0.0010	6	0.0019	14	0.0024	16	0.0028	29	0.0030	28	0.0058	19	0.0050	21	0.0271	7
77	closemi-001	0.0136	302	0.0163	267	0.0039	137	0.0054	136	0.0072	143	1.0000	438	0.0094	122	0.0318	223
78	cloudmatrix-001	0.0668	390	0.1141	389	0.0539	380	0.0905	380	0.3509	407	0.9819	406	0.9010	421	0.0636	333
79	cloudmatrix-002	0.0075	219	0.0113	224	0.0084	264	0.0120	245	0.9248	442	0.9997	429	0.9985	442	0.0358	267
80	cloudwalk-hr-003	0.0026	64	0.0041	67	0.0040	144	0.0058	151	0.0060	128	0.9992	422	0.0094	120	0.7206	439
81	cloudwalk-hr-004	0.0009	4	0.0018	10	0.0034	110	0.0028	34	0.0052	107	0.9992	423	0.0093	119	0.1625	386
82	cloudwalk-mt-005	0.0006	2	0.0009	3	0.0025	30	0.0022	7	0.0017	2	0.9286	395	0.5956	396	0.0287	128
83	cloudwalk-mt-006	0.0006	3	0.0006	1	0.0023	10	0.0019	1	0.0016	1	0.0032	1	0.0030	2	0.0290	151
84	codeline-000	0.0057	165	0.0079	167	0.0037	125	0.0053	135	0.2721	401	1.0000	439	0.9763	430	0.0273	15
85	cogent-006	0.0046	130	0.0059	126	0.0036	117	0.0047	115	0.0058	121	0.0113	94	0.0091	115	0.0343	248
86	cogent-007	0.0022	50	0.0038	62	0.0028	67	0.0031	45	0.0040	73	0.0082	56	0.0067	67	0.0438	301
87	cognitec-003	0.0038	112	0.0052	108	0.0054	195	0.0057	148	0.0225	299	0.0416	236	0.0388	289	0.0348	253
88	cognitec-004	0.0036	103	0.0053	112	0.0053	188	0.0056	145	0.0098	199	0.0202	165	0.0154	202	0.0352	263

Table 20: FNMR is the proportion of mated comparisons below a threshold set to achieve the FMR given in the header on the fourth row. FMR is the proportion of impostor comparisons at or above that threshold. The light grey values give rank over all algorithms in that column. The pink columns use only same-sex impostors; others are selected regardless of demographics. The exception, in the green column, uses “matched-covariates” i.e. impostors of the same sex, age group, and country of birth. The second pink column includes effects of extended ageing. Missing entries for border, visa, mugshot and wild images generally mean the algorithm did not run to completion. The VISA columns compare images described in section 2.1. The MUGSHOT columns compare images described in section 2.4. The VISA-BORDER column compare images described in section 2.2 with those of section 2.3. The BORDER column compares images described in section 2.3. The WILD columns compare images described in section 2.6.

Algorithm	FALSE NON-MATCH RATE (FNMR)																
	CONSTRAINED, COOPERATIVE								LESS CONSTRAINED, NON-COOP.								
	Name	VISAMC	VISA	MUGSHOT	MUGSHOT12+YRS	VISABORDER	BORDER	BORDER	WILD								
FMR	0.0001	1E-06	1E-05	1E-05	1E-06	1E-06	1E-06	1E-05	0.0001	0.0277	41						
89	cor-001	0.0075	218	0.0113	222	0.0055	199	0.0084	209	0.0091	181	0.0148	117	0.0092	117	0.0277	41
90	coretech-000	0.7699	457	1.0000	462	1.0000	457	-	1.0000	460	1.0000	456	1.0000	458	1.0000	457	
91	coretech-001	0.0052	147	0.0067	140	0.0083	262	0.0092	220	0.0346	332	0.1363	292	0.0252	261	0.0793	353
92	corsight-002	0.0053	152	0.0068	141	0.0030	79	0.0041	96	0.0039	68	0.0079	51	0.0054	37	0.0276	36
93	corsight-003	0.0026	63	0.0040	65	0.0028	64	0.0045	110	0.0035	56	0.0059	21	0.0046	17	0.0279	58
94	csc-002	0.0099	256	0.0132	239	0.0077	246	0.0142	279	0.0126	231	0.0195	158	0.0146	194	0.1779	391
95	csc-003	0.0053	153	0.0065	134	0.0037	126	0.0047	116	0.0074	145	0.0124	105	0.0112	150	0.1773	390
96	ctbcbank-000	0.0168	326	0.0250	321	0.0146	327	0.0224	324	0.0211	296	0.8964	388	0.3779	380	1.0000	463
97	ctbcbank-001	0.0155	319	0.0235	316	0.0148	332	0.0243	329	0.0207	293	0.9279	394	0.3469	375	1.0000	459
98	cubox-001	0.0064	191	0.0080	168	0.0037	123	0.0055	140	0.0060	125	0.0111	91	0.0077	86	0.0300	185
99	cubox-002	0.0034	99	0.0041	70	0.0025	27	0.0025	20	0.0033	44	0.0064	27	0.0058	45	0.0480	310
100	cudocommunication-001	0.4777	436	1.0000	463	0.4373	418	0.5360	415	1.0000	461	1.0000	454	1.0000	460	1.0000	458
101	cukee-001	0.0036	104	0.0045	88	0.0031	92	0.0046	113	0.0051	106	0.0095	76	0.0079	89	0.1492	381
102	cybercore-002	0.0092	246	0.0119	227	0.0049	175	0.0072	182	0.9105	441	1.0000	443	1.0000	448	0.5484	432
103	cybercore-003	0.0155	318	0.0164	268	0.0032	99	0.0033	58	0.0024	10	0.9719	404	0.8213	416	0.0705	344
104	cyberextruder-003	0.0109	270	0.0169	273	0.0071	235	0.0112	241	0.0165	266	0.0410	235	0.0272	268	0.0302	192
105	cyberextruder-004	0.0118	281	0.0181	283	0.0081	257	0.0133	266	0.0191	288	0.0329	212	0.0268	266	0.0679	339
106	cyberlink-009	0.0018	37	0.0027	36	0.0047	166	0.0046	111	0.0040	76	0.0086	65	0.0062	57	0.0280	75
107	cyberlink-010	0.0011	9	0.0019	15	0.0041	146	0.0041	92	0.0039	66	0.1829	299	0.0054	38	0.0280	69
108	dahua-006	0.0027	65	0.0039	63	0.0031	90	0.0039	89	0.0039	67	0.0067	32	0.0058	44	0.0280	67
109	dahua-007	0.0017	32	0.0023	22	0.0026	42	0.0032	50	0.0033	41	0.0060	22	0.0054	36	0.0278	46
110	daon-000	0.0095	252	0.0117	226	0.0068	225	0.0077	196	0.0092	185	0.0174	146	0.0137	181	0.0331	237
111	decatur-000	0.0714	391	0.1115	388	0.0608	386	0.1106	388	0.0866	370	1.0000	441	0.0714	323	0.0658	336
112	decatur-001	0.0424	374	0.0711	378	0.0237	352	0.0458	355	0.0447	348	1.0000	435	0.9969	439	0.0280	72
113	deepglint-004	0.0025	61	0.0034	50	0.0039	138	0.0061	162	0.0050	102	0.0091	69	0.0082	96	0.0285	119
114	deepglint-005	0.0052	148	0.0059	127	0.0030	75	0.0031	46	0.0033	46	0.7620	371	0.1535	349	0.0320	226
115	deepsea-001	0.0136	303	0.0215	303	0.0142	324	0.0214	321	0.0163	264	0.0250	183	0.0192	235	0.0347	251
116	deepsense-000	0.0145	310	0.0265	329	0.0113	307	0.0196	314	0.0151	253	0.0215	170	0.0129	173	0.0290	150
117	deepsense-001	0.0013	19	0.0019	12	0.0024	21	0.0025	18	0.0027	21	0.0115	98	0.0053	30	0.0285	113
118	dermalog-009	0.0067	196	0.0094	189	0.0051	183	0.0069	177	0.0116	223	0.0312	206	0.0177	220	0.0270	6
119	dermalog-010	0.0030	78	0.0041	68	0.0034	113	0.0037	79	0.0075	146	0.5181	344	0.2530	360	0.0275	23
120	dicio-001	0.5486	445	0.6442	439	0.7516	438	0.8607	436	0.8678	435	0.8268	381	0.7034	405	0.3605	420
121	didiglobalface-001	0.0055	161	0.0092	188	0.0030	78	0.0045	109	0.0088	173	0.0119	102	0.0085	105	0.0282	91
122	digitida-000	0.0967	398	0.1410	394	0.2596	409	0.3462	407	0.0293	324	0.0363	226	0.0212	247	0.0310	208
123	digitida-001	0.0224	348	0.0352	347	0.0330	367	0.0570	367	0.0109	213	0.0481	245	0.0123	168	0.0288	131
124	digitalbarriers-002	0.3360	425	0.3690	417	0.0877	394	0.1557	394	0.0971	376	0.0951	276	0.0497	304	0.0436	300
125	dps-000	0.0115	277	0.0176	279	0.0149	334	0.0185	309	0.0173	276	0.0275	194	0.0180	223	0.1067	371
126	dsk-000	0.1526	407	0.2169	405	0.3787	414	0.5426	417	0.3115	403	0.3089	321	0.1994	356	0.2201	399
127	einetworks-000	0.0099	257	0.0180	282	0.0088	274	0.0140	276	0.0130	233	0.0225	175	0.0147	196	0.0293	163
128	ekin-002	0.1168	401	0.2042	402	0.1530	404	0.2524	403	0.1777	391	0.2773	318	0.1347	343	0.4801	429
129	enface-000	0.0028	70	0.0049	101	0.0043	153	0.0072	180	0.0058	122	0.0150	119	0.0090	114	0.0290	157
130	enface-001	0.0072	213	0.0107	214	0.0071	232	0.0138	272	0.0068	138	0.0151	248	0.0094	123	0.0284	108
131	eocortex-000	0.3485	426	0.6943	446	0.1122	396	0.1574	395	0.2155	398	0.2257	311	0.1606	353	0.2546	410
132	ercacat-001	0.0036	105	0.0044	83	0.0033	102	0.0047	117	0.0106	208	0.0202	164	0.0184	228	0.0258	1

Table 21: FNMR is the proportion of mated comparisons below a threshold set to achieve the FMR given in the header on the fourth row. FMR is the proportion of impostor comparisons at or above that threshold. The light grey values give rank over all algorithms in that column. The pink columns use only same-sex impostors; others are selected regardless of demographics. The exception, in the green column, uses “matched-covariates” i.e. impostors of the same sex, age group, and country of birth. The second pink column includes effects of extended ageing. Missing entries for border, visa, mugshot and wild images generally mean the algorithm did not run to completion. The VISA columns compare images described in section 2.1. The MUGSHOT columns compare images described in section 2.4. The VISA-BORDER column compare images described in section 2.2 with those of section 2.3. The BORDER column compares images described in section 2.3. The WILD columns compare images described in section 2.6.

Algorithm	FALSE NON-MATCH RATE (FNMR)									
	CONSTRAINED, COOPERATIVE								LESS CONSTRAINED, NON-COOP.	
	Name	VISAMC	VISA	MUGSHOT	MUGSHOT12+YRS	VISABORDER	BORDER	BORDER	WILD	
FMR	0.0001	1E-06	1E-05	1E-05	1E-06	1E-06	1E-06	1E-05	0.0001	
133	euronovate-001	0.2786	419	0.3608	416	0.4489	420	0.6105	421	0.5010
134	expasoft-001	0.0328	367	0.0488	359	0.0211	346	0.0342	345	0.0629
135	expasoft-002	0.0170	329	0.0274	331	0.0787	393	0.0768	375	0.1629
136	f8-001	0.0249	351	0.0336	342	0.0178	339	0.0232	325	0.0303
137	f8-002	0.0340	369	0.0591	374	0.0213	348	0.0374	348	0.0452
138	faceonline-001	0.0269	356	0.0359	349	0.0387	372	0.0721	374	0.0246
139	faceonline-002	0.0121	286	0.0135	242	0.0033	104	0.0041	94	0.0037
140	facephi-000	0.0044	127	0.0059	123	0.0047	168	0.0057	149	0.0088
141	facesoft-000	0.0085	237	0.0112	221	0.0064	218	0.0107	236	0.0091
142	facetag-000	0.2836	420	0.4081	422	0.2933	411	0.4303	411	0.3448
143	facetag-002	0.0098	255	0.0147	252	0.0064	219	0.0110	238	0.0116
144	facex-001	1.0000	462	1.0000	460	1.0000	456	-	1.0000	455
145	facex-002	0.0803	393	0.1404	393	0.1283	399	0.1979	400	0.1440
146	farfaces-001	0.4890	439	0.5860	438	0.5650	426	0.7268	428	0.8015
147	fiberhome-nanjing-003	0.0090	240	0.0139	246	0.0082	259	0.0144	280	0.0110
148	fiberhome-nanjing-004	0.0037	111	0.0056	120	0.0031	87	0.0043	102	0.0043
149	fincore-000	0.0309	365	0.0502	361	0.0281	359	0.0510	362	0.0521
150	firstcreditKZ-001	0.0024	59	0.0034	48	0.0024	25	0.0024	14	0.0034
151	frpkauai-001	0.0023	54	0.0035	55	0.0026	36	0.0030	42	0.0040
152	fujitsulab-002	0.0091	243	0.0124	234	0.0105	293	0.0156	289	0.0169
153	fujitsulab-003	0.0045	128	0.0065	136	0.0057	204	0.0083	207	0.0080
154	g42-intelibrain-001	0.0006	1	0.0009	2	0.0037	124	0.0044	106	0.0030
155	geo-002	0.0171	333	0.0187	288	0.0035	116	0.0051	130	0.0064
156	geo-004	0.0030	76	0.0041	71	0.0025	33	0.0030	39	0.0035
157	glory-004	0.0077	222	0.0123	231	0.0074	243	0.0098	230	0.0122
158	glory-005	0.0056	162	0.0076	155	0.0054	196	0.0072	183	0.0075
159	gorilla-007	0.0074	217	0.0111	220	0.0065	221	0.0126	255	0.0100
160	gorilla-008	0.0058	173	0.0091	186	0.0049	174	0.0079	203	0.0079
161	graymatics-001	0.1039	399	0.1620	397	0.1344	401	0.1917	398	0.1648
162	griaule-000	0.0071	210	0.0099	200	0.0050	178	0.0072	179	0.0160
163	griaule-001	0.0057	163	0.0078	162	0.0045	162	0.0065	172	0.0070
164	hertasecurity-001	0.0249	352	0.0309	338	0.0105	294	0.0161	292	0.0245
165	hertasecurity-002	0.0206	344	0.0315	339	0.0060	210	0.0078	199	0.0253
166	hik-001	0.0096	254	0.0125	235	0.0093	283	0.0164	297	0.0108
167	hisign-001	0.0036	106	0.0050	102	0.0034	108	0.0046	112	0.0079
168	hisign-002	0.0029	72	0.0044	84	0.0027	57	0.0032	52	0.0028
169	hyperverge-002	0.0050	137	0.0066	137	0.0035	115	0.0051	127	0.0062
170	hyperverge-003	0.0019	39	0.0030	41	0.0025	28	0.0029	37	0.0027
171	hzailiu-002	0.0051	142	0.0072	146	0.0038	133	0.0055	142	0.0040
172	hzailiu-003	0.0178	335	0.0291	336	0.0031	93	0.0042	100	0.0035
173	icm-003	0.0138	306	0.0222	309	0.0149	333	0.0282	336	0.0227
174	icm-004	0.0079	226	0.0120	228	0.0074	241	0.0107	235	0.0091
175	ichttc-000	0.0260	354	0.0396	354	0.0207	345	0.0339	344	0.0291
176	id3-006	0.0072	214	0.0103	207	0.0049	176	0.0074	188	0.0095

Table 22: FNMR is the proportion of mated comparisons below a threshold set to achieve the FMR given in the header on the fourth row. FMR is the proportion of impostor comparisons at or above that threshold. The light grey values give rank over all algorithms in that column. The pink columns use only same-sex impostors; others are selected regardless of demographics. The exception, in the green column, uses “matched-covariates” i.e. impostors of the same sex, age group, and country of birth. The second pink column includes effects of extended ageing. Missing entries for border, visa, mugshot and wild images generally mean the algorithm did not run to completion. The VISA columns compare images described in section 2.1. The MUGSHOT columns compare images described in section 2.4. The VISA-BORDER column compare images described in section 2.2 with those of section 2.3. The BORDER column compares images described in section 2.3. The WILD columns compare images described in section 2.6.

Algorithm	Name	FALSE NON-MATCH RATE (FNMR)								LESS CONSTRAINED, NON-COOP.							
		CONSTRAINED, COOPERATIVE															
		VISAMC	VISA	MUGSHOT	MUGSHOT12+YRS	VISA BORDER	BORDER	BORDER	WILD								
FMR		0.0001	1E-06	1E-05	1E-05	1E-06	1E-06	1E-05	0.0001								
177	id3-008	0.0039	115	0.0055	117	0.0032	97	0.0042	98	0.0081	160	0.0155	128	0.0134	176	0.8856	443
178	idemia-008	0.0023	55	0.0032	44	0.0023	12	0.0028	28	0.0034	49	0.0067	31	0.0056	40	0.0290	153
179	idemia-009	0.0022	48	0.0030	42	0.0022	5	0.0023	12	0.0023	9	0.0046	6	0.0039	8	0.0285	112
180	iit-002	0.0111	274	0.0177	281	0.0085	266	0.0140	275	0.0193	289	0.0332	215	0.0260	263	0.1373	379
181	iit-003	0.0082	232	0.0151	259	0.0053	190	0.0084	210	0.0122	227	0.0199	162	0.0137	180	0.0407	286
182	imds-software-001	0.0126	296	0.0228	310	0.0130	320	0.0221	323	0.0231	302	0.0469	243	0.0199	242	0.0365	271
183	imperial-000	0.0067	197	0.0108	217	0.0080	254	0.0134	269	0.0087	171	0.0581	252	0.0102	133	0.0281	80
184	imperial-002	0.0058	171	0.0081	170	0.0055	198	0.0085	213	0.0083	164	0.0157	129	0.0103	134	0.0273	17
185	incode-010	0.0041	122	0.0063	132	0.0028	68	0.0043	101	0.0047	96	0.0077	48	0.0061	53	0.0296	178
186	incode-011	0.0032	82	0.0044	82	0.0026	44	0.0034	63	0.0032	38	0.0359	224	0.0140	185	0.0295	173
187	infocert-001	0.0105	265	0.0172	275	0.0078	249	0.0125	252	0.0159	257	0.1573	294	0.0565	312	0.0307	203
188	innefulabs-000	0.0122	288	0.0199	295	0.0112	306	0.0197	315	0.0222	298	0.0372	229	0.0271	267	0.0348	254
189	innovativetechnologyltd-001	0.0578	386	0.0938	386	0.0501	378	0.0981	381	0.0592	357	0.0779	268	0.0422	293	0.0449	305
190	innovativetechnologyltd-002	0.0451	376	0.0716	379	0.0541	381	0.1009	383	0.0506	353	0.0682	261	0.0371	287	0.0804	355
191	innovatrics-007	0.0040	120	0.0054	115	0.0057	203	0.0078	197	0.0079	152	0.0123	103	0.0088	111	0.0282	93
192	innovatrics-008	0.0047	133	0.0064	133	0.0038	131	0.0052	131	0.0053	109	0.0088	66	0.0069	72	0.0287	126
193	insightface-001	0.0009	5	0.0014	4	0.0027	49	0.0024	13	0.0035	54	0.0070	35	0.0065	61	0.0279	61
194	insightface-003	0.0015	24	0.0021	17	0.0045	161	0.0034	64	0.1298	380	1.0000	463	0.9407	424	0.0277	39
195	inspur-000	0.0060	184	0.0078	161	0.7415	437	0.9093	445	0.2838	402	0.9996	426	0.9976	440	0.0283	99
196	intellicloudai-001	0.0142	308	0.0234	314	0.0092	280	0.0145	281	0.0162	262	0.0371	228	0.0171	215	0.0409	289
197	intellicloudai-002	0.0059	178	0.0085	176	0.0060	211	0.0069	178	0.0108	210	0.2477	315	0.0171	214	0.0303	193
198	intellifusion-001	0.0072	211	0.0094	193	0.0056	202	0.0085	214	0.0111	217	0.0212	168	0.0143	190	0.0289	143
199	intellifusion-002	0.0059	176	0.0077	156	0.0040	143	0.0074	187	0.0085	168	0.5352	345	0.0104	139	0.0305	197
200	intellivision-003	0.1177	402	0.2006	401	0.0760	391	0.1244	392	0.1069	379	0.1431	293	0.0839	328	0.0829	359
201	intellivision-004	0.0271	357	0.0559	370	0.0294	364	0.0503	361	0.0327	331	0.0461	241	0.0293	275	0.0645	335
202	intellivix-001	0.0064	192	0.0087	178	0.0046	164	0.0063	166	0.0072	142	0.9233	392	0.7856	411	0.0340	247
203	intellivix-002	0.0062	185	0.0085	175	0.0039	136	0.0056	144	0.0060	127	0.3464	325	0.0857	331	0.0289	144
204	intelresearch-004	0.0025	62	0.0035	52	0.0032	95	0.0038	83	0.0049	101	0.0094	72	0.0072	75	0.0290	155
205	intelresearch-005	0.0016	27	0.0023	21	0.0028	61	0.0034	61	0.0042	83	0.0084	58	0.0066	65	0.0290	152
206	intema-000	0.0012	13	0.0017	8	0.0023	6	0.0022	8	0.0022	8	0.0172	143	0.0061	52	0.0279	60
207	intsysmsu-001	0.9543	460	0.9888	458	0.9923	452	-	0.9977	447	0.9955	416	0.9892	432	0.7871	443	
208	intsysmsu-002	0.0130	299	0.0254	323	0.0137	322	0.0267	334	0.0160	259	0.0267	190	0.0145	193	0.0289	147
209	ionetworks-000	0.0060	183	0.0087	182	0.0044	155	0.0058	154	0.0080	159	0.0144	115	0.0112	148	0.0319	224
210	iqface-000	0.0091	245	0.0143	247	0.0075	244	0.0110	239	0.0171	275	0.2234	309	0.0359	283	0.0381	276
211	iqface-003	0.0058	170	0.0079	165	0.0051	184	0.0058	155	0.0104	206	0.0200	163	0.0193	236	0.0402	281
212	irex-000	0.0052	146	0.0099	201	0.0056	201	0.0083	208	0.0137	242	0.0163	136	0.0078	87	0.0285	114
213	isap-001	0.5092	441	0.6588	442	0.6899	433	0.7978	431	0.7200	420	0.7253	363	0.5373	391	0.1931	394
214	isap-002	0.0114	276	0.0186	287	0.0087	272	0.0151	287	0.0156	256	0.5134	342	0.0333	276	0.0354	264
215	isityou-000	0.5682	447	0.7033	448	1.0000	461	-	1.0000	458	1.0000	448	1.0000	454	1.0000	454	454
216	isystems-001	0.0149	315	0.0245	319	0.0138	323	0.0210	319	0.0209	295	0.0332	214	0.0223	252	0.0524	321
217	isystems-002	0.0118	279	0.0182	284	0.0111	303	0.0162	295	0.0166	267	0.0284	200	0.0195	238	0.0516	315
218	itmo-007	0.0080	228	0.0125	236	0.0107	296	0.0185	307	0.0167	269	0.0222	173	0.0144	192	0.0300	186
219	itmo-008	0.0090	241	0.0150	256	0.0058	206	0.0059	157	0.0187	284	0.0355	223	0.0339	277	0.1498	382
220	ivacognitive-001	0.0189	338	0.0351	346	0.0123	316	0.0235	326	0.0198	291	0.0274	193	0.0155	203	0.0296	175

Table 23: FNMR is the proportion of mated comparisons below a threshold set to achieve the FMR given in the header on the fourth row. FMR is the proportion of impostor comparisons at or above that threshold. The light grey values give rank over all algorithms in that column. The pink columns use only same-sex impostors; others are selected regardless of demographics. The exception, in the green column, uses “matched-covariates” i.e. impostors of the same sex, age group, and country of birth. The second pink column includes effects of extended ageing. Missing entries for border, visa, mugshot and wild images generally mean the algorithm did not run to completion. The VISA columns compare images described in section 2.1. The MUGSHOT columns compare images described in section 2.4. The VISA-BORDER column compare images described in section 2.2 with those of section 2.3. The BORDER column compares images described in section 2.3. The WILD columns compare images described in section 2.6.

	Algorithm	FALSE NON-MATCH RATE (FNMR)										LESS CONSTRAINED, NON-COOP.							
		CONSTRAINED, COOPERATIVE								WILD									
		Name	VISAMC	VISA	MUGSHOT	MUGSHOT12+YRS	VISABORDER	BORDER	BORDER										
		FMR	0.0001	1E-06	1E-05	1E-05	1E-06	1E-06	1E-05	0.0001									
221	iws-000	0.4824	437	0.5801	435	0.6859	432	0.8155	432	0.8251	428	0.7756	373	0.6400	400	0.3251	418		
222	jaakit-001	0.5830	448	0.7146	449	0.8173	444	0.8893	442	0.8950	438	0.8387	384	0.7091	406	0.5849	435		
223	kakao-007	0.0019	41	0.0028	37	0.0024	15	0.0026	22	0.0033	43	0.0061	23	0.0053	31	0.0427	295		
224	kakao-008	0.0011	11	0.0018	11	0.0023	7	0.0023	10	0.0021	7	0.0041	4	0.0035	3	0.0427	296		
225	kakaopay-001	0.0152	317	0.0252	322	0.0145	326	0.0270	335	0.0232	303	0.0344	220	0.0194	237	0.0416	292		
226	kasikornlabs-000	0.0112	275	0.0184	285	0.0086	268	0.0137	271	0.0130	235	0.0225	174	0.0148	198	0.0674	337		
227	kasikornlabs-001	0.0138	305	0.0206	297	0.0087	271	0.0139	274	0.0142	245	0.0236	178	0.0171	213	0.0729	346		
228	kedacom-000	0.0055	159	0.0081	171	0.0111	305	0.0120	246	0.0415	342	0.0966	278	0.0686	320	0.2511	407		
229	kiwitech-000	0.0076	221	0.0105	210	0.0081	258	0.0128	261	0.0096	193	0.0163	135	0.0101	130	0.0279	63		
230	kneron-003	0.0542	385	0.0902	384	0.0346	370	0.0562	365	0.0919	373	0.1251	288	0.0973	336	0.3053	415		
231	kneron-005	0.0157	320	0.0259	325	0.0126	319	0.0212	320	0.0406	341	0.0693	264	0.0542	310	0.0471	308		
232	knowutech-000	0.0039	116	0.0055	118	0.0028	70	0.0042	97	0.0042	80	0.0077	46	0.0059	49	0.0271	9		
233	kookmin-002	0.0054	156	0.0077	158	0.0043	152	0.0065	171	0.0123	229	0.7591	370	0.0198	241	0.0285	117		
234	krungthai-002	0.0105	267	0.0161	264	0.0091	277	0.0141	277	0.7350	422	0.9889	411	0.9605	427	0.0620	331		
235	kuke3d-001	0.0058	167	0.0104	209	0.0083	261	0.0093	222	0.0270	319	0.9901	412	0.8341	417	0.0404	282		
236	kuke3d-002	0.0077	223	0.0135	243	0.0069	229	0.0098	229	0.0111	216	1.0000	445	1.0000	451	0.0316	220		
237	lebentech-000	0.5940	449	0.7032	447	0.8854	448	0.9511	447	0.9089	440	0.9970	417	0.9861	431	0.6250	436		
238	lemalabs-001	0.0111	273	0.0175	278	0.0088	273	0.0142	278	0.0143	247	0.0228	176	0.0140	184	0.0281	77		
239	lineclova-001	0.0025	60	0.0040	64	0.0026	48	0.0034	65	0.0045	90	0.4127	334	0.0080	93	0.0283	101		
240	lineclova-002	0.0021	46	0.0035	54	0.0025	26	0.0027	26	0.0041	77	0.0086	62	0.0072	76	0.0279	53		
241	lookman-002	0.0297	362	0.0547	369	0.0339	368	0.0562	364	0.0614	359	0.0960	277	0.0790	326	0.2640	412		
242	lookman-004	0.0074	216	0.0099	202	0.0124	318	0.0149	285	0.0430	345	0.0866	271	0.0694	321	0.2516	408		
243	luxand-000	0.2056	411	0.2814	410	0.4053	416	0.5365	416	0.3497	406	0.3743	329	0.2605	362	0.2222	401		
244	mantra-000	0.0037	109	0.0052	110	0.0054	193	0.0056	146	0.0097	197	0.0181	151	0.0151	201	0.0350	257		
245	maxvision-001	0.0305	364	0.0528	367	0.1028	395	0.1921	399	0.0650	362	0.3001	320	0.1553	351	0.0539	322		
246	maxvision-002	0.0070	203	0.0107	213	0.0061	212	0.0093	221	0.0080	156	0.5726	348	0.2943	369	0.0372	273		
247	megvii-005	0.0010	7	0.0015	5	0.0026	41	0.0031	49	0.0019	4	0.0500	247	0.0057	41	0.0292	161		
248	megvii-006	0.0011	8	0.0016	6	0.0026	45	0.0033	57	0.0025	14	0.0050	10	0.0048	20	0.0296	176		
249	meituau-001	0.0164	325	0.1886	399	0.0025	29	0.0026	21	0.0030	31	0.0074	41	0.0051	23	0.1157	375		
250	meituau-002	0.0017	31	0.0025	27	0.0024	18	0.0023	9	0.0024	13	0.0067	33	0.0044	16	0.0312	214		
251	meiya-001	0.0171	331	0.0275	332	0.0159	336	0.0261	333	0.0311	328	0.2250	310	0.0245	259	0.0363	270		
252	mendaxiatech-000	0.0027	66	0.0036	56	0.0029	72	0.0036	75	0.0031	36	0.0057	18	0.0051	24	0.0275	26		
253	metsakuurcompany-001	0.0068	200	0.0087	179	0.0068	227	0.0078	198	0.0095	191	0.8972	389	0.5635	392	0.0351	259		
254	metsakuurcompany-002	0.0048	134	0.0071	143	0.0030	81	0.0043	104	0.0032	40	0.2059	307	0.0665	319	0.0408	287		
255	microfocus-001	0.4482	434	0.5524	434	0.7256	436	0.8416	435	0.7301	421	0.6926	361	0.5180	390	0.2567	411		
256	microfocus-002	0.3605	427	0.5057	429	0.5783	428	0.7223	427	0.5909	416	0.5963	351	0.4160	384	0.1582	384		
257	minivision-000	0.0033	88	0.0048	96	0.0038	130	0.0049	121	0.0055	113	0.0094	75	0.0079	91	0.0273	14		
258	mobai-000	0.0360	371	0.0439	358	0.0372	371	0.0700	372	0.0367	336	0.0939	274	0.0795	327	0.2640	413		
259	mobai-001	0.0199	342	0.0219	306	0.0047	169	0.0061	159	0.0093	188	0.0174	145	0.0138	183	0.1045	370		
260	mobbl-001	0.3208	421	0.4375	423	0.5680	427	0.7193	426	0.6282	417	0.5783	349	0.3984	382	0.1866	393		
261	mobbl-003	0.0087	238	0.0134	241	0.0062	214	0.0087	216	0.0099	200	0.0197	159	0.0122	167	0.0312	212		
262	mopipintech-000	0.0090	242	0.0149	255	0.0039	142	0.0057	147	0.0115	221	0.0465	242	0.0182	225	0.0315	219		
263	moreedian-000	0.3874	428	0.4912	428	0.9988	454	-				0.9990	449	0.9999	432	0.9998	445	0.4788	428
264	mukh-001	0.0170	330	0.0285	334	0.0225	350	0.0405	351	0.0272	320	0.0950	275	0.0291	274	0.0301	188		

Table 24: FNMR is the proportion of mated comparisons below a threshold set to achieve the FMR given in the header on the fourth row. FMR is the proportion of impostor comparisons at or above that threshold. The light grey values give rank over all algorithms in that column. The pink columns use only same-sex impostors; others are selected regardless of demographics. The exception, in the green column, uses “matched-covariates” i.e. impostors of the same sex, age group, and country of birth. The second pink column includes effects of extended ageing. Missing entries for border, visa, mugshot and wild images generally mean the algorithm did not run to completion. The VISA columns compare images described in section 2.1. The MUGSHOT columns compare images described in section 2.4. The VISA-BORDER column compare images described in section 2.2 with those of section 2.3. The BORDER column compares images described in section 2.3. The WILD columns compare images described in section 2.6.

	Algorithm	FALSE NON-MATCH RATE (FNMR)										LESS CONSTRAINED, NON-COOP.					
		CONSTRAINED, COOPERATIVE															
		Name	VISAMC	VISA	MUGSHOT	MUGSHOT12+YRS	VISABORDER	BORDER	BORDER	WILD							
	FMR	0.0001	1E-06	1E-05	1E-05	1E-05	1E-06	1E-06	1E-05	0.0001							
265	multimodality-000	0.0034	97	0.0047	94	0.0036	122	0.0044	107	0.0077	150	0.9976	419	0.4456	386	0.0287	127
266	multimodality-001	0.0029	74	0.0042	75	0.0031	85	0.0035	67	0.0038	63	0.0071	37	0.0059	48	0.0281	79
267	mvision-001	0.0191	339	0.0233	312	0.0204	344	0.0356	346	0.0198	292	0.0337	217	0.0242	258	0.0431	297
268	nazhai-000	0.0040	117	0.0059	125	0.0036	118	0.0048	119	0.0057	118	0.0125	106	0.0083	100	0.0275	28
269	neosystems-004	0.0279	359	0.0495	360	0.0289	361	0.0585	369	0.0439	347	0.9621	401	0.1296	341	0.0333	240
270	neosystems-005	0.0060	180	0.0077	157	0.0045	160	0.0064	169	0.0062	129	0.5811	350	0.0117	158	0.0278	49
271	netbridge-tech-001	0.4749	435	0.6599	443	0.4438	419	0.5676	418	0.4491	412	1.0000	437	0.9541	426	0.1098	374
272	netbridge-tech-002	0.0101	260	0.0166	270	0.0077	247	0.0127	258	0.0133	238	0.8215	379	0.0523	308	0.0351	260
273	neurotechnology-013	0.0032	85	0.0045	89	0.0026	47	0.0036	71	0.0037	61	0.0068	34	0.0052	29	0.0278	47
274	neurotechnology-015	0.0022	51	0.0036	58	0.0024	14	0.0028	31	0.0030	29	0.0052	12	0.0041	11	0.0276	33
275	rhn-002	0.0068	199	0.0096	194	0.0057	205	0.0087	218	0.0136	241	0.0253	185	0.0186	232	0.0302	190
276	rhn-003	0.0033	89	0.0048	98	0.0027	54	0.0038	82	0.0036	59	0.0198	160	0.0071	74	0.0285	120
277	nodeflux-002	0.0186	337	0.0340	343	0.0261	357	0.0451	354	0.0548	355	1.0000	442	1.0000	450	0.0299	182
278	notiontag-001	0.6846	453	0.8006	453	0.3955	415	0.5247	414	0.8669	433	0.8313	383	0.6362	399	0.2221	400
279	notiontag-002	0.0066	194	0.0089	183	0.0045	159	0.0061	160	0.0077	151	0.0137	111	0.0104	137	0.0299	181
280	nsensecorp-003	0.0251	353	0.0295	337	0.0212	347	0.0305	339	0.0131	236	0.2139	308	0.0141	188	0.0872	362
281	nsensecorp-004	0.1370	406	0.1397	392	0.0066	223	0.0094	224	1.0000	457	1.0000	447	1.0000	453	0.0805	356
282	ntechlab-011	0.0012	16	0.0019	13	0.0024	19	0.0028	35	0.0029	27	0.0055	14	0.0047	19	0.0288	136
283	ntechlab-012	0.0011	10	0.0016	7	0.0023	13	0.0030	40	0.0026	16	0.0050	11	0.0043	13	0.0280	73
284	omface-000	0.2573	417	0.3835	420	0.3590	413	0.4903	413	0.3956	411	0.5003	341	0.2595	361	0.2400	404
285	omface-001	0.0137	304	0.0212	302	0.0114	311	0.0187	310	0.0174	278	1.0000	453	0.0214	249	0.0789	352
286	omnigarde-001	0.0168	327	0.0260	326	0.0203	343	0.0402	349	0.0243	311	0.0327	211	0.0177	218	0.0288	134
287	omnigarde-002	0.0033	95	0.0046	92	0.0027	58	0.0039	85	0.0041	78	0.0076	44	0.0059	51	0.0278	51
288	openface-001	0.1804	408	0.2921	411	0.2878	410	0.3906	410	0.2054	396	0.2338	313	0.1549	350	0.2445	405
289	oz-003	0.0095	253	0.0143	248	0.0054	194	0.0077	195	0.0096	195	0.0175	148	0.0118	161	0.0288	139
290	oz-004	0.0033	94	0.0049	100	0.0038	132	0.0055	139	0.0081	161	0.0163	137	0.0142	189	0.0329	235
291	palit-000	0.0062	187	0.0084	174	0.0039	135	0.0055	138	0.0055	114	0.4610	338	0.2468	359	0.0280	71
292	palit-001	0.0050	138	0.0068	142	0.0032	100	0.0047	118	0.0045	89	0.0110	90	0.0058	46	0.0287	129
293	pangiam-000	0.0031	80	0.0043	80	0.0026	37	0.0030	44	0.0038	64	0.0071	38	0.0061	56	0.0424	294
294	papago-001	0.0067	198	0.0096	197	0.0051	185	0.0077	194	0.0071	140	0.0126	107	0.0086	108	0.0816	358
295	papsav1923-001	0.0078	224	0.0130	238	0.0068	226	0.0105	234	0.0119	224	0.0221	172	0.0136	178	0.0293	164
296	papsav1923-002	0.0021	47	0.0034	49	0.0026	38	0.0030	43	0.0048	97	0.0093	71	0.0086	106	0.0312	213
297	paravision-008	0.0018	35	0.0025	28	0.0024	17	0.0025	17	0.0036	58	0.0070	36	0.0063	59	0.0279	59
298	paravision-010	0.0012	17	0.0021	16	0.0022	4	0.0021	5	0.0027	20	0.0055	15	0.0050	22	0.0288	140
299	pensees-001	0.0087	239	0.0133	240	0.0071	234	0.0122	250	0.0145	250	0.0252	184	0.0195	239	0.0283	98
300	pixelall-008	0.0015	23	0.0023	23	0.0034	114	0.0049	120	0.0031	35	0.0057	17	0.0052	25	0.0278	44
301	pixelall-009	0.0018	36	0.0025	29	0.0024	22	0.0026	23	0.0031	37	0.3475	326	0.0053	32	0.0276	31
302	psl-010	0.0017	33	0.0035	53	0.0023	8	0.0025	15	0.0035	53	0.0104	82	0.0052	28	0.0282	84
303	psl-011	0.0013	18	0.0026	31	0.0021	1	0.0021	4	0.0024	11	0.0047	7	0.0035	4	0.0285	116
304	ptakuratsatu-000	0.0060	179	0.0089	184	0.0070	231	0.0104	233	0.0096	196	0.0152	124	0.0100	127	0.0284	104
305	pxl-001	0.0488	379	0.0752	381	0.0586	384	0.1087	384	0.0946	374	0.1065	281	0.0625	317	0.1088	372
306	pyramid-000	0.0136	301	0.0233	313	0.0117	313	0.0192	312	0.0185	283	0.0322	210	0.0206	245	0.0304	196
307	qazbs-000	0.0058	168	0.0083	172	0.0046	165	0.0072	181	0.0130	234	0.0244	181	0.0196	240	0.0297	180
308	qnap-001	0.0148	312	0.0215	304	0.0103	289	0.0162	294	0.0183	282	0.0301	202	0.0186	231	0.0360	269

Table 25: FNMR is the proportion of mated comparisons below a threshold set to achieve the FMR given in the header on the fourth row. FMR is the proportion of impostor comparisons at or above that threshold. The light grey values give rank over all algorithms in that column. The pink columns use only same-sex impostors; others are selected regardless of demographics. The exception, in the green column, uses “matched-covariates” i.e. impostors of the same sex, age group, and country of birth. The second pink column includes effects of extended ageing. Missing entries for border, visa, mugshot and wild images generally mean the algorithm did not run to completion. The VISA columns compare images described in section 2.1. The MUGSHOT columns compare images described in section 2.4. The VISA-BORDER column compare images described in section 2.2 with those of section 2.3. The BORDER column compares images described in section 2.3. The WILD columns compare images described in section 2.6.

Algorithm	FALSE NON-MATCH RATE (FNMR)																
	CONSTRAINED, COOPERATIVE																
	Name	VISAMC	VISA	MUGSHOT	MUGSHOT12+YRS	VISABORDER	BORDER	BORDER	WILD								
FMR	0.0001	1E-06	1E-05	1E-05	1E-06	1E-06	1E-05	1E-05	0.0001								
309	qnap-002	0.0122	287	0.0191	290	0.0075	245	0.0095	227	0.0146	251	0.0281	199	0.0184	227	0.0352	262
310	quantasoft-003	0.0081	231	0.0113	223	0.0056	200	0.0076	191	0.0091	183	0.0161	134	0.0107	144	0.0414	291
311	rankone-012	0.0043	125	0.0058	121	0.0031	94	0.0038	81	0.0047	94	0.0081	54	0.0065	62	0.0358	266
312	rankone-013	0.0028	68	0.0041	69	0.0026	39	0.0033	55	0.0028	24	0.0055	16	0.0040	9	0.0291	159
313	realnetworks-006	0.0040	118	0.0056	119	0.8657	447	-		0.0059	123	0.0112	92	0.0085	104	0.1790	392
314	realnetworks-007	0.0031	81	0.0051	106	0.0028	66	0.0035	68	0.0048	98	0.0091	68	0.0074	82	0.0279	54
315	regula-000	0.0184	336	0.0376	352	0.0103	290	0.0185	306	0.0120	225	0.9983	421	0.0231	254	0.0273	16
316	regula-001	0.0072	212	0.0107	216	0.0102	287	0.0179	304	0.0123	230	0.0333	216	0.0174	216	0.0295	168
317	remarkai-001	0.0144	309	0.0256	324	0.0102	286	0.0159	291	0.0162	263	0.0582	253	0.0185	229	0.0308	206
318	remarkai-003	0.0047	132	0.0063	131	0.0033	105	0.0049	122	0.0054	110	0.0100	80	0.0072	78	0.0275	29
319	rendip-000	0.0055	160	0.0077	159	0.0048	172	0.0060	158	0.0080	157	0.0142	114	0.0110	147	0.0433	299
320	revealmedia-005	0.0050	139	0.0074	153	0.0050	179	0.0068	176	0.0075	148	0.0124	104	0.0104	140	0.3960	423
321	revealmedia-006	0.0040	119	0.0067	139	0.0041	148	0.0056	143	0.0056	115	0.0085	61	0.0068	69	0.0278	50
322	rokid-000	0.0093	249	0.0145	250	0.0073	240	0.0102	232	0.0164	265	0.0280	196	0.0214	248	0.0857	361
323	rokid-001	0.0105	266	0.0162	265	0.0094	285	0.0163	296	0.0181	279	0.0276	195	0.0165	210	0.0325	230
324	s1-005	0.0024	57	0.0036	57	0.0025	35	0.0029	38	0.0026	17	0.0048	8	0.0038	7	0.0359	268
325	s1-006	0.0029	73	0.0044	85	0.0028	62	0.0033	53	0.0035	52	0.0073	39	0.0044	15	0.0367	272
326	saffe-001	0.4339	432	0.5261	431	0.7539	440	0.8736	441	0.7977	425	0.9810	405	0.7435	409	0.3887	422
327	saffe-002	0.0119	282	0.0206	296	0.0107	299	0.0177	302	0.0244	312	0.9998	431	0.2785	366	0.0308	205
328	samsungsds-001	0.0015	25	0.0026	33	0.0023	11	0.0023	11	0.0024	12	0.1660	296	0.0536	309	0.0282	83
329	samsungsds-002	0.0017	34	0.0027	35	0.0023	9	0.0022	6	0.0021	6	0.0043	5	0.0036	6	0.0283	96
330	samttech-001	0.0197	341	0.0365	350	0.0146	330	0.0241	328	0.0238	310	0.0394	232	0.0251	260	0.0337	241
331	scanovate-002	0.0175	334	0.0355	348	0.0146	328	0.0286	337	0.0269	318	0.0301	201	0.0178	221	0.0301	189
332	scanovate-003	0.0054	155	0.0080	169	0.0054	191	0.0072	185	0.0312	329	0.0599	254	0.0568	313	0.0283	97
333	sdc-000	0.0303	363	0.0526	365	0.0572	383	0.1094	386	0.0867	371	0.6230	352	0.3682	378	0.1201	378
334	securifai-004	0.0136	300	0.0192	291	0.0064	217	0.0099	231	0.0115	220	0.0272	191	0.0127	170	0.0347	250
335	securifai-005	0.0125	292	0.0190	289	0.0080	255	0.0126	256	0.0134	239	0.9861	408	0.9205	422	0.0329	234
336	sensetime-006	0.0014	21	0.0024	25	0.0021	2	0.0020	2	0.0021	5	0.0040	3	0.0036	5	0.0272	12
337	sensetime-007	0.0012	12	0.0022	18	0.0021	3	0.0020	3	0.0018	3	0.0034	2	0.0029	1	0.0280	68
338	sertis-000	0.0118	280	0.0208	298	0.0080	252	0.0127	257	0.0110	215	0.0176	149	0.0114	153	0.0285	118
339	sertis-002	0.0049	135	0.0061	128	0.0039	141	0.0061	163	0.0055	112	0.0099	79	0.0070	73	0.0281	78
340	seventhsense-001	0.0034	98	0.0047	95	0.0025	34	0.0031	48	0.0029	26	0.0338	218	0.0109	146	0.0279	56
341	seventhsense-002	0.0036	108	0.0050	103	0.0028	65	0.0036	72	0.0035	51	0.0811	269	0.0183	226	0.0278	48
342	shaman-000	0.9297	459	0.9774	457	0.9990	455	-		0.9999	450	1.0000	440	0.9999	447	0.9575	449
343	shaman-001	0.3346	424	0.4616	424	0.2368	407	0.3723	409	0.3574	408	0.3527	327	0.2304	358	0.1498	383
344	shu-002	-	0.0079	166	0.0146	329	0.0308	340	1.0000	451	0.0183	152	0.0115	155	0.0284	105	
345	shu-003	0.0028	69	0.0041	74	0.0050	177	0.0088	219	0.0081	162	0.0133	110	0.0094	121	0.0283	102
346	siat-002	0.0091	244	0.0126	237	0.0109	300	0.0190	311	0.0276	321	0.0516	249	0.0464	301	0.0520	317
347	siat-005	0.0021	43	0.0038	61	0.0059	207	0.0049	123	0.0742	364	0.9623	402	0.6801	402	0.0279	57
348	sjtu-003	0.0017	29	0.0033	45	0.0030	80	0.0037	78	0.0058	119	0.0104	83	0.0081	95	0.0284	110
349	sjtu-004	0.0014	20	0.0025	26	0.0027	51	0.0028	36	0.0046	91	0.0086	64	0.0073	80	0.0272	10
350	sktelecom-000	0.0038	113	0.0054	114	0.0031	83	0.0051	129	0.0042	79	0.3418	323	0.0061	55	0.0293	165
351	smartbiometrik-001	0.5485	444	0.6442	440	0.7550	441	0.8611	438	0.8677	434	0.8270	382	0.7030	404	0.3144	417
352	smartengines-000	0.6240	450	0.7562	451	0.9552	450	0.9784	449	0.9515	445	0.9288	397	0.8200	415	0.8037	444

Table 26: FNMR is the proportion of mated comparisons below a threshold set to achieve the FMR given in the header on the fourth row. FMR is the proportion of impostor comparisons at or above that threshold. The light grey values give rank over all algorithms in that column. The pink columns use only same-sex impostors; others are selected regardless of demographics. The exception, in the green column, uses “matched-covariates” i.e. impostors of the same sex, age group, and country of birth. The second pink column includes effects of extended ageing. Missing entries for border, visa, mugshot and wild images generally mean the algorithm did not run to completion. The VISA columns compare images described in section 2.1. The MUGSHOT columns compare images described in section 2.4. The VISA-BORDER column compare images described in section 2.2 with those of section 2.3. The BORDER column compares images described in section 2.3. The WILD columns compare images described in section 2.6.

	Algorithm	FALSE NON-MATCH RATE (FNMR)										LESS CONSTRAINED, NON-COOP.					
		CONSTRAINED, COOPERATIVE								WILD							
		Name	VISAMC	VISA	MUGSHOT	MUGSHOT12+YRS	VISA BORDER	BORDER	BORDER								
	FMR	0.0001	1E-06	1E-05	1E-05	1E-06	1E-06	1E-06	1E-05		0.0001						
353	smartengines-001	0.6434	452	0.7666	452	0.9446	449	0.9750	448	0.9387	444	0.9556	400	0.8647	420	0.7748	442
354	smartvist-000	0.0912	395	0.1587	396	0.1163	398	0.1841	396	0.1397	383	0.9372	398	0.7107	407	0.0779	349
355	smilart-002	0.2440	413	0.3532	415	-	-	-	-	0.3785	409	0.4145	335	0.2611	363	-	-
356	smilart-003	0.6944	454	0.8836	454	0.0695	389	0.1193	390	0.0894	372	0.1221	287	0.0737	324	0.1190	377
357	sodec-000	0.0033	93	0.0044	87	0.0040	145	0.0053	134	0.0054	111	0.0096	77	0.0080	92	0.0274	19
358	sqisoft-001	0.1220	403	0.2088	403	0.1978	406	0.3386	406	0.2111	397	0.2798	319	0.1474	348	0.0519	316
359	sqisoft-002	0.0082	233	0.0124	232	0.0051	182	0.0086	215	0.0102	204	0.0183	153	0.0122	166	0.0287	130
360	staqu-000	0.0139	307	0.0208	299	0.0104	291	0.0145	283	0.0156	255	0.8063	377	0.1408	346	0.0332	238
361	starhybrid-001	0.0108	268	0.0138	244	0.0081	256	0.0113	242	0.0152	254	0.0265	189	0.0189	233	0.0350	258
362	sukshi-000	0.5409	442	0.6612	444	0.4556	421	0.6567	423	0.9296	443	0.8898	386	0.7384	408	0.6892	438
363	suprema-002	0.0030	77	0.0041	72	0.0034	111	0.0040	90	0.0045	87	0.0085	60	0.0072	79	0.0295	169
364	suprema-003	0.0028	71	0.0041	73	0.0034	109	0.0039	86	0.0030	32	0.3095	322	0.0580	315	0.0284	106
365	supremaid-001	0.0053	154	0.0073	150	0.0045	158	0.0066	173	0.0099	202	0.0186	154	0.0148	197	0.0352	261
366	supremaid-002	0.0063	189	0.0094	192	0.0044	154	0.0062	164	0.0072	144	0.0229	177	0.0095	124	0.0345	249
367	surrey-cvssp-000	0.9084	458	0.9909	459	0.9923	453	0.9950	451	0.9981	448	0.9994	424	0.9979	441	0.9389	446
368	surrey-cvssp-001	1.0000	461	1.0000	461	0.0077	248	0.0079	202	0.0266	317	0.3822	330	0.0551	311	1.0000	462
369	synesis-006	0.0070	204	0.0096	196	0.0107	297	0.0166	298	-	-	0.0128	109	0.0089	112	0.0292	160
370	synesis-007	0.0050	140	0.0073	151	0.0062	215	0.0076	190	-	-	0.0105	84	0.0080	94	0.0288	132
371	synology-000	0.0149	314	0.0238	317	0.0148	331	0.0261	331	0.0221	297	0.0331	213	0.0209	246	0.0330	236
372	synology-002	0.0104	264	0.0153	260	0.0107	298	0.0184	305	0.0189	286	0.2032	305	0.0180	222	0.0312	210
373	sztu-000	0.0092	247	0.0139	245	0.0091	276	0.0201	317	0.0136	240	0.0685	262	0.0118	162	0.0270	5
374	sztu-001	0.0031	79	0.0043	81	0.0025	31	0.0028	33	0.0051	103	0.0113	95	0.0089	113	0.0275	22
375	t4isb-000	0.0058	169	0.0087	181	0.0041	149	0.0064	170	0.0083	165	0.0157	130	0.0103	135	0.0282	89
376	tech5-004	0.0123	289	0.0234	315	0.0086	269	0.0162	293	0.0065	135	0.0112	93	0.0082	98	0.0281	82
377	tech5-005	0.0054	157	0.0072	145	0.0069	228	0.0122	249	0.0060	126	0.0094	74	0.0066	64	0.0349	256
378	techsign-000	0.0325	366	0.0511	363	0.0435	375	0.0710	373	0.0746	365	0.1104	284	0.0841	329	0.0639	334
379	techsign-001	0.0110	271	0.0196	294	0.0067	224	0.0120	247	0.0087	172	0.2475	314	0.0883	333	0.0299	183
380	tevian-007	0.0019	40	0.0027	34	0.0032	98	0.0041	93	0.0045	88	0.0086	63	0.0078	88	0.0310	209
381	tevian-008	0.0012	15	0.0017	9	0.0033	101	0.0042	99	0.0042	81	0.0081	53	0.0068	70	0.0290	148
382	tiger-005	0.0624	387	0.2450	407	0.0292	363	0.0556	363	0.0430	344	1.0000	434	0.9964	437	0.0278	45
383	tiger-006	0.0066	195	0.0101	206	0.0050	181	0.0075	189	0.0089	177	0.0158	131	0.0117	159	0.0290	158
384	tinkoff-001	0.0145	311	0.0244	318	0.0318	366	0.0636	371	0.0236	308	1.0000	457	0.0339	278	0.0563	327
385	tongyi-005	0.0073	215	0.0146	251	0.0187	340	0.0421	353	0.0161	261	0.0215	169	0.0149	199	0.0399	280
386	toppanidgate-000	0.0021	44	0.0033	46	0.0026	40	0.0028	30	0.0039	69	0.0075	42	0.0068	68	0.0376	275
387	toshiba-004	0.0030	75	0.0042	76	0.0025	32	0.0027	27	0.0034	48	0.0063	26	0.0053	35	0.0278	43
388	toshiba-006	0.0022	49	0.0035	51	0.0024	23	0.0025	19	0.0027	19	0.7425	365	0.3070	371	0.0275	27
389	touchlessid-000	0.3296	423	0.4804	426	0.4111	417	0.6026	420	0.5324	415	0.9996	427	0.9964	438	0.2521	409
390	touchlessid-001	0.0076	220	0.0104	208	0.0680	388	0.0842	378	0.1358	381	1.0000	436	0.9995	444	0.0499	312
391	trueface-002	0.0060	181	0.0096	195	0.0048	171	0.0061	161	0.0112	218	0.0198	161	0.0155	204	0.0793	354
392	trueface-003	0.0070	202	0.0094	191	0.0053	189	0.0081	206	0.0122	226	0.0217	171	0.0159	207	0.0785	351
393	tuputech-000	0.3218	422	0.3696	418	-	-	-	-	0.3237	404	0.4304	336	0.2973	370	0.9415	447
394	turingtechchip-001	0.0330	368	0.0540	368	0.0458	376	0.1007	382	0.4715	413	0.9286	396	0.8448	419	0.4035	424
395	turingtechchip-002	0.0126	297	0.0163	266	0.0092	281	0.0118	244	0.2264	399	1.0000	455	0.9925	434	0.2144	398
396	turkcell-000	0.1134	400	0.1288	391	0.0770	392	0.1112	389	0.2570	400	1.0000	433	0.9999	446	0.9556	448

Table 27: FNMR is the proportion of mated comparisons below a threshold set to achieve the FMR given in the header on the fourth row. FMR is the proportion of impostor comparisons at or above that threshold. The light grey values give rank over all algorithms in that column. The pink columns use only same-sex impostors; others are selected regardless of demographics. The exception, in the green column, uses “matched-covariates” i.e. impostors of the same sex, age group, and country of birth. The second pink column includes effects of extended ageing. Missing entries for border, visa, mugshot and wild images generally mean the algorithm did not run to completion. The VISA columns compare images described in section 2.1. The MUGSHOT columns compare images described in section 2.4. The VISA-BORDER column compare images described in section 2.2 with those of section 2.3. The BORDER column compares images described in section 2.3. The WILD columns compare images described in section 2.6.

	Algorithm	FALSE NON-MATCH RATE (FNMR)												LESS CONSTRAINED, NON-COOP.			
		CONSTRAINED, COOPERATIVE															
		Name	VISAMC	VISA	MUGSHOT	MUGSHOT12+YRS	VISABORDER	BORDER	BORDER	1E-06	1E-05	0.0001	WILD				
	FMR	0.0001	1E-06	1E-05	1E-05	1E-05	1E-06	1E-06	1E-05								
397	twface-000	0.0051	143	0.0072	148	0.0041	147	0.0058	150	0.0071	141	0.0153	125	0.0100	126	0.0276	32
398	twface-001	0.0036	101	0.0051	104	0.0031	91	0.0038	80	0.0049	99	0.0091	70	0.0075	84	0.0277	37
399	ulsee-001	0.0151	316	0.0246	320	0.0113	308	0.0185	308	0.0187	285	0.6766	359	0.0181	224	0.0316	221
400	ultinous-000	0.2343	412	0.3484	414	-	-	-	-	-	-	-	-	-	-		
401	ultinous-001	0.2485	414	0.4003	421	-	-	-	-	-	-	-	-	-	-		
402	uluface-002	0.0081	229	0.0123	230	0.0071	233	0.0095	228	0.0107	209	1.0000	450	0.0140	186	0.0444	302
403	uluface-003	0.0100	259	0.0150	257	0.0079	250	0.0128	260	-	-	-	-	-	-	0.0635	332
404	unissey-001	0.0095	251	0.0160	263	0.0134	321	0.0150	286	0.0147	252	0.0253	186	0.0163	208	0.0946	366
405	unissey-002	0.0094	250	0.0151	258	0.0079	251	0.0110	237	0.0114	219	0.4424	337	0.1914	355	0.0420	293
406	upc-001	0.0234	349	0.0519	364	0.0291	362	0.0490	360	0.0294	325	0.2316	312	0.0389	290	0.0314	216
407	uxlabs-001	0.0534	382	0.0570	372	0.0118	314	0.0131	264	0.0237	309	0.0399	233	0.0288	271	0.0876	363
408	vcog-002	0.7522	456	0.9033	455	-	-	-	-	-	-	-	-	-	-	-	
409	vd-002	0.0429	375	0.0704	377	0.0569	382	0.0844	379	0.0801	367	0.0937	272	0.0577	314	0.0556	326
410	vd-003	0.0199	343	0.0222	308	0.0115	312	0.0130	263	0.0138	243	0.0239	179	0.0177	219	0.0389	277
411	veridas-007	0.0063	188	0.0083	173	0.0044	156	0.0058	153	0.0080	158	0.0152	123	0.0120	165	0.0284	107
412	veridas-008	0.0032	84	0.0045	90	0.0030	77	0.0033	56	0.0085	169	0.0206	166	0.0143	191	0.0288	137
413	veridium-000	0.0726	392	0.1248	390	0.5226	424	0.6652	424	0.6425	418	0.8150	378	0.7989	414	0.4988	431
414	verigram-000	0.0032	83	0.0043	79	0.0031	84	0.0034	60	0.0093	187	0.0175	147	0.0164	209	0.0276	30
415	verigram-001	0.0032	86	0.0044	86	0.0027	52	0.0032	51	0.0030	30	0.9995	425	0.9953	436	0.0276	34
416	verihubs-inteligensia-000	0.0070	205	0.0098	199	0.0048	173	0.0076	193	0.0092	184	0.0160	133	0.0117	157	0.0283	100
417	verihubs-inteligensia-001	0.0071	206	0.0114	225	0.0050	180	0.0076	192	0.0096	194	0.0165	139	0.0114	154	0.0282	87
418	verijelas-000	0.2488	415	0.3431	413	0.4861	422	0.6004	419	0.0811	368	0.1148	285	0.0440	296	0.0524	320
419	via-000	0.0216	346	0.0365	351	0.0177	338	0.0287	338	0.0296	326	0.0572	251	0.0290	273	0.0349	255
420	via-001	0.0149	313	0.0229	311	0.0114	310	0.0177	303	0.0183	281	0.4056	333	0.0176	217	0.0373	274
421	videmo-001	0.0295	361	0.0417	355	0.0164	337	0.0261	332	0.0355	334	0.0603	255	0.0442	298	0.1473	380
422	videmo-002	0.0158	321	0.0288	335	0.0149	335	0.0249	330	0.0230	301	0.3429	324	0.1468	347	0.0294	167
423	videonetics-001	0.5483	443	0.6446	441	0.7517	439	0.8607	437	0.8664	432	0.8255	380	0.6956	403	0.2986	414
424	videonetics-002	0.4274	430	0.5329	432	0.6081	429	0.7438	429	0.7775	423	0.7297	364	0.5756	393	0.1976	396
425	viettelhightech-000	0.0117	278	0.0166	271	0.0110	302	0.0198	316	0.0167	270	0.0249	182	0.0158	205	0.0409	290
426	vigilantsolutions-010	0.0109	269	0.0164	269	0.0074	242	0.0095	226	0.0209	294	0.0365	227	0.0233	255	0.0277	38
427	vigilantsolutions-011	0.0124	290	0.0176	280	0.0073	238	0.0095	225	0.0196	290	0.0360	225	0.0221	251	0.0274	18
428	vinai-000	0.0081	230	0.0124	233	0.0045	157	0.0072	184	0.0089	176	0.1814	298	0.0112	149	0.0274	20
429	vinbigdata-001	0.2576	418	0.2763	409	0.1404	402	0.1988	401	0.1407	384	0.1150	286	0.0703	322	0.9767	450
430	vinbigdata-002	0.0102	261	0.0175	277	0.0071	236	0.0084	211	0.0090	178	0.8017	376	0.3134	372	0.0304	195
431	vion-000	0.0419	373	0.0590	373	0.0422	374	0.0478	357	0.0581	356	0.0968	279	0.0847	330	0.2479	406
432	visage-000	0.0933	396	0.1441	395	0.1316	400	0.2416	402	0.1395	382	0.1920	302	0.1001	337	0.0500	313
433	visionbox-001	0.0159	323	0.0270	330	0.0111	304	0.0173	301	0.0190	287	0.0315	207	0.0205	244	0.0389	278
434	visionbox-002	0.0058	166	0.0079	164	0.0060	209	0.0074	186	0.0084	167	0.0149	118	0.0113	152	0.0447	304
435	visionlabs-010	0.0017	30	0.0024	24	0.0026	43	0.0030	41	0.0033	45	0.0061	24	0.0052	27	0.0282	92
436	visionlabs-011	0.0012	14	0.0022	19	0.0024	24	0.0026	24	0.0028	22	0.0053	13	0.0046	18	0.0280	70
437	visteam-003	0.0804	394	0.2166	404	0.0613	387	0.1204	391	0.0963	375	0.1269	289	0.0441	297	0.0296	177
438	visteam-004	0.0541	384	0.5202	430	0.0406	373	0.0827	377	0.1879	392	0.1795	297	0.0347	281	0.0289	142
439	vixvizion-005	0.0276	358	0.0420	356	0.0302	365	0.0629	370	0.0288	322	0.0447	238	0.0235	257	0.0265	2
440	vixvizion-006	0.0082	234	0.0122	229	0.0093	282	0.0194	313	0.0099	201	0.0169	141	0.0108	145	0.0268	4

Table 28: FNMR is the proportion of mated comparisons below a threshold set to achieve the FMR given in the header on the fourth row. FMR is the proportion of impostor comparisons at or above that threshold. The light grey values give rank over all algorithms in that column. The pink columns use only same-sex impostors; others are selected regardless of demographics. The exception, in the green column, uses “matched-covariates” i.e. impostors of the same sex, age group, and country of birth. The second pink column includes effects of extended ageing. Missing entries for border, visa, mugshot and wild images generally mean the algorithm did not run to completion. The VISA columns compare images described in section 2.1. The MUGSHOT columns compare images described in section 2.4. The VISA-BORDER column compare images described in section 2.2 with those of section 2.3. The BORDER column compares images described in section 2.3. The WILD columns compare images described in section 2.6.

	Algorithm	FALSE NON-MATCH RATE (FNMR)										LESS CONSTRAINED, NON-COOP.					
		CONSTRAINED, COOPERATIVE								WILD							
		Name	VISAMC	VISA	MUGSHOT	MUGSHOT12+YRS	VISABORDER	BORDER	BORDER								
	FMR	0.0001	1E-06	1E-05	1E-05	1E-05	1E-06	1E-06	1E-05			0.0001					
441	vnpt-004	0.0058	175	0.0078	163	0.0037	127	0.0053	133	0.0051	104	0.4640	339	0.1384	344	0.0275	25
442	vnpt-005	0.0036	102	0.0052	109	0.0027	53	0.0031	47	0.0036	57	0.0066	30	0.0056	39	0.0286	123
443	vocord-009	0.0022	52	0.0029	40	0.0036	119	0.0046	114	0.0052	108	0.0098	78	0.0086	109	0.0284	109
444	vocord-010	0.0024	58	0.0031	43	0.0036	120	0.0049	125	0.0025	15	0.0065	28	0.0040	10	0.0280	66
445	vts-000	0.0103	262	0.0174	276	0.0080	253	0.0129	262	0.0250	315	0.0450	240	0.0372	288	0.0596	328
446	vts-001	0.0033	90	0.0048	97	0.0027	55	0.0036	73	0.0032	39	0.6519	356	0.3563	377	0.0338	244
447	wicket-000	0.0018	38	0.0028	38	0.0024	20	0.0027	25	0.0031	34	0.7968	375	0.4340	385	0.0323	227
448	winsense-001	0.0062	186	0.0099	203	0.0092	279	0.0210	318	0.0093	186	0.0144	116	0.0098	125	0.0320	225
449	winsense-002	0.0050	141	0.0073	152	0.0038	129	0.0059	156	0.0064	133	0.0118	101	0.0084	102	0.0307	202
450	wiseai-001	0.0658	388	0.0964	387	0.7743	443	0.8956	443	0.1967	393	0.7526	369	0.3419	374	0.5780	434
451	wuhanianyu-001	0.0163	324	0.0262	328	0.0281	360	0.0569	366	0.0316	330	0.0486	246	0.0344	279	0.0324	228
452	x-laboratory-000	0.0071	207	0.0106	211	0.0123	317	0.0138	273	0.0419	343	0.5629	347	0.2852	368	0.0295	174
453	x-laboratory-001	0.0059	177	0.0110	219	0.0054	192	0.0078	200	0.0094	189	0.0142	113	0.0100	128	0.0294	166
454	xforwardai-001	0.0021	42	0.0034	47	0.0027	56	0.0028	32	0.0046	93	0.0088	67	0.0079	90	0.0281	81
455	xforwardai-002	0.0016	28	0.0023	20	0.0026	46	0.0025	16	0.0040	74	0.0081	55	0.0074	81	0.0282	85
456	xm-000	0.0015	22	0.0026	32	0.0031	89	0.0038	84	0.0058	120	0.0105	85	0.0082	99	0.0282	90
457	yisheng-004	0.1988	409	0.3329	412	0.1147	397	0.1849	397	0.2044	395	-	-	-	-	0.0908	364
458	yitu-003	0.0015	26	0.0026	30	0.0066	222	0.0085	212	0.0064	134	0.0114	96	0.0103	136	0.0325	231
459	yoonik-002	0.0052	150	0.0062	129	0.0029	73	0.0034	62	0.0615	360	0.1279	290	0.1166	339	0.0549	324
460	yoonik-003	0.0034	96	0.0047	93	0.0032	96	0.0037	76	0.0816	369	0.2033	306	0.1601	352	0.0699	343
461	ytu-000	0.0057	164	0.0087	180	0.0121	315	0.0238	327	0.0047	95	0.0078	50	0.0059	50	0.0286	124
462	yuan-004	0.0058	174	0.0078	160	0.0039	139	0.0055	141	0.0234	305	0.0442	237	0.0353	282	0.0299	184
463	yuan-005	0.0037	110	0.0046	91	0.0027	59	0.0035	69	0.0033	42	0.2706	317	0.0876	332	0.0288	141

Table 29: FNMR is the proportion of mated comparisons below a threshold set to achieve the FMR given in the header on the fourth row. FMR is the proportion of impostor comparisons at or above that threshold. The light grey values give rank over all algorithms in that column. The pink columns use only same-sex impostors; others are selected regardless of demographics. The exception, in the green column, uses “matched-covariates” i.e. impostors of the same sex, age group, and country of birth. The second pink column includes effects of extended ageing. Missing entries for border, visa, mugshot and wild images generally mean the algorithm did not run to completion. The VISA columns compare images described in section 2.1. The MUGSHOT columns compare images described in section 2.4. The VISA-BORDER column compare images described in section 2.2 with those of section 2.3. The BORDER column compares images described in section 2.3. The WILD columns compare images described in section 2.6.

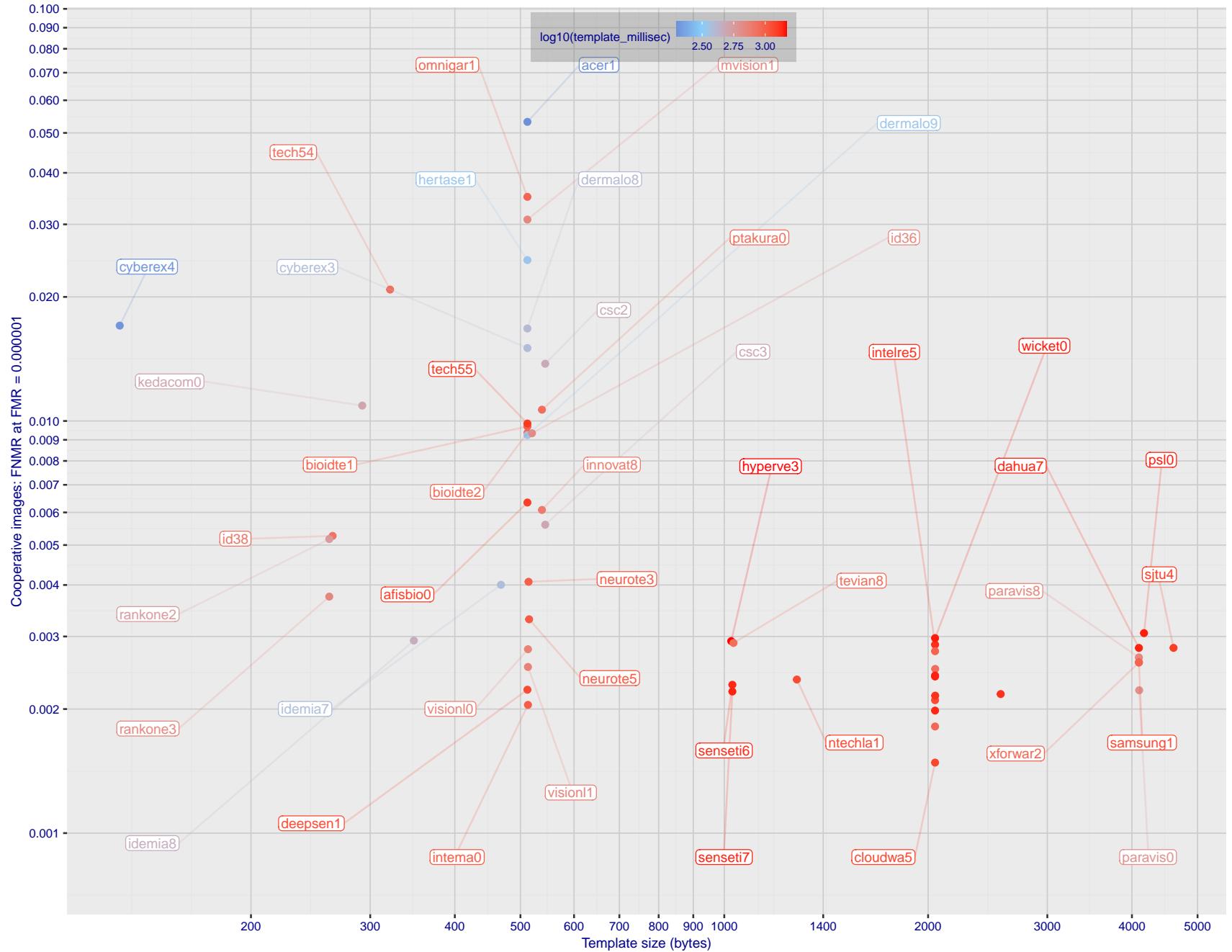


Figure 1: The points show false non-match rates (FNMR) versus the size of the encoded template. FNMR is the geometric mean of FNMR values for visa and mugshot images (from Figs. 86 and 110) at the false match rate (FMR) given in the y-axis label. The color of the points encodes template generation time - which spans at least one order of magnitude. Durations are measured on a single core of a c. 2016 Intel Xeon CPU E5-2630 v4 running at 2.20GHz. Algorithms with poor FNMR are omitted.

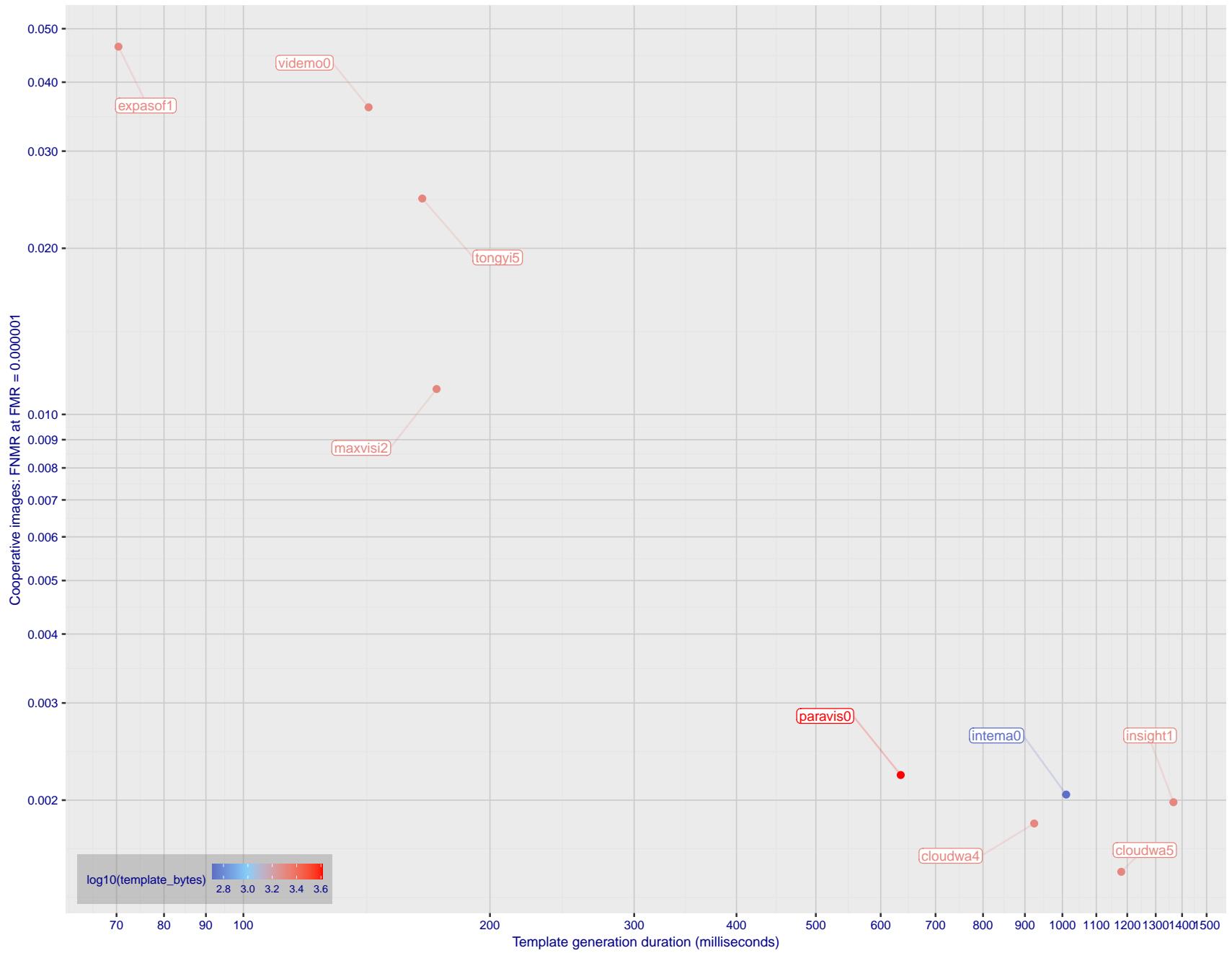


Figure 2: The points show false non-match rates (FNMR) versus the duration of the template generation operation. FNMR is the geometric mean of FNMR values for visa and mugshot images (from Figs. 86 and 110) at a false match rate (FMR) given in the y-axis label. Template generation time is a median estimated over 640 x 480 pixel portraits. It is measured on a single core of a c. 2016 Intel Xeon CPU E5-2630 v4 running at 2.20GHz. The color of the points encodes template size - which span two orders of magnitude. Algorithms with poor FNMR are omitted.

1 Metrics

1.1 Core accuracy

Given a vector of N genuine scores, u , the false non-match rate (FNMR) is computed as the proportion below some threshold, T:

$$\text{FNMR}(T) = 1 - \frac{1}{N} \sum_{i=1}^N H(u_i - T) \quad (1)$$

where $H(x)$ is the unit step function, and $H(0)$ taken to be 1.

Similarly, given a vector of N impostor scores, v , the false match rate (FMR) is computed as the proportion above T:

$$\text{FMR}(T) = \frac{1}{N} \sum_{i=1}^N H(v_i - T) \quad (2)$$

The threshold, T, can take on any value. We typically generate a set of thresholds from quantiles of the observed impostor scores, v , as follows. Given some interesting false match rate range, $[\text{FMR}_L, \text{FMR}_U]$, we form a vector of K thresholds corresponding to FMR measurements evenly spaced on a logarithmic scale

$$T_k = Q_v(1 - \text{FMR}_k) \quad (3)$$

where Q is the quantile function, and FMR_k comes from

$$\log_{10} \text{FMR}_k = \log_{10} \text{FMR}_L + \frac{k}{K} [\log_{10} \text{FMR}_U - \log_{10} \text{FMR}_L] \quad (4)$$

Error tradeoff characteristics are plots of FNMR(T) vs. FMR(T). These are plotted with $\text{FMR}_U \rightarrow 1$ and FMR_L as low as is sustained by the number of impostor comparisons, N. This is somewhat higher than the “rule of three” limit $3/N$ because samples are not independent, due to re-use of images.

1.2 Multi-template scoring methodology

There are some scenarios when one or more people exist and are detected in an image, and some of the proposed test images include $K > 1$ persons for some images and situations where the subject of interest may or may not be the foreground face (largest face in the image). The NIST FRVT 1:1 API supports this by allowing generation of multiple templates representing each person detected in an image. When this occurs, NIST will match all templates generated from the enrollment image with all templates generated from the verification image and use the **maximum** similarity score across all template comparisons. This scoring approach will be used in our calculation of FMR and FNMR (this applies to both genuine and imposter comparisons).

2 Datasets

2.1 Visa images

- ▷ The number of images is on the order of 10^5 .
- ▷ The number of subjects is on the order of 10^5 .
- ▷ The number of subjects with two images is on the order of 10^4 .
- ▷ The images have geometry in reasonable conformance with the ISO/IEC 19794-5 Full Frontal image type. Pose is generally excellent.
- ▷ The images are of size 252x300 pixels. The mean interocular distance (IOD) is 69 pixels.
- ▷ The images are of subjects from greater than 100 countries, with significant imbalance due to visa issuance patterns.
- ▷ The images are of subjects of all ages, including children, again with imbalance due to visa issuance demand.
- ▷ Many of the images are live capture. A substantial number of the images are photographs of paper photographs.
- ▷ When these images are input to the algorithm, they are labelled as being of type "ISO" - see Table 4 of the FRVT API.

2.2 Application images

- ▷ The number of images is on the order of 10^6 .
- ▷ The number of subjects is on the order of 10^6 .
- ▷ The number of subjects with two images is on the order of 10^6 .
- ▷ The images have geometry in good conformance with the ISO/IEC 19794-5 Full Frontal image type. Pose is generally excellent.
- ▷ The images are of size 300x300 pixels. The mean interocular distance (IOD) is 61 pixels.
- ▷ The images are of subjects from greater than 100 countries, with significant imbalance due to population and immigration patterns.
- ▷ The images are of subjects of adults with imbalance due to population and immigration patterns and demand.
- ▷ All of the images are live capture.
- ▷ When these images are input to the algorithm, they are labelled as being of type "ISO" - see Table 4 of the FRVT API.

2.3 Border crossing images

- ▷ The number of images is on the order of 10^6 .
- ▷ The number of subjects is on the order of 10^6 .
- ▷ The number of subjects with two images is on the order of 10^6 .
- ▷ The images are taken with a camera oriented by an attendant toward a cooperating subject. This is done under time constraints so there are roll, pitch and yaw angle variations. Also background illumination is sometimes strong, so the face is under-exposed. There is some perspective distortion due to close range images. Some faces are partially cropped.
- ▷ The images have mean IOD of 38 pixels.
- ▷ The images are of subjects of adults and children aged 12 or above.

- ▷ The images are of subjects from greater than 100 countries, with significant imbalance due to population and immigration patterns.
- ▷ The images are all live capture.
- ▷ When these images are input to the algorithm, they are labelled as being of type "WILD" - see Table 4 of the FRVT API.

2.4 Mugshot images

- ▷ The number of images is on the order of 10^6 .
- ▷ The number of subjects is on the order of 10^6 .
- ▷ The number of subjects with two images is on the order of 10^6 .
- ▷ The images have geometry in reasonable conformance with the ISO/IEC 19794-5 Full Frontal image type.
- ▷ The images are of variable sizes. The median IOD is 105 pixels. The mean IOD is 113 pixels. The 1-st, 5-th, 10-th, 25-th, 75-th, 90-th and 99-th percentiles are 34, 58, 70, 87, 121, 161 and 297 pixels.
- ▷ The images are of subjects from the United States.
- ▷ The images are of adults.
- ▷ The images are all live capture.
- ▷ When these images are input to the algorithm, they are labelled as being of type "mugshot" - see Table 4 of the FRVT API.

2.5 Kiosk images

- ▷ The number of images is on the order of 10^6 .
- ▷ The number of subjects is on the order of 10^5 .
- ▷ The number of subjects with multiple images is the order of 10^5 .
- ▷ The images are taken at kiosk equipped with a camera intended to capture a centered face. However the images have specific quality defects arising from the camera triggering before the subject looks at it. These are downward pitch of the face relative to the optical axis; cropping of the forehead; and cropping of left or right part of the face. Partial cropping affects perhaps 10% of the images. Resolution does not vary widely.
- ▷ The images are of adults.
- ▷ The images have mean IOD of 44 pixels, with maximum below 75, and minimum when both eyes are present above 25 pixels.
- ▷ All of the images are live capture, none are scanned.
- ▷ When these images are input to the algorithm, they are labelled as being of type "WILD" - see Table 4 of the FRVT API.

2.6 Wild images

- ▷ The number of images is on the order of 10^5 .
- ▷ The number of subjects is on the order of 10^4 .
- ▷ The number of subjects with two images on the order of 10^4 .
- ▷ The images include many photojournalism-style images. Images are given to the algorithm using a variable but generally tight crop of the head. Resolution varies very widely. The images are very unconstrained, with wide yaw and pitch pose variation. Faces can be occluded, including hair and hands.

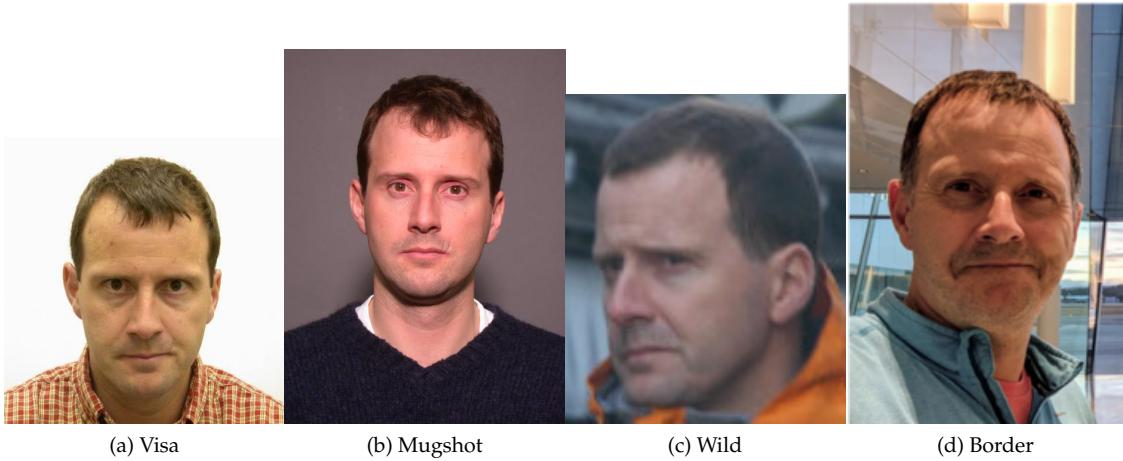


Figure 3: The figure gives simulated samples of image types used in this report.

- ▷ The images are of adults.
- ▷ All of the images are live capture, none are scanned.
- ▷ When these images are input to the algorithm, they are labelled as being of type "WILD" - see Table 4 of the FRVT API.

3 Results

3.1 Test goals

- ▷ To state absolute accuracy for different kinds of images, including those with and without subject cooperation.
- ▷ To state comparative accuracy, across algorithms.

3.2 Test design

Method: For visa images:

- ▷ The comparisons are of visa photos against visa photos.
- ▷ The number of genuine comparisons is on the order of 10^4 .
- ▷ The number of impostor comparisons is on the order of 10^{10} .
- ▷ The comparisons are fully zero-effort, meaning impostors are paired without attention to sex, age or other covariates. However, later analysis is conducted on subsets.
- ▷ The number of persons is on the order of 10^5 .
- ▷ The number of images used to make 1 template is 1.
- ▷ The number of templates used to make each comparison score is two corresponding to simple one-to-one verification.

Method: For mugshot images:

- ▷ The comparisons are of mugshot photos against mugshot photos.

- ▷ The number of genuine comparisons is on the order of 10^6 .
- ▷ The number of impostor comparisons is on the order of 10^8 .
- ▷ The impostors are paired by sex, but not by age or other covariates.
- ▷ The number of persons is on the order of 10^6 .
- ▷ The number of images used to make 1 template is 1.
- ▷ The number of templates used to make each comparison score is two corresponding to simple one-to-one verification.

Method: For visa-border comparisons:

- ▷ The comparisons are of visa-like frontals against border crossing webcam photos.
- ▷ The number of genuine comparisons is on the order of 10^6 .
- ▷ The number of impostor comparisons is on the order of 10^8 .
- ▷ The impostors are paired by sex, but not by age or other covariates.
- ▷ The number of persons is on the order of 10^6 .
- ▷ The number of images used to make 1 template is 1.
- ▷ The number of templates used to make each comparison score is two corresponding to simple one-to-one verification.

Method: For kiosk-border comparisons:

- ▷ The comparisons are of visa-like frontals against kiosk-style photos.
- ▷ The number of genuine comparisons is on the order of 10^6 .
- ▷ The number of impostor comparisons is on the order of 10^8 .
- ▷ The impostors are paired by sex, but not by age or other covariates.
- ▷ The number of persons is on the order of 10^5 .
- ▷ The number of images used to make 1 template is 1.
- ▷ The number of templates used to make each comparison score is two corresponding to simple one-to-one verification.

Method: For border-border comparisons:

- ▷ The comparisons are of border crossing webcam photos.
- ▷ The number of genuine comparisons is on the order of 10^6 .
- ▷ The number of impostor comparisons is on the order of 10^8 .
- ▷ The impostors are paired by sex, but not by age or other covariates.
- ▷ The number of persons is on the order of 10^6 .
- ▷ The number of images used to make 1 template is 1.
- ▷ The number of templates used to make each comparison score is two corresponding to simple one-to-one verification.

Method: For wild images:

- ▷ The comparisons are of wild photos against wild photos.

- ▷ The number of genuine comparisons is on the order of 10^6 .
- ▷ The number of impostor comparisons is on the order of 10^8 .
- ▷ The comparisons are fully zero-effort, meaning impostors are paired without attention to sex, age or other covariates.
- ▷ The number of persons is on the order of 10^4 .
- ▷ The number of images used to make 1 template is 1.
- ▷ The number of templates used to make each comparison score is two corresponding to simple one-to-one verification.

Method: For child exploitation images:

- ▷ The comparisons are of unconstrained child exploitation photos against others of the same type.
- ▷ The number of genuine comparisons is on the order of 10^4 .
- ▷ The number of impostor comparisons is on the order of 10^7 .
- ▷ The comparisons are fully zero-effort, meaning impostors are paired without attention to sex, age or other covariates.
- ▷ The number of persons is on the order of 10^3 .
- ▷ The number of images used to make 1 template is 1.
- ▷ The number of templates used to make each comparison score is two corresponding to simple one-to-one verification.
- ▷ We produce two performance statements. First, is a DET as used for visa and mugshot images. The second is a cumulative match characteristic (CMC) summarizing a simulated one-to-many search process. This is done as follows.
 - We regard M enrollment templates as items in a gallery.
 - These M templates come from $M > N$ individuals, because multiple images of a subject are present in the gallery under separate identifiers.
 - We regard the verification templates as search templates.
 - For each search we compute the rank of the highest scoring mate.
 - This process should properly be conducted with a 1:N algorithm, such as those tested in NIST IR 8009. We use the 1:1 algorithms in a simulated 1:N mode here to a) better reflect what a child exploitation analyst does, and b) to show algorithm efficacy is better than that revealed in the verification DETs.

3.3 Failure to enroll

	Algorithm	Failure to Enrol Rate ¹											
		APPLICATION		BORDER		KIOSK	MUGSHOT	VISA	WILD				
Name	SEC. 2.2	SEC. 2.3	SEC. 2.5	SEC. 2.4	SEC. 2.1	SEC. 2.6							
1	20face-000	0.0000	225	0.0008	236	0.0217	171	0.0000	136	0.0004	258	0.0004	194
2	20face-001	0.0000	259	0.0008	237	0.0000	8	0.0000	134	0.0004	260	0.0004	198
3	3divi-006	0.0000	241	0.0007	206	0.0214	169	0.0001	243	0.0002	140	0.0005	250
4	3divi-007	0.0000	226	0.0007	205	0.0214	168	0.0001	245	0.0002	139	0.0005	251
5	acer-001	0.0000	223	0.0011	293	-	425	0.0001	215	0.0004	277	0.0004	207
6	acer-002	0.0000	378	0.0008	229	0.0191	148	0.0003	333	0.0004	278	0.0011	307
7	acisw-007	0.0000	190	0.0000	105	0.0000	31	0.0000	6	0.0000	110	0.0000	82
8	acisw-008	0.0000	263	0.0009	258	0.0173	133	0.0004	358	0.0004	201	0.0007	283
9	adera-002	0.0000	360	0.0034	380	-	457	0.0003	340	0.0005	375	0.0505	423
10	adera-003	0.0000	361	0.0034	381	0.0403	237	0.0003	339	0.0005	376	0.0505	424
11	advance-003	0.0000	348	0.0012	303	0.0247	186	0.0001	270	0.0004	328	0.0011	306
12	advance-004	0.0001	410	0.0010	284	0.0157	124	0.0008	405	0.0006	389	0.0222	404
13	afisbiometrics-000	0.0000	205	0.0008	219	0.0213	166	0.0000	137	0.0004	276	0.0003	183
14	afrengine-000	0.0000	238	0.0015	320	0.0254	194	0.0008	404	0.0004	219	0.0265	411
15	aifirst-001	0.0000	156	0.0000	84	-	350	0.0000	47	0.0000	87	0.0000	109
16	aigen-001	0.0000	26	0.0000	15	-	413	0.0000	101	0.0000	14	0.0000	2
17	aigen-002	0.0000	11	0.0000	8	0.0000	40	0.0000	116	0.0000	11	0.0000	16
18	ailabs-001	0.0000	227	0.0090	421	-	435	0.0007	398	0.0005	350	0.0016	320
19	aimall-002	0.0000	363	0.0043	398	-	393	0.0012	416	0.0005	367	0.0005	261
20	aimall-003	0.0000	343	0.0012	308	-	318	0.0004	353	0.0005	344	0.0004	224
21	aiseemu-001	0.0000	141	0.0000	77	0.0000	15	0.0000	39	0.0000	81	0.0000	51
22	aiunionface-000	0.0000	23	0.0000	13	-	402	0.0000	98	0.0000	17	0.0000	111
23	aise-001	0.0001	411	0.0040	393	0.0652	254	0.0026	437	0.0022	440	0.0058	359
24	aise-002	0.0000	97	0.0014	318	0.0230	180	0.0005	381	0.0004	259	0.0071	365
25	ajou-001	0.0000	250	0.0020	343	-	304	0.0001	248	0.0004	334	0.0045	350
26	alchera-003	0.0001	423	0.0013	313	0.0317	212	0.0002	314	0.0004	289	0.0036	343
27	alchera-004	0.0000	208	0.0009	256	0.0228	178	0.0001	278	0.0004	217	0.0003	175
28	alfabeta-001	0.0005	435	0.0650	456	0.2142	283	0.0024	433	0.0018	435	0.1071	444
29	alice-000	0.0000	4	0.0006	177	0.0133	108	0.0000	155	0.0004	212	0.0004	223
30	alleyes-000	0.0000	216	0.0010	274	-	401	0.0002	287	0.0004	302	0.0004	233
31	allgvision-000	0.0007	439	0.0062	415	-	329	0.0026	436	0.0052	452	0.0131	385
32	alphaface-001	0.0000	240	0.0012	297	-	450	0.0000	200	0.0004	303	0.0004	200
33	alphaface-002	0.0000	269	0.0012	299	-	323	0.0000	198	0.0004	308	0.0004	202
34	amplifiedgroup-001	0.0114	455	0.1023	458	-	424	0.0189	457	0.0279	460	0.1390	452
35	androvideo-000	0.0000	5	0.0000	5	-	388	0.0000	113	0.0000	7	0.0002	127
36	anke-004	0.0000	210	0.0011	289	-	392	0.0001	259	0.0004	310	0.0006	277
37	anke-005	0.0000	278	0.0012	300	-	348	0.0001	272	0.0004	324	0.0007	281
38	antheus-000	0.0000	110	0.0000	57	-	301	0.0000	56	0.0000	54	0.0242	407
39	antheus-001	0.0000	130	0.0000	70	-	324	0.0000	32	0.0000	84	0.0242	406
40	anyvision-004	0.0000	347	0.0017	332	-	294	0.0001	273	0.0004	270	0.0080	369
41	anyvision-005	0.0000	264	0.0013	309	-	320	0.0000	169	0.0004	215	0.0004	227
42	armatura-001	0.0000	369	0.0021	348	0.0257	197	0.0005	374	0.0005	354	0.0357	420
43	armatura-002	0.0000	350	0.0018	334	0.0206	158	0.0003	348	0.0004	329	0.0314	414
44	asusaics-000	0.0000	21	0.0000	12	-	399	0.0000	121	0.0000	10	0.0000	20
45	asusaics-001	0.0000	103	0.0000	54	-	291	0.0000	48	0.0000	60	0.0000	58
46	authenmetric-003	0.0000	48	0.0000	26	0.0000	47	0.0000	88	0.0000	28	0.0000	36
47	authenmetric-004	0.0000	137	0.0000	71	0.0000	14	0.0000	37	0.0000	78	0.0000	48
48	aware-005	0.0000	330	0.0020	340	-	368	0.0001	286	0.0004	316	0.0011	301
49	aware-006	0.0000	271	0.0009	253	0.0249	188	0.0000	173	0.0004	274	0.0006	274
50	awiros-001	0.0039	443	0.0369	448	-	404	0.0386	458	0.0872	463	0.3415	457
51	awiros-002	0.0000	381	0.0038	391	-	366	0.0007	397	0.0012	425	0.0208	400
52	aximetria-001	0.0000	329	0.0010	286	0.0217	172	0.0001	285	0.0004	264	0.0024	331
53	ayftech-001	0.0002	426	0.0046	402	-	382	0.0043	446	0.0011	412	0.0091	374
54	ayonix-000	0.0053	447	0.0341	445	-	461	0.0113	455	0.0137	457	0.1194	448
55	beethedata-000	0.0005	433	0.0042	397	0.0366	228	0.0002	297	0.0010	406	0.0006	266
56	beyneai-000	0.0000	168	0.0000	90	0.0000	21	0.0000	20	0.0000	94	0.0000	95
57	biocube-001	0.0006	437	0.0391	449	0.1207	275	0.0015	421	0.0020	438	0.0253	410
58	boidtechswiss-001	0.0000	203	0.0007	201	-	384	0.0000	161	0.0004	293	0.0025	333

Table 30: FTE is the proportion of failed template generation attempts. Failures can occur because the software throws an exception, or because the software electively refuses to process the input image. This would typically occur if a face is not detected. FTE is measured as the number of function calls that give EITHER a non-zero error code OR that give a “small” template. This is defined as one whose size is less than 0.3 times the median template size for that algorithm. This second rule is needed because some algorithms incorrectly fail to return a non-zero error code when template generation fails.

A hyphen “-” indicates the dataset was not produced.¹ The effects of FTE are included in the accuracy results of this report by regarding any template comparison involving a failed template to produce a low similarity score. Thus higher FTE results in higher FNMR and lower FMR.

	Algorithm	Failure to Enrol Rate ¹											
		APPLICATION	BORDER	KIOSK	MUGSHOT	VISA	WILD	SEC. 2.2	SEC. 2.3	SEC. 2.5	SEC. 2.4	SEC. 2.1	SEC. 2.6
59	bioditechswiss-002	0.0000	290	0.0007	204	-	363	0.0000	162	0.0004	292	0.0005	263
60	bm-001	0.0000	146	0.0000	80	-	337	0.0000	123	0.0000	91	0.0000	54
61	boetech-001	0.0087	451	0.0272	439	0.2117	281	0.0032	443	0.0160	458	0.0946	439
62	boetech-002	0.0087	452	0.0272	440	0.2117	280	0.0032	442	0.0160	459	0.0946	440
63	bresee-001	0.0000	215	0.0010	280	-	405	0.0002	298	0.0003	170	0.0003	138
64	bresee-002	0.0000	358	0.0020	346	0.0219	173	0.0008	399	0.0004	249	0.0031	341
65	camvi-002	0.0000	60	0.0000	30	-	443	0.0000	97	0.0000	32	0.0000	44
66	camvi-004	0.0000	167	0.0000	120	-	357	0.0000	21	0.0000	95	0.0000	96
67	canon-003	0.0000	231	0.0008	220	0.0234	184	0.0000	195	0.0004	280	0.0003	180
68	canon-004	0.0000	267	0.0008	221	0.0234	183	0.0000	194	0.0004	282	0.0003	181
69	ceiec-003	0.0000	98	0.0013	316	-	289	0.0001	224	0.0004	296	0.0004	197
70	ceiec-004	0.0000	32	0.0008	234	-	415	0.0000	168	0.0004	218	0.0004	234
71	chosun-001	0.0000	38	0.0000	24	-	422	0.0000	109	0.0000	21	0.0000	9
72	chosun-002	0.0000	81	0.0000	42	-	456	0.0000	80	0.0000	51	0.0000	29
73	chtface-004	0.0000	76	0.0017	329	0.0320	214	0.0000	182	0.0004	305	0.0020	328
74	chtface-005	0.0000	72	0.0017	328	0.0320	213	0.0000	181	0.0004	304	0.0020	327
75	cist-001	0.0000	86	0.0005	172	0.0087	91	0.0000	84	0.0000	47	0.0000	33
76	clearviewai-000	0.0000	300	0.0003	139	0.0081	88	0.0000	184	0.0003	157	0.0003	139
77	closeli-001	0.0000	199	0.0000	113	0.0000	36	0.0000	13	0.0000	121	0.0001	124
78	cloudmatrix-001	0.0000	323	0.0028	360	0.0225	176	0.0001	217	0.0004	208	0.0004	219
79	cloudmatrix-002	0.0000	318	0.0028	359	0.0225	175	0.0001	220	0.0004	205	0.0004	220
80	cloudwalk-hr-003	0.0000	304	0.0008	238	-	378	0.0001	229	0.0004	216	0.0113	380
81	cloudwalk-hr-004	0.0000	256	0.0011	296	-	314	0.0004	355	0.0003	187	0.0129	384
82	cloudwalk-mt-005	0.0000	261	0.0005	163	0.0130	107	0.0003	329	0.0004	312	0.0004	209
83	cloudwalk-mt-006	0.0000	295	0.0006	179	0.0158	125	0.0002	308	0.0004	317	0.0004	205
84	codeline-000	0.0000	140	0.0000	73	0.0000	12	0.0000	35	0.0000	75	0.0000	46
85	cogent-006	0.0000	174	0.0000	95	0.0000	24	0.0000	28	0.0000	109	0.0000	101
86	cogent-007	0.0000	356	0.0000	116	0.0000	60	0.0000	170	0.0000	127	0.0001	119
87	cognitec-003	0.0001	402	0.0194	434	0.0820	269	0.0003	346	0.0005	352	0.0039	346
88	cognitec-004	0.0001	403	0.0037	390	0.0580	248	0.0003	345	0.0005	353	0.0035	342
89	cor-001	0.0000	257	0.0006	183	-	315	0.0002	324	0.0004	273	0.0004	247
90	coretech-000	0.0000	99	0.0000	55	0.0000	1	0.0000	51	0.0000	63	0.0000	60
91	coretech-001	0.0000	397	0.0033	376	0.0677	259	0.0005	379	0.0011	418	0.0027	336
92	corsight-002	0.0000	207	0.0005	174	0.0152	120	0.0001	262	0.0004	250	0.0003	179
93	corsight-003	0.0000	276	0.0006	190	0.0175	134	0.0001	252	0.0004	261	0.0003	187
94	csc-002	0.0015	442	0.0033	375	-	330	0.0006	390	0.0006	393	0.0968	442
95	csc-003	0.0015	441	0.0033	374	0.0445	243	0.0006	391	0.0006	392	0.0968	441
96	ctbcbank-000	0.0001	406	0.0051	408	-	407	0.0011	414	0.0019	436	0.0868	435
97	ctbcbank-001	0.0000	379	0.0036	389	-	298	0.0005	375	0.0010	404	0.0844	432
98	cubox-001	0.0000	102	0.0000	53	-	290	0.0000	49	0.0000	61	0.0000	57
99	cubox-002	0.0000	322	0.0006	186	0.0159	127	0.0002	323	0.0005	371	0.0016	319
100	cudocommunication-001	0.0000	129	0.0000	69	0.0000	10	0.0000	33	0.0000	83	0.0000	110
101	cuhkee-001	0.0000	281	0.0011	295	-	351	0.0000	132	0.0004	256	0.1278	450
102	cybercore-002	0.0000	368	0.0001	126	0.0014	67	0.0002	291	0.0002	135	0.0018	323
103	cybercore-003	0.0000	204	0.0003	140	0.0060	76	0.0005	380	0.0003	158	0.0192	399
104	cyberextruder-003	0.0000	364	0.0077	420	0.0887	272	0.0001	281	0.0006	387	0.0009	296
105	cyberextruder-004	0.0000	362	0.0097	422	0.1025	274	0.0001	275	0.0007	394	0.0213	401
106	cyberlink-009	0.0000	169	0.0004	157	0.0106	99	0.0000	128	0.0003	172	0.0002	137
107	cyberlink-010	0.0000	165	0.0004	156	0.0106	98	0.0000	127	0.0003	171	0.0002	136
108	dahua-006	0.0000	189	0.0000	115	-	373	0.0000	186	0.0003	189	0.0000	81
109	dahua-007	0.0000	122	0.0000	114	0.0000	61	0.0000	189	0.0003	188	0.0000	71
110	daon-000	0.0000	386	0.0028	363	0.0577	247	0.0014	420	0.0015	429	0.0030	340
111	decatur-000	0.0000	325	0.0020	339	-	345	0.0004	362	0.0005	345	0.0236	405
112	decatur-001	0.0000	244	0.0009	261	0.0194	150	0.0001	233	0.0004	241	0.0004	238
113	deepglint-004	0.0000	272	0.0005	160	0.0130	106	0.0002	320	0.0004	225	0.0003	161
114	deepglint-005	0.0000	341	0.0019	336	0.0438	242	0.0006	387	0.0006	390	0.0028	339
115	deepsea-001	0.0000	164	0.0000	88	-	354	0.0000	19	0.0000	103	0.0000	94
116	deepsense-000	0.0000	75	0.0006	191	-	447	0.0000	150	0.0004	193	0.0003	164

Table 31: FTE is the proportion of failed template generation attempts. Failures can occur because the software throws an exception, or because the software electively refuses to process the input image. This would typically occur if a face is not detected. FTE is measured as the number of function calls that give EITHER a non-zero error code OR that give a “small” template. This is defined as one whose size is less than 0.3 times the median template size for that algorithm. This second rule is needed because some algorithms incorrectly fail to return a non-zero error code when template generation fails.

A hyphen “-” indicates the dataset was not produced.¹ The effects of FTE are included in the accuracy results of this report by regarding any template comparison involving a failed template to produce a low similarity score. Thus higher FTE results in higher FNMR and lower FMR.

	Algorithm	Failure to Enrol Rate ¹							
		APPLICATION	BORDER	KIOSK	MUGSHOT	VISA	WILD	SEC. 2.1	SEC. 2.6
	Name	SEC. 2.2	SEC. 2.3	SEC. 2.5	SEC. 2.4	SEC. 2.1	SEC. 2.6	SEC. 2.1	SEC. 2.6
117	deepsense-001	0.0000	15	0.0006	193	0.0191	147	0.0000	156
118	dermalog-009	0.0000	374	0.0031	370	0.0148	117	0.0006	385
119	dermalog-010	0.0000	375	0.0031	371	0.0148	116	0.0006	383
120	dicio-001	0.0005	436	0.0649	453	0.2136	282	0.0024	431
121	didiglobalface-001	0.0000	258	0.0012	298	-	313	0.0000	199
122	digidata-000	0.0000	219	0.0023	350	0.0375	233	0.0004	368
123	digidata-001	0.0000	222	0.0023	351	0.0375	232	0.0004	367
124	digitalbarriers-002	0.0001	414	0.0045	400	-	387	0.0028	439
125	dps-000	0.0000	181	0.0000	98	0.0000	27	0.0000	29
126	dsk-000	0.0000	147	0.0000	79	-	338	0.0000	43
127	einetworks-000	0.0000	380	0.0017	330	-	321	0.0002	312
128	ekin-002	0.0000	31	0.0000	118	0.0004	66	0.0000	130
129	enface-000	0.0000	162	0.0012	307	0.0305	210	0.0000	178
130	enface-001	0.0000	192	0.0012	305	0.0304	209	0.0000	158
131	eocortex-000	0.0095	453	0.0602	452	-	356	0.0094	453
132	ercacat-001	0.0000	184	0.0005	167	-	369	0.0000	177
133	euronovate-001	0.0255	459	0.0102	424	0.0517	245	0.0021	428
134	expasoft-001	0.0000	194	0.0000	111	-	376	0.0000	10
135	expasoft-002	0.0000	13	0.0000	9	0.0000	41	0.0000	117
136	f8-001	0.0003	427	0.0059	413	-	385	0.0035	444
137	f8-002	0.0000	400	0.0150	432	0.0685	263	0.0005	370
138	faceonlive-001	0.0000	392	0.0029	367	0.0481	244	0.0013	418
139	faceonlive-002	0.0002	424	0.0009	264	0.0075	82	0.0008	401
140	facephi-000	0.0000	35	0.0004	144	0.0090	92	0.0001	260
141	facesoft-000	0.0000	47	0.0000	25	-	434	0.0000	89
142	facetag-000	0.0000	160	0.0000	85	0.0000	20	0.0000	17
143	facetag-002	0.0000	195	0.0000	110	0.0000	34	0.0000	12
144	facex-001	0.0001	422	0.0360	447	-	374	0.0047	448
145	facex-002	0.0001	421	0.0360	446	0.2663	285	0.0047	449
146	farfaces-001	0.0000	377	0.0007	203	0.0061	77	0.0003	342
147	fiberhome-nanjing-003	0.0000	176	0.0004	151	-	361	0.0000	27
148	fiberhome-nanjing-004	0.0000	28	0.0004	150	-	418	0.0000	104
149	fimcore-000	0.0000	282	0.0008	240	0.0185	142	0.0001	208
150	firstcreditKZ-001	0.0000	340	0.0019	338	0.0321	215	0.0000	197
151	frpkauai-001	0.0000	337	0.0024	354	0.0360	226	0.0001	222
152	fujitsulab-002	0.0000	153	0.0009	249	-	346	0.0001	269
153	fujitsulab-003	0.0000	125	0.0008	227	0.0166	131	0.0001	257
154	g42-intellibrain-001	0.0000	120	0.0000	66	0.0000	7	0.0000	64
155	geo-002	0.0000	297	0.0015	319	0.0332	219	0.0001	204
156	geo-004	0.0000	245	0.0005	173	0.0138	111	0.0001	244
157	glory-004	0.0000	310	0.0020	344	0.0345	222	0.0001	265
158	glory-005	0.0000	327	0.0020	345	0.0345	221	0.0001	264
159	gorilla-007	0.0000	270	0.0009	268	0.0252	192	0.0001	231
160	gorilla-008	0.0000	237	0.0009	267	0.0259	198	0.0001	232
161	graymatics-001	0.0000	188	0.0010	269	0.0210	161	0.0001	280
162	griaule-000	0.0000	388	0.0026	358	0.0531	246	0.0004	366
163	griaule-001	0.0000	117	0.0012	306	0.0366	229	0.0000	149
164	hertasecurity-001	0.0000	49	0.0000	121	0.0000	63	0.0000	143
165	hertasecurity-002	0.0000	177	0.0000	96	0.0000	25	0.0000	139
166	hik-001	0.0000	107	0.0000	123	-	302	0.0000	58
167	hisign-001	0.0000	186	0.0000	104	0.0000	28	0.0000	1
168	hisign-002	0.0000	311	0.0006	187	0.0150	118	0.0001	267
169	hyperverge-002	0.0000	42	0.0008	226	0.0210	163	0.0002	326
170	hyperverge-003	0.0000	73	0.0008	224	0.0210	162	0.0002	325
171	hzailou-002	0.0000	370	0.0015	322	0.0424	238	0.0003	347
172	hzailou-003	0.0000	288	0.0004	145	0.0081	89	0.0002	292
173	icm-003	0.0000	123	0.0001	125	0.0023	68	0.0000	67
174	icm-004	0.0000	387	0.0033	379	0.0698	264	0.0006	389
								0.0010	410
								0.0026	335

Table 32: FTE is the proportion of failed template generation attempts. Failures can occur because the software throws an exception, or because the software electively refuses to process the input image. This would typically occur if a face is not detected. FTE is measured as the number of function calls that give EITHER a non-zero error code OR that give a “small” template. This is defined as one whose size is less than 0.3 times the median template size for that algorithm. This second rule is needed because some algorithms incorrectly fail to return a non-zero error code when template generation fails.

A hyphen “-” indicates the dataset was not produced.¹ The effects of FTE are included in the accuracy results of this report by regarding any template comparison involving a failed template to produce a low similarity score. Thus higher FTE results in higher FNMR and lower FMR.

	Algorithm	Failure to Enrol Rate ¹											
		APPLICATION	BORDER	KIOSK	MUGSHOT	VISA	WILD	SEC. 2.2	SEC. 2.3	SEC. 2.5	SEC. 2.4	SEC. 2.1	SEC. 2.6
175	icthtc-000	0.0001	420	0.0047	405	-	362	0.0028	440	0.0029	447	0.0086	371
176	id3-006	0.0000	345	0.0009	266	-	341	0.0004	357	0.0005	363	0.0008	292
177	id3-008	0.0000	50	0.0006	189	0.0184	139	0.0001	279	0.0004	200	0.0003	141
178	idemria-008	0.0000	173	0.0004	158	0.0078	87	0.0000	138	0.0003	177	0.0003	154
179	idemria-009	0.0000	111	0.0004	154	0.0077	84	0.0000	142	0.0003	176	0.0003	158
180	iit-002	0.0000	385	0.0021	347	-	397	0.0009	410	0.0005	373	0.0443	421
181	iit-003	0.0000	253	0.0008	239	-	316	0.0000	166	0.0004	207	0.0069	363
182	imds-software-001	0.0000	1	0.0000	1	0.0000	39	0.0000	112	0.0000	6	0.0000	13
183	imperial-000	0.0000	78	0.0000	40	-	452	0.0000	77	0.0000	39	0.0000	26
184	imperial-002	0.0000	40	0.0000	23	-	423	0.0000	108	0.0000	20	0.0000	8
185	incode-010	0.0000	333	0.0009	255	0.0255	195	0.0002	299	0.0004	238	0.0007	288
186	incode-011	0.0000	312	0.0009	254	0.0255	196	0.0002	301	0.0004	234	0.0007	287
187	infocert-001	0.0000	352	0.0059	414	0.0424	239	0.0001	234	0.0006	379	0.0018	324
188	innneflabs-000	0.0000	220	0.0024	353	-	420	0.0003	343	0.0005	359	0.0004	218
189	innovativetechnologyltd-001	0.0001	418	0.0050	407	-	343	0.0024	434	0.0025	443	0.0055	356
190	innovativetechnologyltd-002	0.0000	338	0.0046	401	-	417	0.0057	452	0.0005	360	0.0247	409
191	innovatrics-007	0.0000	232	0.0007	213	-	441	0.0001	207	0.0003	164	0.0003	156
192	innovatrics-008	0.0000	283	0.0009	259	0.0204	154	0.0000	175	0.0004	195	0.0003	190
193	insightface-001	0.0000	198	0.0000	112	0.0000	37	0.0000	14	0.0000	122	0.0000	89
194	insightface-003	0.0000	62	0.0000	32	0.0000	50	0.0000	95	0.0000	30	0.0000	42
195	inspur-000	0.0000	127	0.0000	67	0.0000	9	0.0000	68	0.0000	68	0.0000	74
196	intellicloudai-001	0.0000	175	0.0000	94	-	360	0.0000	26	0.0000	108	0.0001	121
197	intellicloudai-002	0.0000	25	0.0008	230	-	406	0.0000	167	0.0004	199	0.0012	310
198	intellifusion-001	0.0000	279	0.0005	169	-	349	0.0001	227	0.0003	182	0.0005	258
199	intellifusion-002	0.0000	150	0.0000	119	-	342	0.0000	124	0.0000	93	0.0001	120
200	intellivision-003	0.0000	249	0.0012	302	0.0308	211	0.0003	336	0.0004	341	0.0185	397
201	intellivision-004	0.0000	285	0.0011	290	0.0266	202	0.0002	327	0.0004	338	0.0179	395
202	intellivix-001	0.0000	94	0.0000	50	0.0000	3	0.0000	54	0.0000	65	0.0000	62
203	intellivix-002	0.0000	54	0.0009	265	0.0184	140	0.0000	92	0.0000	33	0.0000	40
204	intelresearch-004	0.0000	255	0.0006	181	-	308	0.0000	153	0.0004	224	0.0003	165
205	intelresearch-005	0.0000	262	0.0006	182	0.0144	114	0.0000	154	0.0004	223	0.0003	166
206	intemta-000	0.0000	201	0.0005	161	0.0126	104	0.0000	187	0.0004	210	0.0003	153
207	intsysmsu-001	0.0000	106	0.0010	278	-	296	0.0001	247	0.0004	271	0.0004	230
208	intsysmsu-002	0.0000	41	0.0010	276	-	429	0.0001	251	0.0004	265	0.0004	228
209	ionetworks-000	0.0000	124	0.0016	326	0.0387	234	0.0004	351	0.0005	351	0.0004	239
210	iqface-000	0.0000	187	0.0000	102	-	370	0.0000	3	0.0000	113	0.0000	76
211	iqface-003	0.0000	382	0.0076	419	-	448	0.0006	384	0.0005	377	0.0069	362
212	irex-000	0.0000	351	0.0009	263	-	381	0.0000	185	0.0005	346	0.0003	182
213	isap-001	0.0000	96	0.0000	49	-	293	0.0000	52	0.0000	64	0.0000	61
214	isap-002	0.0000	179	0.0000	97	-	365	0.0000	31	0.0000	106	0.0000	105
215	isityou-000	0.0068	450	0.0316	443	-	453	0.0023	430	0.0010	408	0.0663	429
216	isystems-001	0.0000	391	0.0035	386	-	339	0.0010	411	0.0007	396	0.0128	383
217	isystems-002	0.0000	390	0.0035	385	-	431	0.0010	412	0.0007	395	0.0128	382
218	itm0-007	0.0000	10	0.0009	248	-	391	0.0003	349	0.0000	3	0.0004	208
219	itm0-008	0.0000	22	0.0135	429	0.1239	276	0.0024	435	0.0000	18	0.0836	431
220	ivacognitive-001	0.0000	316	0.0011	292	-	462	0.0001	221	0.0004	323	0.0011	302
221	iws-000	0.0005	434	0.0650	455	-	432	0.0024	432	0.0012	421	0.0936	438
222	jaakit-001	0.0008	440	0.0858	457	0.2713	286	0.0042	445	0.0021	439	0.1062	443
223	kakao-007	0.0000	79	0.0007	194	0.0165	130	0.0001	240	0.0004	221	0.0097	378
224	kakao-008	0.0000	80	0.0009	251	0.0209	160	0.0001	239	0.0004	220	0.0097	377
225	kakaopay-001	0.0000	308	0.0013	314	0.0322	216	0.0001	226	0.0004	326	0.0078	368
226	kasikornlabs-000	0.0000	396	0.0035	384	0.0713	265	0.0004	363	0.0012	424	0.0270	412
227	kasikornlabs-001	0.0001	419	0.0050	406	0.0885	271	0.0006	392	0.0035	451	0.0305	413
228	kedacom-000	0.0000	61	0.0000	31	-	442	0.0000	96	0.0000	31	0.0000	43
229	kiwitech-000	0.0000	293	0.0009	247	-	371	0.0004	359	0.0005	349	0.0004	244
230	kneron-003	0.0239	457	0.0306	441	-	319	0.0044	447	0.0016	433	0.1823	454
231	kneron-005	0.0000	393	0.0226	435	-	411	0.0006	382	0.0005	357	0.0097	376
232	knowutech-000	0.0000	252	0.0008	222	0.0215	170	0.0000	172	0.0004	281	0.0003	188

Table 33: FTE is the proportion of failed template generation attempts. Failures can occur because the software throws an exception, or because the software electively refuses to process the input image. This would typically occur if a face is not detected. FTE is measured as the number of function calls that give EITHER a non-zero error code OR that give a “small” template. This is defined as one whose size is less than 0.3 times the median template size for that algorithm. This second rule is needed because some algorithms incorrectly fail to return a non-zero error code when template generation fails.

A hyphen “-” indicates the dataset was not produced.¹ The effects of FTE are included in the accuracy results of this report by regarding any template comparison involving a failed template to produce a low similarity score. Thus higher FTE results in higher FNMR and lower FMR.

	Algorithm	Failure to Enrol Rate ¹											
		APPLICATION	BORDER	KIOSK	MUGSHOT	VISA	WILD	SEC. 2.2	SEC. 2.3	SEC. 2.5	SEC. 2.4	SEC. 2.1	SEC. 2.6
233	kookmin-002	0.0000	142	0.0000	76	-	331	0.0000	40	0.0000	80	0.0000	50
234	krungthai-002	0.0000	305	0.0005	164	0.0111	101	0.0002	310	0.0003	190	0.0005	248
235	kuke3d-001	0.0000	171	0.0000	91	0.0000	23	0.0000	24	0.0000	97	0.0000	98
236	kuke3d-002	0.0000	74	0.0000	39	0.0000	53	0.0000	74	0.0000	36	0.0000	24
237	lebentech-000	0.0042	444	0.0029	369	0.0252	191	0.0051	451	0.0066	454	0.0154	389
238	lemalabs-001	0.0000	65	0.0005	171	0.0141	112	0.0002	309	0.0004	204	0.0004	199
239	lineclova-001	0.0000	70	0.0000	38	0.0000	54	0.0000	76	0.0000	38	0.0001	122
240	lineclova-002	0.0000	157	0.0007	195	0.0181	137	0.0000	46	0.0000	86	0.0000	108
241	lockman-002	0.0000	64	0.0000	33	-	444	0.0000	70	0.0000	41	0.0000	21
242	lockman-004	0.0000	7	0.0000	6	-	389	0.0000	114	0.0000	1	0.0000	15
243	luxand-000	0.0000	172	0.0000	93	-	359	0.0000	25	0.0000	107	0.0000	100
244	mantra-000	0.0001	404	0.0041	396	0.0680	262	0.0003	341	0.0004	339	0.0037	344
245	maxvision-001	0.0000	101	0.0000	52	0.0000	2	0.0000	50	0.0000	62	0.0000	59
246	maxvision-002	0.0000	218	0.0009	244	0.0229	179	0.0002	289	0.0004	252	0.0004	245
247	megvii-005	0.0000	246	0.0010	271	0.0206	156	0.0002	319	0.0004	306	0.0011	303
248	megvii-006	0.0000	294	0.0010	272	0.0206	157	0.0002	318	0.0004	309	0.0011	304
249	meituuan-001	0.0000	213	0.0014	317	0.0295	208	0.0001	254	0.0004	286	0.0013	315
250	meituuan-002	0.0000	234	0.0013	312	0.0251	190	0.0001	253	0.0004	279	0.0020	326
251	meiya-001	0.0000	389	0.0028	364	-	311	0.0004	364	0.0010	409	0.0025	332
252	mendaxiatech-000	0.0000	206	0.0010	270	0.0206	155	0.0002	322	0.0004	301	0.0011	305
253	metsakuurcompany-001	0.0000	112	0.0011	288	0.0208	159	0.0002	316	0.0004	222	0.0003	178
254	metsakuurcompany-002	0.0000	152	0.0000	83	0.0000	18	0.0000	45	0.0000	85	0.0000	56
255	microfocus-001	0.0001	415	0.0053	410	-	427	0.0008	403	0.0016	431	0.0220	403
256	microfocus-002	0.0001	417	0.0053	411	-	322	0.0008	402	0.0016	432	0.0220	402
257	minivision-000	0.0000	93	0.0000	51	-	292	0.0000	53	0.0000	66	0.0000	63
258	mobai-000	0.0000	355	0.0114	426	-	436	0.0003	344	0.0012	423	0.1242	449
259	mobai-001	0.0000	309	0.0040	392	-	428	0.0001	261	0.0012	422	0.0523	426
260	mobabl-001	0.0000	383	0.0052	409	0.0678	260	0.0002	294	0.0005	364	0.0181	396
261	mobabl-003	0.0000	394	0.0029	368	0.0633	253	0.0002	313	0.0009	403	0.0026	334
262	mobilpintech-000	0.0000	85	0.0000	45	0.0000	56	0.0000	81	0.0000	52	0.0000	30
263	moredian-000	0.0000	221	0.0009	245	-	421	0.0004	361	0.0005	348	0.0004	241
264	mukh-001	0.0000	66	0.0010	277	0.0154	122	0.0001	258	0.0003	144	0.0010	298
265	multimodality-000	0.0000	36	0.0000	22	0.0000	46	0.0000	107	0.0000	24	0.0000	7
266	multimodality-001	0.0000	44	0.0009	243	0.0259	199	0.0000	87	0.0000	27	0.0000	35
267	mvision-001	0.0000	77	0.0000	41	-	451	0.0000	78	0.0000	40	0.0000	27
268	nazhaiai-000	0.0000	82	0.0000	43	-	455	0.0000	79	0.0000	50	0.0000	28
269	neosystems-004	0.0000	71	0.0000	37	0.0000	55	0.0000	75	0.0000	37	0.0000	25
270	neosystems-005	0.0000	185	0.0000	103	0.0000	29	0.0000	2	0.0000	114	0.0000	77
271	netbridgetech-001	0.0000	29	0.0000	18	-	414	0.0000	103	0.0000	15	0.0000	3
272	netbridgetech-002	0.0000	182	0.0000	101	-	372	0.0000	5	0.0000	116	0.0000	80
273	neurotechnology-013	0.0000	58	0.0008	241	0.0185	141	0.0000	135	0.0001	129	0.0004	216
274	neurotechnology-015	0.0000	17	0.0004	146	0.0082	90	0.0000	120	0.0000	124	0.0003	140
275	nhn-002	0.0000	144	0.0004	159	0.0091	93	0.0000	164	0.0003	156	0.0003	143
276	nhn-003	0.0000	335	0.0000	16	0.0000	42	0.0001	284	0.0004	287	0.0010	299
277	nodeflux-002	0.0000	280	0.0261	438	-	352	0.0008	400	0.0005	361	0.0008	294
278	notiontag-001	0.0000	138	0.0000	74	-	328	0.0027	438	0.0000	77	0.0132	386
279	notiontag-002	0.0000	193	0.0000	106	0.0000	33	0.0000	7	0.0000	111	0.0000	83
280	nsensecorp-003	0.0000	109	0.0000	124	0.0002	64	0.0000	152	0.0007	398	0.0150	387
281	nsensecorp-004	0.0406	460	0.0035	383	0.0181	136	0.0016	423	0.0760	462	0.0509	425
282	ntechlab-011	0.0000	43	0.0003	130	0.0057	74	0.0000	192	0.0004	191	0.0003	167
283	ntechlab-012	0.0000	128	0.0003	131	0.0057	73	0.0000	190	0.0004	194	0.0003	173
284	omface-000	0.0000	68	0.0000	34	0.0000	52	0.0000	73	0.0000	45	0.1160	447
285	omface-001	0.0000	63	0.0000	117	0.0000	62	0.0000	71	0.0000	42	0.0000	106
286	omnigarde-001	0.0000	229	0.0008	217	0.0213	165	0.0000	160	0.0004	266	0.0003	185
287	omnigarde-002	0.0000	303	0.0008	218	0.0213	164	0.0000	157	0.0004	275	0.0003	189
288	openface-001	0.0000	366	0.0104	425	0.0668	255	0.0004	356	0.0006	391	0.0856	434
289	oz-003	0.0000	89	0.0002	128	0.0042	70	0.0000	129	0.0003	143	0.0002	128
290	oz-004	0.0000	372	0.0003	135	0.0041	69	0.0000	133	0.0002	133	0.0006	265

Table 34: FTE is the proportion of failed template generation attempts. Failures can occur because the software throws an exception, or because the software electively refuses to process the input image. This would typically occur if a face is not detected. FTE is measured as the number of function calls that give EITHER a non-zero error code OR that give a “small” template. This is defined as one whose size is less than 0.3 times the median template size for that algorithm. This second rule is needed because some algorithms incorrectly fail to return a non-zero error code when template generation fails.

A hyphen “-” indicates the dataset was not produced.¹ The effects of FTE are included in the accuracy results of this report by regarding any template comparison involving a failed template to produce a low similarity score. Thus higher FTE results in higher FNMR and lower FMR.

	Algorithm	Failure to Enrol Rate ¹									
		APPLICATION		BORDER		KIOSK		MUGSHOT		VISA	
Name	SEC. 2.2	SEC. 2.3	SEC. 2.5	SEC. 2.4	SEC. 2.1	SEC. 2.6				WILD	
291	palit-000	0.0000	265	0.0005	165	0.0134	109	0.0002	304	0.0004	226
292	palit-001	0.0000	298	0.0007	216	0.0201	153	0.0002	302	0.0004	228
293	pangiam-000	0.0000	95	0.0021	349	0.0364	227	0.0001	205	0.0005	347
294	papago-001	0.0000	315	0.0008	225	0.0159	128	0.0002	328	0.0004	248
295	papsav1923-001	0.0000	301	0.0007	207	-	375	0.0001	242	0.0002	141
296	papsav1923-002	0.0000	291	0.0018	335	0.0268	203	0.0000	179	0.0004	284
297	paravision-008	0.0000	145	0.0010	275	0.0201	151	0.0001	236	0.0004	202
298	paravision-010	0.0000	9	0.0010	273	0.0201	152	0.0001	238	0.0004	197
299	pensees-001	0.0000	274	0.0000	78	-	340	0.0000	42	0.0000	89
300	pixelall-008	0.0000	126	0.0008	232	0.0247	187	0.0000	69	0.0000	75
301	pixelall-009	0.0000	191	0.0000	107	0.0000	32	0.0000	8	0.0000	112
302	psl-010	0.0000	287	0.0004	149	0.0095	94	0.0000	122	0.0004	196
303	psl-011	0.0000	211	0.0003	132	0.0063	79	0.0000	126	0.0003	175
304	ptakuratsatu-000	0.0000	242	0.0007	214	-	458	0.0001	206	0.0003	166
305	pxl-001	0.0000	401	0.0044	399	-	408	0.0005	373	0.0022	441
306	pyramid-000	0.0001	413	0.0041	395	-	300	0.0005	372	0.0007	397
307	qazbs-000	0.0000	154	0.0009	252	0.0265	201	0.0000	147	0.0004	245
308	qnap-001	0.0000	299	0.0000	122	0.0002	65	0.0000	180	0.0001	130
309	qnap-002	0.0000	384	0.0033	373	0.0761	267	0.0004	354	0.0002	132
310	quantasoft-003	0.0000	353	0.0015	323	0.0355	224	0.0005	371	0.0006	386
311	rankone-012	0.0000	139	0.0000	72	0.0000	13	0.0000	36	0.0000	76
312	rankone-013	0.0000	16	0.0005	162	0.0126	105	0.0000	146	0.0003	146
313	realnetworks-006	0.0000	251	0.0002	129	0.0045	71	0.0000	125	0.0002	142
314	realnetworks-007	0.0000	224	0.0013	315	0.0425	240	0.0000	131	0.0004	253
315	regula-000	0.0000	30	0.0000	19	0.0000	43	0.0000	102	0.0000	16
316	regula-001	0.0000	197	0.0000	108	0.0000	35	0.0000	9	0.0000	117
317	remarkai-001	0.0000	91	0.0000	47	-	463	0.0000	85	0.0000	48
318	remarkai-003	0.0000	233	0.0007	202	0.0187	143	0.0000	183	0.0004	213
319	rendip-000	0.0000	344	0.0016	325	0.0293	207	0.0002	300	0.0004	336
320	revealmedia-005	0.0000	349	0.0007	209	0.0189	145	0.0009	409	0.0004	343
321	revealmedia-006	0.0000	200	0.0009	260	0.0238	185	0.0001	255	0.0004	300
322	rokid-000	0.0000	52	0.0072	417	-	438	0.0001	241	0.0005	358
323	rokid-001	0.0000	56	0.0013	311	-	440	0.0000	93	0.0000	34
324	s1-005	0.0000	134	0.0004	152	0.0120	103	0.0001	218	0.0002	134
325	s1-006	0.0000	45	0.0003	133	0.0074	81	0.0001	214	0.0002	136
326	saffe-001	0.0000	105	0.0000	56	-	295	0.0000	55	0.0000	67
327	saffe-002	0.0000	6	0.0000	7	-	390	0.0000	115	0.0000	2
328	samsungsds-001	0.0000	163	0.0005	168	0.0146	115	0.0001	235	0.0003	184
329	samsungsds-002	0.0000	100	0.0004	153	0.0119	102	0.0001	237	0.0003	173
330	samtech-001	0.0001	412	0.0032	372	-	419	0.0004	360	0.0008	399
331	scanovate-002	0.0000	314	0.0018	333	-	454	0.0000	201	0.0004	332
332	scanovate-003	0.0000	313	0.0233	436	0.3371	288	0.0006	386	0.0004	340
333	sdc-000	0.0000	399	0.0035	382	0.0678	261	0.0005	378	0.0011	417
334	securifai-004	0.0000	133	0.0000	68	0.0000	11	0.0000	34	0.0000	82
335	securifai-005	0.0000	151	0.0000	82	0.0000	17	0.0000	44	0.0000	92
336	sensetime-006	0.0000	88	0.0004	147	0.0106	97	0.0000	165	0.0003	165
337	sensetime-007	0.0000	136	0.0004	148	0.0106	96	0.0000	163	0.0003	167
338	sertis-000	0.0000	37	0.0007	208	-	426	0.0000	203	0.0004	233
339	sertis-002	0.0000	131	0.0007	198	0.0152	119	0.0000	196	0.0004	236
340	seventhsense-001	0.0000	230	0.0006	192	0.0184	138	0.0001	210	0.0004	268
341	seventhsense-002	0.0000	46	0.0003	143	0.0076	83	0.0000	202	0.0004	192
342	shaman-000	0.0000	27	0.0000	17	-	412	0.0000	100	0.0000	13
343	shaman-001	0.0000	148	0.0000	81	-	335	0.0000	41	0.0000	88
344	shu-002	0.0000	320	0.0010	281	-	312	0.0005	369	0.0004	320
345	shu-003	0.0000	132	0.0007	196	-	325	0.0001	211	0.0003	159
346	siat-002	0.0000	254	0.0012	304	-	309	0.0000	176	0.0004	255
347	siat-005	0.0000	2	0.0000	3	0.0000	59	0.0000	111	0.0000	5
348	sjtu-003	0.0000	20	0.0005	175	-	398	0.0000	193	0.0003	155
											0.0003
											169

Table 35: FTE is the proportion of failed template generation attempts. Failures can occur because the software throws an exception, or because the software electively refuses to process the input image. This would typically occur if a face is not detected. FTE is measured as the number of function calls that give EITHER a non-zero error code OR that give a "small" template. This is defined as one whose size is less than 0.3 times the median template size for that algorithm. This second rule is needed because some algorithms incorrectly fail to return a non-zero error code when template generation fails.

A hyphen "-" indicates the dataset was not produced.¹ The effects of FTE are included in the accuracy results of this report by regarding any template comparison involving a failed template to produce a low similarity score. Thus higher FTE results in higher FNMR and lower FMR.

	Algorithm	Failure to Enrol Rate ¹											
		APPLICATION	BORDER	KIOSK	MUGSHOT	VISA	WILD	SEC. 2.2	SEC. 2.3	SEC. 2.5	SEC. 2.4		
	Name	SEC. 2.2	SEC. 2.3	SEC. 2.5	SEC. 2.4	SEC. 2.1	SEC. 2.6						
349	sjtu-004	0.0000	183	0.0000	100	0.0000	30	0.0000	4	0.0003	154	0.0000	79
350	sktelecom-000	0.0000	284	0.0008	233	0.0190	146	0.0000	188	0.0004	283	0.0013	314
351	smartbiometrik-001	0.0005	432	0.0649	454	0.2147	284	0.0017	424	0.0008	400	0.0123	381
352	smartengines-000	0.0066	449	0.0150	431	0.1656	277	0.0022	429	0.0013	426	0.0826	430
353	smartengines-001	0.0003	428	0.0073	418	0.0714	266	0.0007	393	0.0005	362	0.0169	393
354	smartvist-000	0.0000	39	0.0026	357	0.0357	225	0.0002	288	0.0011	415	0.0152	388
355	smilart-002	0.0000	395	0.0036	387	-	400	-	462	0.0011	414	-	460
356	smilart-003	0.0003	429	0.0100	423	-	336	0.0014	419	0.0013	428	0.0555	427
357	sodec-000	0.0000	143	0.0000	75	0.0000	16	0.0000	38	0.0000	79	0.0000	49
358	sqisoft-001	0.0000	149	0.0003	141	0.0078	85	0.0000	140	0.0003	183	0.0003	149
359	sqisoft-002	0.0000	92	0.0003	137	0.0078	86	0.0000	145	0.0003	186	0.0003	148
360	stachu-000	0.0000	196	0.0000	109	-	377	0.0000	11	0.0000	118	0.0000	87
361	starhybrid-001	0.0001	416	0.0033	378	-	306	0.0009	408	0.0023	442	0.0044	347
362	sukshi-000	0.0000	116	0.0000	62	0.0000	6	0.0000	63	0.0000	71	0.0000	70
363	suprema-002	0.0000	328	0.0010	285	0.0271	205	0.0002	296	0.0004	237	0.0005	256
364	suprema-003	0.0000	202	0.0008	235	0.0231	181	0.0000	144	0.0004	229	0.0003	174
365	supremaid-001	0.0000	236	0.0020	342	0.0330	218	0.0001	249	0.0004	333	0.0045	348
366	supremaid-002	0.0000	235	0.0020	341	0.0330	217	0.0001	250	0.0004	331	0.0045	349
367	surrey-cvssp-000	0.0000	115	0.0000	59	0.0000	5	0.0000	60	0.0000	57	0.0000	67
368	surrey-cvssp-001	0.0173	456	0.0007	199	0.0179	135	0.0011	415	0.0015	430	0.0038	345
369	synesis-006	0.0000	84	0.0003	142	-	460	0.0000	191	0.0003	148	0.0002	131
370	synesis-007	0.0000	214	0.0013	310	-	396	0.0002	317	0.0004	251	0.0005	249
371	synology-000	0.0000	113	0.0000	61	-	303	0.0000	61	0.0000	59	0.0000	69
372	synology-002	0.0000	158	0.0000	87	-	353	0.0000	18	0.0000	102	0.0000	93
373	sztu-000	0.0000	83	0.0000	44	-	459	0.0000	82	0.0000	53	0.0000	31
374	sztu-001	0.0000	33	0.0000	21	0.0000	44	0.0000	106	0.0000	23	0.0000	6
375	t4isb-000	0.0000	51	0.0000	27	0.0000	48	0.0000	90	0.0000	25	0.0000	38
376	tech5-004	0.0000	228	0.0008	223	-	437	0.0003	335	0.0004	327	0.0006	269
377	tech5-005	0.0000	239	0.0007	215	-	449	0.0000	159	0.0004	294	0.0049	353
378	techsign-000	0.0007	438	0.0334	444	0.2093	279	0.0020	427	0.0011	413	0.0170	394
379	techsign-001	0.0000	286	0.0008	242	0.0253	193	0.0002	305	0.0004	262	0.0004	225
380	tevian-007	0.0000	289	0.0015	324	0.0429	241	0.0002	311	0.0004	285	0.0008	290
381	tevian-008	0.0000	268	0.0006	178	0.0109	100	0.0000	151	0.0003	160	0.0004	226
382	tiger-005	0.0000	306	0.0009	262	0.0194	149	0.0001	230	0.0004	247	0.0004	240
383	tiger-006	0.0000	326	0.0011	294	0.0396	235	0.0001	277	0.0004	342	0.0009	295
384	tinkoff-001	0.0000	321	0.0008	231	0.0171	132	0.0001	271	0.0004	244	0.0014	317
385	tongyi-005	0.0000	108	0.0000	58	-	299	0.0000	57	0.0000	55	0.0000	65
386	toppanidgate-000	0.0000	260	0.0008	228	0.0232	182	0.0004	352	0.0004	272	0.0005	262
387	toshiba-004	0.0000	87	0.0000	46	0.0000	57	0.0000	83	0.0000	46	0.0000	32
388	toshiba-006	0.0000	302	0.0004	155	0.0050	72	0.0001	274	0.0003	162	0.0003	147
389	touchlessid-000	0.0042	445	0.0133	428	0.2009	278	0.0018	426	0.0032	450	0.0457	422
390	touchlessid-001	0.0000	161	0.0036	388	0.0923	273	0.0000	15	0.0000	99	0.0000	90
391	trueface-002	0.0000	319	0.0046	403	-	307	0.0003	332	0.0005	370	0.0330	417
392	trueface-003	0.0000	331	0.0046	404	0.0397	236	0.0003	330	0.0005	372	0.0330	418
393	tuputech-000	0.0003	430	0.0116	427	-	433	-	461	0.0081	456	0.6383	458
394	turingtechvip-001	0.0001	408	0.0007	211	0.0061	78	0.0007	394	0.0006	381	0.0057	358
395	turingtechvip-002	0.0001	407	0.0017	331	0.0097	95	0.0007	395	0.0006	380	0.0057	357
396	turkcell-000	0.0110	454	0.0234	437	0.0350	223	0.0103	454	0.0306	461	0.7213	459
397	twface-000	0.0000	55	0.0000	29	0.0000	49	0.0000	94	0.0000	35	0.0000	41
398	twface-001	0.0000	180	0.0000	99	0.0000	26	0.0000	30	0.0000	105	0.0000	104
399	ulsee-001	0.0000	118	0.0000	63	-	305	0.0000	62	0.0000	70	0.0001	115
400	ultinous-000	-	461	-	460	-	403	-	463	0.0003	168	-	461
401	ultinous-001	-	463	-	463	-	380	-	459	0.0003	169	-	463
402	uluface-002	0.0000	19	0.0000	11	-	394	0.0000	118	0.0000	8	0.0000	18
403	uluface-003	0.0000	178	0.0001	127	-	367	0.0002	290	0.0002	137	0.0244	408
404	unissey-001	0.0000	3	0.0000	4	0.0000	38	0.0000	110	0.0000	4	0.0000	12
405	unissey-002	0.0000	114	0.0000	60	0.0000	4	0.0000	59	0.0000	58	0.0000	68
406	upc-001	0.0000	371	0.0003	136	-	379	0.0003	334	0.0003	179	0.0011	300

Table 36: FTE is the proportion of failed template generation attempts. Failures can occur because the software throws an exception, or because the software electively refuses to process the input image. This would typically occur if a face is not detected. FTE is measured as the number of function calls that give EITHER a non-zero error code OR that give a “small” template. This is defined as one whose size is less than 0.3 times the median template size for that algorithm. This second rule is needed because some algorithms incorrectly fail to return a non-zero error code when template generation fails.

A hyphen “-” indicates the dataset was not produced.¹ The effects of FTE are included in the accuracy results of this report by regarding any template comparison involving a failed template to produce a low similarity score. Thus higher FTE results in higher FNMR and lower FMR.

	Algorithm	Failure to Enrol Rate ¹							
		APPLICATION	BORDER	KIOSK	MUGSHOT	VISA	WILD	SEC. 2.1	SEC. 2.6
	Name	SEC. 2.2	SEC. 2.3	SEC. 2.5	SEC. 2.4				
407	uxlabs-001	0.0000	90	0.0000	48	0.0000	58	0.0000	86
408	vcog-002	-	462	-	461	-	332	-	460
409	vd-002	0.0000	121	0.0000	65	1.0000	310	0.0000	65
410	vd-003	0.0001	409	0.0041	394	0.0676	258	0.0030	441
411	veridas-007	0.0000	367	0.0026	356	0.0595	249	0.0001	263
412	veridas-008	0.0000	365	0.0026	355	0.0595	250	0.0001	266
413	veridium-000	0.0061	448	0.5956	459	0.2889	287	0.0050	450
414	verigram-000	0.0000	342	0.0068	416	0.0822	270	0.0003	350
415	verigram-001	0.0000	332	0.0003	138	0.0060	75	0.0002	315
416	verihubs-inteligensia-000	0.0000	307	0.0029	366	0.0669	257	0.0001	216
417	verihubs-inteligensia-001	0.0000	275	0.0029	365	0.0669	256	0.0001	219
418	verijelas-000	0.0000	296	0.0023	352	0.0375	231	0.0004	365
419	via-000	0.0000	24	0.0000	14	-	410	0.0000	99
420	via-001	0.0000	119	0.0000	64	-	317	0.0000	66
421	videmo-001	0.0000	354	0.0170	433	0.0332	220	0.0010	413
422	videmo-002	0.0000	8	0.0006	188	0.0189	144	0.0001	246
423	videonetics-001	0.0004	431	0.0309	442	-	334	0.0015	422
424	videonetics-002	0.0000	336	0.0459	451	-	416	0.0006	388
425	viettelhightech-000	0.0000	373	0.0019	337	0.0368	230	0.0007	396
426	vigilantsolutions-010	0.0000	357	0.0028	361	0.0609	251	0.0001	225
427	vigilantsolutions-011	0.0000	359	0.0028	362	0.0609	252	0.0001	223
428	vinai-000	0.0000	53	0.0000	28	-	439	0.0000	91
429	vinbigdata-001	0.0000	166	0.0000	89	0.0000	22	0.0000	22
430	vinbigdata-002	0.0000	155	0.0015	321	0.0250	189	0.0000	171
431	vion-000	0.0050	446	0.0392	450	-	383	0.0130	456
432	visage-000	0.0000	376	0.0054	412	-	344	0.0009	406
433	visionbox-001	0.0000	398	0.0033	377	-	355	0.0005	377
434	visionbox-002	0.0000	14	0.0017	327	0.0270	204	0.0000	174
435	visionlabs-010	0.0000	346	0.0009	250	-	445	0.0001	276
436	visionlabs-011	0.0000	57	0.0006	185	0.0156	123	0.0001	228
437	visteam-003	0.0000	209	0.0010	282	0.0225	177	0.0001	213
438	visteam-004	0.0000	212	0.0010	283	0.0225	174	0.0001	256
439	vixvizion-005	0.0000	67	0.0000	35	0.0000	51	0.0000	72
440	vixvizion-006	0.0000	159	0.0000	86	0.0000	19	0.0000	16
441	vnpt-004	0.0000	243	0.0006	180	0.0160	129	0.0002	295
442	vnpt-005	0.0000	12	0.0006	176	0.0154	121	0.0002	306
443	vocord-009	0.0000	248	0.0006	184	-	297	0.0001	282
444	vocord-010	0.0000	324	0.0005	170	0.0141	113	0.0002	307
445	vts-000	0.0000	339	0.0011	291	-	430	0.0001	283
446	vts-001	0.0000	104	0.0003	134	0.0073	80	0.0000	141
447	wicket-000	0.0000	247	0.0009	246	0.0260	200	0.0000	148
448	winsense-001	0.0000	18	0.0000	10	-	395	0.0000	119
449	winsense-002	0.0000	170	0.0000	92	-	358	0.0000	23
450	wiseai-001	0.0001	405	0.0137	430	0.0768	268	0.0018	425
451	wuhantianyu-001	0.0000	59	0.0007	200	0.0159	126	0.0001	209
452	x-laboratory-000	0.0247	458	0.0000	2	-	386	0.0005	376
453	x-laboratory-001	0.0000	277	0.0012	301	-	347	0.0001	268
454	xforwardai-001	0.0000	217	0.0007	210	-	409	0.0003	338
455	xforwardai-002	0.0000	266	0.0007	212	-	326	0.0003	337
456	xm-000	0.0000	135	0.0007	197	-	327	0.0001	212
457	yisheng-004	0.0002	425	-	462	-	364	0.0013	417
458	yitu-003	0.0000	69	0.0000	36	-	446	0.0009	407
459	yoonik-002	0.0000	334	0.0010	279	0.0284	206	0.0003	331
460	yoonik-003	0.0000	317	0.0009	257	0.0214	167	0.0002	293
461	ytu-000	0.0000	273	0.0010	287	-	333	0.0002	321
462	yuan-004	0.0000	34	0.0000	20	0.0000	45	0.0000	105
463	yuan-005	0.0000	292	0.0005	166	0.0134	110	0.0002	303

Table 37: FTE is the proportion of failed template generation attempts. Failures can occur because the software throws an exception, or because the software electively refuses to process the input image. This would typically occur if a face is not detected. FTE is measured as the number of function calls that give EITHER a non-zero error code OR that give a “small” template. This is defined as one whose size is less than 0.3 times the median template size for that algorithm. This second rule is needed because some algorithms incorrectly fail to return a non-zero error code when template generation fails.

A hyphen “-” indicates the dataset was not produced.¹ The effects of FTE are included in the accuracy results of this report by regarding any template comparison involving a failed template to produce a low similarity score. Thus higher FTE results in higher FNMR and lower FMR.

3.4 Recognition accuracy

Core algorithm accuracy is stated via:

▷ **Cooperative subjects**

- The summary table of Figure 29;
- The visa image DETs of Figure 86;
- The mugshot DETs of Figure 110;
- The mugshot ageing profiles of Figure 355;
- The human-difficult pairs of Figure 39

▷ **Non-cooperative subjects**

- The photojournalism DET of Figure 130

Figure 287 shows dependence of false match rate on algorithm score threshold. This allows a deployer to set a threshold to target a particular false match rate appropriate to the security objectives of the application.

Figure 239 likewise shows FMR(T) but for mugshots, and specially four subsets of the population.

Note that in both the mugshot and visa sets false match rates vary with the ethnicity, age, and sex, of the enrollee and impostor. For example figure 152 summarizes FMR for impostors paired from four groups black females, black males, white females, white males.

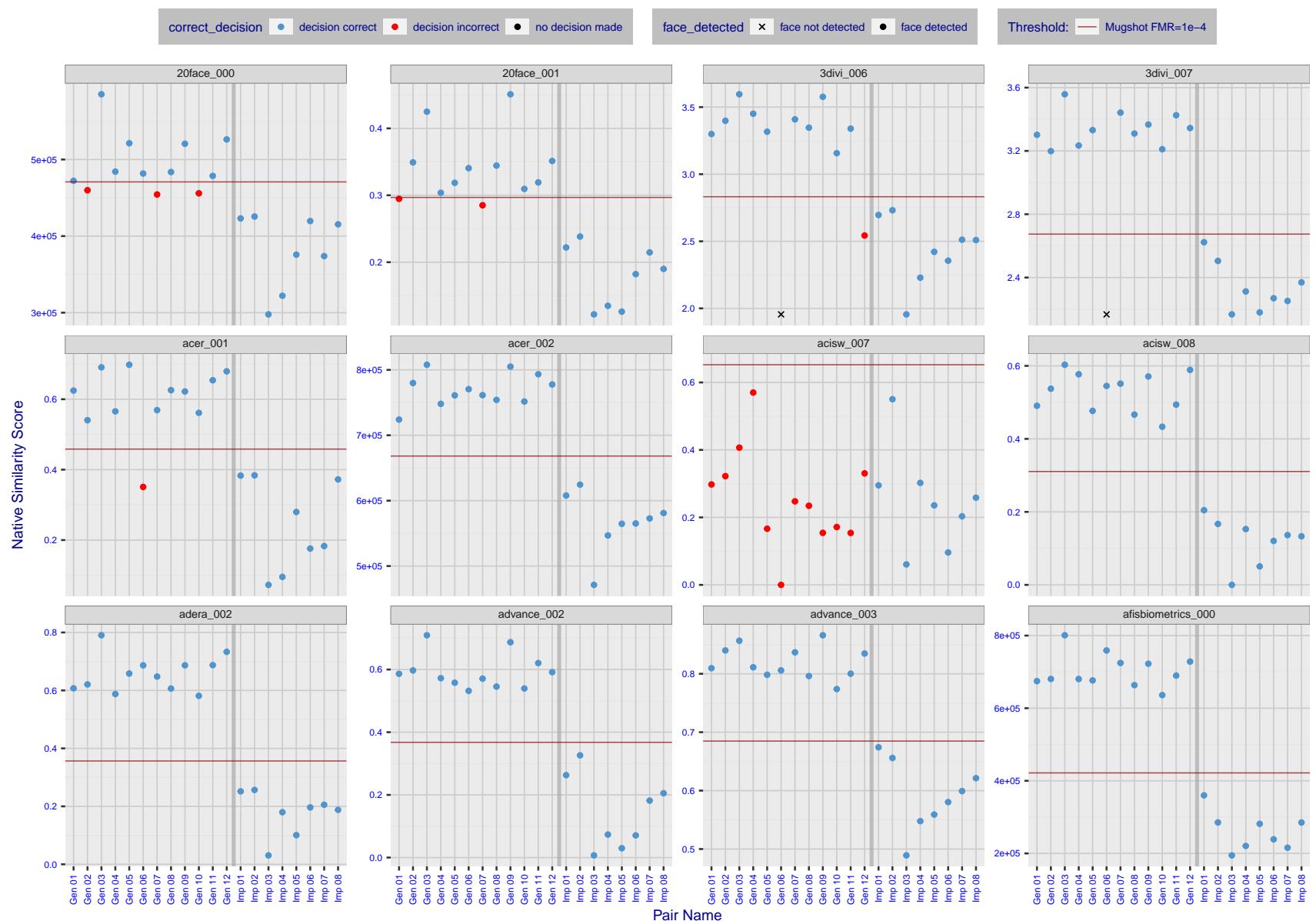


Figure 4: The figure shows algorithms' similarity scores for 12 genuine and 8 impostor image pairs used in a May 2018 paper by Phillips et al. ([1]). The threshold (red horizontal line) is a value calibrated to give $FMR = 0.0001$ on mugshot images. Points above the threshold correspond to pairs determined to be genuine, and points below the threshold correspond to pairs determined to be impostors. If the determined class (genuine or impostor) matches the real class, points will be blue; if not, red. An X represents face detection failure in either of the images in the pair. Note that the sample size ($n=20$) is small, and the figure may change substantially if larger or different sets are used. The images can be viewed on p. 13 of the Appendix, where Gen 01 corresponds to Same-Identity Pair 1, Gen 02 corresponds to Same-Identity Pair 2, and so on.

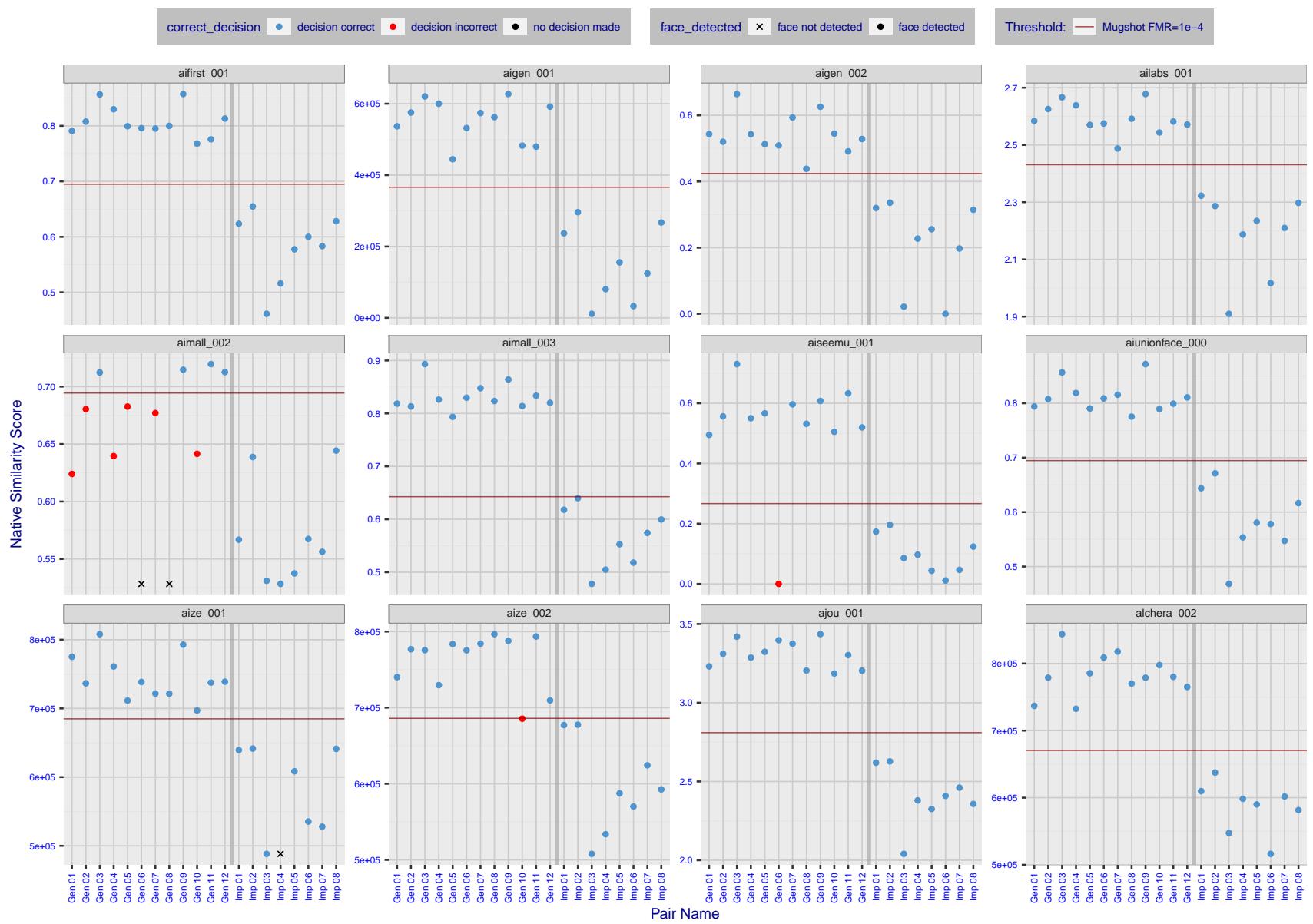


Figure 5: The figure shows algorithms' similarity scores for 12 genuine and 8 impostor image pairs used in a May 2018 paper by Phillips et al. ([1]). The threshold (red horizontal line) is a value calibrated to give $FMR = 0.0001$ on mugshot images. Points above the threshold correspond to pairs determined to be genuine, and points below the threshold correspond to pairs determined to be impostors. If the determined class (genuine or impostor) matches the real class, points will be blue; if not, red. An X represents face detection failure in either of the images in the pair. Note that the sample size ($n=20$) is small, and the figure may change substantially if larger or different sets are used. The images can be viewed on p. 13 of the Appendix, where Gen 01 corresponds to Same-Identity Pair 1, Gen 02 corresponds to Same-Identity Pair 2, and so on.

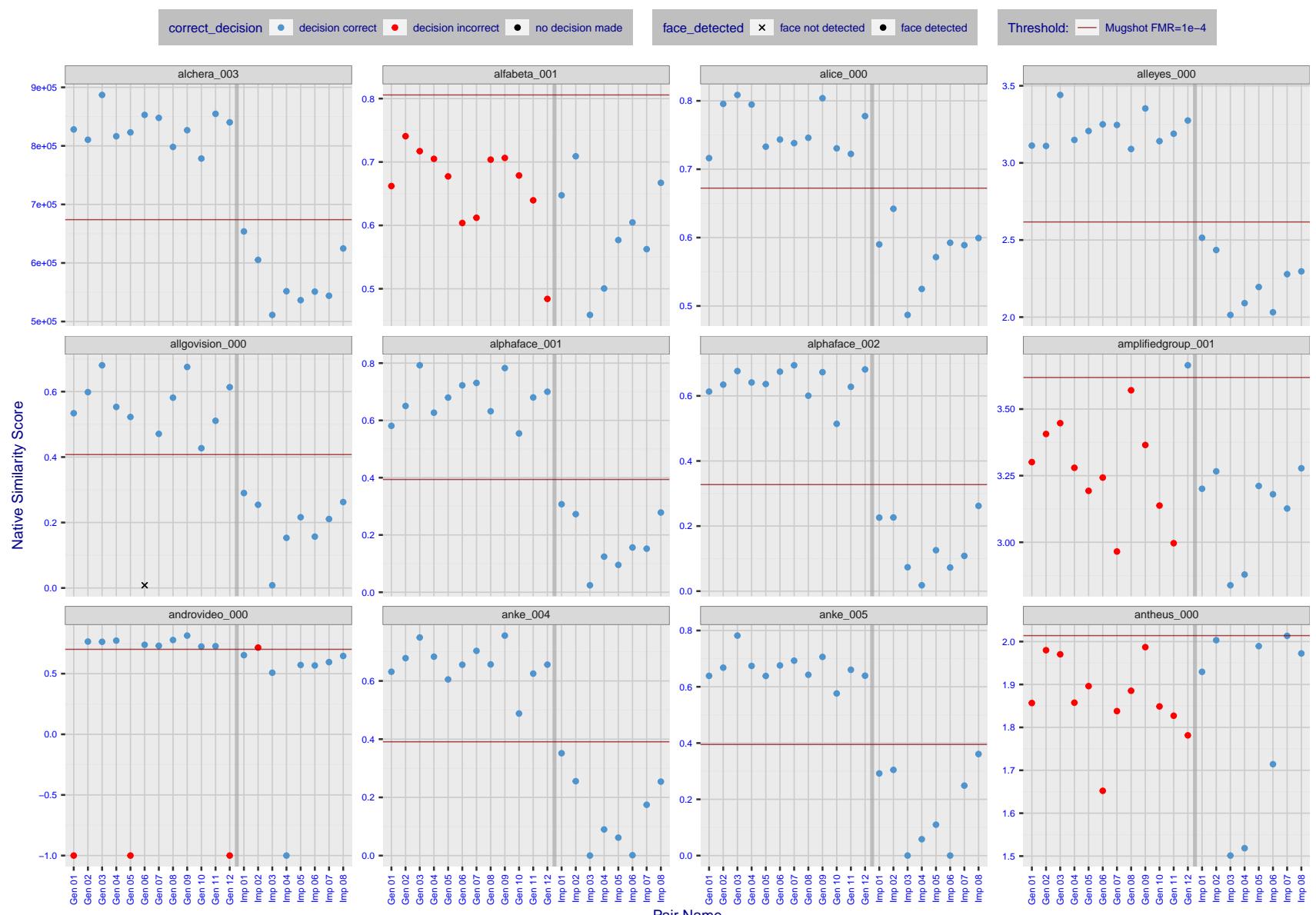


Figure 6: The figure shows algorithms' similarity scores for 12 genuine and 8 impostor image pairs used in a May 2018 paper by Phillips et al. ([1]). The threshold (red horizontal line) is a value calibrated to give $FMR = 0.0001$ on mugshot images. Points above the threshold correspond to pairs determined to be genuine, and points below the threshold correspond to pairs determined to be impostors. If the determined class (genuine or impostor) matches the real class, points will be blue; if not, red. An X represents face detection failure in either of the images in the pair. Note that the sample size ($n=20$) is small, and the figure may change substantially if larger or different sets are used. The images can be viewed on p. 13 of the Appendix, where Gen 01 corresponds to Same-Identity Pair 1, Gen 02 corresponds to Same-Identity Pair 2, and so on.

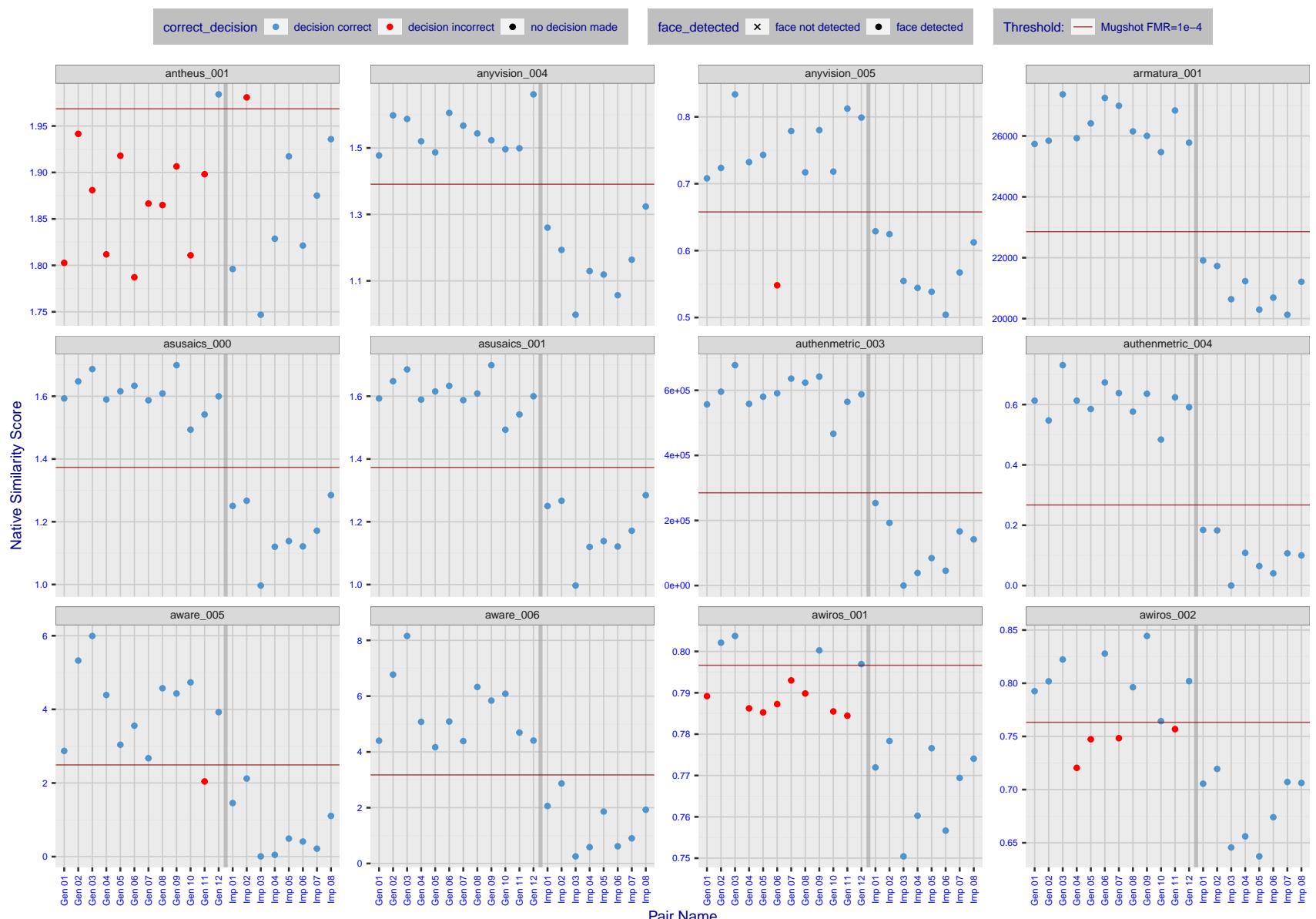


Figure 7: The figure shows algorithms' similarity scores for 12 genuine and 8 impostor image pairs used in a May 2018 paper by Phillips et al. ([1]). The threshold (red horizontal line) is a value calibrated to give $FMR = 0.0001$ on mugshot images. Points above the threshold correspond to pairs determined to be genuine, and points below the threshold correspond to pairs determined to be impostors. If the determined class (genuine or impostor) matches the real class, points will be blue; if not, red. An X represents face detection failure in either of the images in the pair. Note that the sample size ($n=20$) is small, and the figure may change substantially if larger or different sets are used. The images can be viewed on p. 13 of the Appendix, where Gen 01 corresponds to Same-Identity Pair 1, Gen 02 corresponds to Same-Identity Pair 2, and so on.

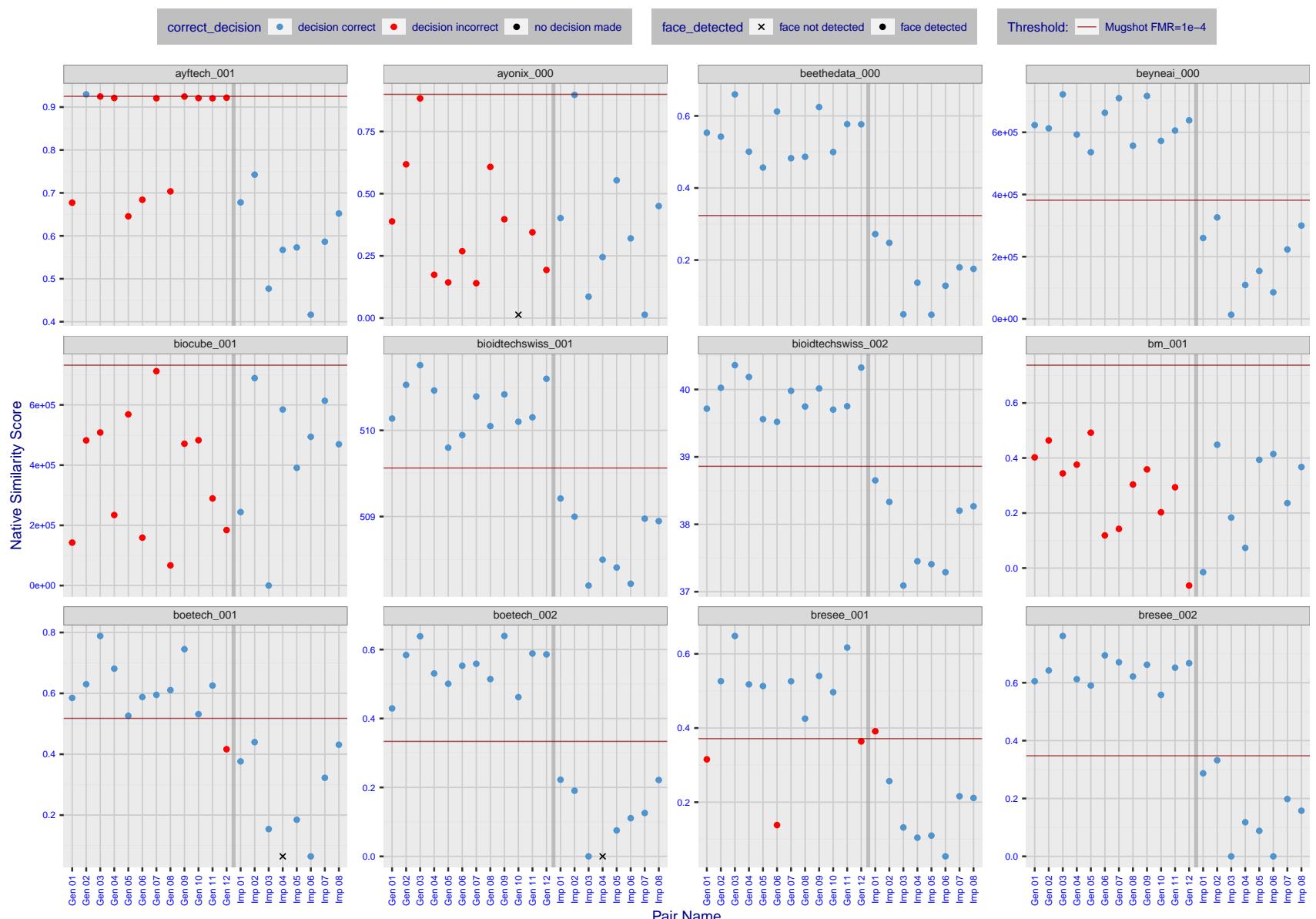


Figure 8: The figure shows algorithms' similarity scores for 12 genuine and 8 impostor image pairs used in a May 2018 paper by Phillips et al. ([1]). The threshold (red horizontal line) is a value calibrated to give $FMR = 0.0001$ on mugshot images. Points above the threshold correspond to pairs determined to be genuine, and points below the threshold correspond to pairs determined to be impostors. If the determined class (genuine or impostor) matches the real class, points will be blue; if not, red. An X represents face detection failure in either of the images in the pair. Note that the sample size ($n=20$) is small, and the figure may change substantially if larger or different sets are used. The images can be viewed on p. 13 of the Appendix, where Gen 01 corresponds to Same-Identity Pair 1, Gen 02 corresponds to Same-Identity Pair 2, and so on.

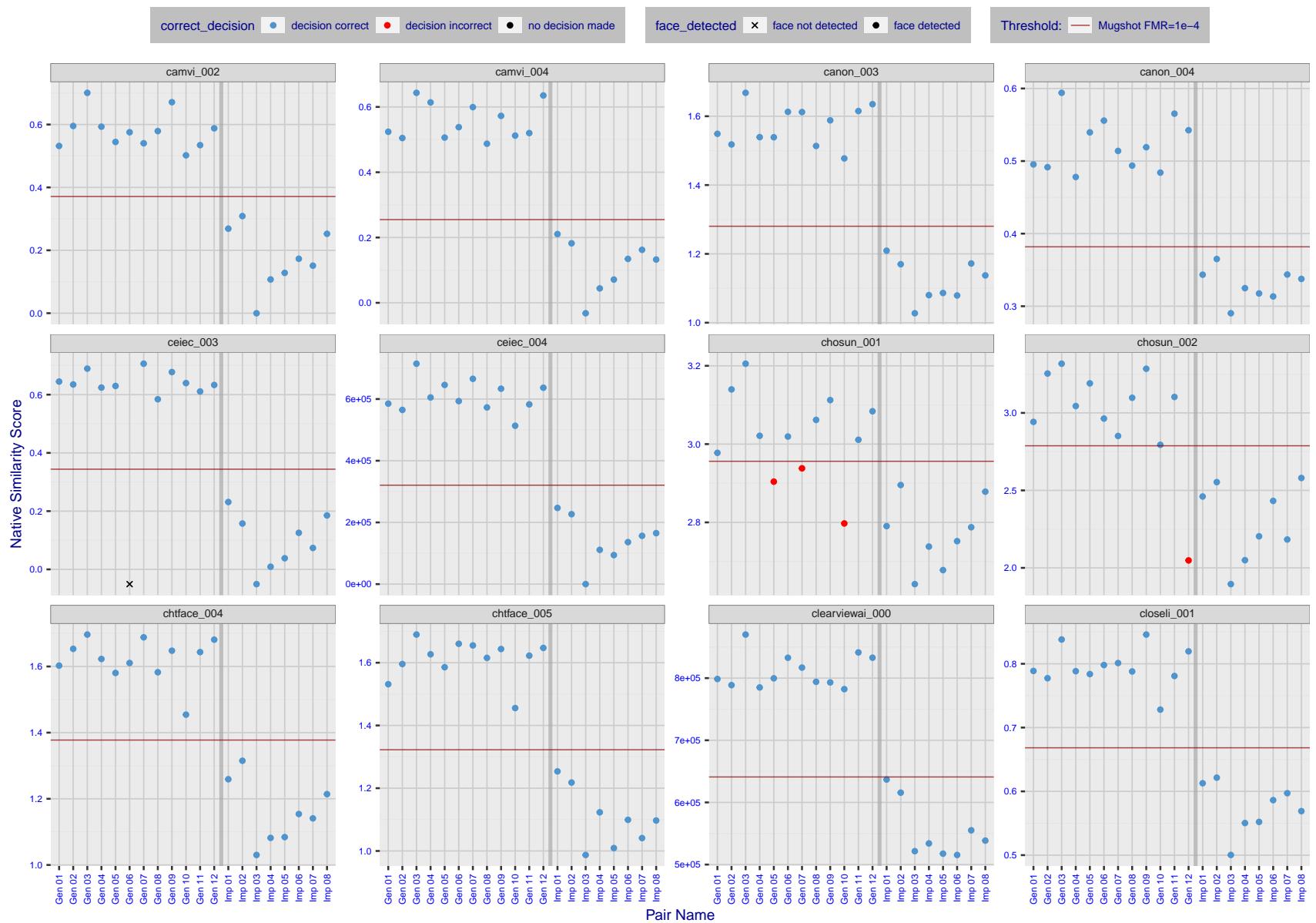


Figure 9: The figure shows algorithms' similarity scores for 12 genuine and 8 impostor image pairs used in a May 2018 paper by Phillips et al. ([1]). The threshold (red horizontal line) is a value calibrated to give $FMR = 0.0001$ on mugshot images. Points above the threshold correspond to pairs determined to be genuine, and points below the threshold correspond to pairs determined to be impostors. If the determined class (genuine or impostor) matches the real class, points will be blue; if not, red. An X represents face detection failure in either of the images in the pair. Note that the sample size ($n=20$) is small, and the figure may change substantially if larger or different sets are used. The images can be viewed on p. 13 of the Appendix, where Gen 01 corresponds to Same-Identity Pair 1, Gen 02 corresponds to Same-Identity Pair 2, and so on.

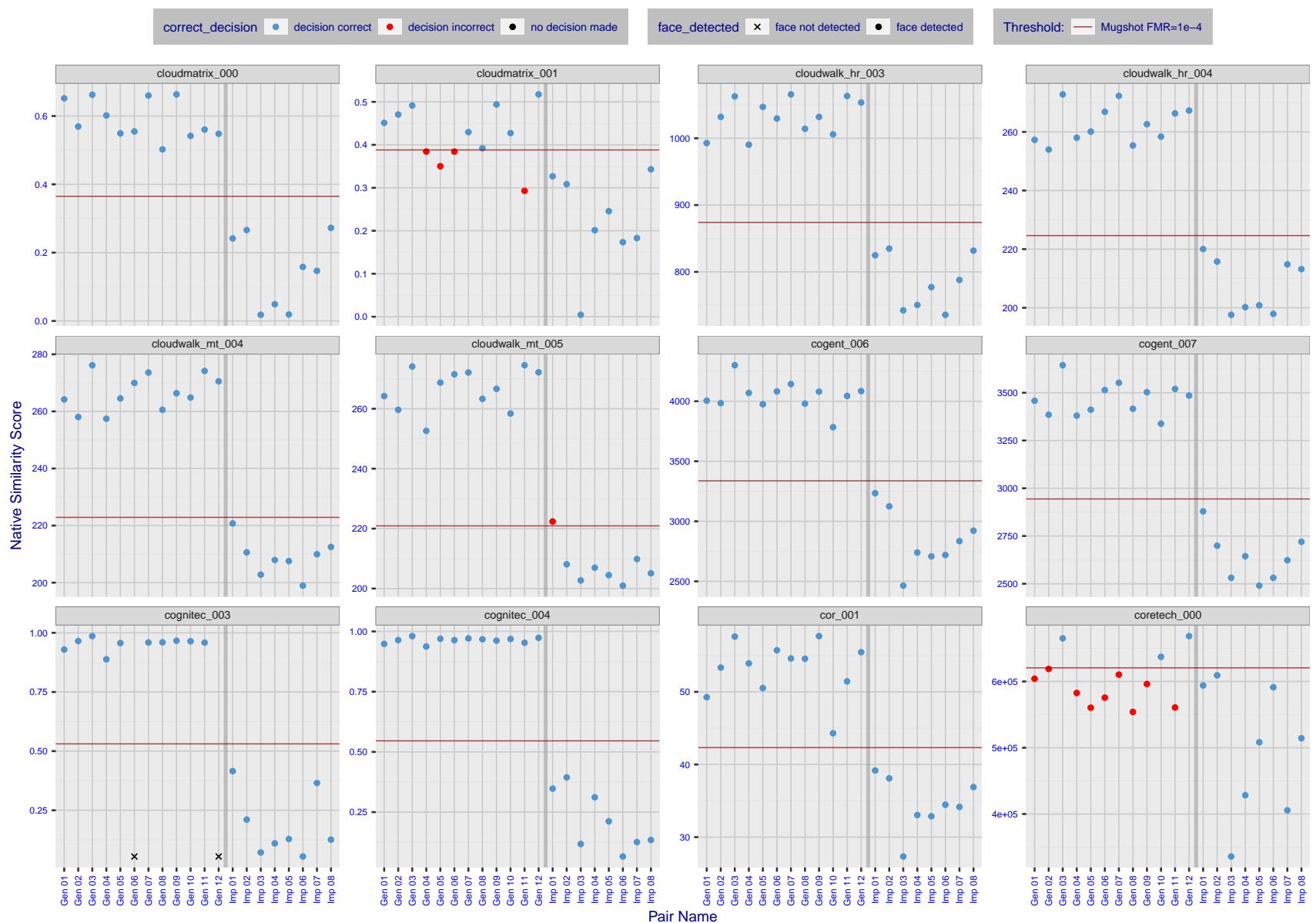


Figure 10: The figure shows algorithms' similarity scores for 12 genuine and 8 impostor image pairs used in a May 2018 paper by Phillips et al. ([1]). The threshold (red horizontal line) is a value calibrated to give $FMR = 0.0001$ on mugshot images. Points above the threshold correspond to pairs determined to be genuine, and points below the threshold correspond to pairs determined to be impostors. If the determined class (genuine or impostor) matches the real class, points will be blue; if not, red. An X represents face detection failure in either of the images in the pair. Note that the sample size ($n=20$) is small, and the figure may change substantially if larger or different sets are used. The images can be viewed on p. 13 of the Appendix, where Gen 01 corresponds to Same-Identity Pair 1, Gen 02 corresponds to Same-Identity Pair 2, and so on.

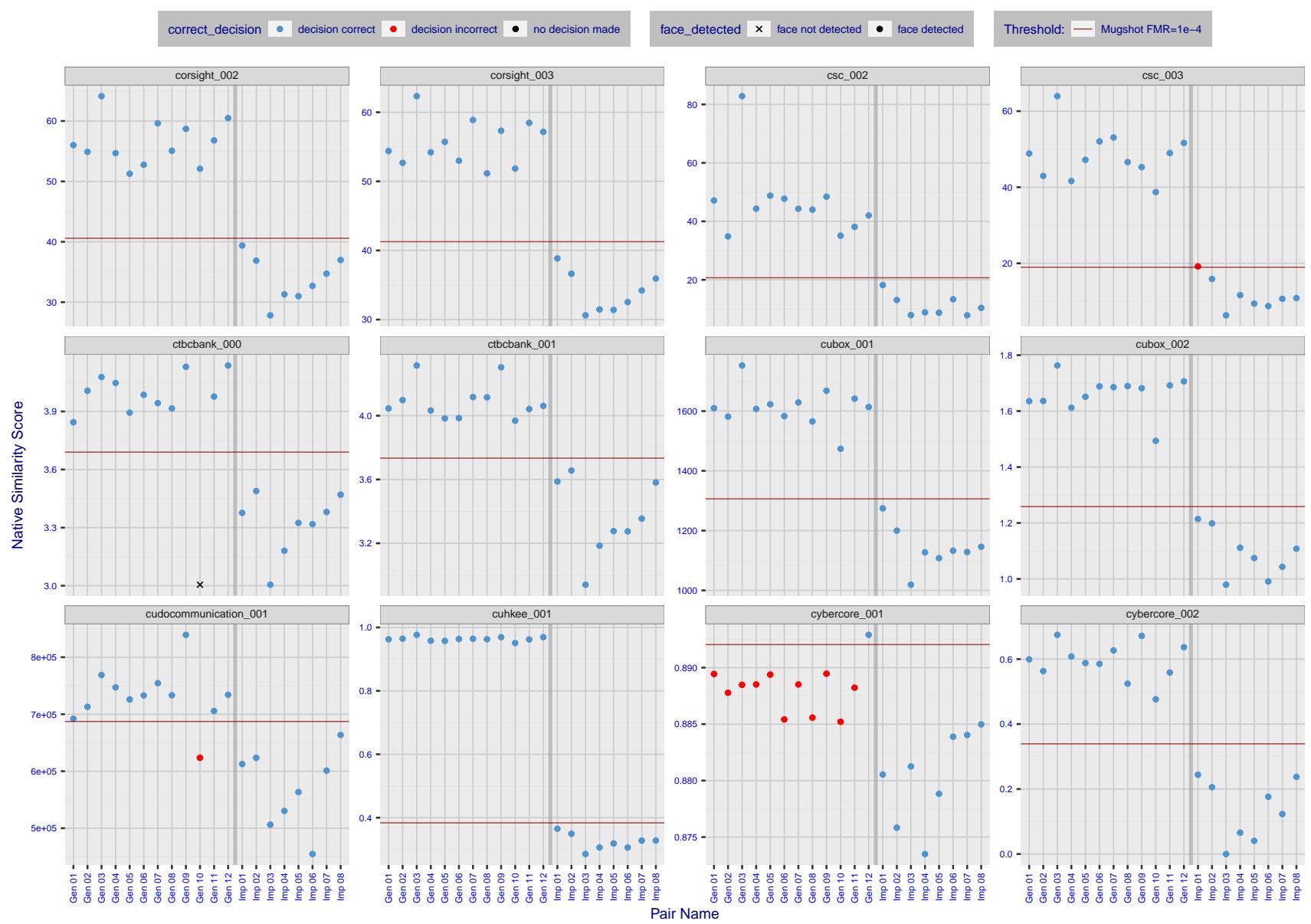


Figure 11: The figure shows algorithms' similarity scores for 12 genuine and 8 impostor image pairs used in a May 2018 paper by Phillips et al. ([1]). The threshold (red horizontal line) is a value calibrated to give $FMR = 0.0001$ on mugshot images. Points above the threshold correspond to pairs determined to be genuine, and points below the threshold correspond to pairs determined to be impostors. If the determined class (genuine or impostor) matches the real class, points will be blue; if not, red. An X represents face detection failure in either of the images in the pair. Note that the sample size ($n=20$) is small, and the figure may change substantially if larger or different sets are used. The images can be viewed on p. 13 of the Appendix, where Gen 01 corresponds to Same-Identity Pair 1, Gen 02 corresponds to Same-Identity Pair 2, and so on.

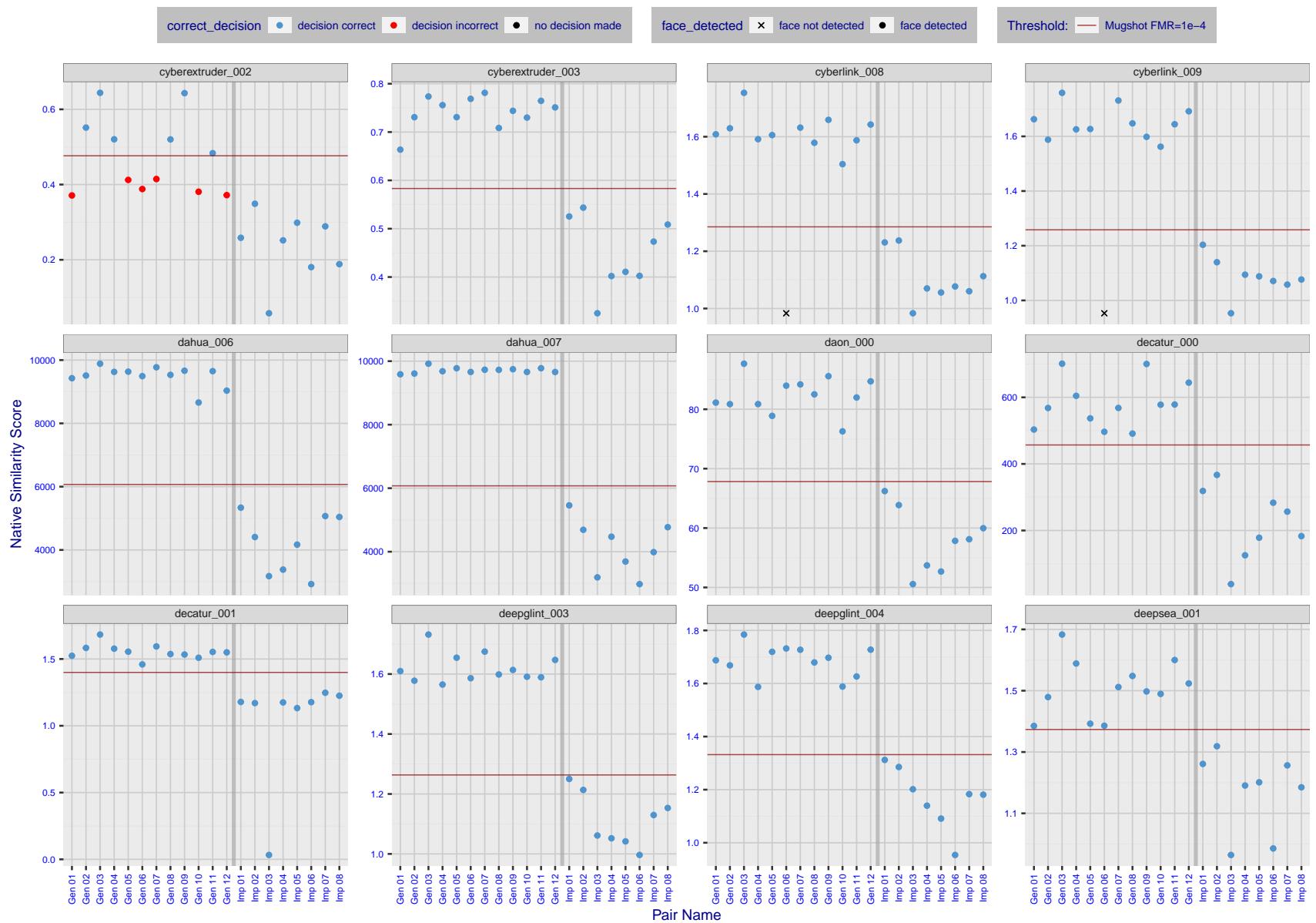


Figure 12: The figure shows algorithms' similarity scores for 12 genuine and 8 impostor image pairs used in a May 2018 paper by Phillips et al. ([1]). The threshold (red horizontal line) is a value calibrated to give $FMR = 0.0001$ on mugshot images. Points above the threshold correspond to pairs determined to be genuine, and points below the threshold correspond to pairs determined to be impostors. If the determined class (genuine or impostor) matches the real class, points will be blue; if not, red. An X represents face detection failure in either of the images in the pair. Note that the sample size ($n=20$) is small, and the figure may change substantially if larger or different sets are used. The images can be viewed on p. 13 of the Appendix, where Gen 01 corresponds to Same-Identity Pair 1, Gen 02 corresponds to Same-Identity Pair 2, and so on.

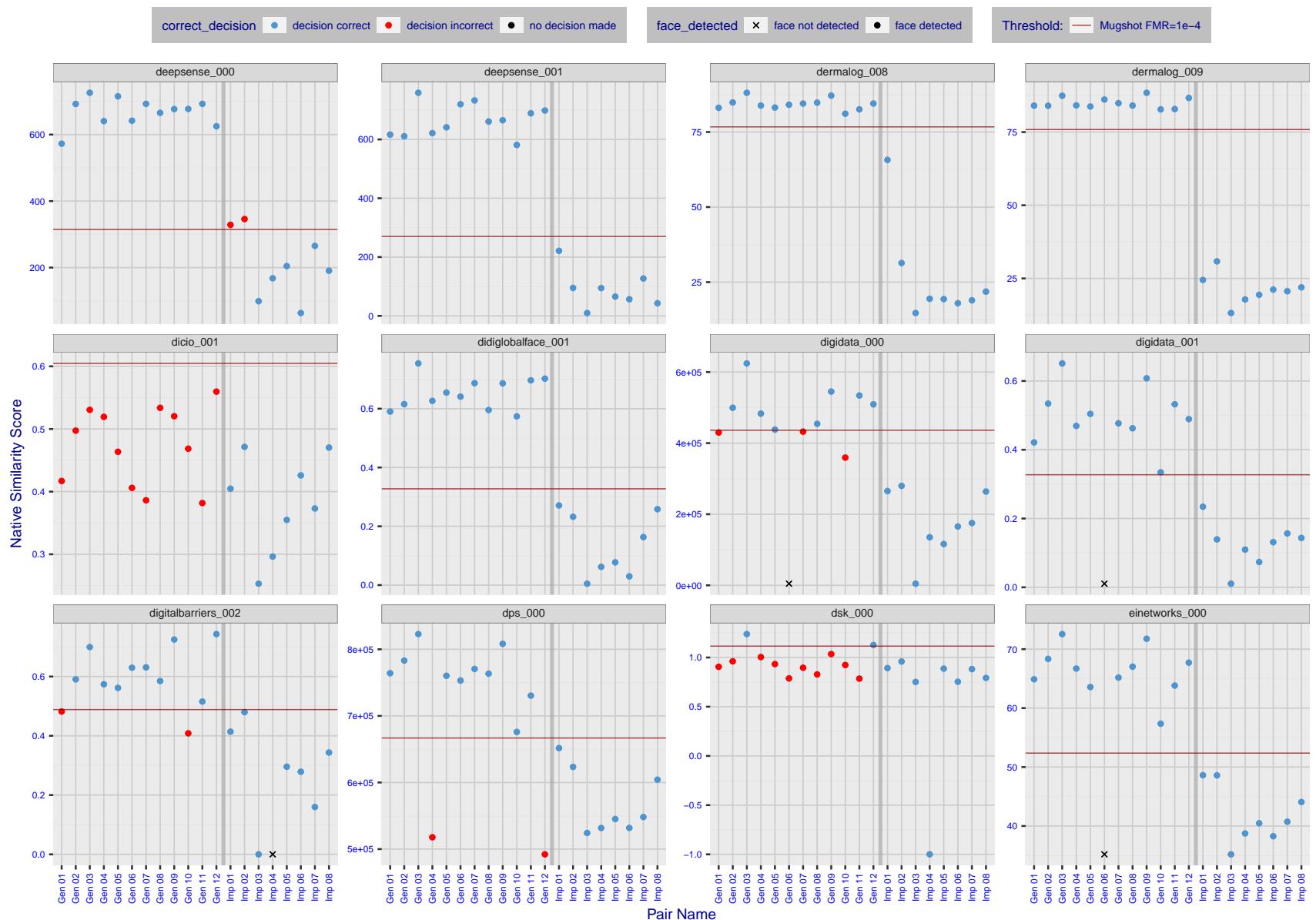


Figure 13: The figure shows algorithms' similarity scores for 12 genuine and 8 impostor image pairs used in a May 2018 paper by Phillips et al. ([1]). The threshold (red horizontal line) is a value calibrated to give $FMR = 0.0001$ on mugshot images. Points above the threshold correspond to pairs determined to be genuine, and points below the threshold correspond to pairs determined to be impostors. If the determined class (genuine or impostor) matches the real class, points will be blue; if not, red. An X represents face detection failure in either of the images in the pair. Note that the sample size ($n=20$) is small, and the figure may change substantially if larger or different sets are used. The images can be viewed on p. 13 of the Appendix, where Gen 01 corresponds to Same-Identity Pair 1, Gen 02 corresponds to Same-Identity Pair 2, and so on.

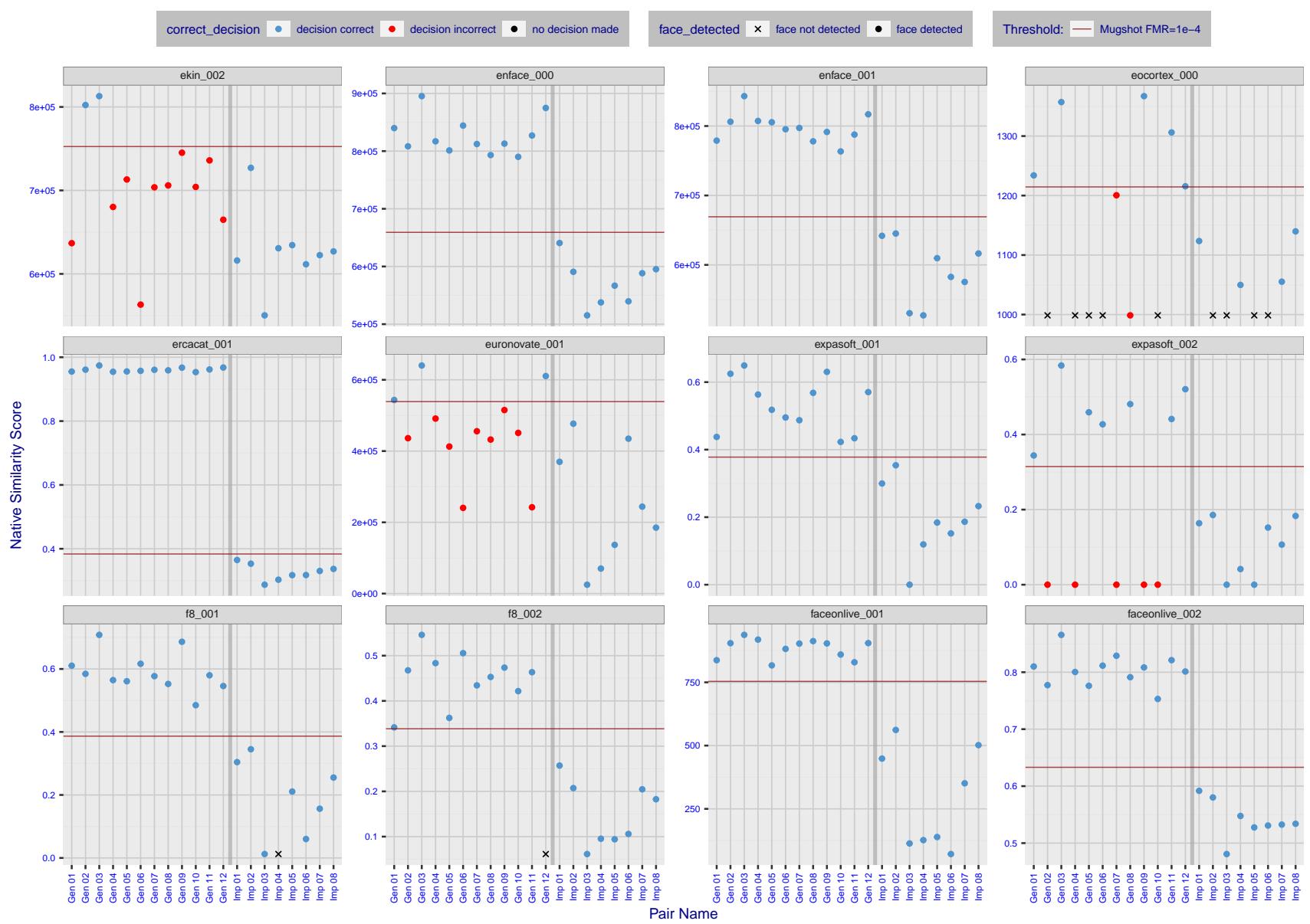


Figure 14: The figure shows algorithms' similarity scores for 12 genuine and 8 impostor image pairs used in a May 2018 paper by Phillips et al. ([1]). The threshold (red horizontal line) is a value calibrated to give $FMR = 0.0001$ on mugshot images. Points above the threshold correspond to pairs determined to be genuine, and points below the threshold correspond to pairs determined to be impostors. If the determined class (genuine or impostor) matches the real class, points will be blue; if not, red. An X represents face detection failure in either of the images in the pair. Note that the sample size ($n=20$) is small, and the figure may change substantially if larger or different sets are used. The images can be viewed on p. 13 of the Appendix, where Gen 01 corresponds to Same-Identity Pair 1, Gen 02 corresponds to Same-Identity Pair 2, and so on.

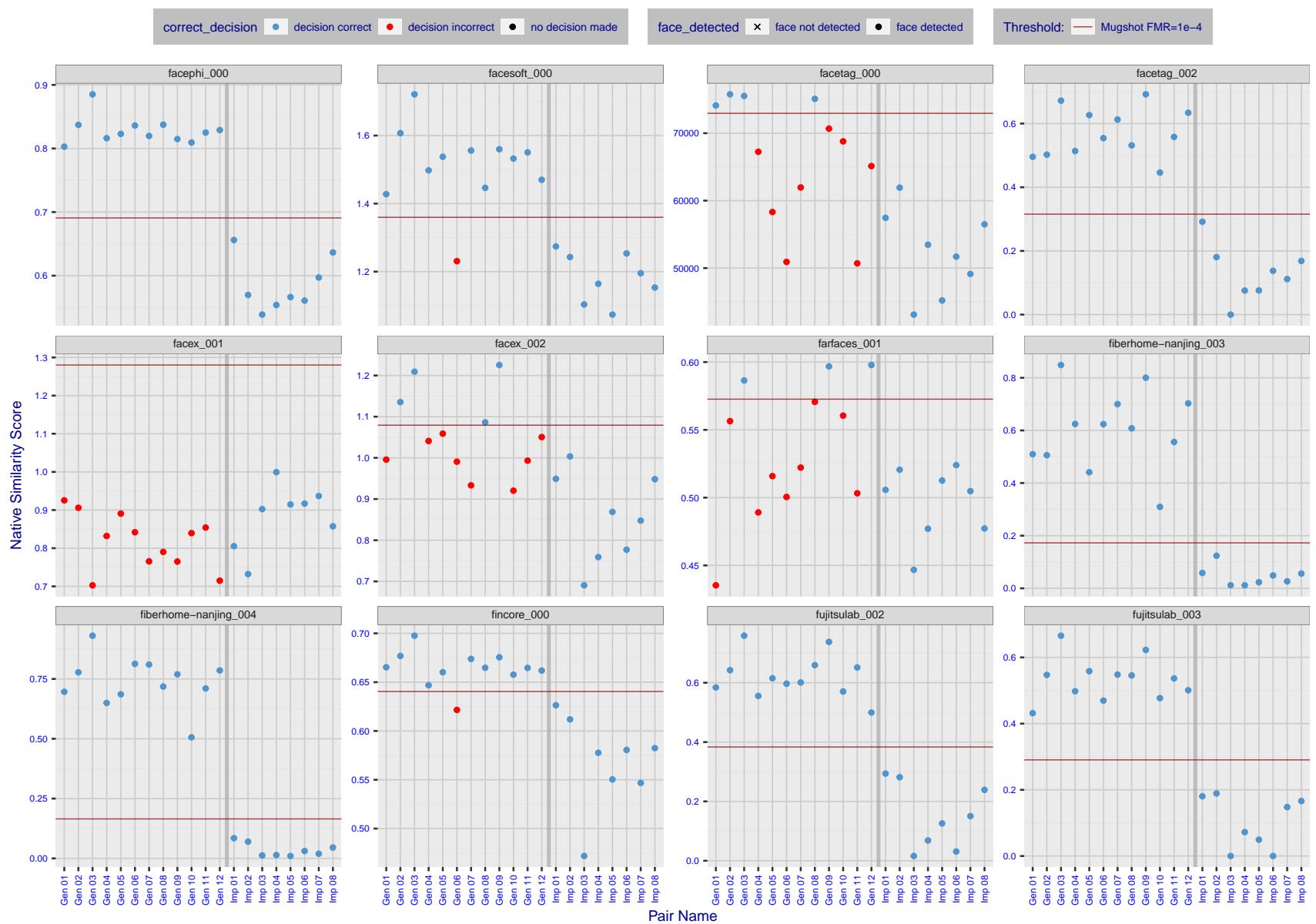


Figure 15: The figure shows algorithms' similarity scores for 12 genuine and 8 impostor image pairs used in a May 2018 paper by Phillips et al. ([1]). The threshold (red horizontal line) is a value calibrated to give $FMR = 0.0001$ on mugshot images. Points above the threshold correspond to pairs determined to be genuine, and points below the threshold correspond to pairs determined to be impostors. If the determined class (genuine or impostor) matches the real class, points will be blue; if not, red. An X represents face detection failure in either of the images in the pair. Note that the sample size ($n=20$) is small, and the figure may change substantially if larger or different sets are used. The images can be viewed on p. 13 of the Appendix, where Gen 01 corresponds to Same-Identity Pair 1, Gen 02 corresponds to Same-Identity Pair 2, and so on.

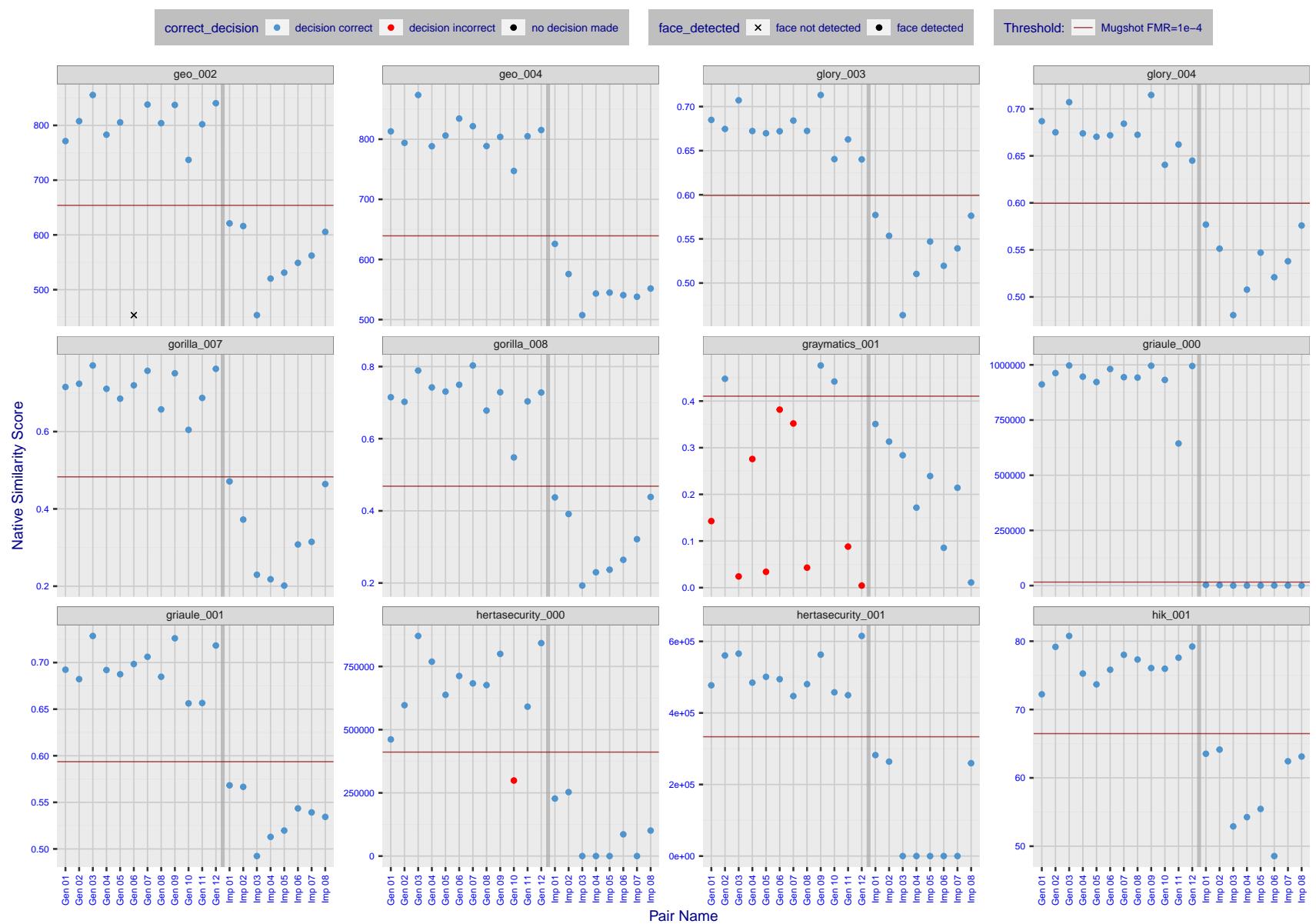


Figure 16: The figure shows algorithms' similarity scores for 12 genuine and 8 impostor image pairs used in a May 2018 paper by Phillips et al. ([1]). The threshold (red horizontal line) is a value calibrated to give $FMR = 0.0001$ on mugshot images. Points above the threshold correspond to pairs determined to be genuine, and points below the threshold correspond to pairs determined to be impostors. If the determined class (genuine or impostor) matches the real class, points will be blue; if not, red. An X represents face detection failure in either of the images in the pair. Note that the sample size ($n=20$) is small, and the figure may change substantially if larger or different sets are used. The images can be viewed on p. 13 of the Appendix, where Gen 01 corresponds to Same-Identity Pair 1, Gen 02 corresponds to Same-Identity Pair 2, and so on.

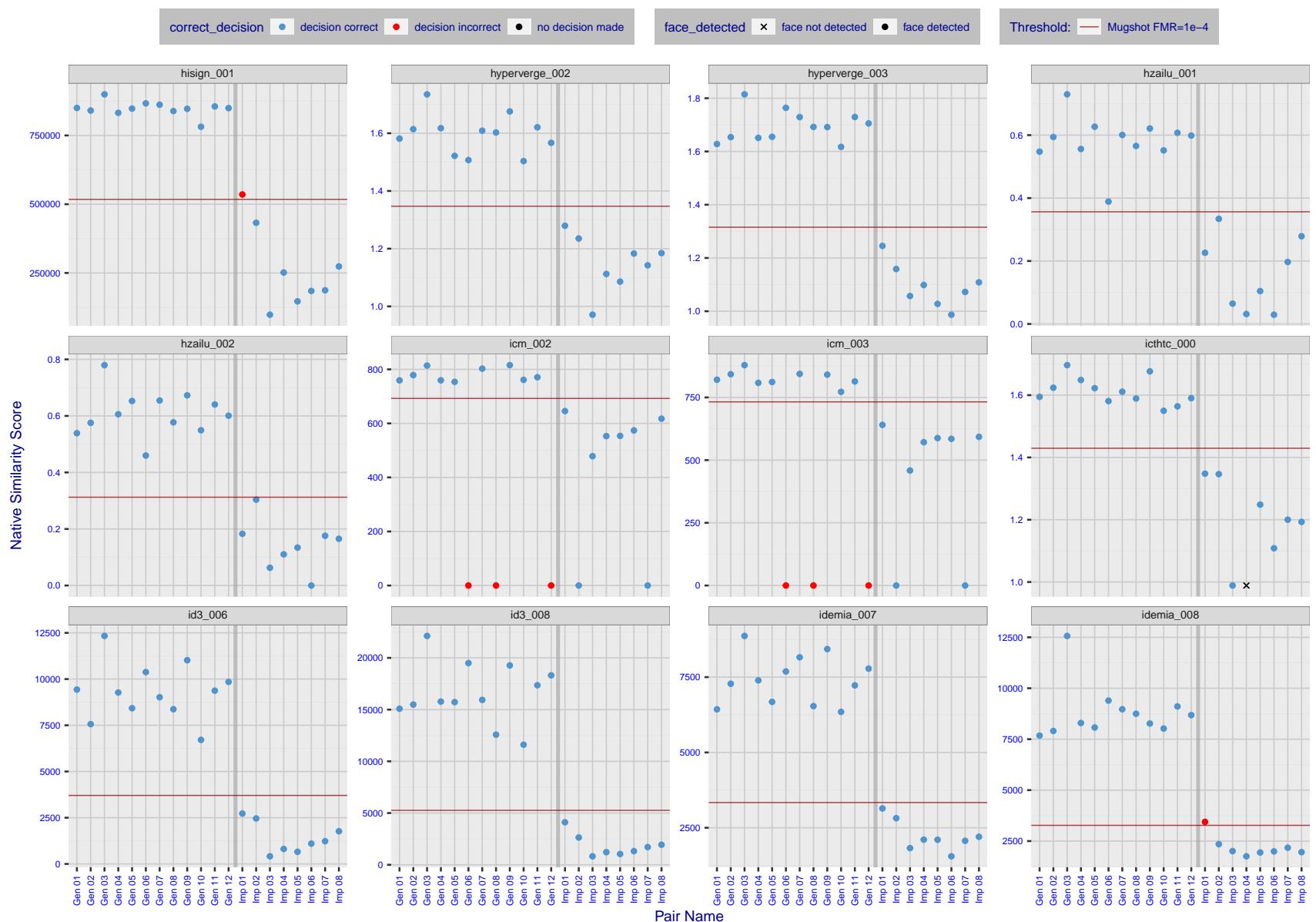


Figure 17: The figure shows algorithms' similarity scores for 12 genuine and 8 impostor image pairs used in a May 2018 paper by Phillips et al. ([1]). The threshold (red horizontal line) is a value calibrated to give $\text{FMR} = 0.0001$ on mugshot images. Points above the threshold correspond to pairs determined to be genuine, and points below the threshold correspond to pairs determined to be impostors. If the determined class (genuine or impostor) matches the real class, points will be blue; if not, red. An X represents face detection failure in either of the images in the pair. Note that the sample size ($n=20$) is small, and the figure may change substantially if larger or different sets are used. The images can be viewed on p. 13 of the Appendix, where Gen 01 corresponds to Same-Identity Pair 1, Gen 02 corresponds to Same-Identity Pair 2, and so on.

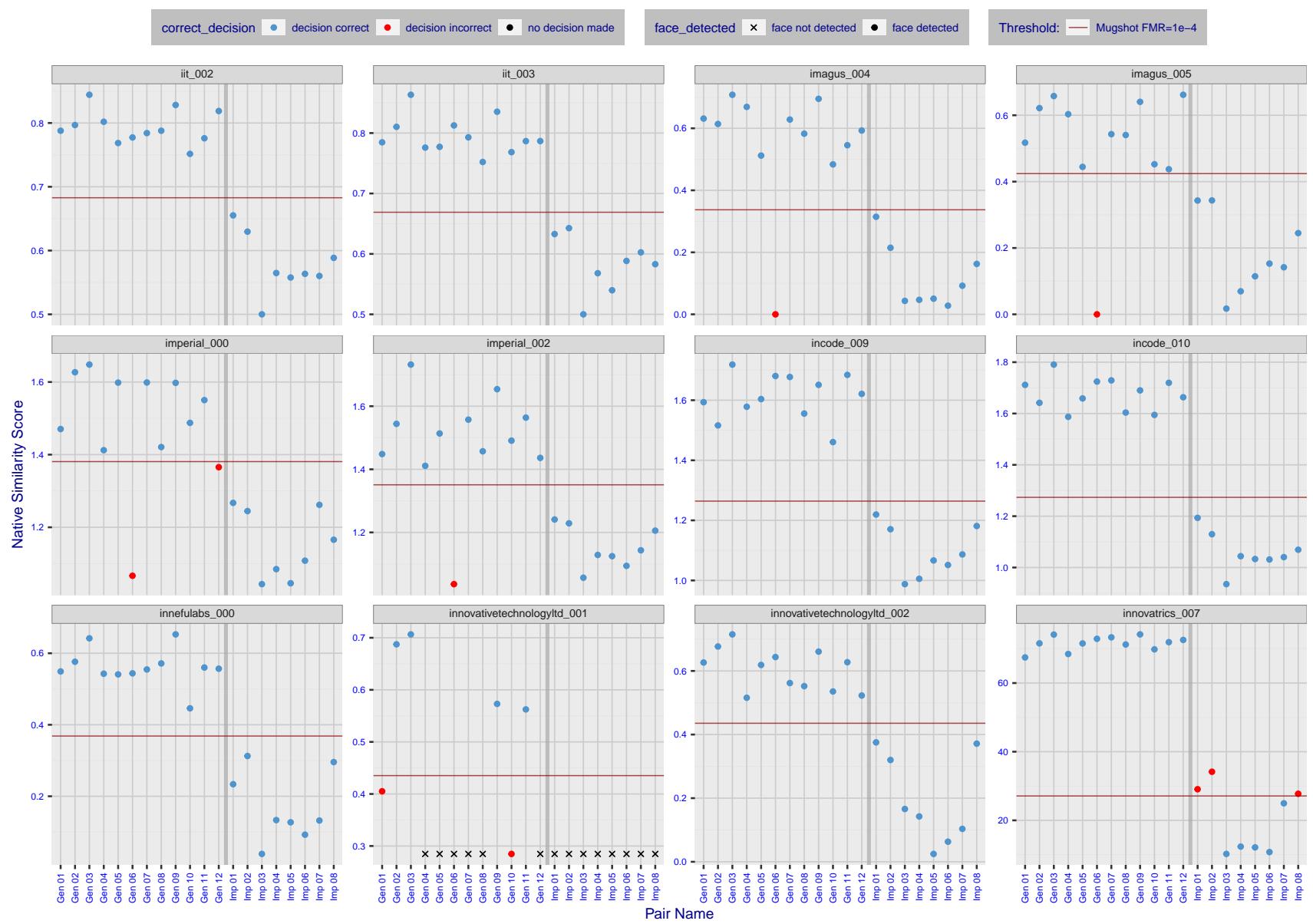


Figure 18: The figure shows algorithms' similarity scores for 12 genuine and 8 impostor image pairs used in a May 2018 paper by Phillips et al. ([1]). The threshold (red horizontal line) is a value calibrated to give $FMR = 0.0001$ on mugshot images. Points above the threshold correspond to pairs determined to be genuine, and points below the threshold correspond to pairs determined to be impostors. If the determined class (genuine or impostor) matches the real class, points will be blue; if not, red. An X represents face detection failure in either of the images in the pair. Note that the sample size ($n=20$) is small, and the figure may change substantially if larger or different sets are used. The images can be viewed on p. 13 of the Appendix, where Gen 01 corresponds to Same-Identity Pair 1, Gen 02 corresponds to Same-Identity Pair 2, and so on.

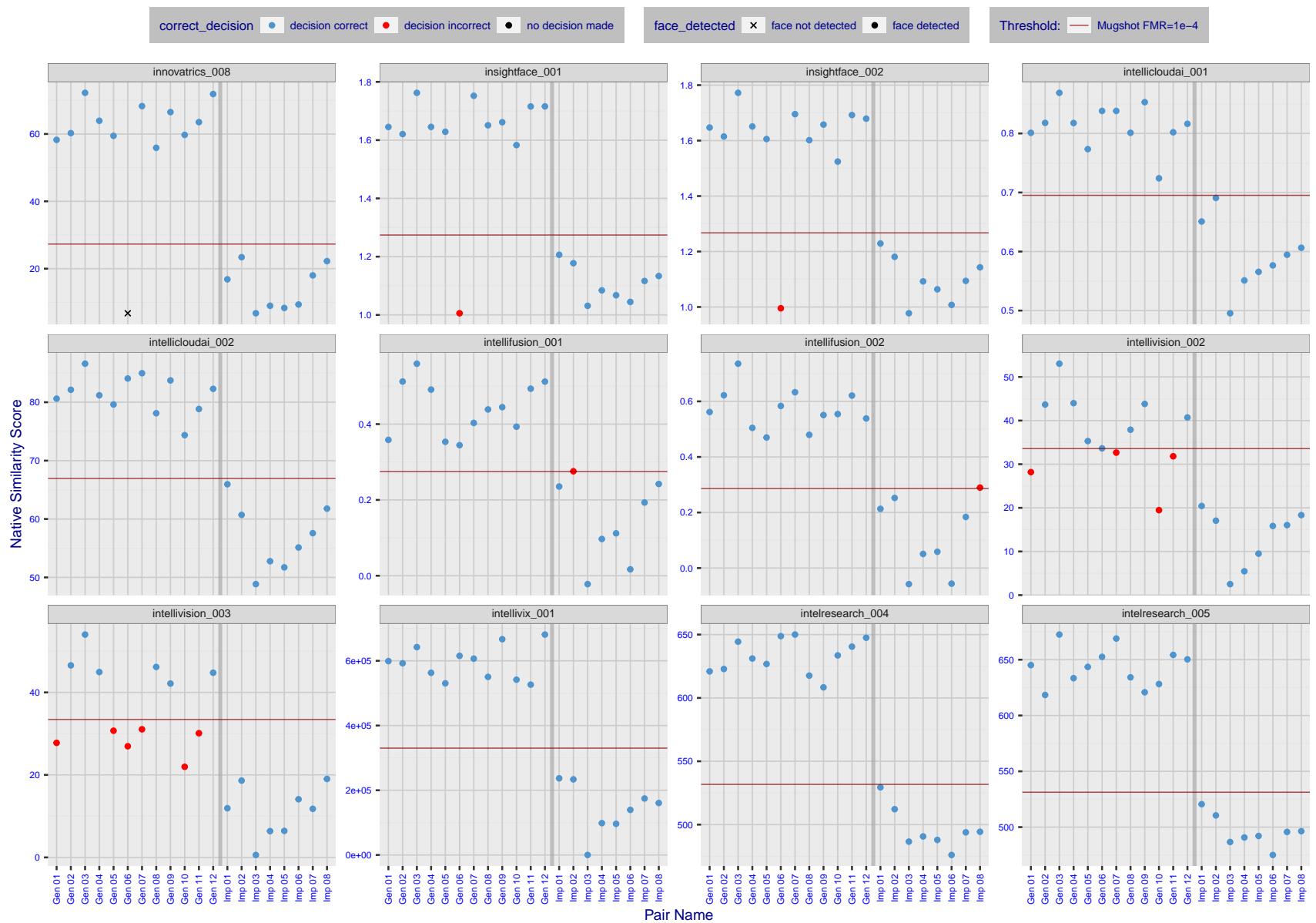


Figure 19: The figure shows algorithms' similarity scores for 12 genuine and 8 impostor image pairs used in a May 2018 paper by Phillips et al. ([1]). The threshold (red horizontal line) is a value calibrated to give $FMR = 0.0001$ on mugshot images. Points above the threshold correspond to pairs determined to be genuine, and points below the threshold correspond to pairs determined to be impostors. If the determined class (genuine or impostor) matches the real class, points will be blue; if not, red. An X represents face detection failure in either of the images in the pair. Note that the sample size ($n=20$) is small, and the figure may change substantially if larger or different sets are used. The images can be viewed on p. 13 of the Appendix, where Gen 01 corresponds to Same-Identity Pair 1, Gen 02 corresponds to Same-Identity Pair 2, and so on.

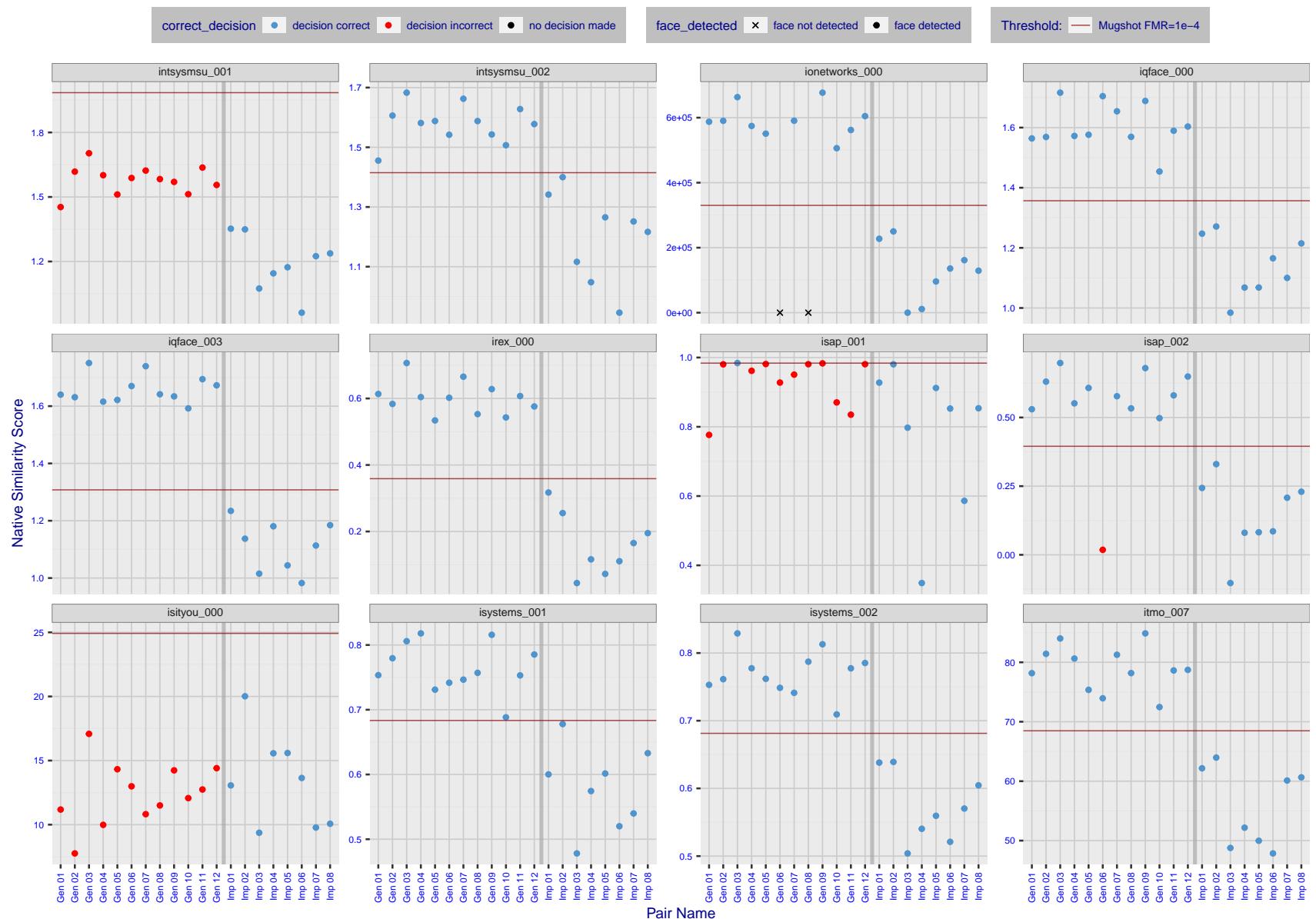


Figure 20: The figure shows algorithms' similarity scores for 12 genuine and 8 impostor image pairs used in a May 2018 paper by Phillips et al. ([1]). The threshold (red horizontal line) is a value calibrated to give $FMR = 0.0001$ on mugshot images. Points above the threshold correspond to pairs determined to be genuine, and points below the threshold correspond to pairs determined to be impostors. If the determined class (genuine or impostor) matches the real class, points will be blue; if not, red. An X represents face detection failure in either of the images in the pair. Note that the sample size ($n=20$) is small, and the figure may change substantially if larger or different sets are used. The images can be viewed on p. 13 of the Appendix, where Gen 01 corresponds to Same-Identity Pair 1, Gen 02 corresponds to Same-Identity Pair 2, and so on.

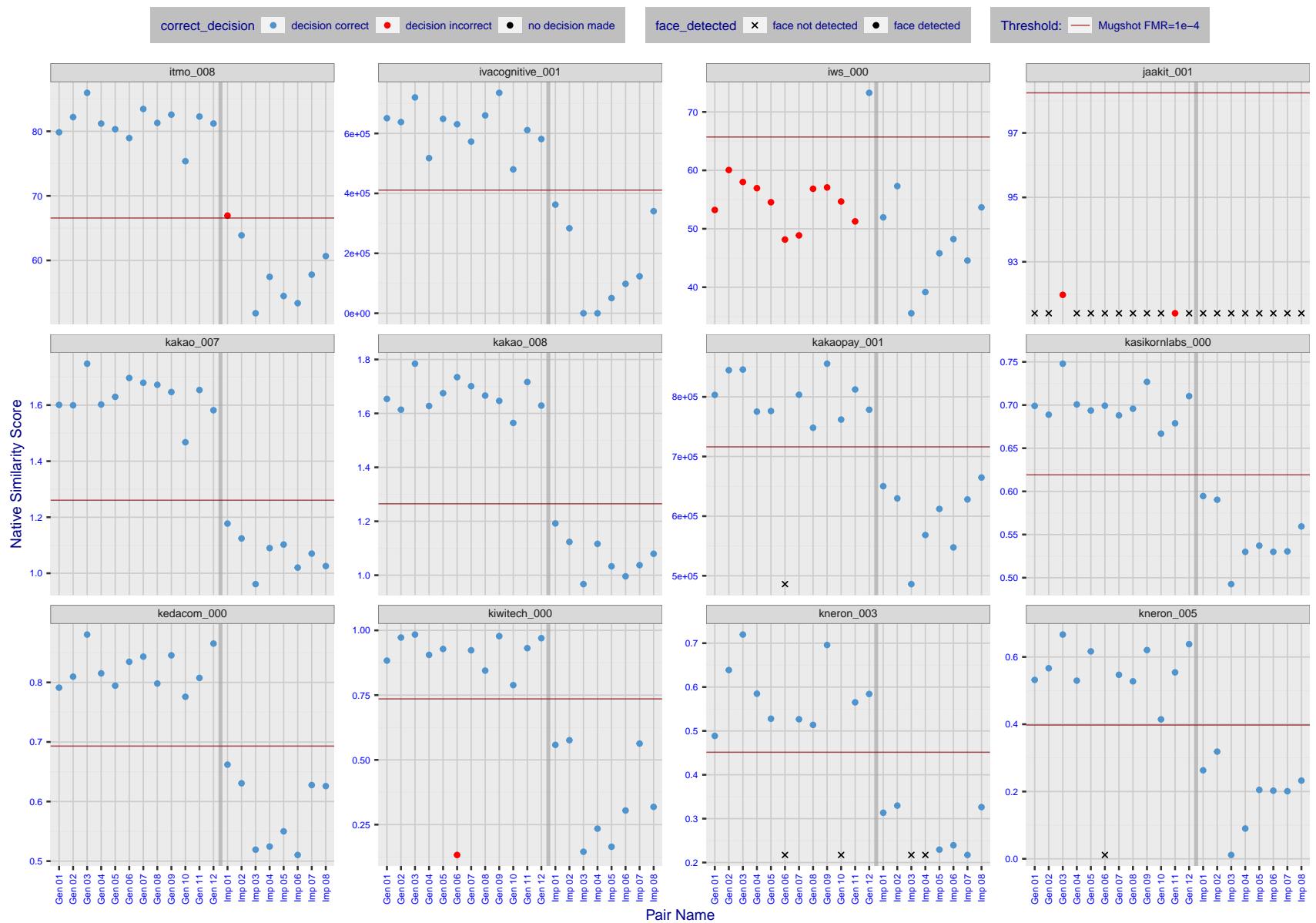


Figure 21: The figure shows algorithms' similarity scores for 12 genuine and 8 impostor image pairs used in a May 2018 paper by Phillips et al. ([1]). The threshold (red horizontal line) is a value calibrated to give $FMR = 0.0001$ on mugshot images. Points above the threshold correspond to pairs determined to be genuine, and points below the threshold correspond to pairs determined to be impostors. If the determined class (genuine or impostor) matches the real class, points will be blue; if not, red. An X represents face detection failure in either of the images in the pair. Note that the sample size ($n=20$) is small, and the figure may change substantially if larger or different sets are used. The images can be viewed on p. 13 of the Appendix, where Gen 01 corresponds to Same-Identity Pair 1, Gen 02 corresponds to Same-Identity Pair 2, and so on.

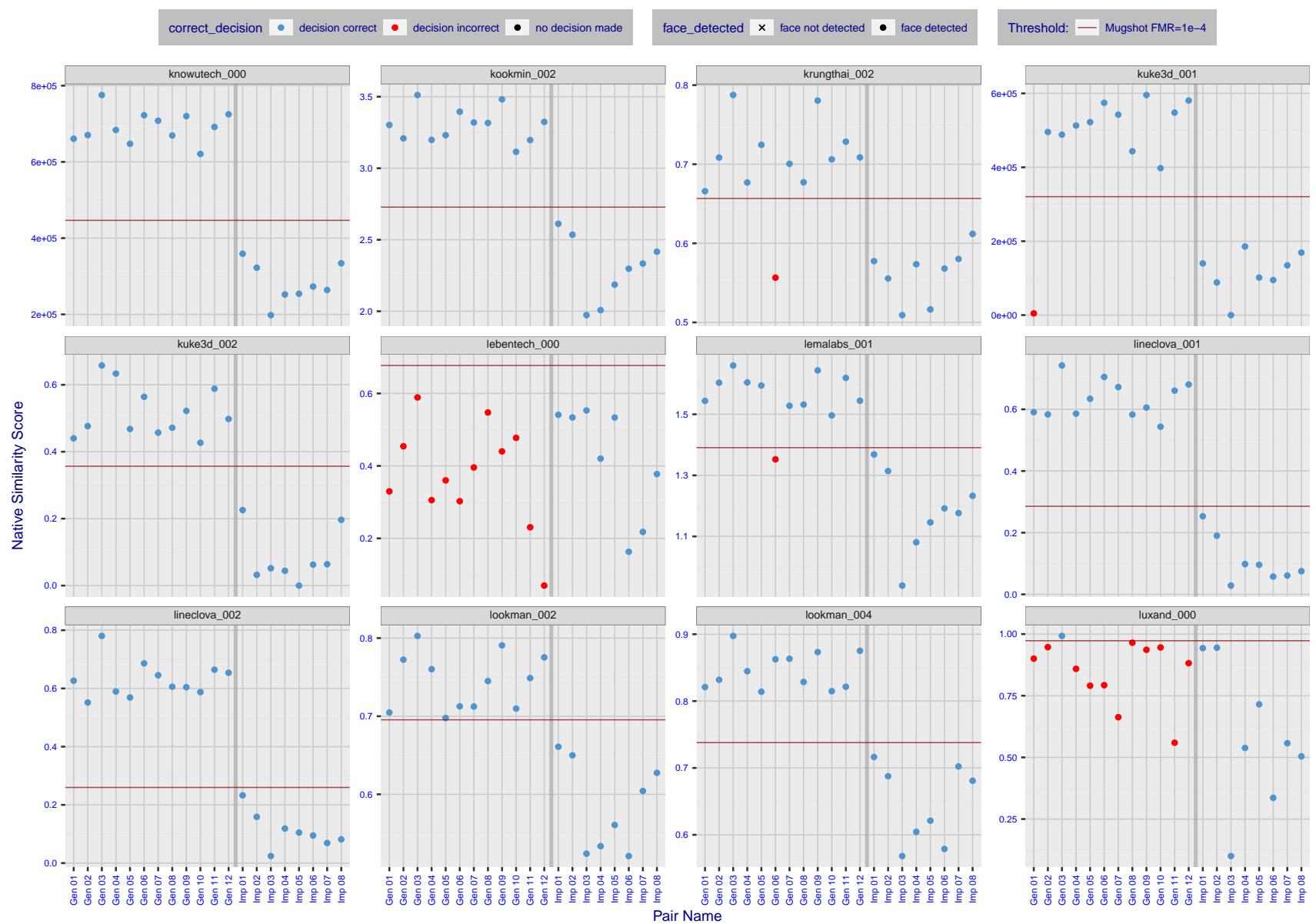


Figure 22: The figure shows algorithms' similarity scores for 12 genuine and 8 impostor image pairs used in a May 2018 paper by Phillips et al. ([1]). The threshold (red horizontal line) is a value calibrated to give $FMR = 0.0001$ on mugshot images. Points above the threshold correspond to pairs determined to be genuine, and points below the threshold correspond to pairs determined to be impostors. If the determined class (genuine or impostor) matches the real class, points will be blue; if not, red. An X represents face detection failure in either of the images in the pair. Note that the sample size ($n=20$) is small, and the figure may change substantially if larger or different sets are used. The images can be viewed on p. 13 of the Appendix, where Gen 01 corresponds to Same-Identity Pair 1, Gen 02 corresponds to Same-Identity Pair 2, and so on.

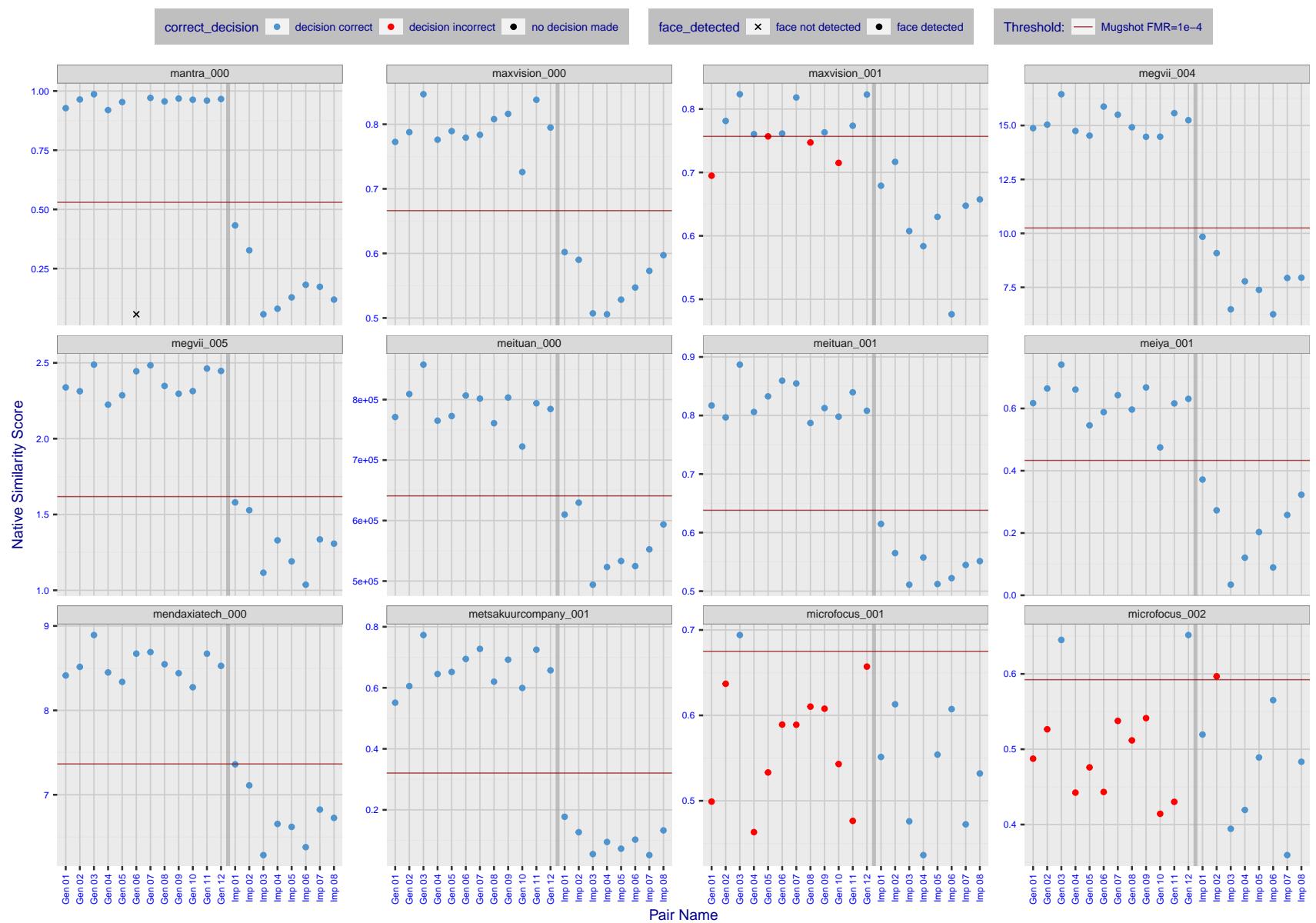


Figure 23: The figure shows algorithms' similarity scores for 12 genuine and 8 impostor image pairs used in a May 2018 paper by Phillips et al. ([1]). The threshold (red horizontal line) is a value calibrated to give $FMR = 0.0001$ on mugshot images. Points above the threshold correspond to pairs determined to be genuine, and points below the threshold correspond to pairs determined to be impostors. If the determined class (genuine or impostor) matches the real class, points will be blue; if not, red. An X represents face detection failure in either of the images in the pair. Note that the sample size ($n=20$) is small, and the figure may change substantially if larger or different sets are used. The images can be viewed on p. 13 of the Appendix, where Gen 01 corresponds to Same-Identity Pair 1, Gen 02 corresponds to Same-Identity Pair 2, and so on.

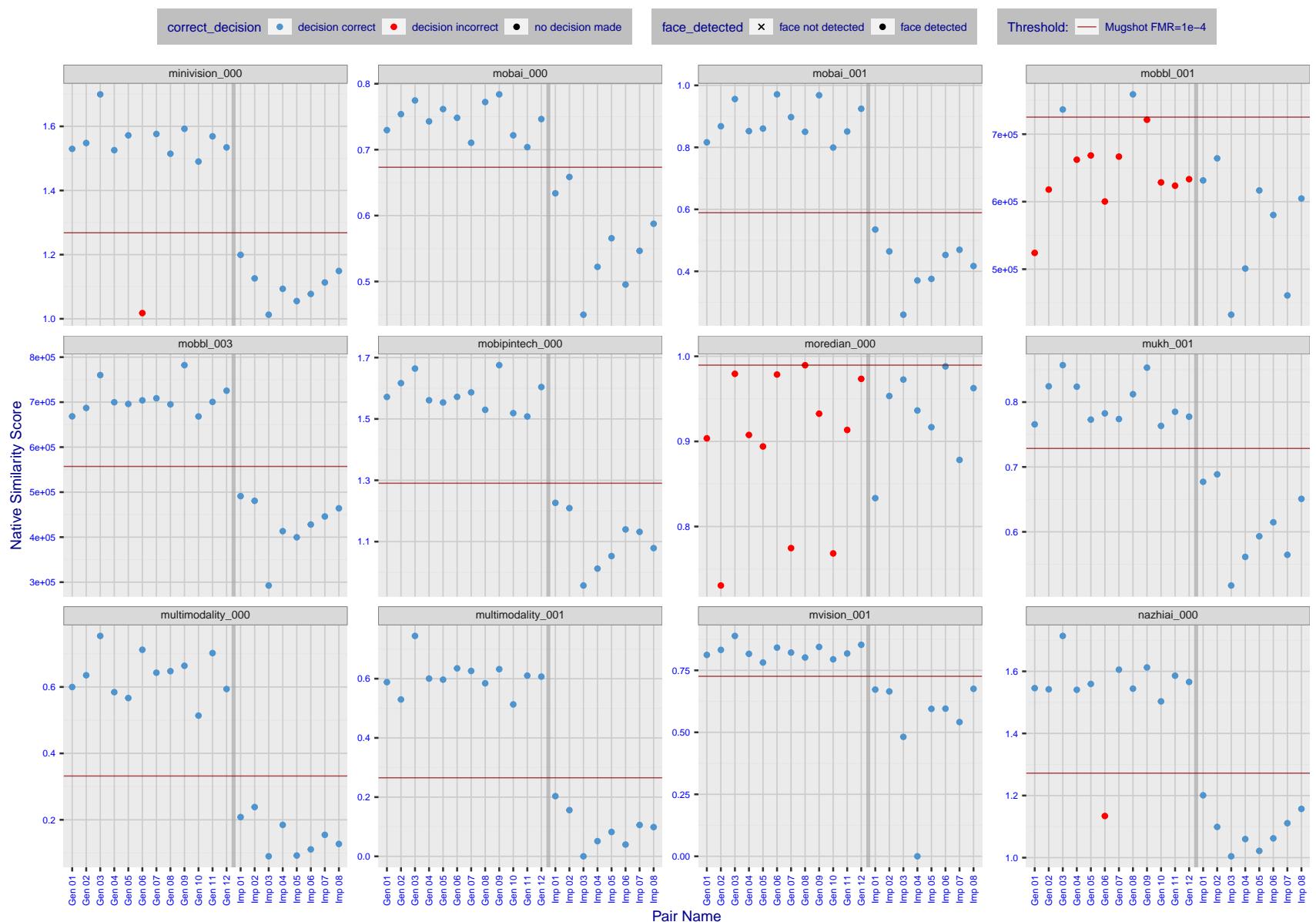


Figure 24: The figure shows algorithms' similarity scores for 12 genuine and 8 impostor image pairs used in a May 2018 paper by Phillips et al. ([1]). The threshold (red horizontal line) is a value calibrated to give $FMR = 0.0001$ on mugshot images. Points above the threshold correspond to pairs determined to be genuine, and points below the threshold correspond to pairs determined to be impostors. If the determined class (genuine or impostor) matches the real class, points will be blue; if not, red. An X represents face detection failure in either of the images in the pair. Note that the sample size ($n=20$) is small, and the figure may change substantially if larger or different sets are used. The images can be viewed on p. 13 of the Appendix, where Gen 01 corresponds to Same-Identity Pair 1, Gen 02 corresponds to Same-Identity Pair 2, and so on.

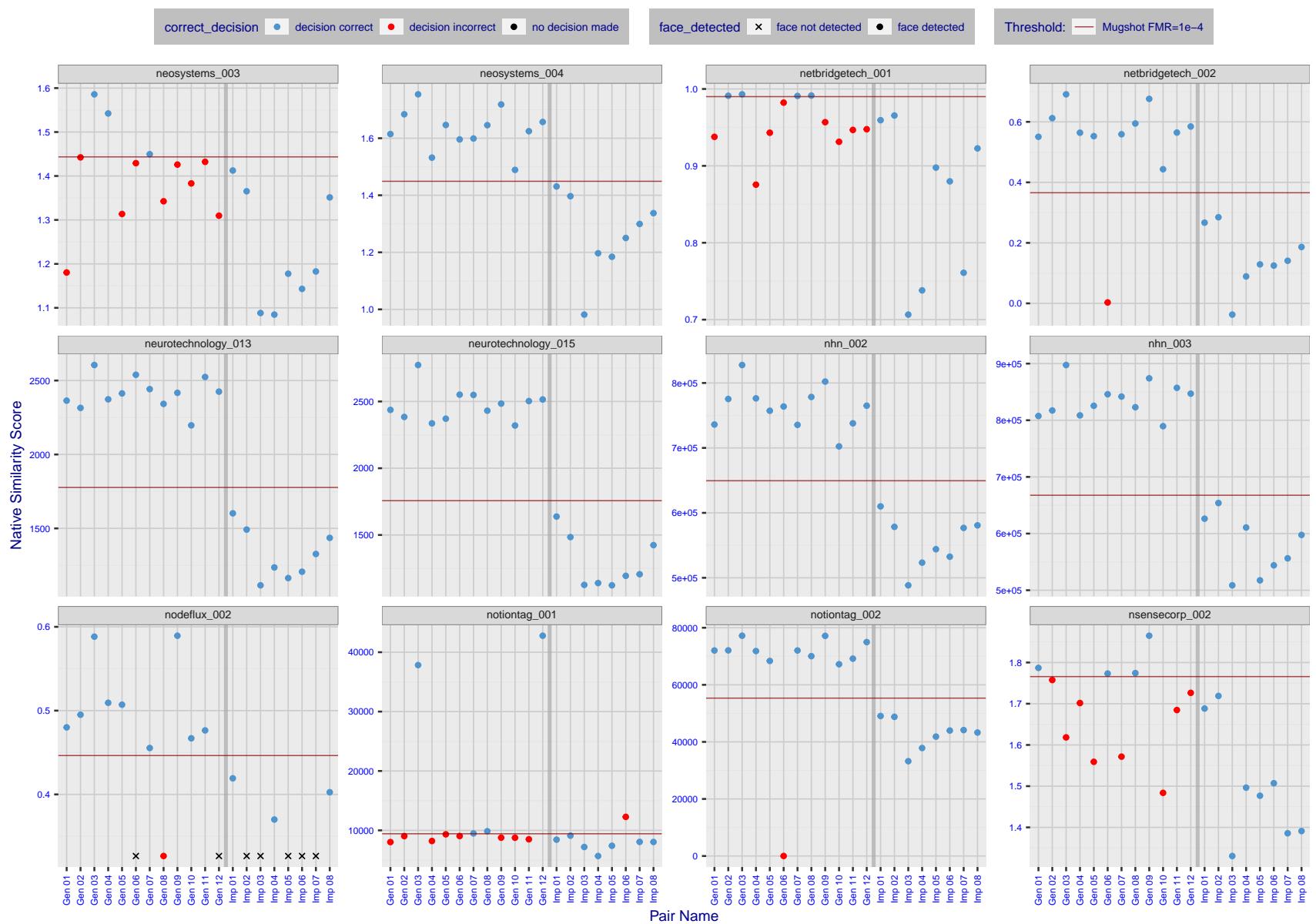


Figure 25: The figure shows algorithms' similarity scores for 12 genuine and 8 impostor image pairs used in a May 2018 paper by Phillips et al. ([1]). The threshold (red horizontal line) is a value calibrated to give $FMR = 0.0001$ on mugshot images. Points above the threshold correspond to pairs determined to be genuine, and points below the threshold correspond to pairs determined to be impostors. If the determined class (genuine or impostor) matches the real class, points will be blue; if not, red. An X represents face detection failure in either of the images in the pair. Note that the sample size ($n=20$) is small, and the figure may change substantially if larger or different sets are used. The images can be viewed on p. 13 of the Appendix, where Gen 01 corresponds to Same-Identity Pair 1, Gen 02 corresponds to Same-Identity Pair 2, and so on.

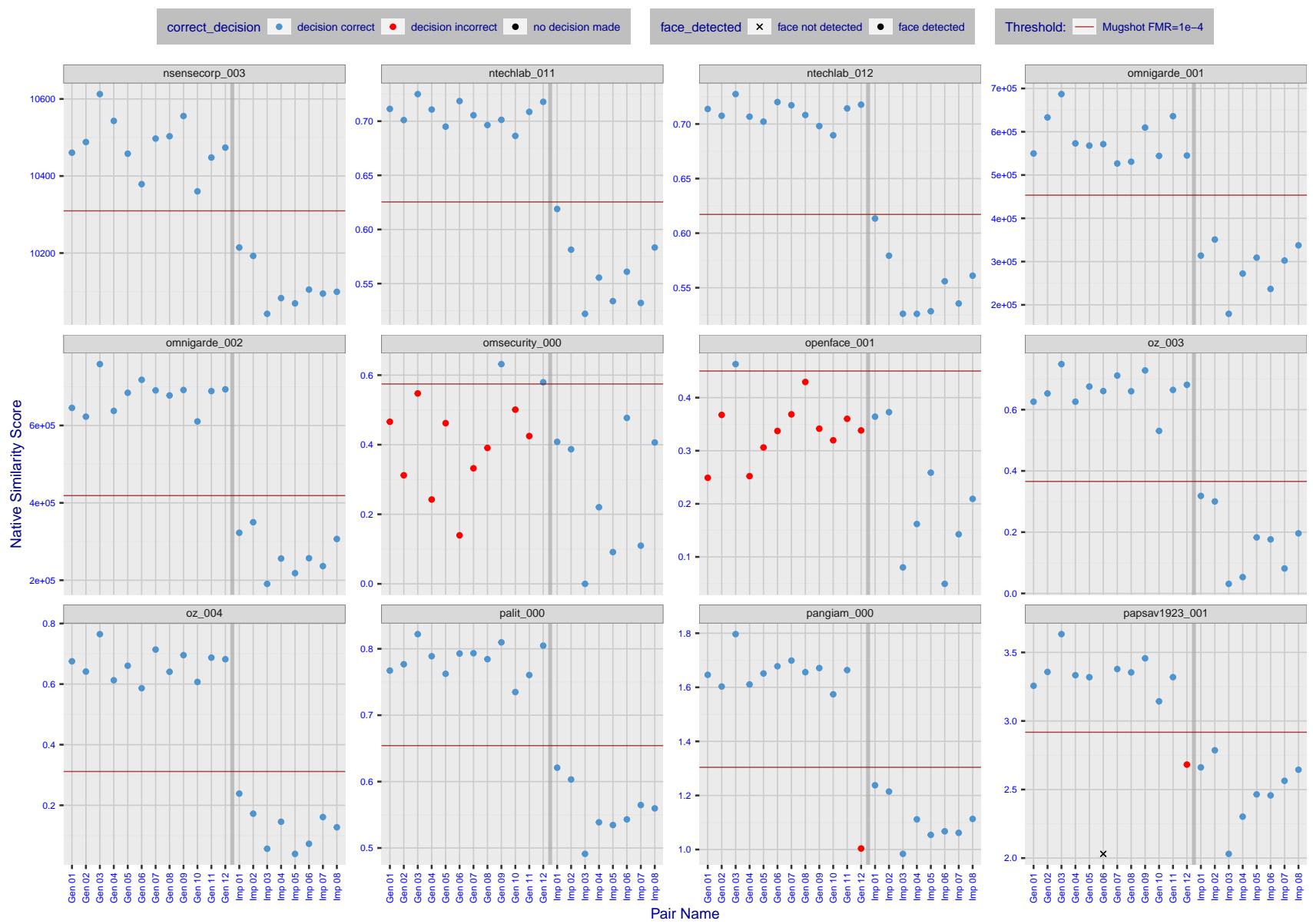


Figure 26: The figure shows algorithms' similarity scores for 12 genuine and 8 impostor image pairs used in a May 2018 paper by Phillips et al. ([1]). The threshold (red horizontal line) is a value calibrated to give $FMR = 0.0001$ on mugshot images. Points above the threshold correspond to pairs determined to be genuine, and points below the threshold correspond to pairs determined to be impostors. If the determined class (genuine or impostor) matches the real class, points will be blue; if not, red. An X represents face detection failure in either of the images in the pair. Note that the sample size ($n=20$) is small, and the figure may change substantially if larger or different sets are used. The images can be viewed on p. 13 of the Appendix, where Gen 01 corresponds to Same-Identity Pair 1, Gen 02 corresponds to Same-Identity Pair 2, and so on.

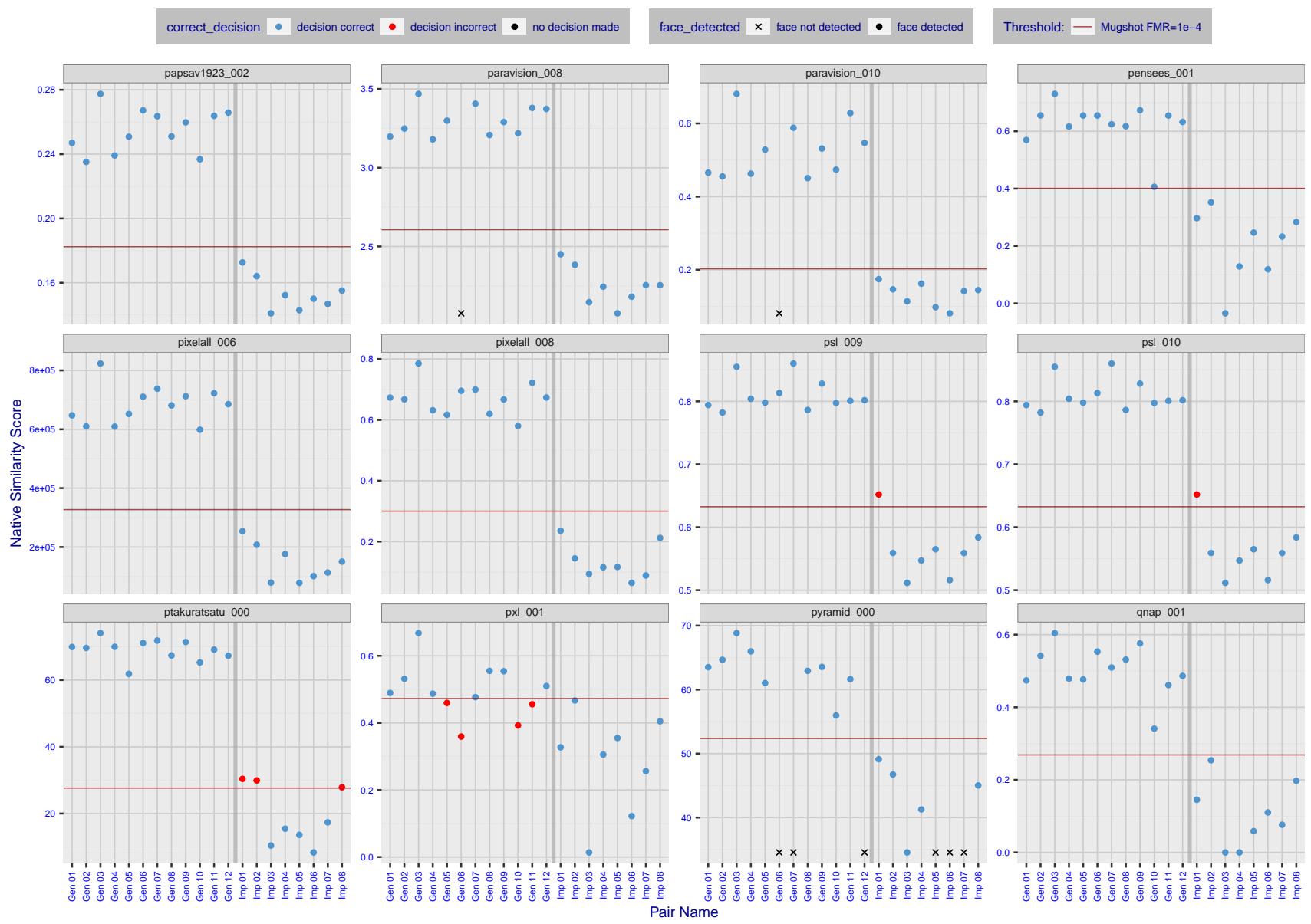


Figure 27: The figure shows algorithms' similarity scores for 12 genuine and 8 impostor image pairs used in a May 2018 paper by Phillips et al. ([1]). The threshold (red horizontal line) is a value calibrated to give $FMR = 0.0001$ on mugshot images. Points above the threshold correspond to pairs determined to be genuine, and points below the threshold correspond to pairs determined to be impostors. If the determined class (genuine or impostor) matches the real class, points will be blue; if not, red. An X represents face detection failure in either of the images in the pair. Note that the sample size ($n=20$) is small, and the figure may change substantially if larger or different sets are used. The images can be viewed on p. 13 of the Appendix, where Gen 01 corresponds to Same-Identity Pair 1, Gen 02 corresponds to Same-Identity Pair 2, and so on.

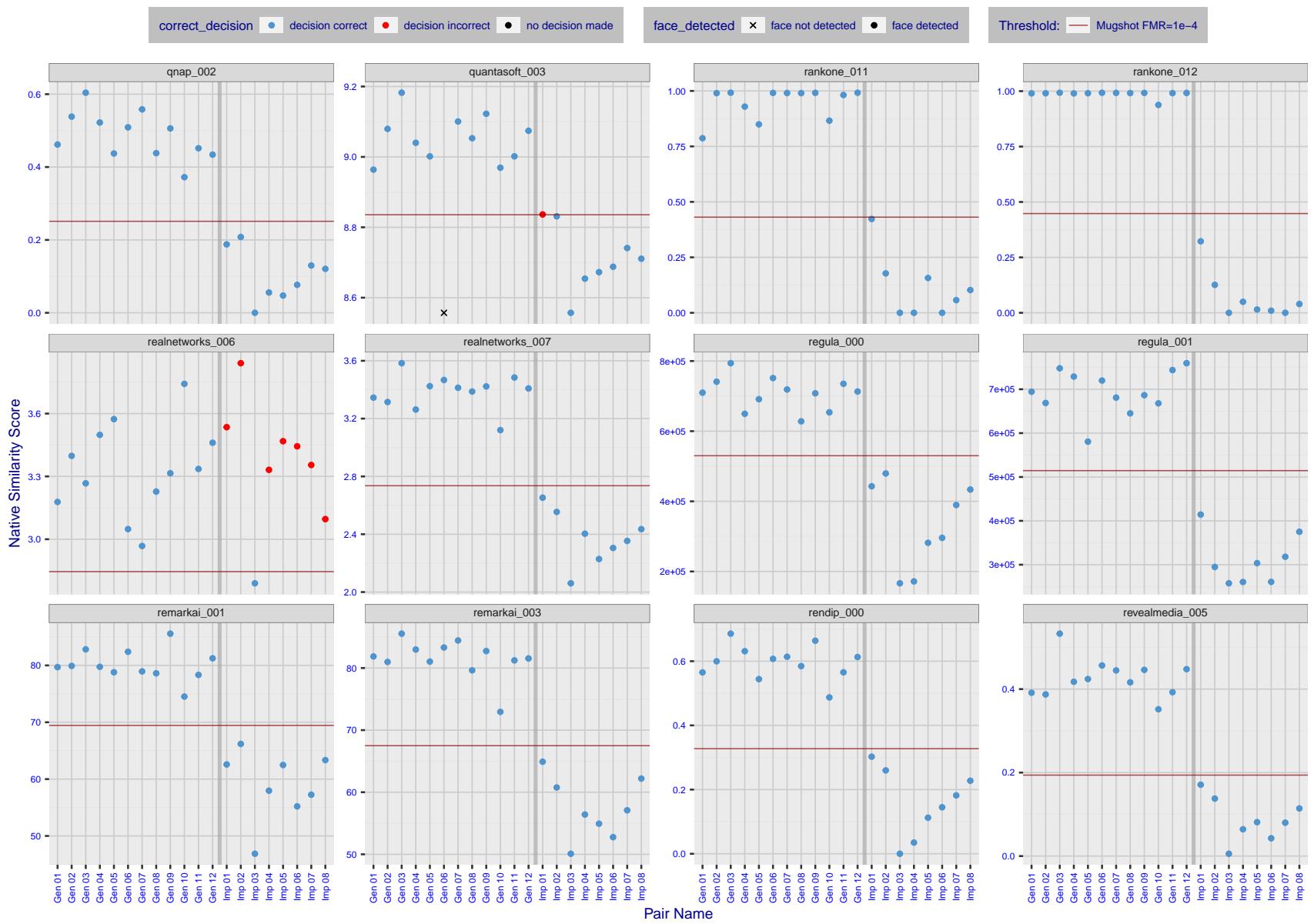


Figure 28: The figure shows algorithms' similarity scores for 12 genuine and 8 impostor image pairs used in a May 2018 paper by Phillips et al. ([1]). The threshold (red horizontal line) is a value calibrated to give $FMR = 0.0001$ on mugshot images. Points above the threshold correspond to pairs determined to be genuine, and points below the threshold correspond to pairs determined to be impostors. If the determined class (genuine or impostor) matches the real class, points will be blue; if not, red. An X represents face detection failure in either of the images in the pair. Note that the sample size ($n=20$) is small, and the figure may change substantially if larger or different sets are used. The images can be viewed on p. 13 of the Appendix, where Gen 01 corresponds to Same-Identity Pair 1, Gen 02 corresponds to Same-Identity Pair 2, and so on.

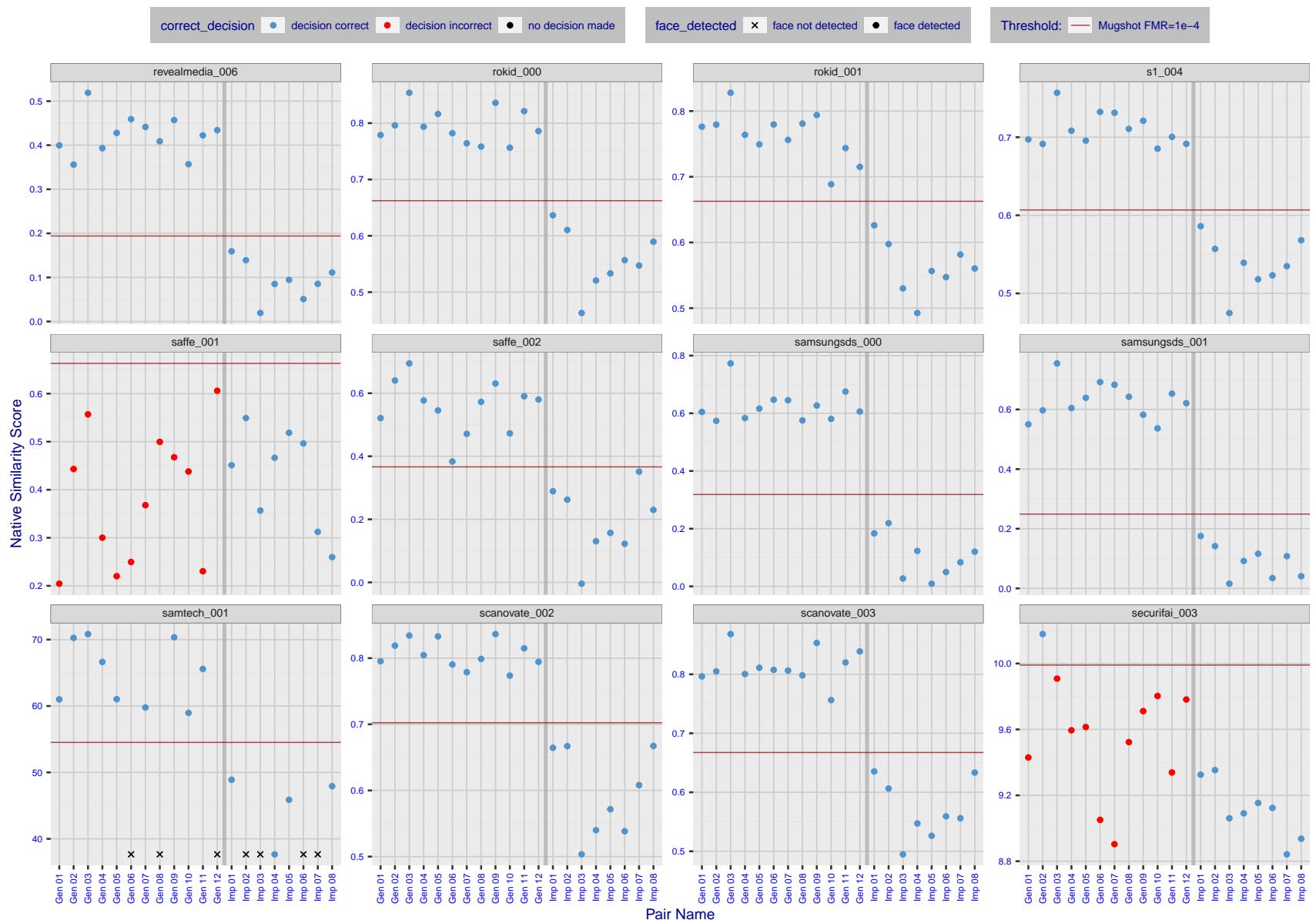


Figure 29: The figure shows algorithms' similarity scores for 12 genuine and 8 impostor image pairs used in a May 2018 paper by Phillips et al. ([1]). The threshold (red horizontal line) is a value calibrated to give $FMR = 0.0001$ on mugshot images. Points above the threshold correspond to pairs determined to be genuine, and points below the threshold correspond to pairs determined to be impostors. If the determined class (genuine or impostor) matches the real class, points will be blue; if not, red. An X represents face detection failure in either of the images in the pair. Note that the sample size ($n=20$) is small, and the figure may change substantially if larger or different sets are used. The images can be viewed on p. 13 of the Appendix, where Gen 01 corresponds to Same-Identity Pair 1, Gen 02 corresponds to Same-Identity Pair 2, and so on.

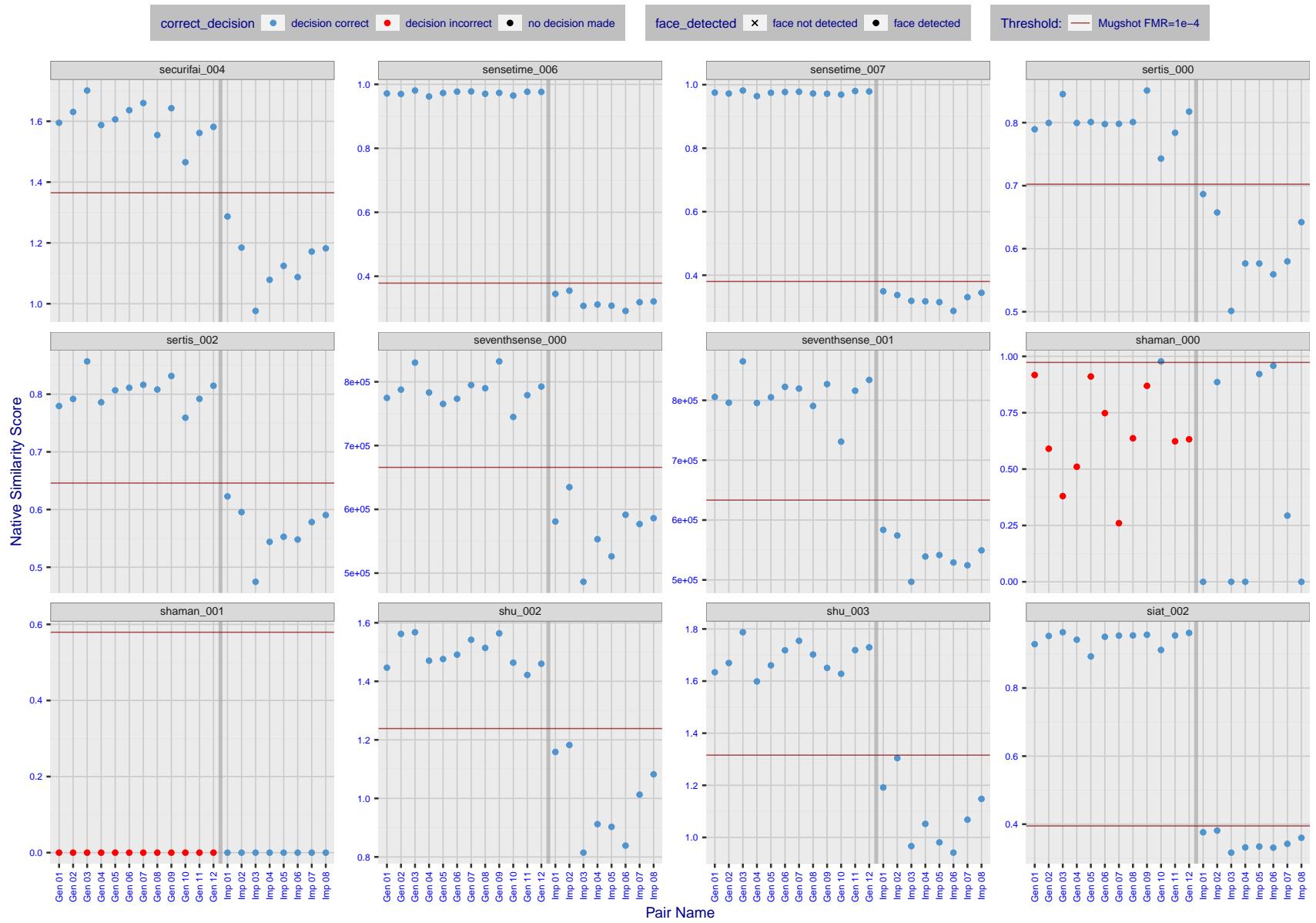


Figure 30: The figure shows algorithms' similarity scores for 12 genuine and 8 impostor image pairs used in a May 2018 paper by Phillips et al. ([1]). The threshold (red horizontal line) is a value calibrated to give $FMR = 0.0001$ on mugshot images. Points above the threshold correspond to pairs determined to be genuine, and points below the threshold correspond to pairs determined to be impostors. If the determined class (genuine or impostor) matches the real class, points will be blue; if not, red. An X represents face detection failure in either of the images in the pair. Note that the sample size ($n=20$) is small, and the figure may change substantially if larger or different sets are used. The images can be viewed on p. 13 of the Appendix, where Gen 01 corresponds to Same-Identity Pair 1, Gen 02 corresponds to Same-Identity Pair 2, and so on.

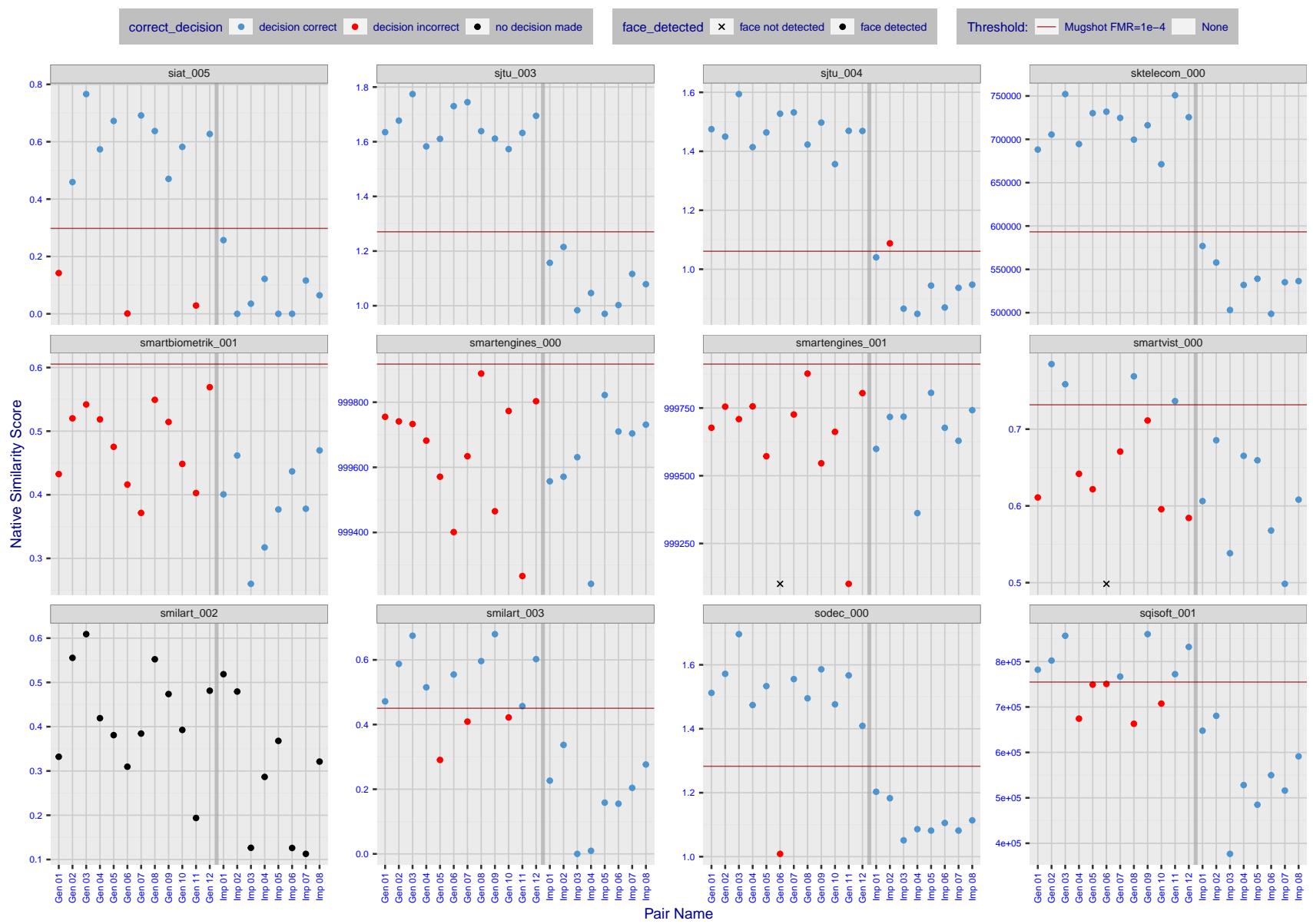


Figure 31: The figure shows algorithms' similarity scores for 12 genuine and 8 impostor image pairs used in a May 2018 paper by Phillips et al. ([1]). The threshold (red horizontal line) is a value calibrated to give $FMR = 0.0001$ on mugshot images. Points above the threshold correspond to pairs determined to be genuine, and points below the threshold correspond to pairs determined to be impostors. If the determined class (genuine or impostor) matches the real class, points will be blue; if not, red. An X represents face detection failure in either of the images in the pair. Note that the sample size ($n=20$) is small, and the figure may change substantially if larger or different sets are used. The images can be viewed on p. 13 of the Appendix, where Gen 01 corresponds to Same-Identity Pair 1, Gen 02 corresponds to Same-Identity Pair 2, and so on.

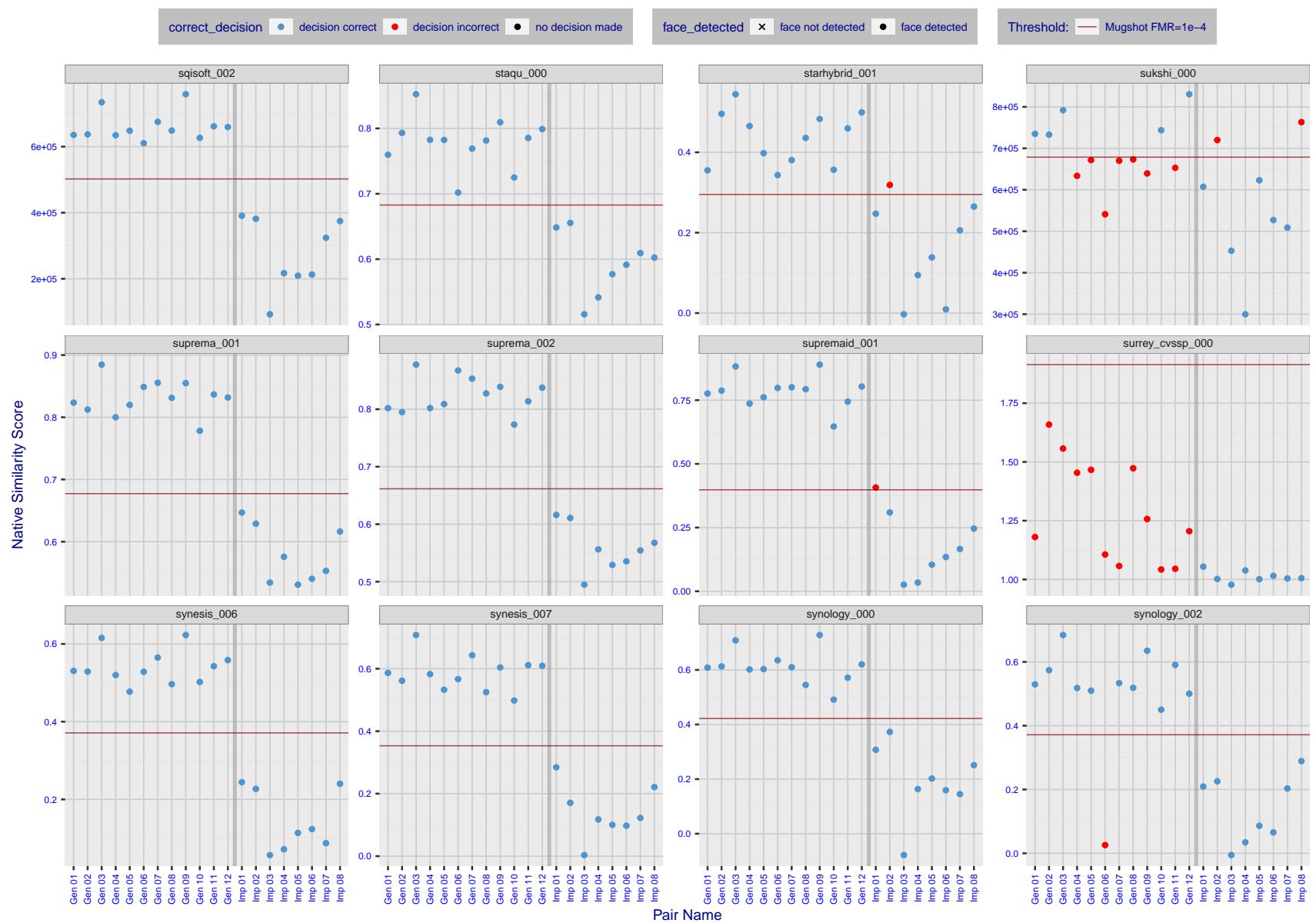


Figure 32: The figure shows algorithms' similarity scores for 12 genuine and 8 impostor image pairs used in a May 2018 paper by Phillips et al. ([1]). The threshold (red horizontal line) is a value calibrated to give $\text{FMR} = 0.0001$ on mugshot images. Points above the threshold correspond to pairs determined to be genuine, and points below the threshold correspond to pairs determined to be impostors. If the determined class (genuine or impostor) matches the real class, points will be blue; if not, red. An X represents face detection failure in either of the images in the pair. Note that the sample size ($n=20$) is small, and the figure may change substantially if larger or different sets are used. The images can be viewed on p. 13 of the Appendix, where Gen 01 corresponds to Same-Identity Pair 1, Gen 02 corresponds to Same-Identity Pair 2, and so on.

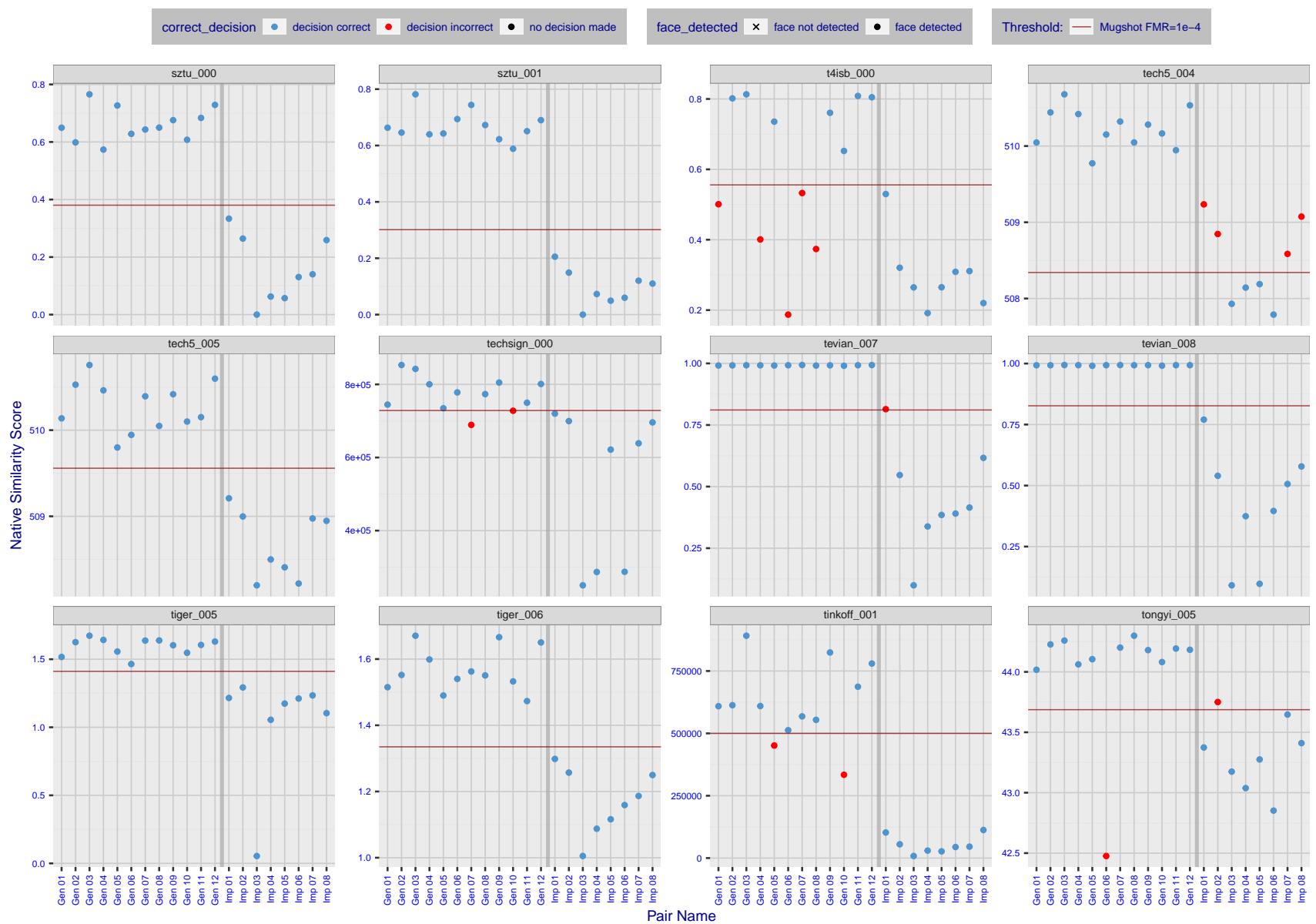


Figure 33: The figure shows algorithms' similarity scores for 12 genuine and 8 impostor image pairs used in a May 2018 paper by Phillips et al. ([1]). The threshold (red horizontal line) is a value calibrated to give $FMR = 0.0001$ on mugshot images. Points above the threshold correspond to pairs determined to be genuine, and points below the threshold correspond to pairs determined to be impostors. If the determined class (genuine or impostor) matches the real class, points will be blue; if not, red. An X represents face detection failure in either of the images in the pair. Note that the sample size ($n=20$) is small, and the figure may change substantially if larger or different sets are used. The images can be viewed on p. 13 of the Appendix, where Gen 01 corresponds to Same-Identity Pair 1, Gen 02 corresponds to Same-Identity Pair 2, and so on.

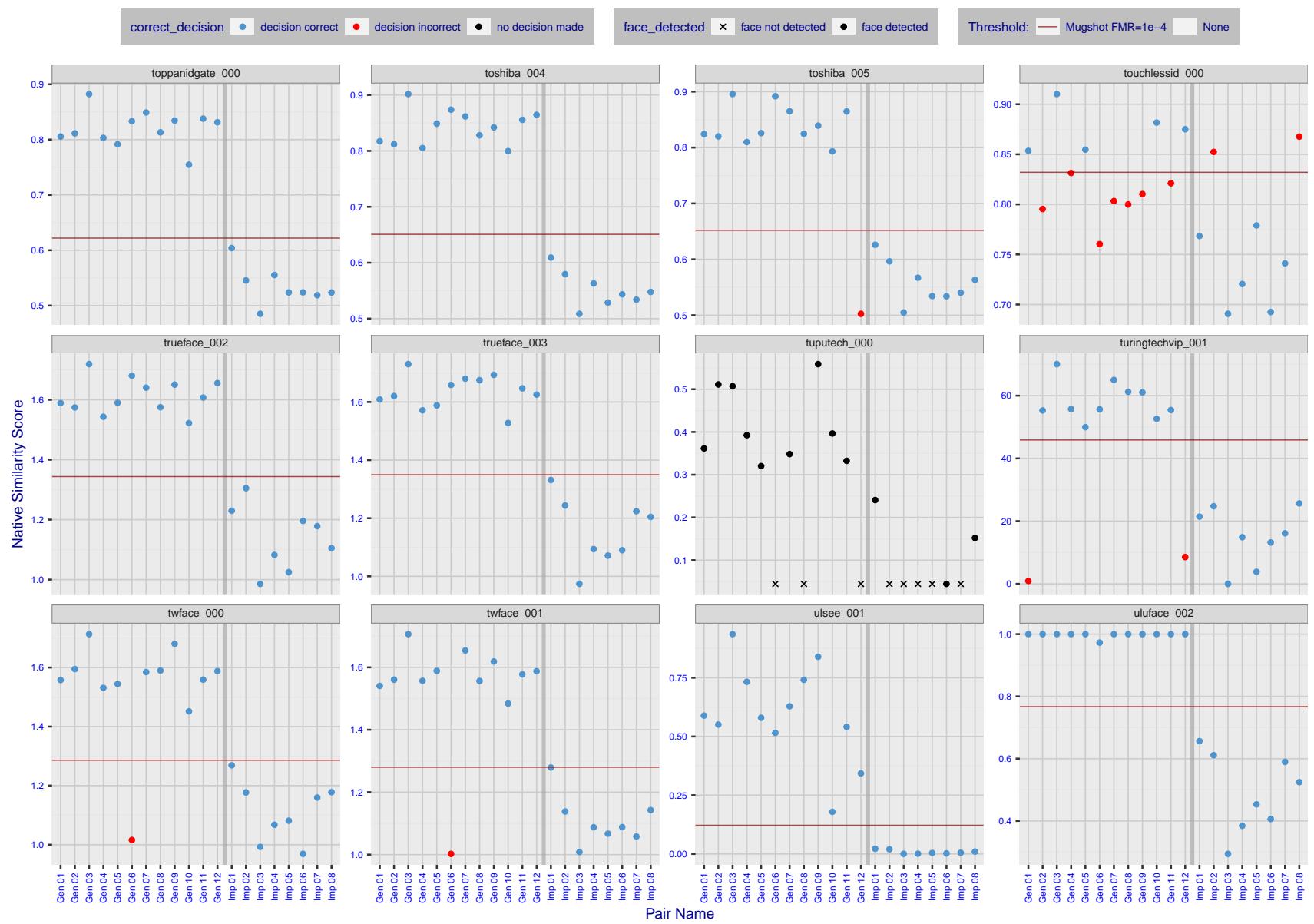


Figure 34: The figure shows algorithms' similarity scores for 12 genuine and 8 impostor image pairs used in a May 2018 paper by Phillips et al. ([1]). The threshold (red horizontal line) is a value calibrated to give $FMR = 0.0001$ on mugshot images. Points above the threshold correspond to pairs determined to be genuine, and points below the threshold correspond to pairs determined to be impostors. If the determined class (genuine or impostor) matches the real class, points will be blue; if not, red. An X represents face detection failure in either of the images in the pair. Note that the sample size ($n=20$) is small, and the figure may change substantially if larger or different sets are used. The images can be viewed on p. 13 of the Appendix, where Gen 01 corresponds to Same-Identity Pair 1, Gen 02 corresponds to Same-Identity Pair 2, and so on.

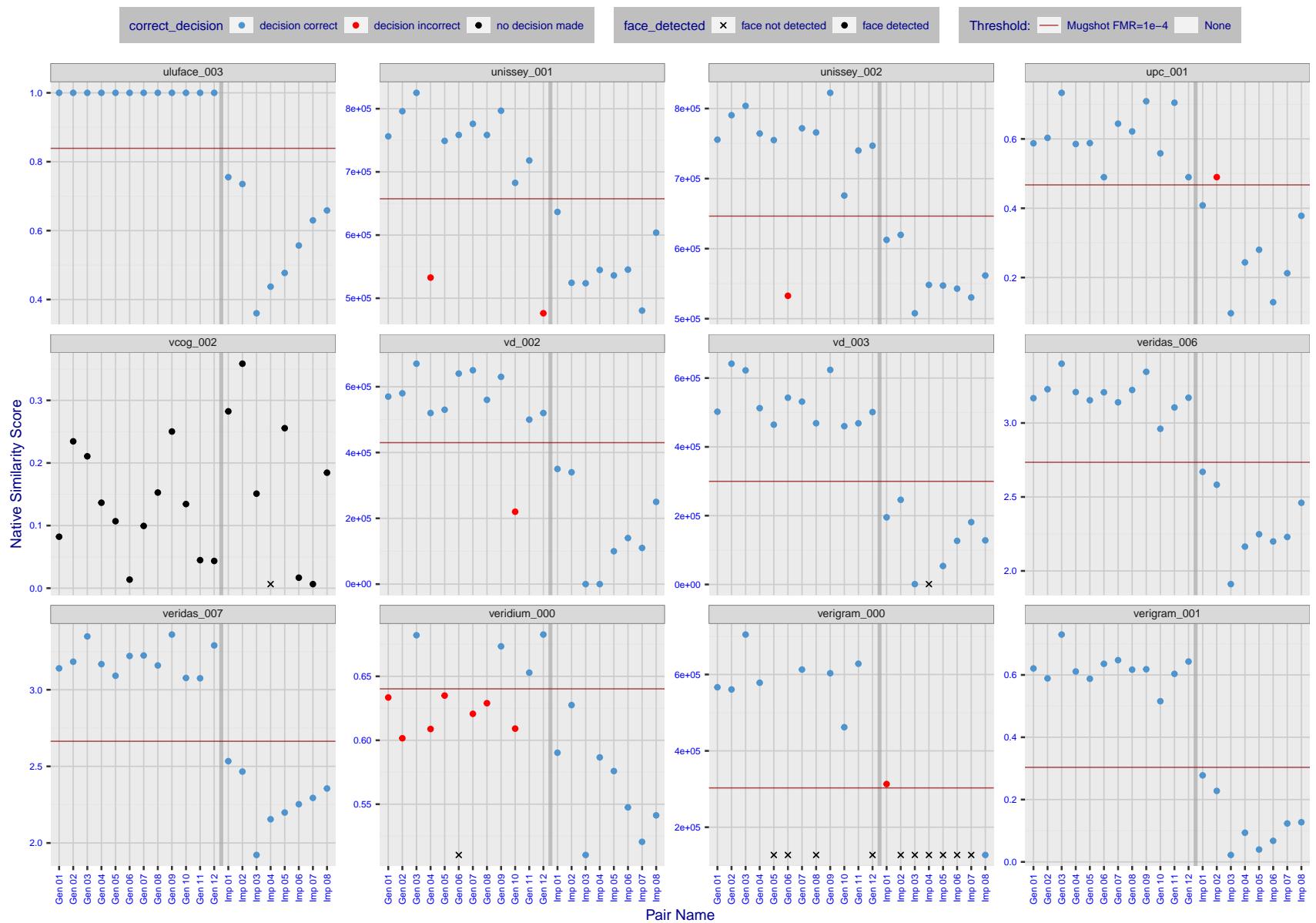


Figure 35: The figure shows algorithms' similarity scores for 12 genuine and 8 impostor image pairs used in a May 2018 paper by Phillips et al. ([1]). The threshold (red horizontal line) is a value calibrated to give $FMR = 0.0001$ on mugshot images. Points above the threshold correspond to pairs determined to be genuine, and points below the threshold correspond to pairs determined to be impostors. If the determined class (genuine or impostor) matches the real class, points will be blue; if not, red. An X represents face detection failure in either of the images in the pair. Note that the sample size ($n=20$) is small, and the figure may change substantially if larger or different sets are used. The images can be viewed on p. 13 of the Appendix, where Gen 01 corresponds to Same-Identity Pair 1, Gen 02 corresponds to Same-Identity Pair 2, and so on.

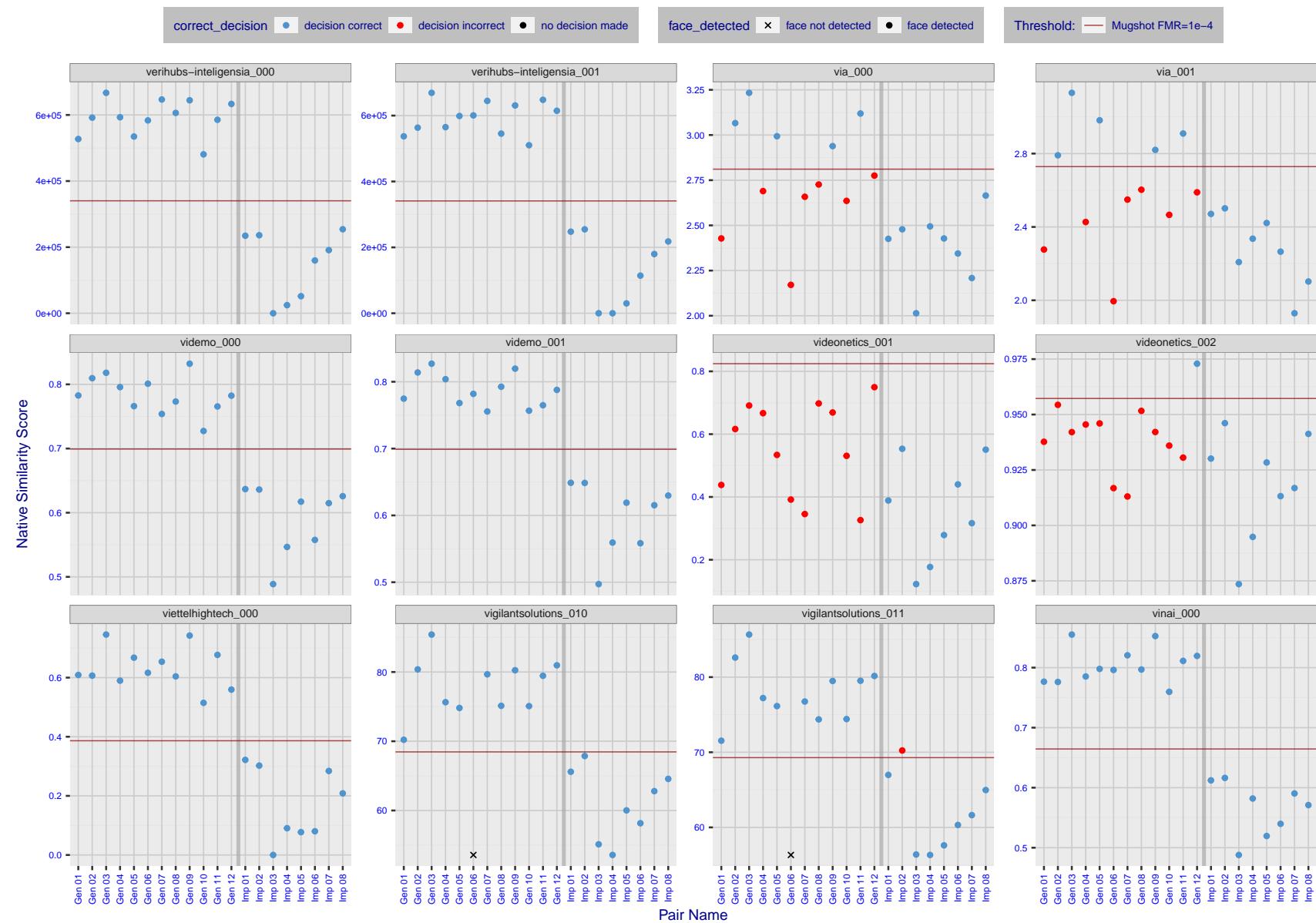


Figure 36: The figure shows algorithms' similarity scores for 12 genuine and 8 impostor image pairs used in a May 2018 paper by Phillips et al. ([1]). The threshold (red horizontal line) is a value calibrated to give $FMR = 0.0001$ on mugshot images. Points above the threshold correspond to pairs determined to be genuine, and points below the threshold correspond to pairs determined to be impostors. If the determined class (genuine or impostor) matches the real class, points will be blue; if not, red. An X represents face detection failure in either of the images in the pair. Note that the sample size ($n=20$) is small, and the figure may change substantially if larger or different sets are used. The images can be viewed on p. 13 of the Appendix, where Gen 01 corresponds to Same-Identity Pair 1, Gen 02 corresponds to Same-Identity Pair 2, and so on.

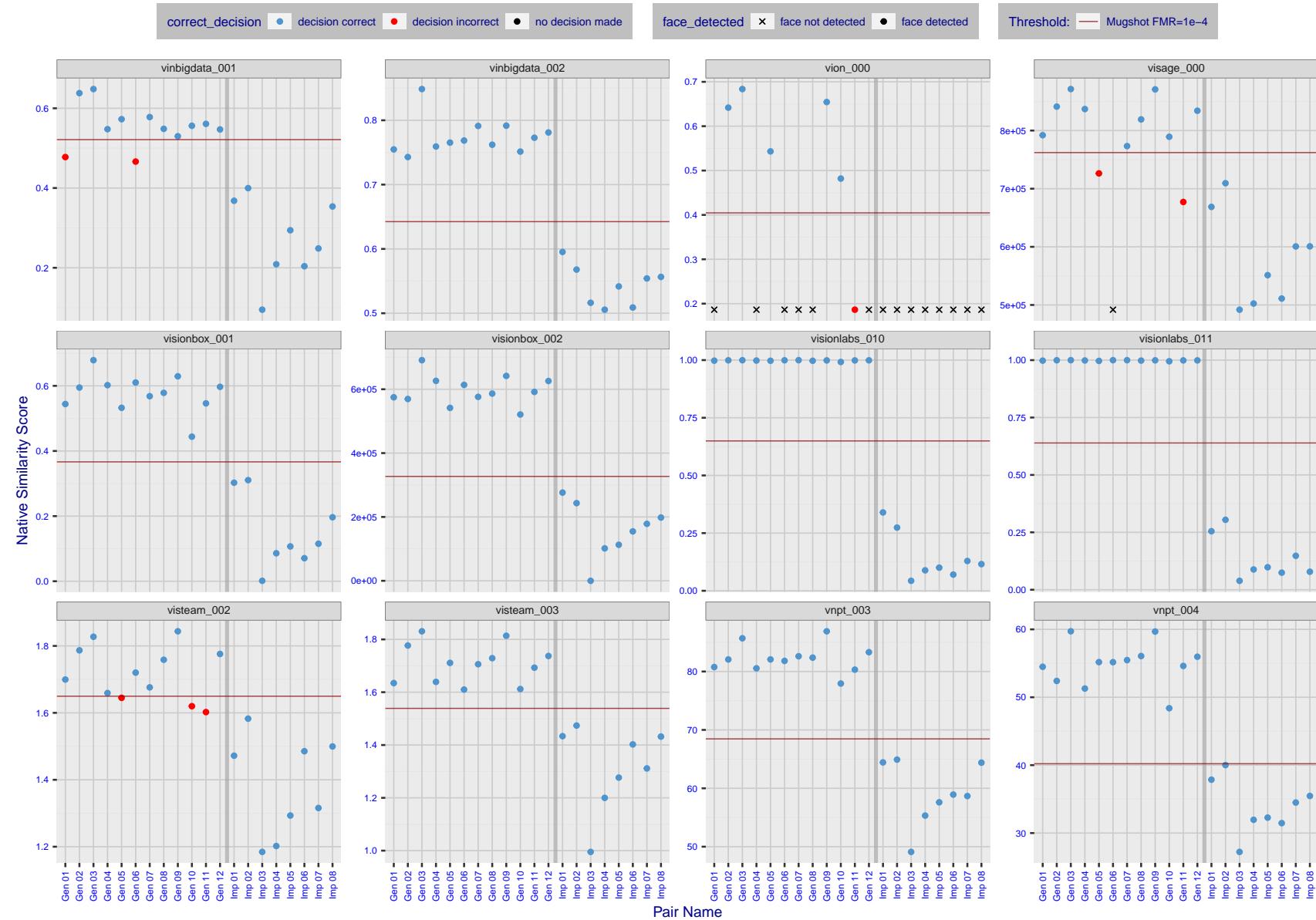


Figure 37: The figure shows algorithms' similarity scores for 12 genuine and 8 impostor image pairs used in a May 2018 paper by Phillips et al. ([1]). The threshold (red horizontal line) is a value calibrated to give $FMR = 0.0001$ on mugshot images. Points above the threshold correspond to pairs determined to be genuine, and points below the threshold correspond to pairs determined to be impostors. If the determined class (genuine or impostor) matches the real class, points will be blue; if not, red. An X represents face detection failure in either of the images in the pair. Note that the sample size ($n=20$) is small, and the figure may change substantially if larger or different sets are used. The images can be viewed on p. 13 of the Appendix, where Gen 01 corresponds to Same-Identity Pair 1, Gen 02 corresponds to Same-Identity Pair 2, and so on.

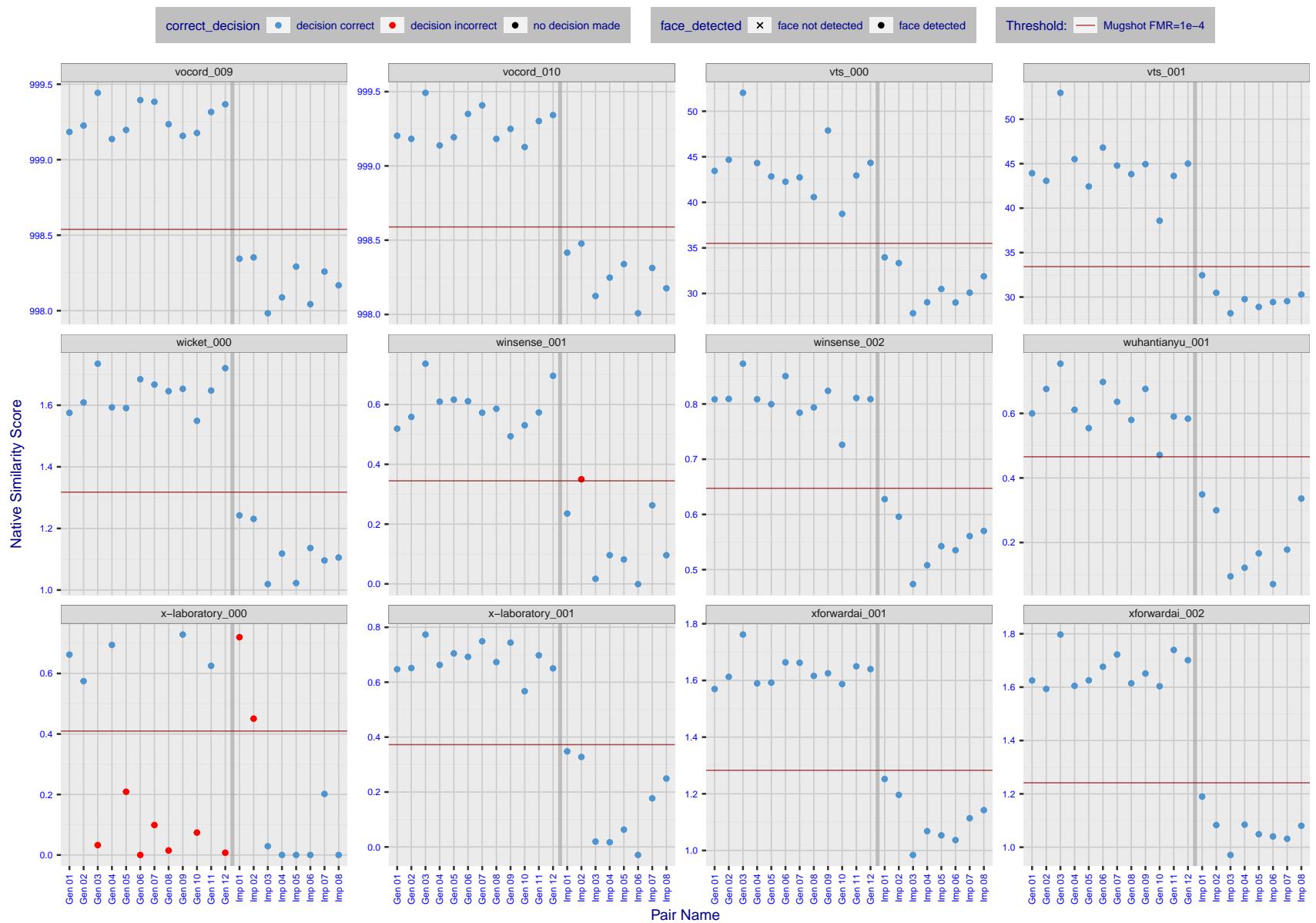


Figure 38: The figure shows algorithms' similarity scores for 12 genuine and 8 impostor image pairs used in a May 2018 paper by Phillips et al. ([1]). The threshold (red horizontal line) is a value calibrated to give $FMR = 0.0001$ on mugshot images. Points above the threshold correspond to pairs determined to be genuine, and points below the threshold correspond to pairs determined to be impostors. If the determined class (genuine or impostor) matches the real class, points will be blue; if not, red. An X represents face detection failure in either of the images in the pair. Note that the sample size ($n=20$) is small, and the figure may change substantially if larger or different sets are used. The images can be viewed on p. 13 of the Appendix, where Gen 01 corresponds to Same-Identity Pair 1, Gen 02 corresponds to Same-Identity Pair 2, and so on.

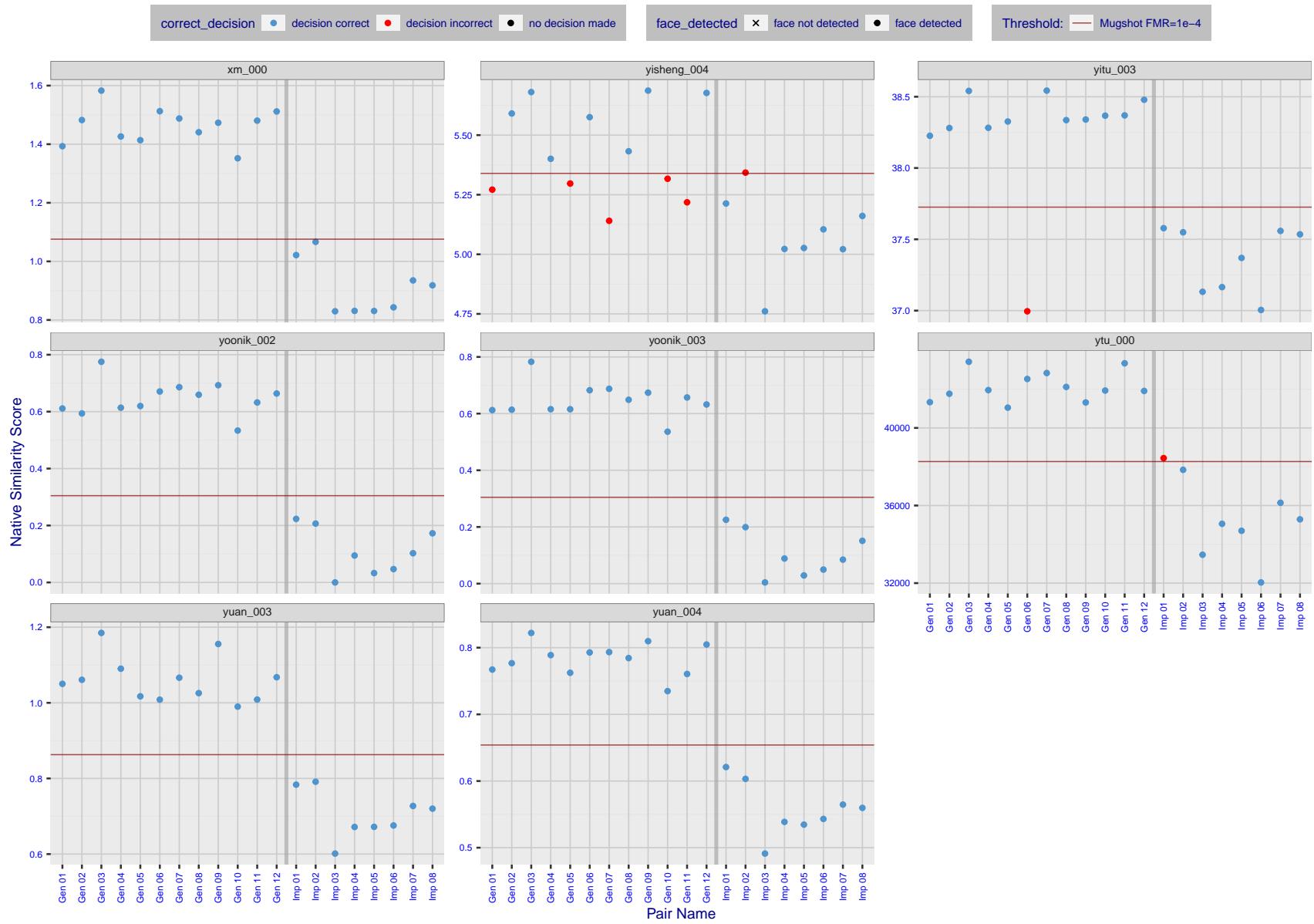


Figure 39: The figure shows algorithms' similarity scores for 12 genuine and 8 impostor image pairs used in a May 2018 paper by Phillips et al. ([1]). The threshold (red horizontal line) is a value calibrated to give $FMR = 0.0001$ on mugshot images. Points above the threshold correspond to pairs determined to be genuine, and points below the threshold correspond to pairs determined to be impostors. If the determined class (genuine or impostor) matches the real class, points will be blue; if not, red. An X represents face detection failure in either of the images in the pair. Note that the sample size ($n=20$) is small, and the figure may change substantially if larger or different sets are used. The images can be viewed on p. 13 of the Appendix, where Gen 01 corresponds to Same-Identity Pair 1, Gen 02 corresponds to Same-Identity Pair 2, and so on.

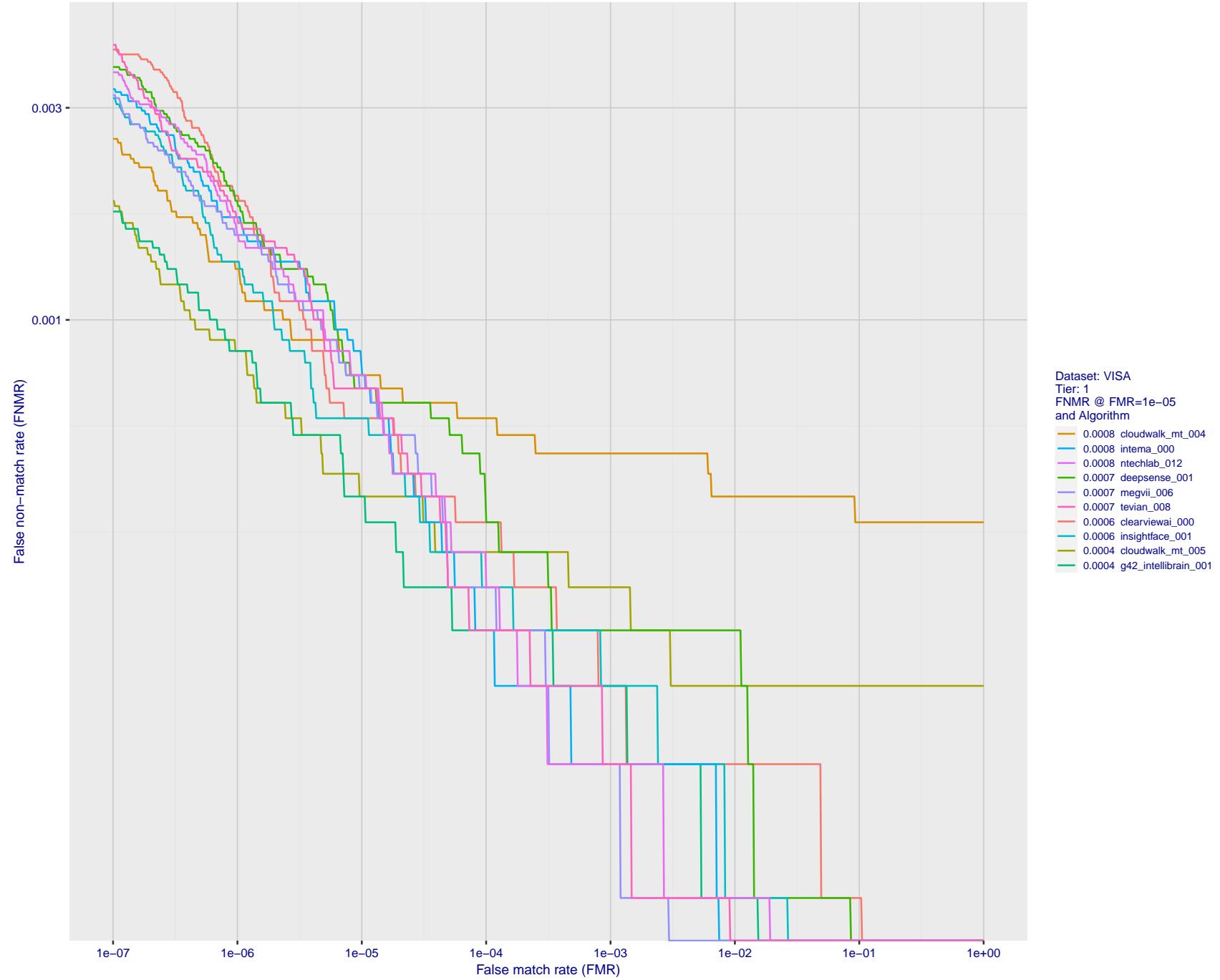


Figure 40: For the visa images, detection error tradeoff (DET) characteristics showing false non-match rate vs. false match rate plotted parametrically on threshold, T . The scales are logarithmic in order to show many decades of FMR.

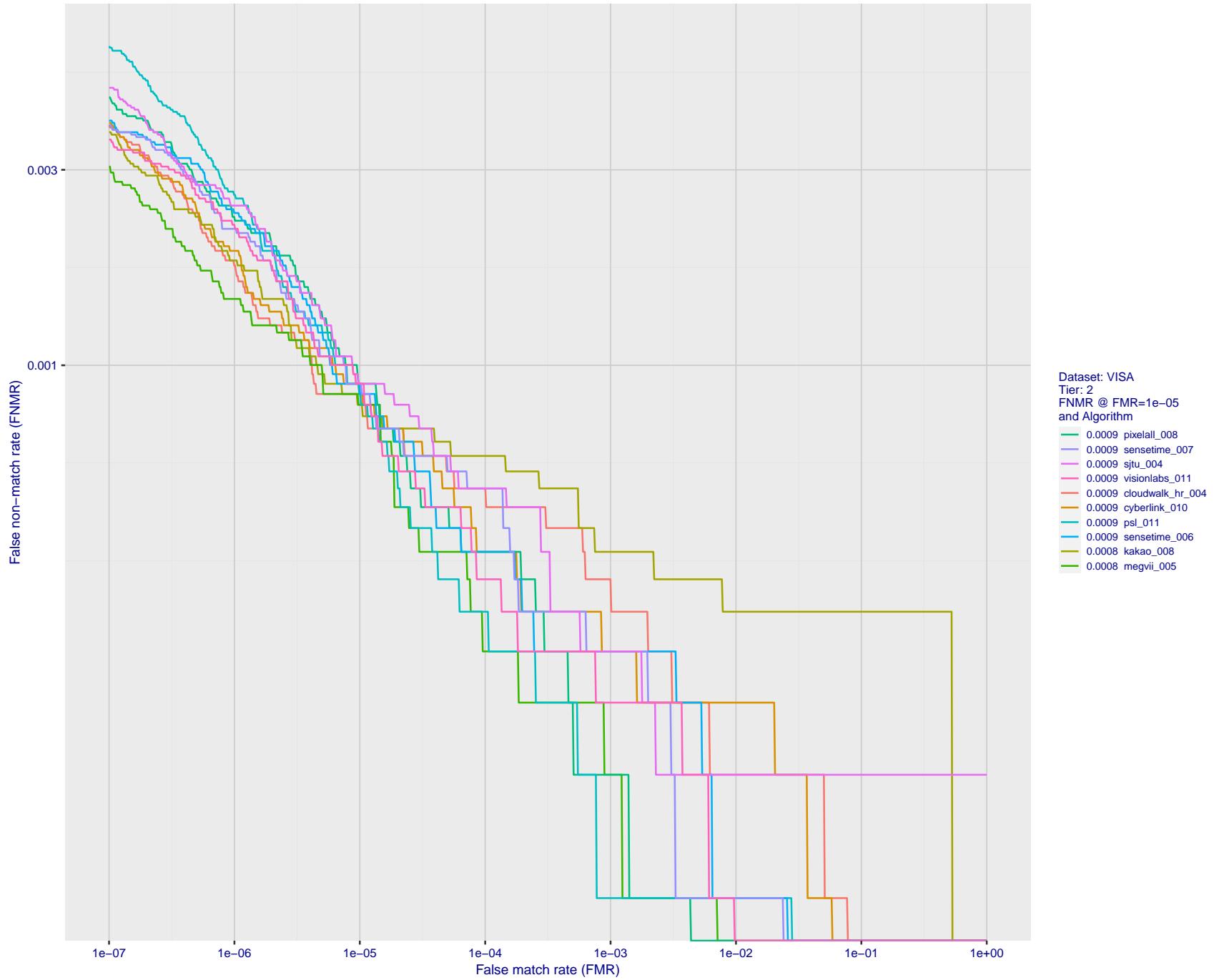


Figure 41: For the visa images, detection error tradeoff (DET) characteristics showing false non-match rate vs. false match rate plotted parametrically on threshold, T . The scales are logarithmic in order to show many decades of FMR.

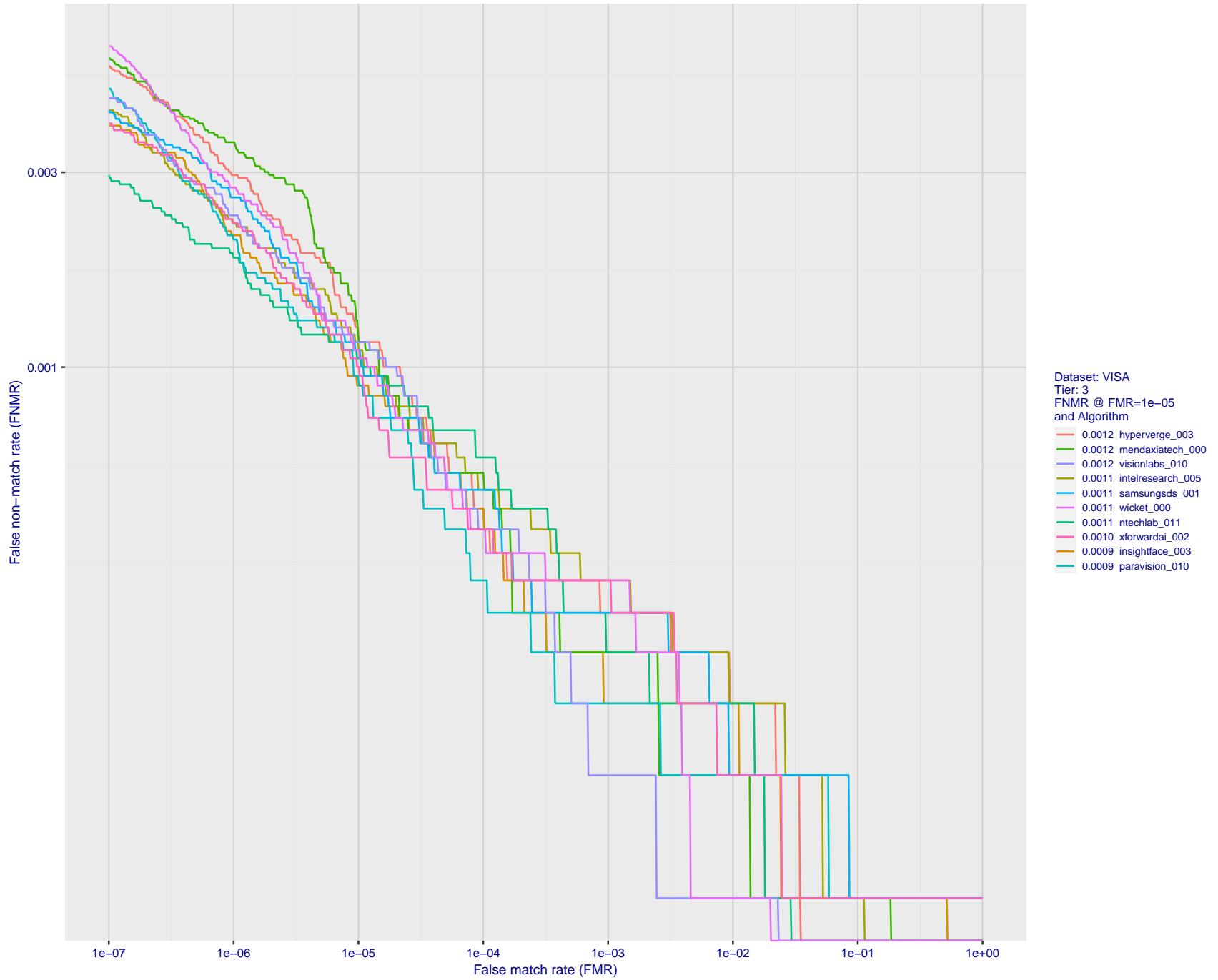


Figure 42: For the visa images, detection error tradeoff (DET) characteristics showing false non-match rate vs. false match rate plotted parametrically on threshold, T . The scales are logarithmic in order to show many decades of FMR.

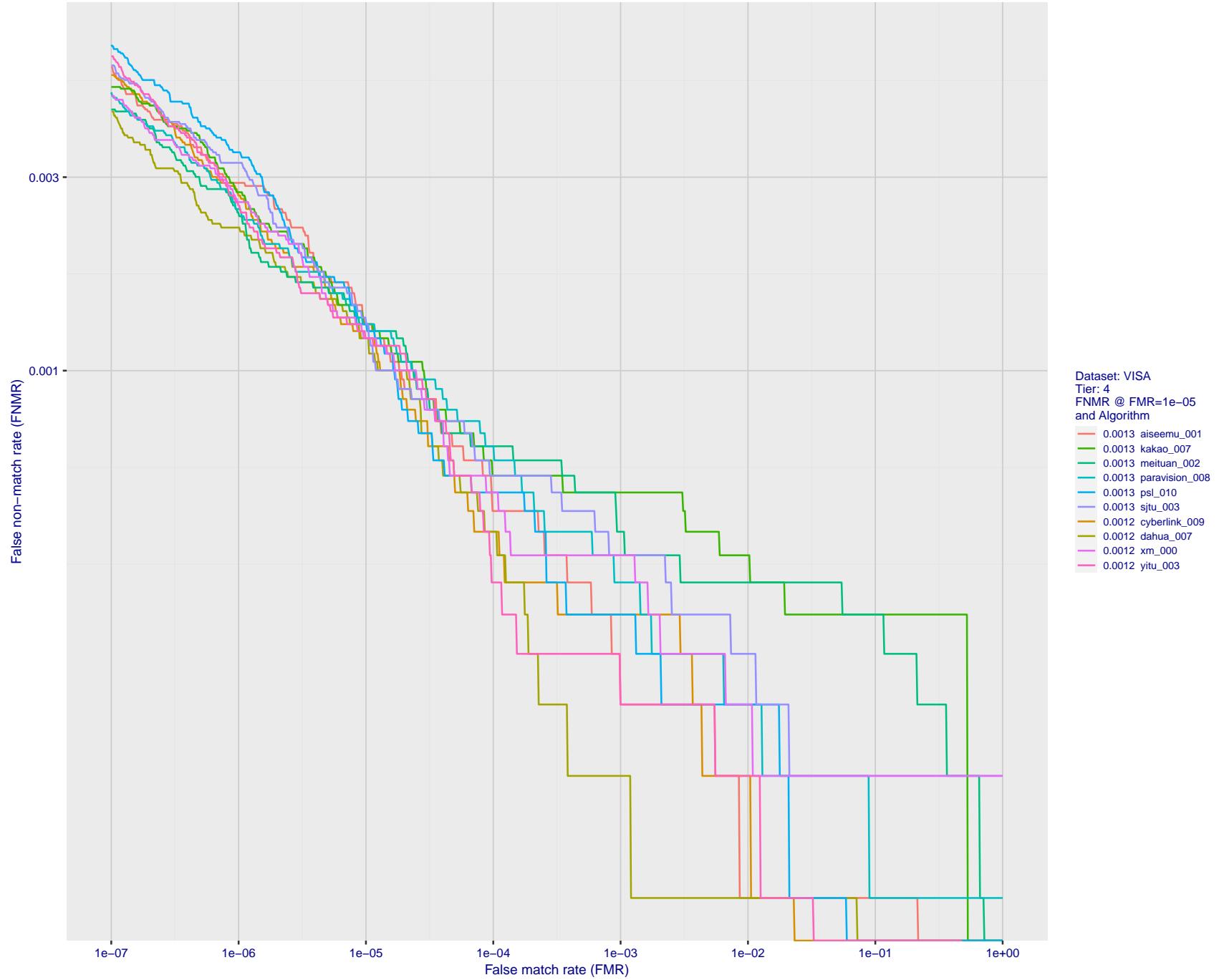


Figure 43: For the visa images, detection error tradeoff (DET) characteristics showing false non-match rate vs. false match rate plotted parametrically on threshold, T . The scales are logarithmic in order to show many decades of FMR.

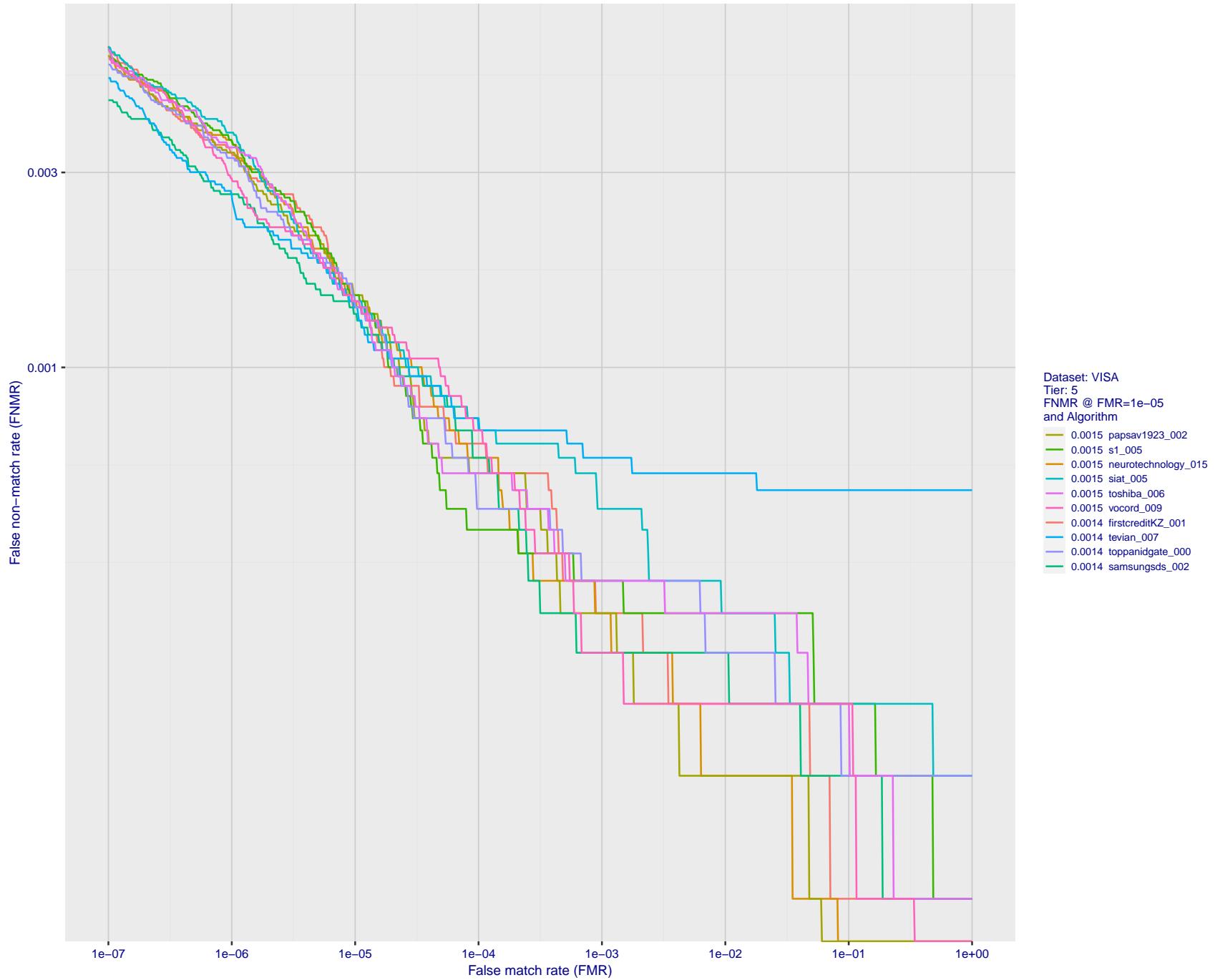


Figure 44: For the visa images, detection error tradeoff (DET) characteristics showing false non-match rate vs. false match rate plotted parametrically on threshold, T . The scales are logarithmic in order to show many decades of FMR.

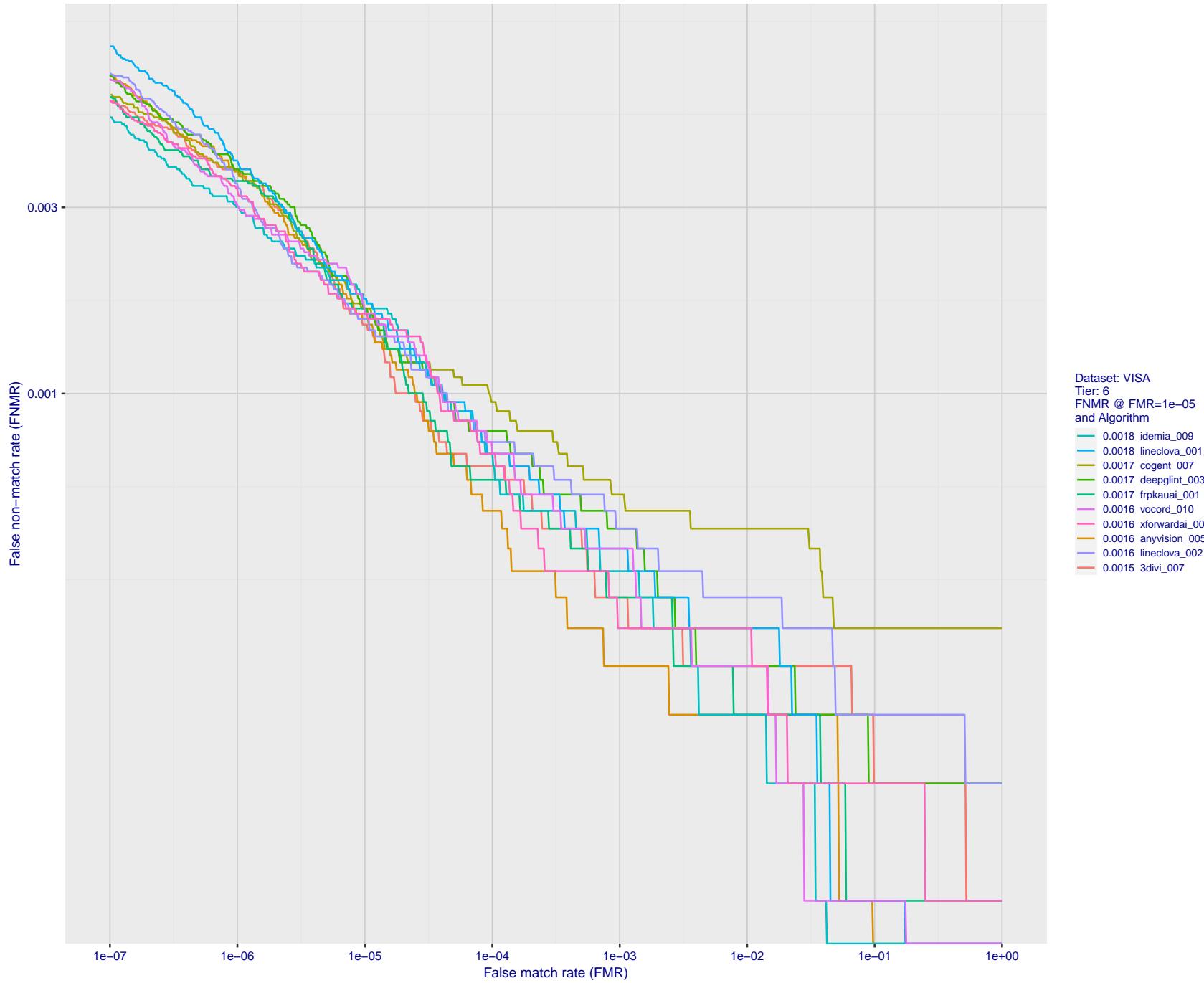


Figure 45: For the visa images, detection error tradeoff (DET) characteristics showing false non-match rate vs. false match rate plotted parametrically on threshold, T . The scales are logarithmic in order to show many decades of FMR.

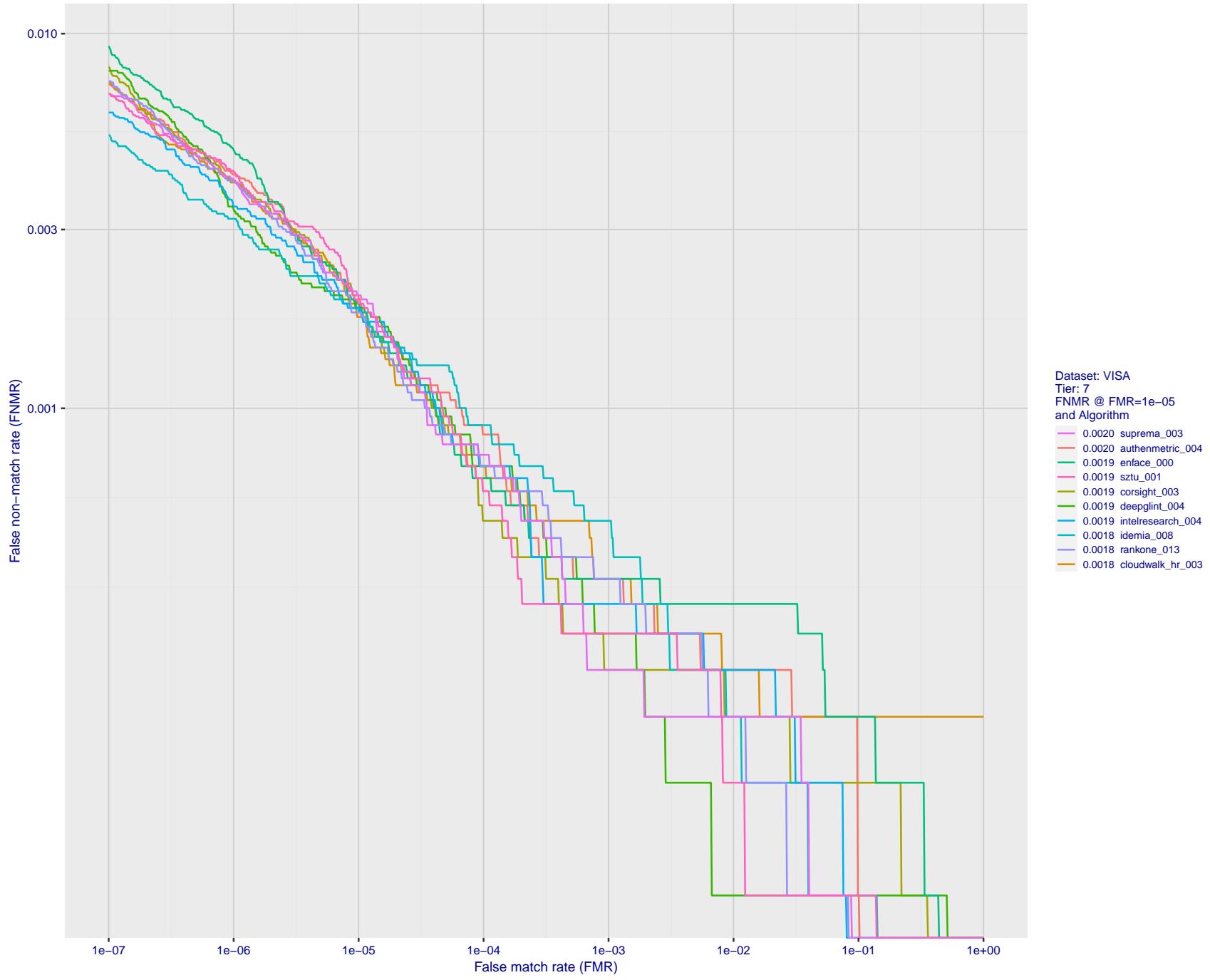


Figure 46: For the visa images, detection error tradeoff (DET) characteristics showing false non-match rate vs. false match rate plotted parametrically on threshold, T . The scales are logarithmic in order to show many decades of FMR.

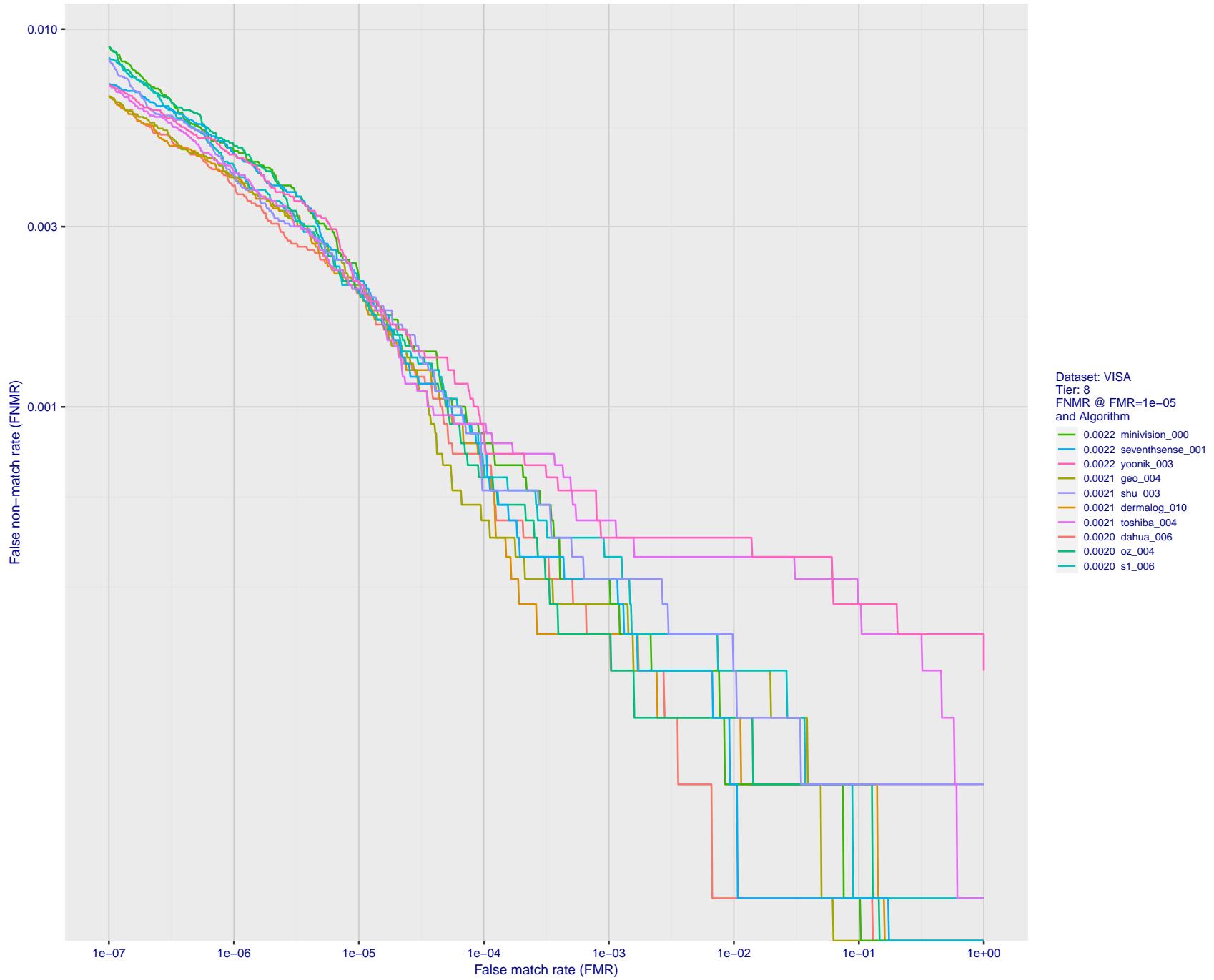


Figure 47: For the visa images, detection error tradeoff (DET) characteristics showing false non-match rate vs. false match rate plotted parametrically on threshold, T . The scales are logarithmic in order to show many decades of FMR.

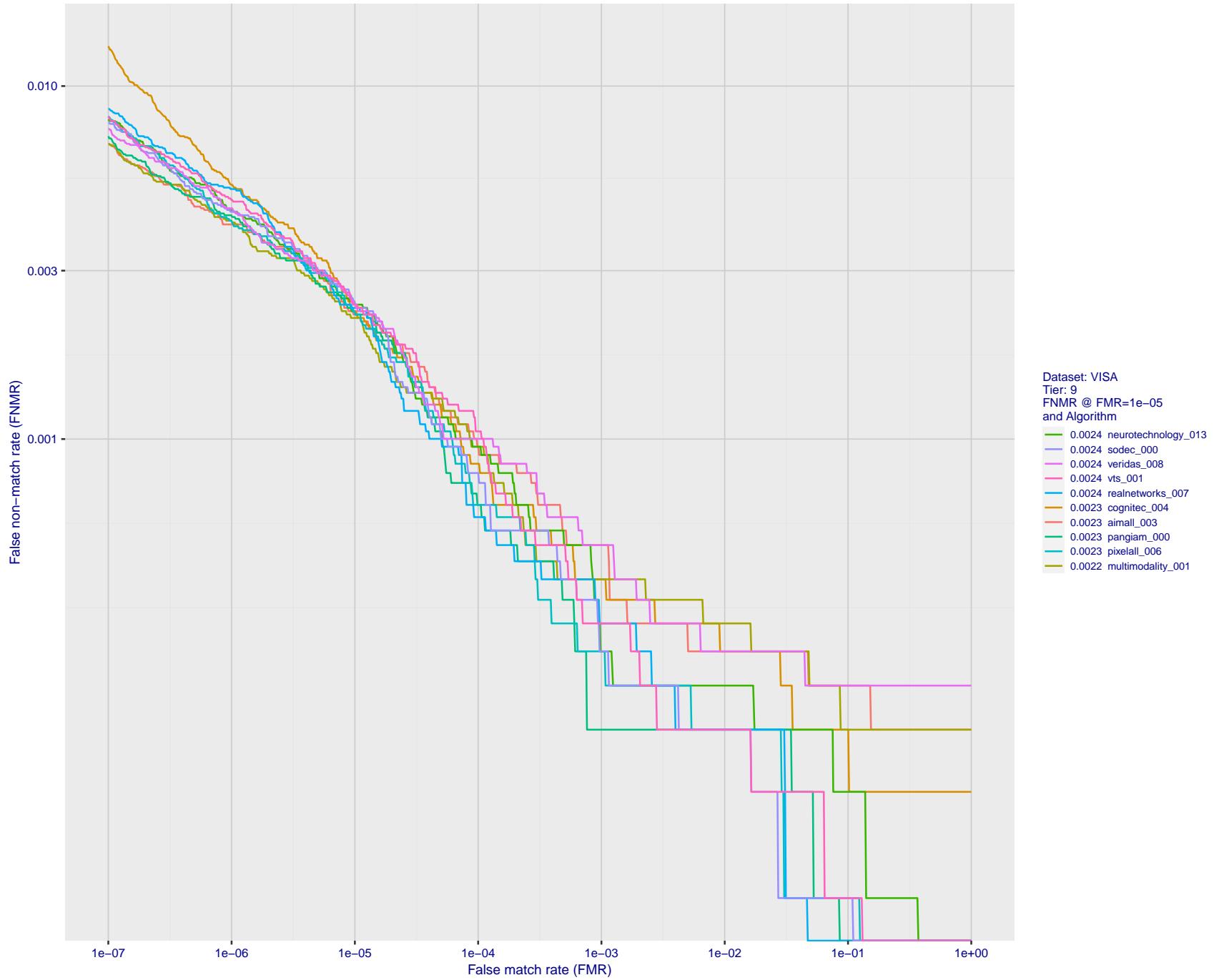


Figure 48: For the visa images, detection error tradeoff (DET) characteristics showing false non-match rate vs. false match rate plotted parametrically on threshold, T . The scales are logarithmic in order to show many decades of FMR.

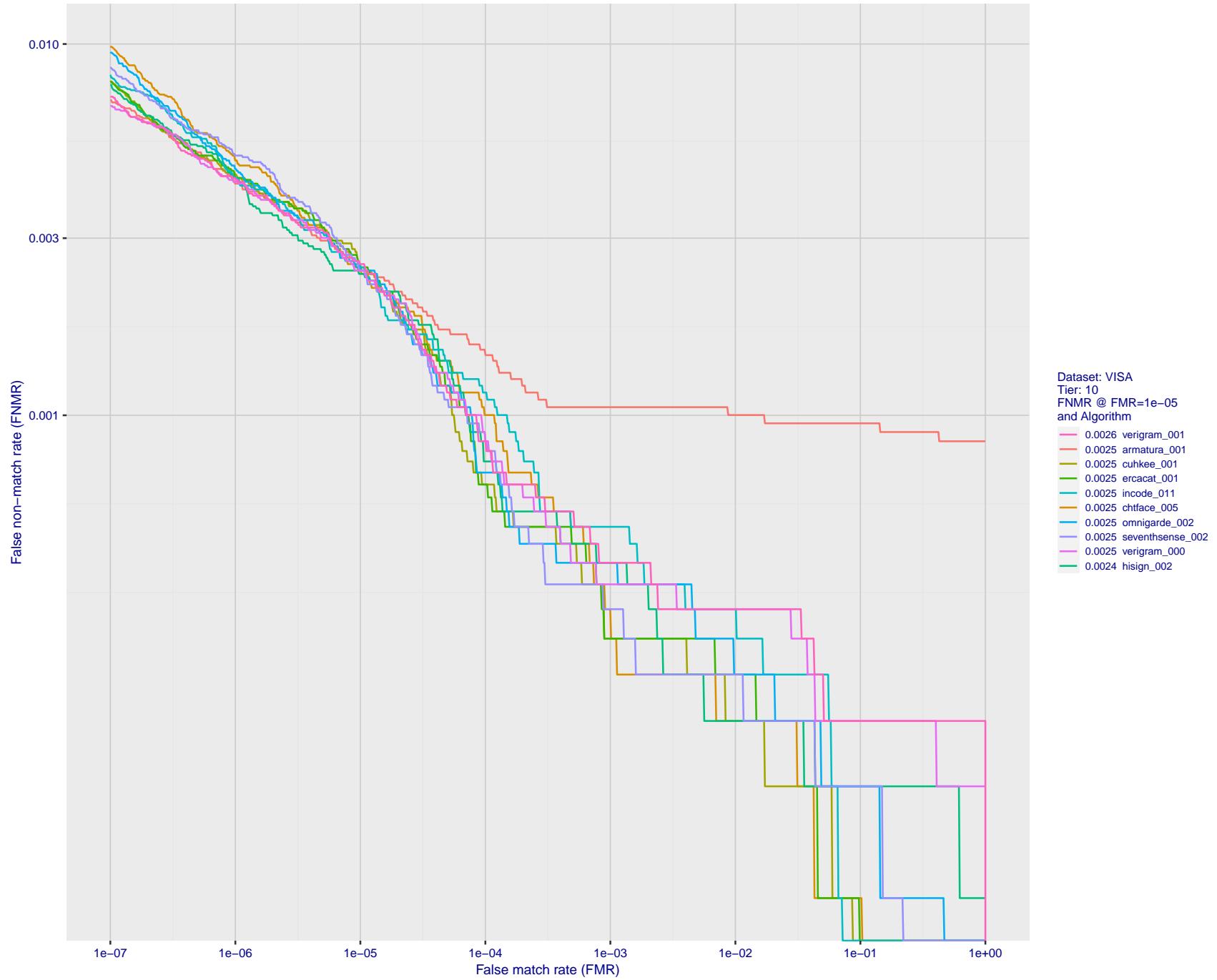


Figure 49: For the visa images, detection error tradeoff (DET) characteristics showing false non-match rate vs. false match rate plotted parametrically on threshold, T . The scales are logarithmic in order to show many decades of FMR.

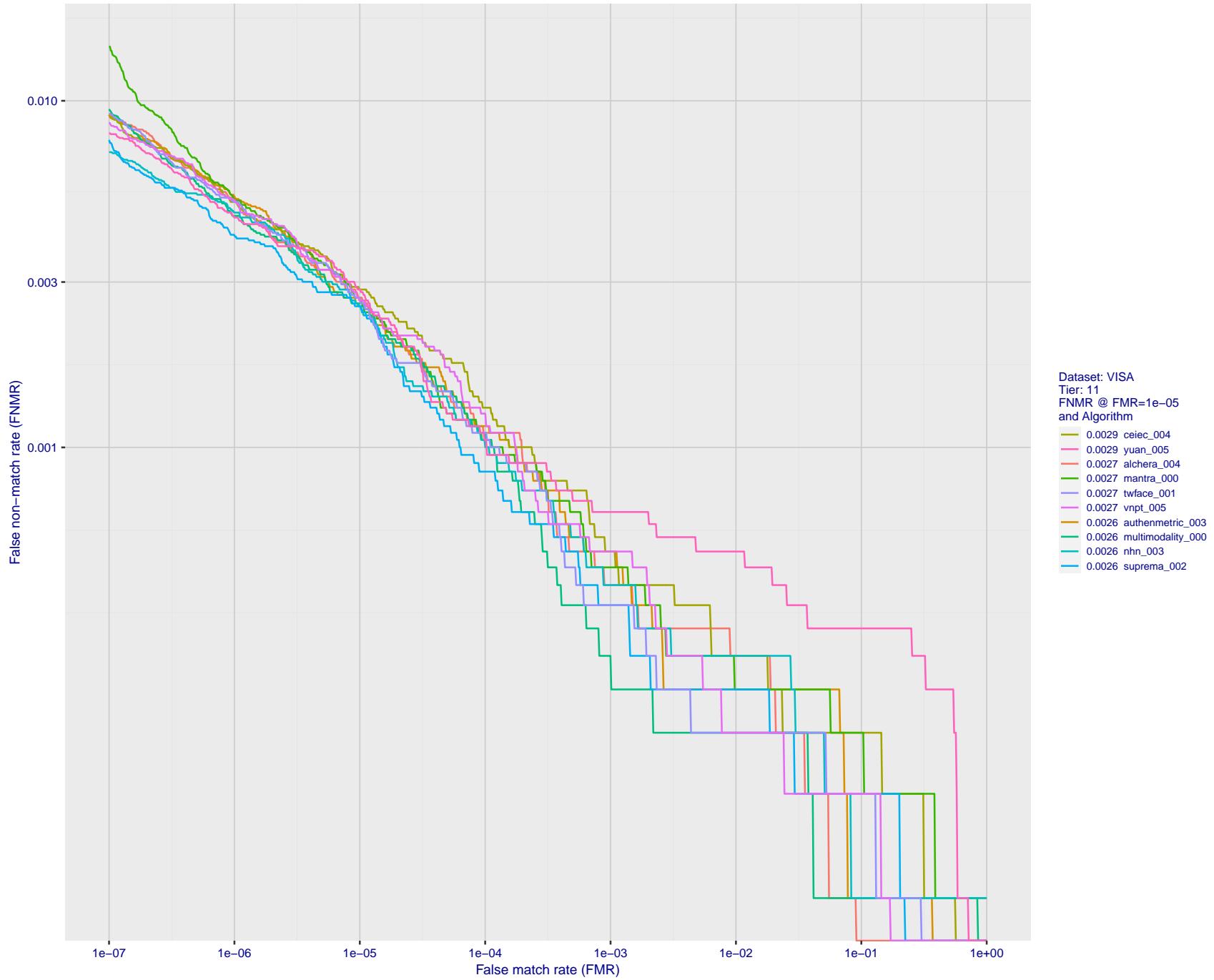


Figure 50: For the visa images, detection error tradeoff (DET) characteristics showing false non-match rate vs. false match rate plotted parametrically on threshold, T . The scales are logarithmic in order to show many decades of FMR.

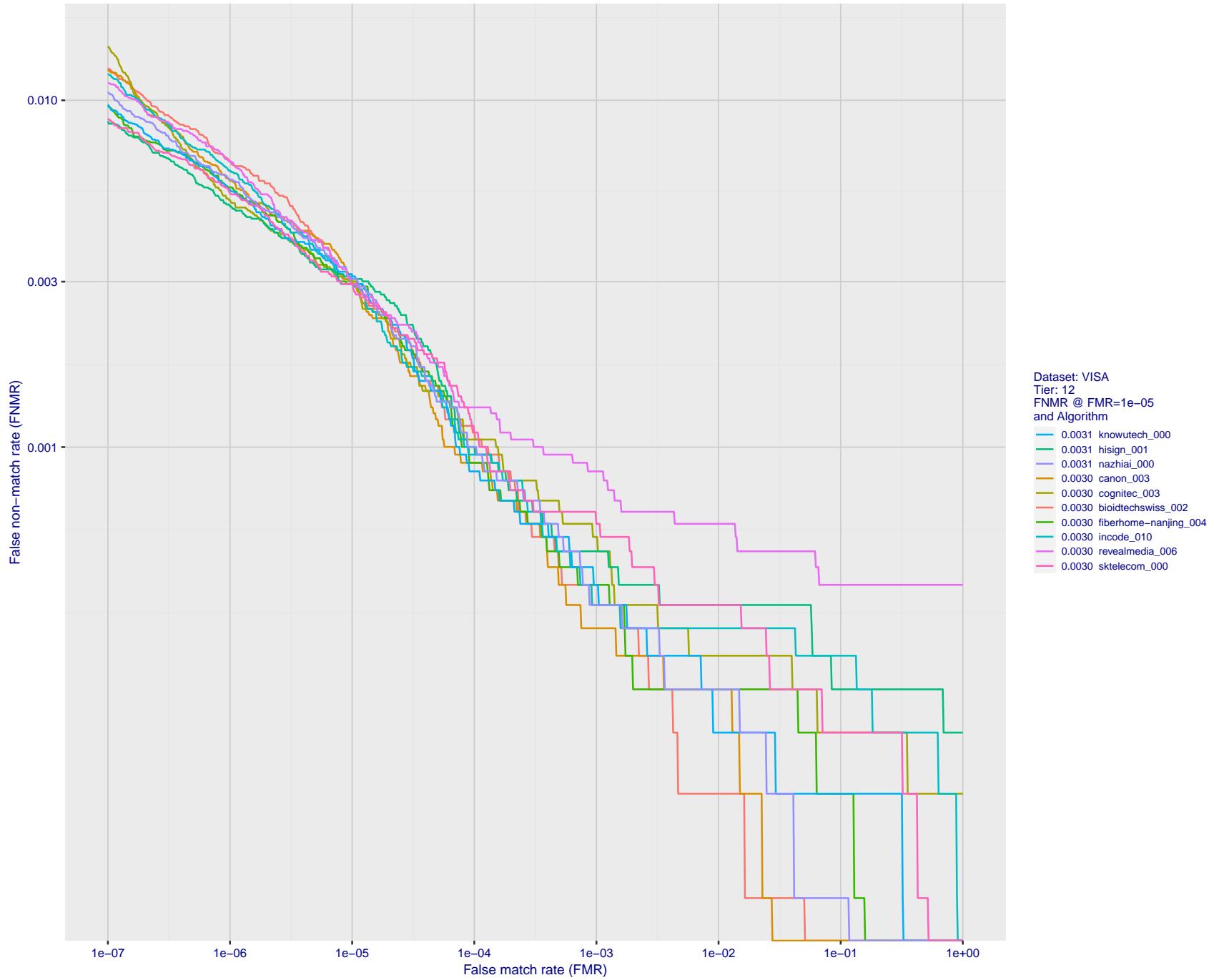


Figure 51: For the visa images, detection error tradeoff (DET) characteristics showing false non-match rate vs. false match rate plotted parametrically on threshold, T . The scales are logarithmic in order to show many decades of FMR.

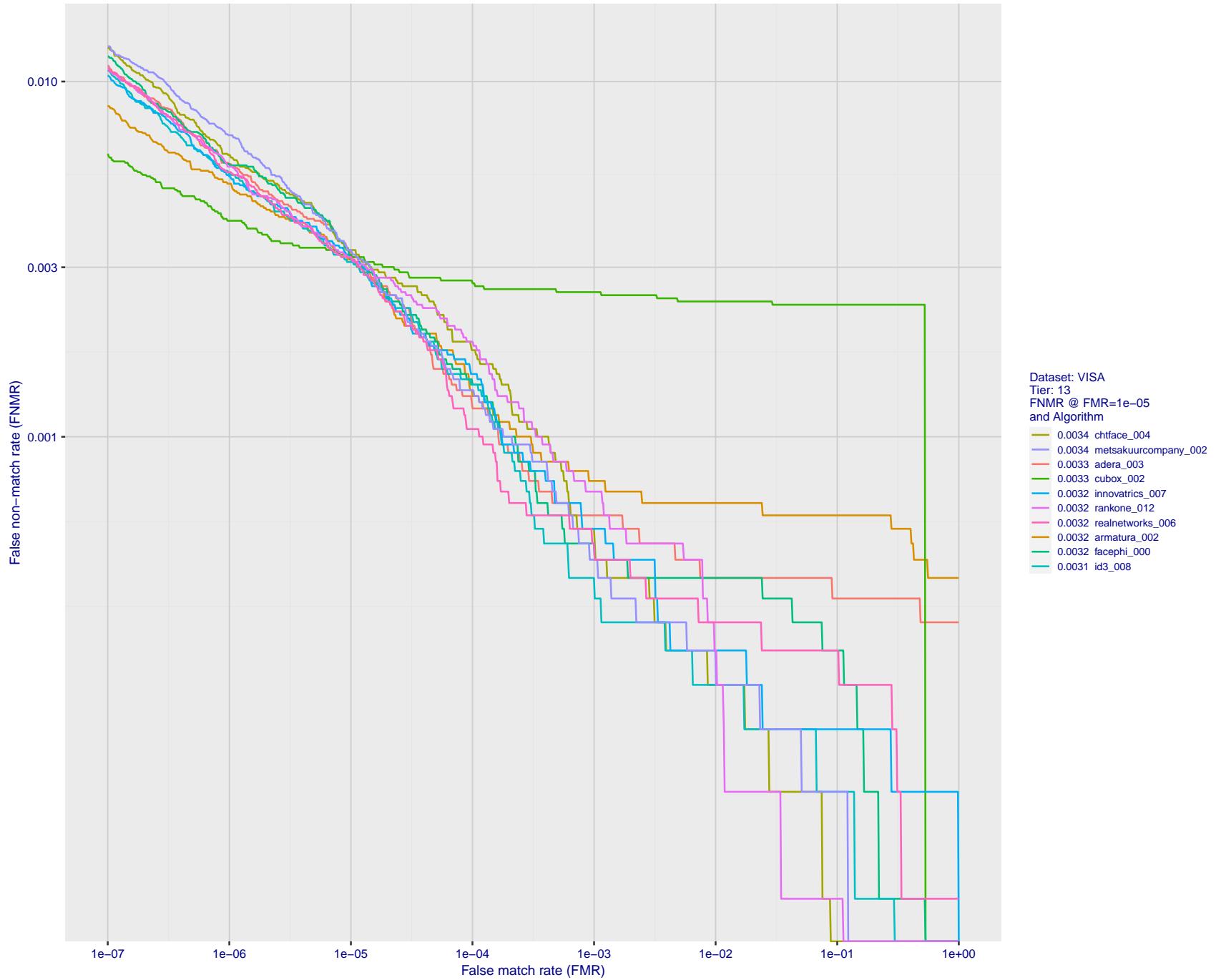


Figure 52: For the visa images, detection error tradeoff (DET) characteristics showing false non-match rate vs. false match rate plotted parametrically on threshold, T . The scales are logarithmic in order to show many decades of FMR.

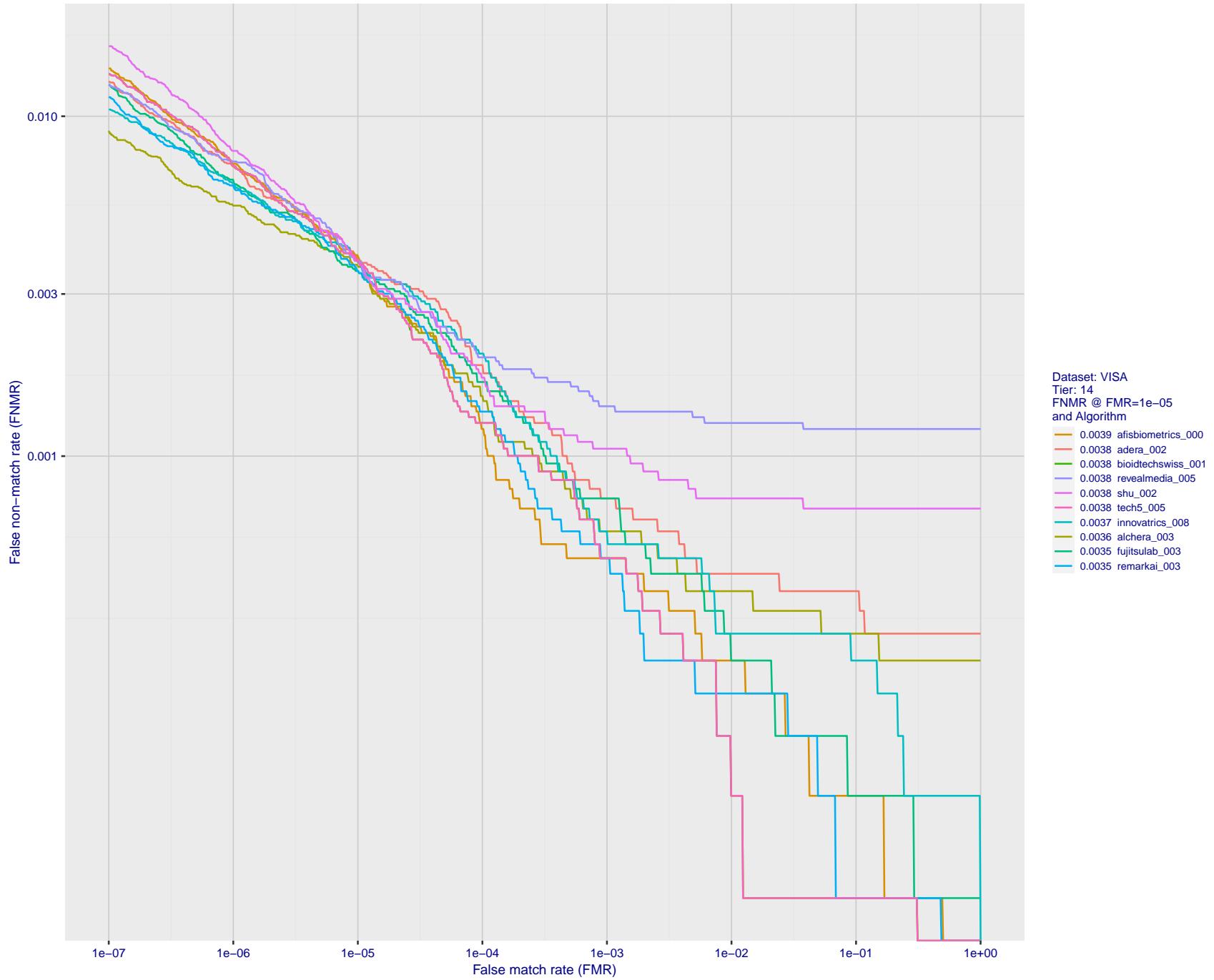


Figure 53: For the visa images, detection error tradeoff (DET) characteristics showing false non-match rate vs. false match rate plotted parametrically on threshold, T . The scales are logarithmic in order to show many decades of FMR.

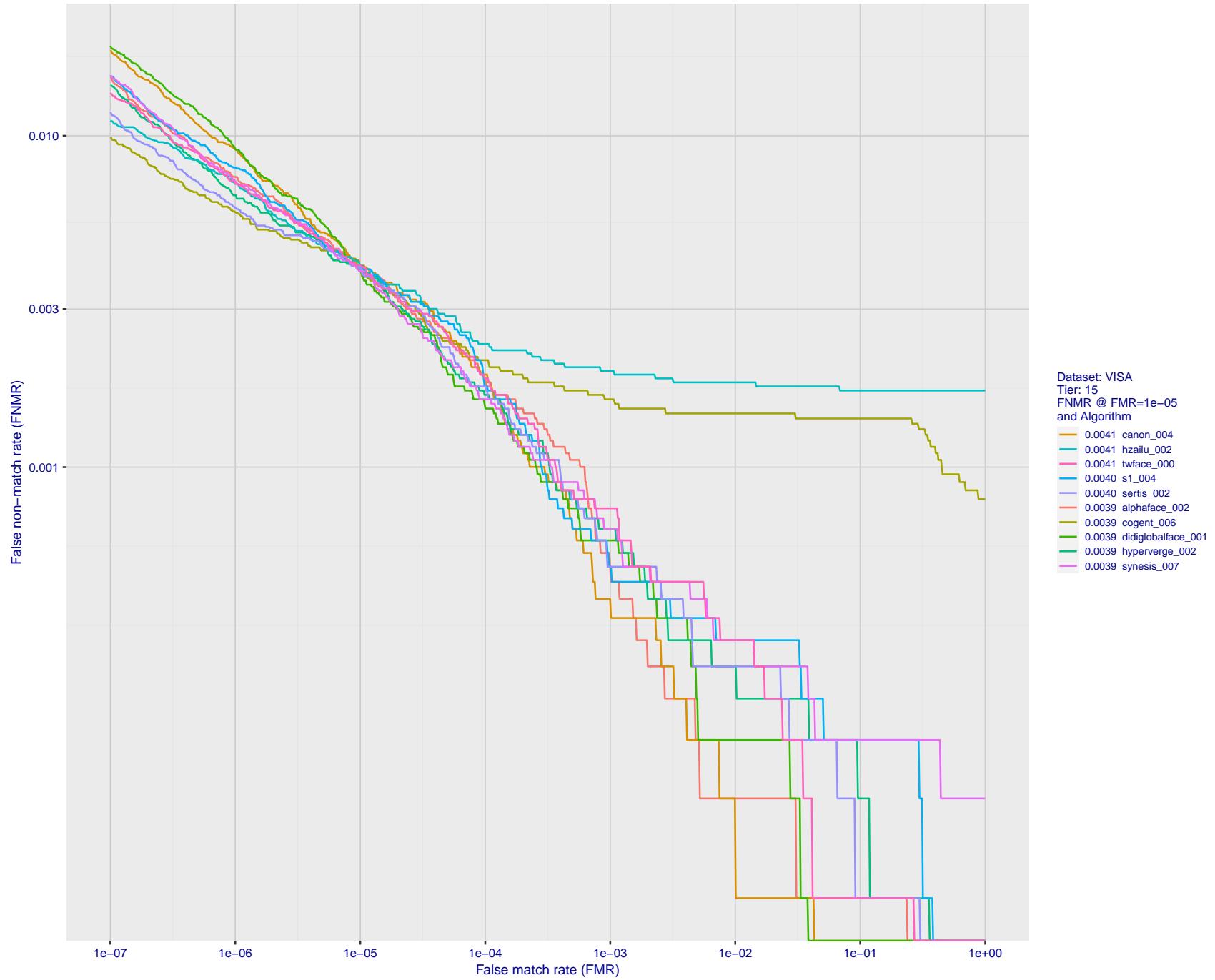


Figure 54: For the visa images, detection error tradeoff (DET) characteristics showing false non-match rate vs. false match rate plotted parametrically on threshold, T . The scales are logarithmic in order to show many decades of FMR.

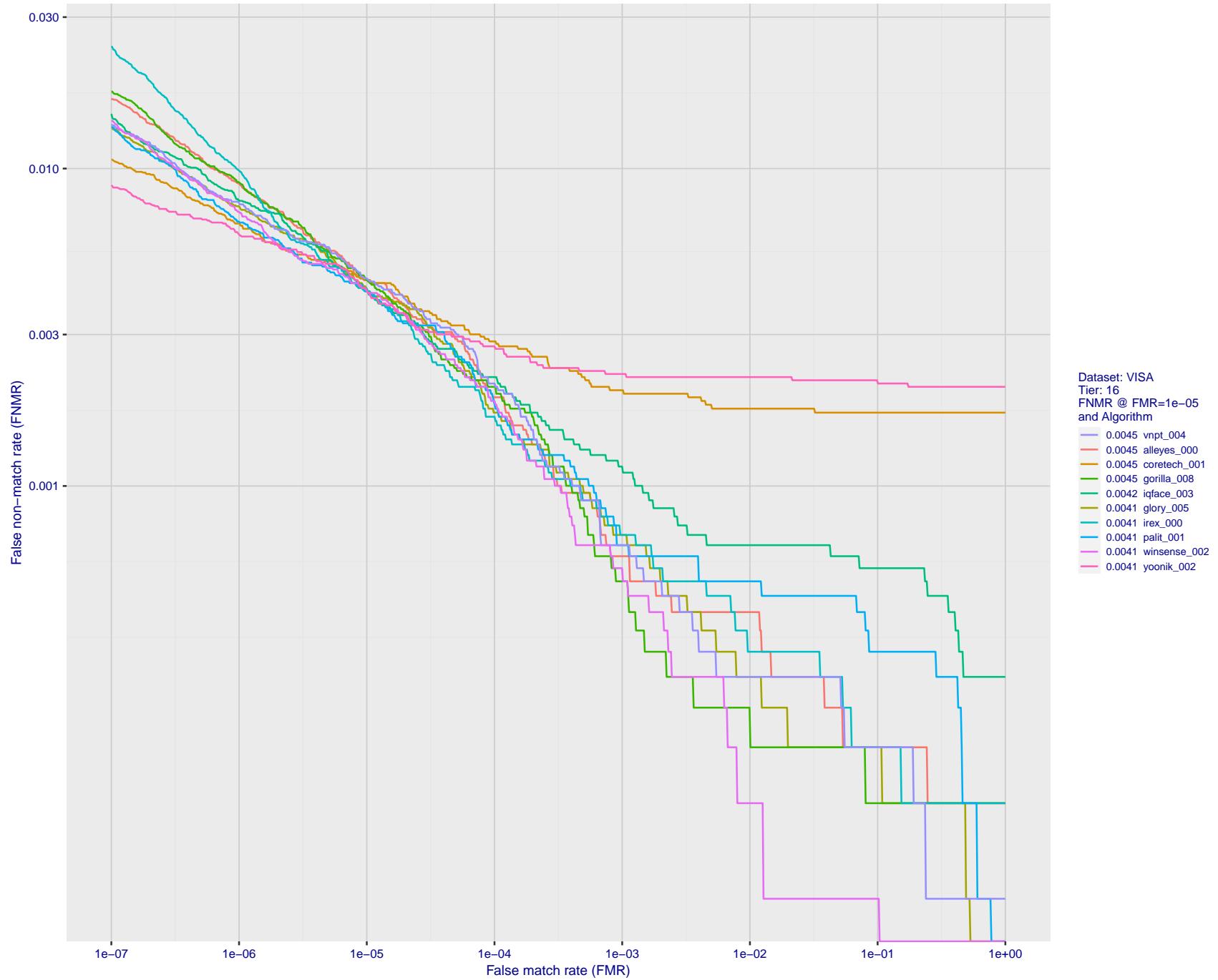


Figure 55: For the visa images, detection error tradeoff (DET) characteristics showing false non-match rate vs. false match rate plotted parametrically on threshold, T . The scales are logarithmic in order to show many decades of FMR.

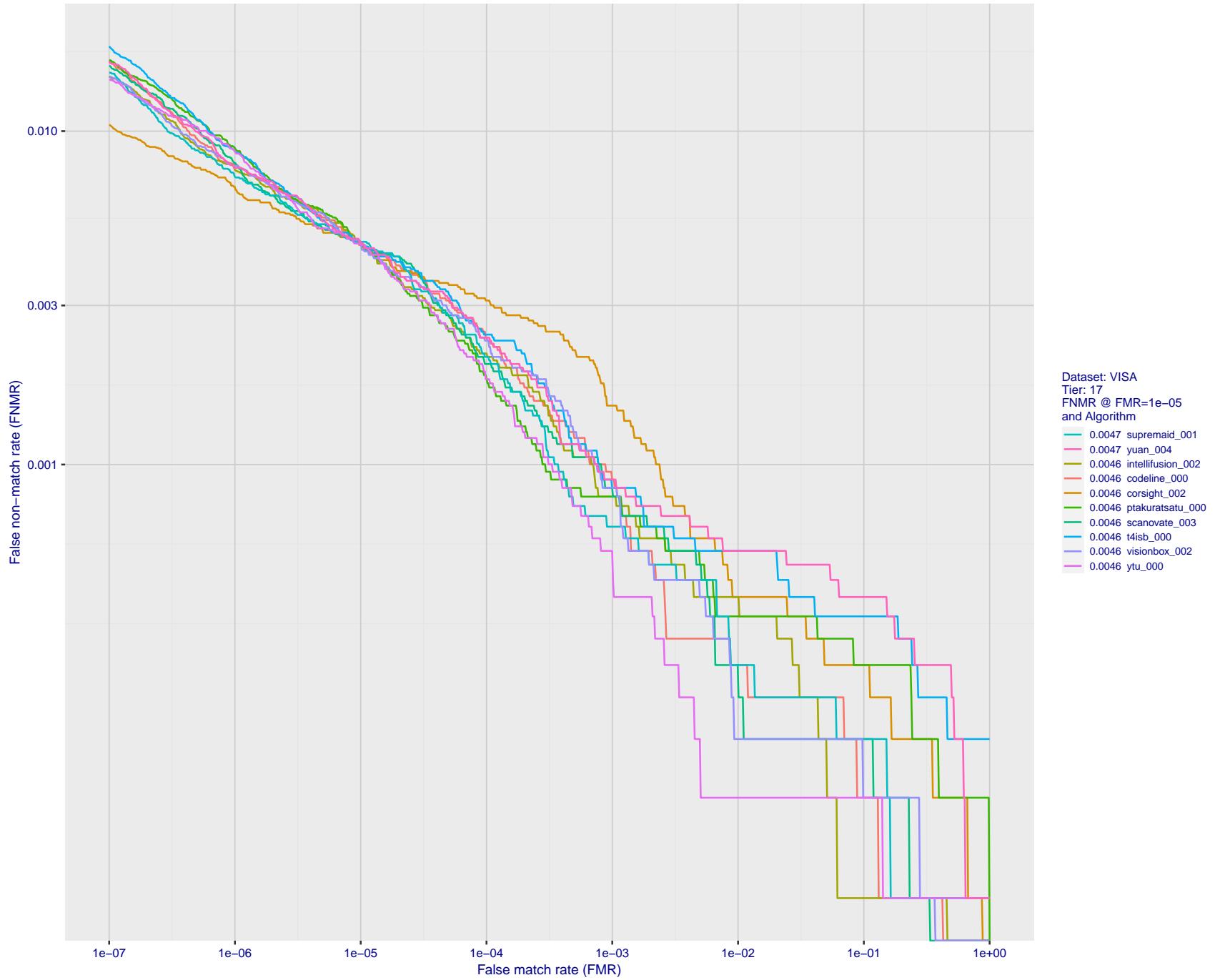


Figure 56: For the visa images, detection error tradeoff (DET) characteristics showing false non-match rate vs. false match rate plotted parametrically on threshold, T . The scales are logarithmic in order to show many decades of FMR.

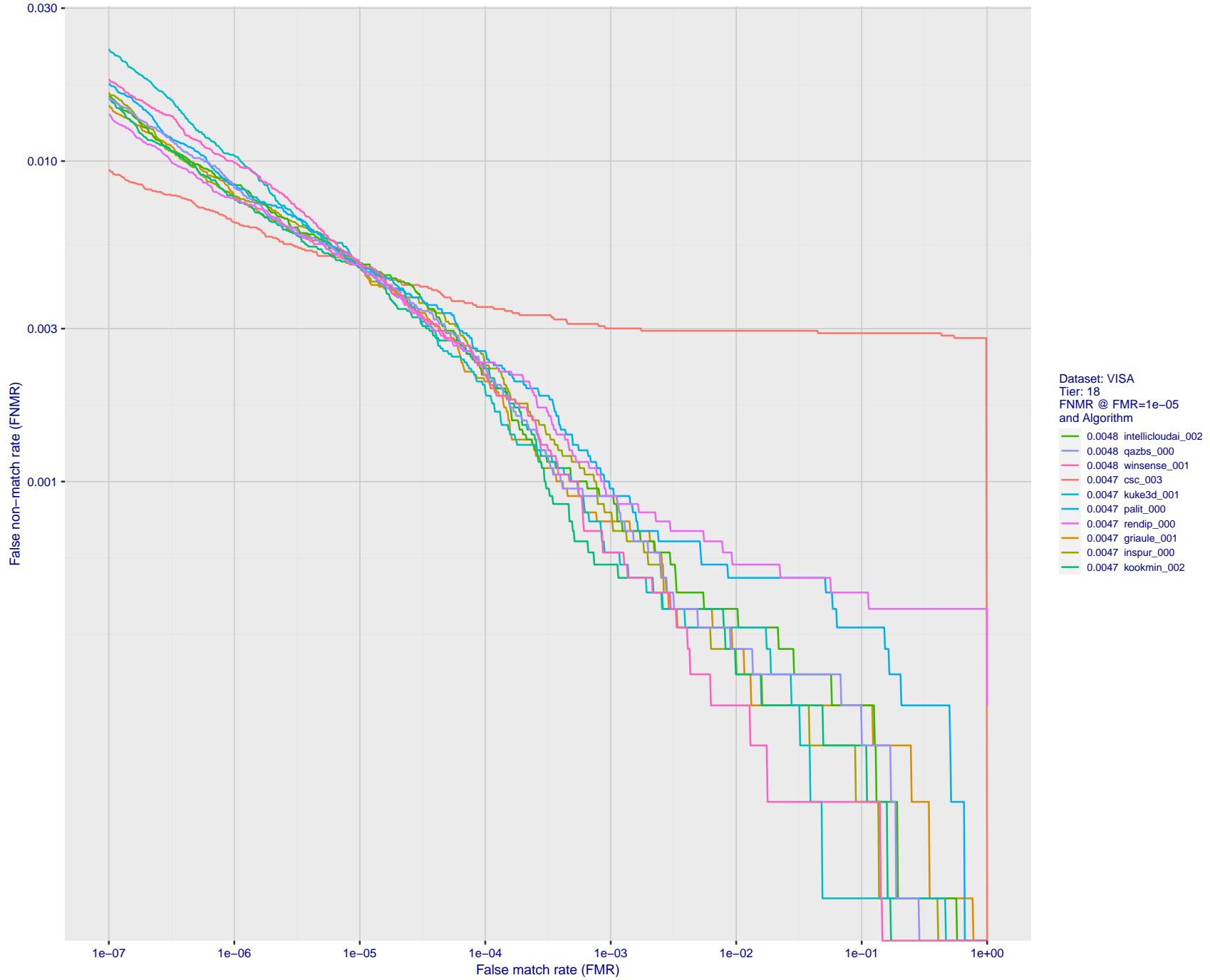


Figure 57: For the visa images, detection error tradeoff (DET) characteristics showing false non-match rate vs. false match rate plotted parametrically on threshold, T . The scales are logarithmic in order to show many decades of FMR.

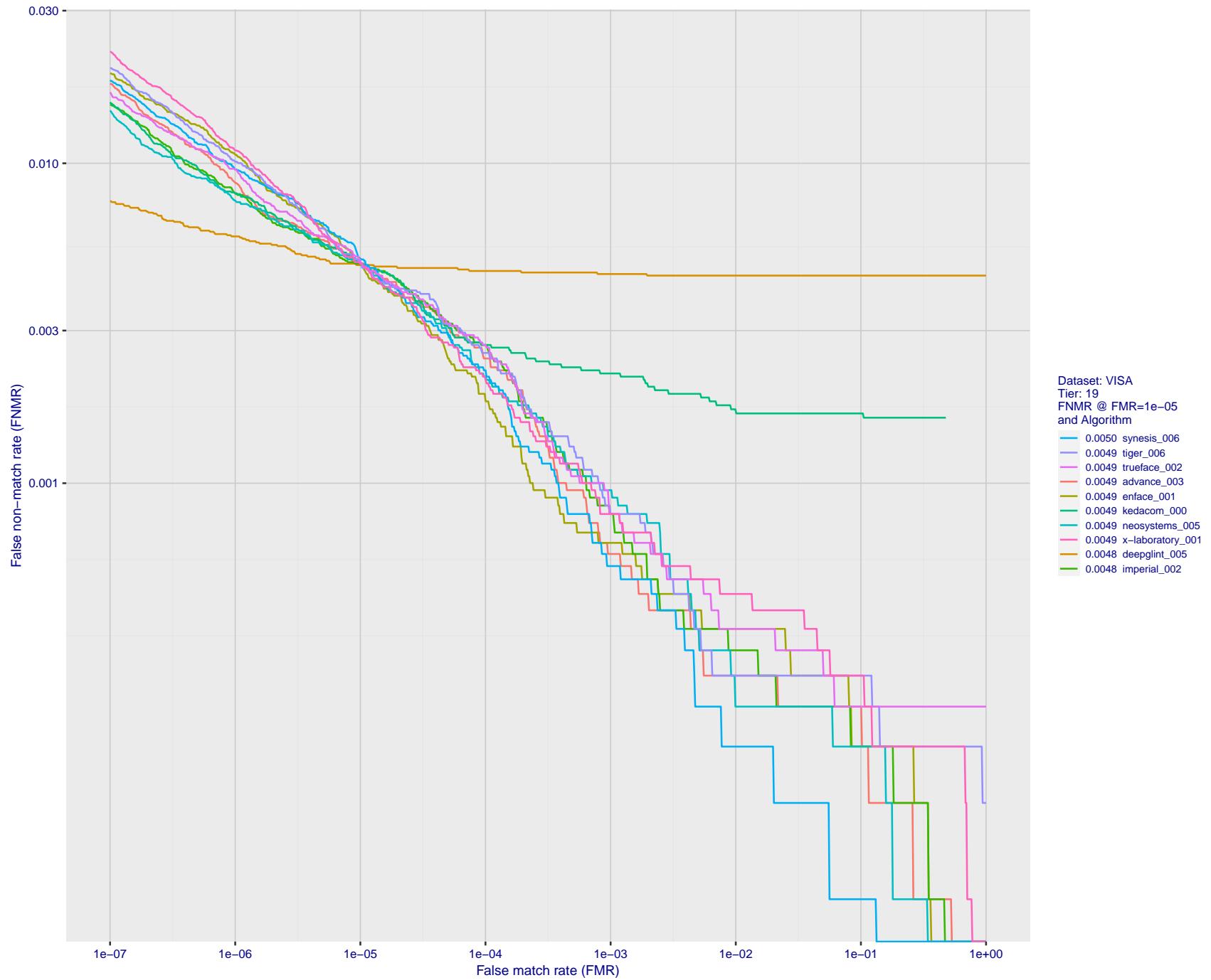


Figure 58: For the visa images, detection error tradeoff (DET) characteristics showing false non-match rate vs. false match rate plotted parametrically on threshold, T . The scales are logarithmic in order to show many decades of FMR.

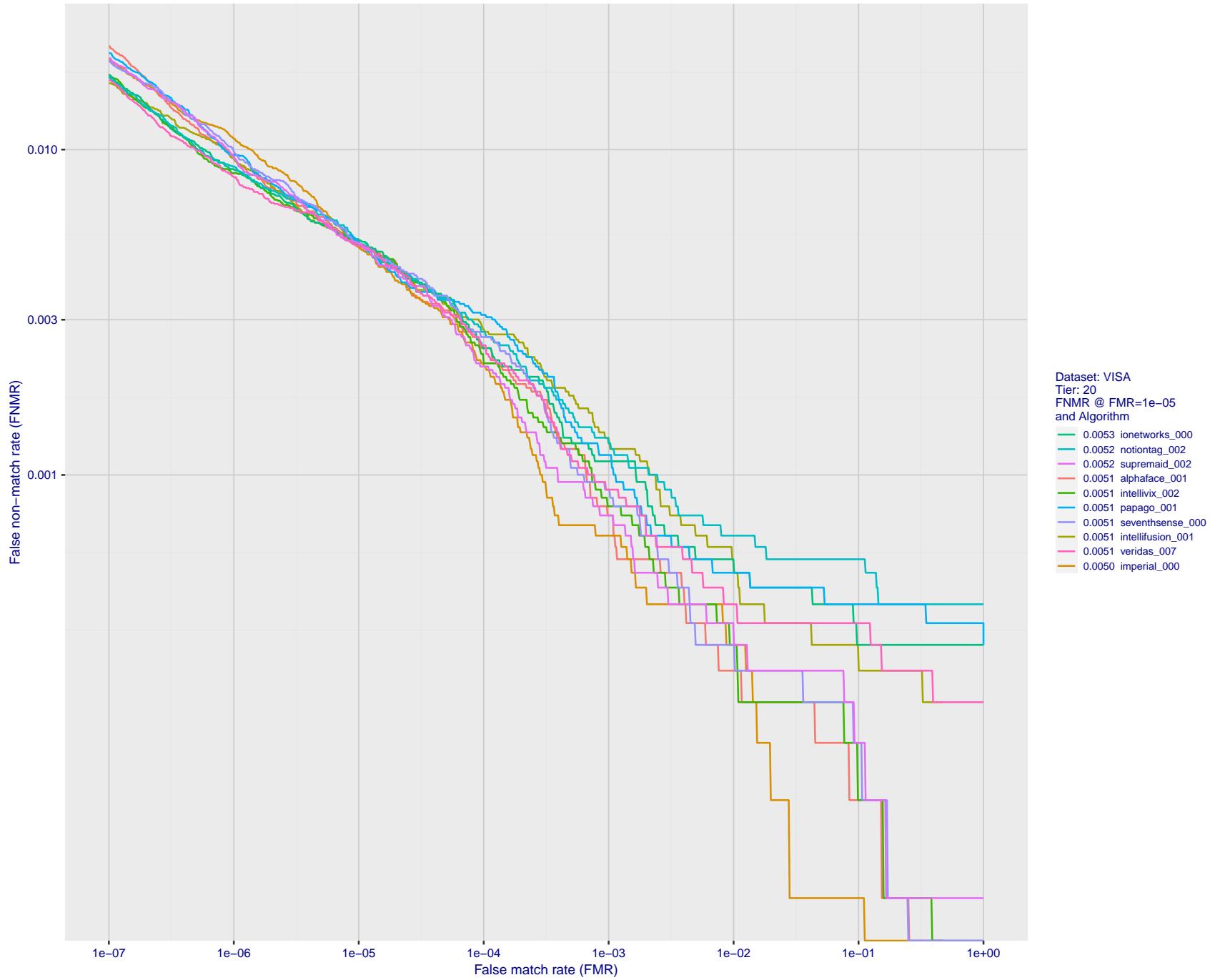


Figure 59: For the visa images, detection error tradeoff (DET) characteristics showing false non-match rate vs. false match rate plotted parametrically on threshold, T . The scales are logarithmic in order to show many decades of FMR.

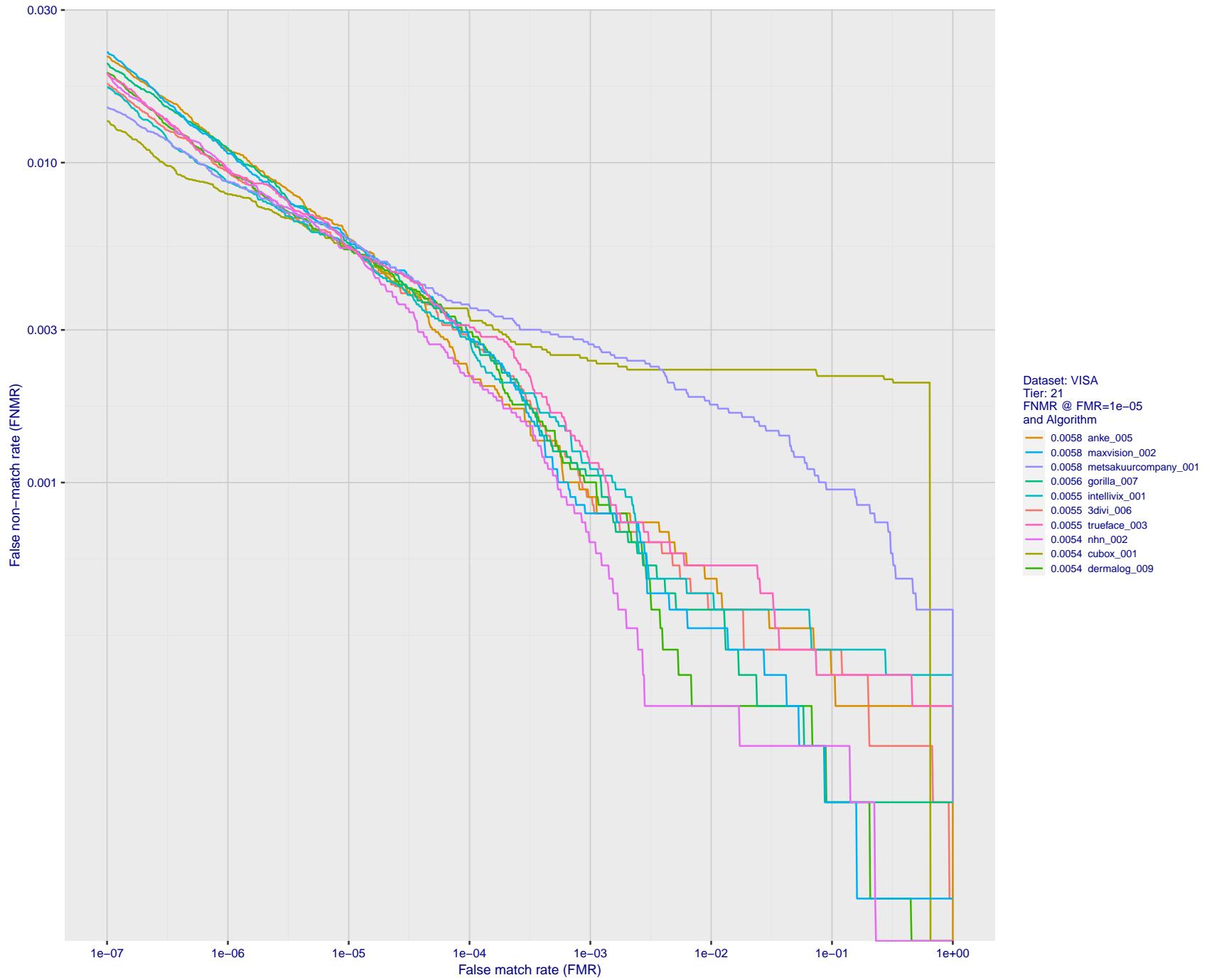


Figure 60: For the visa images, detection error tradeoff (DET) characteristics showing false non-match rate vs. false match rate plotted parametrically on threshold, T . The scales are logarithmic in order to show many decades of FMR.

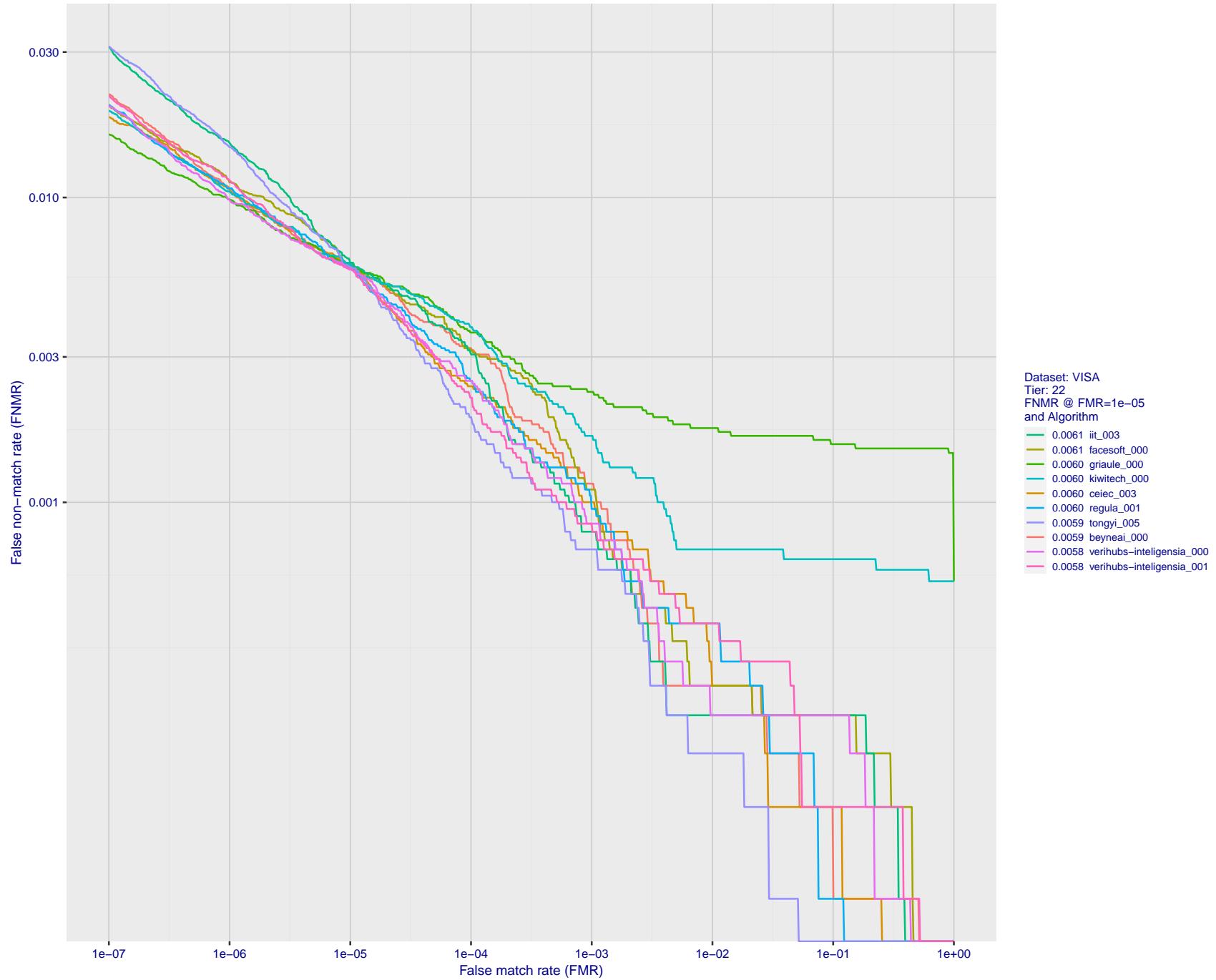


Figure 61: For the visa images, detection error tradeoff (DET) characteristics showing false non-match rate vs. false match rate plotted parametrically on threshold, T . The scales are logarithmic in order to show many decades of FMR.

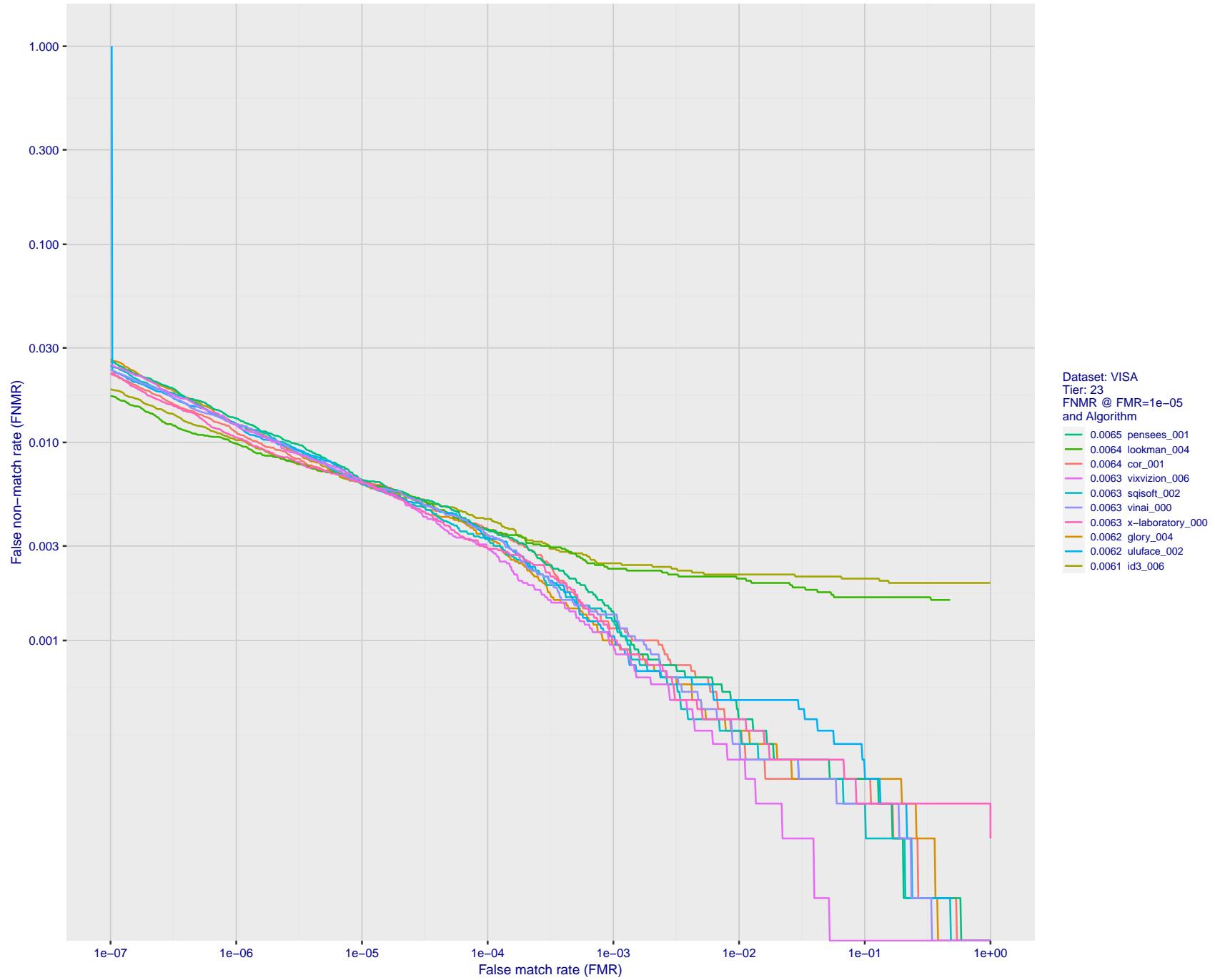


Figure 62: For the visa images, detection error tradeoff (DET) characteristics showing false non-match rate vs. false match rate plotted parametrically on threshold, T . The scales are logarithmic in order to show many decades of FMR.

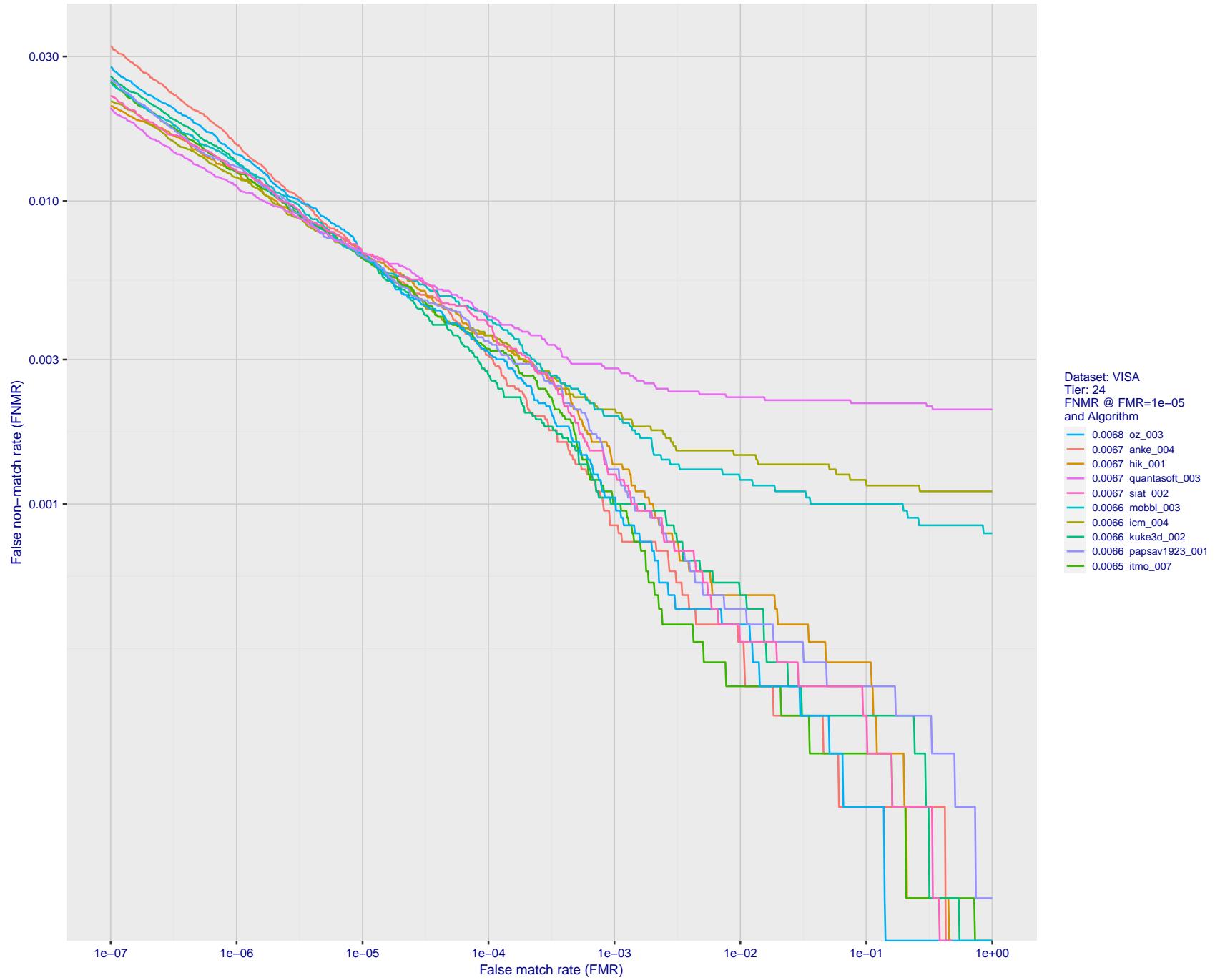


Figure 63: For the visa images, detection error tradeoff (DET) characteristics showing false non-match rate vs. false match rate plotted parametrically on threshold, T . The scales are logarithmic in order to show many decades of FMR.

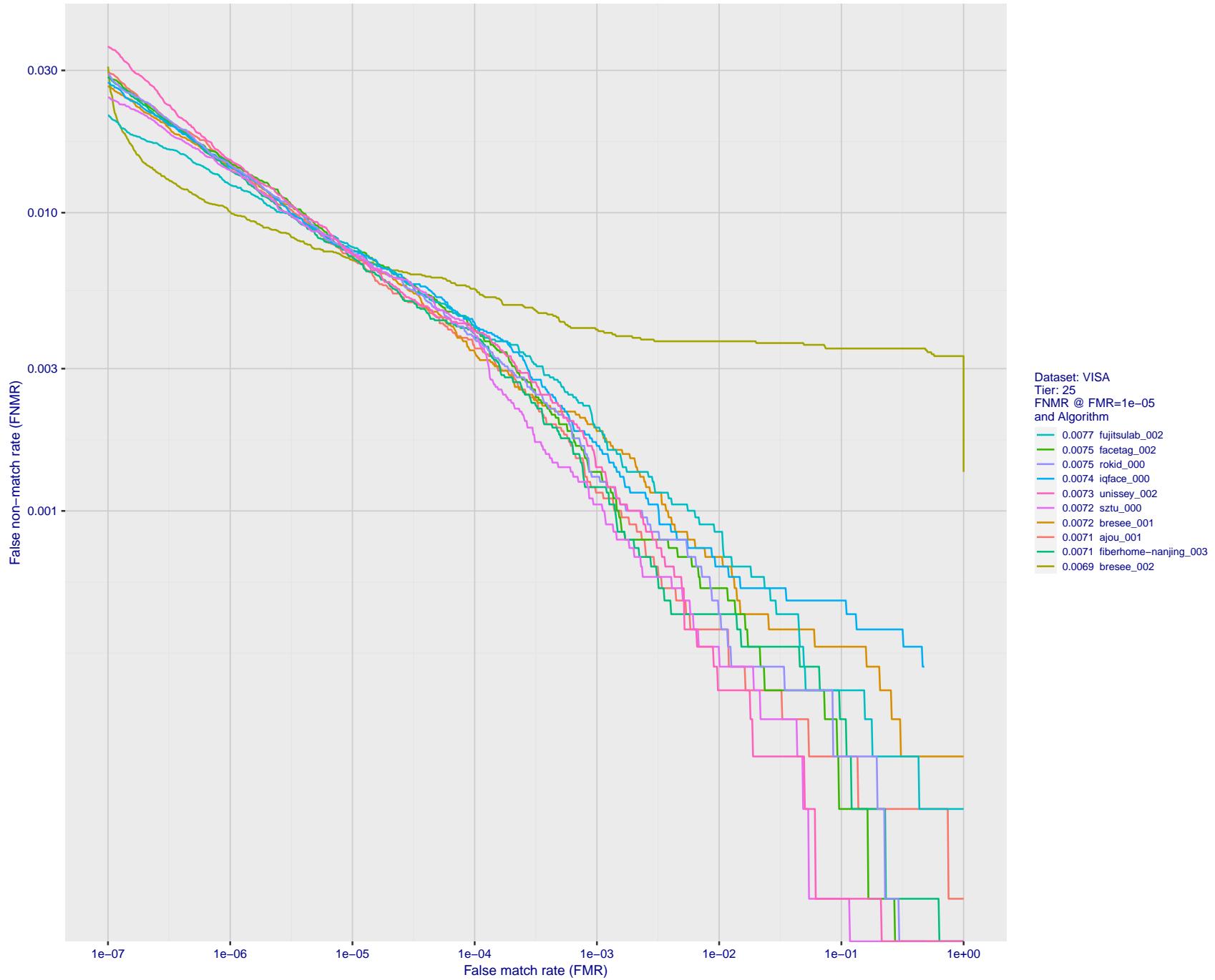


Figure 64: For the visa images, detection error tradeoff (DET) characteristics showing false non-match rate vs. false match rate plotted parametrically on threshold, T . The scales are logarithmic in order to show many decades of FMR.

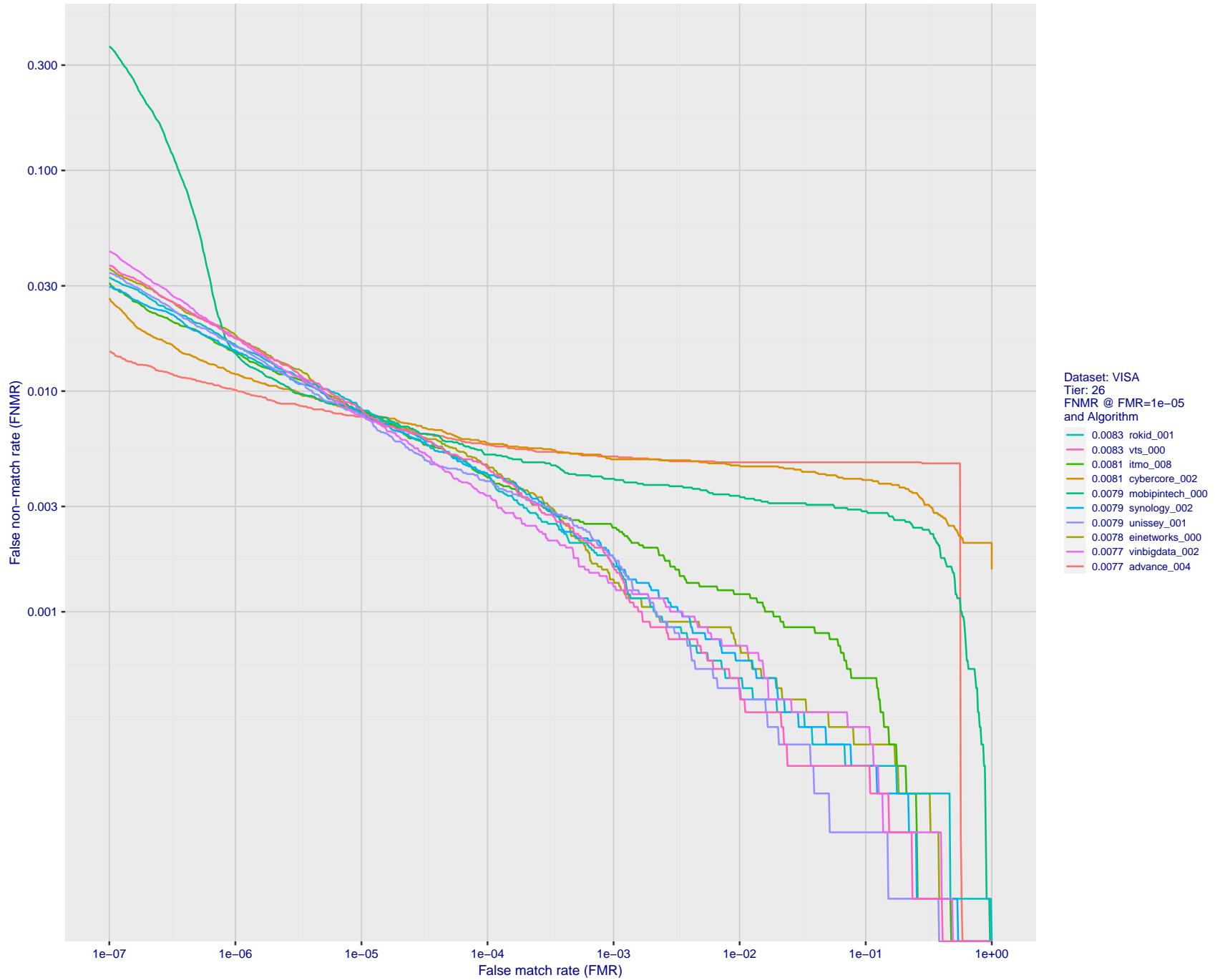


Figure 65: For the visa images, detection error tradeoff (DET) characteristics showing false non-match rate vs. false match rate plotted parametrically on threshold, T . The scales are logarithmic in order to show many decades of FMR.

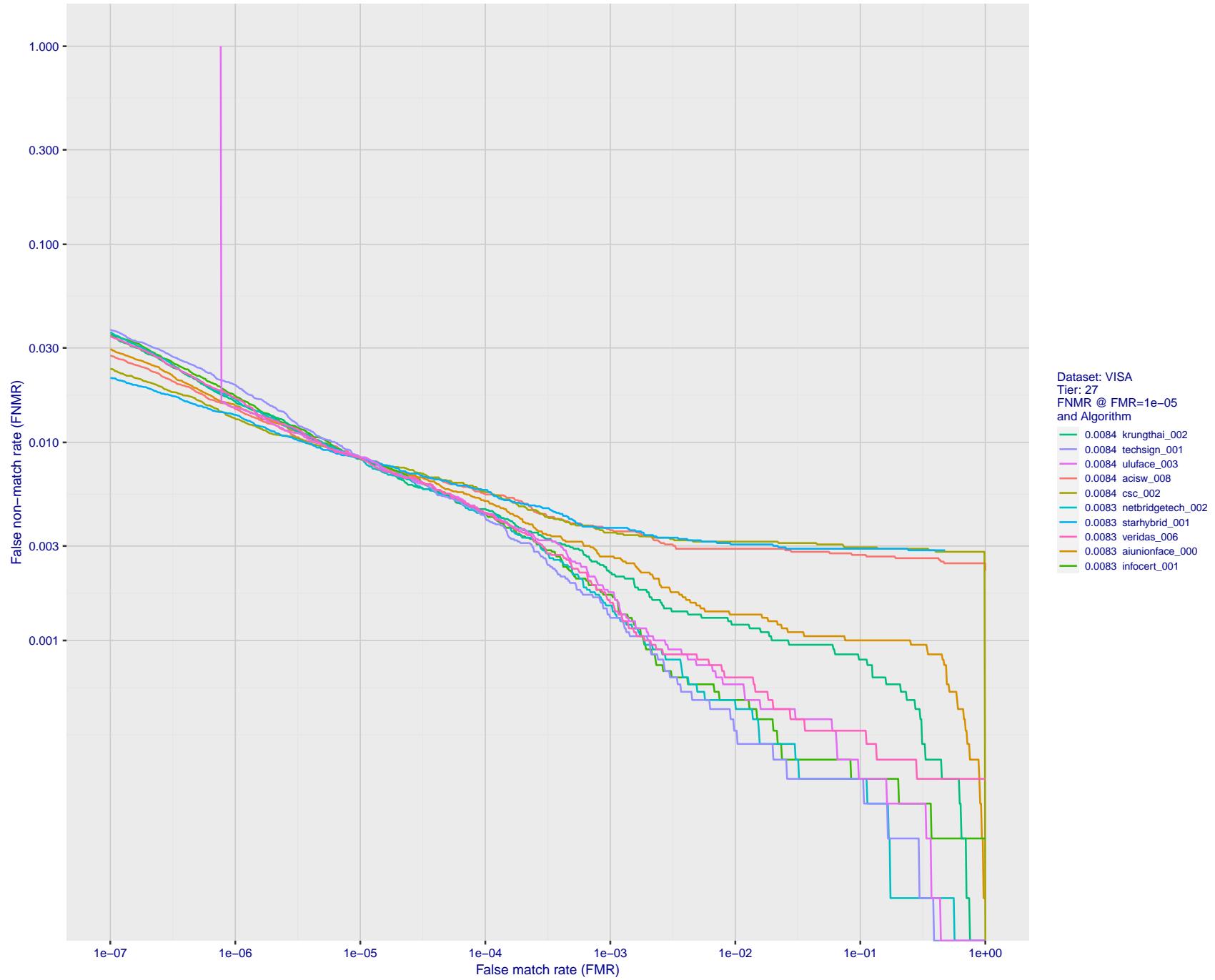


Figure 66: For the visa images, detection error tradeoff (DET) characteristics showing false non-match rate vs. false match rate plotted parametrically on threshold, T . The scales are logarithmic in order to show many decades of FMR.

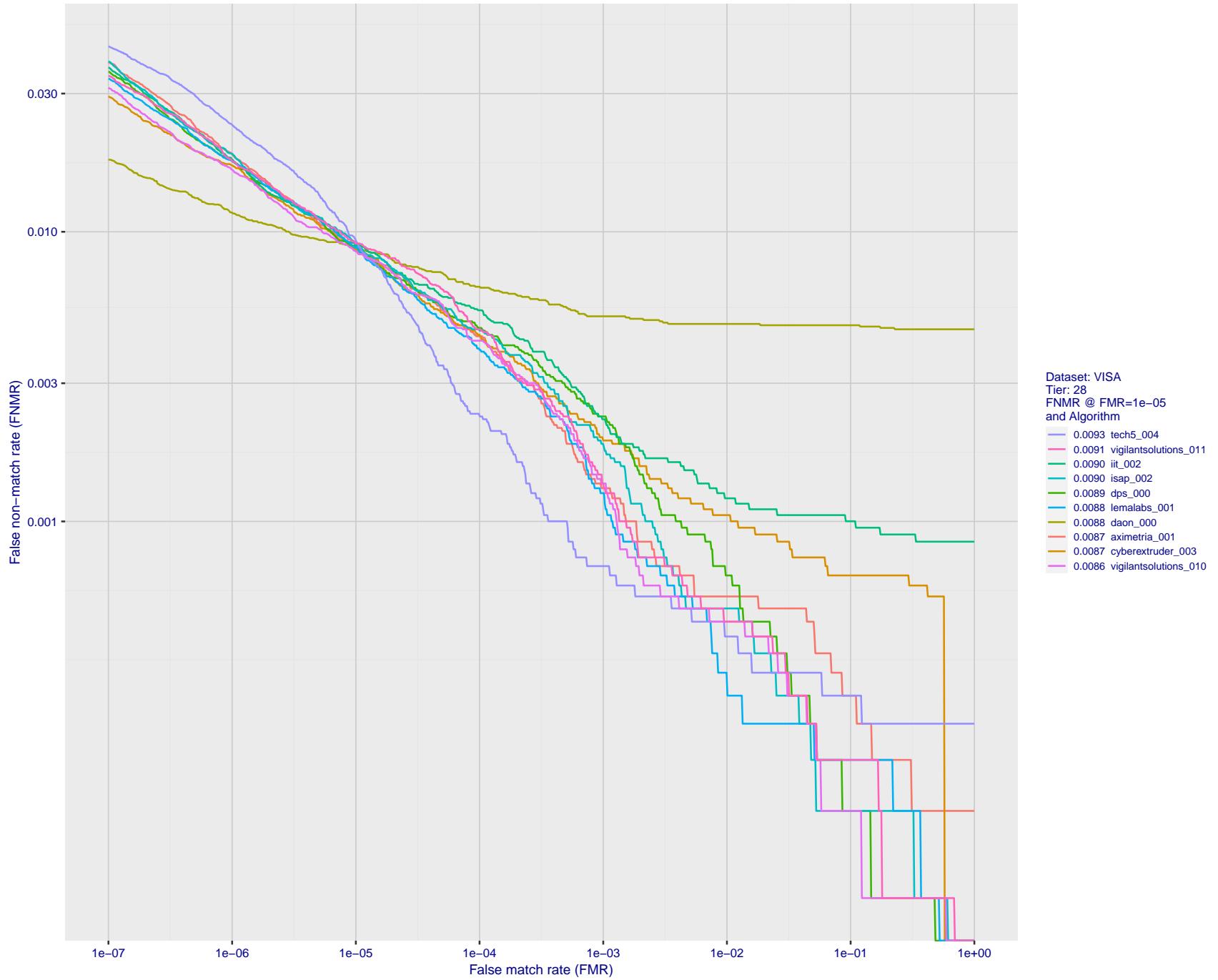


Figure 67: For the visa images, detection error tradeoff (DET) characteristics showing false non-match rate vs. false match rate plotted parametrically on threshold, T . The scales are logarithmic in order to show many decades of FMR.

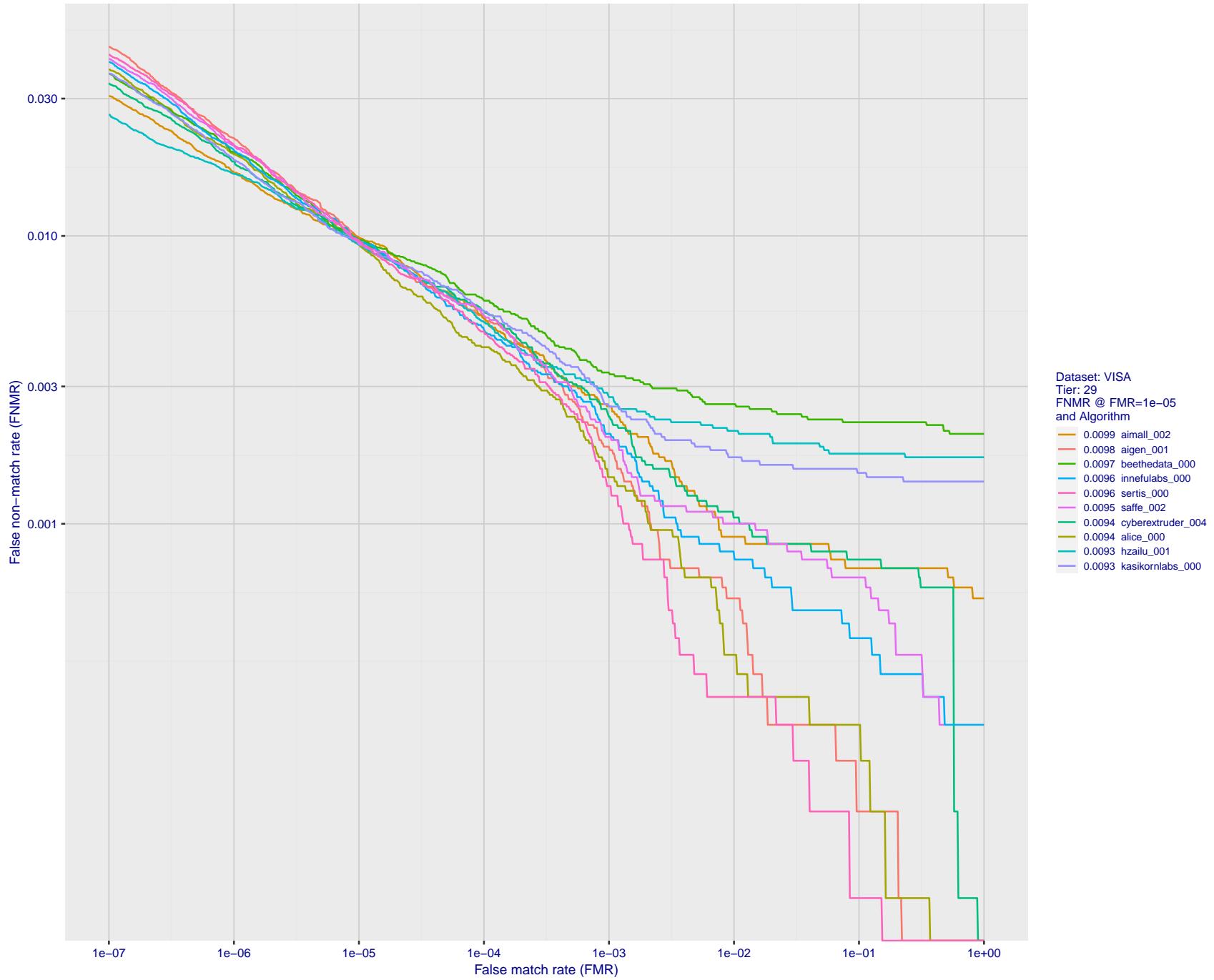


Figure 68: For the visa images, detection error tradeoff (DET) characteristics showing false non-match rate vs. false match rate plotted parametrically on threshold, T . The scales are logarithmic in order to show many decades of FMR.

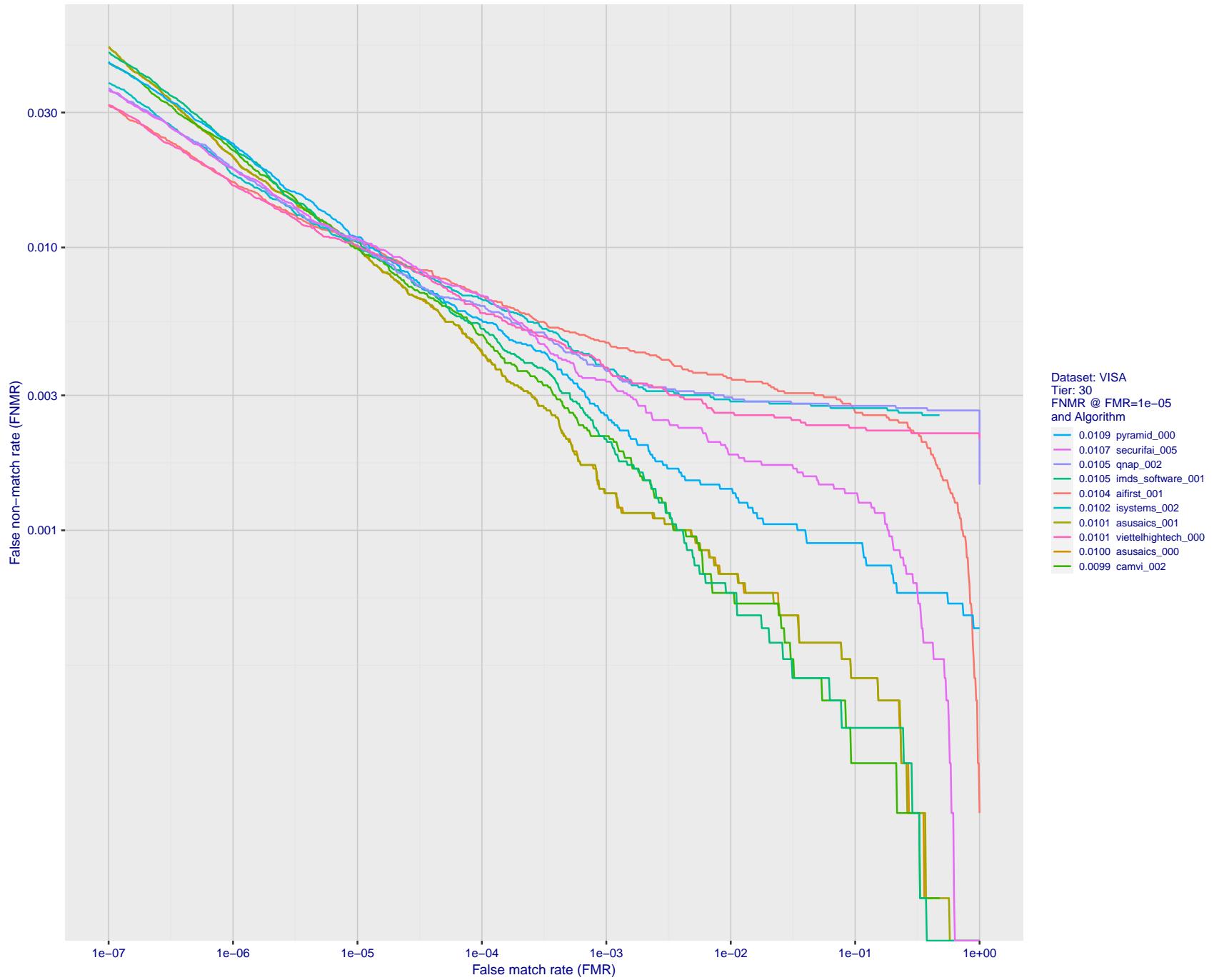


Figure 69: For the visa images, detection error tradeoff (DET) characteristics showing false non-match rate vs. false match rate plotted parametrically on threshold, T . The scales are logarithmic in order to show many decades of FMR.

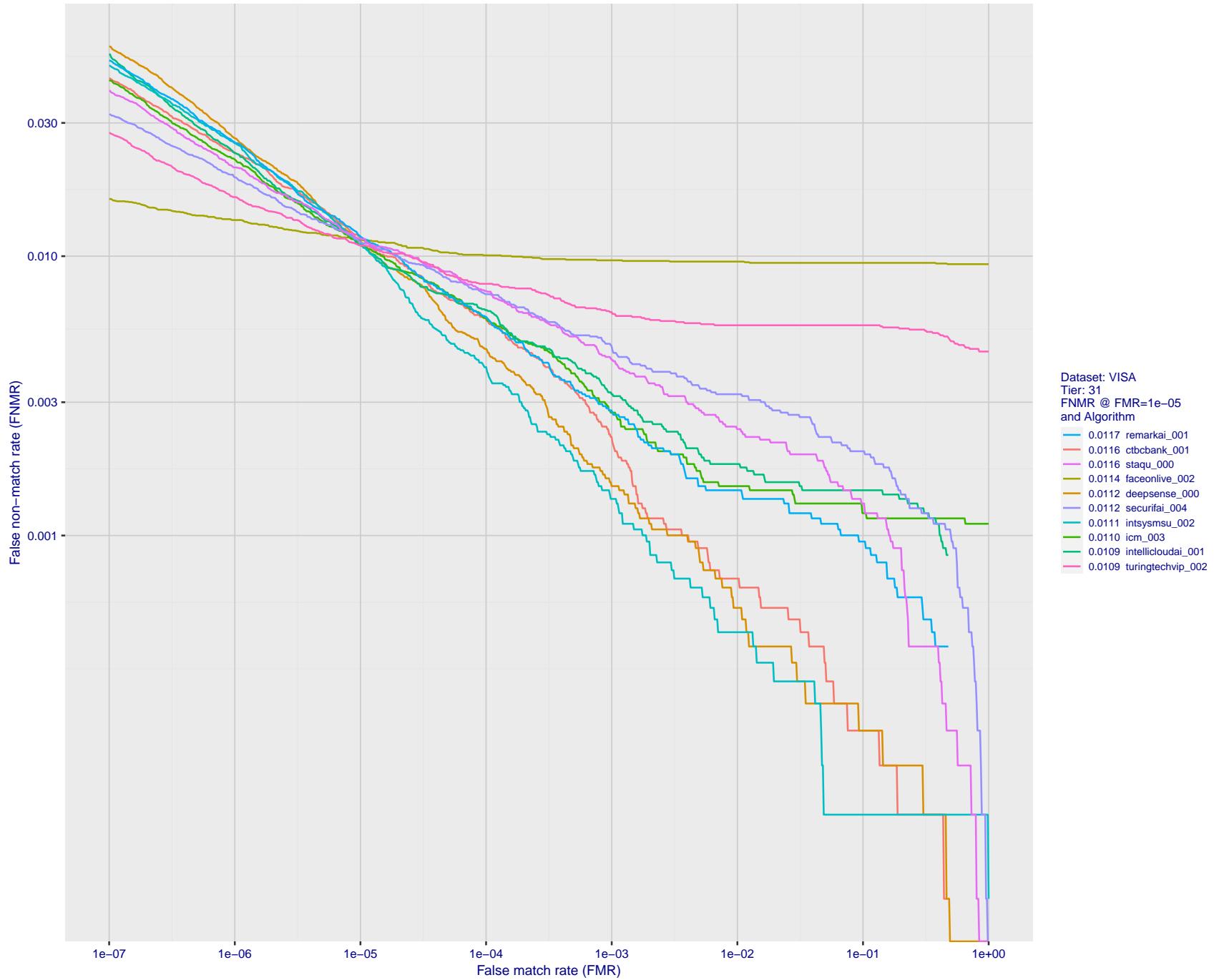


Figure 70: For the visa images, detection error tradeoff (DET) characteristics showing false non-match rate vs. false match rate plotted parametrically on threshold, T . The scales are logarithmic in order to show many decades of FMR.

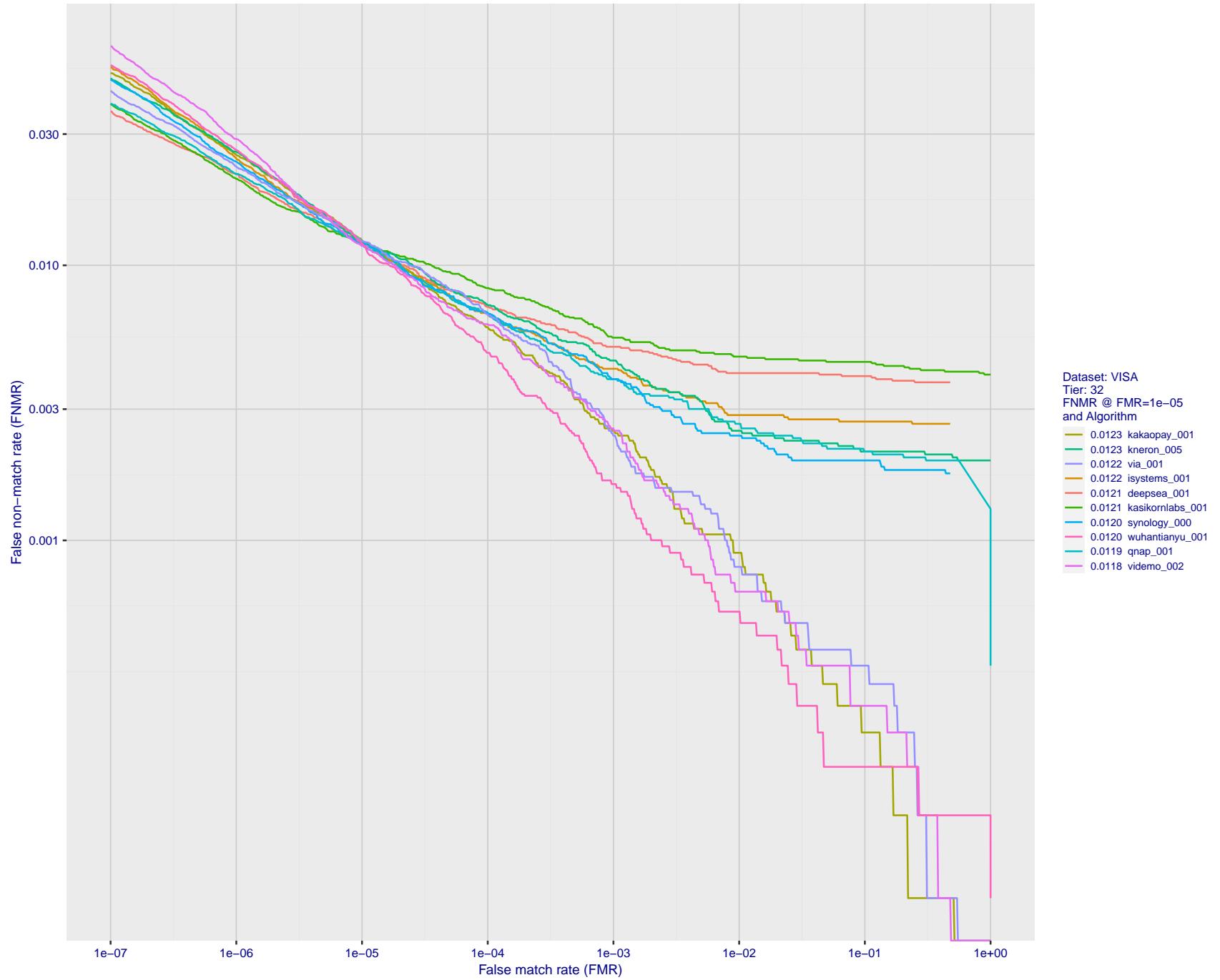


Figure 71: For the visa images, detection error tradeoff (DET) characteristics showing false non-match rate vs. false match rate plotted parametrically on threshold, T . The scales are logarithmic in order to show many decades of FMR.

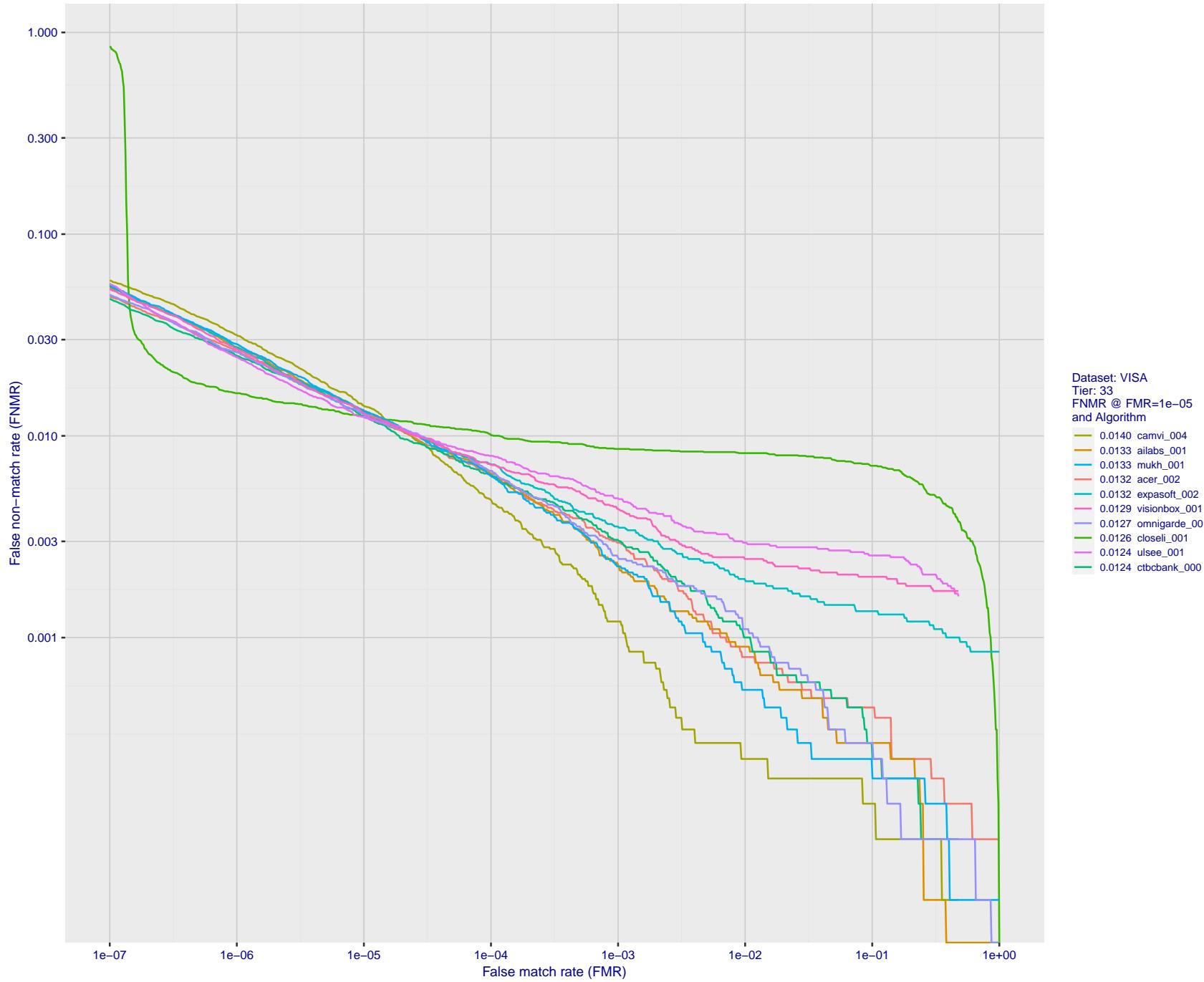


Figure 72: For the visa images, detection error tradeoff (DET) characteristics showing false non-match rate vs. false match rate plotted parametrically on threshold, T . The scales are logarithmic in order to show many decades of FMR.

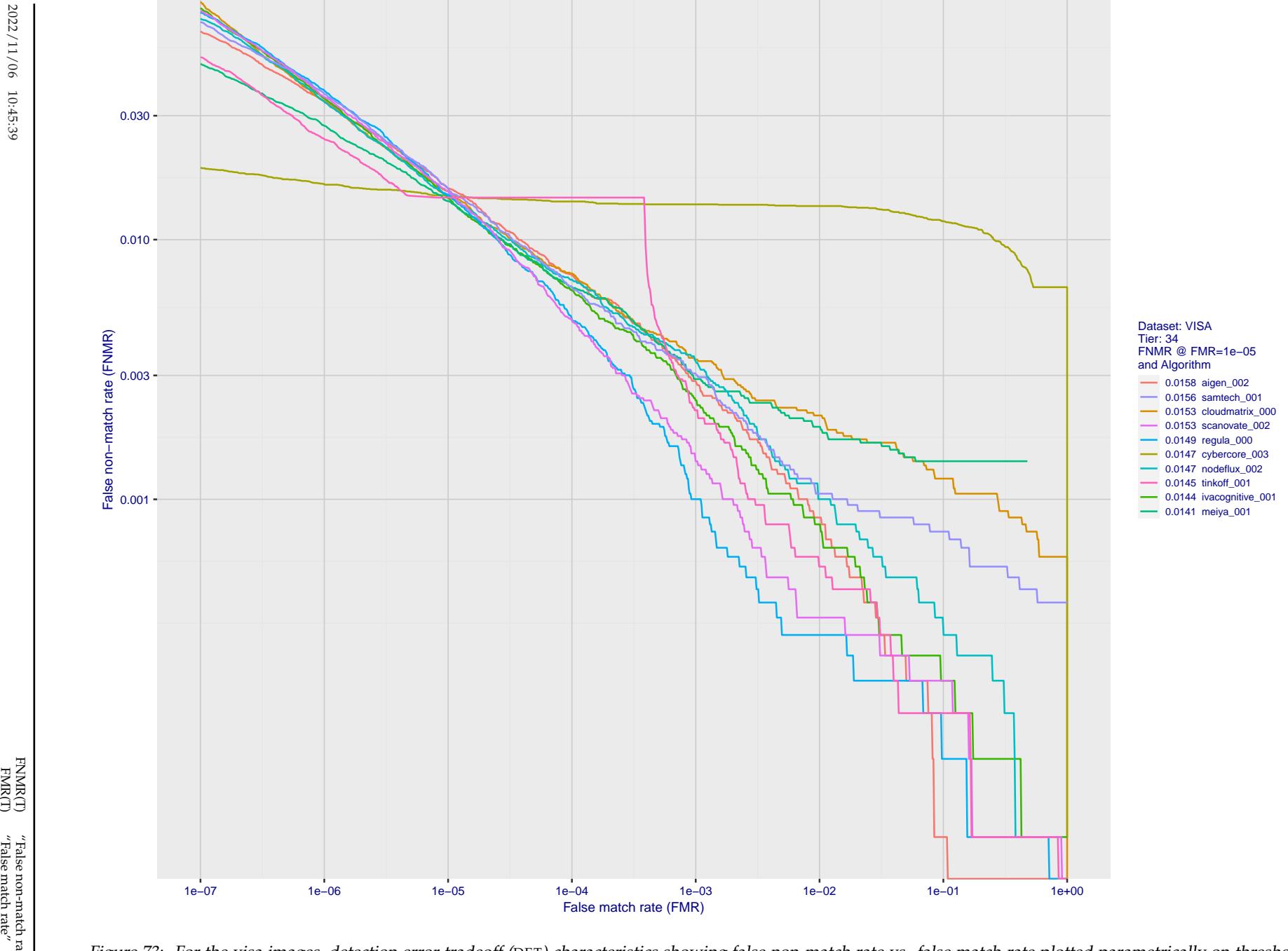


Figure 73: For the visa images, detection error tradeoff (DET) characteristics showing false non-match rate vs. false match rate plotted parametrically on threshold, T . The scales are logarithmic in order to show many decades of FMR.

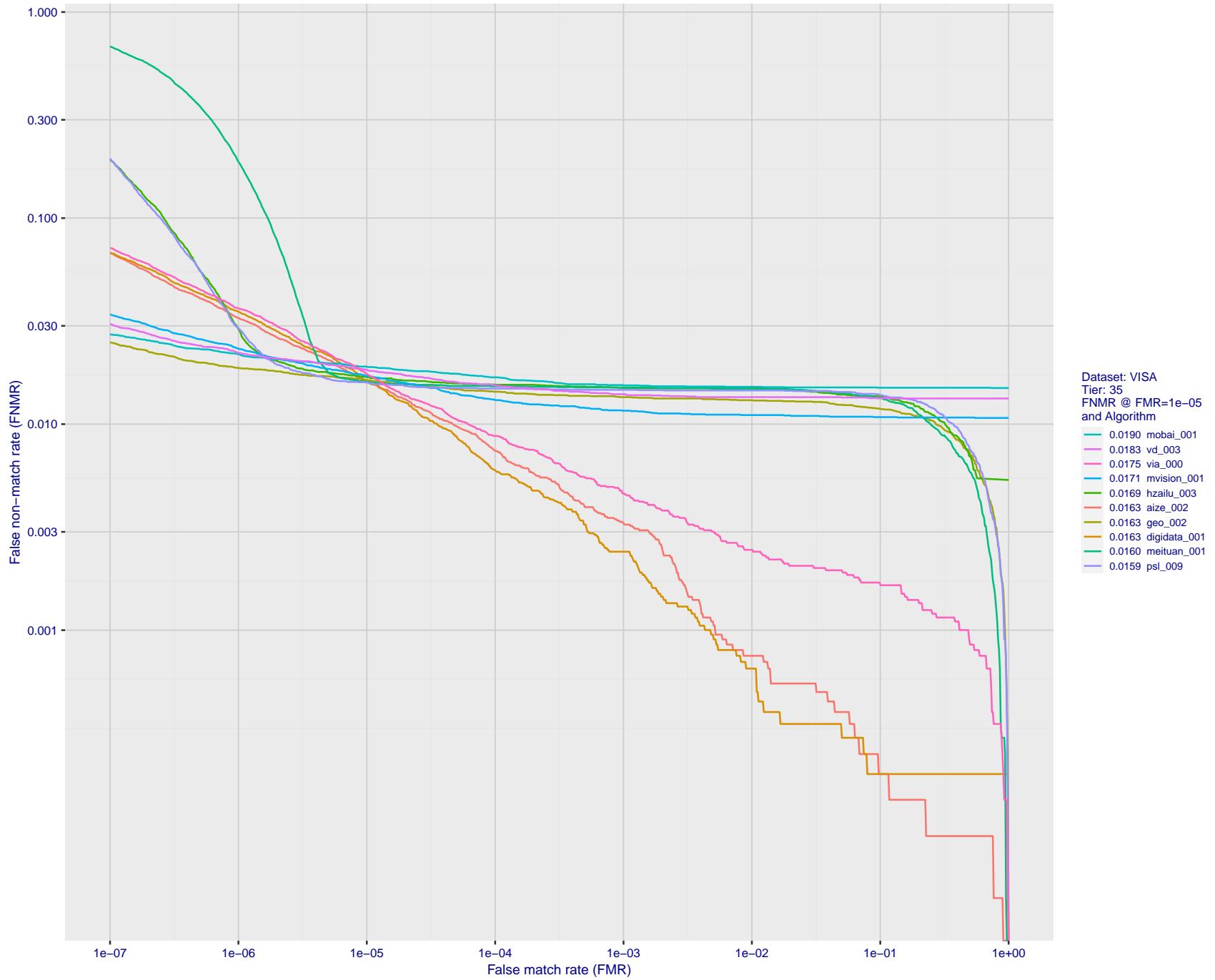


Figure 74: For the visa images, detection error tradeoff (DET) characteristics showing false non-match rate vs. false match rate plotted parametrically on threshold, T . The scales are logarithmic in order to show many decades of FMR.

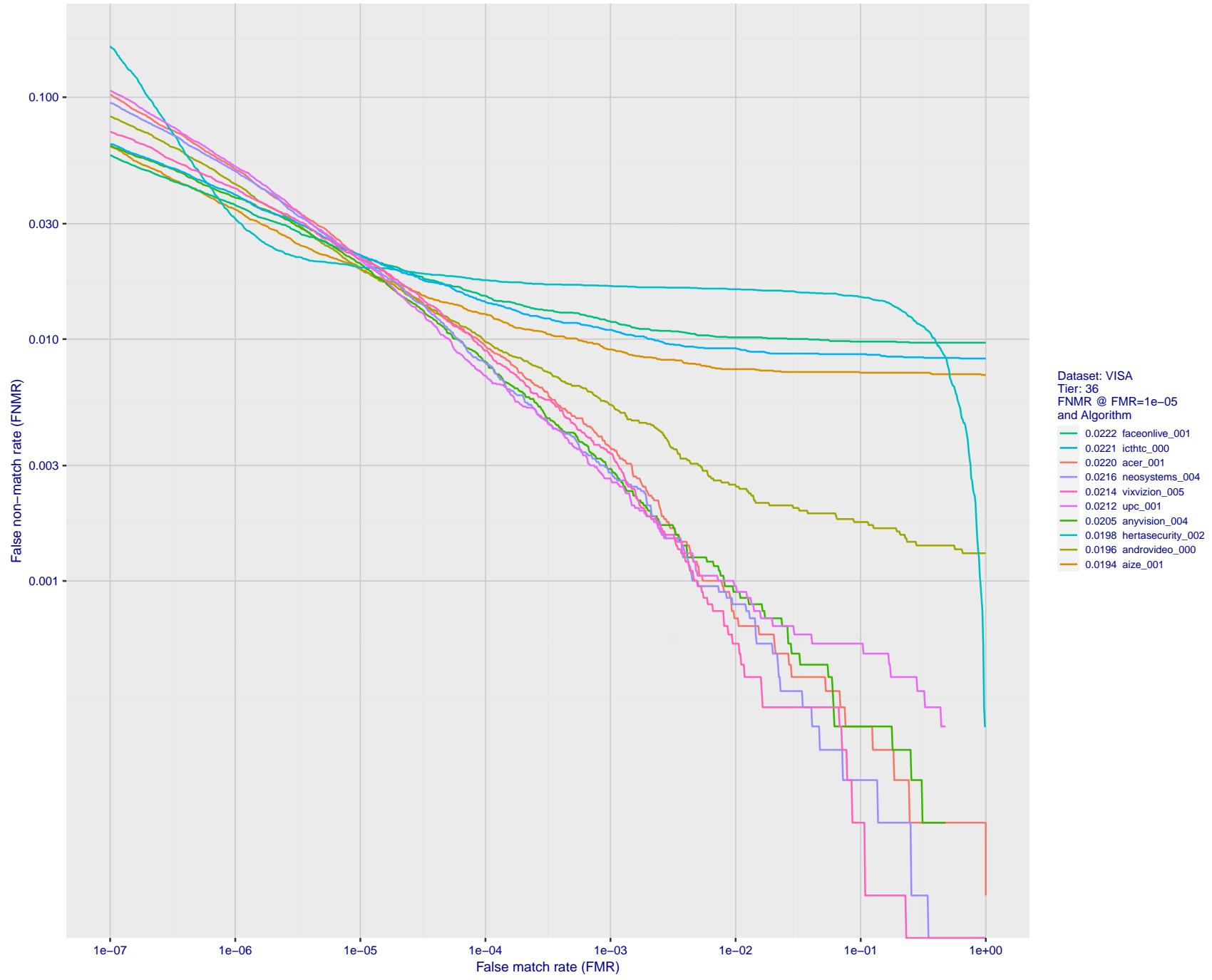


Figure 75: For the visa images, detection error tradeoff (DET) characteristics showing false non-match rate vs. false match rate plotted parametrically on threshold, T . The scales are logarithmic in order to show many decades of FMR.

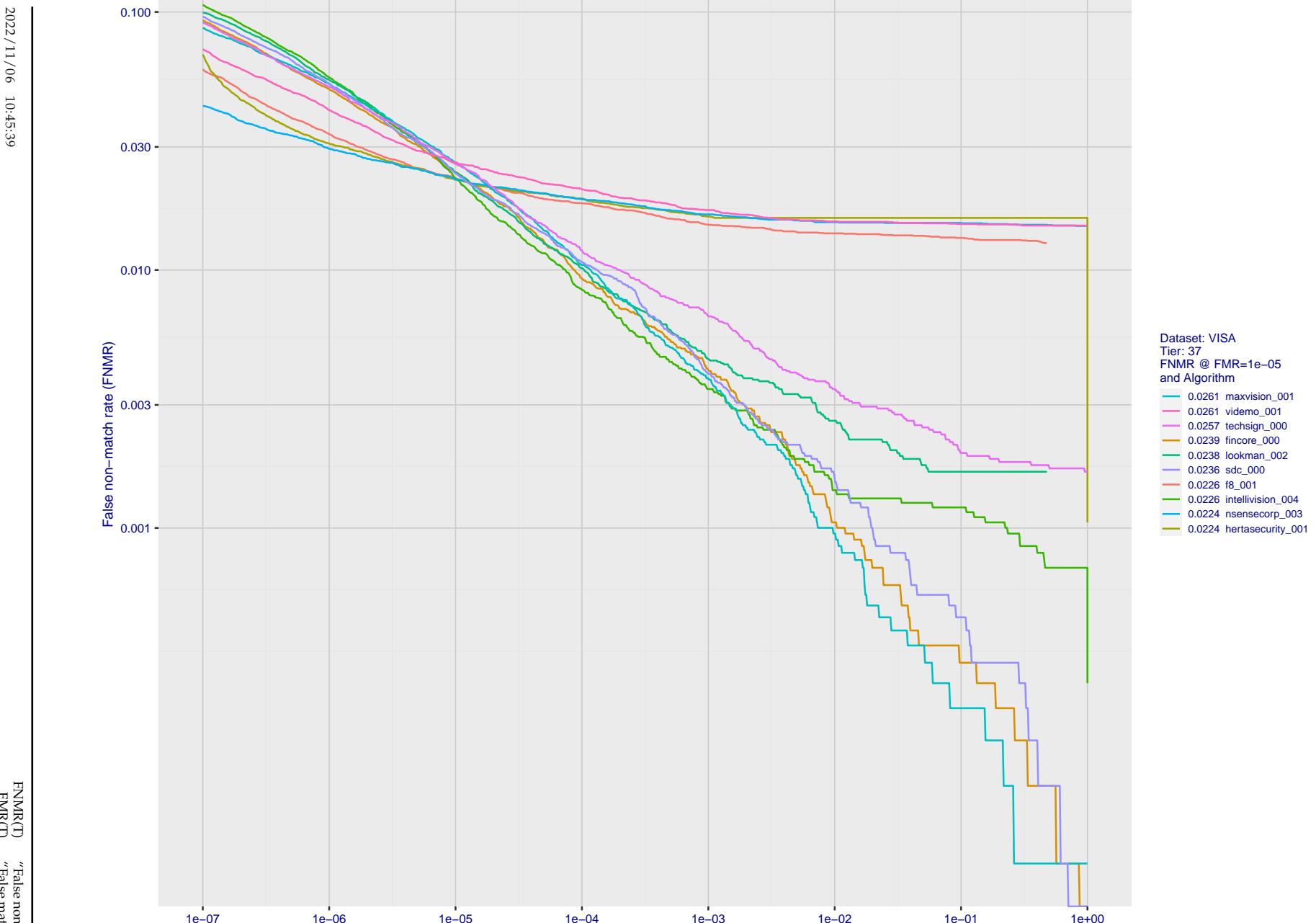


Figure 76: For the visa images, detection error tradeoff (DET) characteristics showing false non-match rate vs. false match rate plotted parametrically on threshold, T . The scales are logarithmic in order to show many decades of FMR.

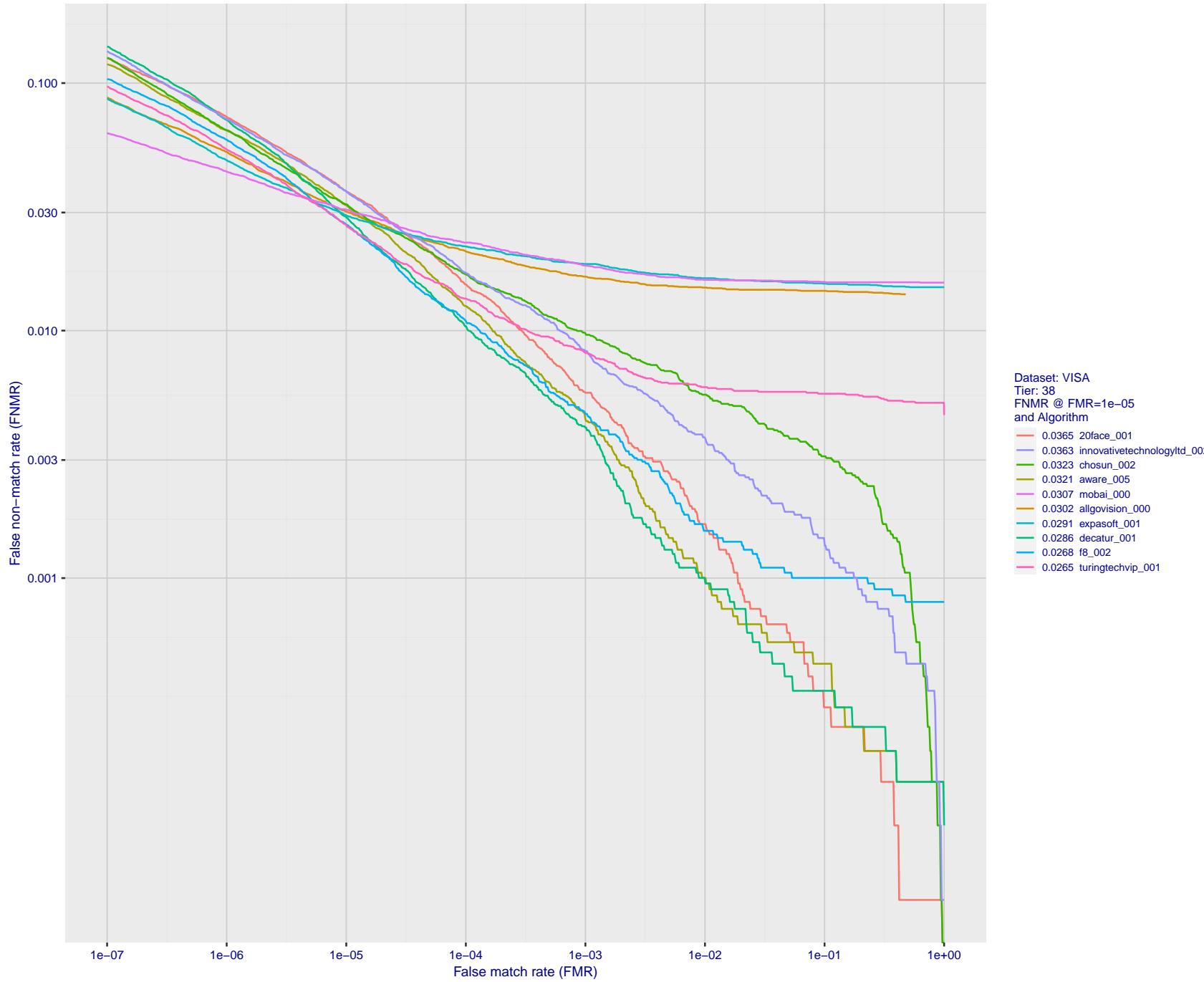


Figure 77: For the visa images, detection error tradeoff (DET) characteristics showing false non-match rate vs. false match rate plotted parametrically on threshold, T . The scales are logarithmic in order to show many decades of FMR.

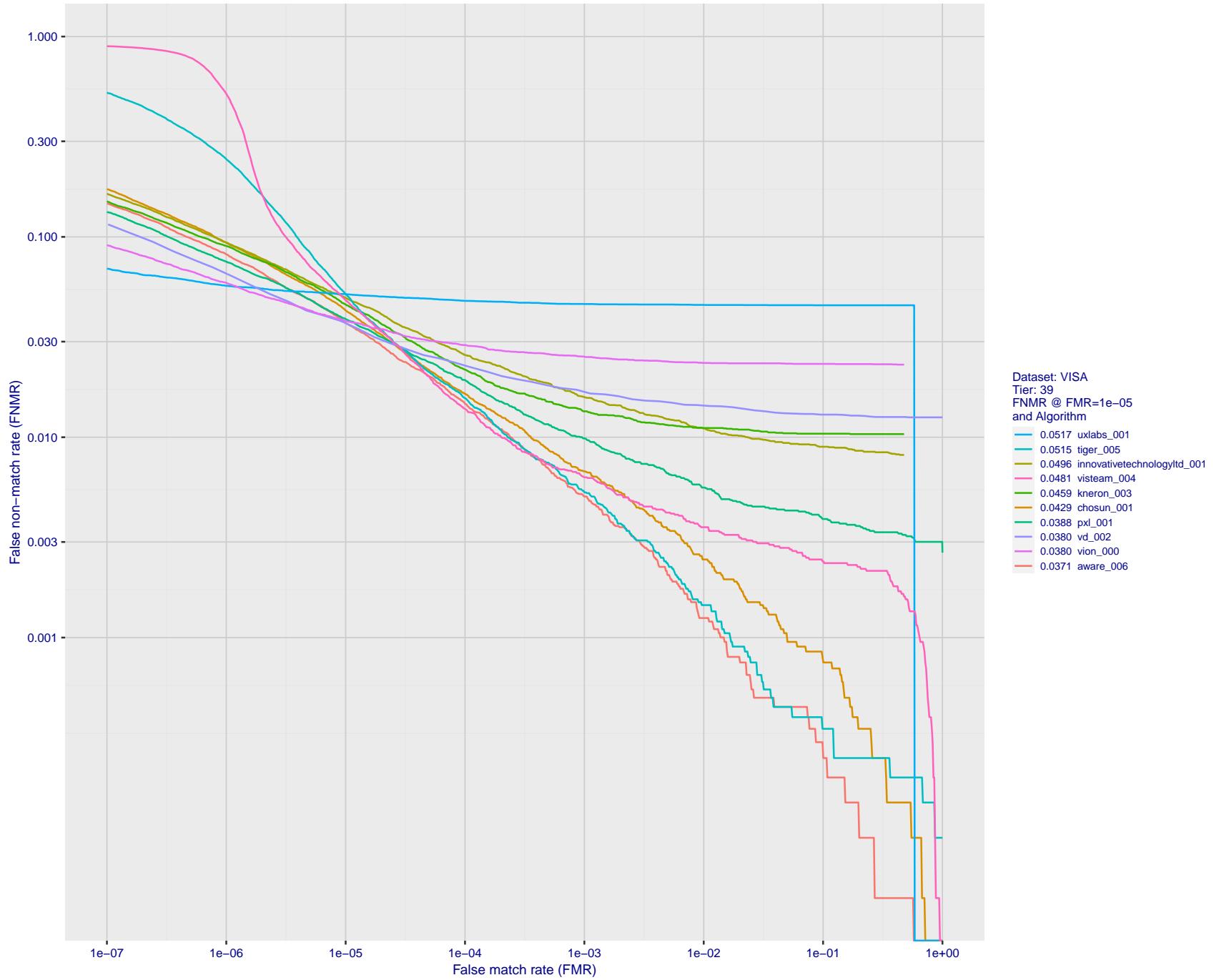


Figure 78: For the visa images, detection error tradeoff (DET) characteristics showing false non-match rate vs. false match rate plotted parametrically on threshold, T . The scales are logarithmic in order to show many decades of FMR.

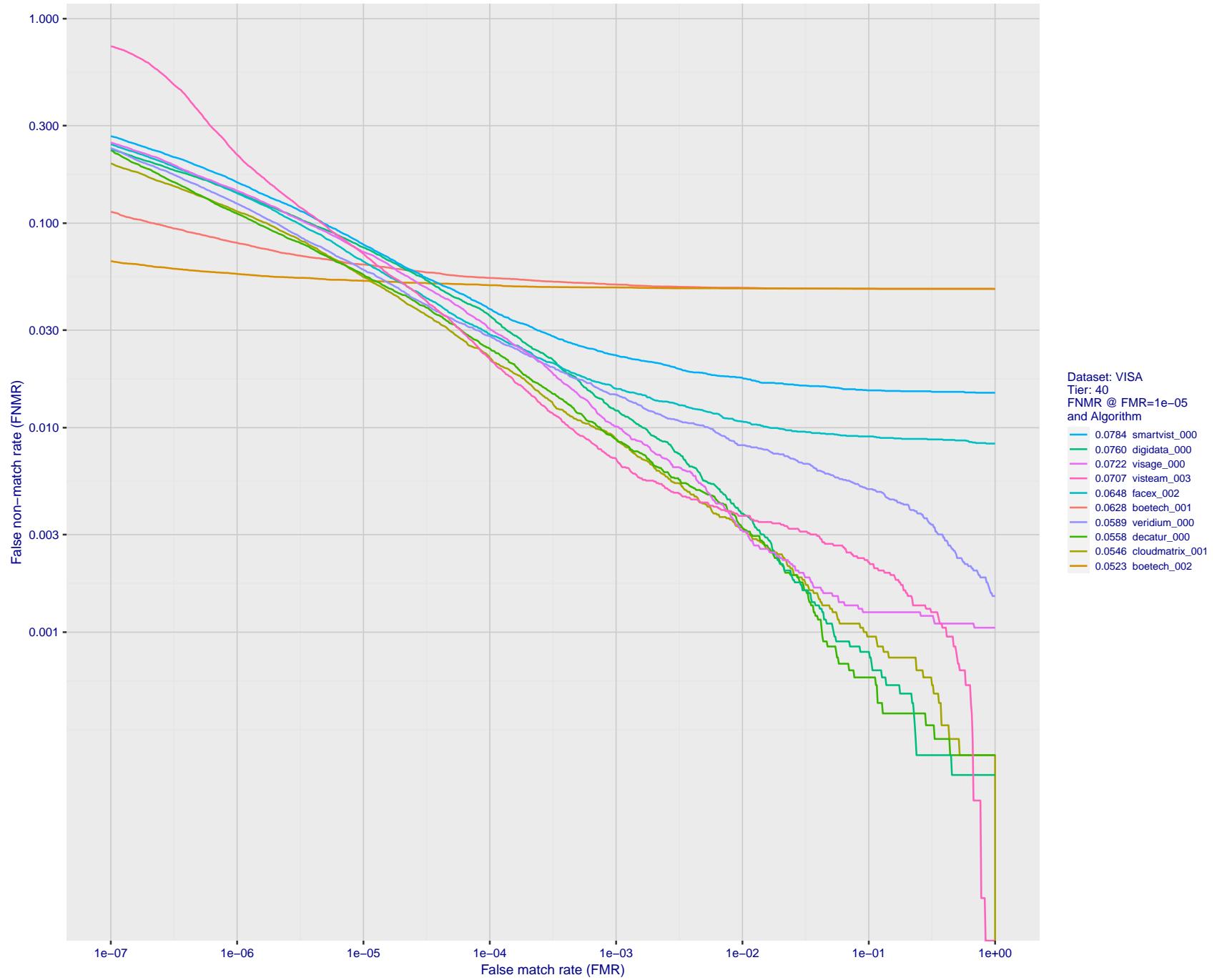


Figure 79: For the visa images, detection error tradeoff (DET) characteristics showing false non-match rate vs. false match rate plotted parametrically on threshold, T . The scales are logarithmic in order to show many decades of FMR.

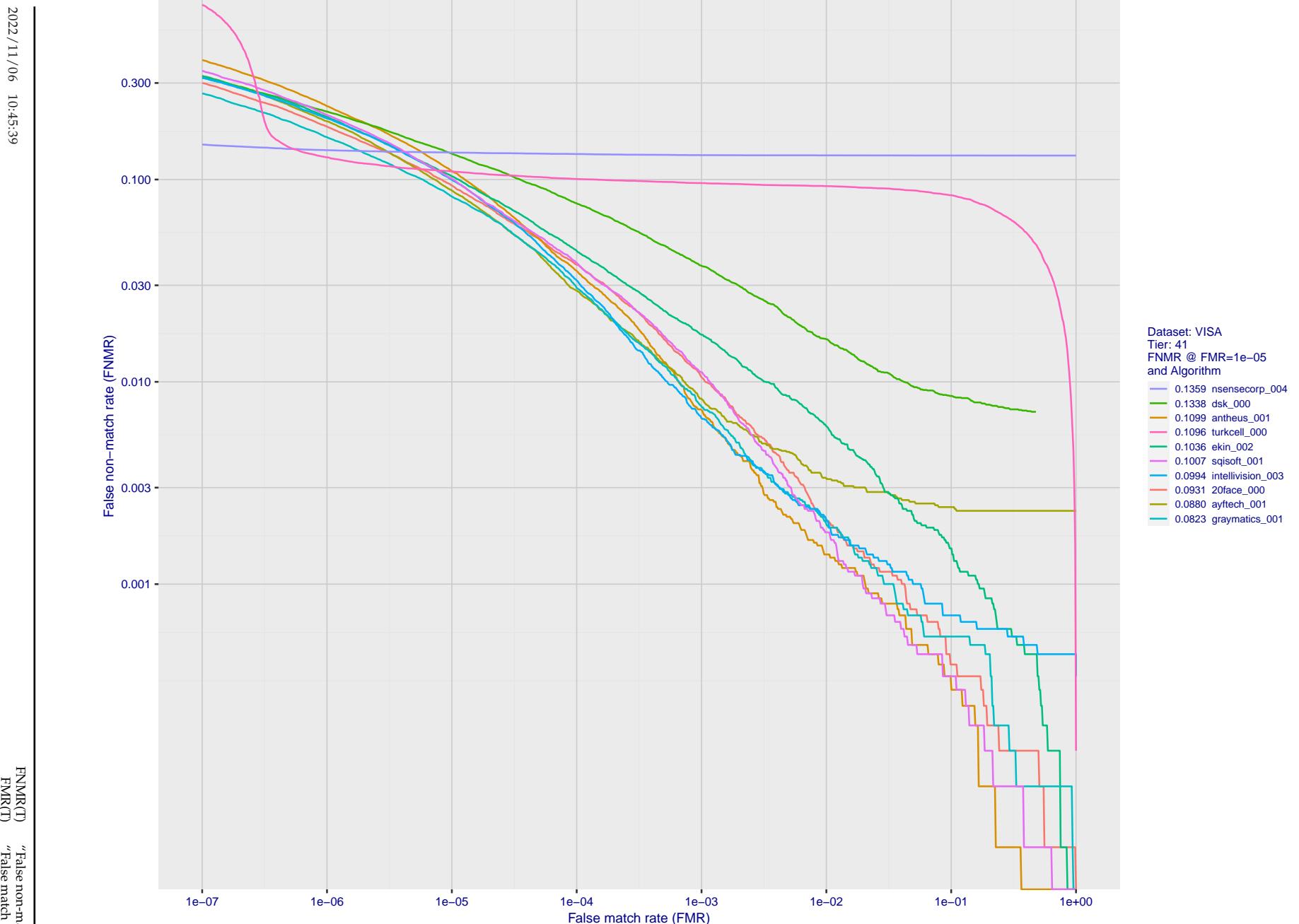


Figure 80: For the visa images, detection error tradeoff (DET) characteristics showing false non-match rate vs. false match rate plotted parametrically on threshold, T . The scales are logarithmic in order to show many decades of FMR.

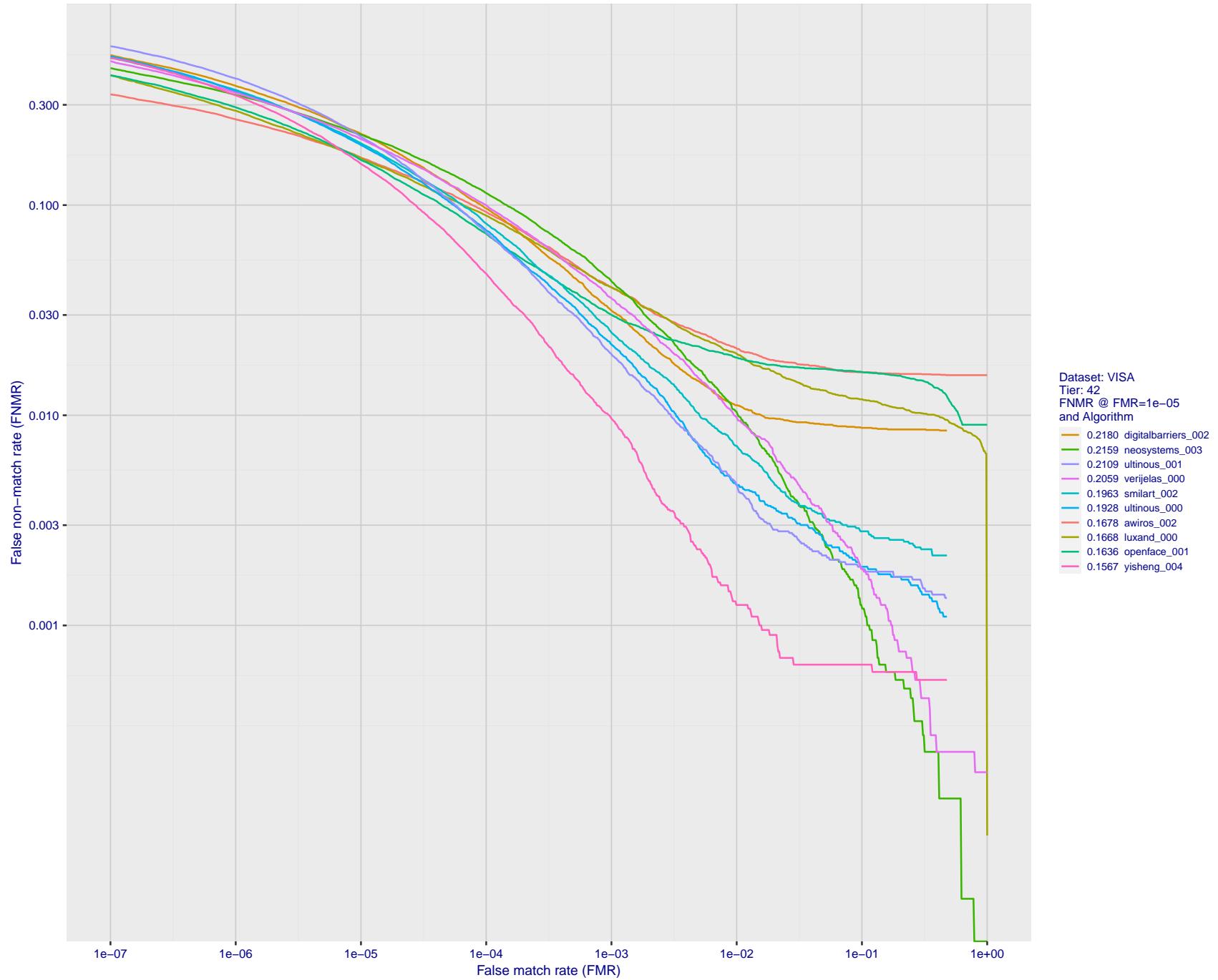


Figure 81: For the visa images, detection error tradeoff (DET) characteristics showing false non-match rate vs. false match rate plotted parametrically on threshold, T . The scales are logarithmic in order to show many decades of FMR.

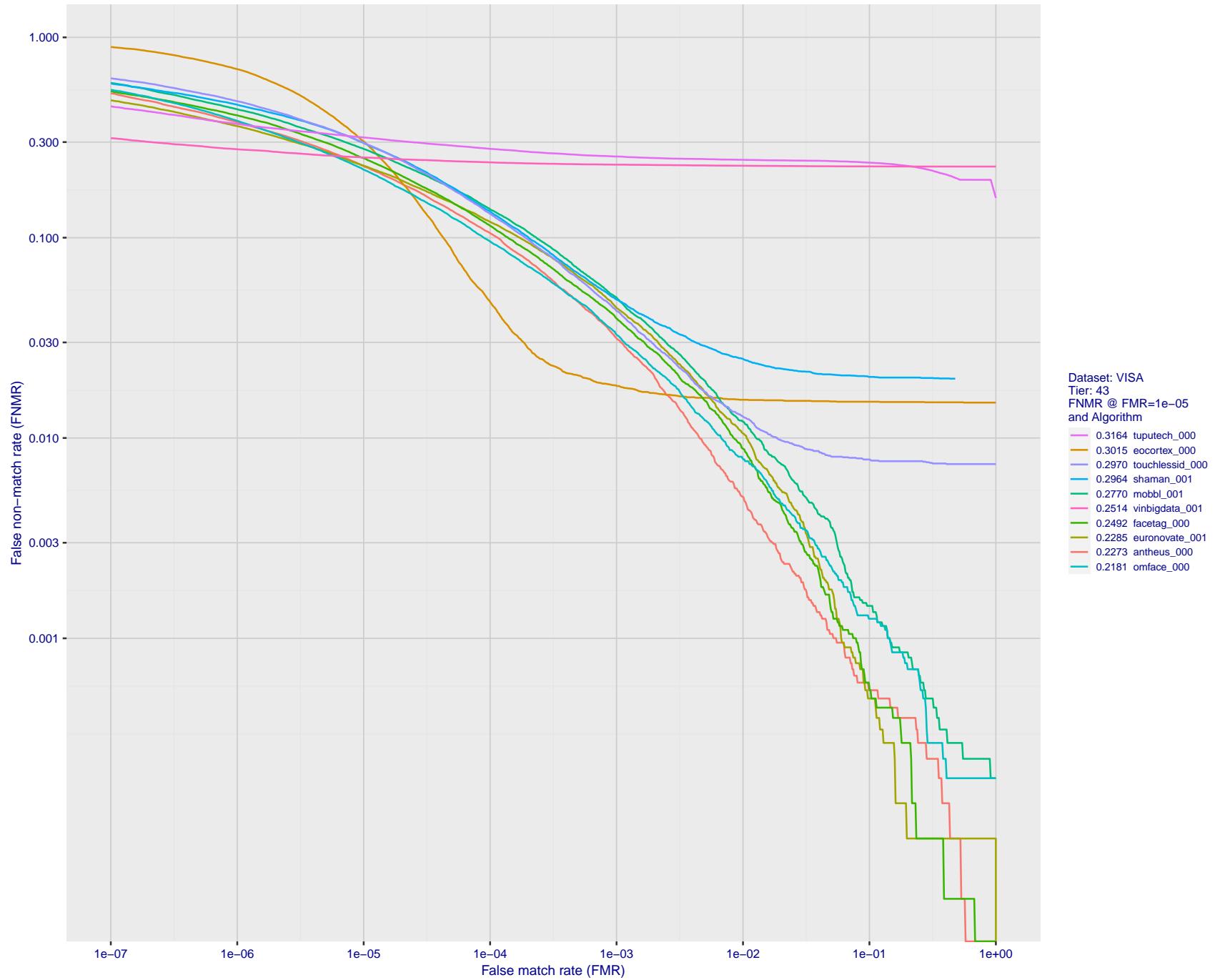


Figure 82: For the visa images, detection error tradeoff (DET) characteristics showing false non-match rate vs. false match rate plotted parametrically on threshold, T . The scales are logarithmic in order to show many decades of FMR.

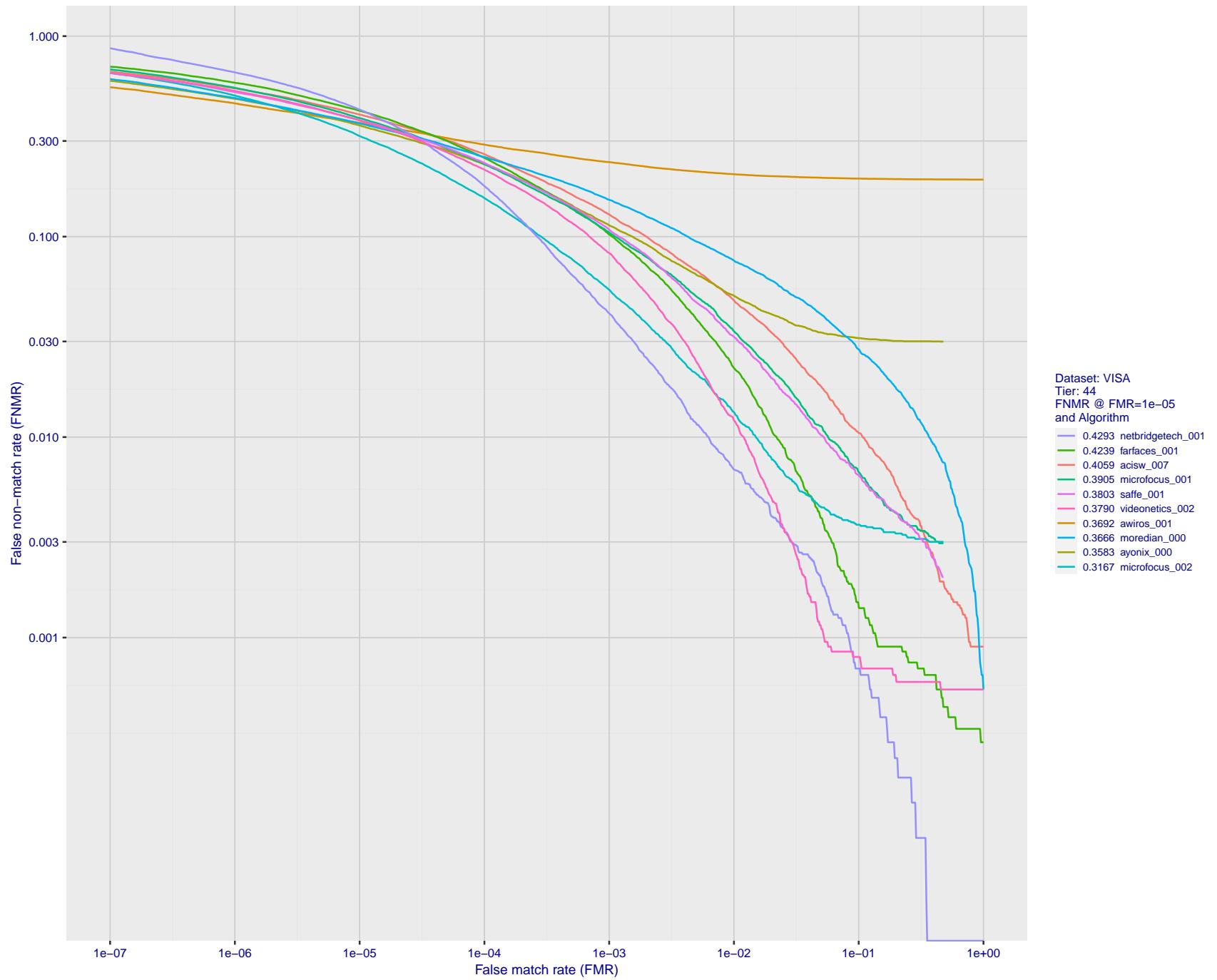


Figure 83: For the visa images, detection error tradeoff (DET) characteristics showing false non-match rate vs. false match rate plotted parametrically on threshold, T . The scales are logarithmic in order to show many decades of FMR.

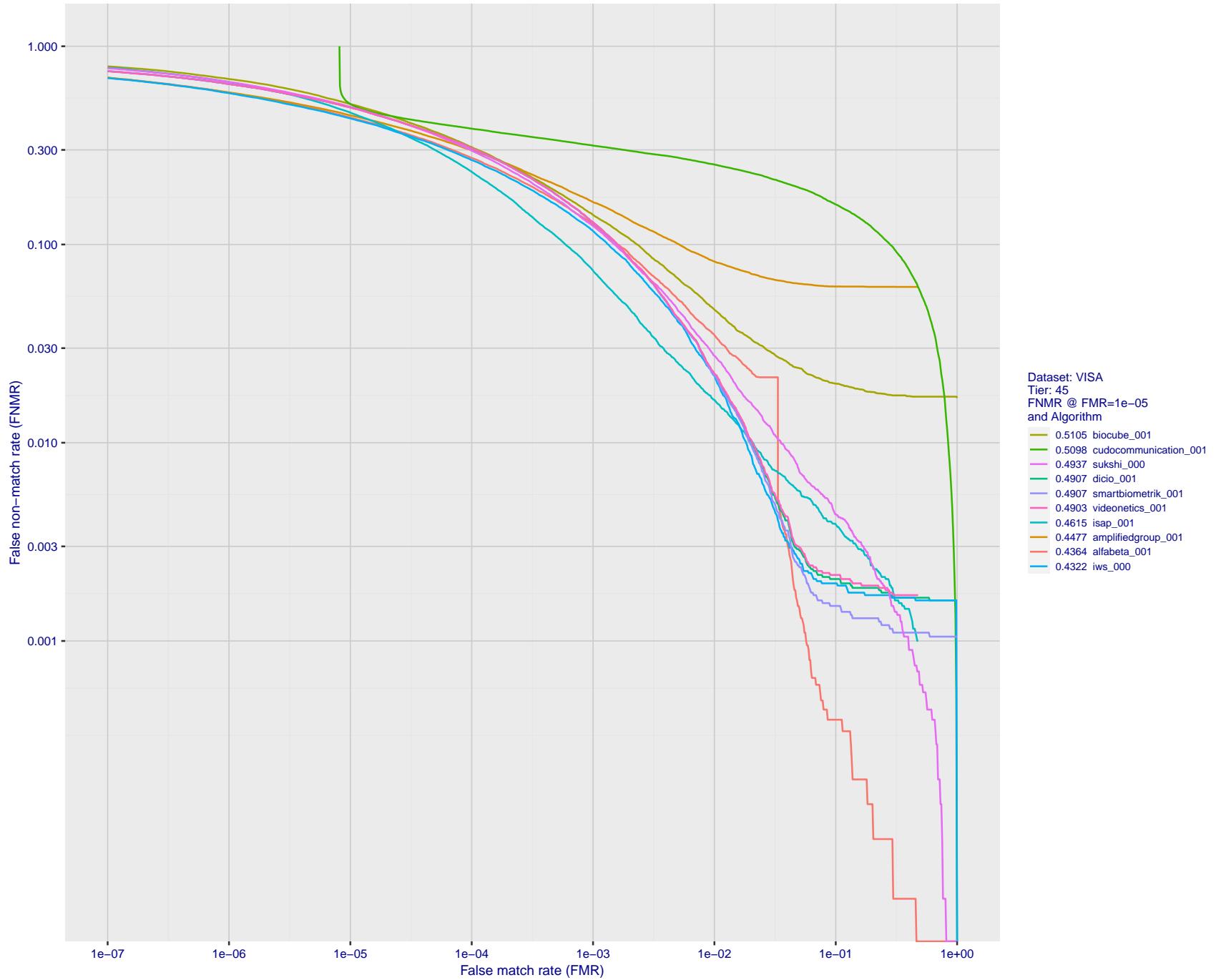


Figure 84: For the visa images, detection error tradeoff (DET) characteristics showing false non-match rate vs. false match rate plotted parametrically on threshold, T . The scales are logarithmic in order to show many decades of FMR.

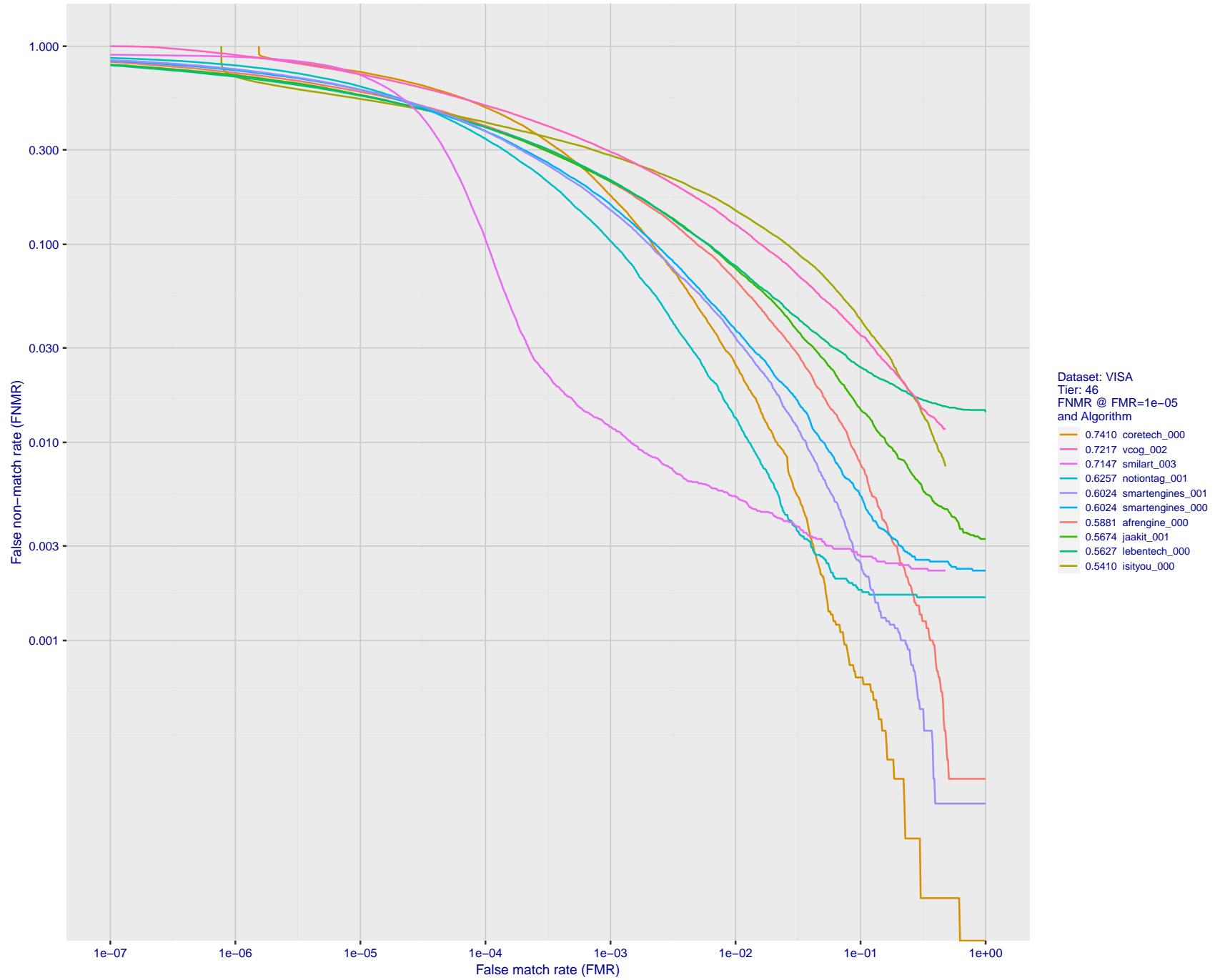


Figure 85: For the visa images, detection error tradeoff (DET) characteristics showing false non-match rate vs. false match rate plotted parametrically on threshold, T . The scales are logarithmic in order to show many decades of FMR.

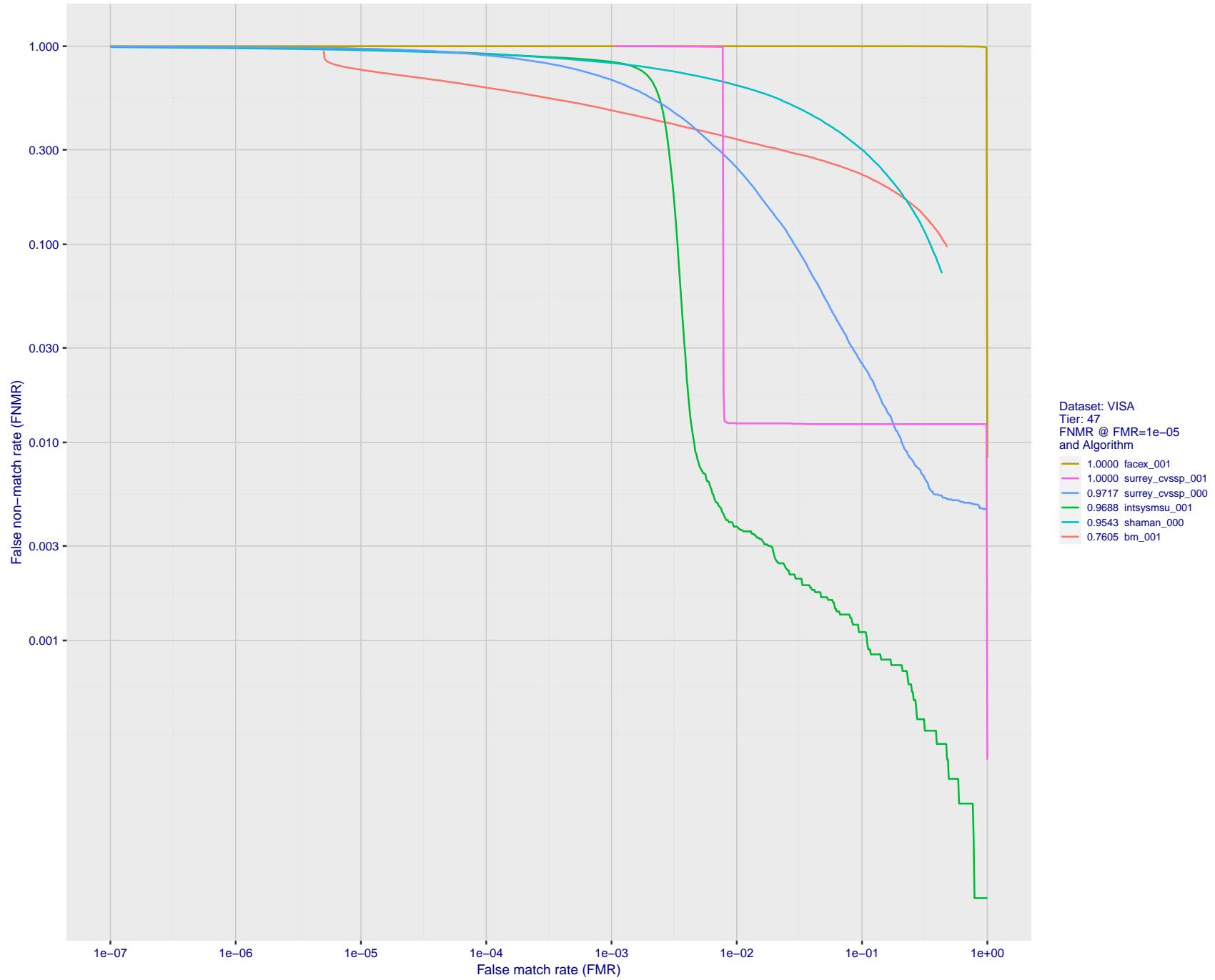


Figure 86: For the visa images, detection error tradeoff (DET) characteristics showing false non-match rate vs. false match rate plotted parametrically on threshold, T . The scales are logarithmic in order to show many decades of FMR.

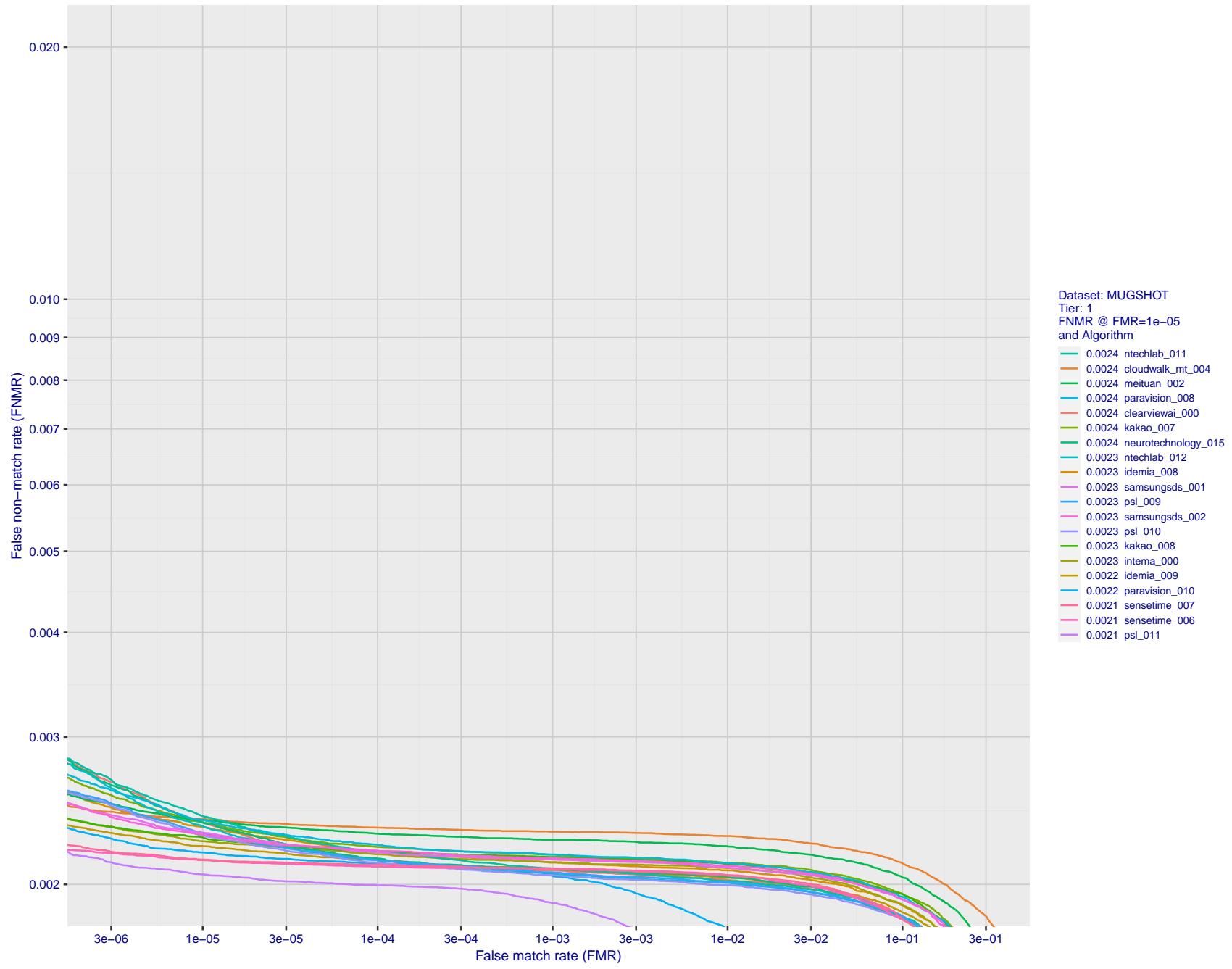


Figure 87: For the mugshot images, detection error tradeoff (DET) characteristics showing false non-match rate vs. false match rate plotted parametrically on threshold, T . The scales are logarithmic in order to show decades of FMR.

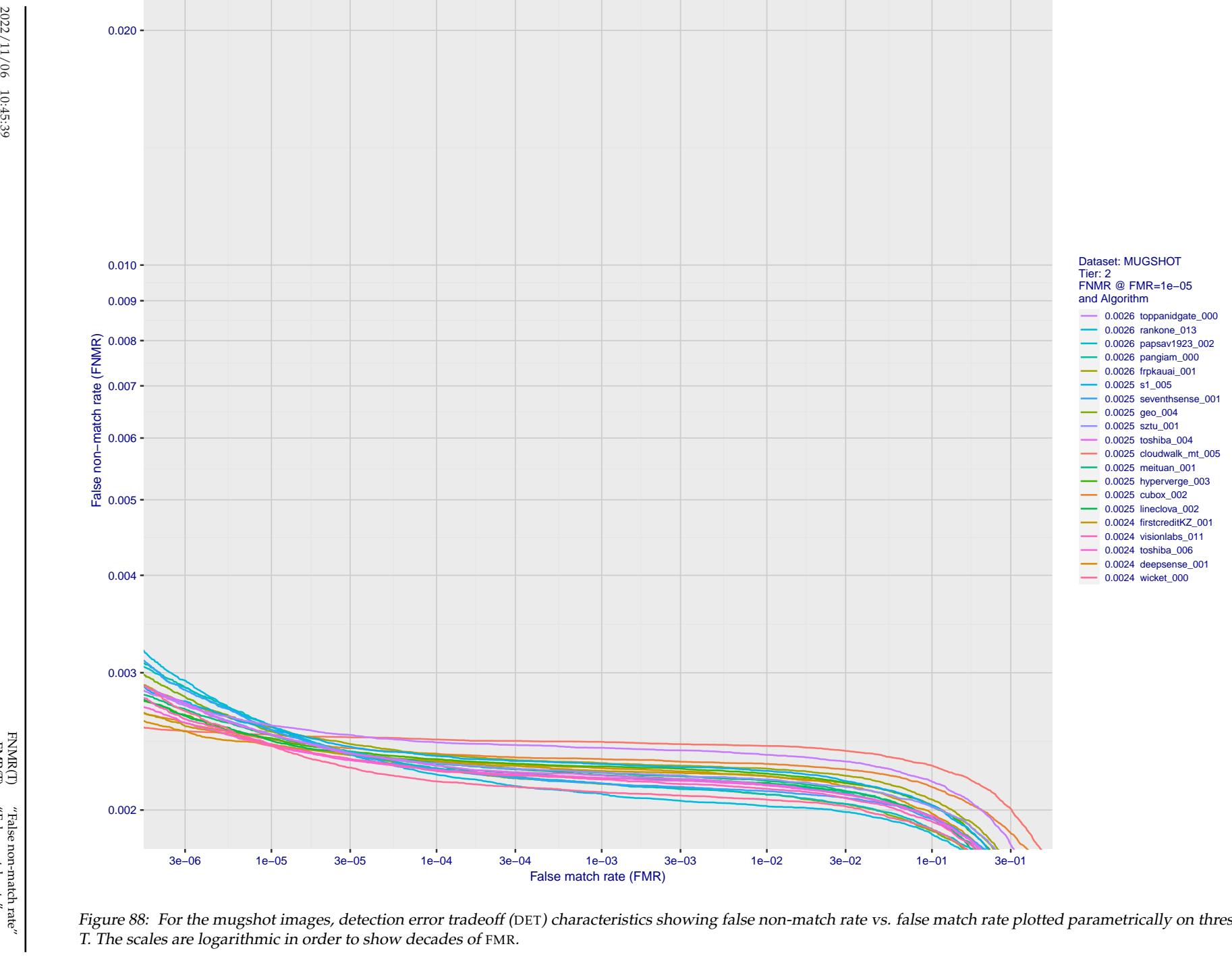
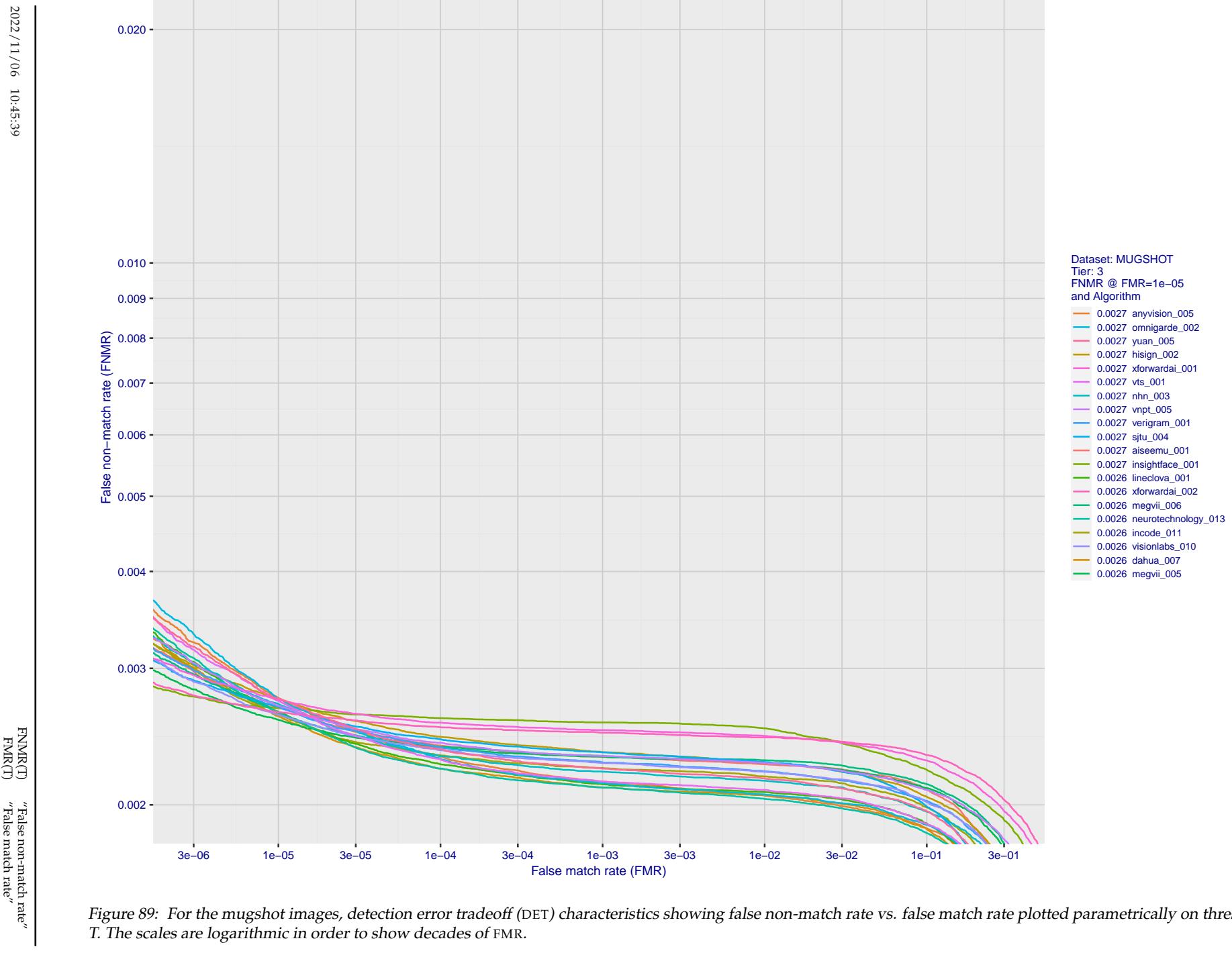


Figure 88: For the mugshot images, detection error tradeoff (DET) characteristics showing false non-match rate vs. false match rate plotted parametrically on threshold, T . The scales are logarithmic in order to show decades of FMR.



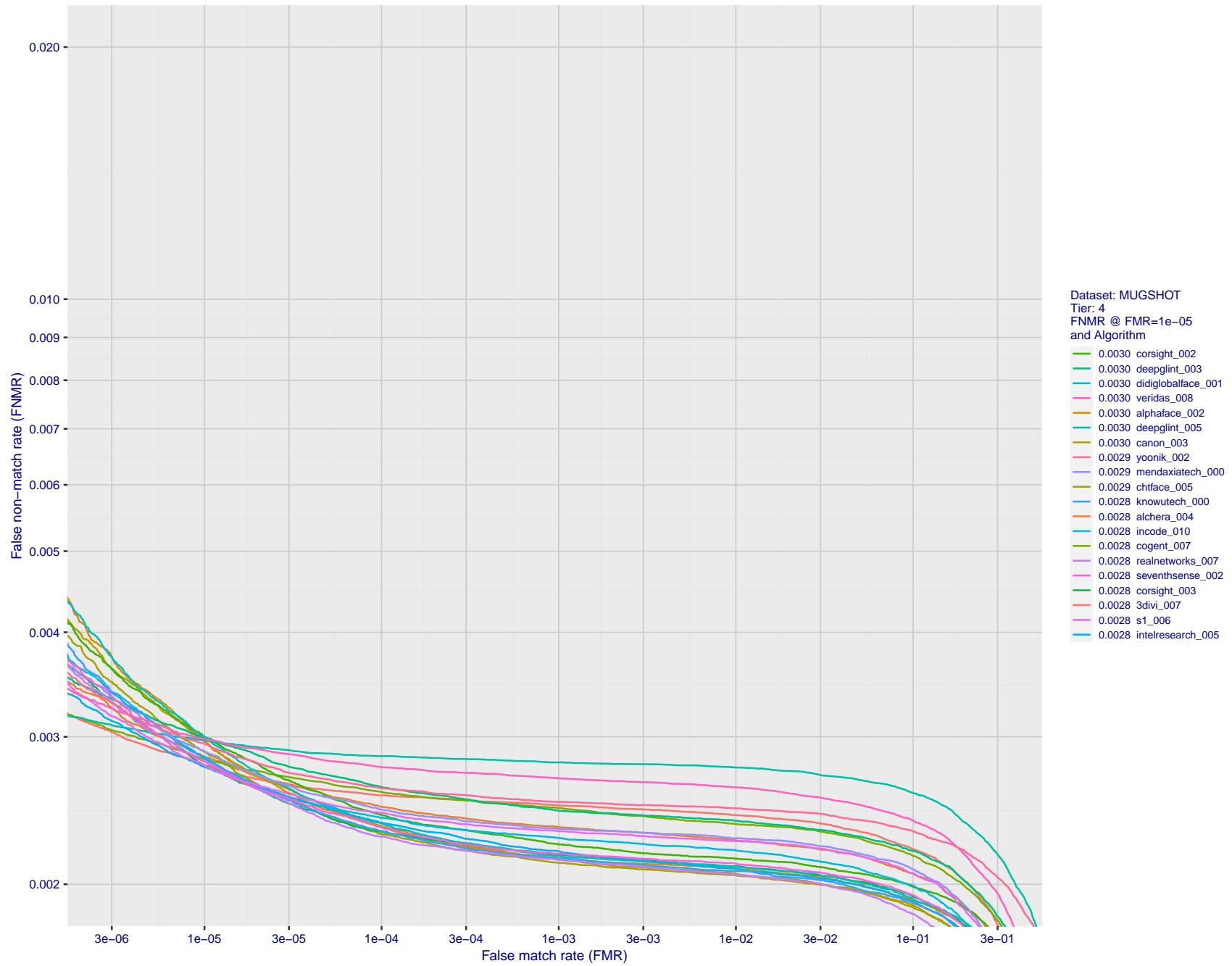


Figure 90: For the mugshot images, detection error tradeoff (DET) characteristics showing false non-match rate vs. false match rate plotted parametrically on threshold, T . The scales are logarithmic in order to show decades of FMR.

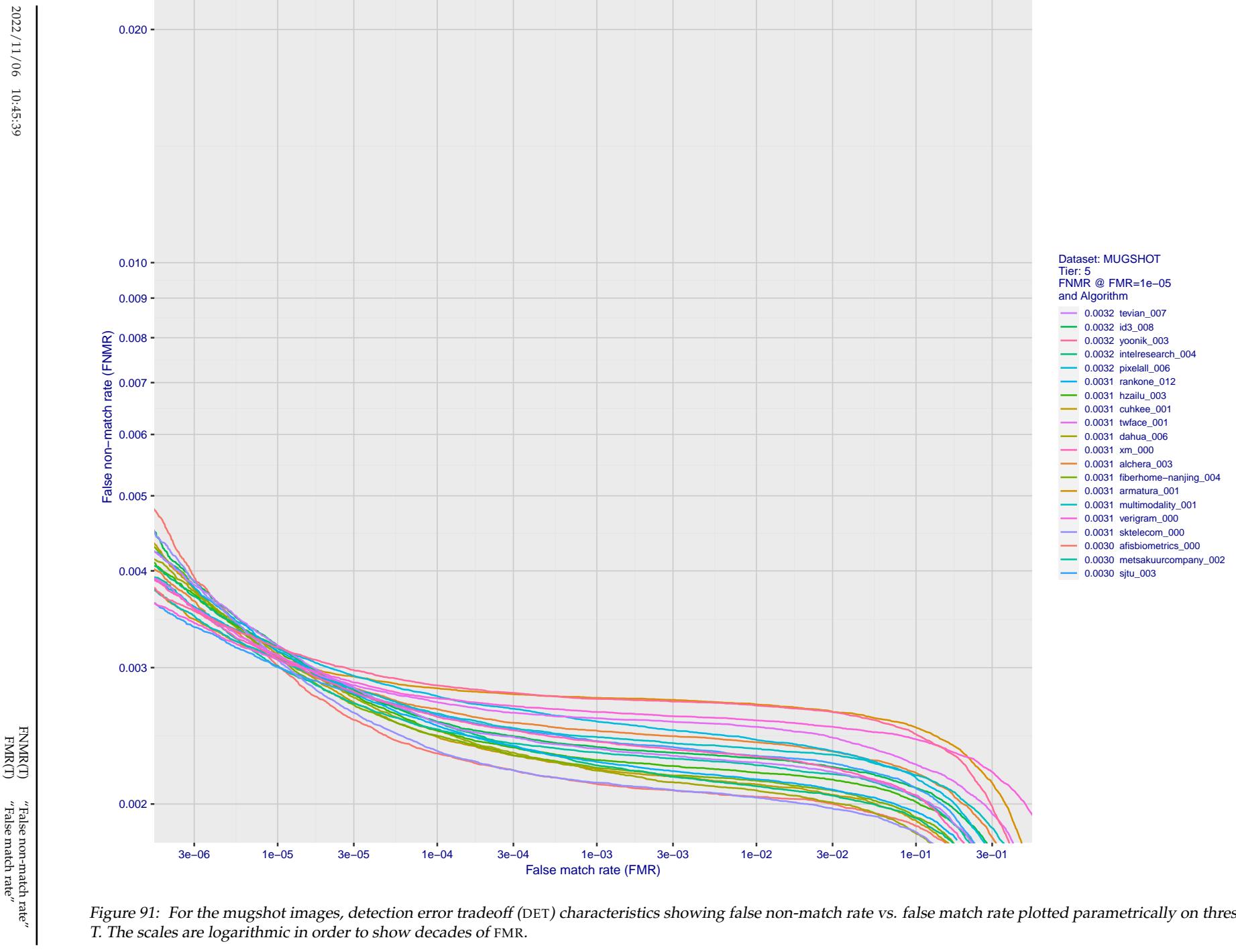


Figure 91: For the mugshot images, detection error tradeoff (DET) characteristics showing false non-match rate vs. false match rate plotted parametrically on threshold, T . The scales are logarithmic in order to show decades of FMR.

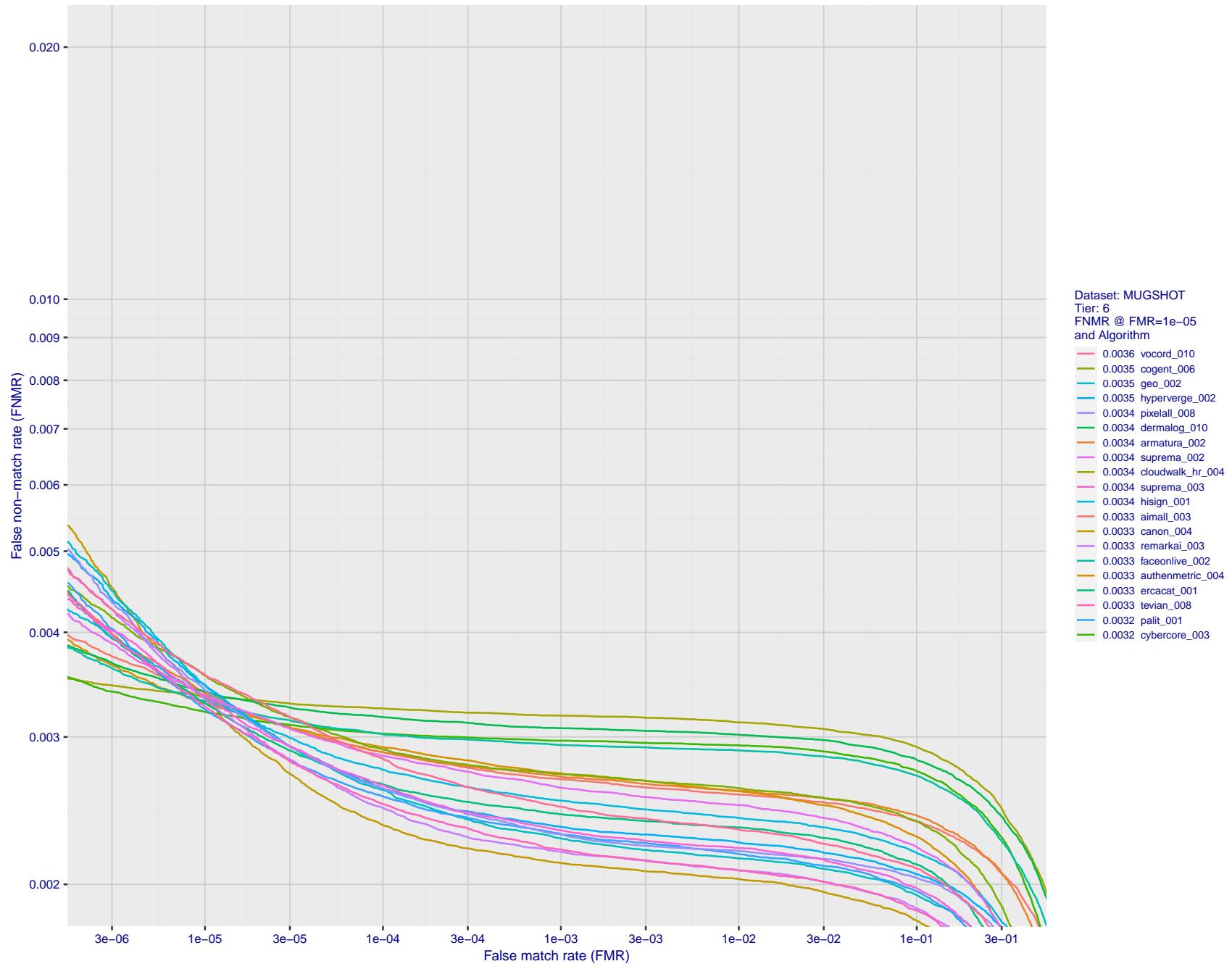


Figure 92: For the mugshot images, detection error tradeoff (DET) characteristics showing false non-match rate vs. false match rate plotted parametrically on threshold, T . The scales are logarithmic in order to show decades of FMR.

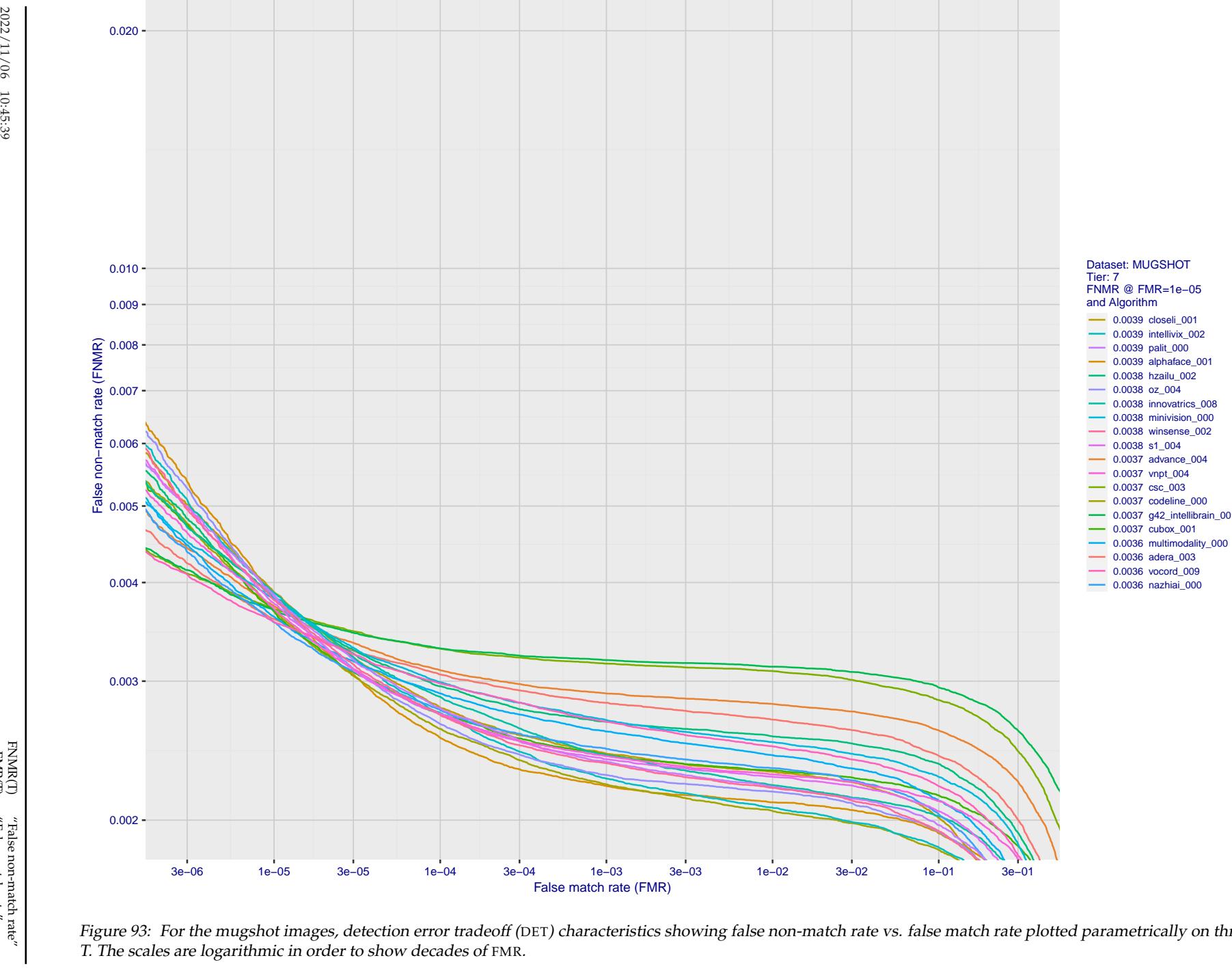


Figure 93: For the mugshot images, detection error tradeoff (DET) characteristics showing false non-match rate vs. false match rate plotted parametrically on threshold, T . The scales are logarithmic in order to show decades of FMR.

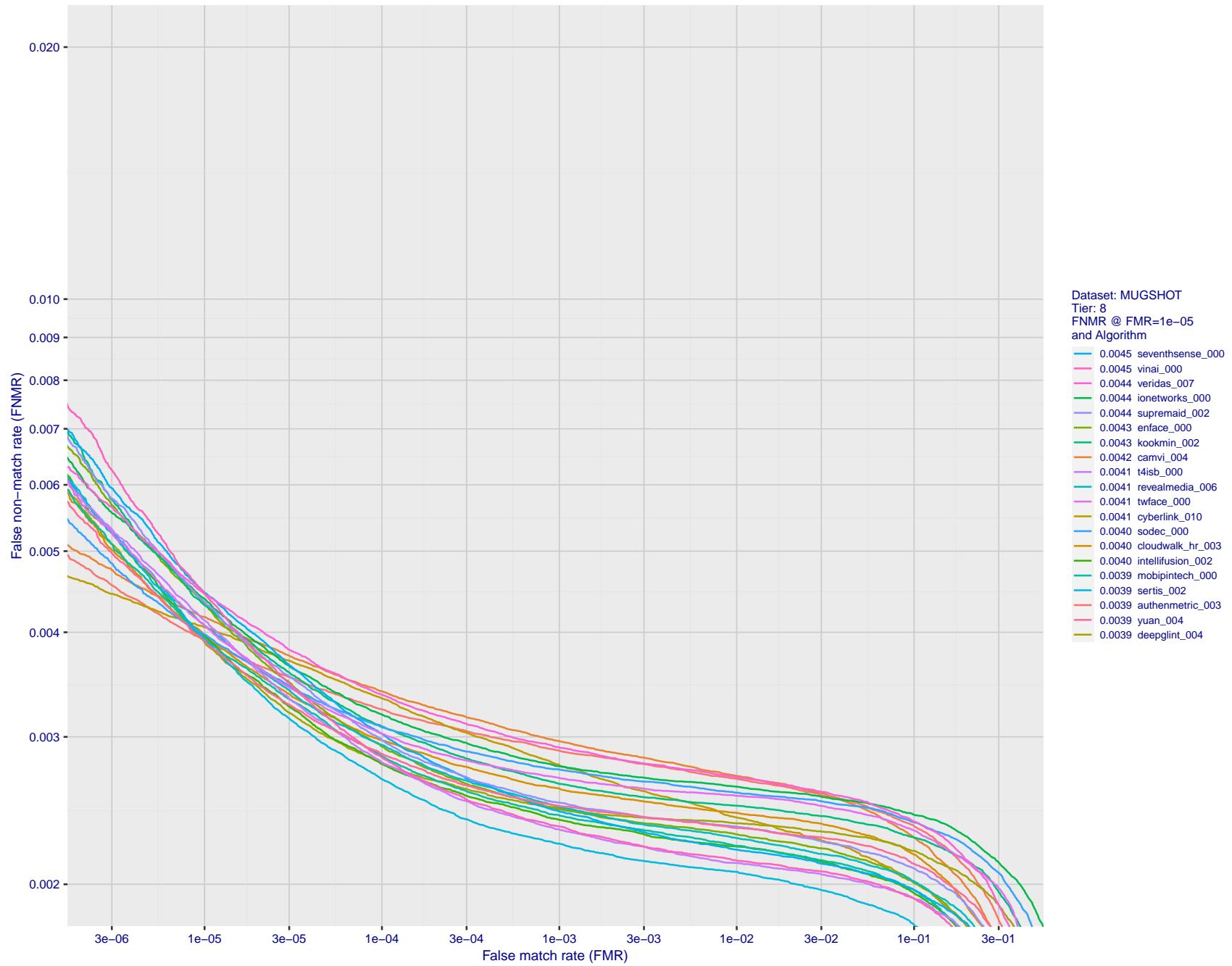


Figure 94: For the mugshot images, detection error tradeoff (DET) characteristics showing false non-match rate vs. false match rate plotted parametrically on threshold, T . The scales are logarithmic in order to show decades of FMR.

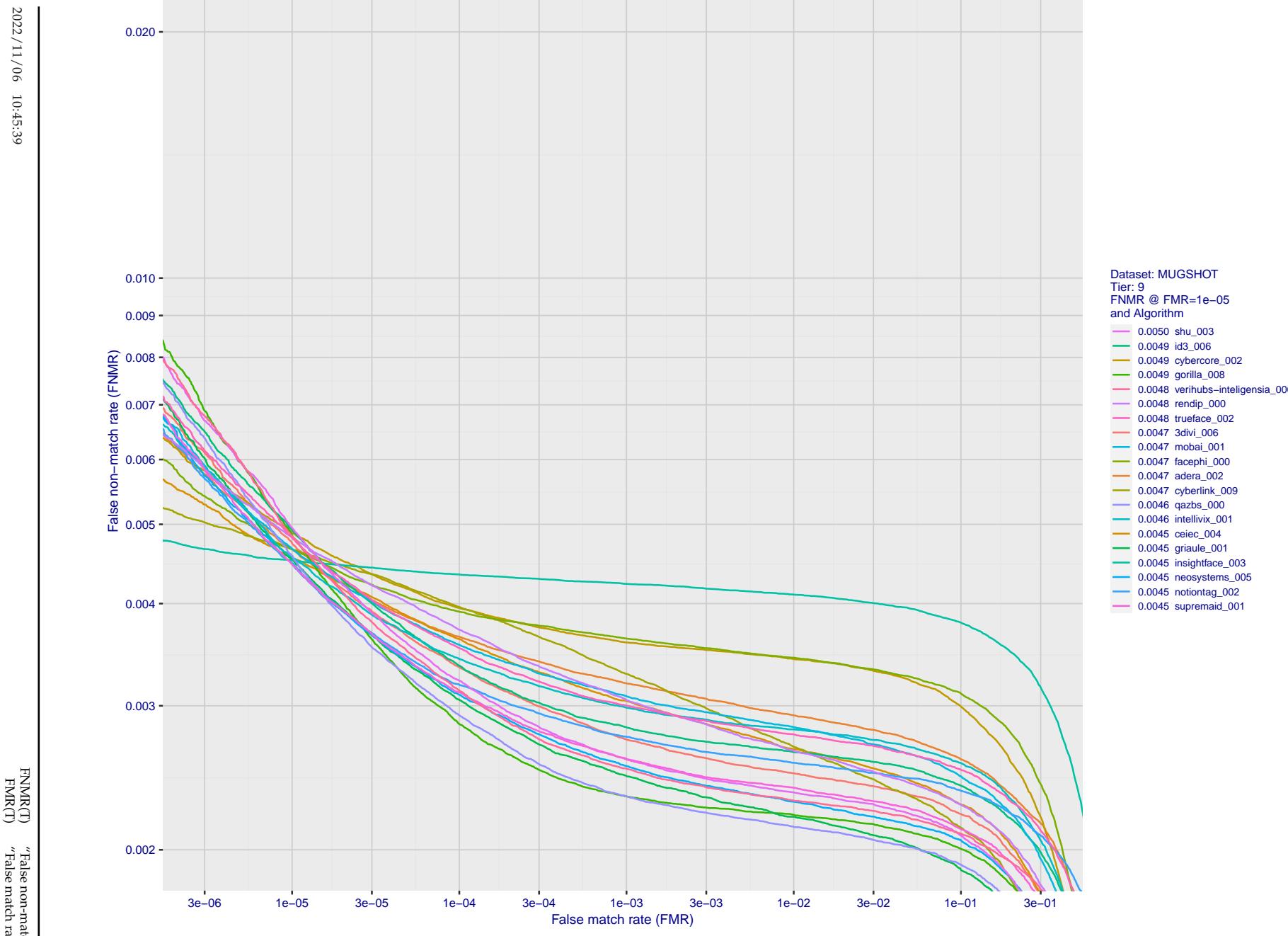


Figure 95: For the mugshot images, detection error tradeoff (DET) characteristics showing false non-match rate vs. false match rate plotted parametrically on threshold, T . The scales are logarithmic in order to show decades of FMR.

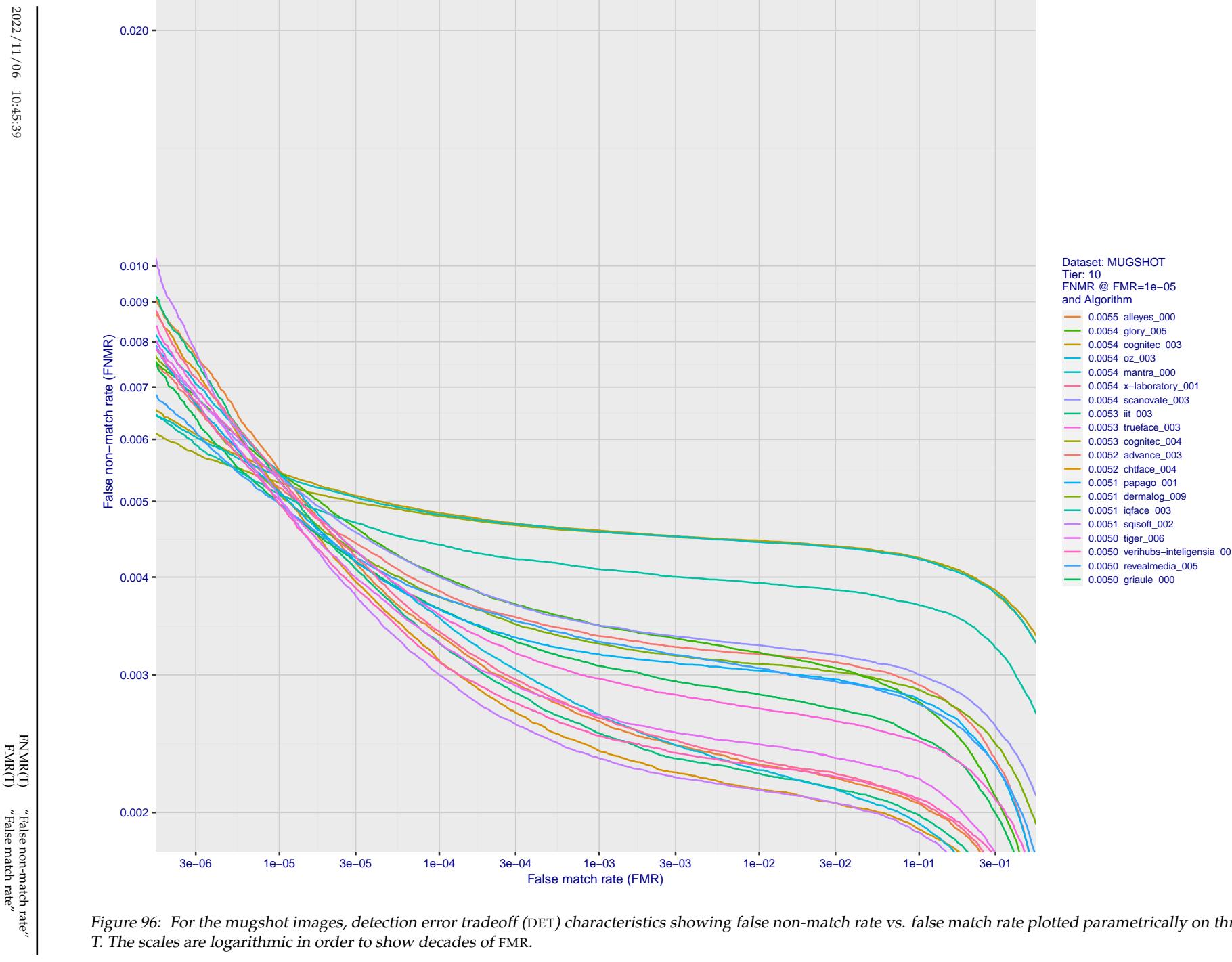


Figure 96: For the mugshot images, detection error tradeoff (DET) characteristics showing false non-match rate vs. false match rate plotted parametrically on threshold, T . The scales are logarithmic in order to show decades of FMR.

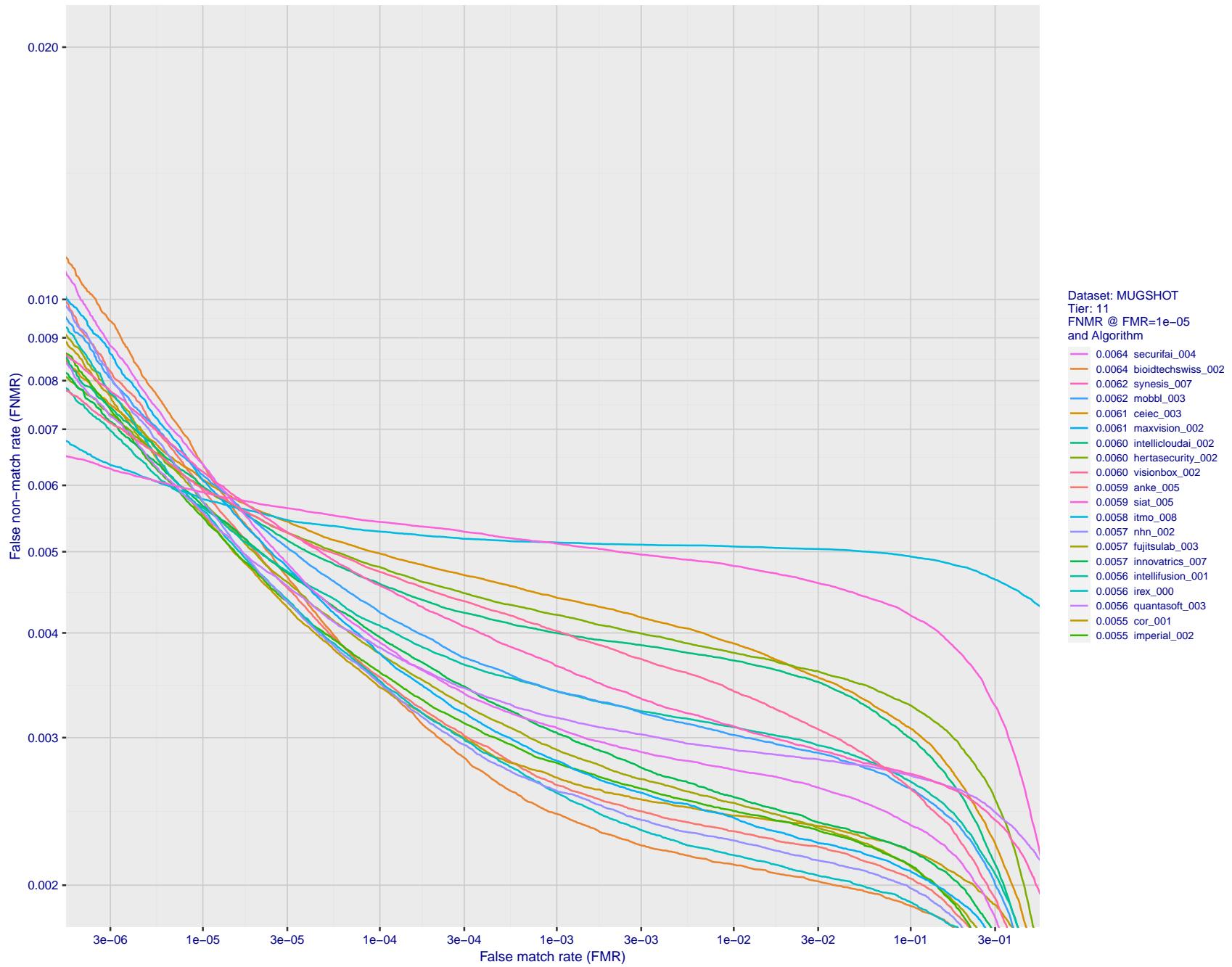


Figure 97: For the mugshot images, detection error tradeoff (DET) characteristics showing false non-match rate vs. false match rate plotted parametrically on threshold, T . The scales are logarithmic in order to show decades of FMR.

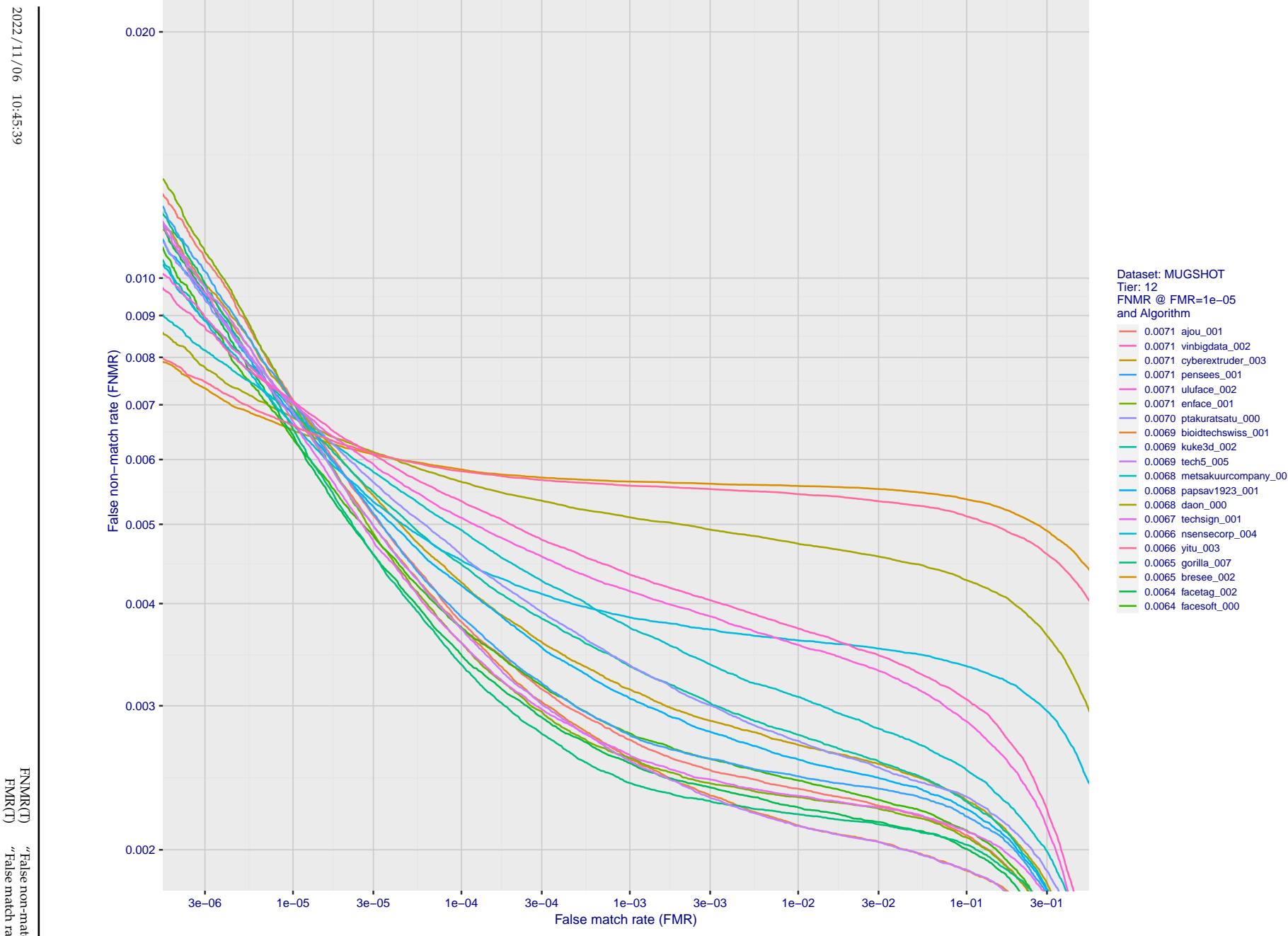


Figure 98: For the mugshot images, detection error tradeoff (DET) characteristics showing false non-match rate vs. false match rate plotted parametrically on threshold, T . The scales are logarithmic in order to show decades of FMR.

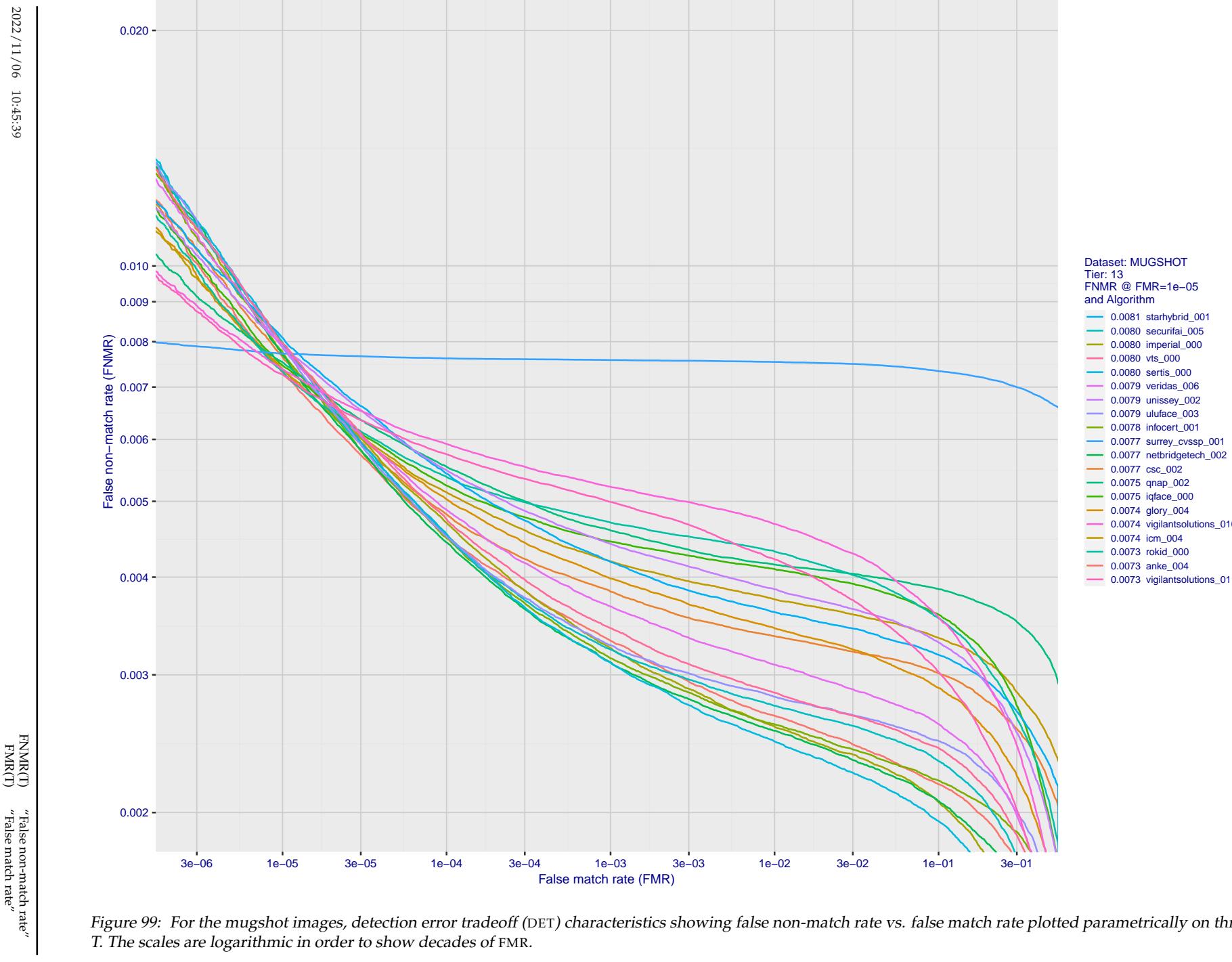


Figure 99: For the mugshot images, detection error tradeoff (DET) characteristics showing false non-match rate vs. false match rate plotted parametrically on threshold, T . The scales are logarithmic in order to show decades of FMR.

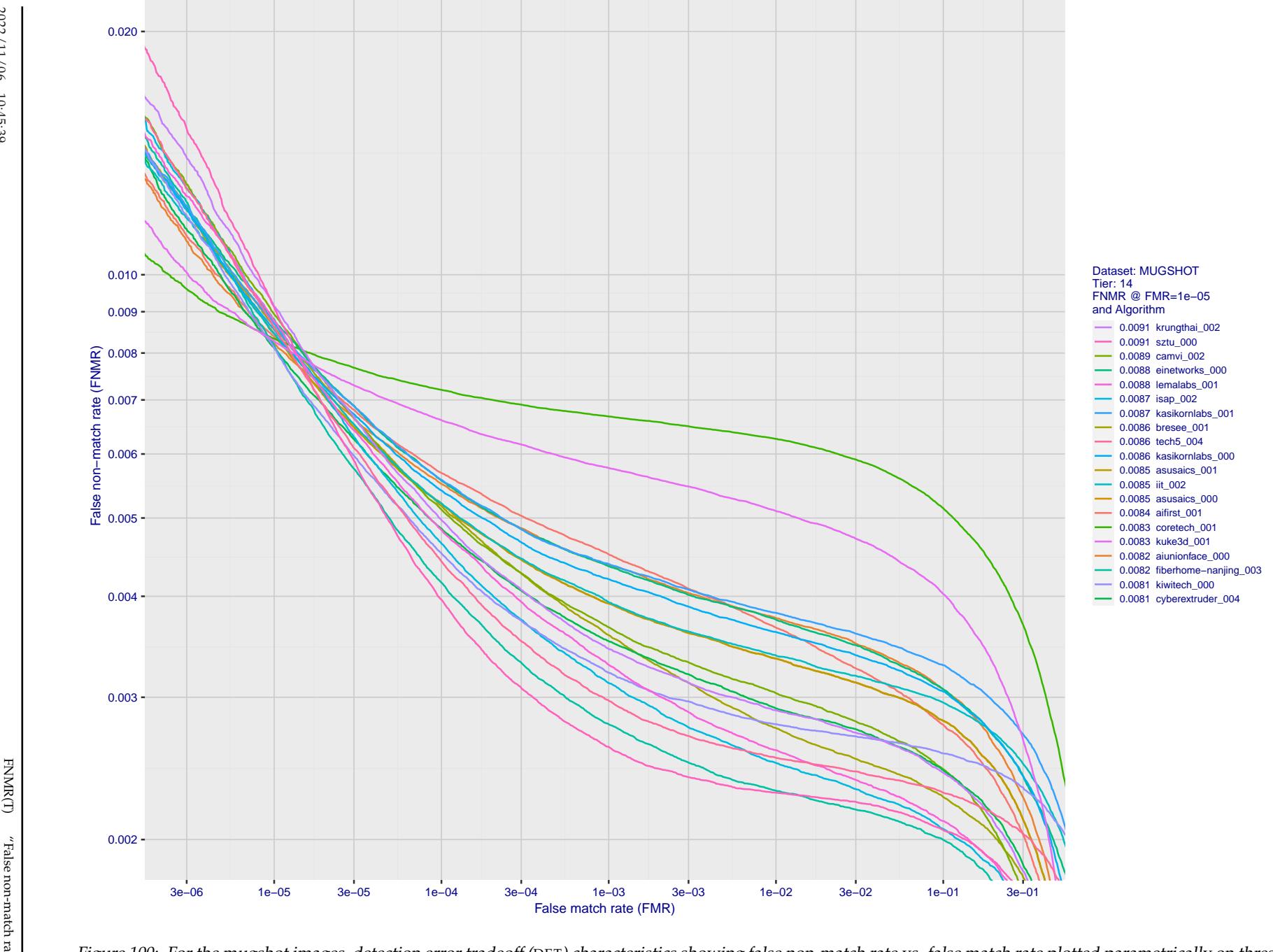


Figure 100: For the mugshot images, detection error tradeoff (DET) characteristics showing false non-match rate vs. false match rate plotted parametrically on threshold, T . The scales are logarithmic in order to show decades of FMR.

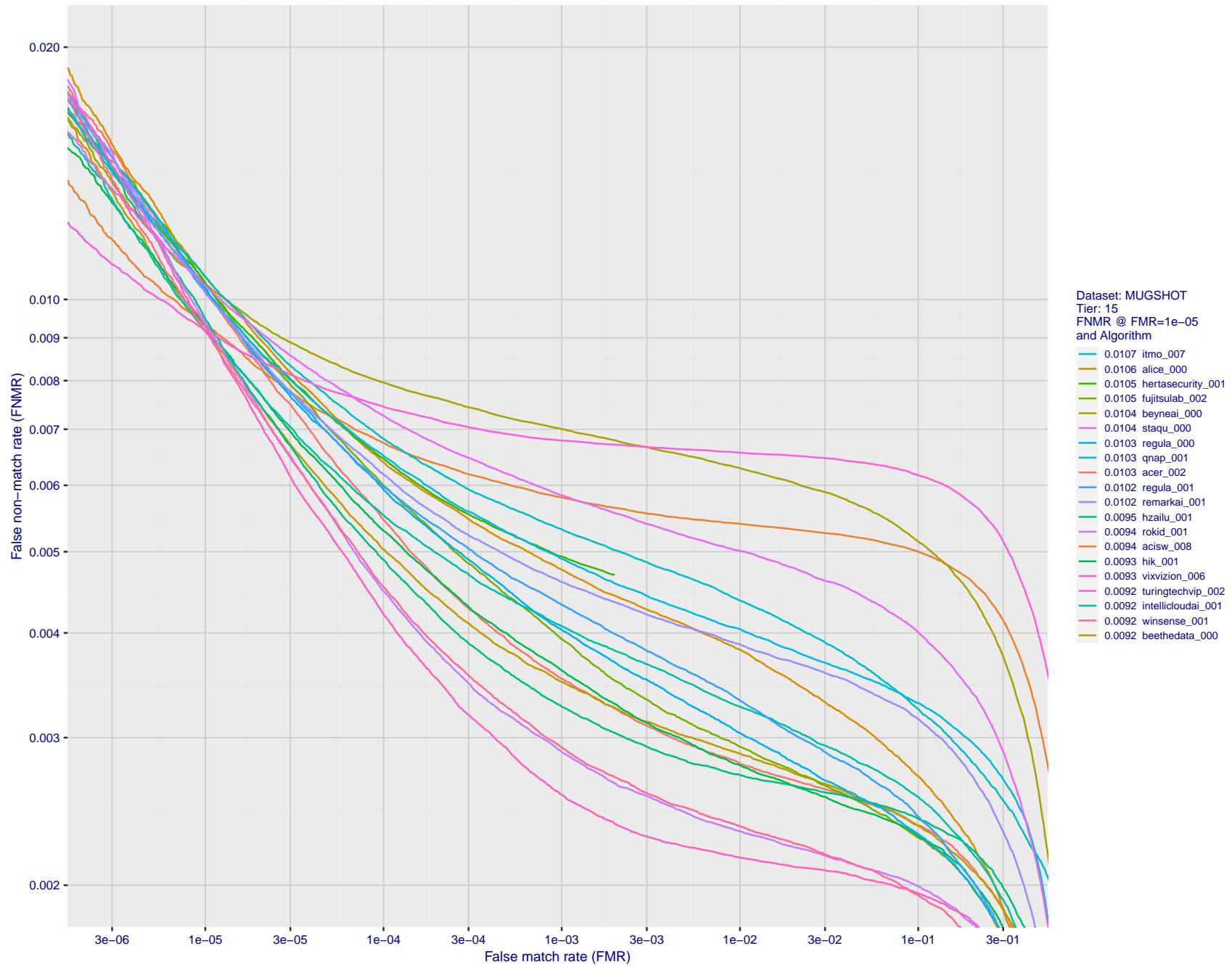


Figure 101: For the mugshot images, detection error tradeoff (DET) characteristics showing false non-match rate vs. false match rate plotted parametrically on threshold, T. The scales are logarithmic in order to show decades of FMR.

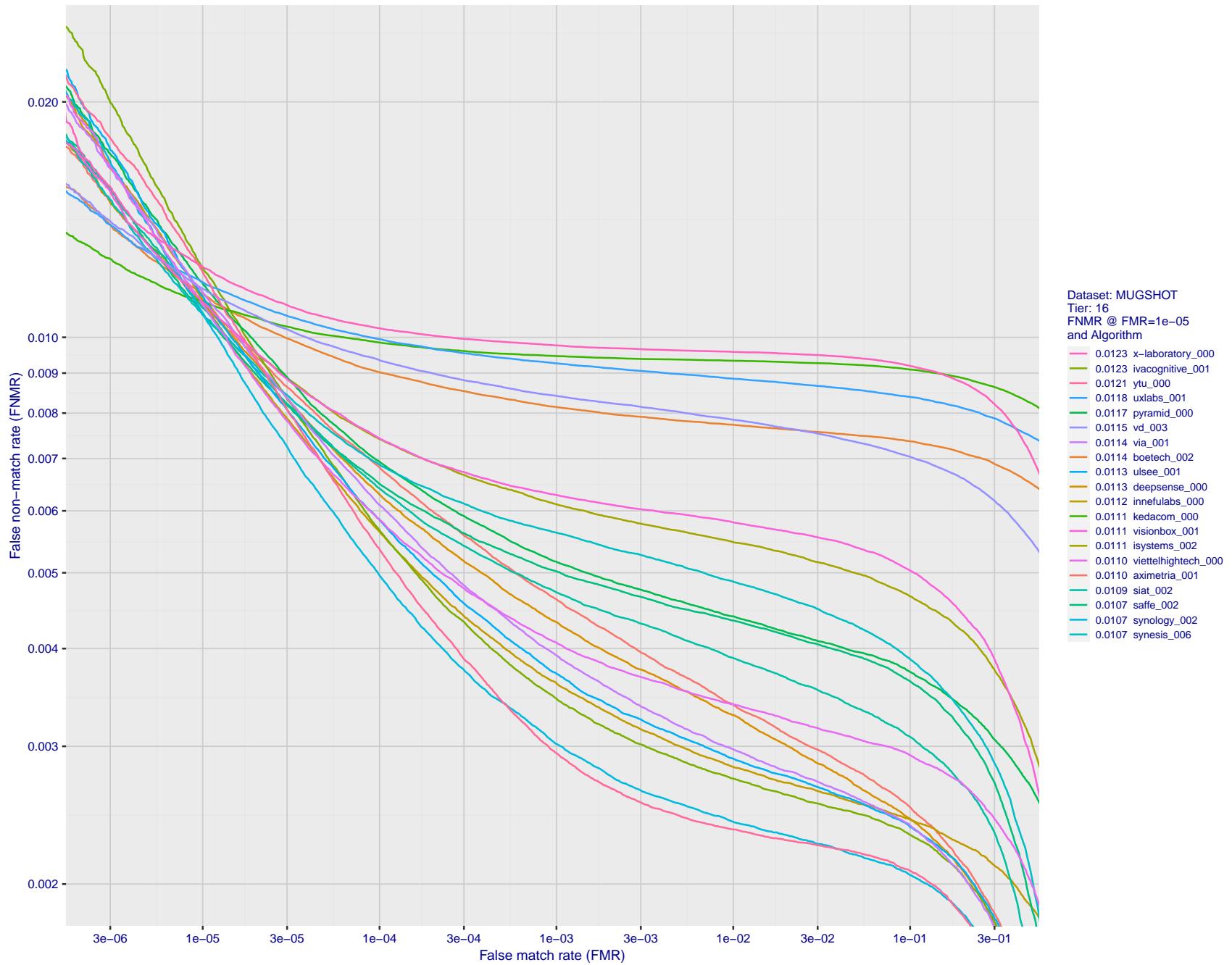


Figure 102: For the mugshot images, detection error tradeoff (DET) characteristics showing false non-match rate vs. false match rate plotted parametrically on threshold, T . The scales are logarithmic in order to show decades of FMR.

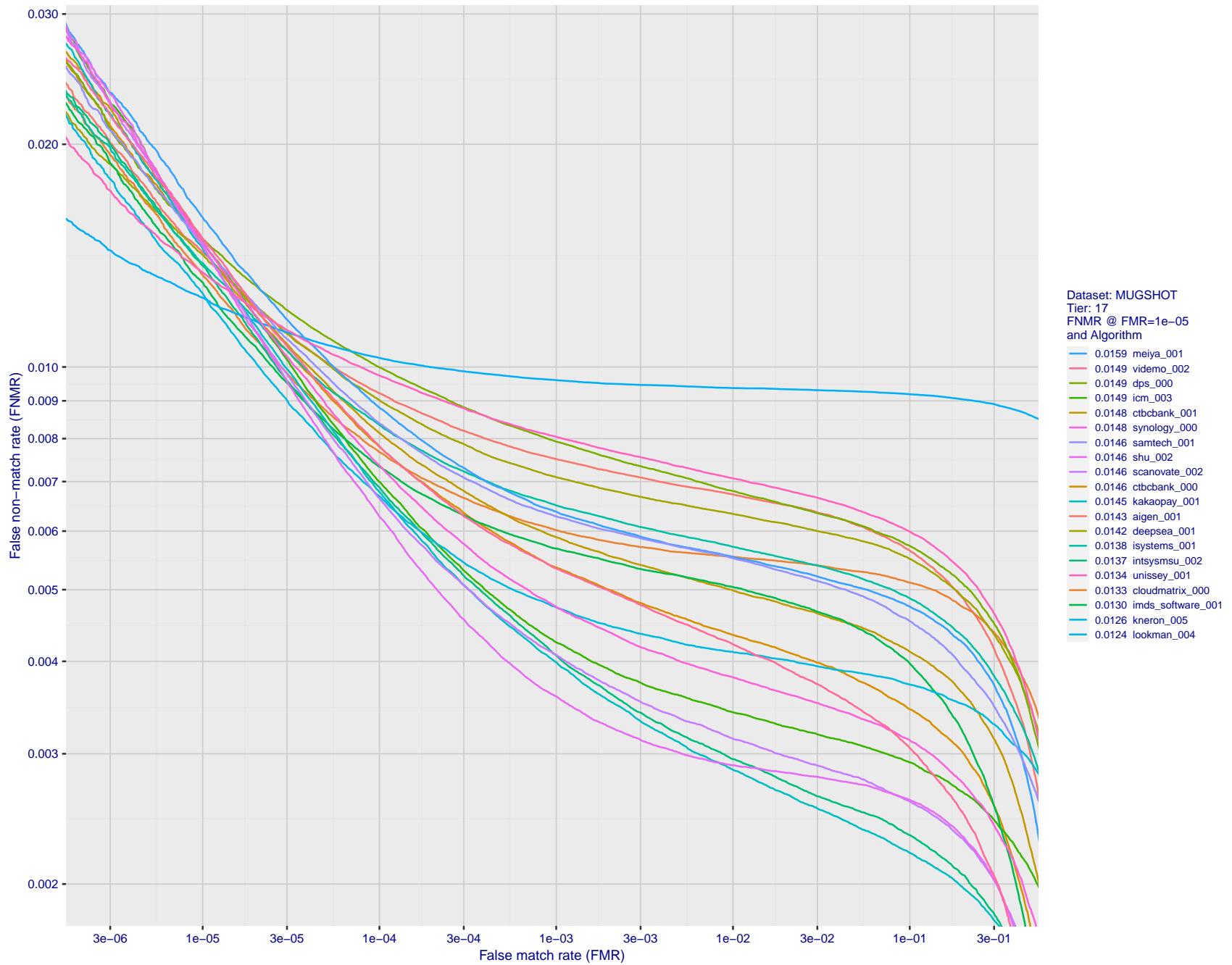


Figure 103: For the mugshot images, detection error tradeoff (DET) characteristics showing false non-match rate vs. false match rate plotted parametrically on threshold, T . The scales are logarithmic in order to show decades of FMR.

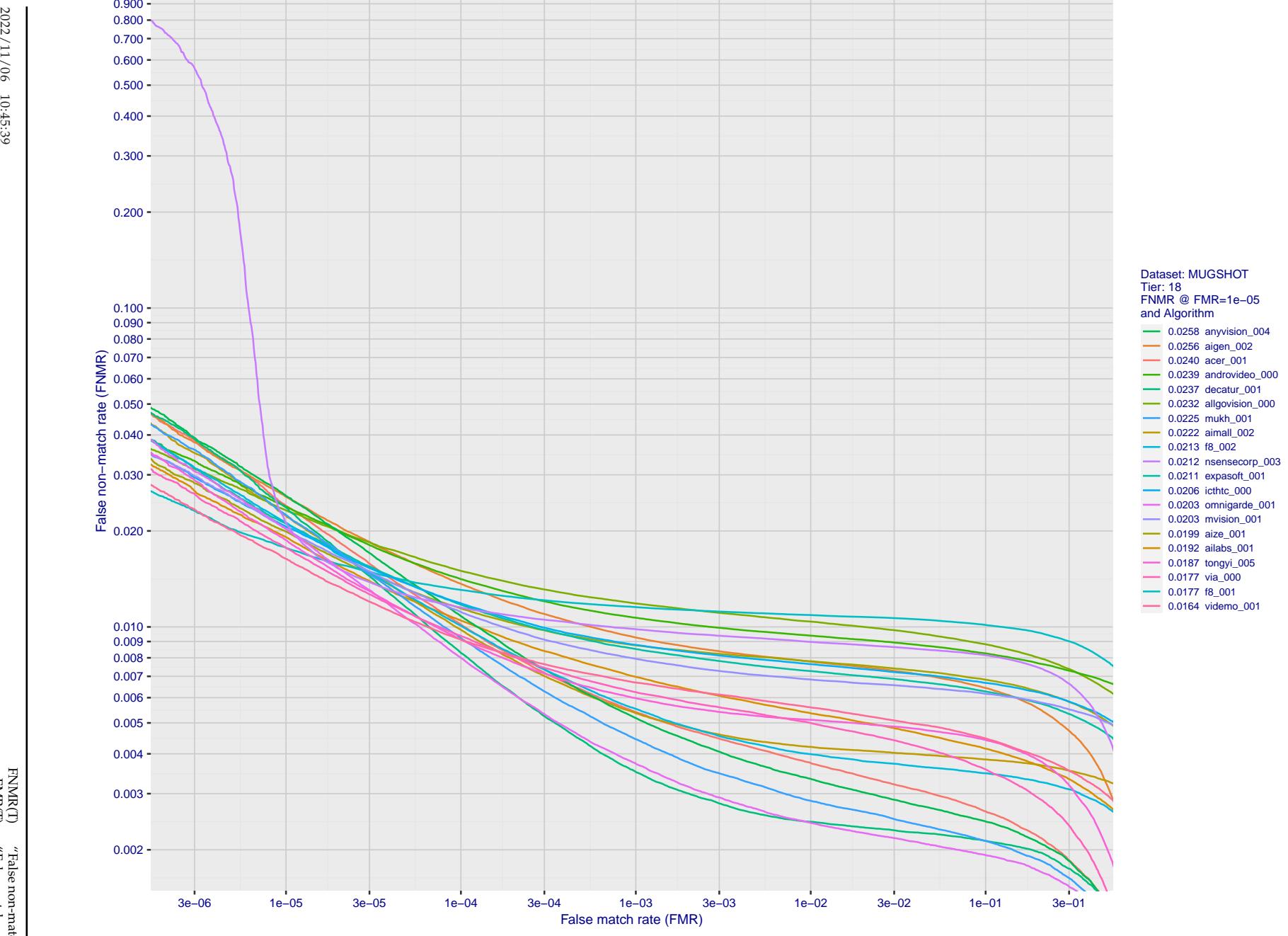


Figure 104: For the mugshot images, detection error tradeoff (DET) characteristics showing false non-match rate vs. false match rate plotted parametrically on threshold, T . The scales are logarithmic in order to show decades of FMR.

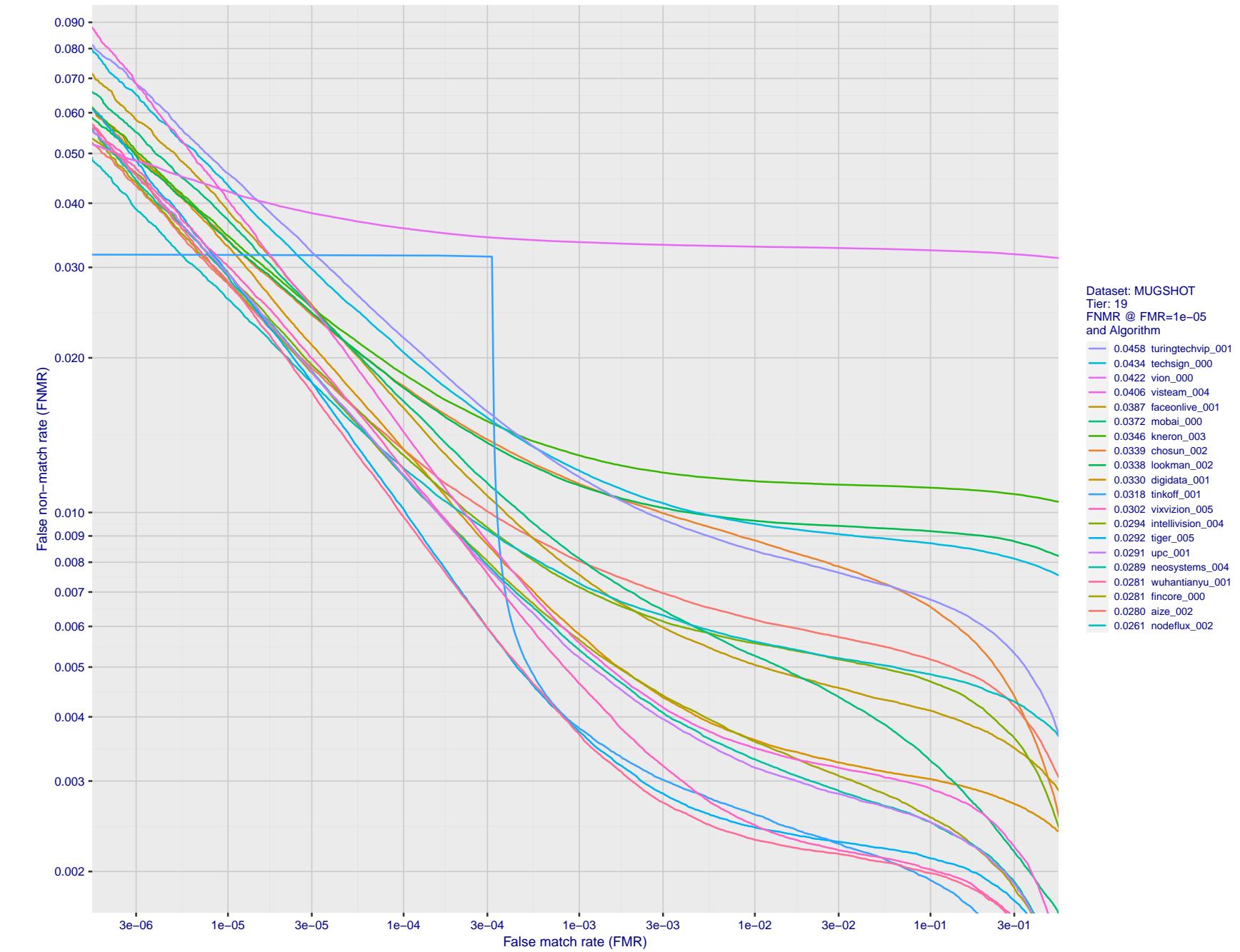


Figure 105: For the mugshot images, detection error tradeoff (DET) characteristics showing false non-match rate vs. false match rate plotted parametrically on threshold, T . The scales are logarithmic in order to show decades of FMR.

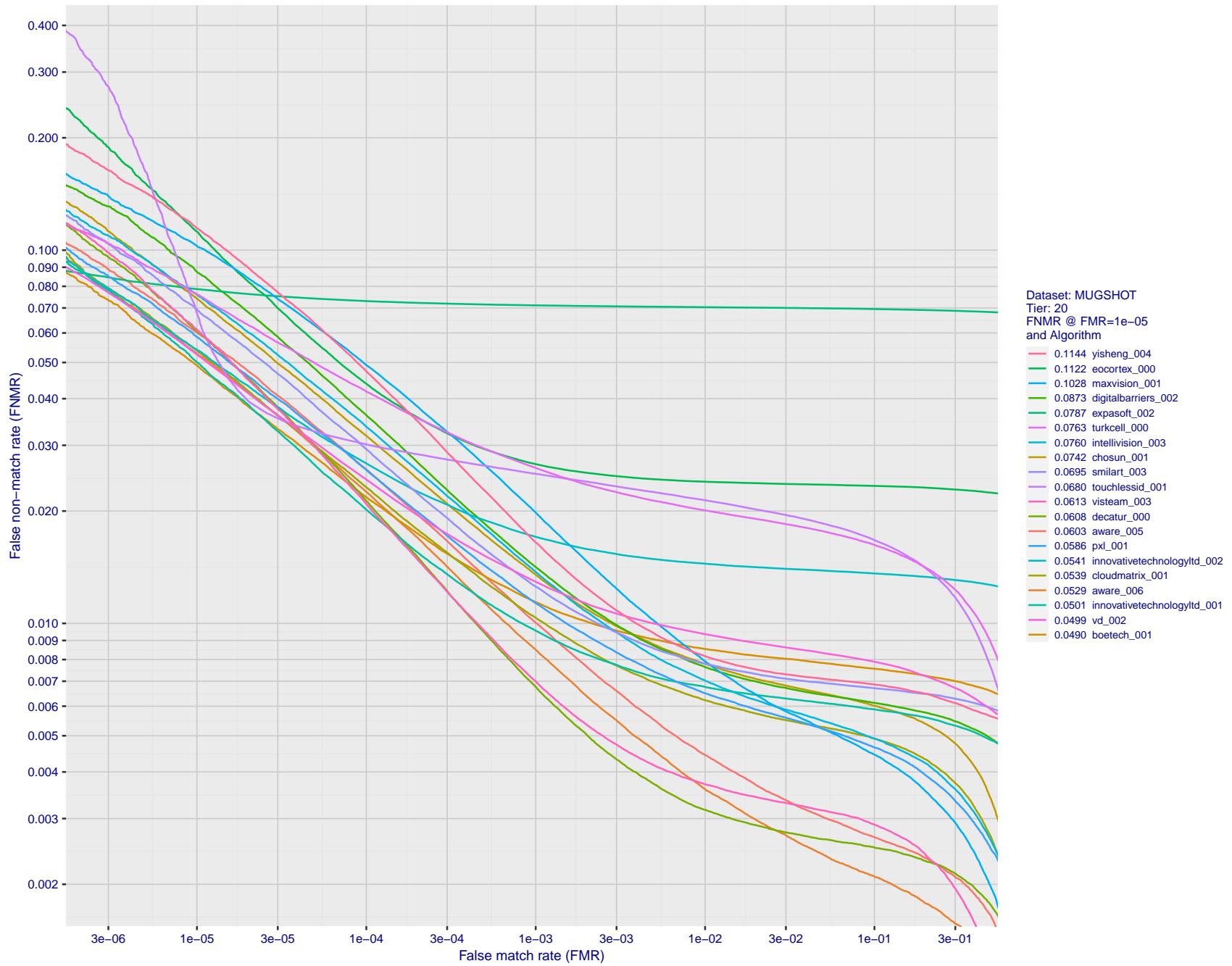


Figure 106: For the mugshot images, detection error tradeoff (DET) characteristics showing false non-match rate vs. false match rate plotted parametrically on threshold, T . The scales are logarithmic in order to show decades of FMR.

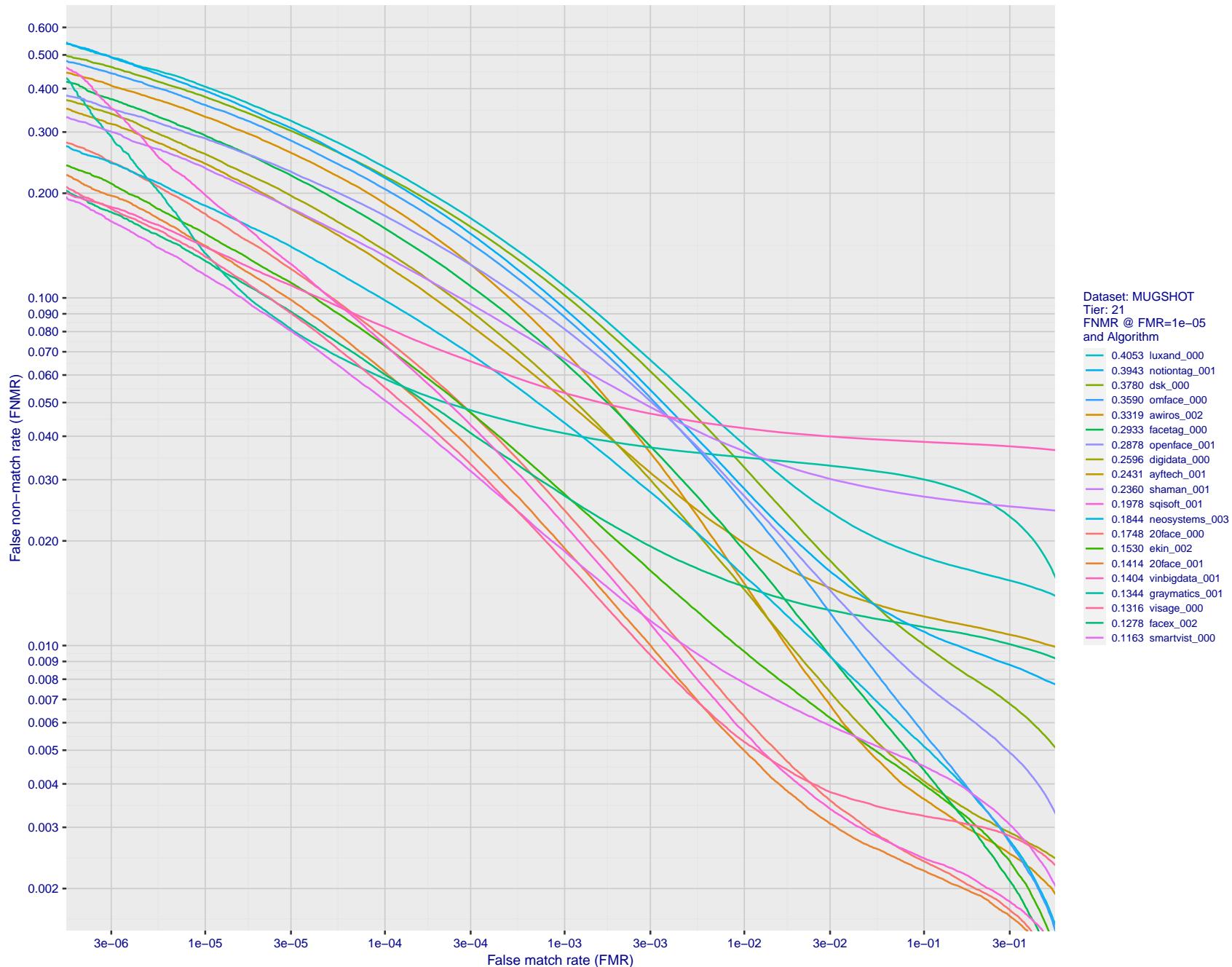


Figure 107: For the mugshot images, detection error tradeoff (DET) characteristics showing false non-match rate vs. false match rate plotted parametrically on threshold, T . The scales are logarithmic in order to show decades of FMR.

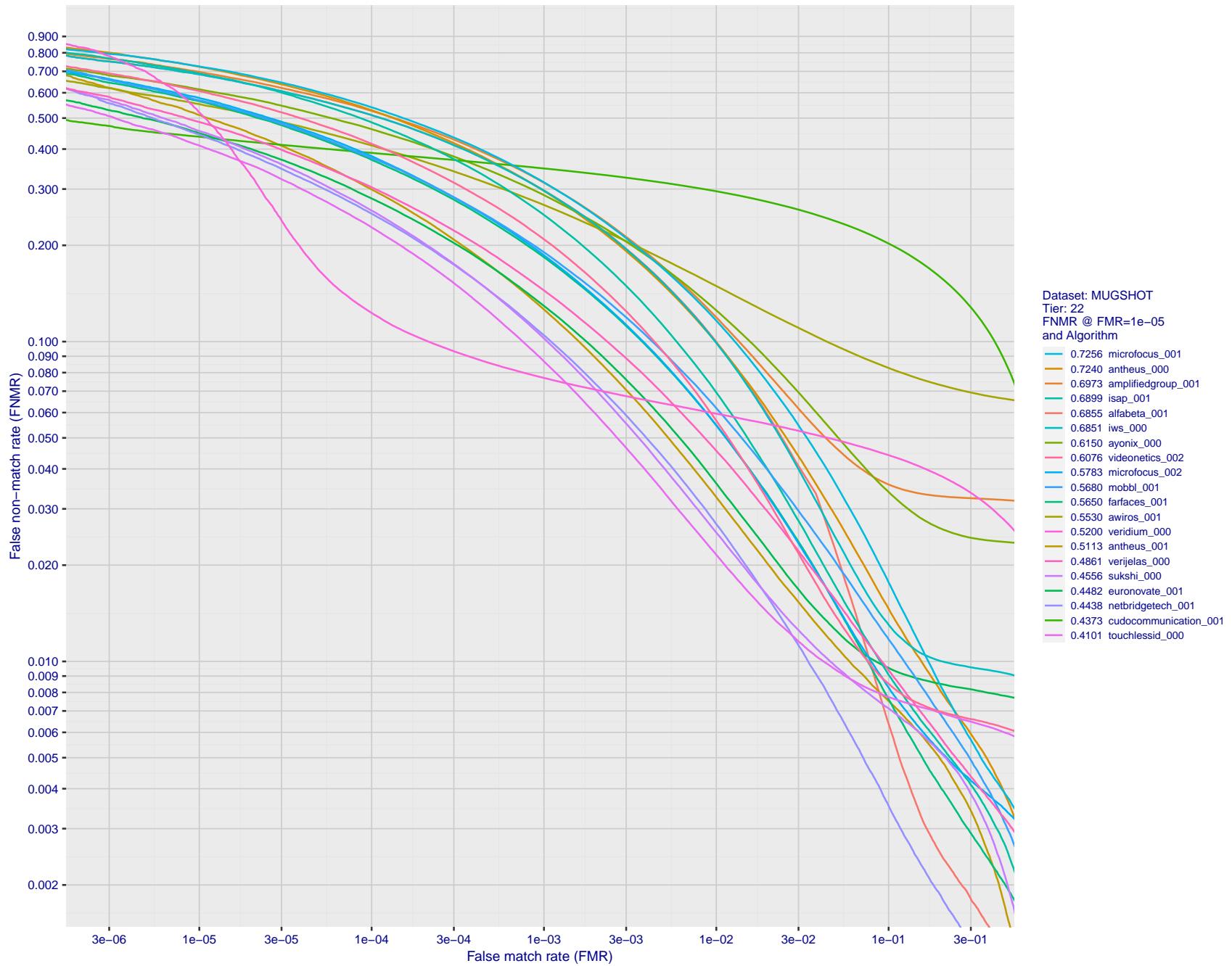


Figure 108: For the mugshot images, detection error tradeoff (DET) characteristics showing false non-match rate vs. false match rate plotted parametrically on threshold, T. The scales are logarithmic in order to show decades of FMR.

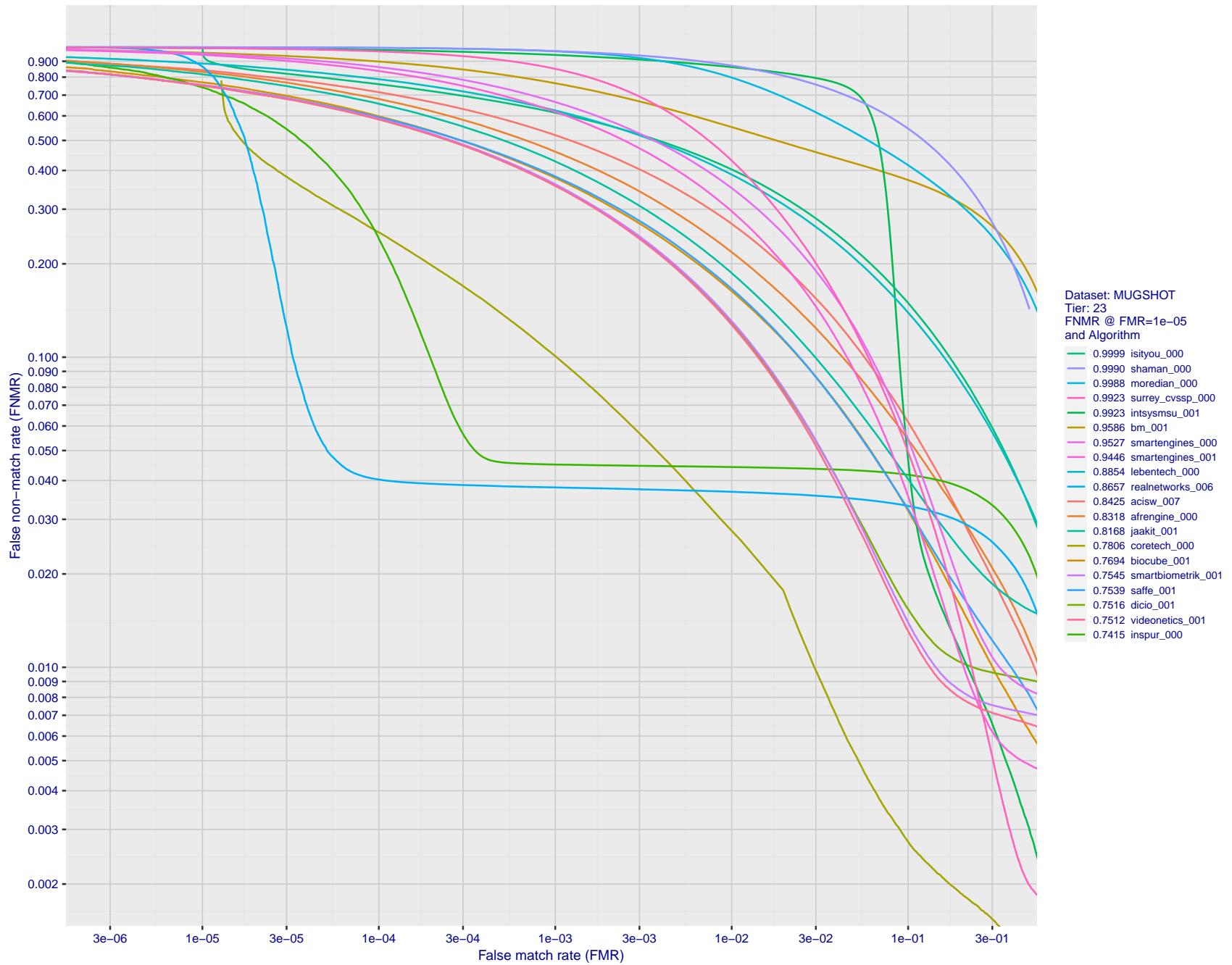


Figure 109: For the mugshot images, detection error tradeoff (DET) characteristics showing false non-match rate vs. false match rate plotted parametrically on threshold, T . The scales are logarithmic in order to show decades of FMR.

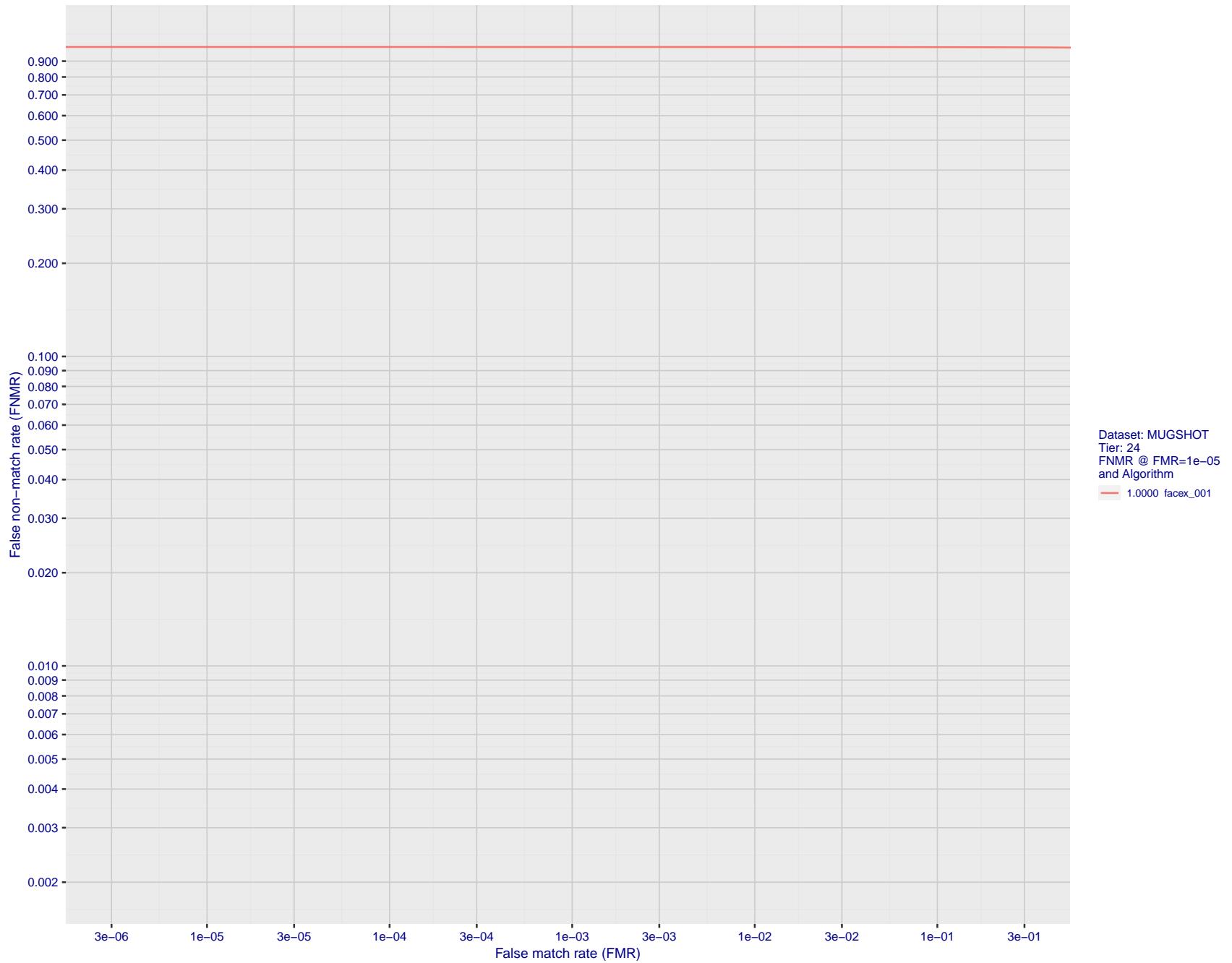


Figure 110: For the mugshot images, detection error tradeoff (DET) characteristics showing false non-match rate vs. false match rate plotted parametrically on threshold, T . The scales are logarithmic in order to show decades of FMR.

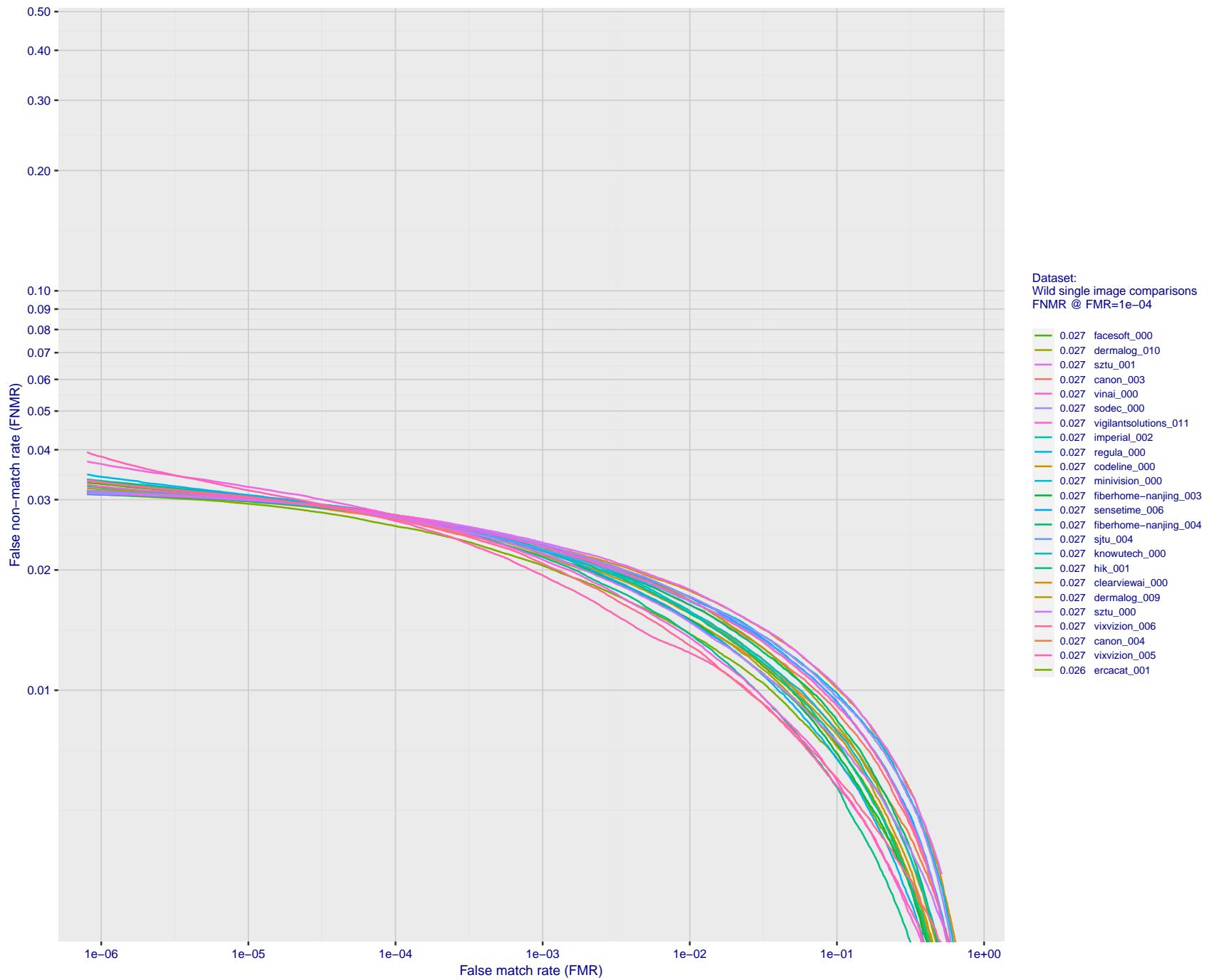


Figure 111: For the 2018 wild image comparisons, detection error tradeoff (DET) characteristics showing false non-match rate vs. false match rate plotted parametrically on threshold, T . The scales are logarithmic in order to show several decades of FMR.

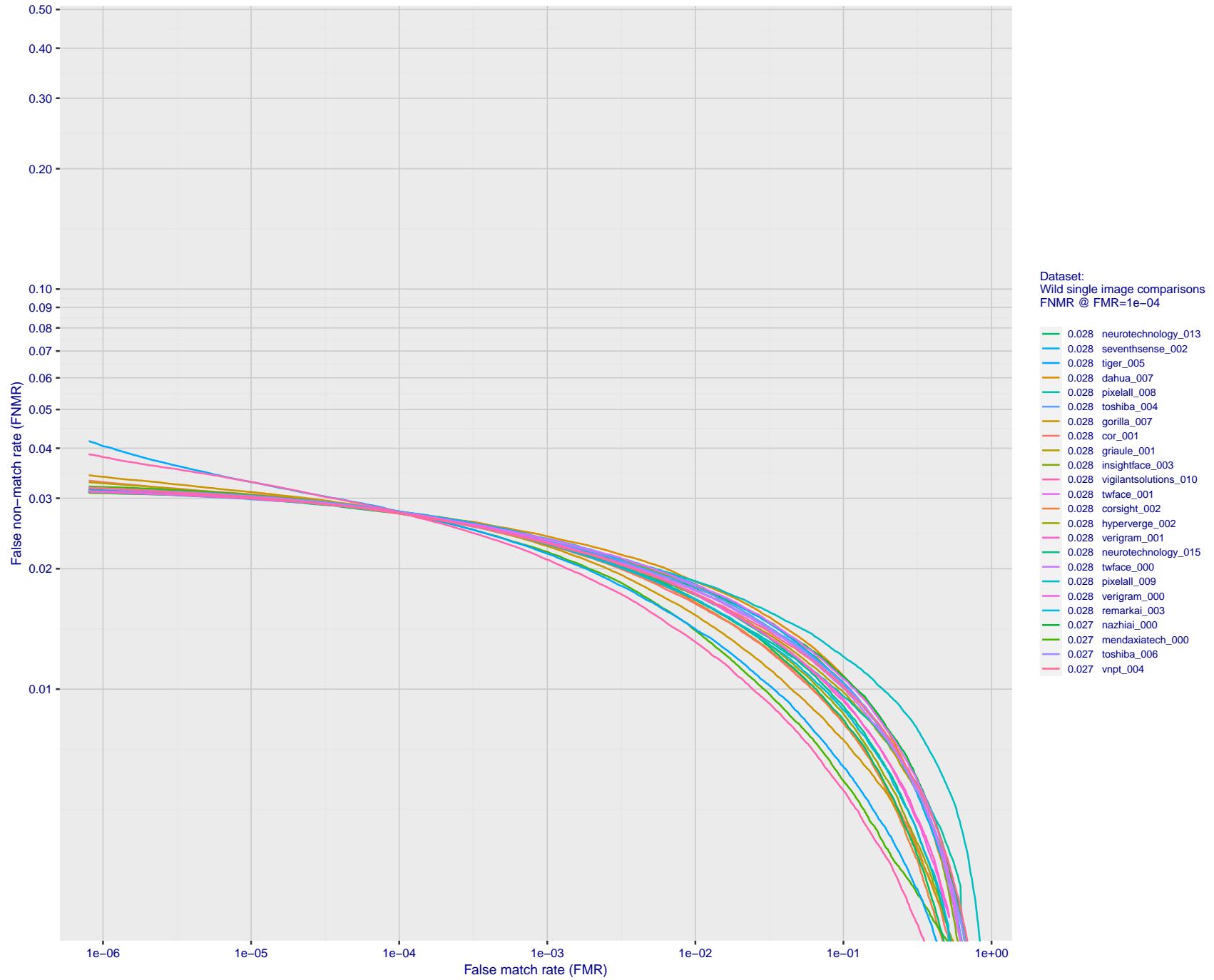


Figure 112: For the 2018 wild image comparisons, detection error tradeoff (DET) characteristics showing false non-match rate vs. false match rate plotted parametrically on threshold, T . The scales are logarithmic in order to show several decades of FMR.

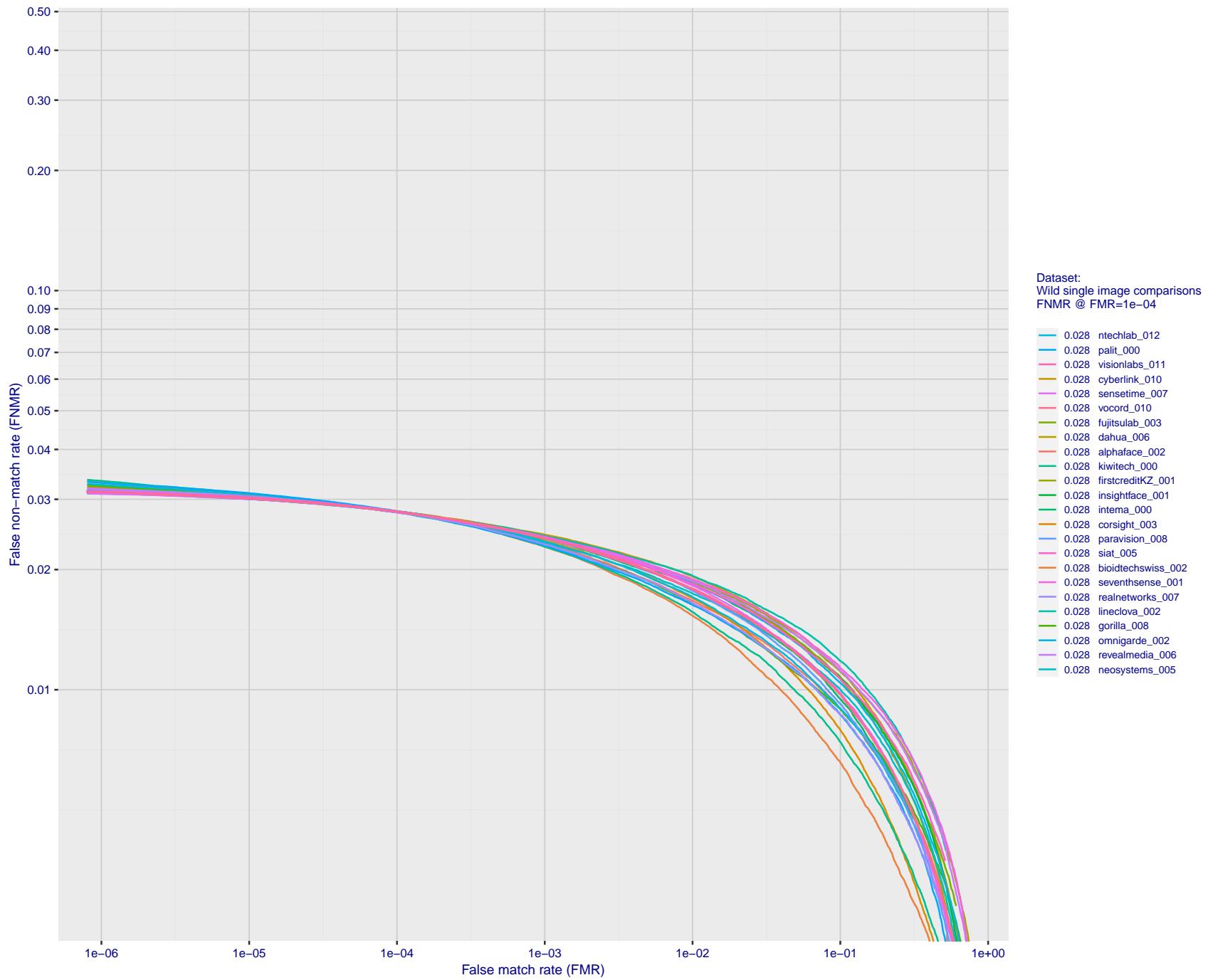


Figure 113: For the 2018 wild image comparisons, detection error tradeoff (DET) characteristics showing false non-match rate vs. false match rate plotted parametrically on threshold, T. The scales are logarithmic in order to show several decades of FMR.

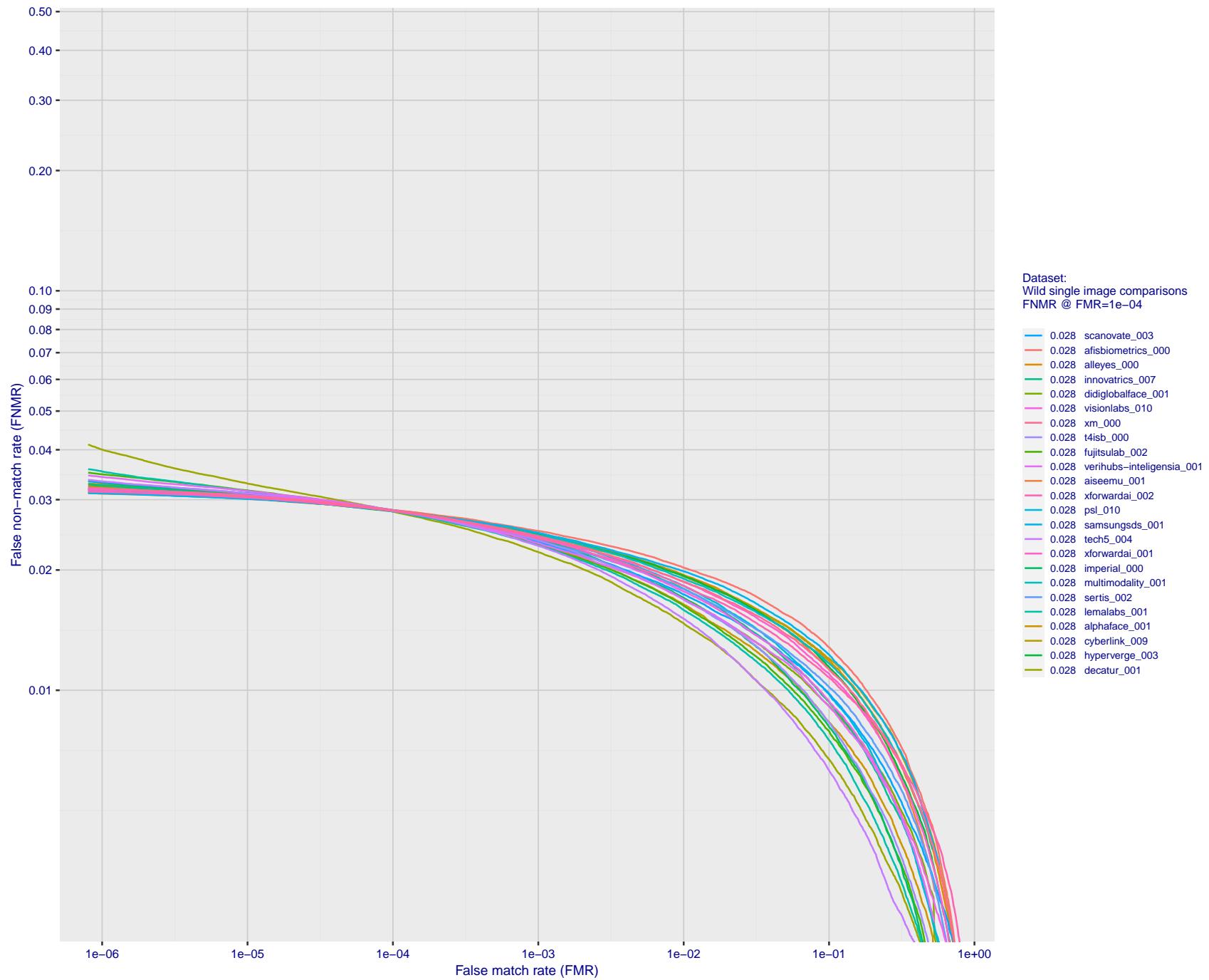


Figure 114: For the 2018 wild image comparisons, detection error tradeoff (DET) characteristics showing false non-match rate vs. false match rate plotted parametrically on threshold, T . The scales are logarithmic in order to show several decades of FMR.

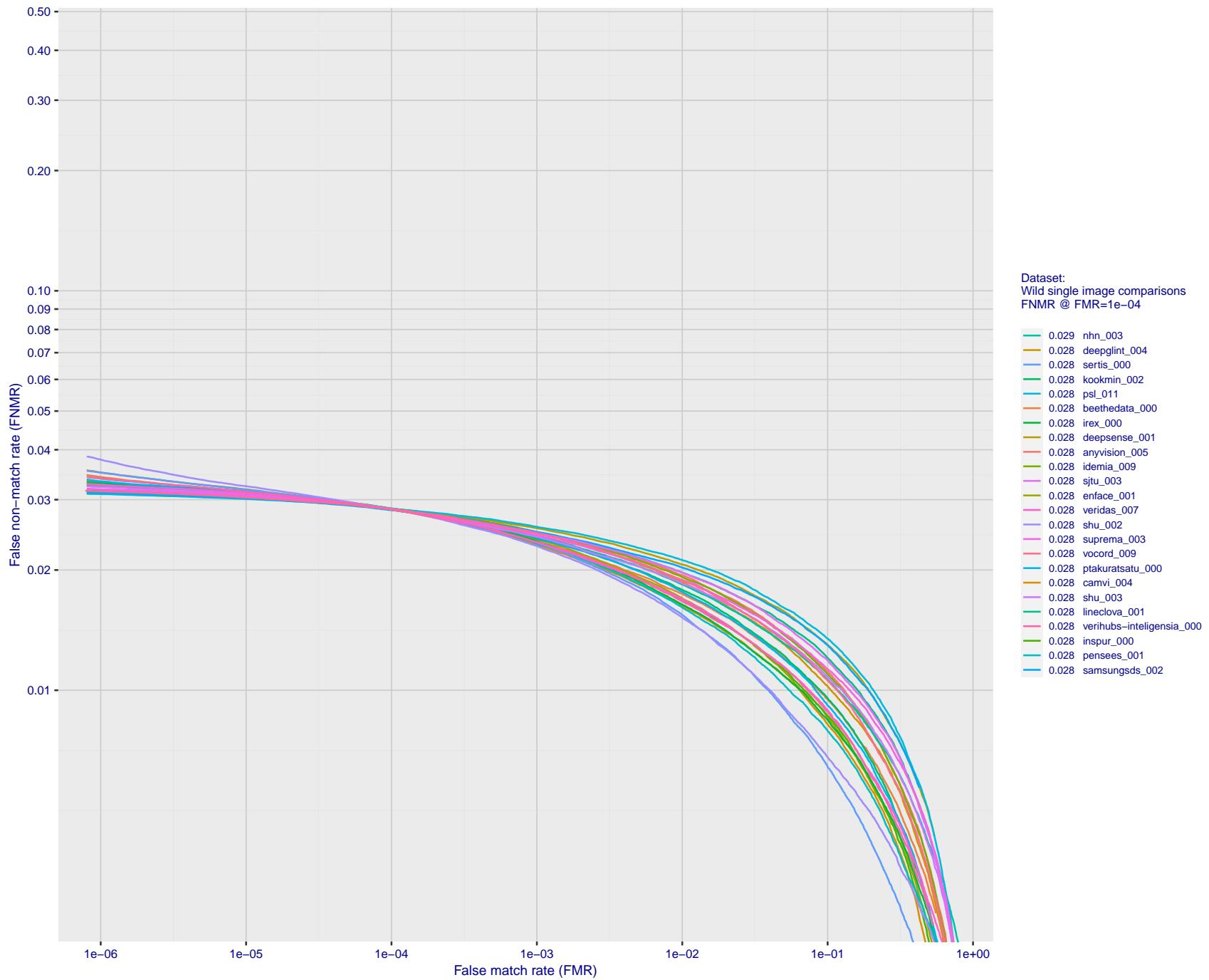


Figure 115: For the 2018 wild image comparisons, detection error tradeoff (DET) characteristics showing false non-match rate vs. false match rate plotted parametrically on threshold, T . The scales are logarithmic in order to show several decades of FMR.

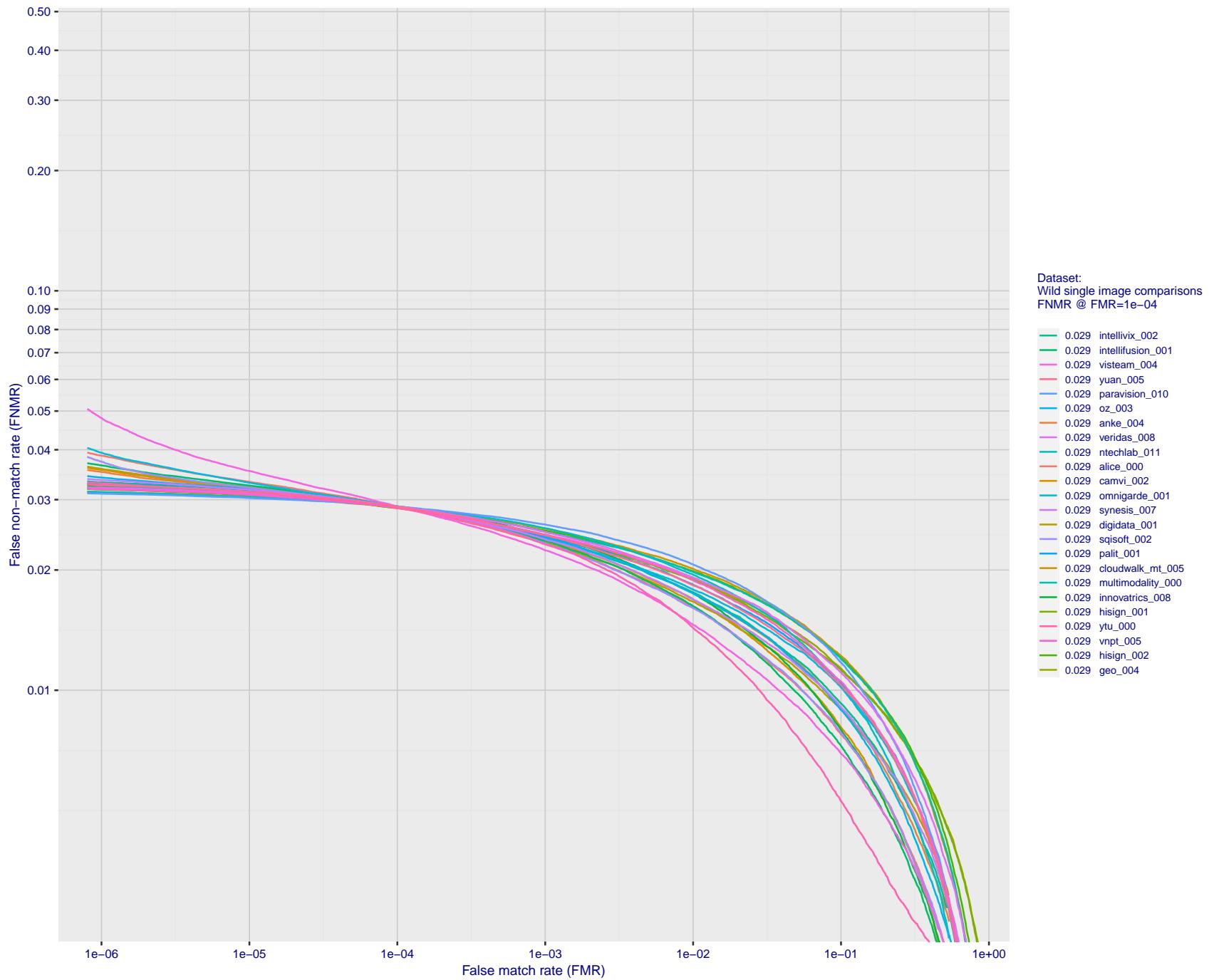


Figure 116: For the 2018 wild image comparisons, detection error tradeoff (DET) characteristics showing false non-match rate vs. false match rate plotted parametrically on threshold, T . The scales are logarithmic in order to show several decades of FMR.

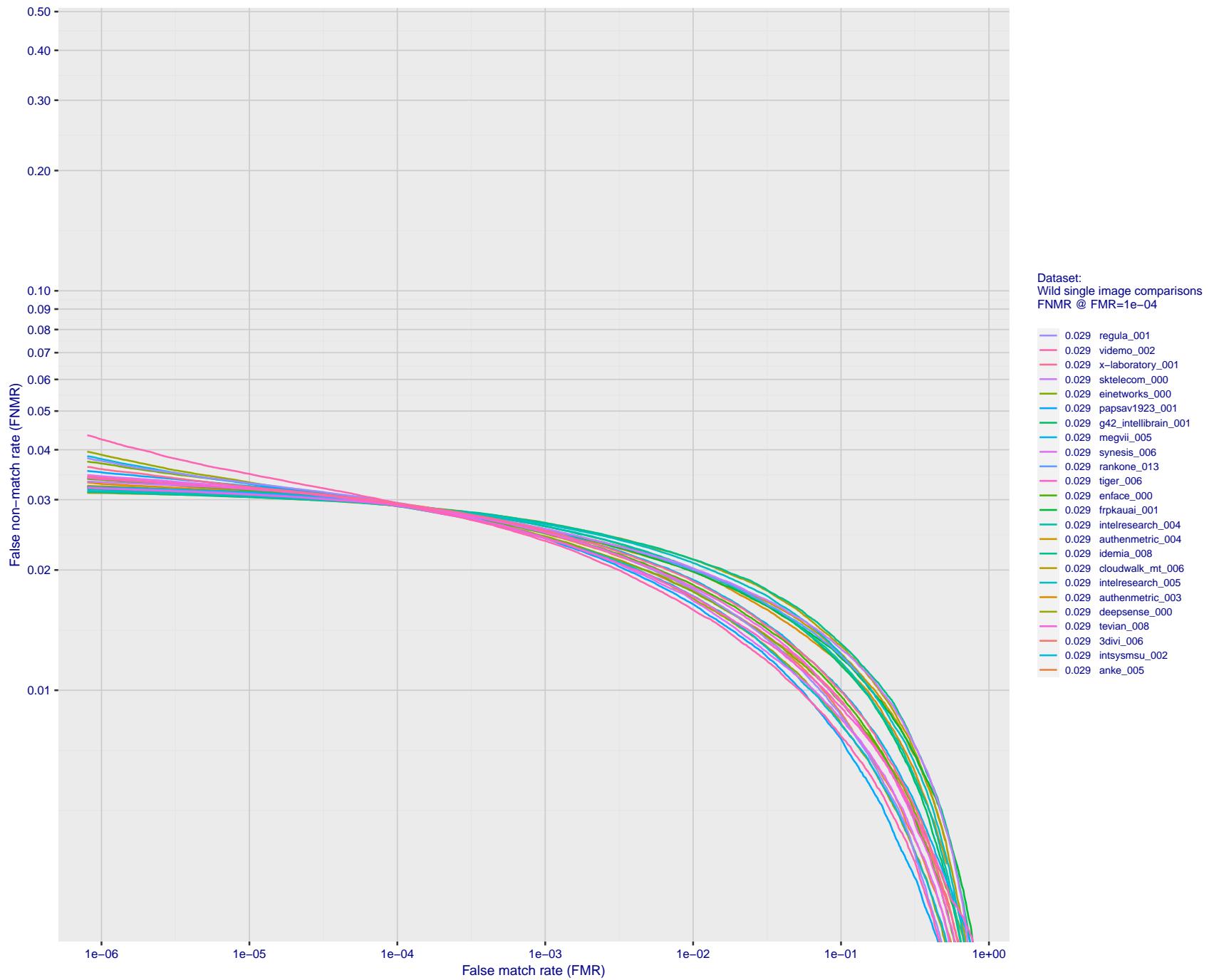


Figure 117: For the 2018 wild image comparisons, detection error tradeoff (DET) characteristics showing false non-match rate vs. false match rate plotted parametrically on threshold, T. The scales are logarithmic in order to show several decades of FMR.

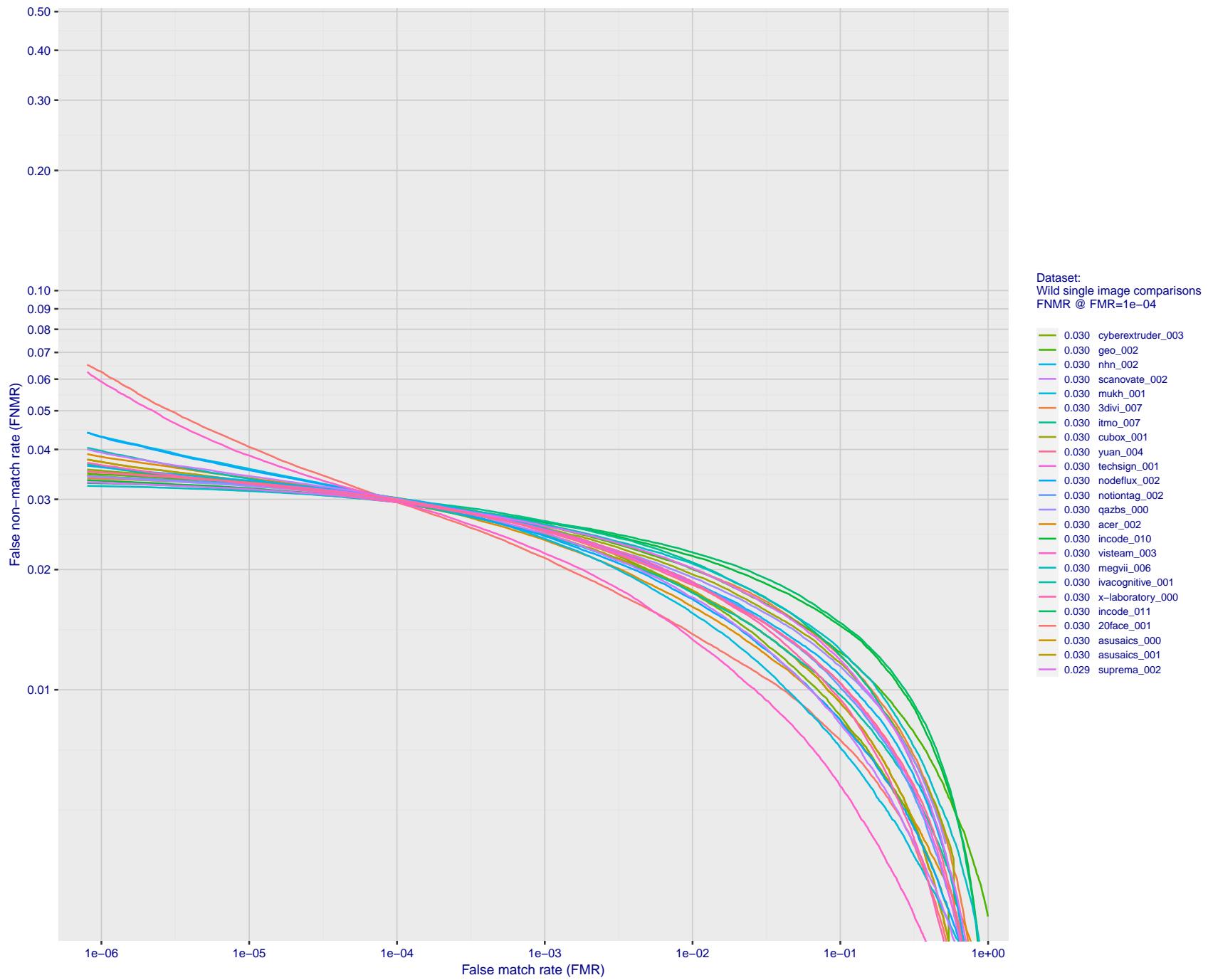


Figure 118: For the 2018 wild image comparisons, detection error tradeoff (DET) characteristics showing false non-match rate vs. false match rate plotted parametrically on threshold, T . The scales are logarithmic in order to show several decades of FMR.

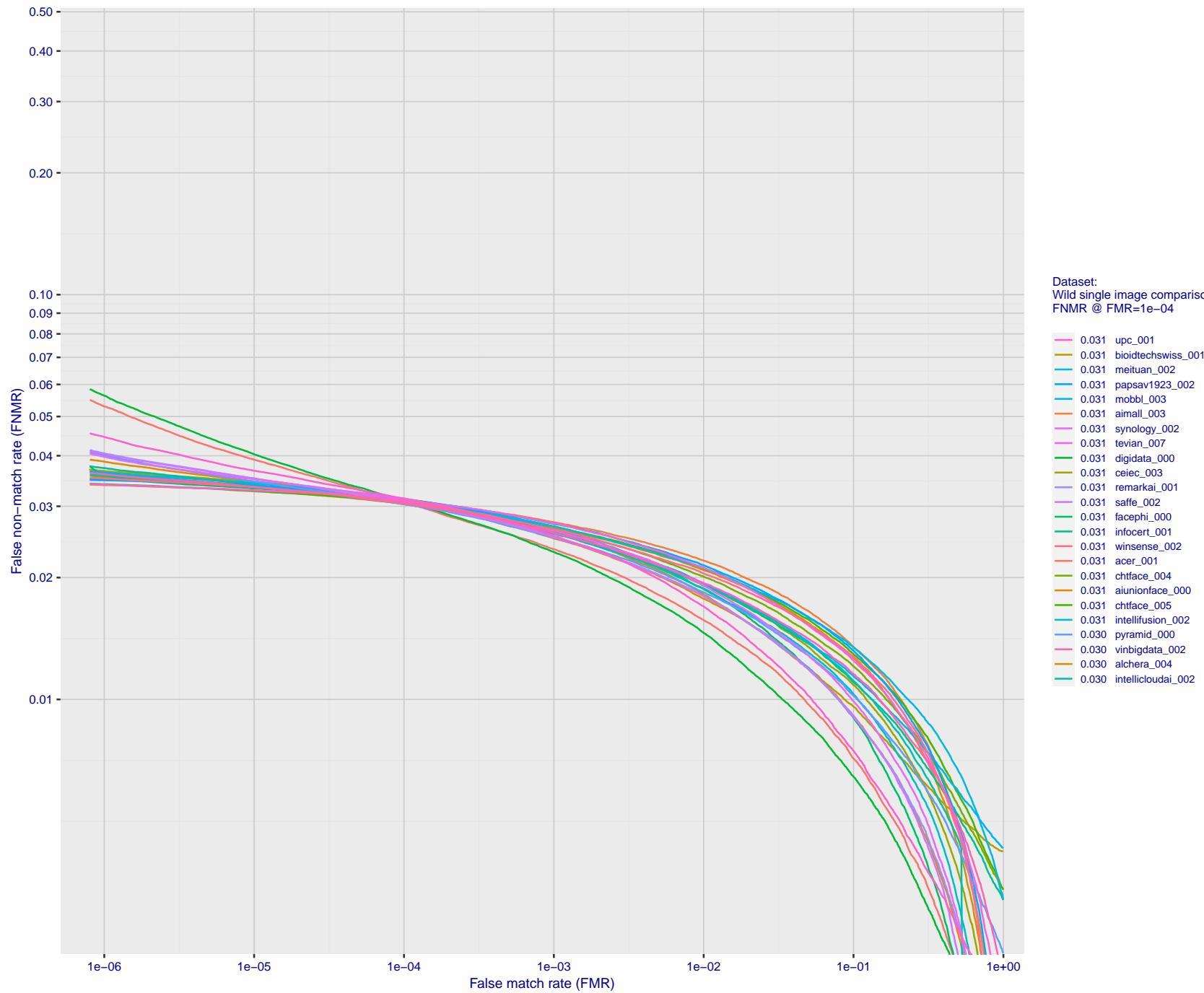


Figure 119: For the 2018 wild image comparisons, detection error tradeoff (DET) characteristics showing false non-match rate vs. false match rate plotted parametrically on threshold, T. The scales are logarithmic in order to show several decades of FMR.

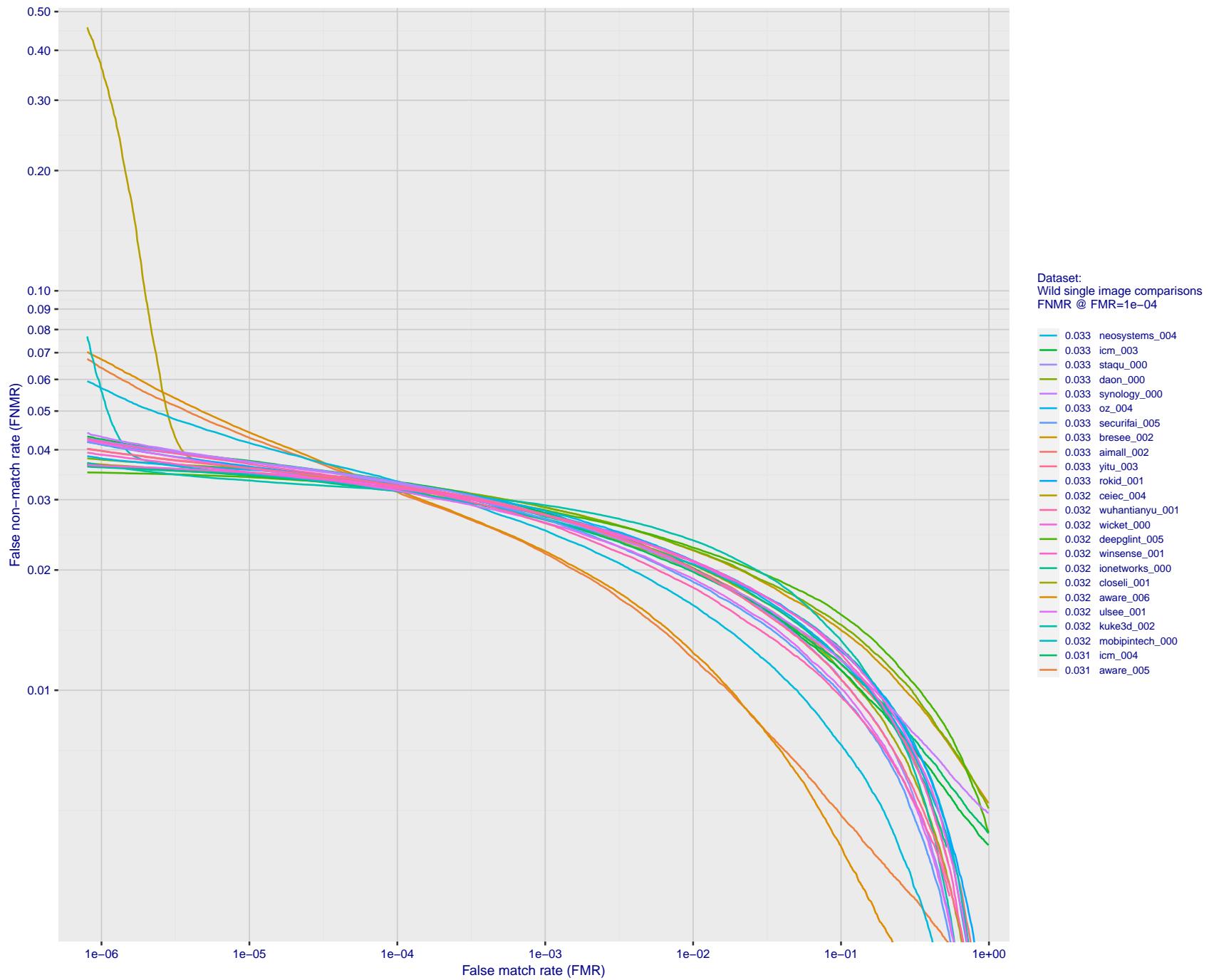


Figure 120: For the 2018 wild image comparisons, detection error tradeoff (DET) characteristics showing false non-match rate vs. false match rate plotted parametrically on threshold, T . The scales are logarithmic in order to show several decades of FMR.

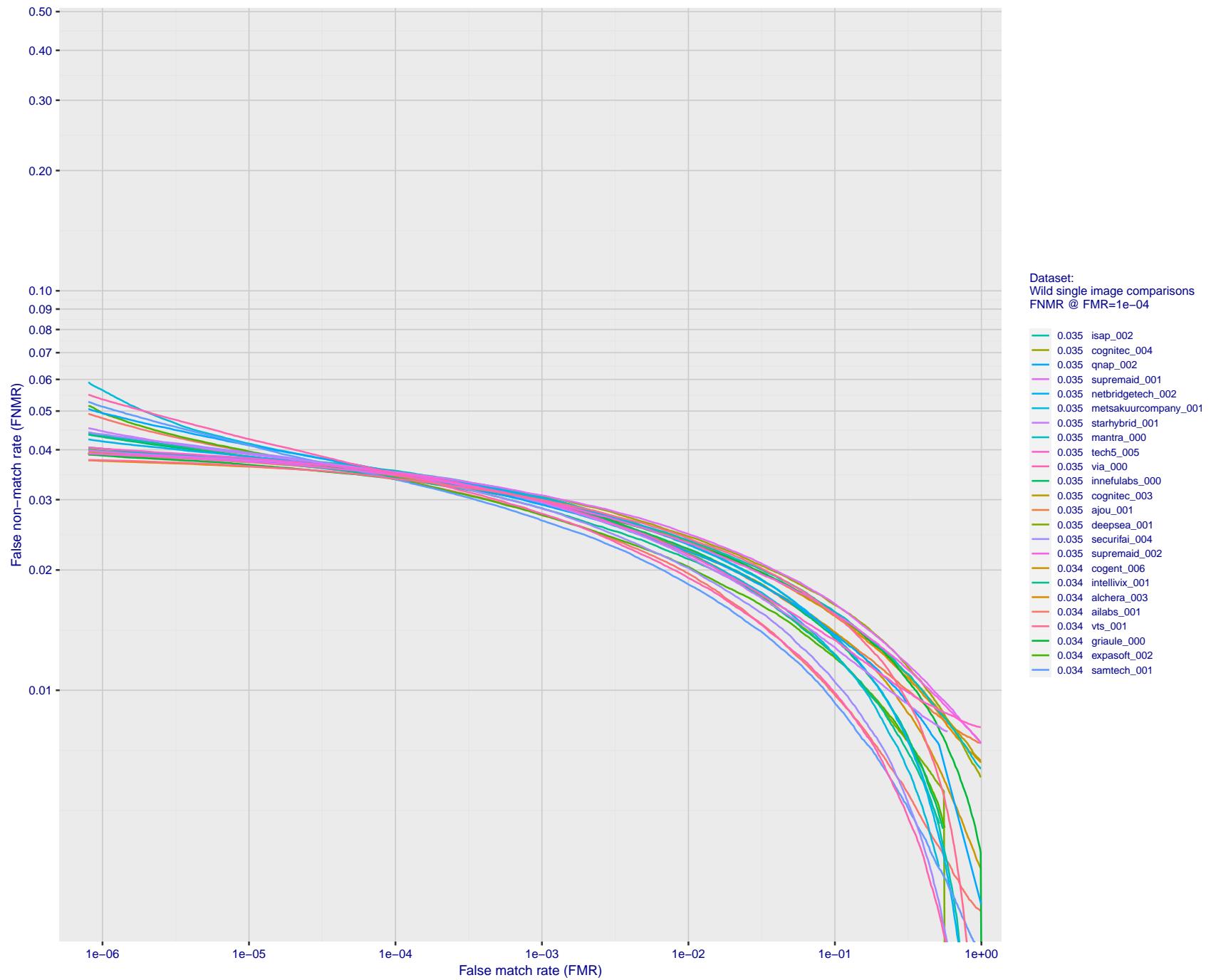


Figure 121: For the 2018 wild image comparisons, detection error tradeoff (DET) characteristics showing false non-match rate vs. false match rate plotted parametrically on threshold, T . The scales are logarithmic in order to show several decades of FMR.

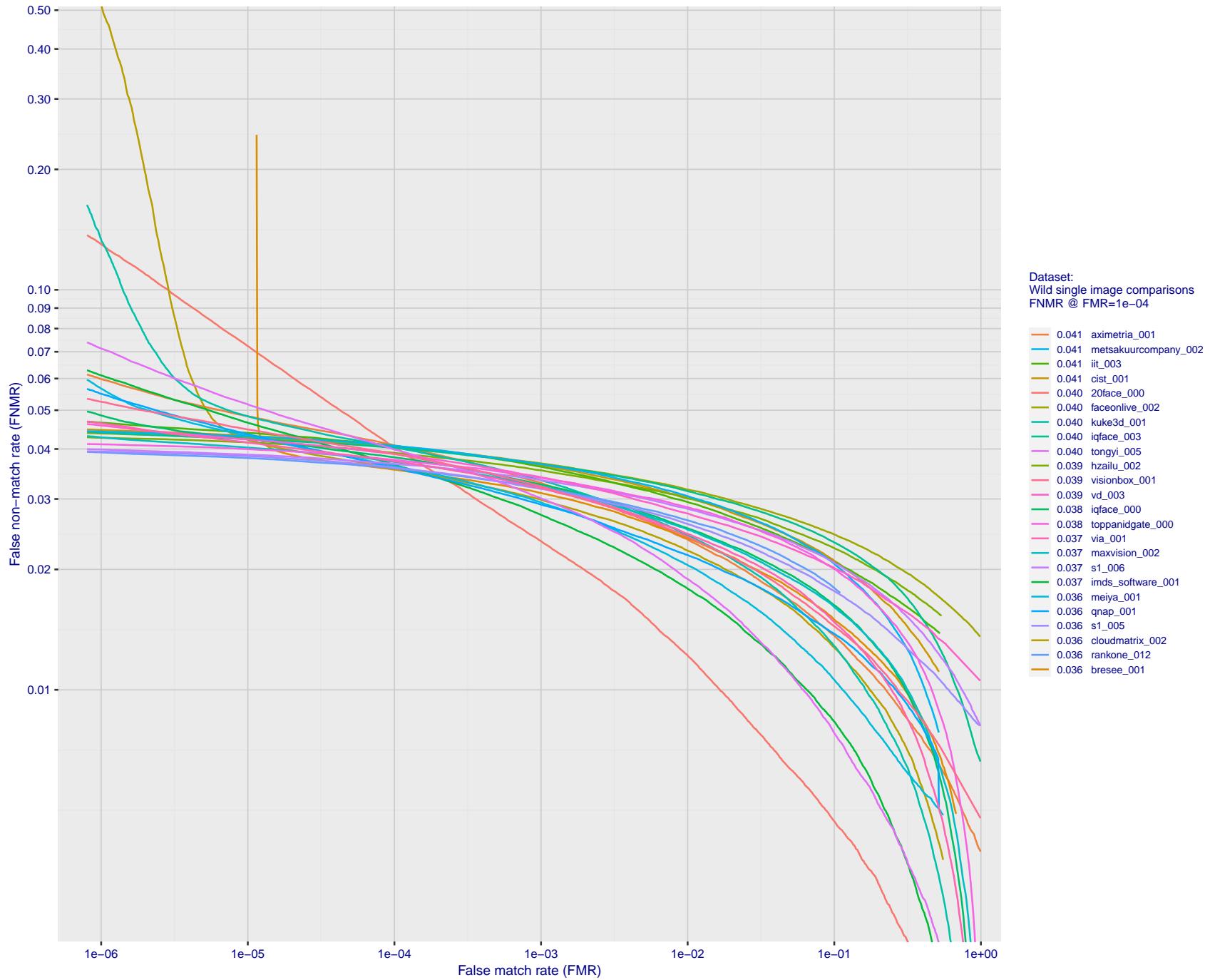


Figure 122: For the 2018 wild image comparisons, detection error tradeoff (DET) characteristics showing false non-match rate vs. false match rate plotted parametrically on threshold, T. The scales are logarithmic in order to show several decades of FMR.

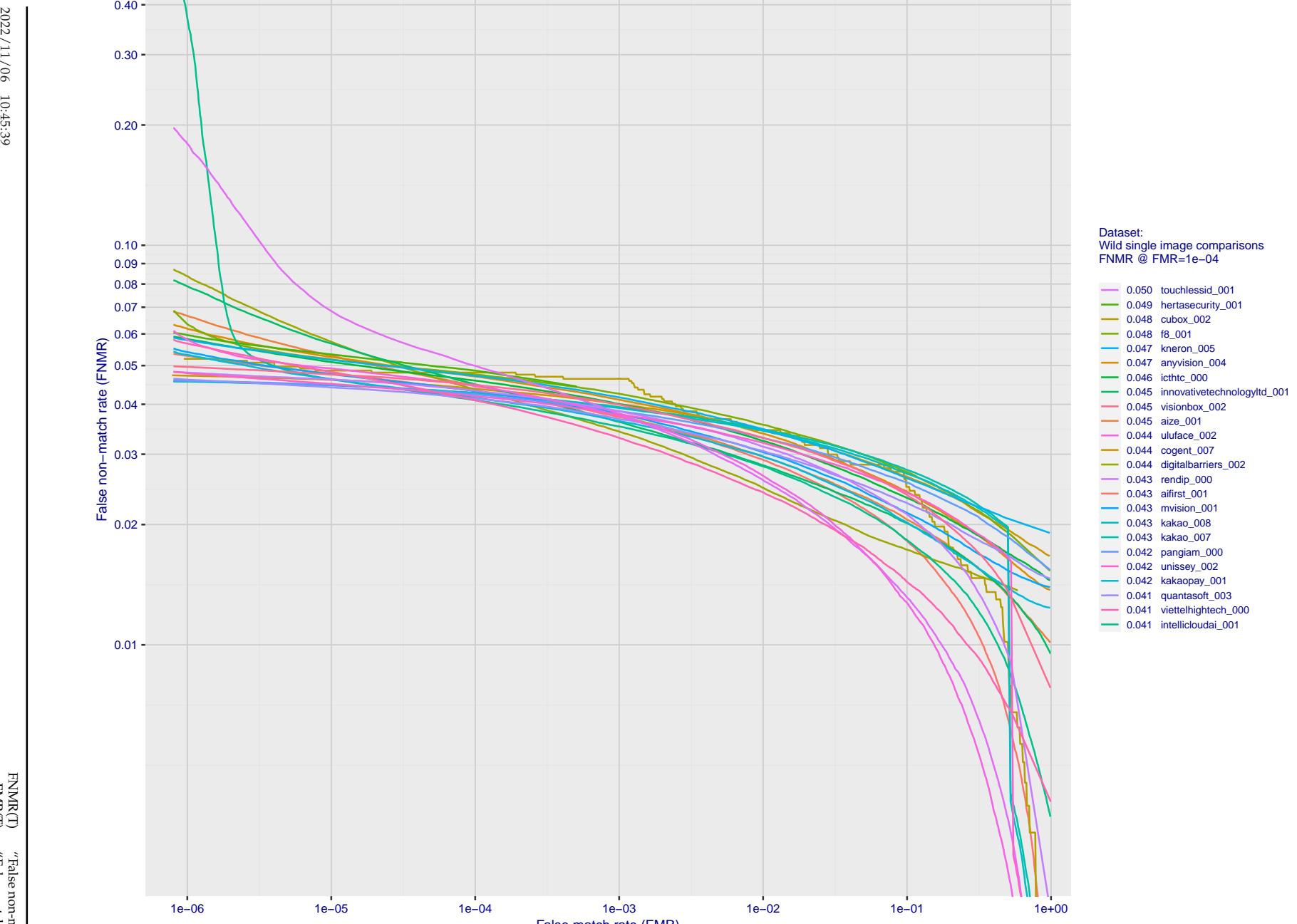


Figure 123: For the 2018 wild image comparisons, detection error tradeoff (DET) characteristics showing false non-match rate vs. false match rate plotted parametrically on threshold, T . The scales are logarithmic in order to show several decades of FMR.

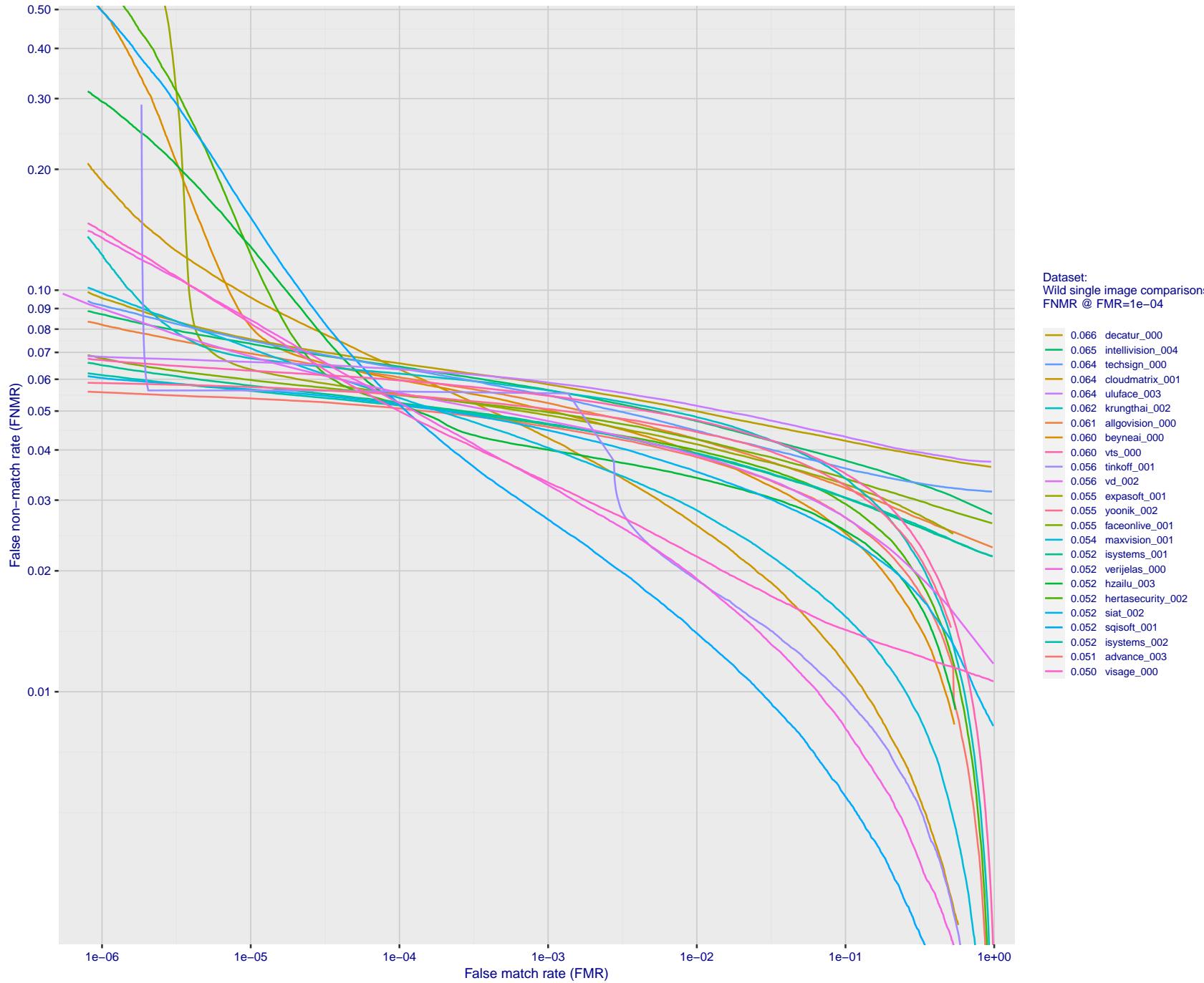


Figure 124: For the 2018 wild image comparisons, detection error tradeoff (DET) characteristics showing false non-match rate vs. false match rate plotted parametrically on threshold, T . The scales are logarithmic in order to show several decades of FMR.

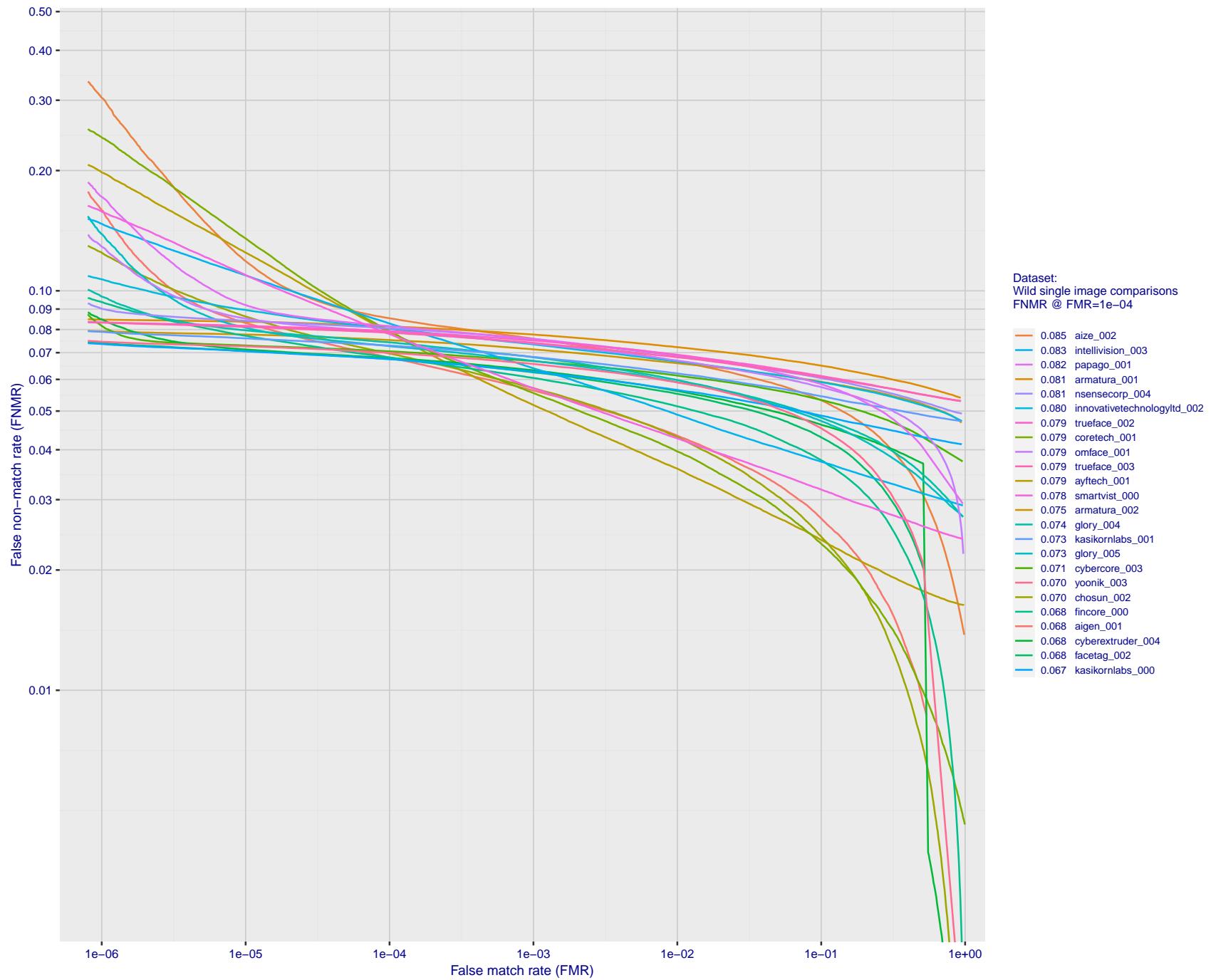


Figure 125: For the 2018 wild image comparisons, detection error tradeoff (DET) characteristics showing false non-match rate vs. false match rate plotted parametrically on threshold, T . The scales are logarithmic in order to show several decades of FMR.

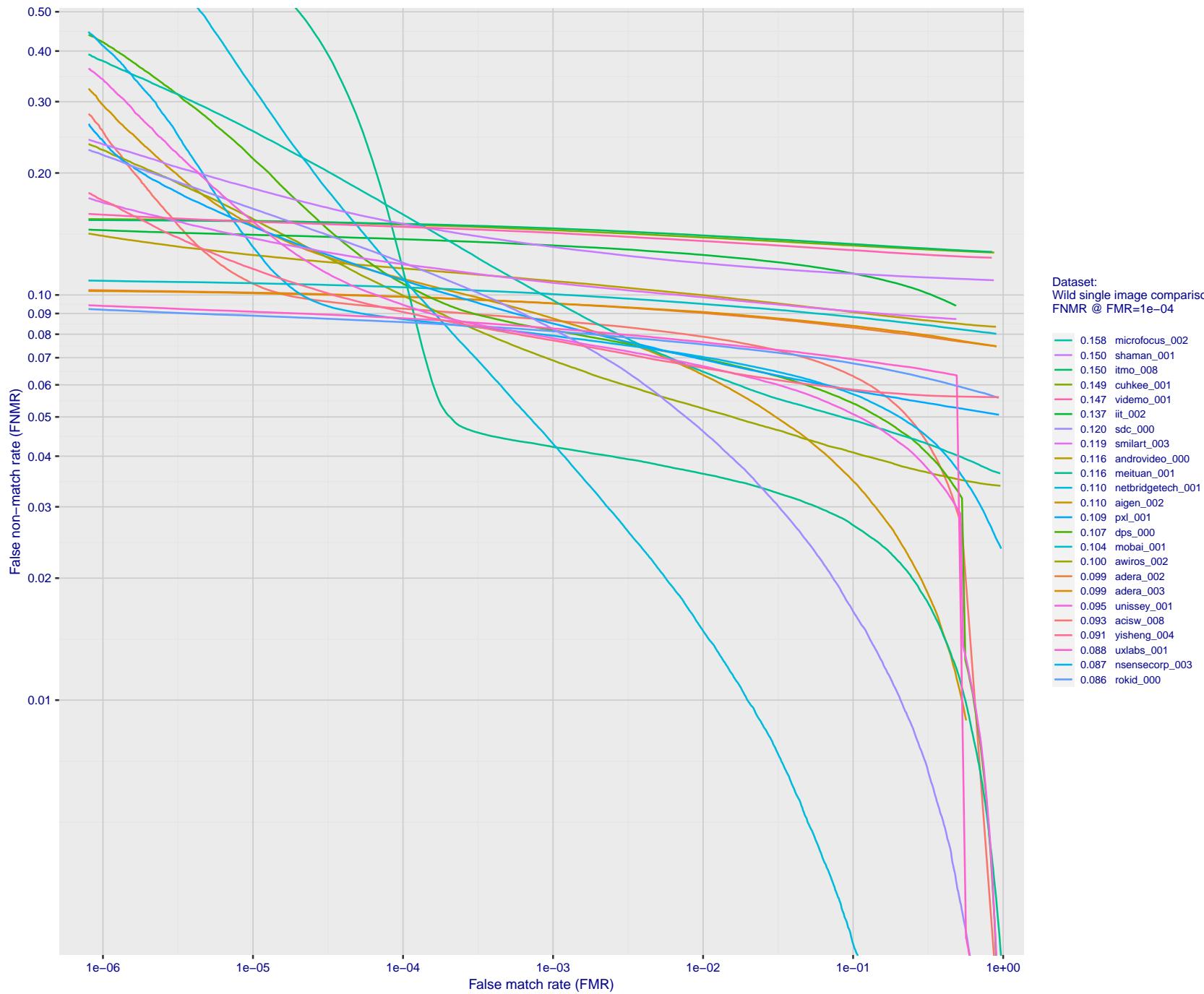
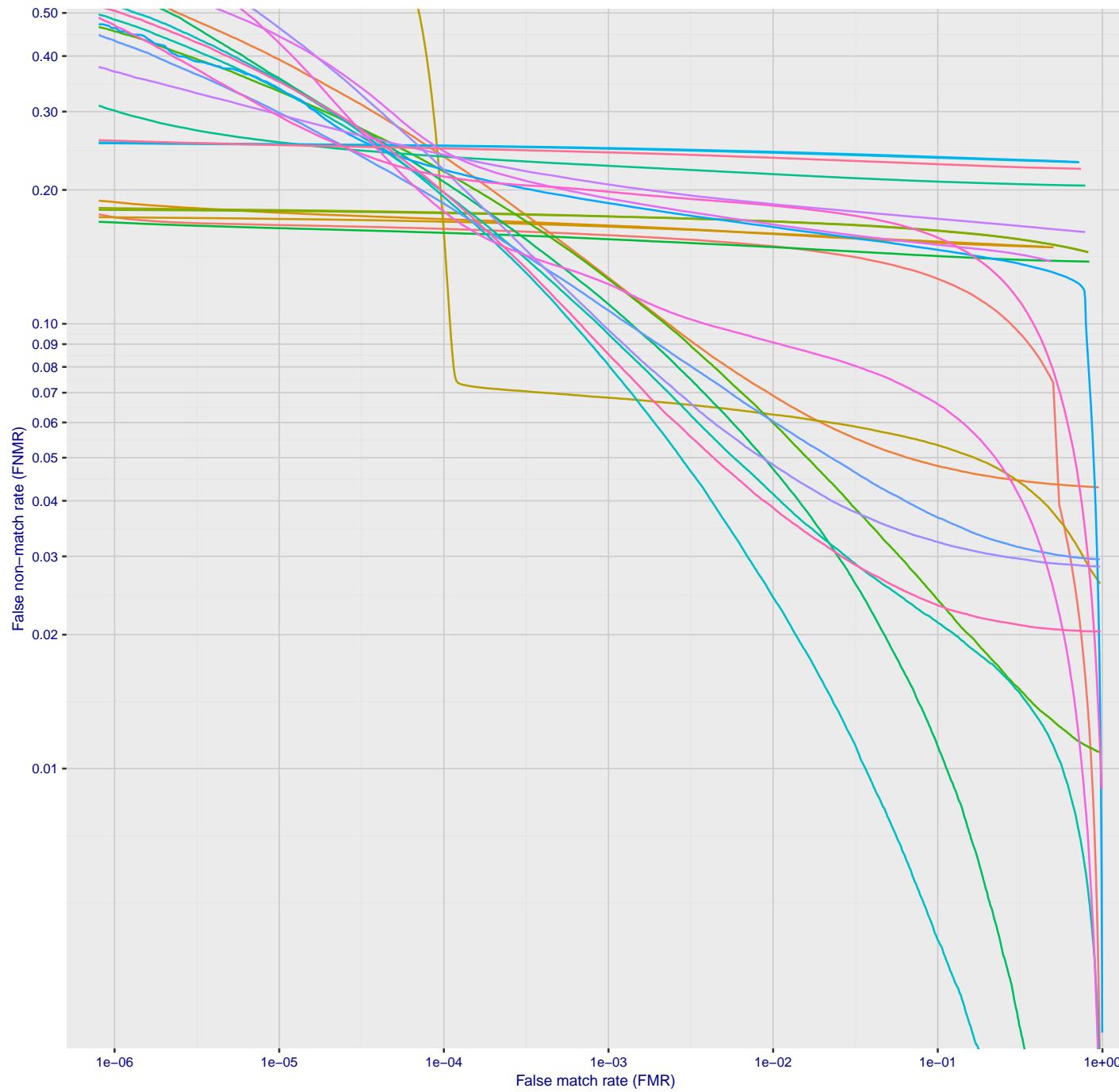


Figure 126: For the 2018 wild image comparisons, detection error tradeoff (DET) characteristics showing false non-match rate vs. false match rate plotted parametrically on threshold, T . The scales are logarithmic in order to show several decades of FMR.

2022/11/06 10:45:39



Dataset:
Wild single image comparisons
FNMR @ FMR=1e-04

Figure 127: For the 2018 wild image comparisons, detection error tradeoff (DET) characteristics showing false non-match rate vs. false match rate plotted parametrically on threshold, T . The scales are logarithmic in order to show several decades of FMR.

2022/11/06 10:45:39

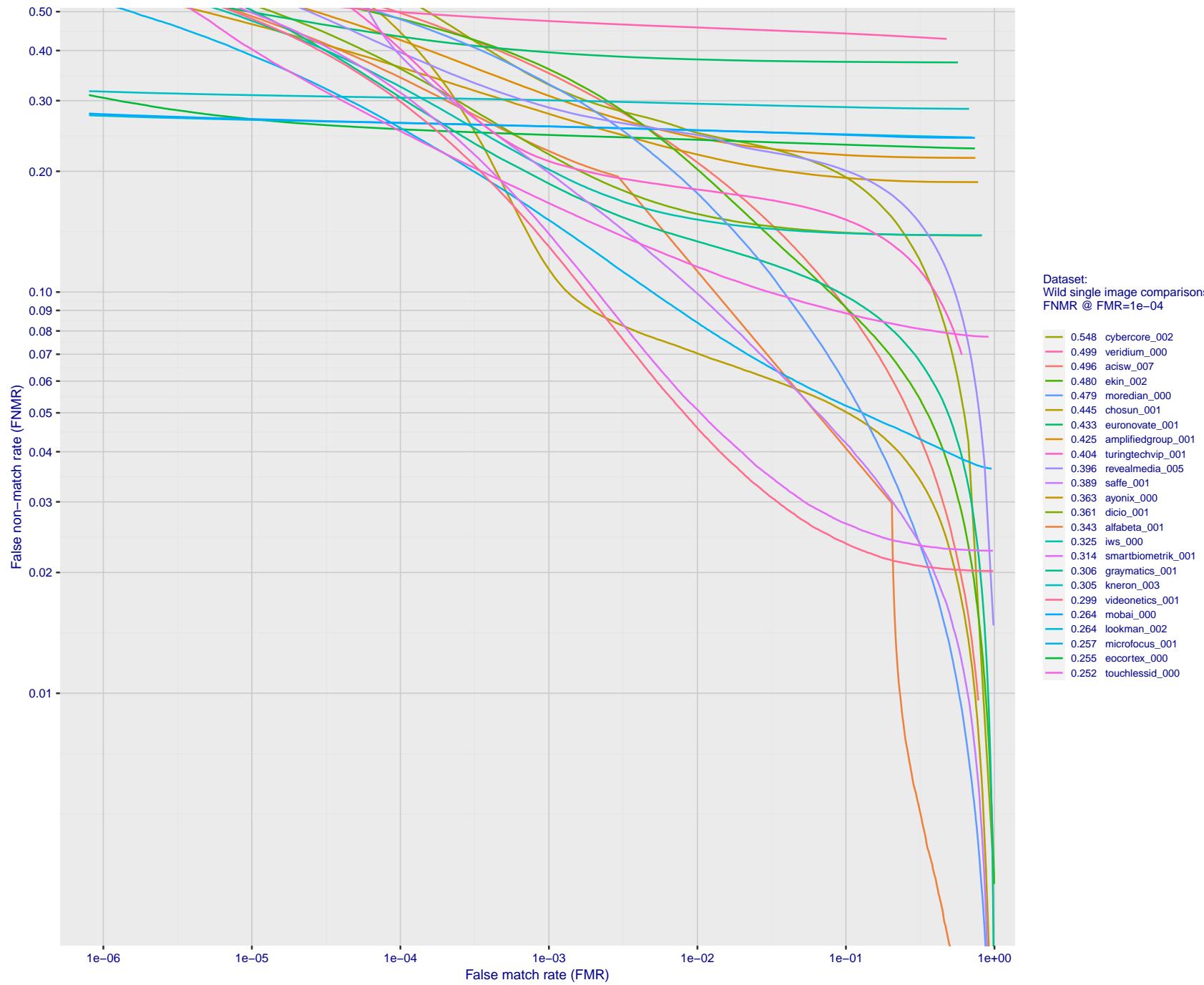


Figure 128: For the 2018 wild image comparisons, detection error tradeoff (DET) characteristics showing false non-match rate vs. false match rate plotted parametrically on threshold, T . The scales are logarithmic in order to show several decades of FMR.

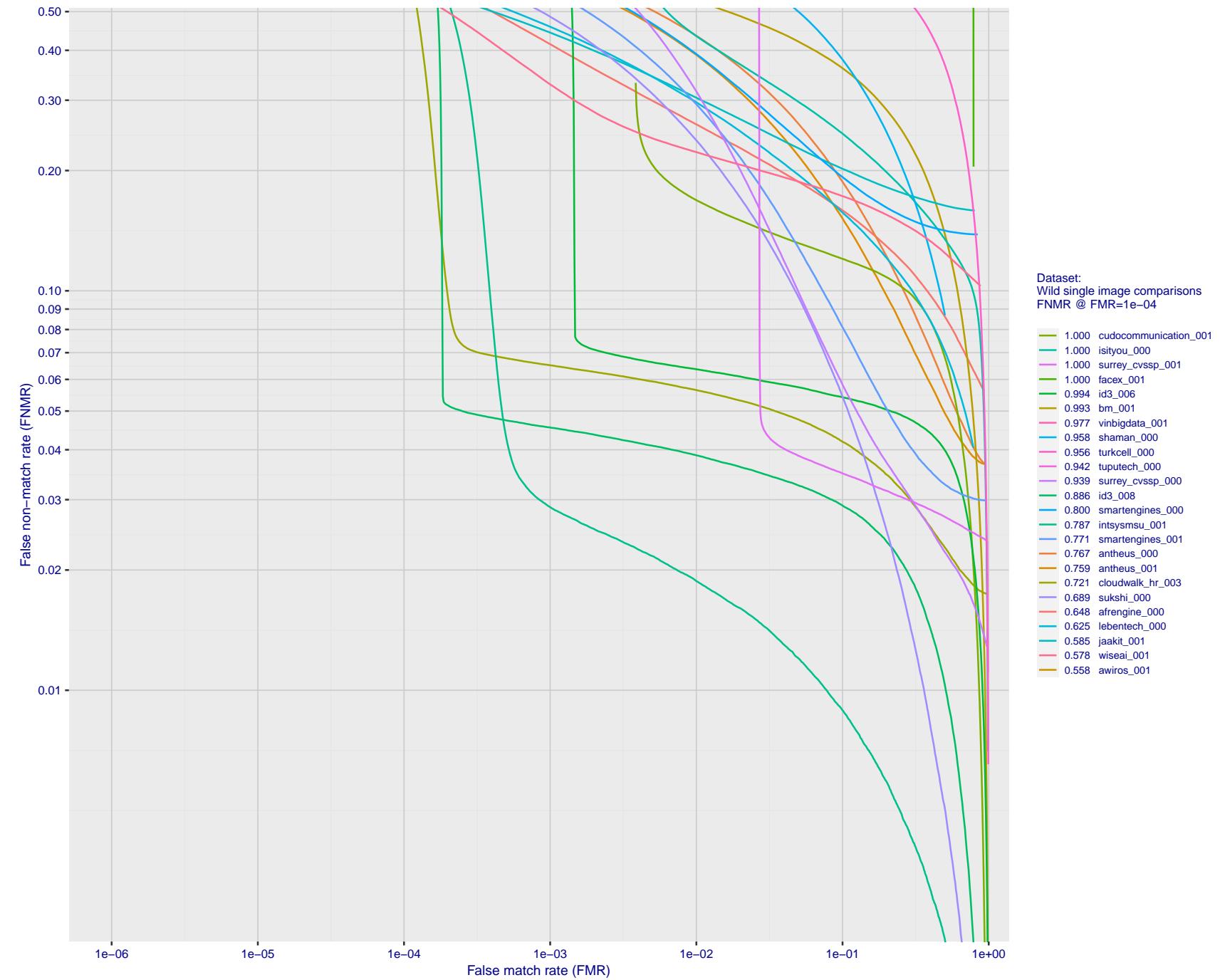
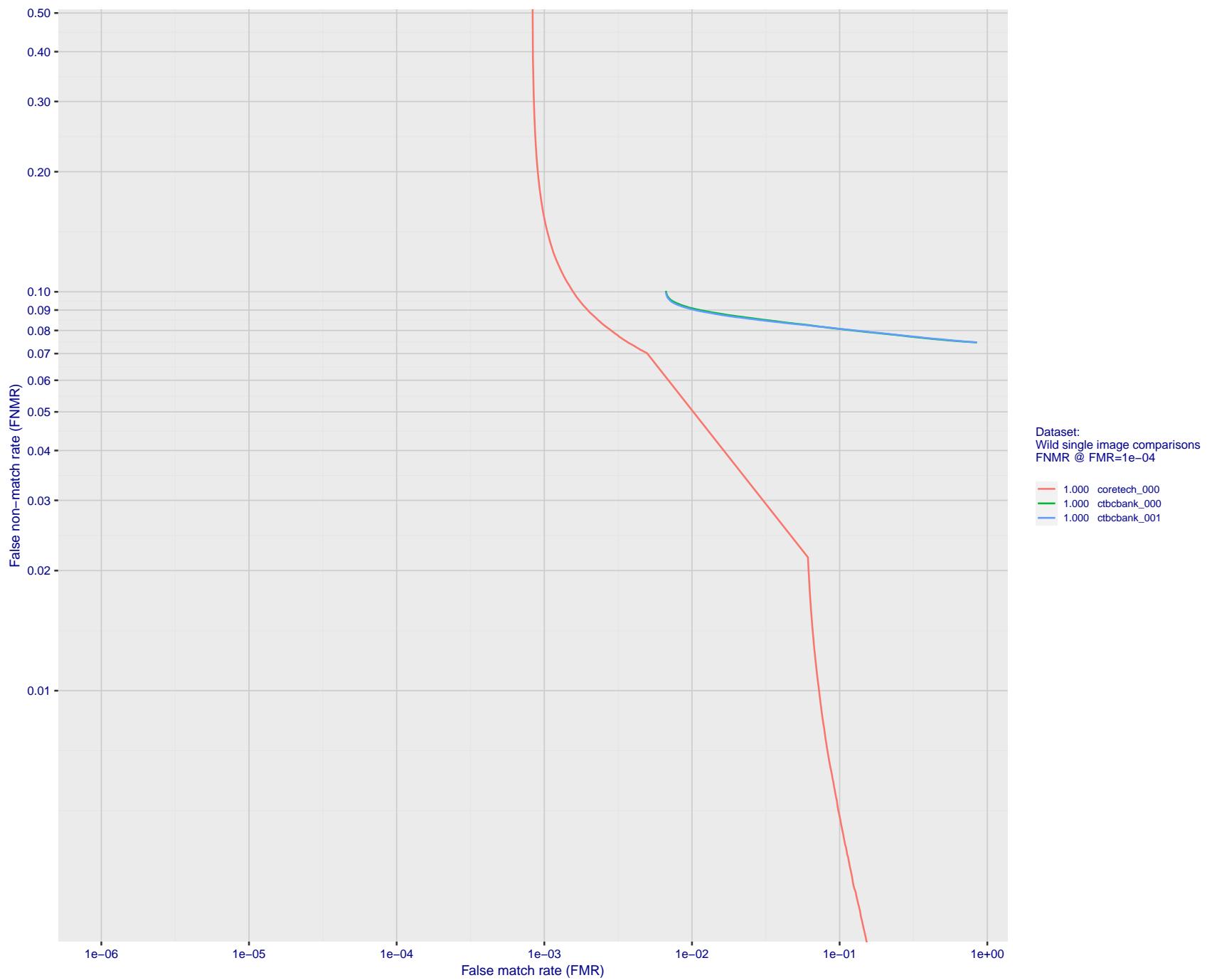


Figure 129: For the 2018 wild image comparisons, detection error tradeoff (DET) characteristics showing false non-match rate vs. false match rate plotted parametrically on threshold, T . The scales are logarithmic in order to show several decades of FMR.



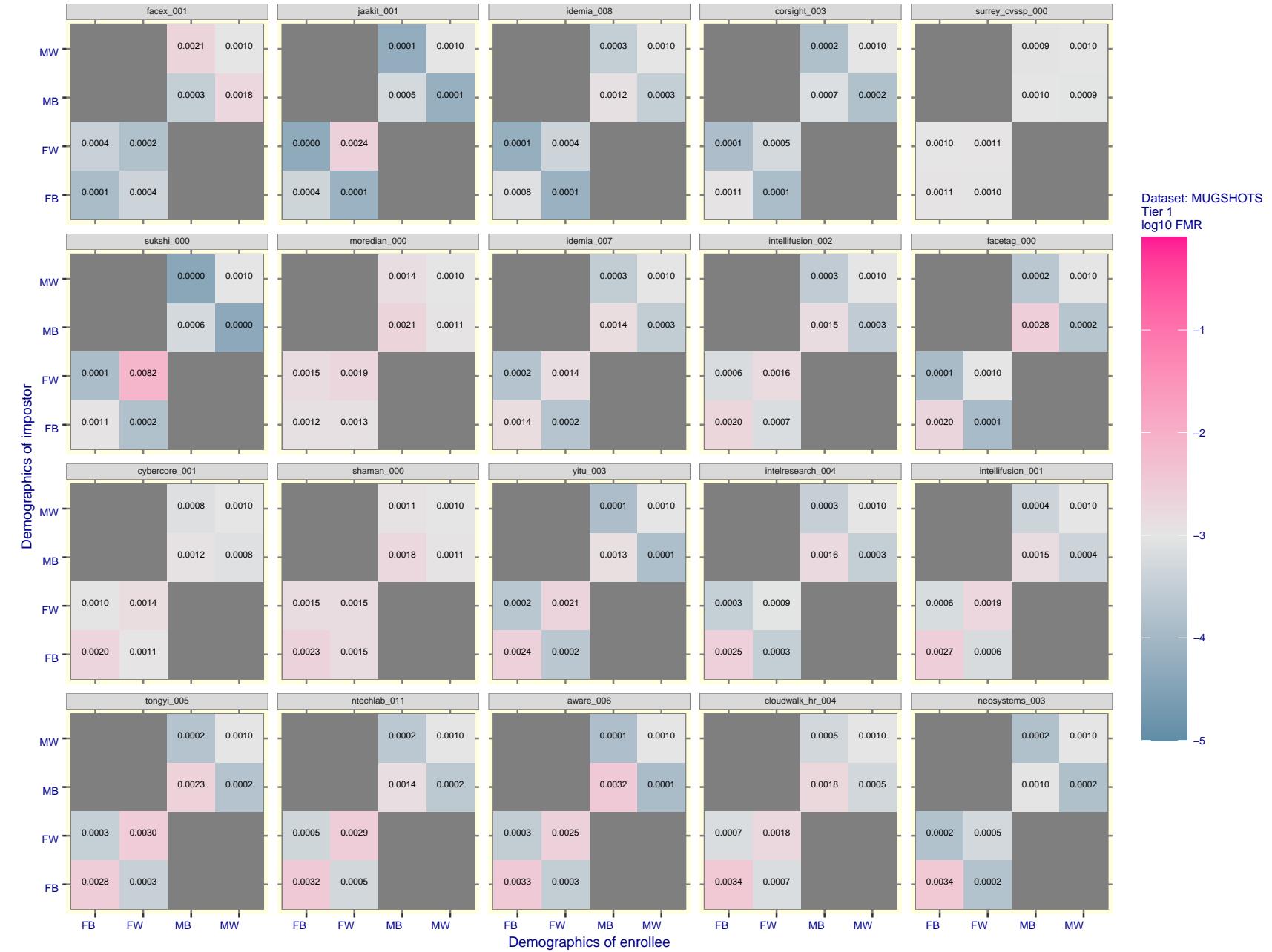


Figure 131: For the mugshot images, FMR for same-sex impostor pairs of images annotated with codes for black female, black male, white female, white male. The threshold is set for each algorithm to give $FMR = 0.001$ for white males which is the demographic that usually gives the lowest FMR. This means the top right box is the same color in all panels. The panels are sorted over multiple pages in order of FMR on black females, which is the demographic that usually gives the highest FMR.

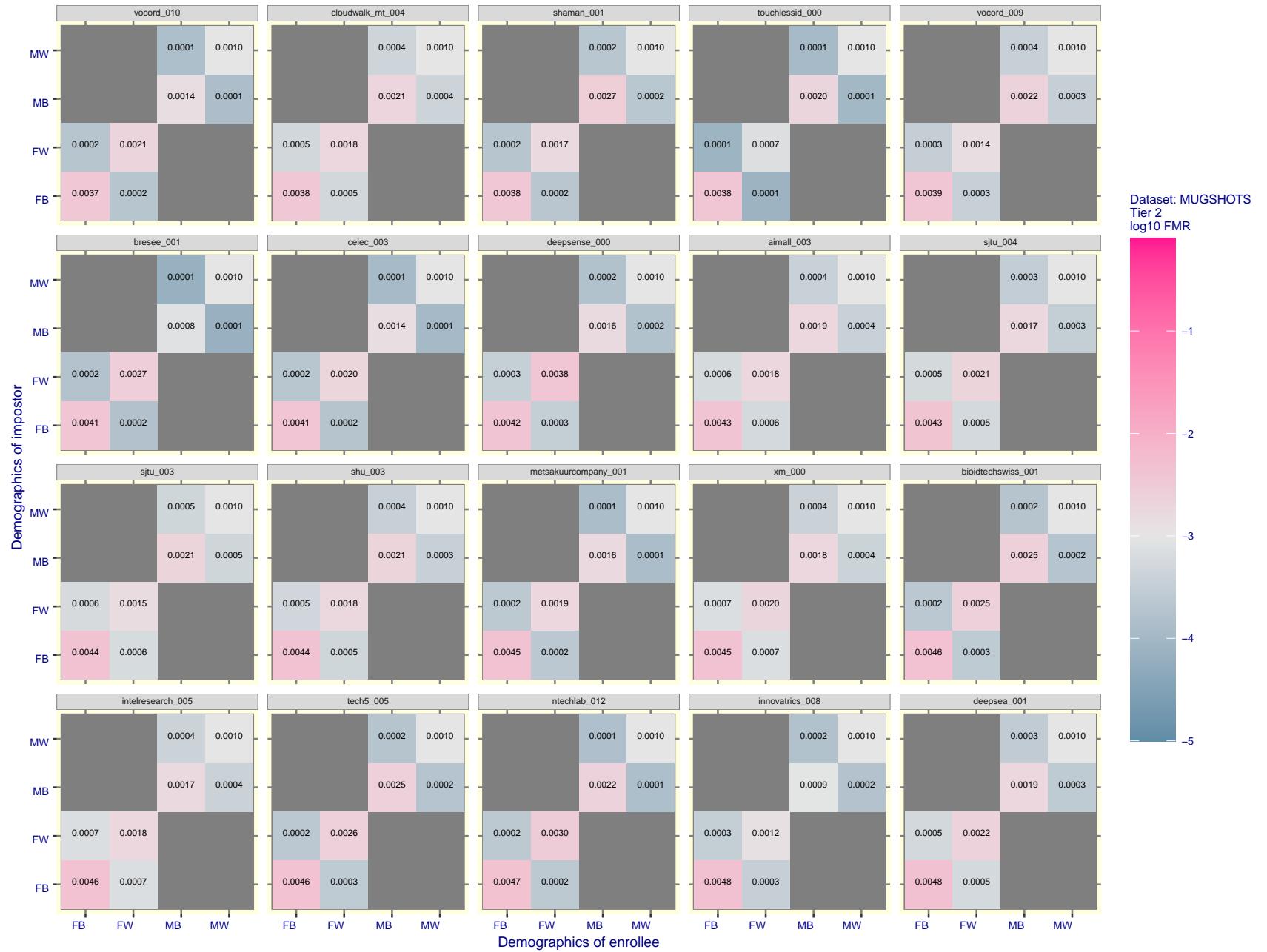


Figure 132: For the mugshot images, FMR for same-sex impostor pairs of images annotated with codes for black female, black male, white female, white male. The threshold is set for each algorithm to give $FMR = 0.001$ for white males which is the demographic that usually gives the lowest FMR. This means the top right box is the same color in all panels. The panels are sorted over multiple pages in order of FMR on black females, which is the demographic that usually gives the highest FMR.

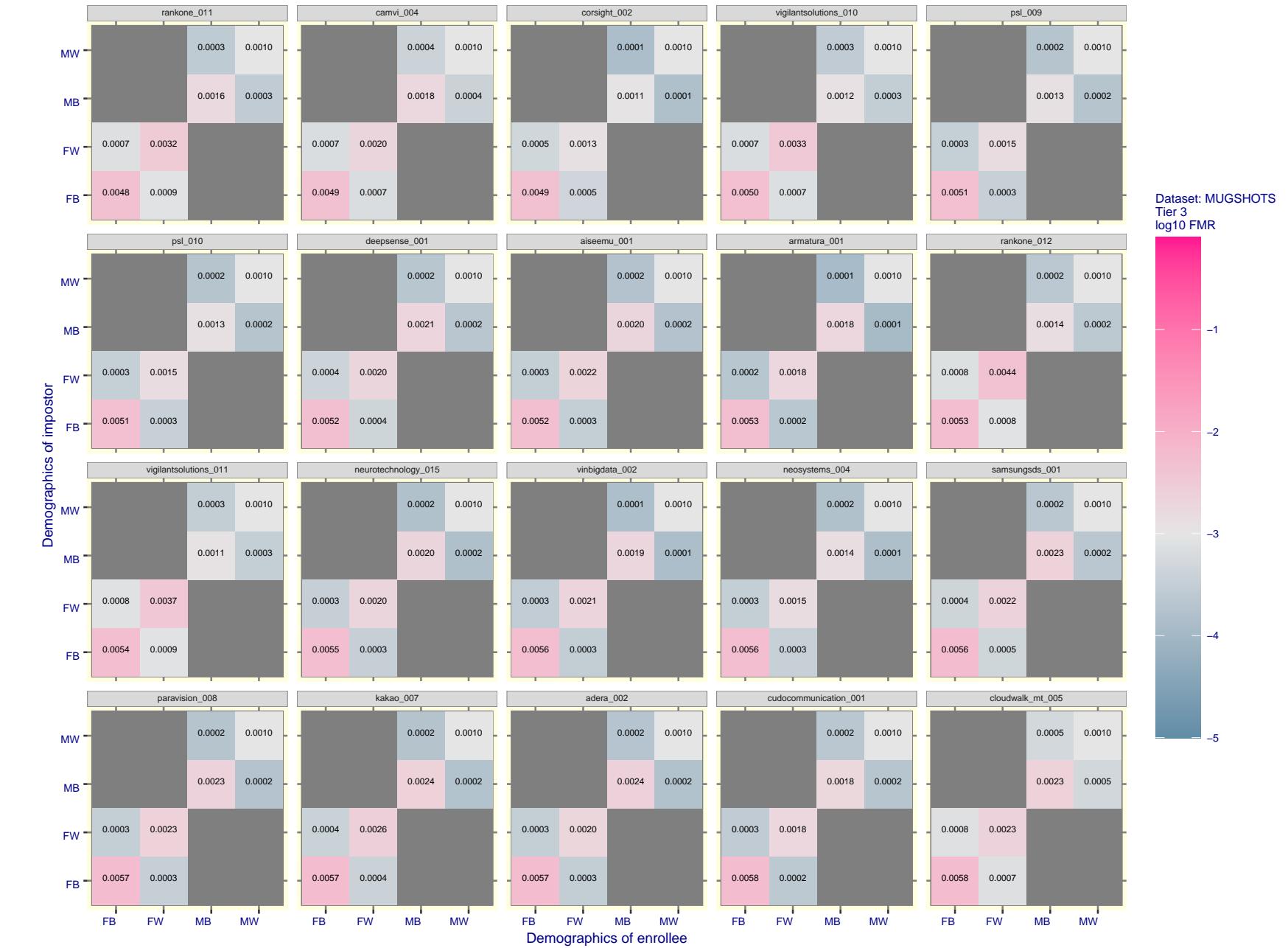


Figure 133: For the mugshot images, FMR for same-sex impostor pairs of images annotated with codes for black female, black male, white female, white male. The threshold is set for each algorithm to give FMR = 0.001 for white males which is the demographic that usually gives the lowest FMR. This means the top right box is the same color in all panels. The panels are sorted over multiple pages in order of FMR on black females, which is the demographic that usually gives the highest FMR.

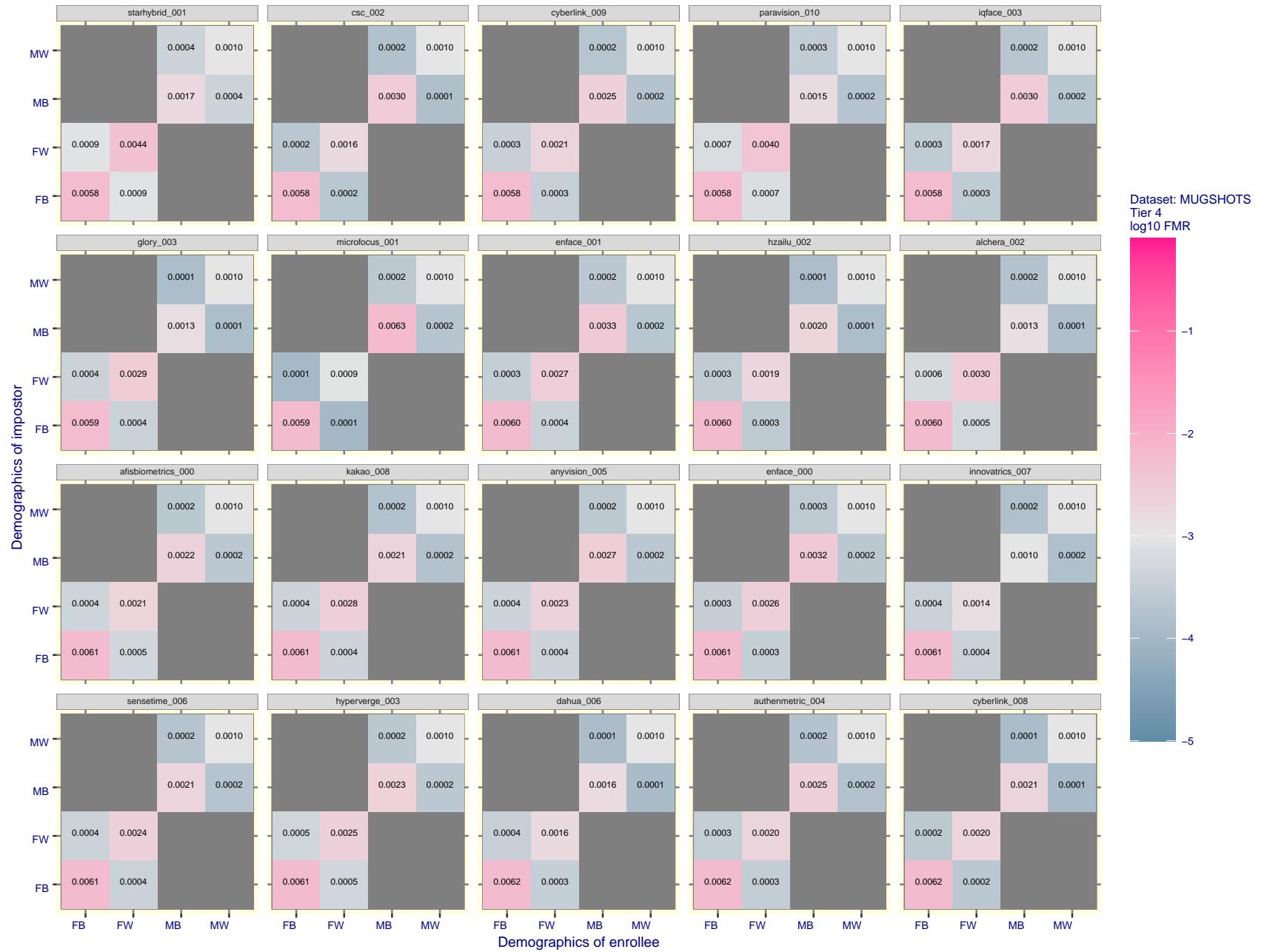


Figure 134: For the mugshot images, FMR for same-sex impostor pairs of images annotated with codes for black female, black male, white female, white male. The threshold is set for each algorithm to give FMR = 0.001 for white males which is the demographic that usually gives the lowest FMR. This means the top right box is the same color in all panels. The panels are sorted over multiple pages in order of FMR on black females, which is the demographic that usually gives the highest FMR.

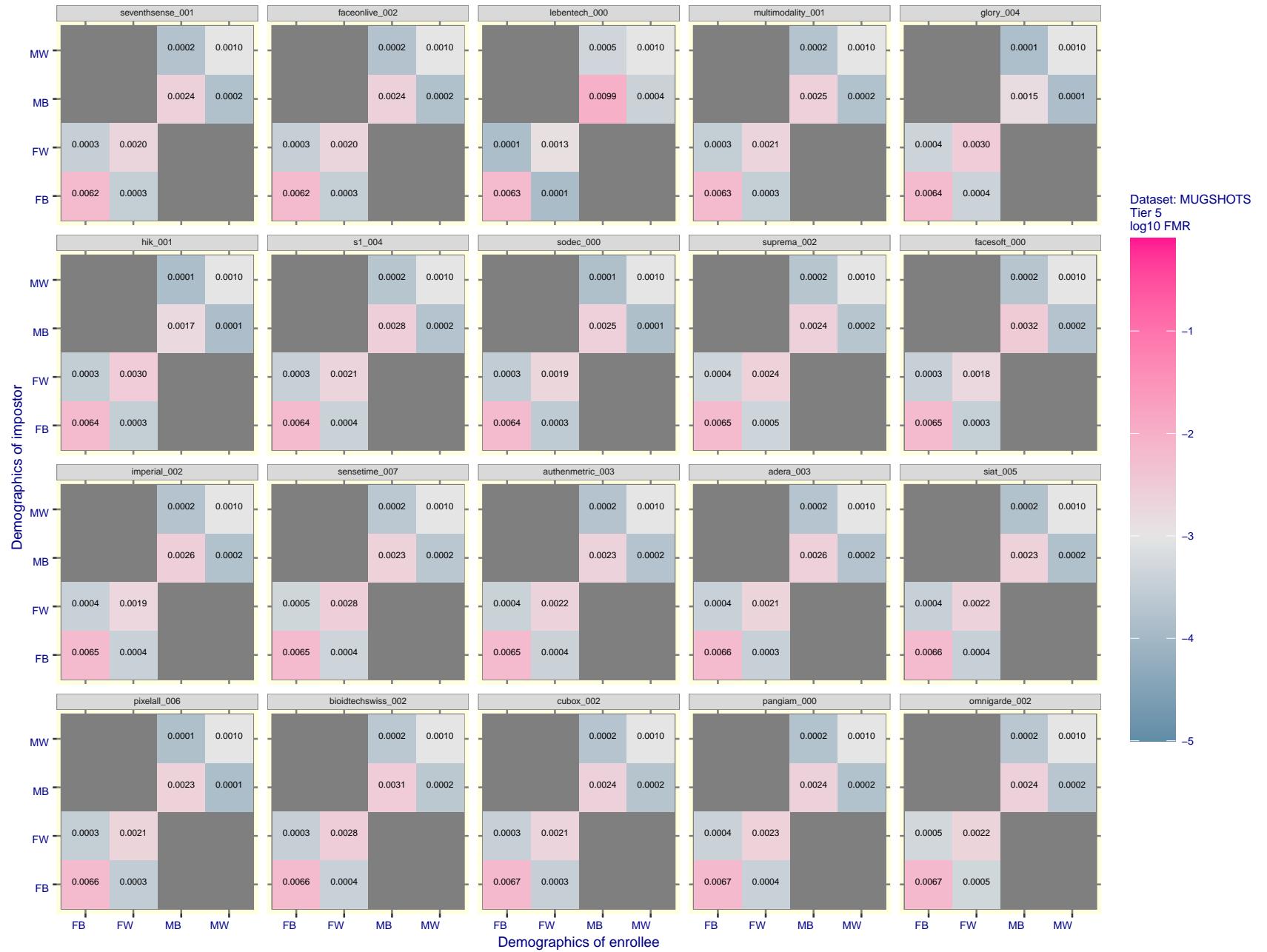


Figure 135: For the mugshot images, FMR for same-sex impostor pairs of images annotated with codes for black female, black male, white female, white male. The threshold is set for each algorithm to give FMR = 0.001 for white males which is the demographic that usually gives the lowest FMR. This means the top right box is the same color in all panels. The panels are sorted over multiple pages in order of FMR on black females, which is the demographic that usually gives the highest FMR.



Figure 136: For the mugshot images, FMR for same-sex impostor pairs of images annotated with codes for black female, black male, white female, white male. The threshold is set for each algorithm to give FMR = 0.001 for white males which is the demographic that usually gives the lowest FMR. This means the top right box is the same color in all panels. The panels are sorted over multiple pages in order of FMR on black females, which is the demographic that usually gives the highest FMR.

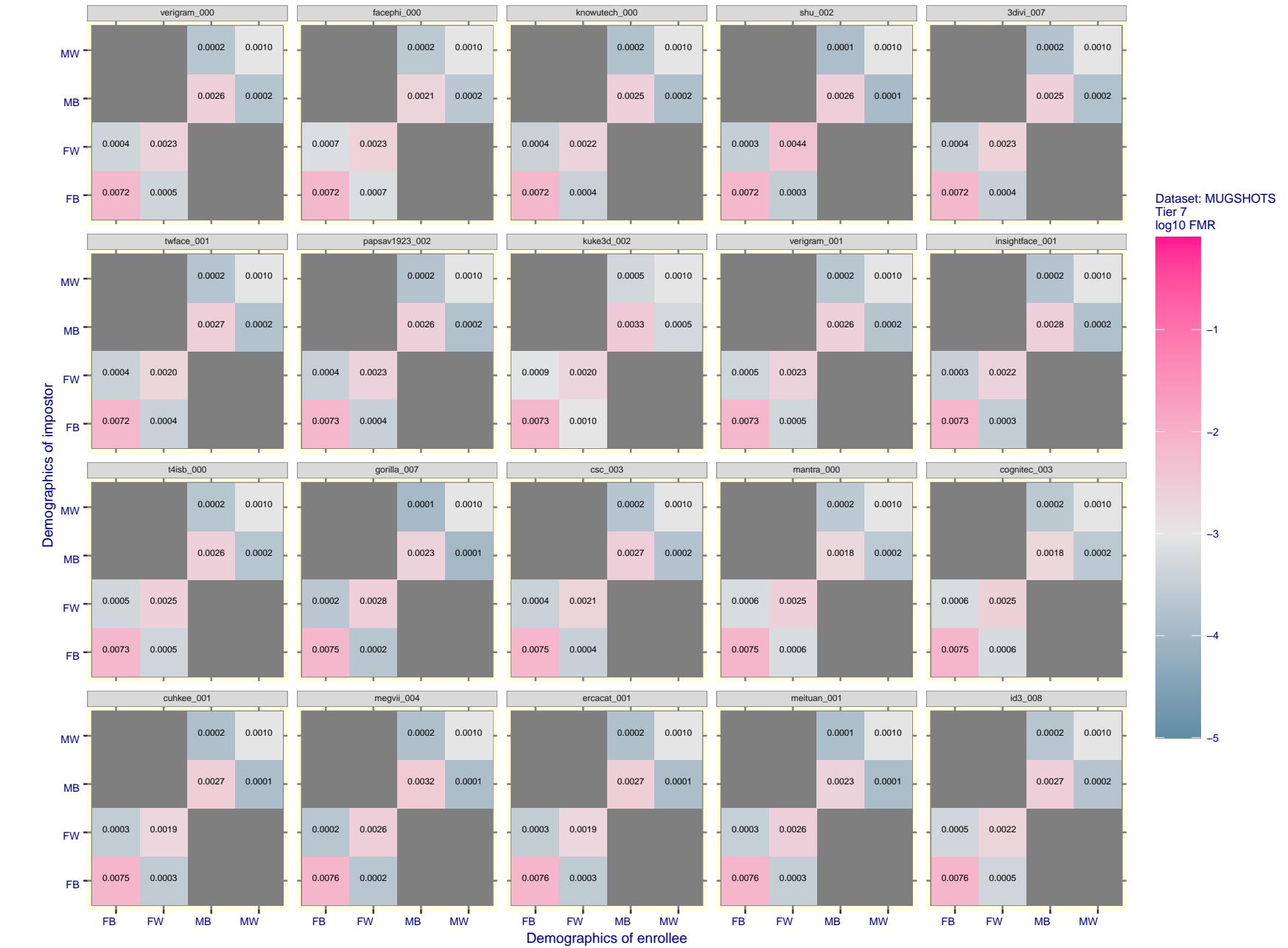


Figure 137: For the mugshot images, FMR for same-sex impostor pairs of images annotated with codes for black female, black male, white female, white male. The threshold is set for each algorithm to give FMR = 0.001 for white males which is the demographic that usually gives the lowest FMR. This means the top right box is the same color in all panels. The panels are sorted over multiple pages in order of FMR on black females, which is the demographic that usually gives the highest FMR.

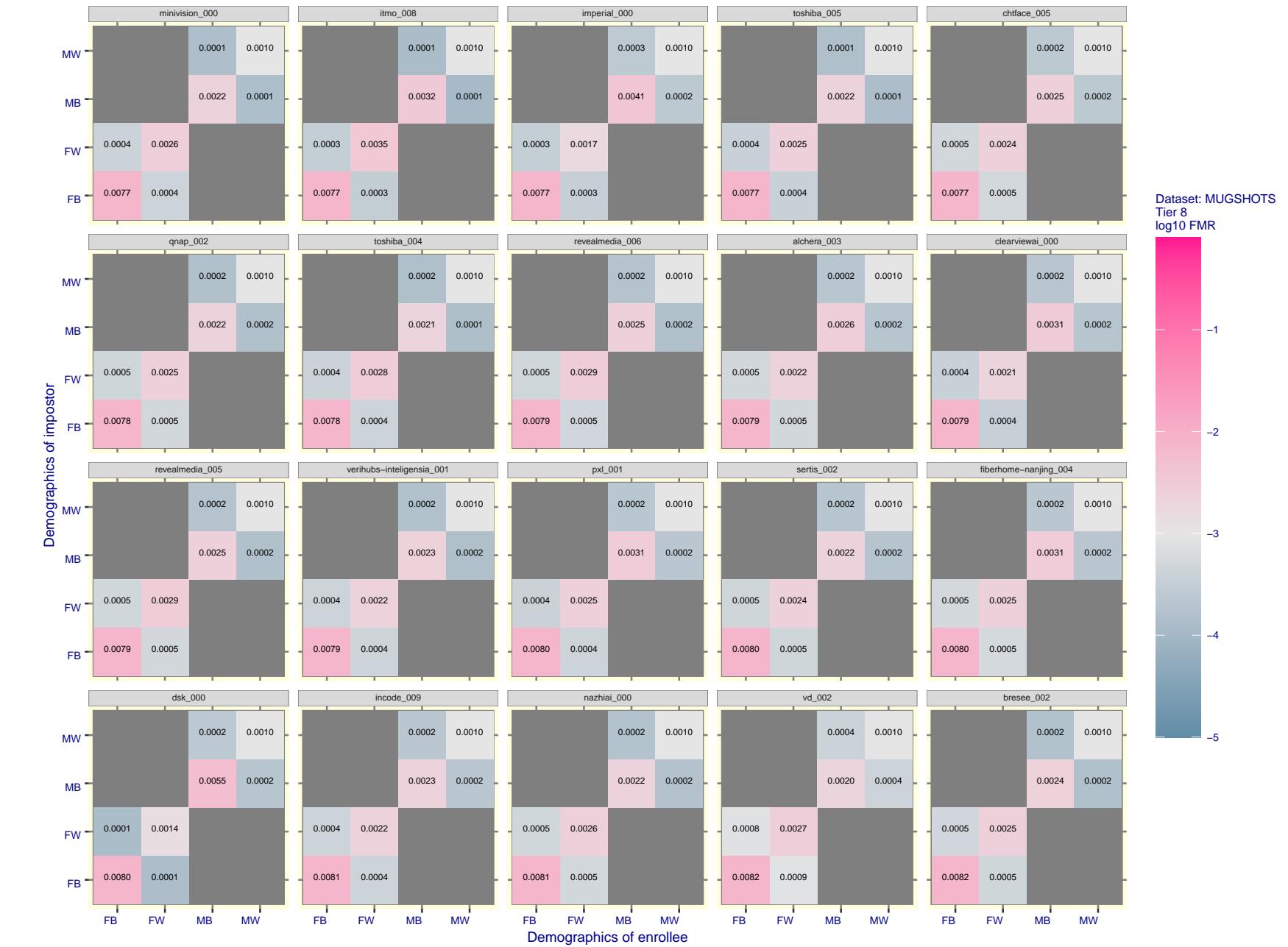


Figure 138: For the mugshot images, FMR for same-sex impostor pairs of images annotated with codes for black female, black male, white female, white male. The threshold is set for each algorithm to give $FMR = 0.001$ for white males which is the demographic that usually gives the lowest FMR. This means the top right box is the same color in all panels. The panels are sorted over multiple pages in order of FMR on black females, which is the demographic that usually gives the highest FMR.

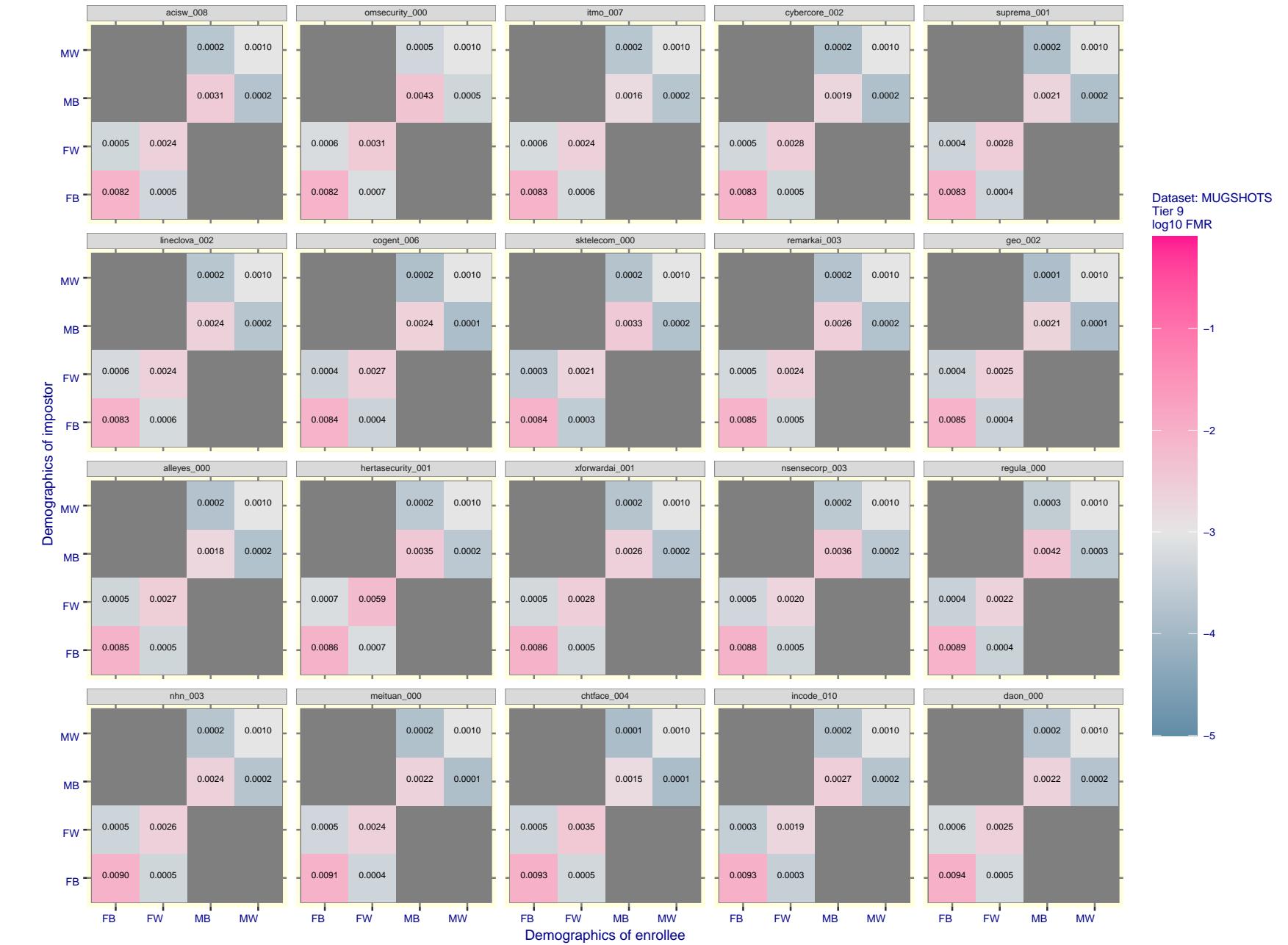


Figure 139: For the mugshot images, FMR for same-sex impostor pairs of images annotated with codes for black female, black male, white female, white male. The threshold is set for each algorithm to give $\text{FMR} = 0.001$ for white males which is the demographic that usually gives the lowest FMR. This means the top right box is the same color in all panels. The panels are sorted over multiple pages in order of FMR on black females, which is the demographic that usually gives the highest FMR.

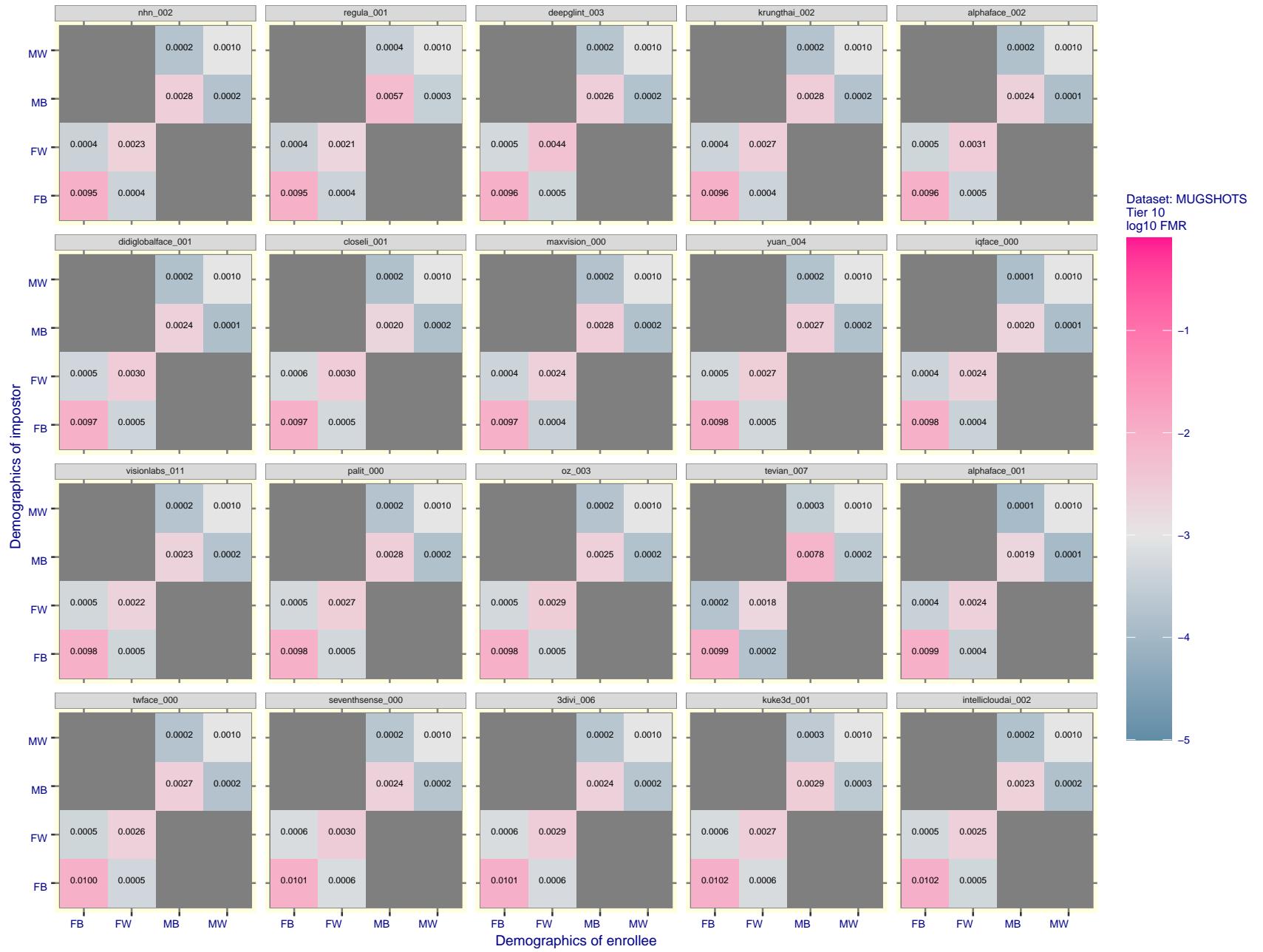


Figure 140: For the mugshot images, FMR for same-sex impostor pairs of images annotated with codes for black female, black male, white female, white male. The threshold is set for each algorithm to give FMR = 0.001 for white males which is the demographic that usually gives the lowest FMR. This means the top right box is the same color in all panels. The panels are sorted over multiple pages in order of FMR on black females, which is the demographic that usually gives the highest FMR.

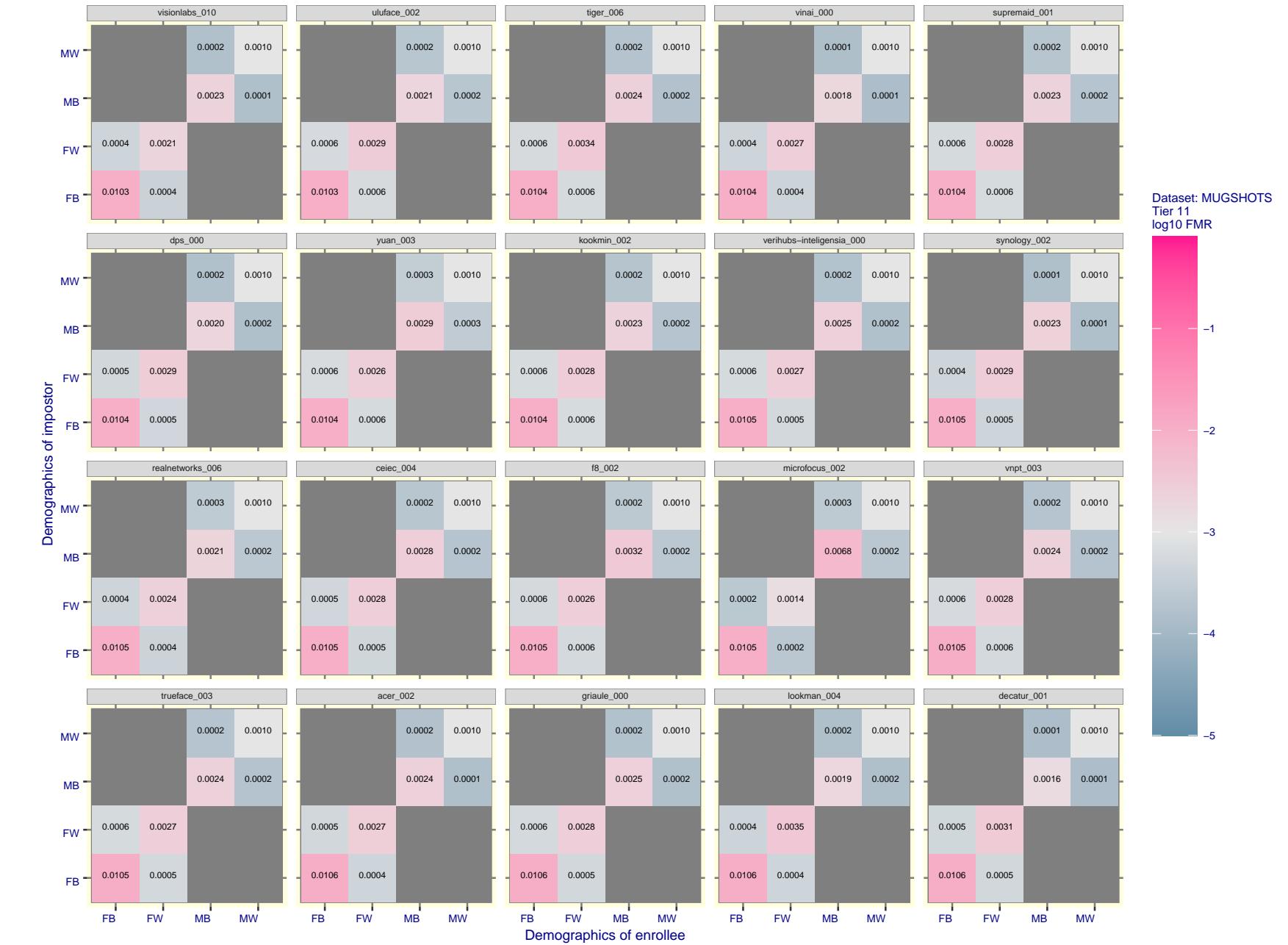


Figure 141: For the mugshot images, FMR for same-sex impostor pairs of images annotated with codes for black female, black male, white female, white male. The threshold is set for each algorithm to give FMR = 0.001 for white males which is the demographic that usually gives the lowest FMR. This means the top right box is the same color in all panels. The panels are sorted over multiple pages in order of FMR on black females, which is the demographic that usually gives the highest FMR.

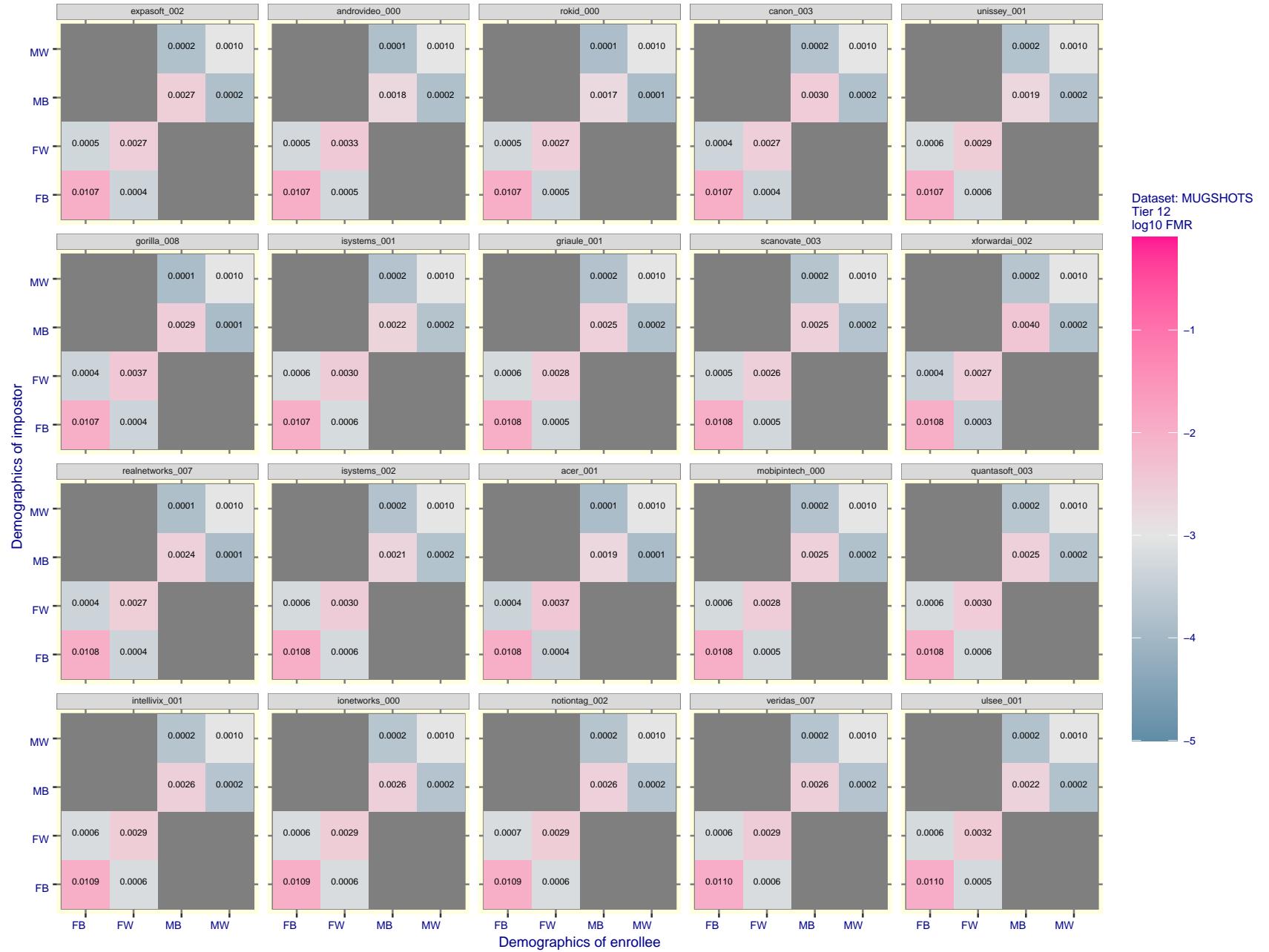


Figure 142: For the mugshot images, FMR for same-sex impostor pairs of images annotated with codes for black female, black male, white female, white male. The threshold is set for each algorithm to give FMR = 0.001 for white males which is the demographic that usually gives the lowest FMR. This means the top right box is the same color in all panels. The panels are sorted over multiple pages in order of FMR on black females, which is the demographic that usually gives the highest FMR.

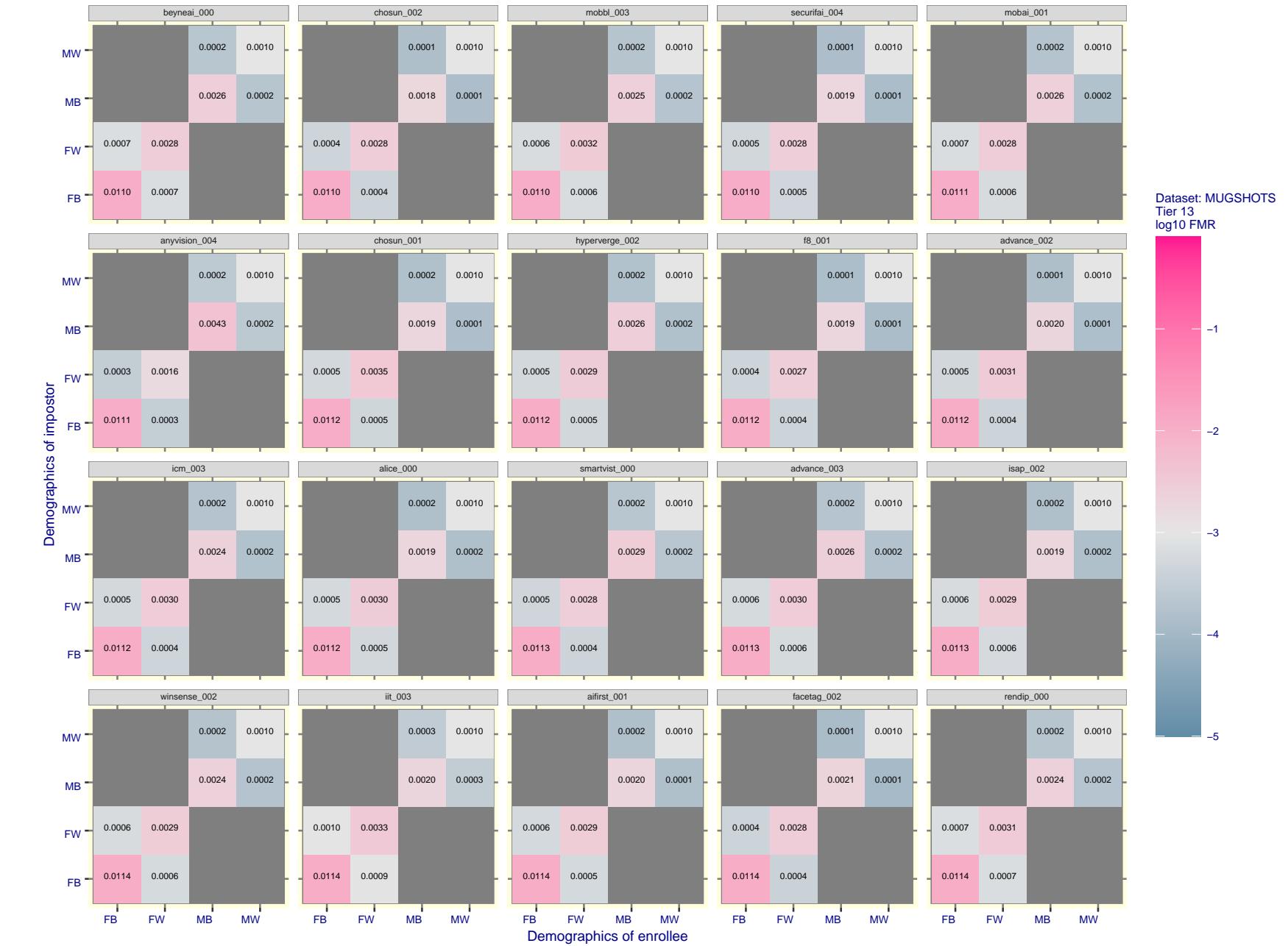


Figure 143: For the mugshot images, FMR for same-sex impostor pairs of images annotated with codes for black female, black male, white female, white male. The threshold is set for each algorithm to give FMR = 0.001 for white males which is the demographic that usually gives the lowest FMR. This means the top right box is the same color in all panels. The panels are sorted over multiple pages in order of FMR on black females, which is the demographic that usually gives the highest FMR.

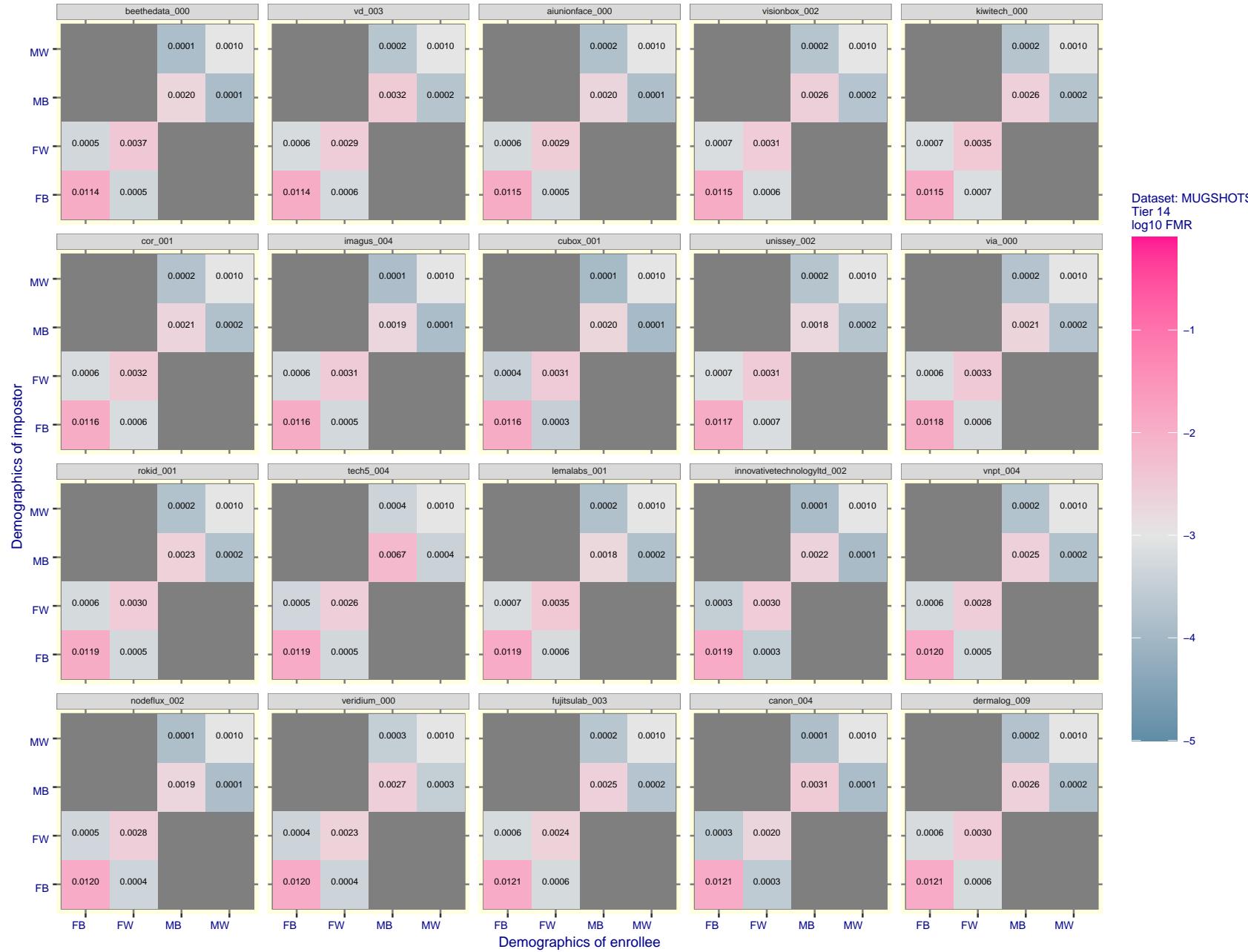


Figure 144: For the mugshot images, FMR for same-sex impostor pairs of images annotated with codes for black female, black male, white female, white male. The threshold is set for each algorithm to give FMR = 0.001 for white males which is the demographic that usually gives the lowest FMR. This means the top right box is the same color in all panels. The panels are sorted over multiple pages in order of FMR on black females, which is the demographic that usually gives the highest FMR.

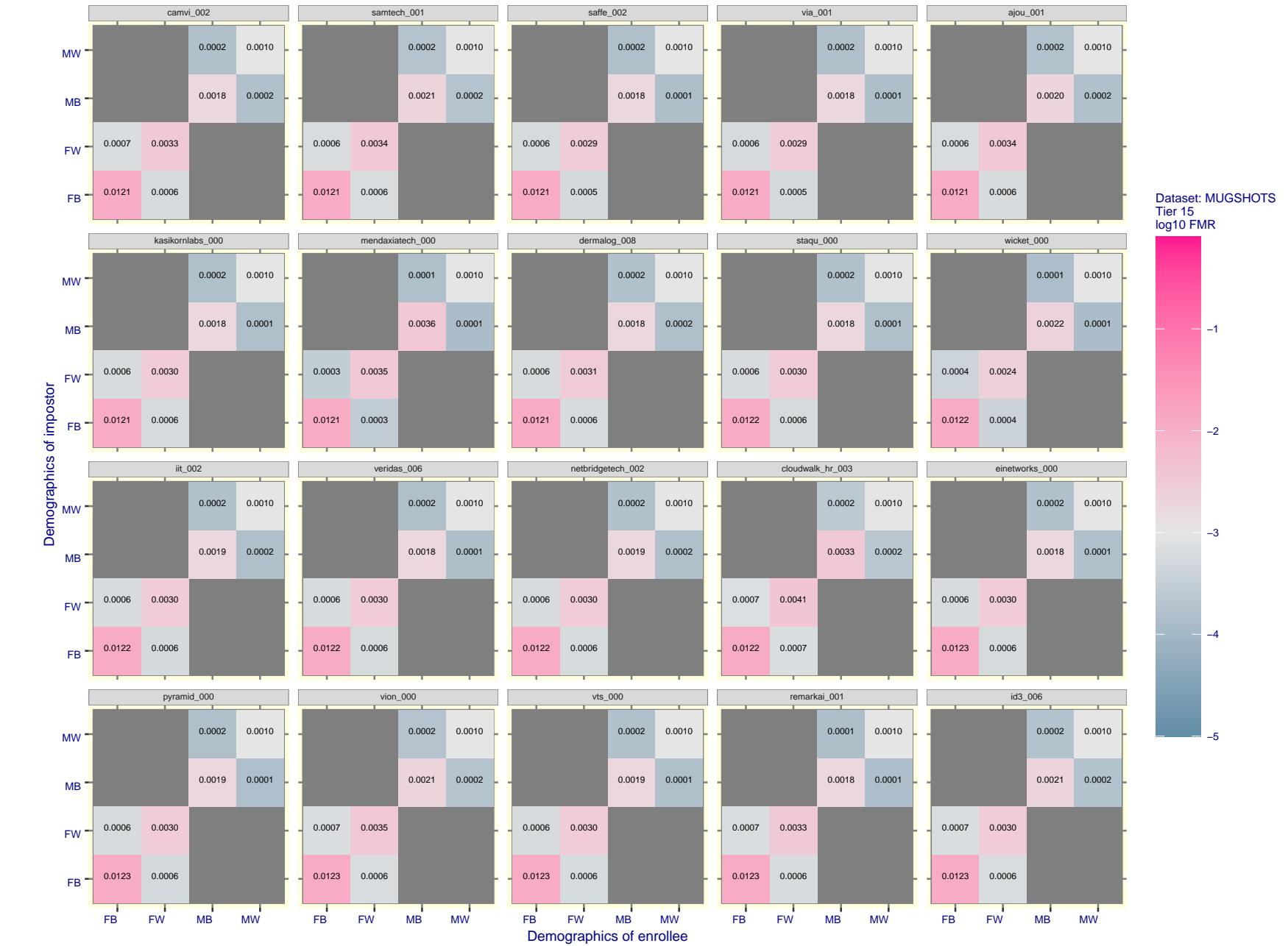


Figure 145: For the mugshot images, FMR for same-sex impostor pairs of images annotated with codes for black female, black male, white female, white male. The threshold is set for each algorithm to give $FMR = 0.001$ for white males which is the demographic that usually gives the lowest FMR. This means the top right box is the same color in all panels. The panels are sorted over multiple pages in order of FMR on black females, which is the demographic that usually gives the highest FMR.

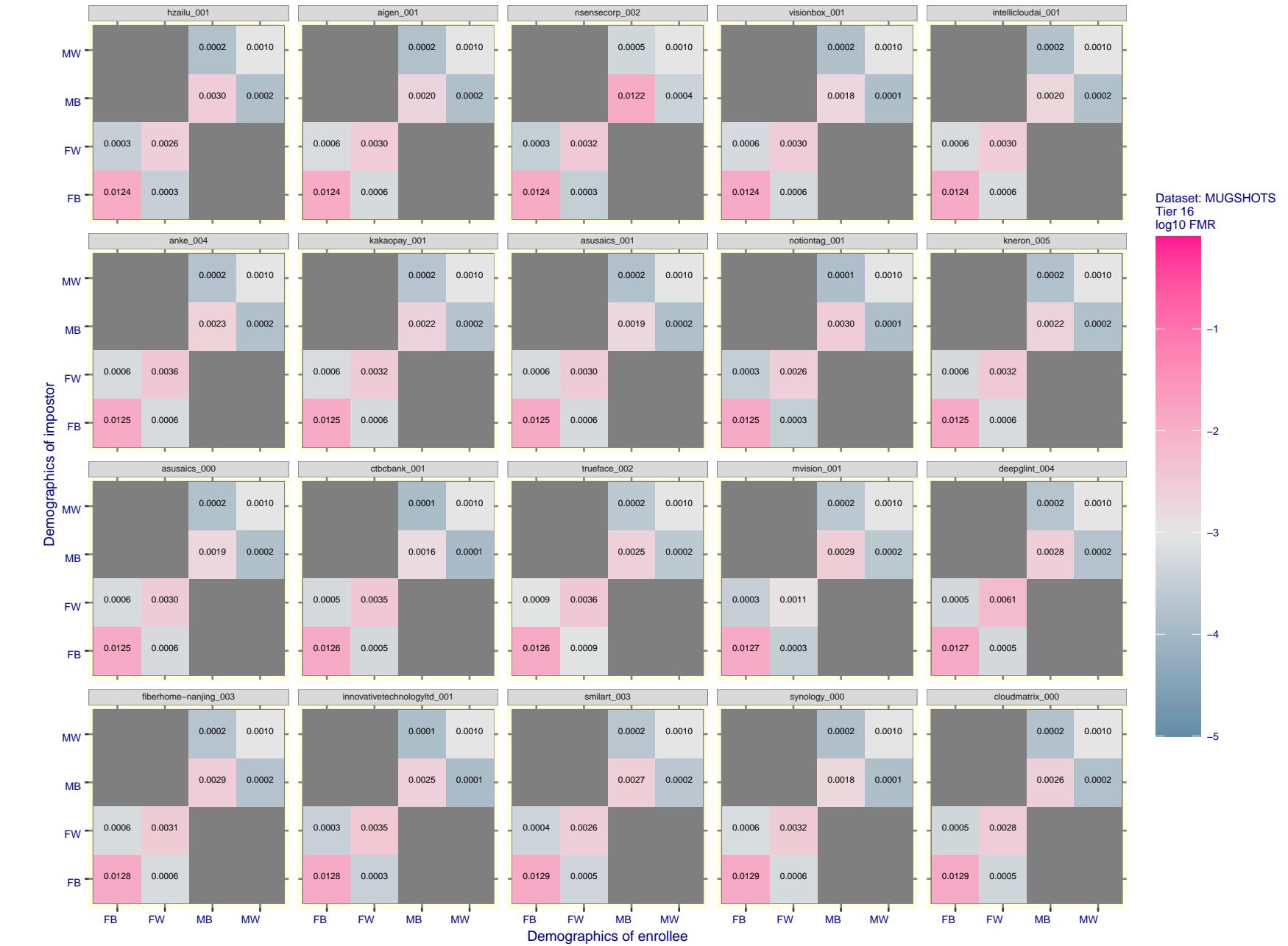


Figure 146: For the mugshot images, FMR for same-sex impostor pairs of images annotated with codes for black female, black male, white female, white male. The threshold is set for each algorithm to give FMR = 0.001 for white males which is the demographic that usually gives the lowest FMR. This means the top right box is the same color in all panels. The panels are sorted over multiple pages in order of FMR on black females, which is the demographic that usually gives the highest FMR.

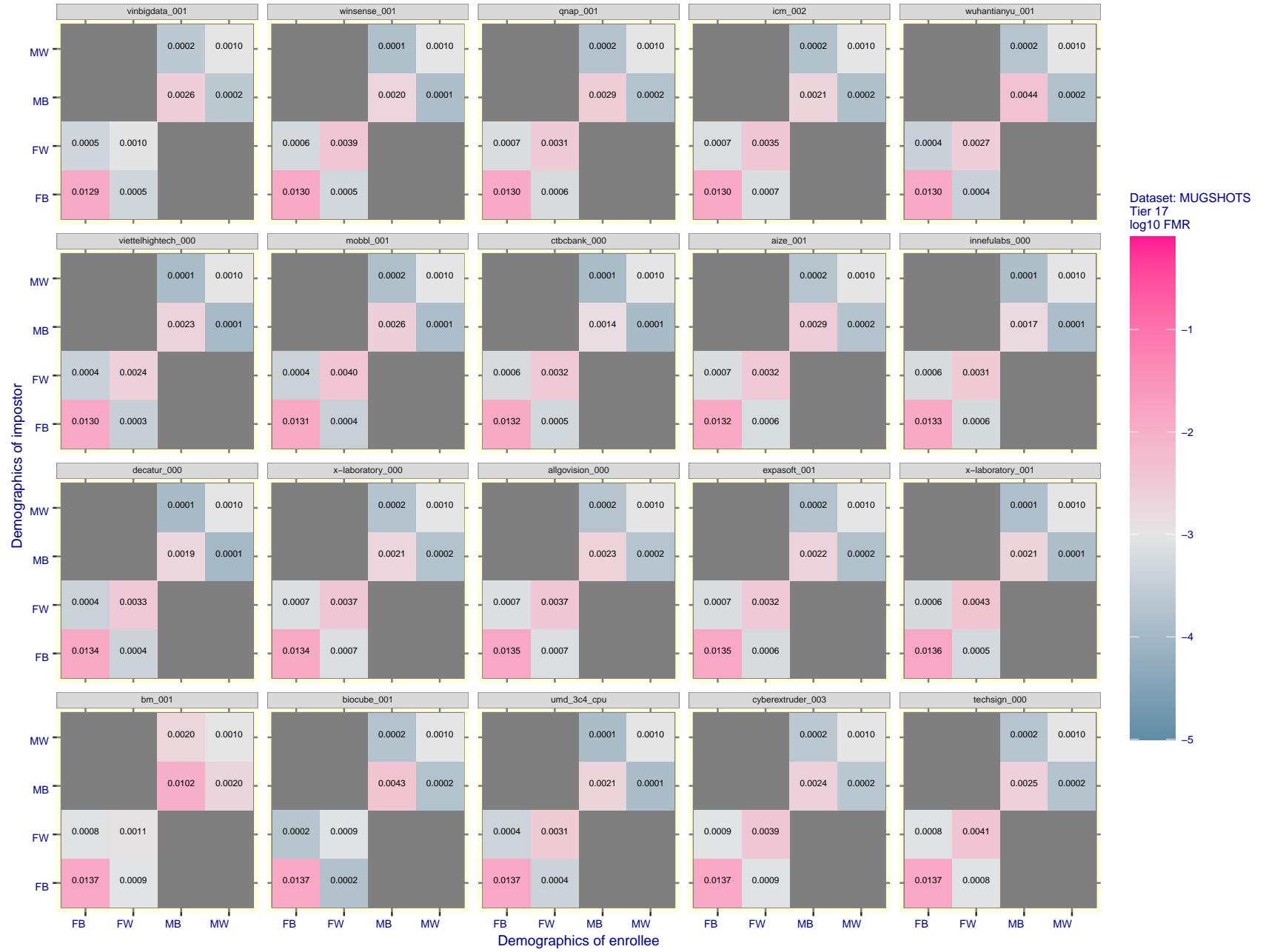


Figure 147: For the mugshot images, FMR for same-sex impostor pairs of images annotated with codes for black female, black male, white female, white male. The threshold is set for each algorithm to give FMR = 0.001 for white males which is the demographic that usually gives the lowest FMR. This means the top right box is the same color in all panels. The panels are sorted over multiple pages in order of FMR on black females, which is the demographic that usually gives the highest FMR.

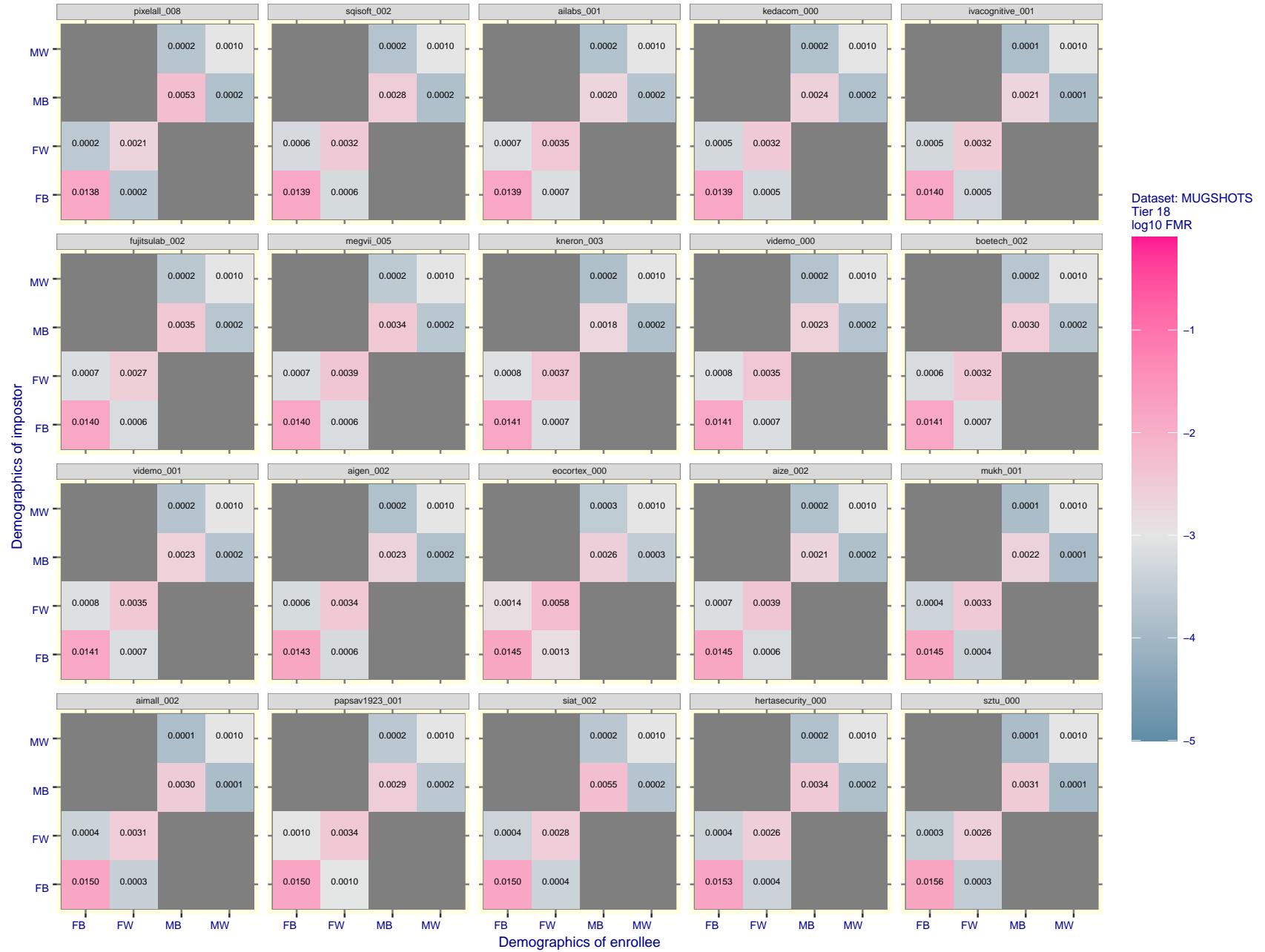


Figure 148: For the mugshot images, FMR for same-sex impostor pairs of images annotated with codes for black female, black male, white female, white male. The threshold is set for each algorithm to give FMR = 0.001 for white males which is the demographic that usually gives the lowest FMR. This means the top right box is the same color in all panels. The panels are sorted over multiple pages in order of FMR on black females, which is the demographic that usually gives the highest FMR.

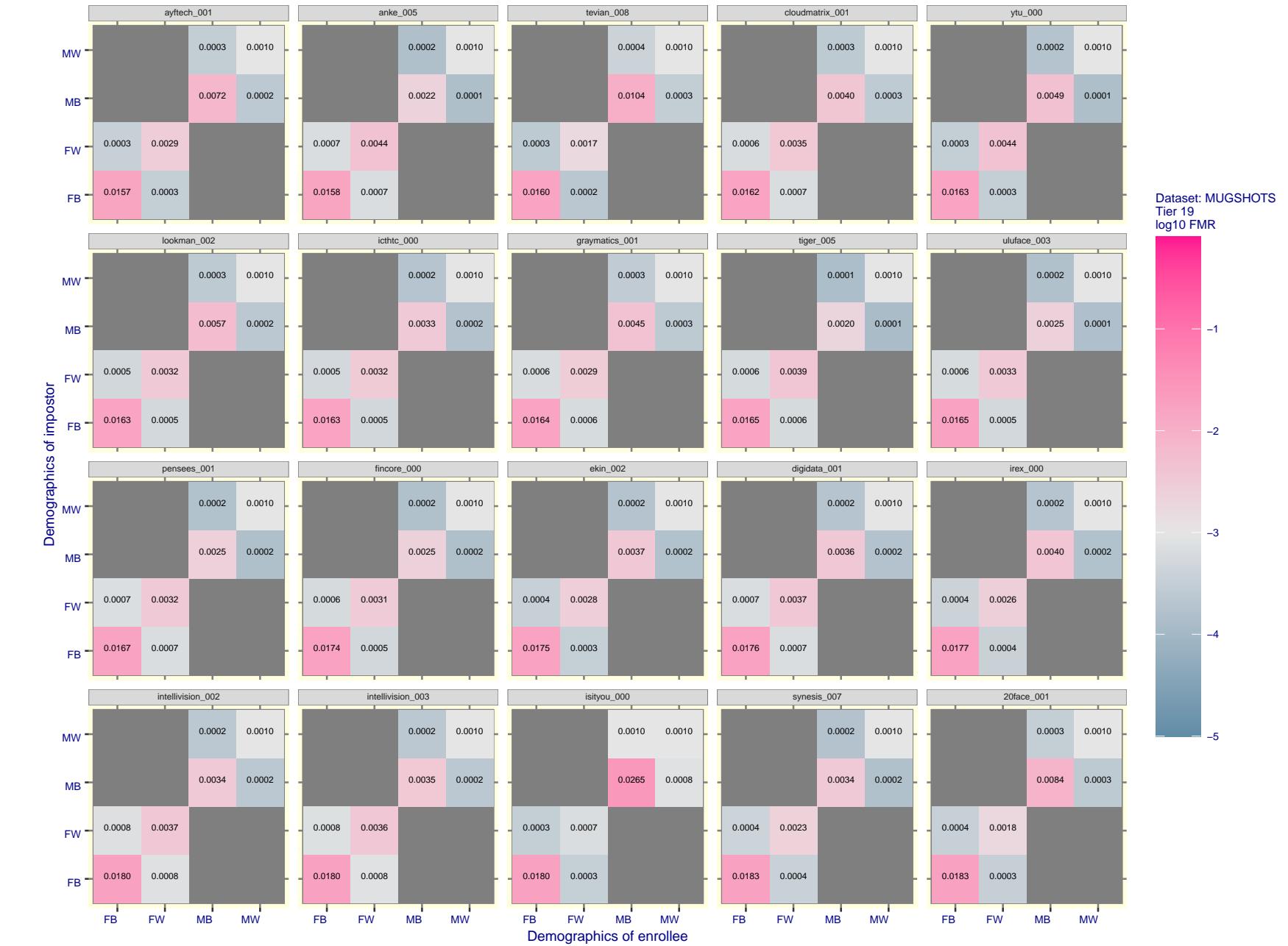


Figure 149: For the mugshot images, FMR for same-sex impostor pairs of images annotated with codes for black female, black male, white female, white male. The threshold is set for each algorithm to give FMR = 0.001 for white males which is the demographic that usually gives the lowest FMR. This means the top right box is the same color in all panels. The panels are sorted over multiple pages in order of FMR on black females, which is the demographic that usually gives the highest FMR.



Figure 150: For the mugshot images, FMR for same-sex impostor pairs of images annotated with codes for black female, black male, white female, white male. The threshold is set for each algorithm to give FMR = 0.001 for white males which is the demographic that usually gives the lowest FMR. This means the top right box is the same color in all panels. The panels are sorted over multiple pages in order of FMR on black females, which is the demographic that usually gives the highest FMR.

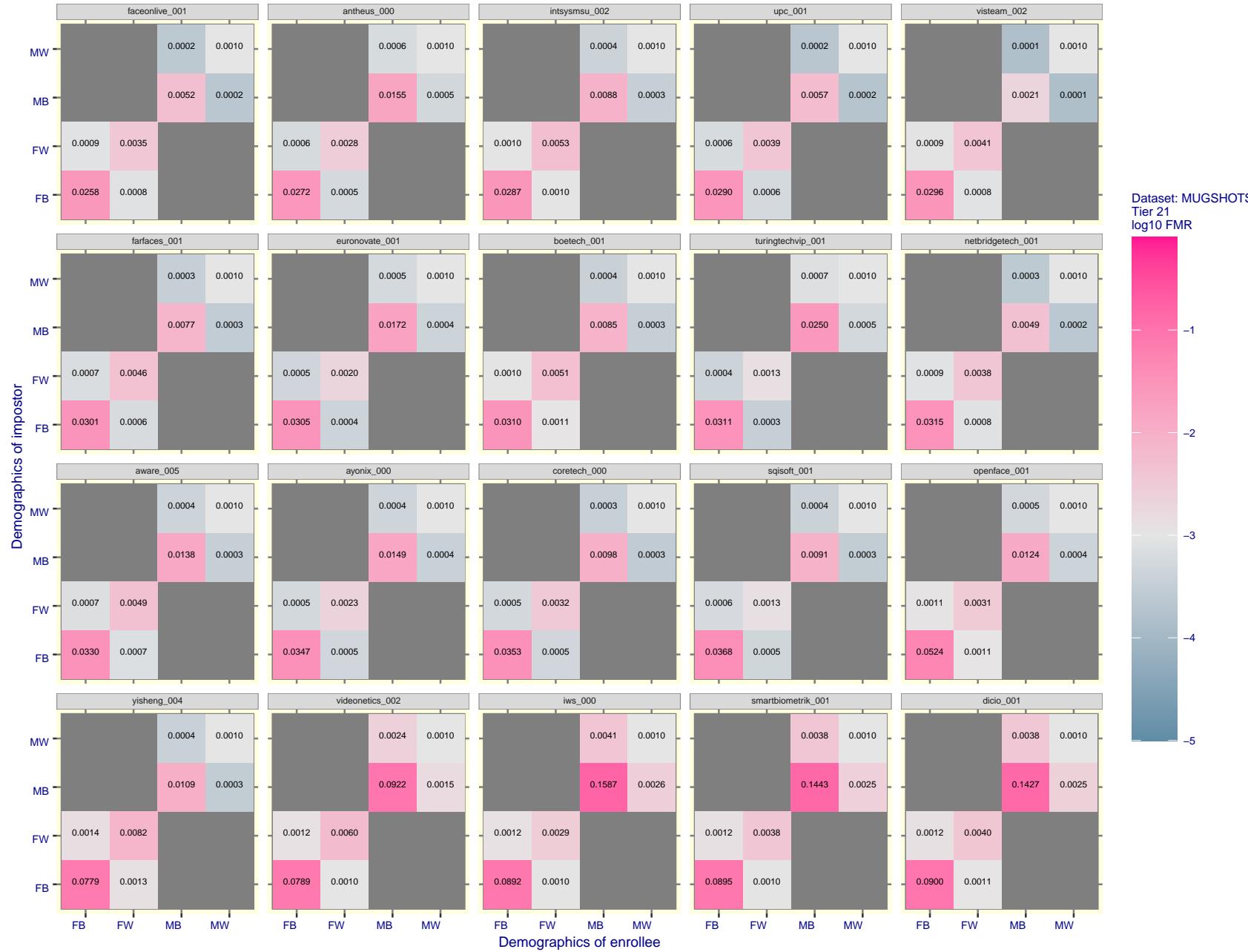


Figure 151: For the mugshot images, FMR for same-sex impostor pairs of images annotated with codes for black female, black male, white female, white male. The threshold is set for each algorithm to give FMR = 0.001 for white males which is the demographic that usually gives the lowest FMR. This means the top right box is the same color in all panels. The panels are sorted over multiple pages in order of FMR on black females, which is the demographic that usually gives the highest FMR.

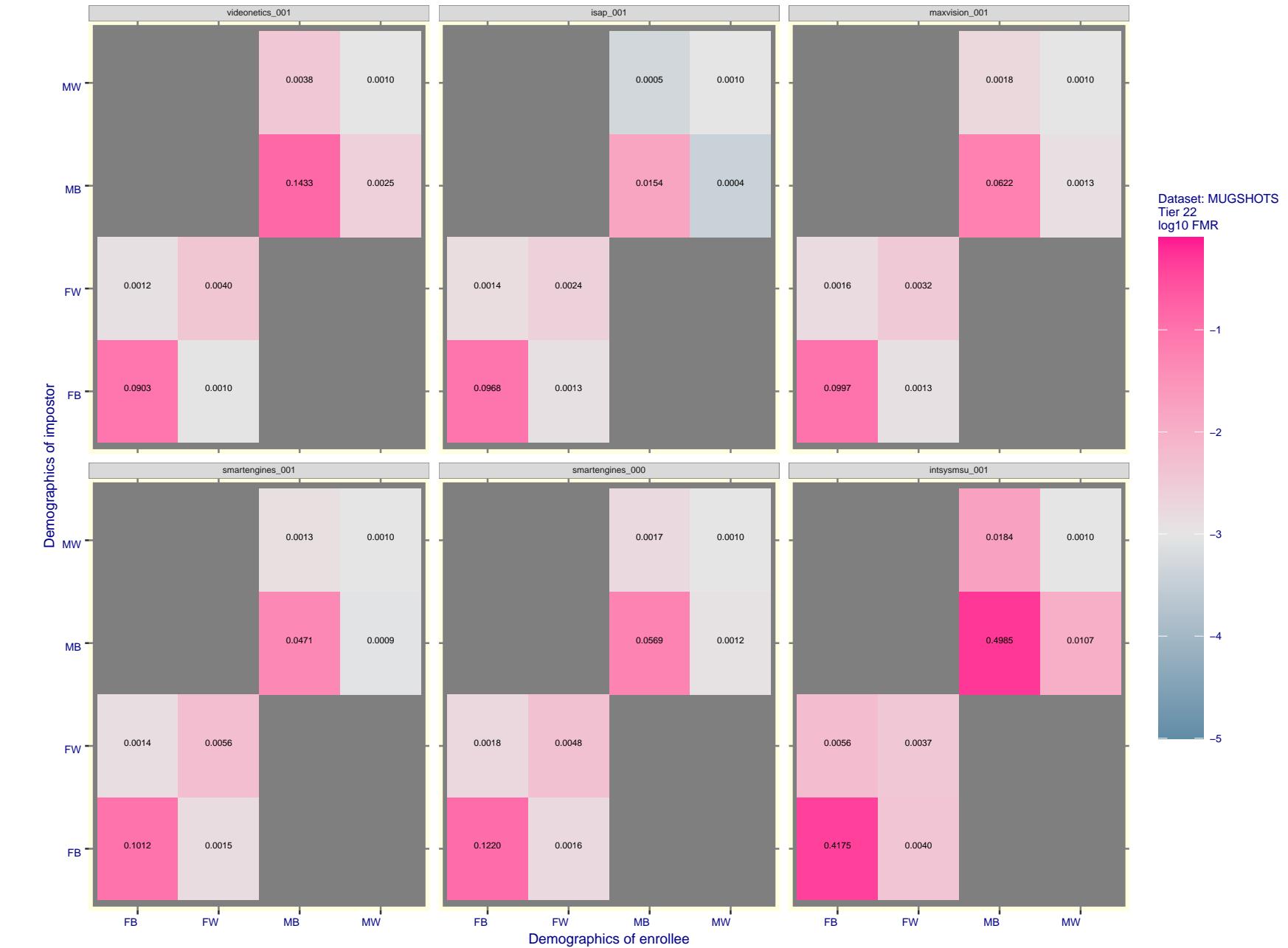


Figure 152: For the mugshot images, FMR for same-sex impostor pairs of images annotated with codes for black female, black male, white female, white male. The threshold is set for each algorithm to give $\text{FMR} = 0.001$ for white males which is the demographic that usually gives the lowest FMR. This means the top right box is the same color in all panels. The panels are sorted over multiple pages in order of FMR on black females, which is the demographic that usually gives the highest FMR.

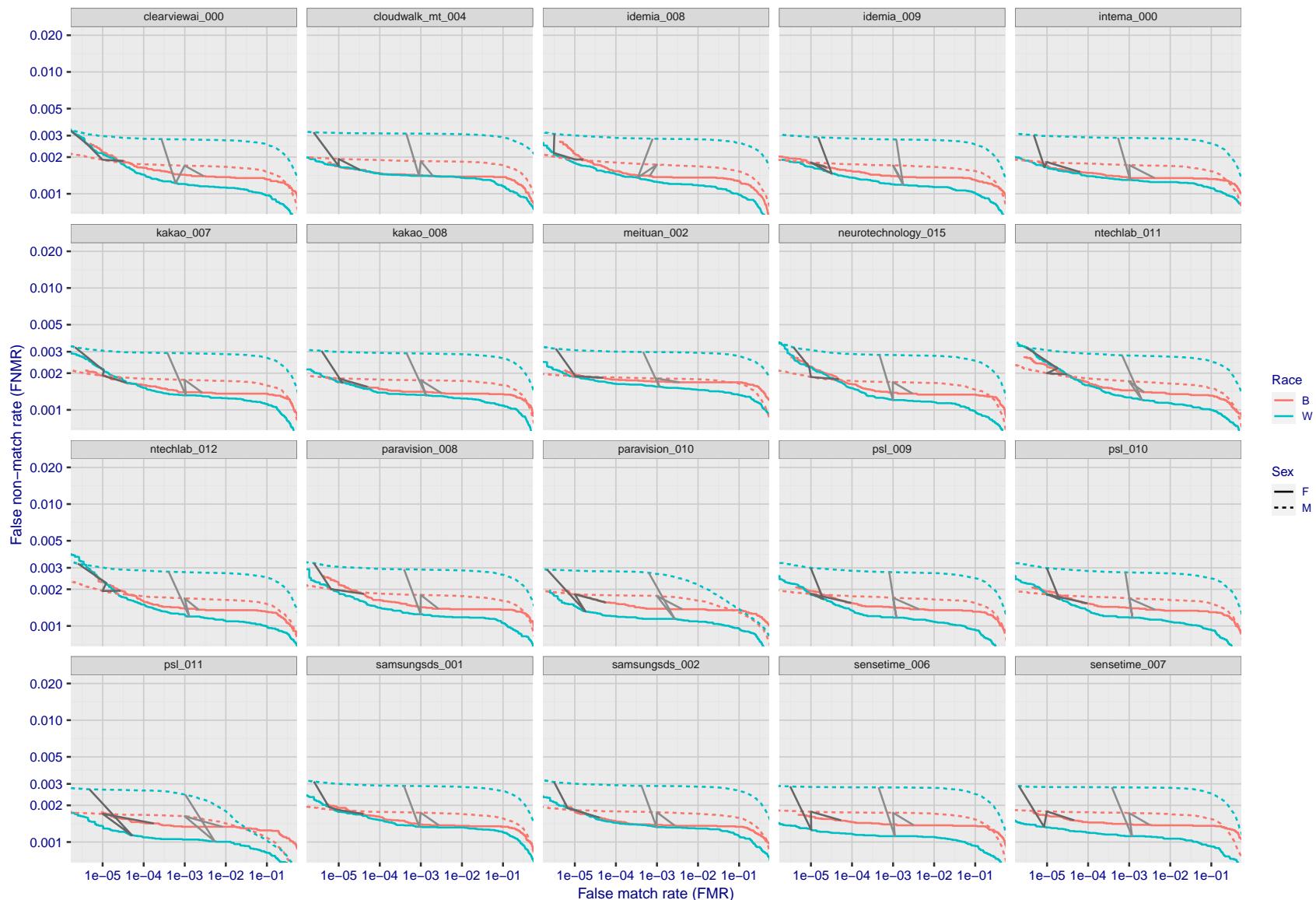


Figure 153: For the mugshot images, error tradeoff characteristics for white females, black females, black males and white males. The Z-shaped grey lines correspond to fixed thresholds, showing both FNMR and FMR vary at one T value. Note: Many of the plots will naively be read as saying women gives worse error rates than men because the solid traces lie above the dotted ones. However, this is misleading and incomplete: The grey lines show the traces reveal horizontal shifts. Thus for the cogent-003 algorithm FNMR for men is higher than for women at a fixed threshold but, at the same time, FMR is higher for women - see Figure 239. As access control systems almost always operate at a fixed threshold, the naive interpretation is incorrect.

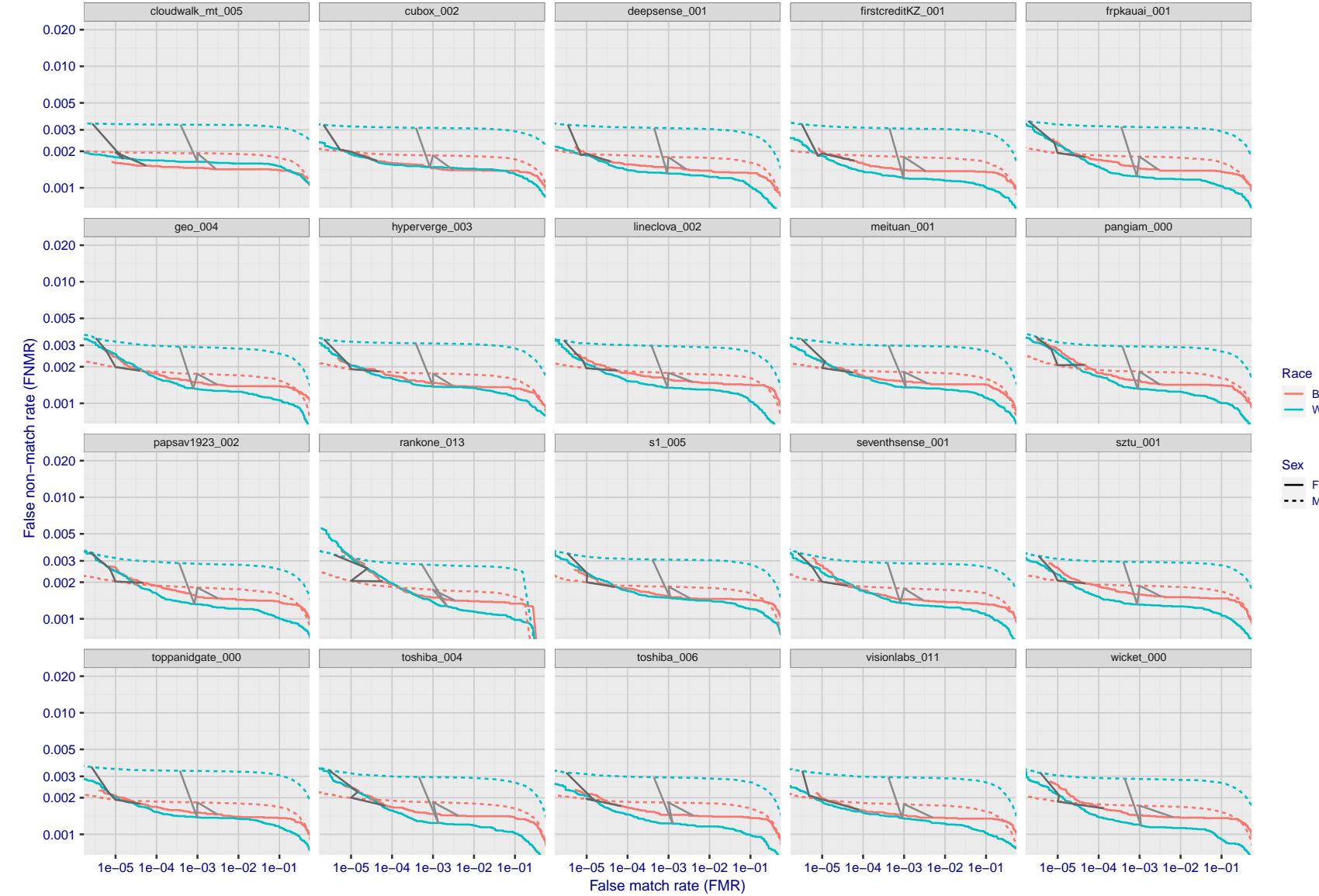


Figure 154: For the mugshot images, error tradeoff characteristics for white females, black females, black males and white males. The Z-shaped grey lines correspond to fixed thresholds, showing both FNMR and FMR vary at one T value. Note: Many of the plots will naively be read as saying women gives worse error rates than men because the solid traces lie above the dotted ones. However, this is misleading and incomplete: The grey lines show the traces reveal horizontal shifts. Thus for the cogent-003 algorithm FNMR for men is higher than for women at a fixed threshold but, at the same time, FMR is higher for women - see Figure 239. As access control systems almost always operate at a fixed threshold, the naive interpretation is incorrect.

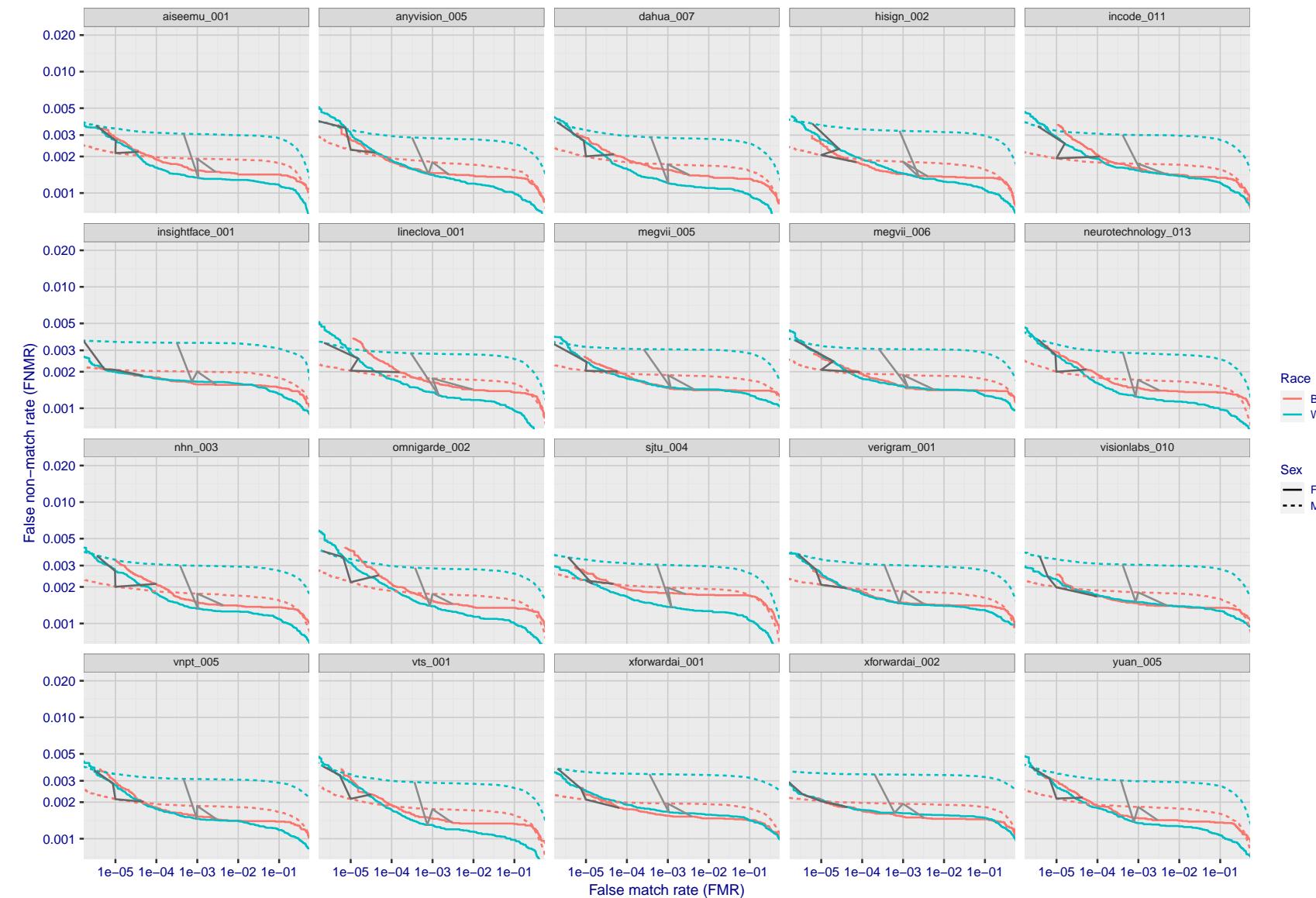


Figure 155: For the mugshot images, error tradeoff characteristics for white females, black females, black males and white males. The Z-shaped grey lines correspond to fixed thresholds, showing both FNMR and FMR vary at one T value. Note: Many of the plots will naively be read as saying women gives worse error rates than men because the solid traces lie above the dotted ones. However, this is misleading and incomplete: The grey lines show the traces reveal horizontal shifts. Thus for the cogent-003 algorithm FNMR for men is higher than for women at a fixed threshold but, at the same time, FMR is higher for women - see Figure 239. As access control systems almost always operate at a fixed threshold, the naive interpretation is incorrect.

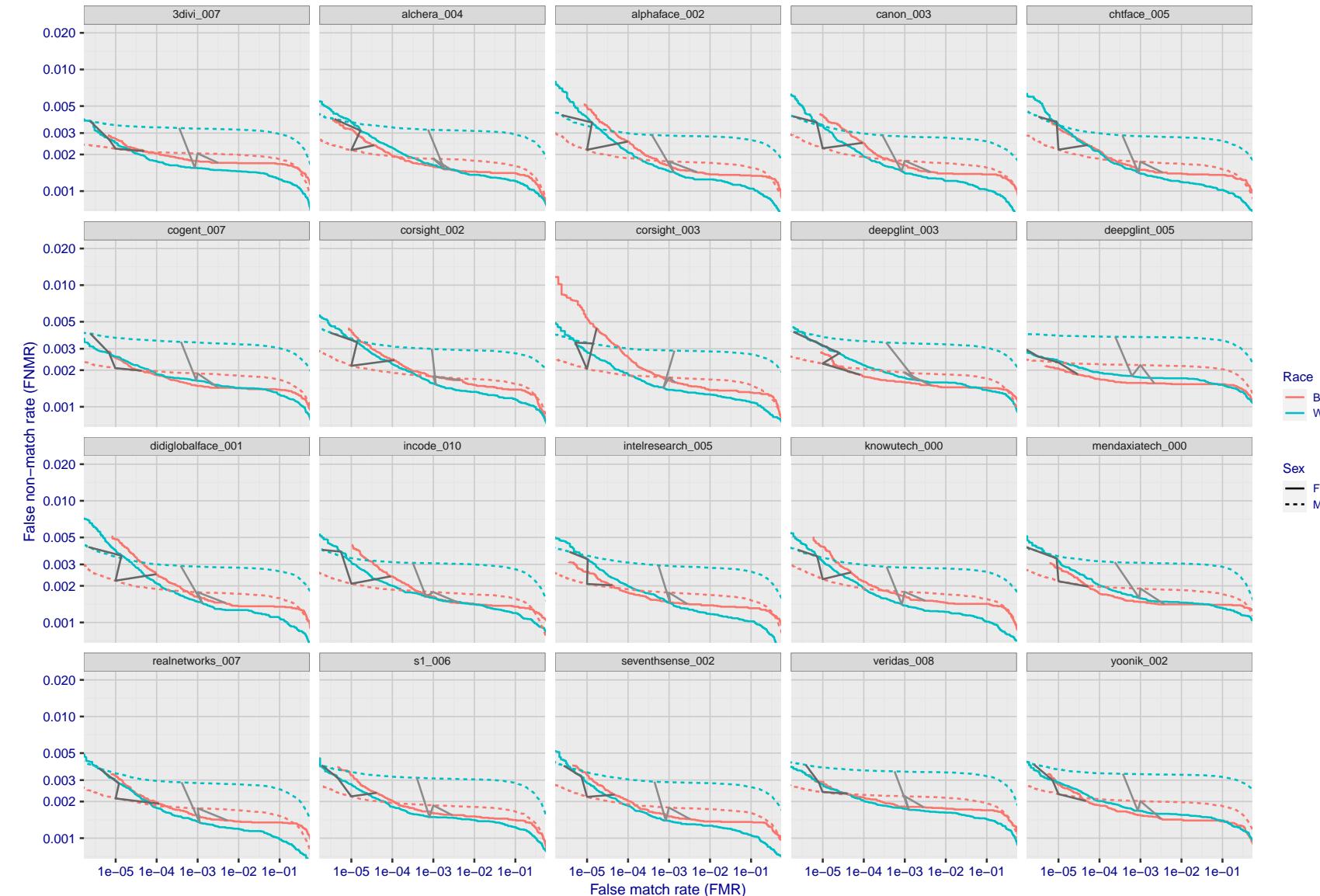


Figure 156: For the mugshot images, error tradeoff characteristics for white females, black females, black males and white males. The Z-shaped grey lines correspond to fixed thresholds, showing both FNMR and FMR vary at one T value. Note: Many of the plots will naively be read as saying women gives worse error rates than men because the solid traces lie above the dotted ones. However, this is misleading and incomplete: The grey lines show the traces reveal horizontal shifts. Thus for the cogent-003 algorithm FNMR for men is higher than for women at a fixed threshold but, at the same time, FMR is higher for women - see Figure 239. As access control systems almost always operate at a fixed threshold, the naive interpretation is incorrect.

2022/11/06 10:45:39

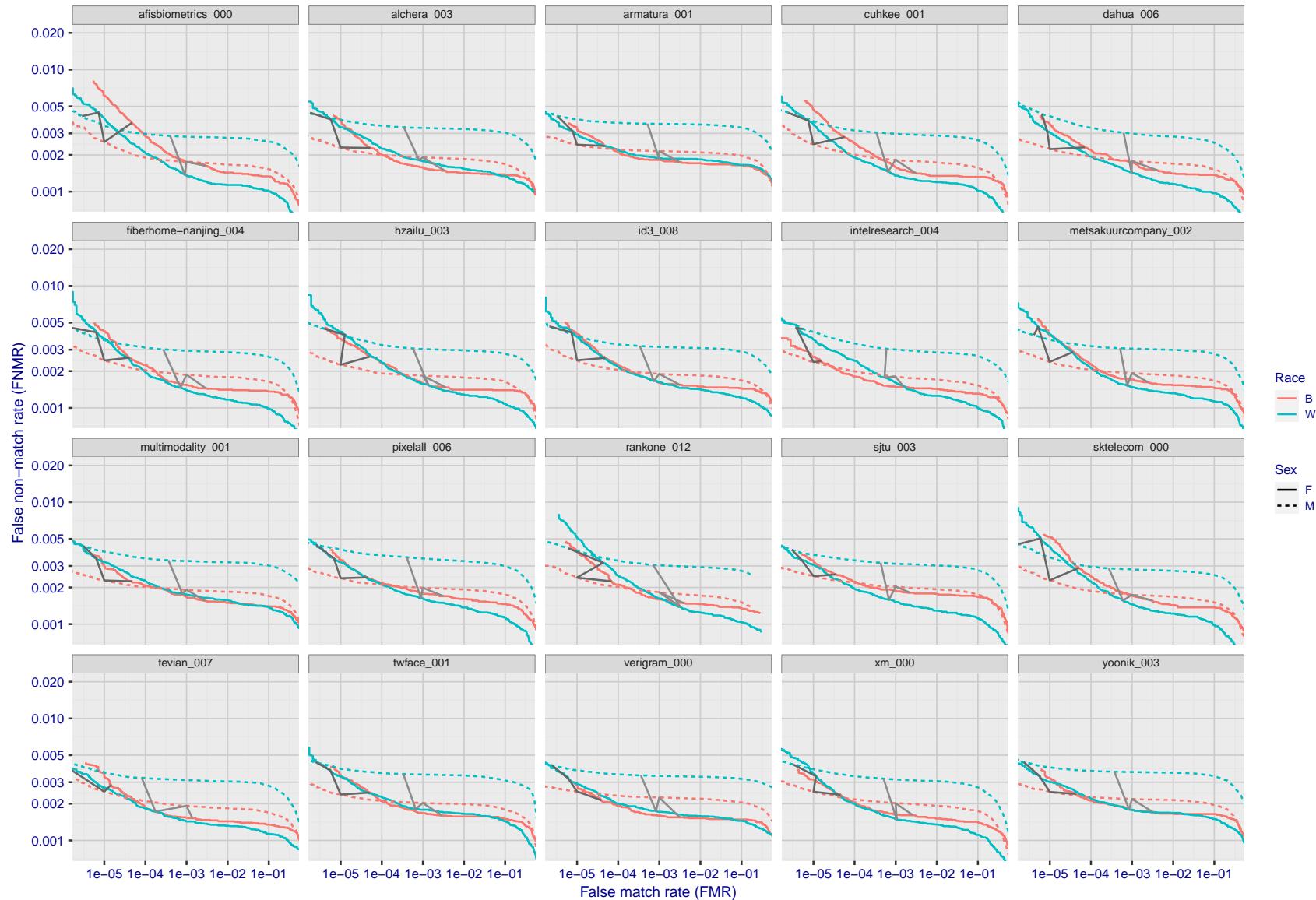


Figure 157: For the mugshot images, error tradeoff characteristics for white females, black females, black males and white males. The Z-shaped grey lines correspond to fixed thresholds, showing both FNMR and FMR vary at one T value. Note: Many of the plots will naively be read as saying women gives worse error rates than men because the solid traces lie above the dotted ones. However, this is misleading and incomplete: The grey lines show the traces reveal horizontal shifts. Thus for the cogent-003 algorithm FNMR for men is higher than for women at a fixed threshold but, at the same time, FMR is higher for women - see Figure 239. As access control systems almost always operate at a fixed threshold, the naive interpretation is incorrect.

FNMR(T)
FMR(T)

"False non-match rate"
"False match rate"

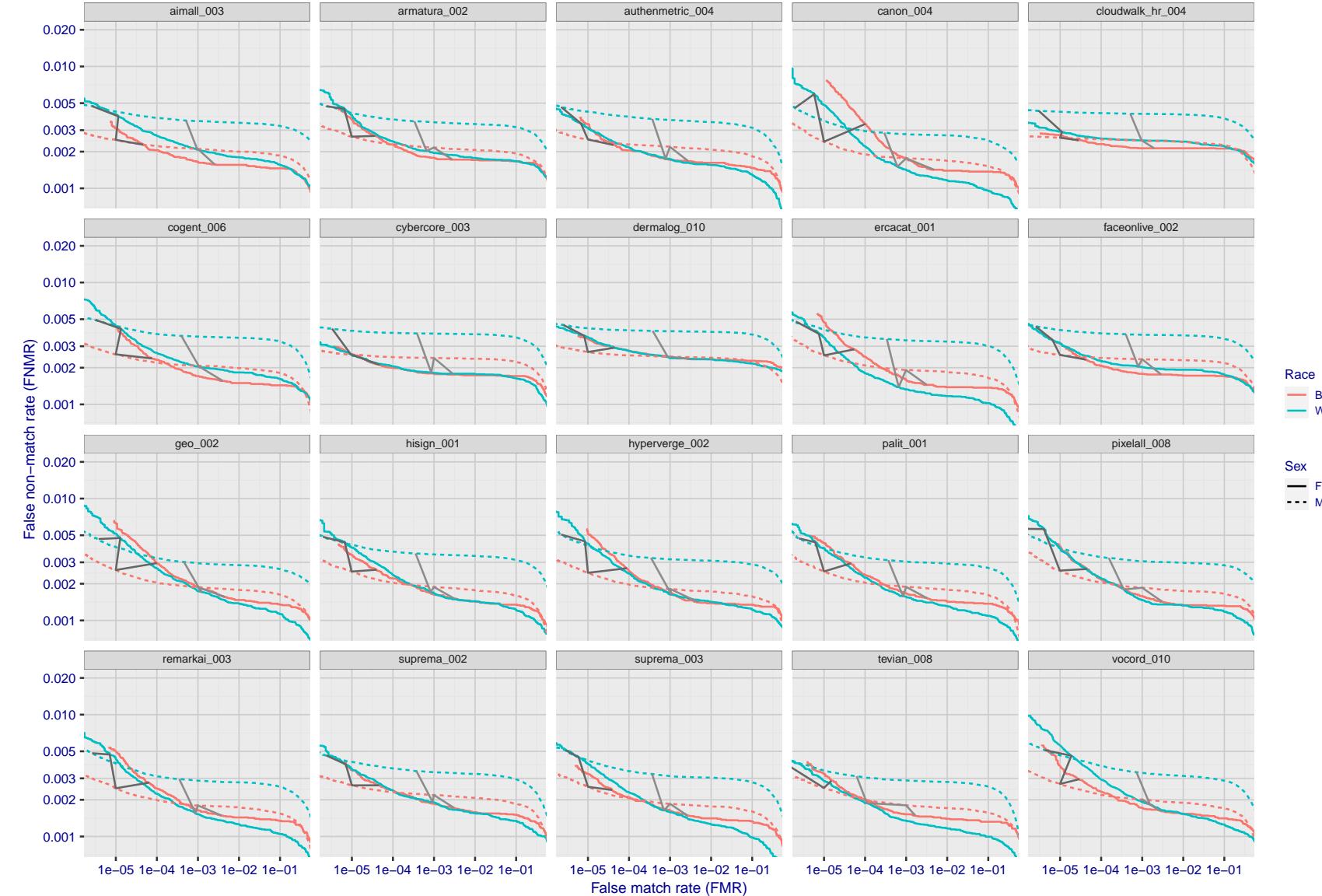


Figure 158: For the mugshot images, error tradeoff characteristics for white females, black females, black males and white males. The Z-shaped grey lines correspond to fixed thresholds, showing both FNMR and FMR vary at one T value. Note: Many of the plots will naively be read as saying women gives worse error rates than men because the solid traces lie above the dotted ones. However, this is misleading and incomplete: The grey lines show the traces reveal horizontal shifts. Thus for the cogent-003 algorithm FNMR for men is higher than for women at a fixed threshold but, at the same time, FMR is higher for women - see Figure 239. As access control systems almost always operate at a fixed threshold, the naive interpretation is incorrect.

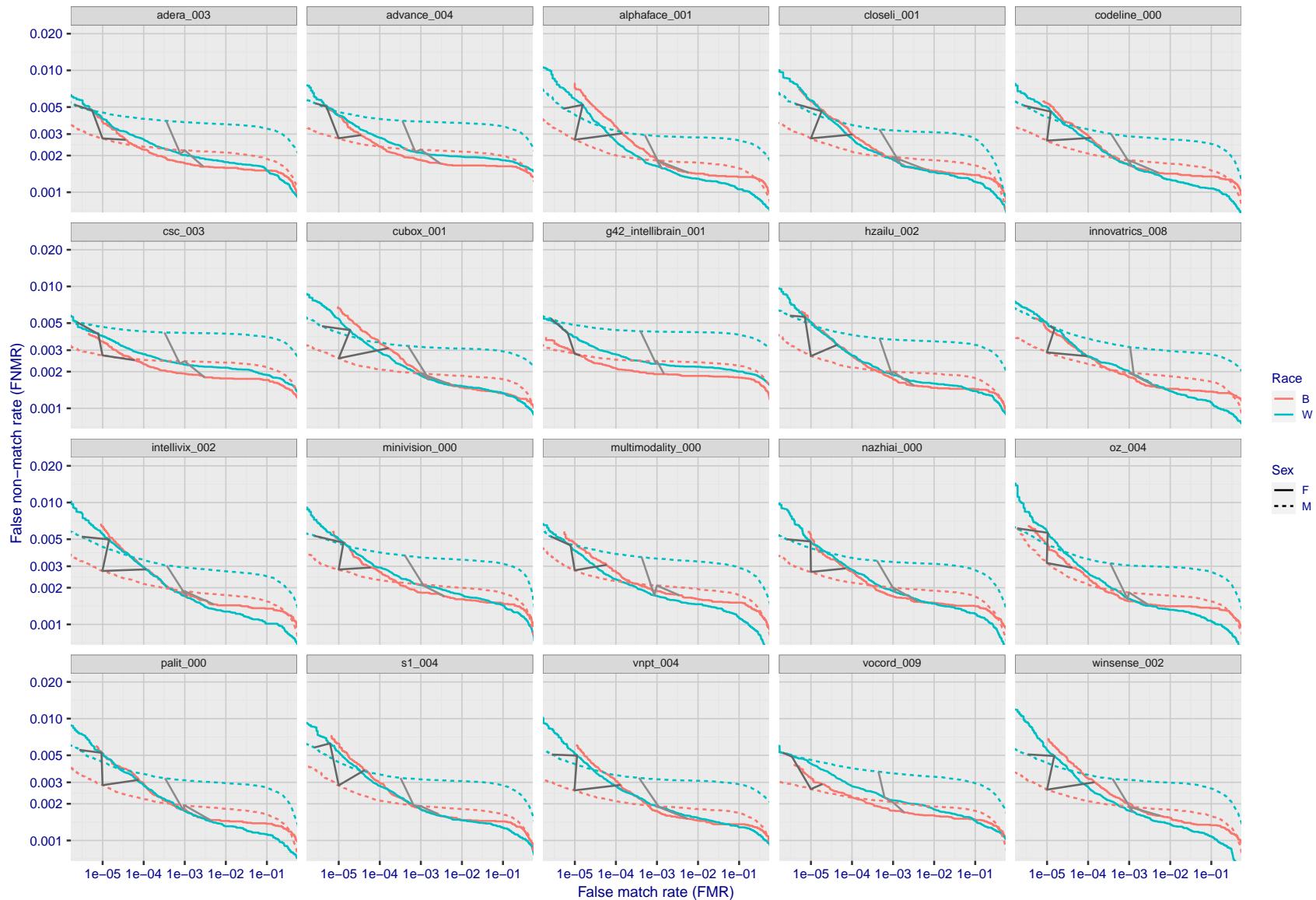


Figure 159: For the mugshot images, error tradeoff characteristics for white females, black females, black males and white males. The Z-shaped grey lines correspond to fixed thresholds, showing both FNMR and FMR vary at one T value. Note: Many of the plots will naively be read as saying women gives worse error rates than men because the solid traces lie above the dotted ones. However, this is misleading and incomplete: The grey lines show the traces reveal horizontal shifts. Thus for the cogent-003 algorithm FNMR for men is higher than for women at a fixed threshold but, at the same time, FMR is higher for women - see Figure 239. As access control systems almost always operate at a fixed threshold, the naive interpretation is incorrect.

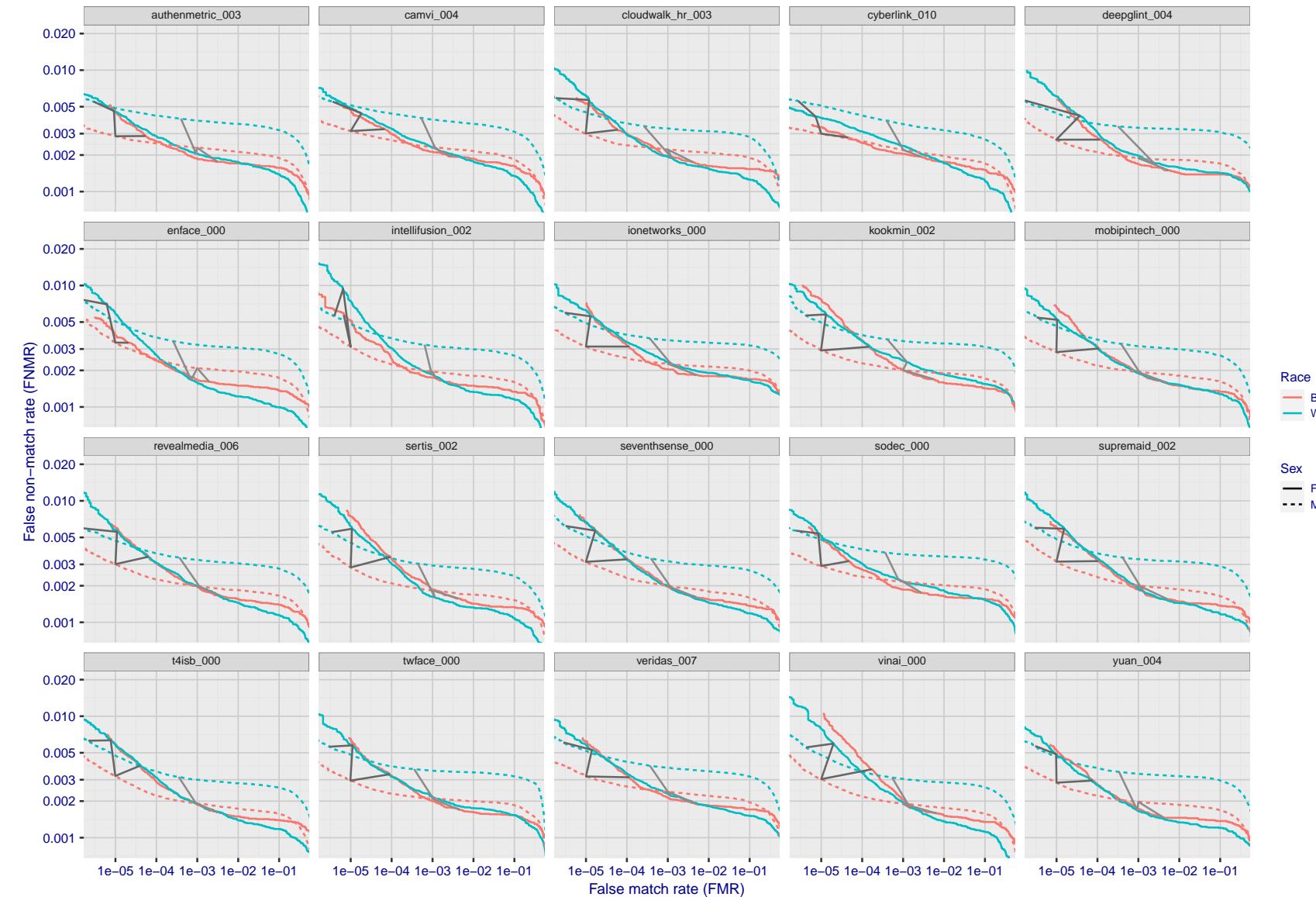


Figure 160: For the mugshot images, error tradeoff characteristics for white females, black females, black males and white males. The Z-shaped grey lines correspond to fixed thresholds, showing both FNMR and FMR vary at one T value. Note: Many of the plots will naively be read as saying women gives worse error rates than men because the solid traces lie above the dotted ones. However, this is misleading and incomplete: The grey lines show the traces reveal horizontal shifts. Thus for the cogent-003 algorithm FNMR for men is higher than for women at a fixed threshold but, at the same time, FMR is higher for women - see Figure 239. As access control systems almost always operate at a fixed threshold, the naive interpretation is incorrect.

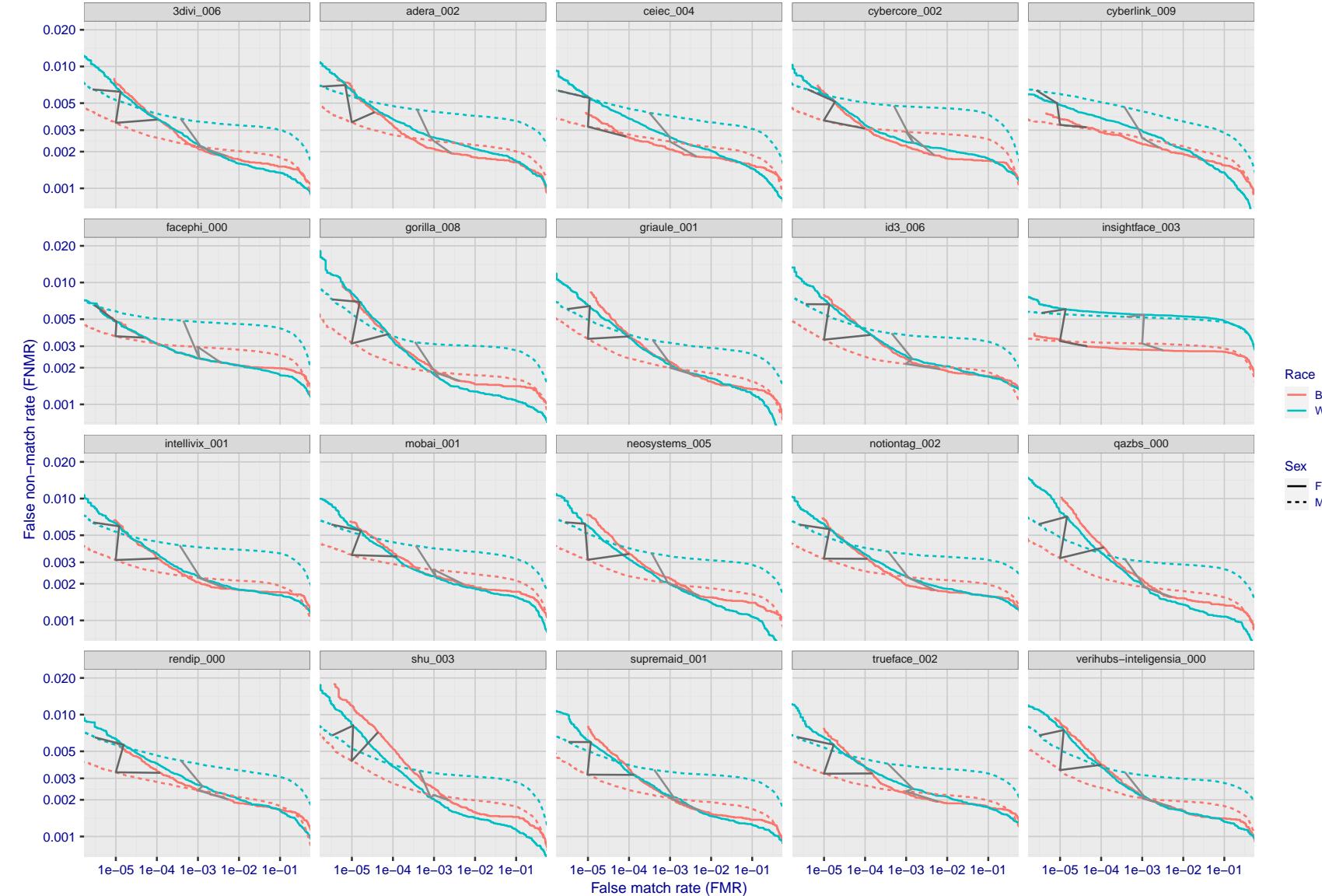


Figure 161: For the mugshot images, error tradeoff characteristics for white females, black females, black males and white males. The Z-shaped grey lines correspond to fixed thresholds, showing both FNMR and FMR vary at one T value. Note: Many of the plots will naively be read as saying women gives worse error rates than men because the solid traces lie above the dotted ones. However, this is misleading and incomplete: The grey lines show the traces reveal horizontal shifts. Thus for the cogent-003 algorithm FNMR for men is higher than for women at a fixed threshold but, at the same time, FMR is higher for women - see Figure 239. As access control systems almost always operate at a fixed threshold, the naive interpretation is incorrect.

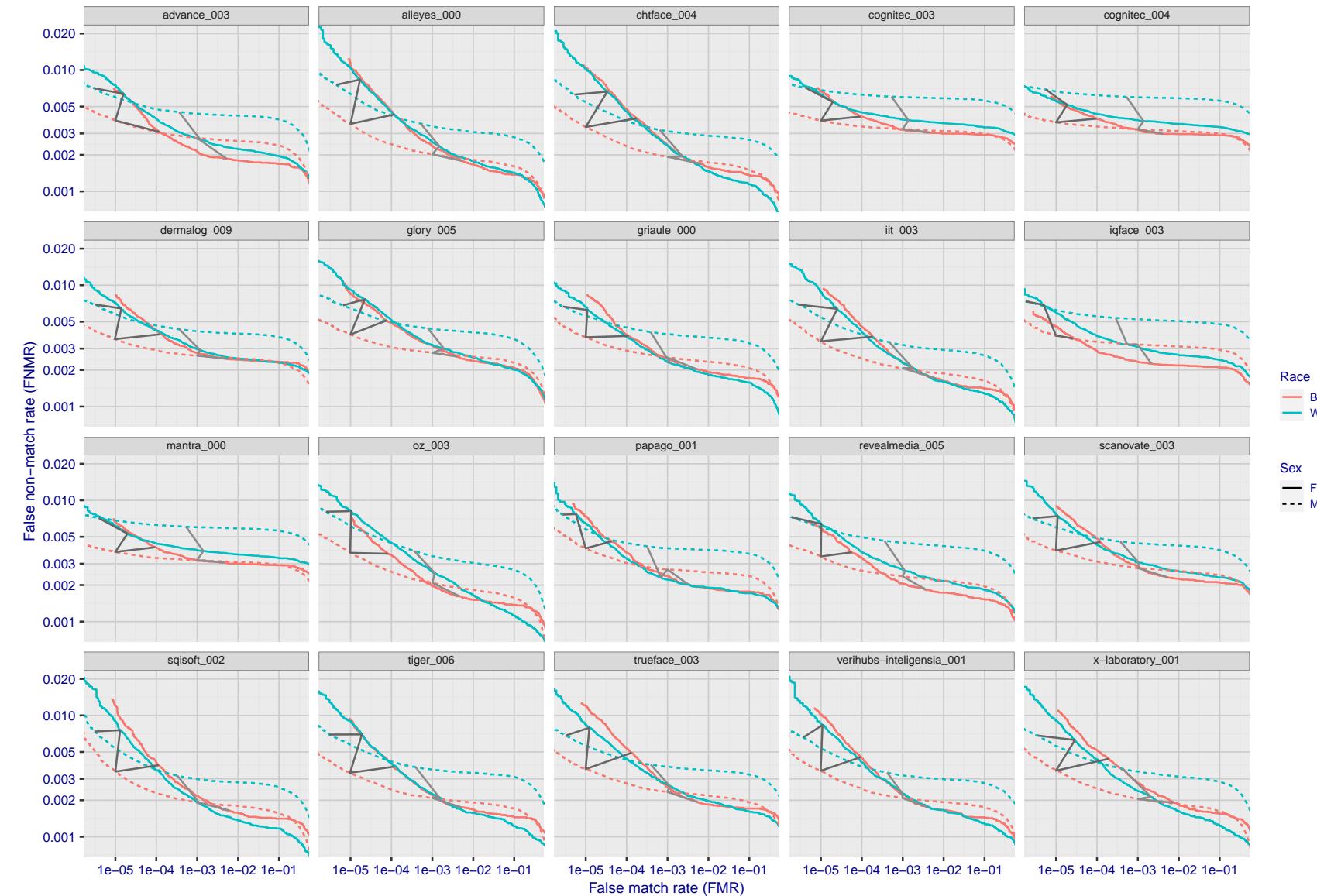


Figure 162: For the mugshot images, error tradeoff characteristics for white females, black females, black males and white males. The Z-shaped grey lines correspond to fixed thresholds, showing both FNMR and FMR vary at one T value. Note: Many of the plots will naively be read as saying women gives worse error rates than men because the solid traces lie above the dotted ones. However, this is misleading and incomplete: The grey lines show the traces reveal horizontal shifts. Thus for the cogent-003 algorithm FNMR for men is higher than for women at a fixed threshold but, at the same time, FMR is higher for women - see Figure 239. As access control systems almost always operate at a fixed threshold, the naive interpretation is incorrect.

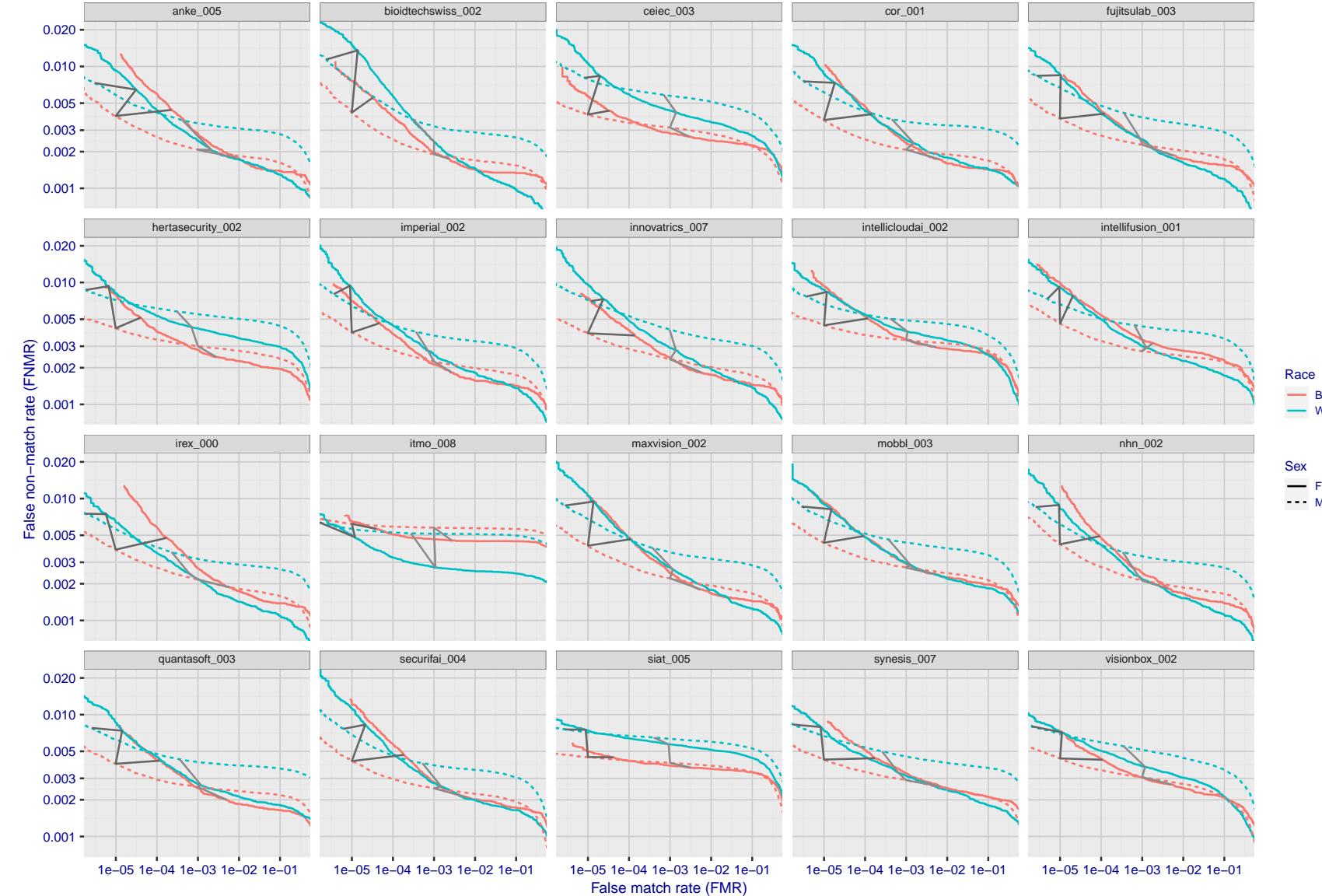


Figure 163: For the mugshot images, error tradeoff characteristics for white females, black females, black males and white males. The Z-shaped grey lines correspond to fixed thresholds, showing both FNMR and FMR vary at one T value. Note: Many of the plots will naively be read as saying women gives worse error rates than men because the solid traces lie above the dotted ones. However, this is misleading and incomplete: The grey lines show the traces reveal horizontal shifts. Thus for the cogent-003 algorithm FNMR for men is higher than for women at a fixed threshold but, at the same time, FMR is higher for women - see Figure 239. As access control systems almost always operate at a fixed threshold, the naive interpretation is incorrect.

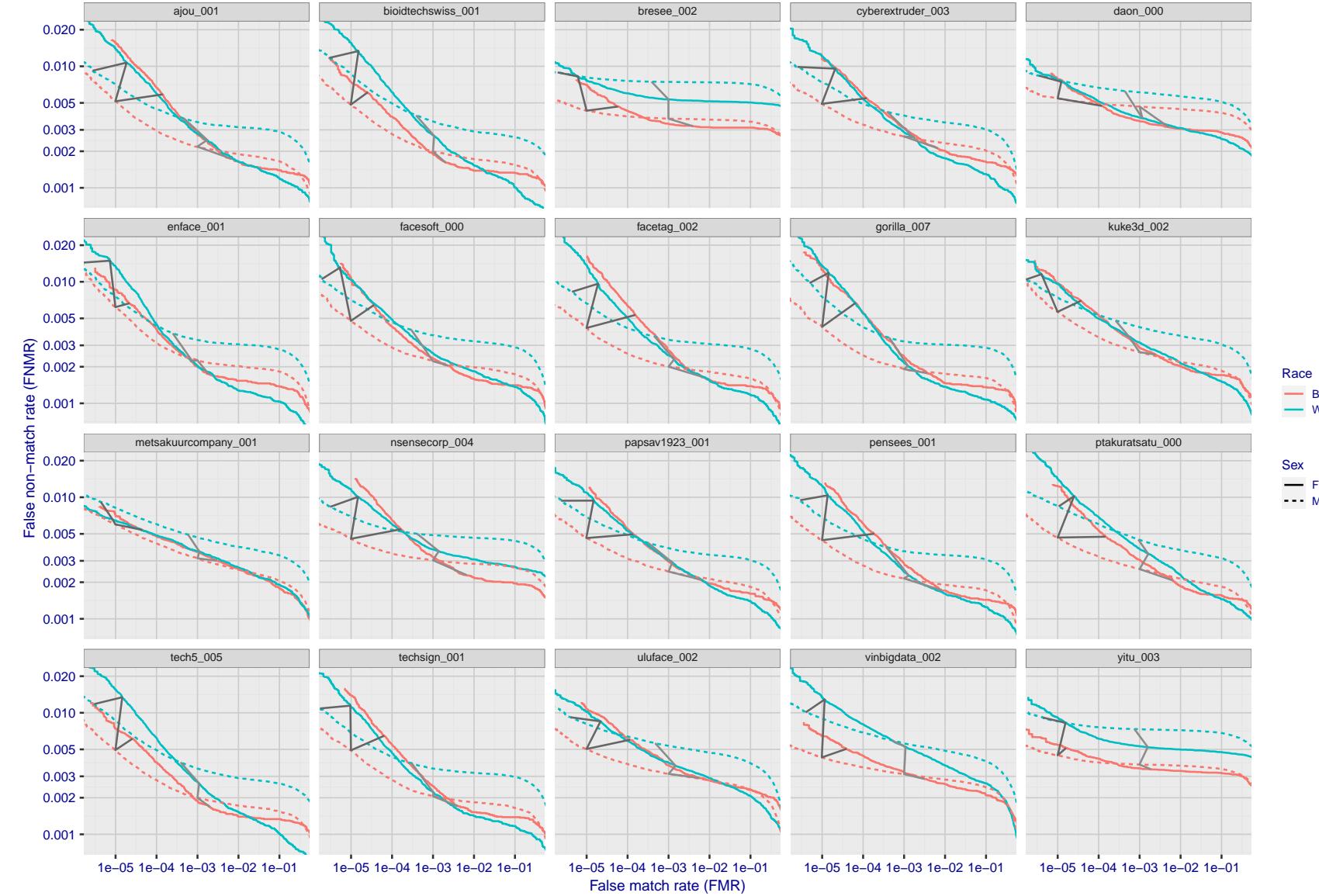


Figure 164: For the mugshot images, error tradeoff characteristics for white females, black females, black males and white males. The Z-shaped grey lines correspond to fixed thresholds, showing both FNMR and FMR vary at one T value. Note: Many of the plots will naively be read as saying women gives worse error rates than men because the solid traces lie above the dotted ones. However, this is misleading and incomplete: The grey lines show the traces reveal horizontal shifts. Thus for the cogent-003 algorithm FNMR for men is higher than for women at a fixed threshold but, at the same time, FMR is higher for women - see Figure 239. As access control systems almost always operate at a fixed threshold, the naive interpretation is incorrect.

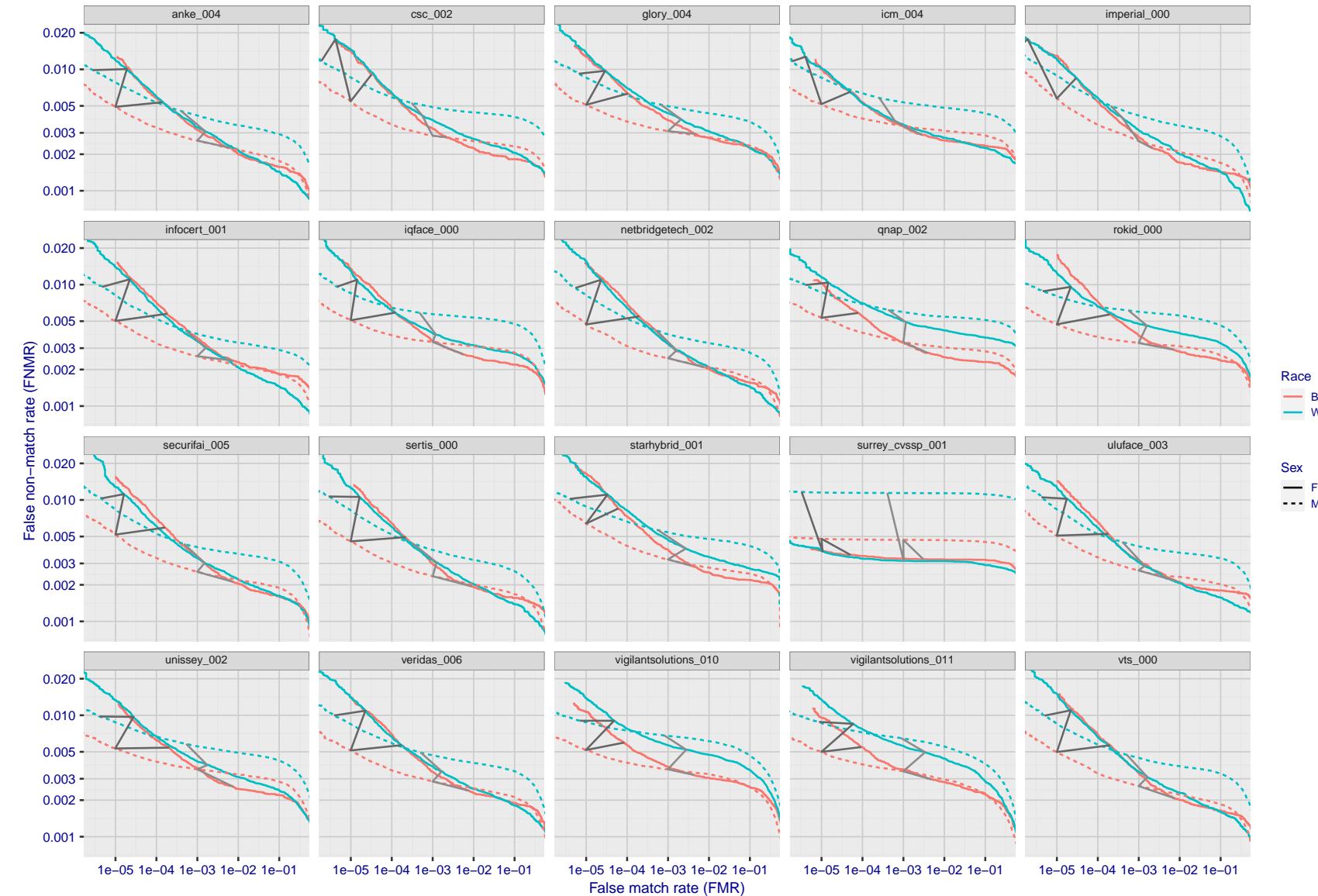


Figure 165: For the mugshot images, error tradeoff characteristics for white females, black females, black males and white males. The Z-shaped grey lines correspond to fixed thresholds, showing both FNMR and FMR vary at one T value. Note: Many of the plots will naively be read as saying women gives worse error rates than men because the solid traces lie above the dotted ones. However, this is misleading and incomplete: The grey lines show the traces reveal horizontal shifts. Thus for the cogent-003 algorithm FNMR for men is higher than for women at a fixed threshold but, at the same time, FMR is higher for women - see Figure 239. As access control systems almost always operate at a fixed threshold, the naive interpretation is incorrect.

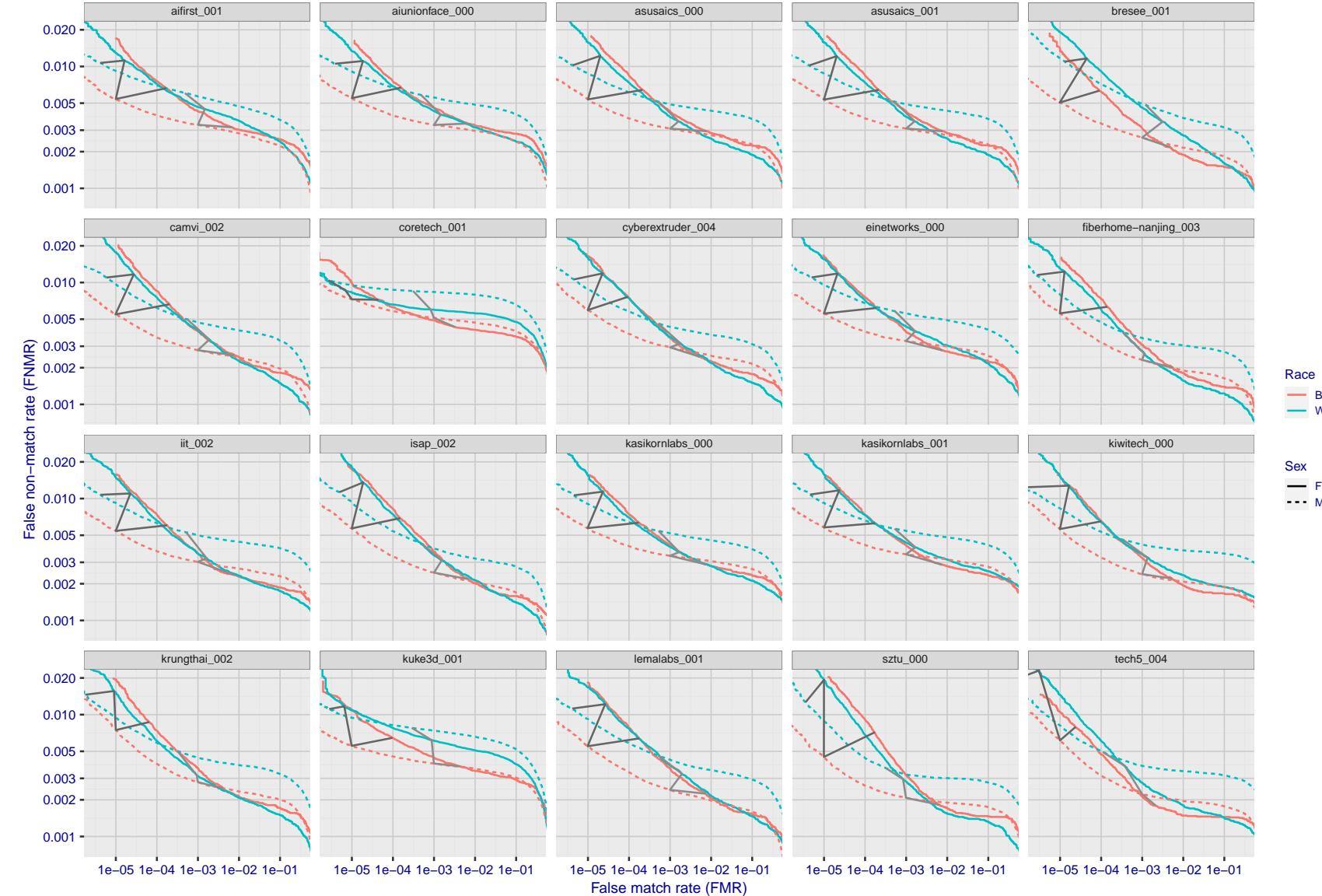


Figure 166: For the mugshot images, error tradeoff characteristics for white females, black females, black males and white males. The Z-shaped grey lines correspond to fixed thresholds, showing both FNMR and FMR vary at one T value. Note: Many of the plots will naively be read as saying women gives worse error rates than men because the solid traces lie above the dotted ones. However, this is misleading and incomplete: The grey lines show the traces reveal horizontal shifts. Thus for the cogent-003 algorithm FNMR for men is higher than for women at a fixed threshold but, at the same time, FMR is higher for women - see Figure 239. As access control systems almost always operate at a fixed threshold, the naive interpretation is incorrect.

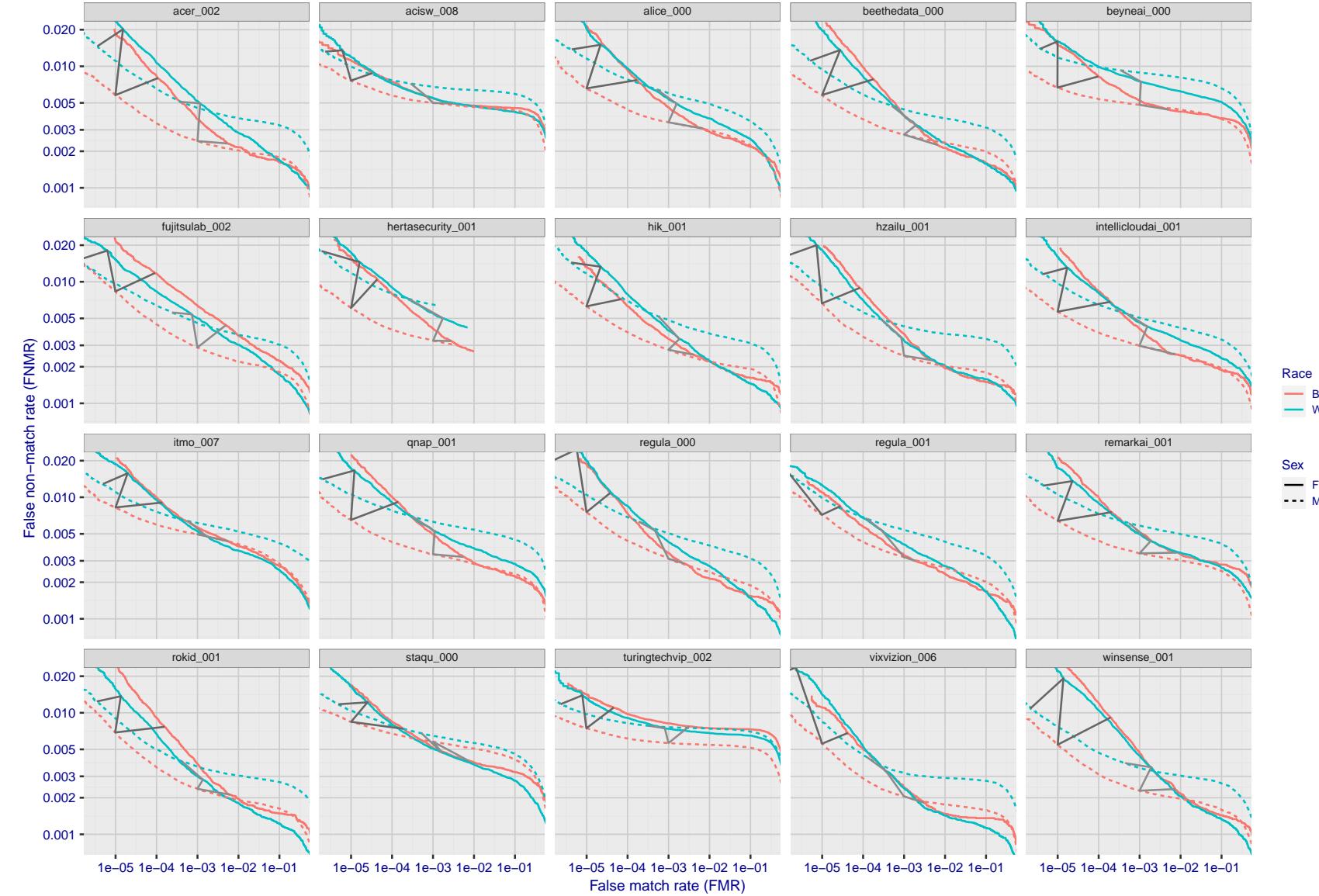


Figure 167: For the mugshot images, error tradeoff characteristics for white females, black females, black males and white males. The Z-shaped grey lines correspond to fixed thresholds, showing both FNMR and FMR vary at one T value. Note: Many of the plots will naively be read as saying women gives worse error rates than men because the solid traces lie above the dotted ones. However, this is misleading and incomplete: The grey lines show the traces reveal horizontal shifts. Thus for the cogent-003 algorithm FNMR for men is higher than for women at a fixed threshold but, at the same time, FMR is higher for women - see Figure 239. As access control systems almost always operate at a fixed threshold, the naive interpretation is incorrect.

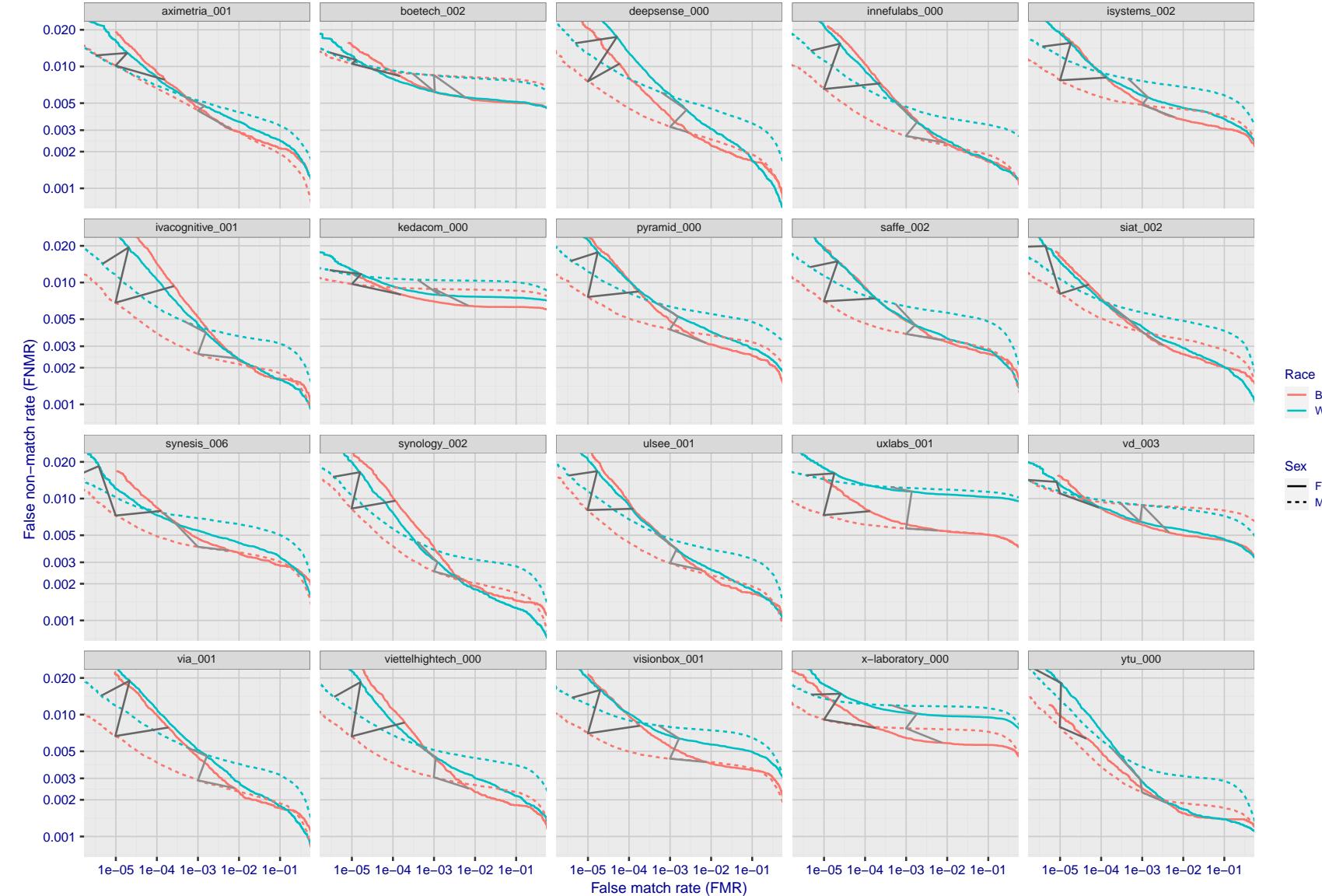


Figure 168: For the mugshot images, error tradeoff characteristics for white females, black females, black males and white males. The Z-shaped grey lines correspond to fixed thresholds, showing both FNMR and FMR vary at one T value. Note: Many of the plots will naively be read as saying women gives worse error rates than men because the solid traces lie above the dotted ones. However, this is misleading and incomplete: The grey lines show the traces reveal horizontal shifts. Thus for the cogent-003 algorithm FNMR for men is higher than for women at a fixed threshold but, at the same time, FMR is higher for women - see Figure 239. As access control systems almost always operate at a fixed threshold, the naive interpretation is incorrect.

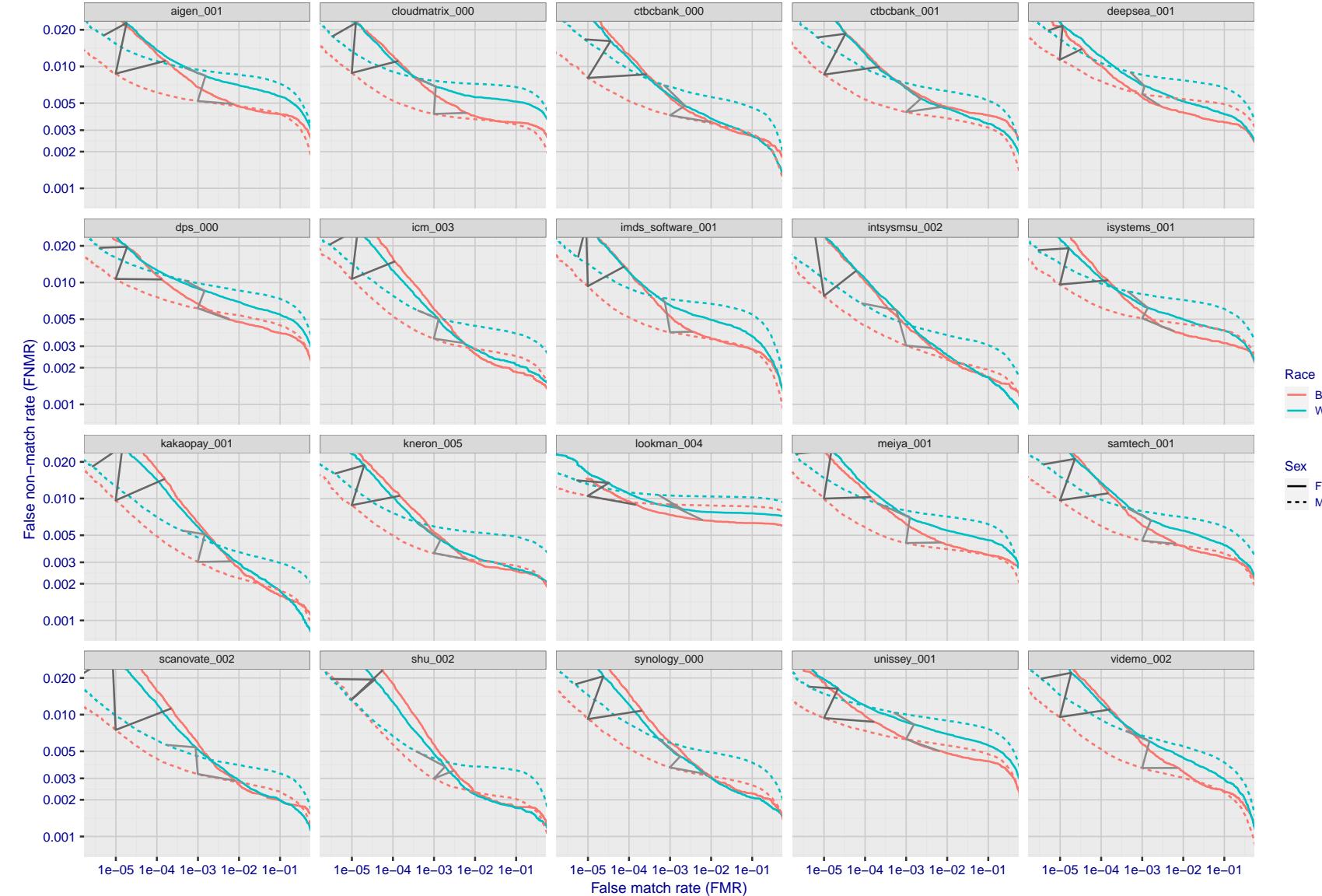


Figure 169: For the mugshot images, error tradeoff characteristics for white females, black females, black males and white males. The Z-shaped grey lines correspond to fixed thresholds, showing both FNMR and FMR vary at one T value. Note: Many of the plots will naively be read as saying women gives worse error rates than men because the solid traces lie above the dotted ones. However, this is misleading and incomplete: The grey lines show the traces reveal horizontal shifts. Thus for the cogent-003 algorithm FNMR for men is higher than for women at a fixed threshold but, at the same time, FMR is higher for women - see Figure 239. As access control systems almost always operate at a fixed threshold, the naive interpretation is incorrect.

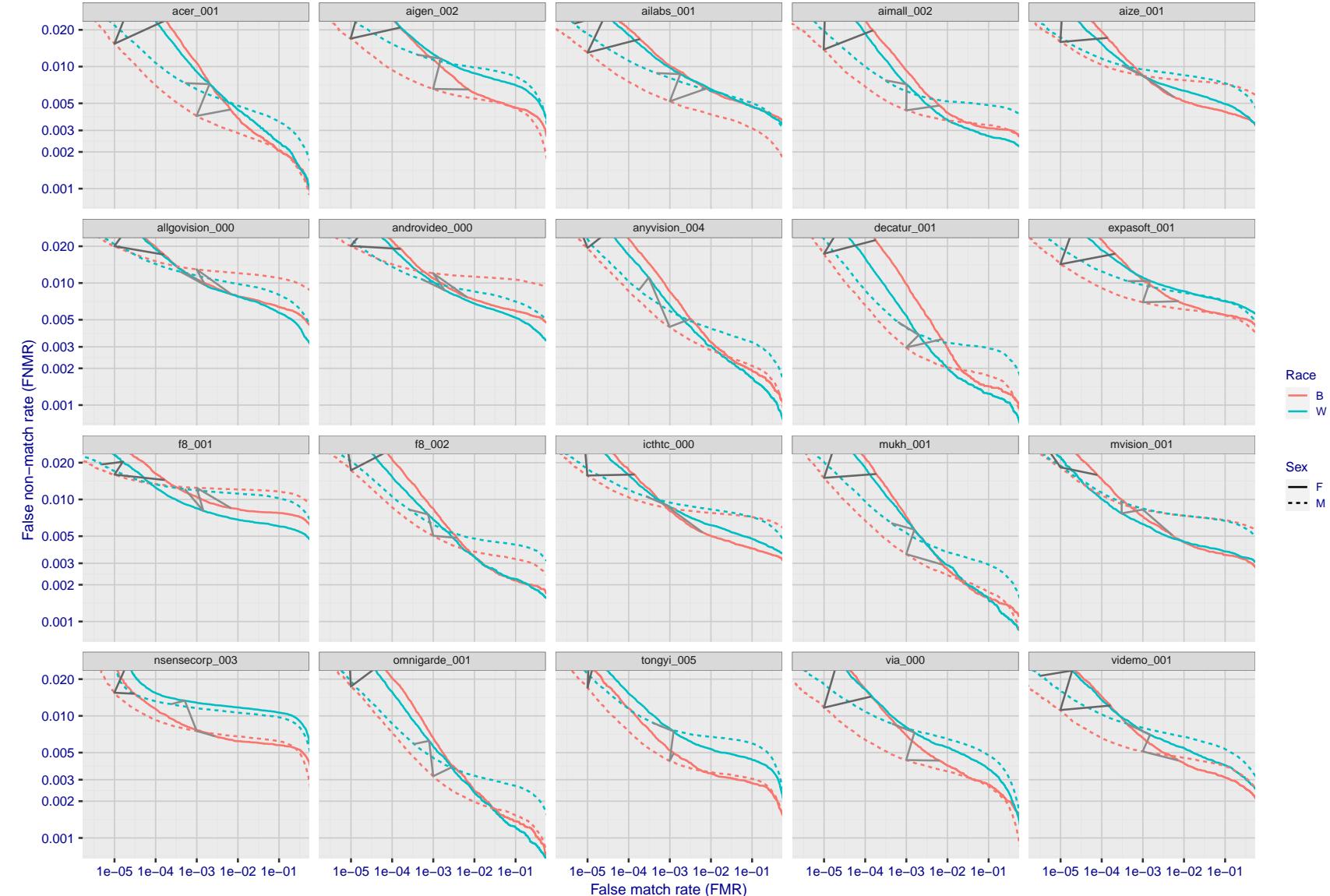


Figure 170: For the mugshot images, error tradeoff characteristics for white females, black females, black males and white males. The Z-shaped grey lines correspond to fixed thresholds, showing both FNMR and FMR vary at one T value. Note: Many of the plots will naively be read as saying women gives worse error rates than men because the solid traces lie above the dotted ones. However, this is misleading and incomplete: The grey lines show the traces reveal horizontal shifts. Thus for the cogent-003 algorithm FNMR for men is higher than for women at a fixed threshold but, at the same time, FMR is higher for women - see Figure 239. As access control systems almost always operate at a fixed threshold, the naive interpretation is incorrect.

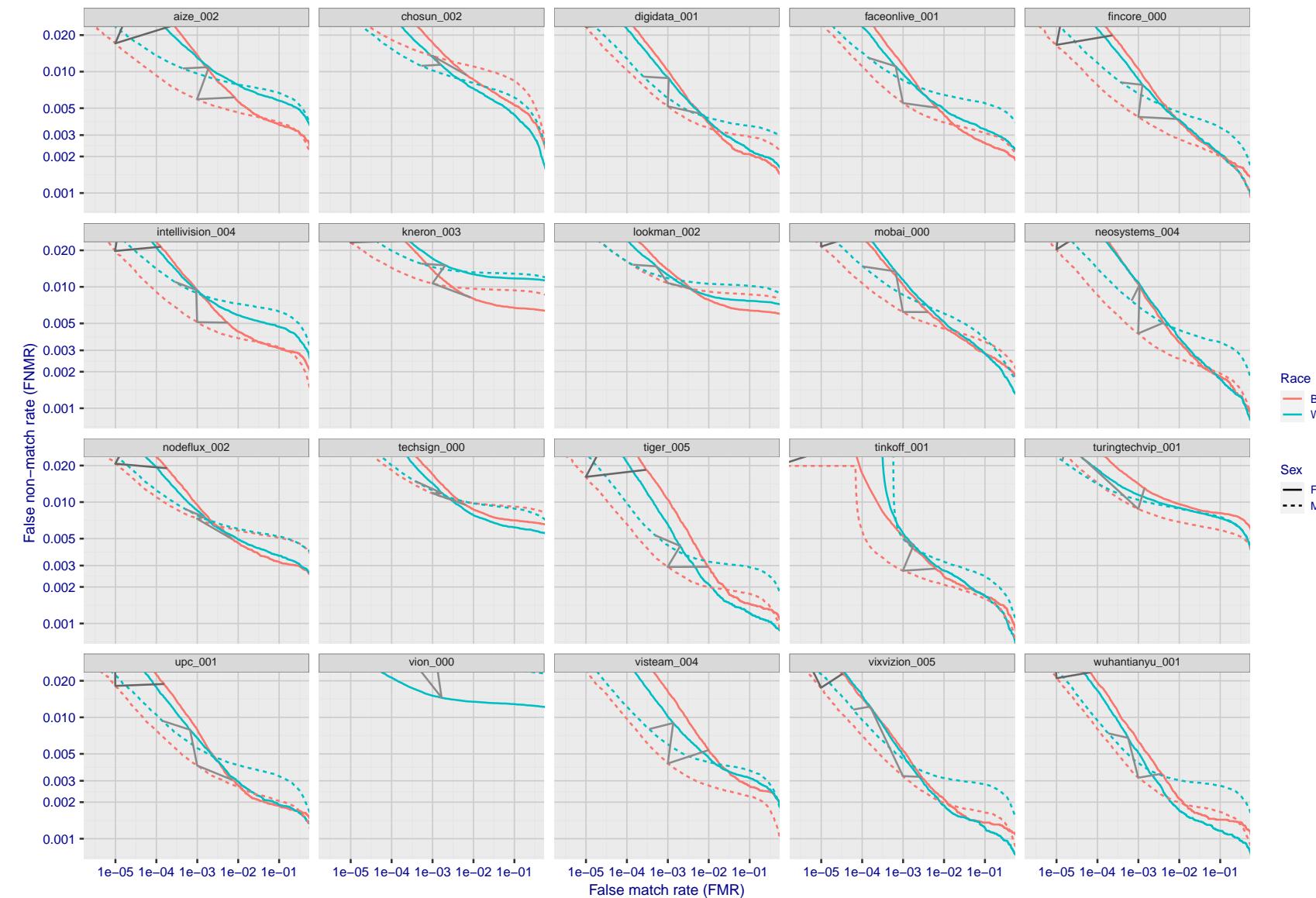


Figure 171: For the mugshot images, error tradeoff characteristics for white females, black females, black males and white males. The Z-shaped grey lines correspond to fixed thresholds, showing both FNMR and FMR vary at one T value. Note: Many of the plots will naively be read as saying women gives worse error rates than men because the solid traces lie above the dotted ones. However, this is misleading and incomplete: The grey lines show the traces reveal horizontal shifts. Thus for the cogent-003 algorithm FNMR for men is higher than for women at a fixed threshold but, at the same time, FMR is higher for women - see Figure 239. As access control systems almost always operate at a fixed threshold, the naive interpretation is incorrect.

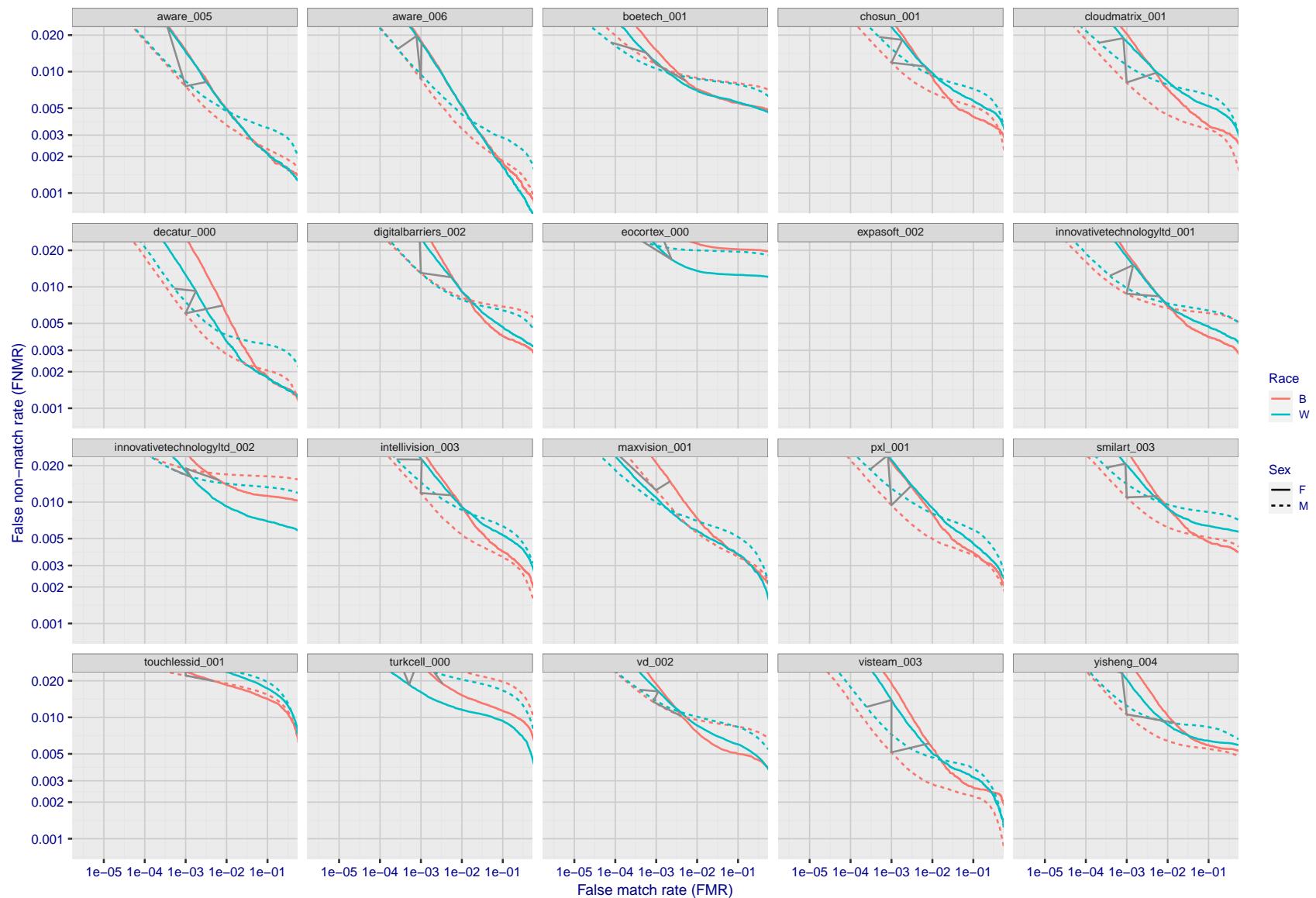


Figure 172: For the mugshot images, error tradeoff characteristics for white females, black females, black males and white males. The Z-shaped grey lines correspond to fixed thresholds, showing both FNMR and FMR vary at one T value. Note: Many of the plots will naively be read as saying women gives worse error rates than men because the solid traces lie above the dotted ones. However, this is misleading and incomplete: The grey lines show the traces reveal horizontal shifts. Thus for the cogent-003 algorithm FNMR for men is higher than for women at a fixed threshold but, at the same time, FMR is higher for women - see Figure 239. As access control systems almost always operate at a fixed threshold, the naive interpretation is incorrect.

2022/11/06 10:45:39

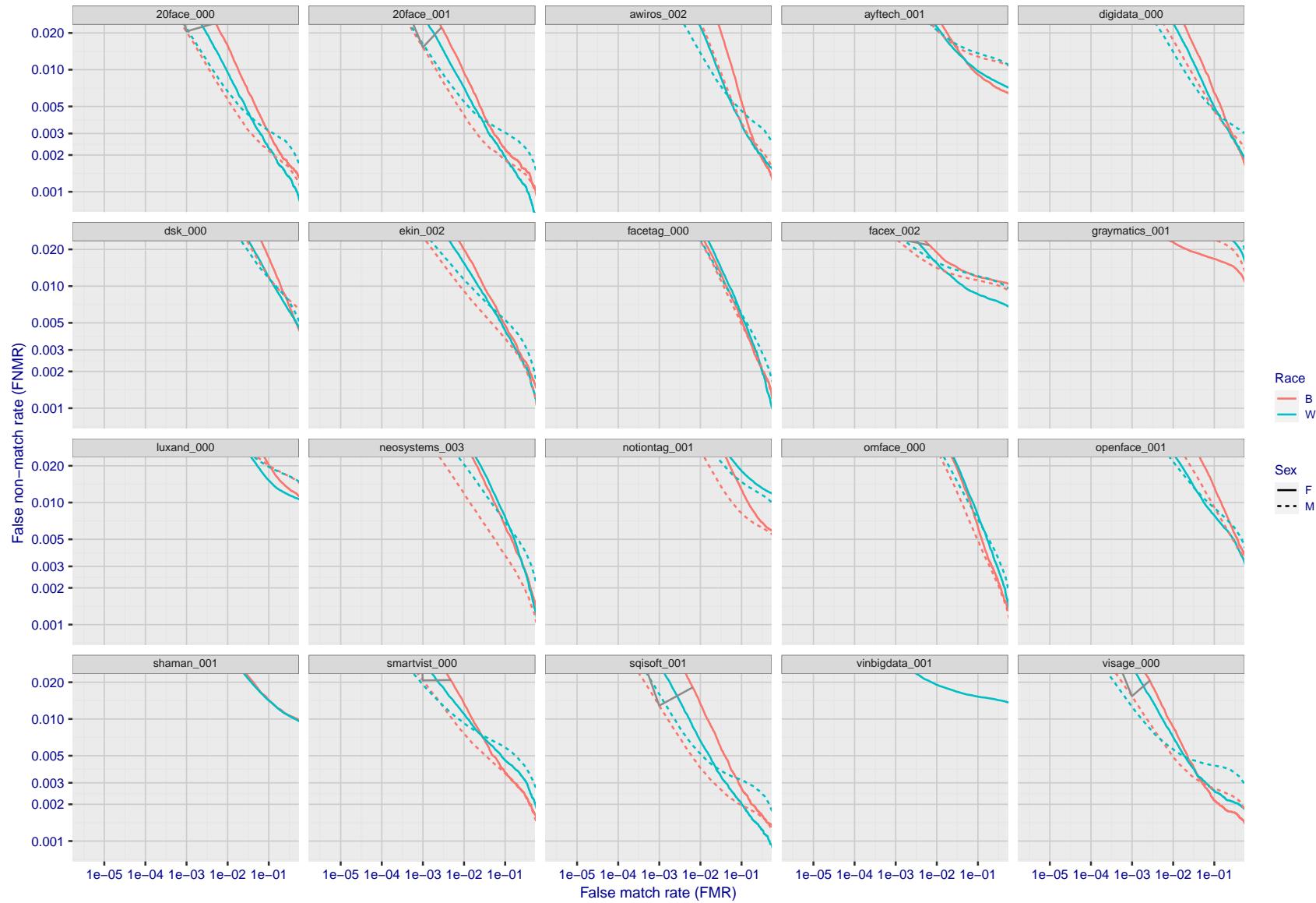


Figure 173: For the mugshot images, error tradeoff characteristics for white females, black females, black males and white males. The Z-shaped grey lines correspond to fixed thresholds, showing both FNMR and FMR vary at one T value. Note: Many of the plots will naively be read as saying women gives worse error rates than men because the solid traces lie above the dotted ones. However, this is misleading and incomplete: The grey lines show the traces reveal horizontal shifts. Thus for the cogent-003 algorithm FNMR for men is higher than for women at a fixed threshold but, at the same time, FMR is higher for women - see Figure 239. As access control systems almost always operate at a fixed threshold, the naive interpretation is incorrect.

FNMR(T)
FMR(T)
"False non-match rate"
"False match rate"

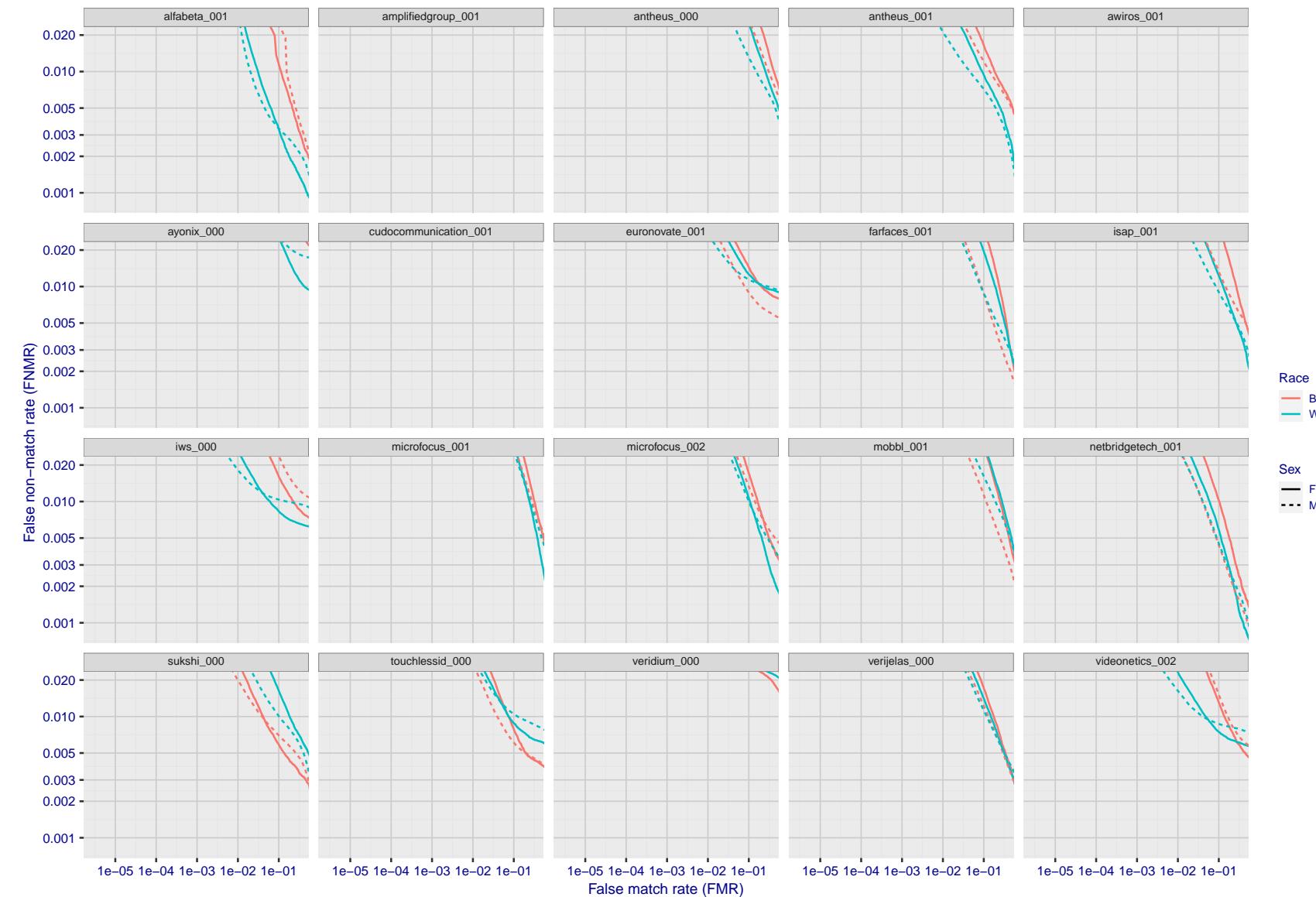


Figure 174: For the mugshot images, error tradeoff characteristics for white females, black females, black males and white males. The Z-shaped grey lines correspond to fixed thresholds, showing both FNMR and FMR vary at one T value. Note: Many of the plots will naively be read as saying women gives worse error rates than men because the solid traces lie above the dotted ones. However, this is misleading and incomplete: The grey lines show the traces reveal horizontal shifts. Thus for the cogent-003 algorithm FNMR for men is higher than for women at a fixed threshold but, at the same time, FMR is higher for women - see Figure 239. As access control systems almost always operate at a fixed threshold, the naive interpretation is incorrect.

2022/11/06 10:45:39

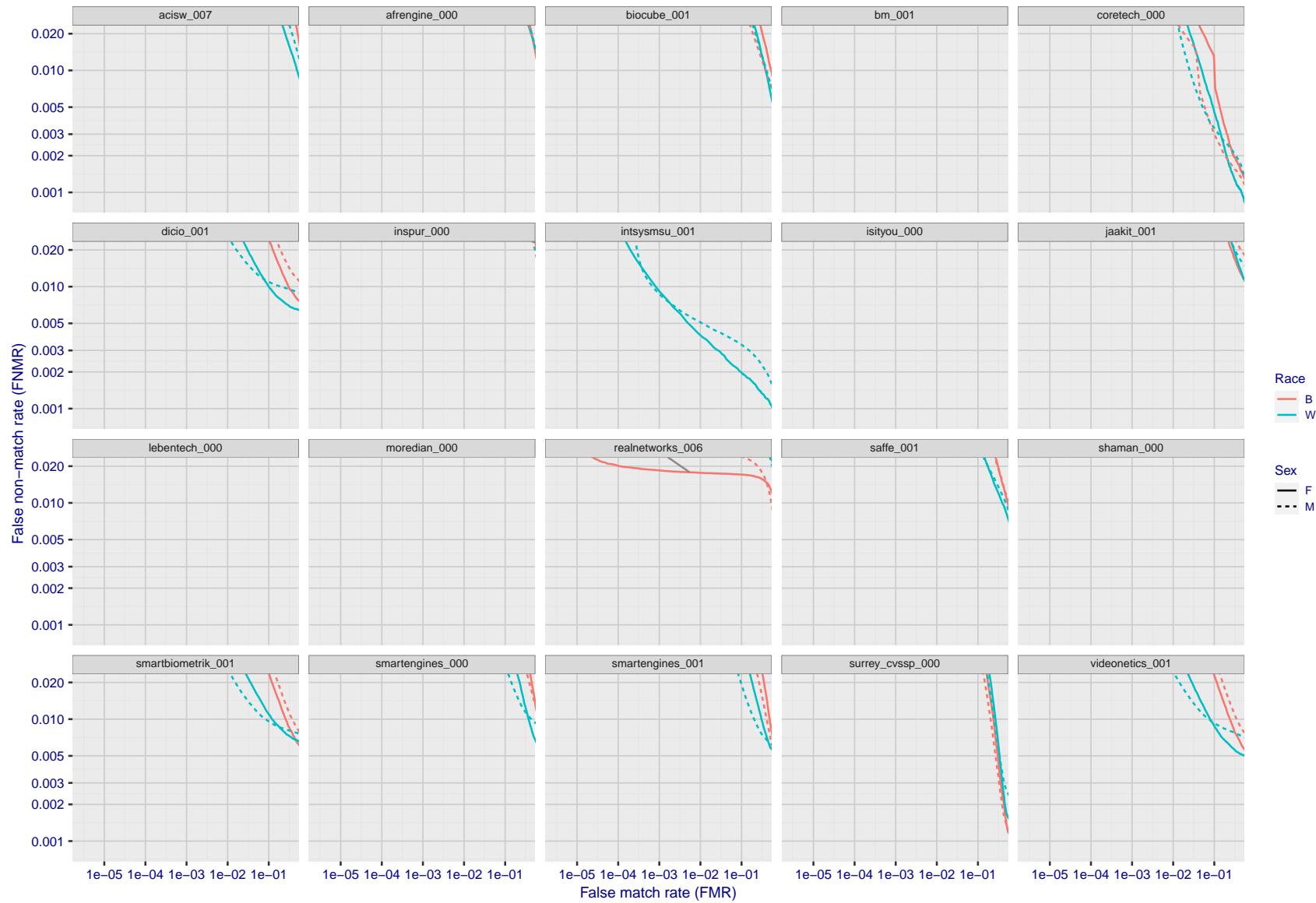


Figure 175: For the mugshot images, error tradeoff characteristics for white females, black females, black males and white males. The Z-shaped grey lines correspond to fixed thresholds, showing both FNMR and FMR vary at one T value. Note: Many of the plots will naively be read as saying women gives worse error rates than men because the solid traces lie above the dotted ones. However, this is misleading and incomplete: The grey lines show the traces reveal horizontal shifts. Thus for the cogent-003 algorithm FNMR for men is higher than for women at a fixed threshold but, at the same time, FMR is higher for women - see Figure 239. As access control systems almost always operate at a fixed threshold, the naive interpretation is incorrect.

FNMR(T)"False non-match rate"
"False match rate"

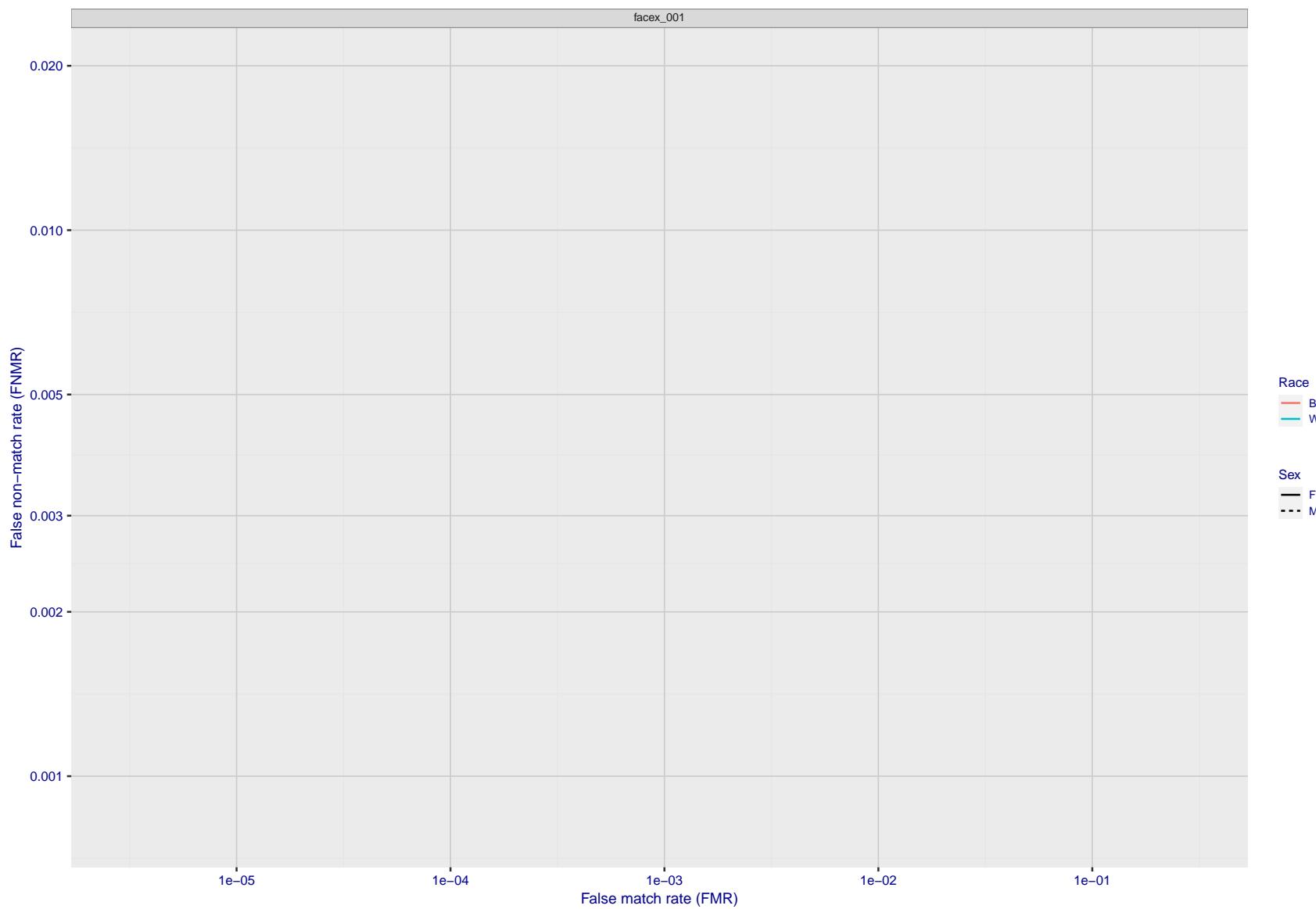


Figure 176: For the mugshot images, error tradeoff characteristics for white females, black females, black males and white males. The Z-shaped grey lines correspond to fixed thresholds, showing both FNMR and FMR vary at one T value. Note: Many of the plots will naively be read as saying women gives worse error rates than men because the solid traces lie above the dotted ones. However, this is misleading and incomplete: The grey lines show the traces reveal horizontal shifts. Thus for the cogent-003 algorithm FNMR for men is higher than for women at a fixed threshold but, at the same time, FMR is higher for women - see Figure 239. As access control systems almost always operate at a fixed threshold, the naive interpretation is incorrect.

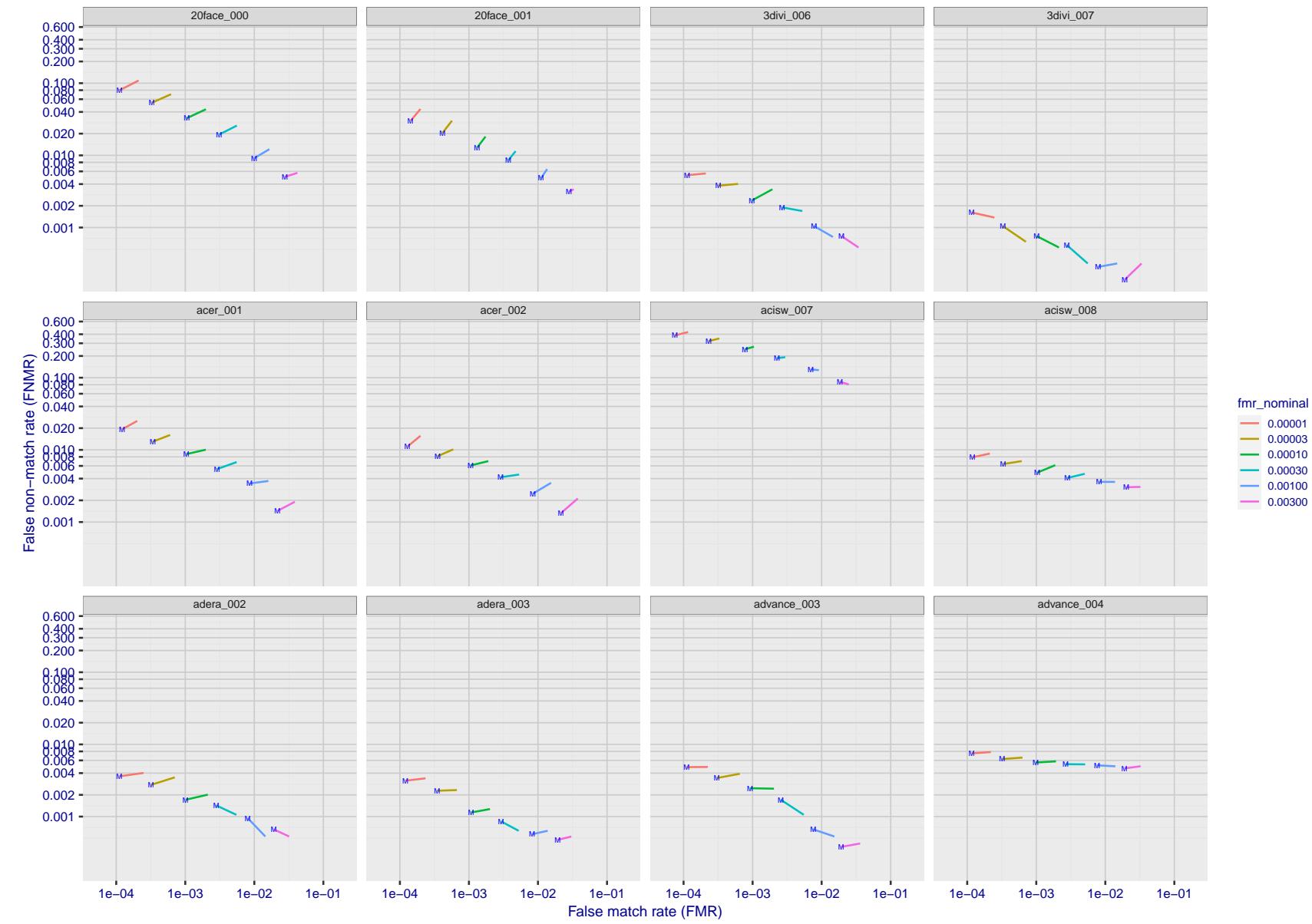


Figure 177: For the visa images, FNMR and FMR at six operating points along the DET characteristic. At each point a line is drawn between $(FMR, FNMR)_{MALE}$ and $(FMR, FNMR)_{FEMALE}$ showing how which sex has lower FMR and/or FNMR. The "M" label denotes male, the other end of the line corresponds to female. The six operating thresholds are selected to give the nominal false match rates given in the legend, and are computed over all impostor pairs regardless of age, sex, and place of birth. The plotted FMR values are broadly an order of magnitude larger than the nominal rates because FMR is computed over demographically-matched impostor pairs i.e individuals of the same sex, from the same geographic region (see section 3.6.1), and the same age group (see section 3.6.2).

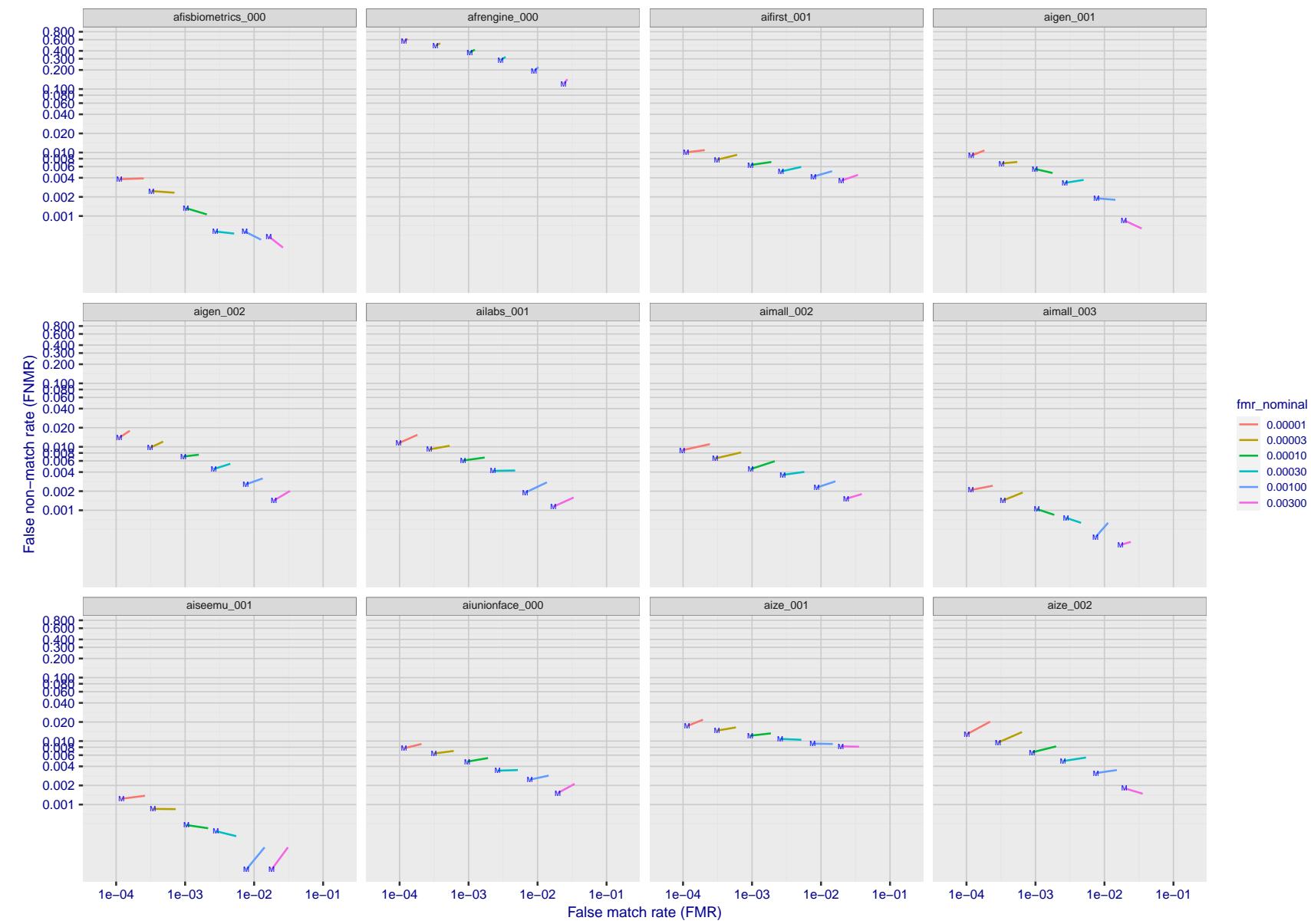


Figure 178: For the visa images, FNMR and FMR at six operating points along the DET characteristic. At each point a line is drawn between $(FMR, FNMR)_{MALE}$ and $(FMR, FNMR)_{FEMALE}$ showing how which sex has lower FMR and/or FNMR. The "M" label denotes male, the other end of the line corresponds to female. The six operating thresholds are selected to give the nominal false match rates given in the legend, and are computed over all impostor pairs regardless of age, sex, and place of birth. The plotted FMR values are broadly an order of magnitude larger than the nominal rates because FMR is computed over demographically-matched impostor pairs i.e individuals of the same sex, from the same geographic region (see section 3.6.1), and the same age group (see section 3.6.2).

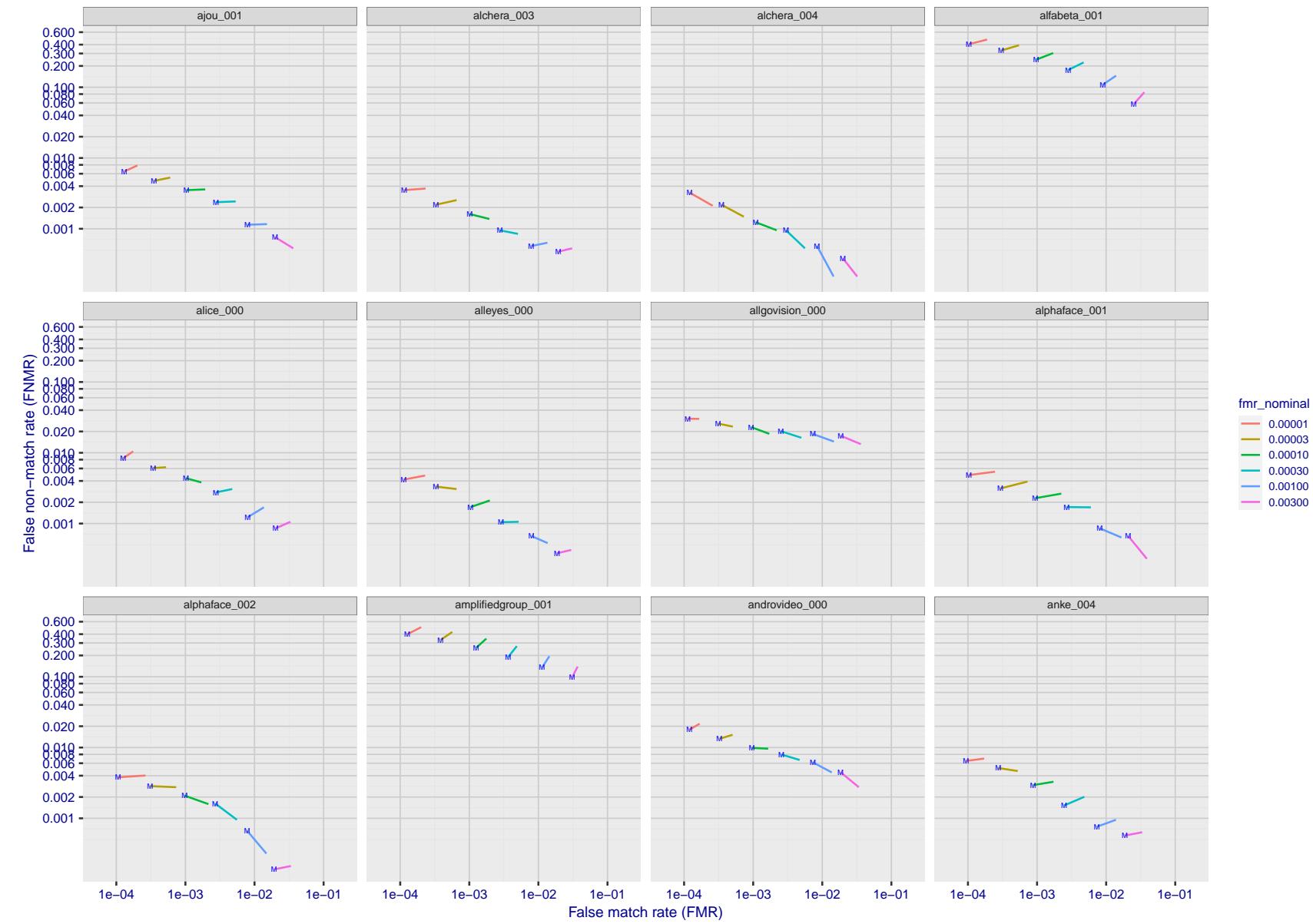


Figure 179: For the visa images, FNMR and FMR at six operating points along the DET characteristic. At each point a line is drawn between $(FMR, FNMR)_{MALE}$ and $(FMR, FNMR)_{FEMALE}$ showing how which sex has lower FMR and/or FNMR. The "M" label denotes male, the other end of the line corresponds to female. The six operating thresholds are selected to give the nominal false match rates given in the legend, and are computed over all impostor pairs regardless of age, sex, and place of birth. The plotted FMR values are broadly an order of magnitude larger than the nominal rates because FMR is computed over demographically-matched impostor pairs i.e individuals of the same sex, from the same geographic region (see section 3.6.1), and the same age group (see section 3.6.2).

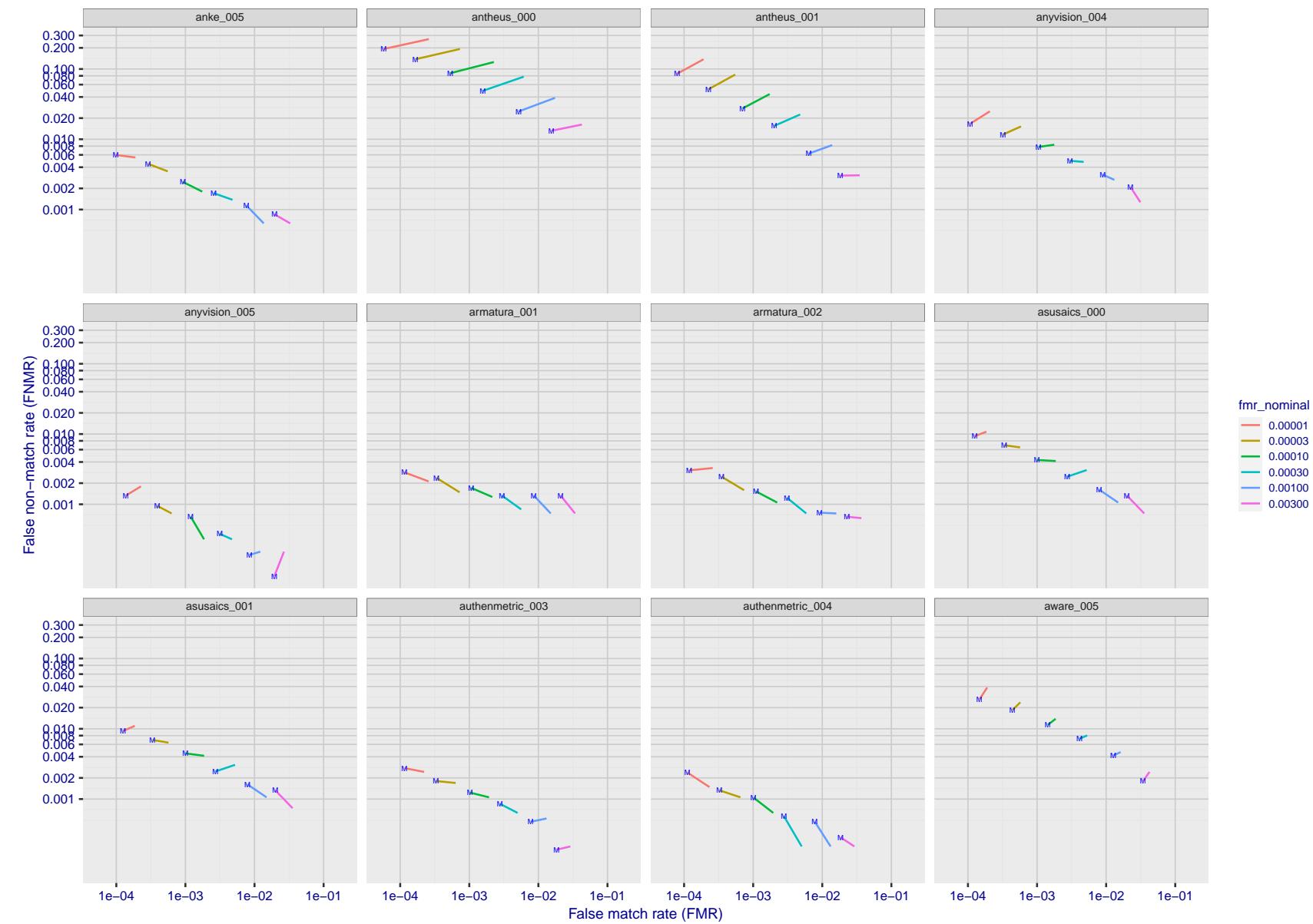


Figure 180: For the visa images, FNMR and FMR at six operating points along the DET characteristic. At each point a line is drawn between $(FMR, FNMR)_{MALE}$ and $(FMR, FNMR)_{FEMALE}$ showing how which sex has lower FMR and/or FNMR. The "M" label denotes male, the other end of the line corresponds to female. The six operating thresholds are selected to give the nominal false match rates given in the legend, and are computed over all impostor pairs regardless of age, sex, and place of birth. The plotted FMR values are broadly an order of magnitude larger than the nominal rates because FMR is computed over demographically-matched impostor pairs i.e individuals of the same sex, from the same geographic region (see section 3.6.1), and the same age group (see section 3.6.2).

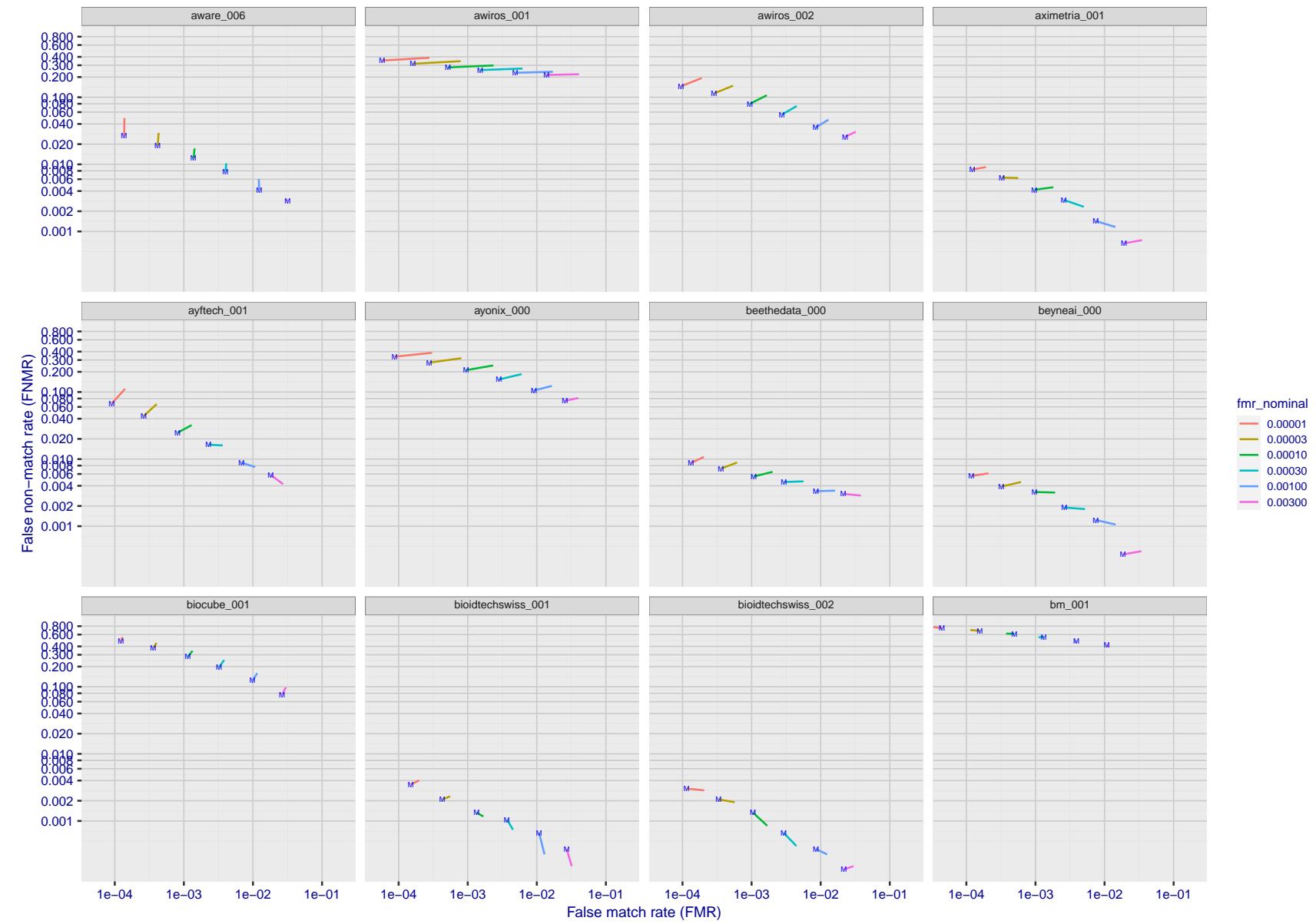


Figure 181: For the visa images, FNMR and FMR at six operating points along the DET characteristic. At each point a line is drawn between $(FMR, FNMR)_{MALE}$ and $(FMR, FNMR)_{FEMALE}$ showing how which sex has lower FMR and/or FNMR. The "M" label denotes male, the other end of the line corresponds to female. The six operating thresholds are selected to give the nominal false match rates given in the legend, and are computed over all impostor pairs regardless of age, sex, and place of birth. The plotted FMR values are broadly an order of magnitude larger than the nominal rates because FMR is computed over demographically-matched impostor pairs i.e individuals of the same sex, from the same geographic region (see section 3.6.1), and the same age group (see section 3.6.2).

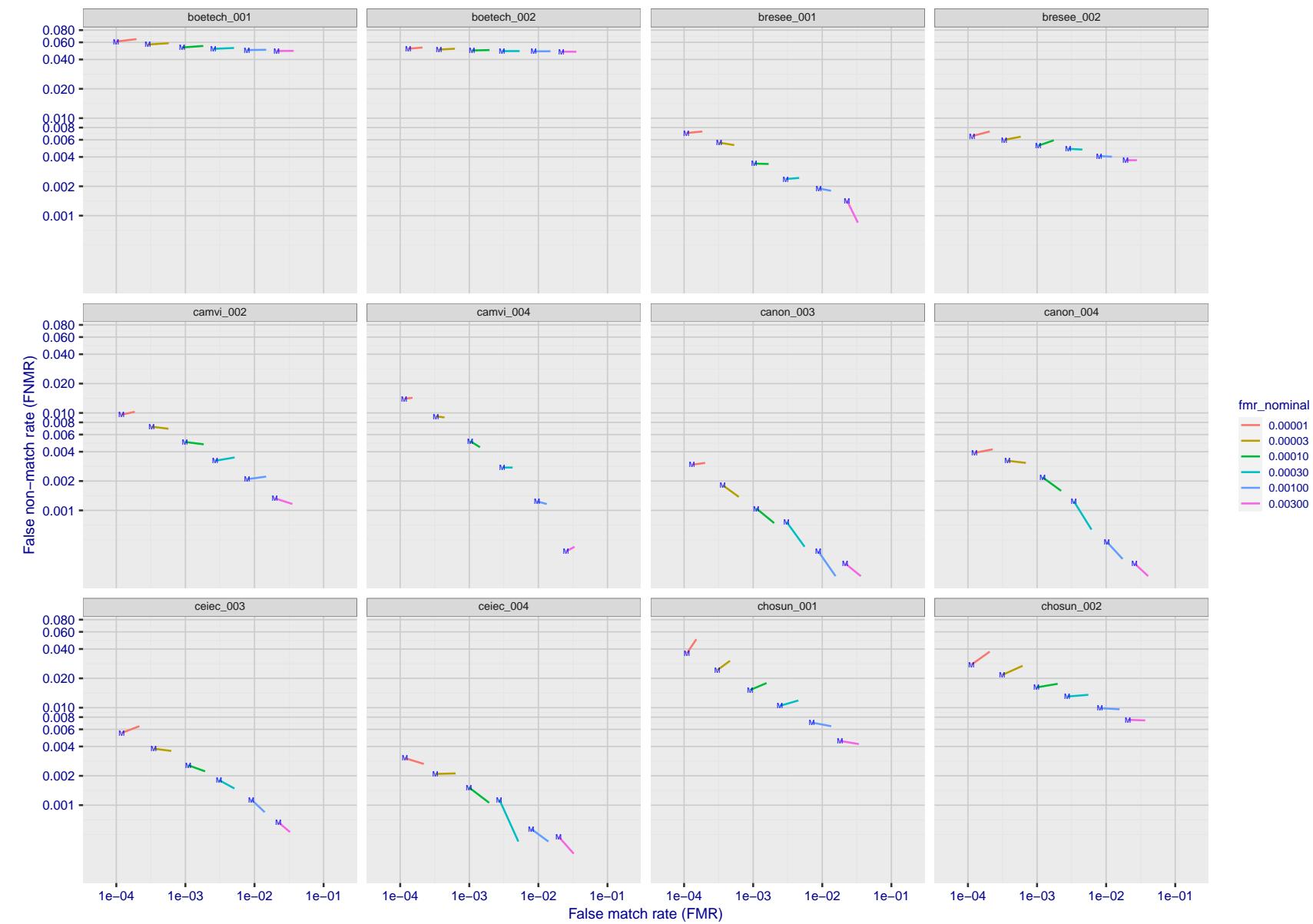


Figure 182: For the visa images, FNMR and FMR at six operating points along the DET characteristic. At each point a line is drawn between $(FMR, FNMR)_{MALE}$ and $(FMR, FNMR)_{FEMALE}$ showing how which sex has lower FMR and/or FNMR. The "M" label denotes male, the other end of the line corresponds to female. The six operating thresholds are selected to give the nominal false match rates given in the legend, and are computed over all impostor pairs regardless of age, sex, and place of birth. The plotted FMR values are broadly an order of magnitude larger than the nominal rates because FMR is computed over demographically-matched impostor pairs i.e individuals of the same sex, from the same geographic region (see section 3.6.1), and the same age group (see section 3.6.2).

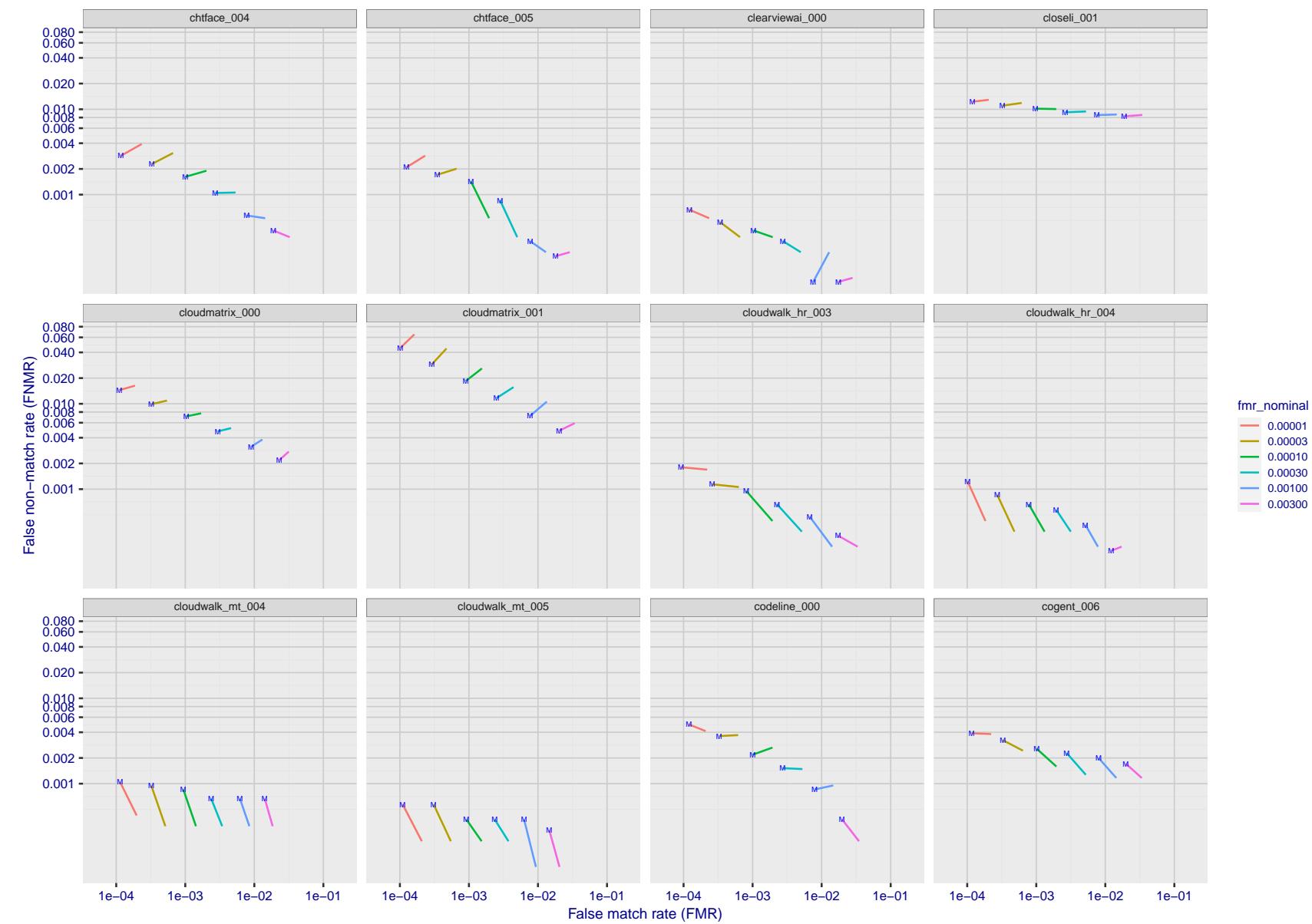


Figure 183: For the visa images, FNMR and FMR at six operating points along the DET characteristic. At each point a line is drawn between $(FMR, FNMR)_{MALE}$ and $(FMR, FNMR)_{FEMALE}$ showing how which sex has lower FMR and/or FNMR. The "M" label denotes male, the other end of the line corresponds to female. The six operating thresholds are selected to give the nominal false match rates given in the legend, and are computed over all impostor pairs regardless of age, sex, and place of birth. The plotted FMR values are broadly an order of magnitude larger than the nominal rates because FMR is computed over demographically-matched impostor pairs i.e individuals of the same sex, from the same geographic region (see section 3.6.1), and the same age group (see section 3.6.2).

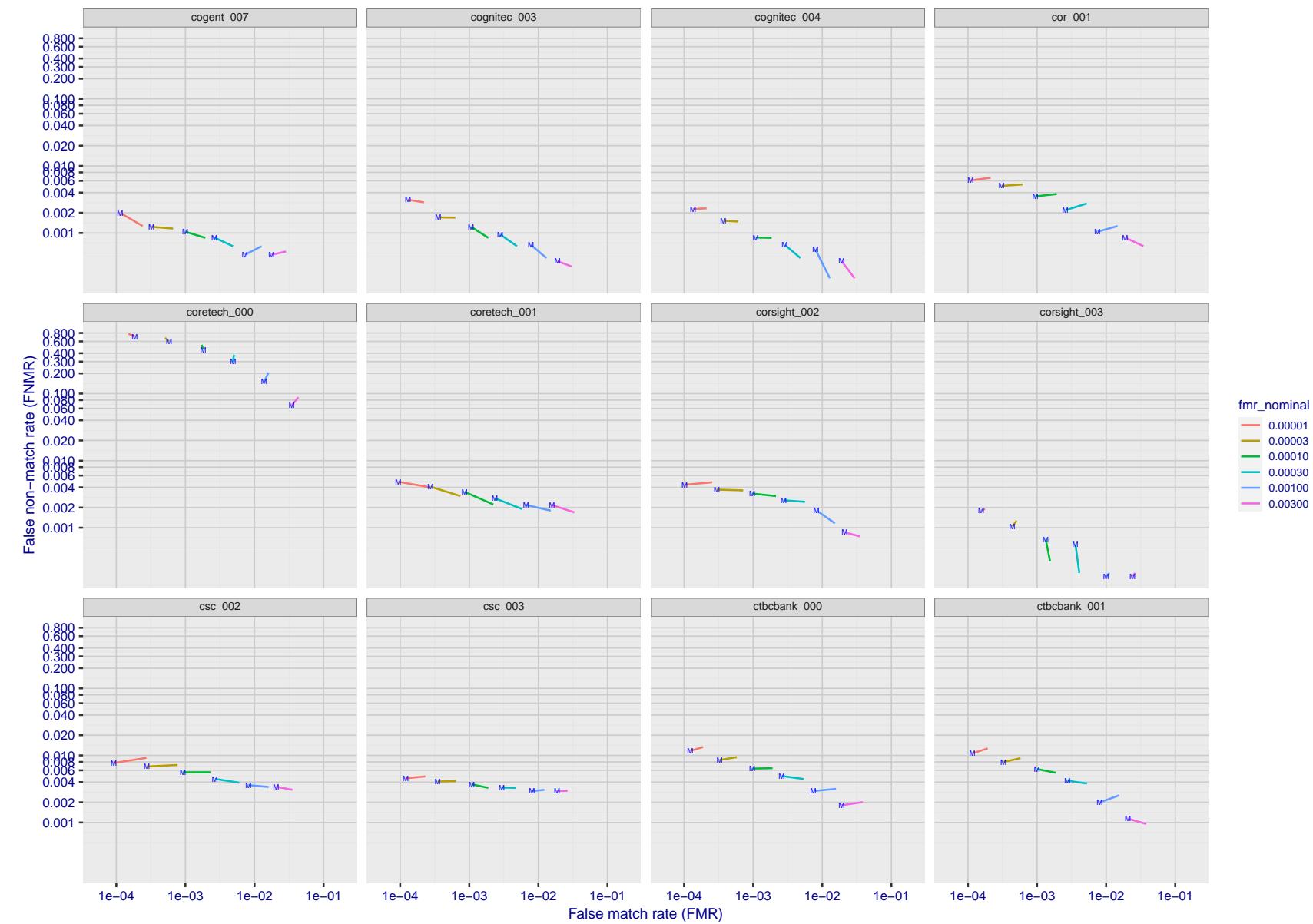


Figure 184: For the visa images, FNMR and FMR at six operating points along the DET characteristic. At each point a line is drawn between $(FMR, FNMR)_{MALE}$ and $(FMR, FNMR)_{FEMALE}$ showing how which sex has lower FMR and/or FNMR. The "M" label denotes male, the other end of the line corresponds to female. The six operating thresholds are selected to give the nominal false match rates given in the legend, and are computed over all impostor pairs regardless of age, sex, and place of birth. The plotted FMR values are broadly an order of magnitude larger than the nominal rates because FMR is computed over demographically-matched impostor pairs i.e individuals of the same sex, from the same geographic region (see section 3.6.1), and the same age group (see section 3.6.2).

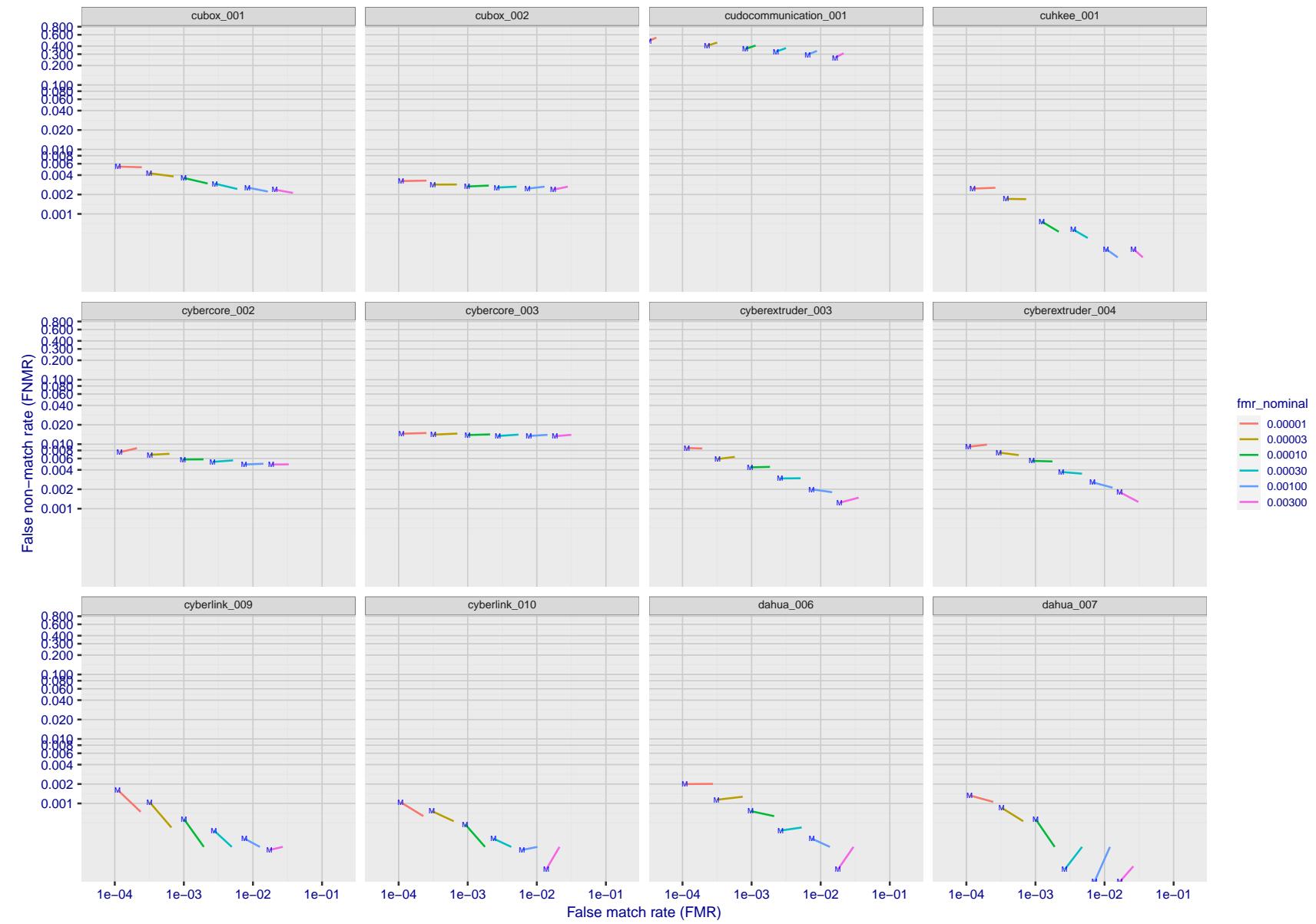


Figure 185: For the visa images, FNMR and FMR at six operating points along the DET characteristic. At each point a line is drawn between $(FMR, FNMR)_{MALE}$ and $(FMR, FNMR)_{FEMALE}$ showing how which sex has lower FMR and/or FNMR. The "M" label denotes male, the other end of the line corresponds to female. The six operating thresholds are selected to give the nominal false match rates given in the legend, and are computed over all impostor pairs regardless of age, sex, and place of birth. The plotted FMR values are broadly an order of magnitude larger than the nominal rates because FMR is computed over demographically-matched impostor pairs i.e individuals of the same sex, from the same geographic region (see section 3.6.1), and the same age group (see section 3.6.2).

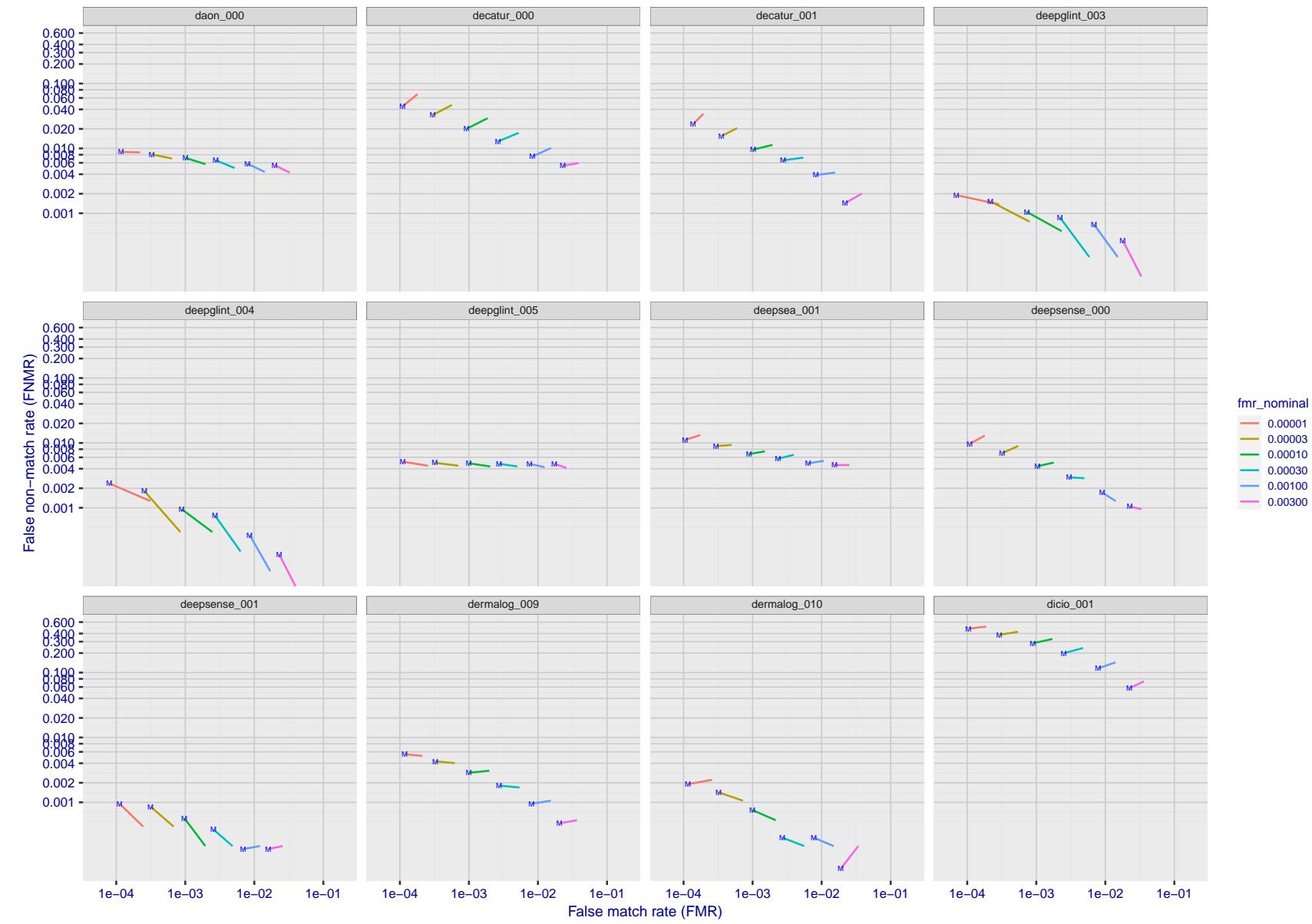


Figure 186: For the visa images, FNMR and FMR at six operating points along the DET characteristic. At each point a line is drawn between $(FMR, FNMR)_{MALE}$ and $(FMR, FNMR)_{FEMALE}$ showing how which sex has lower FMR and/or FNMR. The "M" label denotes male, the other end of the line corresponds to female. The six operating thresholds are selected to give the nominal false match rates given in the legend, and are computed over all impostor pairs regardless of age, sex, and place of birth. The plotted FMR values are broadly an order of magnitude larger than the nominal rates because FMR is computed over demographically-matched impostor pairs i.e individuals of the same sex, from the same geographic region (see section 3.6.1), and the same age group (see section 3.6.2).

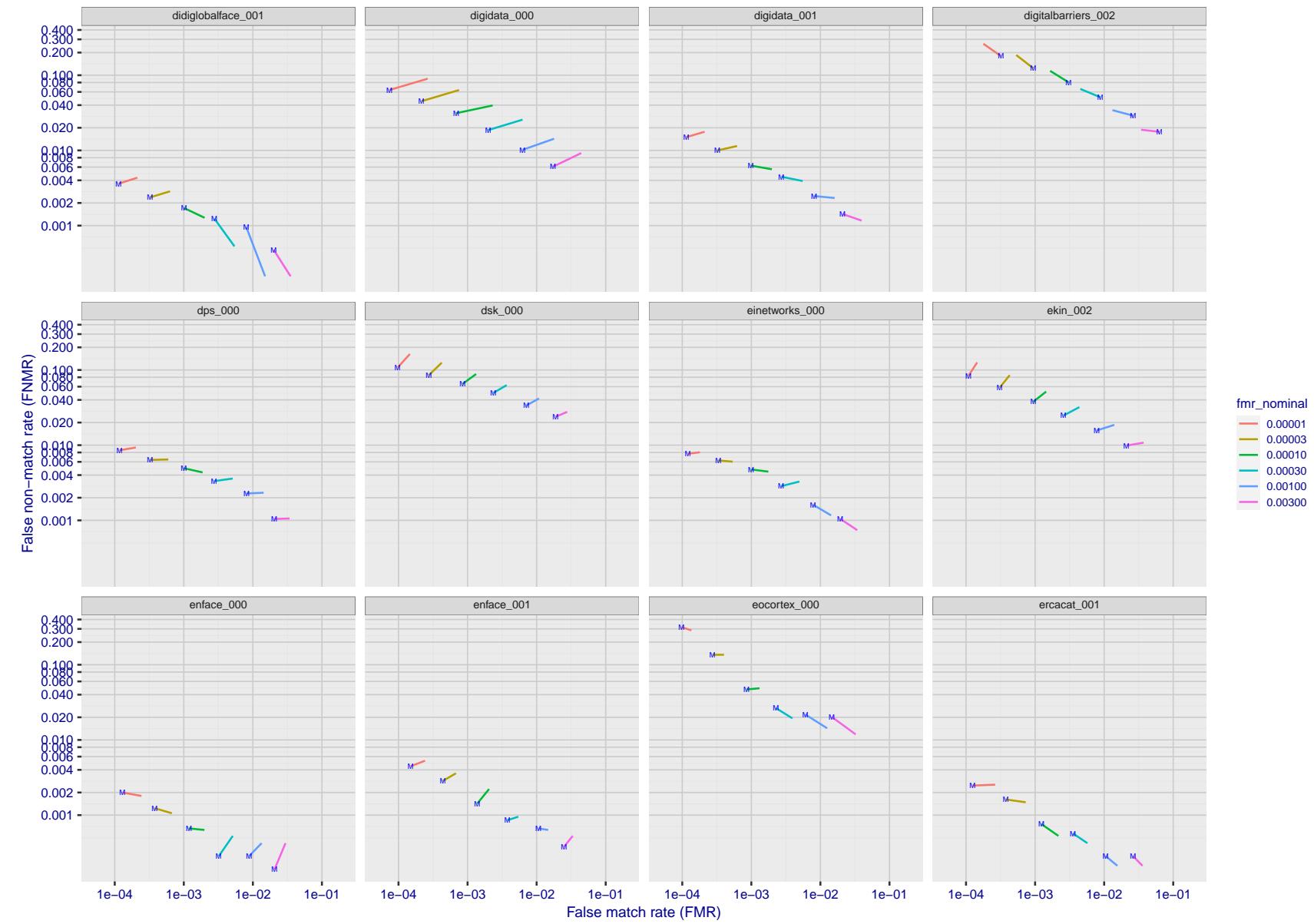


Figure 187: For the visa images, FNMR and FMR at six operating points along the DET characteristic. At each point a line is drawn between $(FMR, FNMR)_{MALE}$ and $(FMR, FNMR)_{FEMALE}$ showing how which sex has lower FMR and/or FNMR. The "M" label denotes male, the other end of the line corresponds to female. The six operating thresholds are selected to give the nominal false match rates given in the legend, and are computed over all impostor pairs regardless of age, sex, and place of birth. The plotted FMR values are broadly an order of magnitude larger than the nominal rates because FMR is computed over demographically-matched impostor pairs i.e individuals of the same sex, from the same geographic region (see section 3.6.1), and the same age group (see section 3.6.2).

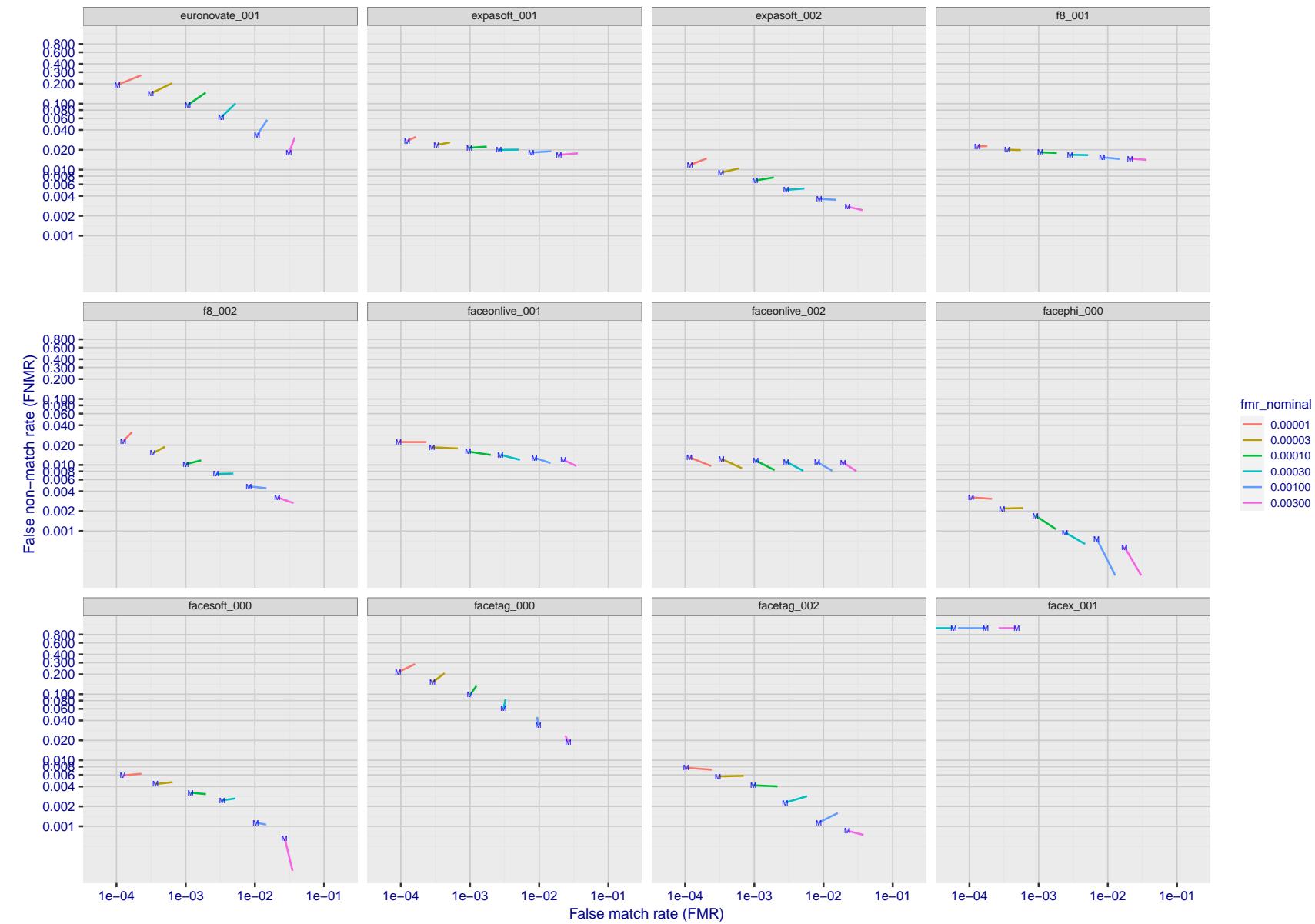


Figure 188: For the visa images, FNMR and FMR at six operating points along the DET characteristic. At each point a line is drawn between $(FMR, FNMR)_{MALE}$ and $(FMR, FNMR)_{FEMALE}$ showing how which sex has lower FMR and/or FNMR. The "M" label denotes male, the other end of the line corresponds to female. The six operating thresholds are selected to give the nominal false match rates given in the legend, and are computed over all impostor pairs regardless of age, sex, and place of birth. The plotted FMR values are broadly an order of magnitude larger than the nominal rates because FMR is computed over demographically-matched impostor pairs i.e individuals of the same sex, from the same geographic region (see section 3.6.1), and the same age group (see section 3.6.2).

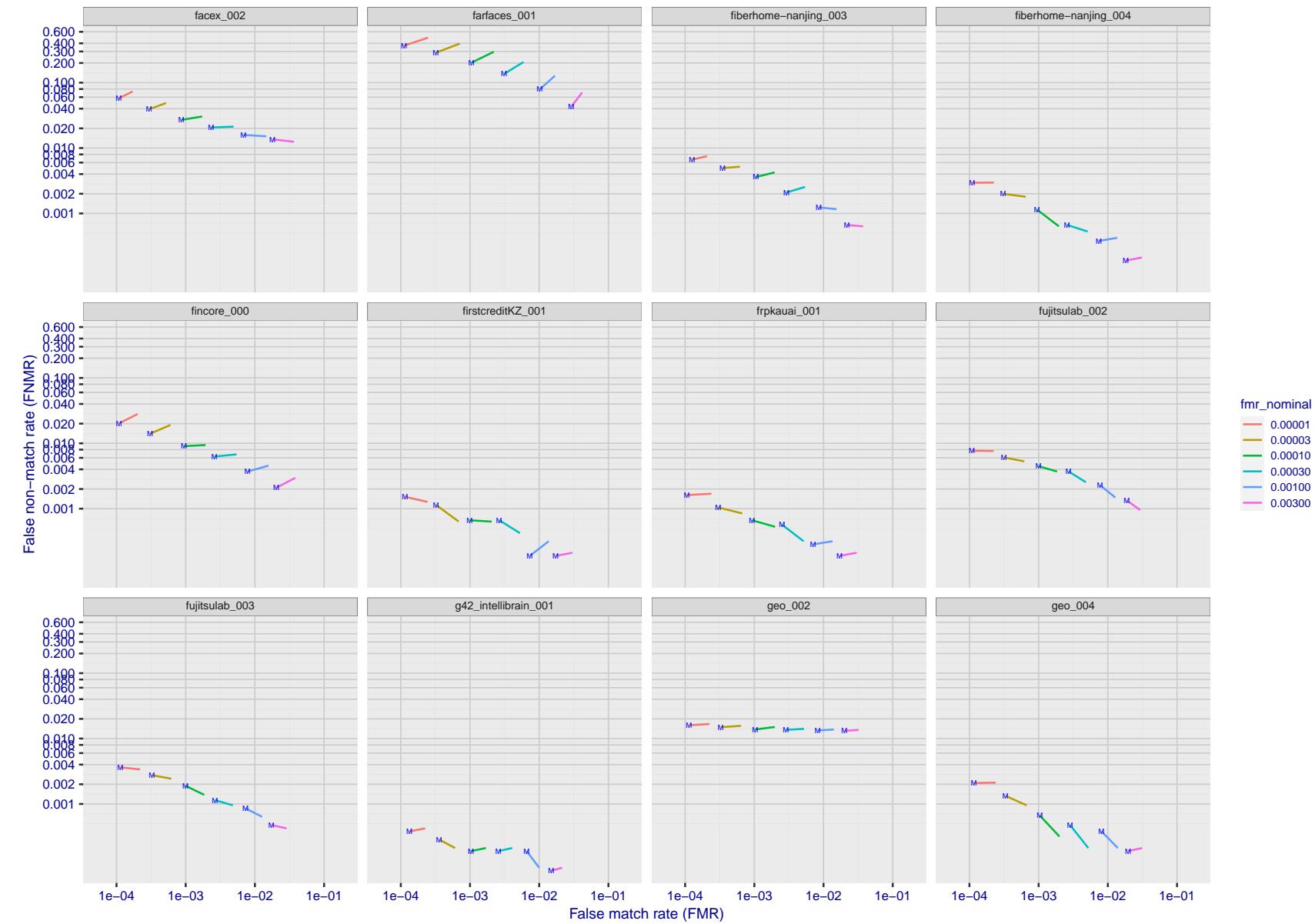


Figure 189: For the visa images, FNMR and FMR at six operating points along the DET characteristic. At each point a line is drawn between $(FMR, FNMR)_{MALE}$ and $(FMR, FNMR)_{FEMALE}$ showing how which sex has lower FMR and/or FNMR. The "M" label denotes male, the other end of the line corresponds to female. The six operating thresholds are selected to give the nominal false match rates given in the legend, and are computed over all impostor pairs regardless of age, sex, and place of birth. The plotted FMR values are broadly an order of magnitude larger than the nominal rates because FMR is computed over demographically-matched impostor pairs i.e individuals of the same sex, from the same geographic region (see section 3.6.1), and the same age group (see section 3.6.2).

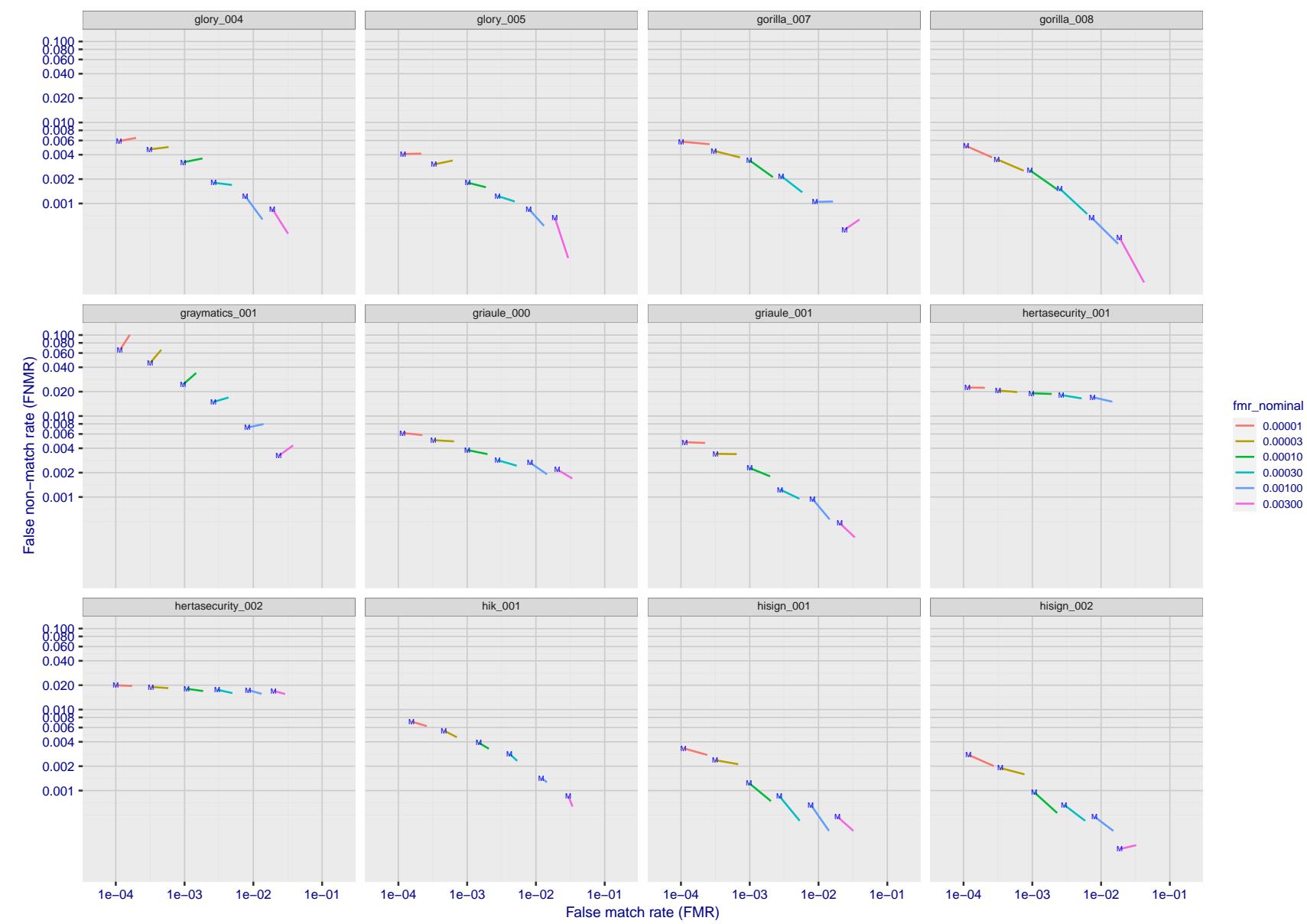


Figure 190: For the visa images, FNMR and FMR at six operating points along the DET characteristic. At each point a line is drawn between $(FMR, FNMR)_{MALE}$ and $(FMR, FNMR)_{FEMALE}$ showing how which sex has lower FMR and/or FNMR. The "M" label denotes male, the other end of the line corresponds to female. The six operating thresholds are selected to give the nominal false match rates given in the legend, and are computed over all impostor pairs regardless of age, sex, and place of birth. The plotted FMR values are broadly an order of magnitude larger than the nominal rates because FMR is computed over demographically-matched impostor pairs i.e individuals of the same sex, from the same geographic region (see section 3.6.1), and the same age group (see section 3.6.2).

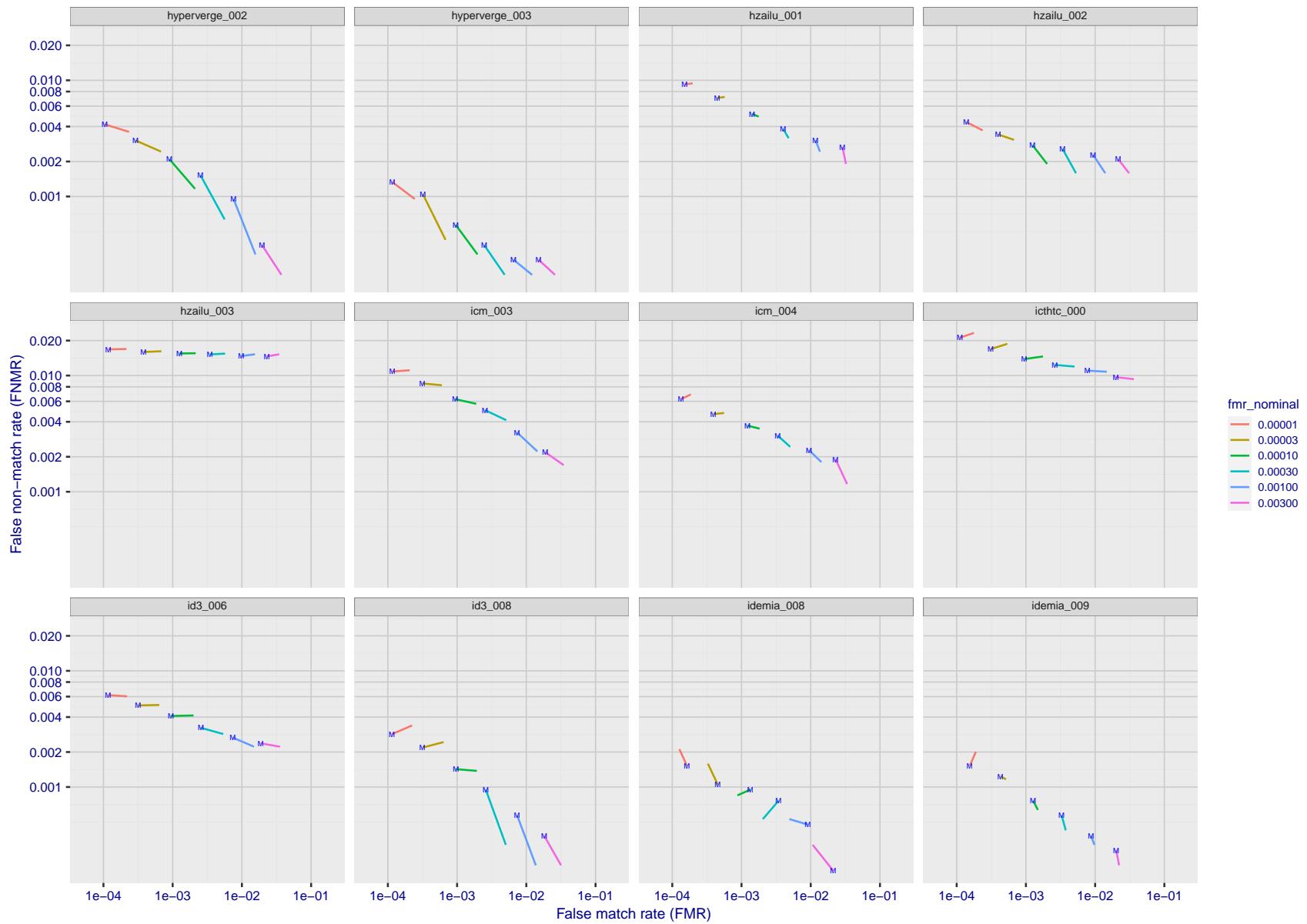


Figure 191: For the visa images, FNMR and FMR at six operating points along the DET characteristic. At each point a line is drawn between $(FMR, FNMR)_{MALE}$ and $(FMR, FNMR)_{FEMALE}$ showing how which sex has lower FMR and/or FNMR. The "M" label denotes male, the other end of the line corresponds to female. The six operating thresholds are selected to give the nominal false match rates given in the legend, and are computed over all impostor pairs regardless of age, sex, and place of birth. The plotted FMR values are broadly an order of magnitude larger than the nominal rates because FMR is computed over demographically-matched impostor pairs i.e individuals of the same sex, from the same geographic region (see section 3.6.1), and the same age group (see section 3.6.2).

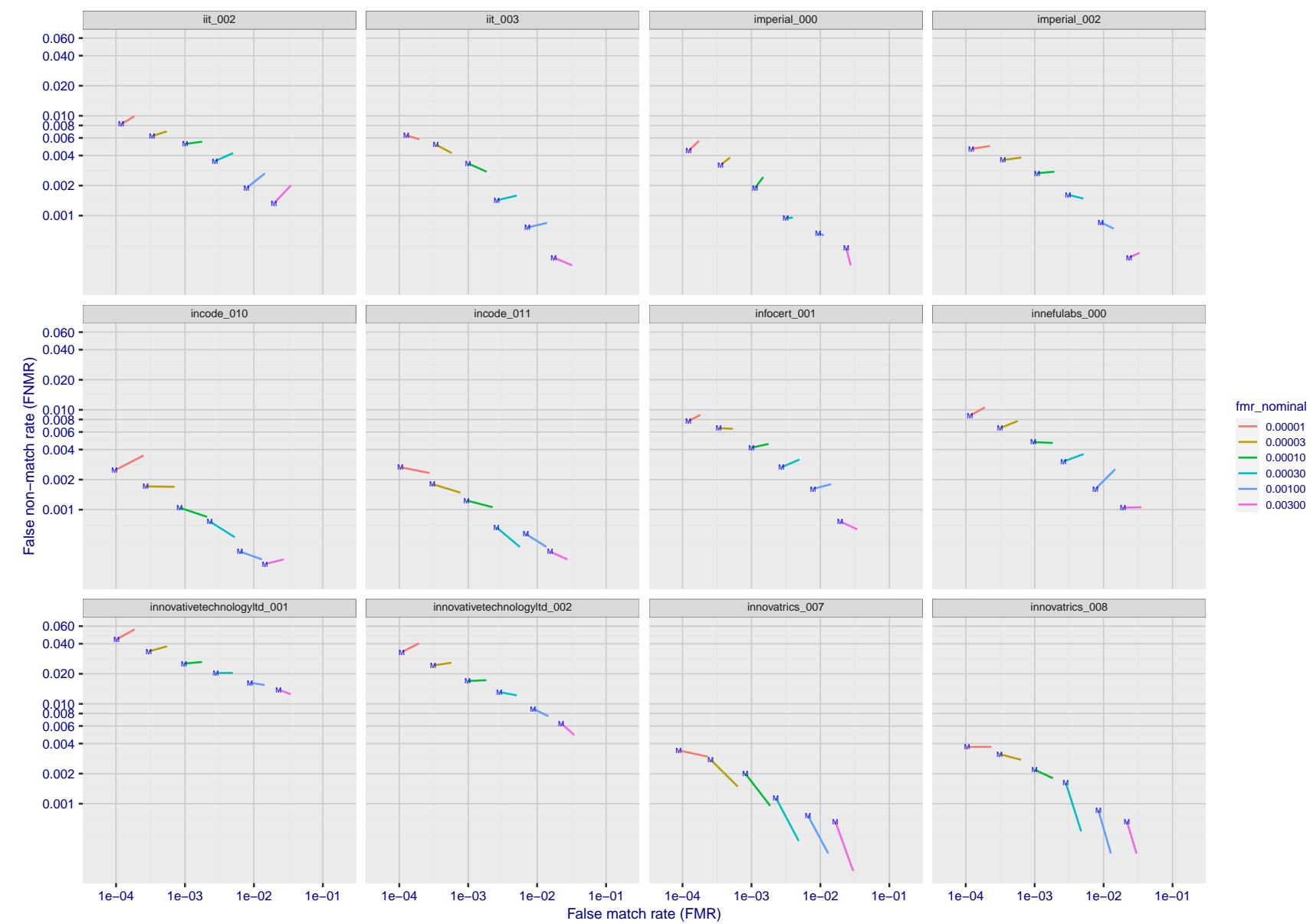


Figure 192: For the visa images, FNMR and FMR at six operating points along the DET characteristic. At each point a line is drawn between $(FMR, FNMR)_{MALE}$ and $(FMR, FNMR)_{FEMALE}$ showing how which sex has lower FMR and/or FNMR. The "M" label denotes male, the other end of the line corresponds to female. The six operating thresholds are selected to give the nominal false match rates given in the legend, and are computed over all impostor pairs regardless of age, sex, and place of birth. The plotted FMR values are broadly an order of magnitude larger than the nominal rates because FMR is computed over demographically-matched impostor pairs i.e individuals of the same sex, from the same geographic region (see section 3.6.1), and the same age group (see section 3.6.2).

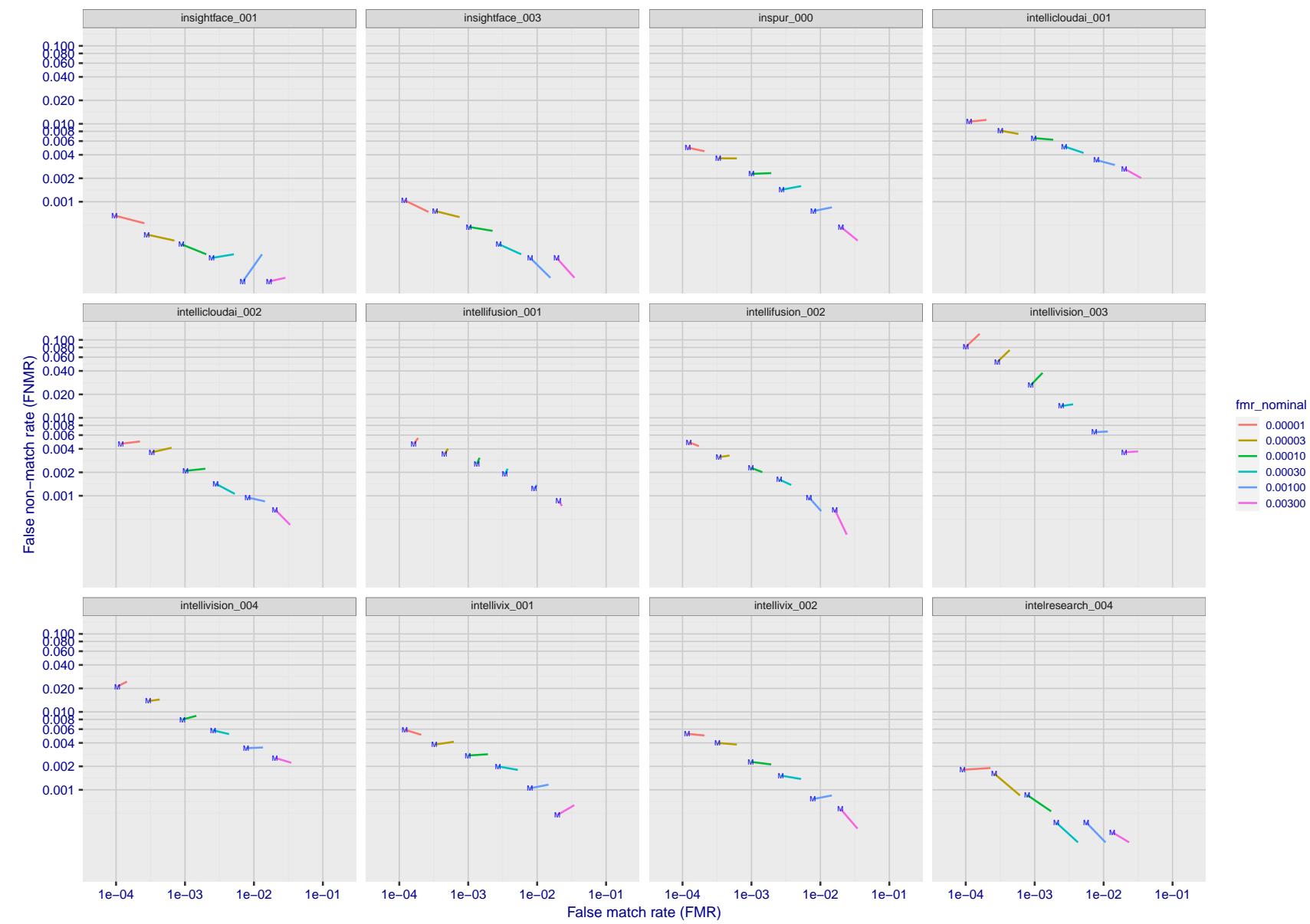


Figure 193: For the visa images, FNMR and FMR at six operating points along the DET characteristic. At each point a line is drawn between $(FMR, FNMR)_{MALE}$ and $(FMR, FNMR)_{FEMALE}$ showing how which sex has lower FMR and/or FNMR. The "M" label denotes male, the other end of the line corresponds to female. The six operating thresholds are selected to give the nominal false match rates given in the legend, and are computed over all impostor pairs regardless of age, sex, and place of birth. The plotted FMR values are broadly an order of magnitude larger than the nominal rates because FMR is computed over demographically-matched impostor pairs i.e individuals of the same sex, from the same geographic region (see section 3.6.1), and the same age group (see section 3.6.2).

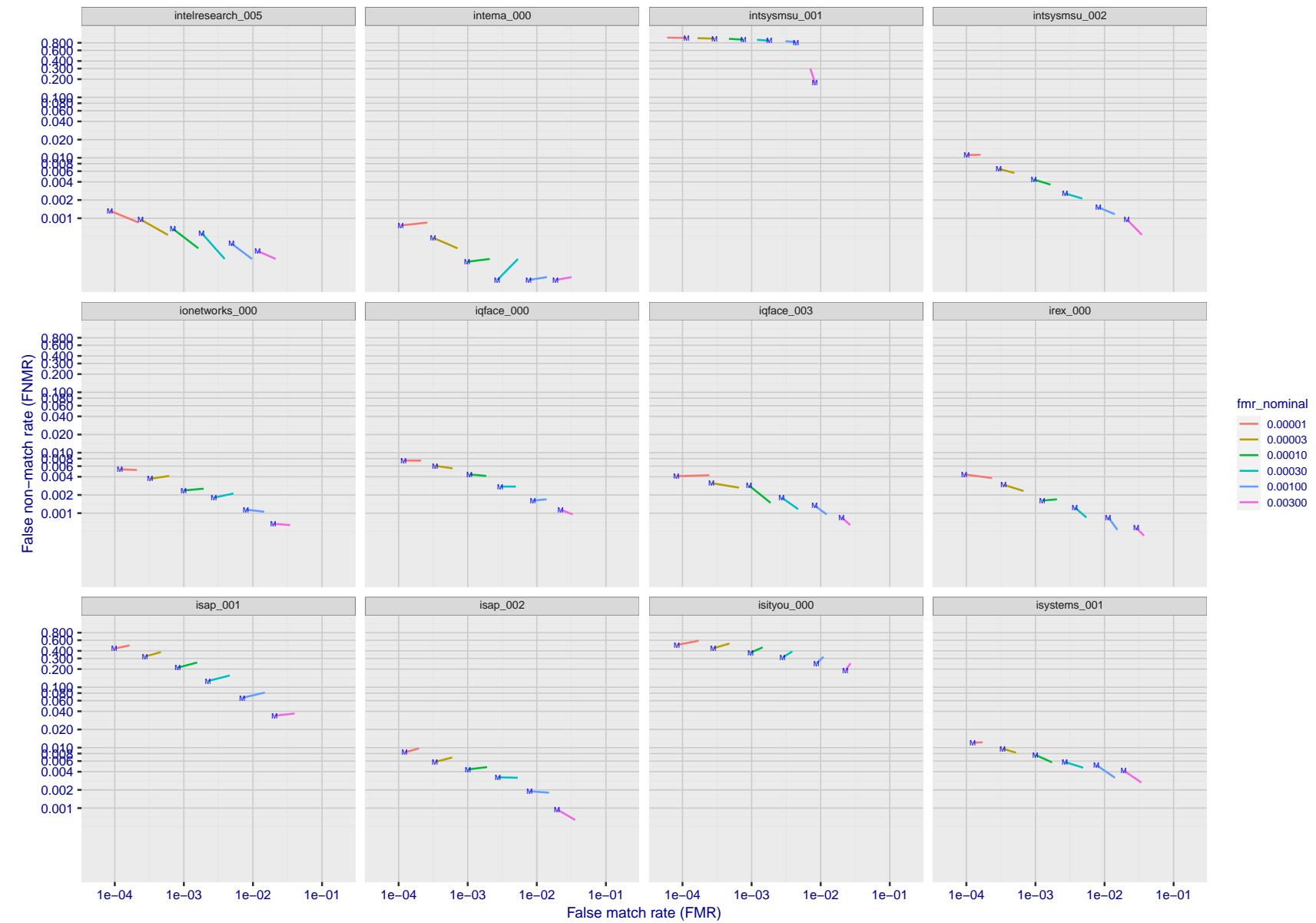


Figure 194: For the visa images, FNMR and FMR at six operating points along the DET characteristic. At each point a line is drawn between $(FMR, FNMR)_{MALE}$ and $(FMR, FNMR)_{FEMALE}$ showing how which sex has lower FMR and/or FNMR. The "M" label denotes male, the other end of the line corresponds to female. The six operating thresholds are selected to give the nominal false match rates given in the legend, and are computed over all impostor pairs regardless of age, sex, and place of birth. The plotted FMR values are broadly an order of magnitude larger than the nominal rates because FMR is computed over demographically-matched impostor pairs i.e individuals of the same sex, from the same geographic region (see section 3.6.1), and the same age group (see section 3.6.2).

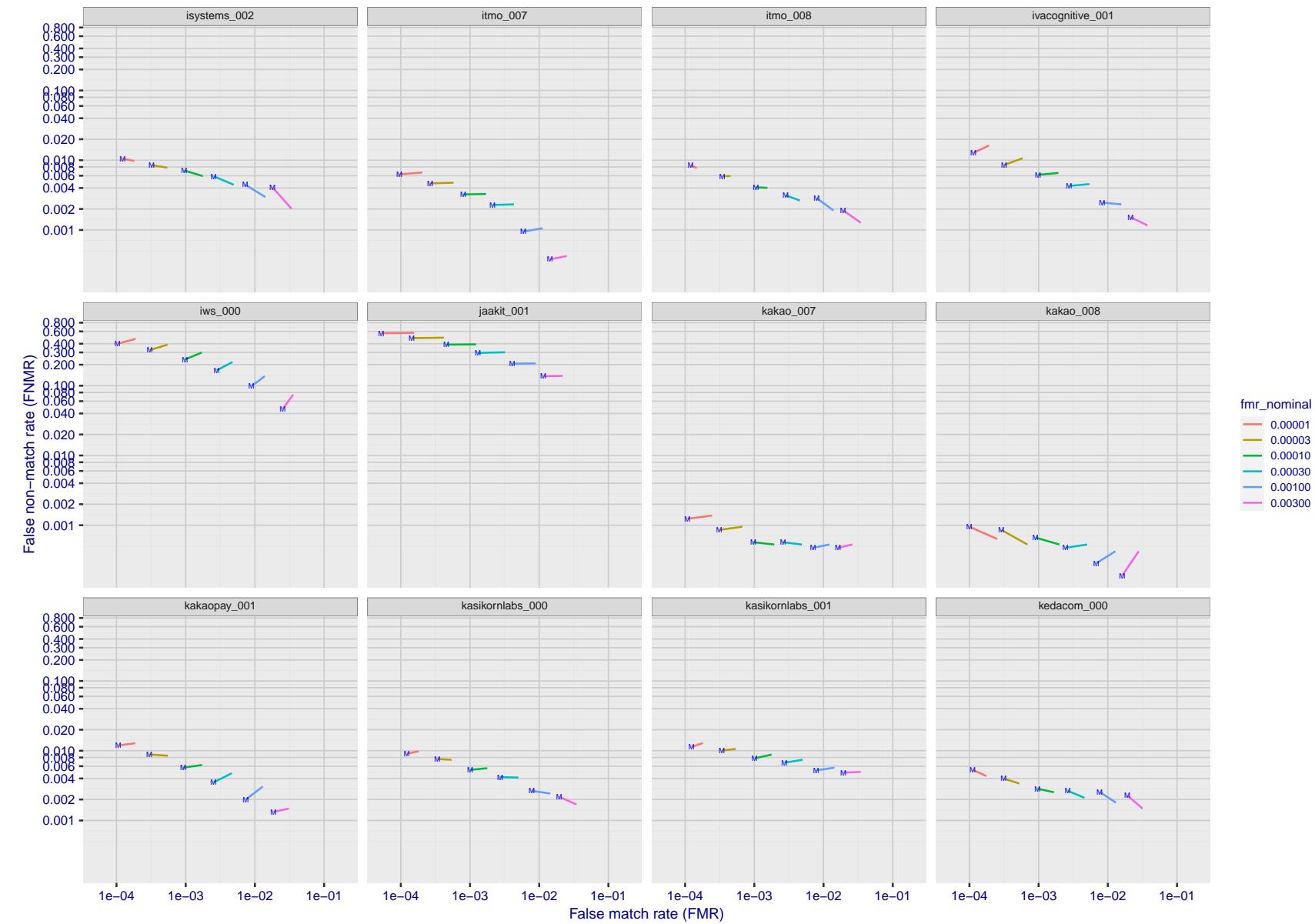


Figure 195: For the visa images, FNMR and FMR at six operating points along the DET characteristic. At each point a line is drawn between $(FMR, FNMR)_{MALE}$ and $(FMR, FNMR)_{FEMALE}$ showing how which sex has lower FMR and/or FNMR. The "M" label denotes male, the other end of the line corresponds to female. The six operating thresholds are selected to give the nominal false match rates given in the legend, and are computed over all impostor pairs regardless of age, sex, and place of birth. The plotted FMR values are broadly an order of magnitude larger than the nominal rates because FMR is computed over demographically-matched impostor pairs i.e individuals of the same sex, from the same geographic region (see section 3.6.1), and the same age group (see section 3.6.2).

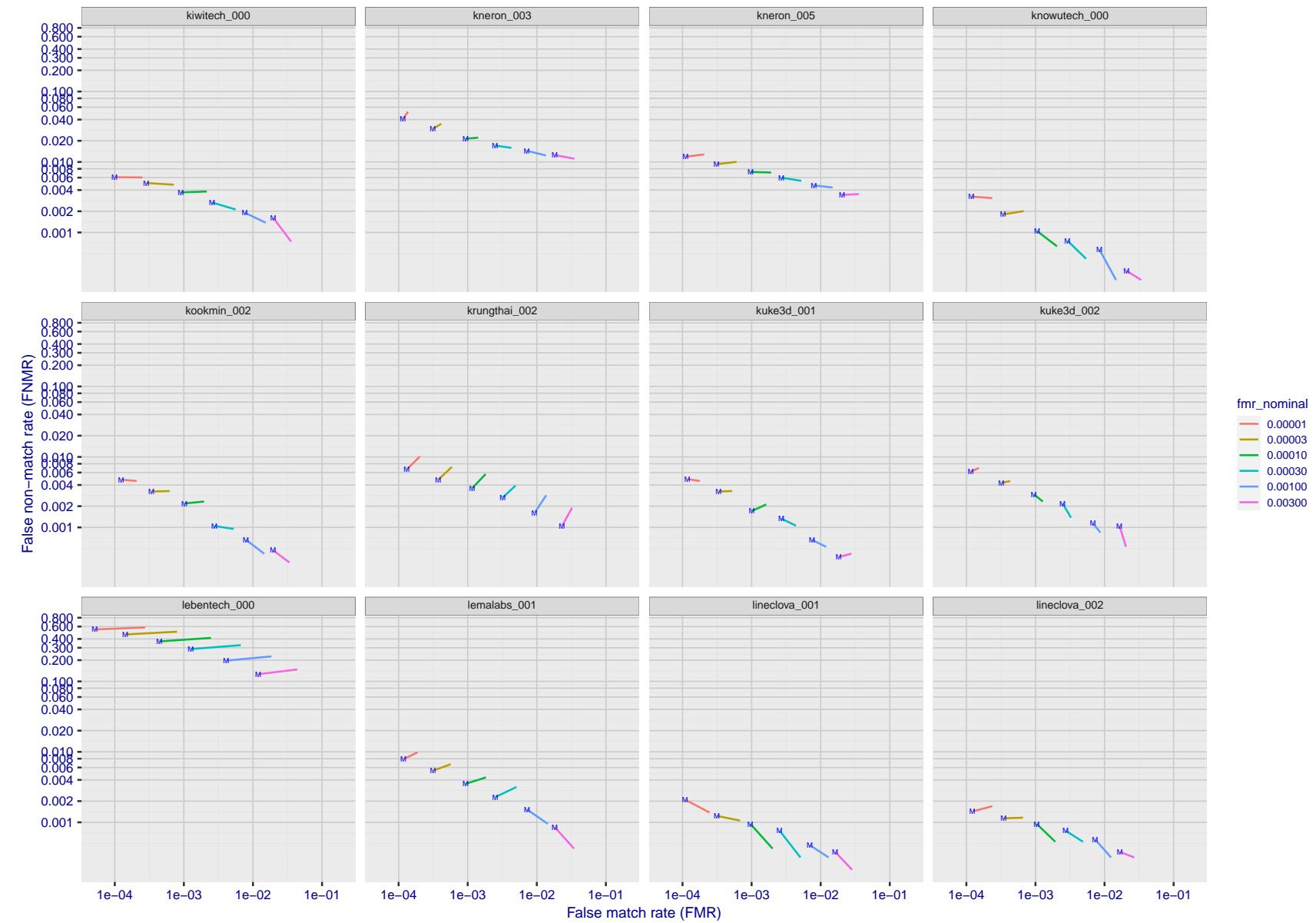


Figure 196: For the visa images, FNMR and FMR at six operating points along the DET characteristic. At each point a line is drawn between $(FMR, FNMR)_{MALE}$ and $(FMR, FNMR)_{FEMALE}$ showing how which sex has lower FMR and/or FNMR. The "M" label denotes male, the other end of the line corresponds to female. The six operating thresholds are selected to give the nominal false match rates given in the legend, and are computed over all impostor pairs regardless of age, sex, and place of birth. The plotted FMR values are broadly an order of magnitude larger than the nominal rates because FMR is computed over demographically-matched impostor pairs i.e individuals of the same sex, from the same geographic region (see section 3.6.1), and the same age group (see section 3.6.2).

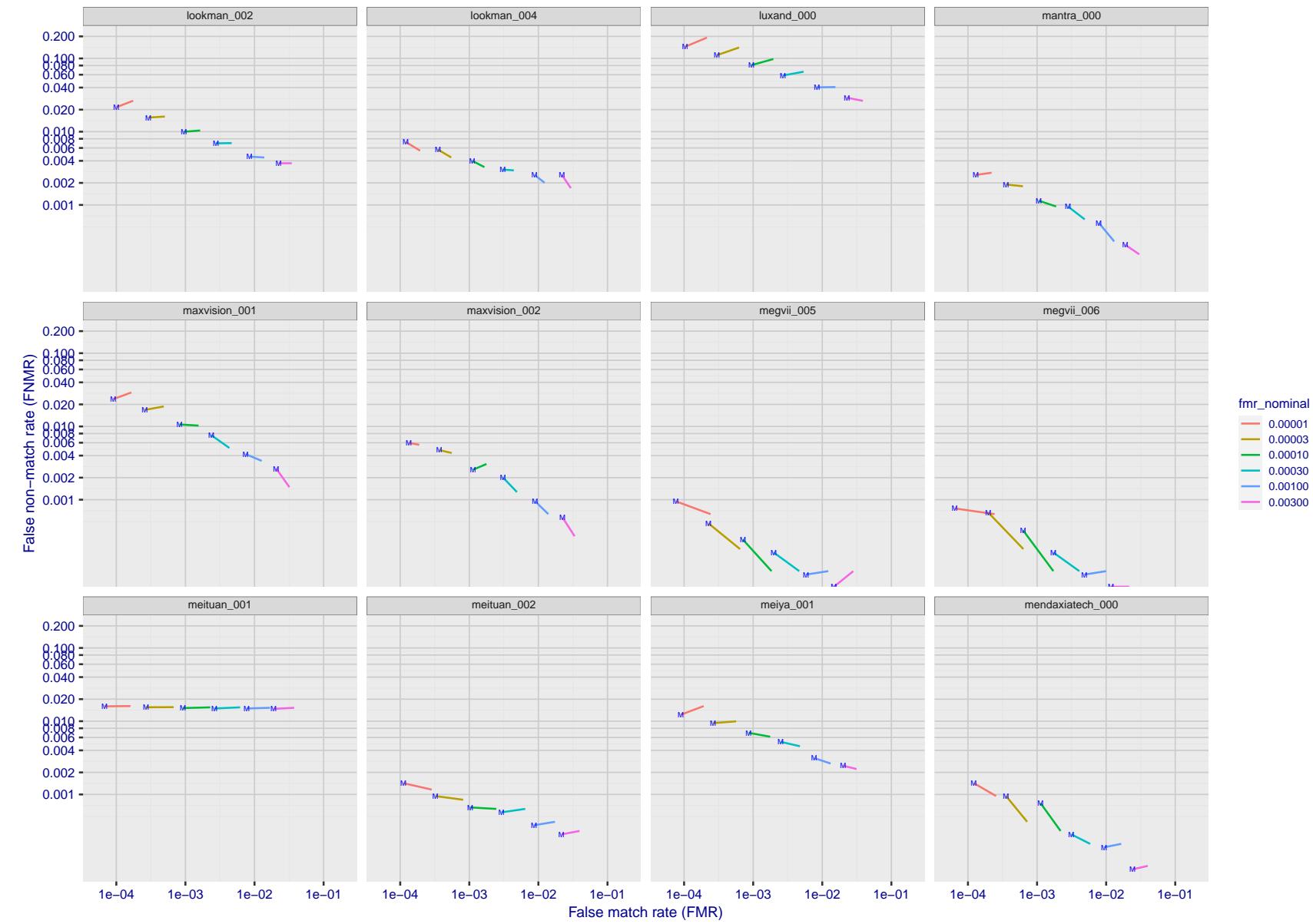


Figure 197: For the visa images, FNMR and FMR at six operating points along the DET characteristic. At each point a line is drawn between $(FMR, FNMR)_{MALE}$ and $(FMR, FNMR)_{FEMALE}$ showing how which sex has lower FMR and/or FNMR. The "M" label denotes male, the other end of the line corresponds to female. The six operating thresholds are selected to give the nominal false match rates given in the legend, and are computed over all impostor pairs regardless of age, sex, and place of birth. The plotted FMR values are broadly an order of magnitude larger than the nominal rates because FMR is computed over demographically-matched impostor pairs i.e individuals of the same sex, from the same geographic region (see section 3.6.1), and the same age group (see section 3.6.2).

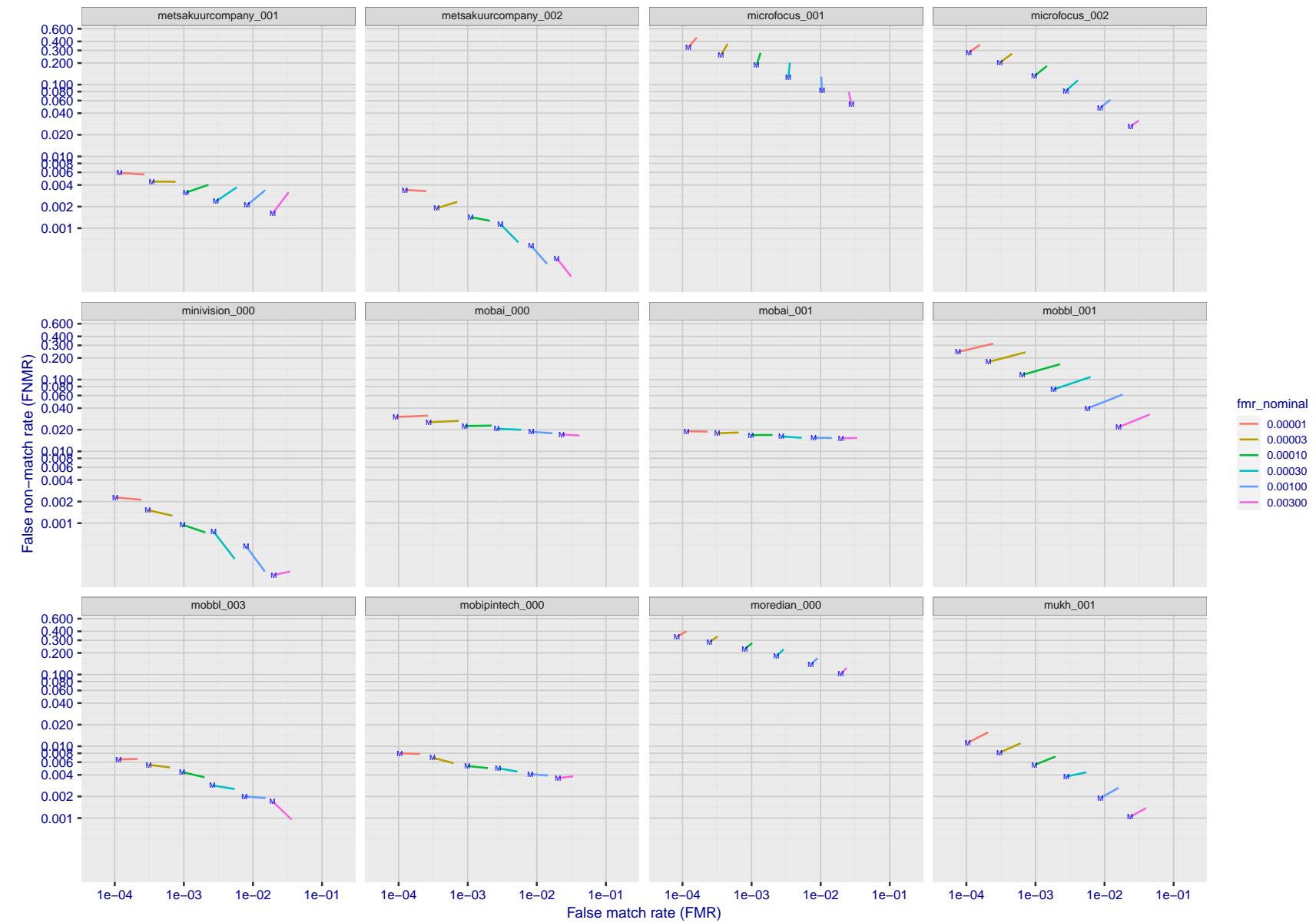


Figure 198: For the visa images, FNMR and FMR at six operating points along the DET characteristic. At each point a line is drawn between $(FMR, FNMR)_{MALE}$ and $(FMR, FNMR)_{FEMALE}$ showing how which sex has lower FMR and/or FNMR. The "M" label denotes male, the other end of the line corresponds to female. The six operating thresholds are selected to give the nominal false match rates given in the legend, and are computed over all impostor pairs regardless of age, sex, and place of birth. The plotted FMR values are broadly an order of magnitude larger than the nominal rates because FMR is computed over demographically-matched impostor pairs i.e individuals of the same sex, from the same geographic region (see section 3.6.1), and the same age group (see section 3.6.2).

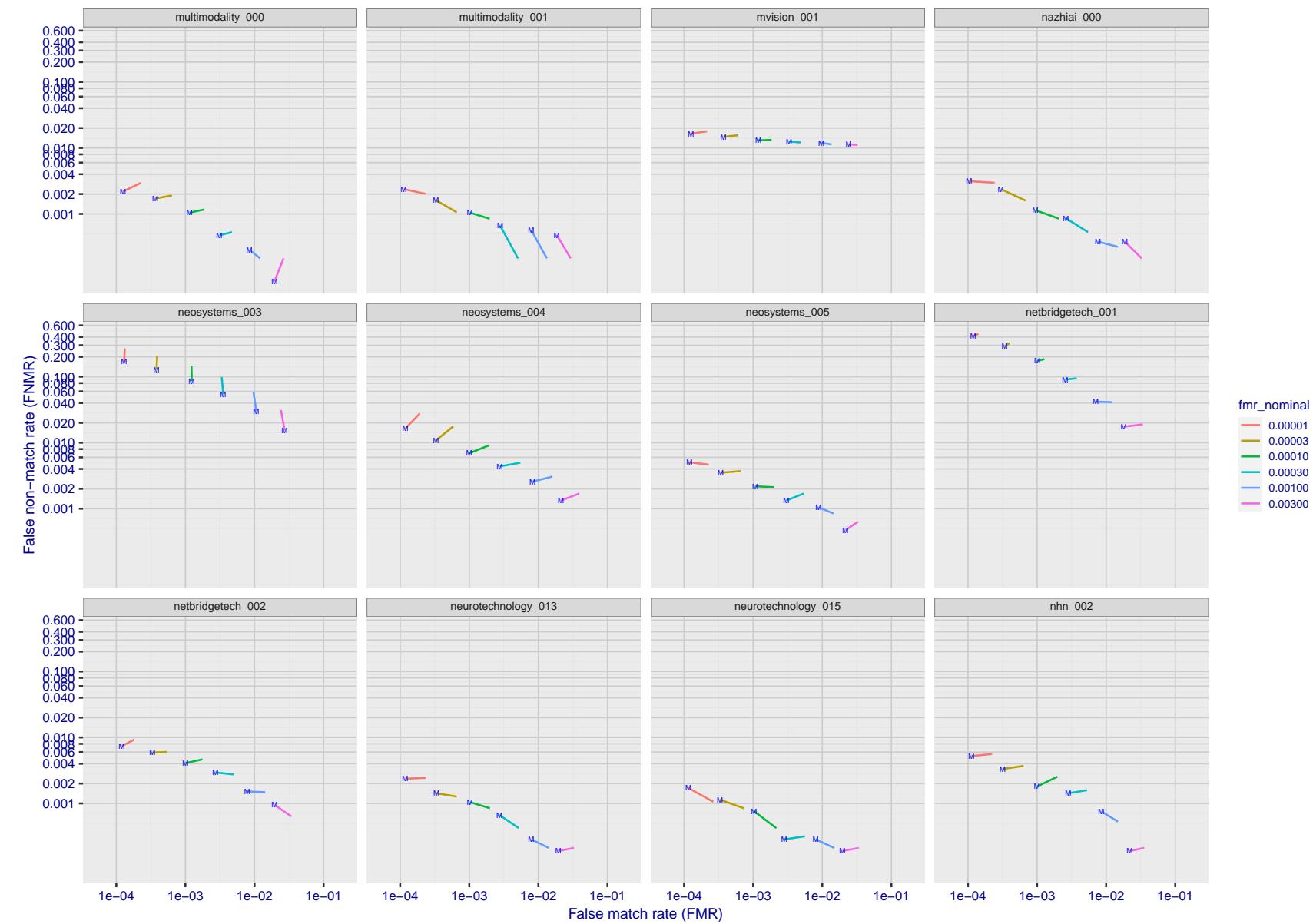


Figure 199: For the visa images, FNMR and FMR at six operating points along the DET characteristic. At each point a line is drawn between $(FMR, FNMR)_{MALE}$ and $(FMR, FNMR)_{FEMALE}$ showing how which sex has lower FMR and/or FNMR. The "M" label denotes male, the other end of the line corresponds to female. The six operating thresholds are selected to give the nominal false match rates given in the legend, and are computed over all impostor pairs regardless of age, sex, and place of birth. The plotted FMR values are broadly an order of magnitude larger than the nominal rates because FMR is computed over demographically-matched impostor pairs i.e individuals of the same sex, from the same geographic region (see section 3.6.1), and the same age group (see section 3.6.2).

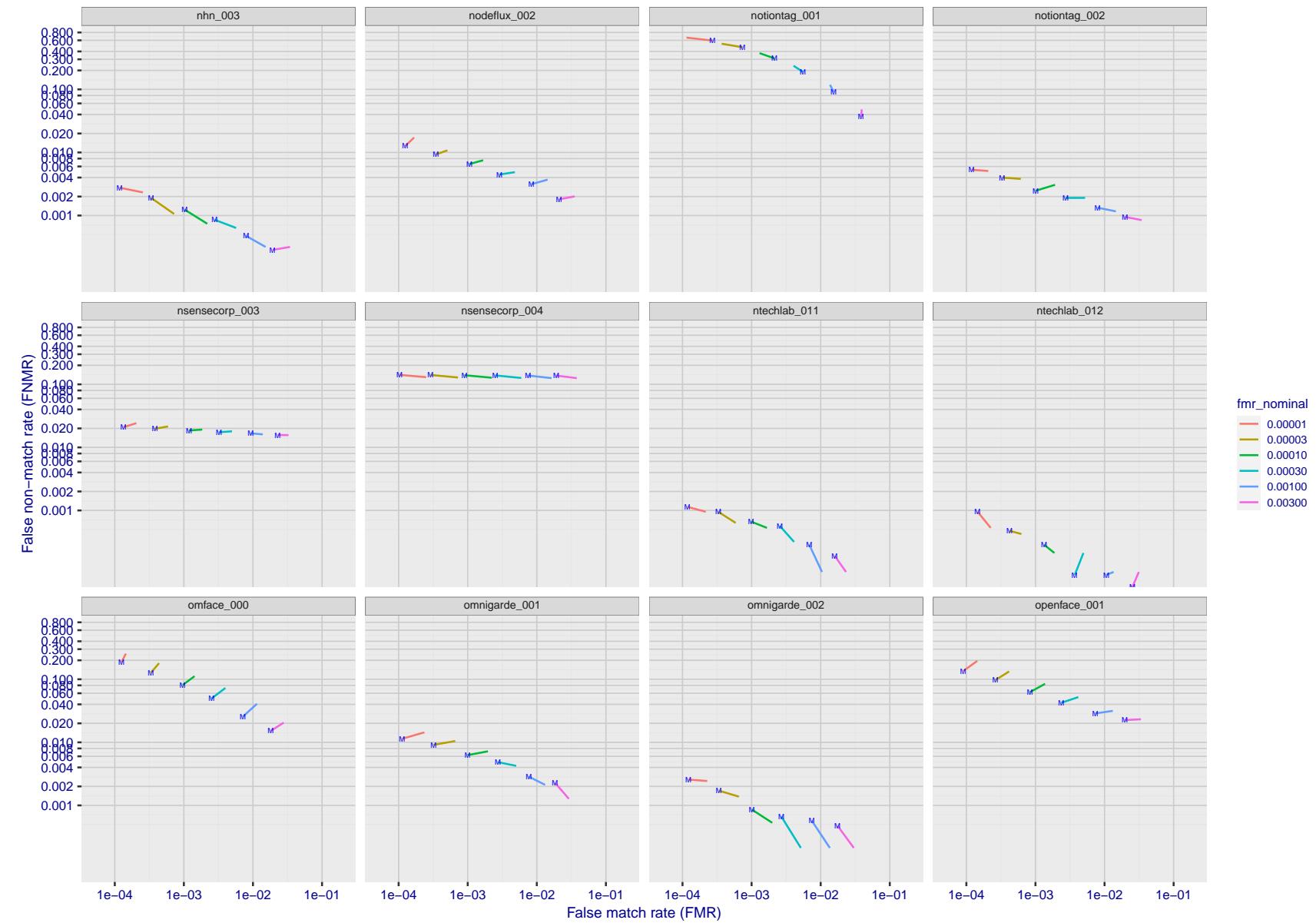


Figure 200: For the visa images, FNMR and FMR at six operating points along the DET characteristic. At each point a line is drawn between $(FMR, FNMR)_{MALE}$ and $(FMR, FNMR)_{FEMALE}$ showing how which sex has lower FMR and/or FNMR. The "M" label denotes male, the other end of the line corresponds to female. The six operating thresholds are selected to give the nominal false match rates given in the legend, and are computed over all impostor pairs regardless of age, sex, and place of birth. The plotted FMR values are broadly an order of magnitude larger than the nominal rates because FMR is computed over demographically-matched impostor pairs i.e individuals of the same sex, from the same geographic region (see section 3.6.1), and the same age group (see section 3.6.2).

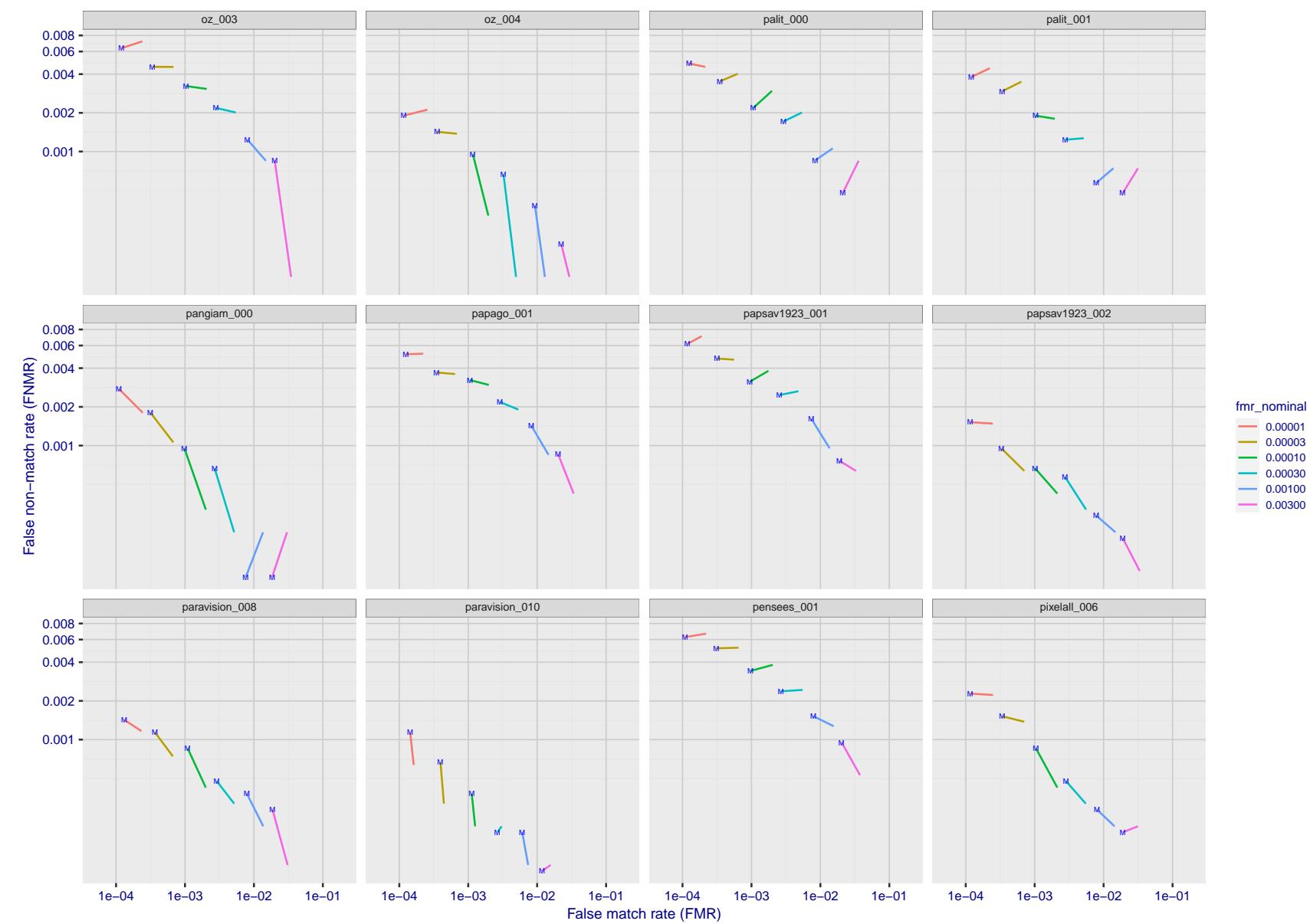


Figure 201: For the visa images, FNMR and FMR at six operating points along the DET characteristic. At each point a line is drawn between $(FMR, FNMR)_{MALE}$ and $(FMR, FNMR)_{FEMALE}$ showing how which sex has lower FMR and/or FNMR. The "M" label denotes male, the other end of the line corresponds to female. The six operating thresholds are selected to give the nominal false match rates given in the legend, and are computed over all impostor pairs regardless of age, sex, and place of birth. The plotted FMR values are broadly an order of magnitude larger than the nominal rates because FMR is computed over demographically-matched impostor pairs i.e individuals of the same sex, from the same geographic region (see section 3.6.1), and the same age group (see section 3.6.2).

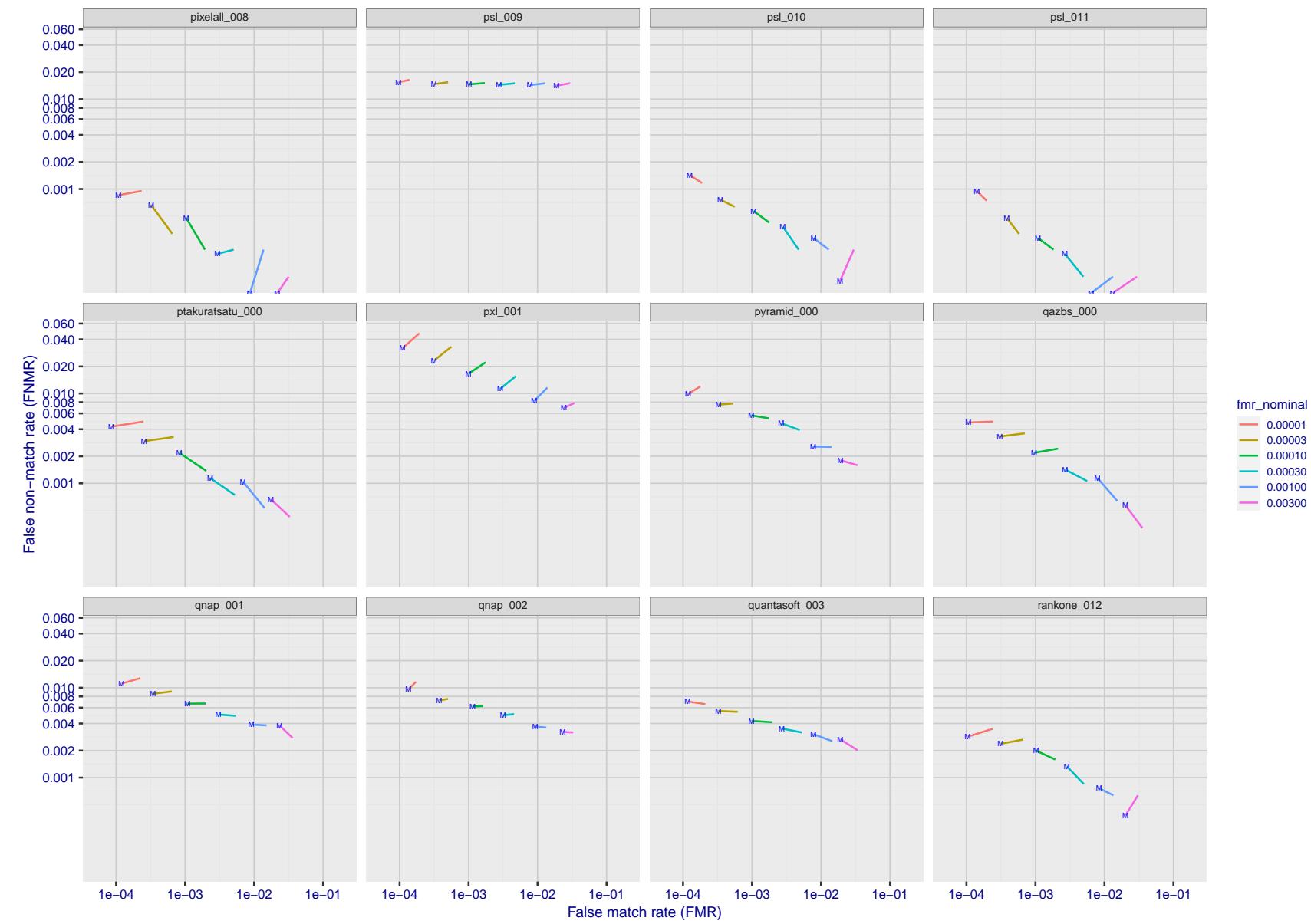


Figure 202: For the visa images, FNMR and FMR at six operating points along the DET characteristic. At each point a line is drawn between $(FMR, FNMR)_{MALE}$ and $(FMR, FNMR)_{FEMALE}$ showing how which sex has lower FMR and/or FNMR. The "M" label denotes male, the other end of the line corresponds to female. The six operating thresholds are selected to give the nominal false match rates given in the legend, and are computed over all impostor pairs regardless of age, sex, and place of birth. The plotted FMR values are broadly an order of magnitude larger than the nominal rates because FMR is computed over demographically-matched impostor pairs i.e individuals of the same sex, from the same geographic region (see section 3.6.1), and the same age group (see section 3.6.2).

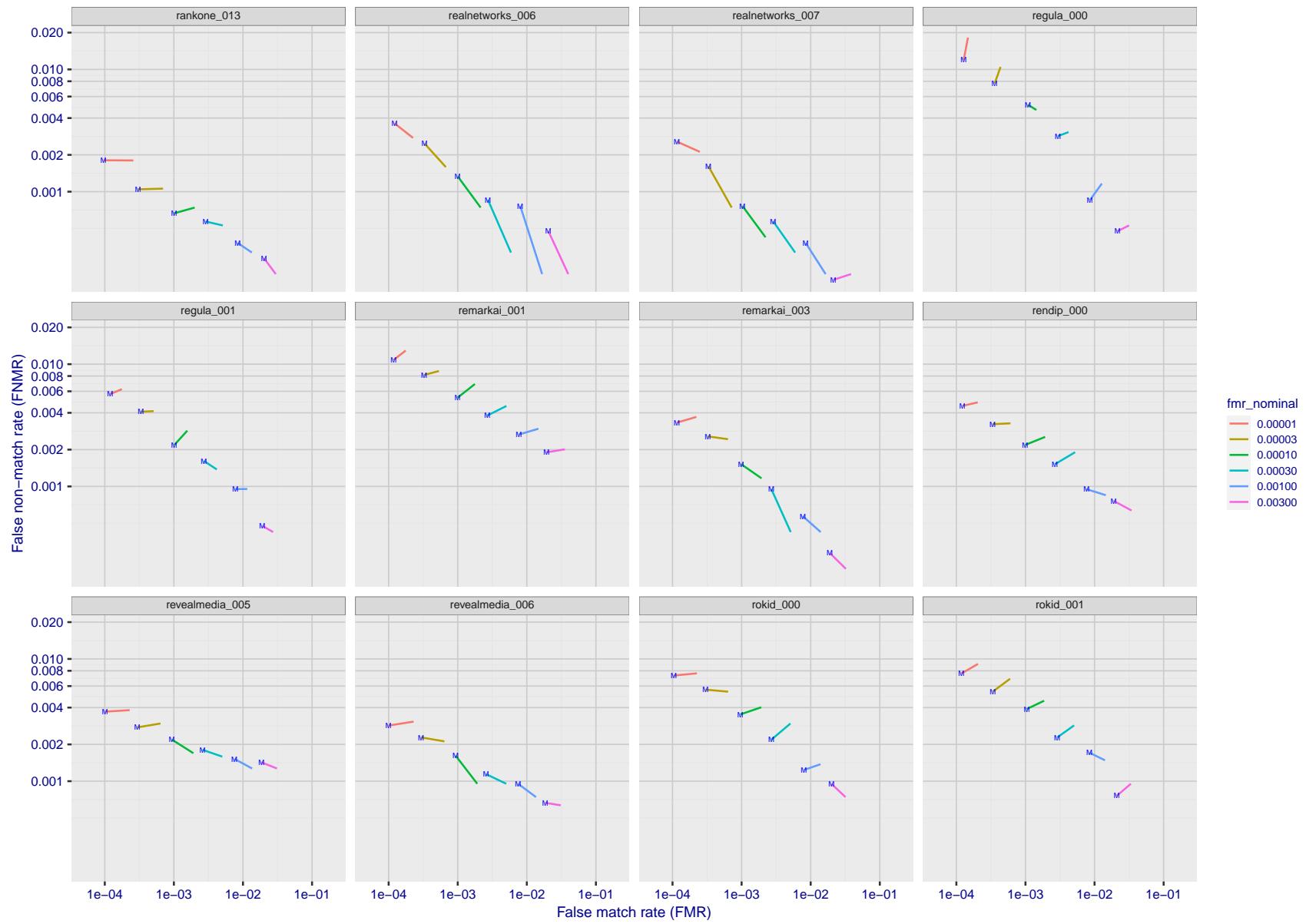


Figure 203: For the visa images, FNMR and FMR at six operating points along the DET characteristic. At each point a line is drawn between $(FMR, FNMR)_{MALE}$ and $(FMR, FNMR)_{FEMALE}$ showing how which sex has lower FMR and/or FNMR. The "M" label denotes male, the other end of the line corresponds to female. The six operating thresholds are selected to give the nominal false match rates given in the legend, and are computed over all impostor pairs regardless of age, sex, and place of birth. The plotted FMR values are broadly an order of magnitude larger than the nominal rates because FMR is computed over demographically-matched impostor pairs i.e individuals of the same sex, from the same geographic region (see section 3.6.1), and the same age group (see section 3.6.2).

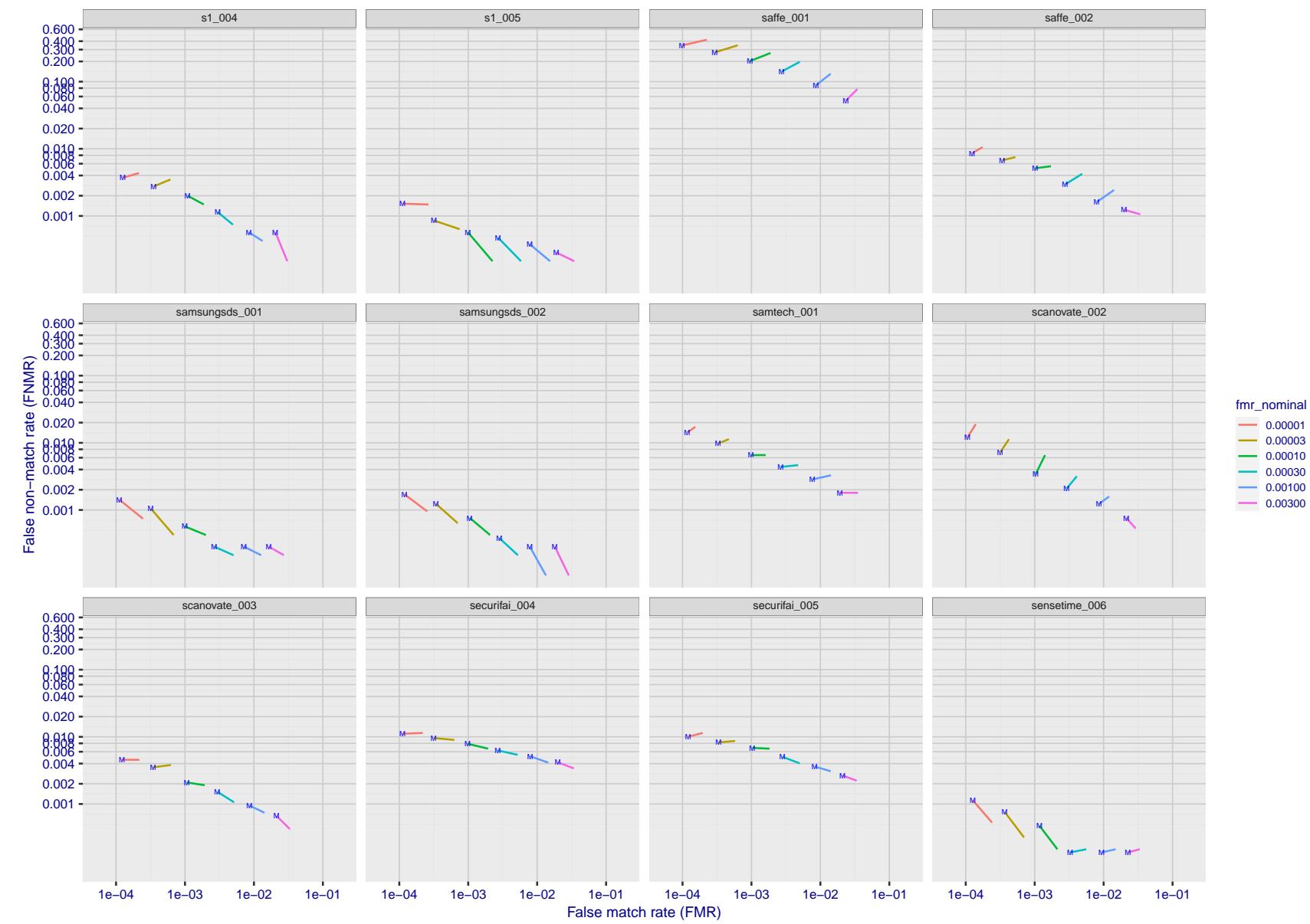


Figure 204: For the visa images, FNMR and FMR at six operating points along the DET characteristic. At each point a line is drawn between $(FMR, FNMR)_{MALE}$ and $(FMR, FNMR)_{FEMALE}$ showing how which sex has lower FMR and/or FNMR. The "M" label denotes male, the other end of the line corresponds to female. The six operating thresholds are selected to give the nominal false match rates given in the legend, and are computed over all impostor pairs regardless of age, sex, and place of birth. The plotted FMR values are broadly an order of magnitude larger than the nominal rates because FMR is computed over demographically-matched impostor pairs i.e individuals of the same sex, from the same geographic region (see section 3.6.1), and the same age group (see section 3.6.2).

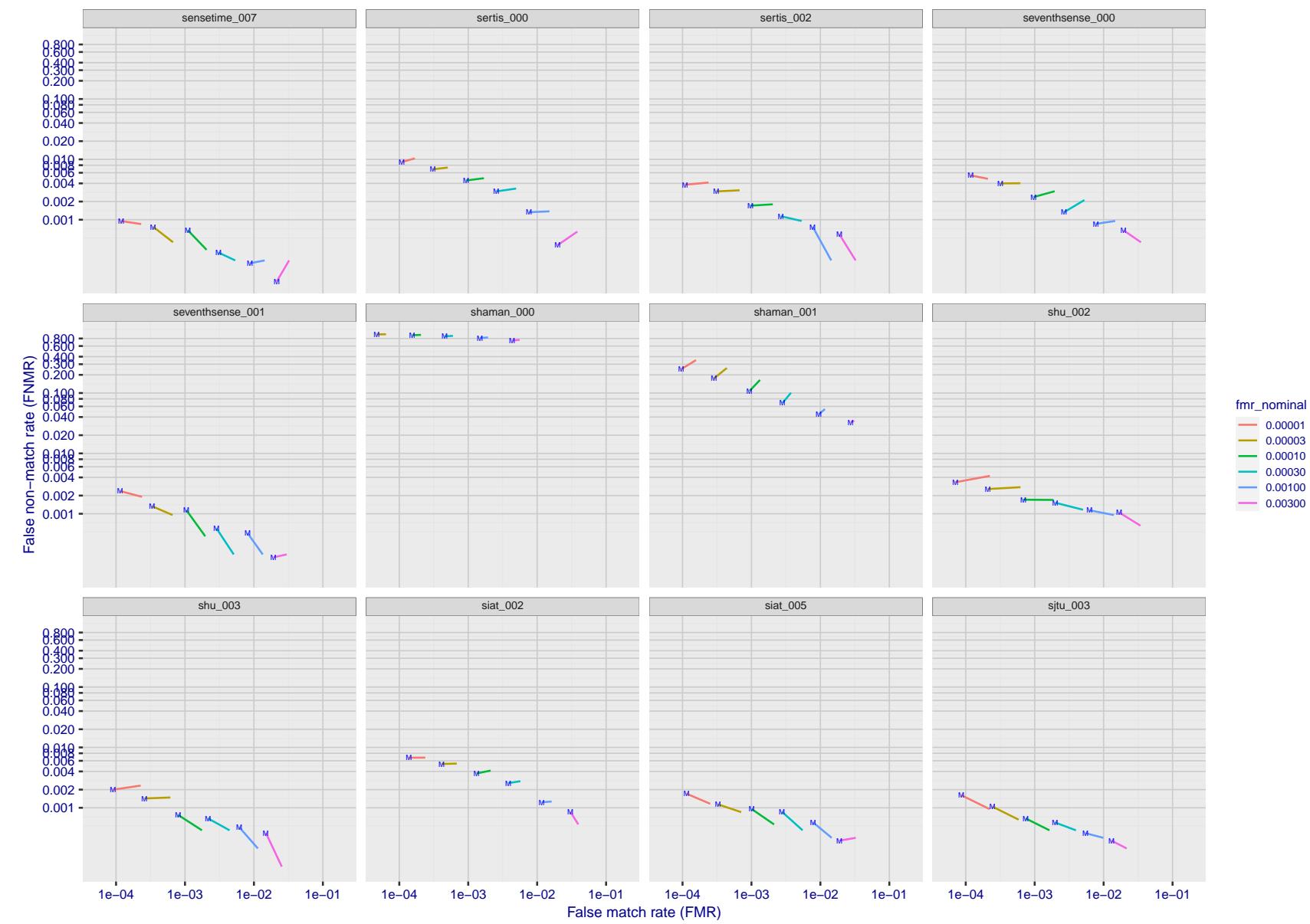


Figure 205: For the visa images, FNMR and FMR at six operating points along the DET characteristic. At each point a line is drawn between $(FMR, FNMR)_{MALE}$ and $(FMR, FNMR)_{FEMALE}$ showing how which sex has lower FMR and/or FNMR. The "M" label denotes male, the other end of the line corresponds to female. The six operating thresholds are selected to give the nominal false match rates given in the legend, and are computed over all impostor pairs regardless of age, sex, and place of birth. The plotted FMR values are broadly an order of magnitude larger than the nominal rates because FMR is computed over demographically-matched impostor pairs i.e individuals of the same sex, from the same geographic region (see section 3.6.1), and the same age group (see section 3.6.2).

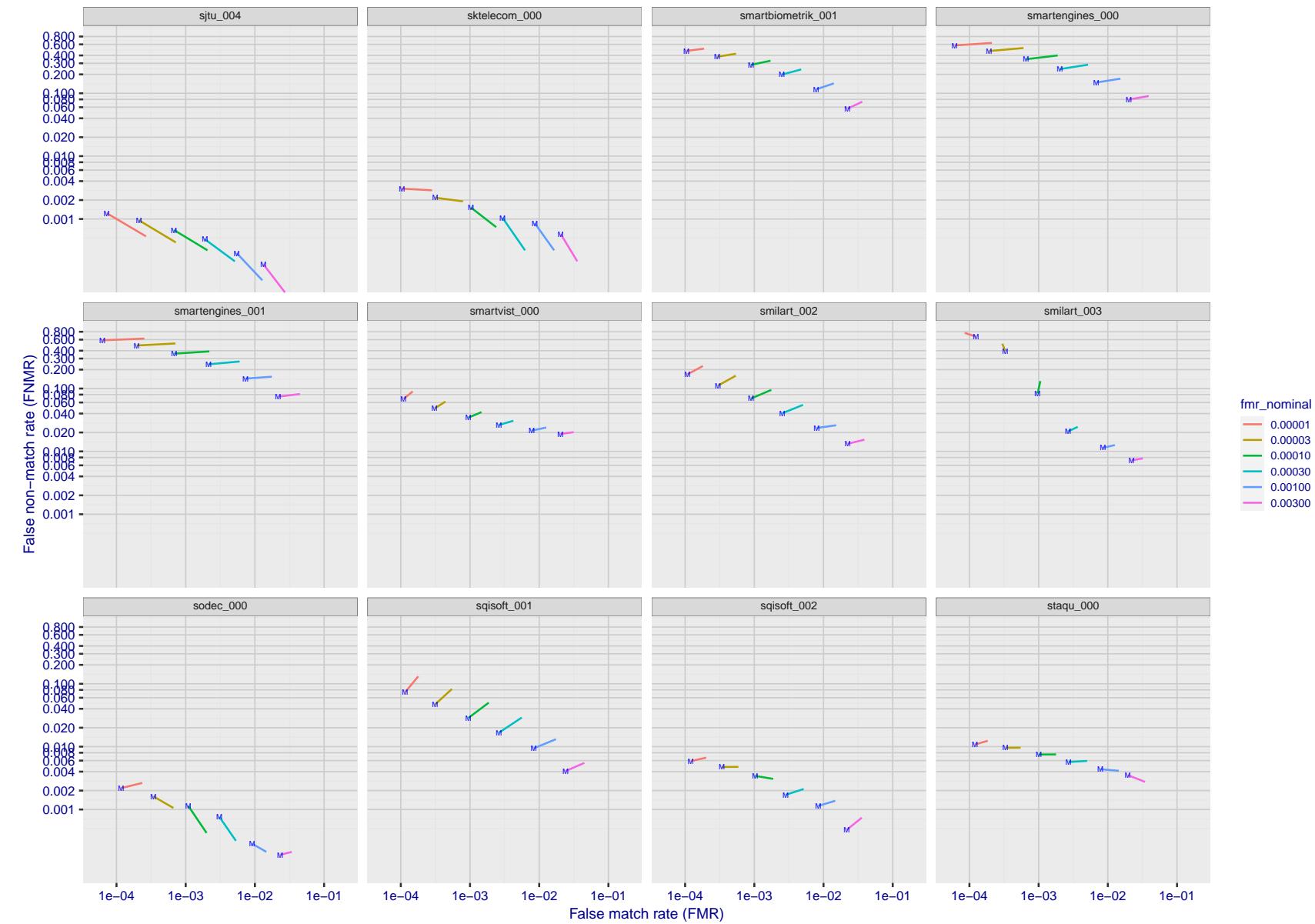


Figure 206: For the visa images, FNMR and FMR at six operating points along the DET characteristic. At each point a line is drawn between $(FMR, FNMR)_{MALE}$ and $(FMR, FNMR)_{FEMALE}$ showing how which sex has lower FMR and/or FNMR. The "M" label denotes male, the other end of the line corresponds to female. The six operating thresholds are selected to give the nominal false match rates given in the legend, and are computed over all impostor pairs regardless of age, sex, and place of birth. The plotted FMR values are broadly an order of magnitude larger than the nominal rates because FMR is computed over demographically-matched impostor pairs i.e individuals of the same sex, from the same geographic region (see section 3.6.1), and the same age group (see section 3.6.2).

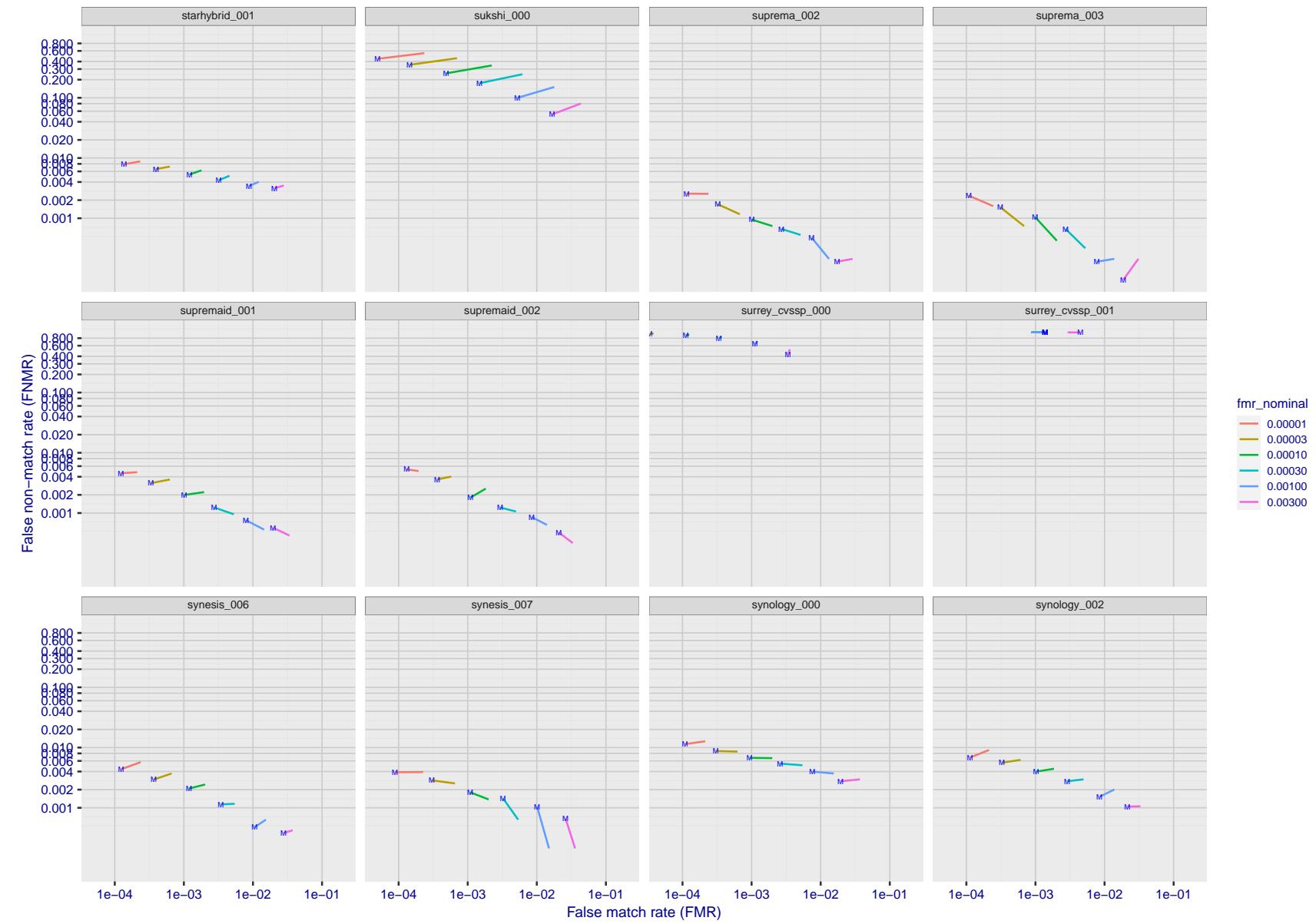


Figure 207: For the visa images, FNMR and FMR at six operating points along the DET characteristic. At each point a line is drawn between $(FMR, FNMR)_{MALE}$ and $(FMR, FNMR)_{FEMALE}$ showing how which sex has lower FMR and/or FNMR. The "M" label denotes male, the other end of the line corresponds to female. The six operating thresholds are selected to give the nominal false match rates given in the legend, and are computed over all impostor pairs regardless of age, sex, and place of birth. The plotted FMR values are broadly an order of magnitude larger than the nominal rates because FMR is computed over demographically-matched impostor pairs i.e individuals of the same sex, from the same geographic region (see section 3.6.1), and the same age group (see section 3.6.2).

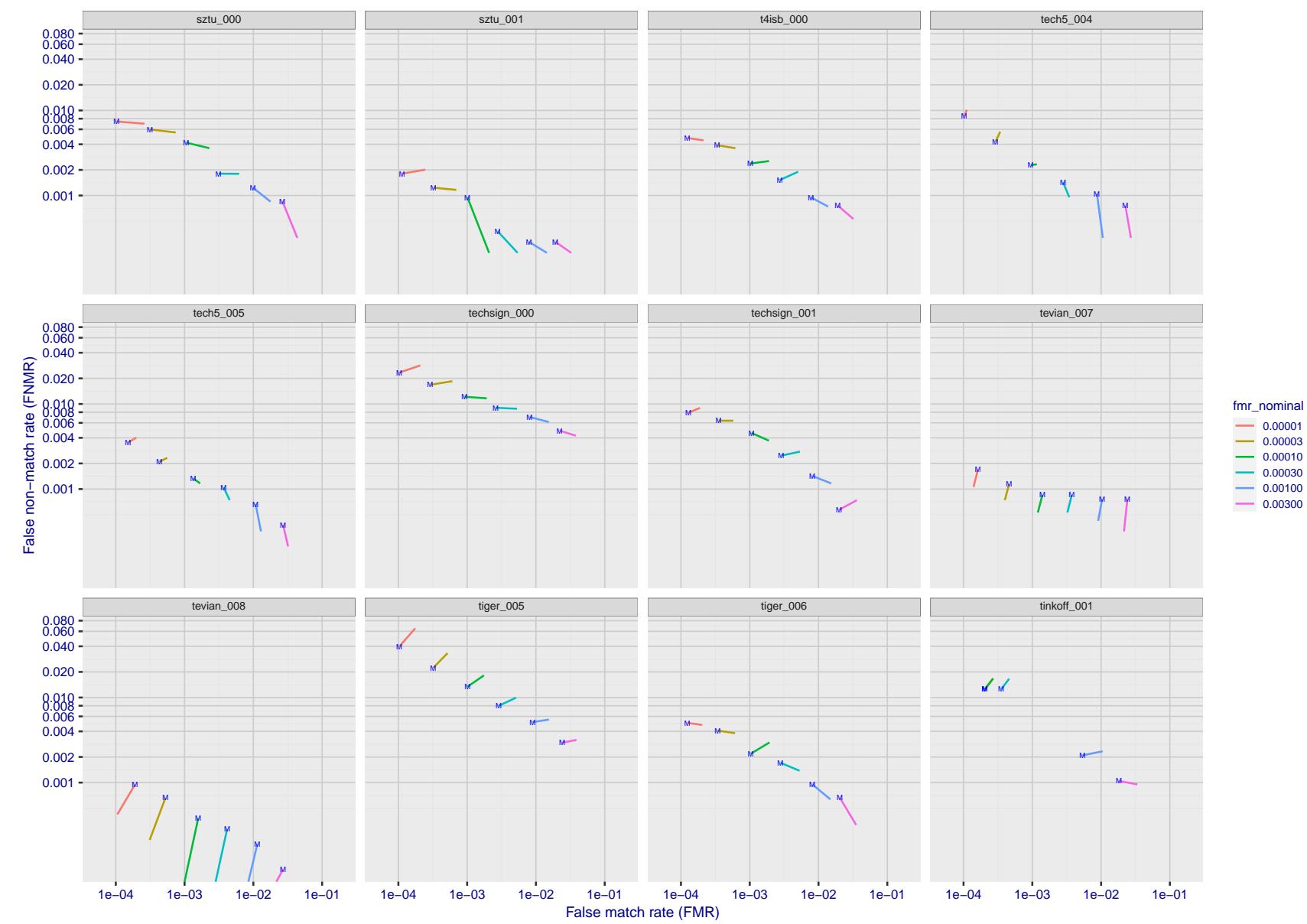


Figure 208: For the visa images, FNMR and FMR at six operating points along the DET characteristic. At each point a line is drawn between $(FMR, FNMR)_{MALE}$ and $(FMR, FNMR)_{FEMALE}$ showing how which sex has lower FMR and/or FNMR. The "M" label denotes male, the other end of the line corresponds to female. The six operating thresholds are selected to give the nominal false match rates given in the legend, and are computed over all impostor pairs regardless of age, sex, and place of birth. The plotted FMR values are broadly an order of magnitude larger than the nominal rates because FMR is computed over demographically-matched impostor pairs i.e individuals of the same sex, from the same geographic region (see section 3.6.1), and the same age group (see section 3.6.2).

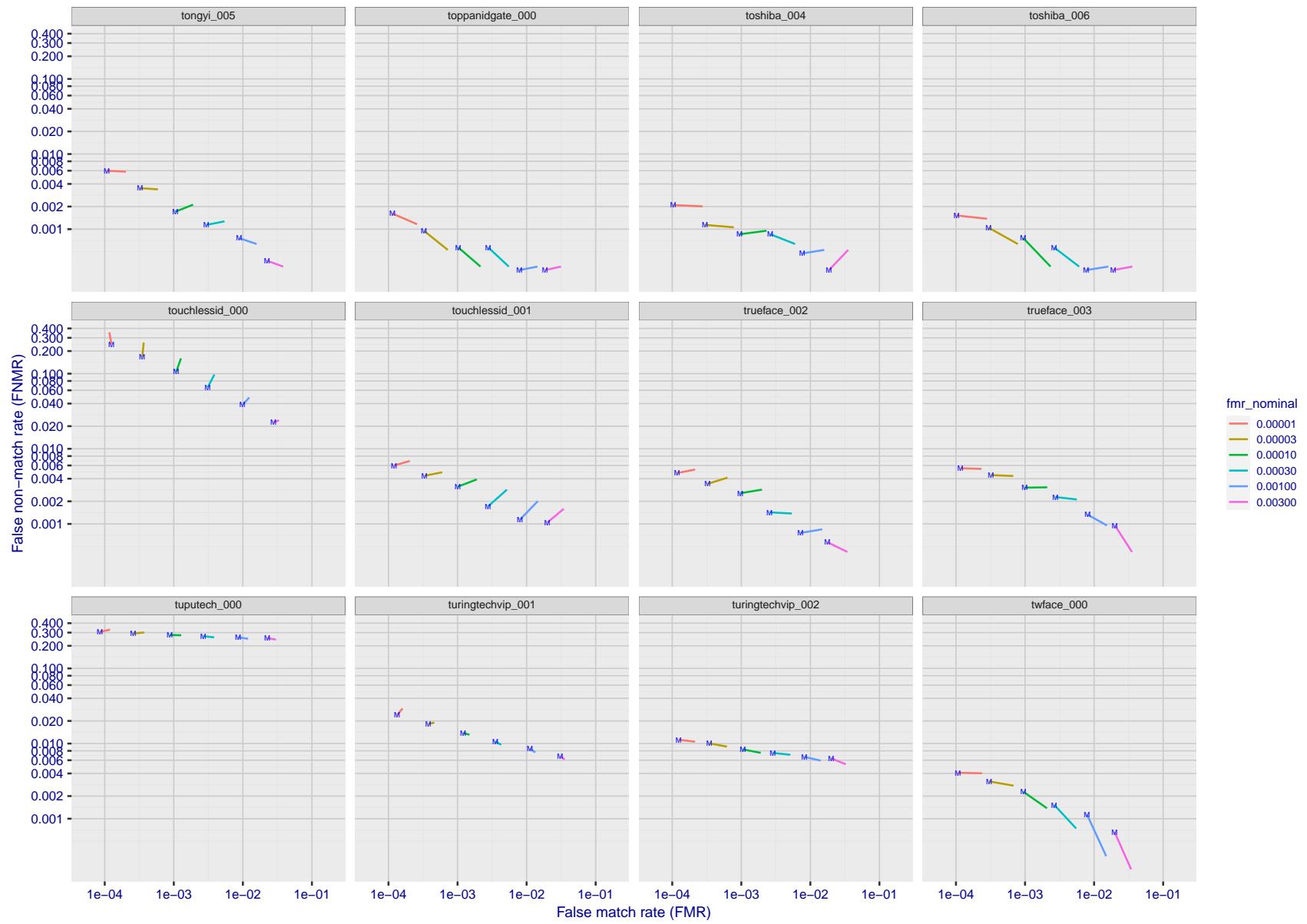


Figure 209: For the visa images, FNMR and FMR at six operating points along the DET characteristic. At each point a line is drawn between $(FMR, FNMR)_{MALE}$ and $(FMR, FNMR)_{FEMALE}$ showing how which sex has lower FMR and/or FNMR. The "M" label denotes male, the other end of the line corresponds to female. The six operating thresholds are selected to give the nominal false match rates given in the legend, and are computed over all impostor pairs regardless of age, sex, and place of birth. The plotted FMR values are broadly an order of magnitude larger than the nominal rates because FMR is computed over demographically-matched impostor pairs i.e individuals of the same sex, from the same geographic region (see section 3.6.1), and the same age group (see section 3.6.2).

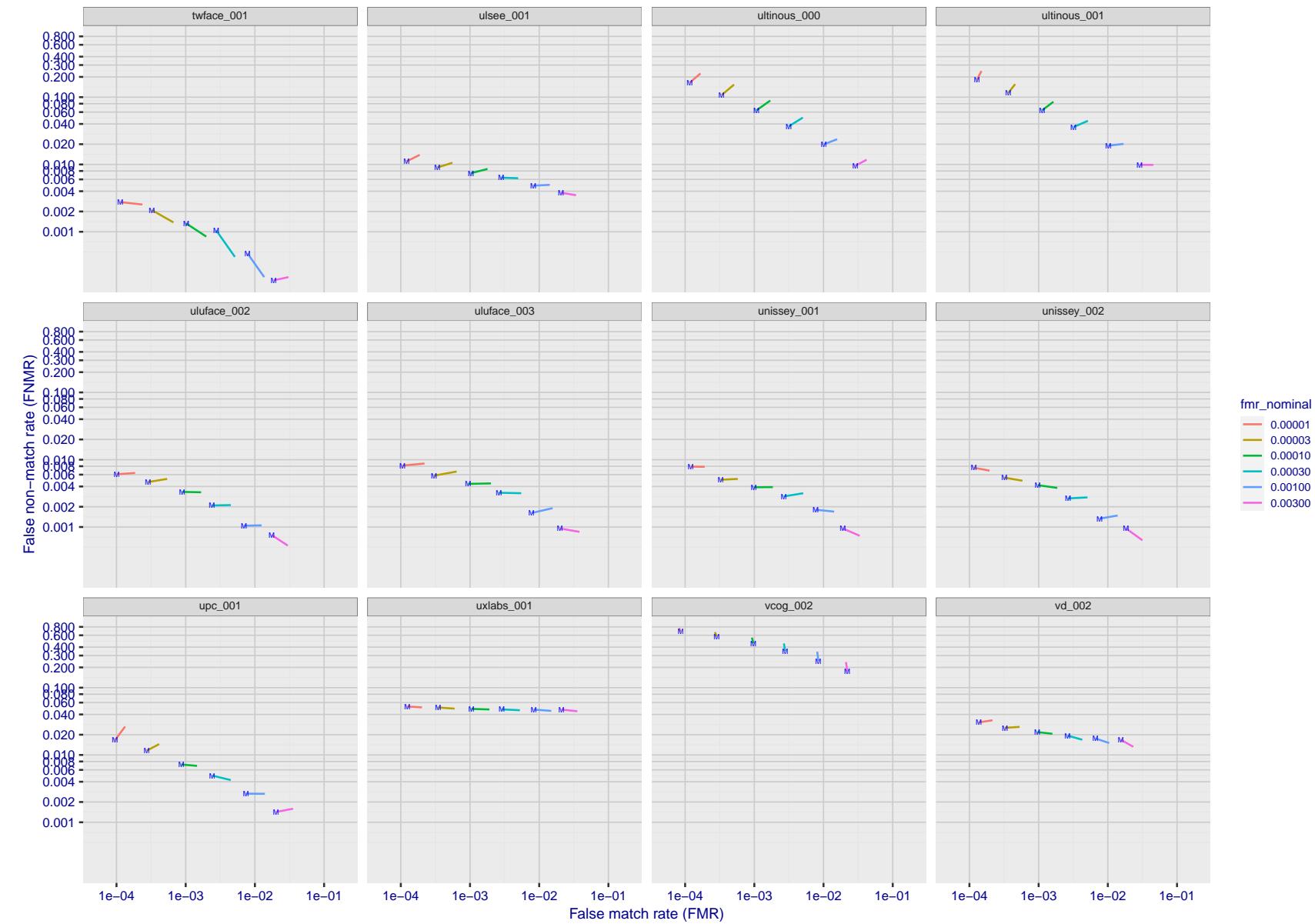


Figure 210: For the visa images, FNMR and FMR at six operating points along the DET characteristic. At each point a line is drawn between $(FMR, FNMR)_{MALE}$ and $(FMR, FNMR)_{FEMALE}$ showing how which sex has lower FMR and/or FNMR. The "M" label denotes male, the other end of the line corresponds to female. The six operating thresholds are selected to give the nominal false match rates given in the legend, and are computed over all impostor pairs regardless of age, sex, and place of birth. The plotted FMR values are broadly an order of magnitude larger than the nominal rates because FMR is computed over demographically-matched impostor pairs i.e individuals of the same sex, from the same geographic region (see section 3.6.1), and the same age group (see section 3.6.2).

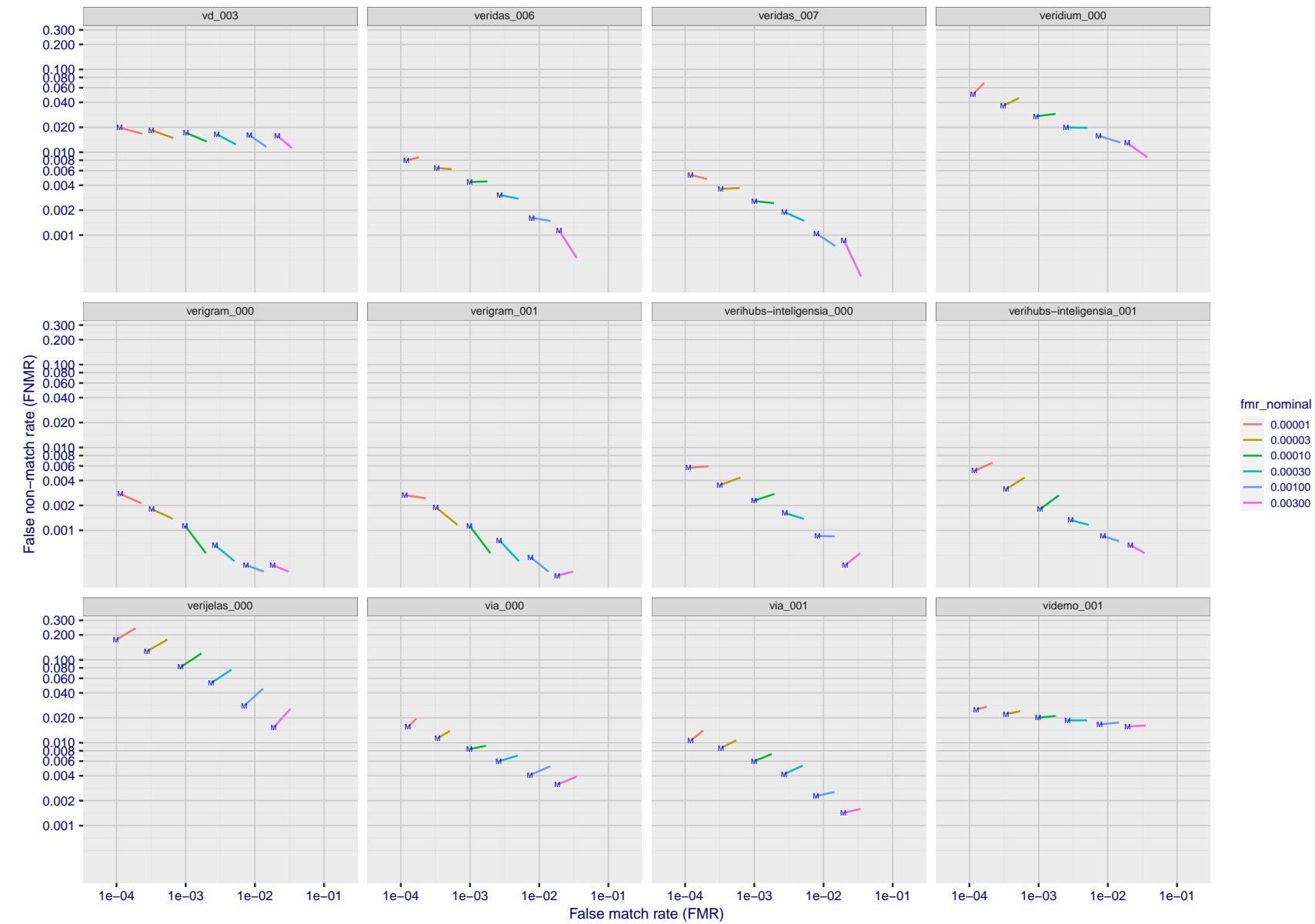


Figure 211: For the visa images, FNMR and FMR at six operating points along the DET characteristic. At each point a line is drawn between $(FMR, FNMR)_{MALE}$ and $(FMR, FNMR)_{FEMALE}$ showing how which sex has lower FMR and/or FNMR. The "M" label denotes male, the other end of the line corresponds to female. The six operating thresholds are selected to give the nominal false match rates given in the legend, and are computed over all impostor pairs regardless of age, sex, and place of birth. The plotted FMR values are broadly an order of magnitude larger than the nominal rates because FMR is computed over demographically-matched impostor pairs i.e individuals of the same sex, from the same geographic region (see section 3.6.1), and the same age group (see section 3.6.2).

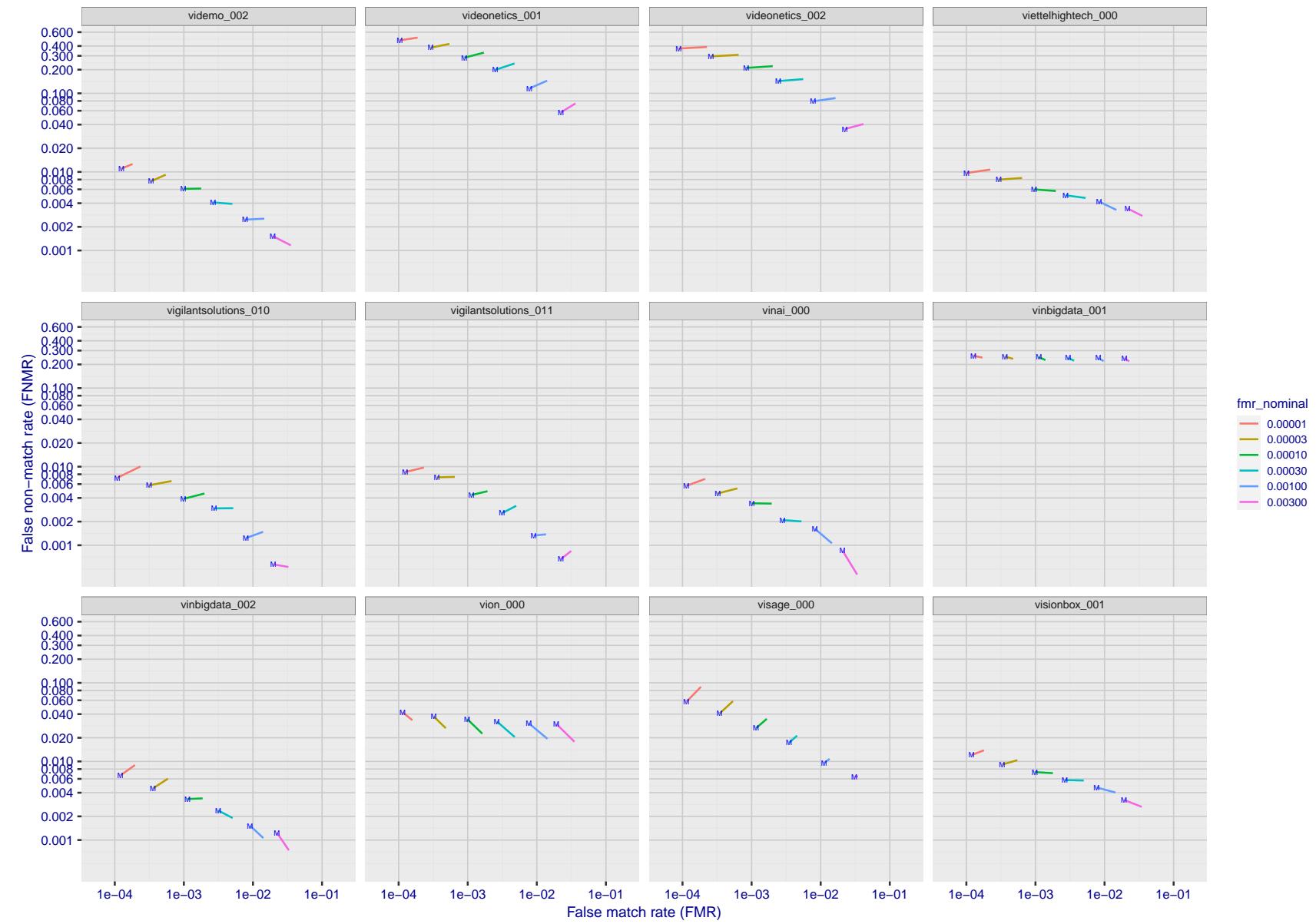


Figure 212: For the visa images, FNMR and FMR at six operating points along the DET characteristic. At each point a line is drawn between $(FMR, FNMR)_{MALE}$ and $(FMR, FNMR)_{FEMALE}$ showing how which sex has lower FMR and/or FNMR. The "M" label denotes male, the other end of the line corresponds to female. The six operating thresholds are selected to give the nominal false match rates given in the legend, and are computed over all impostor pairs regardless of age, sex, and place of birth. The plotted FMR values are broadly an order of magnitude larger than the nominal rates because FMR is computed over demographically-matched impostor pairs i.e individuals of the same sex, from the same geographic region (see section 3.6.1), and the same age group (see section 3.6.2).

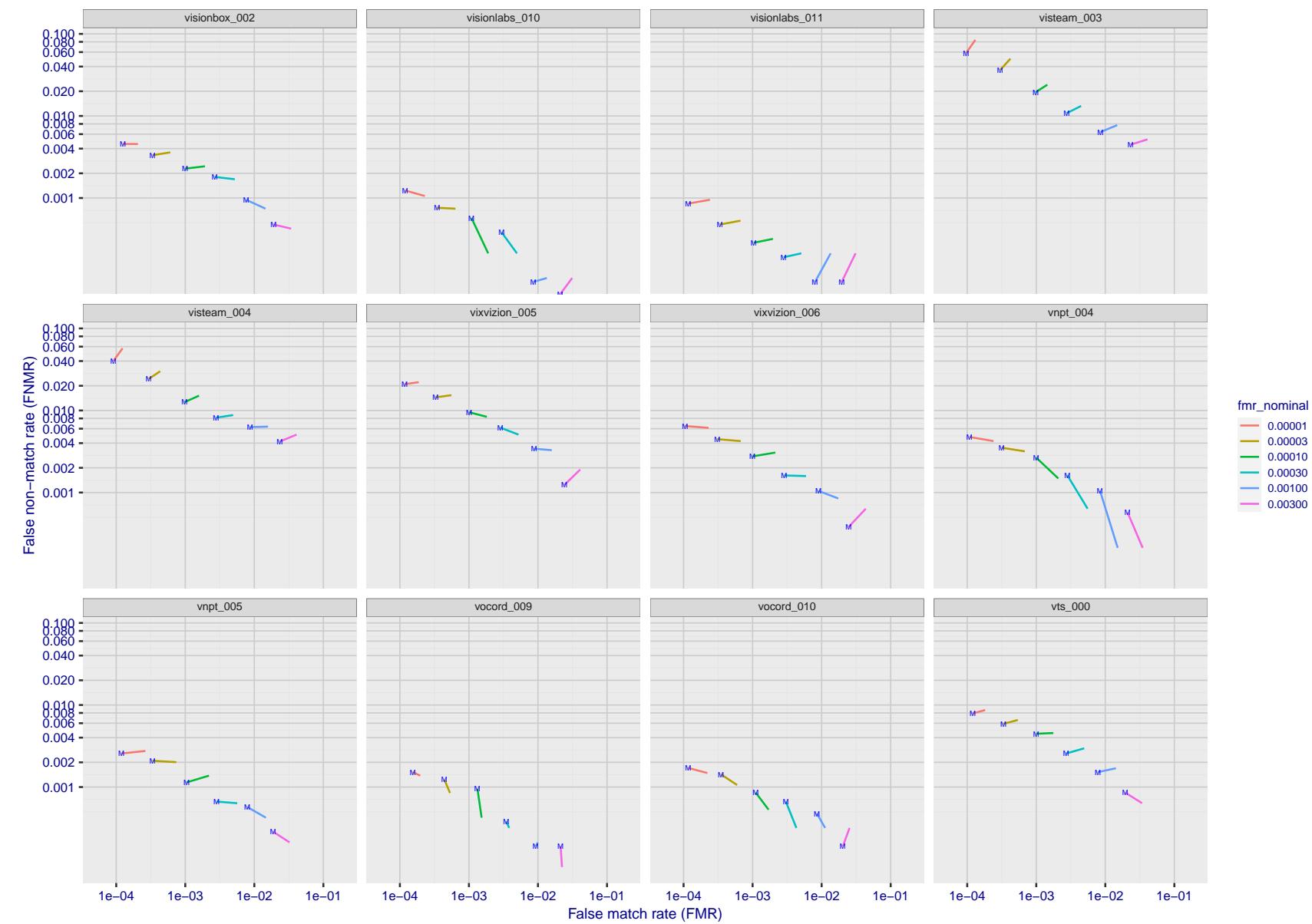


Figure 213: For the visa images, FNMR and FMR at six operating points along the DET characteristic. At each point a line is drawn between $(FMR, FNMR)_{MALE}$ and $(FMR, FNMR)_{FEMALE}$ showing how which sex has lower FMR and/or FNMR. The "M" label denotes male, the other end of the line corresponds to female. The six operating thresholds are selected to give the nominal false match rates given in the legend, and are computed over all impostor pairs regardless of age, sex, and place of birth. The plotted FMR values are broadly an order of magnitude larger than the nominal rates because FMR is computed over demographically-matched impostor pairs i.e individuals of the same sex, from the same geographic region (see section 3.6.1), and the same age group (see section 3.6.2).

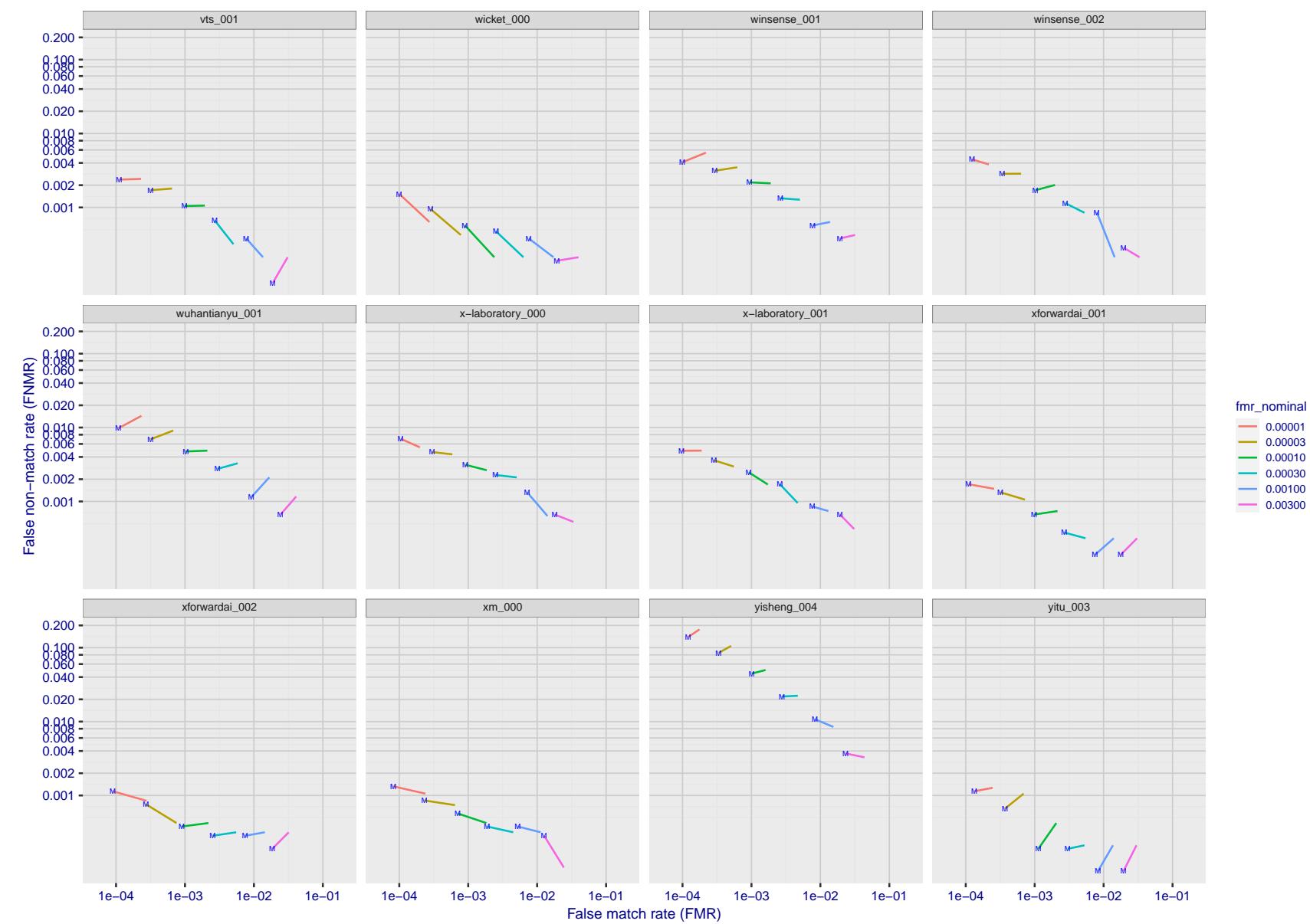


Figure 214: For the visa images, FNMR and FMR at six operating points along the DET characteristic. At each point a line is drawn between $(FMR, FNMR)_{MALE}$ and $(FMR, FNMR)_{FEMALE}$ showing how which sex has lower FMR and/or FNMR. The "M" label denotes male, the other end of the line corresponds to female. The six operating thresholds are selected to give the nominal false match rates given in the legend, and are computed over all impostor pairs regardless of age, sex, and place of birth. The plotted FMR values are broadly an order of magnitude larger than the nominal rates because FMR is computed over demographically-matched impostor pairs i.e individuals of the same sex, from the same geographic region (see section 3.6.1), and the same age group (see section 3.6.2).

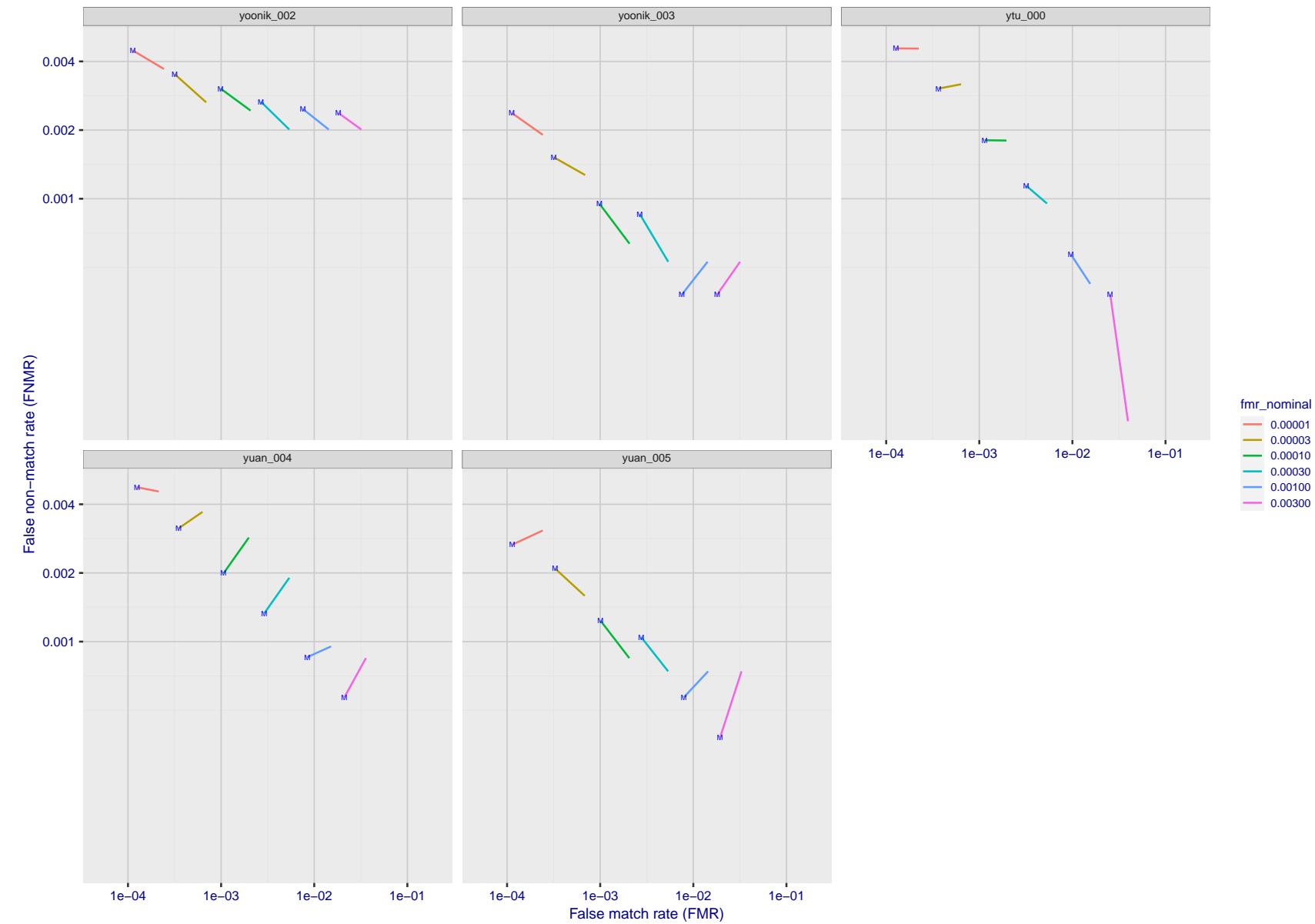


Figure 215: For the visa images, FNMR and FMR at six operating points along the DET characteristic. At each point a line is drawn between $(FMR, FNMR)_{MALE}$ and $(FMR, FNMR)_{FEMALE}$ showing how which sex has lower FMR and/or FNMR. The "M" label denotes male, the other end of the line corresponds to female. The six operating thresholds are selected to give the nominal false match rates given in the legend, and are computed over all impostor pairs regardless of age, sex, and place of birth. The plotted FMR values are broadly an order of magnitude larger than the nominal rates because FMR is computed over demographically-matched impostor pairs i.e individuals of the same sex, from the same geographic region (see section 3.6.1), and the same age group (see section 3.6.2).

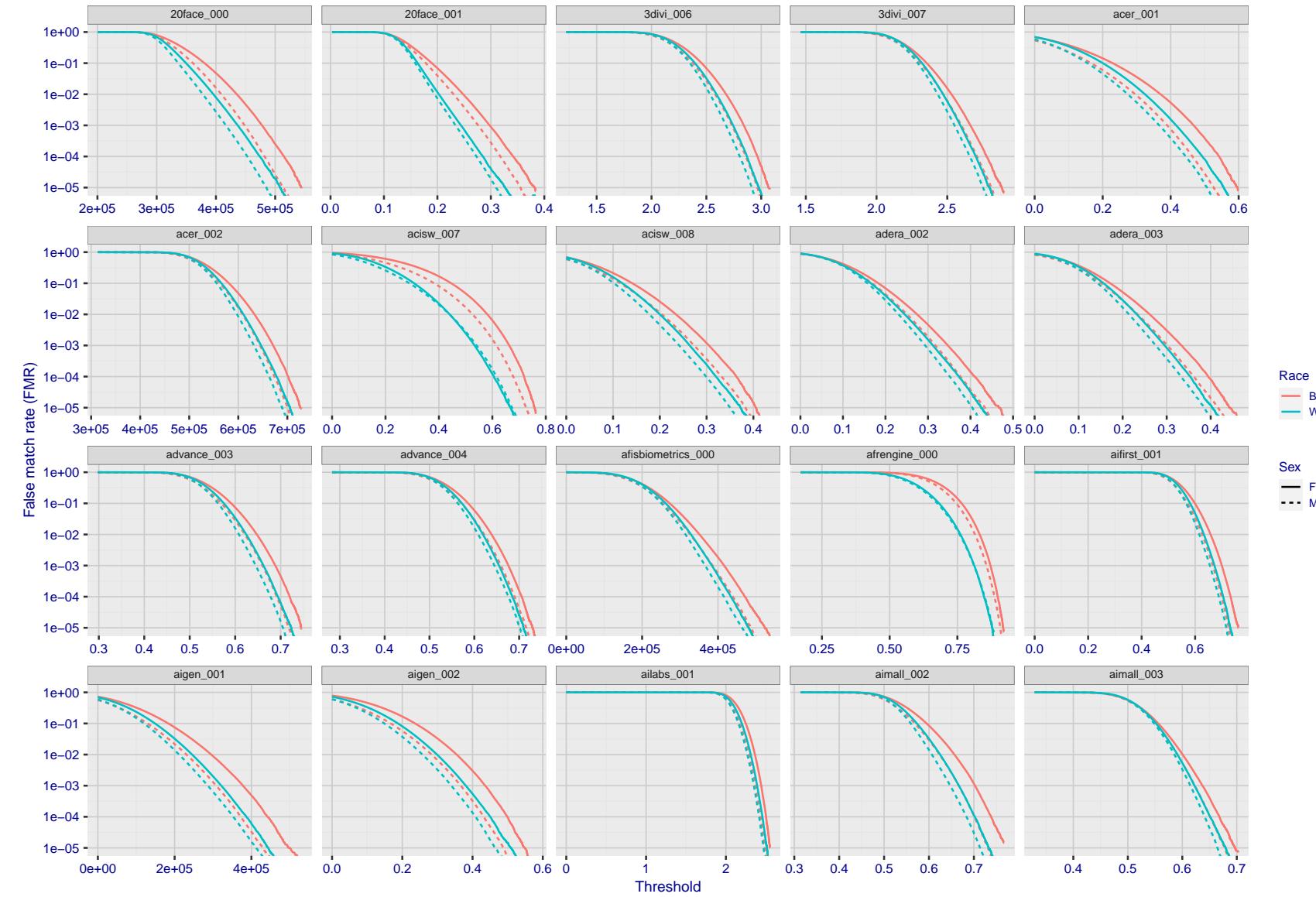


Figure 216: For the mugshot images, the false match calibration curves show false match rate vs. threshold. Separate curves appear for white females, black females, black males and white males.

2022/11/06 10:45:39

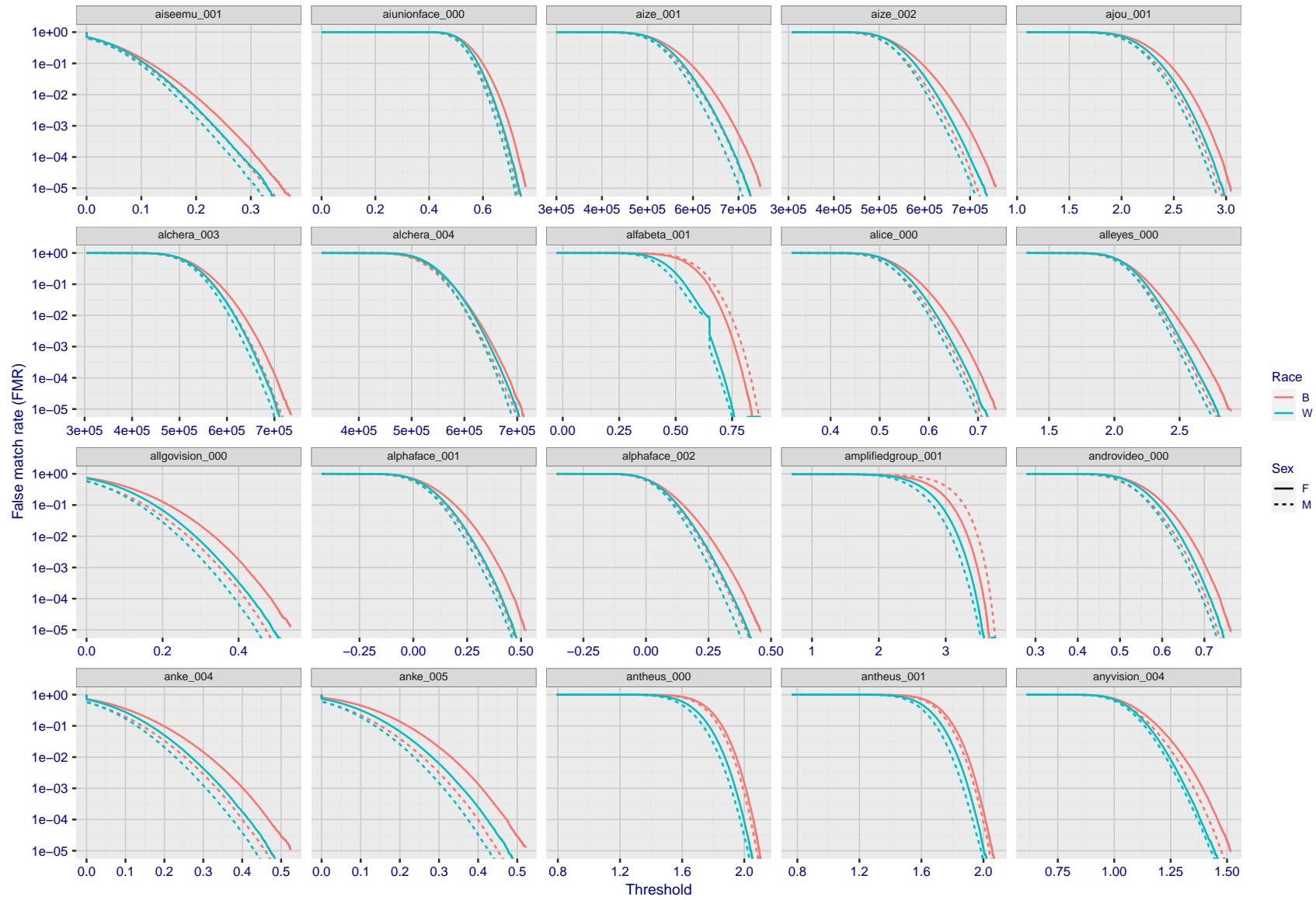


Figure 217: For the mugshot images, the false match calibration curves show false match rate vs. threshold. Separate curves appear for white females, black females, black males and white males.

2022/11/06 10:45:39

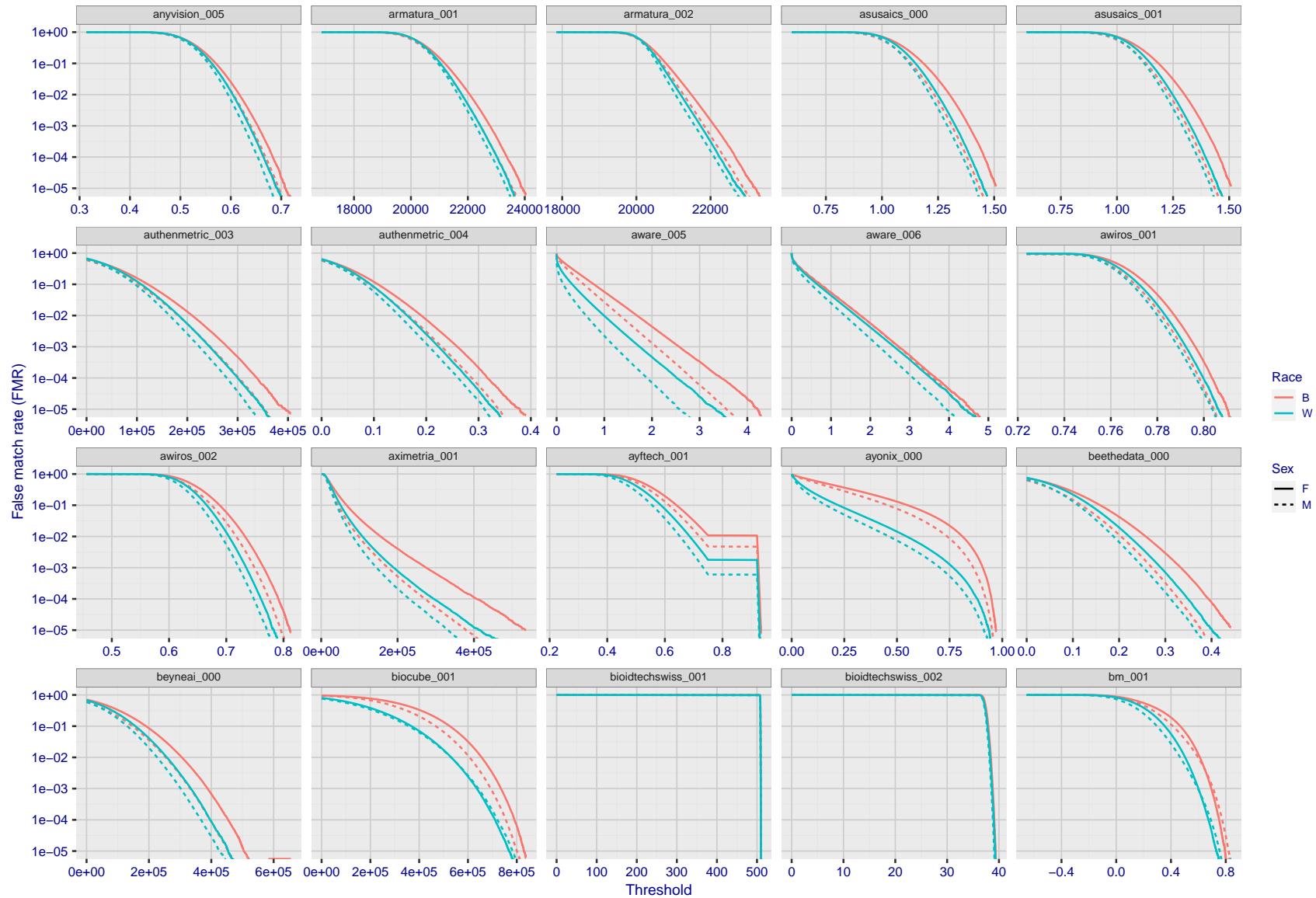


Figure 218: For the mugshot images, the false match calibration curves show false match rate vs. threshold. Separate curves appear for white females, black females, black males and white males.

2022/11/06 10:45:39

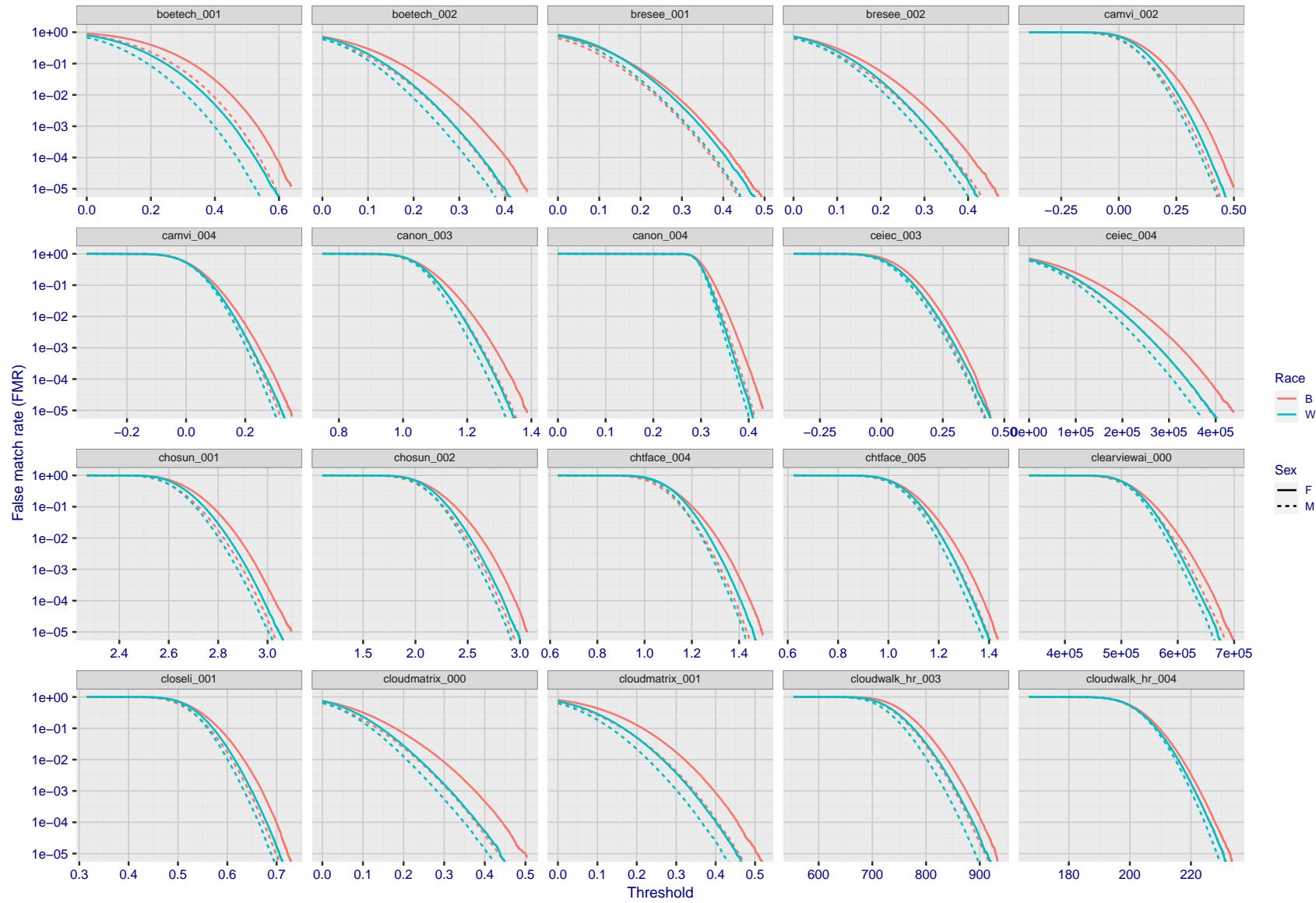


Figure 219: For the mugshot images, the false match calibration curves show false match rate vs. threshold. Separate curves appear for white females, black females, black males and white males.

2022/11/06 10:45:39

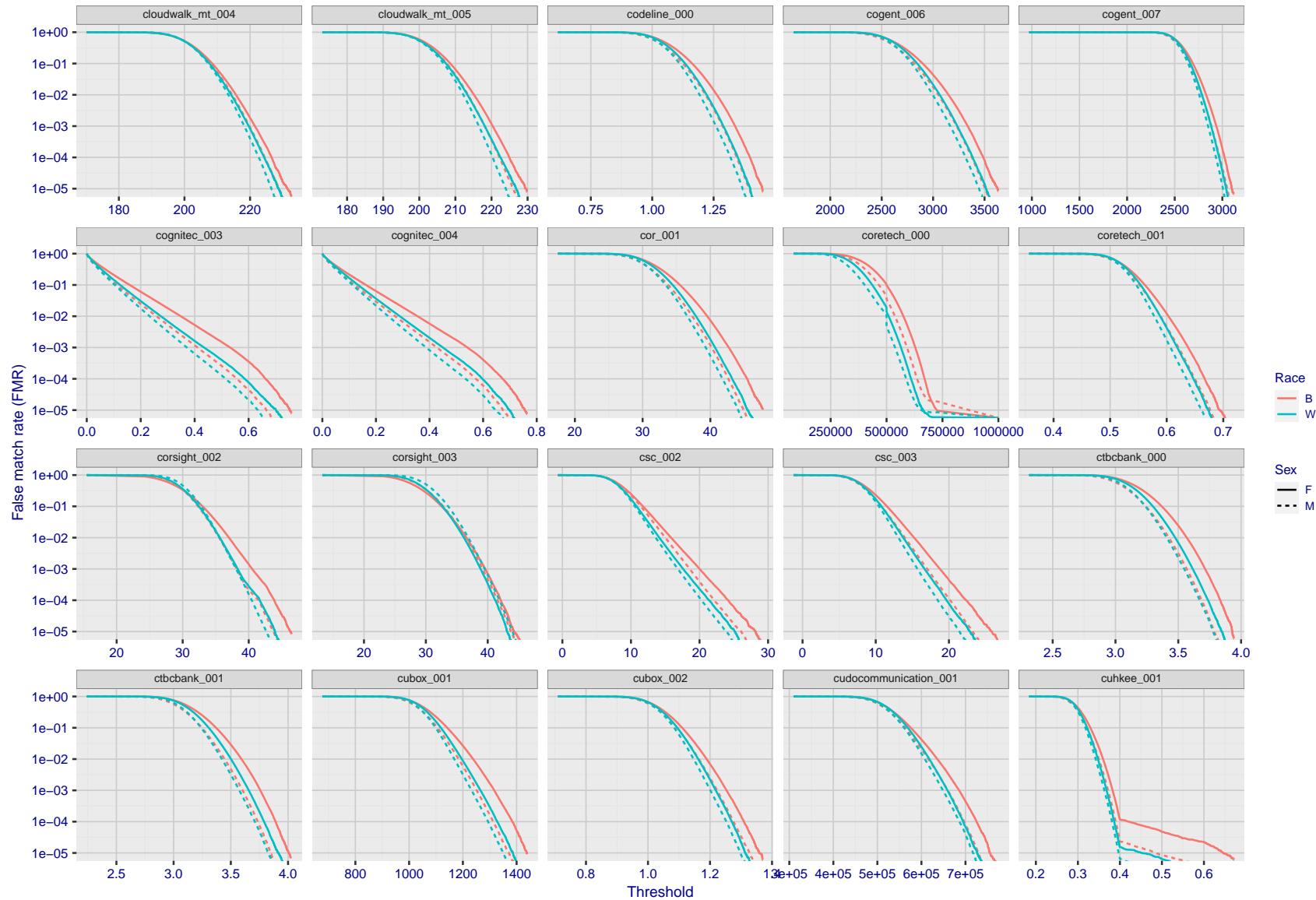


Figure 220: For the mugshot images, the false match calibration curves show false match rate vs. threshold. Separate curves appear for white females, black females, black males and white males.

FNMR(T)
"False non-match rate"
"False match rate"

2022/11/06 10:45:39

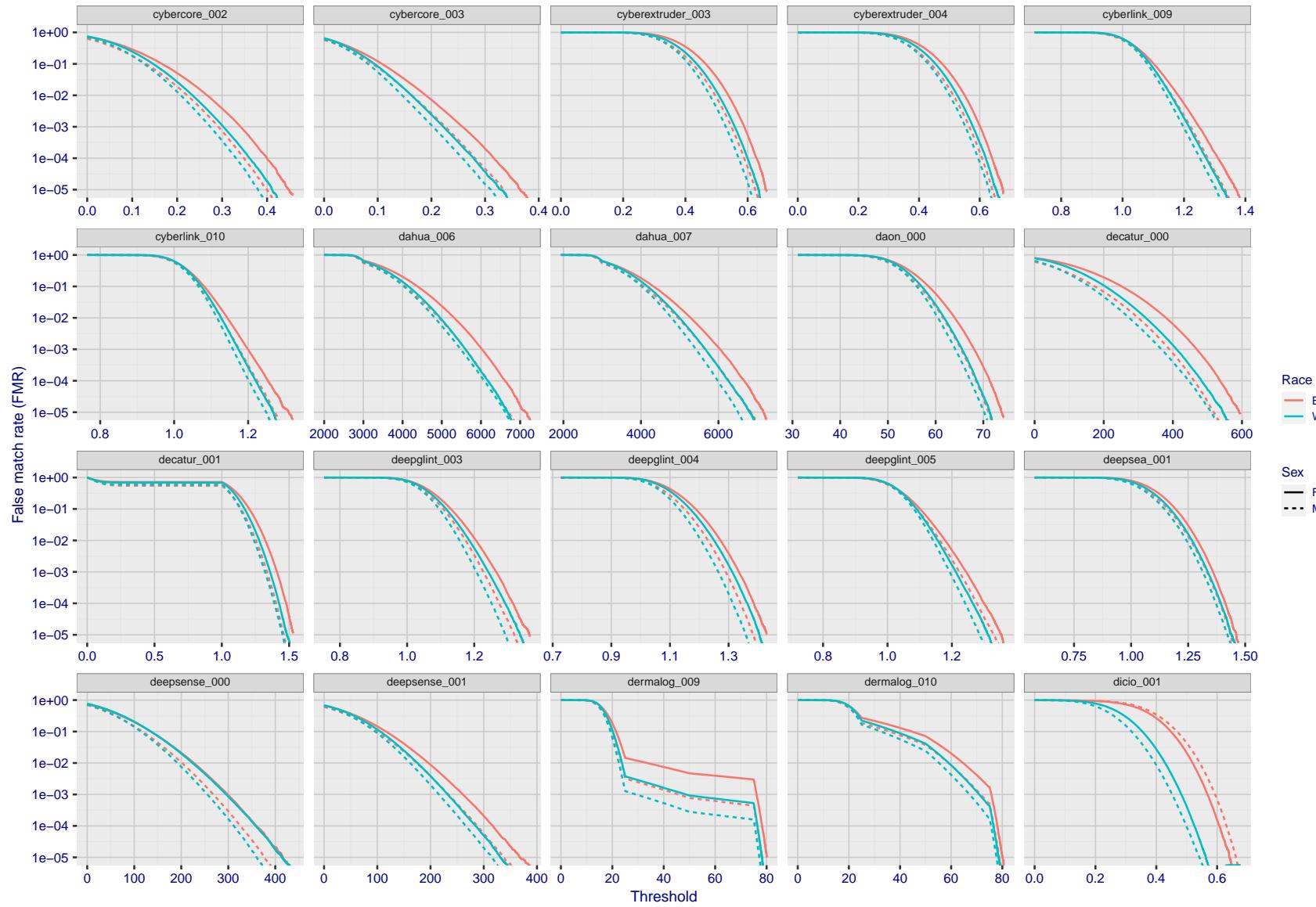


Figure 221: For the mugshot images, the false match calibration curves show false match rate vs. threshold. Separate curves appear for white females, black females, black males and white males.

2022/11/06 10:45:39

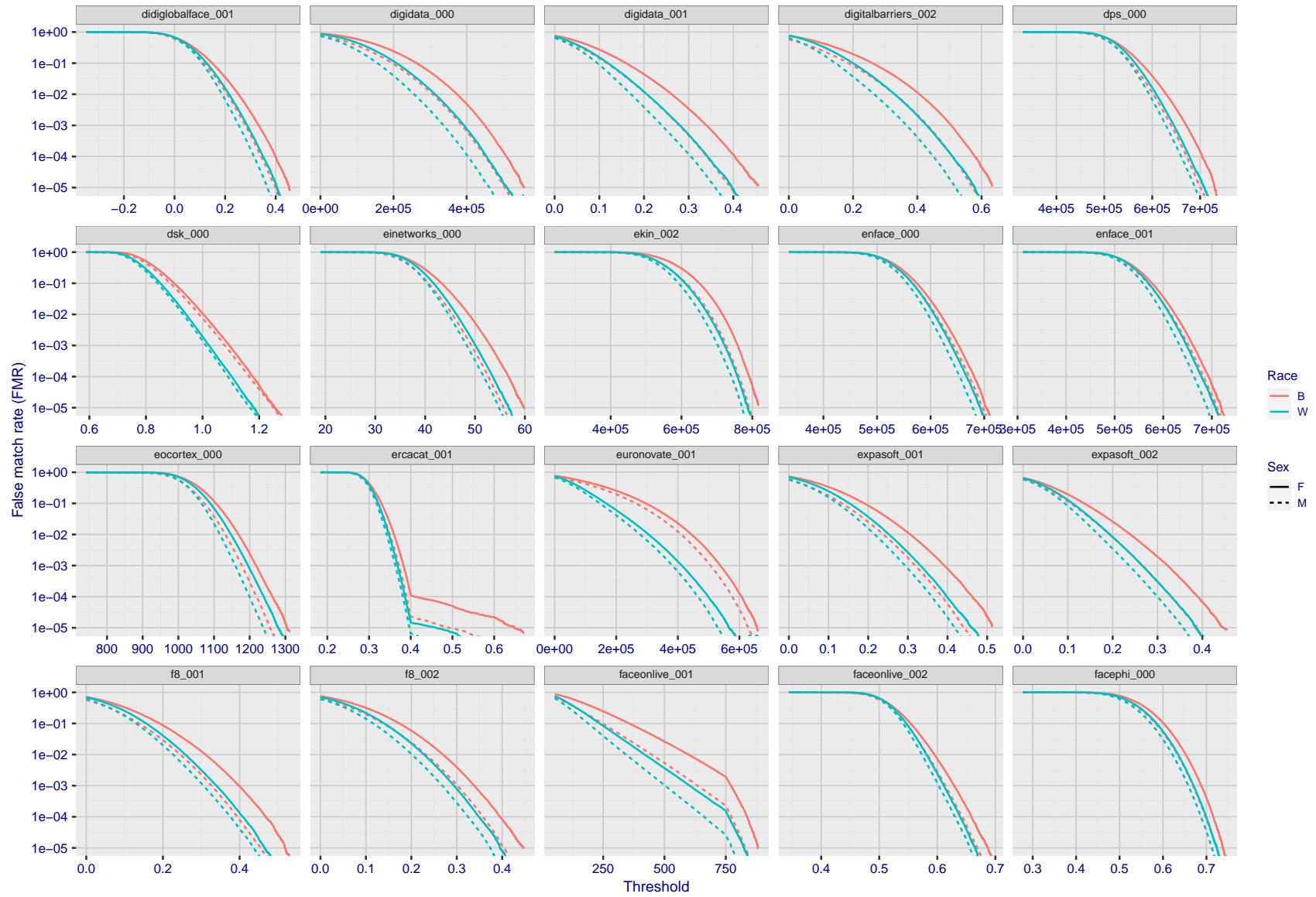


Figure 222: For the mugshot images, the false match calibration curves show false match rate vs. threshold. Separate curves appear for white females, black females, black males and white males.

2022/11/06 10:45:39

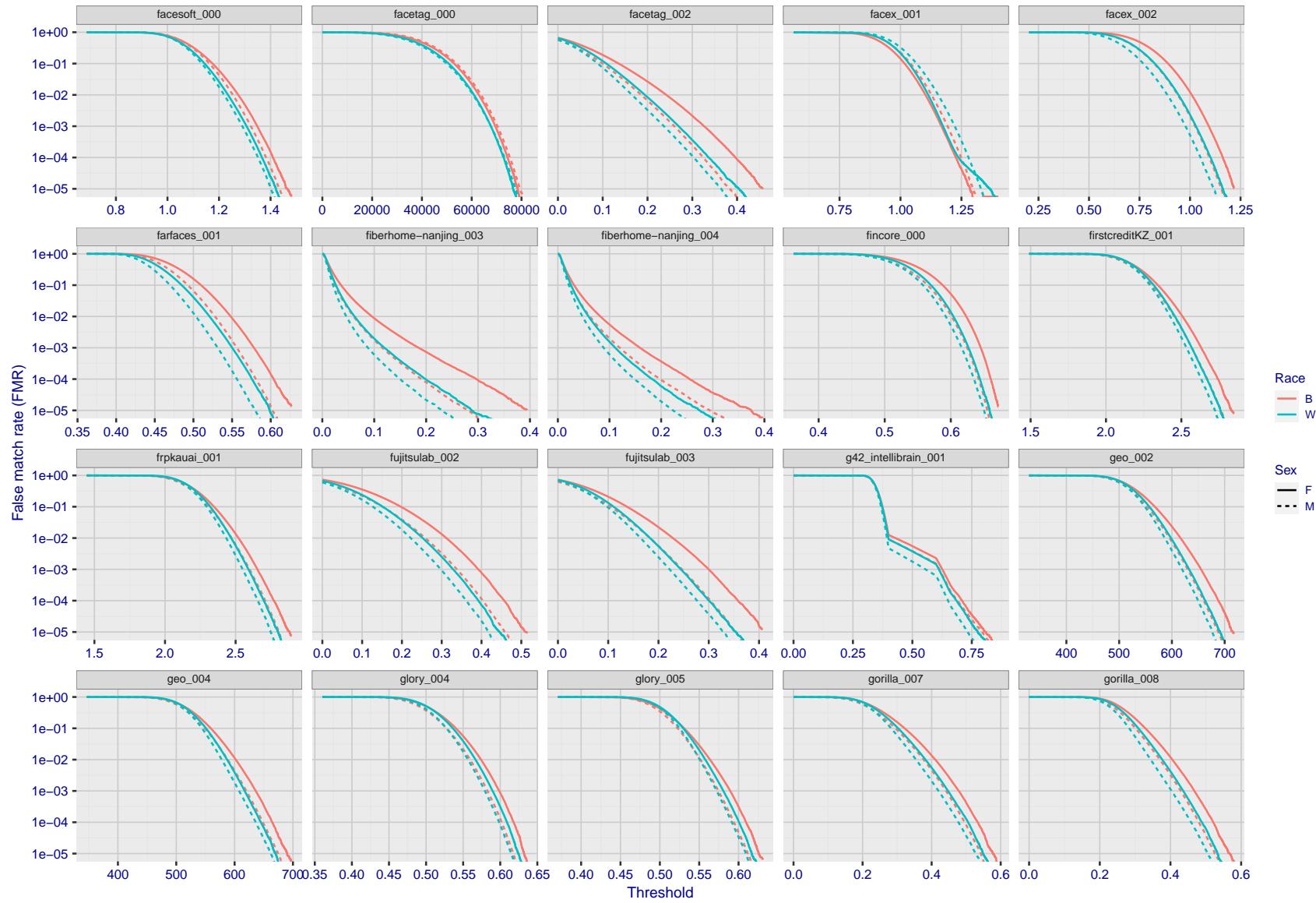


Figure 223: For the mugshot images, the false match calibration curves show false match rate vs. threshold. Separate curves appear for white females, black females, black males and white males.

2022/11/06 10:45:39

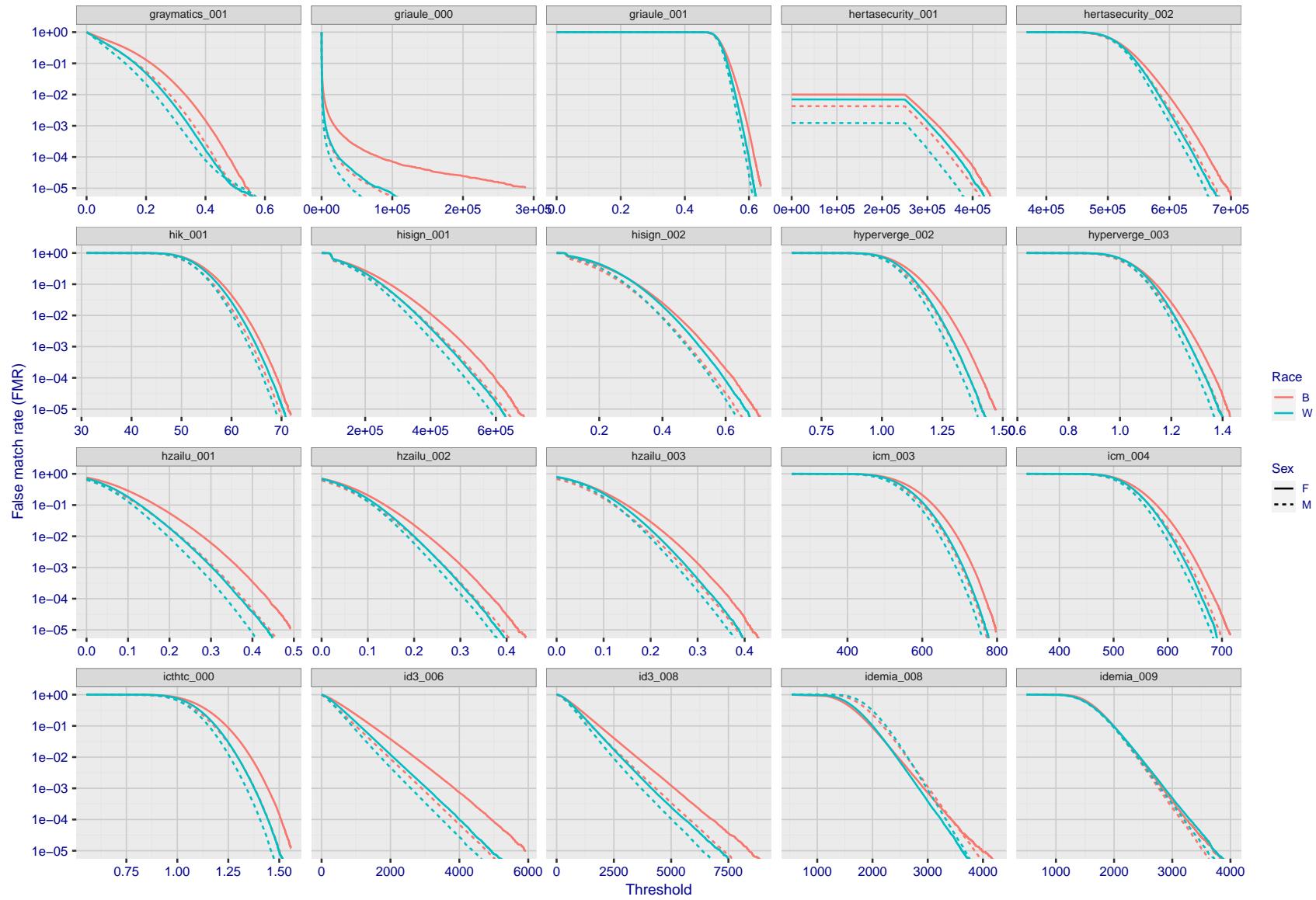


Figure 224: For the mugshot images, the false match calibration curves show false match rate vs. threshold. Separate curves appear for white females, black females, black males and white males.

2022/11/06 10:45:39

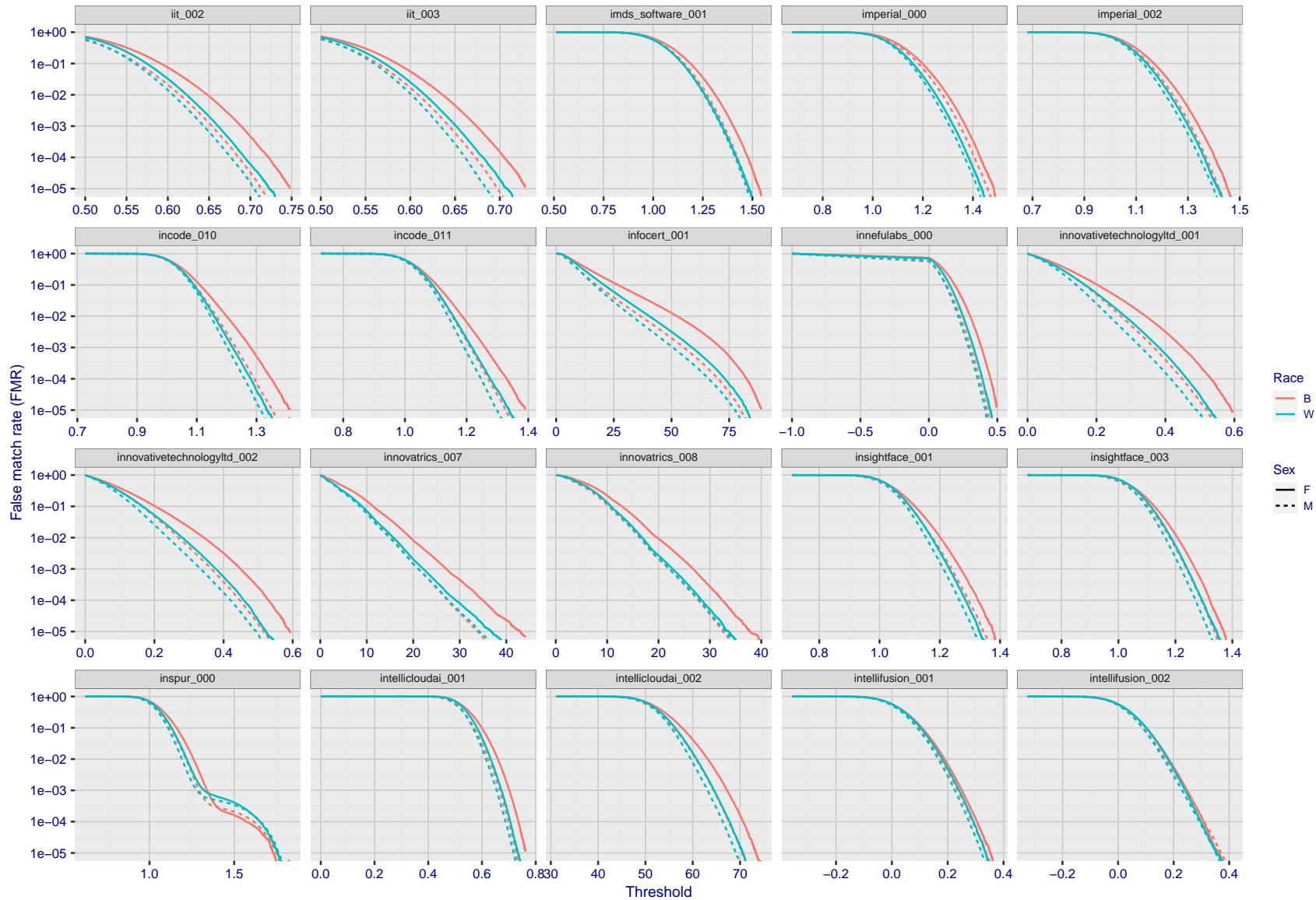


Figure 225: For the mugshot images, the false match calibration curves show false match rate vs. threshold. Separate curves appear for white females, black females, black males and white males.

2022/11/06 10:45:39

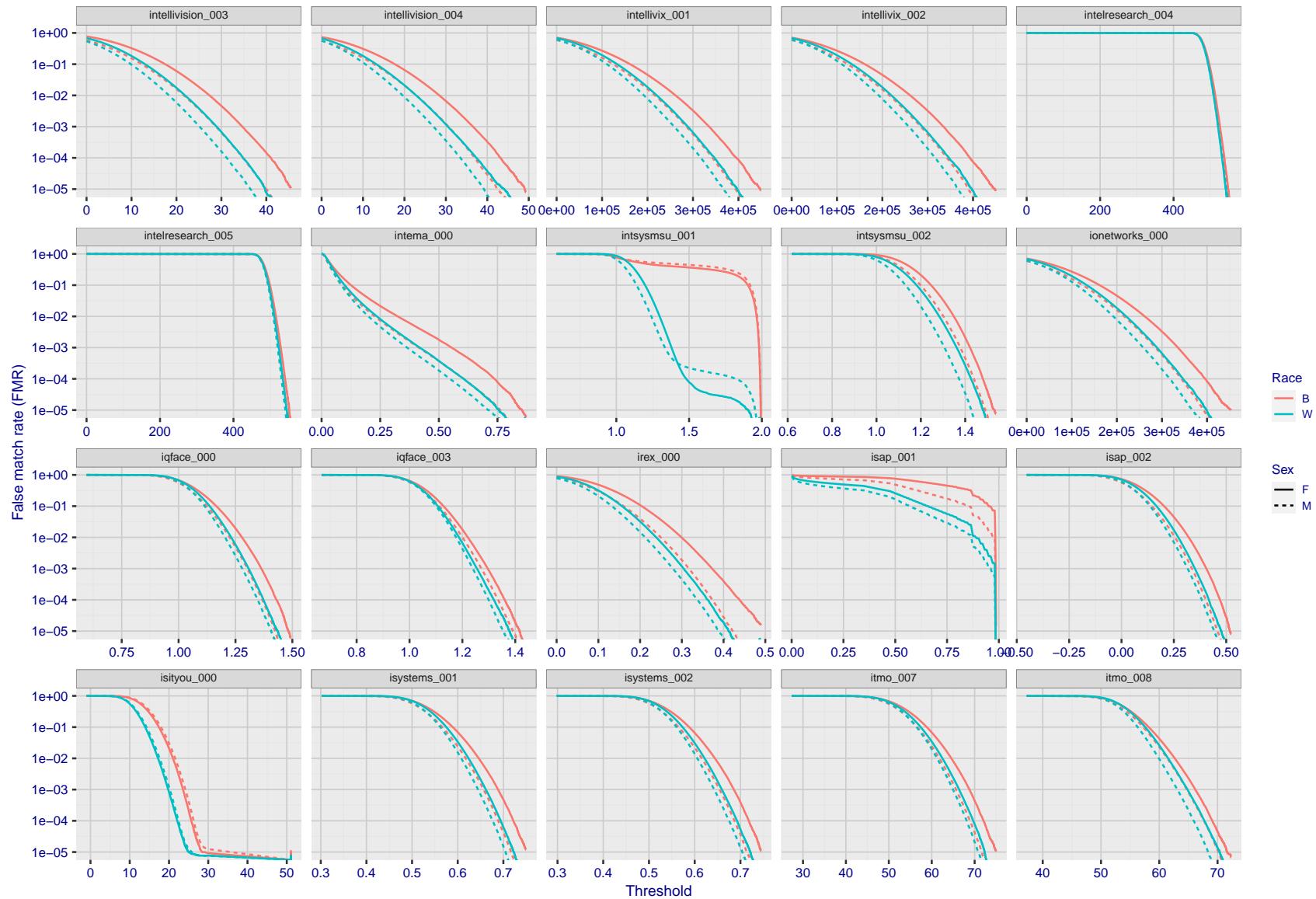


Figure 226: For the mugshot images, the false match calibration curves show false match rate vs. threshold. Separate curves appear for white females, black females, black males and white males.

2022/11/06 10:45:39

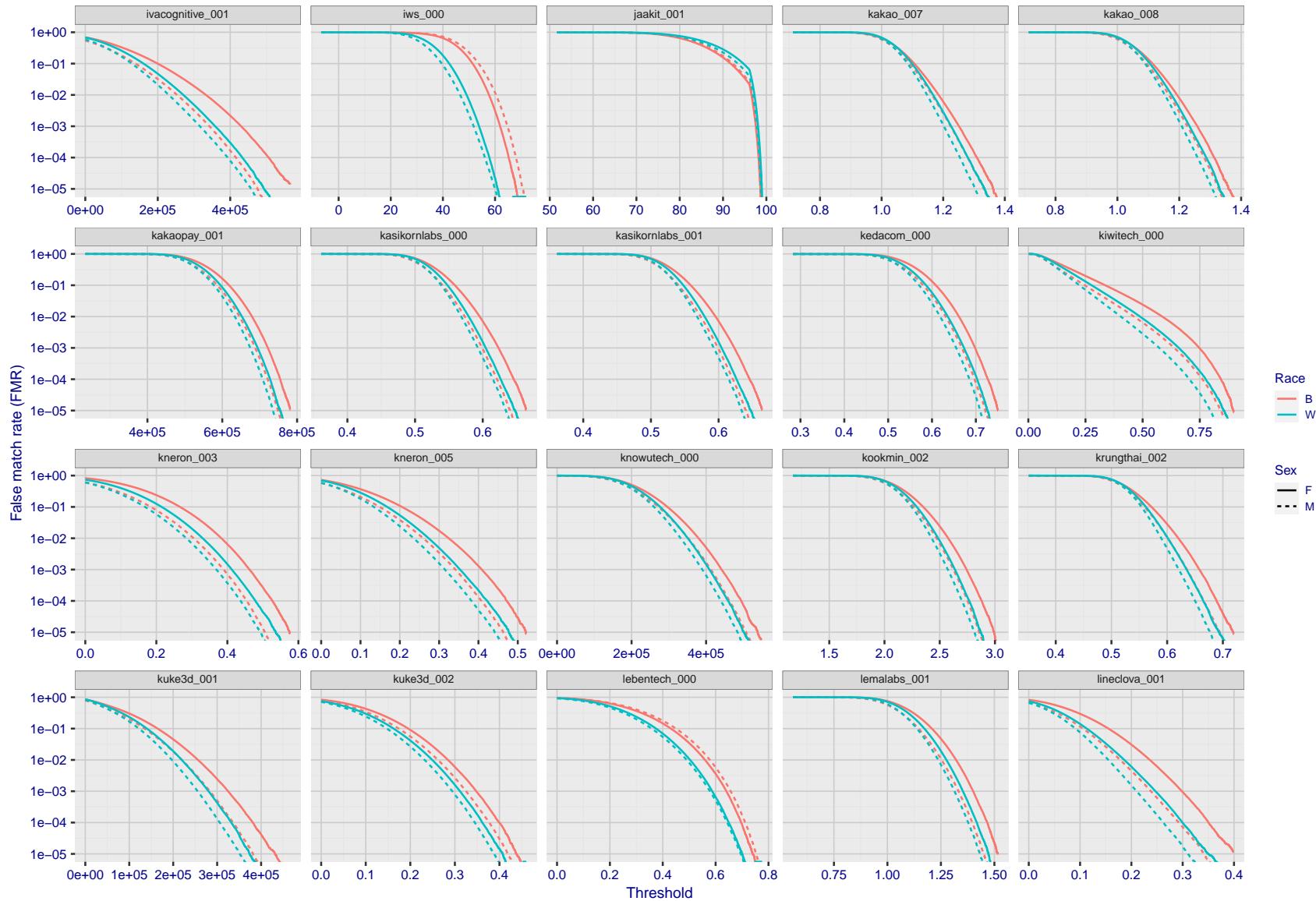


Figure 227: For the mugshot images, the false match calibration curves show false match rate vs. threshold. Separate curves appear for white females, black females, black males and white males.

2022/11/06 10:45:39

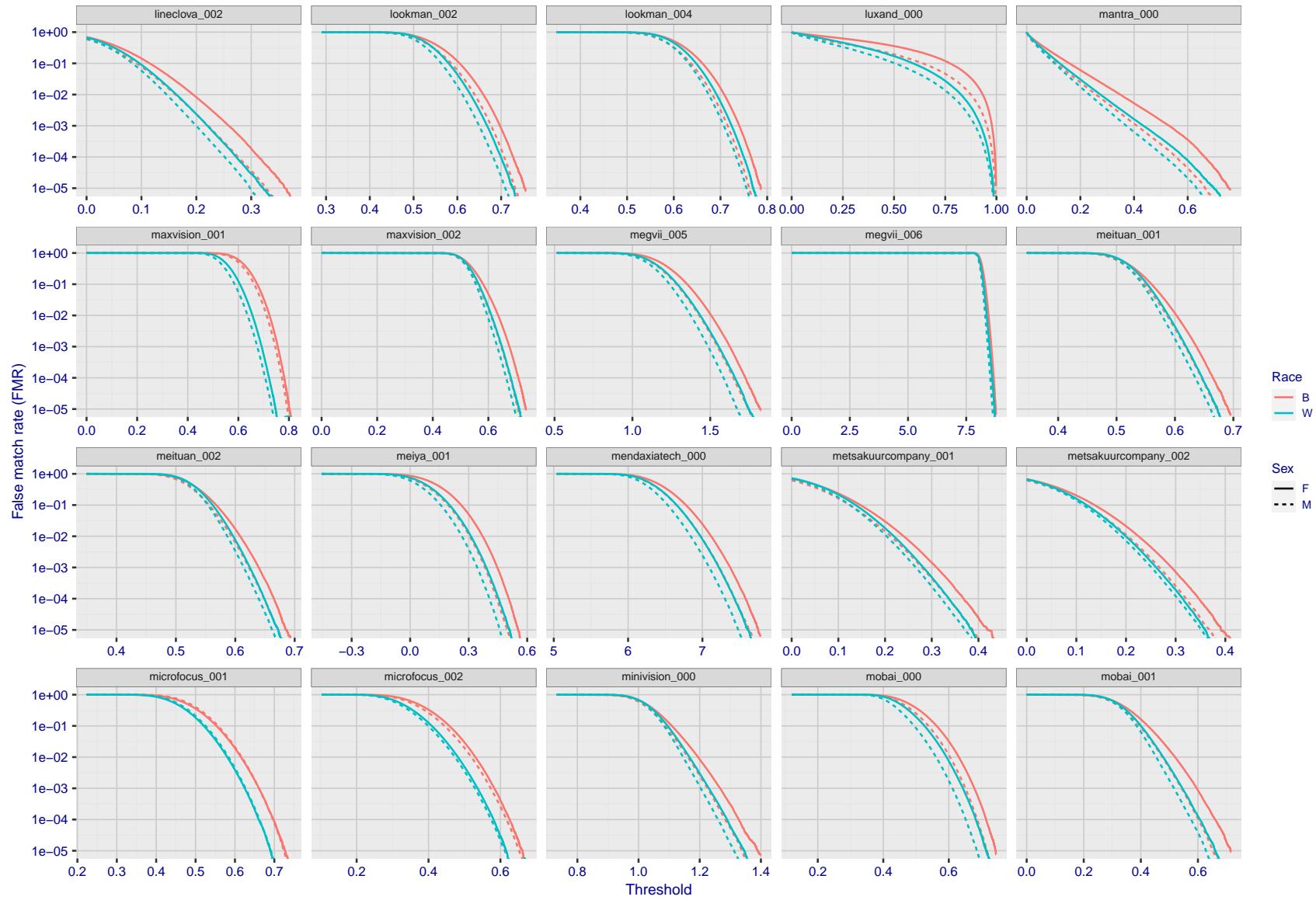


Figure 228: For the mugshot images, the false match calibration curves show false match rate vs. threshold. Separate curves appear for white females, black females, black males and white males.

2022/11/06 10:45:39

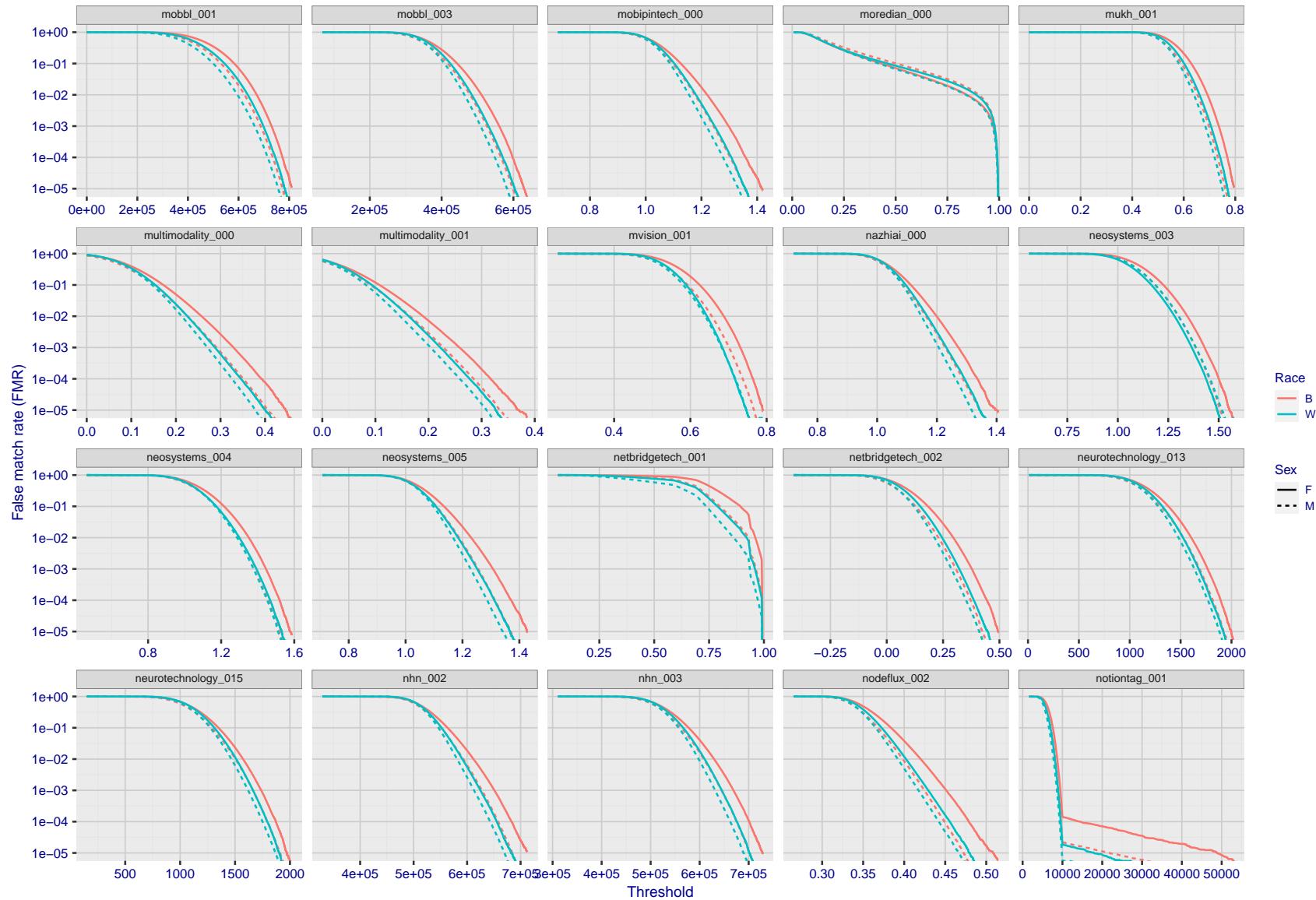


Figure 229: For the mugshot images, the false match calibration curves show false match rate vs. threshold. Separate curves appear for white females, black females, black males and white males.

2022/11/06 10:45:39

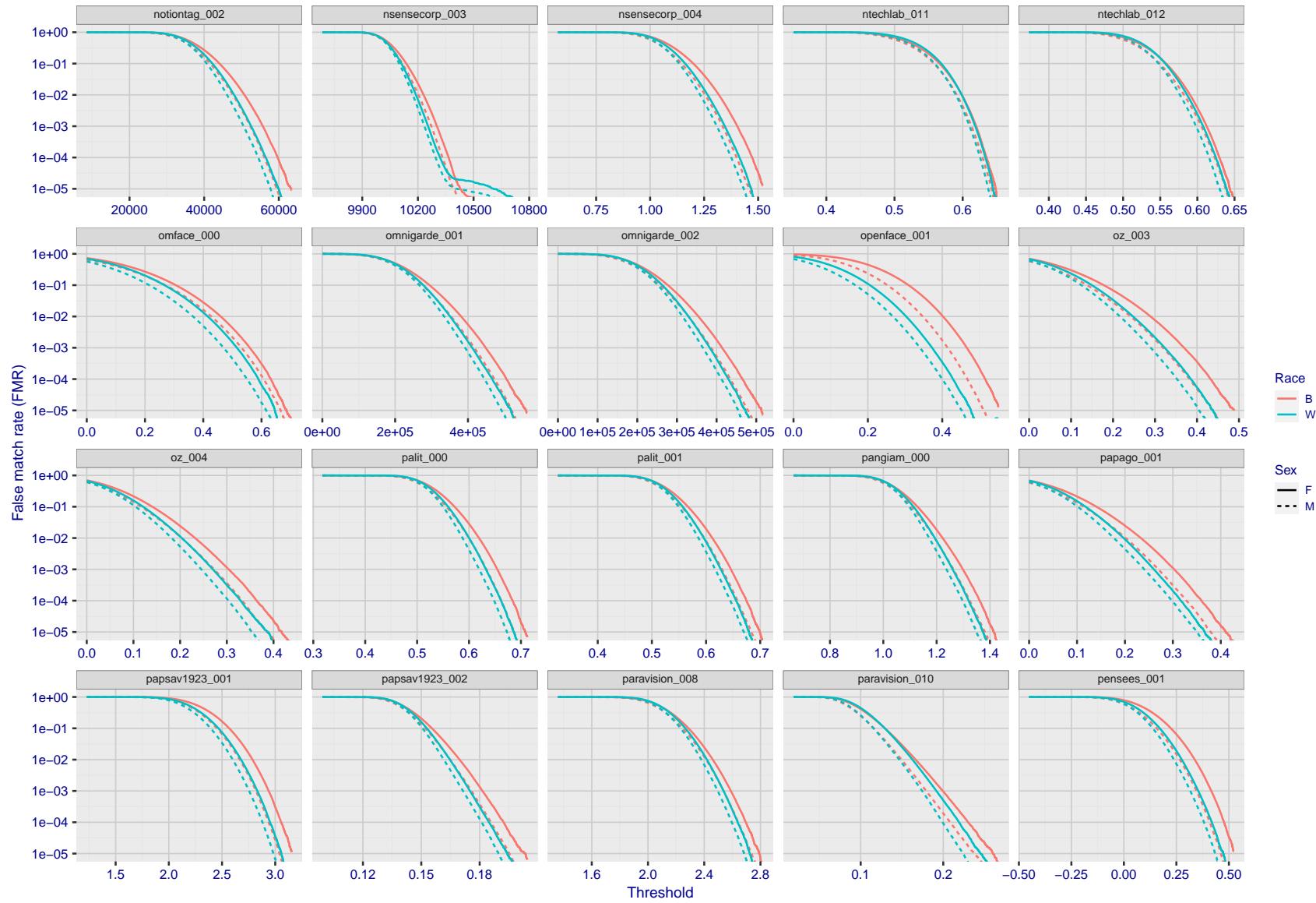


Figure 230: For the mugshot images, the false match calibration curves show false match rate vs. threshold. Separate curves appear for white females, black females, black males and white males.

2022/11/06 10:45:39

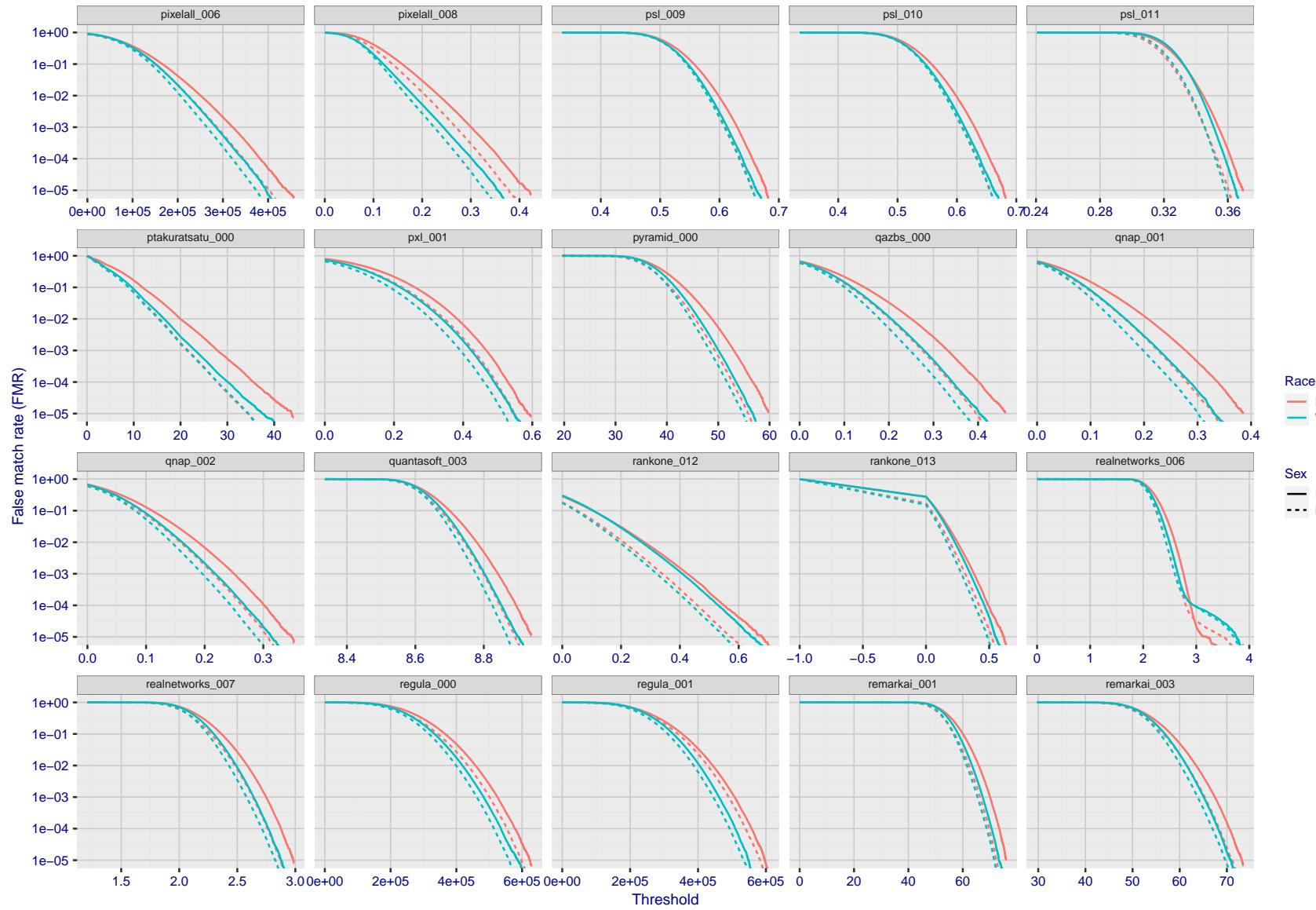


Figure 231: For the mugshot images, the false match calibration curves show false match rate vs. threshold. Separate curves appear for white females, black females, black males and white males.

2022/11/06 10:45:39

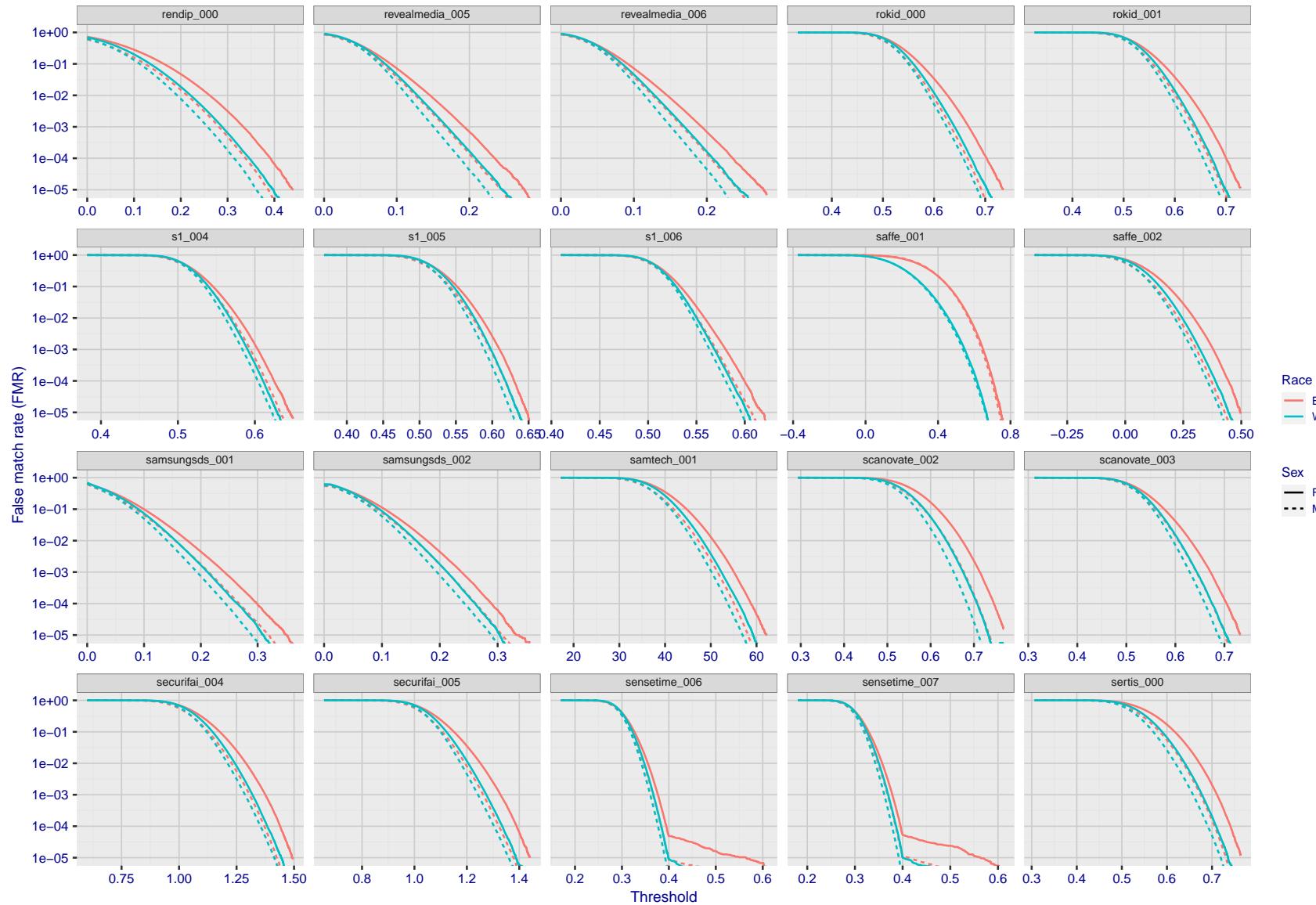


Figure 232: For the mugshot images, the false match calibration curves show false match rate vs. threshold. Separate curves appear for white females, black females, black males and white males.

2022/11/06 10:45:39

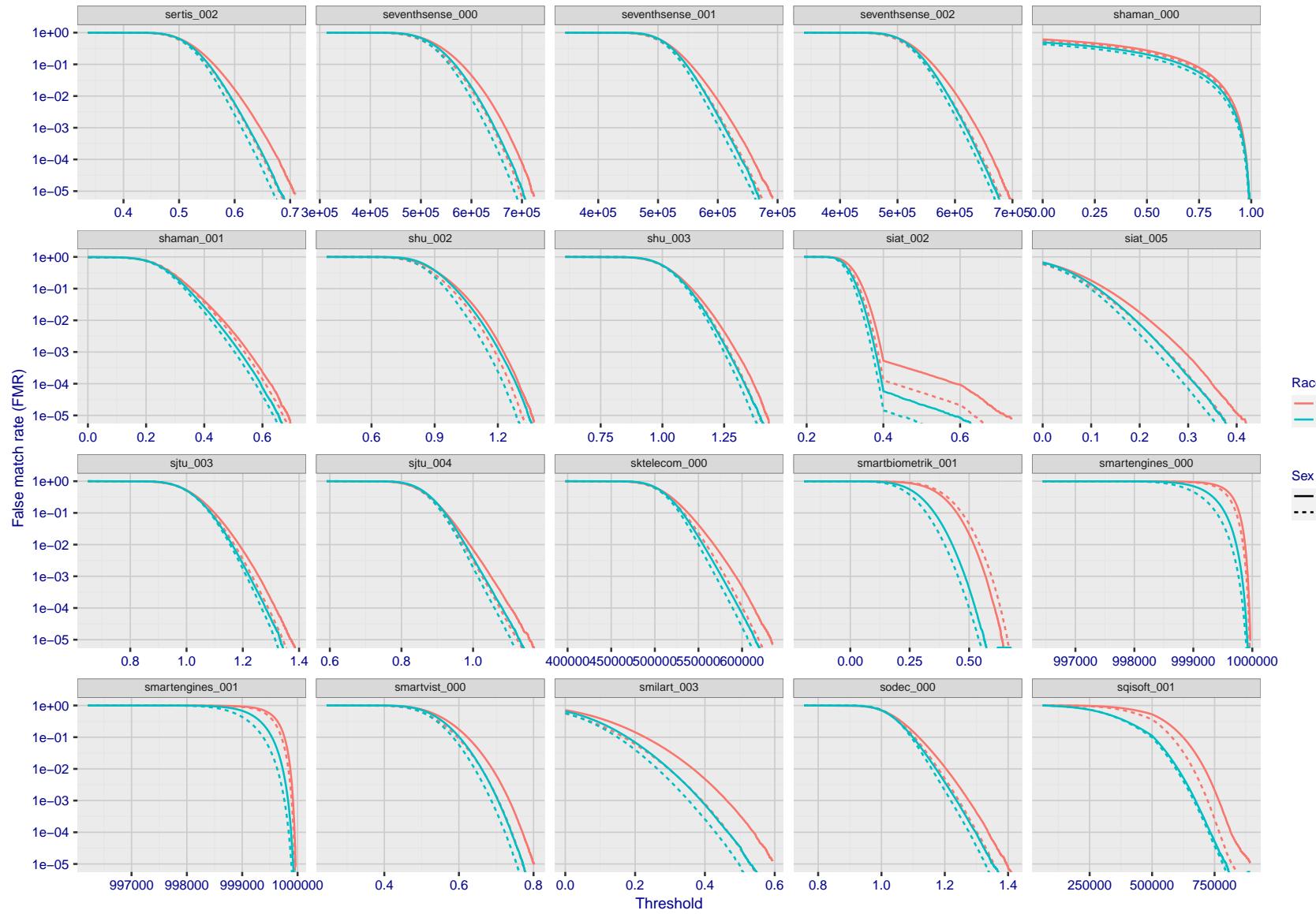


Figure 233: For the mugshot images, the false match calibration curves show false match rate vs. threshold. Separate curves appear for white females, black females, black males and white males.

2022/11/06 10:45:39

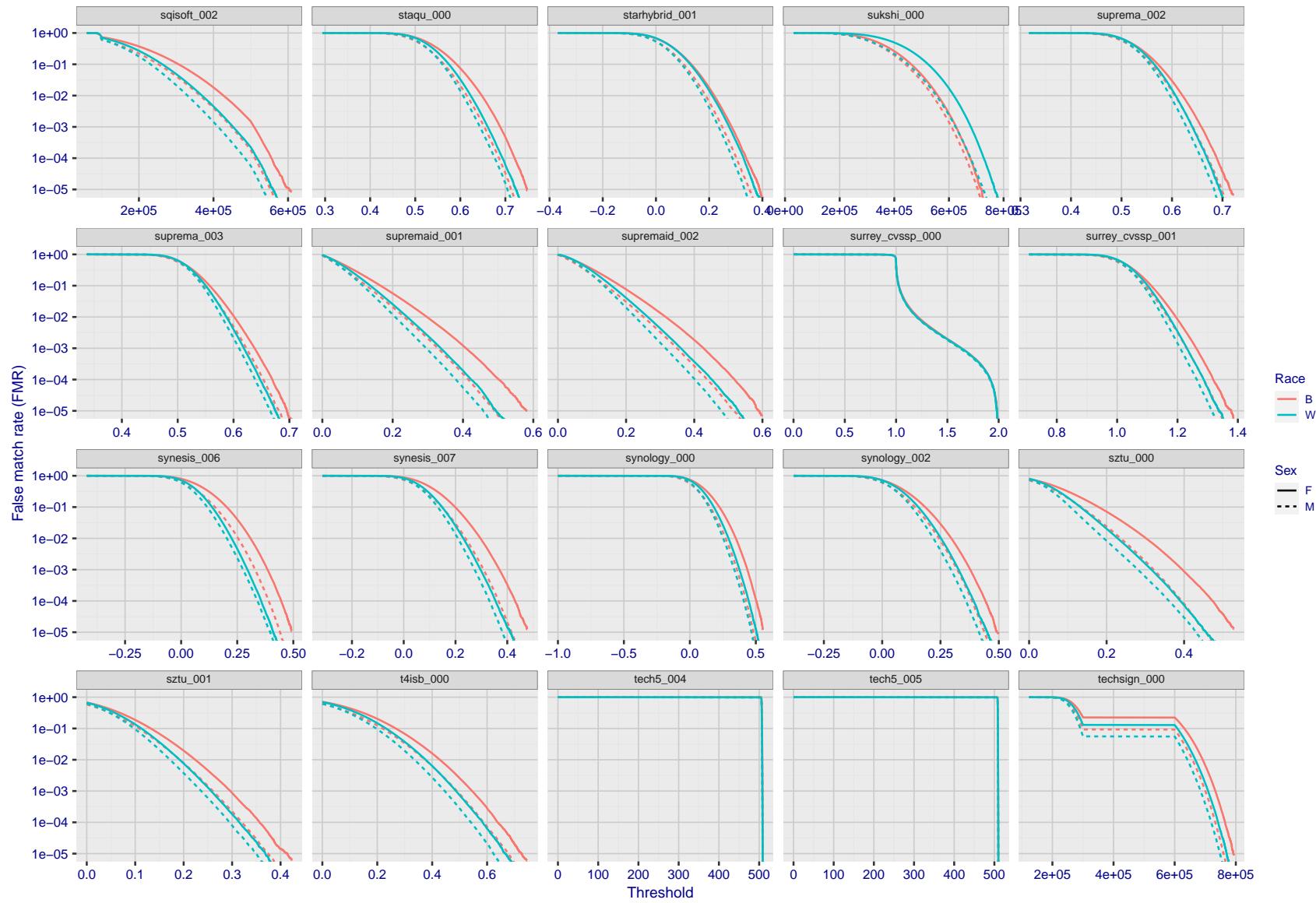


Figure 234: For the mugshot images, the false match calibration curves show false match rate vs. threshold. Separate curves appear for white females, black females, black males and white males.

2022/11/06 10:45:39

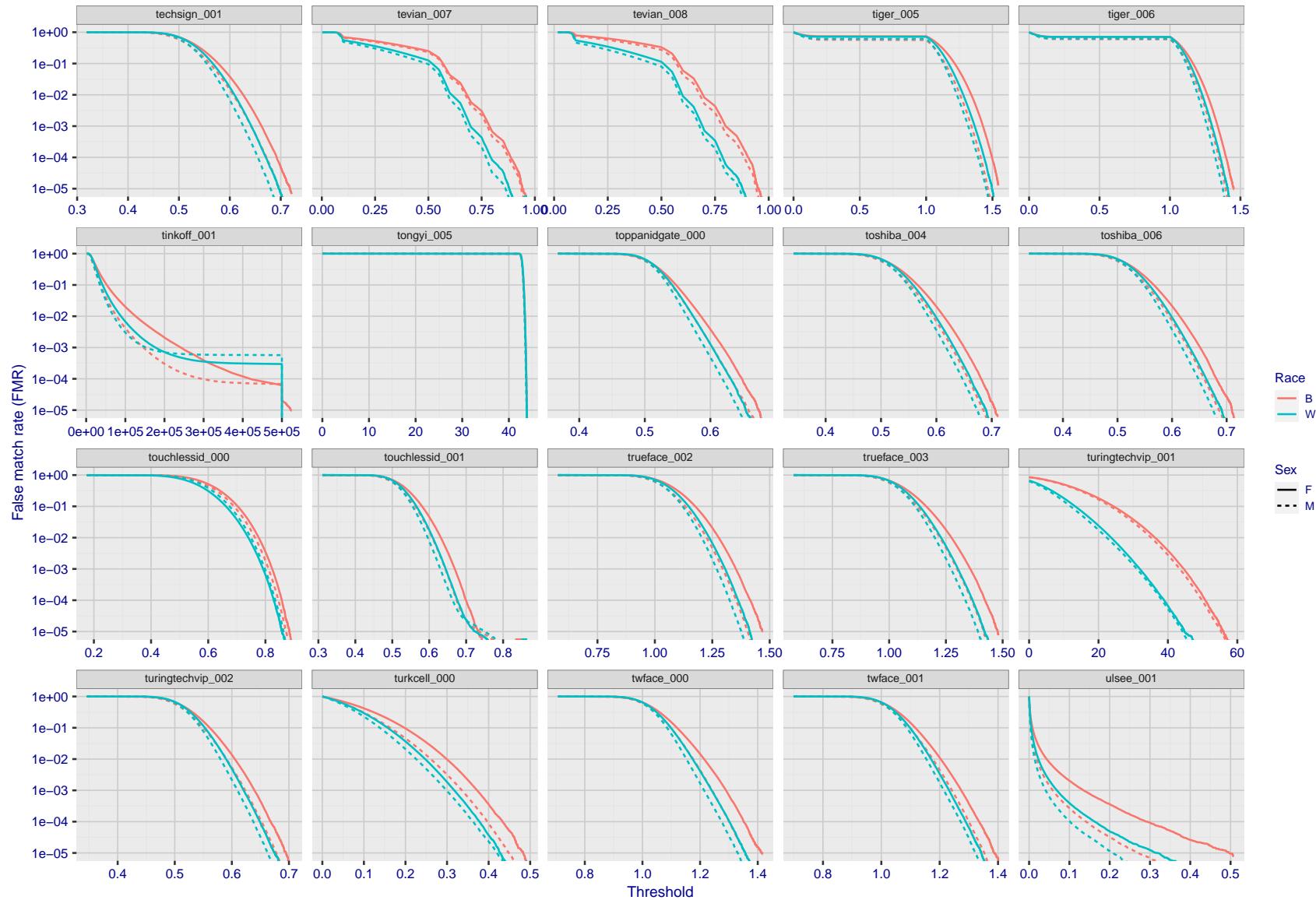


Figure 235: For the mugshot images, the false match calibration curves show false match rate vs. threshold. Separate curves appear for white females, black females, black males and white males.

FNMR(T)

"False non-match rate"

"False match rate"

2022/11/06 10:45:39

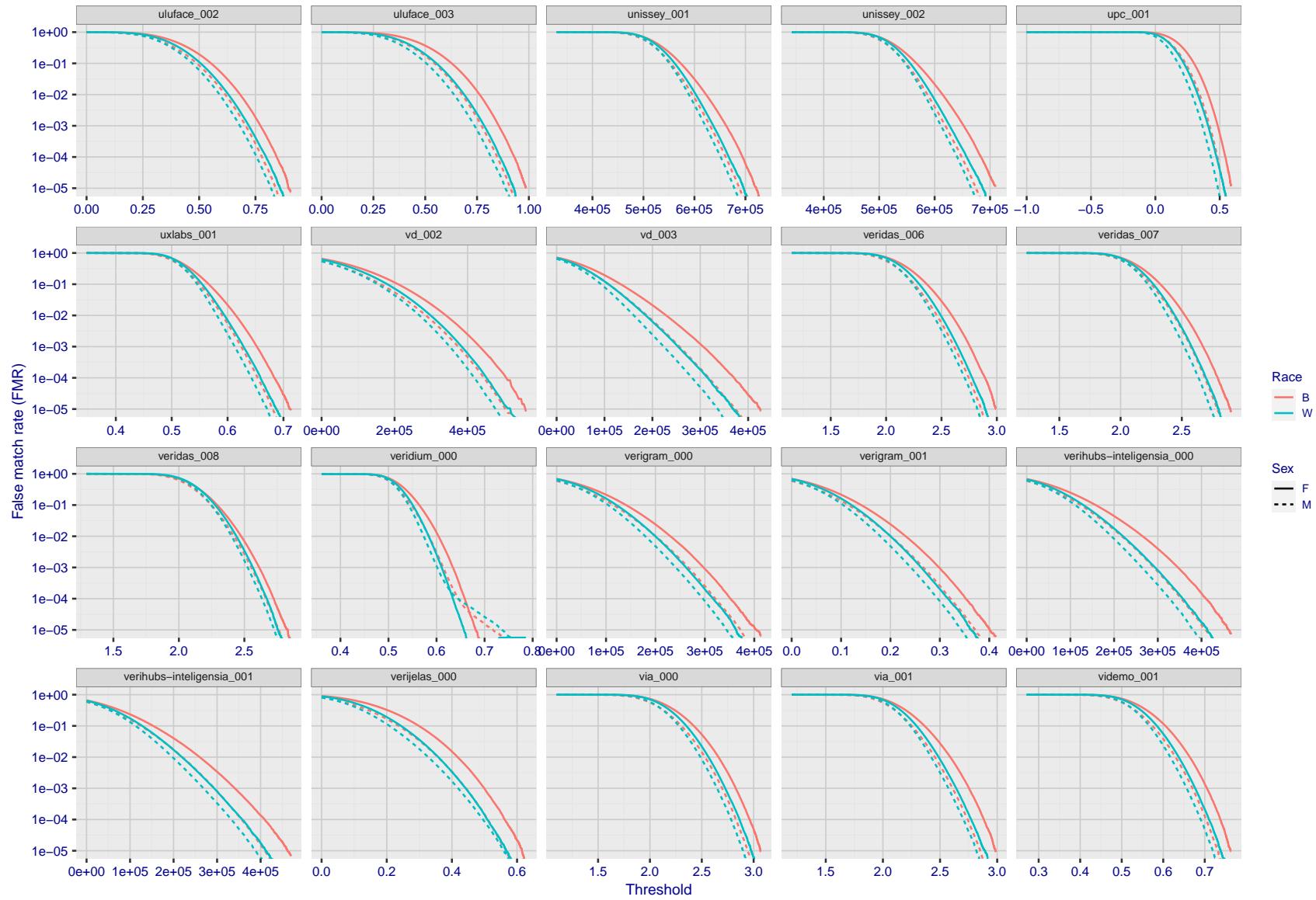


Figure 236: For the mugshot images, the false match calibration curves show false match rate vs. threshold. Separate curves appear for white females, black females, black males and white males.

2022/11/06 10:45:39

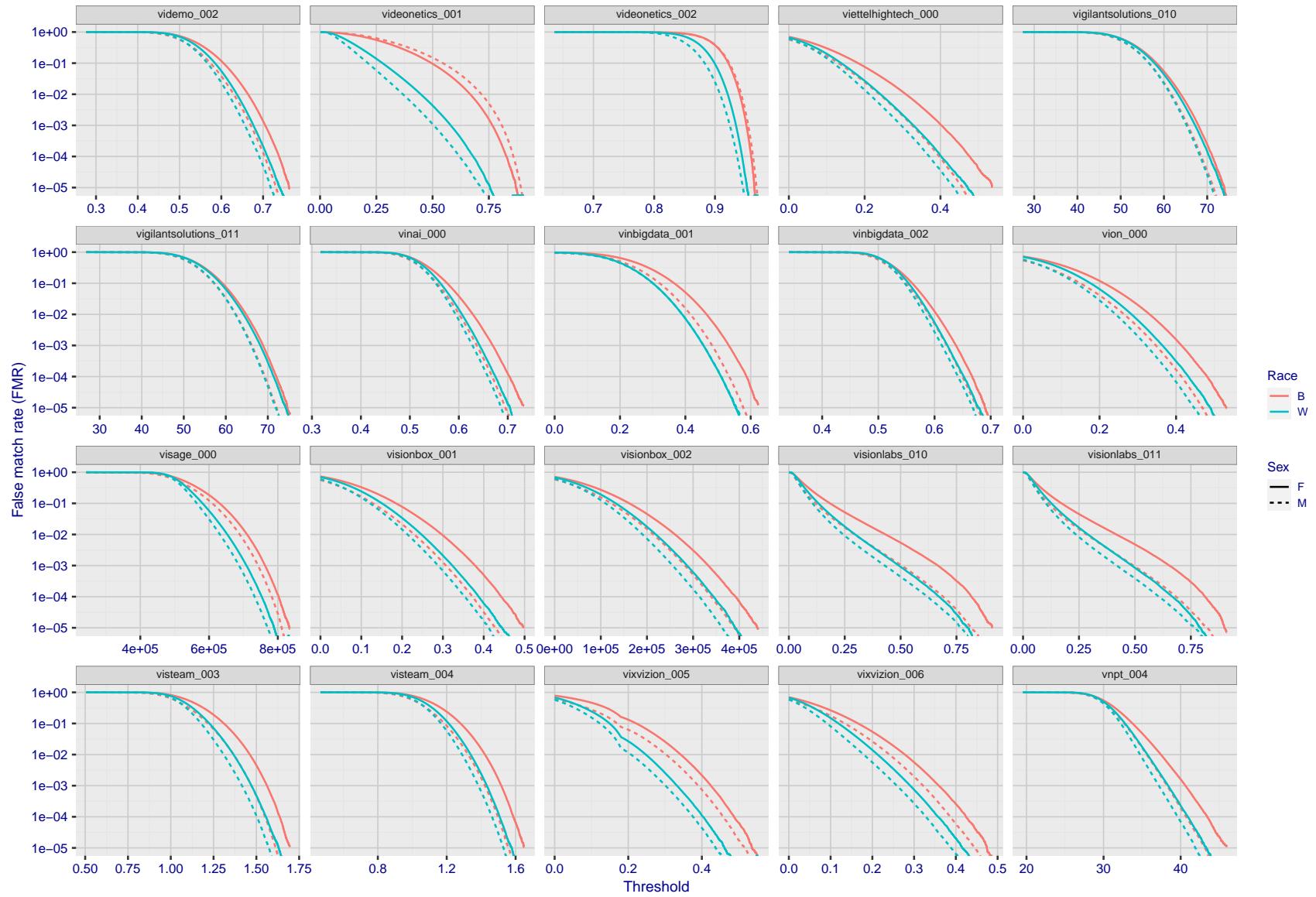


Figure 237: For the mugshot images, the false match calibration curves show false match rate vs. threshold. Separate curves appear for white females, black females, black males and white males.

2022/11/06 10:45:39

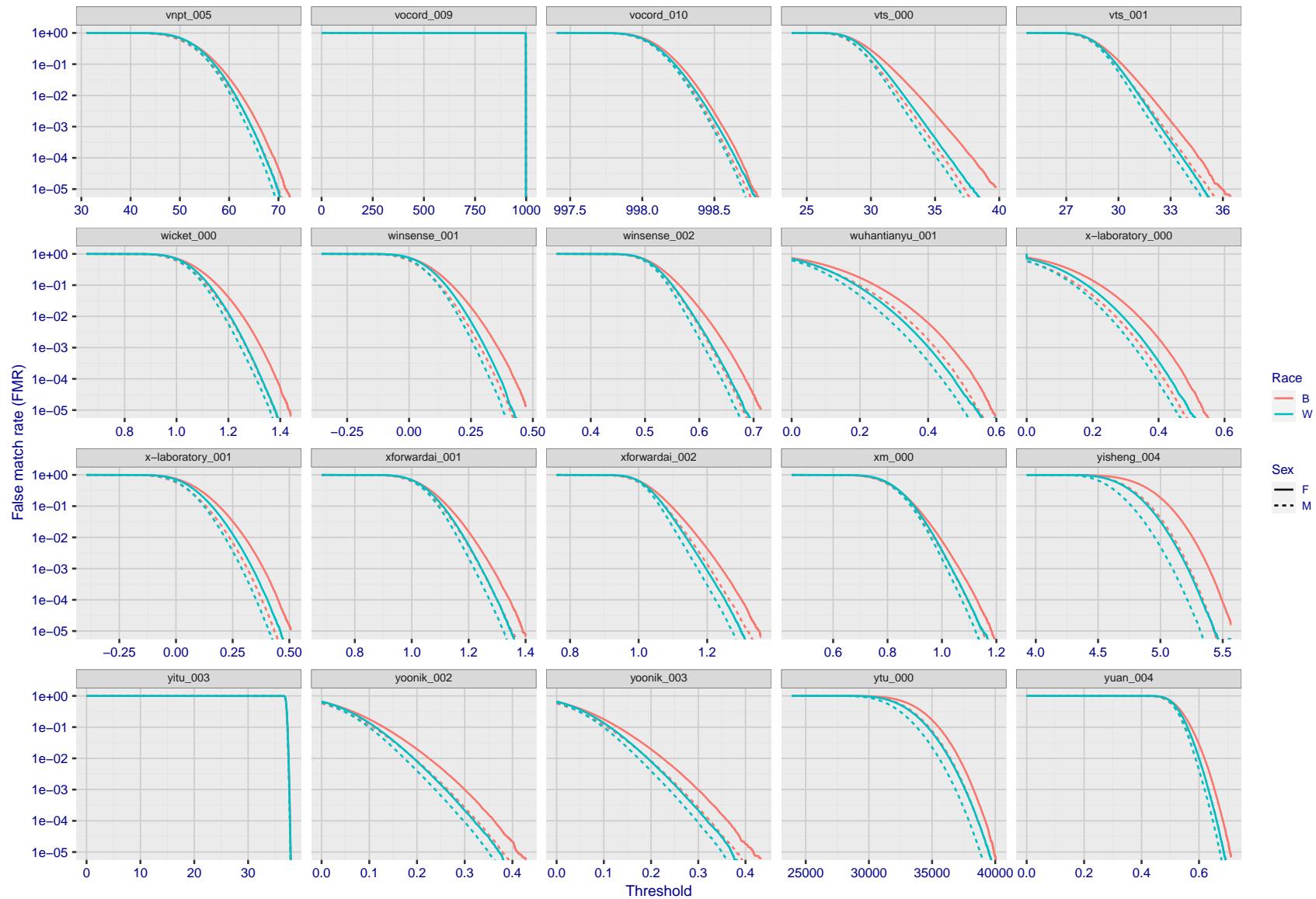


Figure 238: For the mugshot images, the false match calibration curves show false match rate vs. threshold. Separate curves appear for white females, black females, black males and white males.

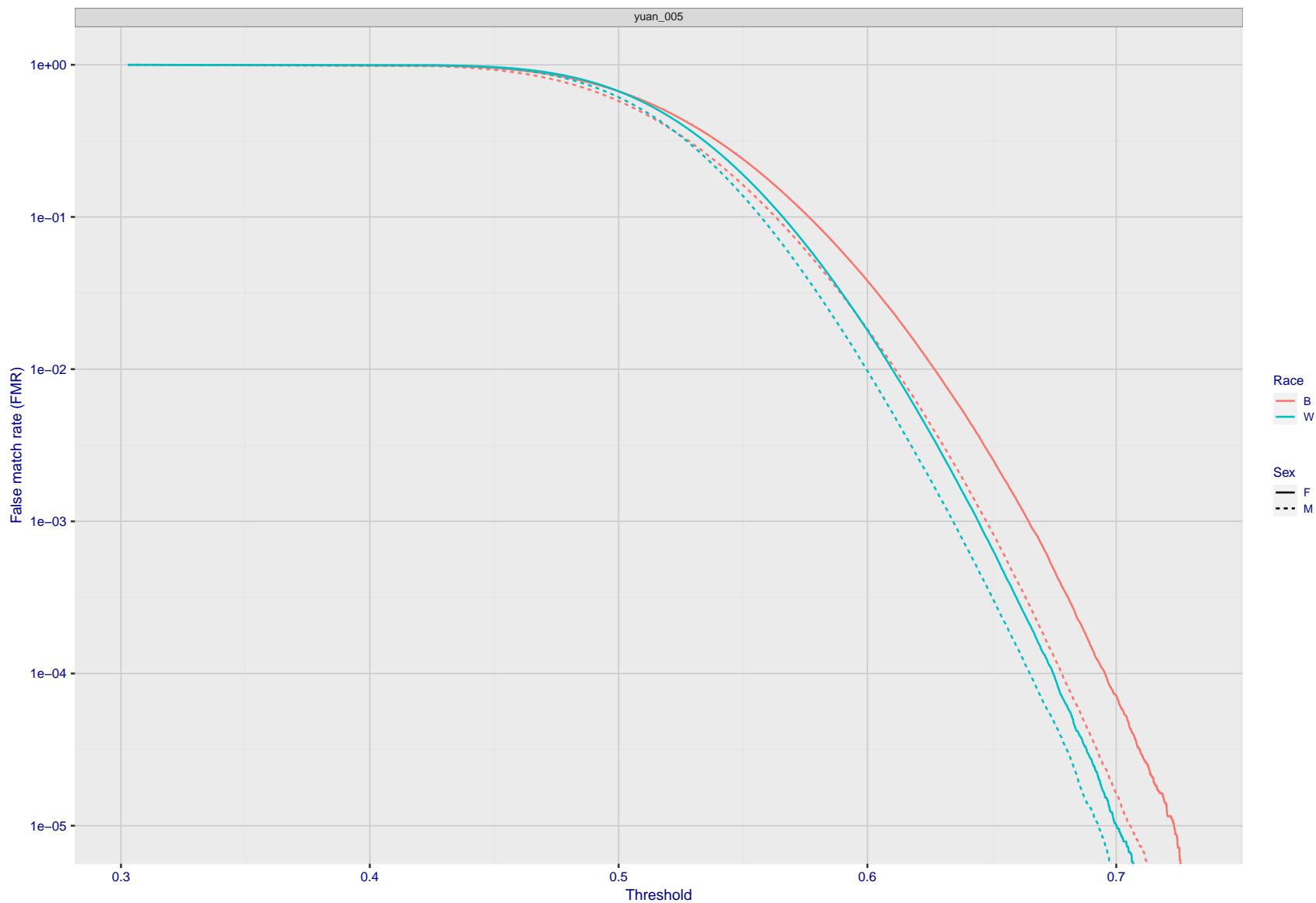


Figure 239: For the mugshot images, the false match calibration curves show false match rate vs. threshold. Separate curves appear for white females, black females, black males and white males.

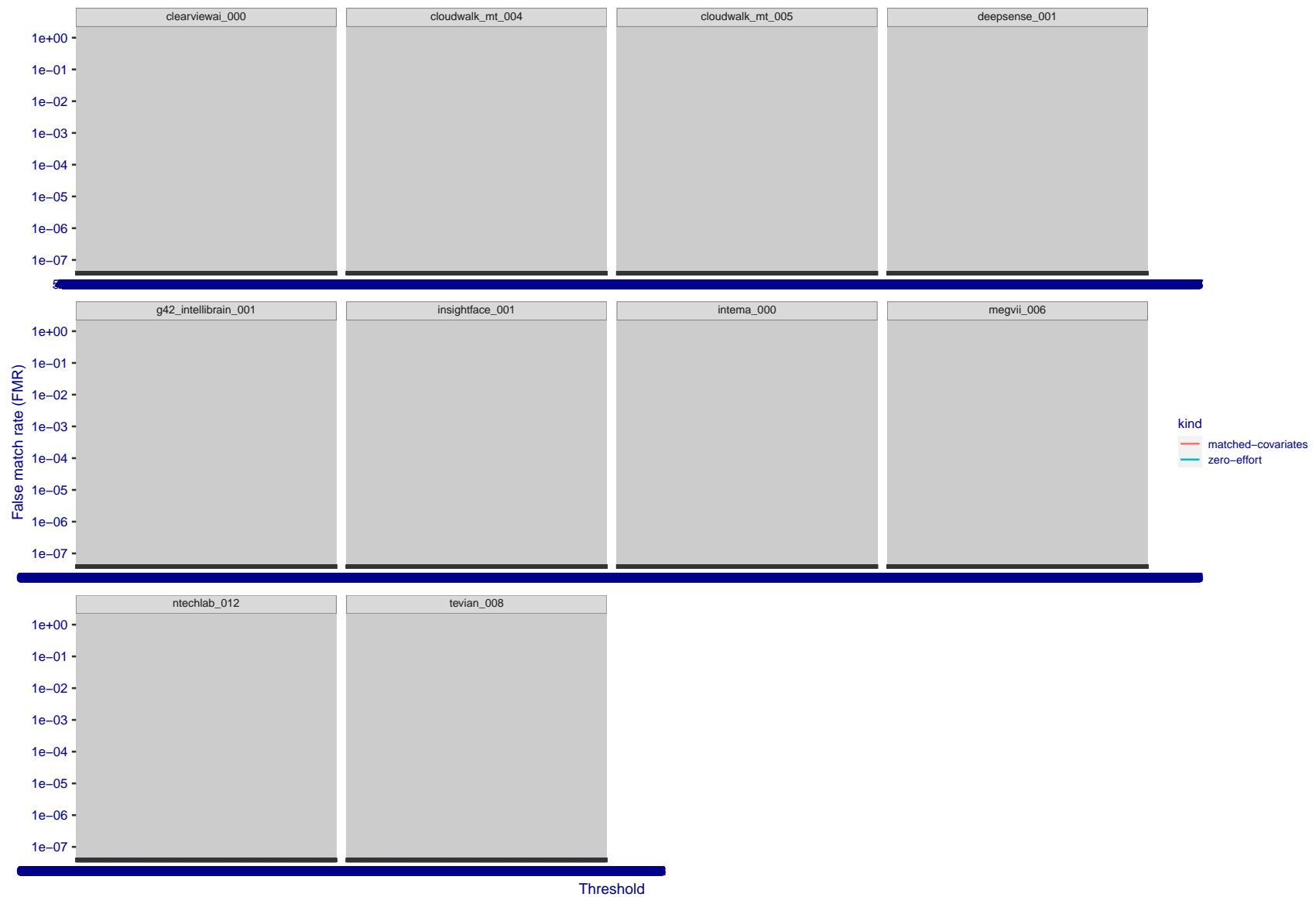


Figure 240: For the visa images, the false match calibration curves show FMR vs. threshold, T . The blue (lower) curves are for zero-effort impostors (i.e. comparing all images against all). The red (upper) curves are for persons of the same-sex, same-age, and same national-origin. This shows that FMR is underestimated (by a factor of 10 or more) by using a zero-effort impostor calculation to calibrate T . As shown later (sec. 3.6), FMR is higher for demographic-matched impostors.

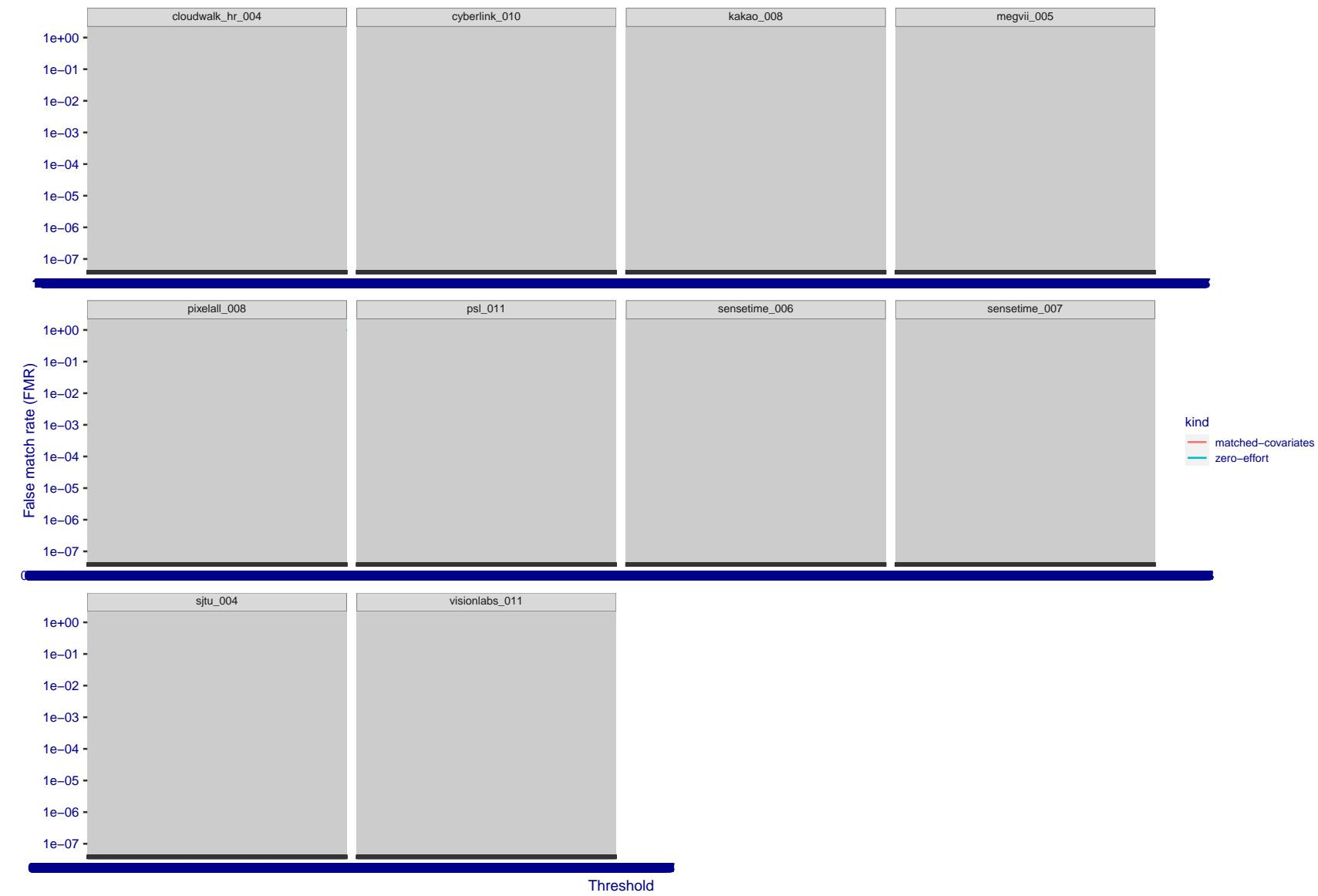


Figure 241: For the visa images, the false match calibration curves show FMR vs. threshold, T . The blue (lower) curves are for zero-effort impostors (i.e. comparing all images against all). The red (upper) curves are for persons of the same-sex, same-age, and same national-origin. This shows that FMR is underestimated (by a factor of 10 or more) by using a zero-effort impostor calculation to calibrate T . As shown later (sec. 3.6), FMR is higher for demographic-matched impostors.

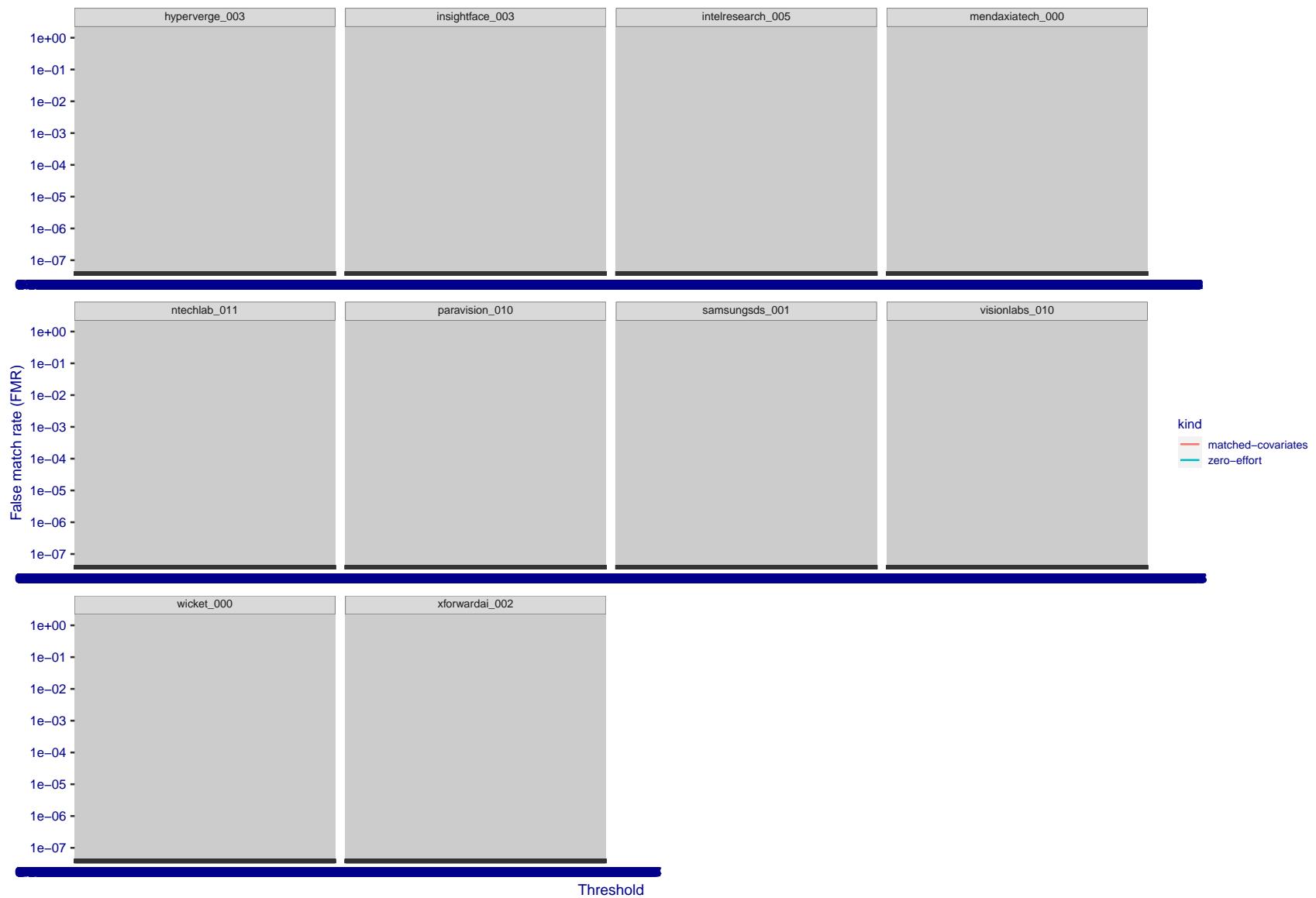


Figure 242: For the visa images, the false match calibration curves show FMR vs. threshold, T . The blue (lower) curves are for zero-effort impostors (i.e. comparing all images against all). The red (upper) curves are for persons of the same-sex, same-age, and same national-origin. This shows that FMR is underestimated (by a factor of 10 or more) by using a zero-effort impostor calculation to calibrate T . As shown later (sec. 3.6), FMR is higher for demographic-matched impostors.

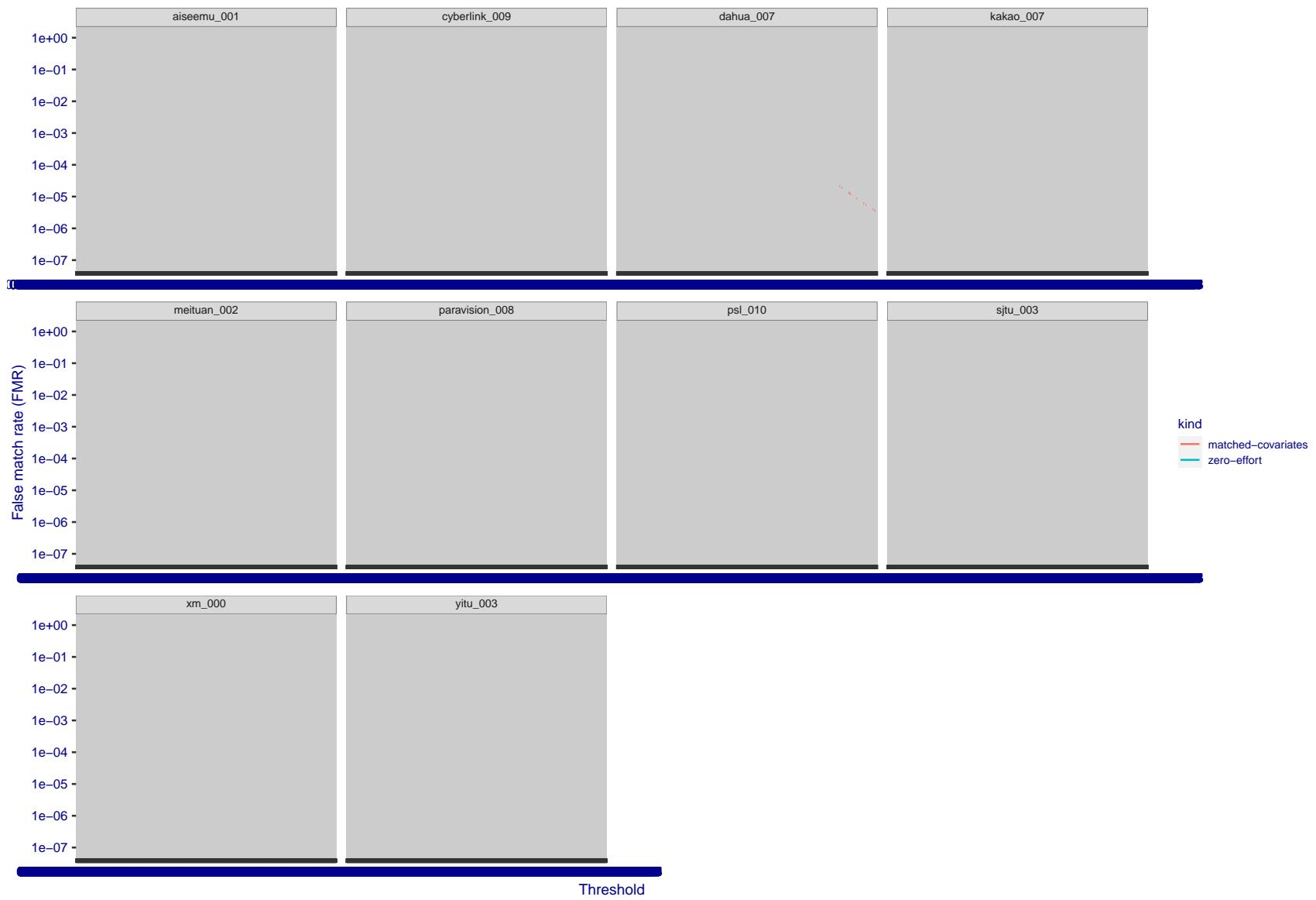


Figure 243: For the visa images, the false match calibration curves show FMR vs. threshold, T . The blue (lower) curves are for zero-effort impostors (i.e. comparing all images against all). The red (upper) curves are for persons of the same-sex, same-age, and same national-origin. This shows that FMR is underestimated (by a factor of 10 or more) by using a zero-effort impostor calculation to calibrate T . As shown later (sec. 3.6), FMR is higher for demographic-matched impostors.

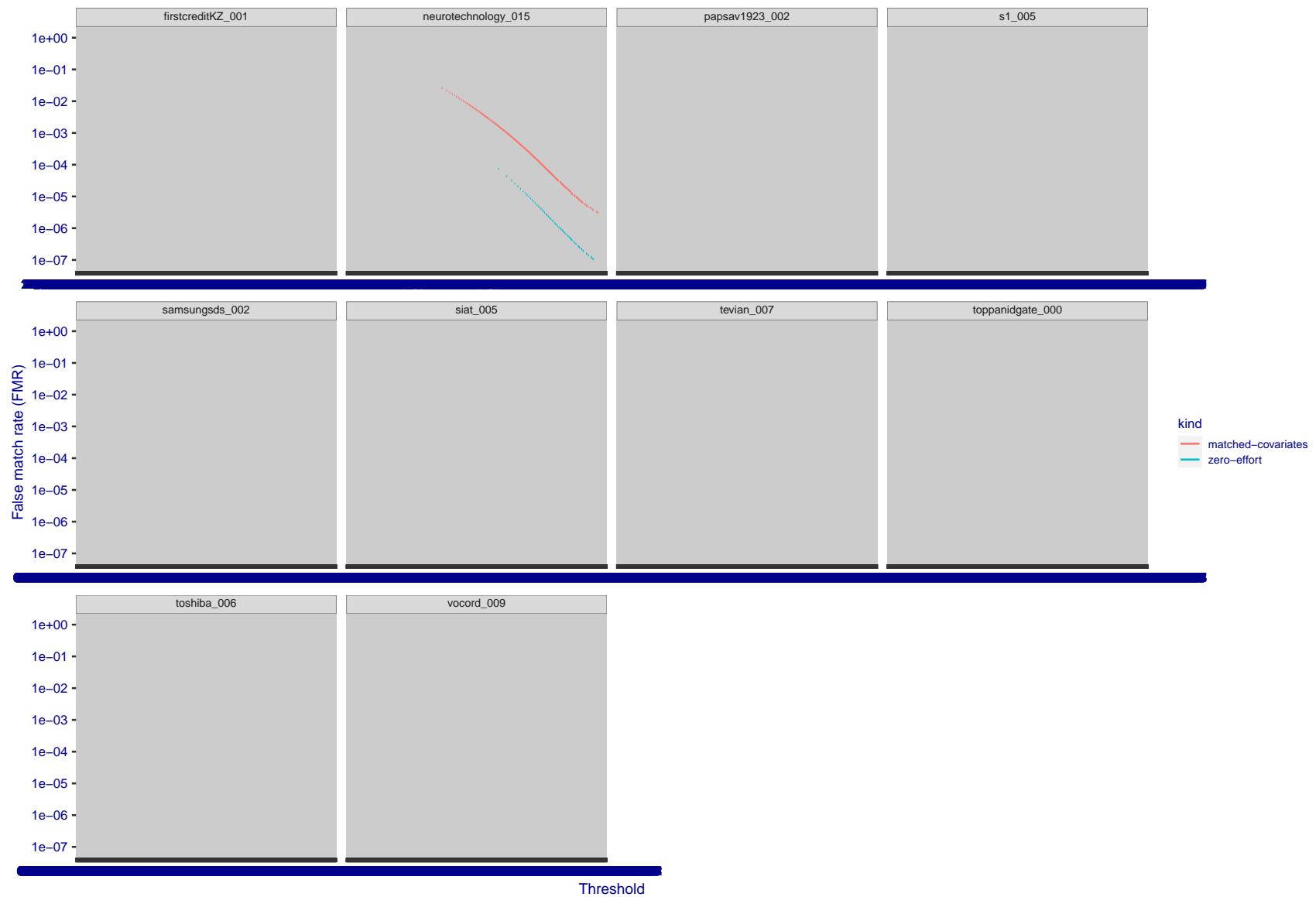


Figure 244: For the visa images, the false match calibration curves show FMR vs. threshold, T . The blue (lower) curves are for zero-effort impostors (i.e. comparing all images against all). The red (upper) curves are for persons of the same-sex, same-age, and same national-origin. This shows that FMR is underestimated (by a factor of 10 or more) by using a zero-effort impostor calculation to calibrate T . As shown later (sec. 3.6), FMR is higher for demographic-matched impostors.

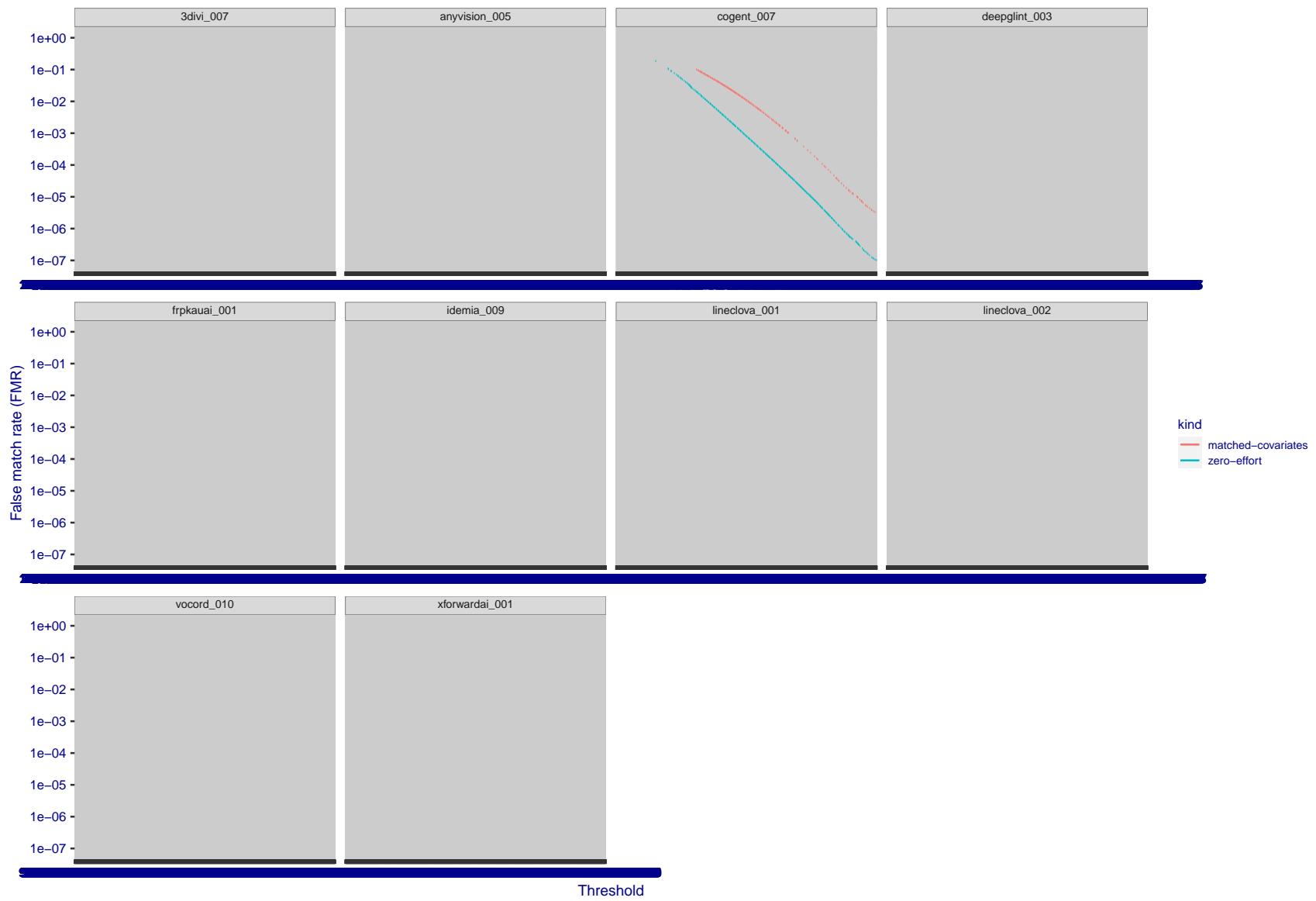


Figure 245: For the visa images, the false match calibration curves show FMR vs. threshold, T . The blue (lower) curves are for zero-effort impostors (i.e. comparing all images against all). The red (upper) curves are for persons of the same-sex, same-age, and same national-origin. This shows that FMR is underestimated (by a factor of 10 or more) by using a zero-effort impostor calculation to calibrate T . As shown later (sec. 3.6), FMR is higher for demographic-matched impostors.

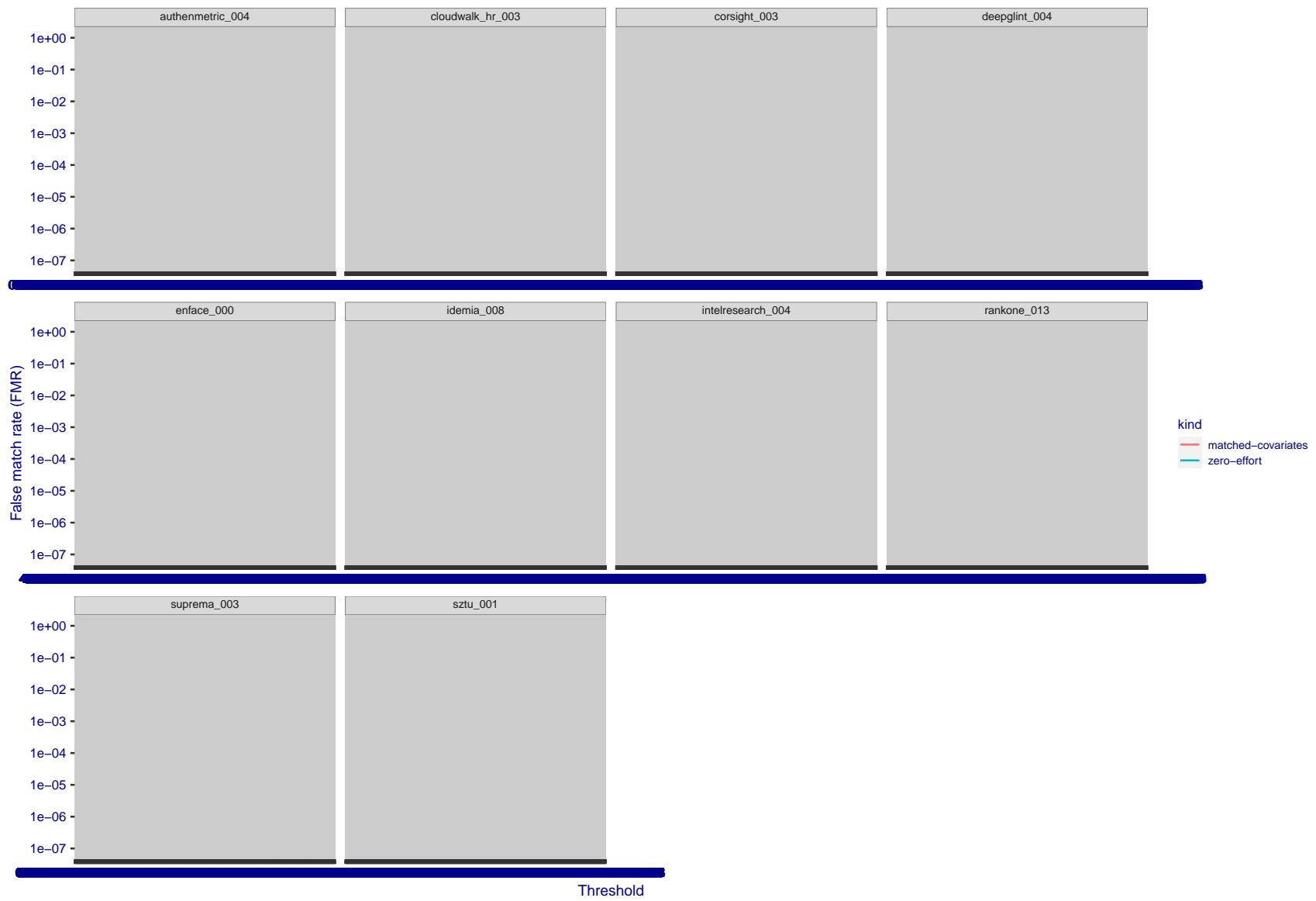


Figure 246: For the visa images, the false match calibration curves show FMR vs. threshold, T . The blue (lower) curves are for zero-effort impostors (i.e. comparing all images against all). The red (upper) curves are for persons of the same-sex, same-age, and same national-origin. This shows that FMR is underestimated (by a factor of 10 or more) by using a zero-effort impostor calculation to calibrate T . As shown later (sec. 3.6), FMR is higher for demographic-matched impostors.

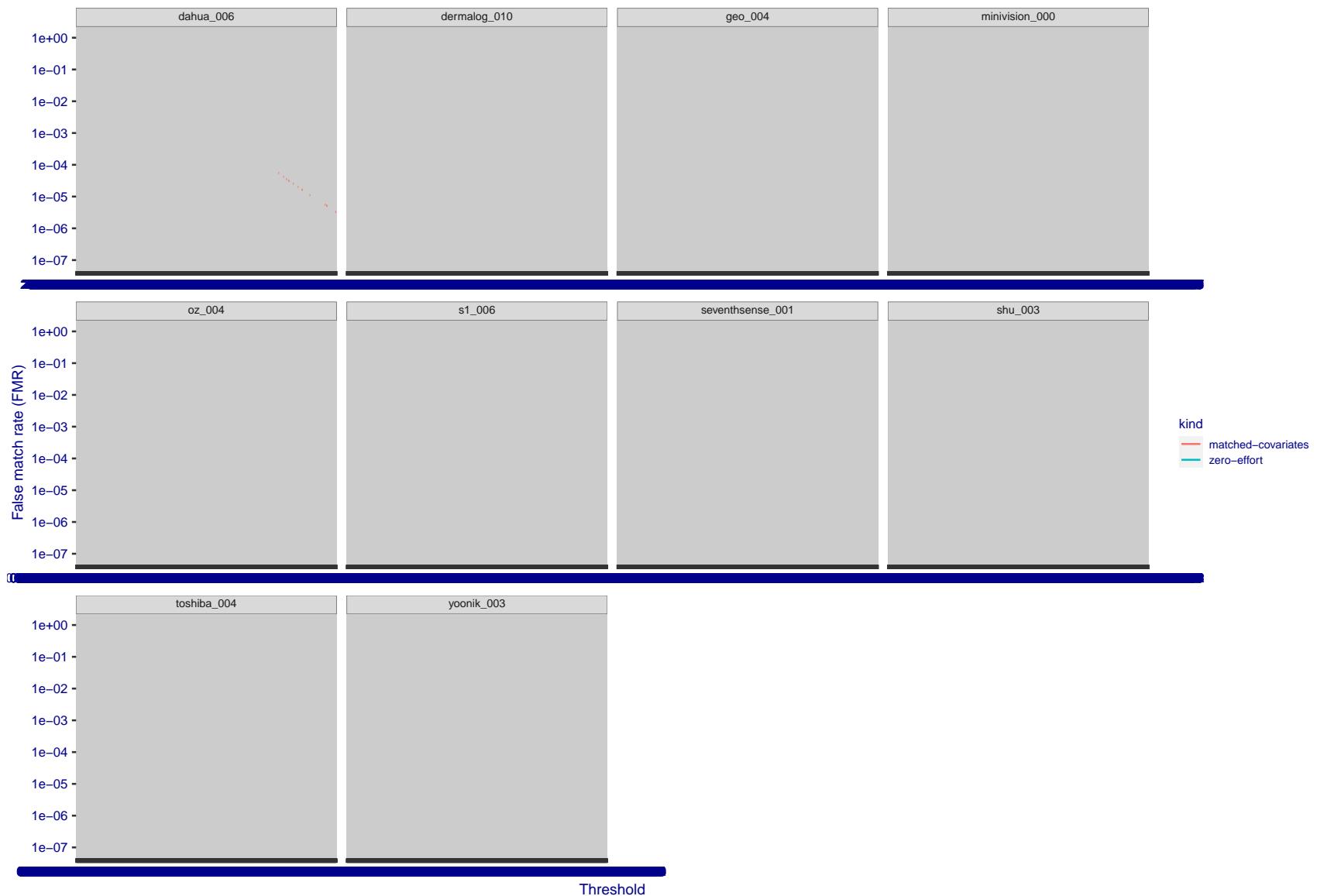


Figure 247: For the visa images, the false match calibration curves show FMR vs. threshold, T . The blue (lower) curves are for zero-effort impostors (i.e. comparing all images against all). The red (upper) curves are for persons of the same-sex, same-age, and same national-origin. This shows that FMR is underestimated (by a factor of 10 or more) by using a zero-effort impostor calculation to calibrate T . As shown later (sec. 3.6), FMR is higher for demographic-matched impostors.

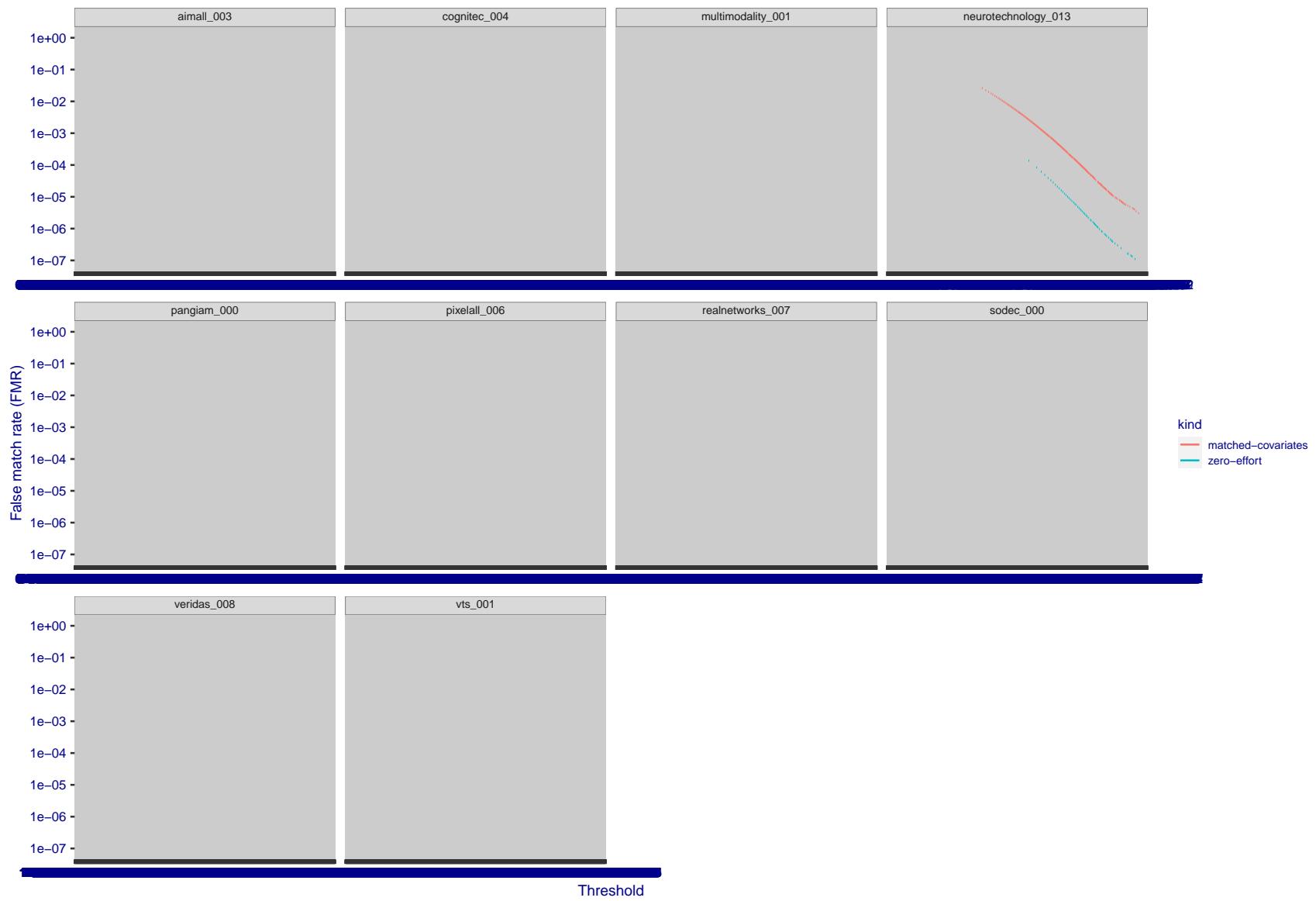


Figure 248: For the visa images, the false match calibration curves show FMR vs. threshold, T . The blue (lower) curves are for zero-effort impostors (i.e. comparing all images against all). The red (upper) curves are for persons of the same-sex, same-age, and same national-origin. This shows that FMR is underestimated (by a factor of 10 or more) by using a zero-effort impostor calculation to calibrate T . As shown later (sec. 3.6), FMR is higher for demographic-matched impostors.

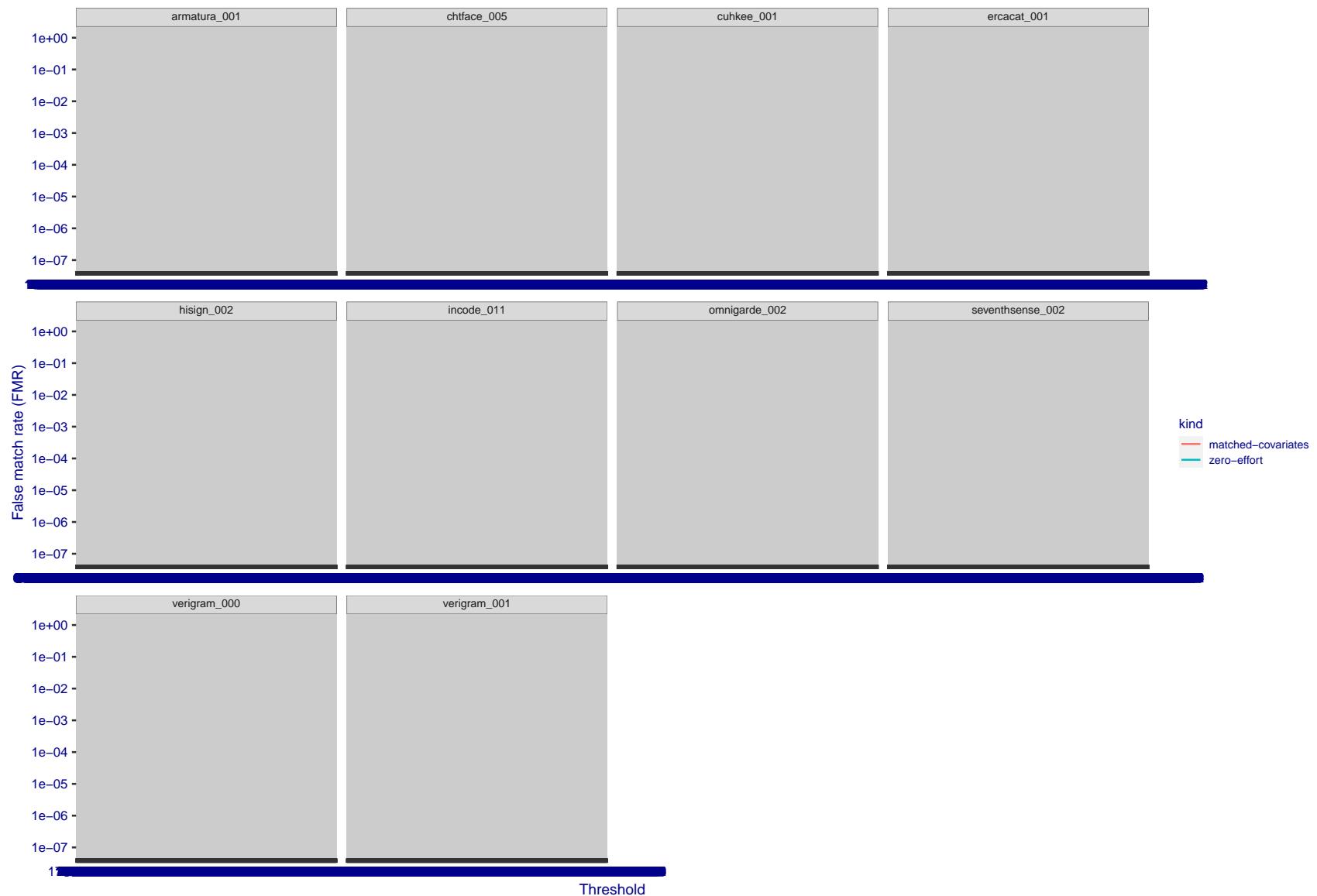


Figure 249: For the visa images, the false match calibration curves show FMR vs. threshold, T . The blue (lower) curves are for zero-effort impostors (i.e. comparing all images against all). The red (upper) curves are for persons of the same-sex, same-age, and same national-origin. This shows that FMR is underestimated (by a factor of 10 or more) by using a zero-effort impostor calculation to calibrate T . As shown later (sec. 3.6), FMR is higher for demographic-matched impostors.

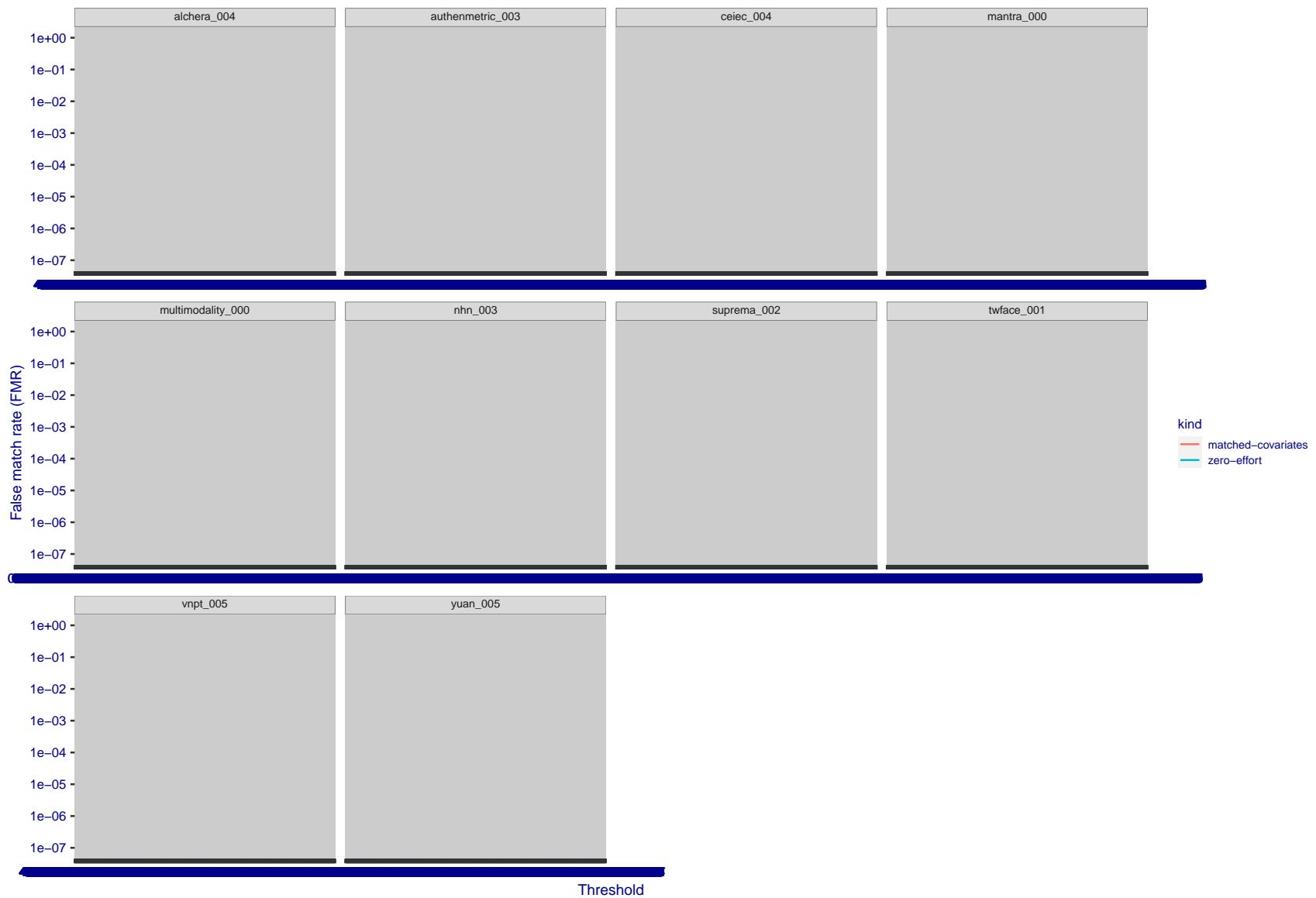


Figure 250: For the visa images, the false match calibration curves show FMR vs. threshold, T . The blue (lower) curves are for zero-effort impostors (i.e. comparing all images against all). The red (upper) curves are for persons of the same-sex, same-age, and same national-origin. This shows that FMR is underestimated (by a factor of 10 or more) by using a zero-effort impostor calculation to calibrate T . As shown later (sec. 3.6), FMR is higher for demographic-matched impostors.

2022/11/06 10:45:39

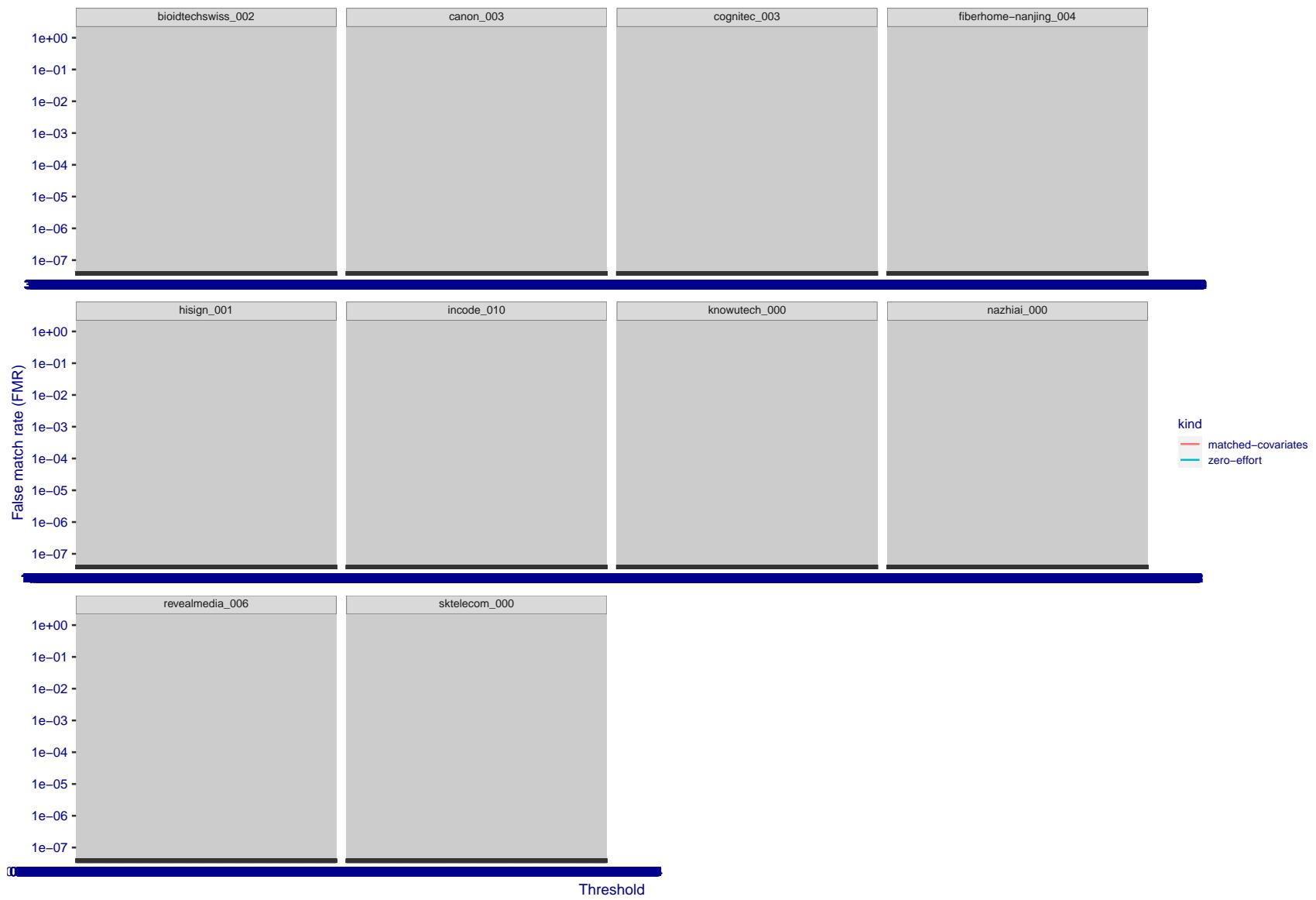


Figure 251: For the visa images, the false match calibration curves show FMR vs. threshold, T . The blue (lower) curves are for zero-effort impostors (i.e. comparing all images against all). The red (upper) curves are for persons of the same-sex, same-age, and same national-origin. This shows that FMR is underestimated (by a factor of 10 or more) by using a zero-effort impostor calculation to calibrate T . As shown later (sec. 3.6), FMR is higher for demographic-matched impostors.

2022/11/06 10:45:39

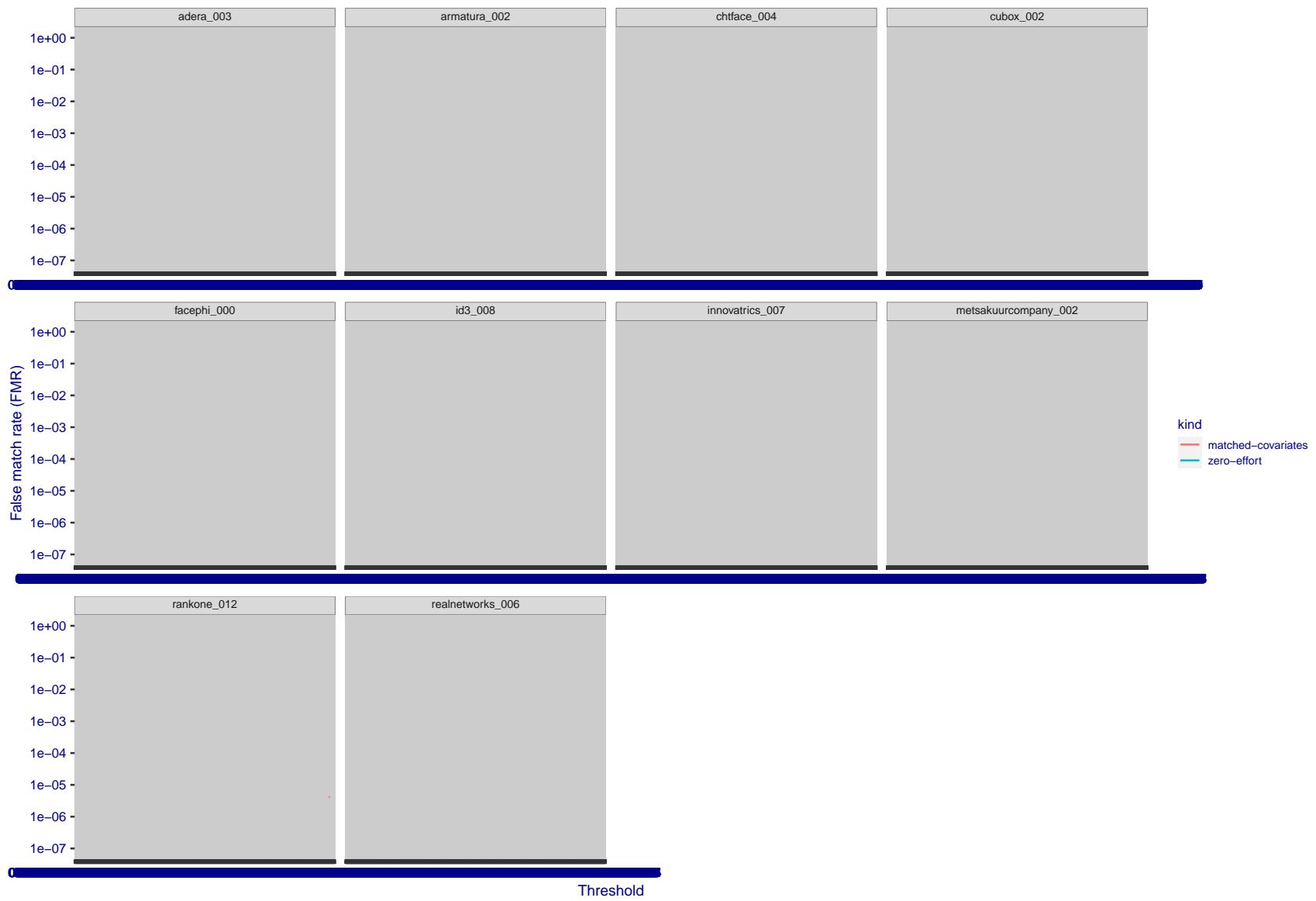


Figure 252: For the visa images, the false match calibration curves show FMR vs. threshold, T . The blue (lower) curves are for zero-effort impostors (i.e. comparing all images against all). The red (upper) curves are for persons of the same-sex, same-age, and same national-origin. This shows that FMR is underestimated (by a factor of 10 or more) by using a zero-effort impostor calculation to calibrate T . As shown later (sec. 3.6), FMR is higher for demographic-matched impostors.

FNMR(T)
FMR(T)
"False non-match rate"
"False match rate"

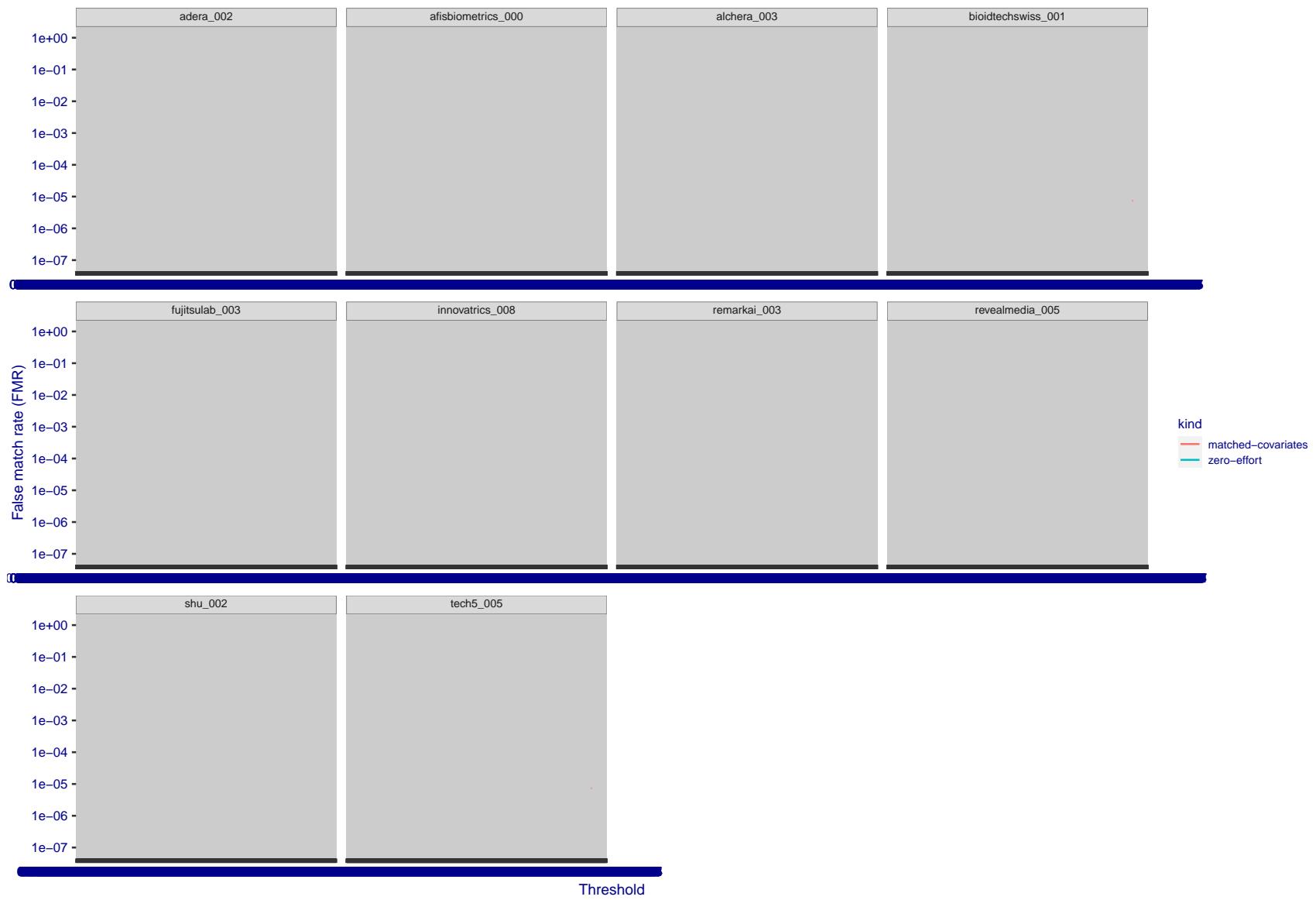


Figure 253: For the visa images, the false match calibration curves show FMR vs. threshold, T . The blue (lower) curves are for zero-effort impostors (i.e. comparing all images against all). The red (upper) curves are for persons of the same-sex, same-age, and same national-origin. This shows that FMR is underestimated (by a factor of 10 or more) by using a zero-effort impostor calculation to calibrate T . As shown later (sec. 3.6), FMR is higher for demographic-matched impostors.

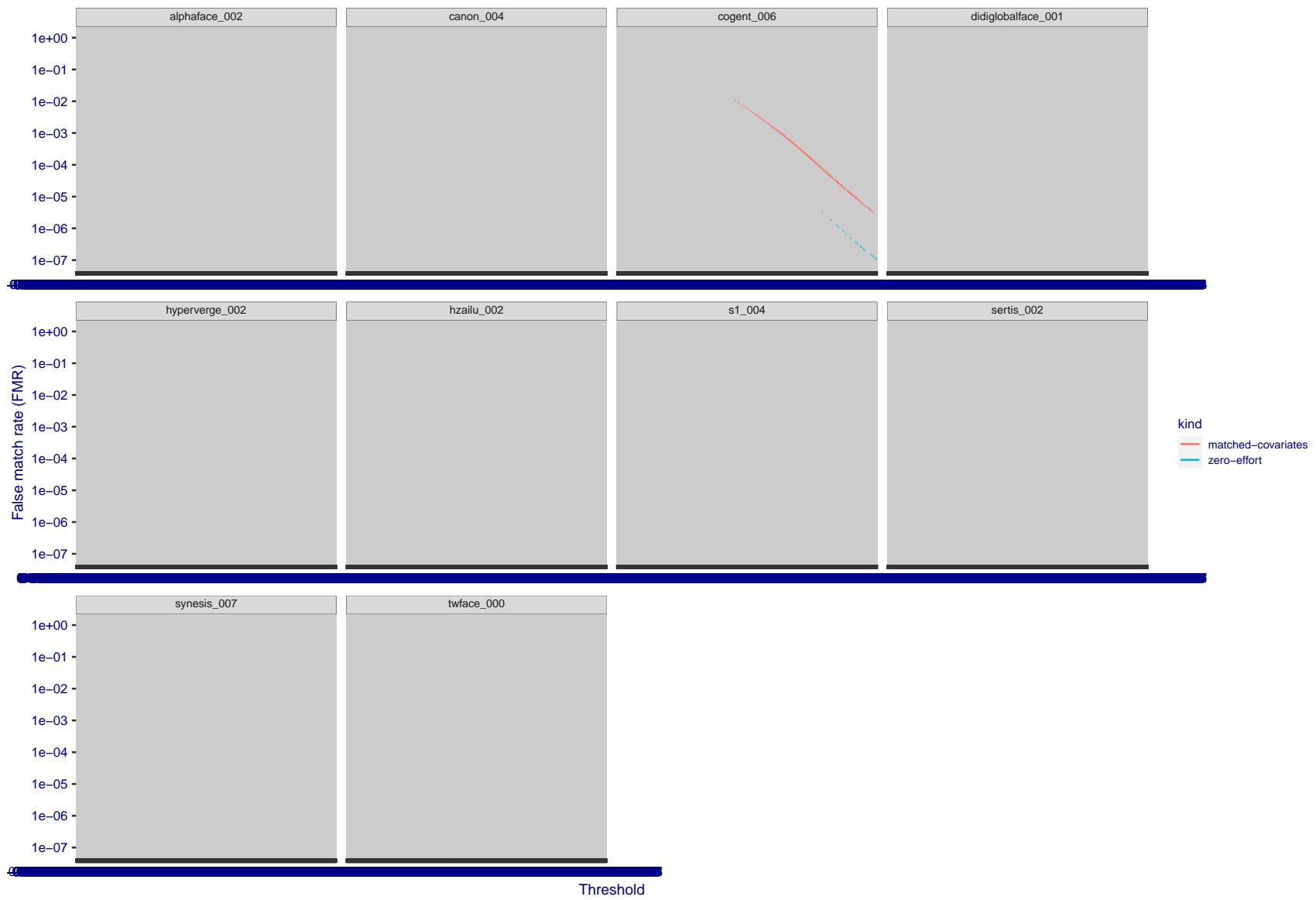


Figure 254: For the visa images, the false match calibration curves show FMR vs. threshold, T . The blue (lower) curves are for zero-effort impostors (i.e. comparing all images against all). The red (upper) curves are for persons of the same-sex, same-age, and same national-origin. This shows that FMR is underestimated (by a factor of 10 or more) by using a zero-effort impostor calculation to calibrate T . As shown later (sec. 3.6), FMR is higher for demographic-matched impostors.

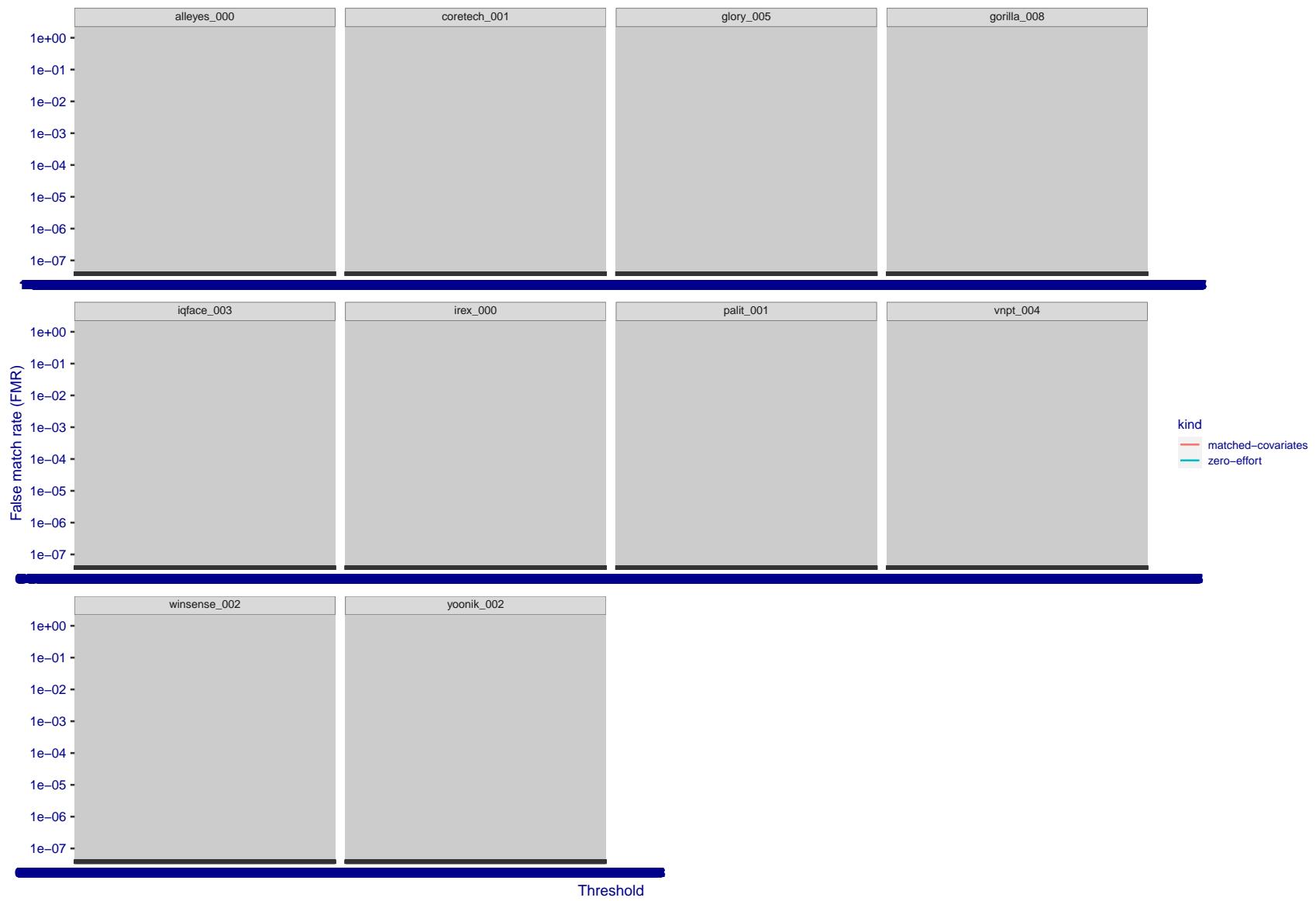


Figure 255: For the visa images, the false match calibration curves show FMR vs. threshold, T . The blue (lower) curves are for zero-effort impostors (i.e. comparing all images against all). The red (upper) curves are for persons of the same-sex, same-age, and same national-origin. This shows that FMR is underestimated (by a factor of 10 or more) by using a zero-effort impostor calculation to calibrate T . As shown later (sec. 3.6), FMR is higher for demographic-matched impostors.

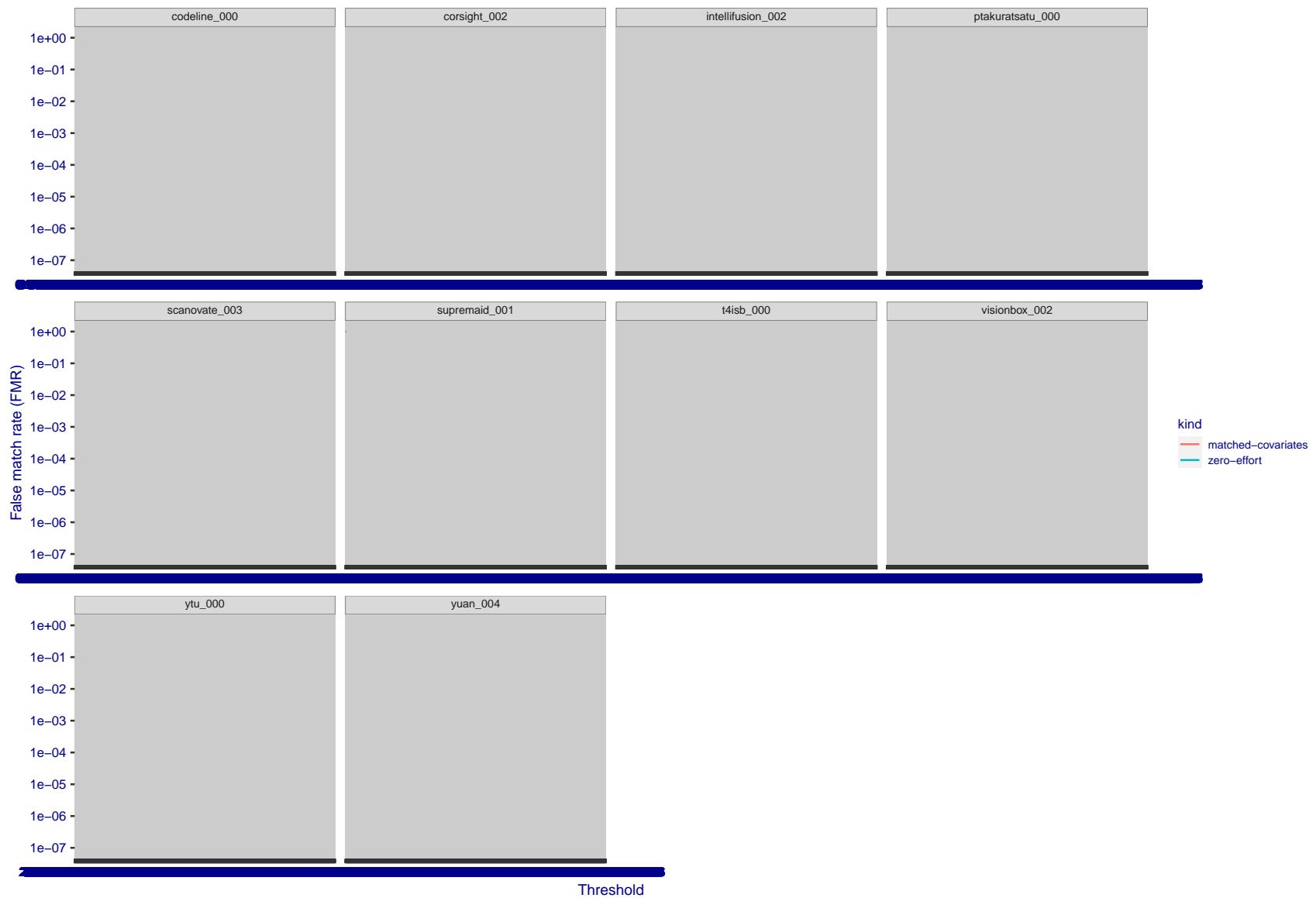


Figure 256: For the visa images, the false match calibration curves show FMR vs. threshold, T . The blue (lower) curves are for zero-effort impostors (i.e. comparing all images against all). The red (upper) curves are for persons of the same-sex, same-age, and same national-origin. This shows that FMR is underestimated (by a factor of 10 or more) by using a zero-effort impostor calculation to calibrate T . As shown later (sec. 3.6), FMR is higher for demographic-matched impostors.

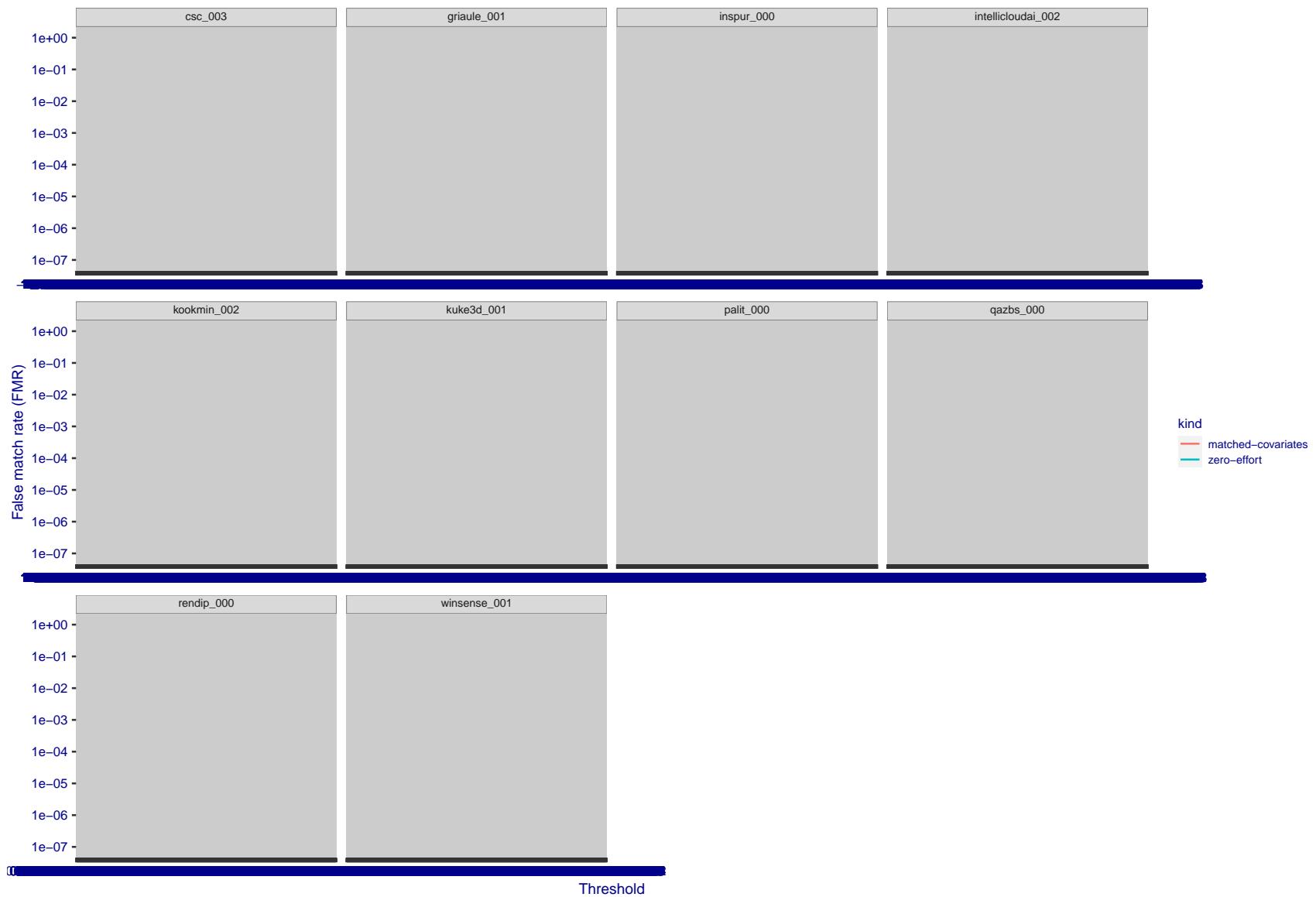


Figure 257: For the visa images, the false match calibration curves show FMR vs. threshold, T . The blue (lower) curves are for zero-effort impostors (i.e. comparing all images against all). The red (upper) curves are for persons of the same-sex, same-age, and same national-origin. This shows that FMR is underestimated (by a factor of 10 or more) by using a zero-effort impostor calculation to calibrate T . As shown later (sec. 3.6), FMR is higher for demographic-matched impostors.

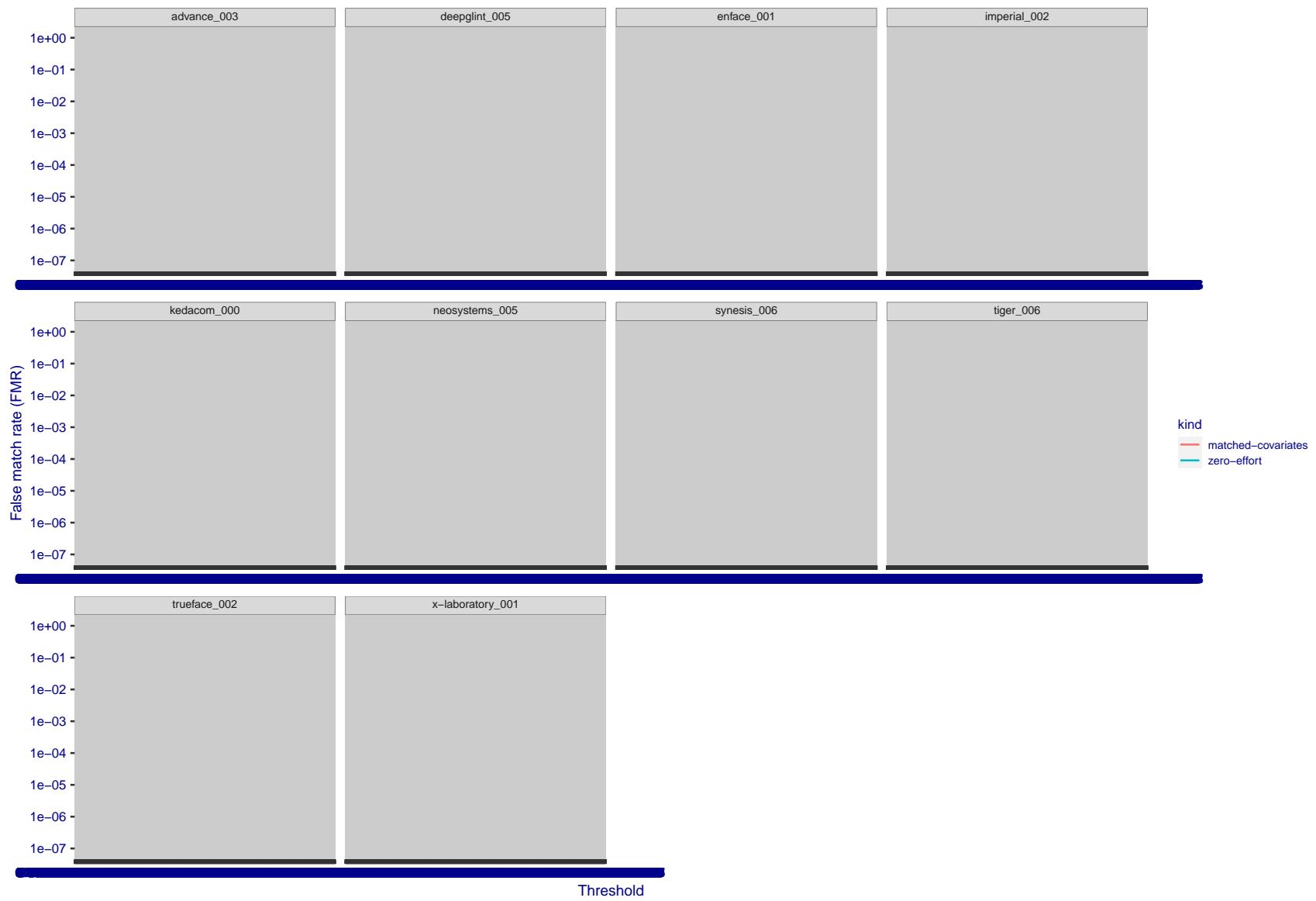


Figure 258: For the visa images, the false match calibration curves show FMR vs. threshold, T . The blue (lower) curves are for zero-effort impostors (i.e. comparing all images against all). The red (upper) curves are for persons of the same-sex, same-age, and same national-origin. This shows that FMR is underestimated (by a factor of 10 or more) by using a zero-effort impostor calculation to calibrate T . As shown later (sec. 3.6), FMR is higher for demographic-matched impostors.

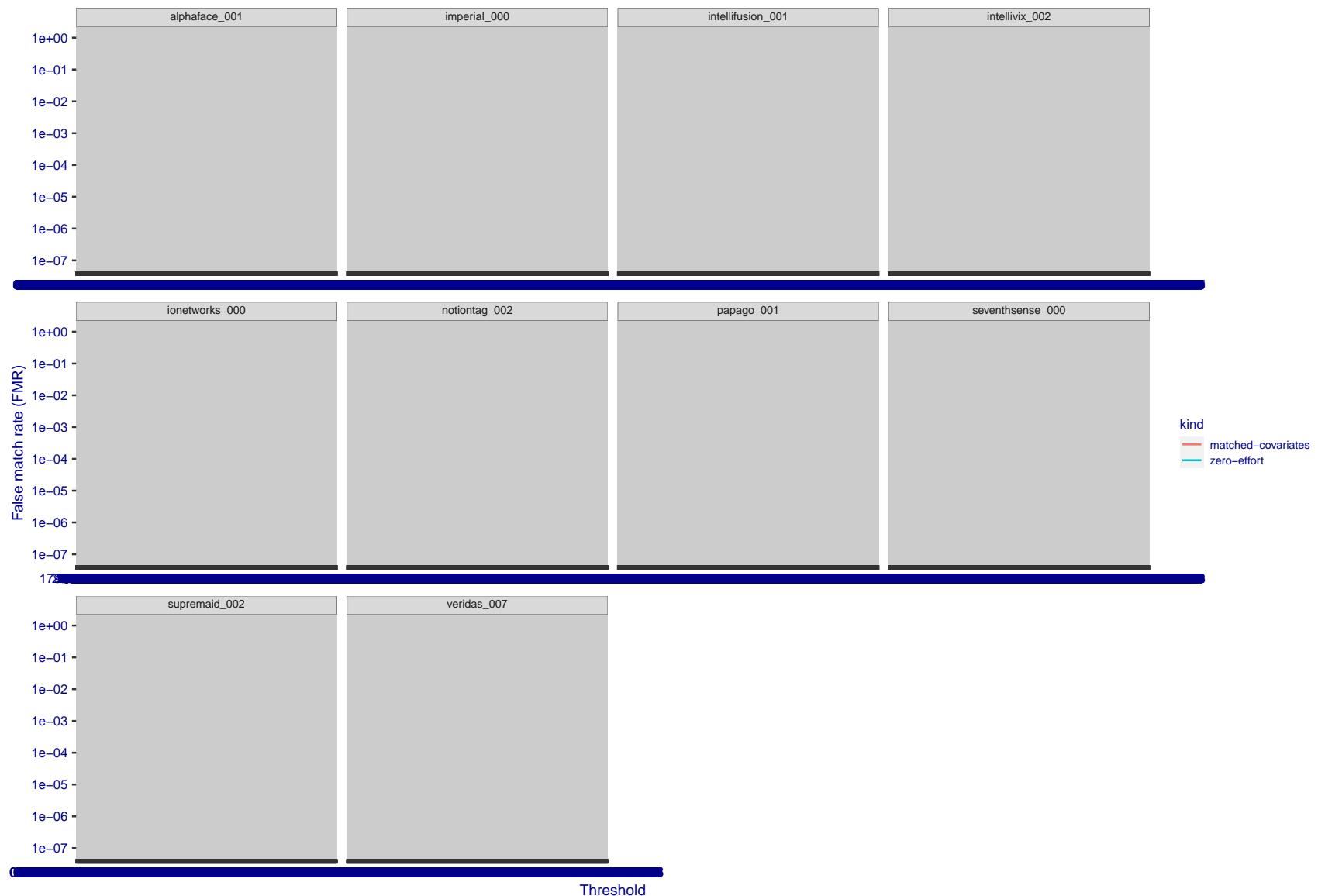


Figure 259: For the visa images, the false match calibration curves show FMR vs. threshold, T . The blue (lower) curves are for zero-effort impostors (i.e. comparing all images against all). The red (upper) curves are for persons of the same-sex, same-age, and same national-origin. This shows that FMR is underestimated (by a factor of 10 or more) by using a zero-effort impostor calculation to calibrate T . As shown later (sec. 3.6), FMR is higher for demographic-matched impostors.

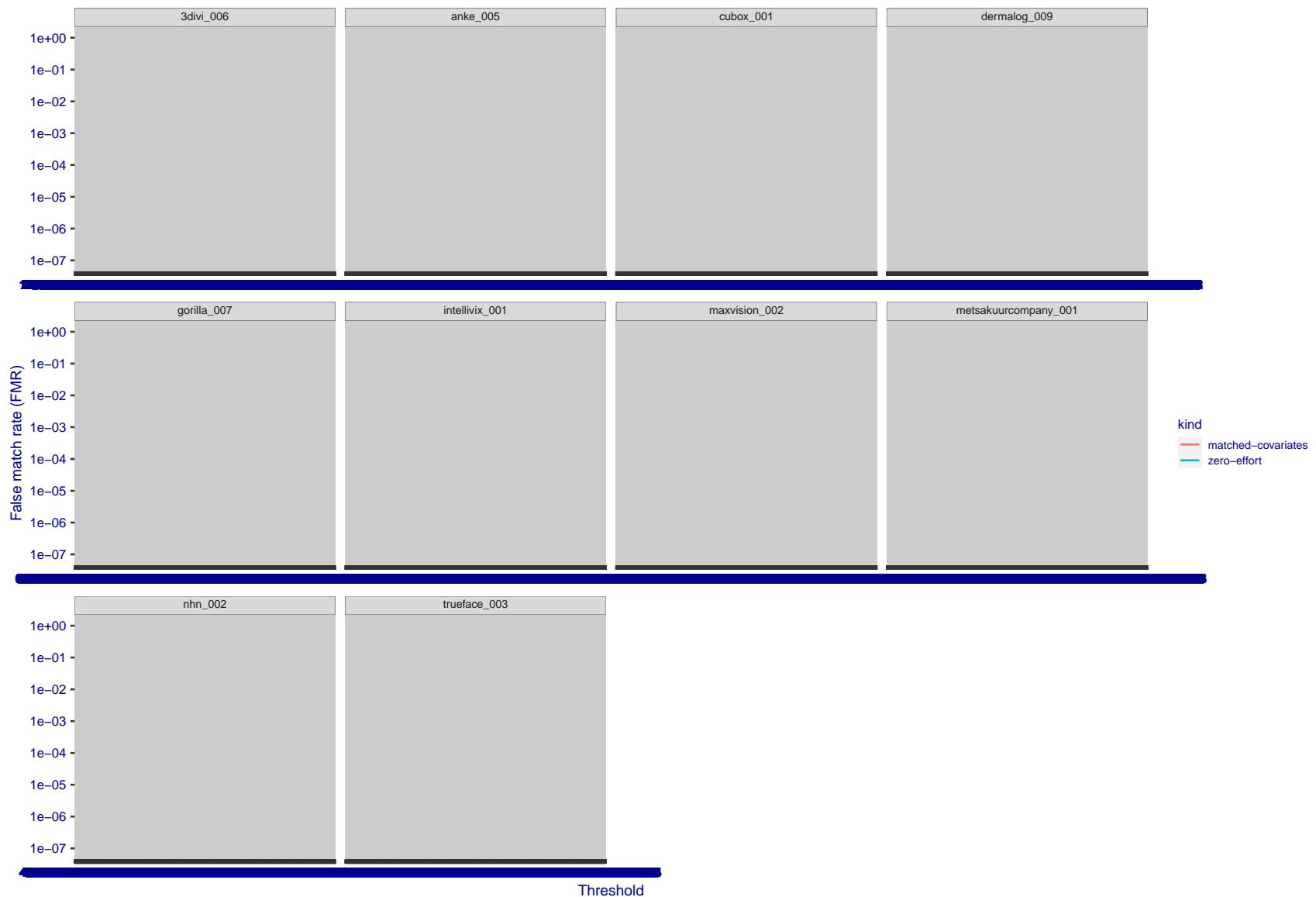


Figure 260: For the visa images, the false match calibration curves show FMR vs. threshold, T . The blue (lower) curves are for zero-effort impostors (i.e. comparing all images against all). The red (upper) curves are for persons of the same-sex, same-age, and same national-origin. This shows that FMR is underestimated (by a factor of 10 or more) by using a zero-effort impostor calculation to calibrate T . As shown later (sec. 3.6), FMR is higher for demographic-matched impostors.

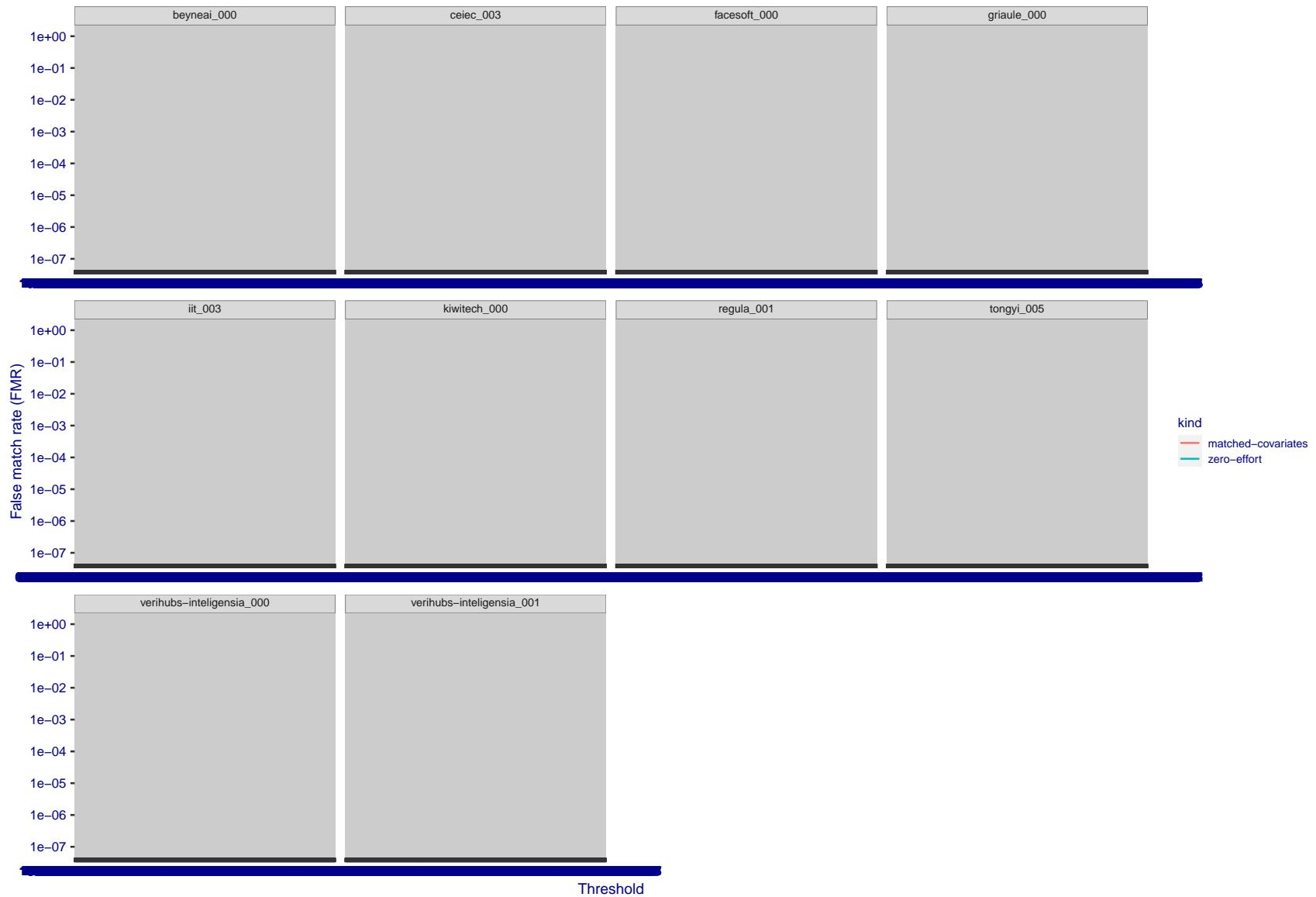


Figure 261: For the visa images, the false match calibration curves show FMR vs. threshold, T . The blue (lower) curves are for zero-effort impostors (i.e. comparing all images against all). The red (upper) curves are for persons of the same-sex, same-age, and same national-origin. This shows that FMR is underestimated (by a factor of 10 or more) by using a zero-effort impostor calculation to calibrate T . As shown later (sec. 3.6), FMR is higher for demographic-matched impostors.

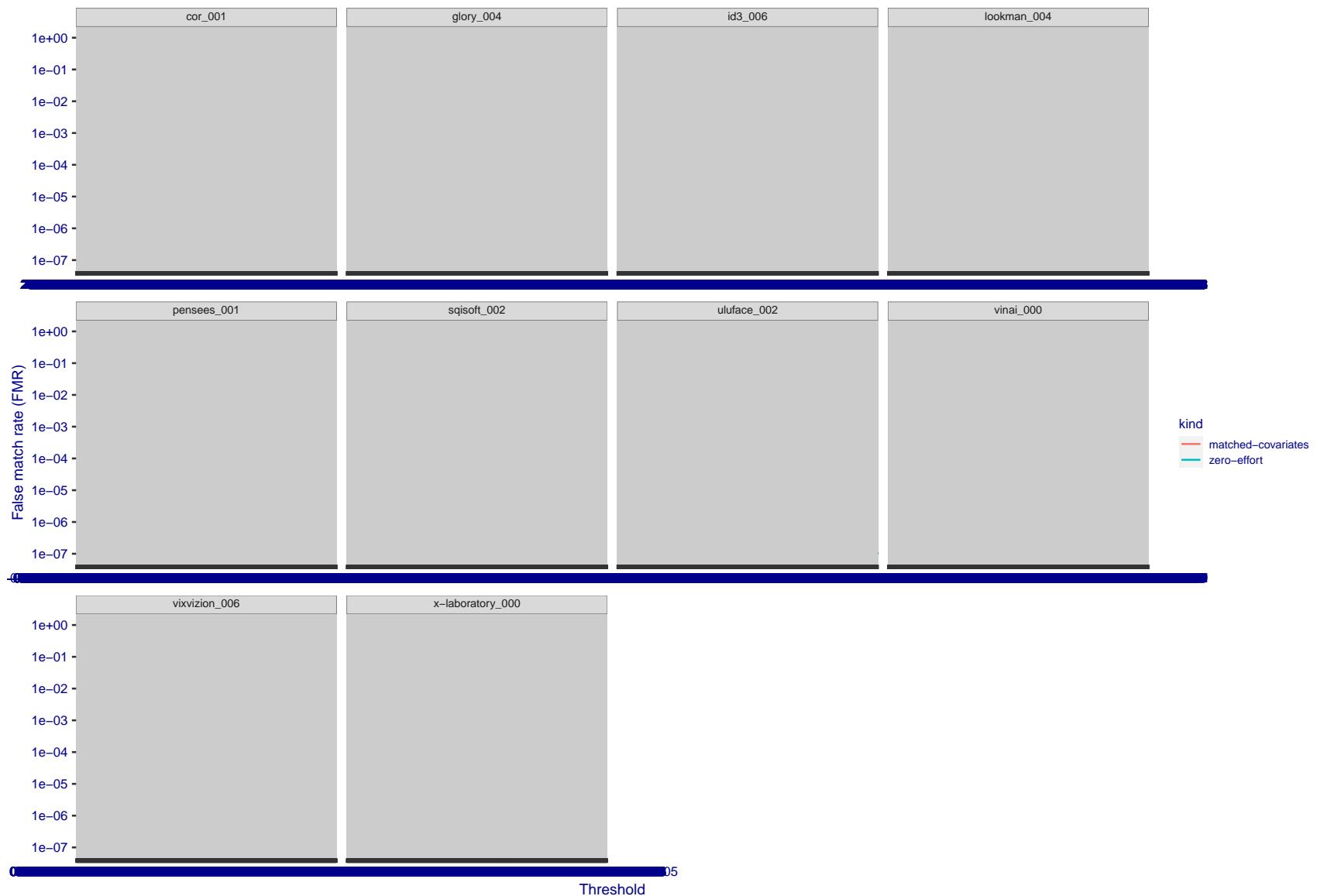


Figure 262: For the visa images, the false match calibration curves show FMR vs. threshold, T . The blue (lower) curves are for zero-effort impostors (i.e. comparing all images against all). The red (upper) curves are for persons of the same-sex, same-age, and same national-origin. This shows that FMR is underestimated (by a factor of 10 or more) by using a zero-effort impostor calculation to calibrate T . As shown later (sec. 3.6), FMR is higher for demographic-matched impostors.

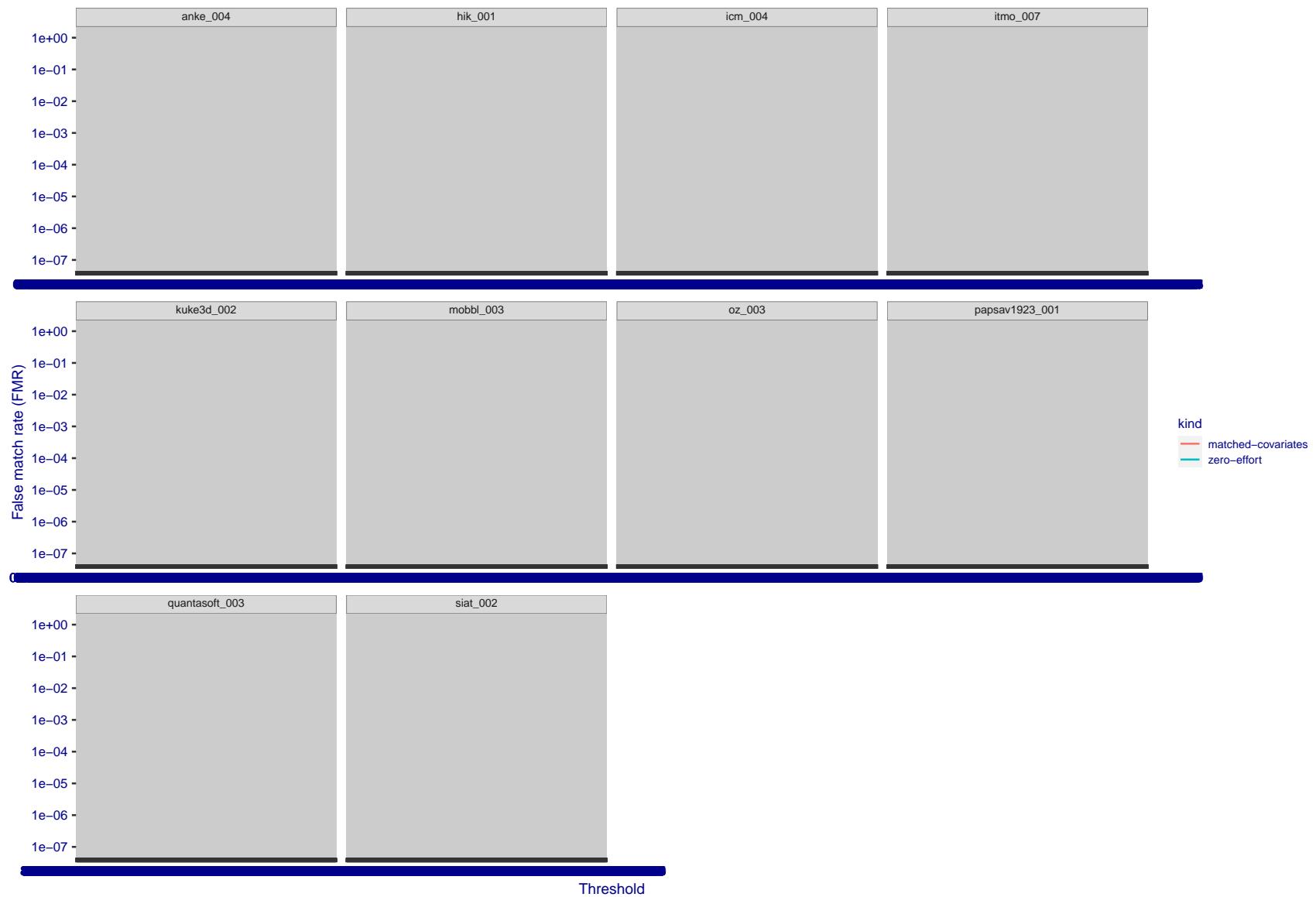


Figure 263: For the visa images, the false match calibration curves show FMR vs. threshold, T . The blue (lower) curves are for zero-effort impostors (i.e. comparing all images against all). The red (upper) curves are for persons of the same-sex, same-age, and same national-origin. This shows that FMR is underestimated (by a factor of 10 or more) by using a zero-effort impostor calculation to calibrate T . As shown later (sec. 3.6), FMR is higher for demographic-matched impostors.

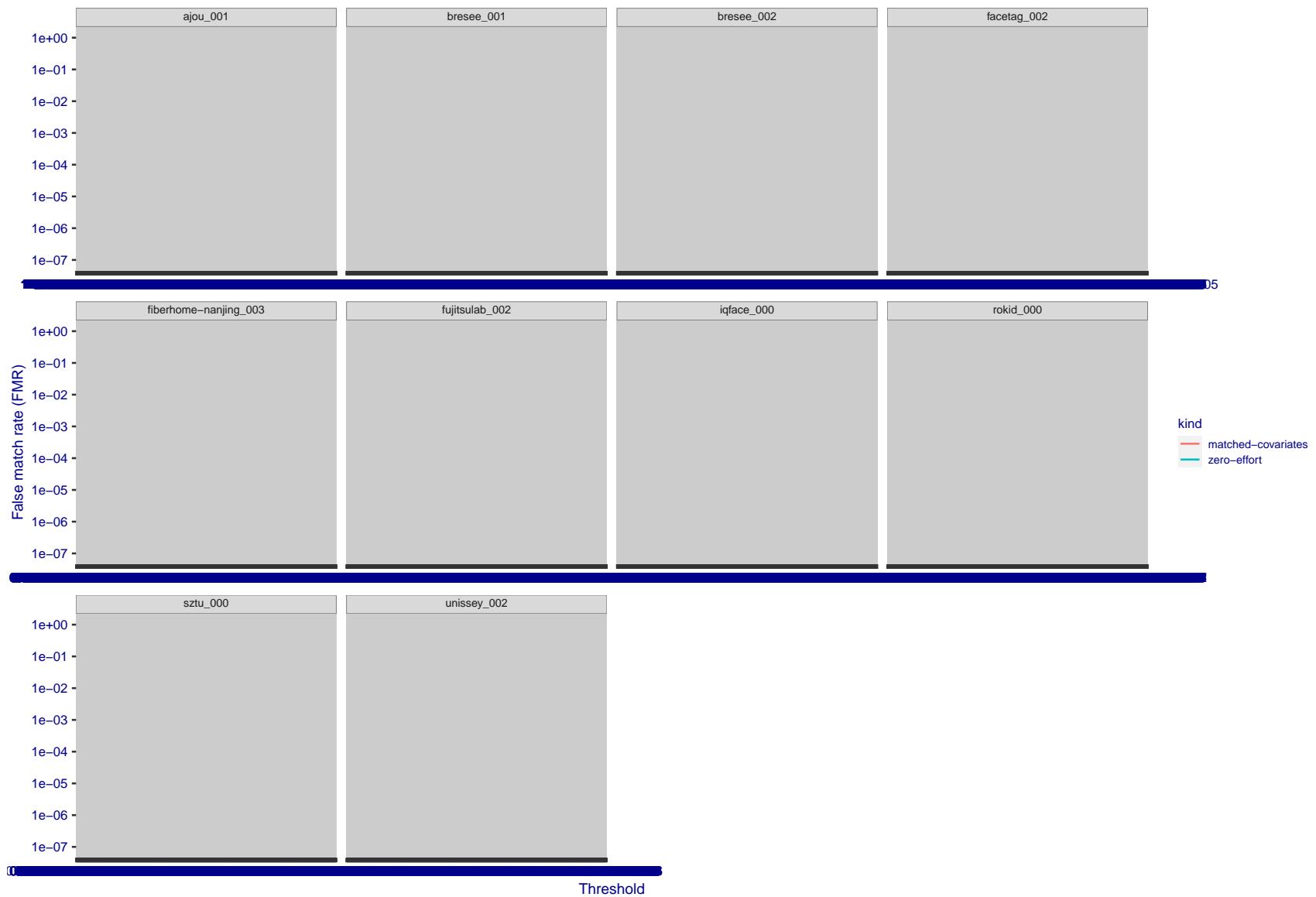


Figure 264: For the visa images, the false match calibration curves show FMR vs. threshold, T . The blue (lower) curves are for zero-effort impostors (i.e. comparing all images against all). The red (upper) curves are for persons of the same-sex, same-age, and same national-origin. This shows that FMR is underestimated (by a factor of 10 or more) by using a zero-effort impostor calculation to calibrate T . As shown later (sec. 3.6), FMR is higher for demographic-matched impostors.

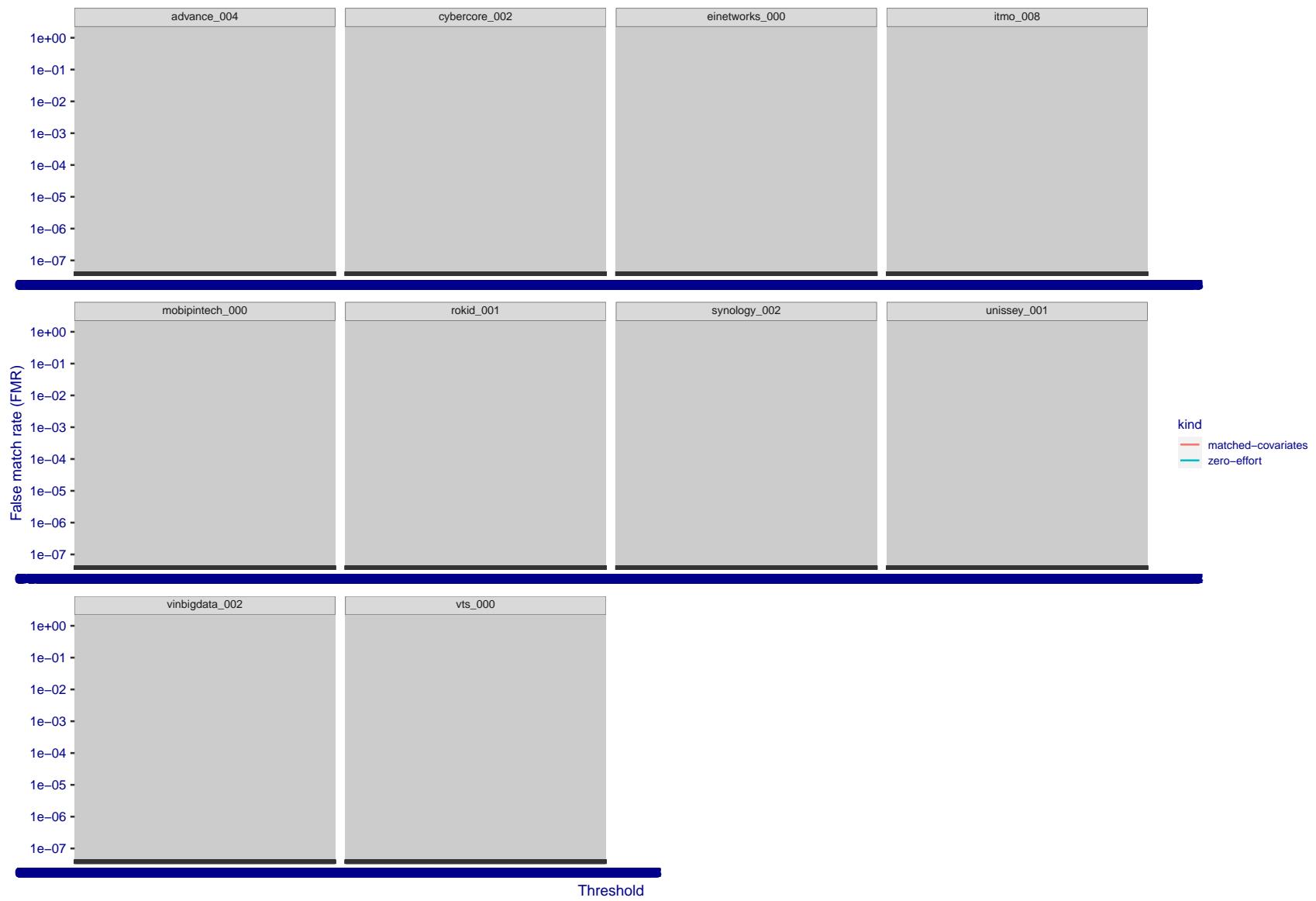


Figure 265: For the visa images, the false match calibration curves show FMR vs. threshold, T . The blue (lower) curves are for zero-effort impostors (i.e. comparing all images against all). The red (upper) curves are for persons of the same-sex, same-age, and same national-origin. This shows that FMR is underestimated (by a factor of 10 or more) by using a zero-effort impostor calculation to calibrate T . As shown later (sec. 3.6), FMR is higher for demographic-matched impostors.

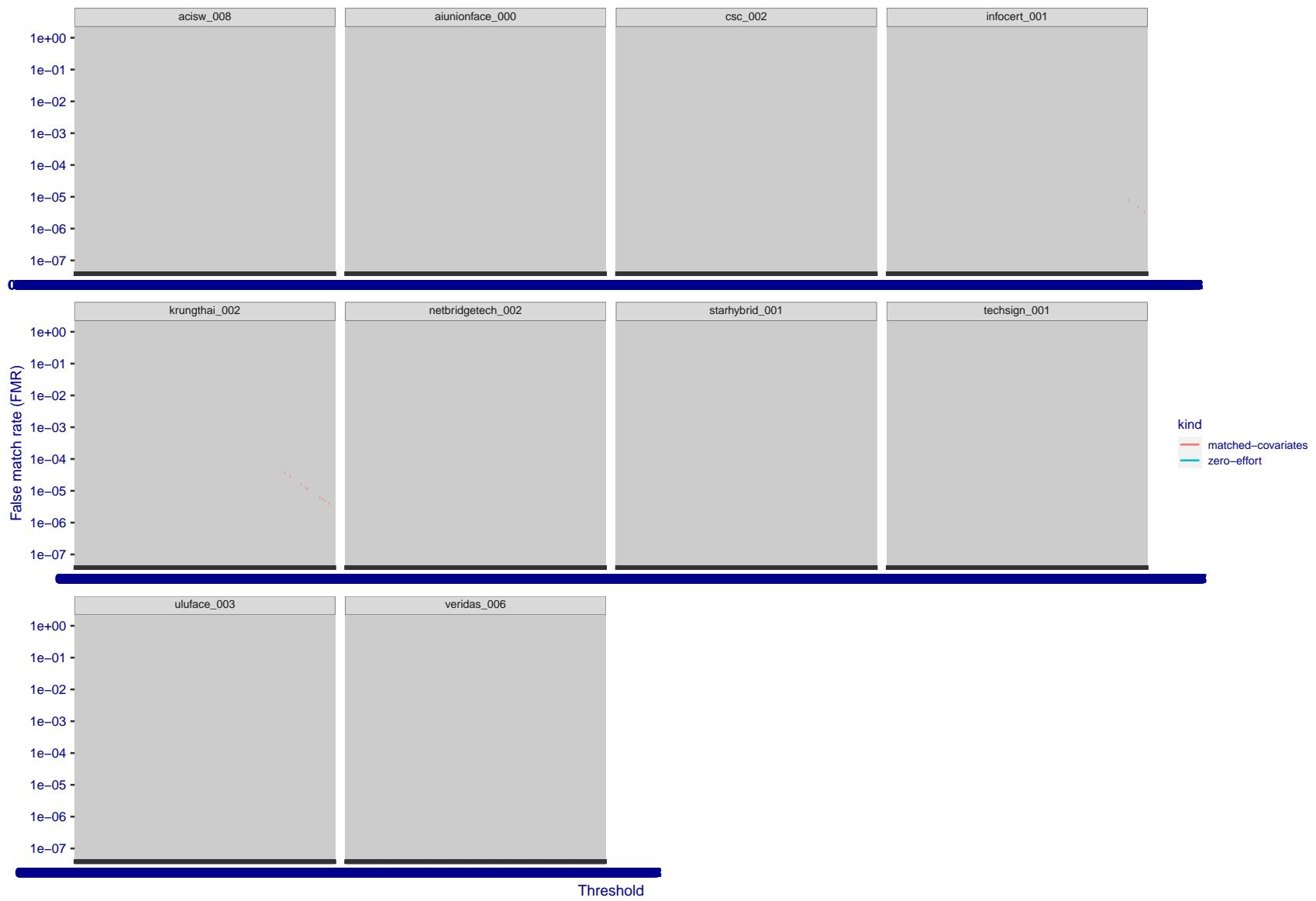


Figure 266: For the visa images, the false match calibration curves show FMR vs. threshold, T . The blue (lower) curves are for zero-effort impostors (i.e. comparing all images against all). The red (upper) curves are for persons of the same-sex, same-age, and same national-origin. This shows that FMR is underestimated (by a factor of 10 or more) by using a zero-effort impostor calculation to calibrate T . As shown later (sec. 3.6), FMR is higher for demographic-matched impostors.

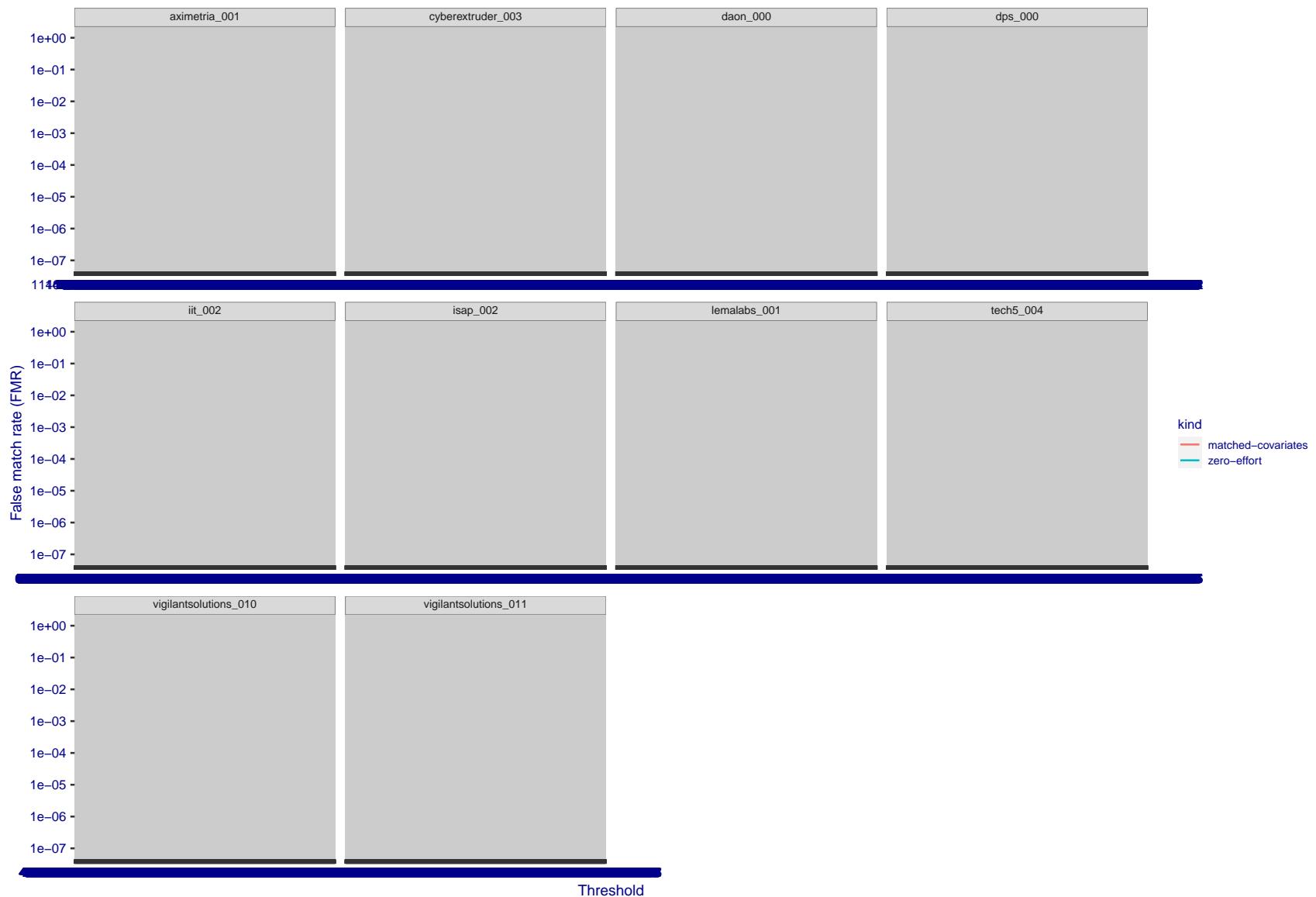


Figure 267: For the visa images, the false match calibration curves show FMR vs. threshold, T . The blue (lower) curves are for zero-effort impostors (i.e. comparing all images against all). The red (upper) curves are for persons of the same-sex, same-age, and same national-origin. This shows that FMR is underestimated (by a factor of 10 or more) by using a zero-effort impostor calculation to calibrate T . As shown later (sec. 3.6), FMR is higher for demographic-matched impostors.

2022/11/06 10:45:39

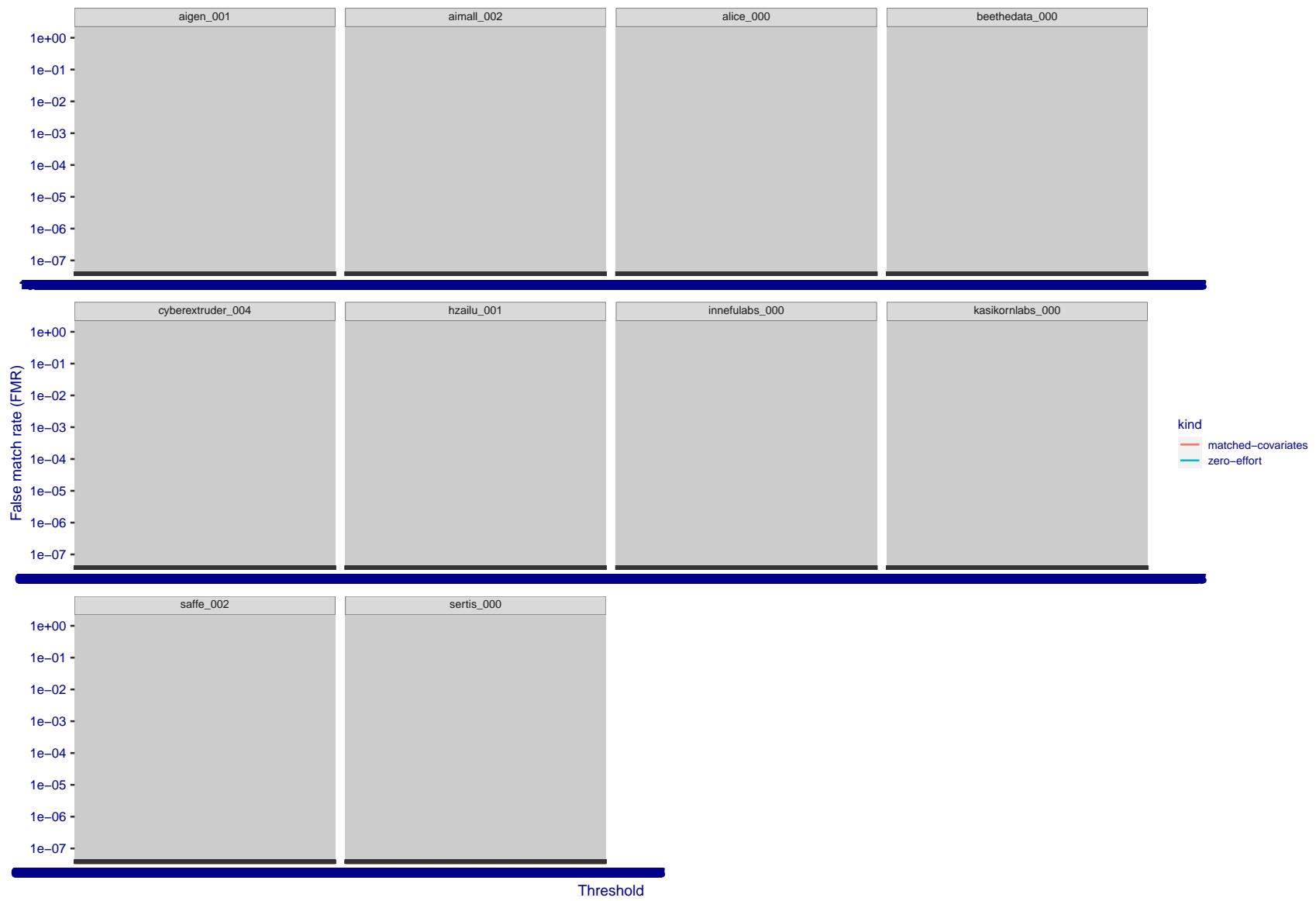


Figure 268: For the visa images, the false match calibration curves show FMR vs. threshold, T . The blue (lower) curves are for zero-effort impostors (i.e. comparing all images against all). The red (upper) curves are for persons of the same-sex, same-age, and same national-origin. This shows that FMR is underestimated (by a factor of 10 or more) by using a zero-effort impostor calculation to calibrate T . As shown later (sec. 3.6), FMR is higher for demographic-matched impostors.

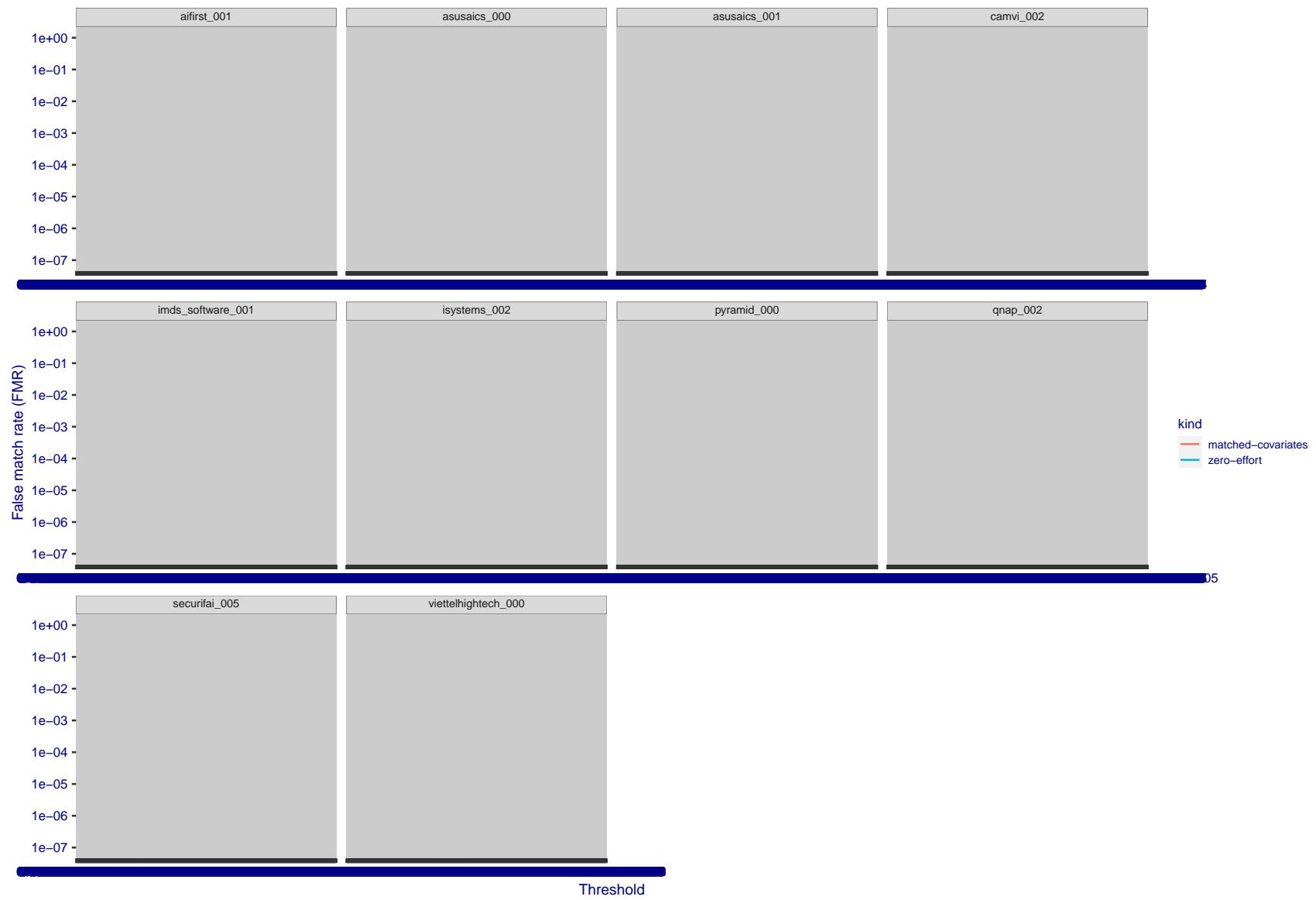


Figure 269: For the visa images, the false match calibration curves show FMR vs. threshold, T . The blue (lower) curves are for zero-effort impostors (i.e. comparing all images against all). The red (upper) curves are for persons of the same-sex, same-age, and same national-origin. This shows that FMR is underestimated (by a factor of 10 or more) by using a zero-effort impostor calculation to calibrate T . As shown later (sec. 3.6), FMR is higher for demographic-matched impostors.

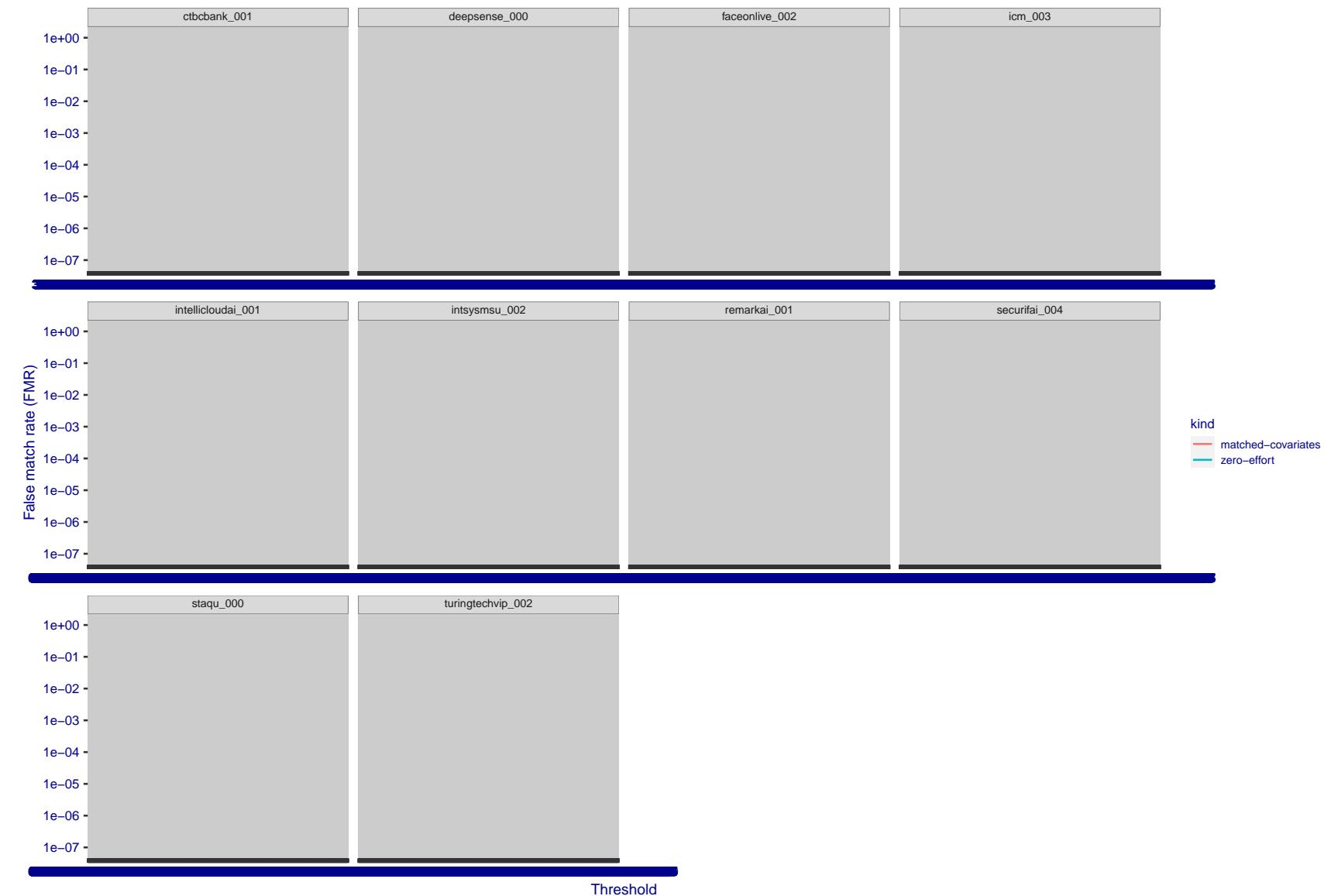


Figure 270: For the visa images, the false match calibration curves show FMR vs. threshold, T . The blue (lower) curves are for zero-effort impostors (i.e. comparing all images against all). The red (upper) curves are for persons of the same-sex, same-age, and same national-origin. This shows that FMR is underestimated (by a factor of 10 or more) by using a zero-effort impostor calculation to calibrate T . As shown later (sec. 3.6), FMR is higher for demographic-matched impostors.

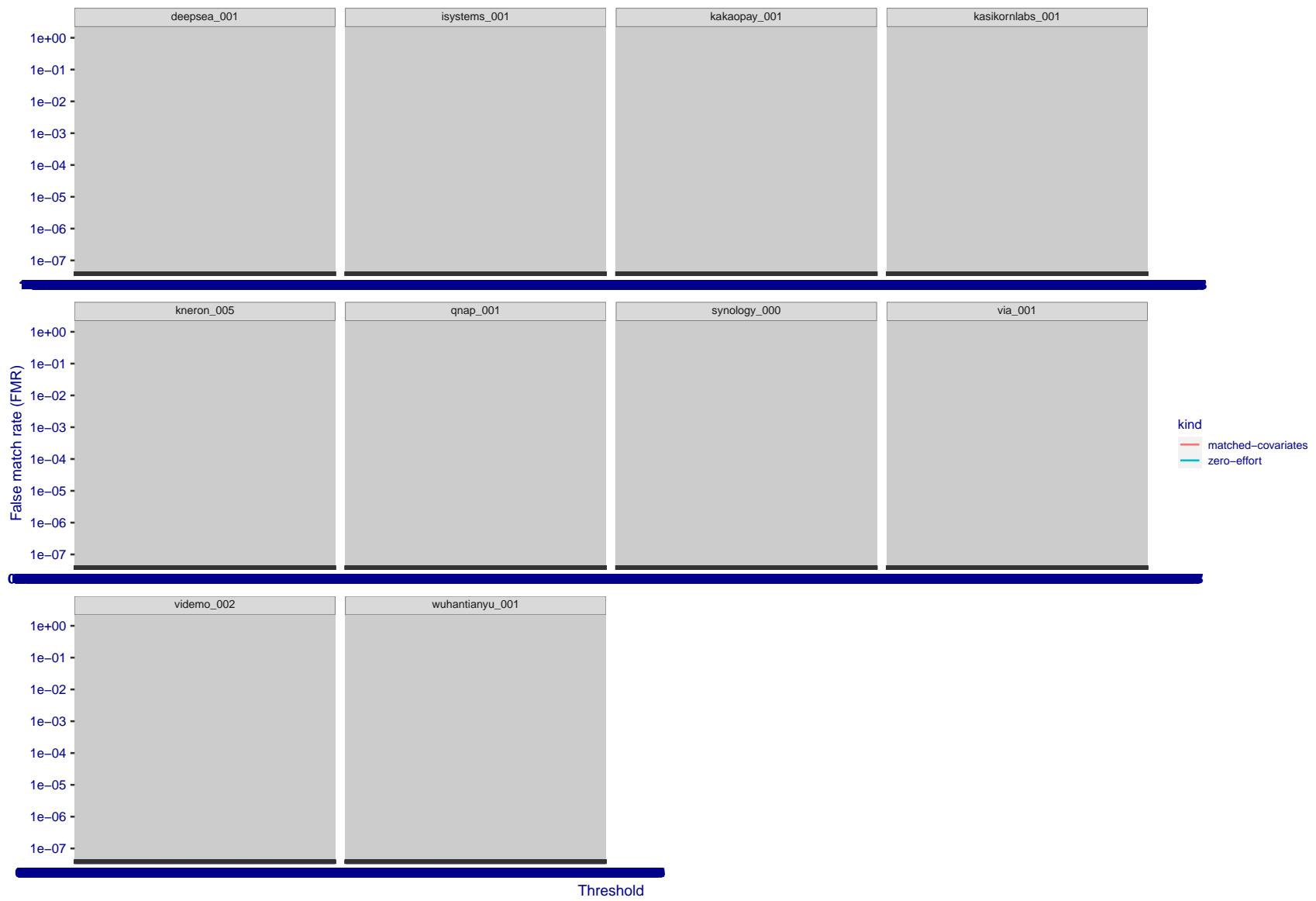


Figure 271: For the visa images, the false match calibration curves show FMR vs. threshold, T . The blue (lower) curves are for zero-effort impostors (i.e. comparing all images against all). The red (upper) curves are for persons of the same-sex, same-age, and same national-origin. This shows that FMR is underestimated (by a factor of 10 or more) by using a zero-effort impostor calculation to calibrate T . As shown later (sec. 3.6), FMR is higher for demographic-matched impostors.

2022/11/06 10:45:39

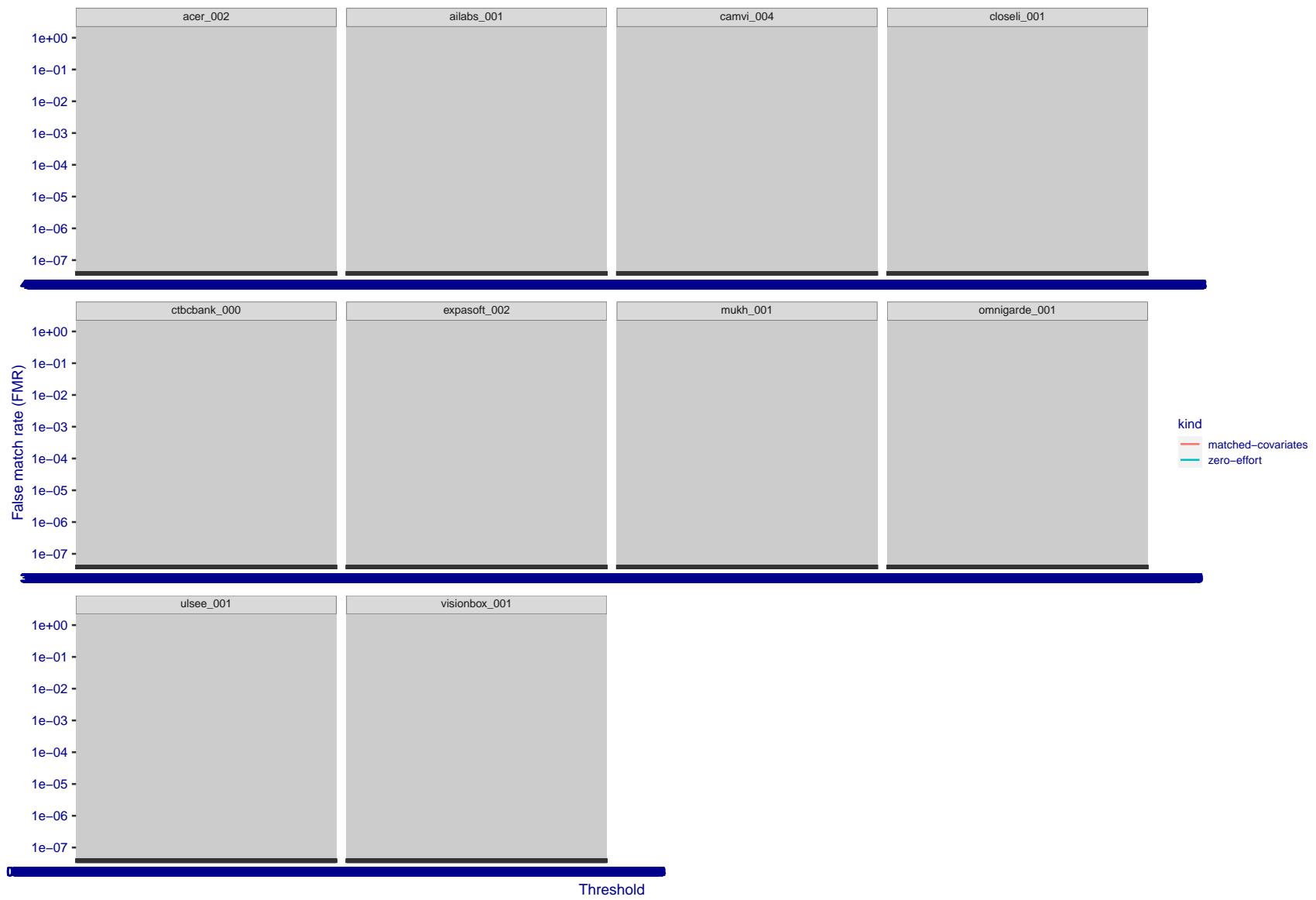


Figure 272: For the visa images, the false match calibration curves show FMR vs. threshold, T . The blue (lower) curves are for zero-effort impostors (i.e. comparing all images against all). The red (upper) curves are for persons of the same-sex, same-age, and same national-origin. This shows that FMR is underestimated (by a factor of 10 or more) by using a zero-effort impostor calculation to calibrate T . As shown later (sec. 3.6), FMR is higher for demographic-matched impostors.

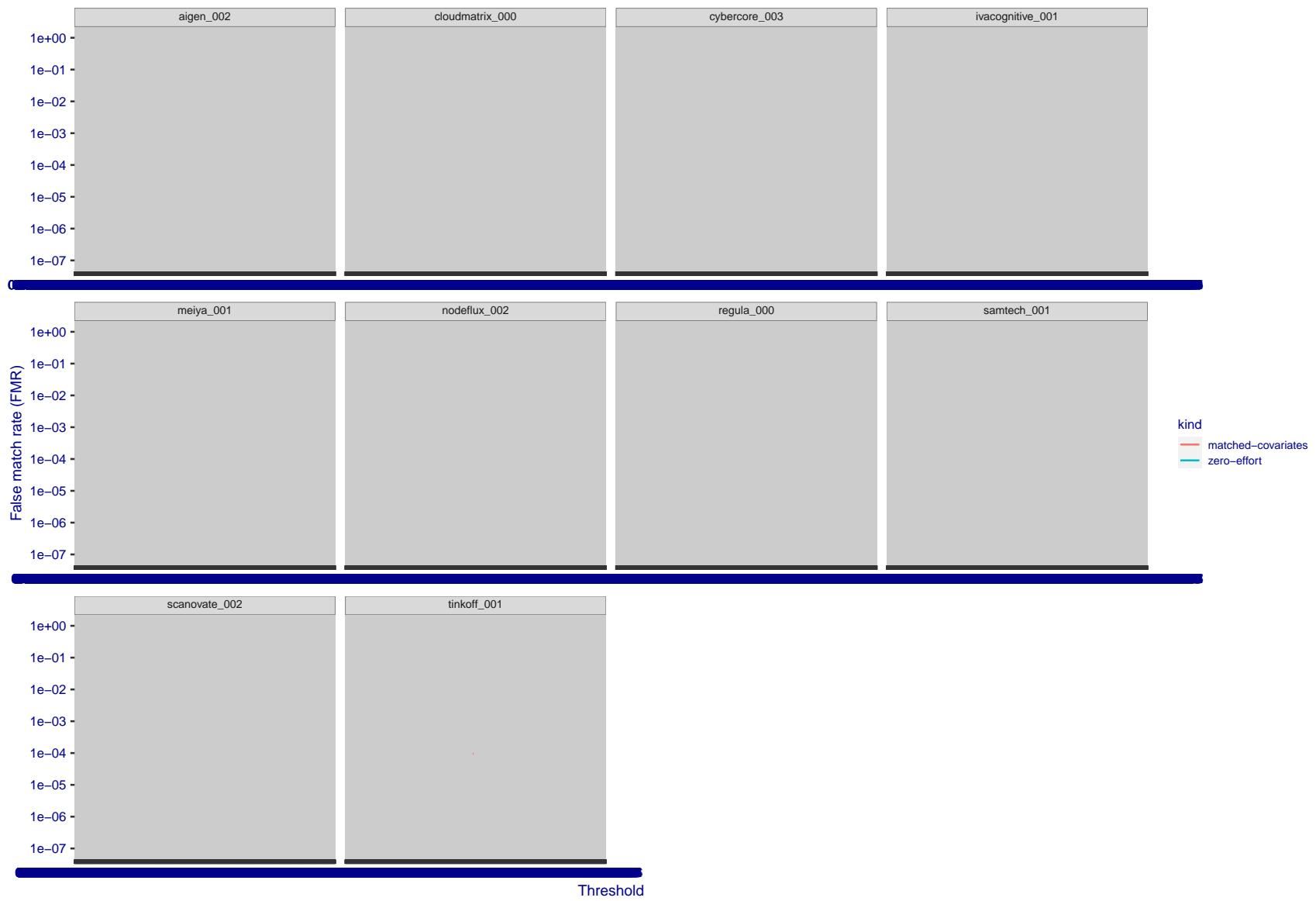


Figure 273: For the visa images, the false match calibration curves show FMR vs. threshold, T . The blue (lower) curves are for zero-effort impostors (i.e. comparing all images against all). The red (upper) curves are for persons of the same-sex, same-age, and same national-origin. This shows that FMR is underestimated (by a factor of 10 or more) by using a zero-effort impostor calculation to calibrate T . As shown later (sec. 3.6), FMR is higher for demographic-matched impostors.

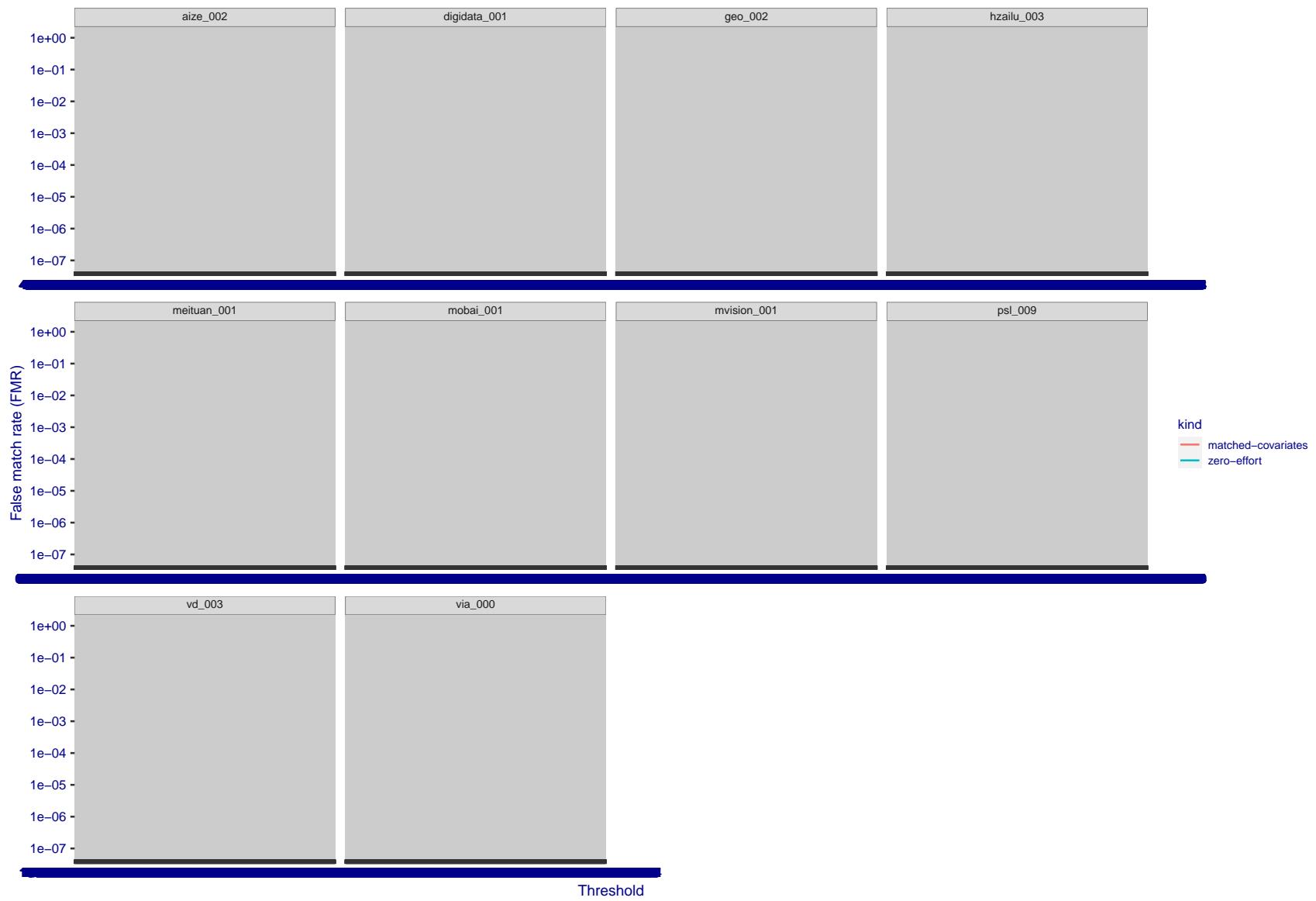


Figure 274: For the visa images, the false match calibration curves show FMR vs. threshold, T . The blue (lower) curves are for zero-effort impostors (i.e. comparing all images against all). The red (upper) curves are for persons of the same-sex, same-age, and same national-origin. This shows that FMR is underestimated (by a factor of 10 or more) by using a zero-effort impostor calculation to calibrate T . As shown later (sec. 3.6), FMR is higher for demographic-matched impostors.

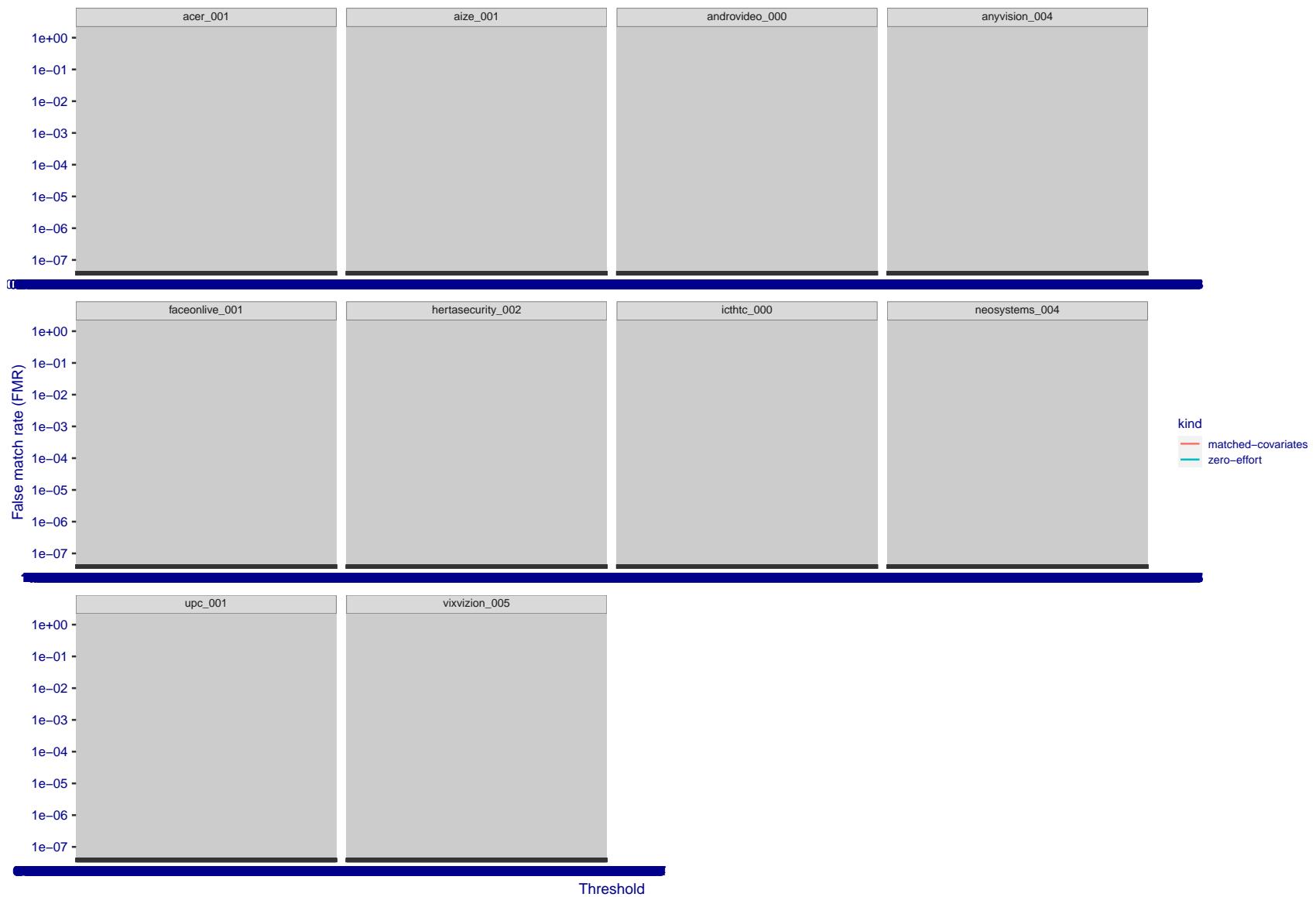


Figure 275: For the visa images, the false match calibration curves show FMR vs. threshold, T . The blue (lower) curves are for zero-effort impostors (i.e. comparing all images against all). The red (upper) curves are for persons of the same-sex, same-age, and same national-origin. This shows that FMR is underestimated (by a factor of 10 or more) by using a zero-effort impostor calculation to calibrate T . As shown later (sec. 3.6), FMR is higher for demographic-matched impostors.

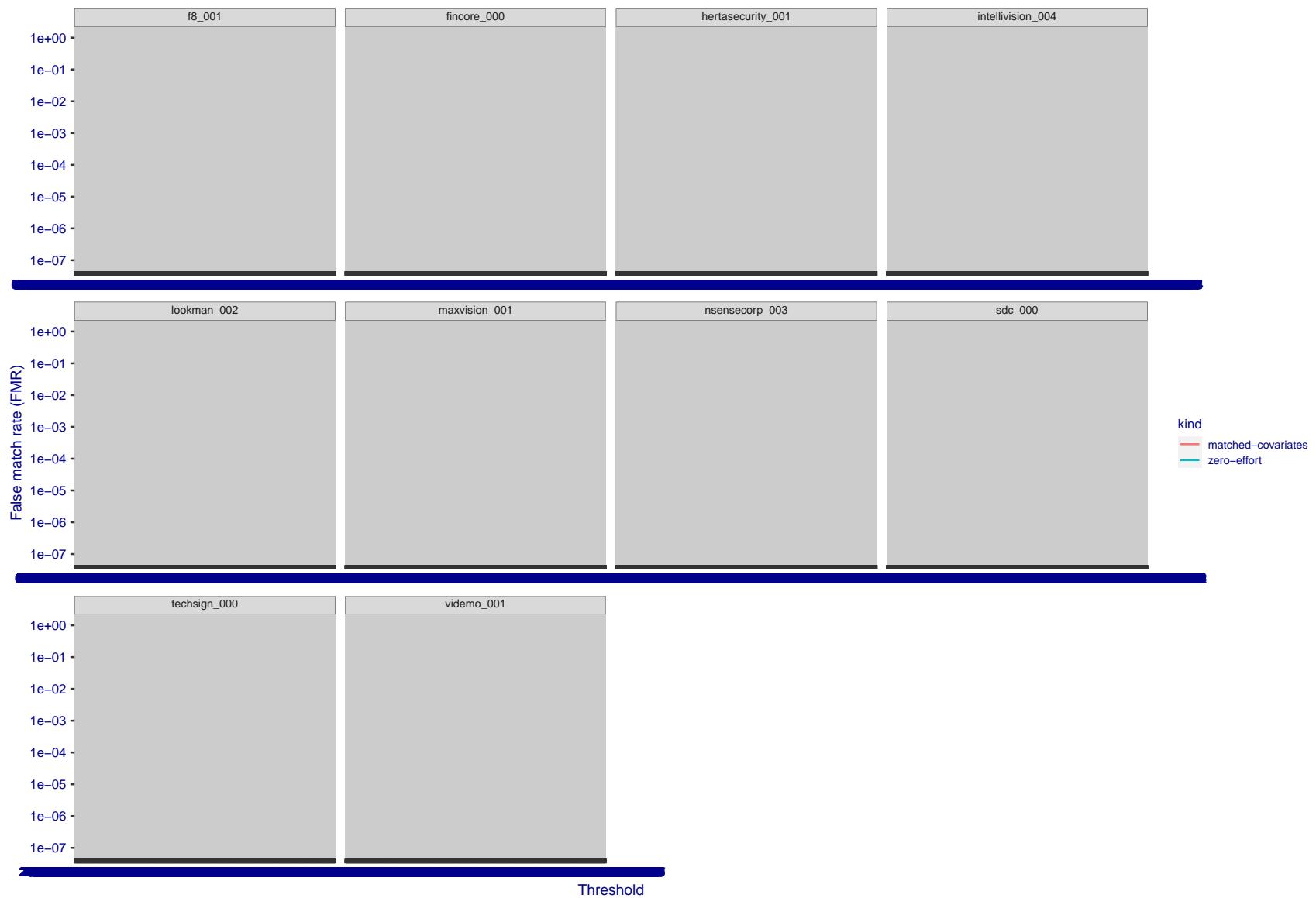


Figure 276: For the visa images, the false match calibration curves show FMR vs. threshold, T . The blue (lower) curves are for zero-effort impostors (i.e. comparing all images against all). The red (upper) curves are for persons of the same-sex, same-age, and same national-origin. This shows that FMR is underestimated (by a factor of 10 or more) by using a zero-effort impostor calculation to calibrate T . As shown later (sec. 3.6), FMR is higher for demographic-matched impostors.

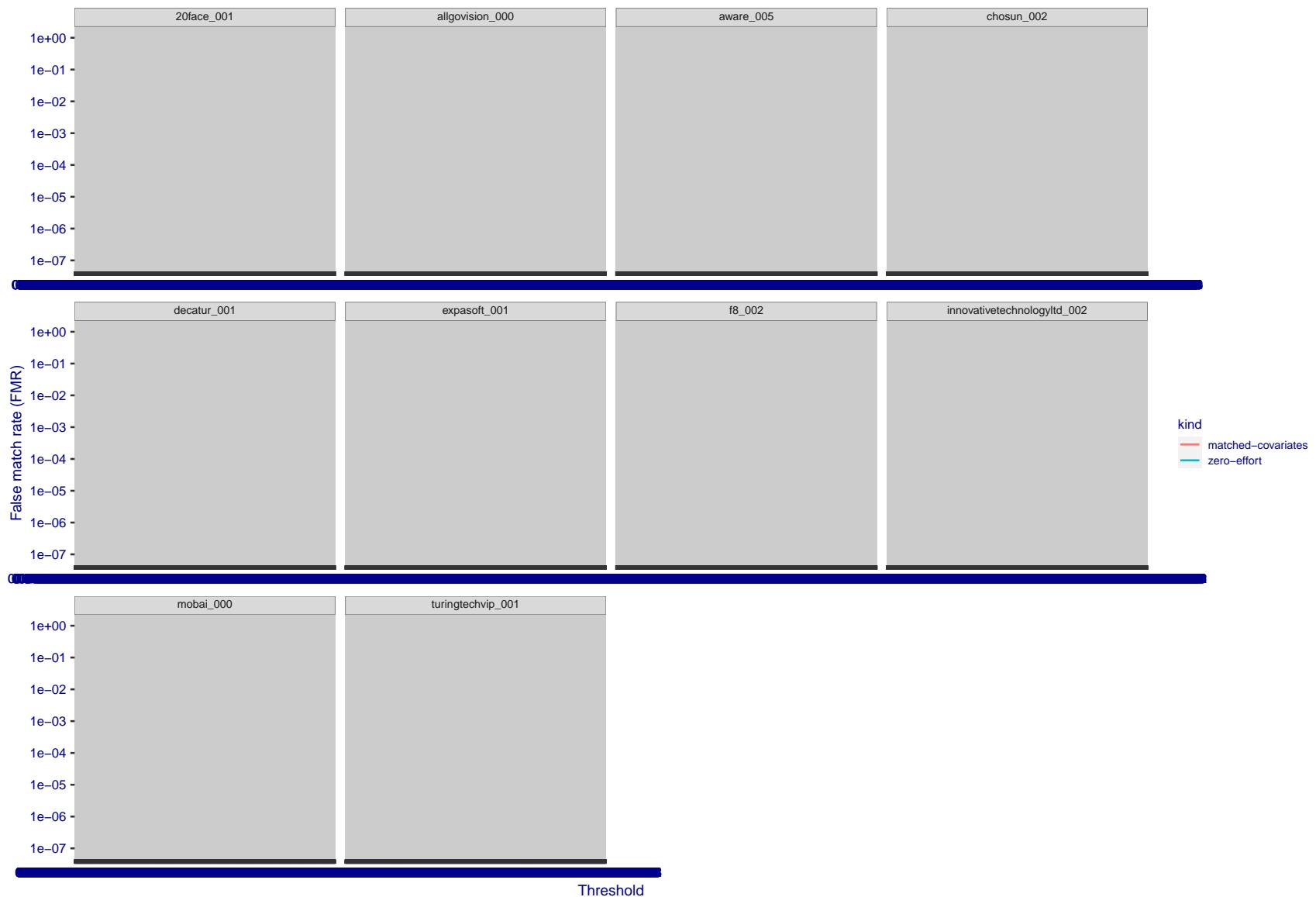


Figure 277: For the visa images, the false match calibration curves show FMR vs. threshold, T . The blue (lower) curves are for zero-effort impostors (i.e. comparing all images against all). The red (upper) curves are for persons of the same-sex, same-age, and same national-origin. This shows that FMR is underestimated (by a factor of 10 or more) by using a zero-effort impostor calculation to calibrate T . As shown later (sec. 3.6), FMR is higher for demographic-matched impostors.

2022/11/06 10:45:39

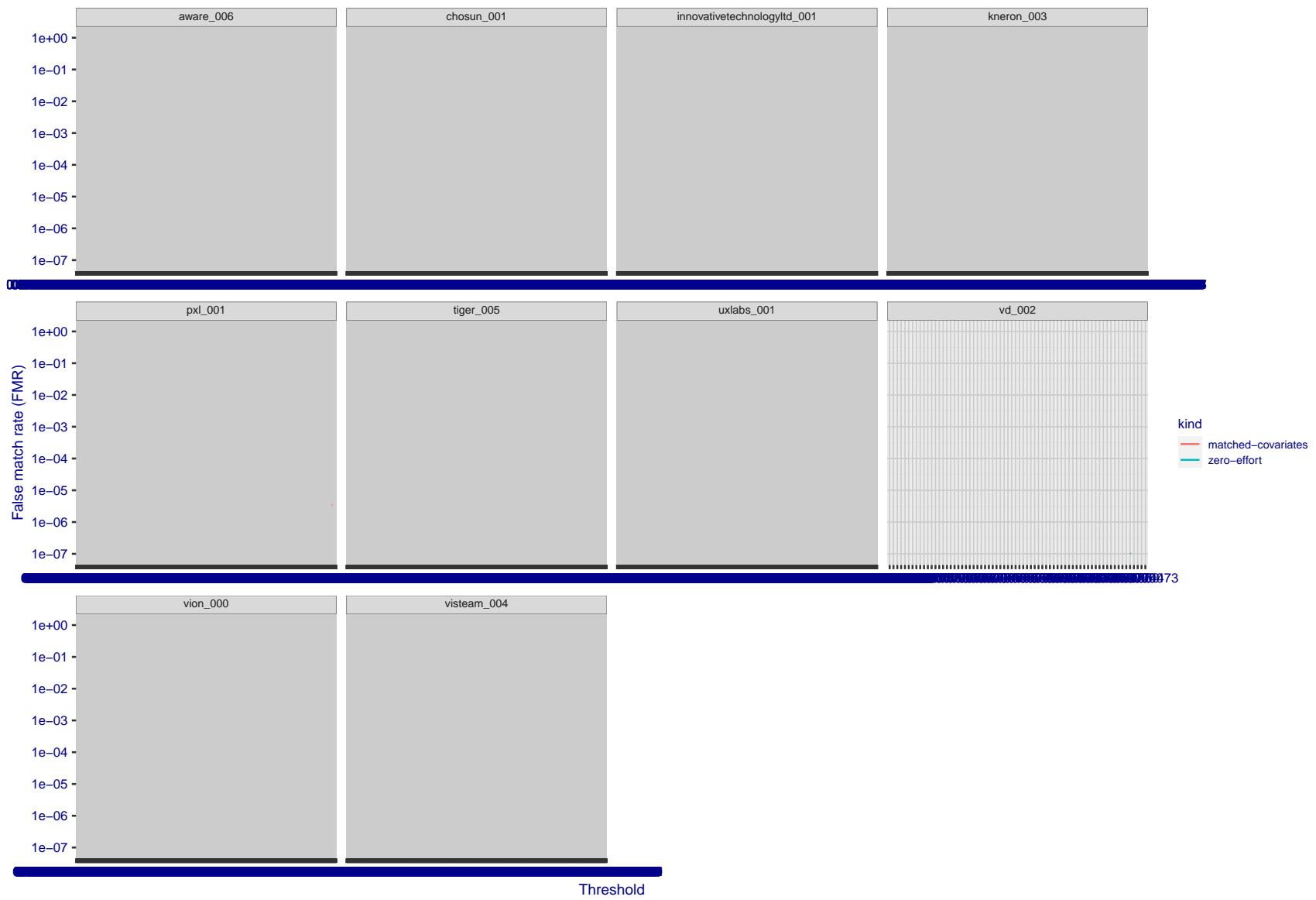


Figure 278: For the visa images, the false match calibration curves show FMR vs. threshold, T . The blue (lower) curves are for zero-effort impostors (i.e. comparing all images against all). The red (upper) curves are for persons of the same-sex, same-age, and same national-origin. This shows that FMR is underestimated (by a factor of 10 or more) by using a zero-effort impostor calculation to calibrate T . As shown later (sec. 3.6), FMR is higher for demographic-matched impostors.

FNMR(T)
FMR(T)
"False non-match rate"
"False match rate"

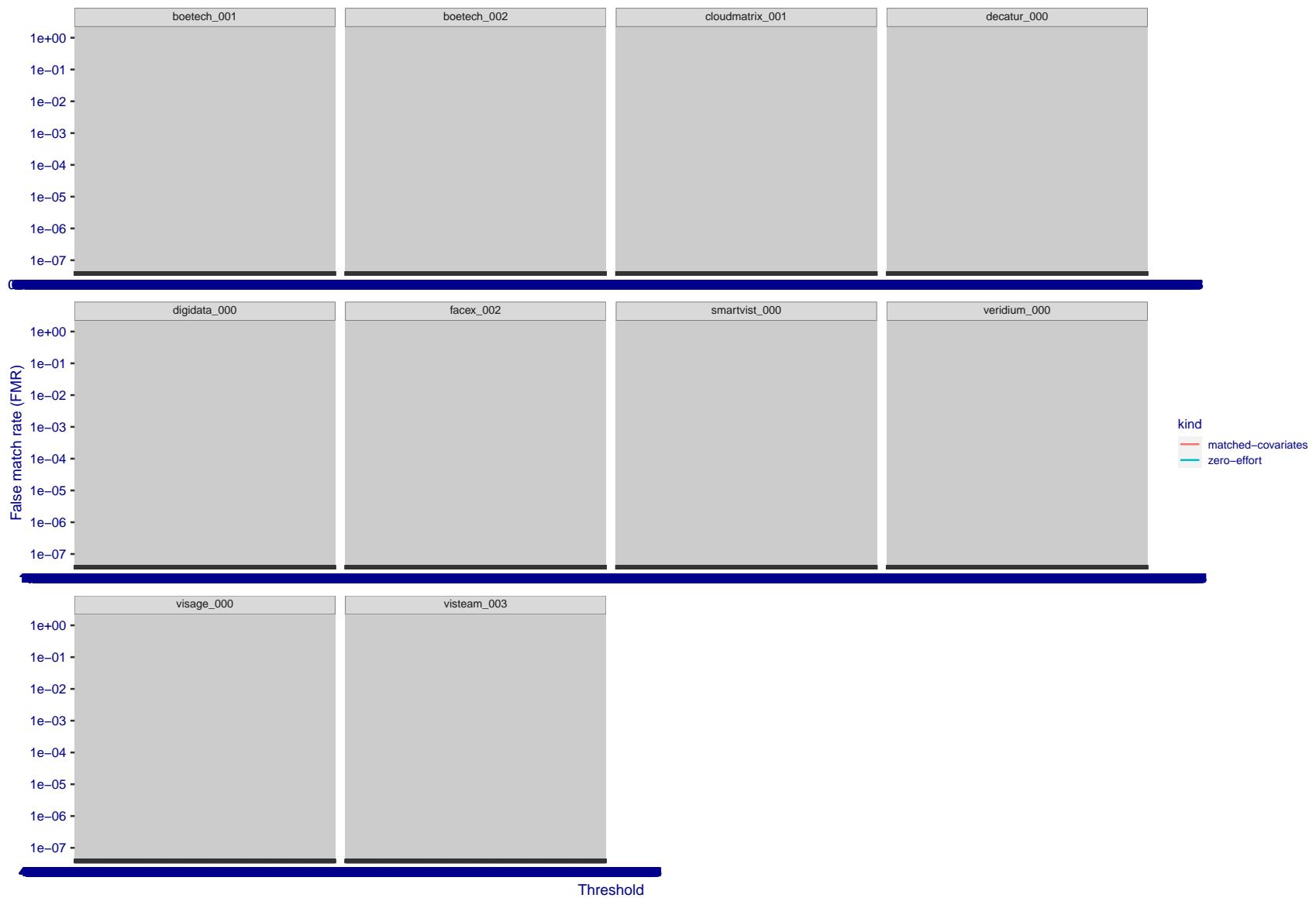


Figure 279: For the visa images, the false match calibration curves show FMR vs. threshold, T . The blue (lower) curves are for zero-effort impostors (i.e. comparing all images against all). The red (upper) curves are for persons of the same-sex, same-age, and same national-origin. This shows that FMR is underestimated (by a factor of 10 or more) by using a zero-effort impostor calculation to calibrate T . As shown later (sec. 3.6), FMR is higher for demographic-matched impostors.

2022/11/06 10:45:39

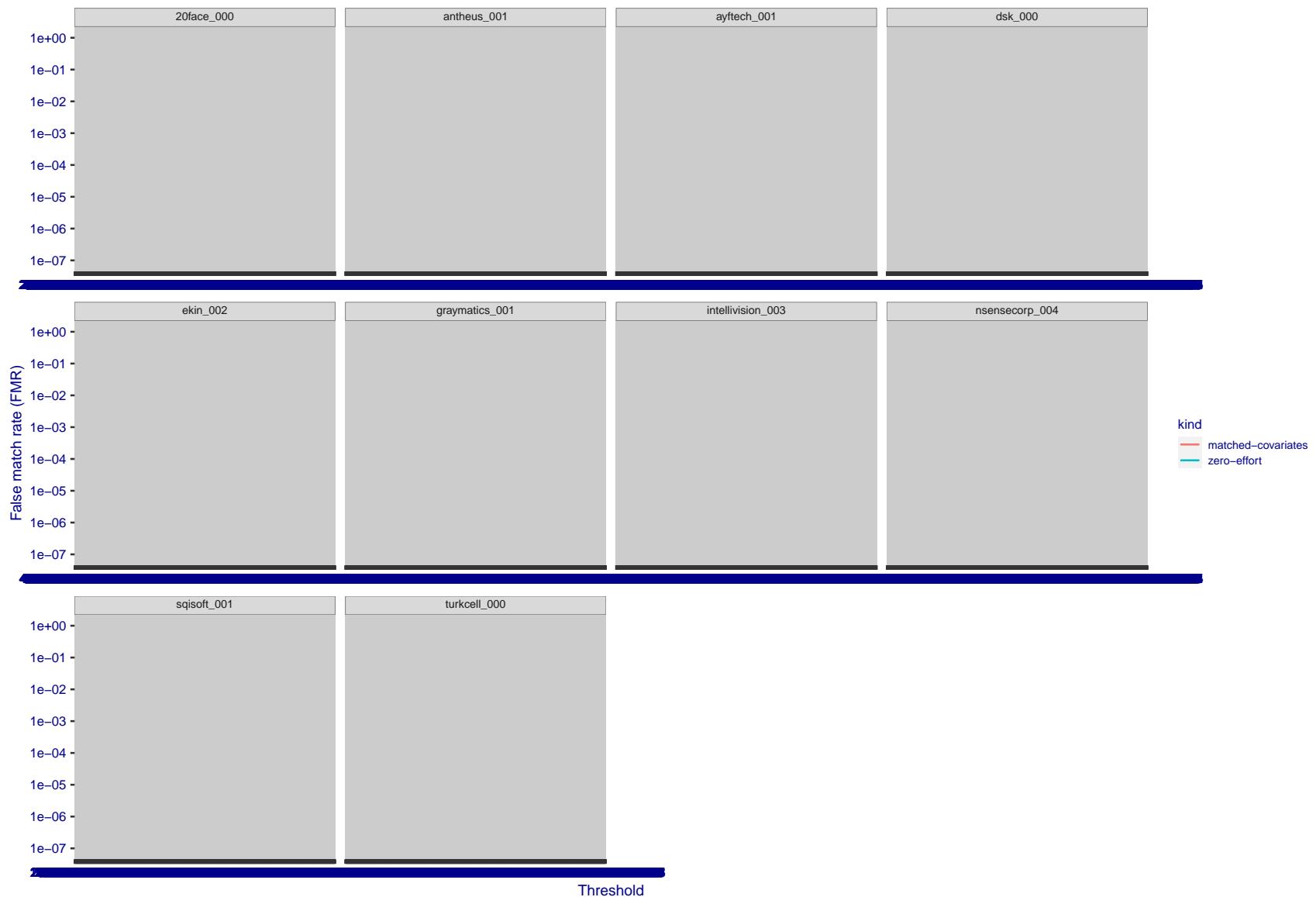


Figure 280: For the visa images, the false match calibration curves show FMR vs. threshold, T . The blue (lower) curves are for zero-effort impostors (i.e. comparing all images against all). The red (upper) curves are for persons of the same-sex, same-age, and same national-origin. This shows that FMR is underestimated (by a factor of 10 or more) by using a zero-effort impostor calculation to calibrate T . As shown later (sec. 3.6), FMR is higher for demographic-matched impostors.

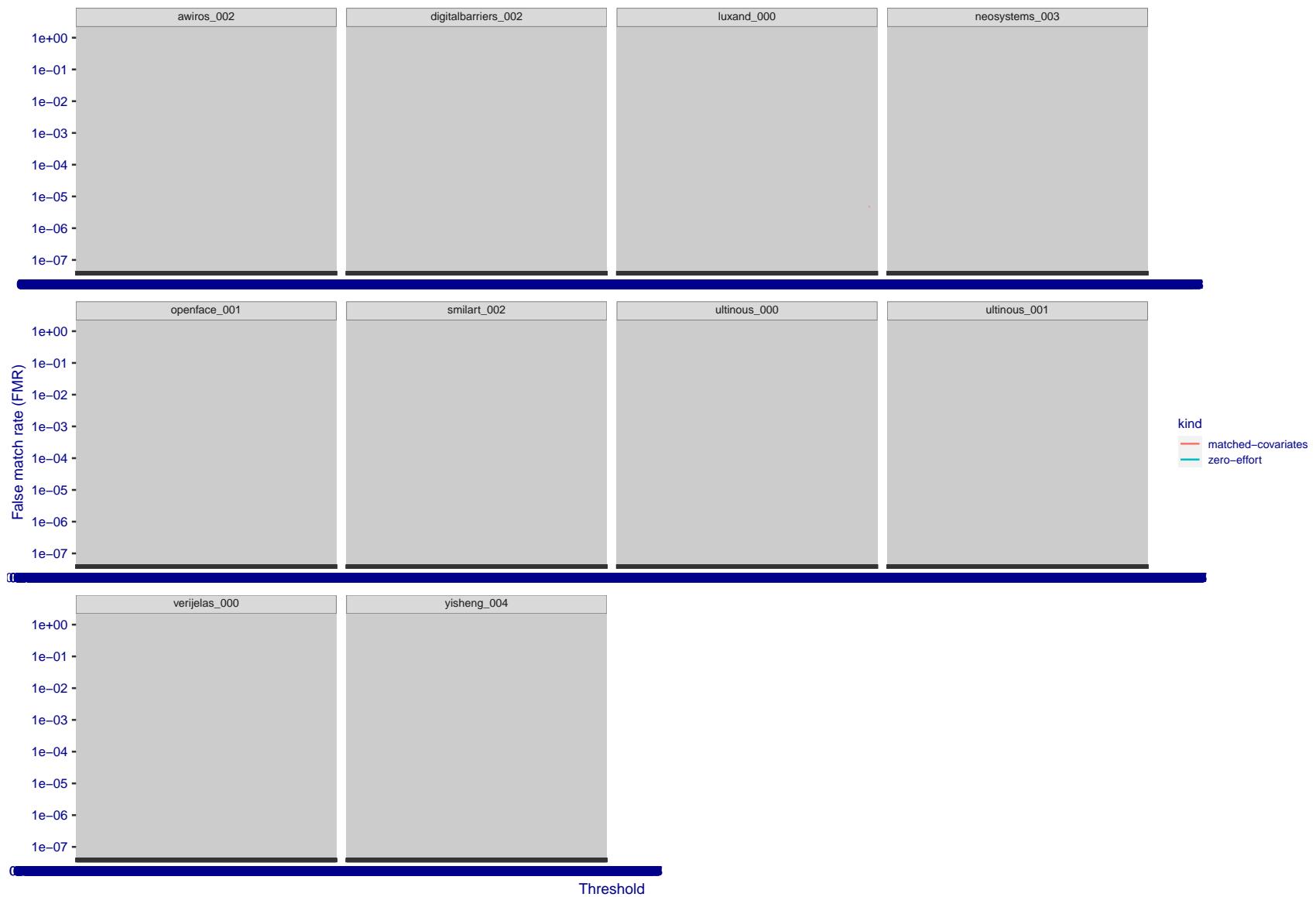


Figure 281: For the visa images, the false match calibration curves show FMR vs. threshold, T . The blue (lower) curves are for zero-effort impostors (i.e. comparing all images against all). The red (upper) curves are for persons of the same-sex, same-age, and same national-origin. This shows that FMR is underestimated (by a factor of 10 or more) by using a zero-effort impostor calculation to calibrate T . As shown later (sec. 3.6), FMR is higher for demographic-matched impostors.

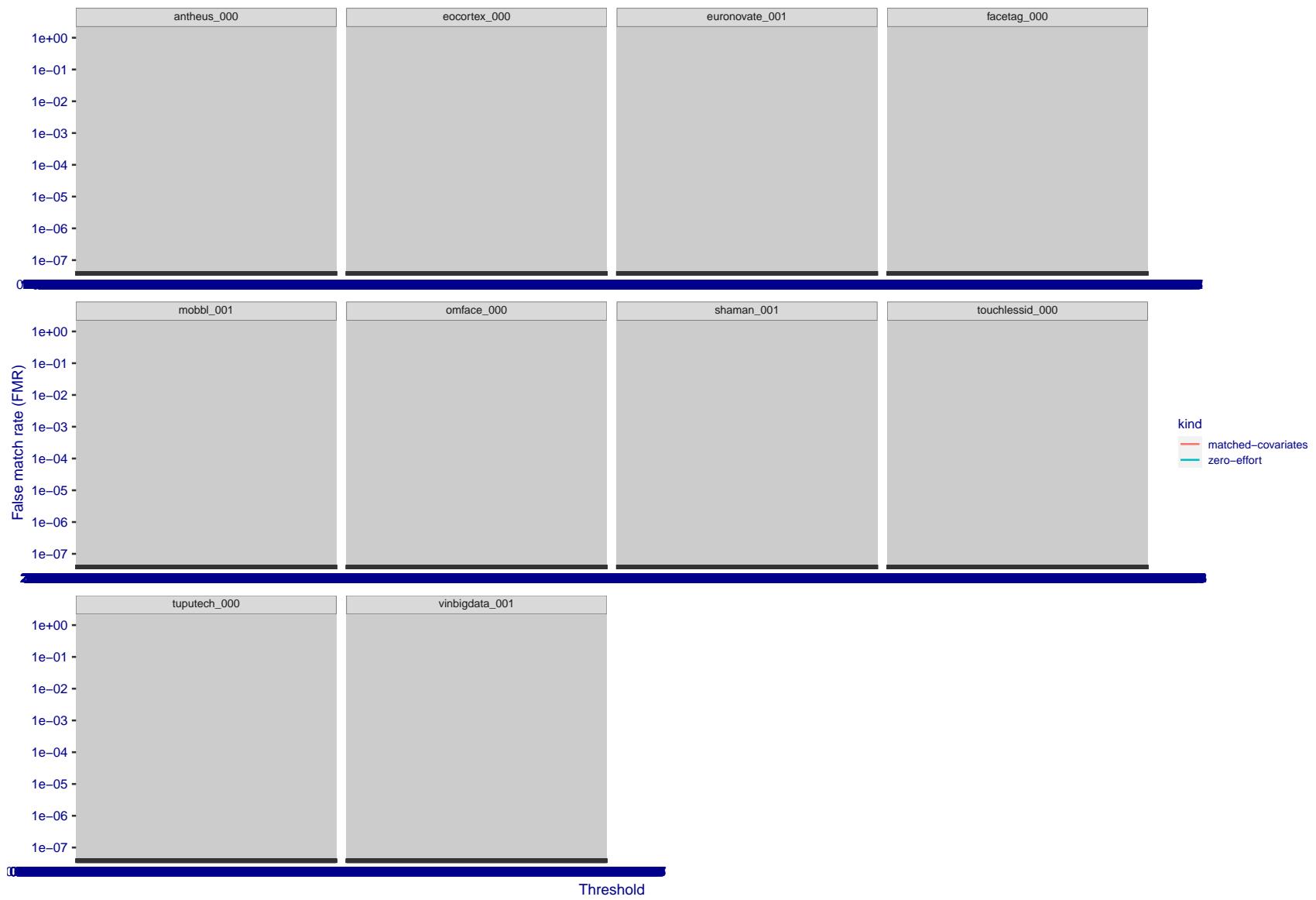


Figure 282: For the visa images, the false match calibration curves show FMR vs. threshold, T . The blue (lower) curves are for zero-effort impostors (i.e. comparing all images against all). The red (upper) curves are for persons of the same-sex, same-age, and same national-origin. This shows that FMR is underestimated (by a factor of 10 or more) by using a zero-effort impostor calculation to calibrate T . As shown later (sec. 3.6), FMR is higher for demographic-matched impostors.

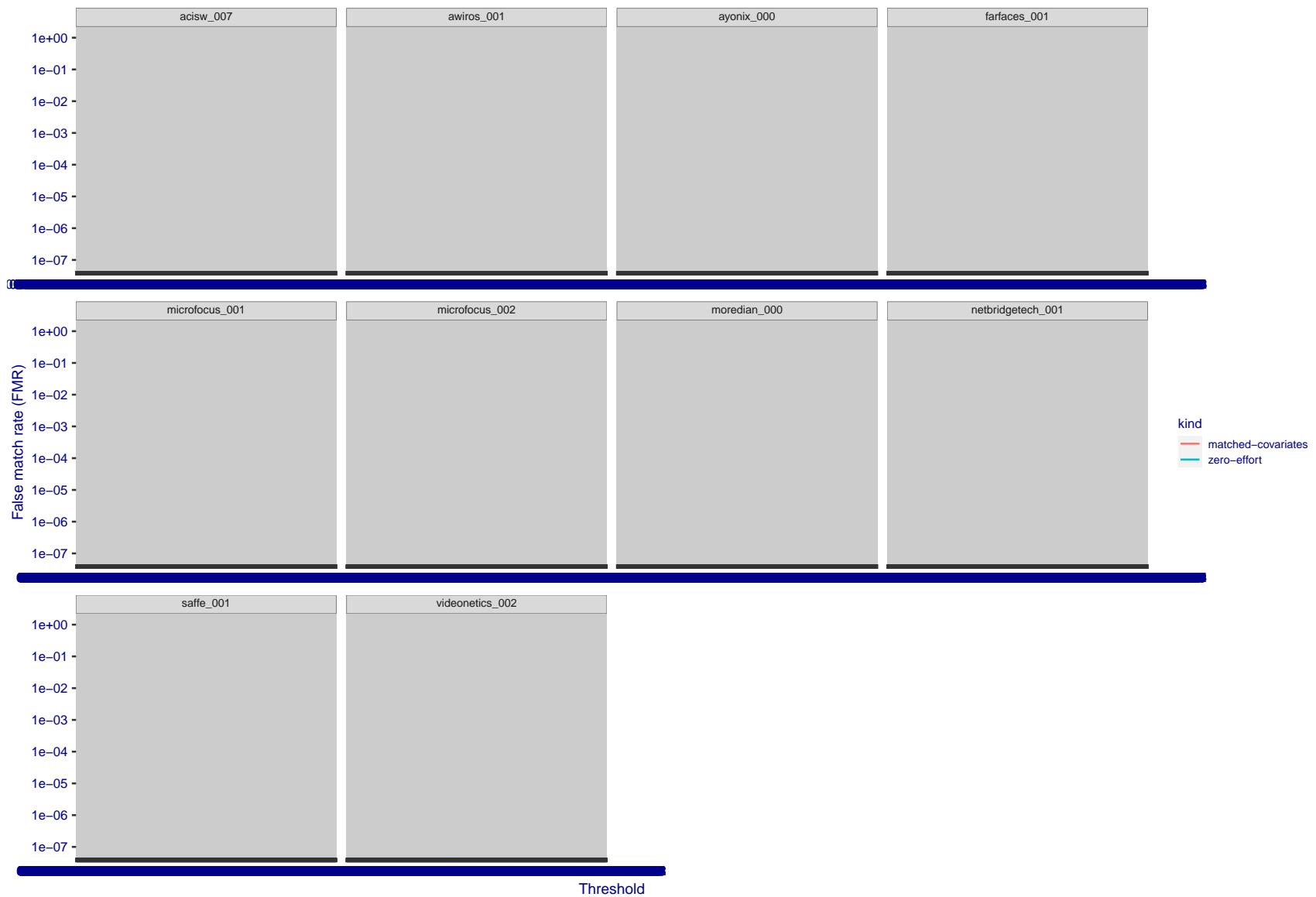


Figure 283: For the visa images, the false match calibration curves show FMR vs. threshold, T . The blue (lower) curves are for zero-effort impostors (i.e. comparing all images against all). The red (upper) curves are for persons of the same-sex, same-age, and same national-origin. This shows that FMR is underestimated (by a factor of 10 or more) by using a zero-effort impostor calculation to calibrate T . As shown later (sec. 3.6), FMR is higher for demographic-matched impostors.

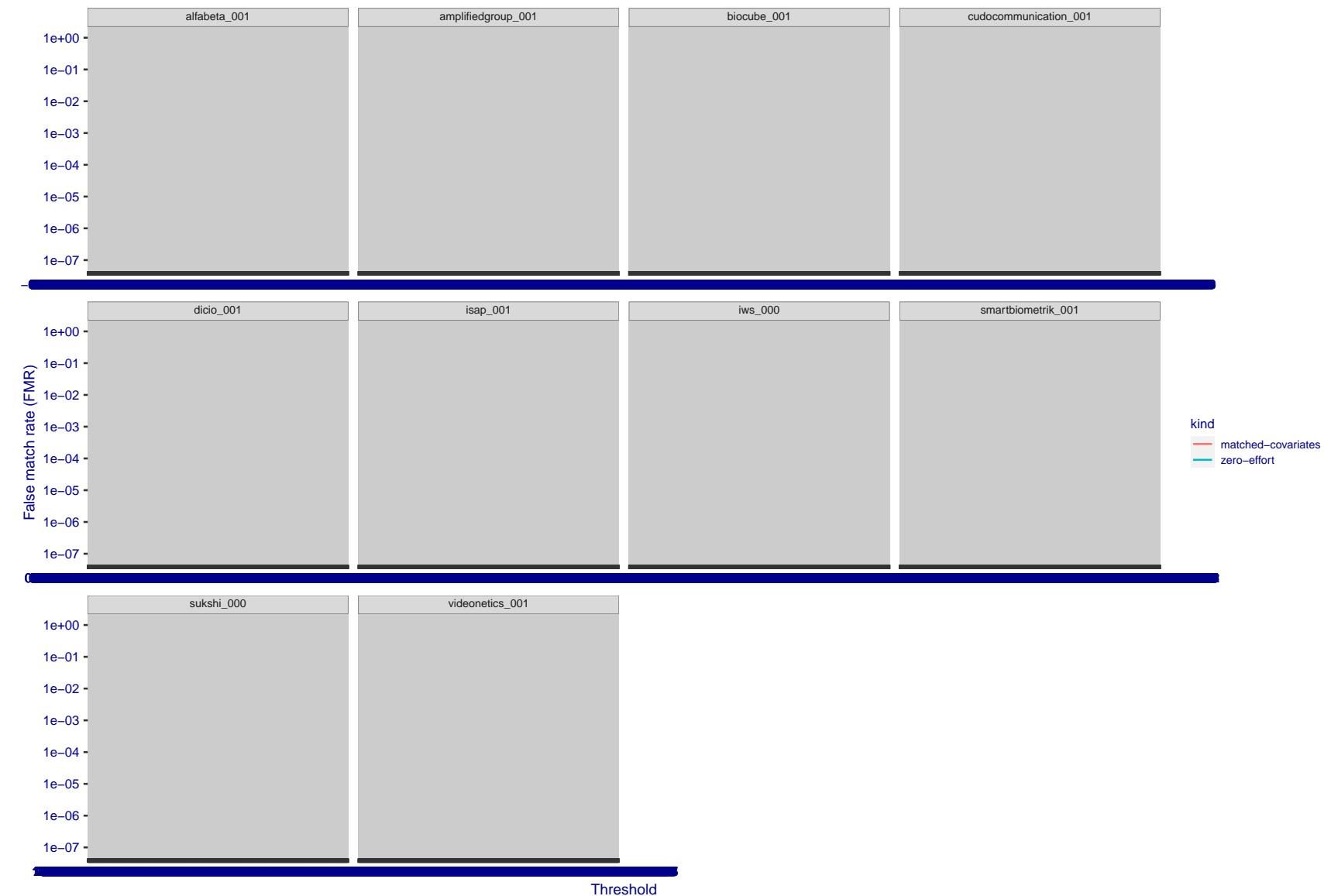


Figure 284: For the visa images, the false match calibration curves show FMR vs. threshold, T . The blue (lower) curves are for zero-effort impostors (i.e. comparing all images against all). The red (upper) curves are for persons of the same-sex, same-age, and same national-origin. This shows that FMR is underestimated (by a factor of 10 or more) by using a zero-effort impostor calculation to calibrate T . As shown later (sec. 3.6), FMR is higher for demographic-matched impostors.

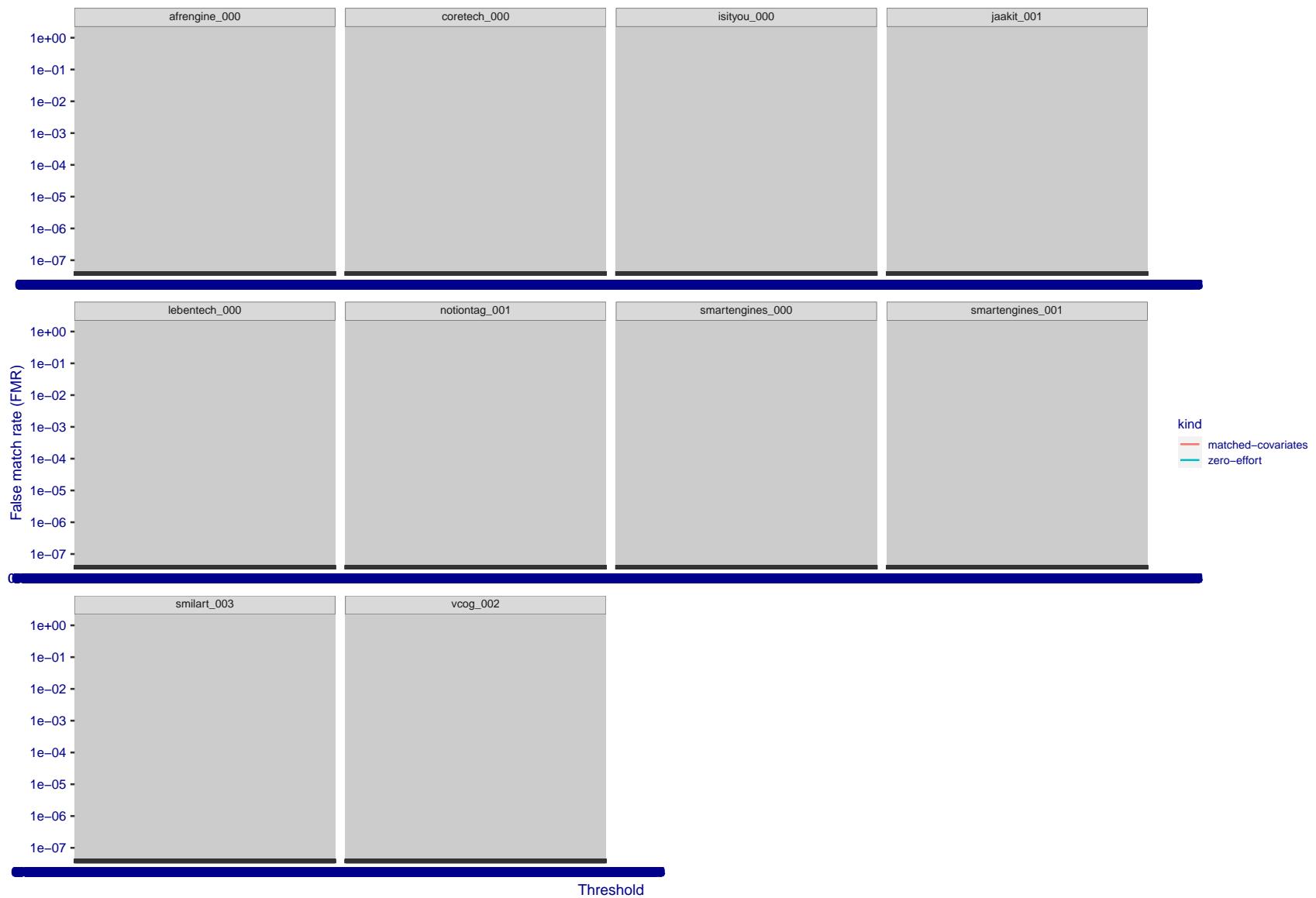


Figure 285: For the visa images, the false match calibration curves show FMR vs. threshold, T . The blue (lower) curves are for zero-effort impostors (i.e. comparing all images against all). The red (upper) curves are for persons of the same-sex, same-age, and same national-origin. This shows that FMR is underestimated (by a factor of 10 or more) by using a zero-effort impostor calculation to calibrate T . As shown later (sec. 3.6), FMR is higher for demographic-matched impostors.

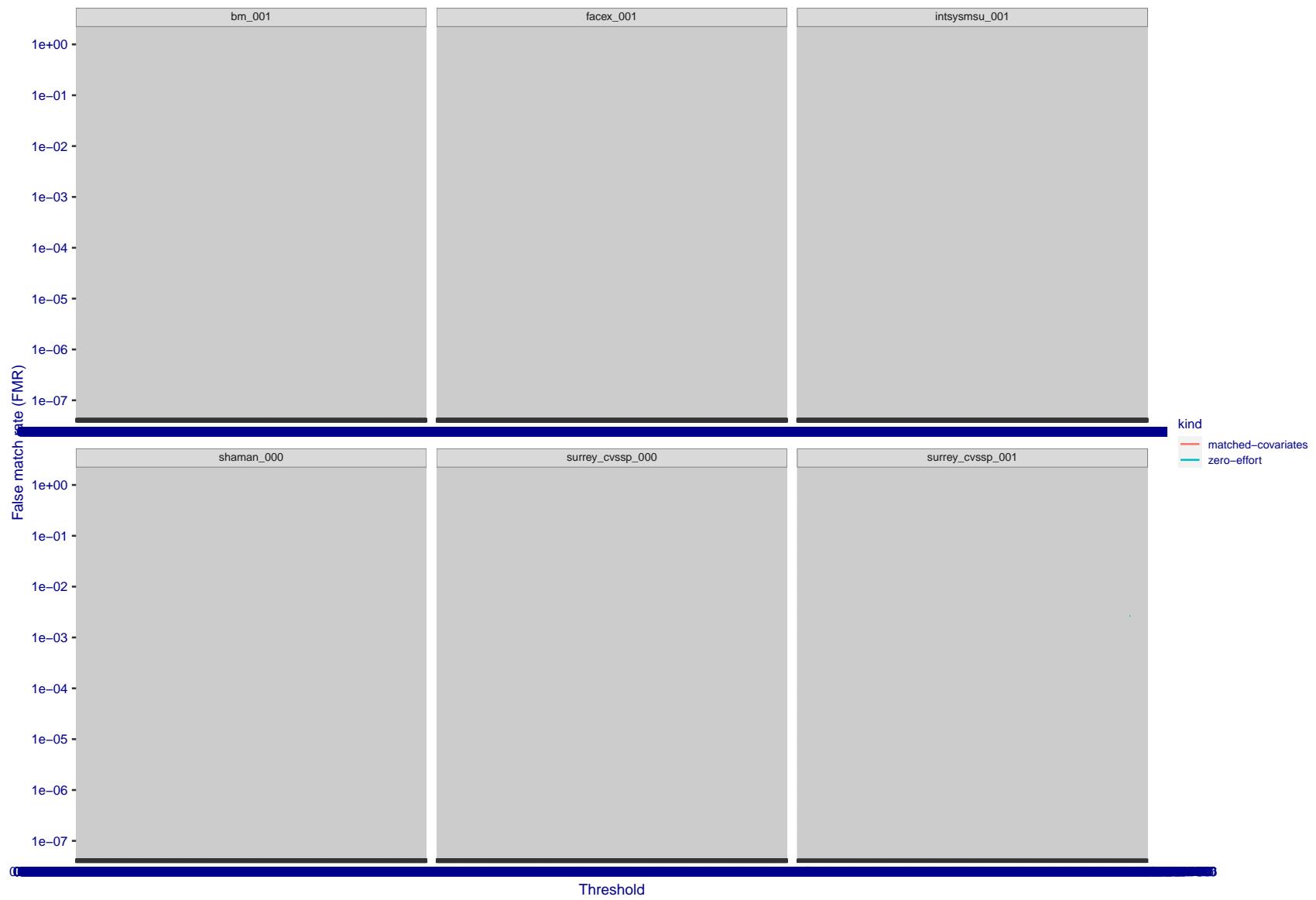


Figure 286: For the visa images, the false match calibration curves show FMR vs. threshold, T . The blue (lower) curves are for zero-effort impostors (i.e. comparing all images against all). The red (upper) curves are for persons of the same-sex, same-age, and same national-origin. This shows that FMR is underestimated (by a factor of 10 or more) by using a zero-effort impostor calculation to calibrate T . As shown later (sec. 3.6), FMR is higher for demographic-matched impostors.



Figure 287: For the visa images, the false match calibration curves show FMR vs. threshold, T . The blue (lower) curves are for zero-effort impostors (i.e. comparing all images against all). The red (upper) curves are for persons of the same-sex, same-age, and same national-origin. This shows that FMR is underestimated (by a factor of 10 or more) by using a zero-effort impostor calculation to calibrate T . As shown later (sec. 3.6), FMR is higher for demographic-matched impostors.

3.5 Genuine distribution stability

3.5.1 Effect of birth place on the genuine distribution

Background: Both skin tone and bone structure vary geographically. Prior studies have reported variations in FNMR and FMR.

Goal: To measure false non-match rate (FNMR) variation with country of birth.

Methods: Thresholds are determined that give $FMR = \{0.001, 0.0001\}$ over the entire impostor set. Then FNMR is measured over 1000 bootstrap replications of the genuine scores. Only those countries with at least 140 individuals are included in the analysis.

Results: Figure 326 shows FNMR by country of birth for the two thresholds.

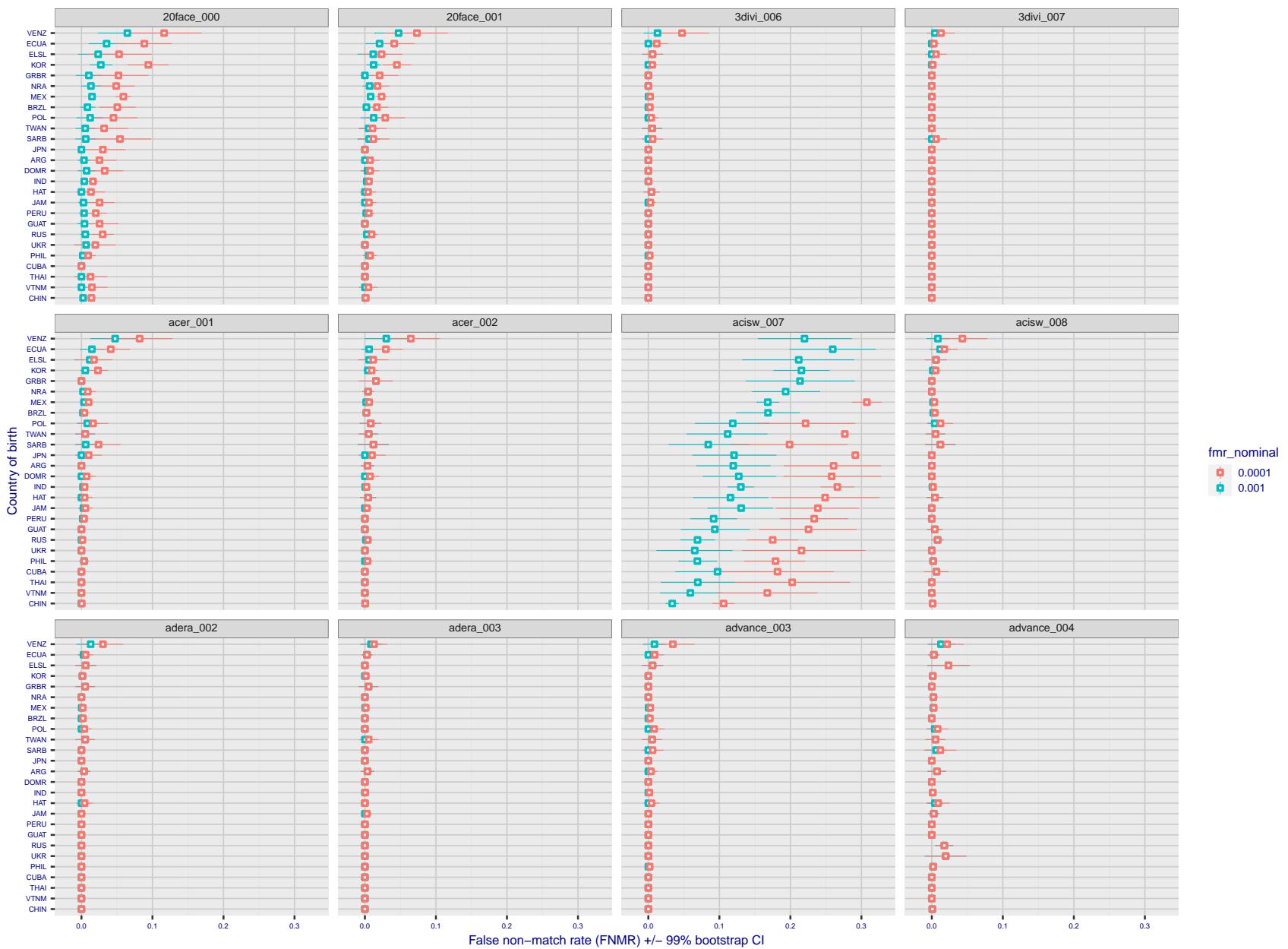


Figure 288: For the visa images, the dots show FNMR by country of birth for two globally set operating thresholds corresponding to $FMR = \{0.001, 0.0001\}$ computed over all on the order of 10^{10} impostor scores. The FMR in each bin will vary also - see subsequent impostor heatmaps in sec. 3.6.1. The figures shows an order of magnitude variation in FNMR across country of birth; these effects are likely due quality variations, then demographics like age and race. The error rates in some cases are zero, and in others the DET is flat so the error rates at the two thresholds are identical. The lines span 1% and 99% of bootstrap replicated FNMR estimates.

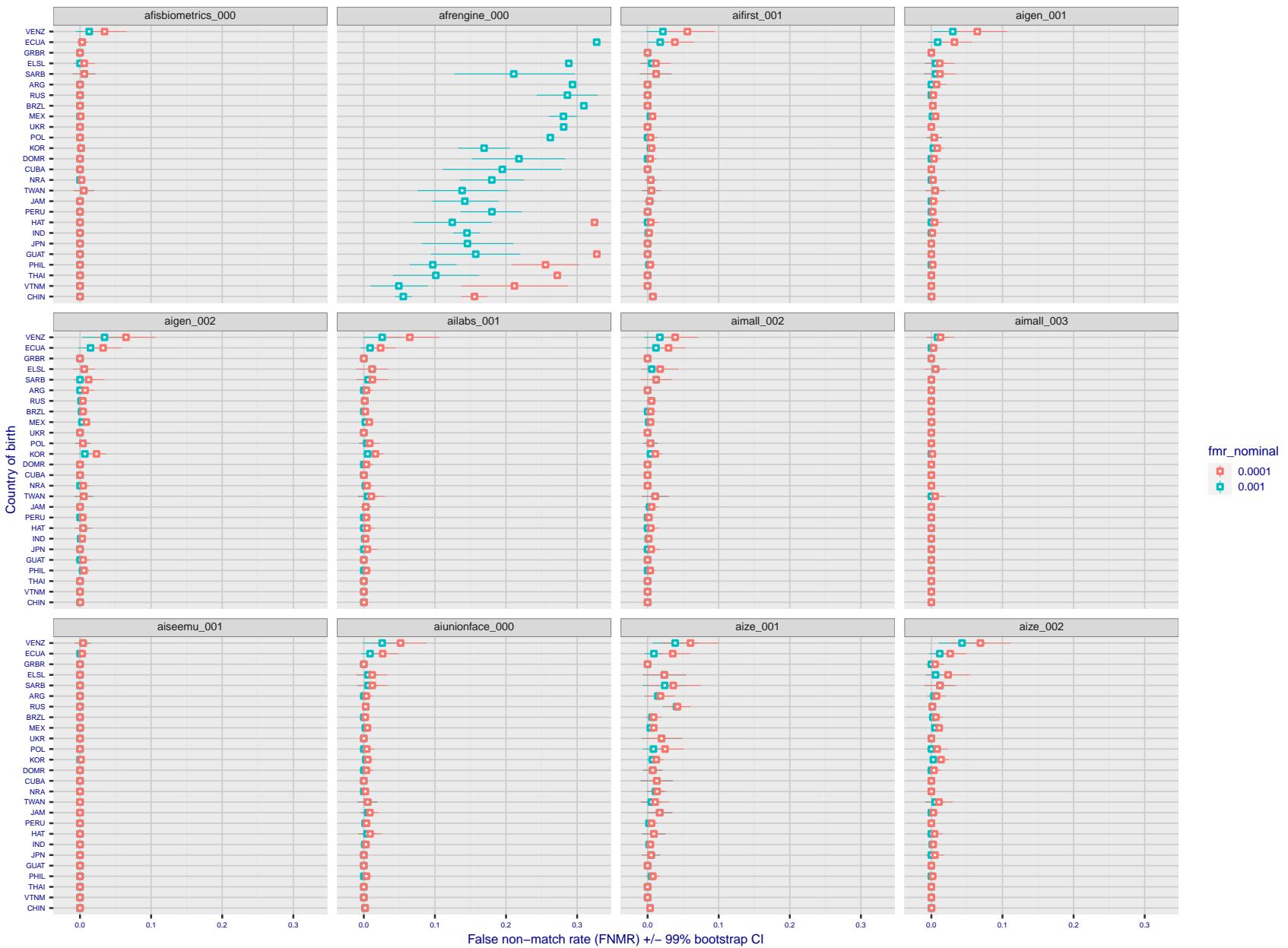


Figure 289: For the visa images, the dots show FNMR by country of birth for two globally set operating thresholds corresponding to $FMR = \{0.001, 0.0001\}$ computed over all on the order of 10^{10} impostor scores. The FMR in each bin will vary also - see subsequent impostor heatmaps in sec. 3.6.1. The figures shows an order of magnitude variation in FNMR across country of birth; these effects are likely due quality variations, then demographics like age and race. The error rates in some cases are zero, and in others the DET is flat so the error rates at the two thresholds are identical. The lines span 1% and 99% of bootstrap replicated FNMR estimates.

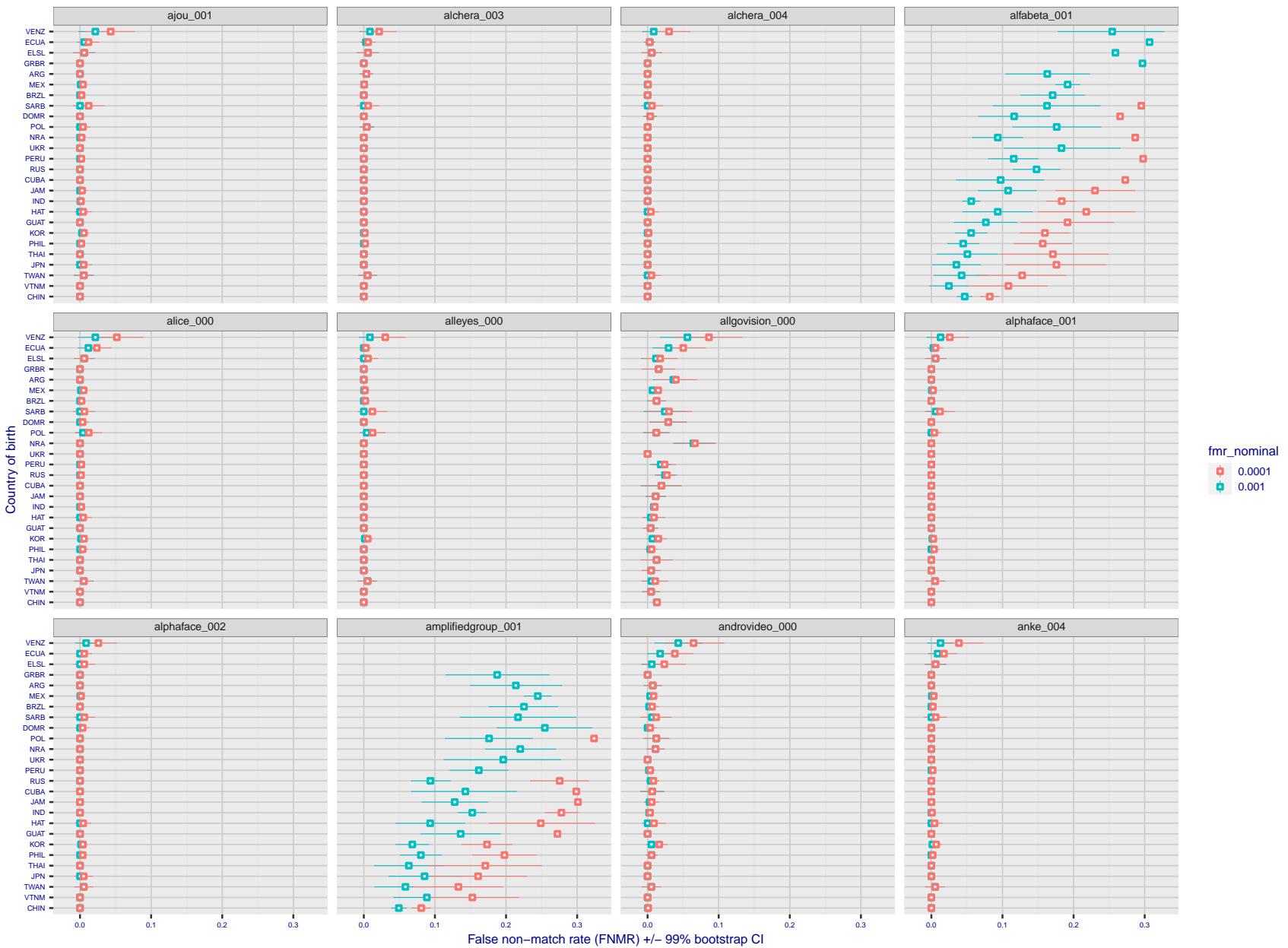


Figure 290: For the visa images, the dots show FNMR by country of birth for two globally set operating thresholds corresponding to $FMR = \{0.001, 0.0001\}$ computed over all on the order of 10^{10} impostor scores. The FMR in each bin will vary also - see subsequent impostor heatmaps in sec. 3.6.1. The figures shows an order of magnitude variation in FNMR across country of birth; these effects are likely due quality variations, then demographics like age and race. The error rates in some cases are zero, and in others the DET is flat so the error rates at the two thresholds are identical. The lines span 1% and 99% of bootstrap replicated FNMR estimates.

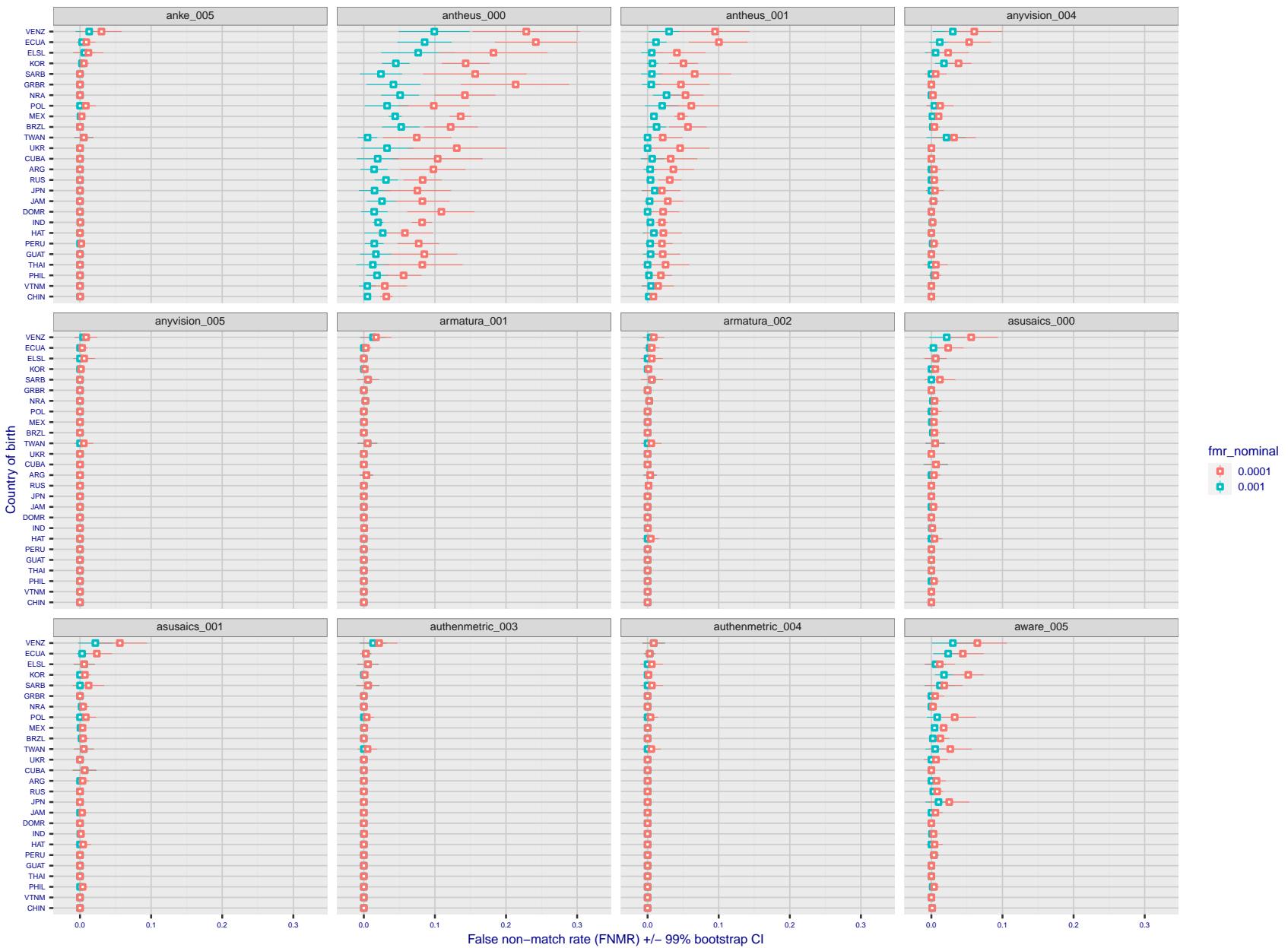


Figure 291: For the visa images, the dots show FNMR by country of birth for two globally set operating thresholds corresponding to $FMR = \{0.001, 0.0001\}$ computed over all on the order of 10^{10} impostor scores. The FMR in each bin will vary also - see subsequent impostor heatmaps in sec. 3.6.1. The figures shows an order of magnitude variation in FNMR across country of birth; these effects are likely due quality variations, then demographics like age and race. The error rates in some cases are zero, and in others the DET is flat so the error rates at the two thresholds are identical. The lines span 1% and 99% of bootstrap replicated FNMR estimates.

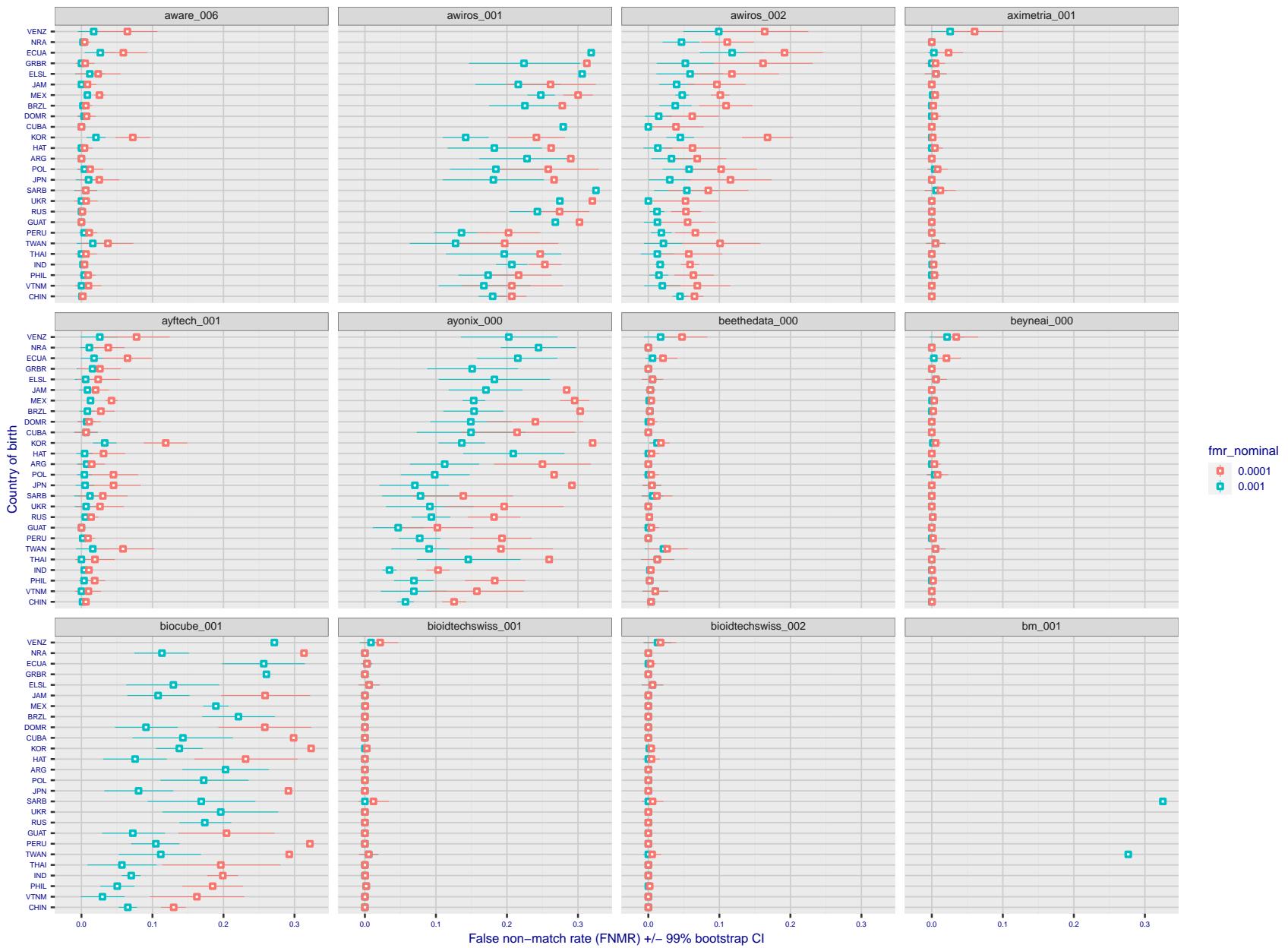


Figure 292: For the visa images, the dots show FNMR by country of birth for two globally set operating thresholds corresponding to $FMR = \{0.001, 0.0001\}$ computed over all on the order of 10^{10} impostor scores. The FMR in each bin will vary also - see subsequent impostor heatmaps in sec. 3.6.1. The figures shows an order of magnitude variation in FNMR across country of birth; these effects are likely due quality variations, then demographics like age and race. The error rates in some cases are zero, and in others the DET is flat so the error rates at the two thresholds are identical. The lines span 1% and 99% of bootstrap replicated FNMR estimates.

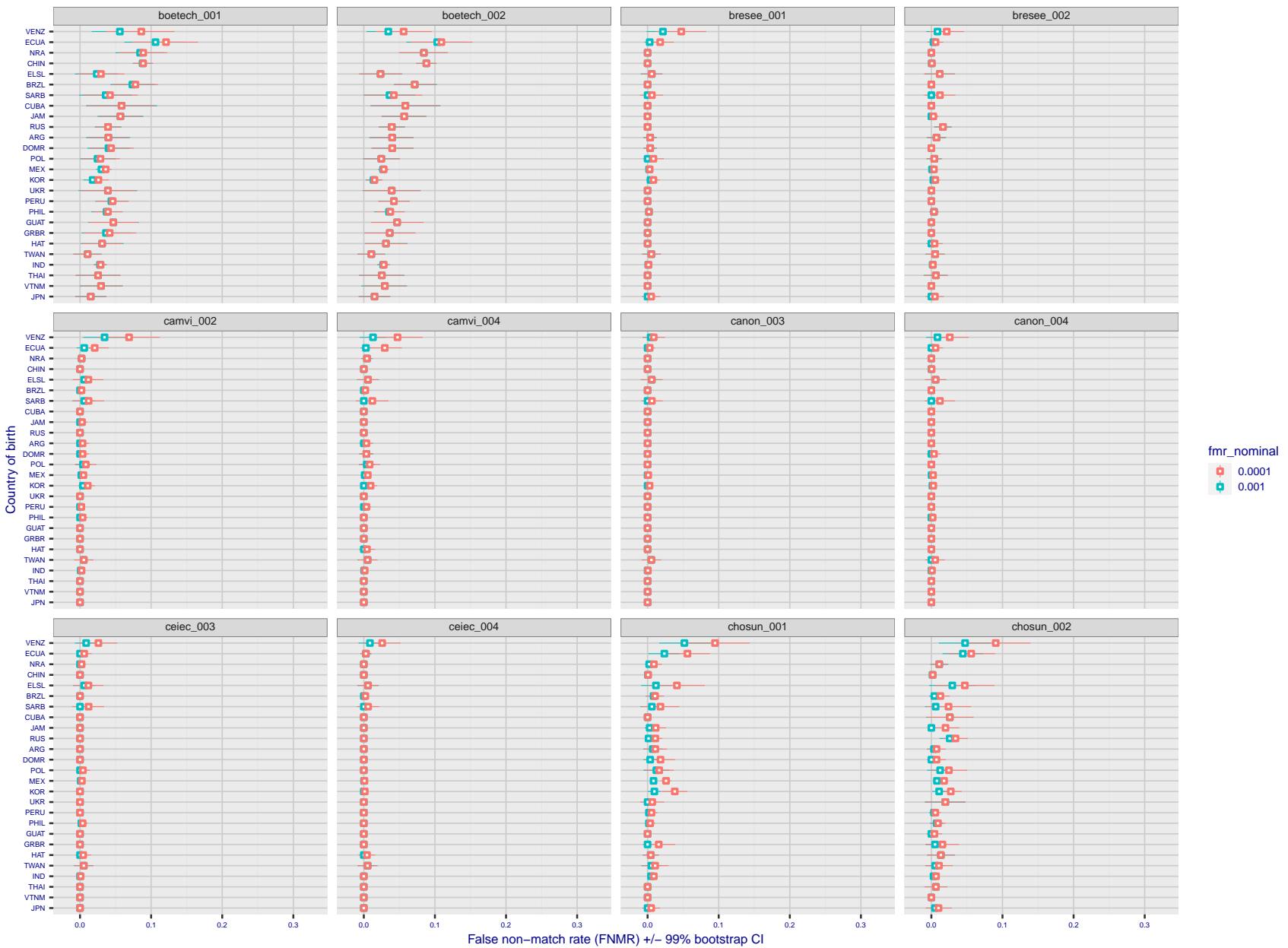


Figure 293: For the visa images, the dots show FNMR by country of birth for two globally set operating thresholds corresponding to $FMR = \{0.001, 0.0001\}$ computed over all on the order of 10^{10} impostor scores. The FMR in each bin will vary also - see subsequent impostor heatmaps in sec. 3.6.1. The figures shows an order of magnitude variation in FNMR across country of birth; these effects are likely due quality variations, then demographics like age and race. The error rates in some cases are zero, and in others the DET is flat so the error rates at the two thresholds are identical. The lines span 1% and 99% of bootstrap replicated FNMR estimates.

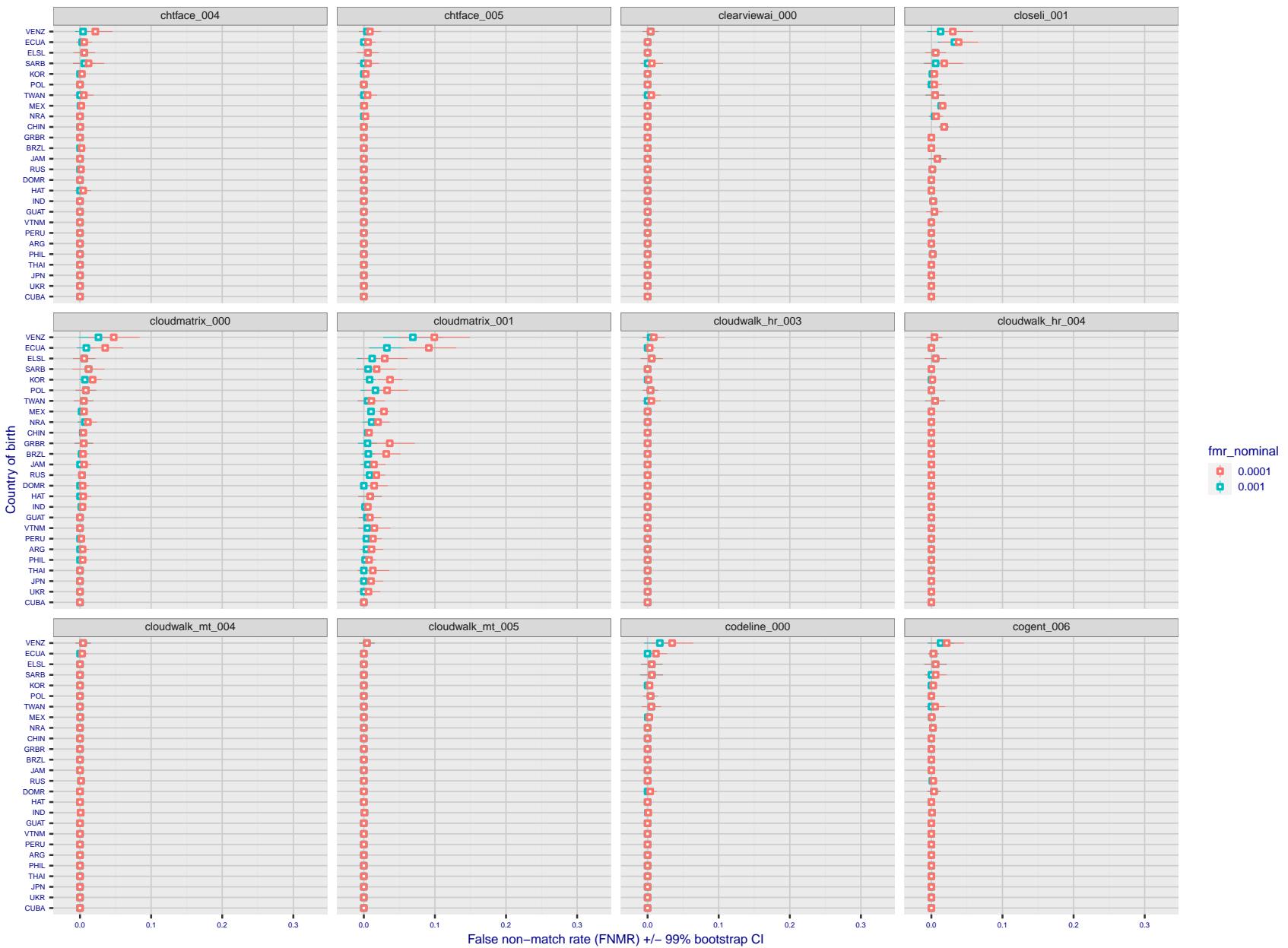


Figure 294: For the visa images, the dots show FNMR by country of birth for two globally set operating thresholds corresponding to $FMR = \{0.001, 0.0001\}$ computed over all on the order of 10^{10} impostor scores. The FMR in each bin will vary also - see subsequent impostor heatmaps in sec. 3.6.1. The figures shows an order of magnitude variation in FNMR across country of birth; these effects are likely due quality variations, then demographics like age and race. The error rates in some cases are zero, and in others the DET is flat so the error rates at the two thresholds are identical. The lines span 1% and 99% of bootstrap replicated FNMR estimates.

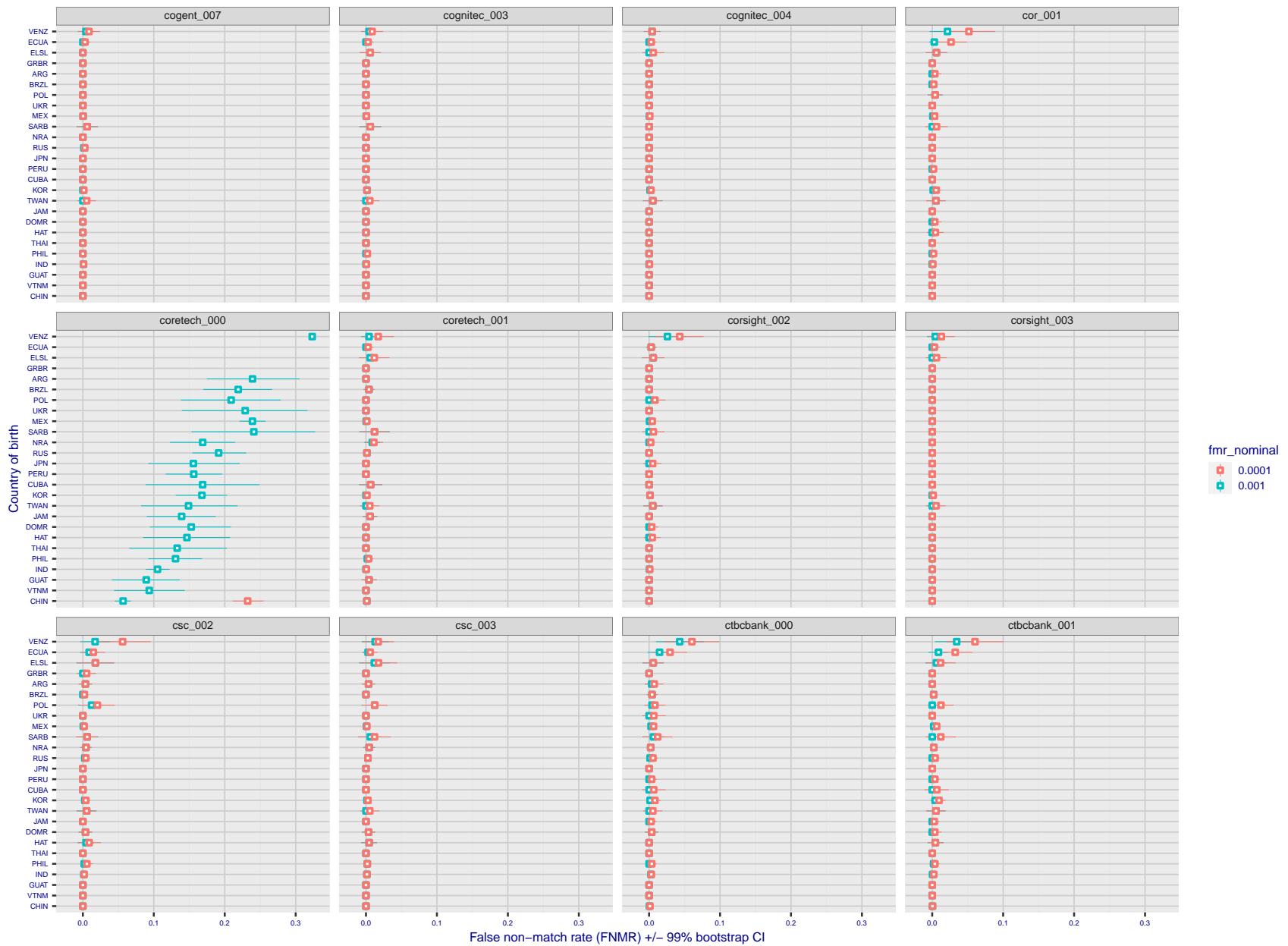


Figure 295: For the visa images, the dots show FNMR by country of birth for two globally set operating thresholds corresponding to $FMR = \{0.001, 0.0001\}$ computed over all on the order of 10^{10} impostor scores. The FMR in each bin will vary also - see subsequent impostor heatmaps in sec. 3.6.1. The figures shows an order of magnitude variation in FNMR across country of birth; these effects are likely due quality variations, then demographics like age and race. The error rates in some cases are zero, and in others the DET is flat so the error rates at the two thresholds are identical. The lines span 1% and 99% of bootstrap replicated FNMR estimates.

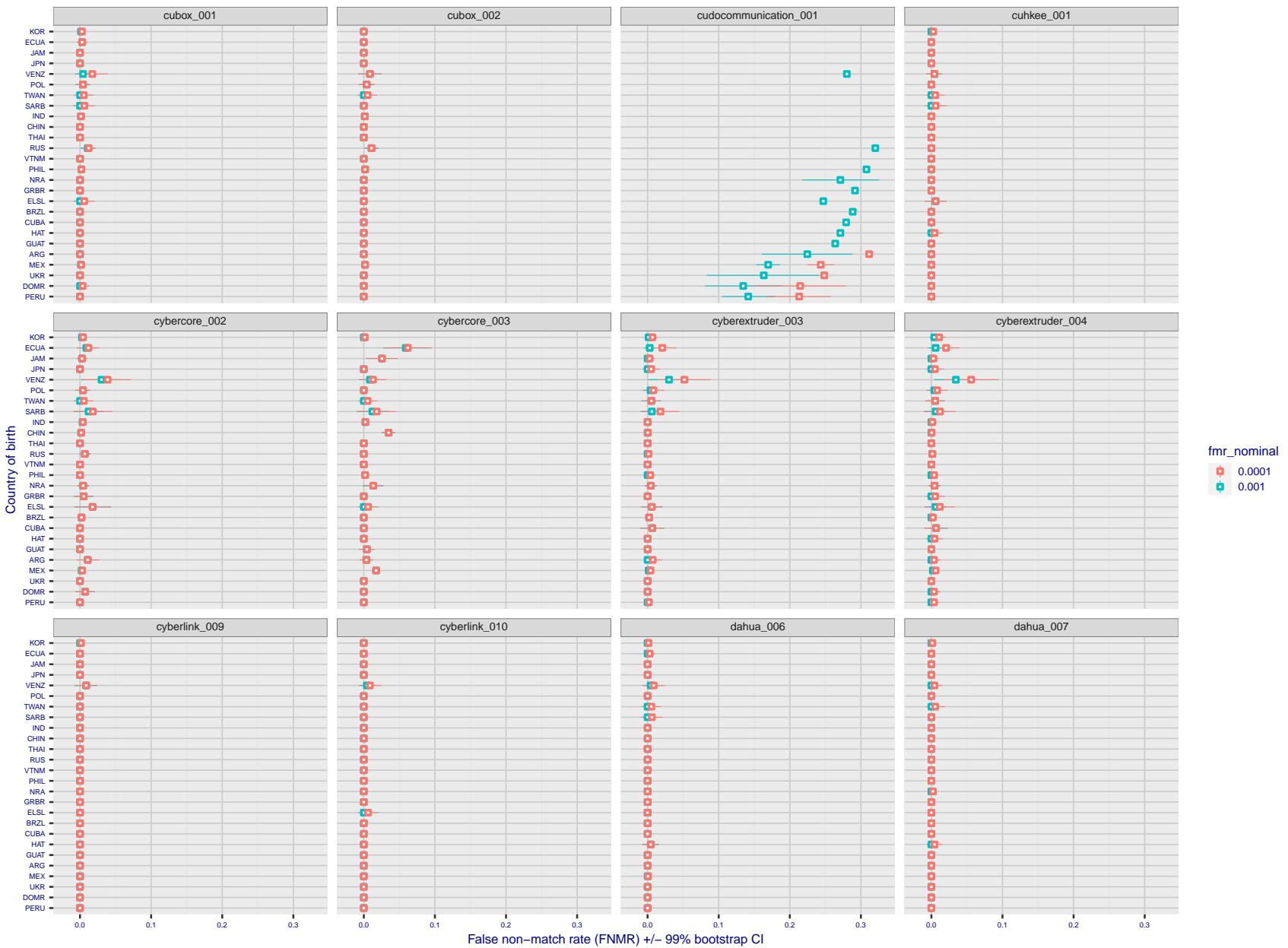


Figure 296: For the visa images, the dots show FNMR by country of birth for two globally set operating thresholds corresponding to $FMR = \{0.001, 0.0001\}$ computed over all on the order of 10^{10} impostor scores. The FMR in each bin will vary also - see subsequent impostor heatmaps in sec. 3.6.1. The figures shows an order of magnitude variation in FNMR across country of birth; these effects are likely due quality variations, then demographics like age and race. The error rates in some cases are zero, and in others the DET is flat so the error rates at the two thresholds are identical. The lines span 1% and 99% of bootstrap replicated FNMR estimates.

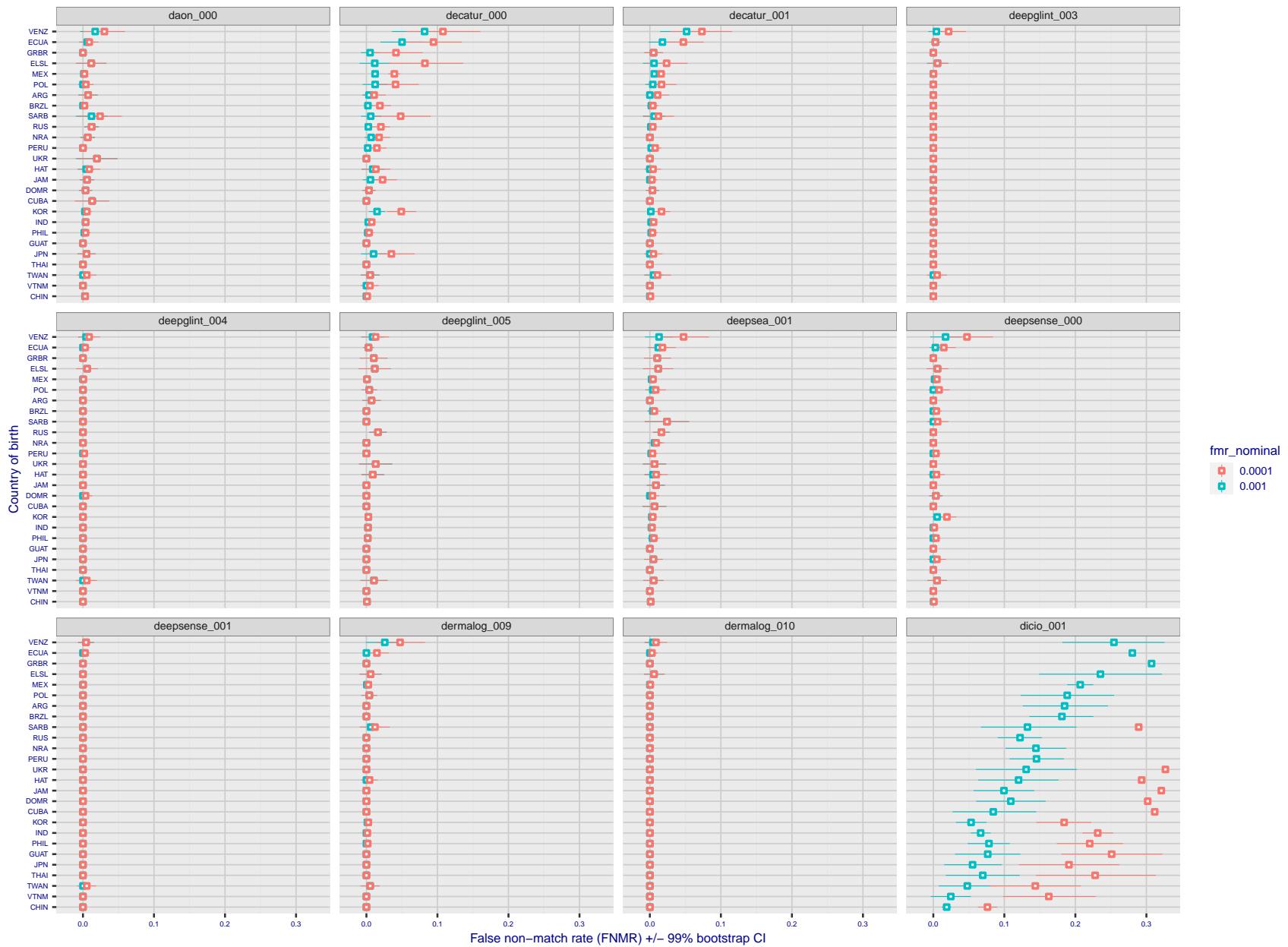


Figure 297: For the visa images, the dots show FNMR by country of birth for two globally set operating thresholds corresponding to $FMR = \{0.001, 0.0001\}$ computed over all on the order of 10^{10} impostor scores. The FMR in each bin will vary also - see subsequent impostor heatmaps in sec. 3.6.1. The figures shows an order of magnitude variation in FNMR across country of birth; these effects are likely due quality variations, then demographics like age and race. The error rates in some cases are zero, and in others the DET is flat so the error rates at the two thresholds are identical. The lines span 1% and 99% of bootstrap replicated FNMR estimates.

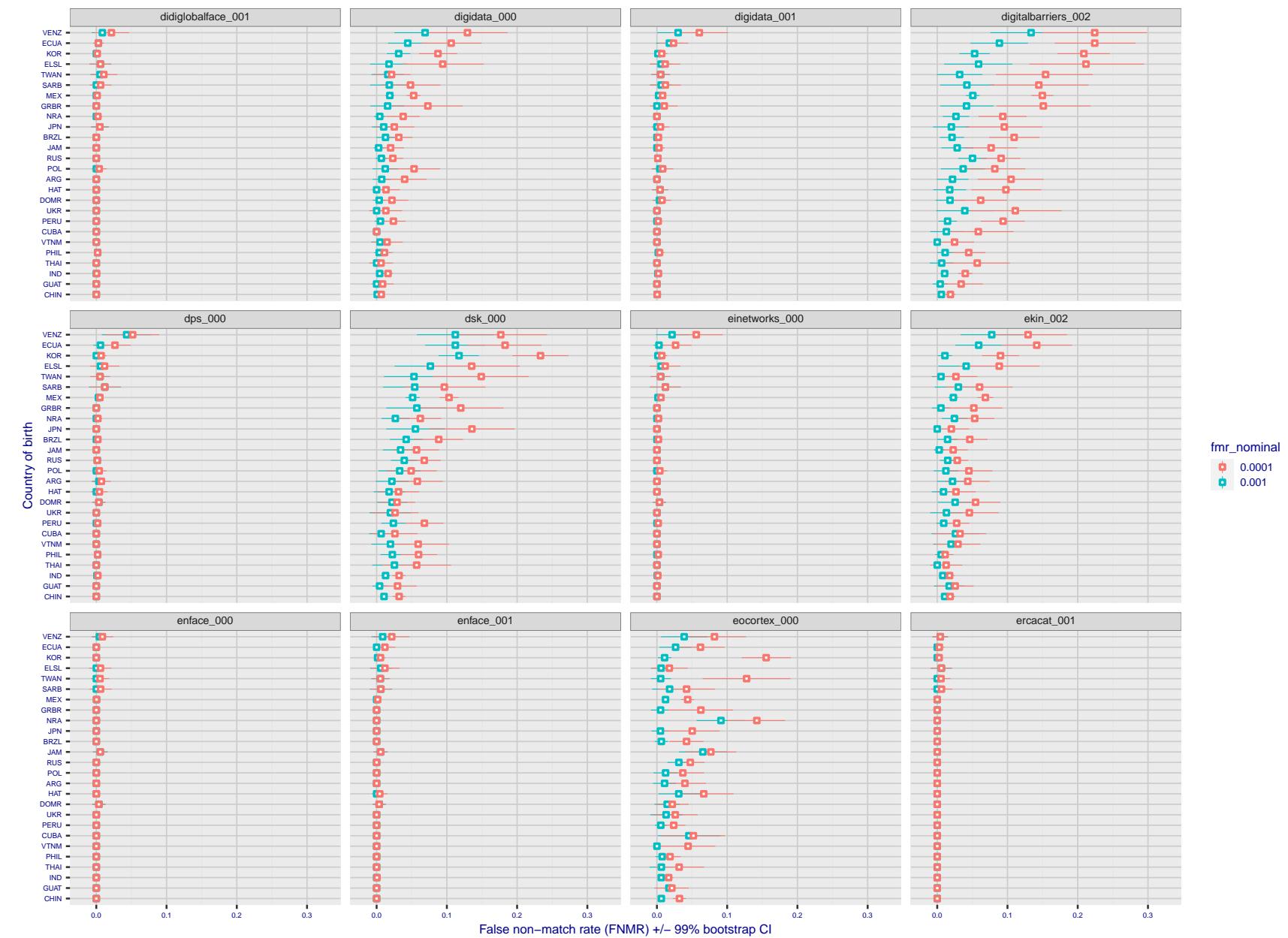


Figure 298: For the visa images, the dots show FNMR by country of birth for two globally set operating thresholds corresponding to $FMR = \{0.001, 0.0001\}$ computed over all on the order of 10^{10} impostor scores. The FMR in each bin will vary also - see subsequent impostor heatmaps in sec. 3.6.1. The figures shows an order of magnitude variation in FNMR across country of birth; these effects are likely due quality variations, then demographics like age and race. The error rates in some cases are zero, and in others the DET is flat so the error rates at the two thresholds are identical. The lines span 1% and 99% of bootstrap replicated FNMR estimates.

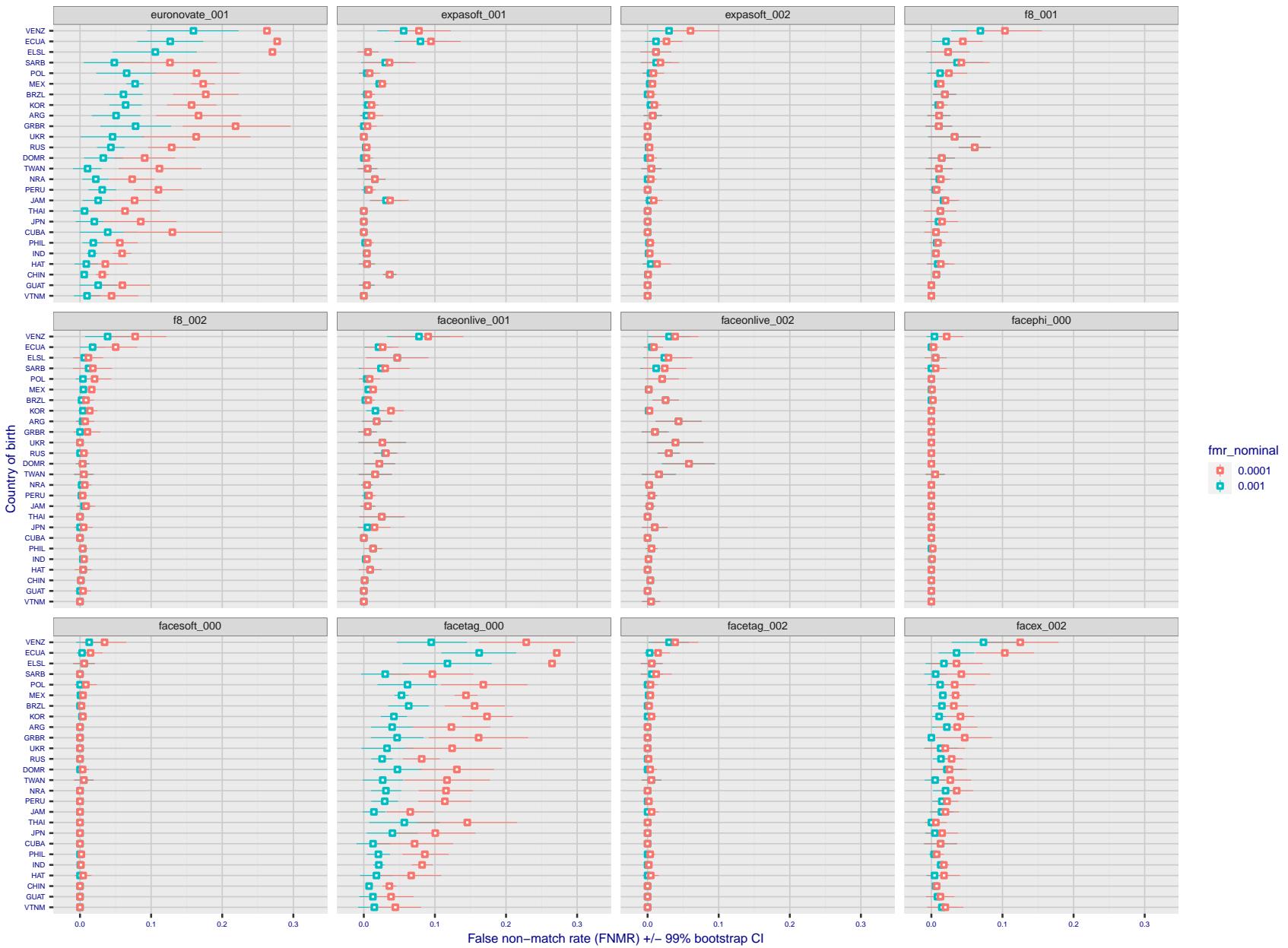


Figure 299: For the visa images, the dots show FNMR by country of birth for two globally set operating thresholds corresponding to $FMR = \{0.001, 0.0001\}$ computed over all on the order of 10^{10} impostor scores. The FMR in each bin will vary also - see subsequent impostor heatmaps in sec. 3.6.1. The figures shows an order of magnitude variation in FNMR across country of birth; these effects are likely due quality variations, then demographics like age and race. The error rates in some cases are zero, and in others the DET is flat so the error rates at the two thresholds are identical. The lines span 1% and 99% of bootstrap replicated FNMR estimates.

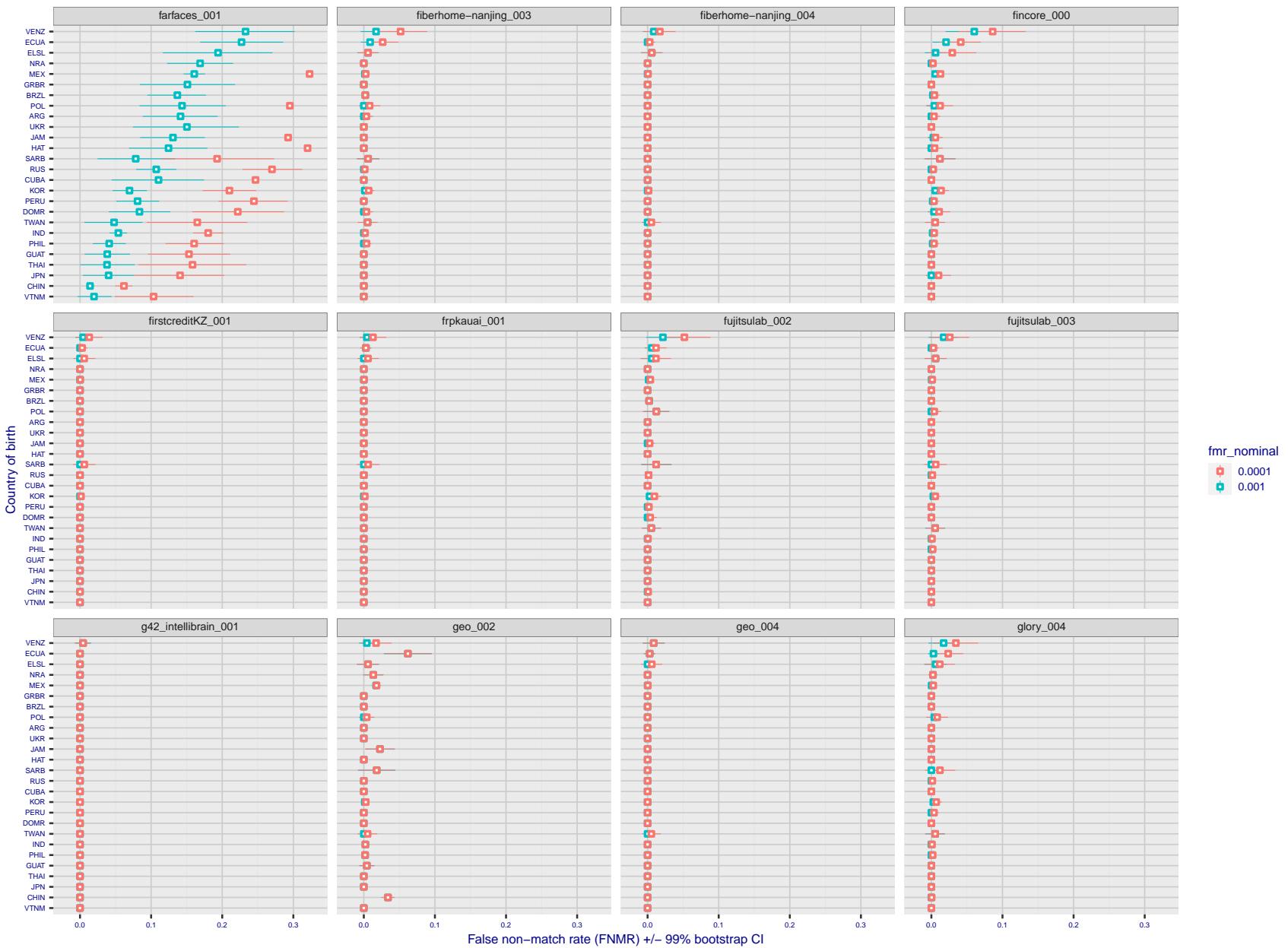


Figure 300: For the visa images, the dots show FNMR by country of birth for two globally set operating thresholds corresponding to $FMR = \{0.001, 0.0001\}$ computed over all on the order of 10^{10} impostor scores. The FMR in each bin will vary also - see subsequent impostor heatmaps in sec. 3.6.1. The figures shows an order of magnitude variation in FNMR across country of birth; these effects are likely due quality variations, then demographics like age and race. The error rates in some cases are zero, and in others the DET is flat so the error rates at the two thresholds are identical. The lines span 1% and 99% of bootstrap replicated FNMR estimates.

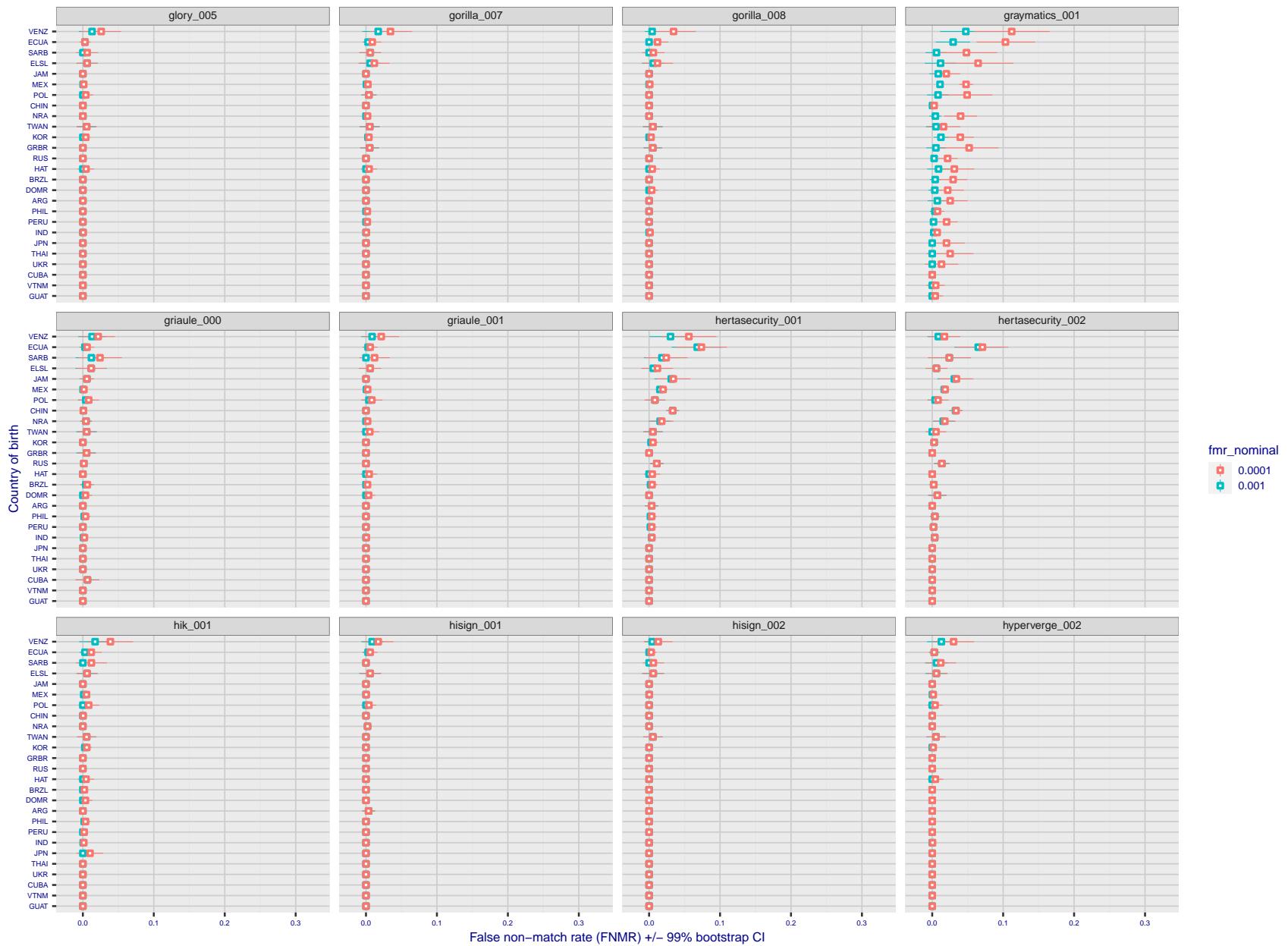


Figure 301: For the visa images, the dots show FNMR by country of birth for two globally set operating thresholds corresponding to $FMR = \{0.001, 0.0001\}$ computed over all on the order of 10^{10} impostor scores. The FMR in each bin will vary also - see subsequent impostor heatmaps in sec. 3.6.1. The figures shows an order of magnitude variation in FNMR across country of birth; these effects are likely due quality variations, then demographics like age and race. The error rates in some cases are zero, and in others the DET is flat so the error rates at the two thresholds are identical. The lines span 1% and 99% of bootstrap replicated FNMR estimates.

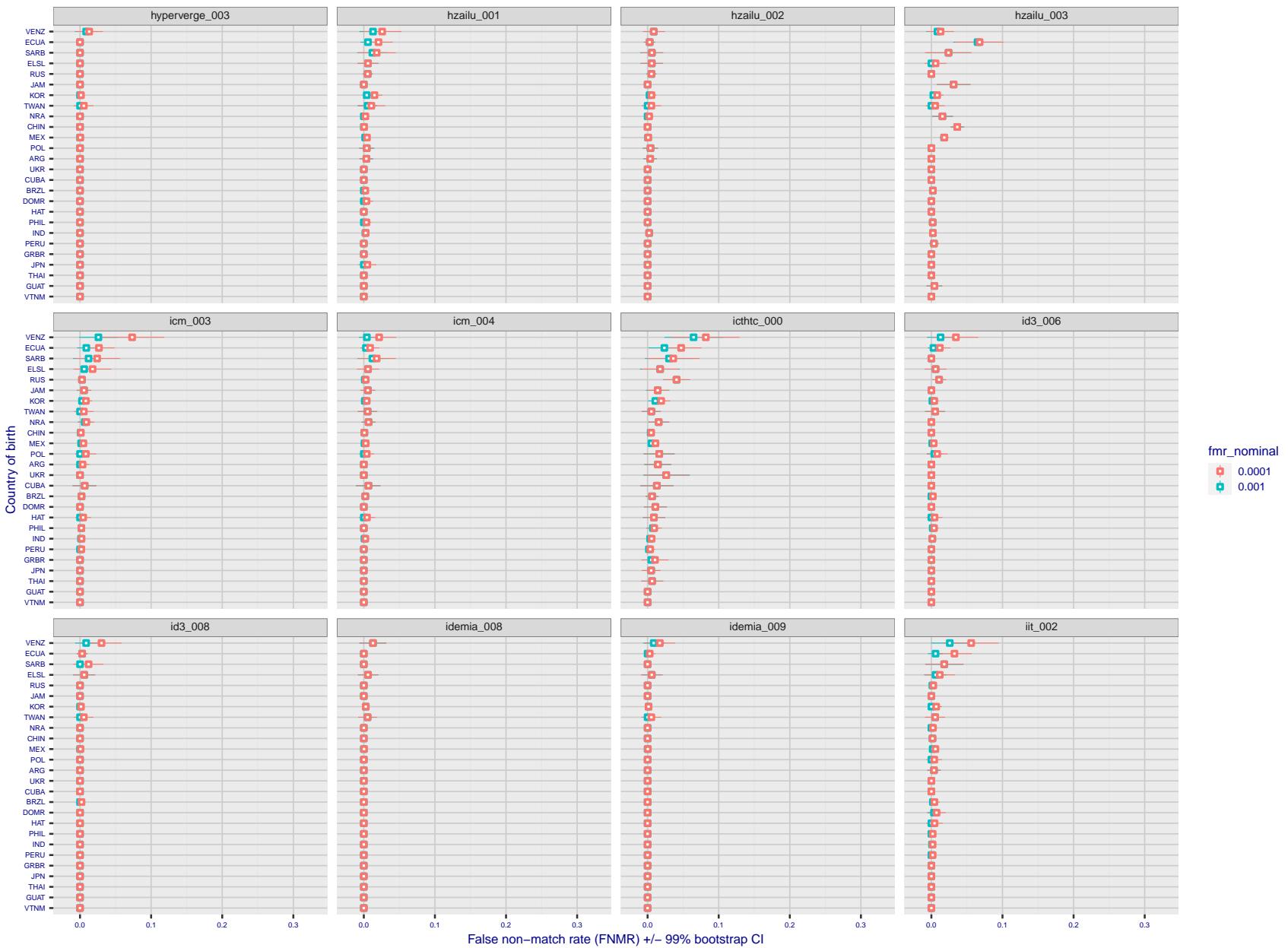


Figure 302: For the visa images, the dots show FNMR by country of birth for two globally set operating thresholds corresponding to $FMR = \{0.001, 0.0001\}$ computed over all on the order of 10^{10} impostor scores. The FMR in each bin will vary also - see subsequent impostor heatmaps in sec. 3.6.1. The figures shows an order of magnitude variation in FNMR across country of birth; these effects are likely due quality variations, then demographics like age and race. The error rates in some cases are zero, and in others the DET is flat so the error rates at the two thresholds are identical. The lines span 1% and 99% of bootstrap replicated FNMR estimates.

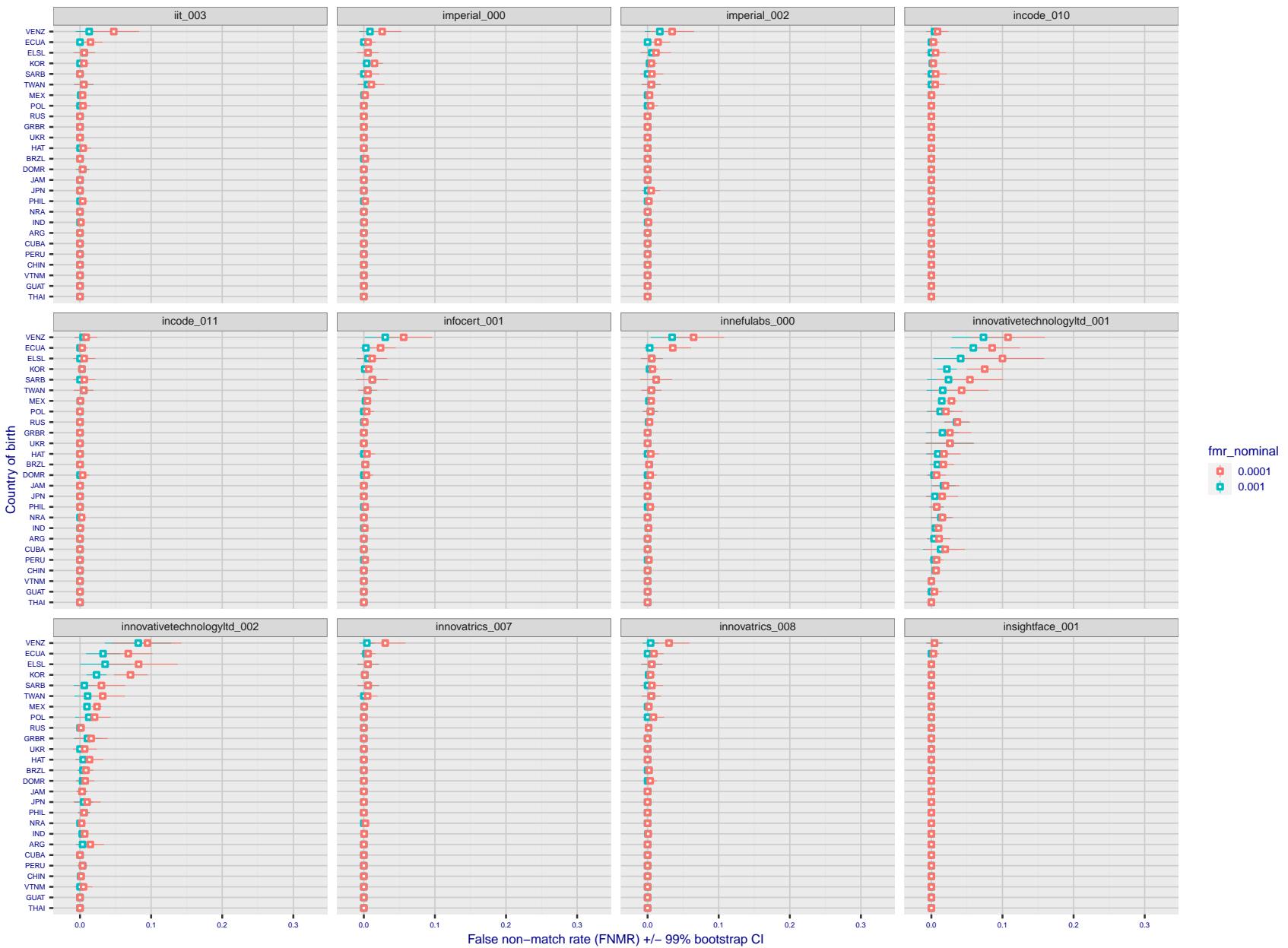


Figure 303: For the visa images, the dots show FNMR by country of birth for two globally set operating thresholds corresponding to $FMR = \{0.001, 0.0001\}$ computed over all on the order of 10^{10} impostor scores. The FMR in each bin will vary also - see subsequent impostor heatmaps in sec. 3.6.1. The figures shows an order of magnitude variation in FNMR across country of birth; these effects are likely due quality variations, then demographics like age and race. The error rates in some cases are zero, and in others the DET is flat so the error rates at the two thresholds are identical. The lines span 1% and 99% of bootstrap replicated FNMR estimates.

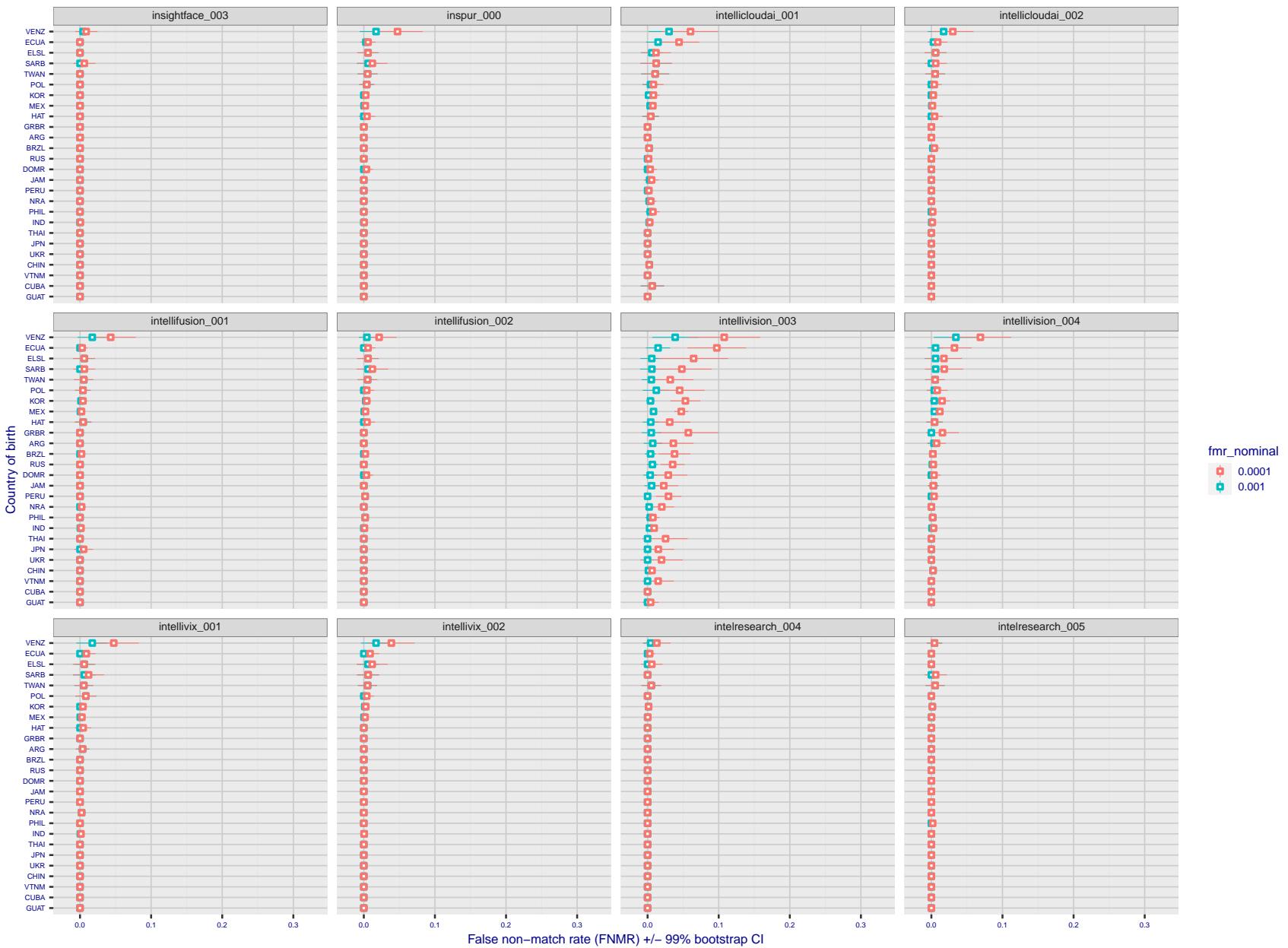


Figure 304: For the visa images, the dots show FNMR by country of birth for two globally set operating thresholds corresponding to $FMR = \{0.001, 0.0001\}$ computed over all on the order of 10^{10} impostor scores. The FMR in each bin will vary also - see subsequent impostor heatmaps in sec. 3.6.1. The figures shows an order of magnitude variation in FNMR across country of birth; these effects are likely due quality variations, then demographics like age and race. The error rates in some cases are zero, and in others the DET is flat so the error rates at the two thresholds are identical. The lines span 1% and 99% of bootstrap replicated FNMR estimates.

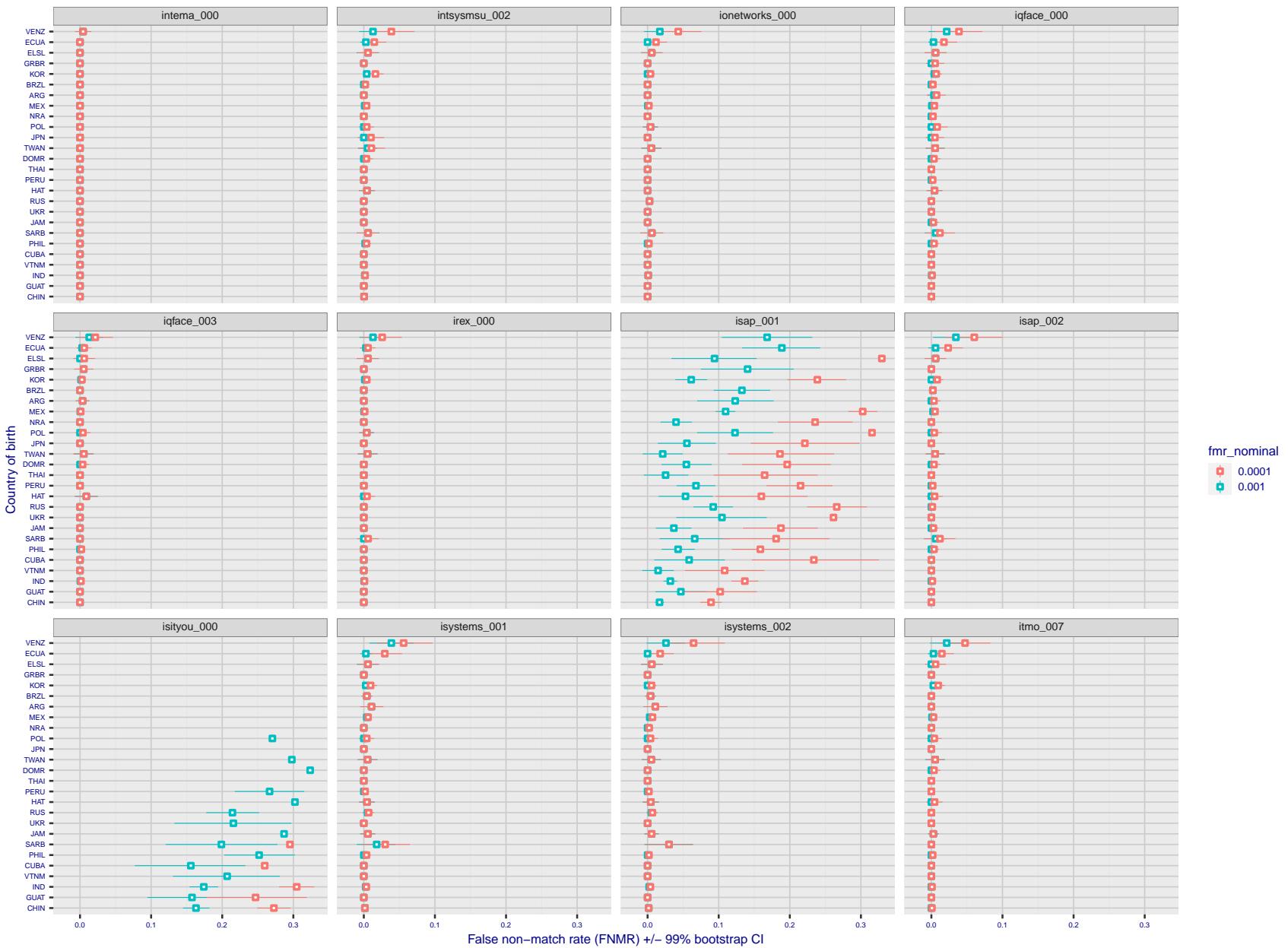


Figure 305: For the visa images, the dots show FNMR by country of birth for two globally set operating thresholds corresponding to $FMR = \{0.001, 0.0001\}$ computed over all on the order of 10^{10} impostor scores. The FMR in each bin will vary also - see subsequent impostor heatmaps in sec. 3.6.1. The figures shows an order of magnitude variation in FNMR across country of birth; these effects are likely due quality variations, then demographics like age and race. The error rates in some cases are zero, and in others the DET is flat so the error rates at the two thresholds are identical. The lines span 1% and 99% of bootstrap replicated FNMR estimates.

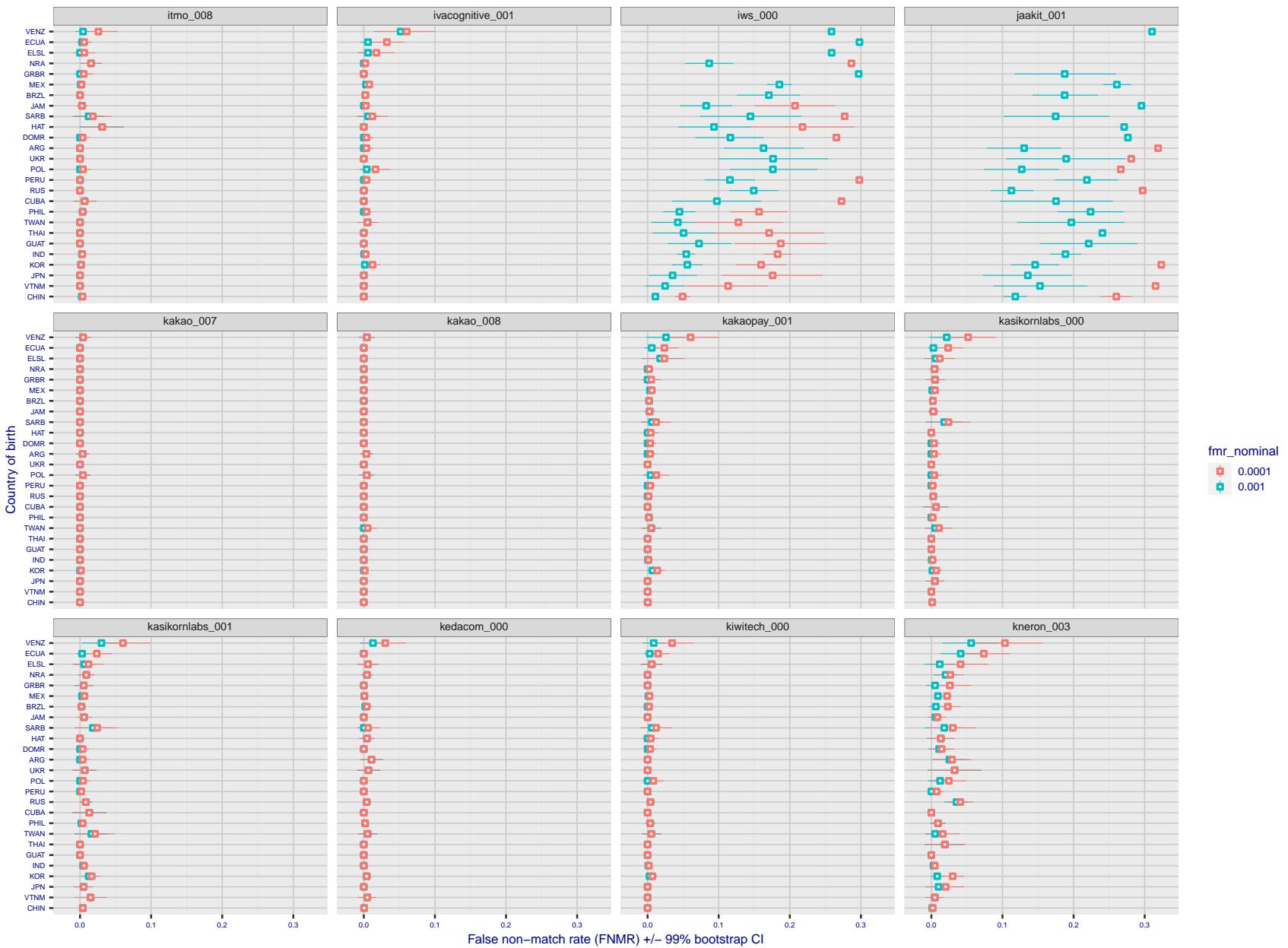


Figure 306: For the visa images, the dots show FNMR by country of birth for two globally set operating thresholds corresponding to $FMR = \{0.001, 0.0001\}$ computed over all on the order of 10^{10} impostor scores. The FMR in each bin will vary also - see subsequent impostor heatmaps in sec. 3.6.1. The figures shows an order of magnitude variation in FNMR across country of birth; these effects are likely due quality variations, then demographics like age and race. The error rates in some cases are zero, and in others the DET is flat so the error rates at the two thresholds are identical. The lines span 1% and 99% of bootstrap replicated FNMR estimates.

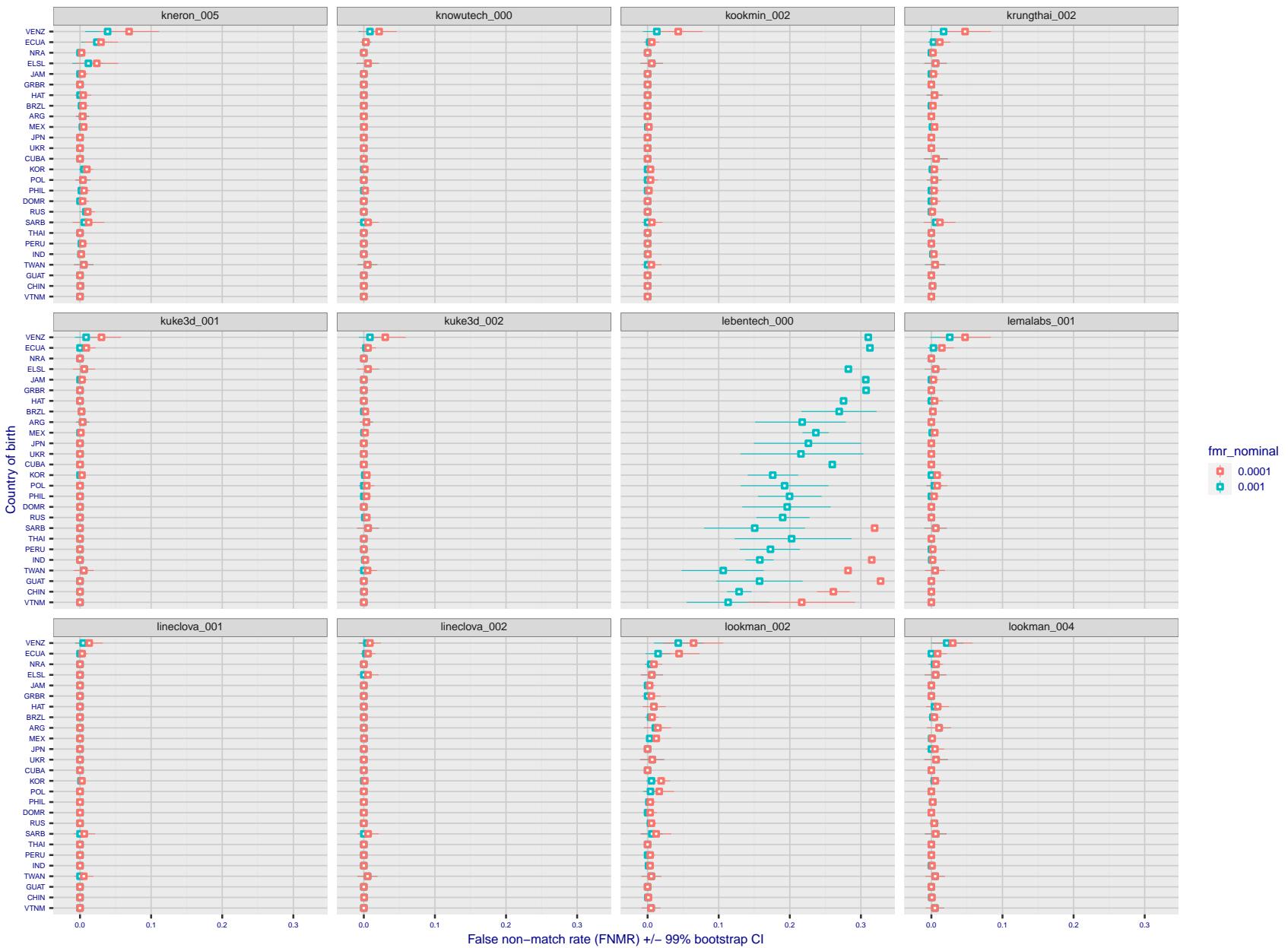


Figure 307: For the visa images, the dots show FNMR by country of birth for two globally set operating thresholds corresponding to $FMR = \{0.001, 0.0001\}$ computed over all on the order of 10^{10} impostor scores. The FMR in each bin will vary also - see subsequent impostor heatmaps in sec. 3.6.1. The figures shows an order of magnitude variation in FNMR across country of birth; these effects are likely due quality variations, then demographics like age and race. The error rates in some cases are zero, and in others the DET is flat so the error rates at the two thresholds are identical. The lines span 1% and 99% of bootstrap replicated FNMR estimates.

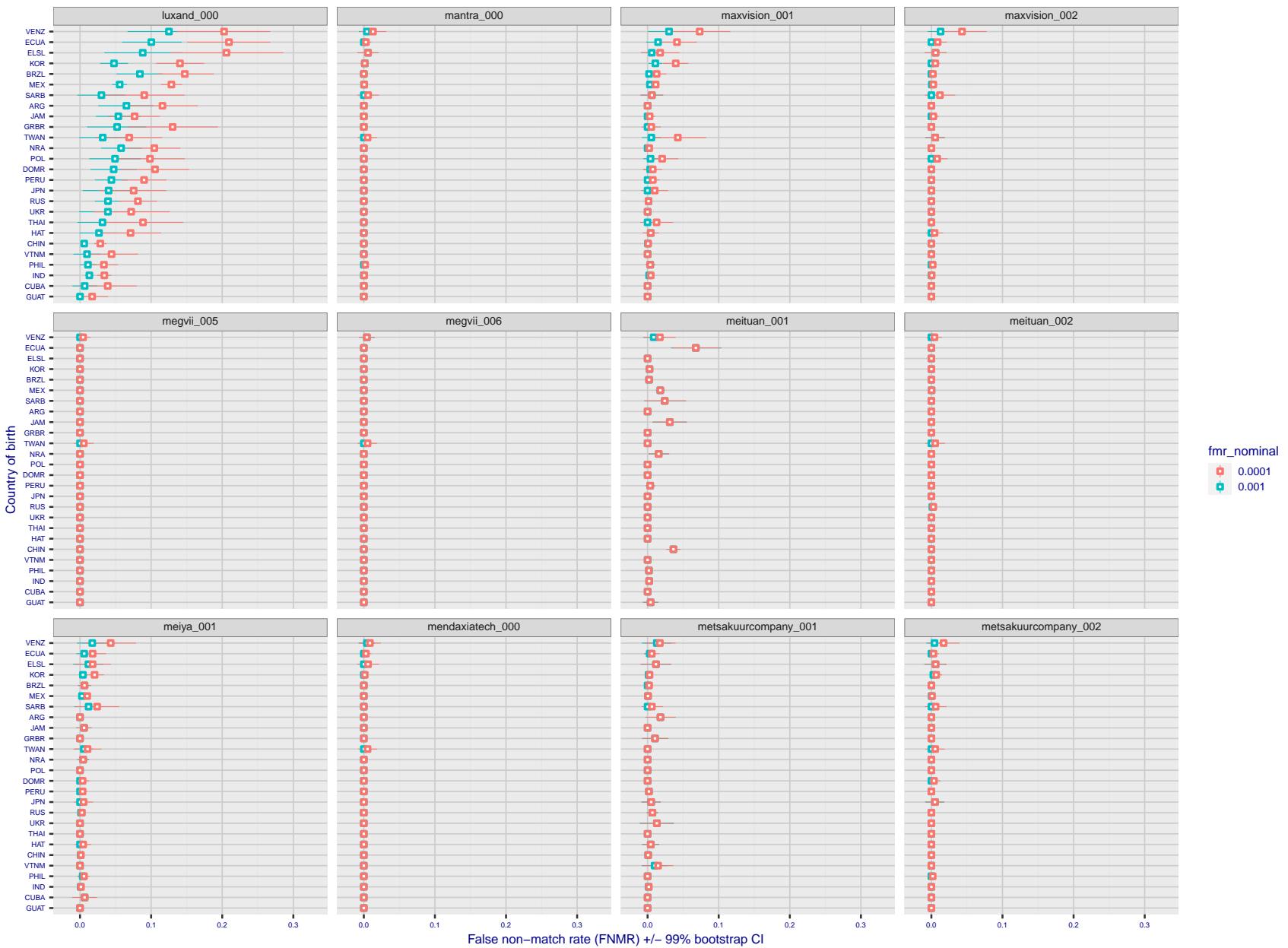


Figure 308: For the visa images, the dots show FNMR by country of birth for two globally set operating thresholds corresponding to $FMR = \{0.001, 0.0001\}$ computed over all on the order of 10^{10} impostor scores. The FMR in each bin will vary also - see subsequent impostor heatmaps in sec. 3.6.1. The figures shows an order of magnitude variation in FNMR across country of birth; these effects are likely due quality variations, then demographics like age and race. The error rates in some cases are zero, and in others the DET is flat so the error rates at the two thresholds are identical. The lines span 1% and 99% of bootstrap replicated FNMR estimates.

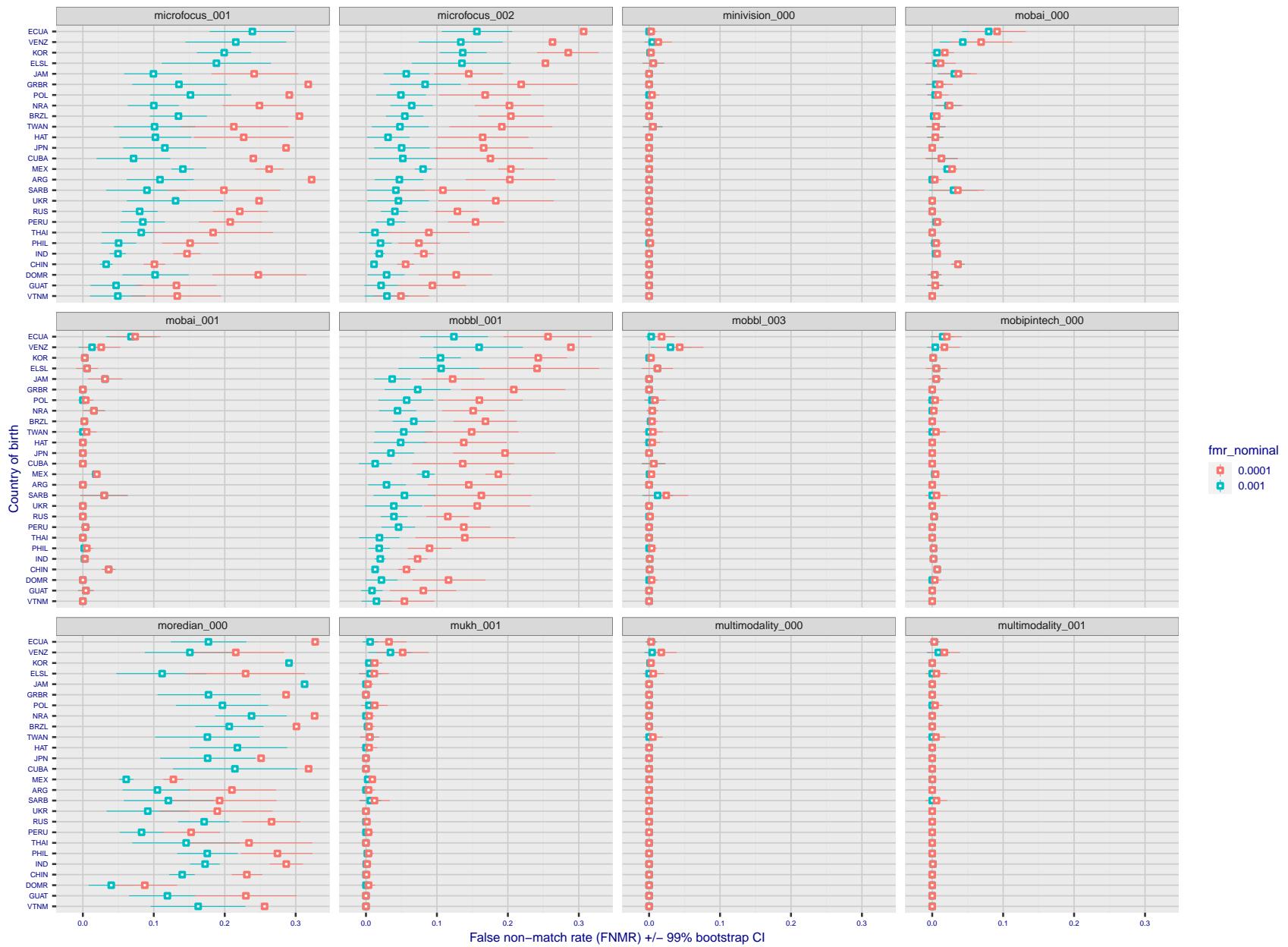


Figure 309: For the visa images, the dots show FNMR by country of birth for two globally set operating thresholds corresponding to $FMR = \{0.001, 0.0001\}$ computed over all on the order of 10^{10} impostor scores. The FMR in each bin will vary also - see subsequent impostor heatmaps in sec. 3.6.1. The figures shows an order of magnitude variation in FNMR across country of birth; these effects are likely due quality variations, then demographics like age and race. The error rates in some cases are zero, and in others the DET is flat so the error rates at the two thresholds are identical. The lines span 1% and 99% of bootstrap replicated FNMR estimates.

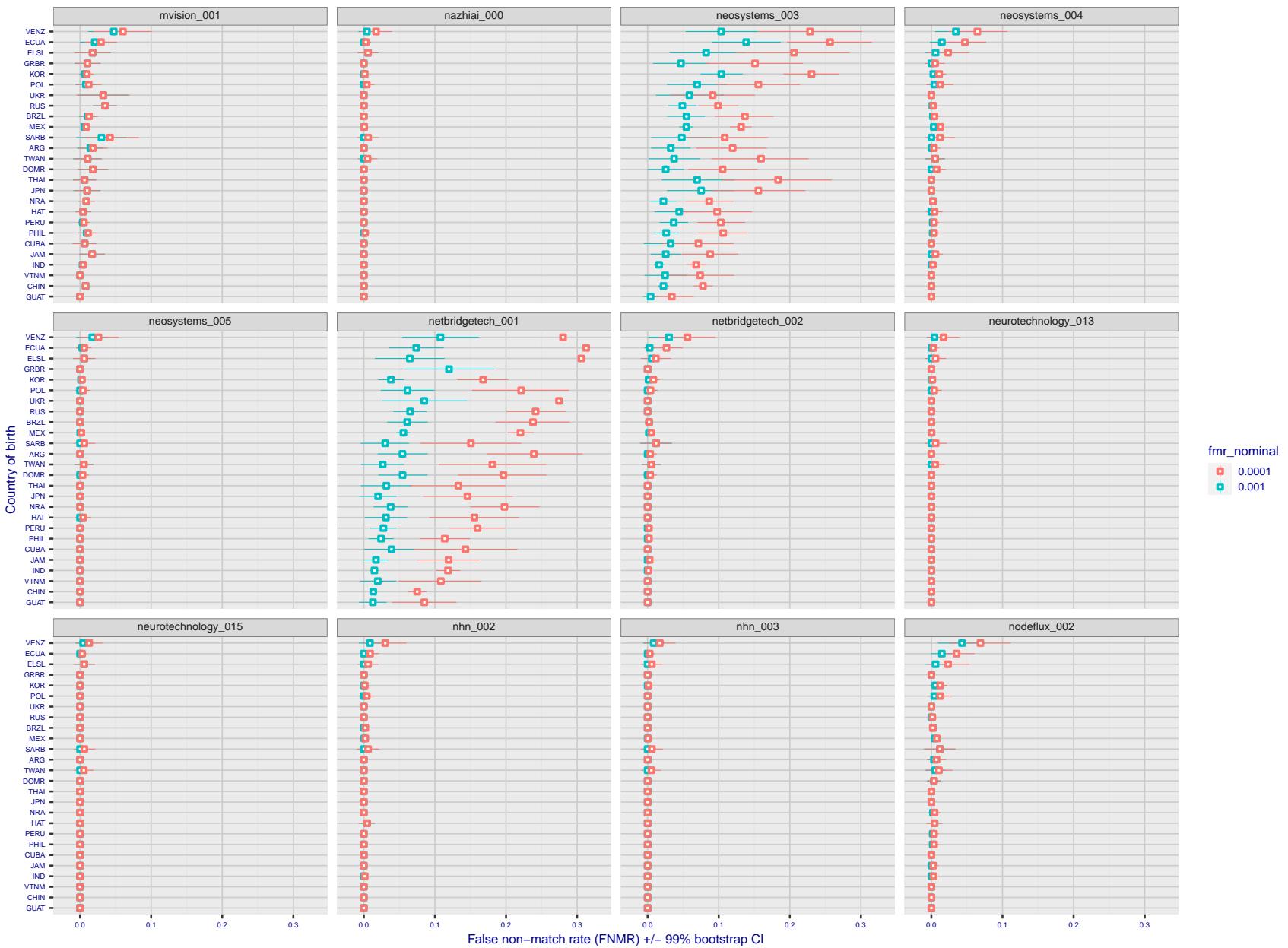


Figure 310: For the visa images, the dots show FNMR by country of birth for two globally set operating thresholds corresponding to $FMR = \{0.001, 0.0001\}$ computed over all on the order of 10^{10} impostor scores. The FMR in each bin will vary also - see subsequent impostor heatmaps in sec. 3.6.1. The figures shows an order of magnitude variation in FNMR across country of birth; these effects are likely due quality variations, then demographics like age and race. The error rates in some cases are zero, and in others the DET is flat so the error rates at the two thresholds are identical. The lines span 1% and 99% of bootstrap replicated FNMR estimates.

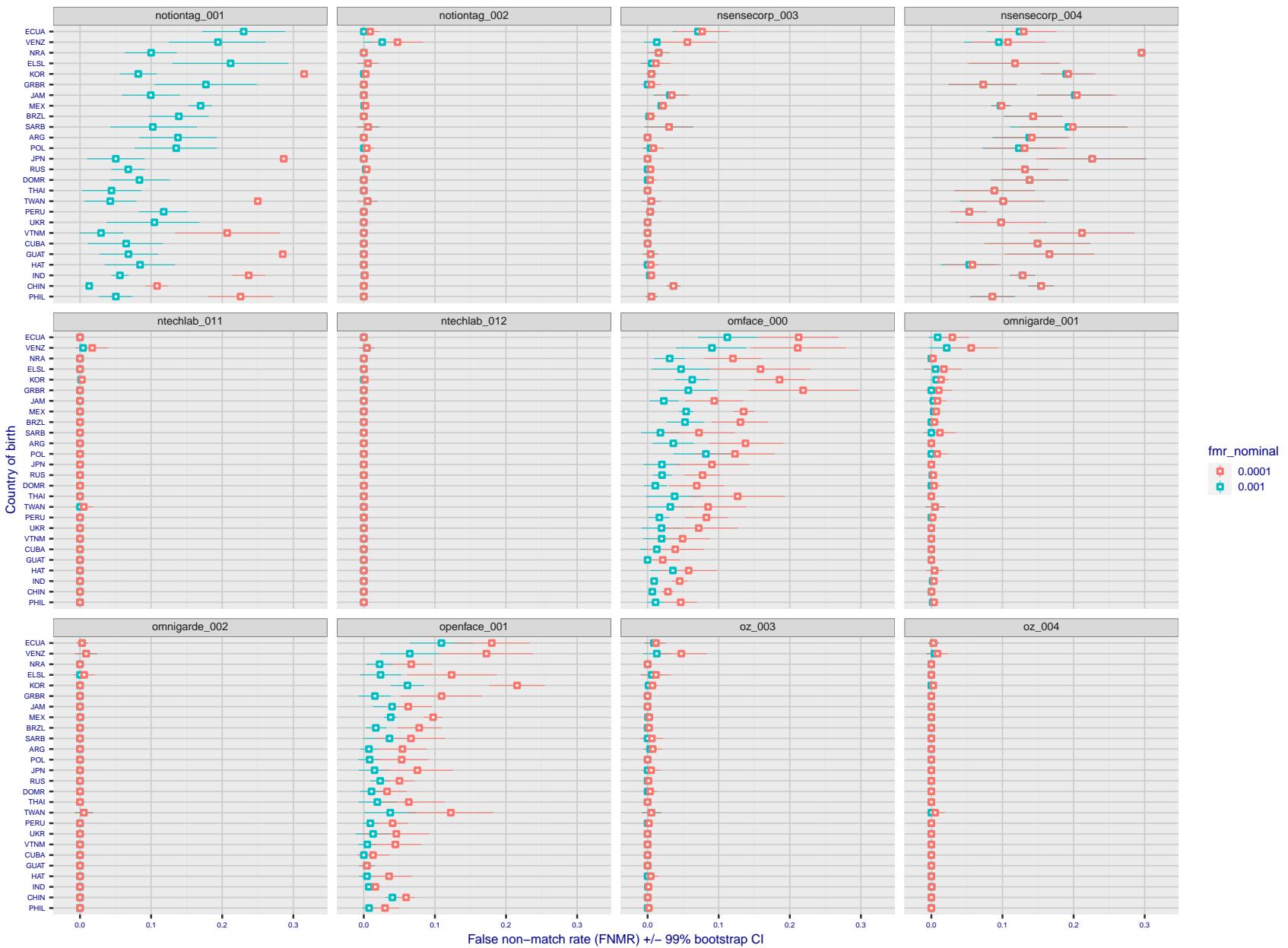


Figure 311: For the visa images, the dots show FNMR by country of birth for two globally set operating thresholds corresponding to $FMR = \{0.001, 0.0001\}$ computed over all on the order of 10^{10} impostor scores. The FMR in each bin will vary also - see subsequent impostor heatmaps in sec. 3.6.1. The figures shows an order of magnitude variation in FNMR across country of birth; these effects are likely due quality variations, then demographics like age and race. The error rates in some cases are zero, and in others the DET is flat so the error rates at the two thresholds are identical. The lines span 1% and 99% of bootstrap replicated FNMR estimates.

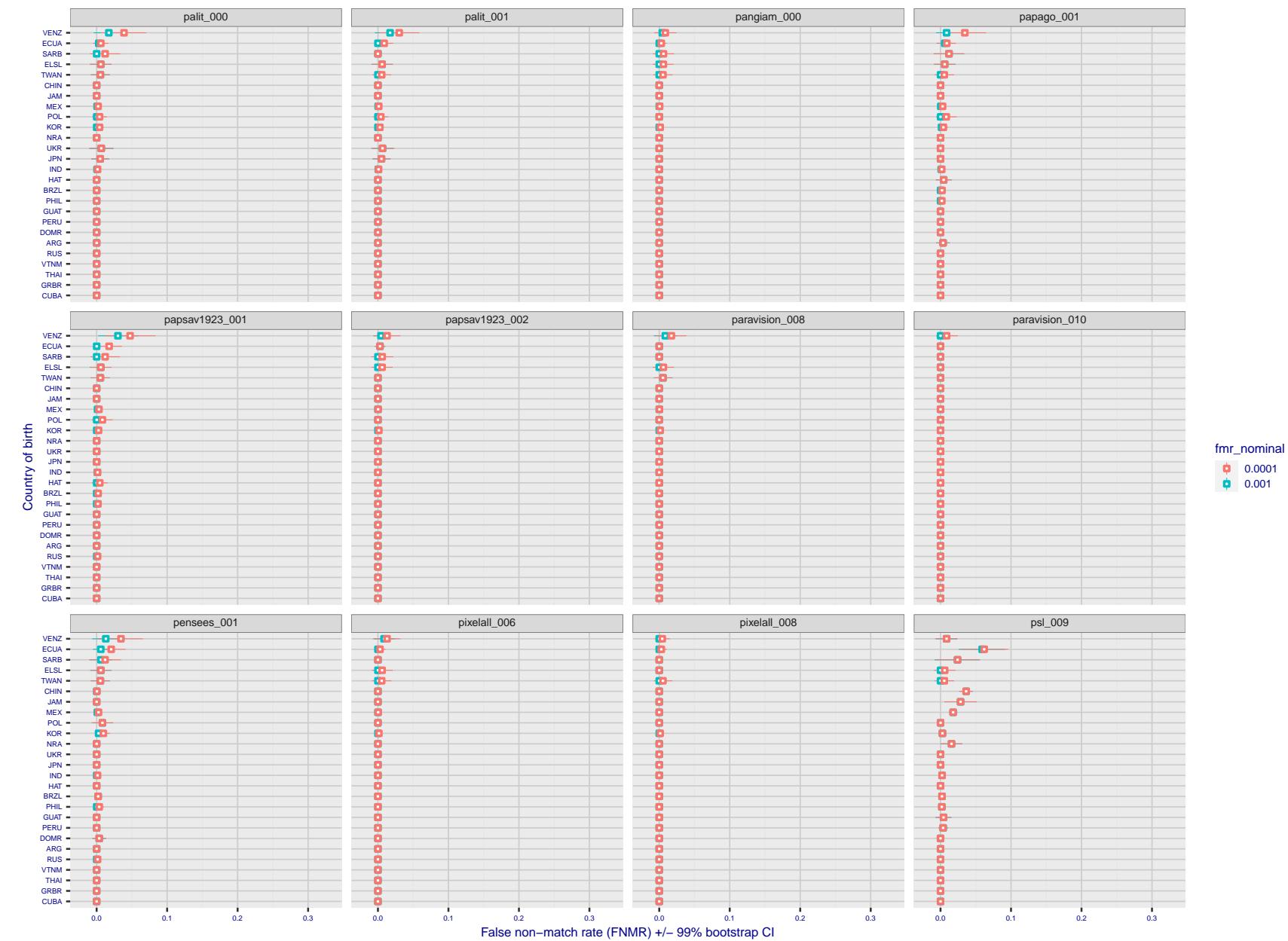


Figure 312: For the visa images, the dots show FNMR by country of birth for two globally set operating thresholds corresponding to $FMR = \{0.001, 0.0001\}$ computed over all on the order of 10^{10} impostor scores. The FMR in each bin will vary also - see subsequent impostor heatmaps in sec. 3.6.1. The figures shows an order of magnitude variation in FNMR across country of birth; these effects are likely due quality variations, then demographics like age and race. The error rates in some cases are zero, and in others the DET is flat so the error rates at the two thresholds are identical. The lines span 1% and 99% of bootstrap replicated FNMR estimates.

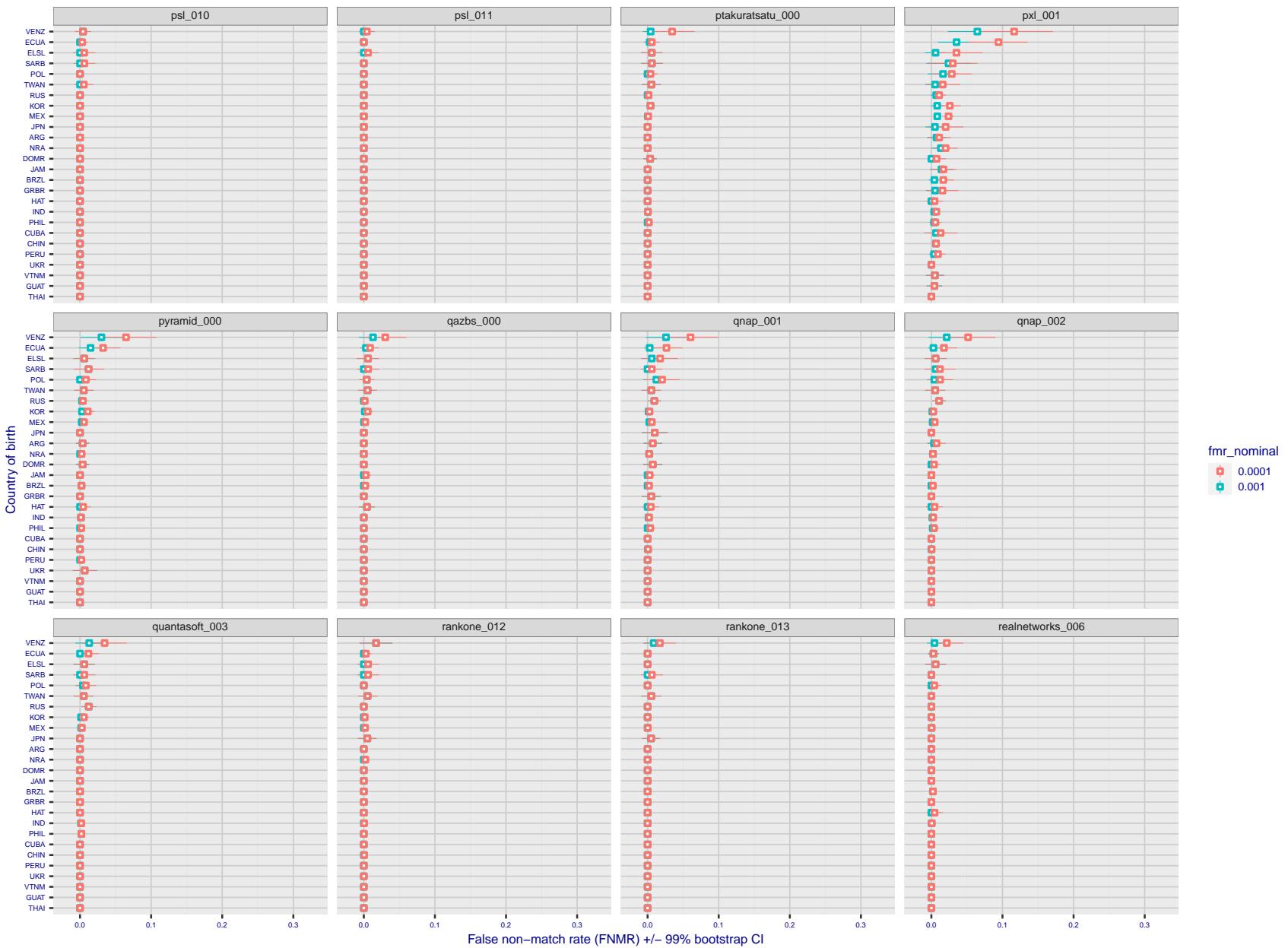


Figure 313: For the visa images, the dots show FNMR by country of birth for two globally set operating thresholds corresponding to $FMR = \{0.001, 0.0001\}$ computed over all on the order of 10^{10} impostor scores. The FMR in each bin will vary also - see subsequent impostor heatmaps in sec. 3.6.1. The figures shows an order of magnitude variation in FNMR across country of birth; these effects are likely due quality variations, then demographics like age and race. The error rates in some cases are zero, and in others the DET is flat so the error rates at the two thresholds are identical. The lines span 1% and 99% of bootstrap replicated FNMR estimates.

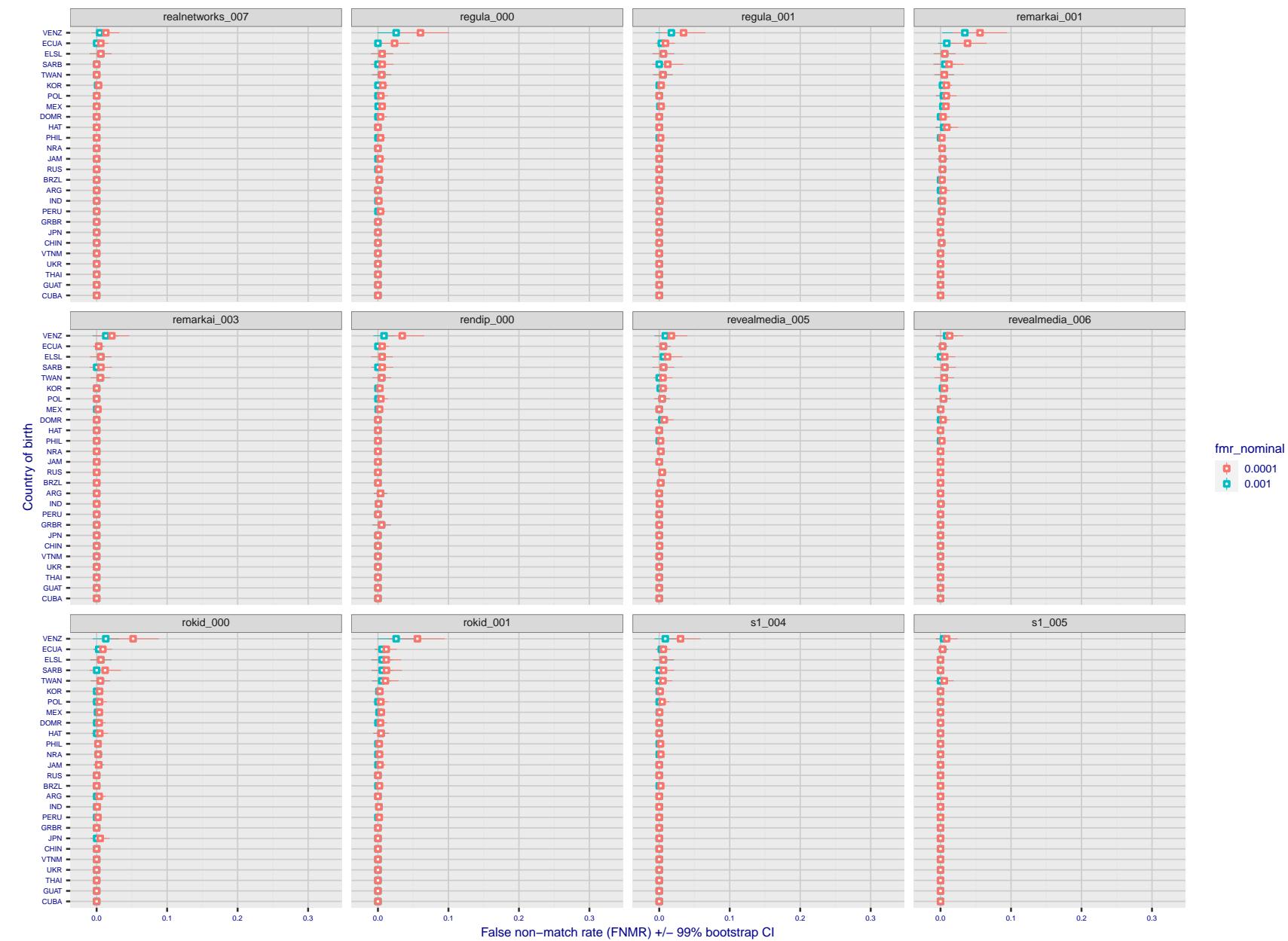


Figure 314: For the visa images, the dots show FNMR by country of birth for two globally set operating thresholds corresponding to $FMR = \{0.001, 0.0001\}$ computed over all on the order of 10^{10} impostor scores. The FMR in each bin will vary also - see subsequent impostor heatmaps in sec. 3.6.1. The figures shows an order of magnitude variation in FNMR across country of birth; these effects are likely due quality variations, then demographics like age and race. The error rates in some cases are zero, and in others the DET is flat so the error rates at the two thresholds are identical. The lines span 1% and 99% of bootstrap replicated FNMR estimates.

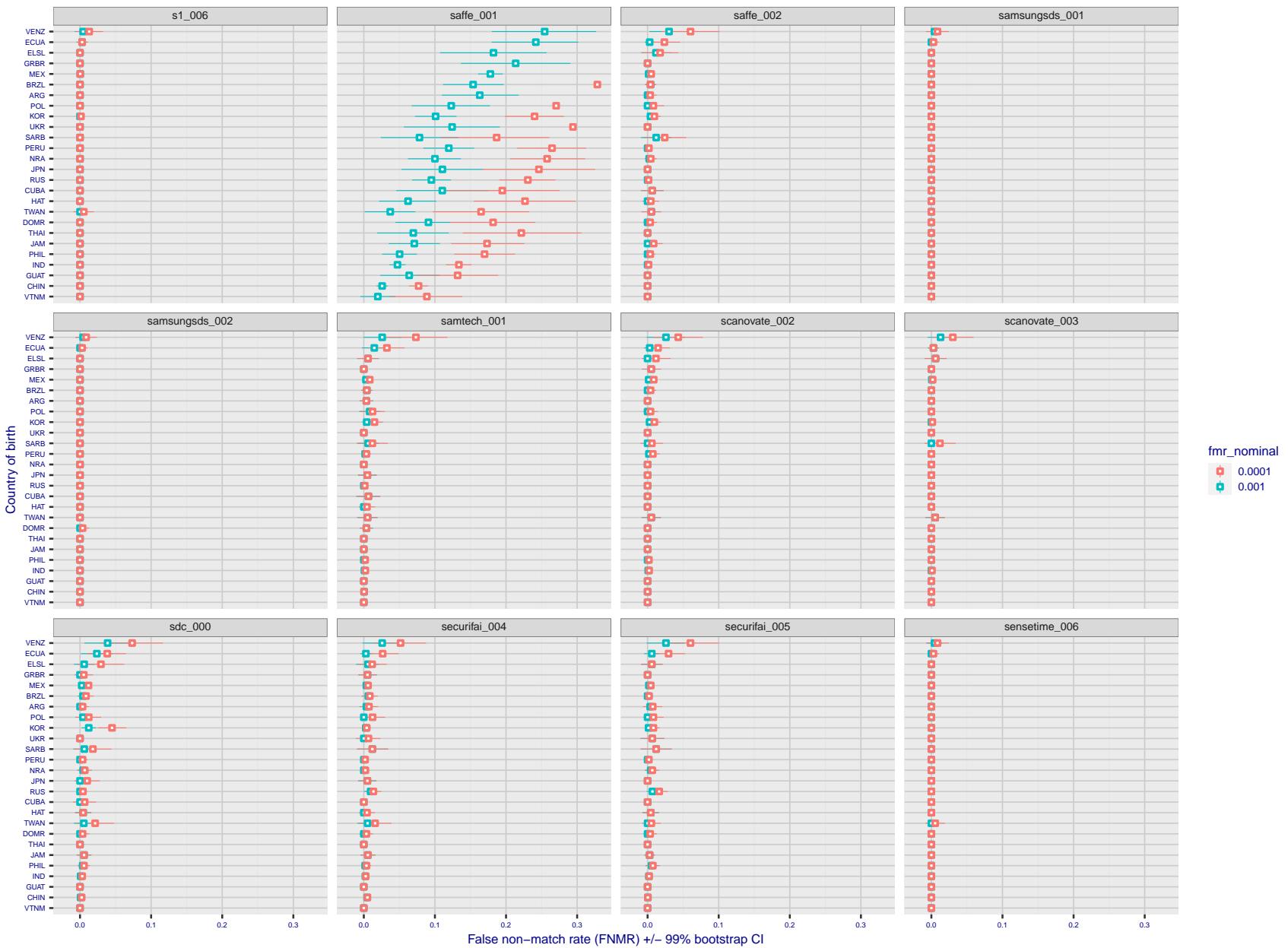


Figure 315: For the visa images, the dots show FNMR by country of birth for two globally set operating thresholds corresponding to $FMR = \{0.001, 0.0001\}$ computed over all on the order of 10^{10} impostor scores. The FMR in each bin will vary also - see subsequent impostor heatmaps in sec. 3.6.1. The figures shows an order of magnitude variation in FNMR across country of birth; these effects are likely due quality variations, then demographics like age and race. The error rates in some cases are zero, and in others the DET is flat so the error rates at the two thresholds are identical. The lines span 1% and 99% of bootstrap replicated FNMR estimates.

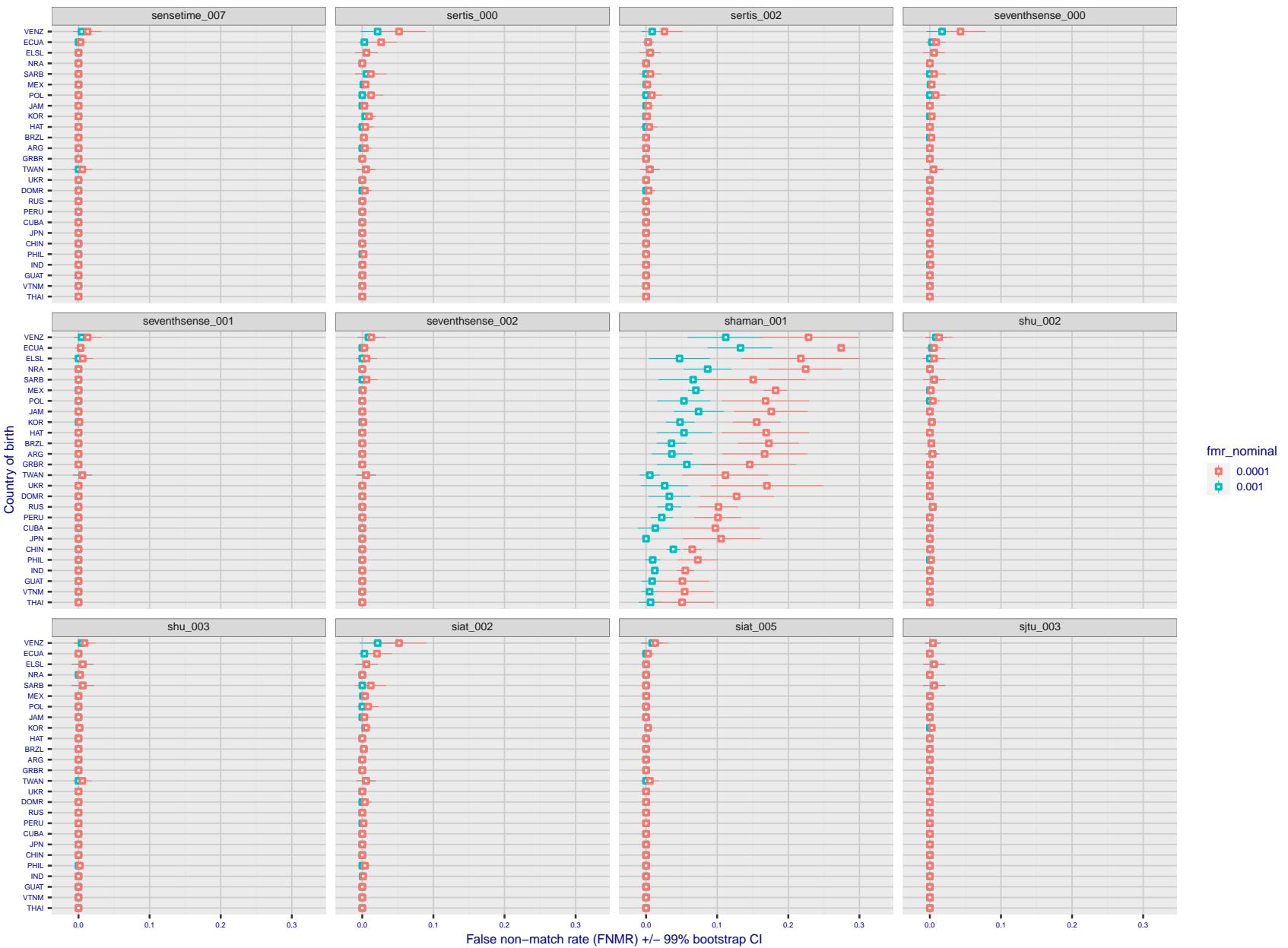


Figure 316: For the visa images, the dots show FNMR by country of birth for two globally set operating thresholds corresponding to $FMR = \{0.001, 0.0001\}$ computed over all on the order of 10^{10} impostor scores. The FMR in each bin will vary also - see subsequent impostor heatmaps in sec. 3.6.1. The figures shows an order of magnitude variation in FNMR across country of birth; these effects are likely due quality variations, then demographics like age and race. The error rates in some cases are zero, and in others the DET is flat so the error rates at the two thresholds are identical. The lines span 1% and 99% of bootstrap replicated FNMR estimates.

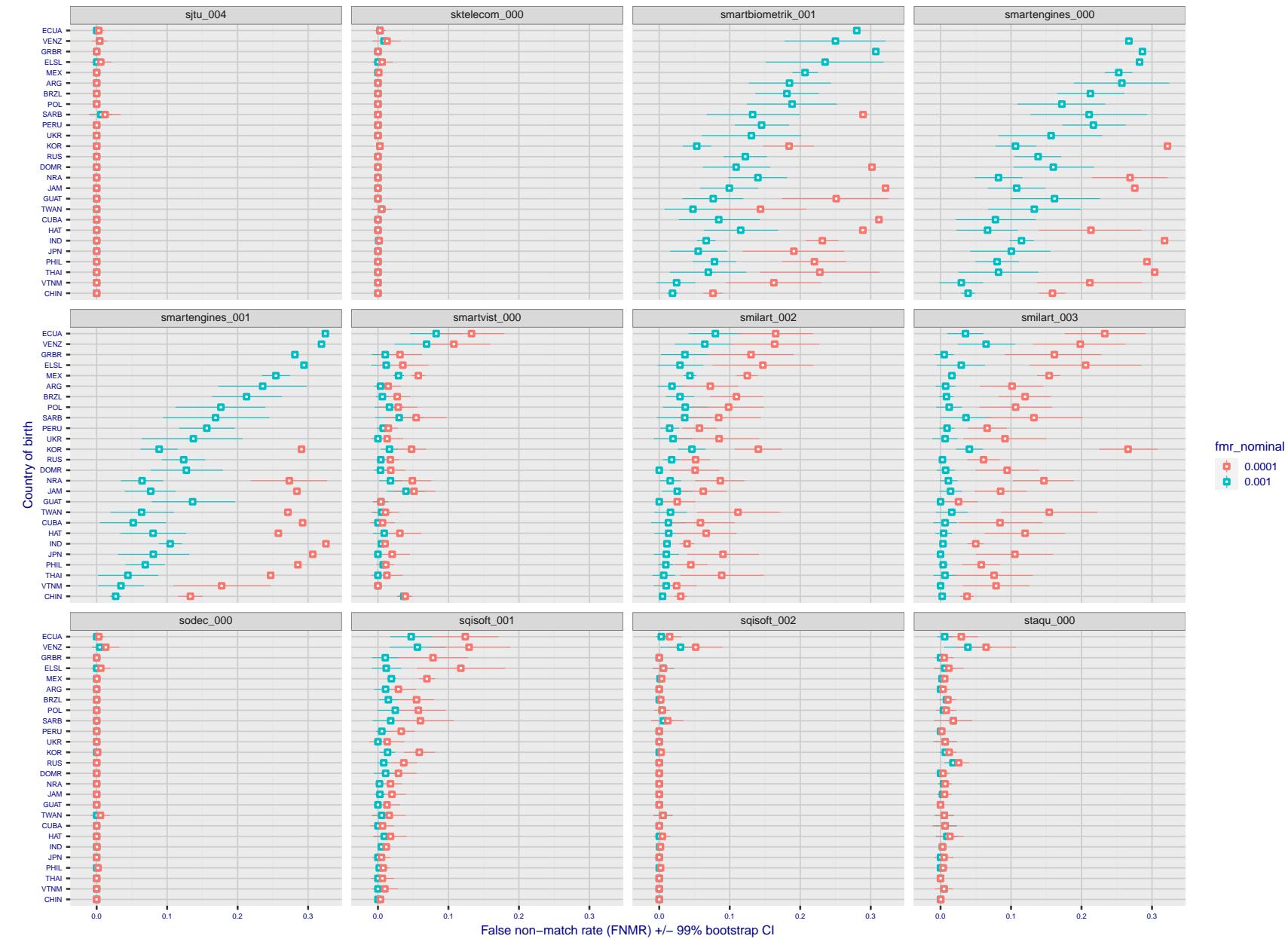


Figure 317: For the visa images, the dots show FNMR by country of birth for two globally set operating thresholds corresponding to $FMR = \{0.001, 0.0001\}$ computed over all on the order of 10^{10} impostor scores. The FMR in each bin will vary also - see subsequent impostor heatmaps in sec. 3.6.1. The figures shows an order of magnitude variation in FNMR across country of birth; these effects are likely due quality variations, then demographics like age and race. The error rates in some cases are zero, and in others the DET is flat so the error rates at the two thresholds are identical. The lines span 1% and 99% of bootstrap replicated FNMR estimates.

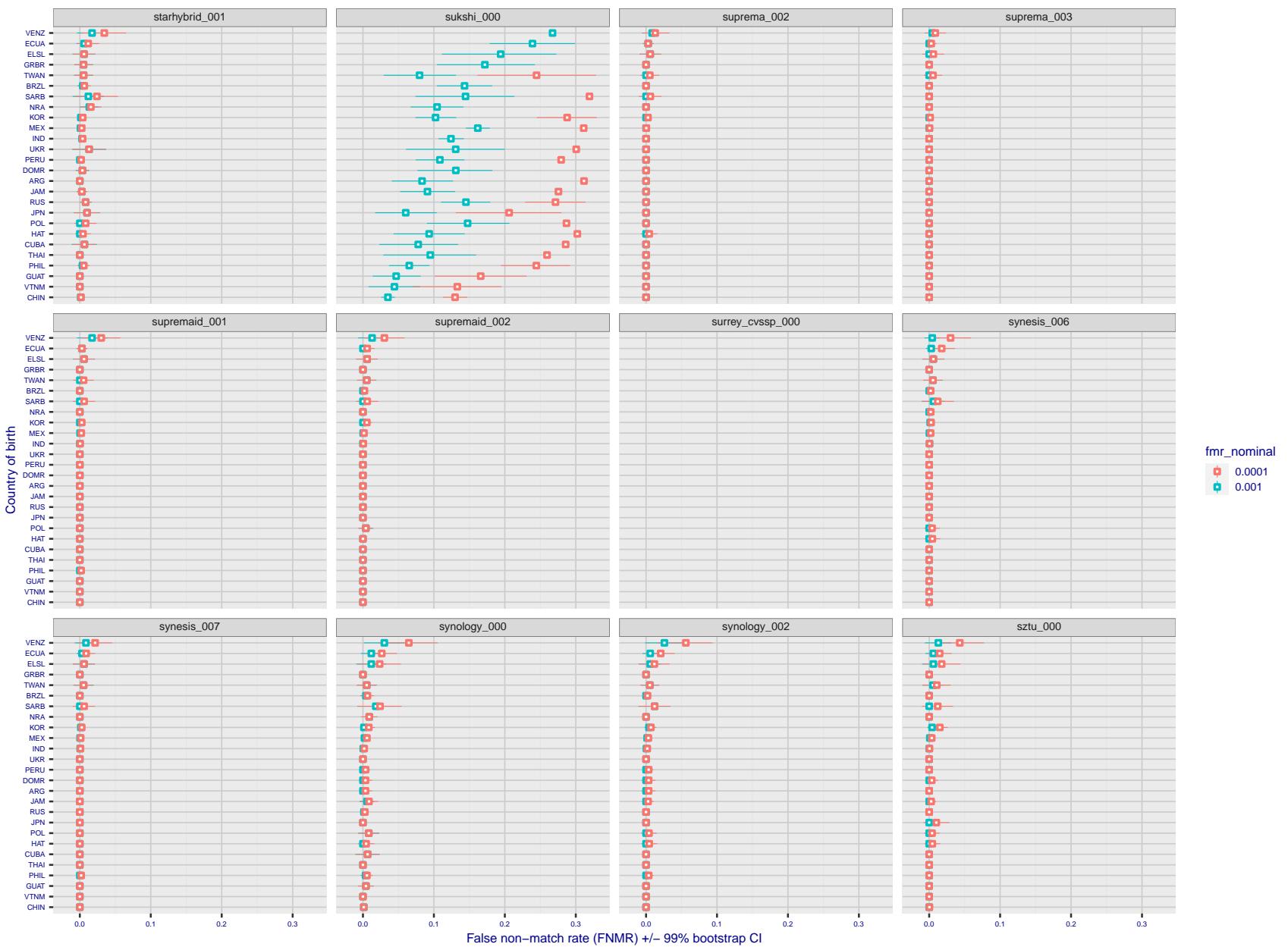


Figure 318: For the visa images, the dots show FNMR by country of birth for two globally set operating thresholds corresponding to $FMR = \{0.001, 0.0001\}$ computed over all on the order of 10^{10} impostor scores. The FMR in each bin will vary also - see subsequent impostor heatmaps in sec. 3.6.1. The figures shows an order of magnitude variation in FNMR across country of birth; these effects are likely due quality variations, then demographics like age and race. The error rates in some cases are zero, and in others the DET is flat so the error rates at the two thresholds are identical. The lines span 1% and 99% of bootstrap replicated FNMR estimates.

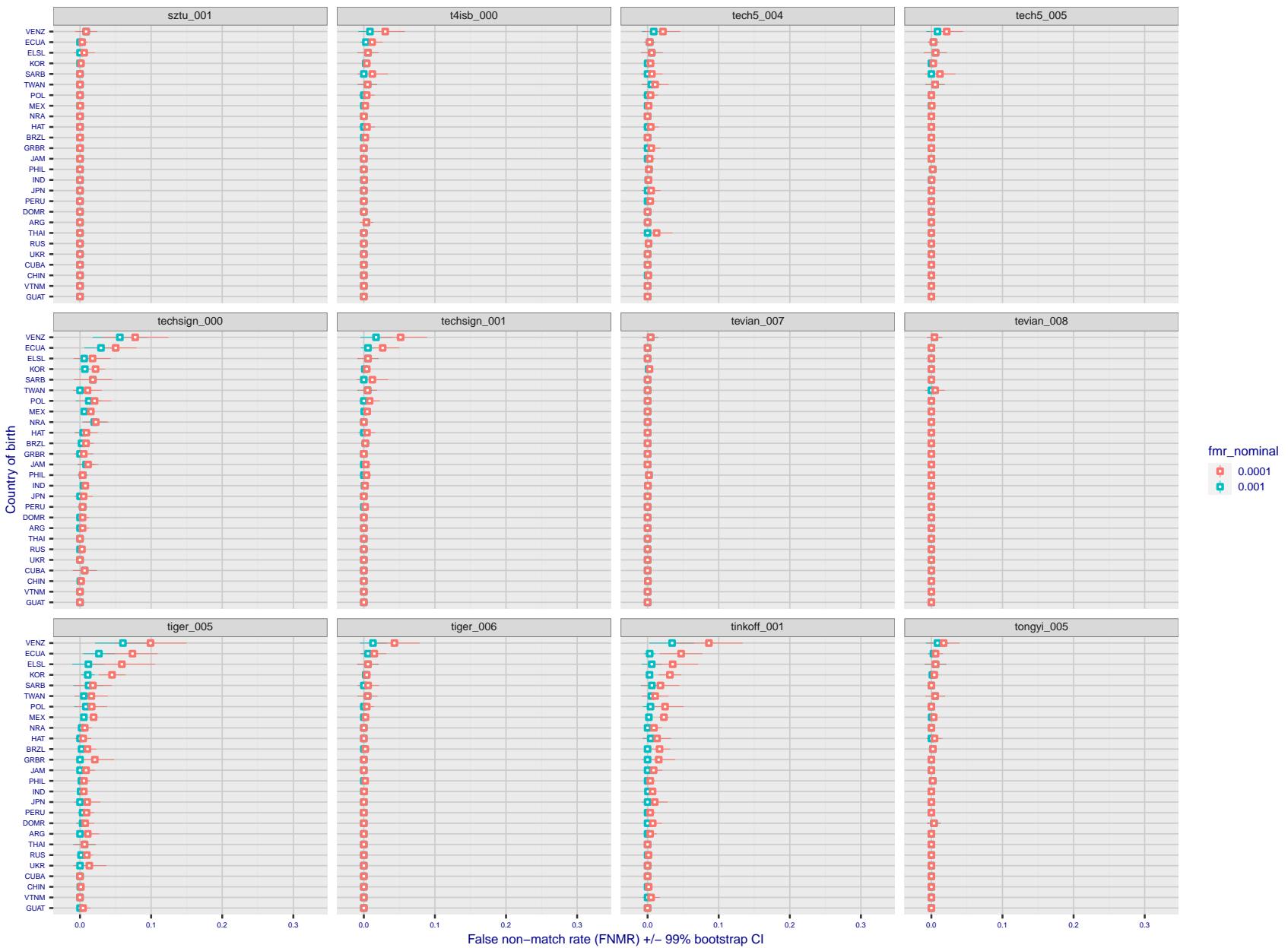


Figure 319: For the visa images, the dots show FNMR by country of birth for two globally set operating thresholds corresponding to $FMR = \{0.001, 0.0001\}$ computed over all on the order of 10^{10} impostor scores. The FMR in each bin will vary also - see subsequent impostor heatmaps in sec. 3.6.1. The figures shows an order of magnitude variation in FNMR across country of birth; these effects are likely due quality variations, then demographics like age and race. The error rates in some cases are zero, and in others the DET is flat so the error rates at the two thresholds are identical. The lines span 1% and 99% of bootstrap replicated FNMR estimates.

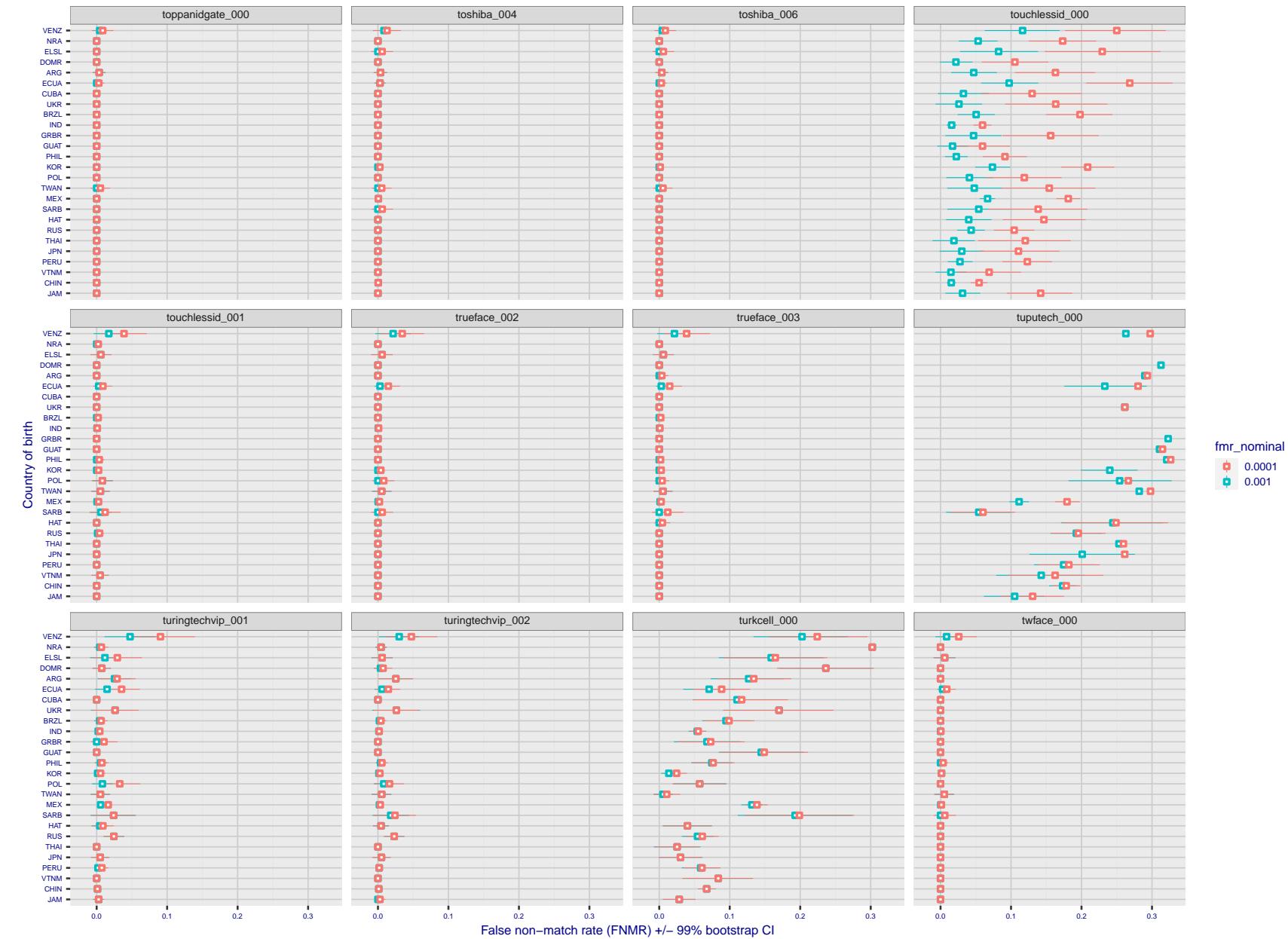


Figure 320: For the visa images, the dots show FNMR by country of birth for two globally set operating thresholds corresponding to $FMR = \{0.001, 0.0001\}$ computed over all on the order of 10^{10} impostor scores. The FMR in each bin will vary also - see subsequent impostor heatmaps in sec. 3.6.1. The figures shows an order of magnitude variation in FNMR across country of birth; these effects are likely due quality variations, then demographics like age and race. The error rates in some cases are zero, and in others the DET is flat so the error rates at the two thresholds are identical. The lines span 1% and 99% of bootstrap replicated FNMR estimates.

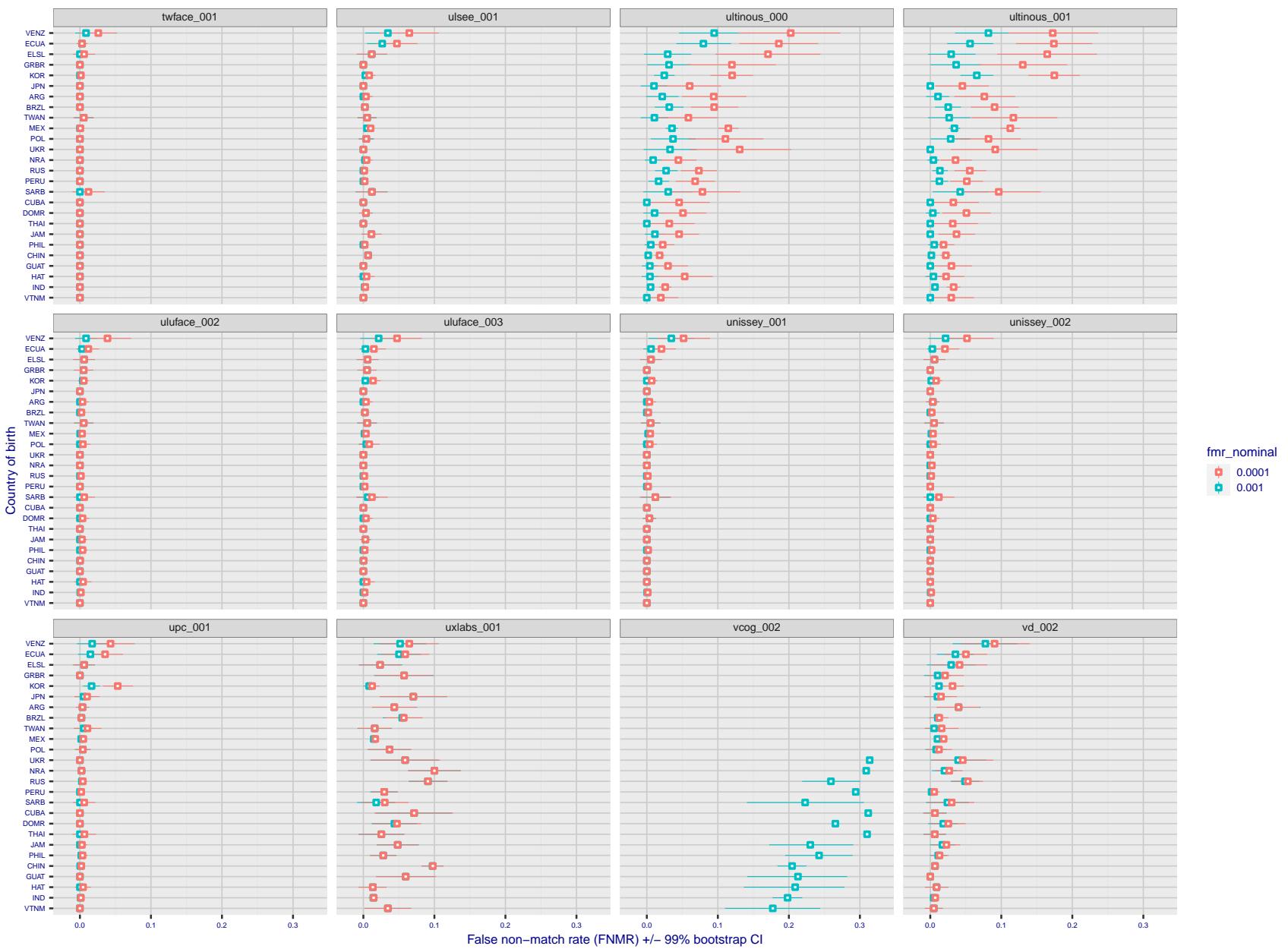


Figure 321: For the visa images, the dots show FNMR by country of birth for two globally set operating thresholds corresponding to $FMR = \{0.001, 0.0001\}$ computed over all on the order of 10^{10} impostor scores. The FMR in each bin will vary also - see subsequent impostor heatmaps in sec. 3.6.1. The figures shows an order of magnitude variation in FNMR across country of birth; these effects are likely due quality variations, then demographics like age and race. The error rates in some cases are zero, and in others the DET is flat so the error rates at the two thresholds are identical. The lines span 1% and 99% of bootstrap replicated FNMR estimates.

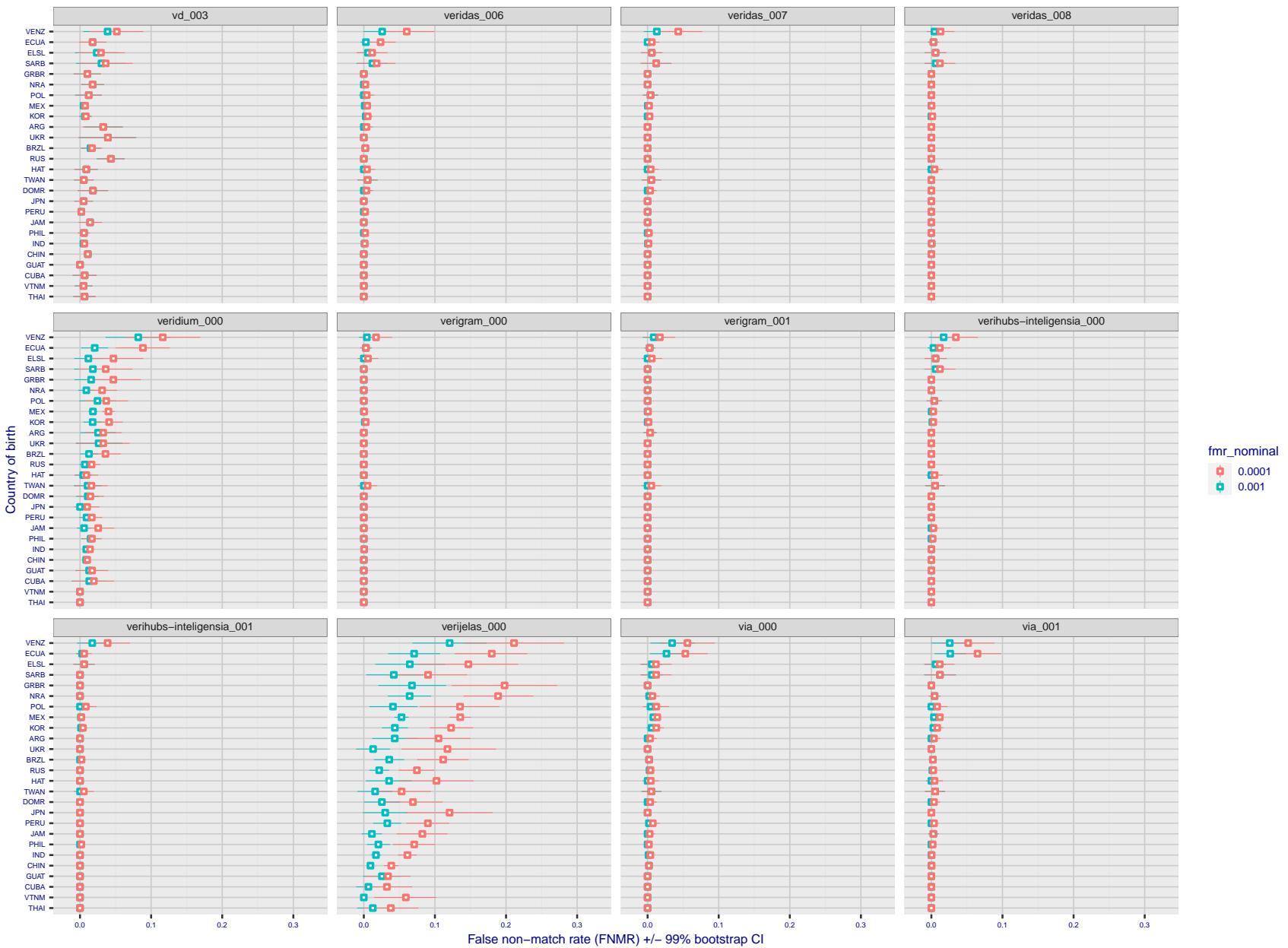


Figure 322: For the visa images, the dots show FNMR by country of birth for two globally set operating thresholds corresponding to $FMR = \{0.001, 0.0001\}$ computed over all on the order of 10^{10} impostor scores. The FMR in each bin will vary also - see subsequent impostor heatmaps in sec. 3.6.1. The figures shows an order of magnitude variation in FNMR across country of birth; these effects are likely due quality variations, then demographics like age and race. The error rates in some cases are zero, and in others the DET is flat so the error rates at the two thresholds are identical. The lines span 1% and 99% of bootstrap replicated FNMR estimates.

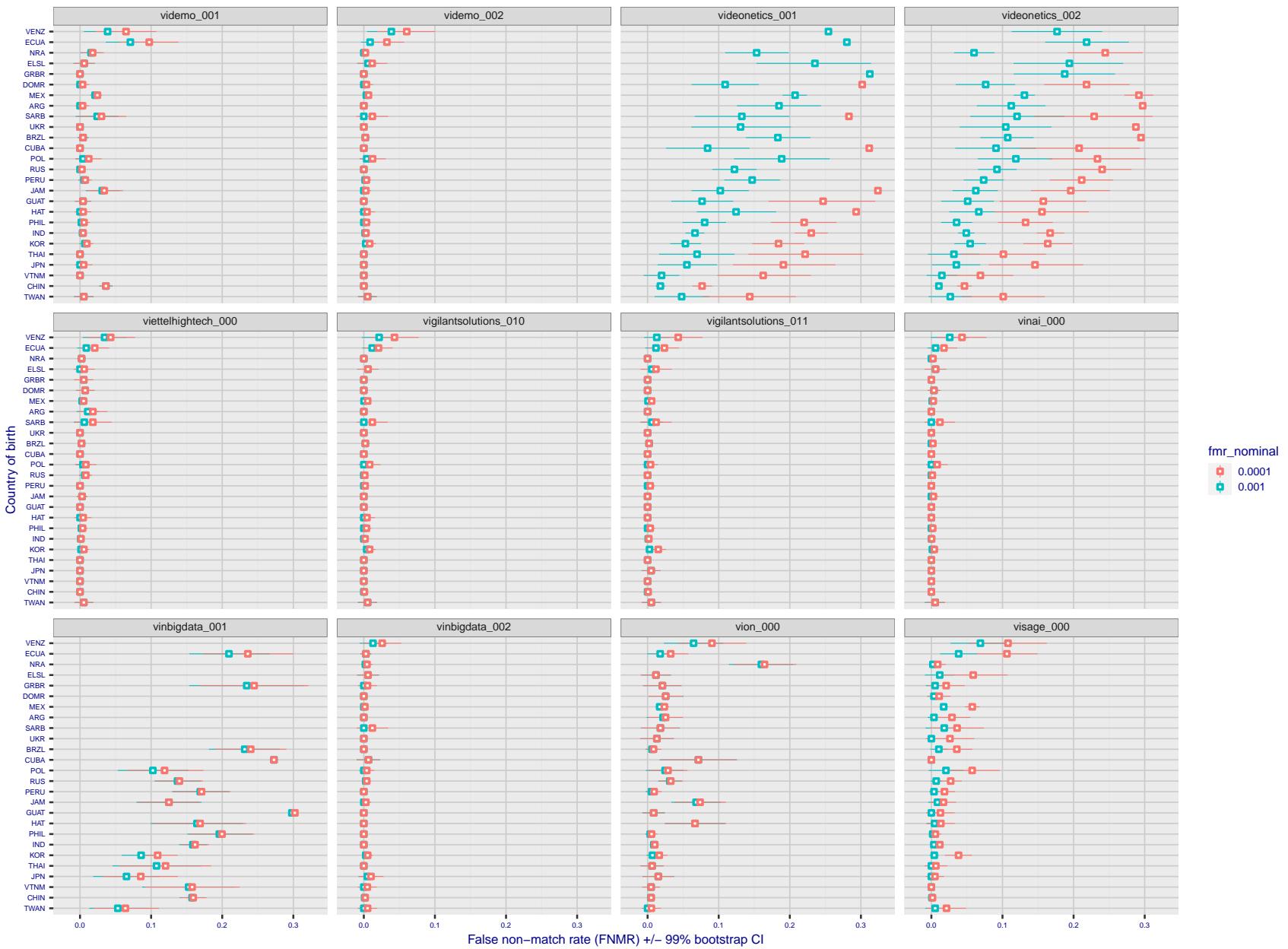


Figure 323: For the visa images, the dots show FNMR by country of birth for two globally set operating thresholds corresponding to $FMR = \{0.001, 0.0001\}$ computed over all on the order of 10^{10} impostor scores. The FMR in each bin will vary also - see subsequent impostor heatmaps in sec. 3.6.1. The figures shows an order of magnitude variation in FNMR across country of birth; these effects are likely due quality variations, then demographics like age and race. The error rates in some cases are zero, and in others the DET is flat so the error rates at the two thresholds are identical. The lines span 1% and 99% of bootstrap replicated FNMR estimates.

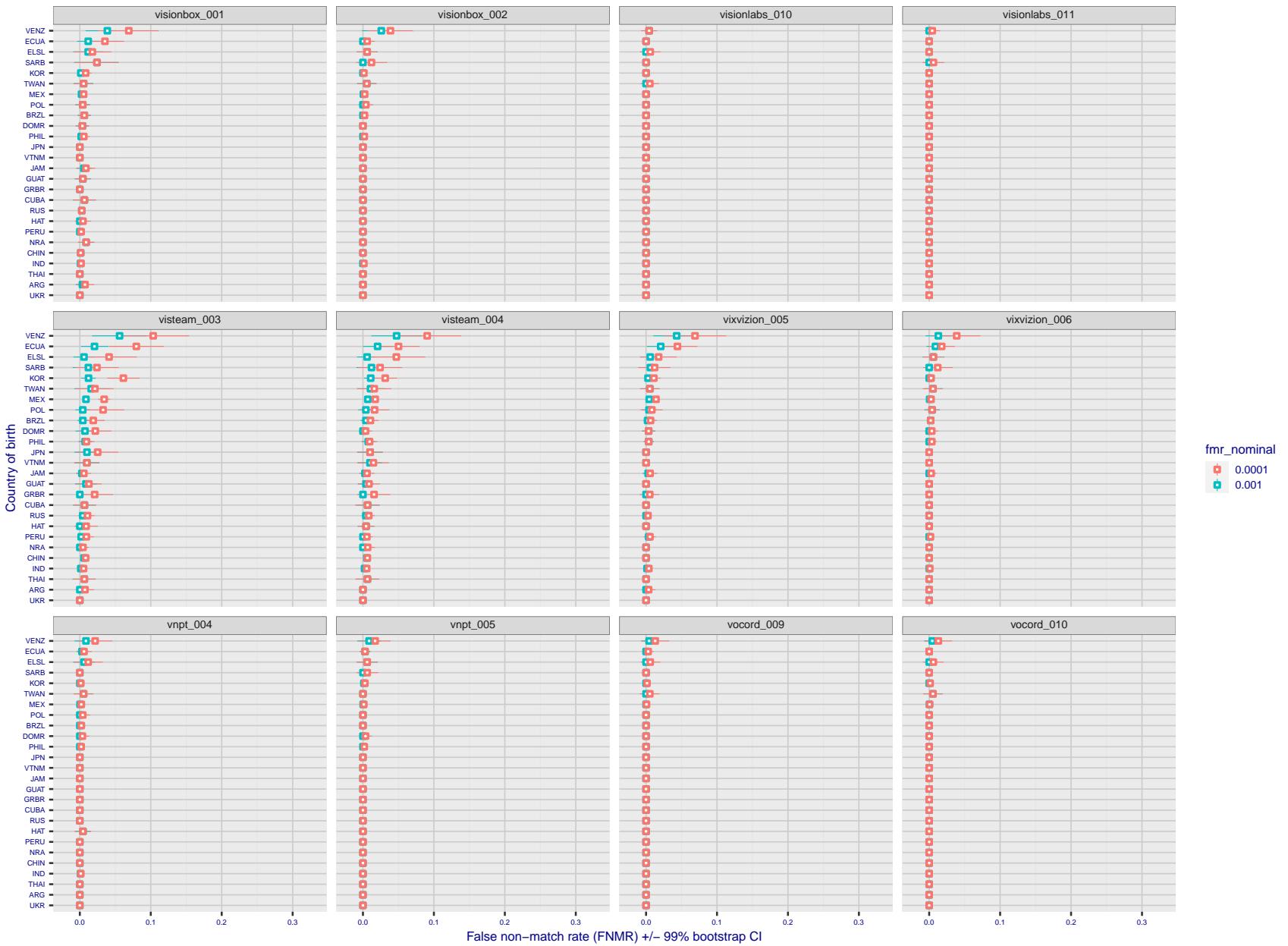


Figure 324: For the visa images, the dots show FNMR by country of birth for two globally set operating thresholds corresponding to $FMR = \{0.001, 0.0001\}$ computed over all on the order of 10^{10} impostor scores. The FMR in each bin will vary also - see subsequent impostor heatmaps in sec. 3.6.1. The figures shows an order of magnitude variation in FNMR across country of birth; these effects are likely due quality variations, then demographics like age and race. The error rates in some cases are zero, and in others the DET is flat so the error rates at the two thresholds are identical. The lines span 1% and 99% of bootstrap replicated FNMR estimates.

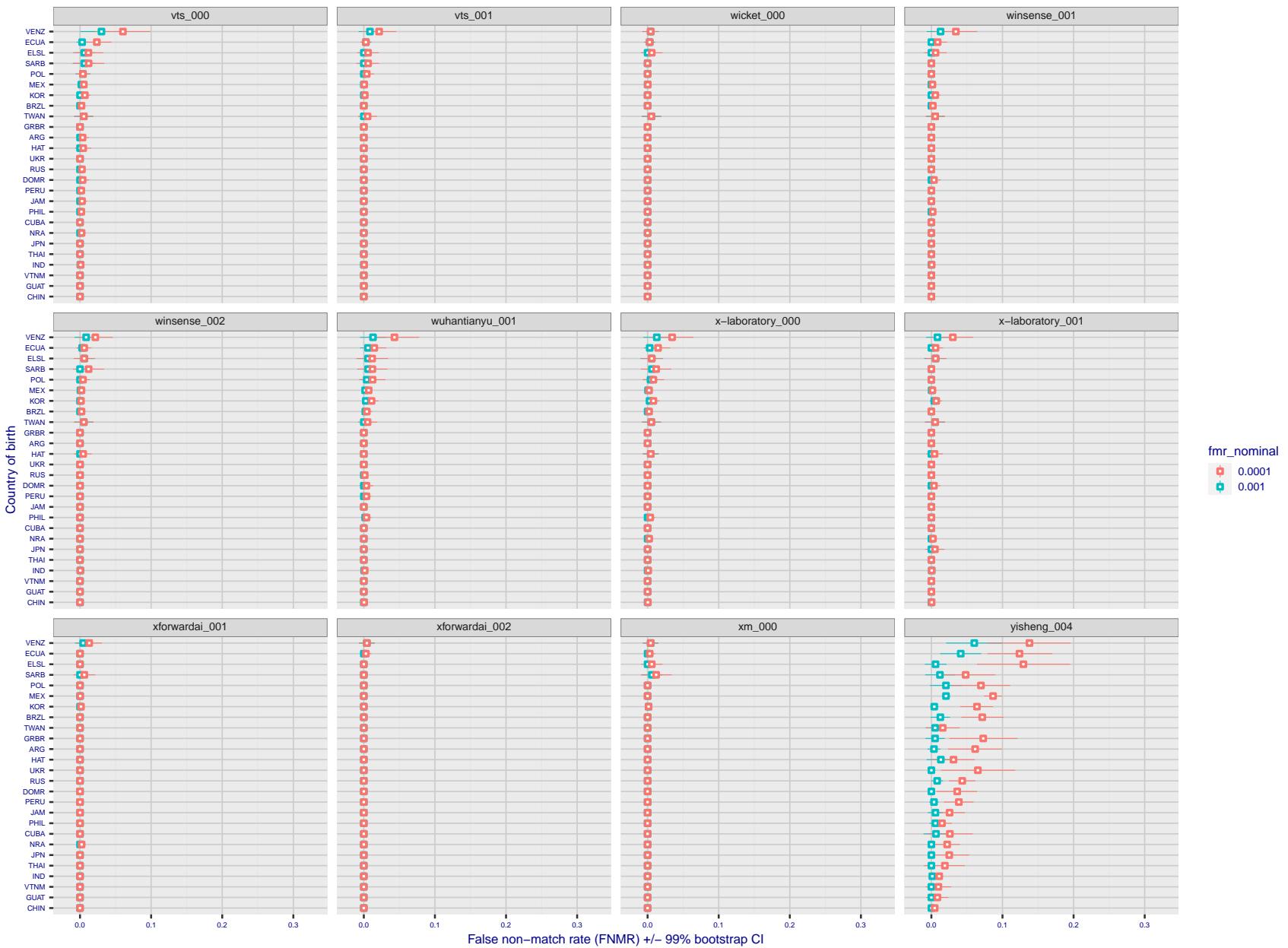


Figure 325: For the visa images, the dots show FNMR by country of birth for two globally set operating thresholds corresponding to $FMR = \{0.001, 0.0001\}$ computed over all on the order of 10^{10} impostor scores. The FMR in each bin will vary also - see subsequent impostor heatmaps in sec. 3.6.1. The figures shows an order of magnitude variation in FNMR across country of birth; these effects are likely due quality variations, then demographics like age and race. The error rates in some cases are zero, and in others the DET is flat so the error rates at the two thresholds are identical. The lines span 1% and 99% of bootstrap replicated FNMR estimates.

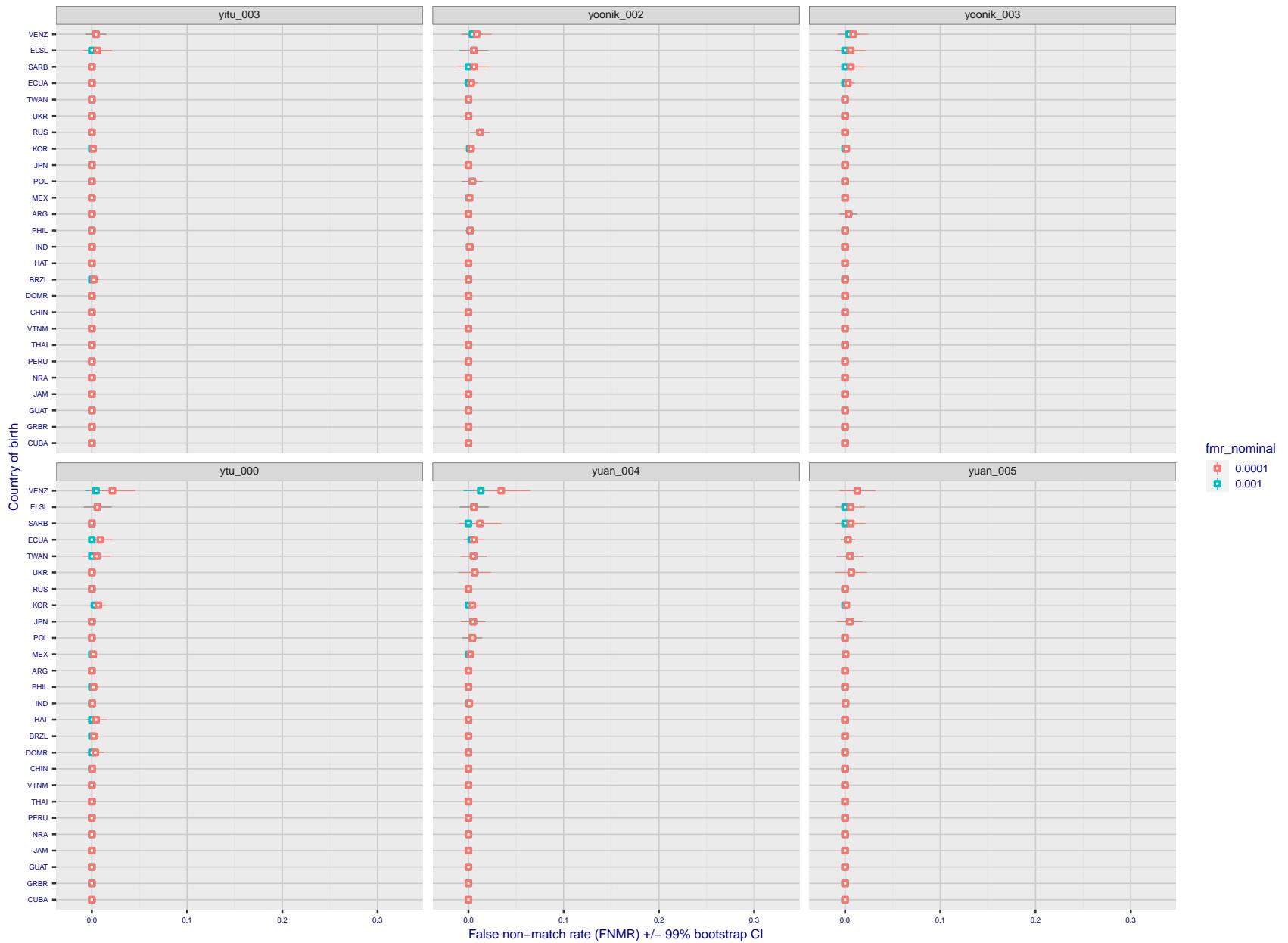


Figure 326: For the visa images, the dots show FNMR by country of birth for two globally set operating thresholds corresponding to $FMR = \{0.001, 0.0001\}$ computed over all on the order of 10^{10} impostor scores. The FMR in each bin will vary also - see subsequent impostor heatmaps in sec. 3.6.1. The figures shows an order of magnitude variation in FNMR across country of birth; these effects are likely due quality variations, then demographics like age and race. The error rates in some cases are zero, and in others the DET is flat so the error rates at the two thresholds are identical. The lines span 1% and 99% of bootstrap replicated FNMR estimates.

Caveats: The results may not relate to subject-specific properties. Instead they could reflect image-specific quality differences, which could occur due to collection protocol or software processing variations.

3.5.2 Effect of ageing

Background: Faces change appearance throughout life. This change gradually reduces similarity of a new image to an earlier image. Face recognition algorithms give reduced similarity scores and more frequent false rejections.

Goal: To quantify false non-match rates (FNMR) as a function of elapsed time in an adult population.

Methods: Using the mugshot images, a threshold is set to give FMR = 0.00001 over the entire impostor set. Then FNMR is measured over 1000 bootstrap replications of the genuine scores.

Results: For the visa images, Figure 355 shows how false non-match rates for genuine users, as a function of age group.

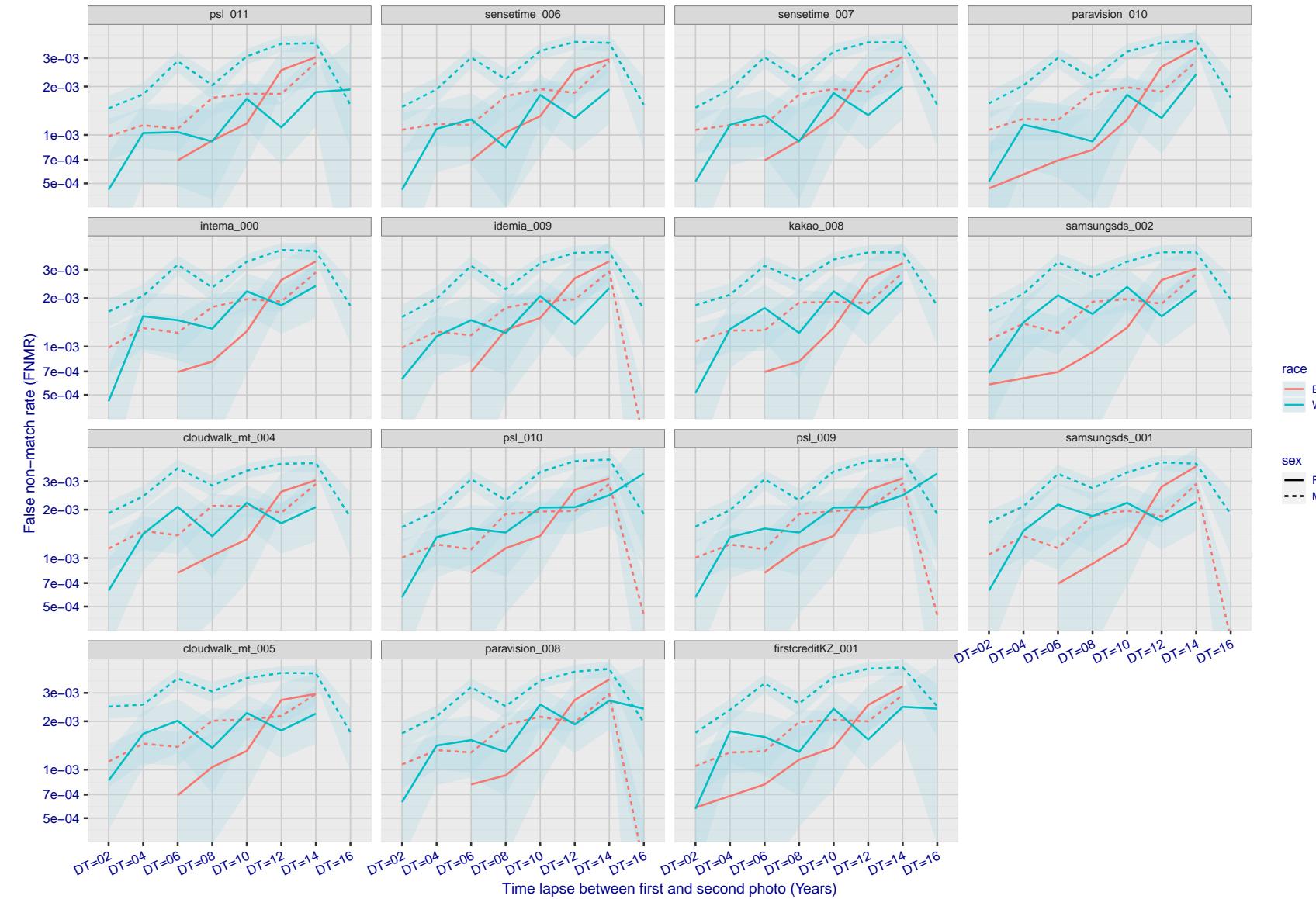


Figure 327: For the mugshot images, FNMR as a function of elapsed time between initial enrollment and second verification images. The panels appear most accurate first, and vertical scale changes on each page. The four traces correspond to images annotated with codes for black female, black male, white female, white male. The threshold is fixed for each algorithm to give $FMR = 0.00001$ over all (10^8) impostor comparisons. For short time-lapses, the most accurate algorithms give very few errors ($FNMR < 0.001$) so that the uncertainty estimates are high.

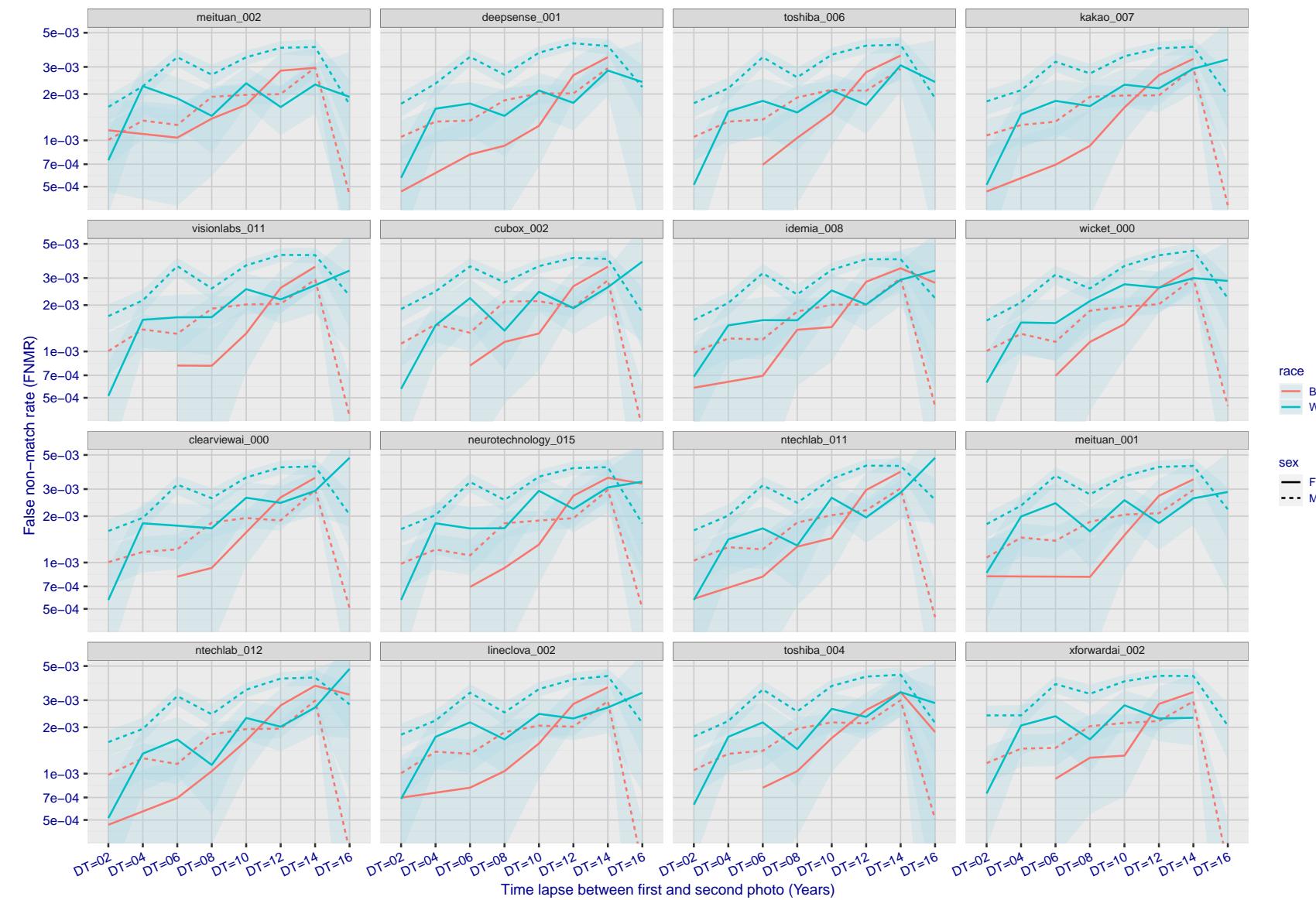


Figure 328: For the mugshot images, FNMR as a function of elapsed time between initial enrollment and second verification images. The panels appear most accurate first, and vertical scale changes on each page. The four traces correspond to images annotated with codes for black female, black male, white female, white male. The threshold is fixed for each algorithm to give FMR = 0.00001 over all (10^8) impostor comparisons. For short time-lapses, the most accurate algorithms give very few errors (FNMR < 0.001) so that the uncertainty estimates are high.

2022/11/06 10:45:39

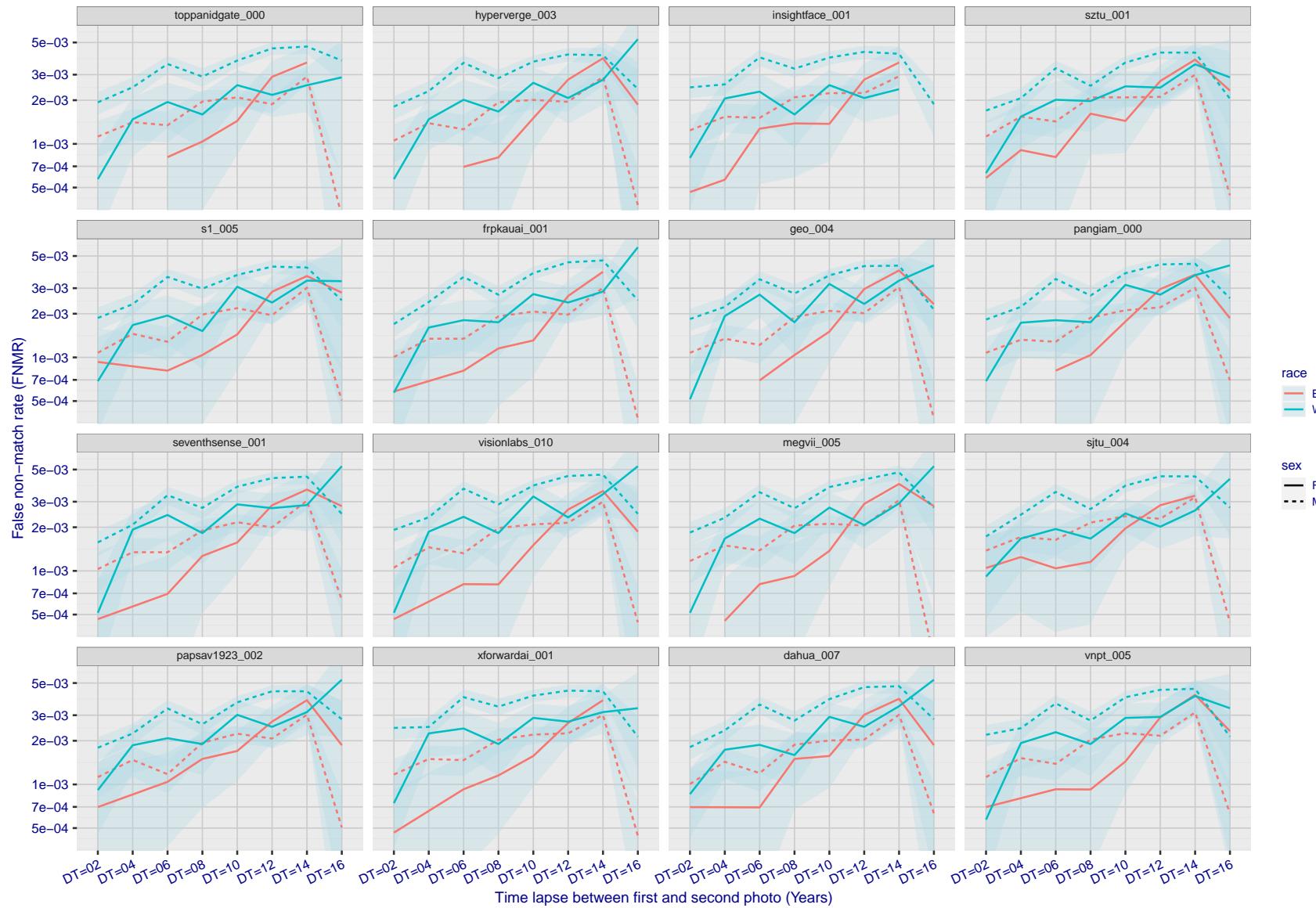


Figure 329: For the mugshot images, FNMR as a function of elapsed time between initial enrollment and second verification images. The panels appear most accurate first, and vertical scale changes on each page. The four traces correspond to images annotated with codes for black female, black male, white female, white male. The threshold is fixed for each algorithm to give FMR = 0.00001 over all (10^8) impostor comparisons. For short time-lapses, the most accurate algorithms give very few errors (FNMR < 0.001) so that the uncertainty estimates are high.

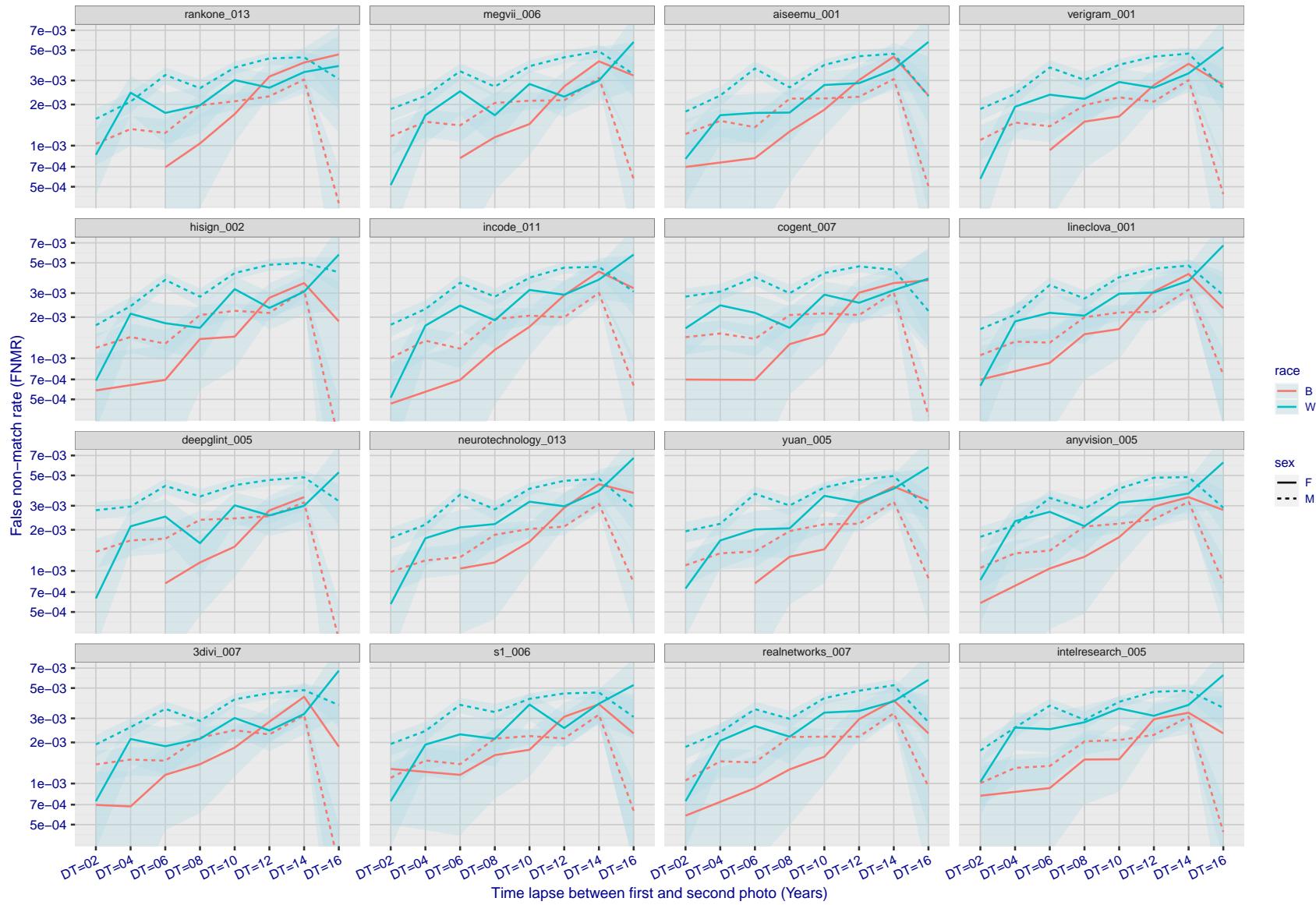


Figure 330: For the mugshot images, FNMR as a function of elapsed time between initial enrollment and second verification images. The panels appear most accurate first, and vertical scale changes on each page. The four traces correspond to images annotated with codes for black female, black male, white female, white male. The threshold is fixed for each algorithm to give $FMR = 0.00001$ over all (10^8) impostor comparisons. For short time-lapses, the most accurate algorithms give very few errors ($FNMR < 0.001$) so that the uncertainty estimates are high.

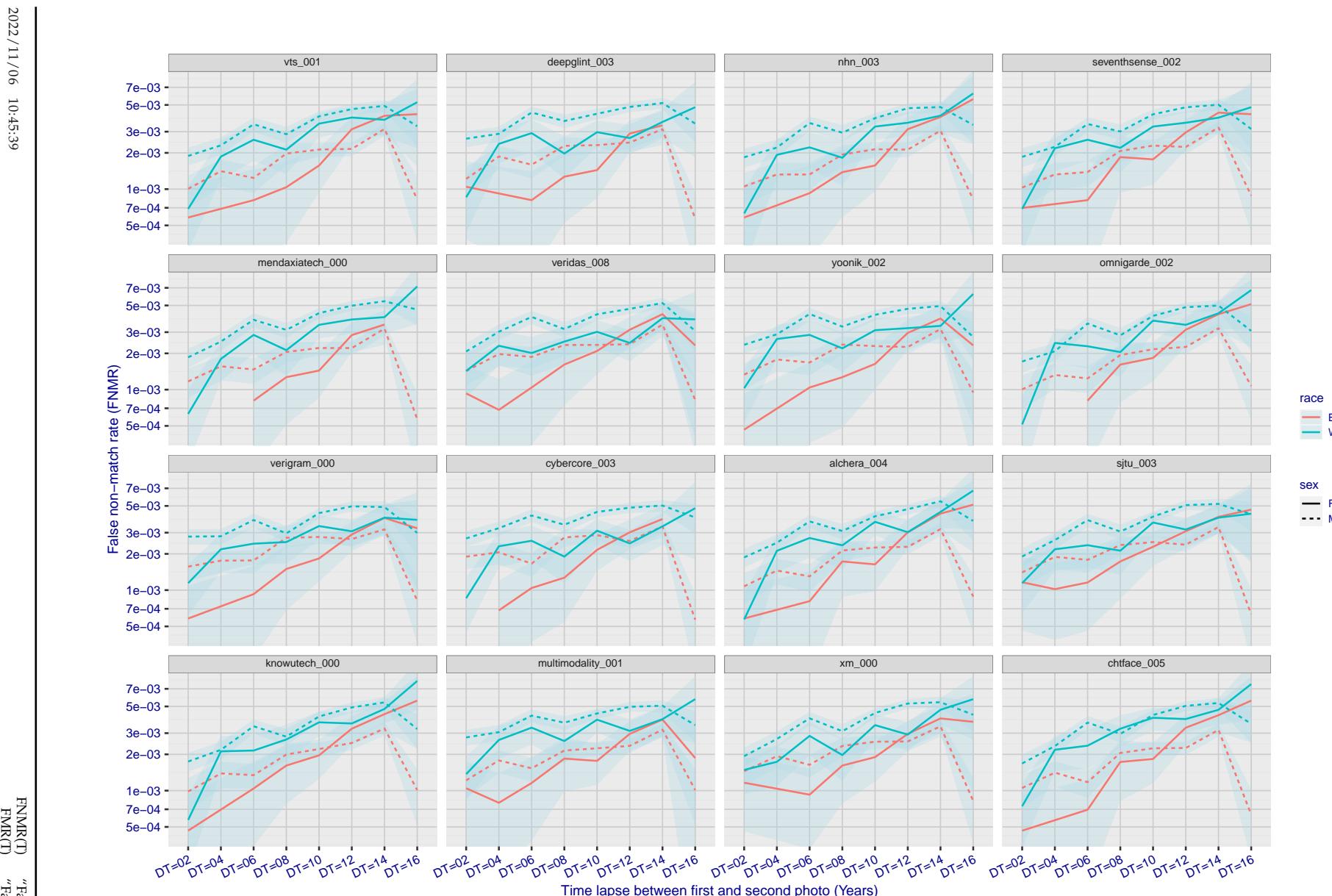


Figure 331: For the mugshot images, FNMR as a function of elapsed time between initial enrollment and second verification images. The panels appear most accurate first, and vertical scale changes on each page. The four traces correspond to images annotated with codes for black female, black male, white female, white male. The threshold is fixed for each algorithm to give FMR = 0.00001 over all (10^8) impostor comparisons. For short time-lapses, the most accurate algorithms give very few errors (FNMR < 0.001) so that the uncertainty estimates are high.

2022/11/06 10:45:39

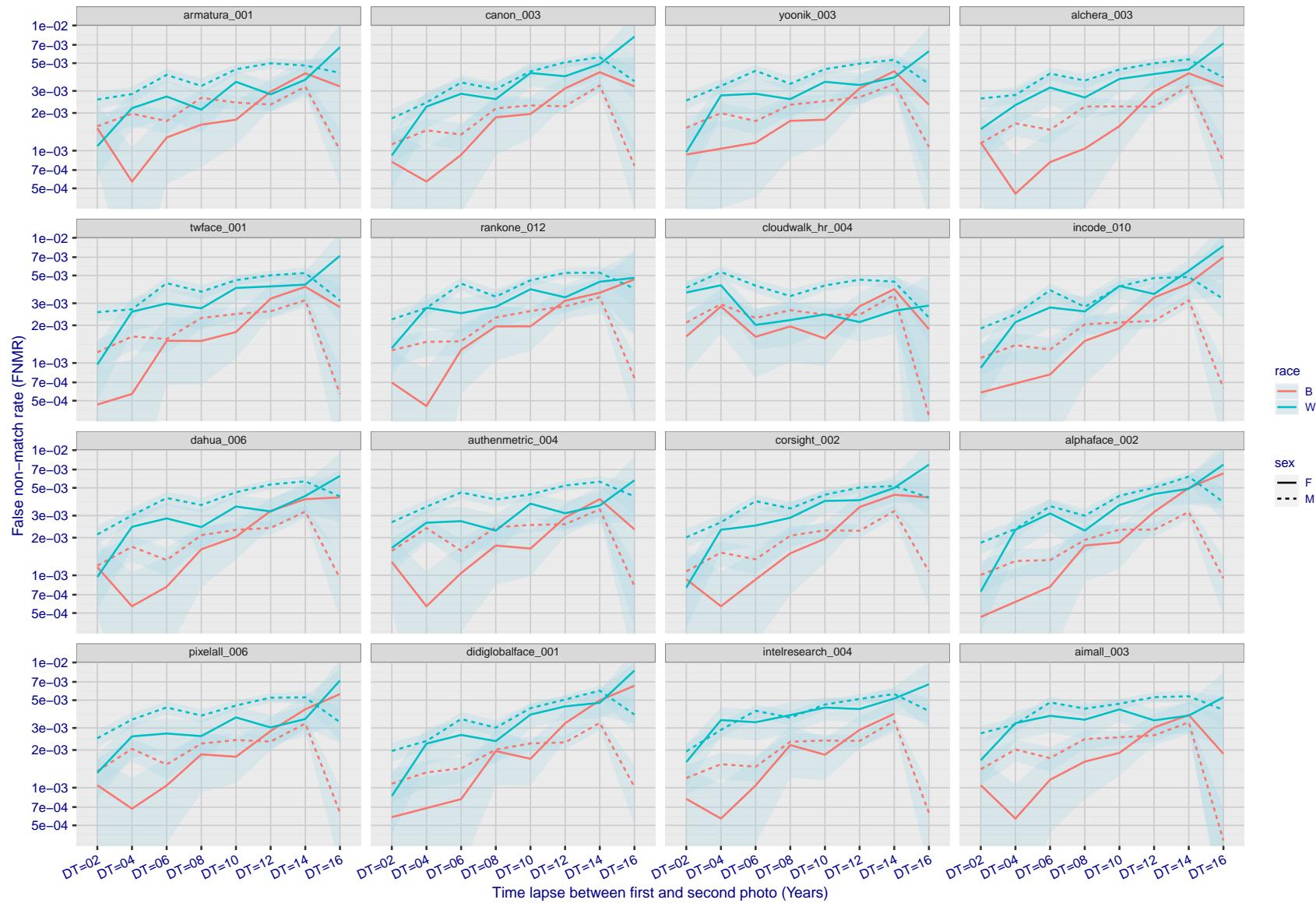


Figure 332: For the mugshot images, FNMR as a function of elapsed time between initial enrollment and second verification images. The panels appear most accurate first, and vertical scale changes on each page. The four traces correspond to images annotated with codes for black female, black male, white female, white male. The threshold is fixed for each algorithm to give FMR = 0.00001 over all (10^8) impostor comparisons. For short time-lapses, the most accurate algorithms give very few errors (FNMR < 0.001) so that the uncertainty estimates are high.

2022/11/06 10:45:39

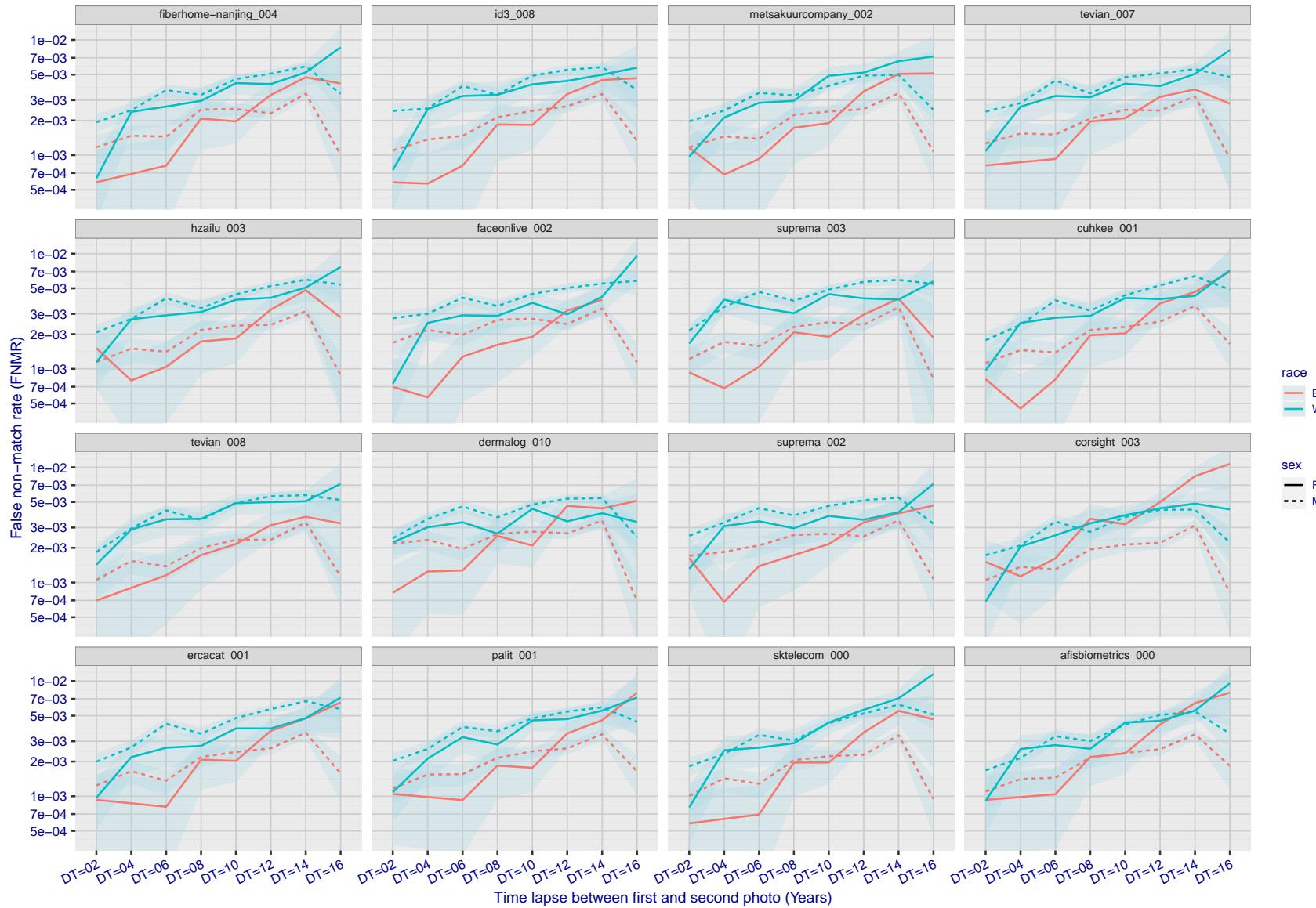


Figure 333: For the mugshot images, FNMR as a function of elapsed time between initial enrollment and second verification images. The panels appear most accurate first, and vertical scale changes on each page. The four traces correspond to images annotated with codes for black female, black male, white female, white male. The threshold is fixed for each algorithm to give FMR = 0.00001 over all (10^8) impostor comparisons. For short time-lapses, the most accurate algorithms give very few errors (FNMR < 0.001) so that the uncertainty estimates are high.

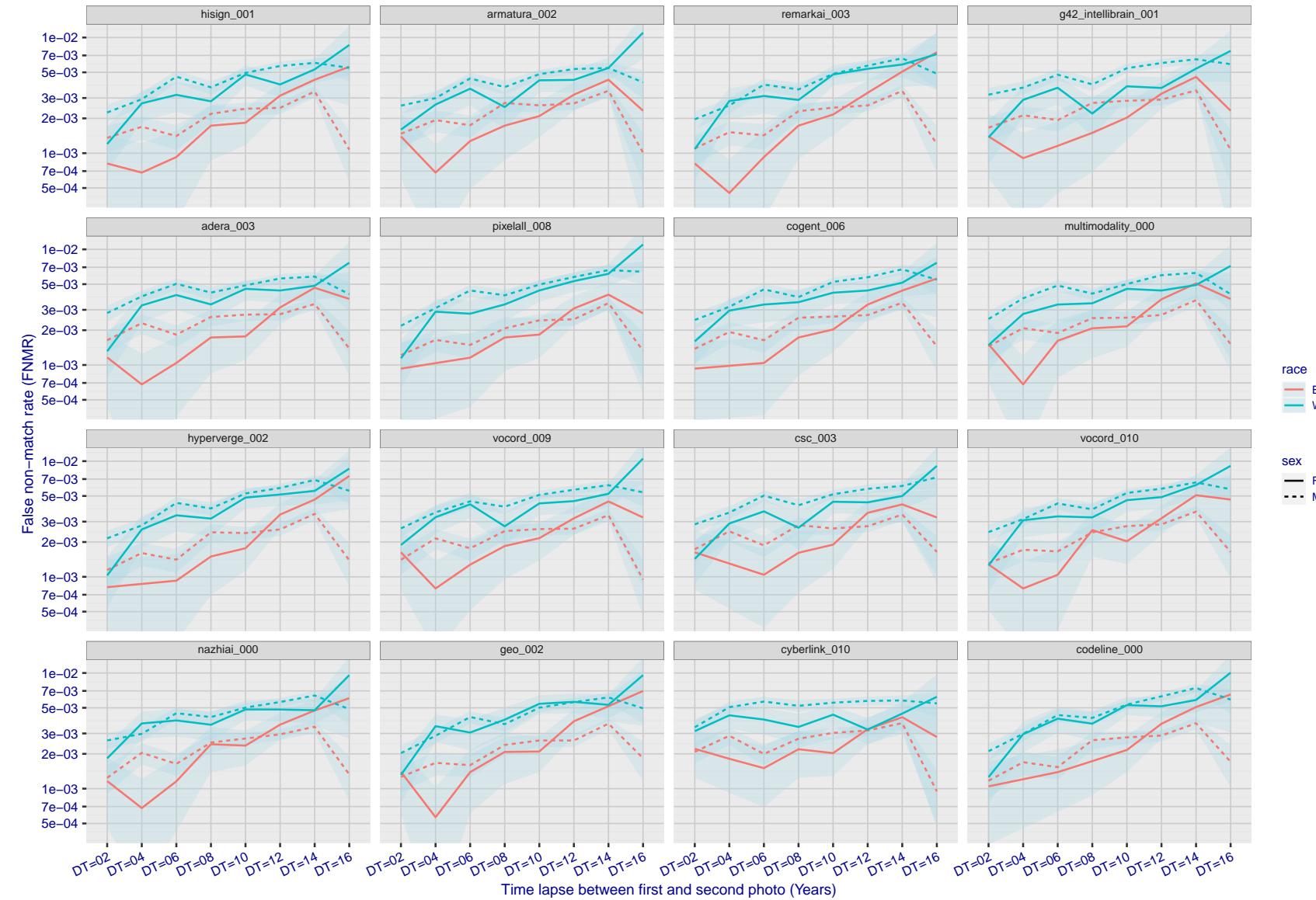


Figure 334: For the mugshot images, FNMR as a function of elapsed time between initial enrollment and second verification images. The panels appear most accurate first, and vertical scale changes on each page. The four traces correspond to images annotated with codes for black female, black male, white female, white male. The threshold is fixed for each algorithm to give $FMR = 0.00001$ over all (10^8) impostor comparisons. For short time-lapses, the most accurate algorithms give very few errors ($FNMR < 0.001$) so that the uncertainty estimates are high.

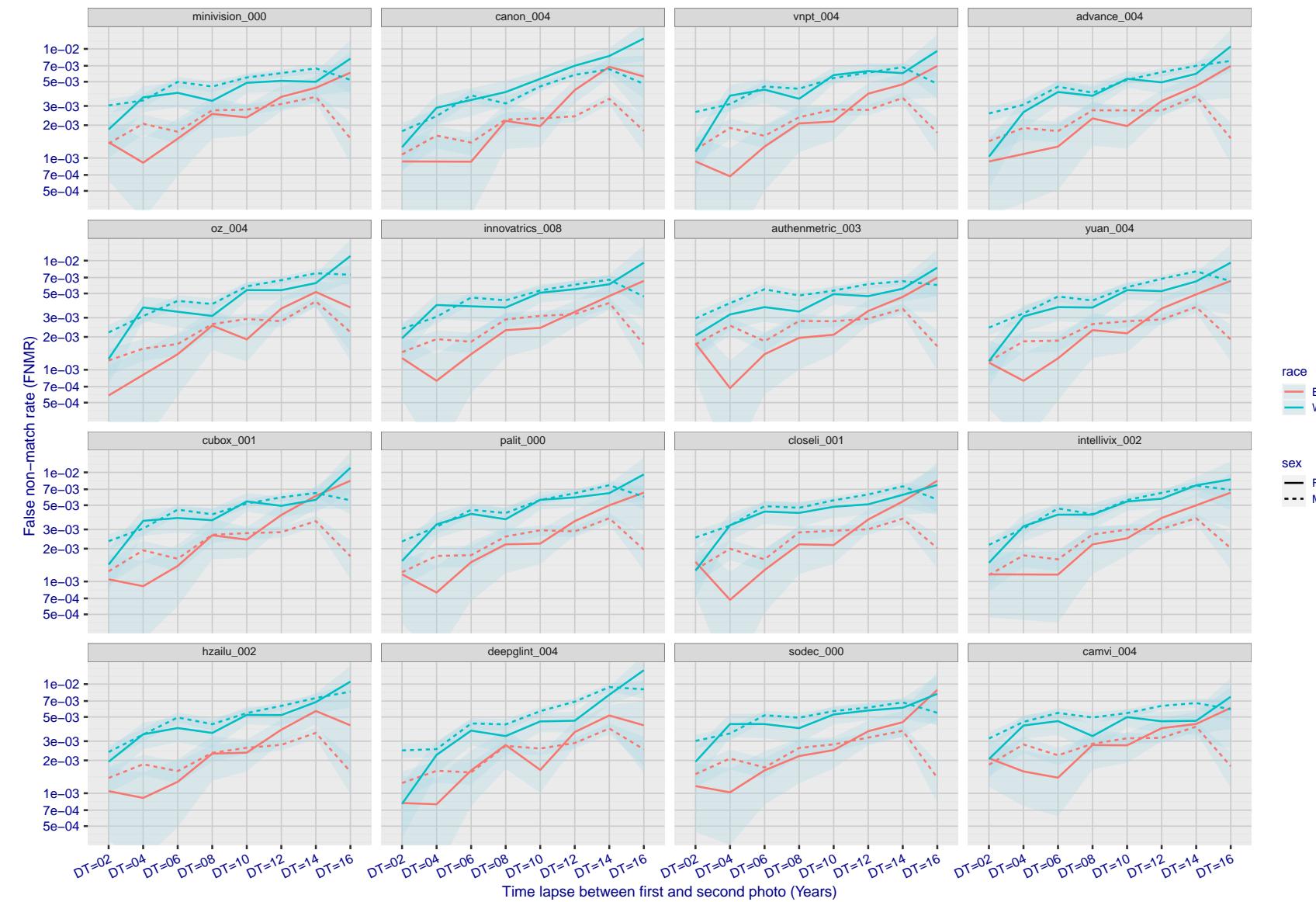


Figure 335: For the mugshot images, FNMR as a function of elapsed time between initial enrollment and second verification images. The panels appear most accurate first, and vertical scale changes on each page. The four traces correspond to images annotated with codes for black female, black male, white female, white male. The threshold is fixed for each algorithm to give FMR = 0.00001 over all (10^8) impostor comparisons. For short time-lapses, the most accurate algorithms give very few errors (FNMR < 0.001) so that the uncertainty estimates are high.

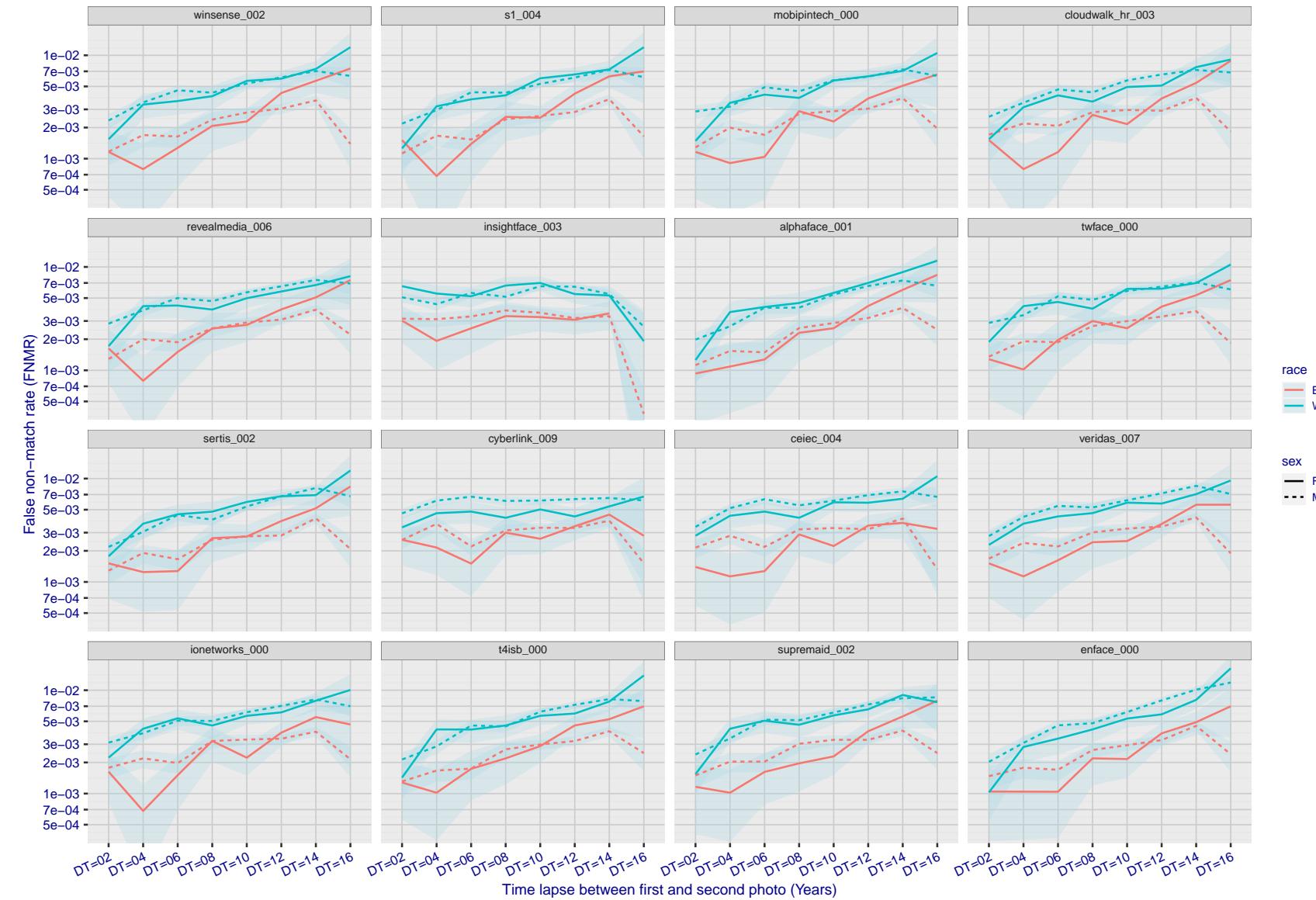


Figure 336: For the mugshot images, FNMR as a function of elapsed time between initial enrollment and second verification images. The panels appear most accurate first, and vertical scale changes on each page. The four traces correspond to images annotated with codes for black female, black male, white female, white male. The threshold is fixed for each algorithm to give FMR = 0.00001 over all (10^8) impostor comparisons. For short time-lapses, the most accurate algorithms give very few errors (FNMR < 0.001) so that the uncertainty estimates are high.

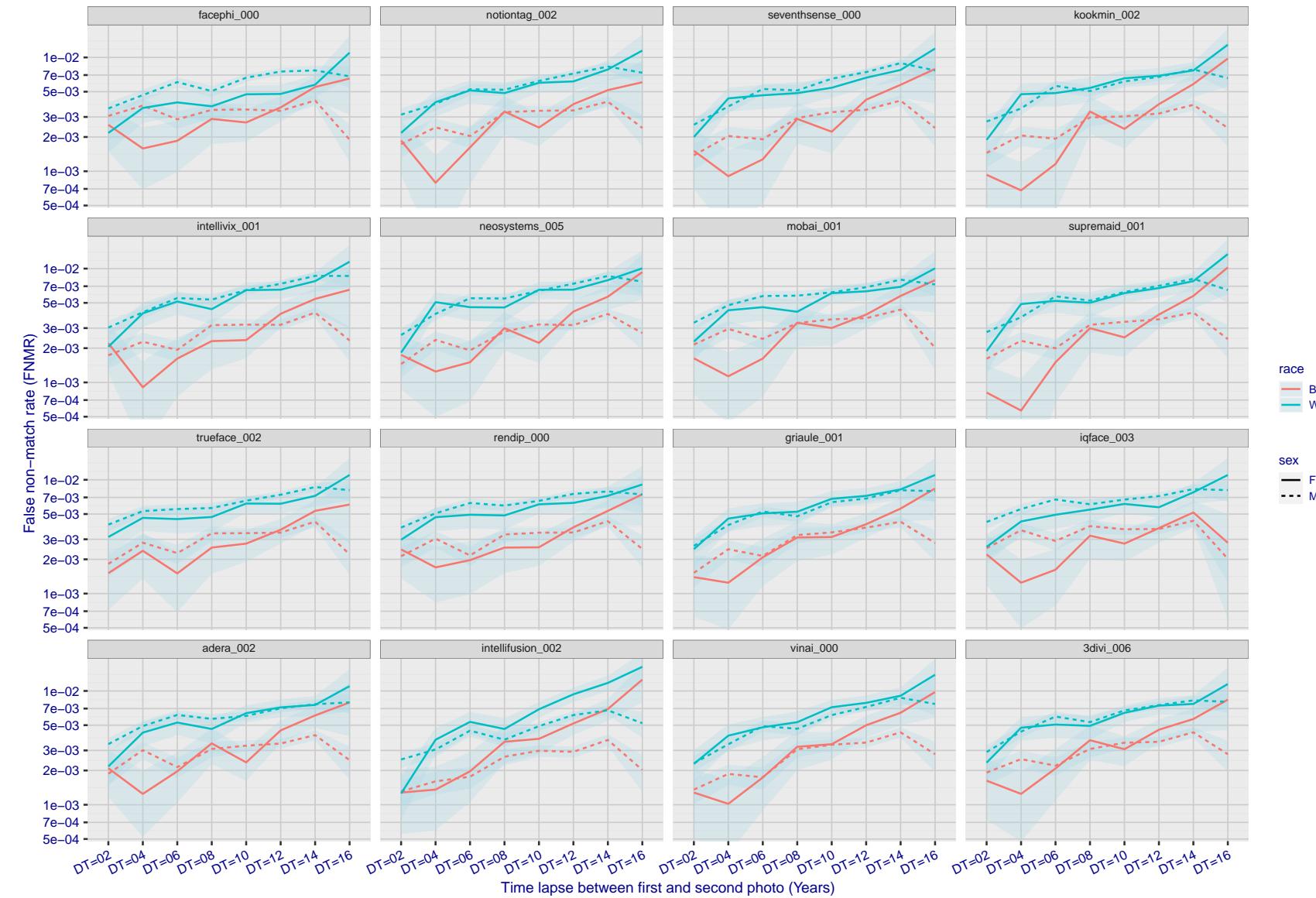


Figure 337: For the mugshot images, FNMR as a function of elapsed time between initial enrollment and second verification images. The panels appear most accurate first, and vertical scale changes on each page. The four traces correspond to images annotated with codes for black female, black male, white female, white male. The threshold is fixed for each algorithm to give FMR = 0.00001 over all (10^8) impostor comparisons. For short time-lapses, the most accurate algorithms give very few errors (FNMR < 0.001) so that the uncertainty estimates are high.

2022/11/06 10:45:39

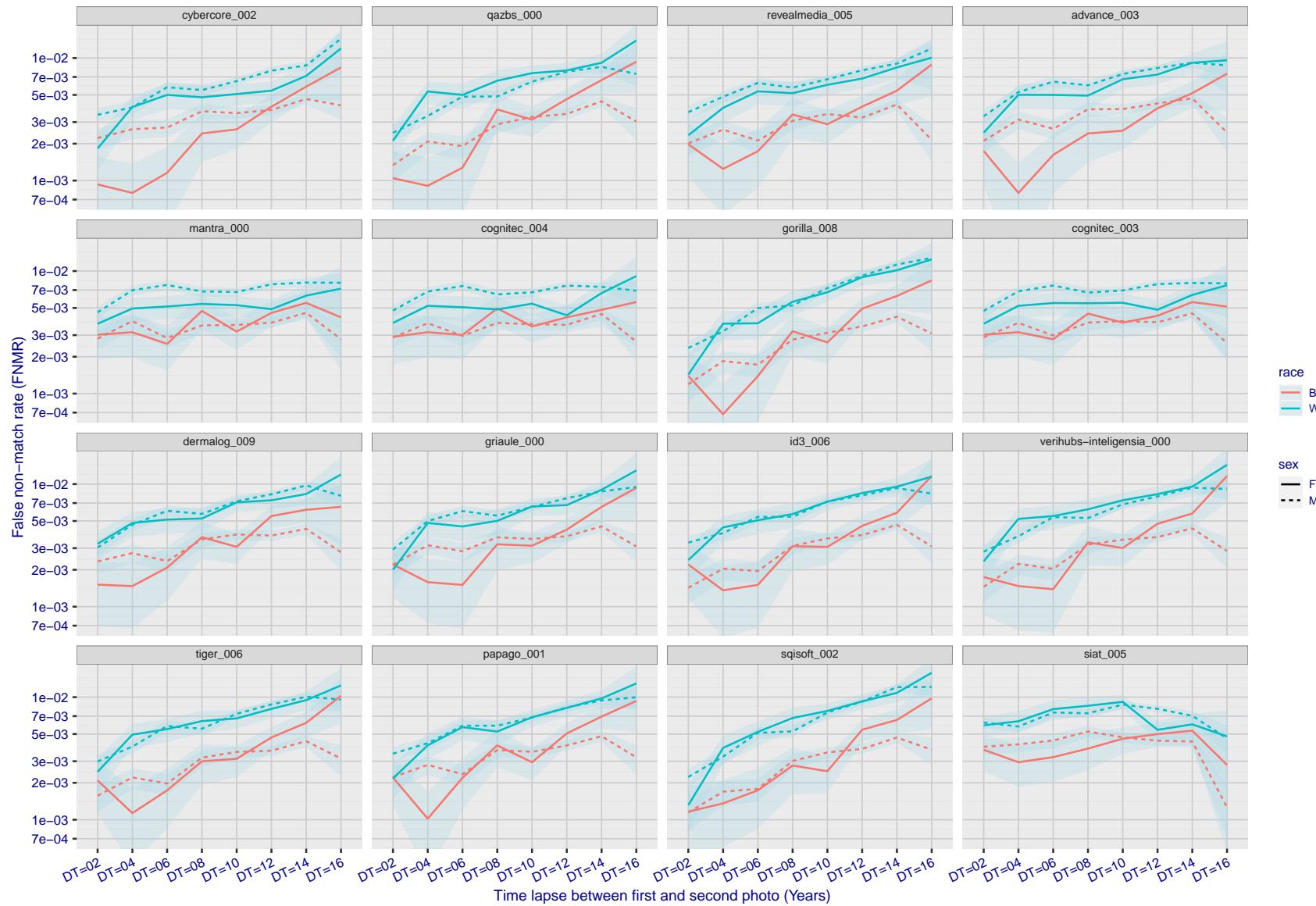


Figure 338: For the mugshot images, FNMR as a function of elapsed time between initial enrollment and second verification images. The panels appear most accurate first, and vertical scale changes on each page. The four traces correspond to images annotated with codes for black female, black male, white female, white male. The threshold is fixed for each algorithm to give $FMR = 0.00001$ over all (10^8) impostor comparisons. For short time-lapses, the most accurate algorithms give very few errors ($FNMR < 0.001$) so that the uncertainty estimates are high.

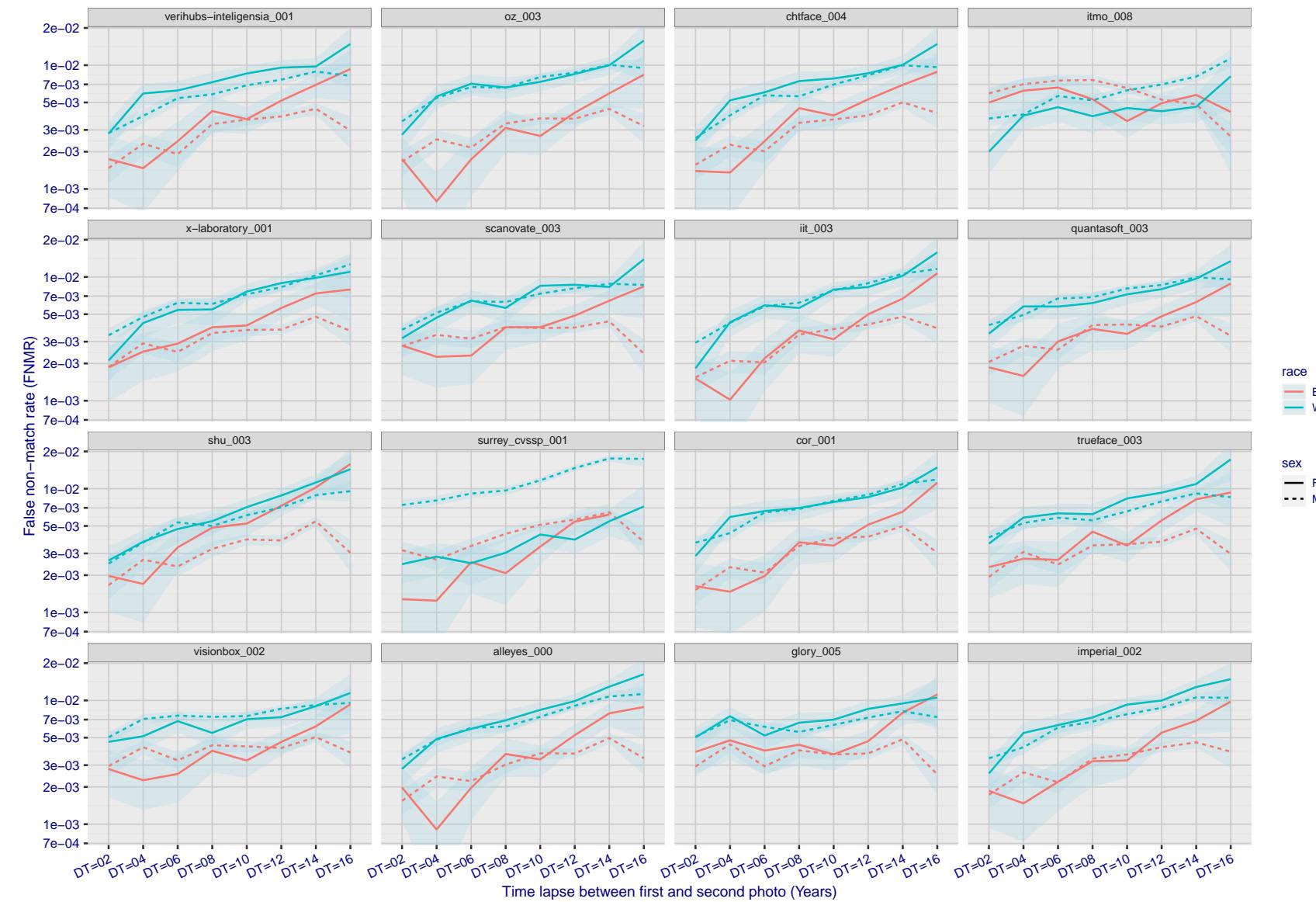


Figure 339: For the mugshot images, FNMR as a function of elapsed time between initial enrollment and second verification images. The panels appear most accurate first, and vertical scale changes on each page. The four traces correspond to images annotated with codes for black female, black male, white female, white male. The threshold is fixed for each algorithm to give $FMR = 0.00001$ over all (10^8) impostor comparisons. For short time-lapses, the most accurate algorithms give very few errors ($FNMR < 0.001$) so that the uncertainty estimates are high.

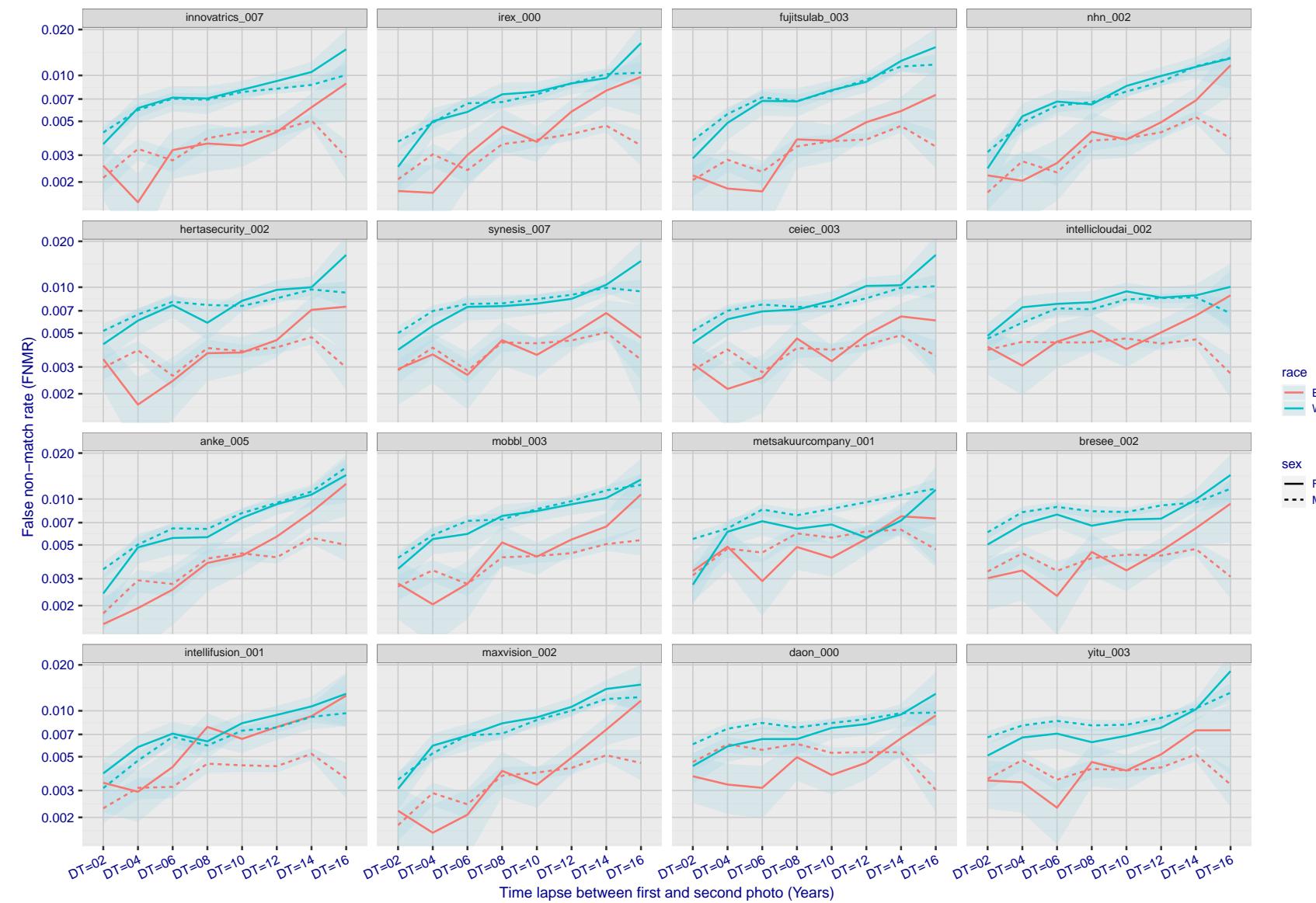


Figure 340: For the mugshot images, FNMR as a function of elapsed time between initial enrollment and second verification images. The panels appear most accurate first, and vertical scale changes on each page. The four traces correspond to images annotated with codes for black female, black male, white female, white male. The threshold is fixed for each algorithm to give FMR = 0.00001 over all (10^8) impostor comparisons. For short time-lapses, the most accurate algorithms give very few errors (FNMR < 0.001) so that the uncertainty estimates are high.

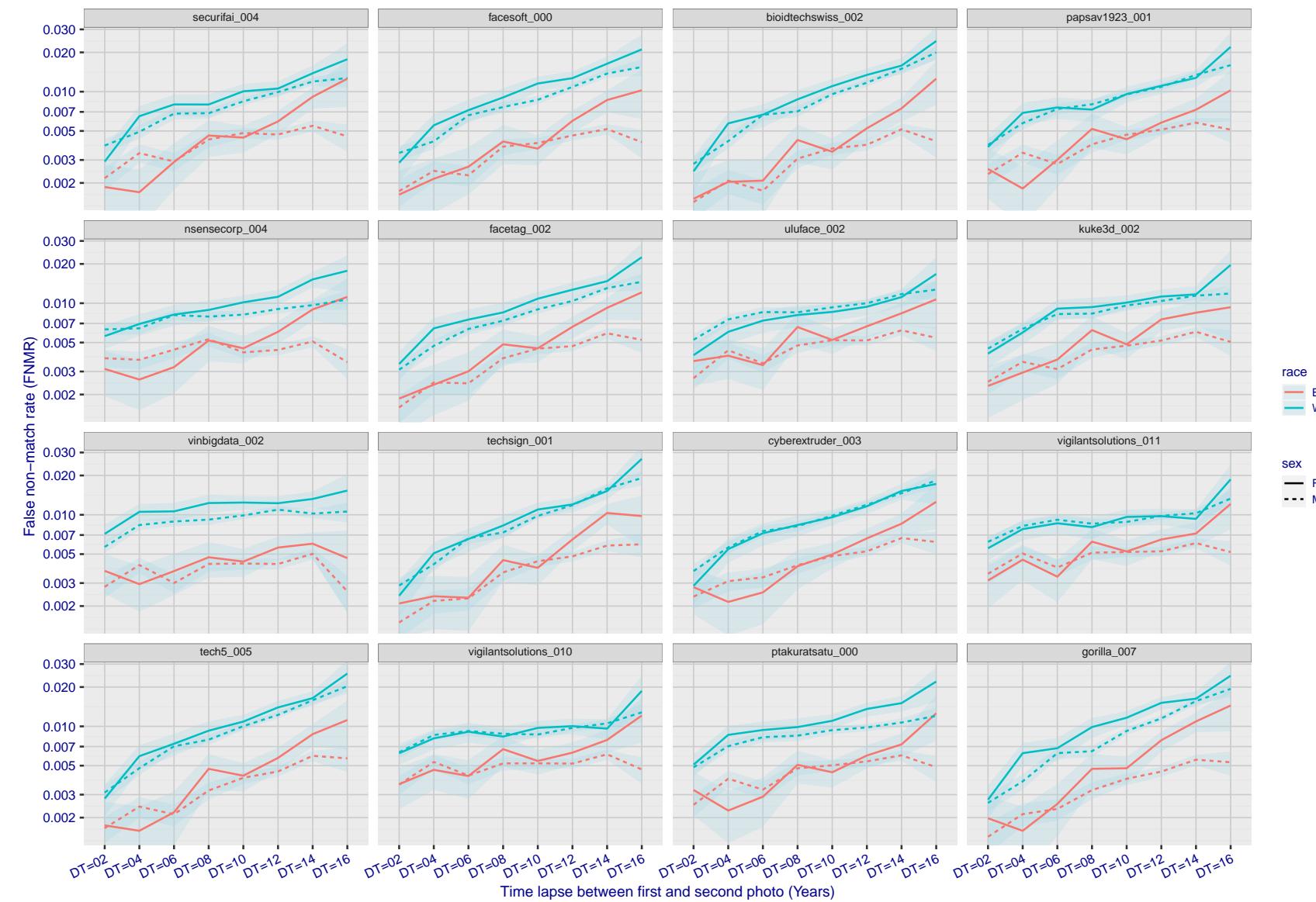


Figure 341: For the mugshot images, FNMR as a function of elapsed time between initial enrollment and second verification images. The panels appear most accurate first, and vertical scale changes on each page. The four traces correspond to images annotated with codes for black female, black male, white female, white male. The threshold is fixed for each algorithm to give FMR = 0.00001 over all (10^8) impostor comparisons. For short time-lapses, the most accurate algorithms give very few errors (FNMR < 0.001) so that the uncertainty estimates are high.

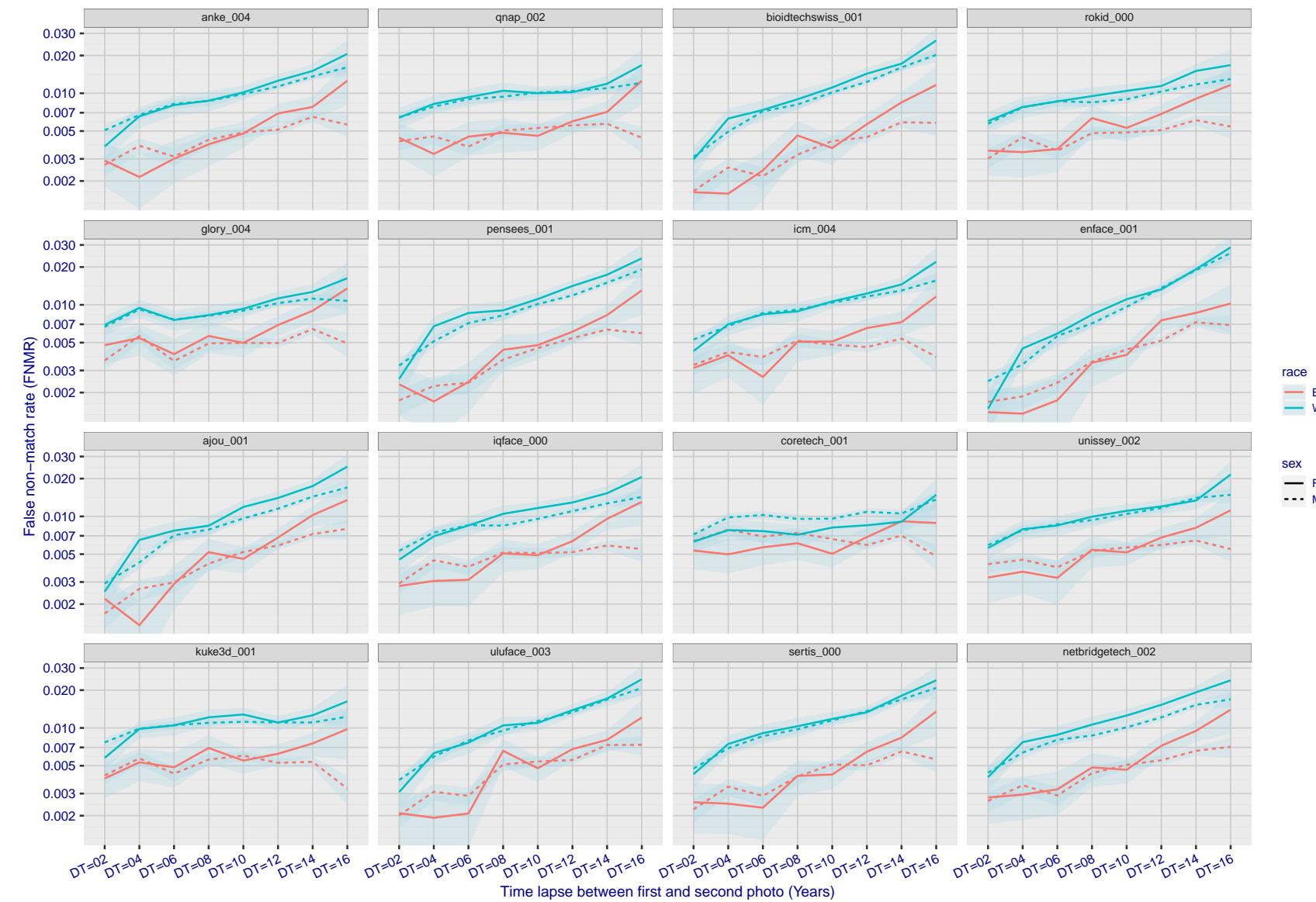


Figure 342: For the mugshot images, FNMR as a function of elapsed time between initial enrollment and second verification images. The panels appear most accurate first, and vertical scale changes on each page. The four traces correspond to images annotated with codes for black female, black male, white female, white male. The threshold is fixed for each algorithm to give FMR = 0.00001 over all (10^8) impostor comparisons. For short time-lapses, the most accurate algorithms give very few errors (FNMR < 0.001) so that the uncertainty estimates are high.

2022/11/06 10:45:39

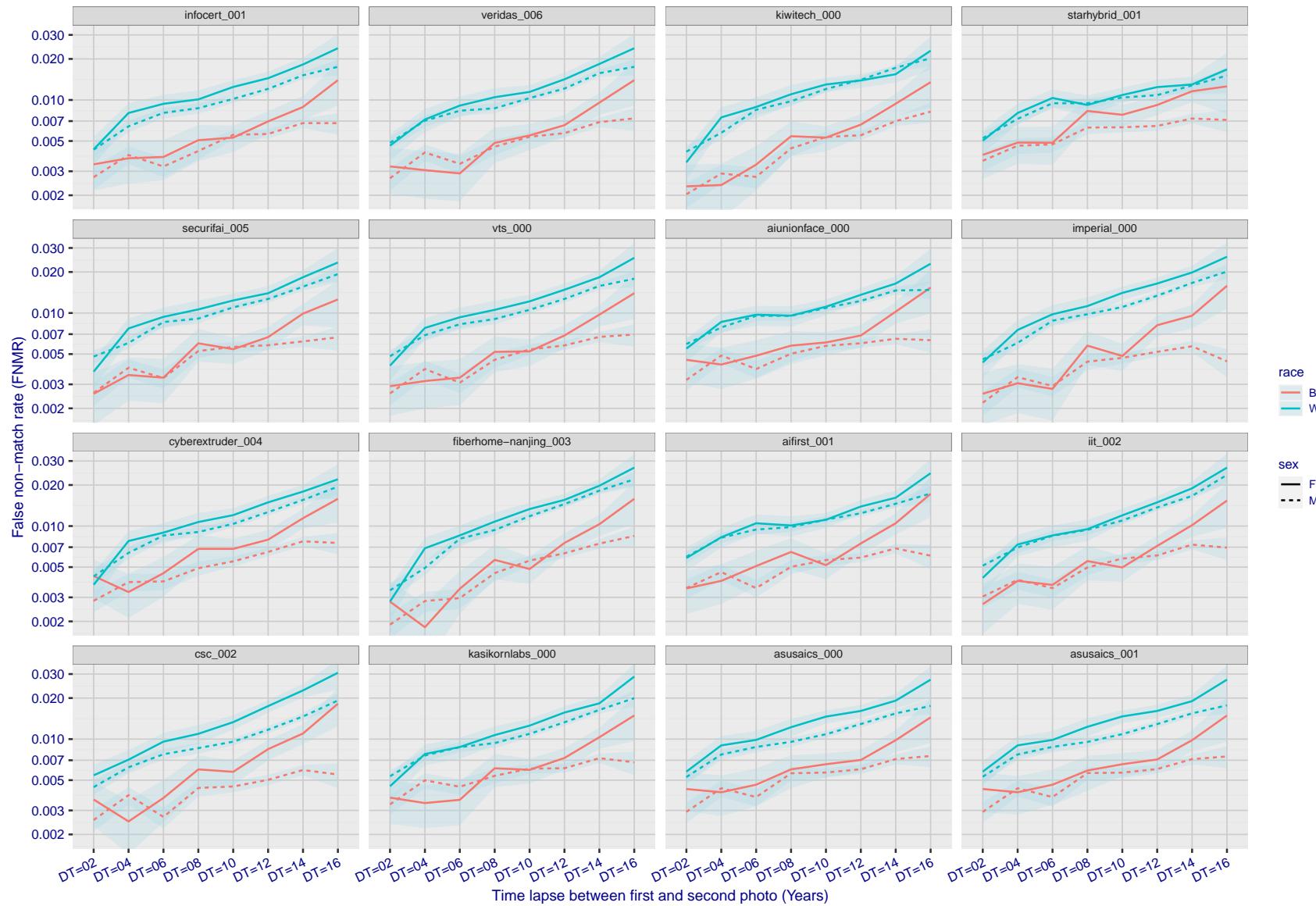


Figure 343: For the mugshot images, FNMR as a function of elapsed time between initial enrollment and second verification images. The panels appear most accurate first, and vertical scale changes on each page. The four traces correspond to images annotated with codes for black female, black male, white female, white male. The threshold is fixed for each algorithm to give FMR = 0.00001 over all (10^8) impostor comparisons. For short time-lapses, the most accurate algorithms give very few errors (FNMR < 0.001) so that the uncertainty estimates are high.

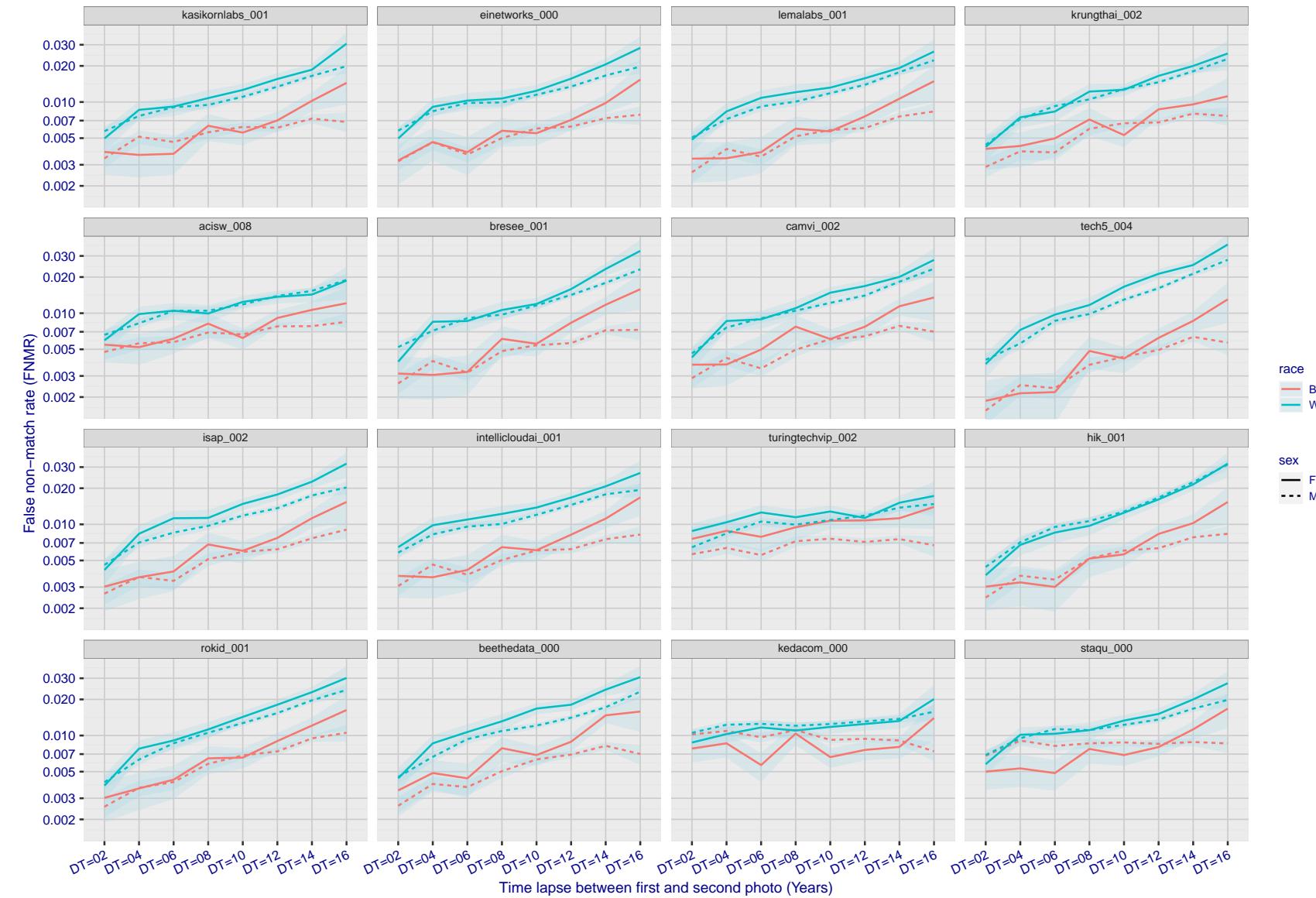


Figure 344: For the mugshot images, FNMR as a function of elapsed time between initial enrollment and second verification images. The panels appear most accurate first, and vertical scale changes on each page. The four traces correspond to images annotated with codes for black female, black male, white female, white male. The threshold is fixed for each algorithm to give FMR = 0.00001 over all (10^8) impostor comparisons. For short time-lapses, the most accurate algorithms give very few errors (FNMR < 0.001) so that the uncertainty estimates are high.

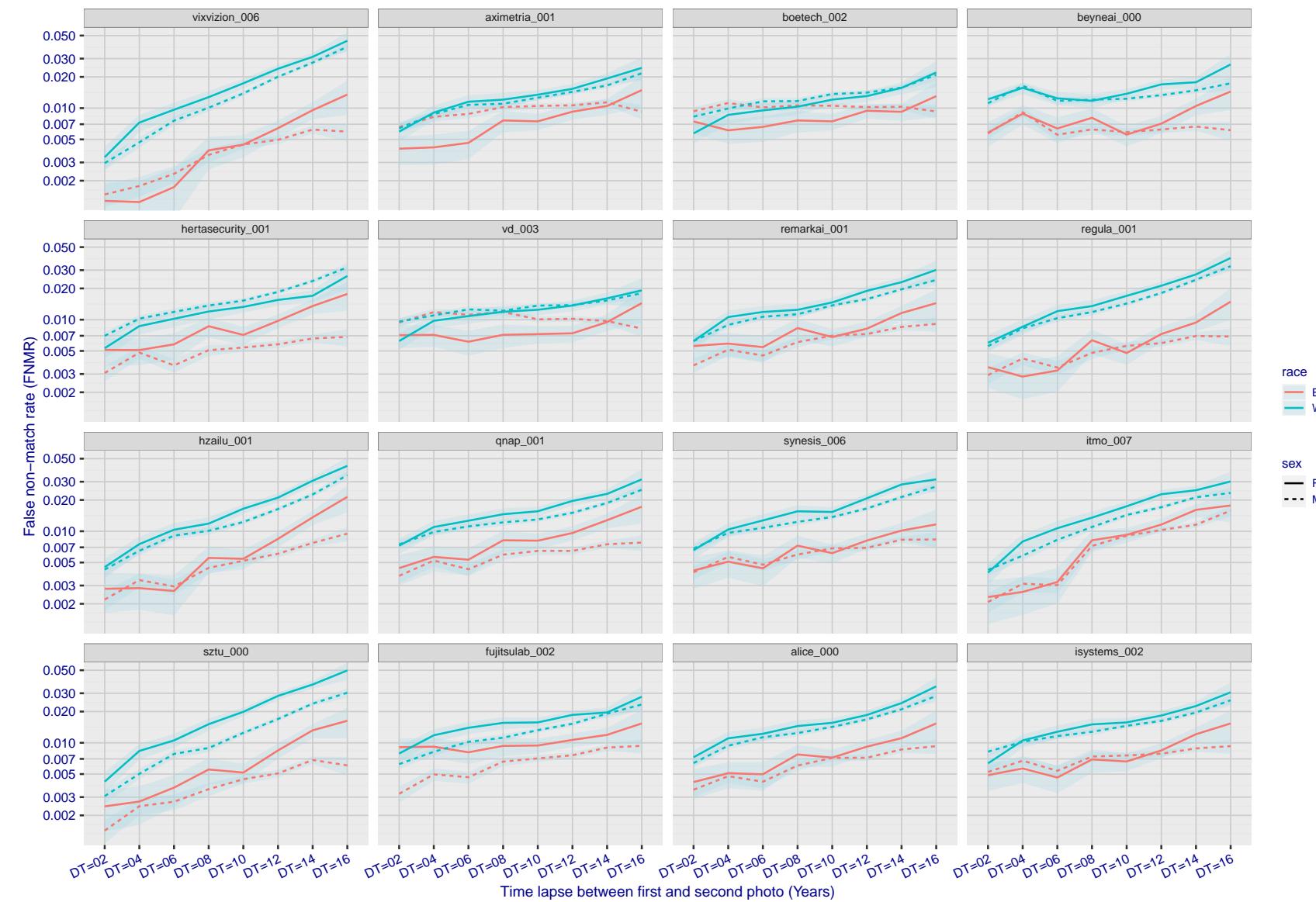


Figure 345: For the mugshot images, FNMR as a function of elapsed time between initial enrollment and second verification images. The panels appear most accurate first, and vertical scale changes on each page. The four traces correspond to images annotated with codes for black female, black male, white female, white male. The threshold is fixed for each algorithm to give FMR = 0.00001 over all (10^8) impostor comparisons. For short time-lapses, the most accurate algorithms give very few errors (FNMR < 0.001) so that the uncertainty estimates are high.

2022/11/06 10:45:39

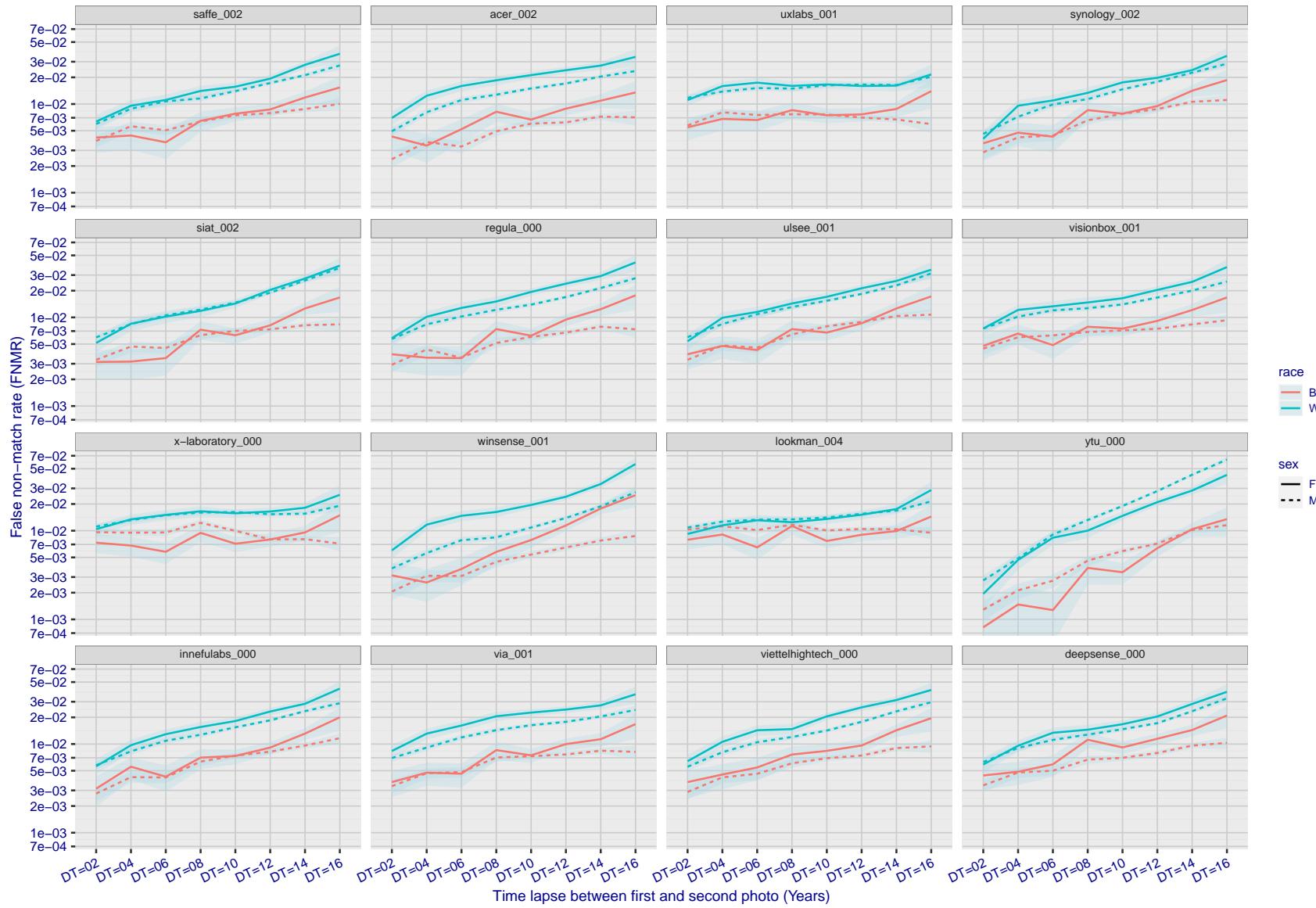


Figure 346: For the mugshot images, FNMR as a function of elapsed time between initial enrollment and second verification images. The panels appear most accurate first, and vertical scale changes on each page. The four traces correspond to images annotated with codes for black female, black male, white female, white male. The threshold is fixed for each algorithm to give $FMR = 0.00001$ over all (10^8) impostor comparisons. For short time-lapses, the most accurate algorithms give very few errors ($FNMR < 0.001$) so that the uncertainty estimates are high.

FNMR(T)
FMR(T)
"False non-match rate"
"False match rate"

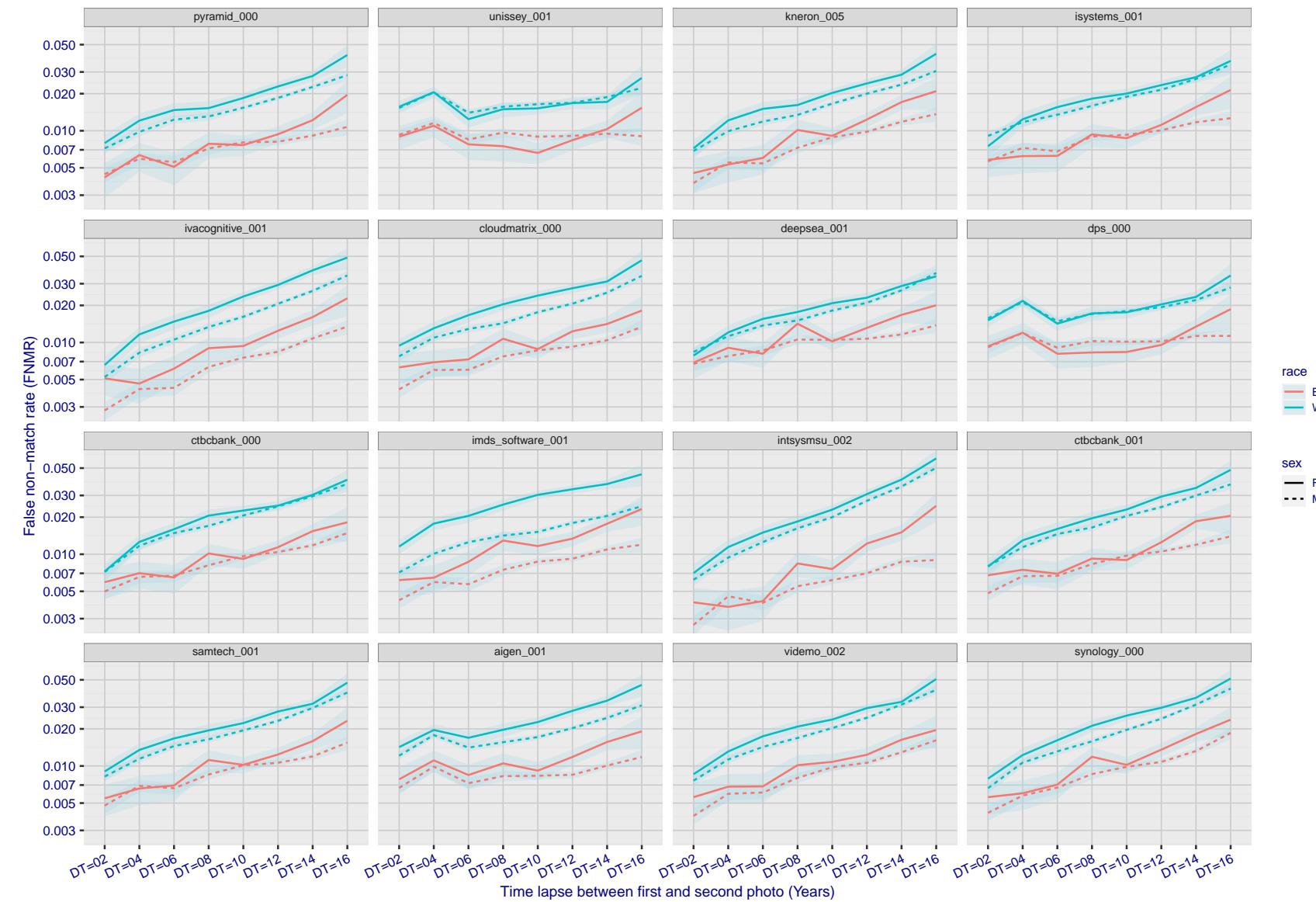


Figure 347: For the mugshot images, FNMR as a function of elapsed time between initial enrollment and second verification images. The panels appear most accurate first, and vertical scale changes on each page. The four traces correspond to images annotated with codes for black female, black male, white female, white male. The threshold is fixed for each algorithm to give FMR = 0.00001 over all (10^8) impostor comparisons. For short time-lapses, the most accurate algorithms give very few errors (FNMR < 0.001) so that the uncertainty estimates are high.

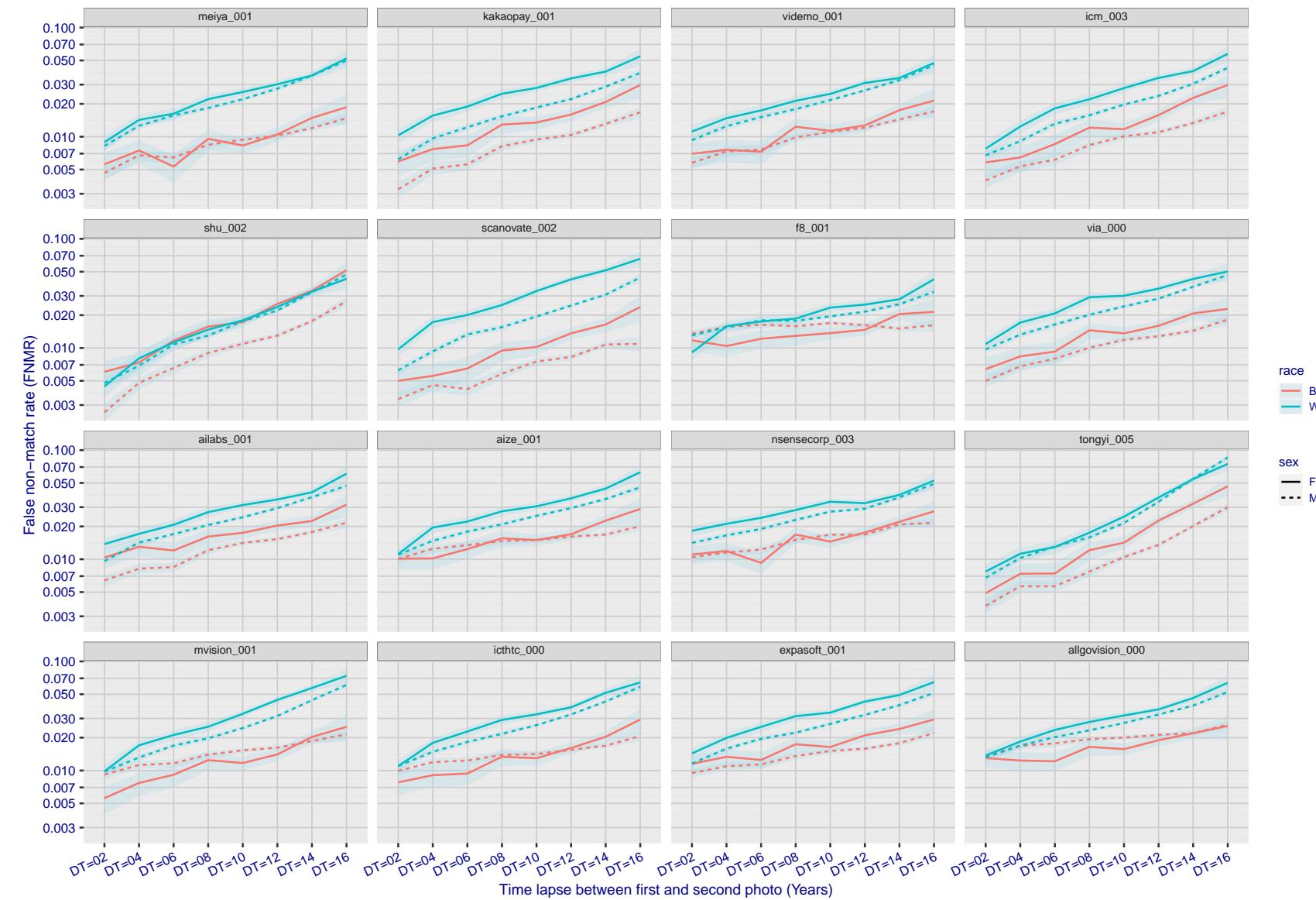


Figure 348: For the mugshot images, FNMR as a function of elapsed time between initial enrollment and second verification images. The panels appear most accurate first, and vertical scale changes on each page. The four traces correspond to images annotated with codes for black female, black male, white female, white male. The threshold is fixed for each algorithm to give FMR = 0.00001 over all (10^8) impostor comparisons. For short time-lapses, the most accurate algorithms give very few errors (FNMR < 0.001) so that the uncertainty estimates are high.

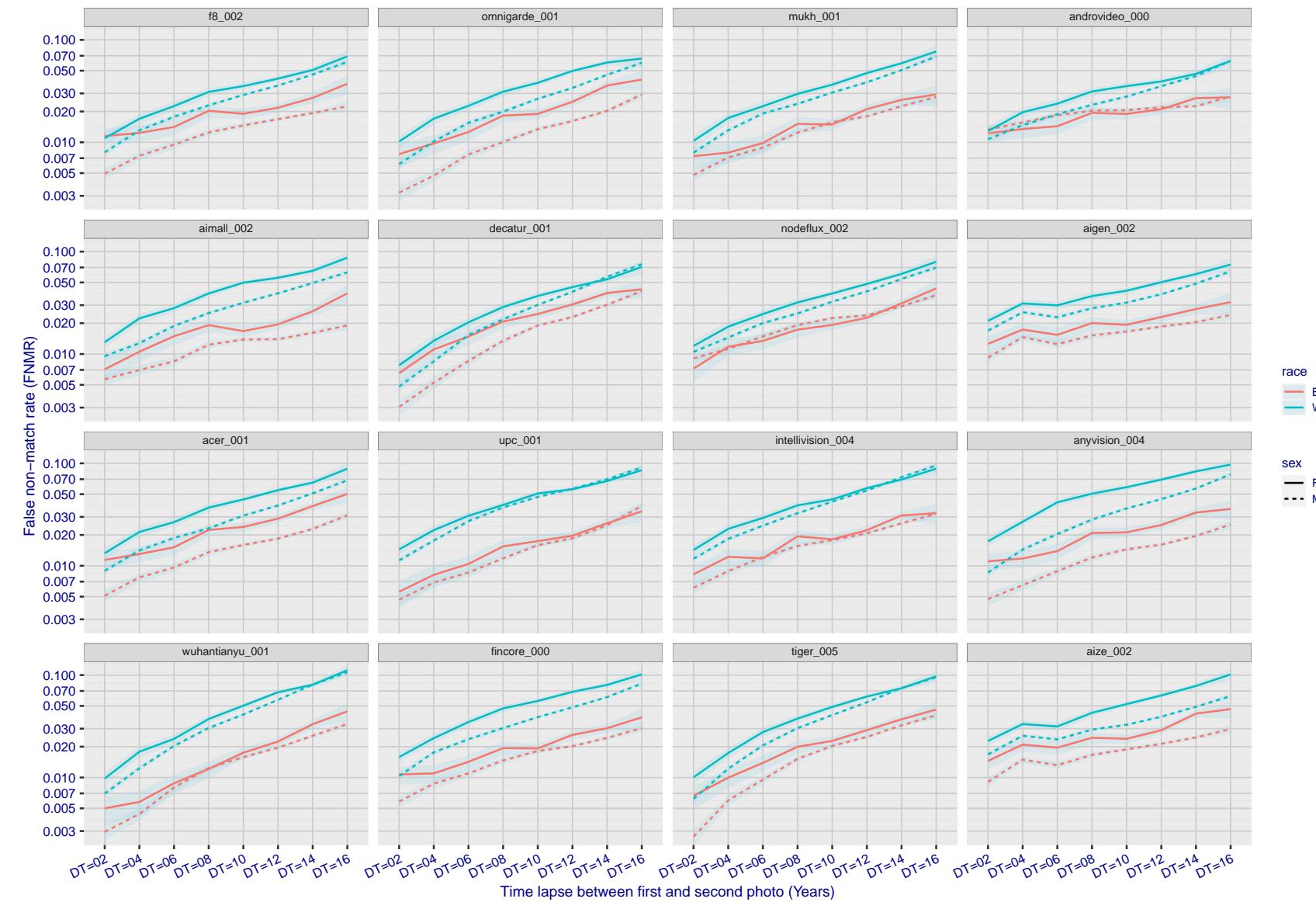


Figure 349: For the mugshot images, FNMR as a function of elapsed time between initial enrollment and second verification images. The panels appear most accurate first, and vertical scale changes on each page. The four traces correspond to images annotated with codes for black female, black male, white female, white male. The threshold is fixed for each algorithm to give FMR = 0.00001 over all (10^8) impostor comparisons. For short time-lapses, the most accurate algorithms give very few errors (FNMR < 0.001) so that the uncertainty estimates are high.

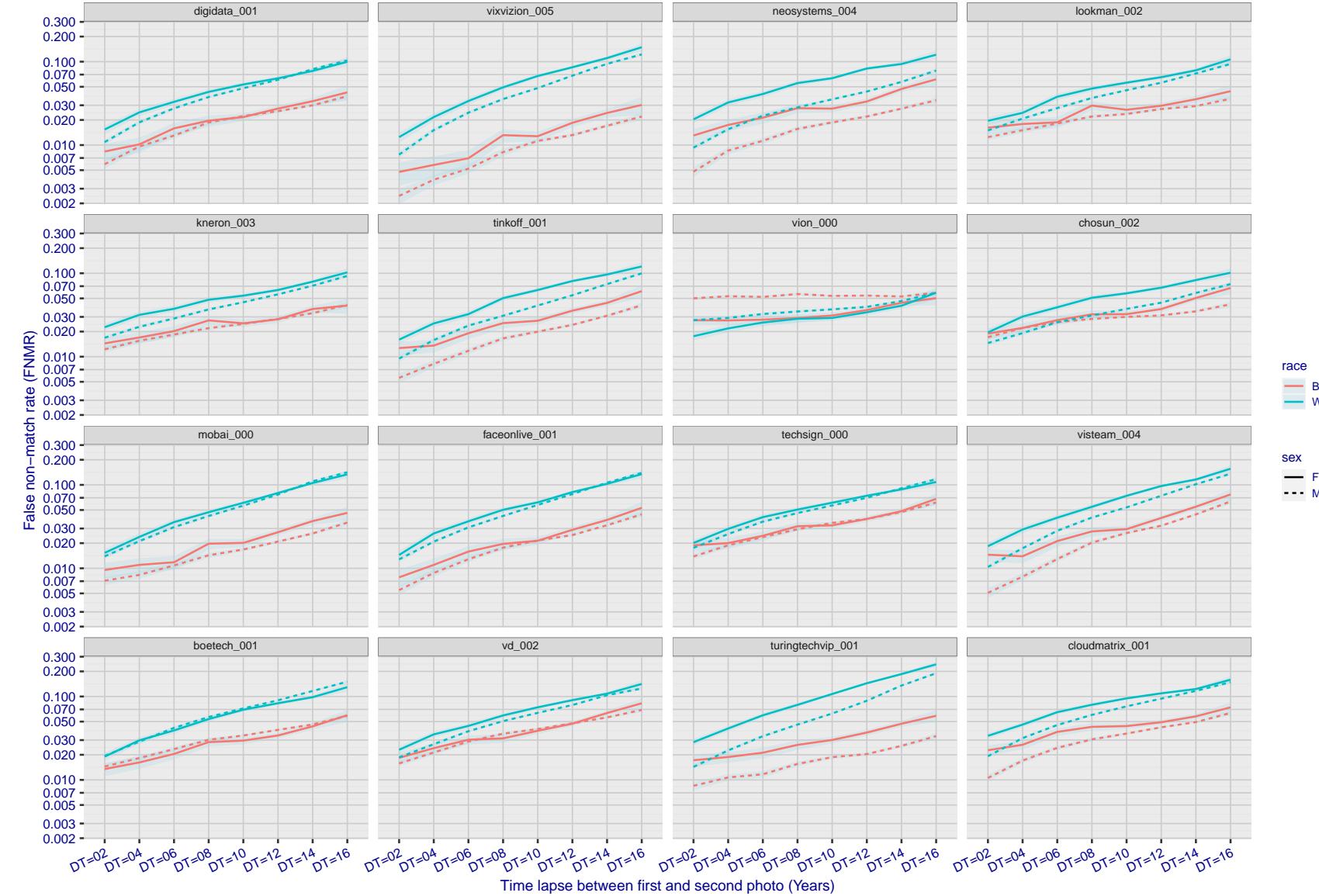


Figure 350: For the mugshot images, FNMR as a function of elapsed time between initial enrollment and second verification images. The panels appear most accurate first, and vertical scale changes on each page. The four traces correspond to images annotated with codes for black female, black male, white female, white male. The threshold is fixed for each algorithm to give FMR = 0.00001 over all (10^8) impostor comparisons. For short time-lapses, the most accurate algorithms give very few errors (FNMR < 0.001) so that the uncertainty estimates are high.

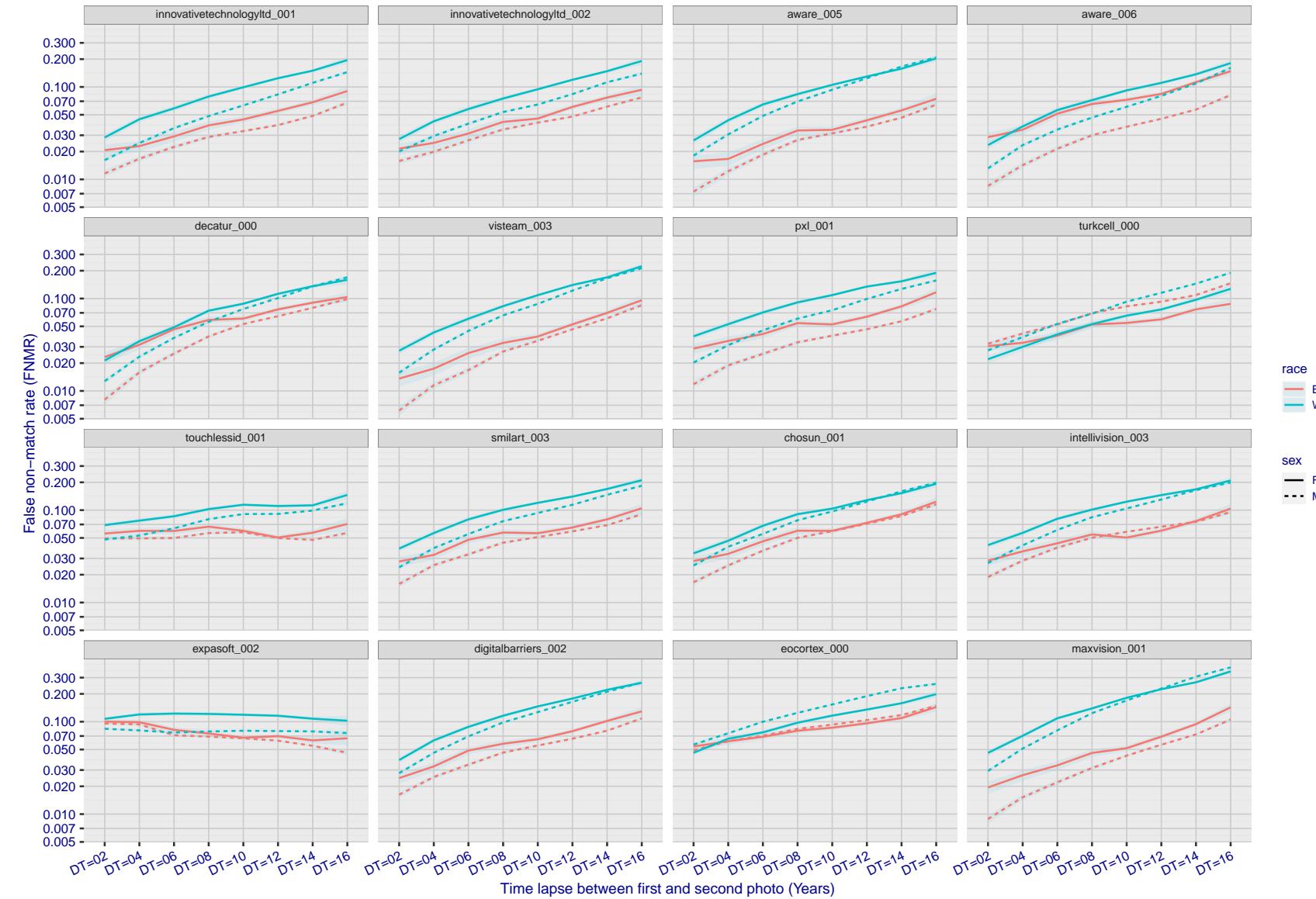


Figure 351: For the mugshot images, FNMR as a function of elapsed time between initial enrollment and second verification images. The panels appear most accurate first, and vertical scale changes on each page. The four traces correspond to images annotated with codes for black female, black male, white female, white male. The threshold is fixed for each algorithm to give FMR = 0.00001 over all (10^8) impostor comparisons. For short time-lapses, the most accurate algorithms give very few errors (FNMR < 0.001) so that the uncertainty estimates are high.

2022/11/06 10:45:39

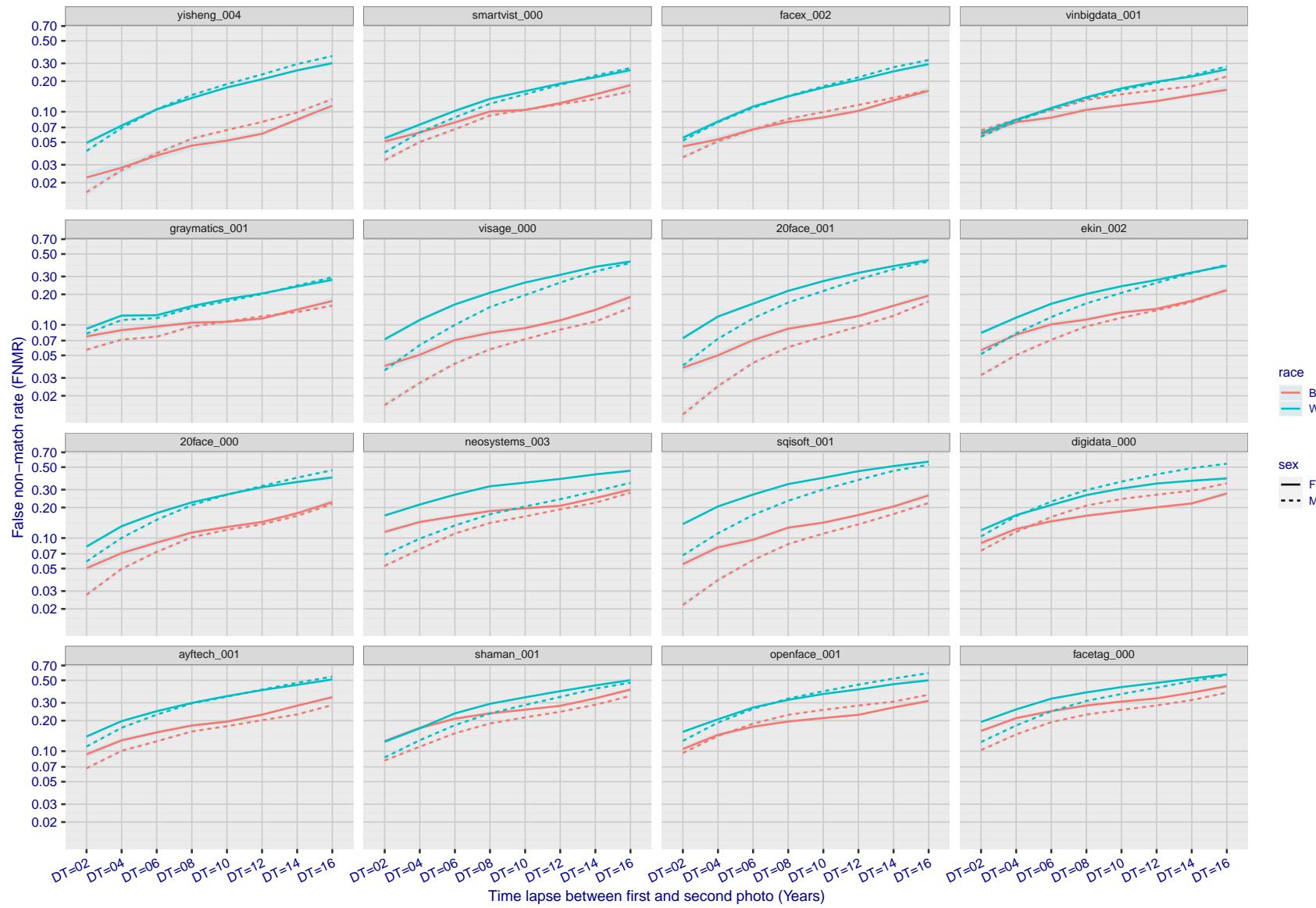


Figure 352: For the mugshot images, FNMR as a function of elapsed time between initial enrollment and second verification images. The panels appear most accurate first, and vertical scale changes on each page. The four traces correspond to images annotated with codes for black female, black male, white female, white male. The threshold is fixed for each algorithm to give FMR = 0.00001 over all (10^8) impostor comparisons. For short time-lapses, the most accurate algorithms give very few errors (FNMR < 0.001) so that the uncertainty estimates are high.

FNMR(T)
FMR(T)
"False non-match rate"
"False match rate"

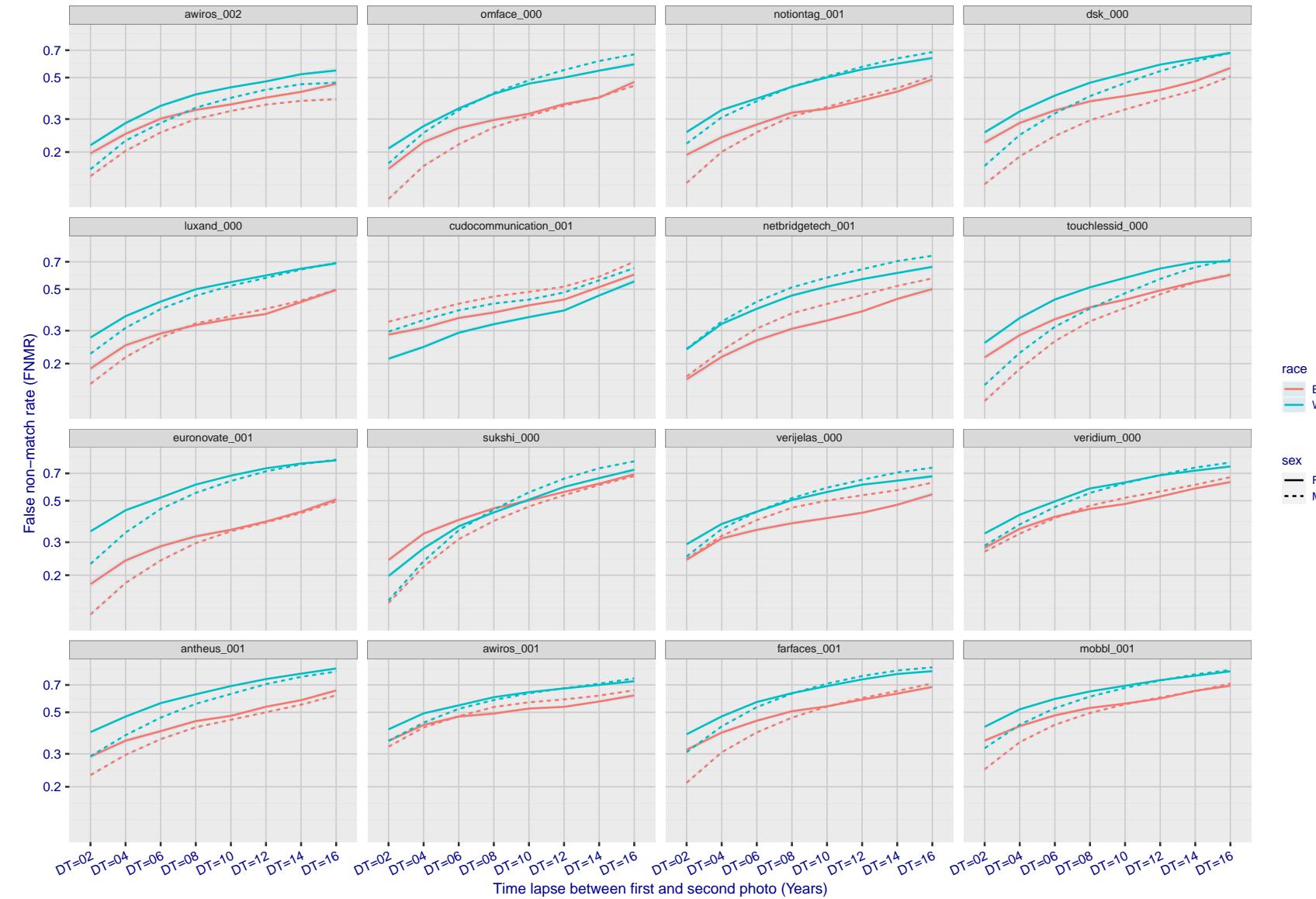


Figure 353: For the mugshot images, FNMR as a function of elapsed time between initial enrollment and second verification images. The panels appear most accurate first, and vertical scale changes on each page. The four traces correspond to images annotated with codes for black female, black male, white female, white male. The threshold is fixed for each algorithm to give FMR = 0.00001 over all (10^8) impostor comparisons. For short time-lapses, the most accurate algorithms give very few errors (FNMR < 0.001) so that the uncertainty estimates are high.

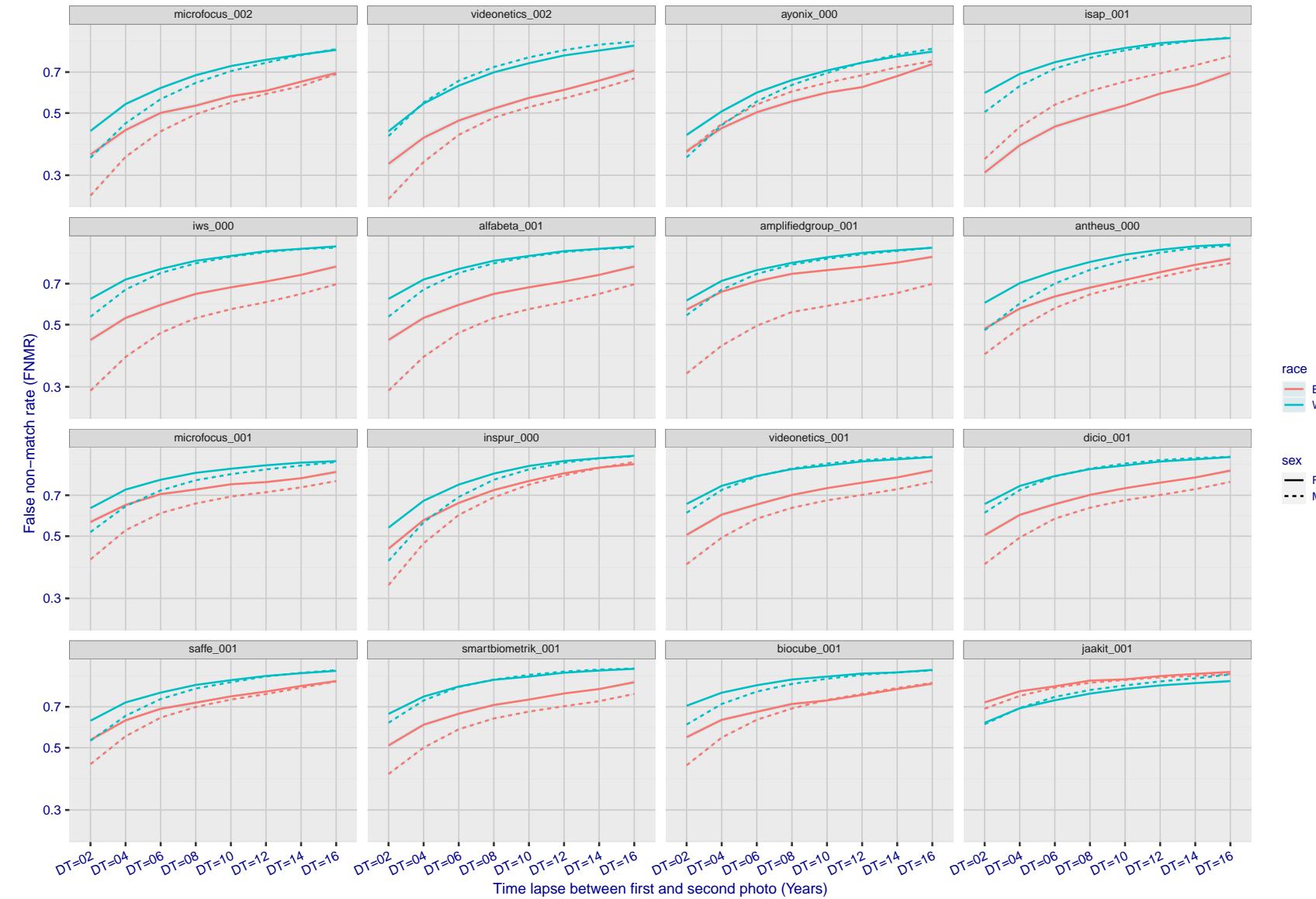


Figure 354: For the mugshot images, FNMR as a function of elapsed time between initial enrollment and second verification images. The panels appear most accurate first, and vertical scale changes on each page. The four traces correspond to images annotated with codes for black female, black male, white female, white male. The threshold is fixed for each algorithm to give FMR = 0.00001 over all (10^8) impostor comparisons. For short time-lapses, the most accurate algorithms give very few errors (FNMR < 0.001) so that the uncertainty estimates are high.

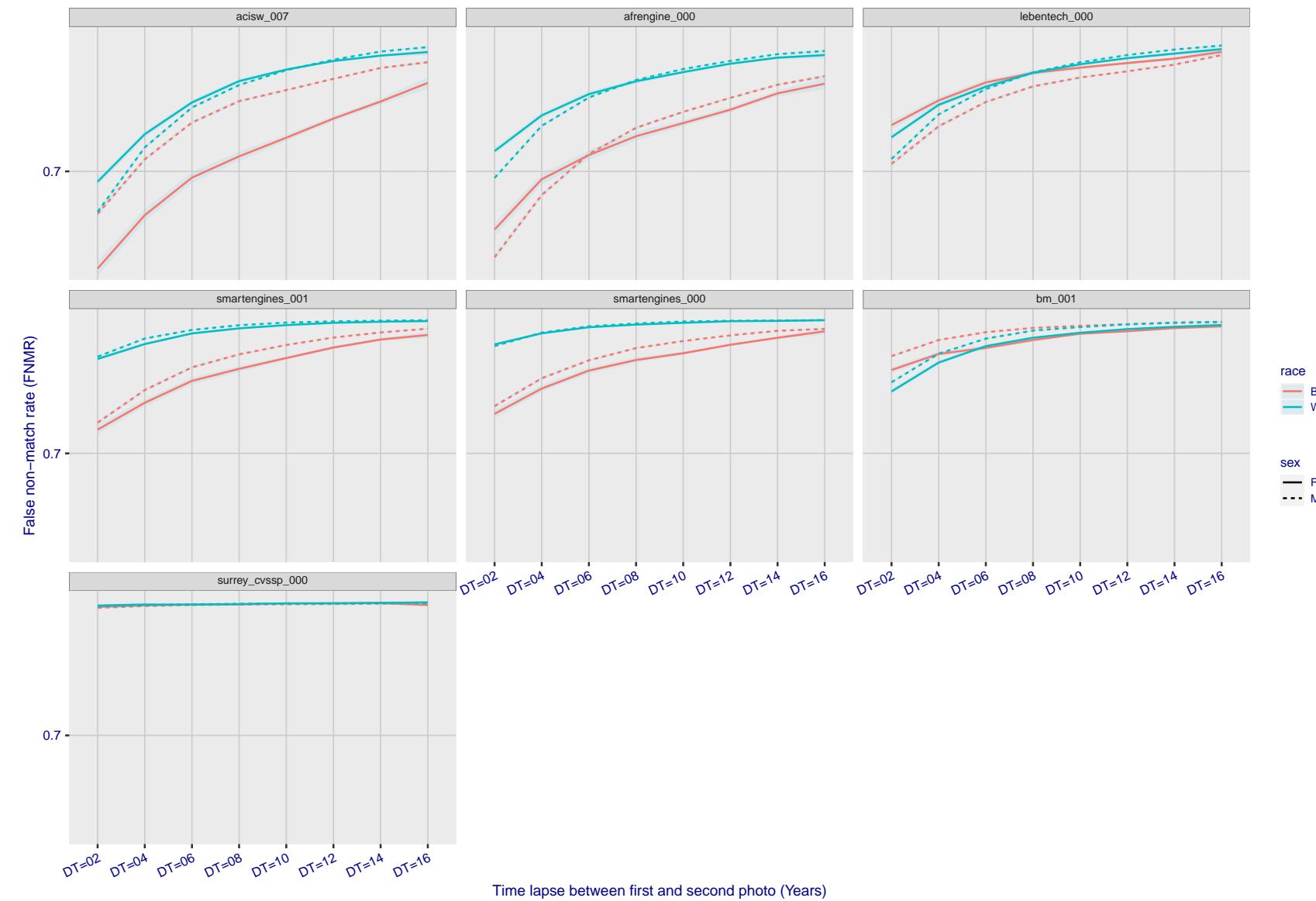


Figure 355: For the mugshot images, FNMR as a function of elapsed time between initial enrollment and second verification images. The panels appear most accurate first, and vertical scale changes on each page. The four traces correspond to images annotated with codes for black female, black male, white female, white male. The threshold is fixed for each algorithm to give FMR = 0.00001 over all (10^8) impostor comparisons. For short time-lapses, the most accurate algorithms give very few errors (FNMR < 0.001) so that the uncertainty estimates are high.

3.5.3 Effect of age on genuine subjects

Background: Faces change appearance throughout life. Face recognition algorithms have previously been reported to give better accuracy on older individuals (See NIST IR 8009).

Goal: To quantify false non-match rates (FNMR) as a function of age, without an ageing component.

Methods: Using the visa images, which span fewer than five years, thresholds are determined that give FMR = 0.001 and 0.0001 over the entire impostor set. Then FNMR is measured over 1000 bootstrap replications of the genuine scores.

Results: For the visa images, Figure 394 shows how false non-match rates for genuine users, as a function of age group.

The notable aspects are:

- ▷ Younger subjects give considerably higher FNMR. This is likely due to rapid growth and change in facial appearance.
- ▷ FNMR trends down throughout life. The last bin, AGE > 72, contains fewer than 140 mated pairs, and may be affected by small sample size.

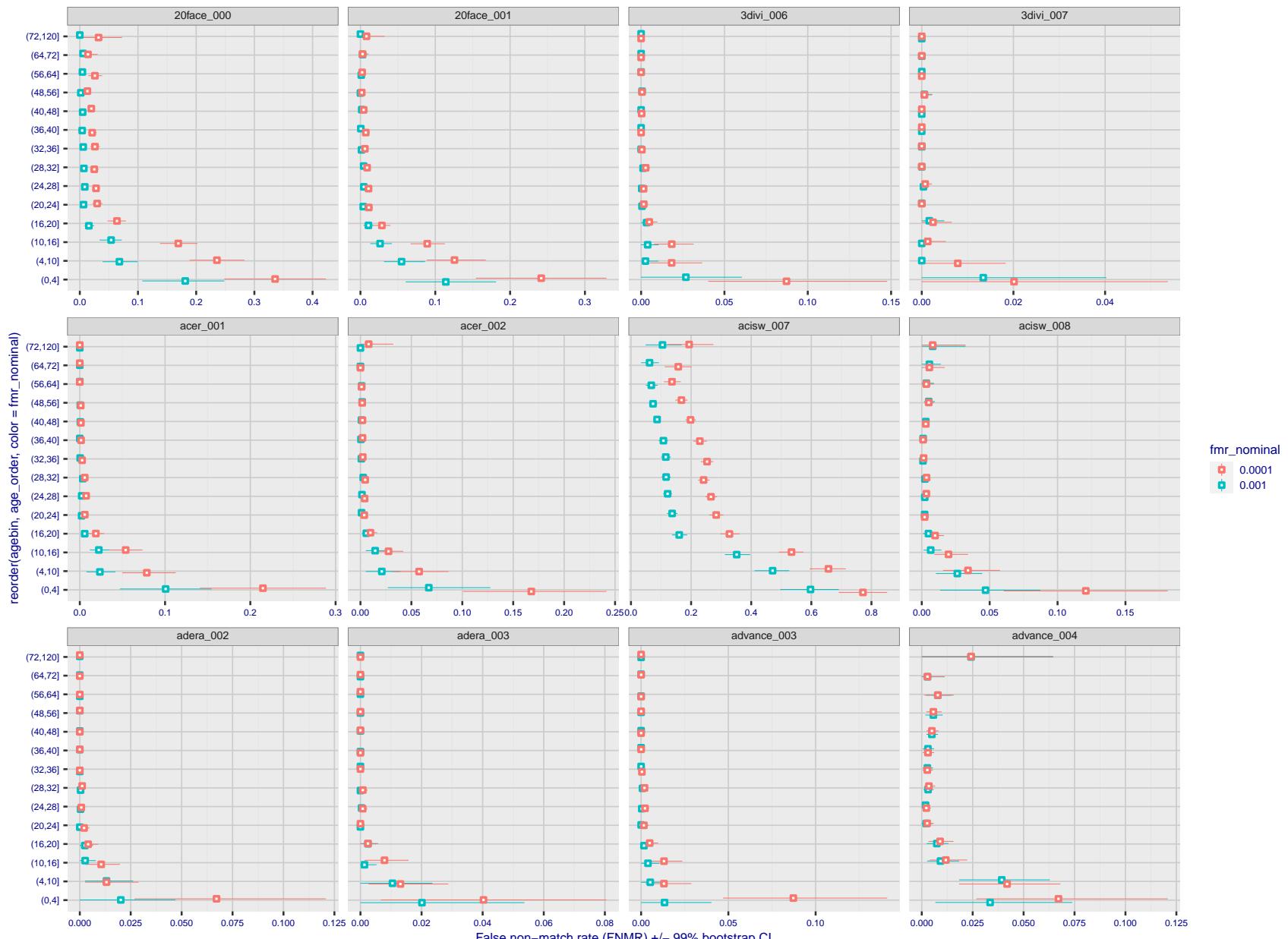


Figure 356: For the visa images, the dots show FNMR by age group for two operating thresholds corresponding to $FMR = \{0.001, 0.0001\}$ computed over all on the order of 10^{10} impostor scores. The FMR in each bin will vary also - see subsequent impostor heatmaps in sec. 3.6.2. Given a pair of face images taken at different times, we assign the comparison to the bin that is the arithmetic average of the subject's ages. This plot shows only the effect of age, not ageing. The number of comparisons in each bin is generally in the thousands, however the first and last bins are computed over 149 and 124 respectively. The error rates in some (adult) cases are zero, and in others the DET is flat so the error rates at the two thresholds are identical. The lines span 1% and 99% of bootstrap replicated FNMR estimates.

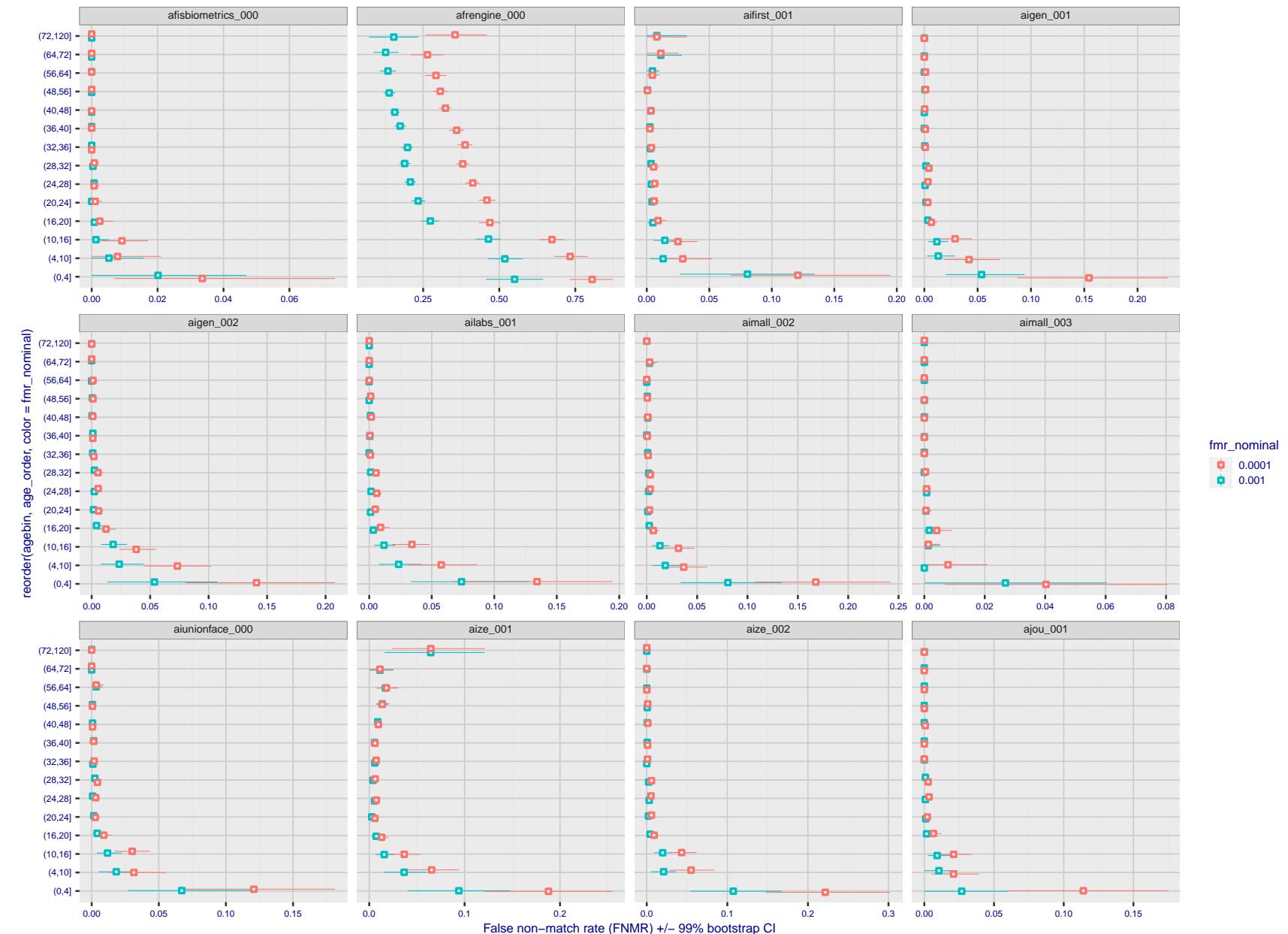


Figure 357: For the visa images, the dots show FNMR by age group for two operating thresholds corresponding to $FMR = \{0.001, 0.0001\}$ computed over all on the order of 10^{10} impostor scores. The FMR in each bin will vary also - see subsequent impostor heatmaps in sec. 3.6.2. Given a pair of face images taken at different times, we assign the comparison to the bin that is the arithmetic average of the subject's ages. This plot shows only the effect of age, not ageing. The number of comparisons in each bin is generally in the thousands, however the first and last bins are computed over 149 and 124 respectively. The error rates in some (adult) cases are zero, and in others the DET is flat so the error rates at the two thresholds are identical. The lines span 1% and 99% of bootstrap replicated FNMR estimates.

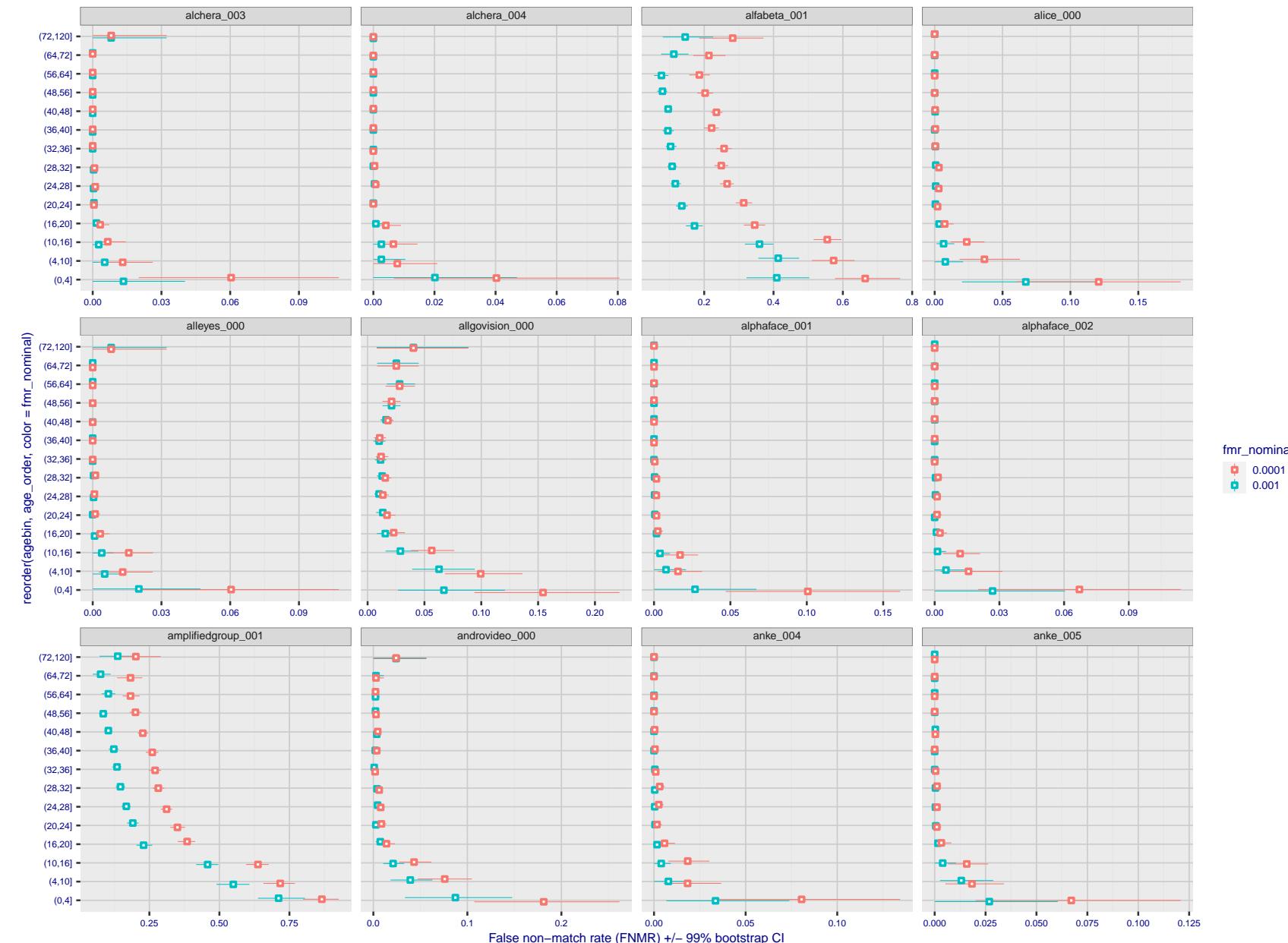


Figure 358: For the visa images, the dots show FNMR by age group for two operating thresholds corresponding to $FMR = \{0.001, 0.0001\}$ computed over all on the order of 10^{10} impostor scores. The FMR in each bin will vary also - see subsequent impostor heatmaps in sec. 3.6.2. Given a pair of face images taken at different times, we assign the comparison to the bin that is the arithmetic average of the subject's ages. This plot shows only the effect of age, not ageing. The number of comparisons in each bin is generally in the thousands, however the first and last bins are computed over 149 and 124 respectively. The error rates in some (adult) cases are zero, and in others the DET is flat so the error rates at the two thresholds are identical. The lines span 1% and 99% of bootstrap replicated FNMR estimates.

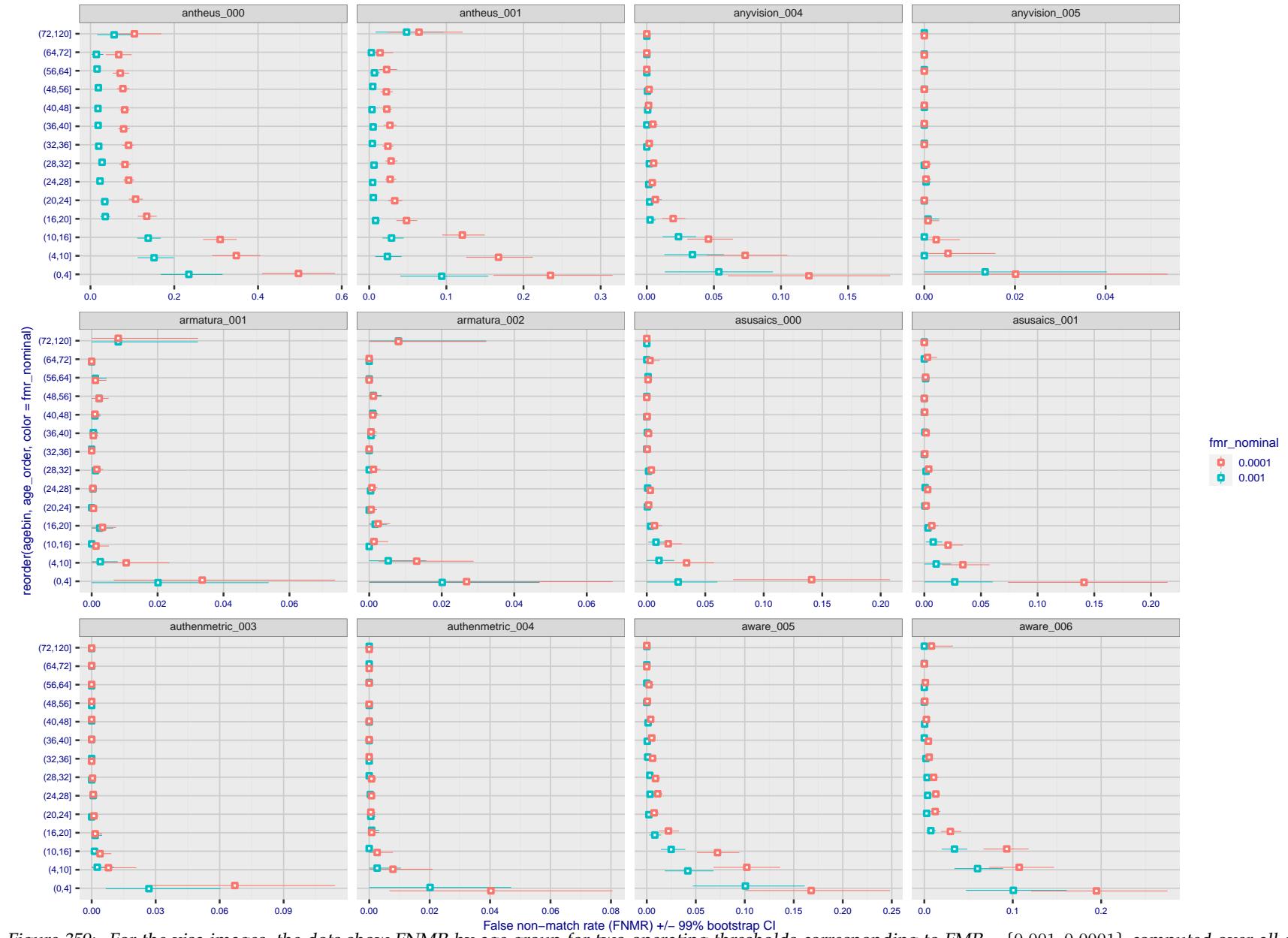


Figure 359: For the visa images, the dots show FNMR by age group for two operating thresholds corresponding to $FMR = \{0.001, 0.0001\}$ computed over all on the order of 10^{10} impostor scores. The FMR in each bin will vary also - see subsequent impostor heatmaps in sec. 3.6.2. Given a pair of face images taken at different times, we assign the comparison to the bin that is the arithmetic average of the subject's ages. This plot shows only the effect of age, not ageing. The number of comparisons in each bin is generally in the thousands, however the first and last bins are computed over 149 and 124 respectively. The error rates in some (adult) cases are zero, and in others the DET is flat so the error rates at the two thresholds are identical. The lines span 1% and 99% of bootstrap replicated FNMR estimates.



Figure 360: For the visa images, the dots show FNMR by age group for two operating thresholds corresponding to $FMR = \{0.001, 0.0001\}$ computed over all on the order of 10^{10} impostor scores. The FMR in each bin will vary also - see subsequent impostor heatmaps in sec. 3.6.2. Given a pair of face images taken at different times, we assign the comparison to the bin that is the arithmetic average of the subject's ages. This plot shows only the effect of age, not ageing. The number of comparisons in each bin is generally in the thousands, however the first and last bins are computed over 149 and 124 respectively. The error rates in some (adult) cases are zero, and in others the DET is flat so the error rates at the two thresholds are identical. The lines span 1% and 99% of bootstrap replicated FNMR estimates.



Figure 361: For the visa images, the dots show FNMR by age group for two operating thresholds corresponding to $FMR = \{0.001, 0.0001\}$ computed over all on the order of 10^{10} impostor scores. The FMR in each bin will vary also - see subsequent impostor heatmaps in sec. 3.6.2. Given a pair of face images taken at different times, we assign the comparison to the bin that is the arithmetic average of the subject's ages. This plot shows only the effect of age, not ageing. The number of comparisons in each bin is generally in the thousands, however the first and last bins are computed over 149 and 124 respectively. The error rates in some (adult) cases are zero, and in others the DET is flat so the error rates at the two thresholds are identical. The lines span 1% and 99% of bootstrap replicated FNMR estimates.



Figure 362: For the visa images, the dots show FNMR by age group for two operating thresholds corresponding to $FMR = \{0.001, 0.0001\}$ computed over all on the order of 10^{10} impostor scores. The FMR in each bin will vary also - see subsequent impostor heatmaps in sec. 3.6.2. Given a pair of face images taken at different times, we assign the comparison to the bin that is the arithmetic average of the subject's ages. This plot shows only the effect of age, not ageing. The number of comparisons in each bin is generally in the thousands, however the first and last bins are computed over 149 and 124 respectively. The error rates in some (adult) cases are zero, and in others the DET is flat so the error rates at the two thresholds are identical. The lines span 1% and 99% of bootstrap replicated FNMR estimates.

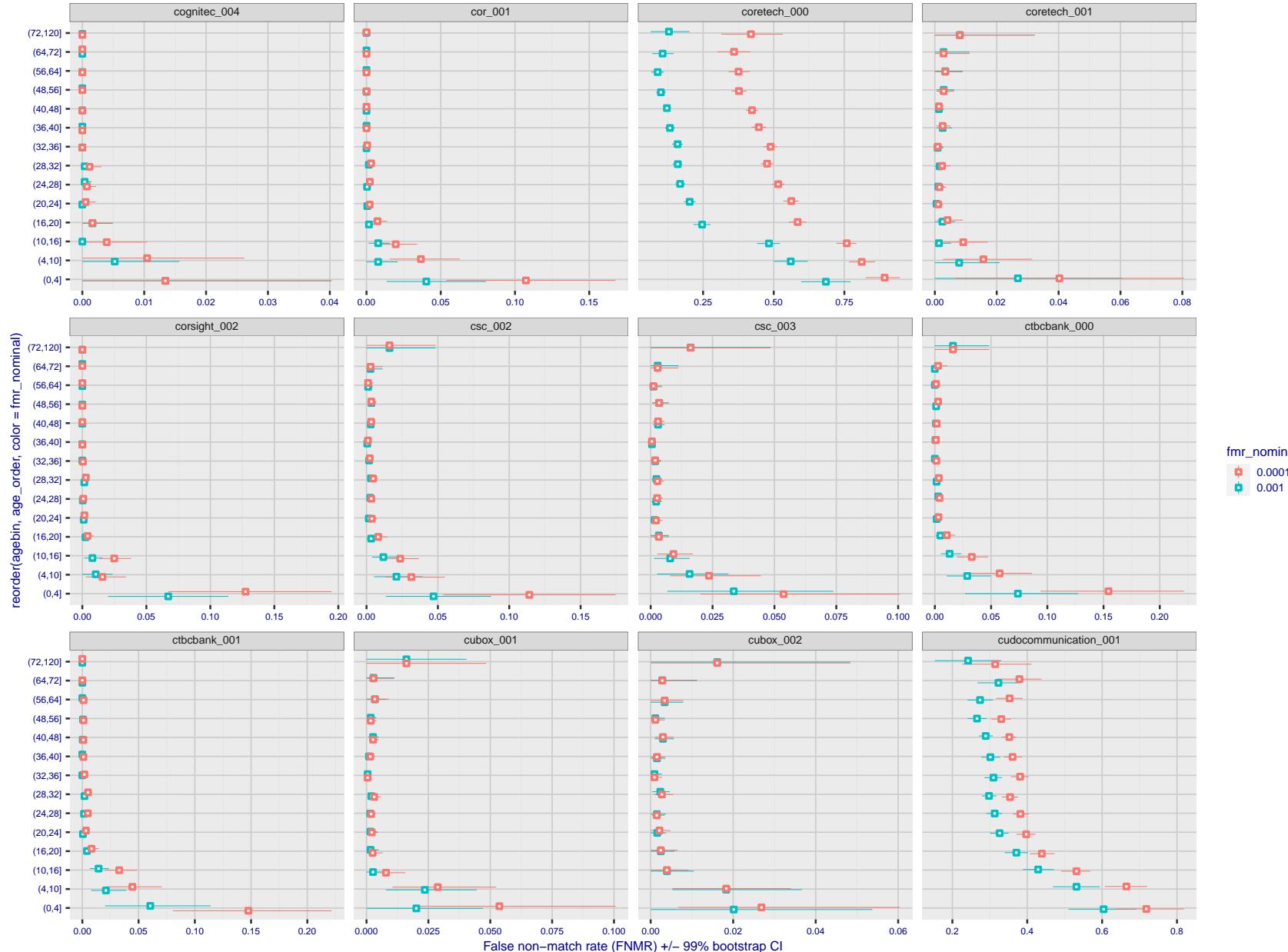


Figure 363: For the visa images, the dots show FNMR by age group for two operating thresholds corresponding to $FMR = \{0.001, 0.0001\}$ computed over all on the order of 10^{10} impostor scores. The FMR in each bin will vary also - see subsequent impostor heatmaps in sec. 3.6.2. Given a pair of face images taken at different times, we assign the comparison to the bin that is the arithmetic average of the subject's ages. This plot shows only the effect of age, not ageing. The number of comparisons in each bin is generally in the thousands, however the first and last bins are computed over 149 and 124 respectively. The error rates in some (adult) cases are zero, and in others the DET is flat so the error rates at the two thresholds are identical. The lines span 1% and 99% of bootstrap replicated FNMR estimates.

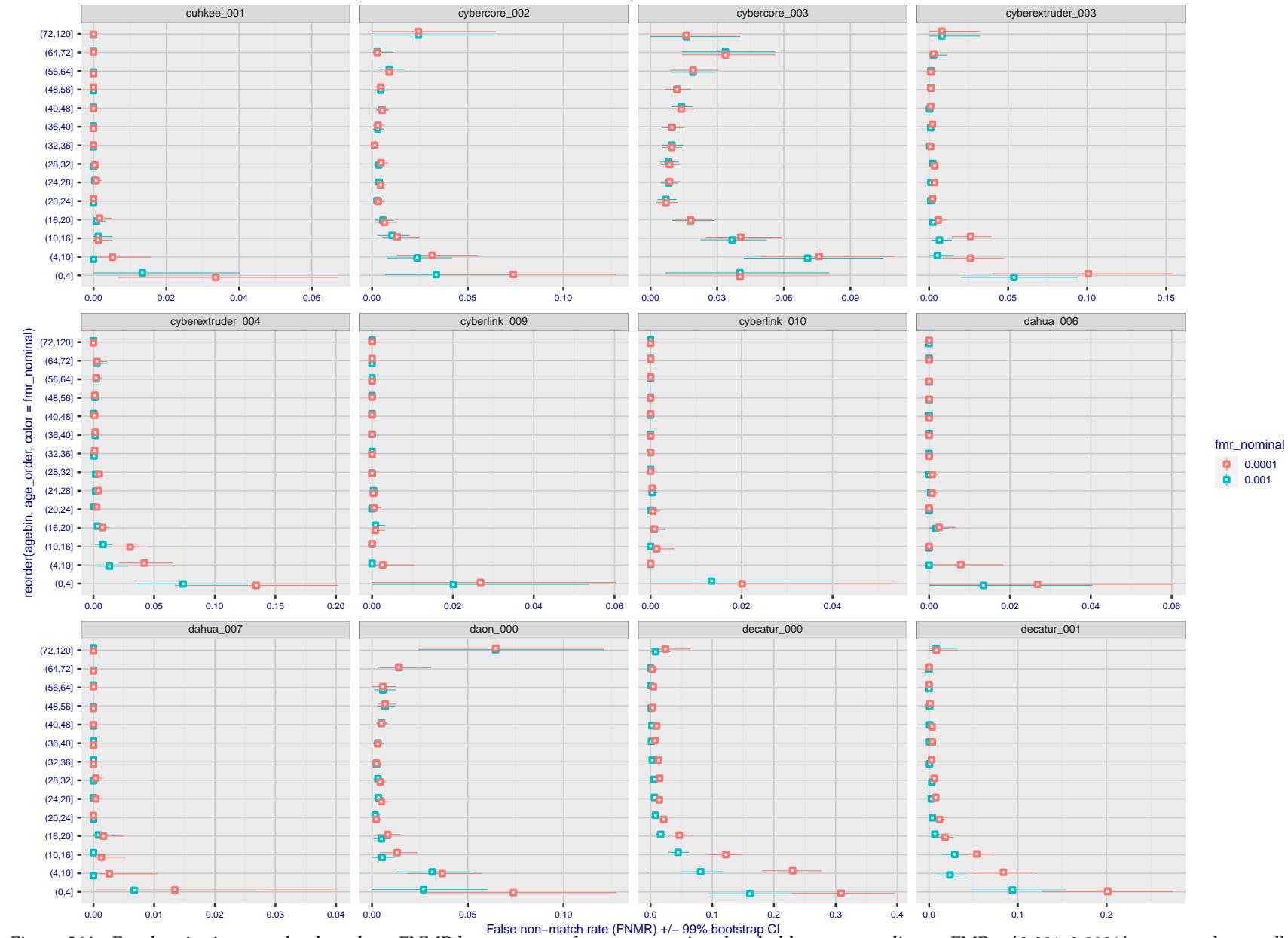


Figure 364: For the visa images, the dots show FNMR by age group for two operating thresholds corresponding to $FMR = \{0.001, 0.0001\}$ computed over all on the order of 10^{10} impostor scores. The FMR in each bin will vary also - see subsequent impostor heatmaps in sec. 3.6.2. Given a pair of face images taken at different times, we assign the comparison to the bin that is the arithmetic average of the subject's ages. This plot shows only the effect of age, not ageing. The number of comparisons in each bin is generally in the thousands, however the first and last bins are computed over 149 and 124 respectively. The error rates in some (adult) cases are zero, and in others the DET is flat so the error rates at the two thresholds are identical. The lines span 1% and 99% of bootstrap replicated FNMR estimates.



Figure 365: For the visa images, the dots show FNMR by age group for two operating thresholds corresponding to $FMR = \{0.001, 0.0001\}$ computed over all on the order of 10^{10} impostor scores. The FMR in each bin will vary also - see subsequent impostor heatmaps in sec. 3.6.2. Given a pair of face images taken at different times, we assign the comparison to the bin that is the arithmetic average of the subject's ages. This plot shows only the effect of age, not ageing. The number of comparisons in each bin is generally in the thousands, however the first and last bins are computed over 149 and 124 respectively. The error rates in some (adult) cases are zero, and in others the DET is flat so the error rates at the two thresholds are identical. The lines span 1% and 99% of bootstrap replicated FNMR estimates.

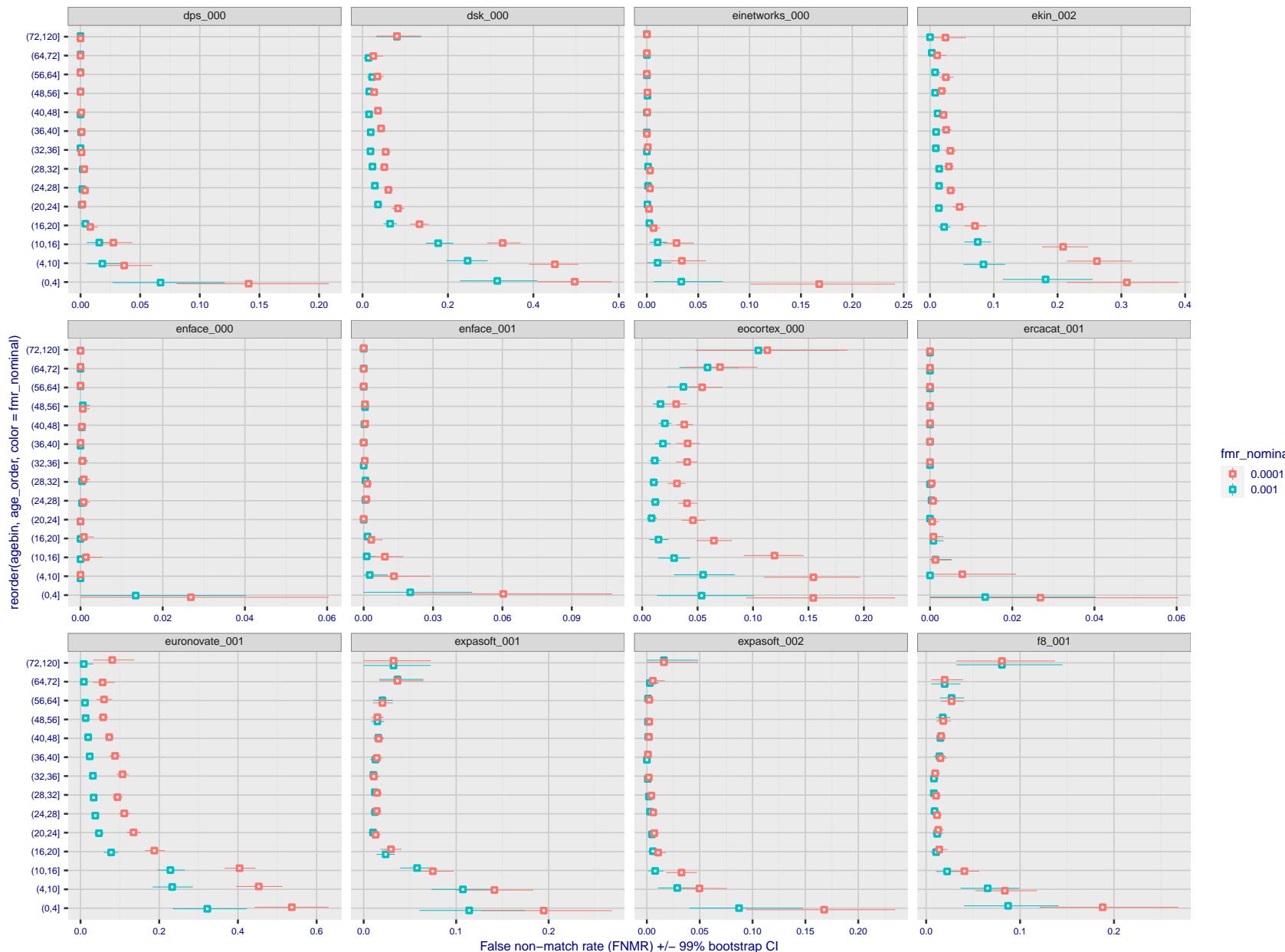


Figure 366: For the visa images, the dots show FNMR by age group for two operating thresholds corresponding to $FMR = \{0.001, 0.0001\}$ computed over all on the order of 10^{10} impostor scores. The FMR in each bin will vary also - see subsequent impostor heatmaps in sec. 3.6.2. Given a pair of face images taken at different times, we assign the comparison to the bin that is the arithmetic average of the subject's ages. This plot shows only the effect of age, not ageing. The number of comparisons in each bin is generally in the thousands, however the first and last bins are computed over 149 and 124 respectively. The error rates in some (adult) cases are zero, and in others the DET is flat so the error rates at the two thresholds are identical. The lines span 1% and 99% of bootstrap replicated FNMR estimates.

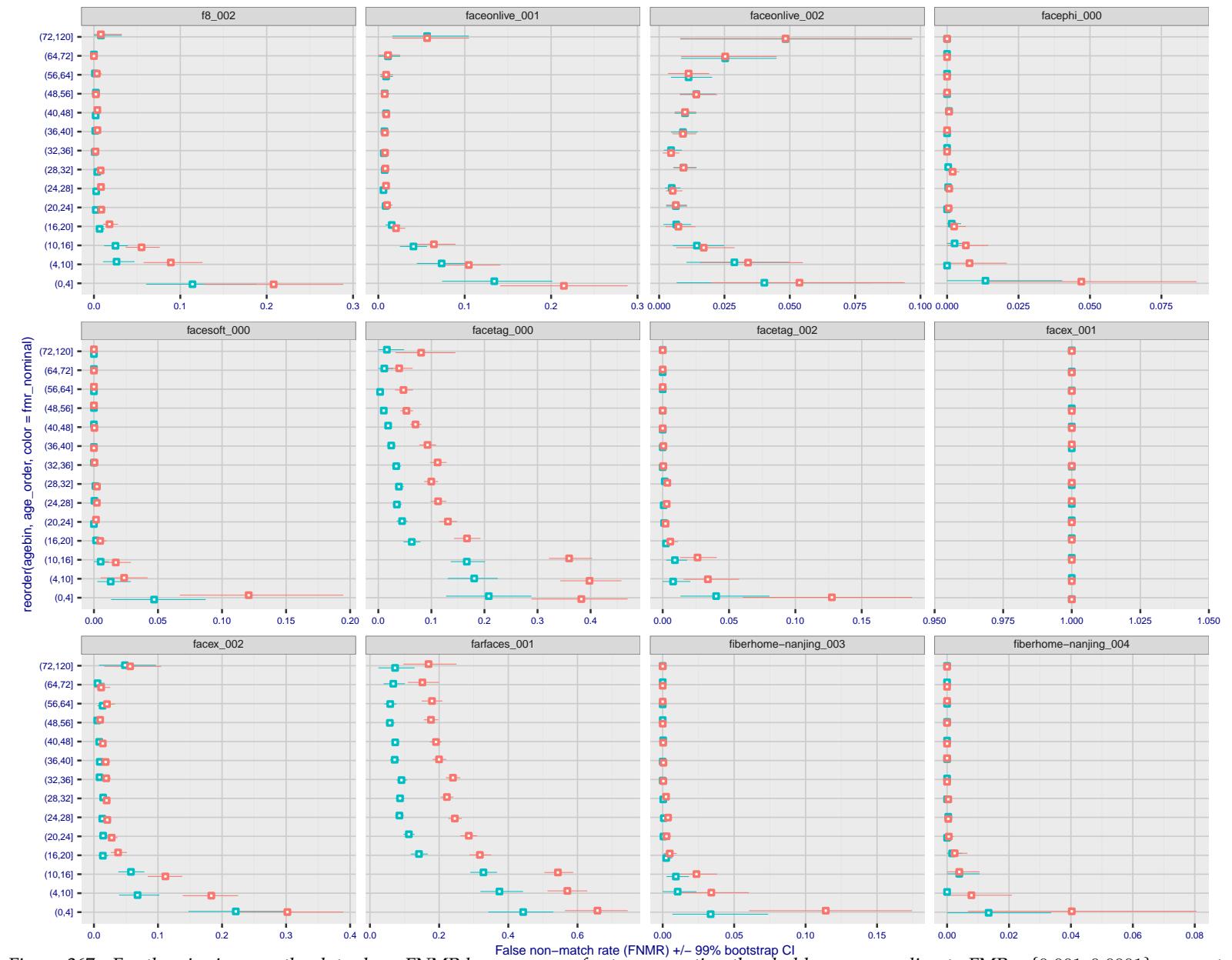


Figure 367: For the visa images, the dots show FNMR by age group for two operating thresholds corresponding to $FMR = \{0.001, 0.0001\}$ computed over all on the order of 10^{10} impostor scores. The FMR in each bin will vary also - see subsequent impostor heatmaps in sec. 3.6.2. Given a pair of face images taken at different times, we assign the comparison to the bin that is the arithmetic average of the subject's ages. This plot shows only the effect of age, not ageing. The number of comparisons in each bin is generally in the thousands, however the first and last bins are computed over 149 and 124 respectively. The error rates in some (adult) cases are zero, and in others the DET is flat so the error rates at the two thresholds are identical. The lines span 1% and 99% of bootstrap replicated FNMR estimates.

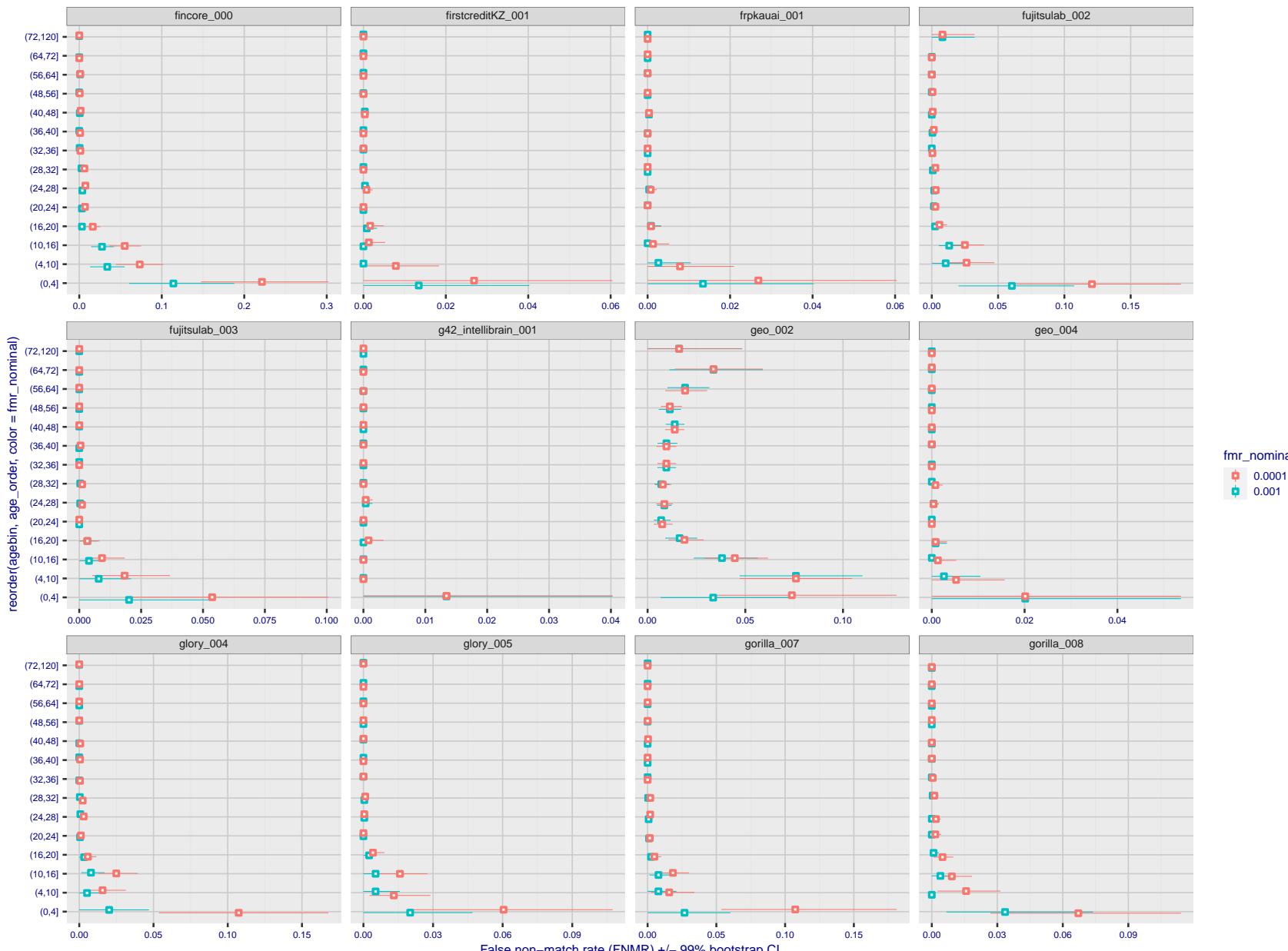


Figure 368: For the visa images, the dots show FNMR by age group for two operating thresholds corresponding to $FMR = \{0.001, 0.0001\}$ computed over all on the order of 10^{10} impostor scores. The FMR in each bin will vary also - see subsequent impostor heatmaps in sec. 3.6.2. Given a pair of face images taken at different times, we assign the comparison to the bin that is the arithmetic average of the subject's ages. This plot shows only the effect of age, not ageing. The number of comparisons in each bin is generally in the thousands, however the first and last bins are computed over 149 and 124 respectively. The error rates in some (adult) cases are zero, and in others the DET is flat so the error rates at the two thresholds are identical. The lines span 1% and 99% of bootstrap replicated FNMR estimates.

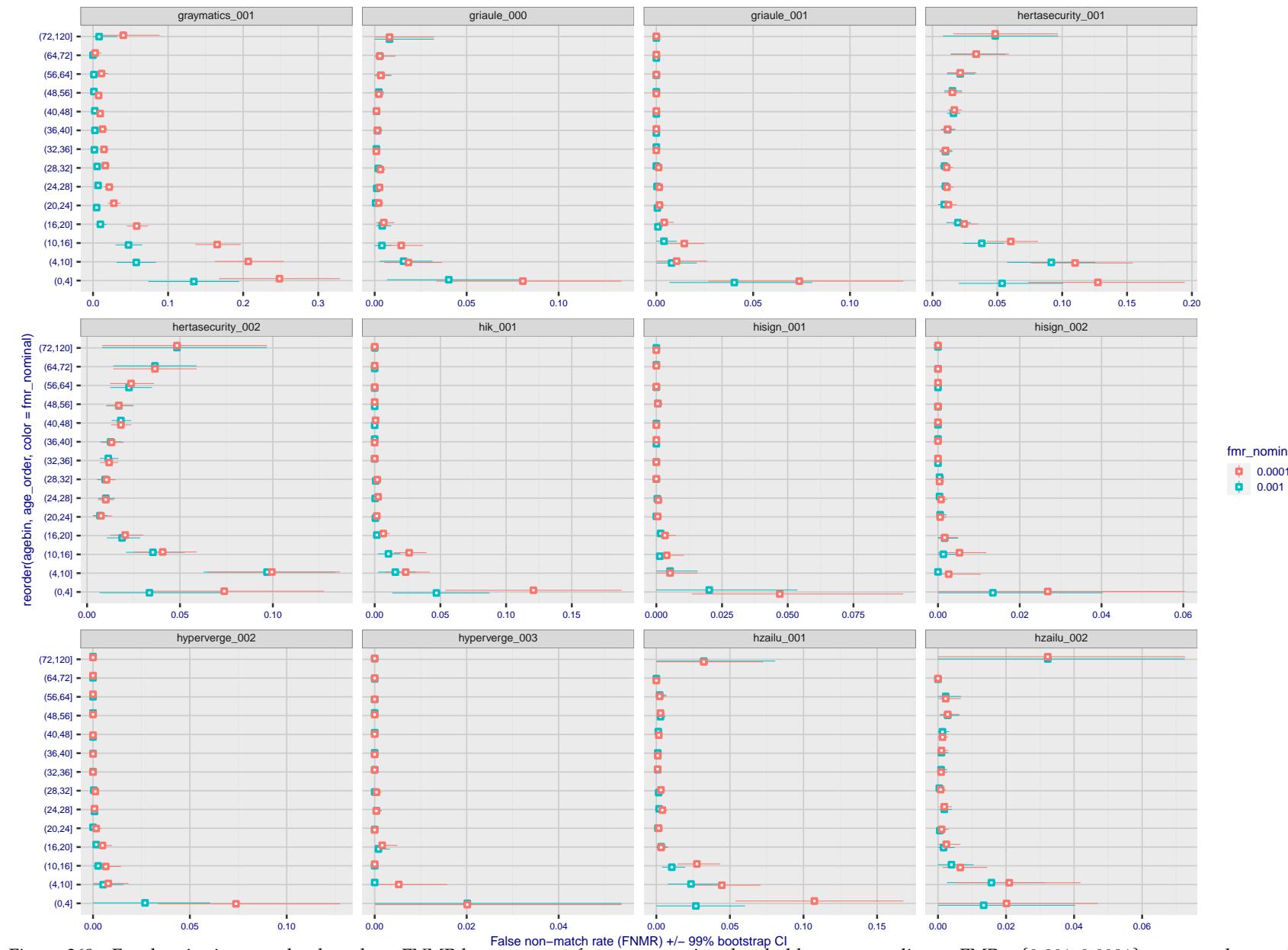


Figure 369: For the visa images, the dots show FNMR by age group for two operating thresholds corresponding to $FMR = \{0.001, 0.0001\}$ computed over all on the order of 10^{10} impostor scores. The FMR in each bin will vary also - see subsequent impostor heatmaps in sec. 3.6.2. Given a pair of face images taken at different times, we assign the comparison to the bin that is the arithmetic average of the subject's ages. This plot shows only the effect of age, not ageing. The number of comparisons in each bin is generally in the thousands, however the first and last bins are computed over 149 and 124 respectively. The error rates in some (adult) cases are zero, and in others the DET is flat so the error rates at the two thresholds are identical. The lines span 1% and 99% of bootstrap replicated FNMR estimates.



Figure 370: For the visa images, the dots show FNMR by age group for two operating thresholds corresponding to $FMR = \{0.001, 0.0001\}$ computed over all on the order of 10^{10} impostor scores. The FMR in each bin will vary also - see subsequent impostor heatmaps in sec. 3.6.2. Given a pair of face images taken at different times, we assign the comparison to the bin that is the arithmetic average of the subject's ages. This plot shows only the effect of age, not ageing. The number of comparisons in each bin is generally in the thousands, however the first and last bins are computed over 149 and 124 respectively. The error rates in some (adult) cases are zero, and in others the DET is flat so the error rates at the two thresholds are identical. The lines span 1% and 99% of bootstrap replicated FNMR estimates.

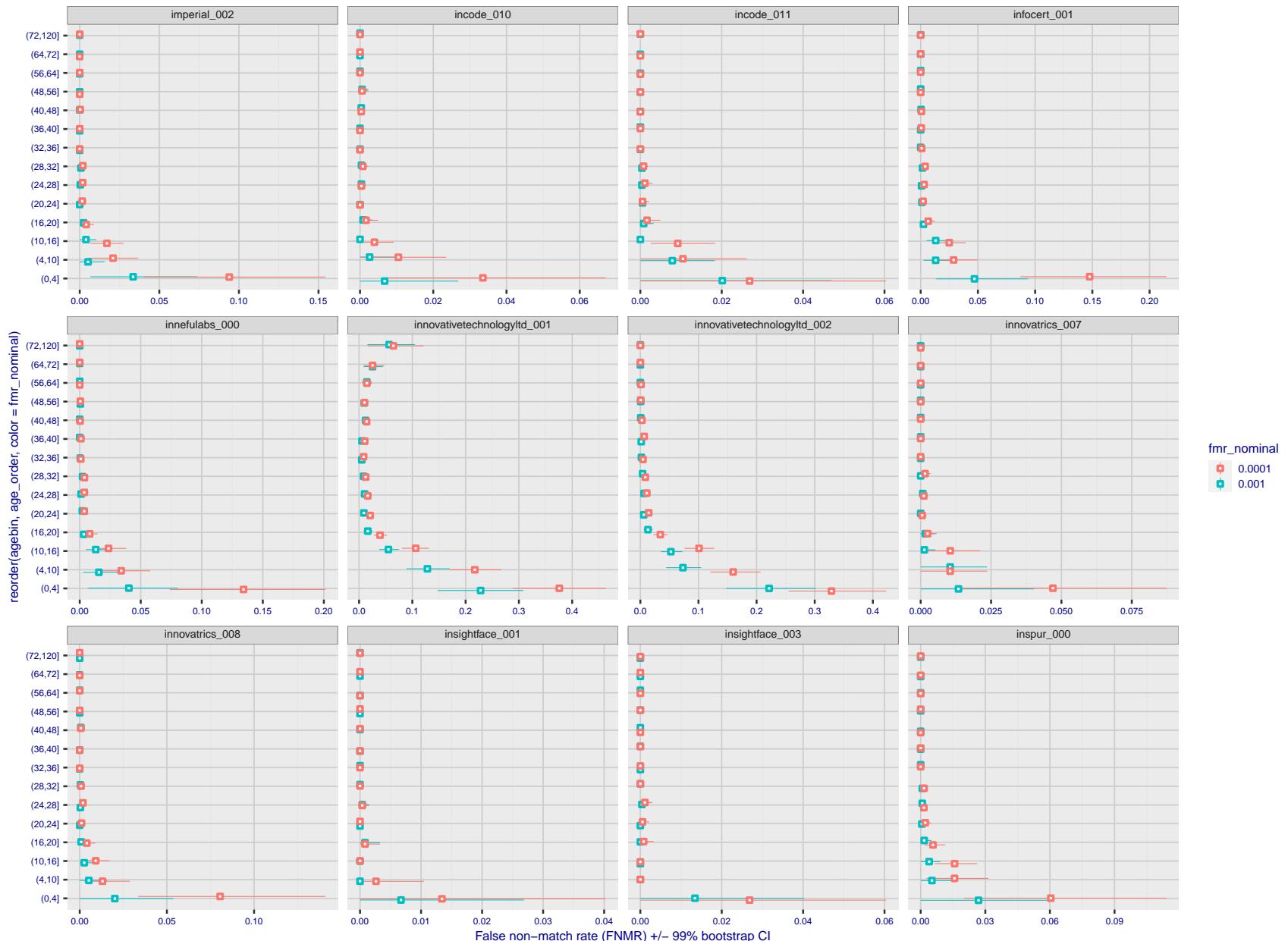


Figure 371: For the visa images, the dots show FNMR by age group for two operating thresholds corresponding to $FMR = \{0.001, 0.0001\}$ computed over all on the order of 10^{10} impostor scores. The FMR in each bin will vary also - see subsequent impostor heatmaps in sec. 3.6.2. Given a pair of face images taken at different times, we assign the comparison to the bin that is the arithmetic average of the subject's ages. This plot shows only the effect of age, not ageing. The number of comparisons in each bin is generally in the thousands, however the first and last bins are computed over 149 and 124 respectively. The error rates in some (adult) cases are zero, and in others the DET is flat so the error rates at the two thresholds are identical. The lines span 1% and 99% of bootstrap replicated FNMR estimates.



Figure 372: For the visa images, the dots show FNMR by age group for two operating thresholds corresponding to $FMR = \{0.001, 0.0001\}$ computed over all on the order of 10^{10} impostor scores. The FMR in each bin will vary also - see subsequent impostor heatmaps in sec. 3.6.2. Given a pair of face images taken at different times, we assign the comparison to the bin that is the arithmetic average of the subject's ages. This plot shows only the effect of age, not ageing. The number of comparisons in each bin is generally in the thousands, however the first and last bins are computed over 149 and 124 respectively. The error rates in some (adult) cases are zero, and in others the DET is flat so the error rates at the two thresholds are identical. The lines span 1% and 99% of bootstrap replicated FNMR estimates.

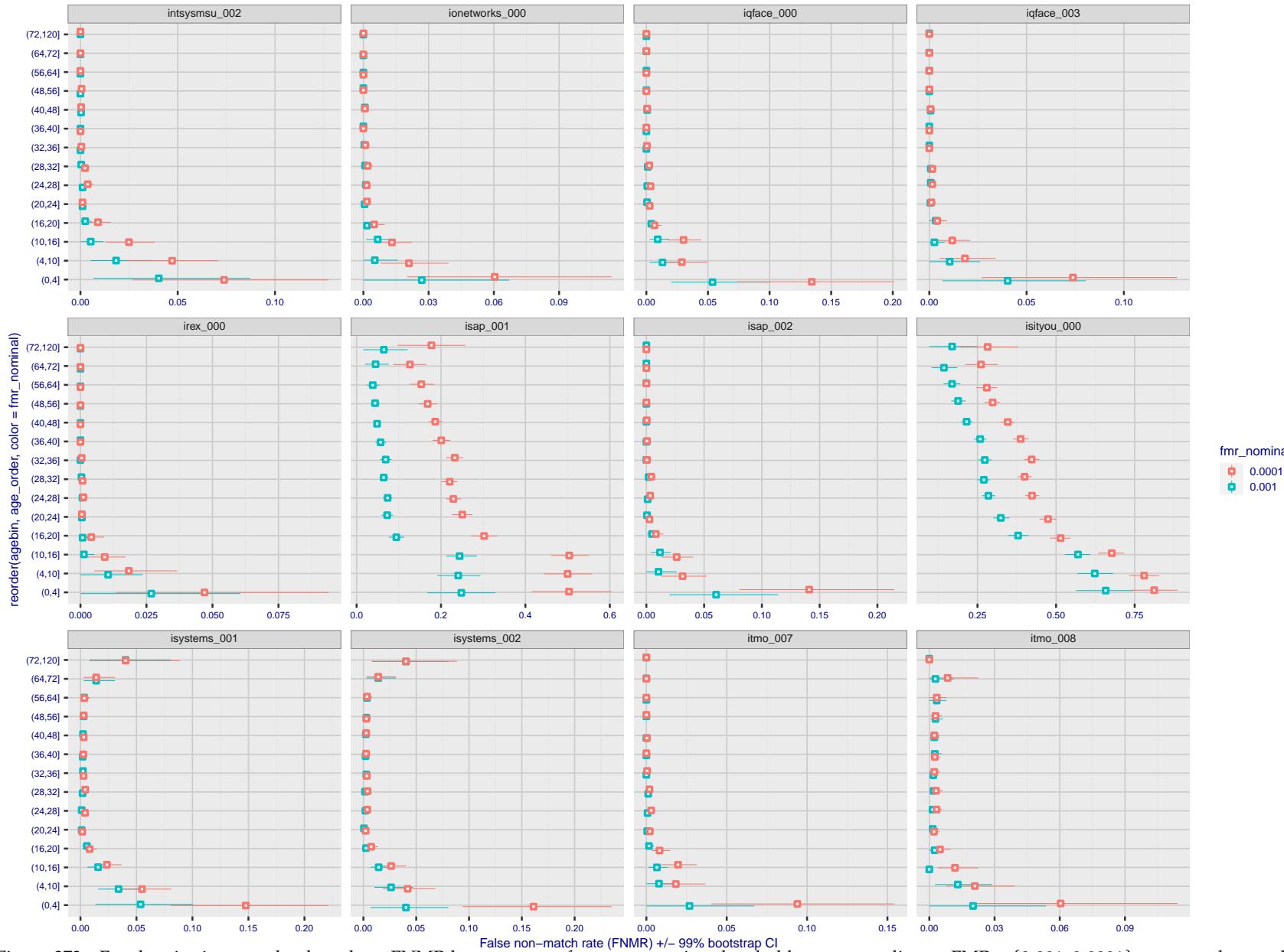


Figure 373: For the visa images, the dots show FNMR by age group for two operating thresholds corresponding to $FMR = \{0.001, 0.0001\}$ computed over all on the order of 10^{10} impostor scores. The FMR in each bin will vary also - see subsequent impostor heatmaps in sec. 3.6.2. Given a pair of face images taken at different times, we assign the comparison to the bin that is the arithmetic average of the subject's ages. This plot shows only the effect of age, not ageing. The number of comparisons in each bin is generally in the thousands, however the first and last bins are computed over 149 and 124 respectively. The error rates in some (adult) cases are zero, and in others the DET is flat so the error rates at the two thresholds are identical. The lines span 1% and 99% of bootstrap replicated FNMR estimates.

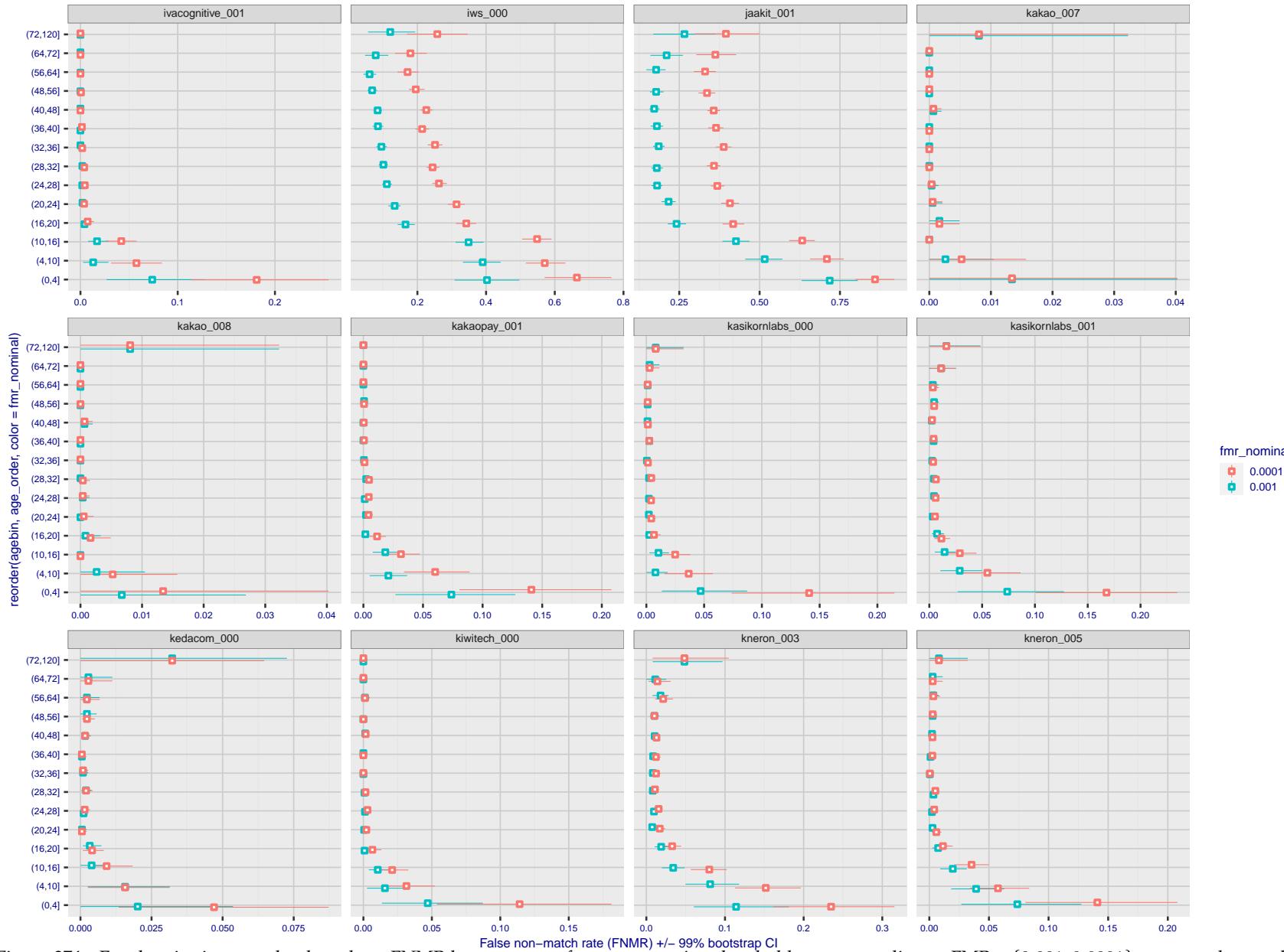


Figure 374: For the visa images, the dots show FNMR by age group for two operating thresholds corresponding to $FMR = \{0.001, 0.0001\}$ computed over all on the order of 10^{10} impostor scores. The FMR in each bin will vary also - see subsequent impostor heatmaps in sec. 3.6.2. Given a pair of face images taken at different times, we assign the comparison to the bin that is the arithmetic average of the subject's ages. This plot shows only the effect of age, not ageing. The number of comparisons in each bin is generally in the thousands, however the first and last bins are computed over 149 and 124 respectively. The error rates in some (adult) cases are zero, and in others the DET is flat so the error rates at the two thresholds are identical. The lines span 1% and 99% of bootstrap replicated FNMR estimates.

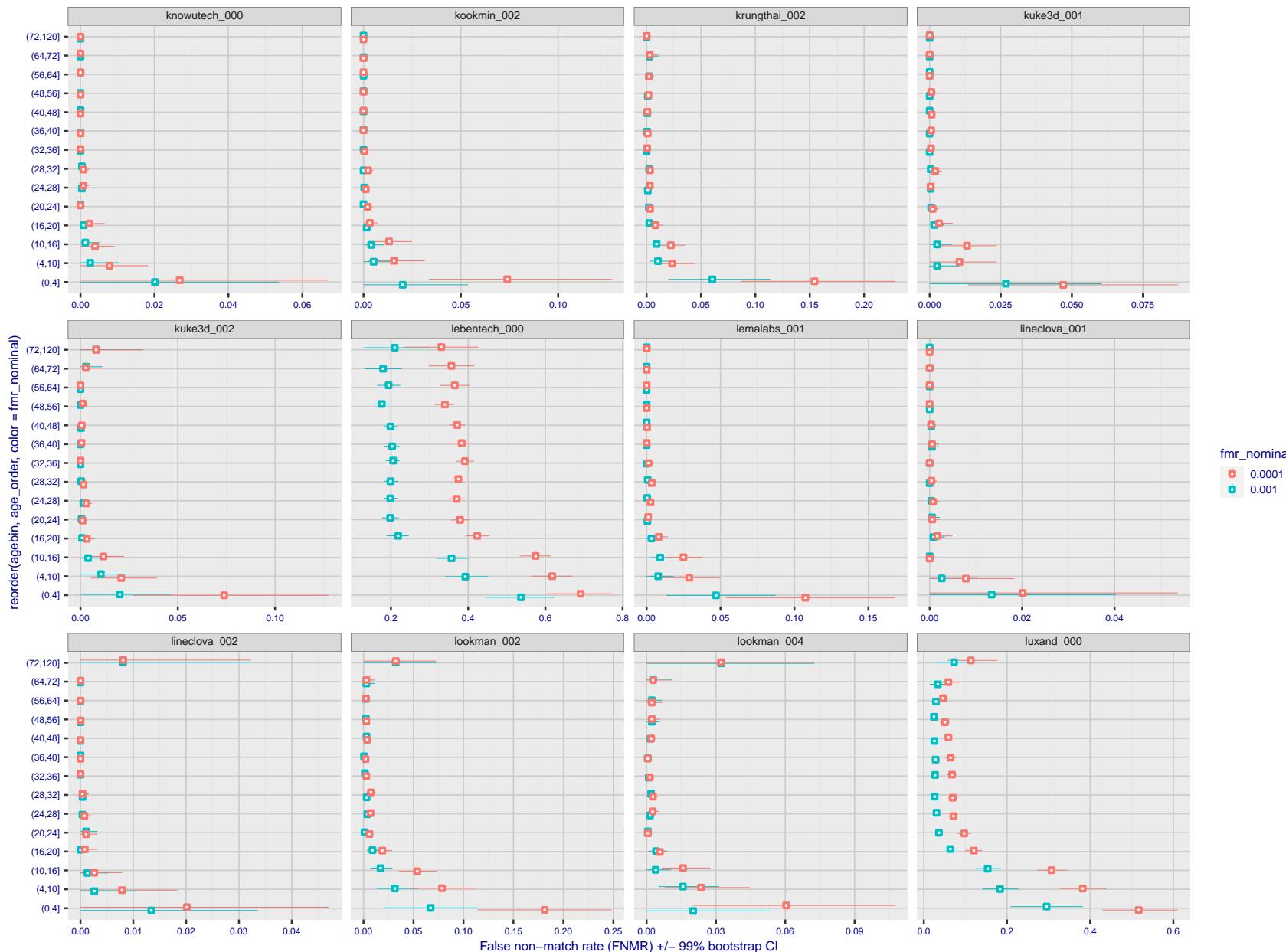


Figure 375: For the visa images, the dots show FNMR by age group for two operating thresholds corresponding to $FMR = \{0.001, 0.0001\}$ computed over all on the order of 10^{10} impostor scores. The FMR in each bin will vary also - see subsequent impostor heatmaps in sec. 3.6.2. Given a pair of face images taken at different times, we assign the comparison to the bin that is the arithmetic average of the subject's ages. This plot shows only the effect of age, not ageing. The number of comparisons in each bin is generally in the thousands, however the first and last bins are computed over 149 and 124 respectively. The error rates in some (adult) cases are zero, and in others the DET is flat so the error rates at the two thresholds are identical. The lines span 1% and 99% of bootstrap replicated FNMR estimates.

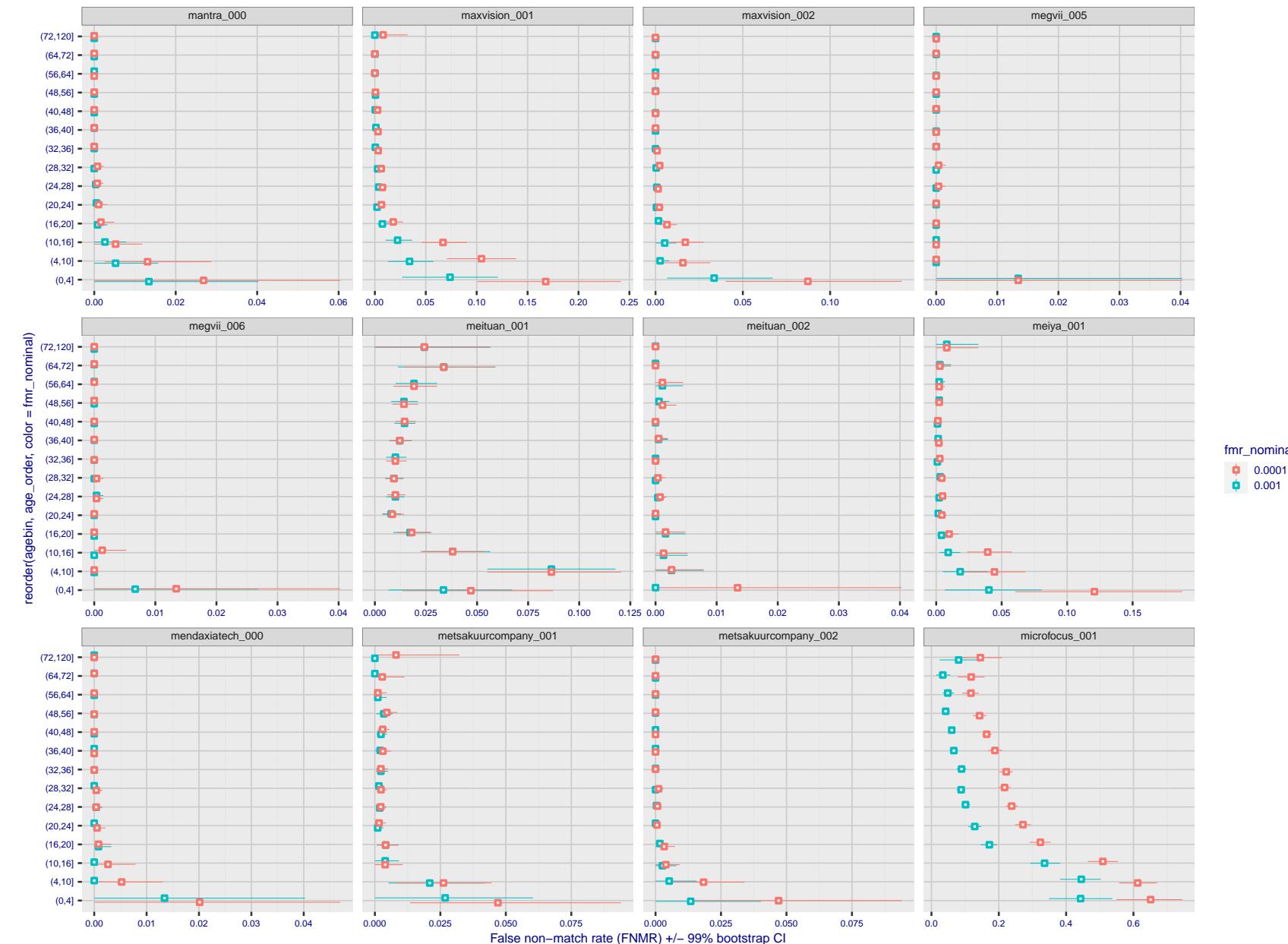


Figure 376: For the visa images, the dots show FNMR by age group for two operating thresholds corresponding to $FMR = \{0.001, 0.0001\}$ computed over all on the order of 10^{10} impostor scores. The FMR in each bin will vary also - see subsequent impostor heatmaps in sec. 3.6.2. Given a pair of face images taken at different times, we assign the comparison to the bin that is the arithmetic average of the subject's ages. This plot shows only the effect of age, not ageing. The number of comparisons in each bin is generally in the thousands, however the first and last bins are computed over 149 and 124 respectively. The error rates in some (adult) cases are zero, and in others the DET is flat so the error rates at the two thresholds are identical. The lines span 1% and 99% of bootstrap replicated FNMR estimates.

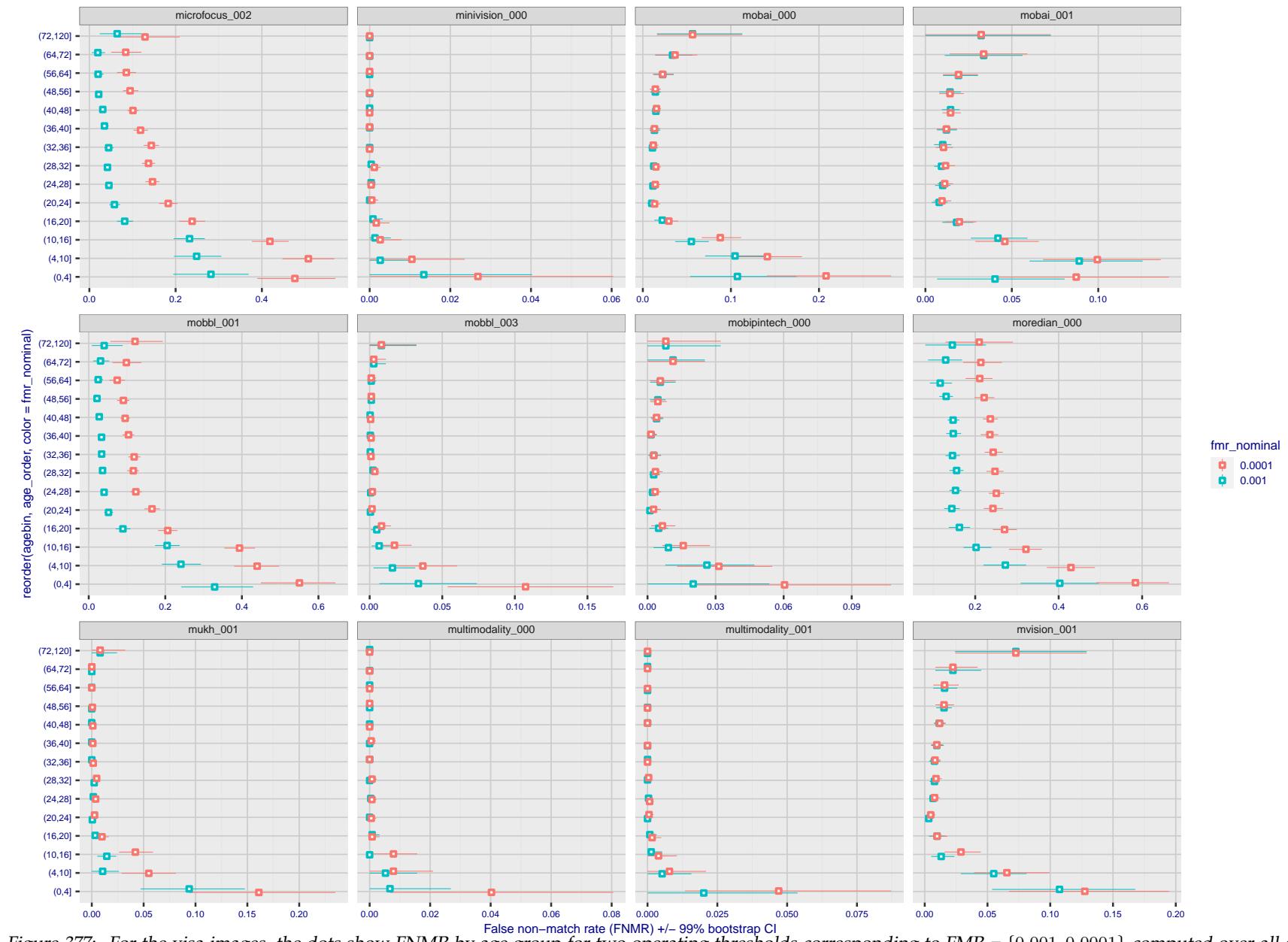


Figure 377: For the visa images, the dots show FNMR by age group for two operating thresholds corresponding to $FMR = \{0.001, 0.0001\}$ computed over all on the order of 10^{10} impostor scores. The FMR in each bin will vary also - see subsequent impostor heatmaps in sec. 3.6.2. Given a pair of face images taken at different times, we assign the comparison to the bin that is the arithmetic average of the subject's ages. This plot shows only the effect of age, not ageing. The number of comparisons in each bin is generally in the thousands, however the first and last bins are computed over 149 and 124 respectively. The error rates in some (adult) cases are zero, and in others the DET is flat so the error rates at the two thresholds are identical. The lines span 1% and 99% of bootstrap replicated FNMR estimates.

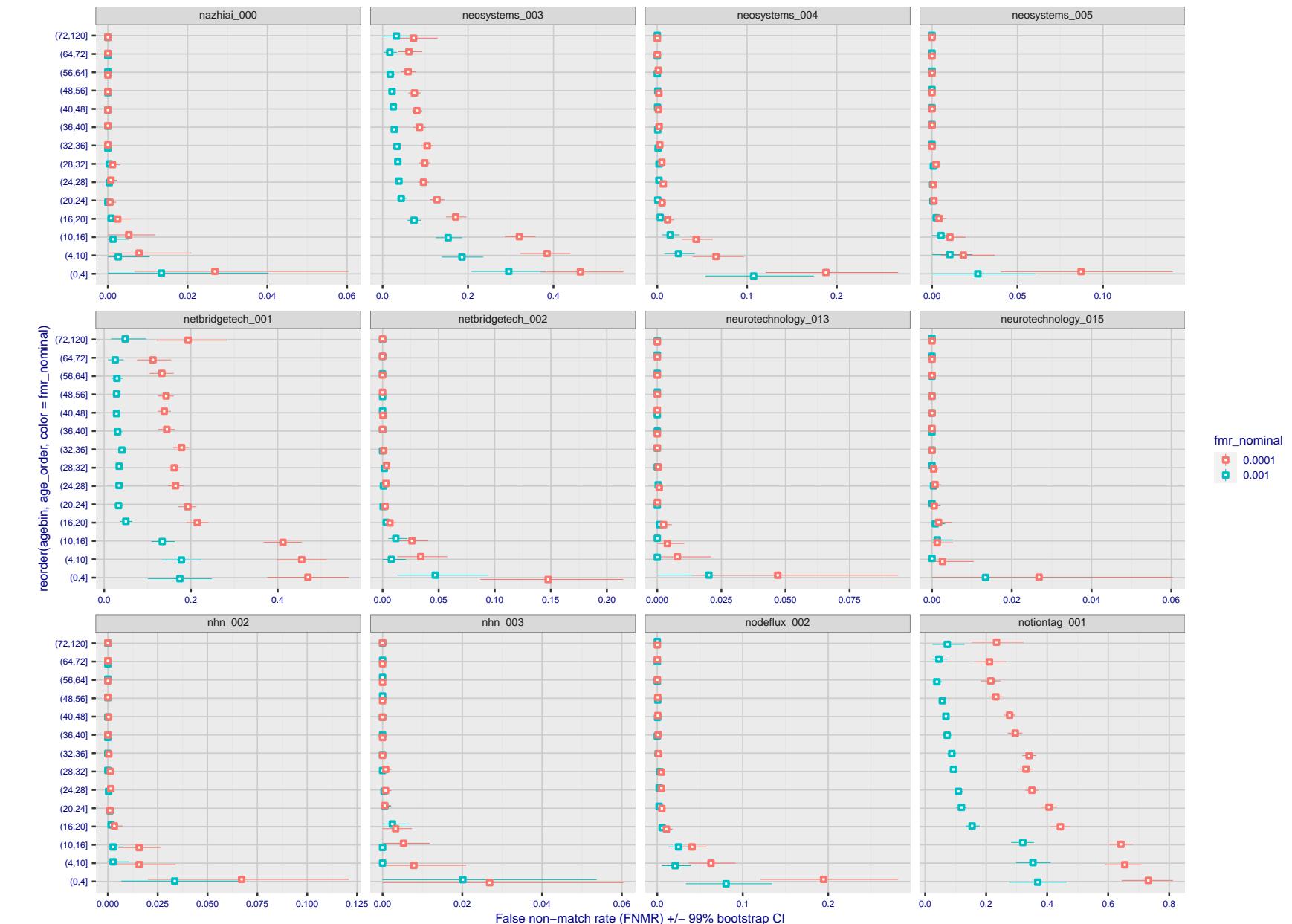


Figure 378: For the visa images, the dots show FNMR by age group for two operating thresholds corresponding to $FMR = \{0.001, 0.0001\}$ computed over all on the order of 10^{10} impostor scores. The FMR in each bin will vary also - see subsequent impostor heatmaps in sec. 3.6.2. Given a pair of face images taken at different times, we assign the comparison to the bin that is the arithmetic average of the subject's ages. This plot shows only the effect of age, not ageing. The number of comparisons in each bin is generally in the thousands, however the first and last bins are computed over 149 and 124 respectively. The error rates in some (adult) cases are zero, and in others the DET is flat so the error rates at the two thresholds are identical. The lines span 1% and 99% of bootstrap replicated FNMR estimates.

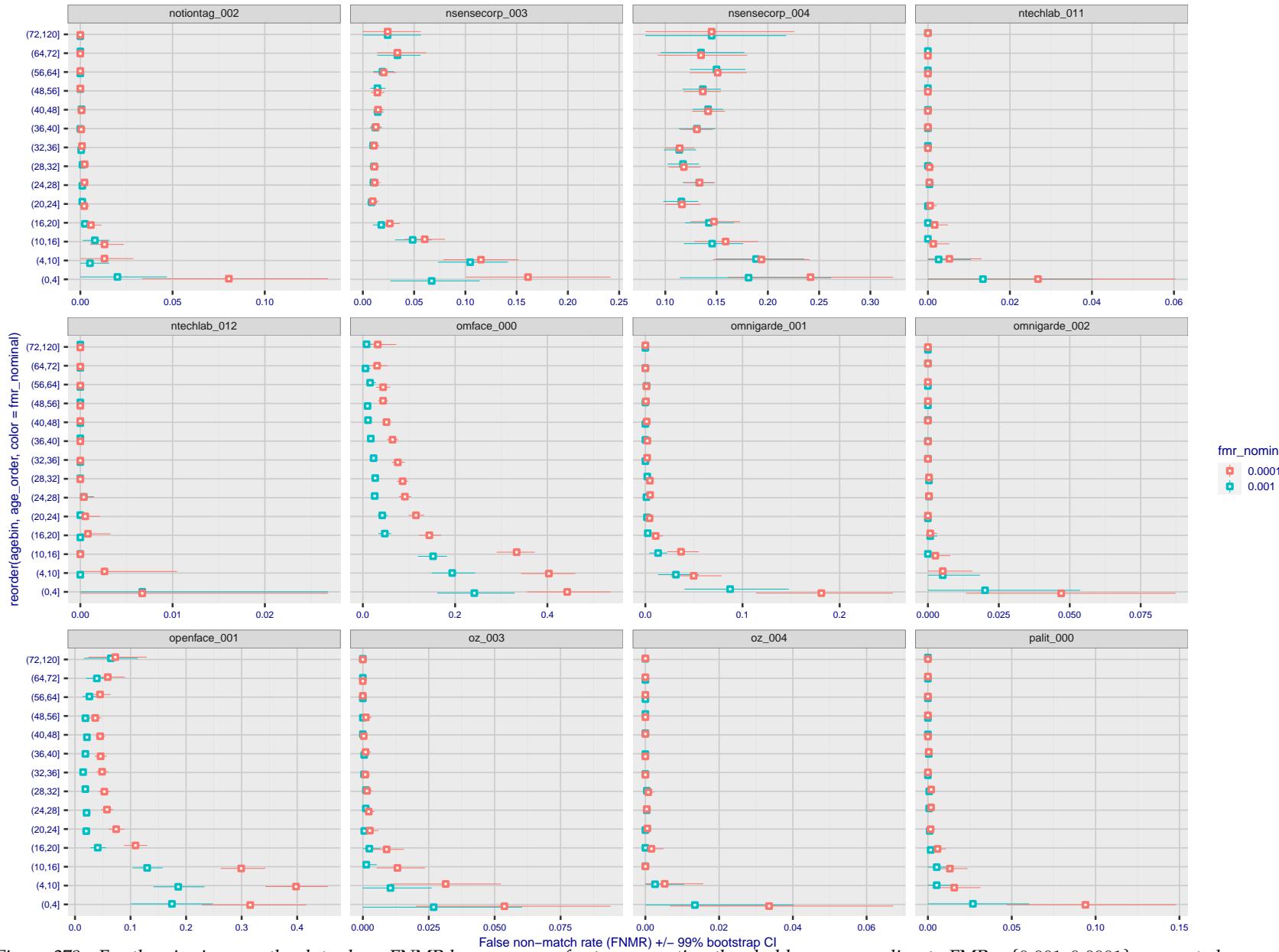


Figure 379: For the visa images, the dots show FNMR by age group for two operating thresholds corresponding to $FMR = \{0.001, 0.0001\}$ computed over all on the order of 10^{10} impostor scores. The FMR in each bin will vary also - see subsequent impostor heatmaps in sec. 3.6.2. Given a pair of face images taken at different times, we assign the comparison to the bin that is the arithmetic average of the subject's ages. This plot shows only the effect of age, not ageing. The number of comparisons in each bin is generally in the thousands, however the first and last bins are computed over 149 and 124 respectively. The error rates in some (adult) cases are zero, and in others the DET is flat so the error rates at the two thresholds are identical. The lines span 1% and 99% of bootstrap replicated FNMR estimates.



Figure 380: For the visa images, the dots show FNMR by age group for two operating thresholds corresponding to $FMR = \{0.001, 0.0001\}$ computed over all on the order of 10^{10} impostor scores. The FMR in each bin will vary also - see subsequent impostor heatmaps in sec. 3.6.2. Given a pair of face images taken at different times, we assign the comparison to the bin that is the arithmetic average of the subject's ages. This plot shows only the effect of age, not ageing. The number of comparisons in each bin is generally in the thousands, however the first and last bins are computed over 149 and 124 respectively. The error rates in some (adult) cases are zero, and in others the DET is flat so the error rates at the two thresholds are identical. The lines span 1% and 99% of bootstrap replicated FNMR estimates.



Figure 381: For the visa images, the dots show FNMR by age group for two operating thresholds corresponding to $FMR = \{0.001, 0.0001\}$ computed over all on the order of 10^{10} impostor scores. The FMR in each bin will vary also - see subsequent impostor heatmaps in sec. 3.6.2. Given a pair of face images taken at different times, we assign the comparison to the bin that is the arithmetic average of the subject's ages. This plot shows only the effect of age, not ageing. The number of comparisons in each bin is generally in the thousands, however the first and last bins are computed over 149 and 124 respectively. The error rates in some (adult) cases are zero, and in others the DET is flat so the error rates at the two thresholds are identical. The lines span 1% and 99% of bootstrap replicated FNMR estimates.



Figure 382: For the visa images, the dots show FNMR by age group for two operating thresholds corresponding to $FMR = \{0.001, 0.0001\}$ computed over all on the order of 10^{10} impostor scores. The FMR in each bin will vary also - see subsequent impostor heatmaps in sec. 3.6.2. Given a pair of face images taken at different times, we assign the comparison to the bin that is the arithmetic average of the subject's ages. This plot shows only the effect of age, not ageing. The number of comparisons in each bin is generally in the thousands, however the first and last bins are computed over 149 and 124 respectively. The error rates in some (adult) cases are zero, and in others the DET is flat so the error rates at the two thresholds are identical. The lines span 1% and 99% of bootstrap replicated FNMR estimates.



Figure 383: For the visa images, the dots show FNMR by age group for two operating thresholds corresponding to $FMR = \{0.001, 0.0001\}$ computed over all on the order of 10^{10} impostor scores. The FMR in each bin will vary also - see subsequent impostor heatmaps in sec. 3.6.2. Given a pair of face images taken at different times, we assign the comparison to the bin that is the arithmetic average of the subject's ages. This plot shows only the effect of age, not ageing. The number of comparisons in each bin is generally in the thousands, however the first and last bins are computed over 149 and 124 respectively. The error rates in some (adult) cases are zero, and in others the DET is flat so the error rates at the two thresholds are identical. The lines span 1% and 99% of bootstrap replicated FNMR estimates.

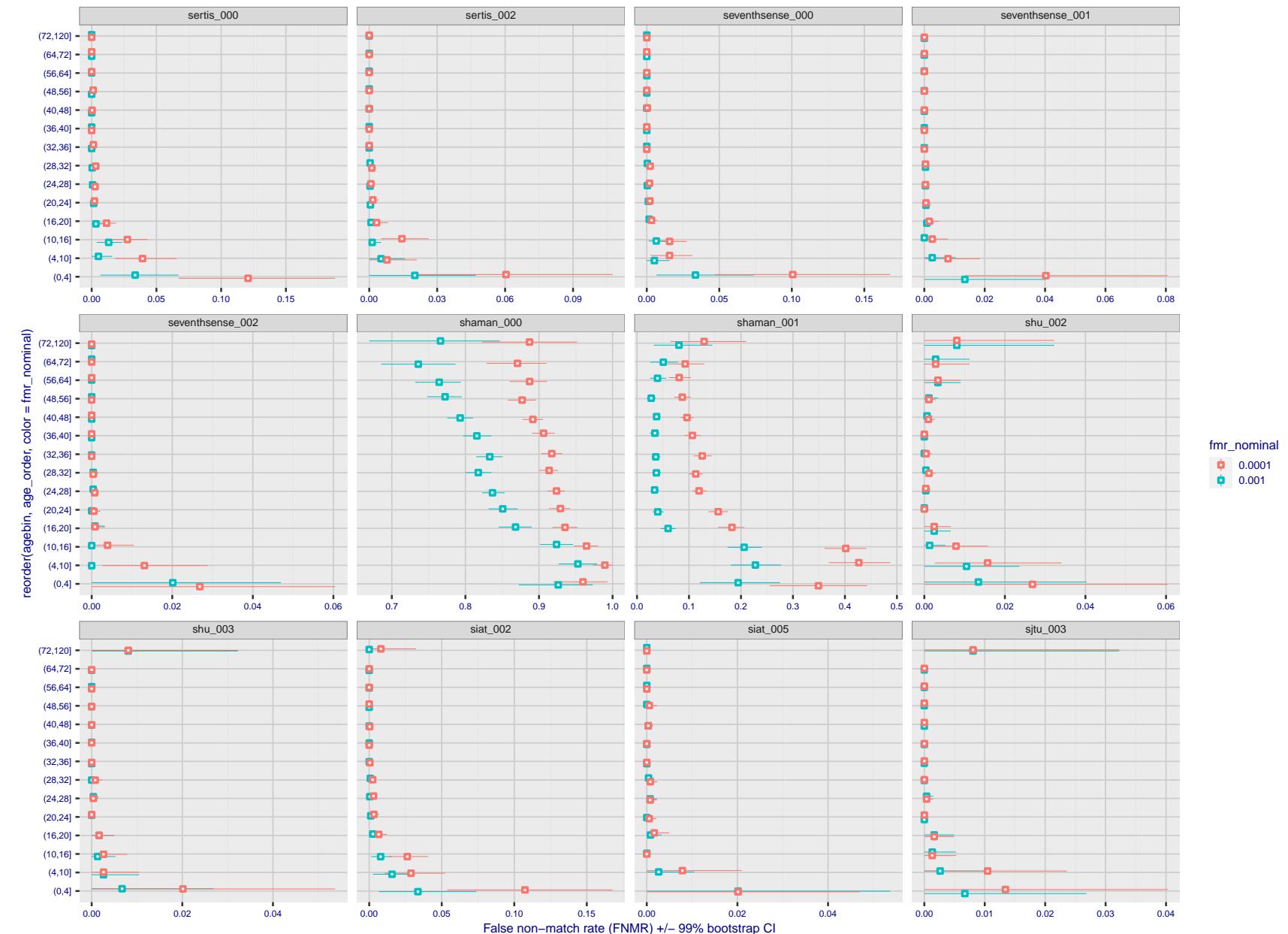


Figure 384: For the visa images, the dots show FNMR by age group for two operating thresholds corresponding to $FMR = \{0.001, 0.0001\}$ computed over all on the order of 10^{10} impostor scores. The FMR in each bin will vary also - see subsequent impostor heatmaps in sec. 3.6.2. Given a pair of face images taken at different times, we assign the comparison to the bin that is the arithmetic average of the subject's ages. This plot shows only the effect of age, not ageing. The number of comparisons in each bin is generally in the thousands, however the first and last bins are computed over 149 and 124 respectively. The error rates in some (adult) cases are zero, and in others the DET is flat so the error rates at the two thresholds are identical. The lines span 1% and 99% of bootstrap replicated FNMR estimates.

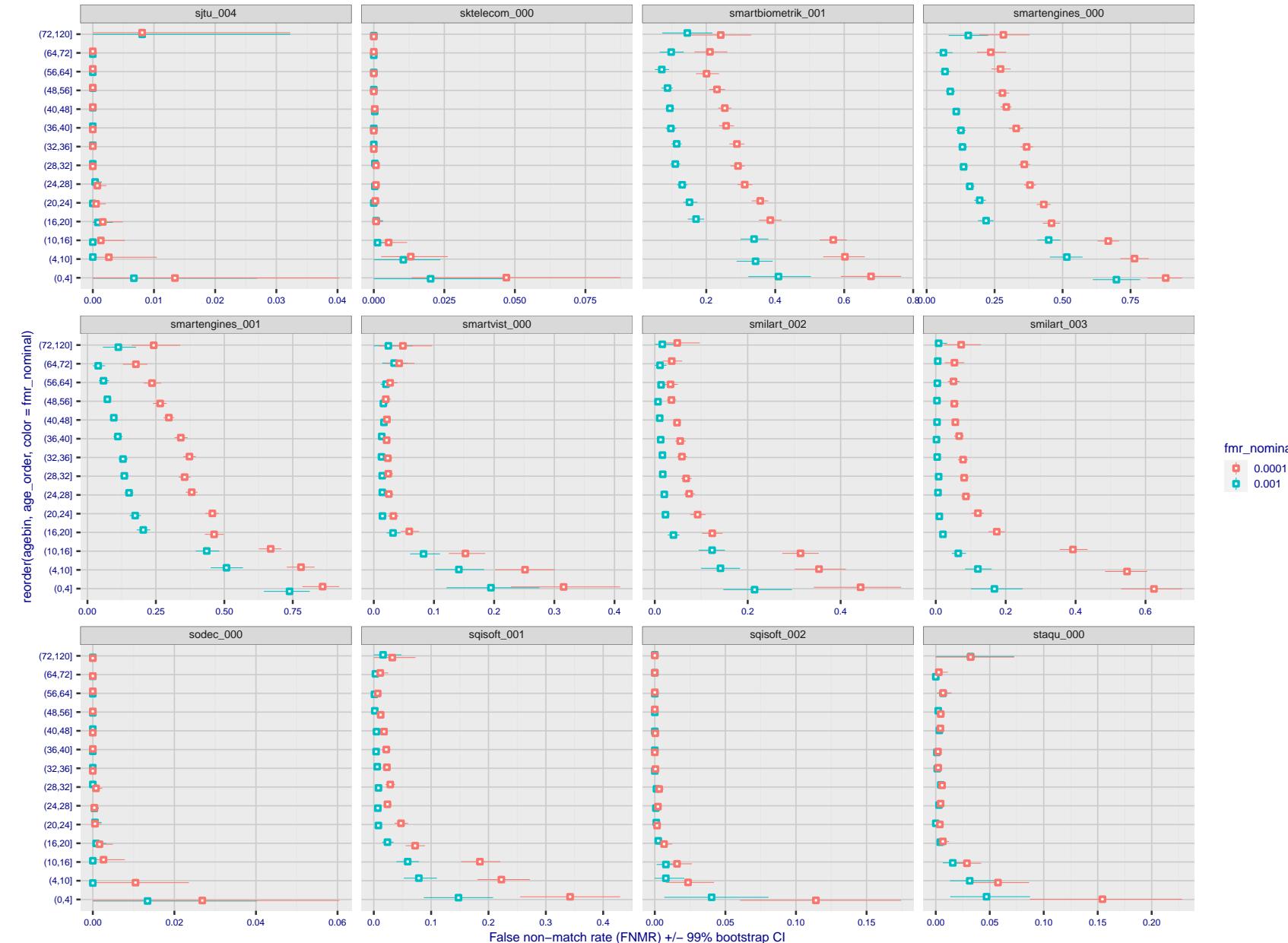


Figure 385: For the visa images, the dots show FNMR by age group for two operating thresholds corresponding to $FMR = \{0.001, 0.0001\}$ computed over all on the order of 10^{10} impostor scores. The FMR in each bin will vary also - see subsequent impostor heatmaps in sec. 3.6.2. Given a pair of face images taken at different times, we assign the comparison to the bin that is the arithmetic average of the subject's ages. This plot shows only the effect of age, not ageing. The number of comparisons in each bin is generally in the thousands, however the first and last bins are computed over 149 and 124 respectively. The error rates in some (adult) cases are zero, and in others the DET is flat so the error rates at the two thresholds are identical. The lines span 1% and 99% of bootstrap replicated FNMR estimates.

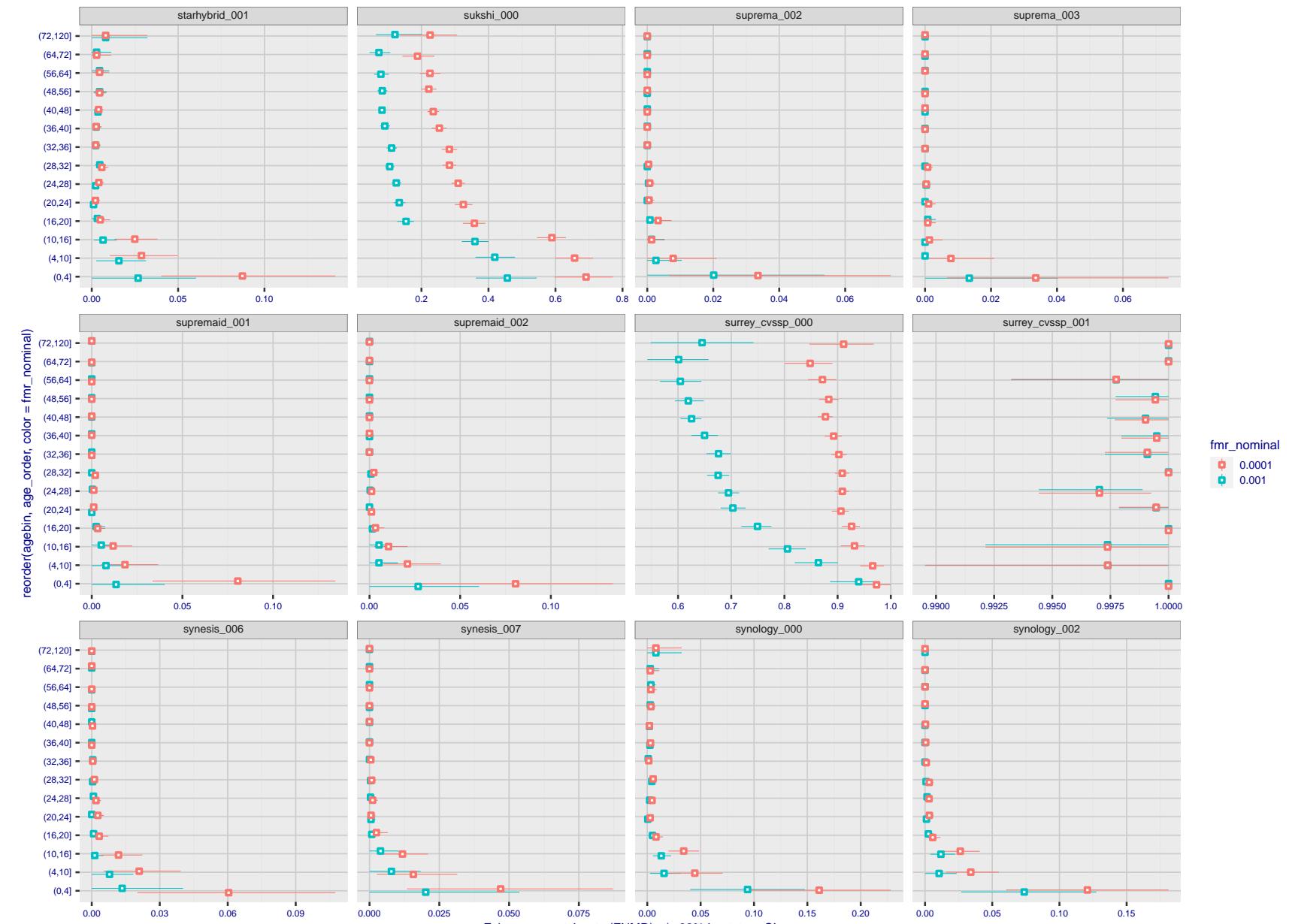


Figure 386: For the visa images, the dots show FNMR by age group for two operating thresholds corresponding to $FMR = \{0.001, 0.0001\}$ computed over all on the order of 10^{10} impostor scores. The FMR in each bin will vary also - see subsequent impostor heatmaps in sec. 3.6.2. Given a pair of face images taken at different times, we assign the comparison to the bin that is the arithmetic average of the subject's ages. This plot shows only the effect of age, not ageing. The number of comparisons in each bin is generally in the thousands, however the first and last bins are computed over 149 and 124 respectively. The error rates in some (adult) cases are zero, and in others the DET is flat so the error rates at the two thresholds are identical. The lines span 1% and 99% of bootstrap replicated FNMR estimates.



Figure 387: For the visa images, the dots show FNMR by age group for two operating thresholds corresponding to $FMR = \{0.001, 0.0001\}$ computed over all on the order of 10^{10} impostor scores. The FMR in each bin will vary also - see subsequent impostor heatmaps in sec. 3.6.2. Given a pair of face images taken at different times, we assign the comparison to the bin that is the arithmetic average of the subject's ages. This plot shows only the effect of age, not ageing. The number of comparisons in each bin is generally in the thousands, however the first and last bins are computed over 149 and 124 respectively. The error rates in some (adult) cases are zero, and in others the DET is flat so the error rates at the two thresholds are identical. The lines span 1% and 99% of bootstrap replicated FNMR estimates.

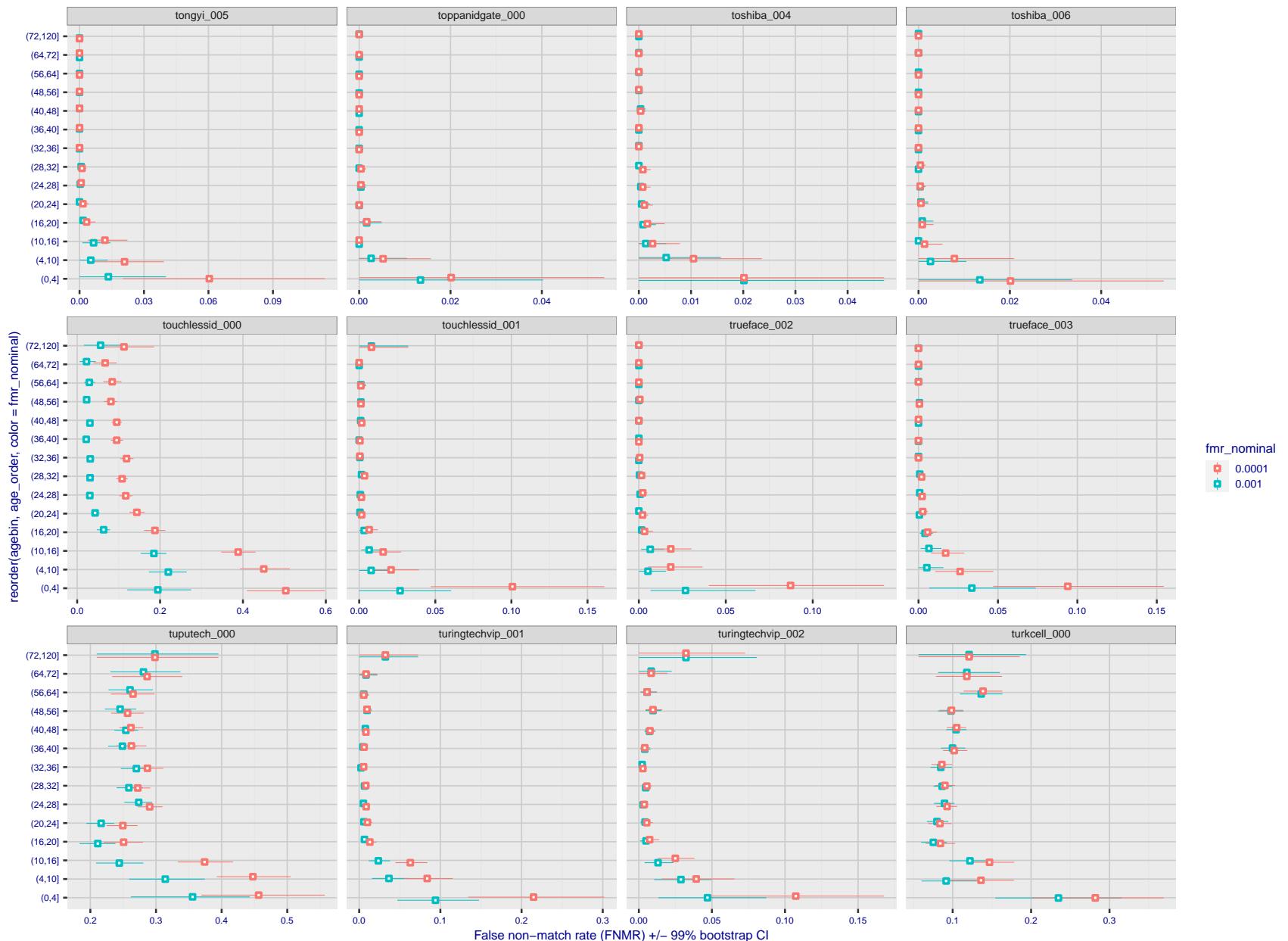


Figure 388: For the visa images, the dots show FNMR by age group for two operating thresholds corresponding to $FMR = \{0.001, 0.0001\}$ computed over all on the order of 10^{10} impostor scores. The FMR in each bin will vary also - see subsequent impostor heatmaps in sec. 3.6.2. Given a pair of face images taken at different times, we assign the comparison to the bin that is the arithmetic average of the subject's ages. This plot shows only the effect of age, not ageing. The number of comparisons in each bin is generally in the thousands, however the first and last bins are computed over 149 and 124 respectively. The error rates in some (adult) cases are zero, and in others the DET is flat so the error rates at the two thresholds are identical. The lines span 1% and 99% of bootstrap replicated FNMR estimates.

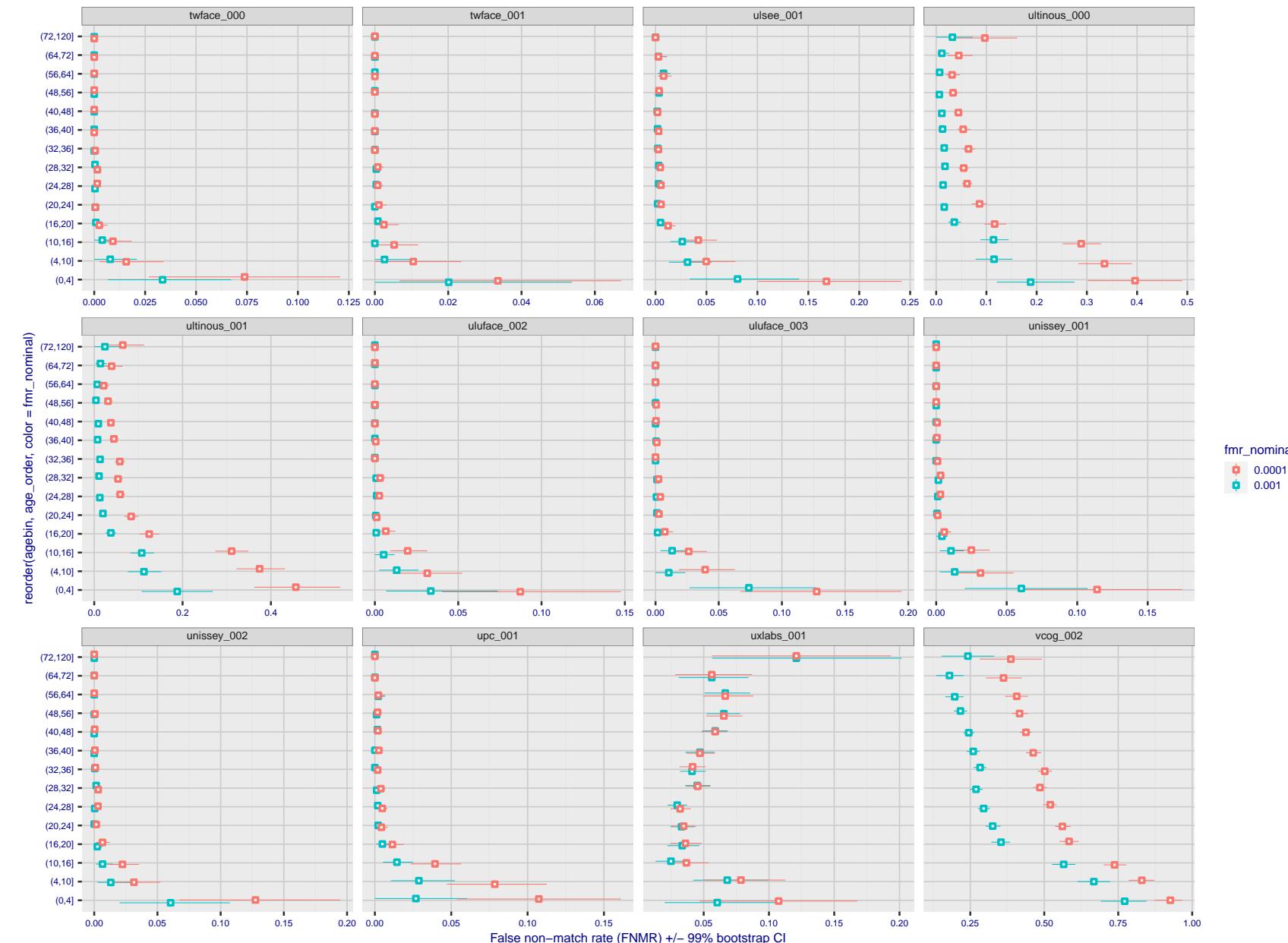


Figure 389: For the visa images, the dots show FNMR by age group for two operating thresholds corresponding to $FMR = \{0.001, 0.0001\}$ computed over all on the order of 10^{10} impostor scores. The FMR in each bin will vary also - see subsequent impostor heatmaps in sec. 3.6.2. Given a pair of face images taken at different times, we assign the comparison to the bin that is the arithmetic average of the subject's ages. This plot shows only the effect of age, not ageing. The number of comparisons in each bin is generally in the thousands, however the first and last bins are computed over 149 and 124 respectively. The error rates in some (adult) cases are zero, and in others the DET is flat so the error rates at the two thresholds are identical. The lines span 1% and 99% of bootstrap replicated FNMR estimates.

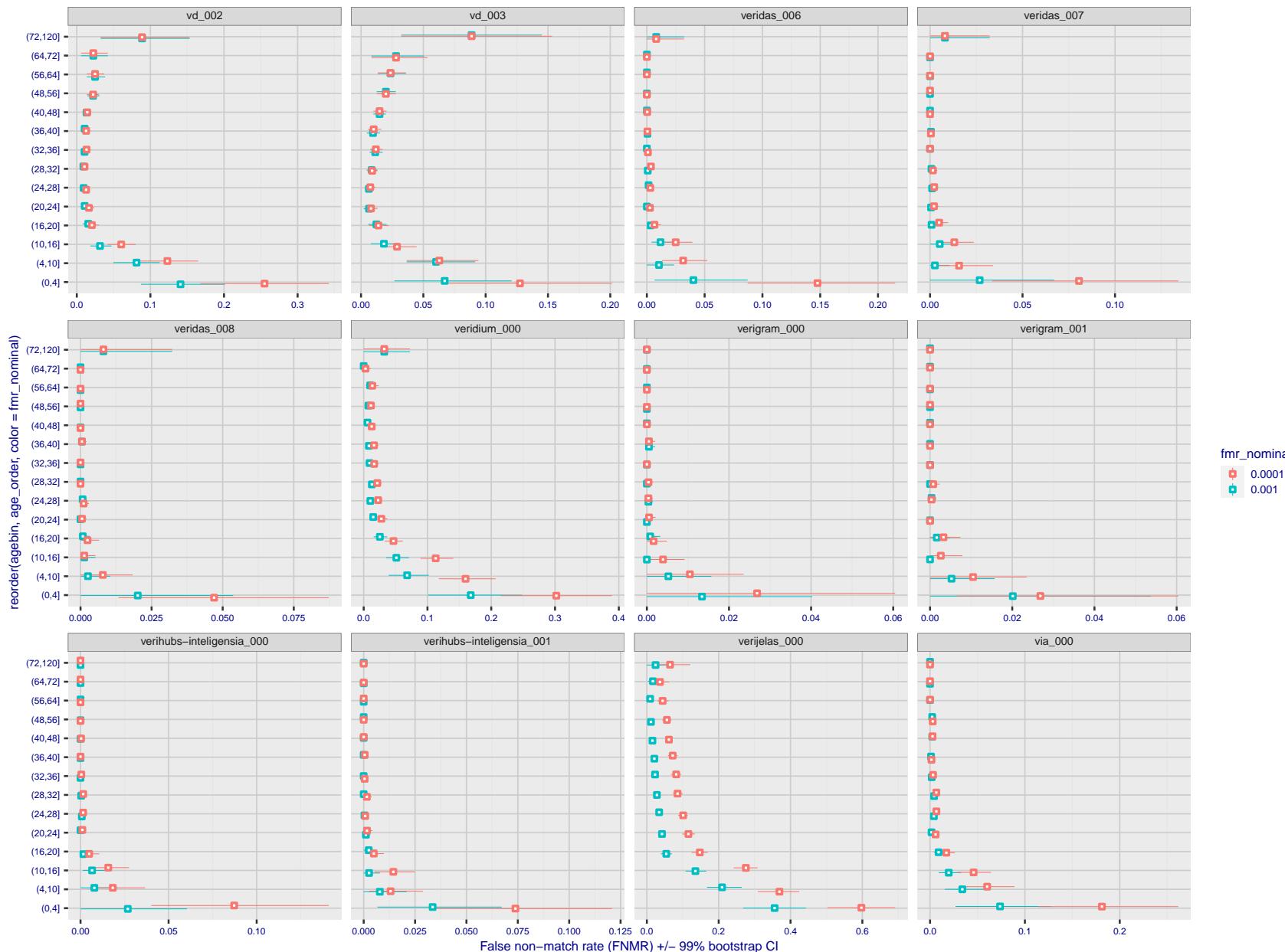


Figure 390: For the visa images, the dots show FNMR by age group for two operating thresholds corresponding to $FMR = \{0.001, 0.0001\}$ computed over all on the order of 10^{10} impostor scores. The FMR in each bin will vary also - see subsequent impostor heatmaps in sec. 3.6.2. Given a pair of face images taken at different times, we assign the comparison to the bin that is the arithmetic average of the subject's ages. This plot shows only the effect of age, not ageing. The number of comparisons in each bin is generally in the thousands, however the first and last bins are computed over 149 and 124 respectively. The error rates in some (adult) cases are zero, and in others the DET is flat so the error rates at the two thresholds are identical. The lines span 1% and 99% of bootstrap replicated FNMR estimates.

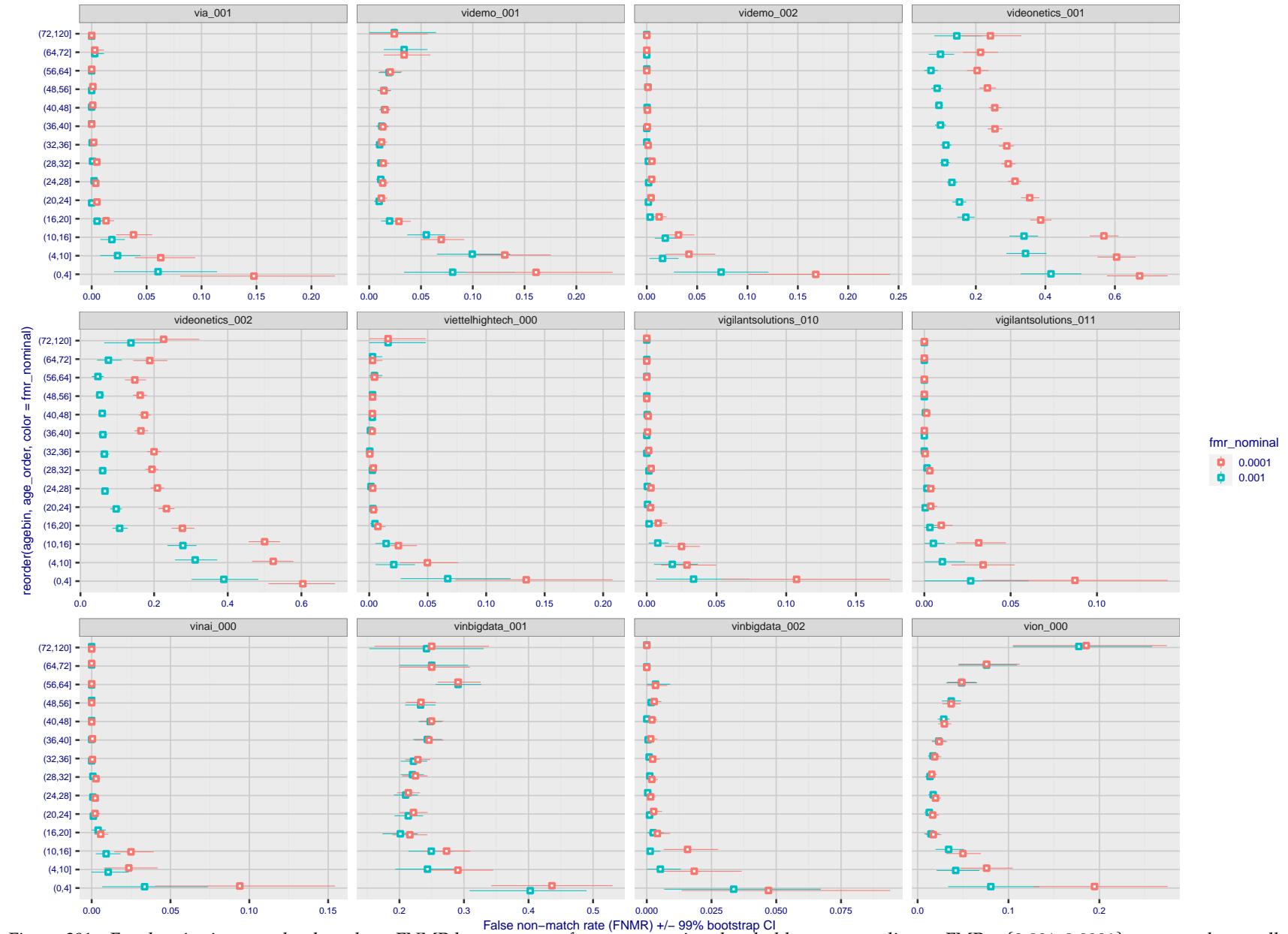


Figure 391: For the visa images, the dots show FNMR by age group for two operating thresholds corresponding to $FMR = \{0.001, 0.0001\}$ computed over all on the order of 10^{10} impostor scores. The FMR in each bin will vary also - see subsequent impostor heatmaps in sec. 3.6.2. Given a pair of face images taken at different times, we assign the comparison to the bin that is the arithmetic average of the subject's ages. This plot shows only the effect of age, not ageing. The number of comparisons in each bin is generally in the thousands, however the first and last bins are computed over 149 and 124 respectively. The error rates in some (adult) cases are zero, and in others the DET is flat so the error rates at the two thresholds are identical. The lines span 1% and 99% of bootstrap replicated FNMR estimates.



FNMR(T)
FMR(T)
"False non-match rate"
"False match rate"

Figure 392: For the visa images, the dots show FNMR by age group for two operating thresholds corresponding to $FMR = \{0.001, 0.0001\}$ computed over all on the order of 10^{10} impostor scores. The FMR in each bin will vary also - see subsequent impostor heatmaps in sec. 3.6.2. Given a pair of face images taken at different times, we assign the comparison to the bin that is the arithmetic average of the subject's ages. This plot shows only the effect of age, not ageing. The number of comparisons in each bin is generally in the thousands, however the first and last bins are computed over 149 and 124 respectively. The error rates in some (adult) cases are zero, and in others the DET is flat so the error rates at the two thresholds are identical. The lines span 1% and 99% of bootstrap replicated FNMR estimates.

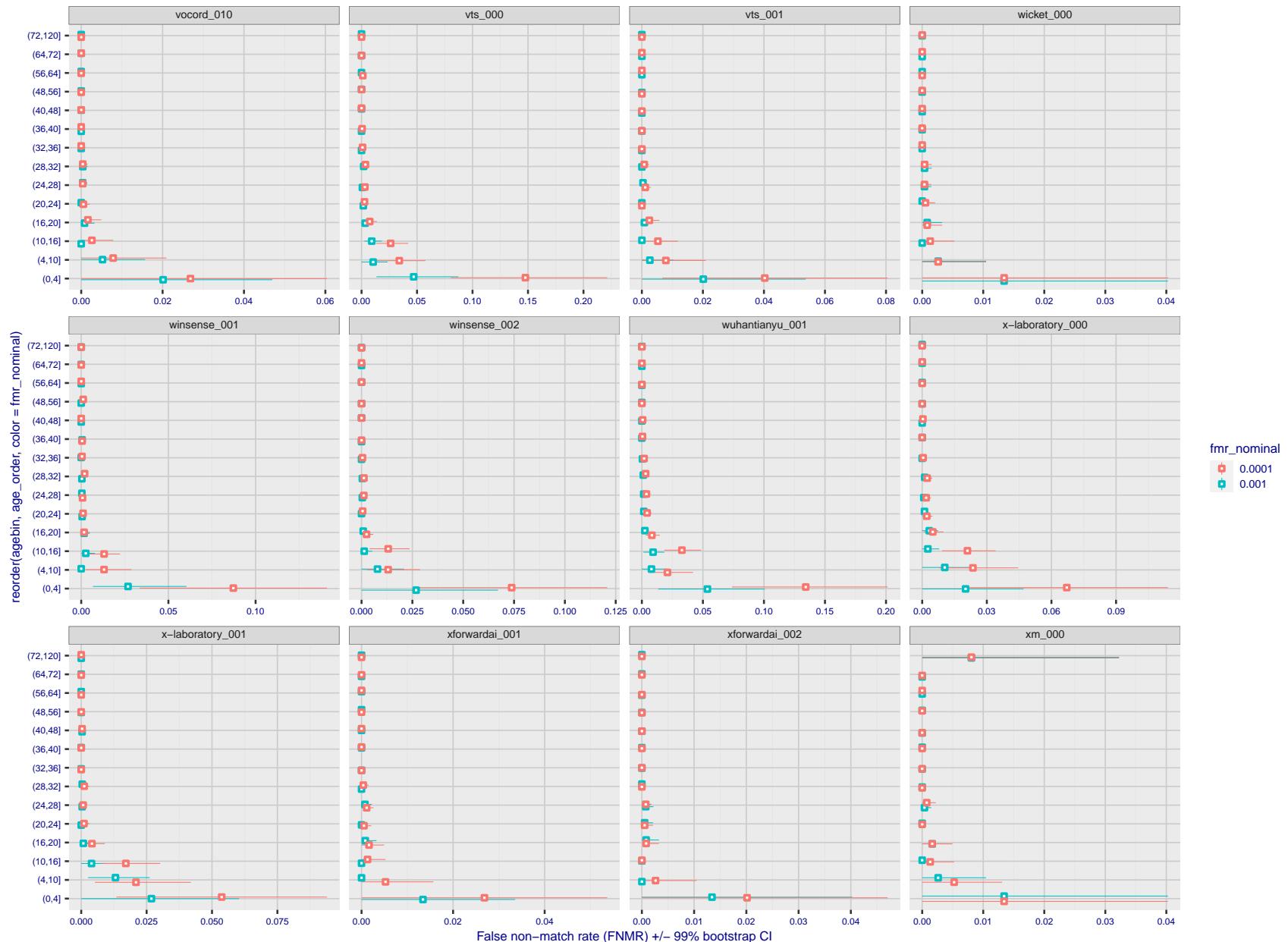


Figure 393: For the visa images, the dots show FNMR by age group for two operating thresholds corresponding to $FMR = \{0.001, 0.0001\}$ computed over all on the order of 10^{10} impostor scores. The FMR in each bin will vary also - see subsequent impostor heatmaps in sec. 3.6.2. Given a pair of face images taken at different times, we assign the comparison to the bin that is the arithmetic average of the subject's ages. This plot shows only the effect of age, not ageing. The number of comparisons in each bin is generally in the thousands, however the first and last bins are computed over 149 and 124 respectively. The error rates in some (adult) cases are zero, and in others the DET is flat so the error rates at the two thresholds are identical. The lines span 1% and 99% of bootstrap replicated FNMR estimates.



False non-match rate (FNMR) +/- 99% bootstrap CI

Figure 394: For the visa images, the dots show FNMR by age group for two operating thresholds corresponding to $FMR = \{0.001, 0.0001\}$ computed over all on the order of 10^{10} impostor scores. The FMR in each bin will vary also - see subsequent impostor heatmaps in sec. 3.6.2. Given a pair of face images taken at different times, we assign the comparison to the bin that is the arithmetic average of the subject's ages. This plot shows only the effect of age, not ageing. The number of comparisons in each bin is generally in the thousands, however the first and last bins are computed over 149 and 124 respectively. The error rates in some (adult) cases are zero, and in others the DET is flat so the error rates at the two thresholds are identical. The lines span 1% and 99% of bootstrap replicated FNMR estimates.

Caveats: None.

3.6 Impostor distribution stability

3.6.1 Effect of birth place on the impostor distribution

Background: Facial appearance varies geographically, both in terms of skin tone, cranio-facial structure and size. This section addresses whether false match rates vary intra- and inter-regionally.

Goals:

- ▷ To show the effect of birth region of the impostor and enrollee on false match rates.
- ▷ To determine whether some algorithms give better impostor distribution stability.

Methods:

- ▷ For the visa images, NIST defined 10 regions: Sub-Saharan Africa, South Asia, Polynesia, North Africa, Middle East, Europe, East Asia, Central and South America, Central Asia, and the Caribbean.
- ▷ For the visa images, NIST mapped each country of birth to a region. There is some arbitrariness to this. For example, Egypt could reasonably be assigned to the Middle East instead of North Africa. An alternative methodology could, for example, assign the Philippines to *both* Polynesia and East Asia.
- ▷ FMR is computed for cases where all face images of impostors born in region r_2 are compared with enrolled face images of persons born in region r_1 .

$$FMR(r_1, r_2, T) = \frac{\sum_{i=1}^{N_{r_1, r_2}} H(s_i - T)}{N_{r_1, r_2}} \quad (5)$$

where the same threshold, T , is used in all cells, and H is the unit step function. The threshold is set to give $FMR(T) = 0.001$ over the entire set of visa image impostor comparisons.

- ▷ This analysis is then repeated by country-pair, but only for those country pairs where both have at least 1000 images available. The countries¹ appear in the axes of graphs that follow.
- ▷ The mean number of impostor scores in any cross-region bin is 33 million. The smallest number of impostor scores in any bin is 135000, for Central Asia - North Africa. While these counts are large enough to support reasonable significance, the number of individual faces is much smaller, on the order of $N^{0.5}$.
- ▷ The numbers of impostor scores in any cross-country bin is shown in Figure 395.

Results: Subsequent figures show heatmaps that use color to represent the base-10 logarithm of the false match rate. Red colors indicate high (bad) false match rates. Dark colors indicate benign false match rates. There are two series of graphs corresponding to aggregated geographical regions, and to countries. The notable observations are:

- ▷ The on-diagonal elements correspond to within-region impostors. FMR is generally above the nominal value of $FMR = 0.001$. Particularly there is usually higher FMR in, Sub-Saharan Africa, South Asia, and the Caribbean. Europe and Central Asia, on the other hand, usually give FMR closer to the nominal value.
- ▷ The off-diagonal elements correspond to across-region impostors. The highest FMR is produced between the Caribbean and Sub-Saharan Africa.
- ▷ Algorithms vary.

¹These are Argentina, Australia, Brazil, Chile, China, Costa Rica, Cuba, Czech Republic, Dominican Republic, Ecuador, Egypt, El Salvador, Germany, Ghana, Great Britain, Greece, Guatemala, Haiti, Hong Kong, Honduras, Indonesia, India, Israel, Jamaica, Japan, Kenya, Korea, Lebanon, Mexico, Malaysia, Nepal, Nigeria, Peru, Philippines, Pakistan, Poland, Romania, Russia, South Africa, Saudi Arabia, Thailand, Trinidad, Turkey, Taiwan, Ukraine, Venezuela, and Vietnam.

- ▷ We computed the same quantities for a global FMR = 0.0001. The effects are similar.

Caveats:

- ▷ The effects of variable impostor rates on one-to-many identification systems may well differ from what's implied by these one-to-one verification results. Two reasons for this are a) the enrollment galleries are usually imbalanced across countries of birth, age and sex; b) one-to-many identification algorithms often implement techniques aimed at stabilizing the impostor distribution. Further research is necessary.
- ▷ In principle, the effects seen in this subsection could be due to differences in the image capture process. We consider this unlikely since the effects are maintained across geography - e.g. Caribbean vs. Africa, or Japan vs. China.

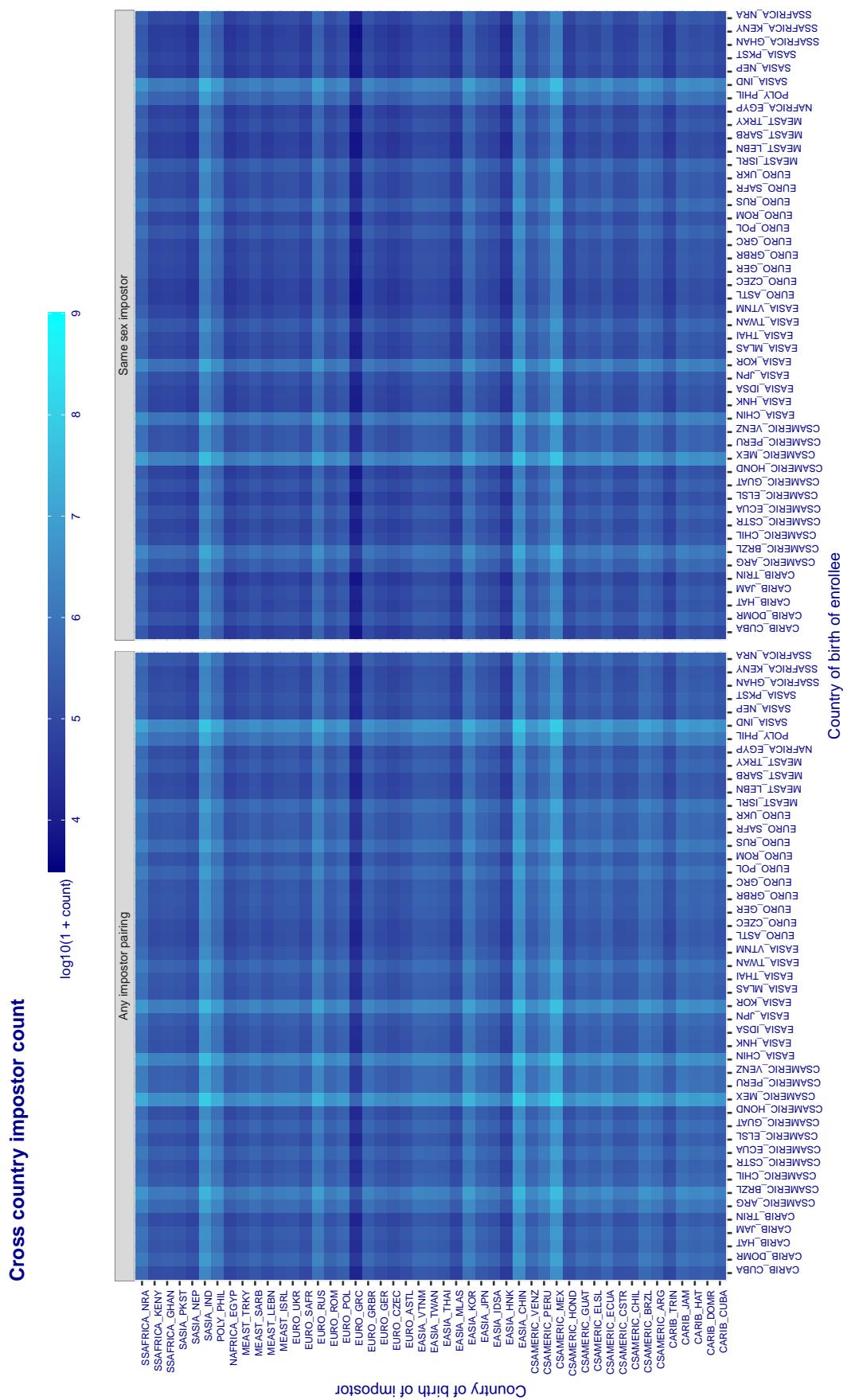


Figure 395: For visa images, the heatmap shows the count of impostor comparisons of faces from different individuals who were born in the given country pair. The FMR heatmaps themselves appear in the 1:1 report cards, for example, [this one](#).

3.6.2 Effect of age on impostors

Background: This section shows the effect of age on the impostor distribution. The ideal behaviour is that the age of the enrollee and the impostor would not affect impostor scores. This would support FMR stability over sub-populations.

Goals:

- ▷ To show the effect of relative ages of the impostor and enrollee on false match rates.
- ▷ To determine whether some algorithms have better impostor distribution stability.

Methods:

- ▷ Define 14 age group bins, spanning 0 to over 100 years old.
- ▷ Compute FMR over all impostor comparisons for which the subjects in the enrollee and impostor images have ages in two bins.
- ▷ Compute FMR over all impostor comparisons for which the subjects are additionally of the same sex, and born in the same geographic region.

Results:

The notable aspects are:

- ▷ Diagonal dominance: Impostors are more likely to be matched against their same age group.
- ▷ Same sex and same region impostors are more successful. On the diagonal, an impostor is more likely to succeed by posing as someone of the same sex. If $\Delta \log_{10} \text{FMR} = 0.2$, then same-sex same-region FMR exceeds the all-pairs FMR by factor of $10^{0.2} = 1.6$.
- ▷ Young children impostors give elevated FMR against young children. Older adult impostor give elevated FMR against older adults. These effects are quite large, for example if $\Delta \log_{10} \text{FMR} = 1.0$ larger than a 32 year old, then these groups have higher FMR by a factor of $10^1 = 10$. This would imply an FMR above 0.01 for a nominal (global) FMR = 0.001.
- ▷ Algorithms vary.
- ▷ We computed the same quantities for a global FMR = 0.0001. The effects are similar.

Note the calculations in this section include impostors paired across all countries of birth.

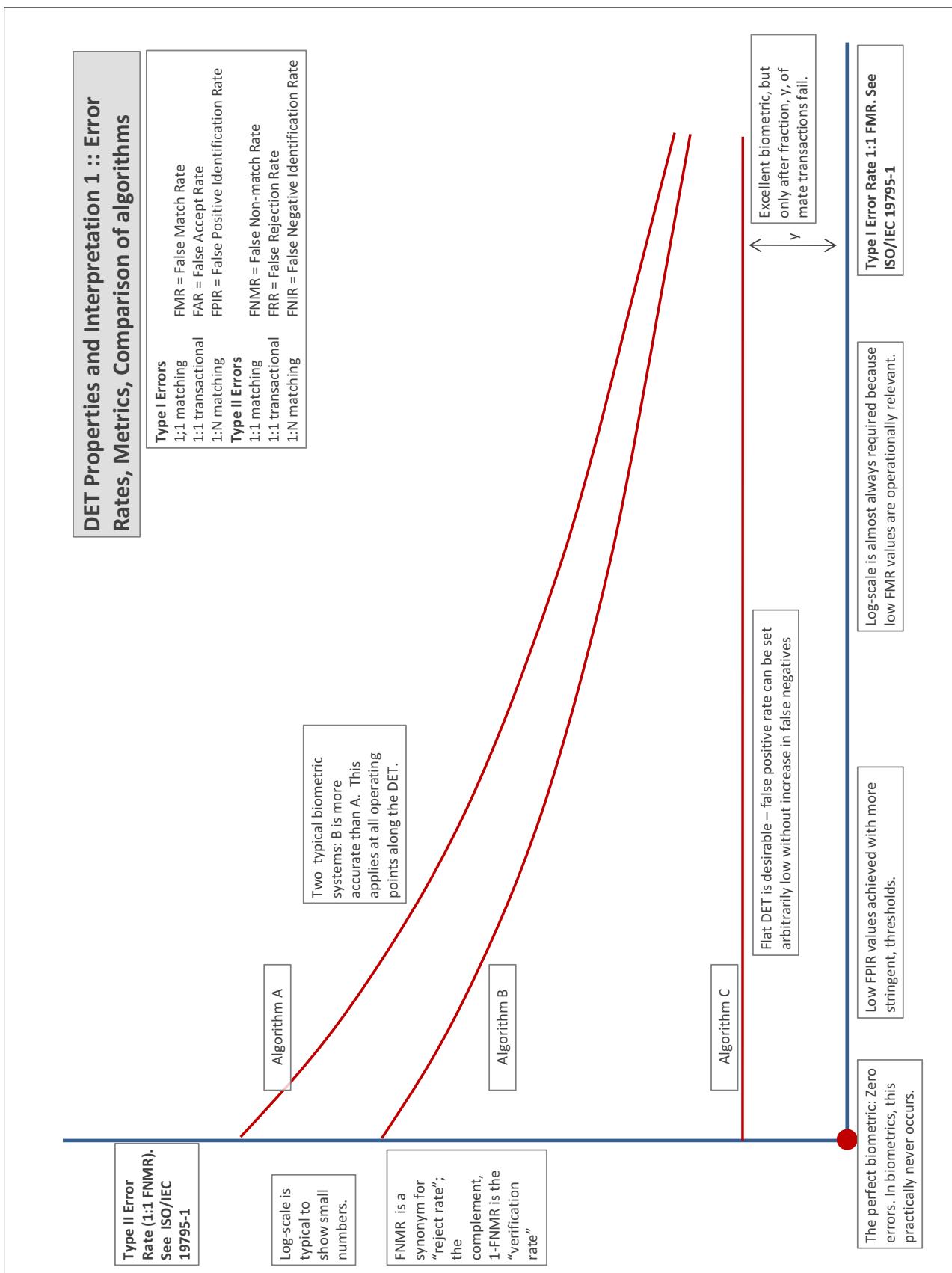
Accuracy Terms + Definitions

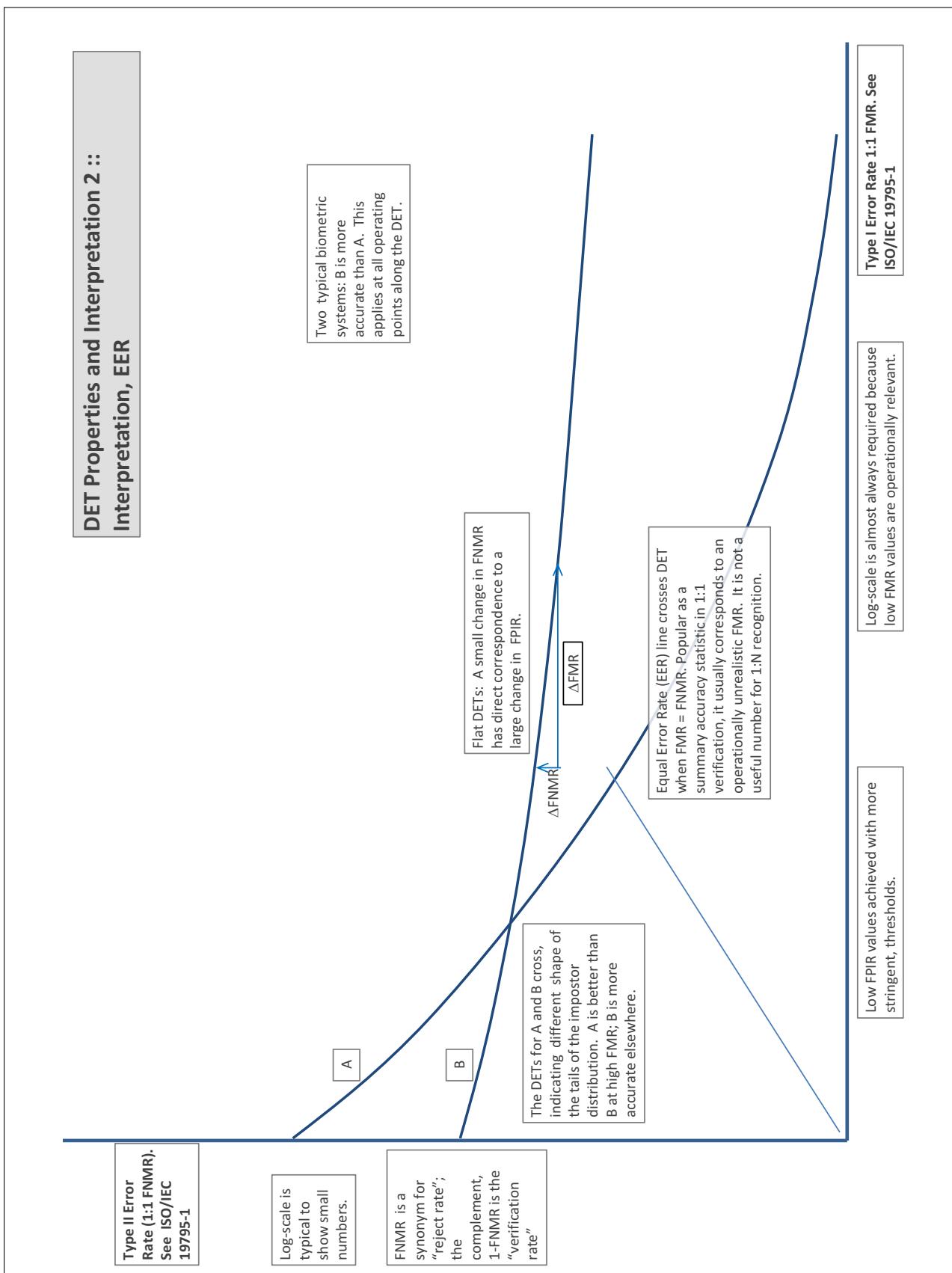
In biometrics, Type II errors occur when two samples of one person do not match – this is called a **false negative**. Correspondingly, Type I errors occur when samples from two persons do match – this is called a **false positive**. Matches are declared by a biometric system when the native comparison score from the recognition algorithm meets some **threshold**. Comparison scores can be either **similarity scores**, in which case higher values indicate that the samples are more likely to come from the same person, or **dissimilarity scores**, in which case higher values indicate different people. Similarity scores are traditionally computed by **fingerprint** and **face** recognition algorithms, while dissimilarities are used in **iris recognition**. In some cases, the dissimilarity score is a distance; this applies only when **metric** properties are obeyed. In any case, scores can be either **mate** scores, coming from a comparison of one person's samples, or **nonmate** scores, coming from comparison of different persons' samples. The words **genuine** or **authentic** are synonyms for mate, and the word **impostor** is used as a synonym for nonmatch. The words mate and nonmatch are traditionally used in identification applications (such as law enforcement search, or background checks) while genuine and impostor are used in verification applications (such as access control).

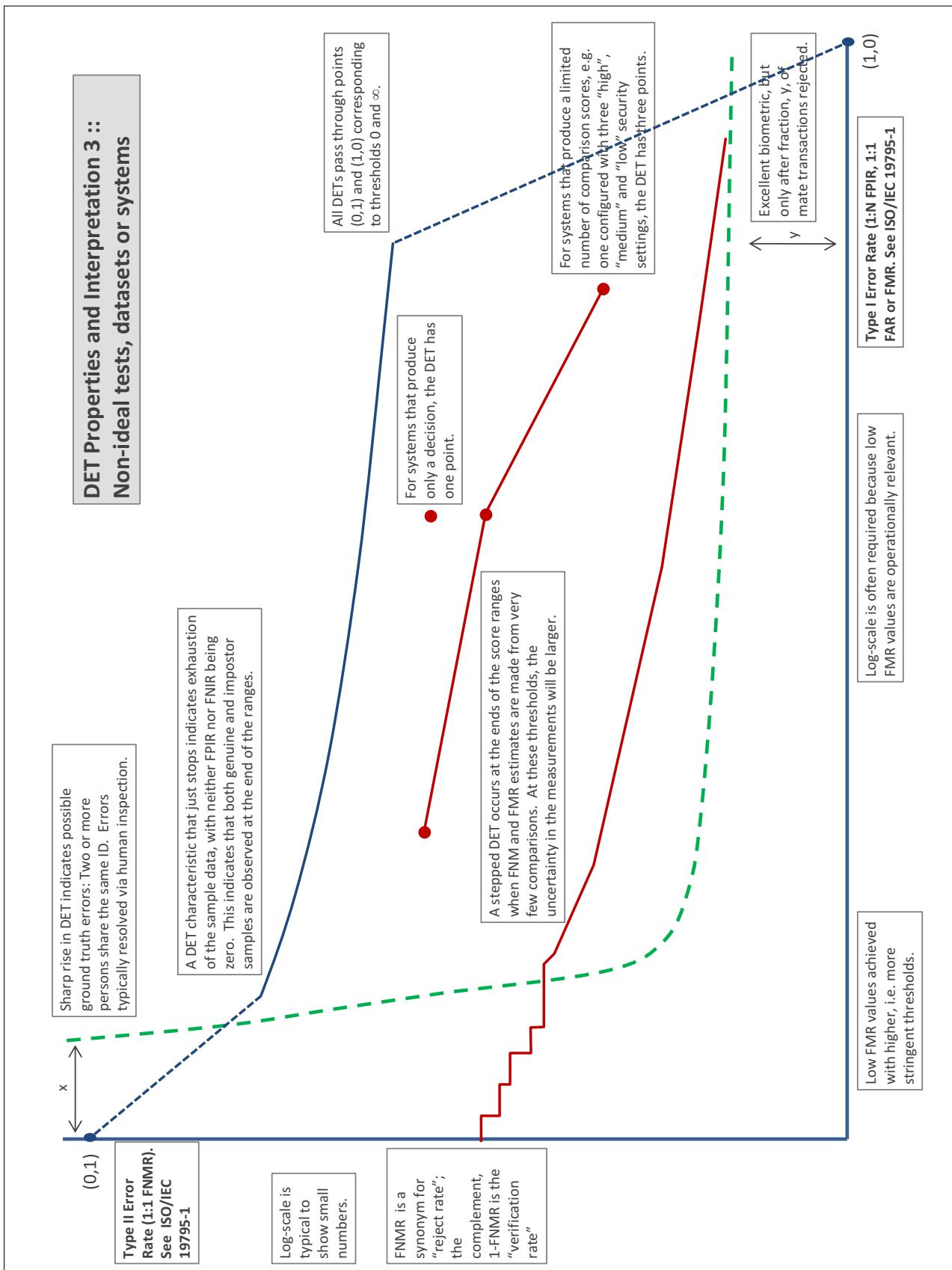
A **error tradeoff** characteristic represents the tradeoff between Type II and Type I classification errors. For verification this plots false non-match rate (FNMR) vs. false match rate (FMR) parametrically with T.

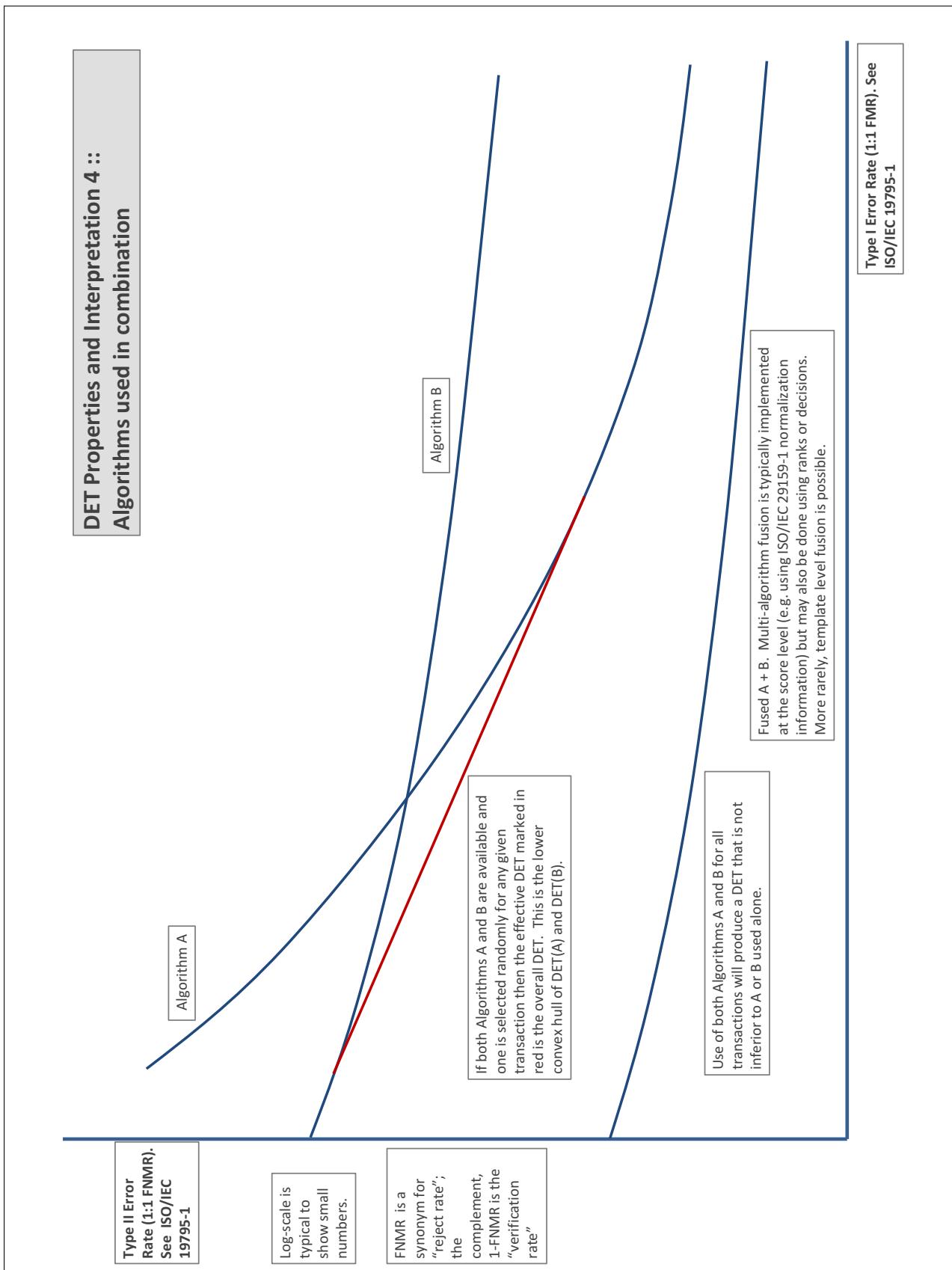
The error tradeoff plots are often called **detection error tradeoff (DET)** characteristics or **receiver operating characteristic (ROC)**. These serve the same function but differ, for example, in plotting the complement of an error rate (e.g., $TMR = 1 - FNMR$) and in transforming the axes most commonly using logarithms, to show multiple decades of FMR. More rarely, the function might be the inverse Gaussian function.

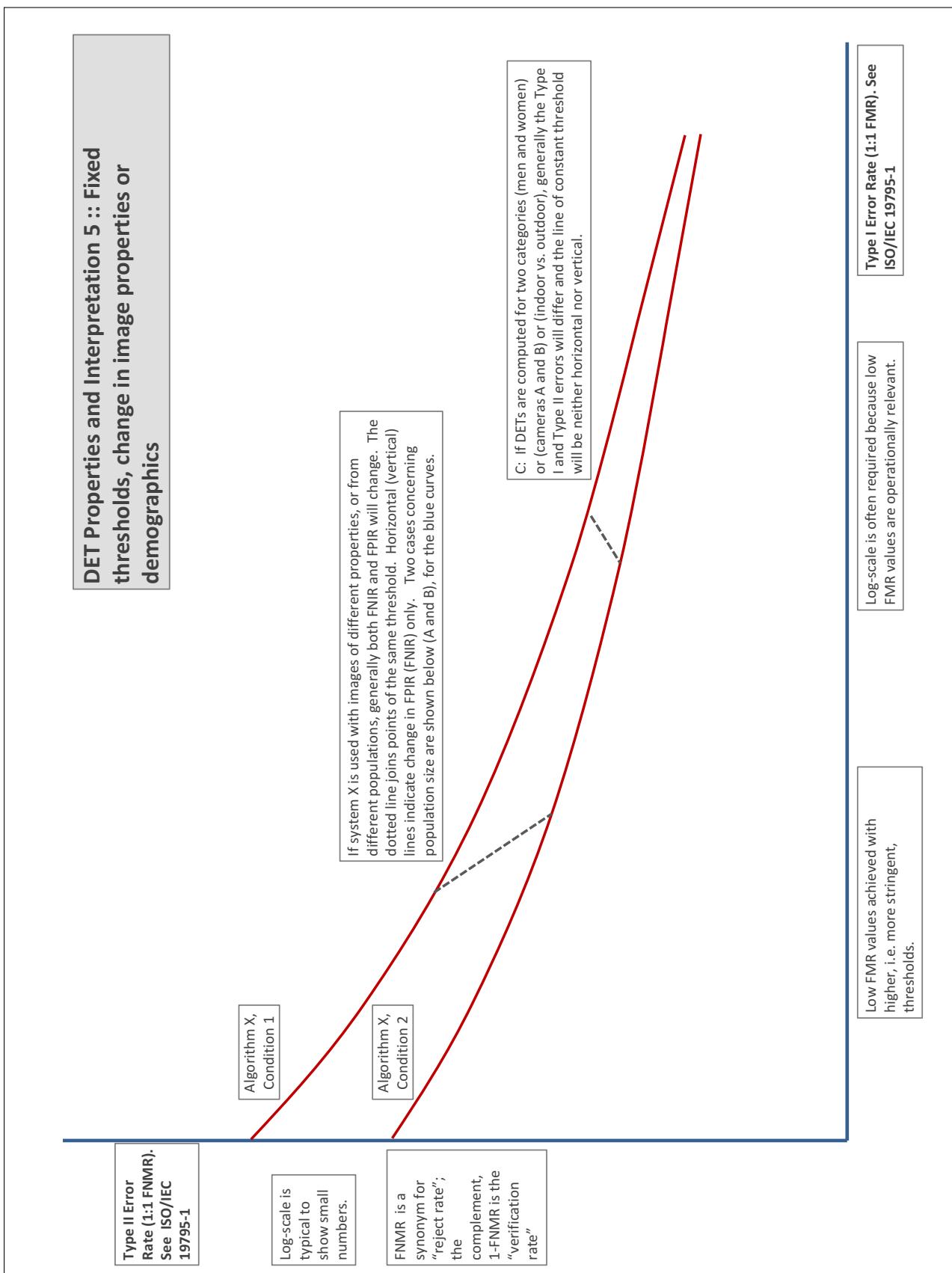
More detail and generality is provided in formal biometrics testing standards, see the various parts of [ISO/IEC 19795 Biometrics Testing and Reporting](#). More terms, including and beyond those to do with accuracy, see [ISO/IEC 2382-37 Information technology -- Vocabulary -- Part 37: Harmonized biometric vocabulary](#)











References

- [1] P. Jonathon Phillips, Amy N. Yates, Ying Hu, Carina A. Hahn, Eilidh Noyes, Kelsey Jackson, Jacqueline G. Cavazos, Géraldine Jeckeln, Rajeev Ranjan, Swami Sankaranarayanan, Jun-Cheng Chen, Carlos D. Castillo, Rama Chellappa, David White, and Alice J. O'Toole. Face recognition accuracy of forensic examiners, superrecognizers, and face recognition algorithms. *Proceedings of the National Academy of Sciences*, 115(24):6171–6176, 2018.